# Foundations of Applied Electromagnetics

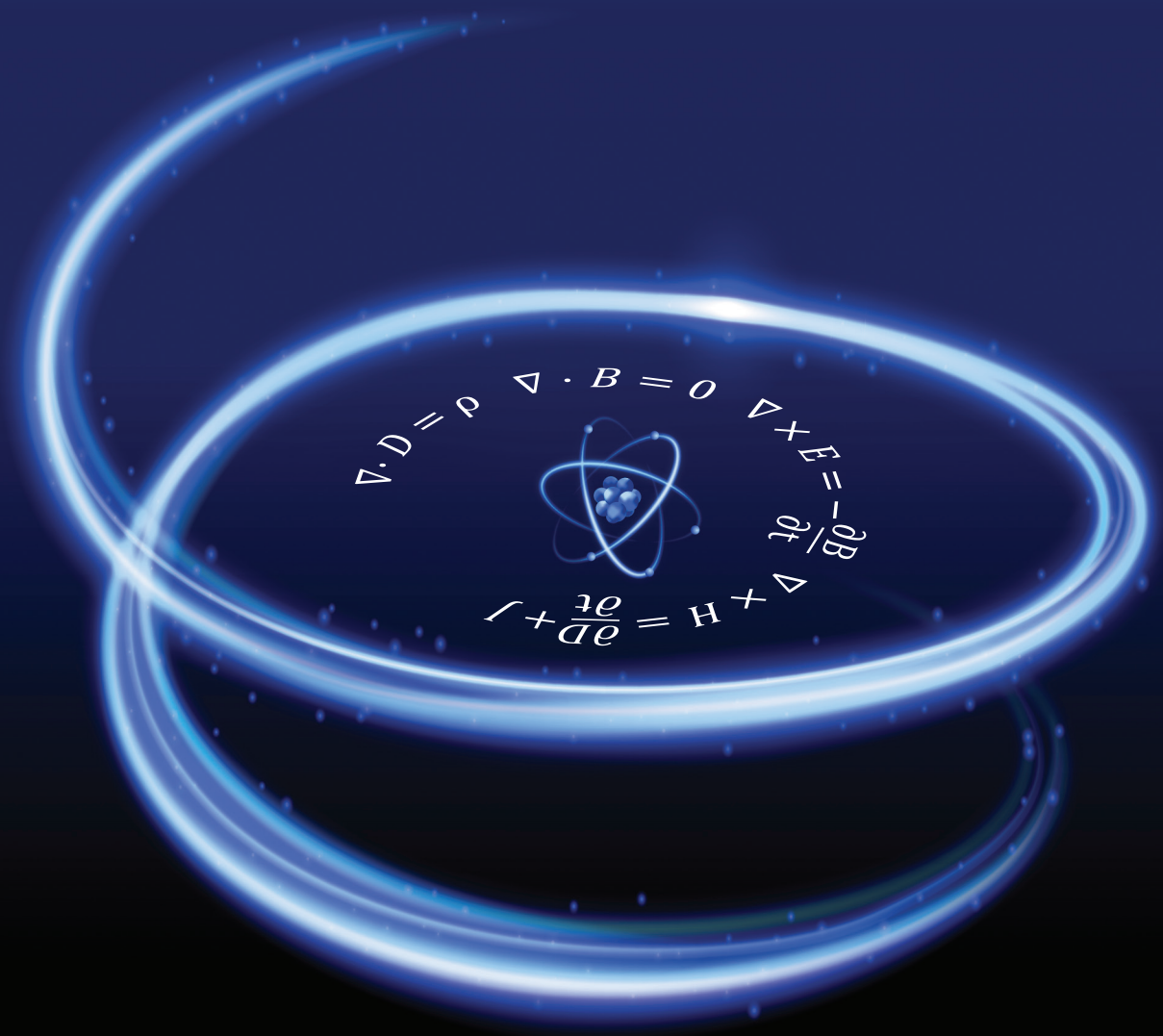


KAMAL SARABANDI

# FOUNDATIONS OF APPLIED ELECTROMAGNETICS

**Kamal Sarabandi**
*The University of Michigan*

Copyright © 2022 Kamal Sarabandi

This book is published by Michigan Publishing under an agreement with the author. It is made available free of charge in electronic form to any student orinstructor interested in the subject matter.

Published in the United States of America by
Michigan Publishing
Manufactured in the United States of America

ISBN 978-1-60785-824-9

The Free ECE Textbook Initiative is sponsored by the ECE Department at the University of Michigan.

The image used in the chapter title pages was taken by the James Webb Space Telescope, courtesy of NASA.

*I dedicate this book to my family:*
*to my wife Shiva and our sons Arya and Sina*
*for their love and support,*
*and to the memory of my parents Abbasali and Jaleh,*
*who instilled in me a passion for science and engineering*

# Preface

Field theory is one of the fundamental pillars of electrical engineering, with many threads interwoven into numerous areas of science and technology. Classical electromagnetic theory may be considered a mature field of science, but because of its importance in wireless transmission of data and energy, it has remained an area of intense research and development for almost two centuries. In recent years, the interest in the field of applied electromagnetics has been fueled by the demand for high data-rate wireless communication, everywhere and at any time. The implementation of such wireless systems relies on innovation in miniaturized wideband and multiband antennas for handheld devices, vehicles, and infrastructures such as base stations and wifi networks. In addition, knowledge of the characteristics of wave propagation and wave interaction with terrain, vegetation, and manmade structures in urban environments is an essential and critical tool for the proper design of wireless communication networks. Moreover, over the past decade we have witnessed a boom in investment focused on the rapid development of autonomous vehicles. Sensors envisioned to enable autonomous functionality include short-range and long-range sensors with different modalities. Some of these sensors are based on electromagnetic waves, such as millimeter-wave radars to provide the range, direction, and velocity of objects present in traffic scenes. For these systems to function with a high degree of reliability, we need to use applicable wave propagation and scattering models together with highly sophisticated directional antennas, all of which requires in-depth understanding of electromagnetic wave theory. In addition, traditional applications of field theory in areas such as microwave remote sensing, military systems, biomedical applications, and space exploration are active and ongoing. Graduate students interested in such exciting fields of research need a strong foundation in field theory, and that was my motivation for writing this book on classical electromagnetics but with an eye on its modern applications.

This book is the outgrowth of my class notes for an entry-level graduate course on electromagnetic theory at the University of Michigan and was inspired by my own research on radar remote sensing, antenna theory, electromagnetic wave propagation, and more recently on bioelectromagnetics.

Any textbook based on a field with more than 200 years of history draws very heavily from the work of an enormous number of scientists and engineers. This book is not an exception and I found it impossible to provide a comprehensive list of references to the original contributors for most topics included in this book.

Publishing this book would not have been possible without the help and encouragement of several colleagues and students. I have to first thank my dear colleague and former advisor Professor Fawwaz Ulaby, who has carefully reviewed and provided valuable comments and suggestions for improving what is presented in this book. I am also indebted to Mr. Richard Carnes, who spent a significant amount of effort typing and formatting the book. I have also to mention the contributions of my students Abdelhamid Nasr, Aditya Varma Muppala, and Behzad Yektakhah for helping with some of the figures and computations presented in the book.

KAMAL SARABANDI
ANN ARBOR, AUGUST 2022

# Contents

**Preface** **iv**

**1 Electromagnetic Fields** **1**
- **1-1** The Field Equations . . . 2
- **1-2** Faraday's Law for a Moving Surface in a Time-Varying Magnetic Field . . . 10
- **1-3** Ampère's Law for a Moving Surface in a Time-Varying Electric Field . . . 13
- **1-4** Constitutive Relations: Macroscopic Properties of Matter . . . 14
- **1-5** Kramers-Krönig Relations . . . 28
- **1-6** Boundary Conditions . . . 30
- **1-7** Drift Current in Metals . . . 33
- **1-8** Hall Effect in Conducting Media . . . 35
- **1-9** Generalized Coordinates . . . 36

**2 Electromagnetic Concepts, Tools, and Theorems** **63**
- **2-1** Equivalent Magnetic Charge and Current Densities . . . 63
- **2-2** Image Theory . . . 68
- **2-3** Method of Images for Other Problems . . . 71
- **2-4** Polarization Current . . . 80
- **2-5** Stored Electromagnetic Energy . . . 83
- **2-6** Flow of Energy . . . 86
- **2-7** Superposition Principle . . . 90
- **2-8** Uniqueness Theorem . . . 90
- **2-9** Equivalence Principle for Electromagnetic Sources . . . 92

**3 The Electromagnetic Potentials and Radiation** **107**
- **3-1** Electromagnetic Potentials . . . 108
- **3-2** Time-Harmonic Electromagnetic Waves . . . 122
- **3-3** Time-Harmonic Retarded Potential . . . 131
- **3-4** Far-Field Distance Criterion . . . 137
- **3-5** Small Loop of Current: A Hertzian Magnetic Dipole . . . 139
- **3-6** Wire Antennas . . . 144
- **3-7** Equivalent Circuit for Receiving Antennas . . . 147

**4 Formal Solutions to Maxwell's Equations and Their Applications 161**
4-1 Formal Solution of the Helmholtz Equation . . . 162
4-2 Solution of the Helmholtz Equation for a Complex Medium . . . 168
4-3 Integral Equations for Electromagnetic Fields . . . 176
4-4 Integral Equation Formulation Based on Equivalent Sources . . . 178
4-5 Integral Equation Formulation for Dielectric Scatterers . . . 181
4-6 Reciprocity Theorem . . . 184
4-7 Applications of the Reciprocity Theorem . . . 189
4-8 Babinet's Principle . . . 205

**5 Electromagnetic Plane Waves 227**
5-1 Plane-Wave Propagation in Homogeneous Media . . . 228
5-2 Polarization of Plane Waves . . . 238
5-3 Plane Waves in Anisotropic Media . . . 241
5-4 kDB Coordinate System for Plane Waves in Bianisotropic Media . . . 247
5-5 Transverse Electric (TE) and Transverse Magnetic (TM) Field Solutions of the Helmholtz Equation . . . 254
5-6 Plane-Wave Reflection at the Interface between a Dielectric Medium and a Good-Conducting Medium . . . 264
5-7 Wave Propagation in an Inhomogeneous Medium: Geometric-Optics Approximation . . . 266
5-8 Plane-Wave Reflection and Transmission from a Half-Space Uniaxial Medium 275
5-9 Plane Waves in Layered Media . . . 281
5-10 Plane-Wave Propagation in a Negative-Index Medium . . . 290
5-11 Negative Refractive-Index Lens . . . 292

**6 Cartesian Wave Functions: Guiding Structures and Resonators 313**
6-1 The Dielectric Plate Waveguide . . . 315
6-2 Guided Waves on Impedance Surfaces . . . 321
6-3 Practical Realization of Reactive Impedance Surfaces . . . 324
6-4 Isotropic Reactive Impedance Surfaces . . . 330
6-5 The Rectangular Waveguide . . . 335
6-6 Transmission-Line Circuit Model for Waveguides . . . 357
6-7 Other Modal Solutions for Rectangular Waveguides . . . 363
6-8 Modal Expansion of Field Quantities . . . 367
6-9 Calculus of Variations for Estimation of Resonant Frequencies in General Cavities . . . 382

**7 Cylindrical Wave Functions and Their Applications 405**
7-1 Wave Functions in the Cylindrical Coordinate System . . . 406
7-2 The Circular Dielectric Waveguide . . . 427
7-3 Radial and Circumferential Waveguides . . . 433
7-4 Green's Functions Solutions for Some Canonical Problems . . . 436
7-5 Scattering from a Metallic Circular Cylinder . . . 455
7-6 Integral Representation of Bessel Functions . . . 464

**7-7** 2-D Green's Function for Homogeneous Media in the Presence of a Metallic Wedge . . . 471
**7-8** Asymptotic Evaluation of a Field Diffracted by a Metallic Wedge . . . 478

**8 Spherical Wave Functions and Their Applications 506**
**8-1** Wave Functions in the Spherical Coordinate System . . . 508
**8-2** Wave Transformation to Spherical Wave Functions . . . 538
**8-3** Multipole Representation of Spherical Waves . . . 543
**8-4** Plane-Wave Scattering from Spheres . . . 547
**8-5** Wave Propagation in a Conical Waveguide . . . 557
**8-6** Biconical Structures . . . 564
**8-7** Other Spherical Waveguides . . . 572

**A Properties of Complex Functions 590**
**A-1** Cauchy–Riemann Conditions . . . 591
**A-2** Conformal Mapping . . . 591
**A-3** Branch Cut and Branch Point . . . 592
**A-4** Cauchy's Theorem . . . 592
**A-5** Cauchy Formulas . . . 594
**A-6** Poles and Residues . . . 594
**A-7** Jordan's Lemma . . . 595

**B Method of Steepest Descent 596**
**B-1** Saddle Point . . . 597
**B-2** Integration along the Steepest Descent Path . . . 598

**C Useful Vector Identities, Operators, and Coordinate Transformations 600**

**Index 605**

# Chapter 1
# Electromagnetic Fields

## Chapter Contents


Overview, 2
1-1 The Field Equations, 2
1-2 Faraday's Law for a Moving Surface in a Time-Varying Magnetic Field, 10
1-3 Ampère's Law for a Moving Surface in a Time-Varying Electric Field, 13
1-4 Constitutive Relations: Macroscopic Properties of Matter, 14
1-6 Boundary Conditions, 30
1-7 Drift Current in Metals, 34
1-8 Hall Effect in Conducting Media, 35
1-9 Generalized Coordinates, 36
Chapter Summary, 44
Problems, 46


## Objectives

Upon learning the material presented in this chapter, you should be able to:

1. Explain the basic physics behind Maxwell's equations.
2. Understand the relations between the field intensities and the flux densities in a material medium (known as the constitutive relations) and their behavior as a function of time and frequency.
3. Incorporate complexities associated with field discontinuities across abrupt boundaries between dissimilar media.
4. Express the expanded form of Maxwell's equations and relevant differential operators in both standard and arbitrary coordinate systems.

## Overview

All material media—from an isolated atom to an entire galaxy of stars and planets—radiate electromagnetic waves, all the time! We are constantly getting bombarded by a spectrum of EM waves, including light waves, microwaves, and radio waves. Electromagnetics, the bidirectional interaction between the electric and magnetic fields, is at the core of what makes electronic circuits function, communication systems transfer data, and computer systems process information. This book is about how electromagnetic fields interact with material media, including reflection by and refraction across boundaries between electromagnetically dissimilar media, transmission across boundaries, absorption by lossy media, and scattering within inhomogeneous media.

Chapter 1 starts with an examination of the four famous equations known as Maxwell's equations, in both differential and integral forms. Maxwell's equations are then formulated for the condition when the electric and magnetic fields are in the presence of a time-varying (moving) surface, and also used to define the constitutive properties of material media, namely the electrical permittivity and magnetic permeability, in both homogeneous and anisotropic materials. These foundational formulations will serve to facilitate the treatments of the various EM-related topics covered in forthcoming chapters.

## 1-1 The Field Equations

Electromagnetism, as the structure of the word implies, encompasses certain laws of physics that define the interrelationships between the electric and magnetic fields. Electromagnetic phenomena are observed only when the two field quantities are time-varying. The nature of the interaction between the time-varying electric and magnetic fields was first discovered by Michael Faraday (1791–1867) and later formulated into mathematical expressions by James Clerk Maxwell (1831–1879). Faraday's significant discovery was based on experimental observations and Maxwell's formulation was based on mathematical deduction. Faraday's extensive experimental work was motivated by the belief that every cause and effect has its converse. That is, if electricity can produce a magnetic field, a phenomenon discovered by Oersted, then, conversely, a magnetic field should be able to produce an electric field.

The fundamental laws of electricity and magnetism are encapsulated by Maxwell's equations:*

$$\nabla \times \mathbf{H} = \mathbf{J} + \frac{\partial \mathbf{D}}{\partial t} \quad (\textit{modified Ampère's law}), \tag{1.1a}$$

$$\nabla \times \mathbf{E} = -\frac{\partial \mathbf{B}}{\partial t} \quad (\textit{Faraday's law}), \tag{1.1b}$$

$$\nabla \cdot \mathbf{D} = \rho \quad (\textit{Gauss' law for electricity}), \tag{1.1c}$$

$$\nabla \cdot \mathbf{B} = 0 \quad (\textit{Gauss' law for magnetism}). \tag{1.1d}$$

*James Clerk Maxwell, *A Treatise on Electricity and Magnetism,* Constable and Co., London, 1873.

where

$$\mathbf{H} = \mathbf{H}(\mathbf{r},t) \quad (\textit{magnetic field intensity}, \text{A/m}),$$
$$\mathbf{E} = \mathbf{E}(\mathbf{r},t) \quad (\textit{electric field intensity}, \text{V/m}),$$
$$\mathbf{D} = \mathbf{D}(\mathbf{r},t) \quad (\textit{electric flux density}, \text{C/m}^2),$$
$$\mathbf{B} = \mathbf{B}(\mathbf{r},t) \quad (\textit{magnetic flux density}, \text{W/m}^2),$$
$$\rho = \rho(\mathbf{r},t) \quad (\textit{volumetric charge density}, \text{C/m}^3),$$
$$\mathbf{J} = \mathbf{J}(\mathbf{r},t) \quad (\textit{current density}, \text{A/m}^2),$$

and $\mathbf{r}$ is the position vector for an ordinary point in the medium. Here ***ordinary point*** refers to a point wherein within its immediate neighborhood the physical properties of the medium are continuous. In other words, the small medium around $\mathbf{r}$ is considered to be ***homogeneous***. If the physical properties of a medium change abruptly as a function of location, the vector field quantities may also do the same. That is, the transition of field vectors across a surface where change in material properties is abrupt may be discontinuous. The nature of these discontinuities will be investigated in detail in later sections.

Equations (1.1a) and (1.1b), in addition to the ***law of conservation of charge***, constitute the necessary and sufficient set of equations required for determining the field quantities.

The phenomena of electricity and magnetism are governed by the presence of static and moving charges. Basically, charges are considered the source of electromagnetic fields without which the field quantities $(\mathbf{E},\mathbf{H},\mathbf{D},\mathbf{B})$ cannot exist.

### 1-1.1 Charge Density

The quantized nature of charges is well established. A charge quantum is equal to the absolute value of the charge of an electron, namely

$$\text{electron charge } e = -1.6 \times 10^{-19} \text{ C}\,.$$

However, Maxwell's equations describe large-scale phenomena, i.e., the macroscopic element of volume must contain a large number of atoms and molecules, in which case a macroscopic particle can assume any real number. If the amount of charge contained in volume element $\Delta V$ is $\Delta q$, then the ***volumetric charge density*** is defined as

$$\rho = \lim_{\Delta V \to 0} \frac{\Delta q}{\Delta V}\,. \tag{1.2}$$

In the strictest sense, Eq. (1.2) does not define a continuous function of position because $\Delta V$ cannot approach zero without limit.

### 1-1.2 Current Density

From a macroscopic point of view, any ordered motion of charge constitutes a current. Hence, a current is represented by a vector quantity whose direction is the direction of

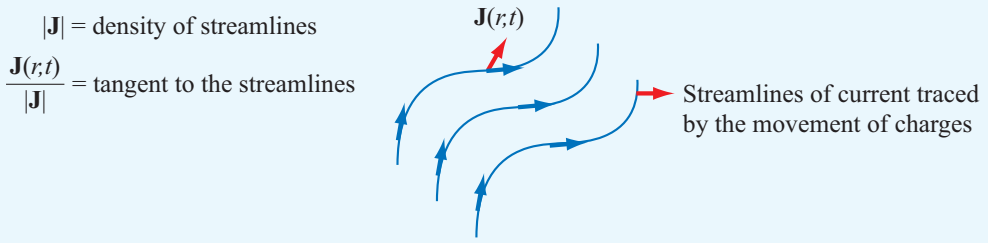


**Figure 1-1:** Streamlines of electric current in a medium, where the intensity of the current density is represented by the density of the streamlines and the unit vector tangent to the lines specifies the direction of flow.

motion of the charges and its magnitude is proportional to the velocity and number density of the charges. To define a current vector more precisely, we do so in terms of the ***current density*** (distribution) defined over the region of space under consideration. Current density (distribution) is characterized by a vector field **J**, as depicted in Fig. 1-1. To better quantify current density, let us consider a differential surface $\Delta S$ whose unit normal is denoted by $\hat{\mathbf{n}}$, as shown in Fig. 1-2. If $\Delta I$ represents the total current crossing the differential area $\Delta S$, then **J** is defined such that

$$\Delta I = \mathbf{J} \cdot \Delta \mathbf{S} \, . \tag{1.3}$$

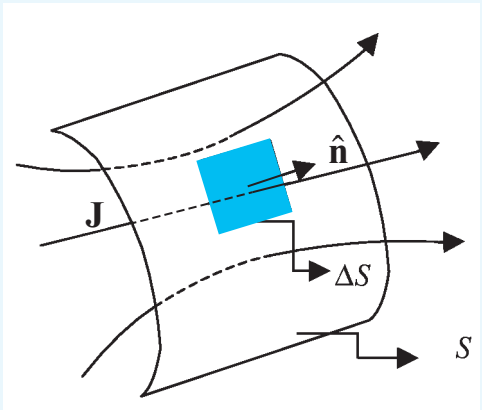


$$\Delta \mathbf{S} = \Delta S \, \hat{\mathbf{n}}$$

**Figure 1-2:** The diagram depicts a surface $S$ intersecting streamlines of an electric current flowing through that surface. The current density **J** is defined as the normalized current flowing through a differential surface.

By extension, the total current crossing an arbitrary surface $S$ can be computed from

$$I = \int_S \mathbf{J} \cdot d\mathbf{s} \, . \tag{1.4}$$

### 1-1.3 Point Form of Law of Conservation of Charge

The law of conservation of charge states that the net value of charge in a closed system remains constant. This means that if there is a certain number of positive charges and a certain number of negative charges in an enclosed medium, nothing can be done to create an excess amount of either kind of charge nor to annihilate only one type of charge. To change the value of net charge in the closed system, charges will have to be either removed from or brought into the system.

Now suppose the surface $S$ is a closed surface. Define $\hat{\mathbf{n}}$ as a unit normal to the surface drawn in the *outward direction*. According to the law of conservation of charges,

$$I = \oiint_S \mathbf{J} \cdot d\mathbf{s} = -\frac{d}{dt} Q = -\frac{d}{dt} \iiint_V \rho \, dv \, , \tag{1.5}$$

where $Q$ is the total charge enclosed and $V$ is the volume enclosed by $S$. If the surface is stationary, then

$$\oiint \mathbf{J} \cdot d\mathbf{s} = \iiint_V -\frac{\partial \rho}{\partial t} \, dv \, . \tag{1.6}$$

According to the divergence theorem,

$$\oiint \mathbf{J} \cdot d\mathbf{s} = \iiint_V \nabla \cdot \mathbf{J} \, dv \, , \tag{1.7}$$

so that in the limit where $V$ is very small, denoted as $\Delta V$,

$$\iiint_{\Delta V} \nabla \cdot \mathbf{J} \, dv = \nabla \cdot \mathbf{J} \, \Delta V \, .$$

This equivalence leads to the following definition for the divergence operation:

$$\nabla \cdot \mathbf{J} \triangleq \lim_{\Delta V \to 0} \frac{1}{\Delta V} \oiint \mathbf{J} \cdot d\mathbf{s} \, . \tag{1.8}$$

Using Eq. (1.7) in Eq. (1.6) leads to the following relation for volume $V$:

$$\iiint_V \nabla \cdot \mathbf{J} \, dv = \iiint_V -\frac{\partial \rho}{\partial t} \, dv \, . \tag{1.9}$$

Since Eq. (1.9) has to be valid for any arbitrary volume, it follows that

$$\nabla \cdot \mathbf{J} = -\frac{\partial \rho}{\partial t} \,, \tag{1.10}$$

which is known as the "law of conservation of charge in the neighborhood of a point," and also known as the ***equation of continuity***.

### 1-1.4 Interdependence of Maxwell's Equations

Equations (1.1c) and (1.1d) of Maxwell's equations (Gauss' laws) *are not independent*.

Noting that for any vector $\mathbf{A}$,

$$\nabla \cdot \nabla \times \mathbf{A} = 0 \,, \qquad \forall \mathbf{A} \tag{1.11}$$

and then applying the divergence operator to both sides of Eq. (1.1a) leads to

$$\nabla \cdot \mathbf{J} + \frac{\partial}{\partial t} \nabla \cdot \mathbf{D} = 0 \,. \tag{1.12}$$

Substituting Eq. (1.10) into Eq. (1.12) gives

$$\frac{\partial}{\partial t} (\nabla \cdot \mathbf{D} - \rho) = 0 \,,$$

which implies that $(\nabla \cdot \mathbf{D} - \rho)$ must be a constant. It makes sense for this constant to be zero as we do not expect a nonzero electric flux to exist at any point in the medium in the absence of charges. Hence,

$$\nabla \cdot \mathbf{D} = \rho \,, \tag{1.13}$$

which is Gauss' law for electricity.

Also, from Eq. (1.1b), applying the divergence operator to both sides and then using Eq. (1.11) leads to

$$\frac{\partial}{\partial t} \nabla \cdot \mathbf{B} = 0 \,,$$

from which it can be concluded that

$$\nabla \cdot \mathbf{B} = 0 \,. \tag{1.14}$$

In summary, Faraday's law, the modified form of Ampère's law, and the equation of continuity constitute a sufficient set of equations to characterize both the electric and magnetic field quantities completely.

### 1-1.5 Integral Form of Maxwell's Equations

To develop the integral-form equivalents of the four Maxwell equations defined by Eqs. (1.1a)–(1.1d), we need to use the basic definition of the curl and divergence operators. The curl of a vector field quantity $\mathbf{A}$ whose components and their first derivatives are

continuous is defined by

$$(\nabla \times \mathbf{A}) \cdot \hat{\mathbf{n}} = \lim_{\Delta s \to 0} \frac{\oint_C \mathbf{A} \cdot d\boldsymbol{\ell}}{\Delta s}, \tag{1.15}$$

where $\hat{\mathbf{n}}$ is the unit normal to surface $\Delta s$ with contour $C$. All three components of $\nabla \times \mathbf{A}$ can be obtained once $\hat{\mathbf{n}}$ is aligned with the coordinate unit vectors. Here, it is important to note that the directions of $\hat{\mathbf{n}}$ and the differential length $d\boldsymbol{\ell}$ are chosen so that they follow the right-hand rule. (That is, if $d\boldsymbol{\ell}$ is along the right-hand fingers, then $\hat{\mathbf{n}}$ would be along the right-hand thumb.)

***Stokes' theorem*** is a natural extension of the curl definition. For a regular closed contour $C$ and any arbitrary surface $S$ bounded by $C$ over which the components of $\mathbf{A}$ and their first derivative are continuous, Stokes' theorem states that

$$\iint_S \nabla \times \mathbf{A} \cdot d\mathbf{s} = \oint_C \mathbf{A} \cdot d\boldsymbol{\ell}. \tag{1.16}$$

Upon applying a surface integral to both sides of Eq. (1.1a) and then incorporating Eq. (1.16) into the result, it can be easily shown that

$$\oint_C \mathbf{H} \cdot d\boldsymbol{\ell} = \iint_S \left( \mathbf{J} + \frac{\partial \mathbf{D}}{\partial t} \right) \cdot d\mathbf{s}. \tag{1.17}$$

Here, $\partial \mathbf{D}/\partial t$ has the unit of A/m$^2$ and is also known as the ***displacement current***. If $S$ is stationary, then

$$\oint_C \mathbf{H} \cdot d\boldsymbol{\ell} = I + \frac{d}{dt} \iint_S \mathbf{D} \cdot d\mathbf{s}, \qquad \textbf{(Ampère's law)} \tag{1.18}$$

where $I = \iint \mathbf{J} \cdot d\mathbf{s}$ is the total conduction current passing through the surface defined by $C$.

In fact, Eq. (1.18) is the physical formulation from which Eq. (1.1a) is derived. This formulation also allows for the surface $S$ and contour $C$ themselves to be time-varying. In a similar manner the integral form of Faraday's law can be obtained and is given by

$$\oint_C \mathbf{E} \cdot d\boldsymbol{\ell} = -\frac{d}{dt} \iint_S \mathbf{B} \cdot d\mathbf{s}, \qquad \textbf{(Faraday's law)} \tag{1.19}$$

which states that the induced voltage around a closed contour is equal to the negative time rate of change of the flux linking the surface.

Applying a volume integral to both sides of Eq. (1.1c) leads to

$$\iiint_V \nabla \cdot D \, dv = \iiint_V \rho \, dv = Q. \tag{1.20}$$

Next, application of the divergence theorem gives:

$$\oiint \mathbf{D} \cdot d\mathbf{s} = Q \,. \qquad \textbf{(Gauss' law for electricity)} \tag{1.21}$$

Similarly it can be shown that

$$\oiint \mathbf{B} \cdot d\mathbf{s} = 0 \,, \qquad \textbf{(Gauss' law for magnetism)} \tag{1.22}$$

which can be interpreted as "the flux lines of the magnetic flux density are continuous."

In summary, Maxwell's equations in integral form are given by

$$\oint_C \mathbf{H} \cdot d\boldsymbol{\ell} = I + \frac{d}{dt} \iint_S \mathbf{D} \cdot d\mathbf{s} \qquad \textbf{(Ampère's law)}, \tag{1.23a}$$

$$\oint_C \mathbf{E} \cdot d\boldsymbol{\ell} = -\frac{d}{dt} \iint_S \mathbf{B} \cdot d\mathbf{s} \qquad \textbf{(Faraday's law)}, \tag{1.23b}$$

$$\oiint \mathbf{D} \cdot d\mathbf{s} = Q \qquad \textbf{(Gauss' law for electricity)}, \tag{1.23c}$$

$$\oiint \mathbf{B} \cdot d\mathbf{s} = 0 \qquad \textbf{(Gauss' law for magnetism)}. \tag{1.23d}$$

## Example 1-1: Deriving Circuit Laws from Maxwell's Equations

Show that the well-known circuit laws can be derived from Maxwell's equations under a ***quasi-static condition***, which refers to a condition where the time rates of change of field quantities are very slow (a condition where $fd/c \ll 1$, where $d$ is a typical dimension of the circuit or circuit element, $f$ is the frequency, and $c$ is the speed of light).

**Solution:** Kirchhoff's current law at an electrical node or junction in a circuit, which states that the sum of electric currents entering a node should add up to zero, is a direct result of the law of conservation of charge. We can use Faraday's law to prove Kirchhoff's voltage law under quasi-static conditions. Starting from the integral form of Faraday's law, as given by Eq. (1.23b), we note that the magnitude of the magnetic flux density is many orders of magnitude smaller than the magnitude of the electric field $\mathbf{E}$ (which will be shown later). We also note that under the quasi-static condition the time rate of change of the linking flux that appears on the right-hand side is very small. Hence, it is concluded that

$$\oint_C \mathbf{E} \cdot d\boldsymbol{\ell} = 0 \,.$$

This equation indicates that the sum of voltage drops over any closed loop in the circuit must add up to zero, which is the statement of Kirchhoff's voltage law.

## Example 1-2: Coulomb's Law of Electricity

Show that Coulomb's law of electricity is not independent of Maxwell's equations.

**Solution:** Coulomb's law was derived experimentally by Charles-Augustine de Coulomb in 1785. This law provides the formula for the force on a test charge created by another charge and is considered the first law of electricity. It is important to realize that this law is not independent of Maxwell's equations, and that in fact it can be derived from Gauss' law of electricity. To show this, let us consider a point charge $q$ centered at the origin of a Cartesian system in a medium with permittivity $\varepsilon$, as shown in Fig. 1-3. At an observation point $\mathbf{r}$ on the surface of sphere $S$, the electric flux density $\mathbf{D}$, according to the integral form of Gauss' law, must satisfy

$$\oiint \mathbf{D} \cdot d\mathbf{s} = q \ .$$

Because of the spherical symmetry of the problem, $\mathbf{D} = D_r \, \hat{\mathbf{r}}$ and $D_r$ is constant on $S$, which leads to

$$4\pi r^2 D_r = q \ ,$$

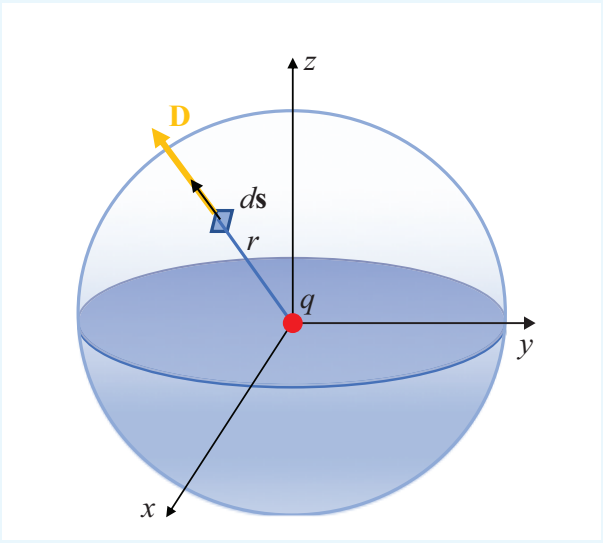


**Figure 1-3:** A point charge $q$ at the origin creates a uniform electric flux density $\mathbf{D}$ on the surface of a sphere $S$ with radius $r$.

from which the electric field of a point charge, consistent with Coulomb's law, is obtained:

$$\mathbf{E} = \frac{q}{4\pi\varepsilon r^2}\,\hat{\mathbf{r}}\,.$$

## 1-2 Faraday's Law for a Moving Surface in a Time-Varying Magnetic Field

Figure 1-4 displays a moving surface $S$ at two points in time, $S(t)$ at time $t$ and the same surface at an incrementally later time $(t + \Delta t)$, denoted $S(t + \Delta t)$. The surface exists in a medium containing a time-varying magnetic flux density $\mathbf{B}(\mathbf{r}, t)$. As we will demonstrate in this section, the configuration in Fig. 1-4 induces an induction voltage difference $V_i$ composed of two components, a transformer induction component $V_{it}$ due to the time-varying magnetic flux density and a motional induction component $V_{im}$ due to the moving surface.

The integral of the electric field intensity over a closed contour on the left-hand side of Eq. (1.19) is equivalent to a voltage. Hence, the right-hand side of the equation represents a

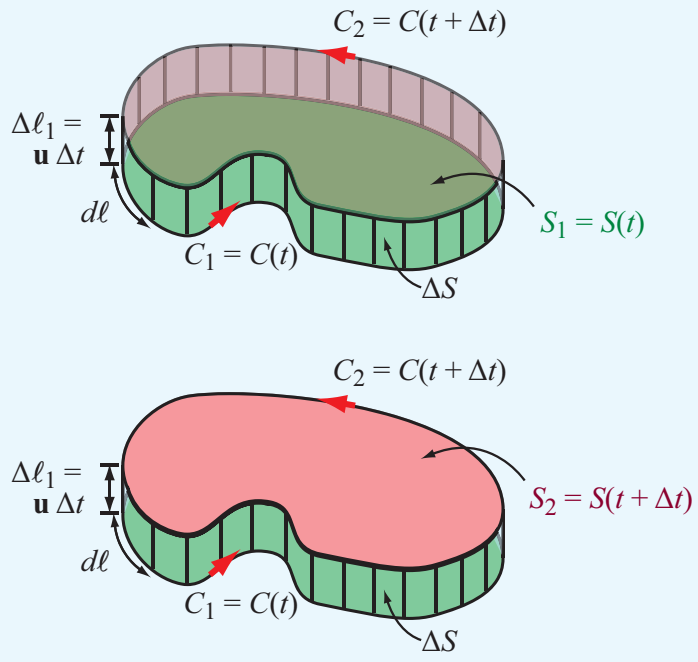


**Figure 1-4:** A moving surface in a magnetic field **B**.

voltage quantity, which we denote by $V_{\rm i}$. Thus,

$$\oint_C \mathbf{E}\cdot d\boldsymbol{\ell} = -\widetilde{V}_{\rm i}\ , \tag{1.24}$$

with

$$\widetilde{V}_{\rm i} = \frac{d}{dt}\iint_{S(t)} \mathbf{B}\cdot d\mathbf{s}\ . \tag{1.25}$$

Next, we use the basic definition of the time derivative to express $V_{\rm i}$ as a sum of two terms:

$$\widetilde{V}_{\rm i} = \lim_{\Delta t\to 0}\frac{1}{\Delta t}\left(\iint_{S(t+\Delta t)} \mathbf{B}(t+\Delta t)\cdot d\mathbf{s} - \iint_{S(t)} \mathbf{B}(t)\cdot d\mathbf{s}\right)\ . \tag{1.26}$$

Noting that for small $\Delta t$

$$\mathbf{B}(t+\Delta t) \approx \mathbf{B}(t) + \frac{\partial \mathbf{B}(t)}{\partial t}\,\Delta t\ ,$$

Eq. (1.26) becomes

$$\widetilde{V}_{\rm i} = \lim_{\Delta t\to 0}\frac{1}{\Delta t}\left[\iint_{S(t+\Delta t)}\left(\mathbf{B}(t) + \frac{\partial \mathbf{B}(t)}{\partial t}\,\Delta t\right)\cdot d\mathbf{s} - \iint_{S(t)} \mathbf{B}(t)\cdot d\mathbf{s}\right]\ , \tag{1.27}$$

which can be rearranged into two components:

$$\widetilde{V}_{\rm i} = V_{\rm it} + V_{\rm im}\ , \tag{1.28}$$

with

$$\widetilde{V}_{\rm it} = \lim_{\Delta t\to 0}\frac{1}{\Delta t}\iint_{S(t+\Delta t)}\left(\frac{\partial \mathbf{B}}{\partial t}\,\Delta t\right)\cdot d\mathbf{s} = \iint_{S(t)}\frac{\partial \mathbf{B}}{\partial t}\cdot d\mathbf{s} \tag{1.29}$$

and

$$\widetilde{V}_{\rm im} = \lim_{\Delta t\to 0}\frac{1}{\Delta t}\left\{\iint_{S(t+\Delta t)} \mathbf{B}(t)\cdot d\mathbf{s} - \iint_{S(t)} \mathbf{B}(t)\cdot d\mathbf{s}\right\}\ . \tag{1.30}$$

For the moving surface $S$ in Fig. 1-4, every point on the contour moves a distance

$$d\boldsymbol{\ell}_1 = \mathbf{u}\,\Delta t\ , \tag{1.31}$$

where $\mathbf{u}$ is the local velocity vector at that point. As the contour moves, it traces a surface on its side. We denote this side surface as $\Delta S$. Next we denote the enclosed surface comprising the lower surface $S(t)$, the top surface $S(t+\Delta t)$, and the side surface $\Delta S$ as $S_0$. Hence, Eq. (1.30) can be rewritten as

$$\widetilde{V}_{\rm im} = \lim_{\Delta t\to 0}\frac{1}{\Delta t}\left\{\oiint_{S_0} \mathbf{B}(t)\cdot d\mathbf{s} - \iint_{\Delta S} \mathbf{B}(t)\cdot d\mathbf{s}\right\}\ . \tag{1.32}$$

The differential surface $d\mathbf{s}$ for the side surface $\Delta S$ is given by

$$d\mathbf{s} = d\boldsymbol{\ell} \times \Delta\boldsymbol{\ell}_1 = d\boldsymbol{\ell} \times \mathbf{u}\,\Delta t\ ,$$

which leads to

$$\lim_{\Delta t\to 0} \frac{1}{\Delta t} \iint_{\Delta s} \mathbf{B}(t)\cdot d\mathbf{s} = \oint_C \mathbf{B}(t)\cdot d\boldsymbol{\ell} \times \mathbf{u}(t)$$
$$= \oint_C [\mathbf{u}(t)\times \mathbf{B}(t)]\cdot d\boldsymbol{\ell}\ . \tag{1.33}$$

Also,

$$\lim_{\Delta t\to 0} \frac{1}{\Delta t} \oiint_{S_0} \mathbf{B}\cdot d\mathbf{s} = \lim_{\Delta t\to 0} \frac{1}{\Delta t} \iiint \nabla\cdot\mathbf{B}\, dv$$
$$= \lim_{\Delta t\to 0} \frac{1}{\Delta t} \iint (\nabla\cdot\mathbf{B})\mathbf{u}\,\Delta t\cdot d\mathbf{s} = \iint (\nabla\cdot\mathbf{B})\mathbf{u}\cdot d\mathbf{s}\ . \tag{1.34}$$

Since $\nabla\cdot\mathbf{B} = 0$, the integral term given by Eq. (1.34) vanishes, and Eq. (1.28) simplifies to

$$\oint_C \mathbf{E}\cdot d\boldsymbol{\ell} = \iint_S -\frac{\partial\mathbf{B}}{\partial t}\cdot d\mathbf{s} + \oint_C (\mathbf{u}\times\mathbf{B})\cdot d\boldsymbol{\ell}\ . \tag{1.35}$$

The first term is referred to as the ***transformer induction*** voltage $\widetilde{V}_{\text{it}}$, and the second term is known as the ***motional induction*** voltage $\widetilde{V}_{\text{im}}$.

It is very important to note that in order to arrive at a nonvanishing motional induction term, *the contour of the surface S has to be moving.* That is, if the contour is fixed and $S(t)$ is still a function of time (such as a fluctuating surface), there will be no motional induction. Physically the contour of the integral (circuit) has to "cut" the flux lines of the magnetic flux density in order to generate "electromotive potential."

This phenomenon can be explained physically using the ***Lorentz force*** $\mathbf{F}$ on a charged particle $q$:

$$\mathbf{F} = q\mathbf{E} + q\mathbf{u}\times\mathbf{B}\ . \tag{1.36}$$

Since the electric field $\mathbf{E}$ is defined in terms of force per unit charge, the equivalent ***induced electric field*** due to moving charges can be defined as

$$\mathbf{E}_{\text{emf}} = \frac{\mathbf{F}_{\text{emf}}}{q} = \mathbf{u}\times\mathbf{B}$$

and

$$V_{\text{emf}} = \oint \mathbf{E}_{\text{emf}}\cdot d\boldsymbol{\ell} = \oint (\mathbf{u}\times\mathbf{B})\cdot d\boldsymbol{\ell}\ . \tag{1.37}$$

Equation (1.37) is consistent with Eq. (1.35). This equivalence indicates that the Lorentz force

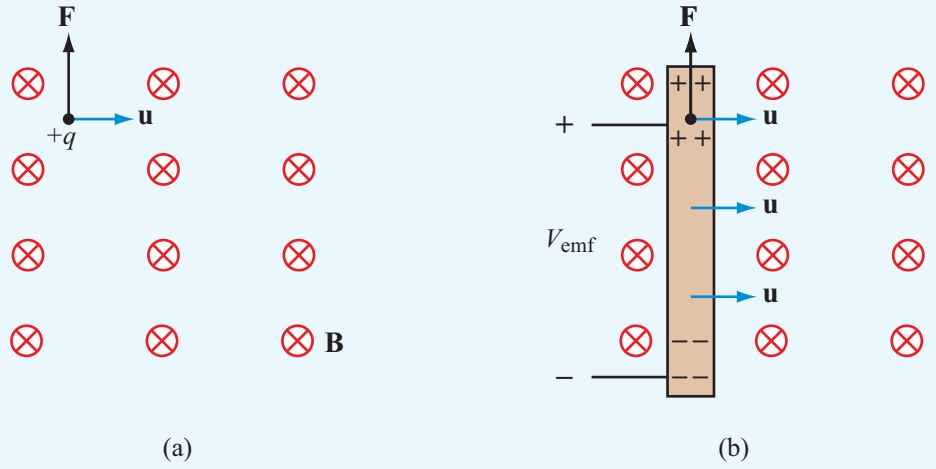


**Figure 1-5:** (a) A positive charge $q$ moving in a magnetic field **B**, and (b) a metallic rod containing many charges moving in a magnetic field, which produces an electromotive voltage $V_{emf}$ across the bar.

equation is not independent of Maxwell's equations.

Figure 1-5(a) depicts the Lorentz force on a moving charge in a magnetic field, and Fig. 1-5(b) shows a conductor moving in the same magnetic field. The Lorentz force acts on free electrons in the conductor and pushes them downward as shown in the figure. Note that the movement of charges in the conductor is confined to within the conductor itself. For a static magnetic field, a dc voltage difference between the two ends of the conductor builds up, and can be computed using Eq. (1.37).

In a medium with distributions of charges and currents, Eq. (1.36) can be used to determine the force per unit volume. For a differential volume $\Delta V$ in a medium with charge density $\rho$ and current density **J**, the charge in $\Delta V$ is $\Delta q = \rho\, \Delta V$ and $\mathbf{J} = \rho\, \mathbf{u}$. The force per unit volume can be calculated from

$$\mathbf{f} = \frac{\mathbf{F}}{\Delta V} = \rho\mathbf{E} + \mathbf{J} \times \mathbf{B}\,. \tag{1.38}$$

## 1-3 Ampère's Law for a Moving Surface in a Time-Varying Electric Field

The sequence of steps that were applied to Faraday's law in the preceding section can also be applied to the integral form of Ampère's law defined by Eq. (1.23a). The process leads to

$$\oint \mathbf{H} \cdot d\boldsymbol{\ell} = I + \iint_S \frac{\partial \mathbf{D}}{\partial t} \cdot d\mathbf{s} + \iint_S (\nabla \cdot \mathbf{D})\mathbf{u} \cdot d\mathbf{s} - \oint_C (\mathbf{u} \times \mathbf{D}) \cdot d\boldsymbol{\ell}\,.$$

Noting from Eq. (1.13) that $\nabla \cdot \mathbf{D} = \rho$, the above expression becomes

$$\oint_C \mathbf{H} \cdot d\boldsymbol{\ell} = I + \iint_S \frac{\partial \mathbf{D}}{\partial t} \cdot d\mathbf{s} + \iint_S \rho \mathbf{u} \cdot d\mathbf{s} - \oint_C (\mathbf{u} \times \mathbf{D}) \cdot d\boldsymbol{\ell} \,, \tag{1.39}$$

in which $I$ represents the ***conduction current***, $\rho\mathbf{u}$ represents the ***drift current***, $\partial\mathbf{D}/\partial t$ represents the ***displacement current***, and $(\mathbf{u} \times \mathbf{D})$ represents the ***motional current***.

Before proceeding to the next section, let us pose the following question: If we were to consider Eq. (1.35) as the correct form of Faraday's law, how would it reduce to its differential form given by Eq. (1.1b)? To answer the question, let us rewrite Eq. (1.35) as

$$\oint_C [\mathbf{E} - \mathbf{u} \times \mathbf{B}] \cdot d\boldsymbol{\ell} = \iint_S -\frac{\partial \mathbf{B}}{\partial t} \cdot d\mathbf{s} \,. \tag{1.40}$$

Now if we apply Stokes' theorem, as given by Eq. (1.16), to the left-hand side to convert the contour integral into a surface integral, the process leads to

$$\iint_S \left( \nabla \times (\mathbf{E} - \mathbf{u} \times \mathbf{B}) + \frac{\partial \mathbf{B}}{\partial t} \right) \cdot d\mathbf{s} = 0 \,. \tag{1.41}$$

Since $S$ is arbitrary, the integrand must vanish. Hence,

$$\nabla \times \mathbf{E} - \nabla \times (\mathbf{u} \times \mathbf{B}) = -\frac{\partial \mathbf{B}}{\partial t} \,. \tag{1.42}$$

As will be shown later, the magnetic flux density $\mathbf{B}$ is many orders of magnitude smaller than the electric field intensity $\mathbf{E}$, and unless $\mathbf{u}$ is close to the speed of light, the second term in Eq. (1.42) can be ignored compared with the first term. As a result, the point form of Faraday's law reduces to

$$\nabla \times \mathbf{E} = -\frac{\partial \mathbf{B}}{\partial t} \,. \tag{1.43}$$

## 1-4 Constitutive Relations: Macroscopic Properties of Matter

As was shown previously in Section 1-1.4, out of the four Maxwell's equations only the modified Ampère's and Faraday's laws (Eqs. (1.1a) and (1.1b)) are truly independent. Considering the fact that it is the charges and currents that are the sources of electromagnetic fields $\mathbf{E}, \mathbf{D}$ and $\mathbf{H}, \mathbf{B}$, we need to impose two additional constraints, in addition to the two independent Maxwell's equations, in order to ensure that the overall system of equations is indeed determinate.

In the most general case, we may consider the relationship among the four field quantities to be of the form

$$\mathbf{D} = \mathbf{D}(\mathbf{E}, \mathbf{H}) \tag{1.44a}$$

and

$$\mathbf{B} = \mathbf{B}(\mathbf{E}, \mathbf{H}) \,, \tag{1.44b}$$

where $\mathbf{D}(\cdot)$ and $\mathbf{B}(\cdot)$ are some general vector functions dependent upon the material in which the field vector quantities are established.

In the treatment of Maxwell's equations considered henceforth, we shall confine our attention to only the small-signal condition wherein the constitutive relations given by Eqs. (1.44a) and (1.44b) are *linear*. That is, if $\mathbf{D}_1$ and $\mathbf{B}_1$ are induced by $\mathbf{E}_1$ and $\mathbf{H}_1$, and $\mathbf{D}_2$ and $\mathbf{B}_2$ are induced by $\mathbf{E}_2$ and $\mathbf{H}_2$, then $\mathbf{D}_1+\mathbf{D}_2$ and $\mathbf{B}_1+\mathbf{B}_2$ are induced by the combination of $\mathbf{E}_1+\mathbf{E}_2$ and $\mathbf{H}_1+\mathbf{H}_2$.

A material medium is considered electromagnetically ***homogeneous*** if the constants of proportionality relating $\mathbf{D}$ and $\mathbf{B}$ to $\mathbf{E}$ and $\mathbf{H}$ are independent of position within the medium. Conversely, the medium is considered ***inhomogeneous*** if the constants of proportionality are position-dependent.

In the absence of any material (vacuum), the constitutive relations are very simple and are given by

$$\mathbf{D}=\varepsilon_0\mathbf{E}\,,\qquad \mathbf{B}=\mu_0\mathbf{H}\,, \tag{1.45}$$

where

$$\varepsilon_0=8.85\times10^{-12}\ \text{(farad/m)}\quad \textbf{(free-space permittivity)}$$

and

$$\mu_0=4\pi\times10^{-7}\ \text{(henry/m)}\qquad \textbf{(free-space permeability)}.$$

Note that the unit for the $\mathbf{D}$ is farad/m $\times$ volt/m $=$ C/m$^2$. Similarly, the unit for the magnetic flux density is henry/m $\times$ ampere/m $=$ W/m$^2$ (magnetic flux per unit area).

The next simplest pair of constitutive relations belongs to materials known as ***isotropic homogeneous materials***. If the physical properties of the medium are the same along all directions (as seen by $\mathbf{E}$ and $\mathbf{H}$) the medium is considered isotropic. Hence $\mathbf{D}$ is parallel to $\mathbf{E}$ and $\mathbf{B}$ is parallel to $\mathbf{H}$ at every location within the medium:

$$\mathbf{D}=\varepsilon\mathbf{E}\qquad\text{and}\qquad\mathbf{B}=\mu\mathbf{H}\,, \tag{1.46}$$

where $\varepsilon=\varepsilon_r\varepsilon_0$ and $\mu=\mu_r\mu_0$.

$$\varepsilon_r=\textbf{relative permittivity}\ \text{(dimensionless)}$$

and

$$\mu_r=\textbf{relative permeability}\ \text{(dimensionless)}.$$

Usually $\varepsilon_r$ and $\mu_r$ are quantities larger than unity. In a homogeneous isotropic material, the applied electric field slightly polarizes the atoms or molecules in a direction parallel to the direction of the applied electric field. That is, the center of mass of the electron cloud around the nucleus shifts slightly in a direction opposite to that of the applied electric field, thereby forming a small electric dipole. The electric field formed by these small dipoles are in the opposite direction to that of the applied field, as shown in Fig. 1-6, and therefore the total electric field in the medium is smaller than the applied electric field. In the presence of external electric and magnetic fields, the material gets polarized and magnetized, respectively.

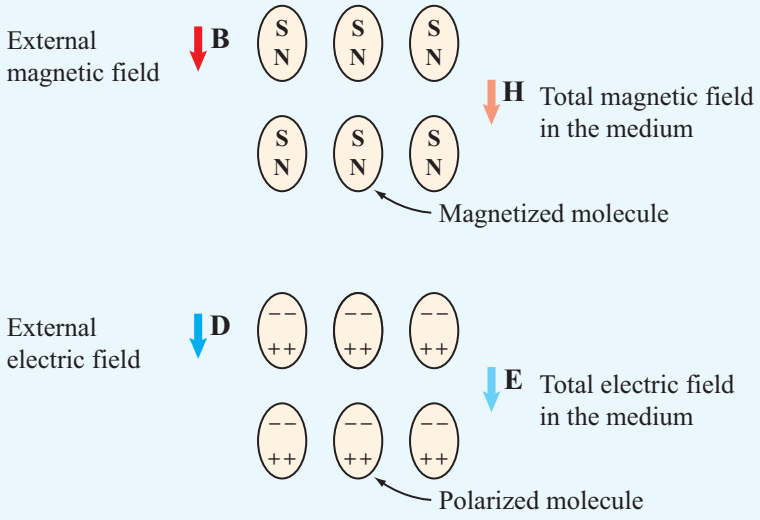


**Figure 1-6:** Magnetized and polarized molecules in the presence of external applied electric and magnetic fields. The total field in such a medium is weaker than the external applied field in the absence of the material.

The in a medium can be written as

$$\mathbf{D} = \varepsilon_0 \mathbf{E} + \mathbf{P} \,, \tag{1.47}$$

where $\mathbf{P}$ is known as the ***polarization vector*** and constitutes a dipole moment per unit volume. If the electric field intensity is not very high, the polarization vector is related linearly to the electric field by $\mathbf{P} = \varepsilon_0 \chi_e \mathbf{E}$, where $\chi_e$ is the electric susceptibility of the medium. Hence, $\mathbf{D}$ can be expressed as

$$\mathbf{D} = \varepsilon \mathbf{E} \,, \tag{1.48a}$$

with

$$\varepsilon = \varepsilon_0 (1 + \chi_e) \,.$$

In a similar manner the magnetic flux density in a magnetic medium, under linearity conditions, can be written as

$$\mathbf{B} = \mu_0 \mathbf{H} + \mu_0 \mathbf{M} \,, \tag{1.49}$$

with $\mathbf{M} = \chi_m \mathbf{H}$, where $\chi_m$ is the magnetic susceptibility of the medium. The quantity $\mathbf{M}$ is known as the ***magnetization vector*** and provides a measure of the induced magnetic dipole moment per unit volume. The manifestation of magnetic dipoles in a medium can be attributed to the electron orbital motion, as well as electron or nuclear spin. An unbalanced net effect of such equivalent atomic currents flowing on a closed loop can give rise to magnetic dipoles within the material. Such an equivalent atomic current loop is characterized by its magnetic moment $\mathbf{m}$. The number of these magnetic moments per unit volume ($N$) is the magnetization

vector $\mathbf{M} = N\mathbf{m}$. From Eq. (1.49) we can show that

$$\mathbf{B} = \mu\mathbf{H} \tag{1.50a}$$

and

$$\mu = \mu_0(1 + \chi_m) \, . \tag{1.50b}$$

In general, magnetic materials can be categorized as:

1. ***Paramagnetic*** ($\mu_r > 1$), which refers to magnetic materials with relatively small magnetic dipoles and which also do not retain permanent magnetism.

2. ***Diamagnetic*** ($\mu_r < 1$), which refers to magnetic materials with induced magnetic moments that are parallel to but in the opposite direction to the applied magnetic field. Such materials are repelled by a permanent magnet. Most materials that are known as nonmagnetic, such as water or gold, are in reality diamagnetic but with a very weak response. For such materials, the magnetic susceptibility is a small negative number.

3. ***Ferromagnetic*** ($\mu_r \gg 1$), which refers to spontaneous magnetization in subdomains. Such materials are highly nonlinear and are characterized by hysteresis (a time-varying phenomenon related to material memory). Above its Curie temperature, the material becomes paramagnetic.

The phenomenon of ferroelectricity has been observed for a variety of materials; for example, barium titanate ($BaTiO_3$) shows a ferroelectric behavior marked by hysteresis, nonlinearity, and very large values for $\varepsilon_r$.

### 1-4.1 Anisotropic Media

For certain materials, their electrical and/or magnetic properties may behave differently along different directions. In such media, vector **B** may not be parallel to vector **H**, and vector **D** may not be parallel to vector **E**. Consequently, the relationships between **D** and **E** and between **B** and **H** should be expressed in terms of ***permittivity*** and ***permeability tensors***:

$$\mathbf{D} = \overline{\overline{\varepsilon}} \cdot \mathbf{E} \, , \qquad \overline{\overline{\varepsilon}} = \varepsilon_0 \overline{\overline{\varepsilon}}_r = \varepsilon_0 \begin{bmatrix} \varepsilon_{xx} & \varepsilon_{xy} & \varepsilon_{xz} \\ \varepsilon_{yx} & \varepsilon_{yy} & \varepsilon_{yz} \\ \varepsilon_{zx} & \varepsilon_{zy} & \varepsilon_{zz} \end{bmatrix} \tag{1.51a}$$

and

$$\mathbf{B} = \overline{\overline{\mu}} \cdot \mathbf{H} \, , \qquad \overline{\overline{\mu}} = \mu_0 \overline{\overline{\mu}}_r = \mu_0 \begin{bmatrix} \mu_{xx} & \mu_{xy} & \mu_{xz} \\ \mu_{yx} & \mu_{yy} & \mu_{yz} \\ \mu_{zx} & \mu_{zy} & \mu_{zz} \end{bmatrix} \, . \tag{1.51b}$$

A material is called ***anisotropic*** if either or both of its permittivity and permeability is/are tensor quantities. It should be noted that the tensor elements are functions of the coordinate system. For materials with axes of symmetry, the permittivity or permeability tensors become symmetric matrices. In that case the matrix (matrices) is (are) diagonizable with real

eigenvalues and eigenvectors that are orthogonal. By rotating the Cartesian coordinate system to align it with the eigenvectors' directions, the tensor becomes diagonal:

$$\overline{\overline{\varepsilon}} = \varepsilon_0 \begin{bmatrix} \varepsilon_x & 0 & 0 \\ 0 & \varepsilon_y & 0 \\ 0 & 0 & \varepsilon_z \end{bmatrix} \qquad \textbf{(biaxial material)}. \tag{1.52}$$

Such a material is known as ***biaxial material***. If there is invariance in any coordinate plane, two of the entries of Eq. (1.52) become equal (say $\varepsilon_x = \varepsilon_y \neq \varepsilon_z$). The material is then called ***uniaxial***.

### 1-4.2 Bianisotropic Media

A ***bianisotropic*** material exhibits *magnetization* when subjected to an externally applied *electric field* and exhibits *polarization* when subjected to an externally applied *magnetic field*, and these cross-field components are in addition to the direct magnetization and polarization components caused by the external fields. The constitutive relationships for these materials are given by

$$\mathbf{D} = \overline{\overline{\varepsilon}} \cdot \mathbf{E} + \overline{\overline{\zeta}} \cdot \mathbf{H} \tag{1.53a}$$

and

$$\mathbf{B} = \overline{\overline{\xi}} \cdot \mathbf{E} + \overline{\overline{\mu}} \cdot \mathbf{H} \,. \tag{1.53b}$$

### 1-4.3 Dispersive Materials

Except for free space, for which neither the permittivity nor the permeability are functions of either time $t$ or the oscillation frequency $\omega$, all other media, strictly speaking, are frequency-dependent. This is due to the fact that all charges that interact with the field quantities have finite masses, which leads to a time delay between the timing of the applied external fields and the formation of the polarization and magnetization vectors.

Under the small-signal approximation (linear), the polarization vector (dipole moment per unit volume) is linearly proportional to the applied electric field. For an isotropic medium,

$$\mathbf{P} = \varepsilon_0 \cdot \chi_e \mathbf{E} \,, \tag{1.54}$$

where $\chi_e$ is called the ***electric susceptibility***. If $\chi_e$ is assumed to be a real constant and independent of frequency, the relationship given by Eq. (1.54) essentially ignores the delay between $\mathbf{E}$ and $\mathbf{P}$. The correct way of thinking about a linear relationship between $\mathbf{P}$ and $\mathbf{E}$ is in terms of a time-domain convolution. If $\chi_e(t)$ represents the true impulse response, then

$$\mathbf{P}(t) = \varepsilon_0 \int_{-\infty}^{t} \chi_e(t-\tau)\, \mathbf{E}(\tau)\, d\tau \,. \tag{1.55}$$

The integral has been truncated at $t$ by imposing the causality condition; i.e., $\chi_e(t) = 0$ for $t < 0$. Hence,

$$\begin{aligned}\mathbf{D}(t) &= \varepsilon_0 \mathbf{E}(t) + \varepsilon_0 \int_{-\infty}^{t} \chi_e(t-\tau)\, \mathbf{E}(\tau)\, d\tau \\ &= \varepsilon_0 \mathbf{E}(t) + \varepsilon_0 \int_{0}^{\infty} \chi_e(\tau)\, \mathbf{E}(t-\tau)\, d\tau\,. \end{aligned} \tag{1.56}$$

Taking the Fourier transform of both sides of Eq. (1.56) gives

$$\int_{-\infty}^{+\infty} \mathbf{D}(t)\, e^{i\omega t}\, dt = \varepsilon_0 \int_{-\infty}^{+\infty} \left( \mathbf{E}(t) + \int_{0}^{\infty} \chi_e(\tau)\, \mathbf{E}(t-\tau)\, d\tau \right) e^{i\omega t}\, dt\,,$$

which is equivalent to

$$\mathbf{D}(\omega) = \varepsilon_0\, \mathbf{E}(\omega) + \varepsilon_0 \int_{0}^{\infty} \chi_e(\tau)\, e^{i\omega\tau} \underbrace{\int_{-\infty}^{+\infty} \mathbf{E}(t-\tau)\, e^{i\omega(t-\tau)}\, dt}_{\mathbf{E}(\omega)}\, d\tau$$

and which leads to

$$\mathbf{D}(\omega) = \varepsilon_0 \left( 1 + \int_{0}^{\infty} \chi_e(\tau)\, e^{i\omega\tau}\, d\tau \right) \mathbf{E}(\omega)\,. \tag{1.57}$$

Therefore, the complex permittivity is given by

$$\varepsilon(\omega) = \varepsilon_0 \left( 1 + \int_{0}^{\infty} \chi_e(\tau)\, e^{i\omega\tau}\, d\tau \right) = \varepsilon_0 [1 + \chi_e(\omega)]\,. \tag{1.58}$$

According to Eq. (1.58), the permittivity of any material (excluding free space) is, in general, a complex function of frequency. If a narrow pulse were to propagate in such a medium, it can be shown that the pulse would spread in time and space as it travels in the medium.

A similar behavior can be shown to be true for magnetic materials:

$$\mathbf{M}(\omega) = \chi_m(\omega)\, \mathbf{H}(\omega)\,. \tag{1.59}$$

The dependence of the permittivity $\varepsilon(\omega)$ and the permeability $\mu(\omega)$ on the frequency $\omega$ may vary significantly among different materials. For most nonpolar materials, $\varepsilon$ and $\mu$ can be approximated by constant quantities at microwave and millimeter-wave parts of the spectrum. Near molecular resonances, however, the variations of the constitutive parameters with frequency must be taken into account carefully.

### 1-4.4 Conducting Media

Another element of the constitutive relations is the relation between the current density $\mathbf{J}$ and the electric field in the medium $\mathbf{E}$. In the absence of magnetic fields, a conducting medium is characterized by

$$\mathbf{J} = \sigma \mathbf{E} \qquad \textbf{(Ohm's law)}, \tag{1.60}$$

where **J** is the conduction current (to be differentiated from any externally impressed source current), **E** is the electric field in the medium, and $\sigma$ is the conductivity of the medium. Equation (1.60) is known as the ***point form of Ohm's law***. In the presence of a magnetic field, the direction of the conduction current is no longer parallel to **E**. This phenomenon is known as the ***Hall effect***, which will be revisited later in this chapter.

Within a conducting medium ($\sigma > 0$) there can be no accumulation of charges. If an initial charge density $\rho_0(\mathbf{r})$ is established in a conducting medium, then according to the equation of continuity given by Eq. (1.10), we have

$$\nabla \cdot \mathbf{J} = -\frac{\partial \rho}{\partial t} , \tag{1.61}$$

and Ohm's law (Eq. (1.60)), we have

$$\nabla \cdot \sigma E = -\frac{\partial \rho}{\partial t} . \tag{1.62}$$

Next, using Gauss' law (Eq. (1.1c)),

$$\sigma \nabla \cdot E = \frac{\sigma}{\varepsilon} \nabla \cdot D = \frac{\sigma}{\varepsilon} \rho , \tag{1.63}$$

and then combining it with Eq. (1.62) leads to

$$\frac{\partial \rho}{\partial t} + \frac{\sigma}{\varepsilon} \rho = 0 \tag{1.64a}$$

$$\Downarrow$$

$$\rho = \rho_0 e^{-(\sigma/\varepsilon)t} . \tag{1.64b}$$

That is, at any point in the medium, charges vanish exponentially. Basically, the positive and negative charges recombine, or move away from each other to be accumulated at the surface of the bounded conducting medium. As charges move in a conducting medium to redistribute themselves over the surface, some of the stored energy is dissipated into heat. After equilibrium has been established, the stored electric energy is lower than that of the cumulative initial condition of the charges in the medium.

### 1-4.5 The Lorentz Dielectric Model

A classical model for the complex dielectric constant of materials was developed by H. A. Lorentz at the turn of the twentieth century. The model is based on a simple oscillatory mechanical system in which bound electrons are allowed to move around stationary ions under the driving force of applied electromagnetic fields. In this model each molecule is considered to be independent of the other modules within the material medium. That is, the motion of

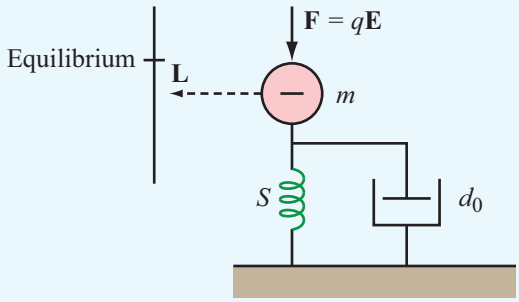


**Figure 1-7:** An equivalent mechanical model describing the motion of bound electrons around ions subjected to an external electric field **E**.

an electron belonging to a particular molecule does not influence the motions of the other electrons and vice versa. Also, under the small signal approximation, the electrostatic force acting on displaced electron clouds around an ion is described by a linear relation. Electron collision is described by a damping coefficient in an equivalent mechanical system, as shown in Fig. 1-7. The equation of motion for an electron cloud of mass $m$ under the influence of the local electric force field **E** is given by

$$m\frac{d^2\mathbf{L}}{dt^2} + d_0\frac{d\mathbf{L}}{dt} + S\mathbf{L} = q\,\mathbf{E}(t)\,, \tag{1.65}$$

where **L** is the *displacement* of the electron cloud's center of mass from the position of equilibrium, $q$ is the charge of the moving electron cloud, $S$ is the ***spring constant*** representing the linearized electrostatic force, and $d_0$ is the ***damping coefficient***. Assuming the excitation to be time-harmonic, i.e., $\mathbf{E}(t) = \Re\mathrm{e}[\widetilde{\mathbf{E}}e^{-i\omega t}]$, the phasor form of displacement is then given by

$$\widetilde{\mathbf{L}} = \frac{(q/m)\widetilde{\mathbf{E}}}{\omega_0^2 - \omega^2 - i\gamma\omega}\,, \tag{1.66}$$

where $\omega_0^2 = S/m$ is the ***natural (resonant) frequency*** of the system and $\gamma = d_0/m$ is the damping factor. Next, assuming there are $N$ independent polarized molecules per unit volume, then the polarization is given by

$$\widetilde{\mathbf{P}} = Nq\widetilde{\mathbf{L}} = \frac{\omega_\mathrm{p}^2}{\omega_0^2 - \omega^2 - i\gamma\omega}\,\varepsilon_0\widetilde{\mathbf{E}}\,, \tag{1.67}$$

where $\omega_\mathrm{p}^2 = Nq^2/m\varepsilon_0$ is defined as the ***plasma frequency***. Recalling that $\widetilde{\mathbf{P}} = \varepsilon_0\chi_\mathrm{e}\widetilde{\mathbf{E}}$ and $\varepsilon = \varepsilon_0(1+\chi_\mathrm{e})$, the dielectric constant of the medium is then given by

$$\varepsilon = \varepsilon_0\left(1 + \frac{\omega_\mathrm{p}^2}{\omega_0^2 - \omega^2 - i\gamma\omega}\right)\,, \tag{1.68}$$

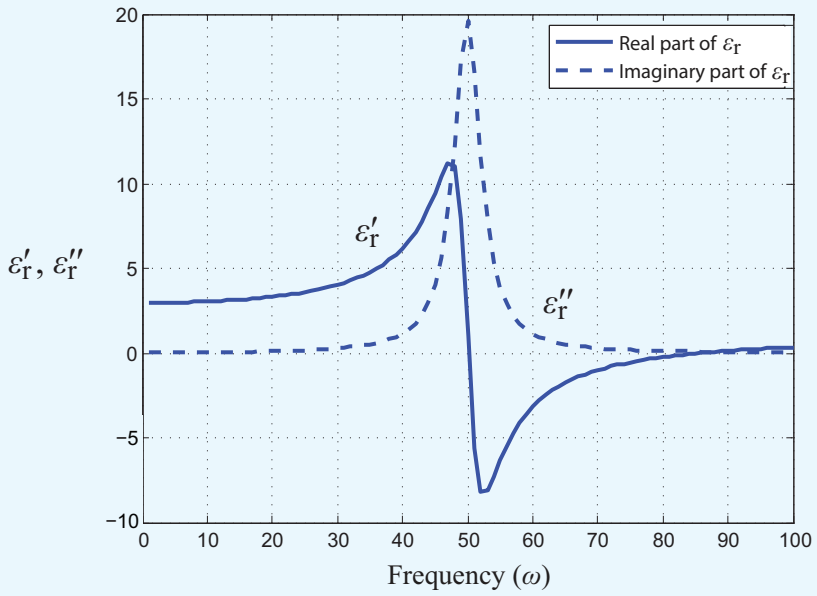


**Figure 1-8:** The real and imaginary parts of the dielectric constant of a material, according to the Lorentz model given by Eq. (1.69) with $\omega_0 = 50$ rad/s, $\omega_p = 70$ rad/s, and $\gamma = 5$ rad/s.

whose real and imaginary parts can be written as

$$\varepsilon' = \varepsilon_0 \left( 1 + \frac{\omega_p^2(\omega_0^2 - \omega^2)}{(\omega_0^2 - \omega^2)^2 + \gamma^2\omega^2} \right) , \tag{1.69a}$$

$$\varepsilon'' = \varepsilon_0 \left( \frac{\omega_p^2 \gamma \omega}{(\omega_0^2 - \omega^2)^2 + \gamma^2\omega^2} \right) . \tag{1.69b}$$

It is interesting to note that near resonance ($\omega \sim \omega_0$) the real part of $\varepsilon$ can become less than unity or even a negative number. The maximum value of $\varepsilon''$ occurs at around $\omega = \omega_0$ and its peak value is approximately equal to $\omega_p^2/\gamma\omega_0$. Figure 1-8 shows plots of $\varepsilon'_r$ and $\varepsilon''_r$ as a function of frequency $\omega$ for some chosen values of $\omega_0$, $\omega_p$, and $\gamma$.

At frequencies much smaller than the resonant frequency ($\omega \ll \omega_0$), it can be easily shown that

$$\varepsilon' \approx \varepsilon_0 \left( 1 + \frac{\omega_p^2}{\omega_0^2} \right) , \qquad (\omega \ll \omega_0) \tag{1.70a}$$

and

$$\varepsilon'' \approx \varepsilon_0 \frac{\gamma\omega_p^2\omega}{\omega_0^4}, \qquad (\omega \ll \omega_0). \tag{1.70b}$$

These expressions indicate that the real part of the dielectric constant is independent of frequency and the ***loss factor***, $\varepsilon''/\varepsilon'$, due to dielectric dispersion, is very small and increases linearly with frequency. Also, at frequencies well above the resonant frequency, approximate expressions for the real and imaginary parts of the dielectric constant can be obtained and are given by

$$\varepsilon' \approx \varepsilon_0 \left(1 - \frac{\omega_p^2}{\omega^2}\right) \qquad (\omega \gg \omega_0) \tag{1.71a}$$

and

$$\varepsilon'' \approx \varepsilon_0 \frac{\gamma\omega_p^2}{\omega^3}. \qquad (\omega \gg \omega_0). \tag{1.71b}$$

It is interesting to note that in the limit as $\omega \to \infty$, the real part of the permittivity approaches that of free space and the imaginary part vanishes.

Some materials may have multiple resonances, for which their spectral dielectric behavior, based on the Lorentz model, can be represented by

$$\varepsilon_1 = \varepsilon_0 + \sum_{j=1}^{N} \frac{\varepsilon_0\omega_{pj}^2}{\omega_{0j}^2 - \omega^2 - i\gamma_j\omega}, \tag{1.72}$$

where $\omega_{0j}$, $\omega_{pj}$, and $\gamma_j$ are the $j$th resonant frequency, plasma frequency, and damping factor respectively.

### 1-4.6 The Drude Model for Metals

Conductors are materials with very high conductivity ($\sigma \gg 1$). As will be shown later, the material conductivity can be expressed in terms of a frequency-dependent imaginary part of the dielectric constant given by

$$\varepsilon''_{\text{cond}} = \frac{\sigma}{\omega}. \tag{1.73}$$

Hence, a standard dielectric model used for metals with finite conductivity is expressed as

$$\varepsilon_{\text{metal}} = \varepsilon_0 \left(1 + i\frac{\sigma}{\omega\varepsilon_0}\right) \qquad \text{(low frequencies)}. \tag{1.74}$$

This model is based on Ohm's law and is valid at low frequencies ($f < 100$ GHz). At higher frequencies, a better approach to describe the spectral behavior of conductors is the Drude model, which can be derived from the Lorentz dielectric model introduced in the previous subsection. Good conductors contain a large number of electrons at the top of the energy distribution and they can be easily excited and moved around within the conduction band. These electrons are essentially free electrons and not bound to specific ions in the material lattice. As a result, the spring constant $S$ in the equivalent mechanical model shown in Fig. 1-7

can be set to zero, which in turn sets $\omega_0 = S/m = 0$ in Eq. (1.68), simplifying it to

$$\varepsilon = \varepsilon_0 \left(1 - \frac{\omega_p^2}{\omega^2 + i\gamma\omega}\right) . \tag{1.75}$$

The explicit expressions for the real and imaginary parts of the dielectric constant are given by

$$\varepsilon_r' = 1 - \frac{\omega_p^2}{\omega^2 + \gamma^2} \tag{1.76a}$$

and **(Drude model for high frequencies)**

$$\varepsilon_r'' = \frac{\omega_p^2 \gamma}{\omega(\omega^2 + \gamma^2)} . \tag{1.76b}$$

At low frequencies where $\omega \ll \gamma$ and $\omega_p \ll \gamma$,

$$\varepsilon_r' \approx 1 \tag{1.77a}$$

and **(Drude model for low frequencies)**

$$\varepsilon_r'' = \frac{\omega_p^2}{\omega\gamma} , \tag{1.77b}$$

which is consistent with the expression for $\varepsilon_{metal}$ at low frequencies. A direct comparison between these expressions reveals the relationship between the conductivity of a metal and its plasma frequency and damping factor:

$$\sigma = \frac{\varepsilon_0 \omega_p^2}{\gamma} = \frac{Nq^2}{m\gamma} \quad \text{S/m.} \tag{1.78}$$

It is important to note that the conductivity of a metal at low frequencies is independent of frequency.

## Example 1-3: Collision Frequency of Copper

It is interesting to examine how some of the parameters in the Drude model can be estimated experimentally. Starting from Eq. (1.78), find the collision frequency $\gamma$ for copper.

**Solution:** Let us consider copper at low frequencies and try to estimate an empirical value for the collision frequency $\gamma$. Assuming one free electron per atom and noting that the molecular

weight of copper is $M_r = 63.54$ g and its density is $d = 8.92$ g/cm$^3$, the number density of electrons per unit volume can be calculated using Avogadro's number ($A = 6.022 \times 10^{23}$):

$$N = \frac{Ad}{M_r} = \frac{6.022 \times 10^{23} \times 8.92 \times 10^6}{63.54} = 8.43 \times 10^{28} \text{ m}^{-3}. \tag{1.79}$$

The conductivity of copper at microwave and lower frequencies is measured to be $\sigma = 5.8 \times 10^7$. Using the charge and mass of an electron ($q = 1.6 \times 10^{-19}$ and $m = 9.1 \times 10^{-31}$) in the Drude conductivity equation given by Eq. (1.78), the estimated collision frequency of copper is found to be

$$\gamma = \frac{Nq^2}{m\sigma} = \frac{8.43 \times 10^{28} \times (1.6 \times 10^{-19})^2}{9.1 \times 10^{-31} \times 5.8 \times 10^7} = 4.08 \times 10^{13} \text{ s}^{-1}.$$

### 1-4.7 Dielectric Relaxation Model for Polar Molecules

Many substances in nature are made up of molecules with a net charge of zero, and yet they exhibit a nonzero electric dipole moment. By definition, a polar molecule is a molecule with one end being slightly positively charged and the other end being slightly negatively charged. Permanent dipole moments are formed in atoms with different electronegativity values like carbon monoxide. The positive charge of the dipole comes from the protons in the carbon nucleus and the negative charge of the dipole comes from the excess electrons orbiting mostly around the oxygen atom. There are also molecular structures in which a significant dipole moment is created from the asymmetry of the bond atoms. The water molecule is one such example. In the atomic structure of a water molecule, the positively charged hydrogen atoms are positioned in an asymmetric manner with respect to the negatively charged oxygen atom. The lines connecting the oxygen and hydrogen atoms form an angle of about 104.5° (instead of 180° for a symmetric structure), giving rise to a permanent electric dipole moment, as shown in Fig. 1-9. In the presence of an applied external electric field **E**, an electric dipole with ***dipole moment*** $\mathbf{p} = q\mathbf{d}$ experiences a ***torque*** given by

$$\mathbf{T} = \mathbf{p} \times \mathbf{E}\,. \tag{1.80}$$

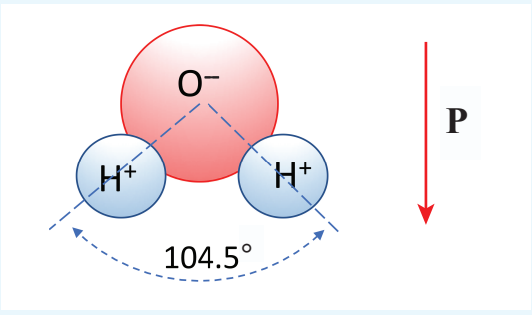


**Figure 1-9:** The atomic structure of a water molecule generates a permanent dipole moment **P**.

Here $q$ refers to the equivalent charge and $\mathbf{d}$ is the displacement vector. Assuming the electric field is along the $z$-axis and denoting the angular momentum of the dipole by $I$, the equation of motion is given by

$$I\,\frac{\partial^2\theta}{\partial t^2} = pE\sin\theta\ , \tag{1.81}$$

where $\theta$ denotes the instantaneous angle between $\mathbf{p}$ and $\mathbf{E}$. The solution of this nonlinear differential equation depends on the time variation of the electric field $\mathbf{E}$. For a static electric field, eventually the dipole will align itself with the electric field and consequently, per Eq. (1.80) the torque disappears. For a small deviation from the equilibrium condition, the sine function can be replaced with its argument, which leads to the second-order differential equation

$$I\,\frac{\partial^2\theta}{\partial t^2} = pE\,\theta\ . \tag{1.82}$$

The natural resonant frequency of the dipole around its equilibrium can easily be calculated from

$$f_0 = \frac{1}{2\pi}\sqrt{\frac{pE}{I}}\ . \tag{1.83}$$

For a polar substance, the equation of motion should also include a damping factor due to the collision, which results in a damped oscillation of the dipoles around the equilibrium condition. For substances in solid or liquid form, the frequency of collision is high and the rate of change of angular velocity with time is very small. This leads to overdamped oscillation, a situation where the dipole "relaxes" to its equilibrium after an initial perturbation.

In an unbiased small region of a medium with polar molecules having random orientations, the net dipole moment can be assumed to be negligible. The sudden application of an electric field, in the form of a step function, causes the medium to get polarized. For such a medium, the polarization vector is composed of two components: The first component is due to the quick motion of electron clouds in the direction opposite of the applied electric field, and the second component is due to the rotation of the permanent dipole moments of the polar molecules. Since the molecules themselves are much heavier than the electron clouds, this latter motion is far slower than the motion of the electron clouds. Denoting the static susceptibility associated with the electron clouds by $\chi_{0e}$ and that of the permanent dipoles by $\chi_{0d}$, and noting that the polarization vector due to the dipole moments reaches the steady-state value in an overdamped manner, the time-domain step response of the ***polarization vector*** can be written as

$$\mathbf{P}_{\text{step}}(t) = \varepsilon_0\mathbf{E}_0[(\chi_{0e}-\chi_{0d})e^{-t/\tau}+\chi_{0d}]\,u(t)\ , \tag{1.84}$$

where $\tau$ is the relaxation time of the overdamped permanent dipoles and $u(t)$ denotes a step function. Here, it is assumed that the polarization due to the electron clouds happens instantaneously (compared with the relaxation time of the dipoles). Hence the impulse response is given by

$$\mathbf{P}(t) = \varepsilon_0\mathbf{E}_0\left(\frac{\chi_{0d}-\chi_{0e}}{\tau}e^{-t/\tau}\,u(t)+\chi_{0e}\,\delta(t)\right)\ , \tag{1.85}$$

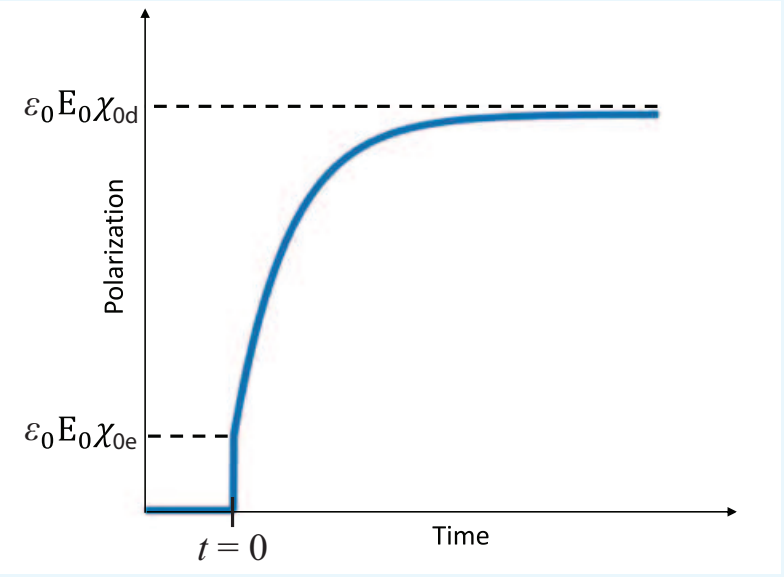


**Figure 1-10:** The step-function response of polarization in a medium with polar molecules.

where $\delta(t)$ denotes a delta function. The step-function response of the polarization as a function of time, as given by Eq. (1.84), is shown in Fig. 1-10.

Upon comparing the expression for $\mathbf{P}(t)$ with the expression given by Eq. (1.54), we obtain the following expression for the susceptibility $\chi_e$:

$$\chi_e(t) = \frac{\chi_{0d} - \chi_{0e}}{\tau} e^{-t/\tau}\, u(t) + \chi_{0e}\, \delta(t)\ . \tag{1.86}$$

Taking the Fourier transform gives

$$\chi_e(\omega) = \chi_{0e} + \frac{\chi_{0d} - \chi_{0e}}{1 - i\omega\tau}\ . \tag{1.87}$$

Incorporating the preceding expression into Eq. (1.58) leads to the following expression for the normalized complex dielectric constant of the medium:

$$\varepsilon_r(\omega) = 1 + \chi_{0e} + \frac{\chi_{0d} - \chi_{0e}}{1 - i\omega\tau}\ . \tag{1.88}$$

For water molecules, the relaxation time has been determined experimentally to be $\tau = 8 \times 10^{-12}$, and the susceptibilities associated with the electron cloud and the permanent dipole moment are also found to be $\chi_{0e} = 4.27$ and $\chi_{0d} = 76.5$, respectively. Using these values, the real and imaginary parts of the relative dielectric constant of water were computed as a function of frequency and then plotted in Fig. 1-11.

It is interesting to note that once water molecules crystallize into ice at low temperatures,

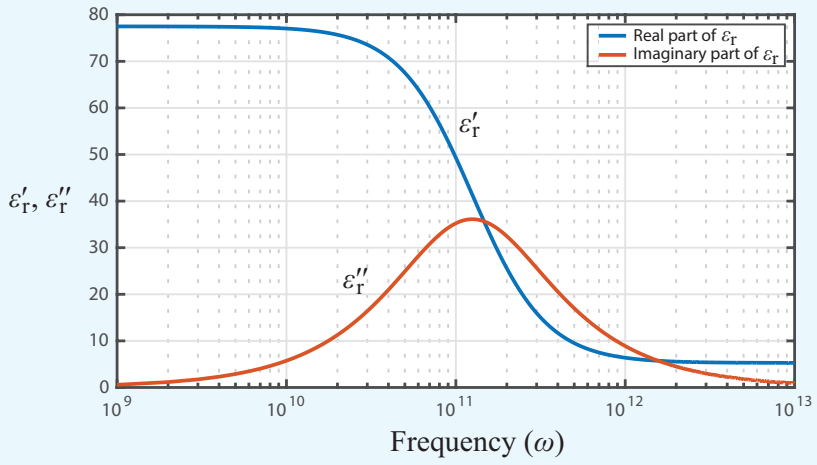


**Figure 1-11:** The real and imaginary parts of the relative dielectric constant of water at 20 °C.

the dielectric constant becomes drastically different from what is shown in Fig. 1-11. Dipoles of water molecules in solid form cannot respond to the applied electric field, and hence the susceptibility associated with the permanent dipoles cannot contribute to the polarization vector (**P**). For ice, the susceptibility $\chi_{e_{ice}}$ associated with the electron clouds is 2.155 at microwave and lower frequencies. Hence $\varepsilon'_{r_{ice}} = 3.155$ and the imaginary part is very small.

An interesting experiment is to place an ice cube in a styrofoam cup with a cap, keeping it in a freezer to ensure that no part of the ice cube has any surface water formed on it. Then the cup is placed in a microwave oven for a minute of time at normal power. After exposure to the microwave power, remove the cap and observe the ice cube in its initial form. The same amount of water in the cup would boil (make sure you don't have the cap on).

## 1-5 Kramers-Krönig Relations

The structure of the expression for the complex permittivity of materials given by Eq. (1.58) is not arbitrary. It can be shown that the real and imaginary parts of the complex permittivity are related to each other. In addition to the causality condition that led to Eq. (1.58), we further postulate that the system of charges in the material is unconditionally stable. That is, the impulse response $\chi_e(t) \to 0$ as $t \to \infty$. This stipulation guarantees that the Fourier transform $\chi_e(\omega)$ has no poles in the upper half-plane of the complex $\omega$-plane corresponding to $\Im\mathrm{m}(\omega) \geq 0$. Equation (1.58) also implies that $\chi_e(\omega) \to 0$ as $\omega \to \infty$ in the upper half-plane.

Now consider the contour integral

$$I = \oint_C \frac{\chi_e(\omega')}{\omega' - \omega}\, d\omega' \,, \tag{1.89}$$

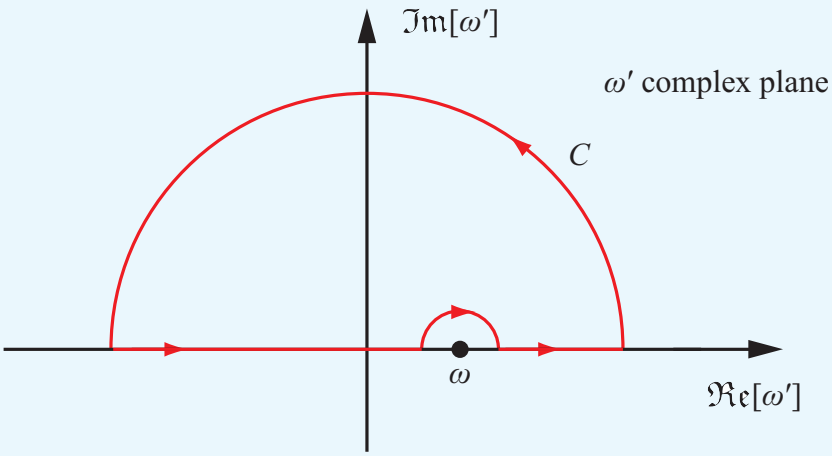


**Figure 1-12:** Complex $\omega'$-plane and closed contour $C$.

where the closed contour $C$ is composed of the real axis and a semicircle in the upper half-plane, as shown in Fig. 1-12, whose radius approaches infinity. Since there are no poles and branch cuts associated with the integrand of Eq. (1.89) within the contour $C$, according to Cauchy's theorem $I = 0$ (see Appendix A). Also, according to Jordan's lemma, the integral over the semicircle of infinite radius vanishes. Defining the principal value of the integral, denoted by $\int\!\!\!\!\!\!-$, as the integral over the real axis except at $\omega = \omega'$, and evaluating one-half of the residue at $\omega = \omega'$, it can be shown that

$$-i\pi\chi_e(\omega) + \int\!\!\!\!\!\!-_{-\infty}^{+\infty} \frac{\chi_e(\omega')}{\omega' - \omega}\, d\omega' = 0\,. \tag{1.90}$$

Representing the real and imaginary parts of the complex susceptibility as $\chi_e(\omega) = \chi_e'(\omega) + i\chi_e''(\omega)$, it can easily be shown that

$$\chi_e'(\omega) = \frac{1}{\pi} \int\!\!\!\!\!\!-_{-\infty}^{+\infty} \frac{\chi_e''(\omega')}{\omega' - \omega}\, d\omega' \tag{1.91a}$$

and

$$\chi_e''(\omega) = -\frac{1}{\pi} \int\!\!\!\!\!\!-_{-\infty}^{+\infty} \frac{\chi_e'(\omega')}{\omega' - \omega}\, d\omega'\,. \tag{1.91b}$$

Clearly, Eqs. (1.91a) and (1.91b) show that the real and imaginary parts of the susceptibility function are related to each other through a pair of integral transforms known as ***Kramers-Krönig relations***. Using Eq. (1.58), a similar relationship between the real and imaginary

parts of the permittivity ($\varepsilon_r(\omega)$) can be obtained and are given by

$$\varepsilon_r'(\omega) - \varepsilon_{r\infty} = \frac{1}{\pi} \int_{-\infty}^{+\infty} \frac{\varepsilon_r''(\omega')}{\omega' - \omega} \, d\omega'$$

and

$$\varepsilon_r''(\omega) = -\frac{1}{\pi} \int_{-\infty}^{+\infty} \frac{\varepsilon_r'(\omega') - \varepsilon_{r\infty}}{\omega' - \omega} \, d\omega' \, .$$

where $\varepsilon_{r\infty}$ is the value of the permittivity at infinite frequency. Strictly speaking, $\varepsilon_{r\infty} = 1$ according to Eq. (1.58).

## 1-6 Boundary Conditions

The Maxwell's equations presented and discussed in the preceding sections are valid in the neighborhood of a point in a medium where all constitutive parameters ($\overline{\overline{\varepsilon}}$, $\overline{\overline{\mu}}$, $\sigma$) are constant functions of position. At interfaces between different media with different constitutive parameters, the sudden discontinuity across the interface may cause the field quantities to become discontinuous. To address this mathematical difficulty, we assume there is a very thin hypothetical layer of width $\Delta z$ in which the constitutive parameters vary continuously between their values in the two distinct media (see Fig. 1-13), and then we evaluate the field

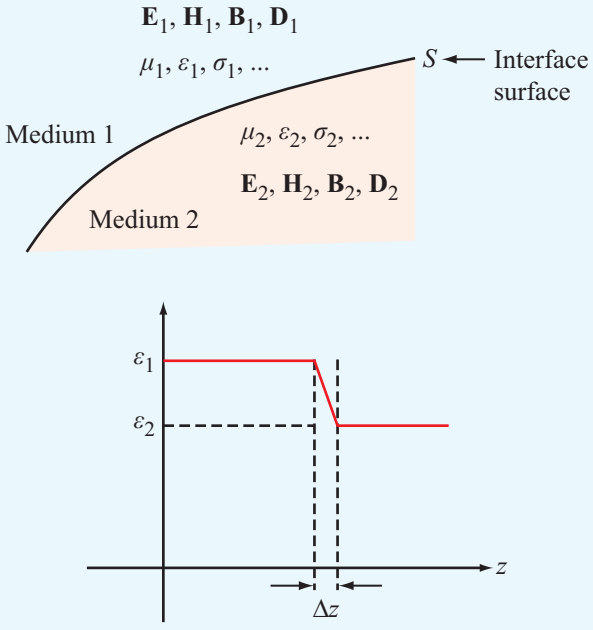


**Figure 1-13:** An abrupt change in the values of constitutive parameters is approximated by inserting a thin layer transitioning the discontinuous parameter in a continuous manner.

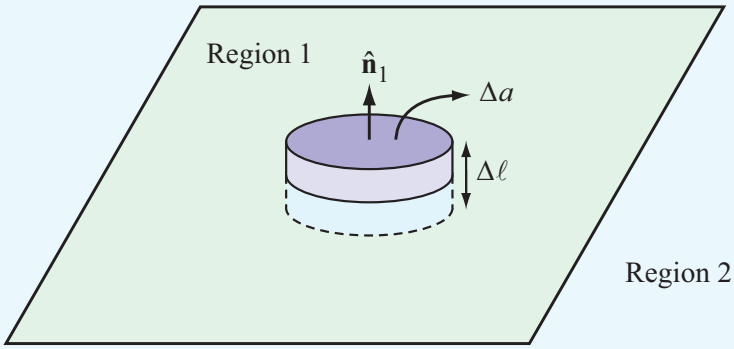


**Figure 1-14:** A small cylindrical volume between two homogeneous media. The base of the cylinder is chosen to be small enough so that the interface can be assumed flat locally.

in the limit as $\Delta z \to 0$. The reason for introducing this fictitious layer is to satisfy the condition that the field quantities and their derivates are continuous throughout the space of interest. It is only under such a continuity condition that theorems such as the divergence theorem and Stokes' theorems can be applied. To derive the solution to Maxwell's equations for a medium composed of two or more homogeneous media, we need to derive relationships between the field quantities across the media interfaces. To establish such relationships, let us consider a thin cylindrical volume between the two media as shown in Fig. 1-14, with the cylinder base being parallel to the interface (locally) and having a very small area $\Delta a$ and height $\Delta \ell$.

Consider a field vector $\mathbf{F}$ whose components and their derivatives are continuous within the volume and on the surface of this cylinder. For this field vector, the following relations hold:

$$\iiint_{\Delta V} \nabla \cdot \mathbf{F}\, d\upsilon = \oiint_{\Delta S} \mathbf{F} \cdot d\mathbf{s} \tag{1.92a}$$

and

$$\iiint_{\Delta V} \nabla \times \mathbf{F}\, d\upsilon = -\oiint_{\Delta S} \mathbf{F} \times d\mathbf{s}\,, \tag{1.92b}$$

where $\Delta V$ and $\Delta S$ refer respectively to the volume and surface of the thin cylinder. Equation (1.92a) is a direct statement of the divergence theorem and Eq. (1.92b) can be derived from the divergence theorem (see Appendix C). Applying the form of Eq. (1.92b) to the electric field $\mathbf{E}$ in Faraday's law (Eq. (1.1c)) leads to

$$\iiint_{\Delta V} \nabla \times \mathbf{E}\, d\upsilon = -\oiint_{\Delta S} \mathbf{E} \times d\mathbf{s} = \iiint_{\Delta V} -\frac{\partial \mathbf{B}}{\partial t}\, d\upsilon\,. \tag{1.93}$$

In the limit as $\Delta\ell \to 0,\ \Delta V \to 0$, and as a result the right-hand side of Eq. (1.93) goes to zero. Then we have

$$\lim_{\Delta\ell\to 0} \oiint_{\Delta S} \mathbf{E}\times d\mathbf{s} = (\mathbf{E}_1\times\hat{\mathbf{n}}_1 + \mathbf{E}_2\times\hat{\mathbf{n}}_2)\,\Delta a = 0\ ,$$

or

$$\hat{\mathbf{n}}\times(\mathbf{E}_1-\mathbf{E}_2) = 0\ , \tag{1.94}$$

where $\hat{\mathbf{n}} = \hat{\mathbf{n}}_1 = -\hat{\mathbf{n}}_2$ and $\hat{\mathbf{n}}_1$ is the unit vector pointing toward medium 1. Equation (1.94) states that the tangential component of the electric field intensity is continuous across a boundary interface between two media. Applying Eq. (1.92b) to the modified Ampère's law, given by Eq. (1.1a), we have

$$\iiint_{V} \nabla\times\mathbf{H}\,d\upsilon = -\oiint_{\Delta S}\mathbf{H}\times d\mathbf{s} = \iiint_{\Delta V}\frac{\partial\mathbf{D}}{\partial t}\,d\upsilon + \iiint_{\Delta V}\mathbf{J}\,d\upsilon\ . \tag{1.95}$$

Following the same recipe using in connection with the derivation leading to Eq. (1.94), as the cylinder shrinks into a circular disk, the contributions from the side wall of the cylinder as well as the volume integrals on the right-hand side of Eq. (1.95) vanish, resulting in

$$\hat{\mathbf{n}}\times(\mathbf{H}_1-\mathbf{H}_2) = 0 \quad \text{(tangent component of } \mathbf{H} \text{ is continuous)}. \tag{1.96}$$

An exception to this boundary condition is when a volumetric current density $\mathbf{J}$ collapses into a surface current density $\mathbf{J}_s$ at the interface. In that case

$$\lim_{\Delta\ell\to 0}\iiint_{\Delta V}\mathbf{J}\,d\upsilon = \mathbf{J}_s\,\Delta a\ ,$$

and the boundary condition given by Eq. (1.96) should be modified to

$$\hat{\mathbf{n}}\times(\mathbf{H}_1-\mathbf{H}_2) = \mathbf{J}_s\ . \tag{1.97}$$

The boundary condition for electric and magnetic flux densities can be obtained from Gauss' law in conjunction with the divergence theorem given by Eq. (1.92a). Upon substituting Gauss' magnetic law, as in Eq. (1.1d), into Eq. (1.92a) and shrinking $\Delta\ell \to 0$, we have

$$\iiint_{\Delta V}\nabla\cdot B = \oiint_{\Delta S}\mathbf{B}\cdot d\mathbf{s} = 0$$

and

$$\lim_{\Delta\ell\to 0}\oiint_{\Delta S}\mathbf{B}\cdot d\mathbf{s} = (\hat{\mathbf{n}}_1\cdot\mathbf{B}_1 + \hat{\mathbf{n}}_2\cdot\mathbf{B}_2)\,\Delta a = 0\ , \tag{1.98}$$

which leads to

$$\hat{\mathbf{n}}_1 \cdot (\mathbf{B}_1 - \mathbf{B}_2) = 0 \quad \text{(normal component of } \mathbf{B} \text{ is continuous).} \tag{1.99}$$

Similarly, substituting the electric flux density for $\mathbf{F}$ into Eq. (1.92a) and using Gauss' law for electricity (Eq. (1.1c)), we get

$$\oiint_{\Delta S} \mathbf{D} \cdot d\mathbf{s} = \iiint_{\Delta V} \rho \, dv \, .$$

As the cylinder shrinks to a disk we can again show that

$$\hat{\mathbf{n}} \cdot (\mathbf{D}_1 - \mathbf{D}_2) = 0 \quad \begin{array}{l}\text{(normal component of } \mathbf{D} \text{ is continuous} \\ \text{across boundary with no surface charge).}\end{array} \tag{1.100}$$

For time-varying field quantities, it should be noted that the continuity of the tangential components of $\mathbf{E}$ and $\mathbf{H}$ at the interface between two media also implies the continuity of the normal components of $\mathbf{B}$ and $\mathbf{D}$ at the interface. That is, if the continuity of the tangential components of $\mathbf{E}$ and $\mathbf{H}$ are imposed at the boundary, there will be no need for imposing the continuity of the normal components of $\mathbf{B}$ and $\mathbf{D}$. In the case where there is a surface charge density at the interface, i.e.,

$$\lim_{\Delta \ell \to 0} \iiint_{\Delta V} \rho \, dv = \rho_s \, \Delta a \, ,$$

then Eq. (1.100) must be modified to

$$\hat{\mathbf{n}} \cdot (\mathbf{D}_1 - \mathbf{D}_2) = \rho_s \quad \begin{array}{l}\text{(continuity of normal component of } \mathbf{D} \\ \text{in presence of surface charge).}\end{array} \tag{1.101}$$

If the second medium is a perfect electric conductor ($\sigma_2 = \infty$), then $\mathbf{E}_2 = 0$ and $\mathbf{D}_2 = 0$ throughout the entire volume of the perfect conductor medium, and therefore Eqs. (1.94), (1.97), and (1.101) reduce to

$$\left[\begin{array}{c} \hat{\mathbf{n}} \times \mathbf{E}_1 = 0 \\ \hat{\mathbf{n}} \times \mathbf{H}_1 = \mathbf{J}_s \\ \hat{\mathbf{n}} \cdot \mathbf{B}_1 = 0 \\ \hat{\mathbf{n}} \cdot \mathbf{D}_1 = \rho_s \end{array}\right] \quad \text{(Medium 2 = perfect conductor).}$$

## 1-7 Drift Current in Metals

As noted earlier, there is a large number of free electrons in the conduction band of good conductors, which facilitates the flow of electric currents without significant resistance. One important fact to keep in mind is that the net charge on the surface of good conductors, as they carry electric current, is zero. Another interesting feature is the speed with which the current flows in conductors. In air, electromagnetic fields propagate at the speed of light, $3 \times 10^8$ m/s. Consider an air-filled coaxial cable along the $z$-axis, supporting an electromagnetic field propagating along the $z$-direction with its magnetic field oriented along $\hat{\boldsymbol{\phi}}$. This magnetic field will generate $z$-directed surface currents on both the inner and outer conductors, which can be calculated from $\mathbf{J}_s = \hat{\mathbf{n}} \times \mathbf{H}$. Since $\mathbf{H}$ is propagating at the speed of light, the electric current on the metal must be moving at that speed. But is it really feasible for electrons in the conduction band to achieve such a high velocity? The answer is obviously no, so how do we reconcile these facts? As is shown in the following example, the charges that make up the surface current move at a much lower velocity known as the ***drift velocity***. For good conductors the drift velocity is on the order of $10^{-5}$ m/s, which depends on the current density and is inversely proportional to the number of free electrons. The apparent contradiction can be resolved by realizing that if an electron moves slightly, the change in the fields as a result of that movement propagates at the speed of light and can act on the other electrons down the line very quickly. The movement of electrons themselves is in fact hampered by collisions. The drift velocity $\mathbf{u}_d$ associated with electrons refers to the average velocity of the electrons in the conductor. For materials with finite conductivity, the field can penetrate to some extent into the conductor and a volumetric current, instead of a surface current, is formed near the surface. If $\rho$ represents the charge density of the moving charges near the surface, the drift current, according to Eq. (1.39), is given by

$$\mathbf{J} = \rho\, \mathbf{u}_d \,. \tag{1.102}$$

As will be shown later, the penetration depth in a good conductor is given by $\delta = 1/\sqrt{\pi\sigma\mu_0 f}$, where $f$ is the frequency. Assuming that the current density is uniform over this thin layer, the volumetric current, in terms of the surface current, assuming the conductor is a perfect conductor, is given by

$$\mathbf{J} = \frac{\mathbf{J}_s}{\delta} = \frac{\hat{\mathbf{n}} \times \mathbf{H}}{\delta} \,.$$

Hence, using Eq. (1.102), the drift velocity can be computed from

$$\mathbf{u}_d = \frac{|\hat{\mathbf{n}} \times \mathbf{H}|}{\delta\rho} = \frac{|\hat{\mathbf{n}} \times \mathbf{H}|\sqrt{\pi\sigma\mu_0 f}}{\rho} \,. \tag{1.103}$$

It follows that the drift velocity increases with increasing the field intensity $\mathbf{H}$, the frequency $f$, and the metal conductivity $\sigma$.

Example 1-4: Drift Velocity

Find the drift velocity in copper at 100 MHz, assuming that the tangential magnetic field intensity is 1 A/m and that there is one free electron available per copper atom.

**Solution:** The conductivity of copper is $\sigma = 5.8 \times 10^7$ S/m. To find the charge density, we first need to find the number $N$ of copper atoms per cubic meter, from which the charge density can be obtained using

$$\rho = eN \, .$$

From Eq. (1.79), $N = 8.43 \times 10^{28}$ m$^{-3}$. Using $\delta = 1/\sqrt{\pi\sigma\mu_0 f}$, the skin depth of copper at $f = 100$ MHz is calculated to be $\delta = 6.6 \times 10^{-6}$ m, and the charge density is $\rho = eN = 1.6 \times 10^{-19} \times 8.43 \times 10^{28} = 1.349 \times 10^{10}$ C/m$^3$. Hence,

$$\mathbf{u}_\mathrm{d} = \frac{\mathbf{H}}{\delta\rho} = \frac{1}{6.6 \times 10^{-6} \times 1.34 \times 10^{10}} = 1.12 \times 10^{-5} \text{ m/s.}$$

## 1-8 Hall Effect in Conducting Media

In a conducting medium, the flow of electric current is influenced by an external magnetic flux density $\mathbf{B}$. This phenomenon is known as the ***Hall effect***, discovered by Edwin H. Hall in 1879. As discussed earlier, the electrons in a conducting medium move with drift velocity $\mathbf{u}_\mathrm{d}$ and thus experience the Lorentz force once the conductor is exposed to an external magnetic flux density $\mathbf{B}$. The electromotive electric field that is perpendicular to $\mathbf{u}_\mathrm{d}$ is given by

$$\mathbf{E}_\perp = \mathbf{u}_\mathrm{d} \times \mathbf{B} \, . \tag{1.104}$$

Calculating the drift velocity from Eq. (1.102) and substituting into Eq. (1.104), we have

$$\mathbf{E}_\perp = \frac{\mathbf{J} \times \mathbf{B}}{\rho} \, . \tag{1.105}$$

There is also a component of the electric field inside the conductor that is parallel to $\mathbf{J}$ given by Ohm's law:

$$\mathbf{E}_\parallel = \frac{\mathbf{J}}{\sigma} \, . \tag{1.106}$$

Hence the direction of the electric field is tilted away from the direction of the current by

$$\theta = \tan^{-1} \frac{|\mathbf{E}_\perp|}{|\mathbf{E}_\parallel|} \approx \frac{|\mathbf{E}_\perp|}{|\mathbf{E}_\parallel|} = \frac{\sigma}{\rho} |\mathbf{B}| \, .$$

If we now consider a metallic strip carrying a current density $\mathbf{J}$ and having a width of $w$ and a magnetic flux density perpendicular to the metallic strip surface, the voltage measured across the strip is given by

$$V_\mathrm{H} = \int_0^w \mathbf{E}_\perp \cdot d\boldsymbol{\ell} = \frac{|\mathbf{J}| \, |\mathbf{B}|}{\rho} w \, . \tag{1.107}$$

For example, using a copper strip with charge density $\rho = 1.349 \times 10^{10}$ C/m$^3$ (see Example 1-4) at a frequency with skin depth 20 $\mu$m carrying 1 A of current, the Hall voltage is measured to be

$$V_{\rm H} = \frac{I}{w\,\delta\rho}\,Bw = \frac{IB}{\delta\rho} = 3.7 \times 10^{-6} B \text{ V}.$$

Hence if $B = 1$ mT, the Hall voltage induced is $V_{\rm H} = 3.7$ nV.

## 1-9 Generalized Coordinates

An important feature of vector calculus is that the equations expressing the physical relationships take the same form independently of any particular system of coordinates. However, to express the field quantities associated with a particular solution of the physical system, it is necessary to do so using a specific coordinate system. Often, depending on the geometry of the boundary between the two media, a particular coordinate system is deemed the most appropriate for a given configuration. The most commonly used coordinate system is the Cartesian coordinate system, in which a position vector specifying a point in three-dimensional space is given by

$$\mathbf{r} = x\,\hat{\mathbf{x}} + y\,\hat{\mathbf{y}} + z\,\hat{\mathbf{z}}\,. \tag{1.108}$$

The differential length in this system is simply given by

$$d\mathbf{r} = d\mathbf{l} = dx\,\hat{\mathbf{x}} + dy\,\hat{\mathbf{y}} + dz\,\hat{\mathbf{z}}\,.$$

We should note that in the general case, when the differential length is applied to a contour or path, the differential increments $dx$, $dy$, and $dz$ may not be necessarily independent.

In a generalized coordinate system, the position of a point is defined by the coordinate triplet $(u_1, u_2, u_3)$. Let $U_1 = f_1(x,y,z)$, $U_2 = f_2(x,y,z)$, and $U_3 = f_3(x,y,z)$ be three independent, single-valued, and continuously differentiable functions of the rectangular coordinates $x, y, z$. In general, there exist three single-valued functions

$$x = X(u_1,u_2,u_3)\,, \quad y = Y(u_1,u_2,u_3)\,, \quad \text{and} \quad z = Z(u_1,u_2,u_3)\,, \tag{1.109}$$

that provide an ordered set $(x,y,z)$ in terms of $(u_1,u_2,u_3)$. The functions $U_1, U_2, U_3$ are called ***general*** or curvilinear coordinates. Functions of the form

$$U_1 = \text{constant}, \quad U_2 = \text{constant}, \quad \text{and} \quad U_3 = \text{constant}$$

define ***coordinate surfaces***. The intersection of two coordinate surfaces creates a ***coordinate curve***. The intersection of two coordinate curves or three coordinate surfaces defines a point. At any point, unit vectors in coordinate surfaces tangent to coordinate curves define the unit vectors $\hat{\mathbf{u}}_1$, $\hat{\mathbf{u}}_2$, and $\hat{\mathbf{u}}_3$ at that point. Henceforth, we shall only consider orthogonal coordinate systems; that is, at any point in space

$$\hat{\mathbf{u}}_i \cdot \hat{\mathbf{u}}_j = \begin{cases} 1 & i = j\,, \\ 0 & i \neq j\,, \end{cases} \tag{1.110}$$

$$\hat{\mathbf{u}}_1 \times \hat{\mathbf{u}}_2 = \hat{\mathbf{u}}_3 \ , \quad \hat{\mathbf{u}}_2 \times \hat{\mathbf{u}}_3 = \hat{\mathbf{u}}_1 \ , \quad \text{and} \quad \hat{\mathbf{u}}_3 \times \hat{\mathbf{u}}_1 = \hat{\mathbf{u}}_2 \ . \tag{1.111}$$

### 1-9.1 Differential Length in the General Coordinate System

In the general coordinate system, the differential length $d\mathbf{r}$ is defined as

$$d\mathbf{r} = \frac{\partial \mathbf{r}}{\partial u_1} du_1 + \frac{\partial \mathbf{r}}{\partial u_2} du_2 + \frac{\partial \mathbf{r}}{\partial u_3} du_3 \ . \tag{1.112}$$

It is obvious that $\partial \mathbf{r}/\partial u_1$ is parallel to $\hat{\mathbf{u}}_1$ (tangent to $u_1$ curve). Similarly, $\partial \mathbf{r}/\partial u_2$ and $\partial \mathbf{r}/\partial u_3$ are parallel to $\hat{\mathbf{u}}_2$ and $\hat{\mathbf{u}}_3$, respectively. The configuration of an orthogonal generalized coordinate system showing the constant coordinate surfaces, coordinate curves, and the unit vectors is shown in Fig. 1-15.

Let us denote

$$\frac{\partial \mathbf{r}}{\partial u_i} = h_i \hat{\mathbf{u}}_i \ , \qquad i = 1, 2, 3$$

where

$$h_i = \left| \frac{\partial \mathbf{r}}{\partial u_i} \right| \ .$$

Hence

$$d\boldsymbol{\ell} = d\mathbf{r} = \sum_{i=1}^{3} h_i \, du_i \, \hat{\mathbf{u}}_i \ . \tag{1.113}$$

The three scaling factors $h_i$ can easily be obtained by noting that

$$\frac{\partial \mathbf{r}}{\partial u_i} = \frac{\partial X}{\partial u_i} \hat{\mathbf{x}} + \frac{\partial Y}{\partial u_i} \hat{\mathbf{y}} + \frac{\partial Z}{\partial u_i} \hat{\mathbf{z}} \ , \tag{1.114}$$

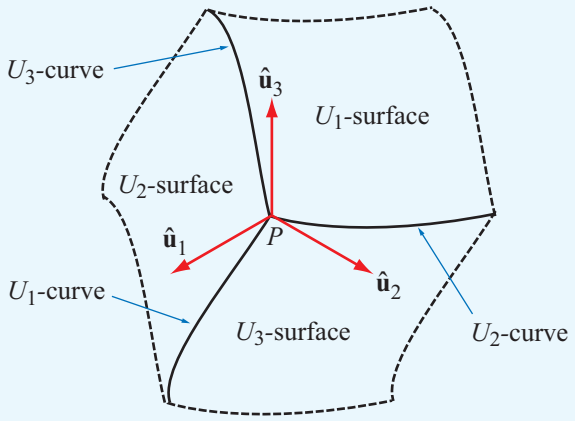


**Figure 1-15:** Orthogonal generalized coordinate system showing constant curves and surfaces.

which leads to

$$h_i = \left[ \left( \frac{\partial X}{\partial u_i} \right)^2 + \left( \frac{\partial Y}{\partial u_i} \right)^2 + \left( \frac{\partial Z}{\partial u_i} \right)^2 \right]^{1/2} . \tag{1.115}$$

Also,

$$\hat{\mathbf{u}}_i = \frac{1}{h_i} \frac{\partial \mathbf{r}}{\partial u_i} . \tag{1.116}$$

**Example 1-5: Scaling Factors and Unit Vectors**

Derive the expressions for the scaling factors and unit vectors in the spherical coordinate system.

**Solution:** Consider a spherical coordinate system with $u_1 = r,\ u_2 = \theta,\ u_3 = \phi$, and

$$X = r \sin\theta \cos\phi , \tag{1.117a}$$
$$Y = r \sin\theta \sin\phi , \tag{1.117b}$$
$$Z = r \cos\theta . \tag{1.117c}$$

Using Eq. (1.115),

$$h_r = [\sin^2\theta \cos^2\phi + \sin^2\theta \sin^2\phi + \cos^2\theta]^{1/2} = 1 , \tag{1.118a}$$
$$h_\theta = [r^2 \cos^2\theta \cos^2\phi + r^2 \cos^2\theta \sin^2\phi + r^2 \sin^2\theta]^{1/2} = r , \tag{1.118b}$$
$$h_\phi = [r^2 \sin^2\theta \sin^2\phi + r^2 \sin^2\theta \cos^2\phi]^{1/2} = r \sin\theta . \tag{1.118c}$$

Also,

$$\hat{\mathbf{u}}_1 = \hat{\mathbf{r}} = \frac{1}{h_r} \frac{\partial \mathbf{r}}{\partial r} = \sin\theta \cos\phi\ \hat{\mathbf{x}} + \sin\theta \sin\phi\ \hat{\mathbf{y}} + \cos\theta\ \hat{\mathbf{z}} , \tag{1.119a}$$
$$\hat{\mathbf{u}}_2 = \hat{\boldsymbol{\theta}} = \frac{1}{h_\theta} \frac{\partial \mathbf{r}}{\partial \theta} = \cos\theta \cos\phi\ \hat{\mathbf{x}} + \cos\theta \sin\phi\ \hat{\mathbf{y}} - \sin\theta\ \hat{\mathbf{z}} , \tag{1.119b}$$
$$\hat{\mathbf{u}}_3 = \hat{\boldsymbol{\phi}} = \frac{1}{h_\phi} \frac{\partial \mathbf{r}}{\partial \phi} = -\sin\phi\ \hat{\mathbf{x}} + \cos\phi\ \hat{\mathbf{y}} . \tag{1.119c}$$

### 1-9.2 Differential Area and Volume

When dealing with electric and magnetic fields in various types of media, we often encounter surface and volume integrals. Depending on the problem at hand, the choice of which coordinate system to use may prove critically important. In general, the differential areas

in constant surfaces are given by

$$d\mathbf{S}_1 = ds_1\ \hat{\mathbf{u}}_1 = h_2\,du_2\ \hat{\mathbf{u}}_2 \times h_3\,du_3\ \hat{\mathbf{u}}_3 = h_2h_3\,du_2\,du_3\ \hat{\mathbf{u}}_1\ , \tag{1.120a}$$

$$d\mathbf{S}_2 = ds_2\ \hat{\mathbf{u}}_2 = h_1h_3\,du_1\,du_3\ \hat{\mathbf{u}}_2\ , \tag{1.120b}$$

$$d\mathbf{S}_3 = h_1h_2\,du_1\,du_2\ \hat{\mathbf{u}}_3\ . \tag{1.120c}$$

Also, in a general coordinate system the differential volume is given by

$$\begin{aligned} d\upsilon &= h_1\,du_1\ \hat{\mathbf{u}}_1 \cdot h_2\,du_2\ \hat{\mathbf{u}}_2 \times h_3\,du_3\ \hat{\mathbf{u}}_3 \\ &= h_1h_2h_3\,du_1\,du_2\,du_3\ . \end{aligned} \tag{1.121}$$

### 1-9.3 Gradient of Scalar Functions

The gradient operator acts on a scalar field quantity and specifies the rate of change of that quantity with respect to distance. For a differentiable scalar field $\psi$, the differential $d\psi$ in a Cartesian coordinate system, is given by

$$d\psi = \frac{\partial\psi}{\partial x}\,dx + \frac{\partial\psi}{\partial y}\,dy + \frac{\partial\psi}{\partial z}\,dz\ ,$$

which can be cast as the dot product of two quantities:

$$d\psi = \left(\frac{\partial\psi}{\partial x}\,\hat{\mathbf{x}} + \frac{\partial\psi}{\partial y}\,\hat{\mathbf{y}} + \frac{\partial\psi}{\partial z}\,\hat{\mathbf{z}}\right) \cdot (dx\,\hat{\mathbf{x}} + dy\,\hat{\mathbf{y}} + dz\,\hat{\mathbf{z}})\ . \tag{1.122}$$

We recognize the quantity in the second parenthesis as the differential length along which the change in $\psi$ is measured. The quantity in the first parenthesis is defined as the gradient $\nabla\psi$ of scalar function $\psi$. Hence, Eq. (1.122) can be rewritten as

$$d\psi = \nabla\psi \cdot d\boldsymbol{\ell}\ .$$

In a similar fashion, we can show that $d\psi$ in a general coordinate system may be written as

$$\begin{aligned} d\psi &= \frac{\partial\psi}{\partial u_1}\,du_1 + \frac{\partial\psi}{\partial u_2}\,du_2 + \frac{\partial\psi}{\partial u_3}\,du_3 \\ &= \left(\frac{1}{h_1}\,\frac{\partial\psi}{\partial u_1}\,\hat{\mathbf{u}}_1 + \frac{1}{h_2}\,\frac{\partial\psi}{\partial u_2}\,\hat{\mathbf{u}}_2 + \frac{1}{h_3}\,\frac{\partial\psi}{\partial u_3}\,\hat{\mathbf{u}}_3\right) \cdot (h_1\,du_1\,\hat{\mathbf{u}}_1 + h_2\,du_2\,\hat{\mathbf{u}}_2 + h_3\,du_3\,\hat{\mathbf{u}}_3)\ . \end{aligned} \tag{1.123}$$

Since $d\boldsymbol{\ell} = \sum_{i=1}^{3} h_i\,du_i\,\hat{\mathbf{u}}_i$, it then can be concluded that

$$\nabla\psi = \sum_{i=1}^{3} \frac{1}{h_i}\,\frac{\partial\psi}{\partial u_i}\,\hat{\mathbf{u}}_i\ . \tag{1.124}$$

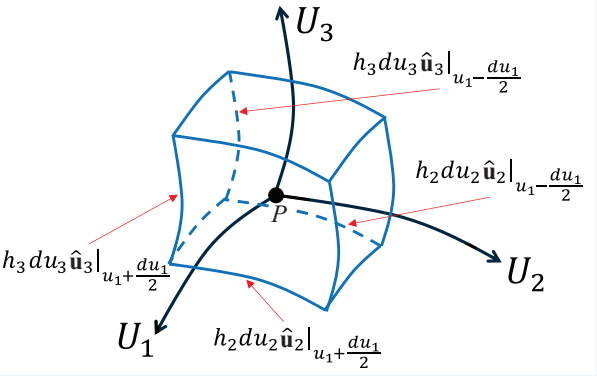


**Figure 1-16:** The curvilinear differential volume and surface used in evaluation of the divergence of a vector function.

### 1-9.4 Divergence of Vector Functions

The divergence of a continuous and differentiable function $\mathbf{F}$ is defined as

$$\nabla \cdot \mathbf{F} = \lim_{\Delta V \to 0} \frac{\sum_i \mathbf{F} \cdot \Delta \mathbf{S}_i}{\Delta V} \,. \tag{1.125}$$

At a specified point in space, the divergence of a vector field quantity represents the normalized outflux of the field from a very small volume surrounding the point. In a generalized coordinate system, referring to Fig. 1-16 it can be shown that

$$\begin{aligned} \sum_i \mathbf{F} \cdot \Delta \mathbf{S}_i = {} & \left(F_1 h_2 h_3|_{u_1+du_1/2} - F_1 h_2 h_3|_{u_1-du_1/2}\right) du_2\, du_3 \\ & + \left(F_2 h_3 h_1|_{u_2+du_2/2} - F_2 h_3 h_1|_{u_2-du_2/2}\right) du_3\, du_1 \\ & + \left(F_3 h_1 h_2|_{u_3+du_3/2} - F_3 h_1 h_2|_{u_3-du_3/2}\right) du_1\, du_2 \,, \end{aligned} \tag{1.126}$$

where $F_1$, $F_2$, and $F_3$ are the components of $\mathbf{F}$ along dimensions $U_1$, $U_2$, and $U_3$, respectively. Noting that

$$\left(F_1 h_2 h_3|_{u_1+du_1/2} - F_1 h_2 h_3|_{u_1-du_1/2}\right) = \frac{\partial (F_1 h_2 h_3)}{\partial u_1} du_1 \tag{1.127}$$

and that similar formulations apply to the second and third terms in Eq. (1.126),

$$\sum \mathbf{F} \cdot \Delta \mathbf{S}_i = \left( \frac{\partial}{\partial u_1}(h_2 h_3 F_1) + \frac{\partial}{\partial u_2}(h_3 h_1 F_2) + \frac{\partial}{\partial u_3}(h_1 h_2 F_3) \right) du_1\, du_2\, du_3 \,. \tag{1.128}$$

Also, $d\upsilon = h_1 h_2 h_3\, du_1\, du_2\, du_3$. Hence,

$$\nabla \cdot \mathbf{F} = \frac{1}{h_1 h_2 h_3} \sum_{i=1}^{3} \frac{\partial}{\partial u_i} \left( \frac{h_1 h_2 h_3}{h_i} F_i \right) . \tag{1.129}$$

### 1-9.5 Curl of a Vector Function

Using Eq. (1.15) with the unit normal $\hat{\mathbf{n}}$ replaced with $\hat{\mathbf{u}}_i$, the curl $\nabla \times \mathbf{F}$ of a vector function $\mathbf{F}$ can be expressed as

$$\hat{\mathbf{u}}_i \cdot \nabla \times \mathbf{F} = \lim_{\Delta S \to 0} \frac{\oint_{\Delta S} \mathbf{F} \cdot d\boldsymbol{\ell}}{\Delta S} = \lim_{\Delta S \to 0} \frac{\sum \mathbf{F} \cdot \Delta \boldsymbol{\ell}}{\Delta S} , \tag{1.130}$$

where $\Delta S$ is the surface whose unit normal is $\hat{\mathbf{u}}_i$. Basically, the curl of a vector field quantity at a point is the normalized circulation of the field quantity along three orthogonal small contours circling the point. Let's first consider $\Delta S$ in the $u_2$–$u_3$ plane as shown in Fig. 1-17, with $\hat{\mathbf{u}}_1$ as its unit normal.

According to Fig. 1-17,

$$\begin{aligned} \sum \mathbf{F} \cdot \Delta \boldsymbol{\ell} &= \left( F_3 h_3 \, du_3 |_{u_2 + du_2/2} - F_3 h_3 \, du_3 |_{u_2 - du_2/2} - F_2 h_2 \, du_2 |_{u_3 + du_3/2} + F_2 h_2 \, du_2 |_{u_3 - du_3/2} \right) \\ &= \left( \frac{\partial (h_3 F_3)}{\partial u_2} - \frac{\partial (h_2 F_2)}{\partial u_3} \right) du_2 \, du_3 . \end{aligned} \tag{1.131}$$

Also, $\Delta S = h_2 h_3 \, du_2 \, du_3$; therefore

$$\hat{\mathbf{u}}_1 \cdot \nabla \times \mathbf{F} = \frac{1}{h_2 h_3} \left( \frac{\partial (h_3 F_3)}{\partial u_2} - \frac{\partial (h_2 F_2)}{\partial u_3} \right) . \tag{1.132a}$$

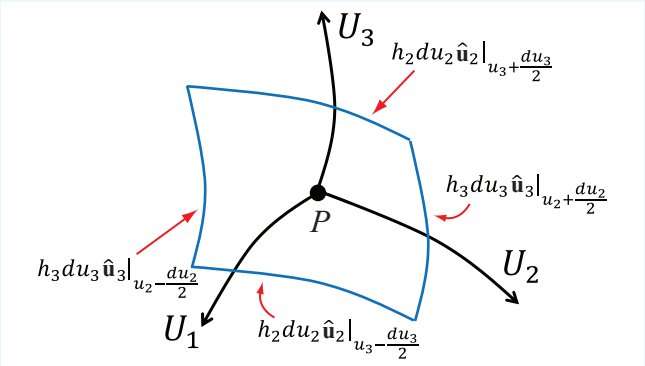


$\Delta S = h_2 h_3 \, du_2 \, du_3$

**Figure 1-17:** A small contour in the constant $U_1$-surface used to compute a component of the curl of a vector field.

Similarly, by permutation it can be shown that

$$\hat{\mathbf{u}}_2 \cdot \nabla \times \mathbf{F} = \frac{1}{h_3 h_1}\left(\frac{\partial}{\partial u_3}(h_1 F_1) - \frac{\partial}{\partial u_1}(h_3 F_3)\right) \tag{1.132b}$$

and

$$\hat{\mathbf{u}}_3 \cdot \nabla \times \mathbf{F} = \frac{1}{h_1 h_2}\left(\frac{\partial}{\partial u_1}(h_2 F_2) - \frac{\partial}{\partial u_2}(h_1 F_1)\right) . \tag{1.132c}$$

Finally,

$$\begin{aligned} \nabla \times \mathbf{F} &= \sum_{i=1}^{3} (\nabla \times \mathbf{F}) \cdot \hat{\mathbf{u}}_i \\ &= \frac{1}{h_1 h_2 h_3} \begin{vmatrix} h_1 \hat{\mathbf{u}}_1 & h_2 \hat{\mathbf{u}}_2 & h_3 \hat{\mathbf{u}}_3 \\ \dfrac{\partial}{\partial u_1} & \dfrac{\partial}{\partial u_2} & \dfrac{\partial}{\partial u_3} \\ h_1 F_1 & h_2 F_2 & h_3 F_3 \end{vmatrix} . \end{aligned} \tag{1.133}$$

## Example 1-6: Spherical Coodinate System

Determine $\nabla \times \mathbf{F}$ in the spherical coordinate system.

**Solution:** From Eq. (1.117) in Example 1-5,

$$h_1 = h_r = 1 , \qquad h_2 = h_\theta = r , \qquad h_3 = h_\phi = r \sin\theta .$$

Application of Eq. (1.133) gives

$$\begin{aligned} \nabla \times \mathbf{F} = {} & \frac{1}{r^2 \sin\theta}\left(\frac{\partial}{\partial \theta}(r \sin\theta \, F_\phi) - \frac{\partial}{\partial \phi}(r F_\theta)\right) \hat{\mathbf{r}} \\ & + \frac{1}{r \sin\theta}\left(\frac{\partial}{\partial \phi}(F_r) - \frac{\partial}{\partial r}(r \sin\theta \, F_\phi)\right) \hat{\boldsymbol{\theta}} \\ & + \frac{1}{r}\left(\frac{\partial}{\partial r}(r F_\theta) - \frac{\partial}{\partial \theta}(F_r)\right) \hat{\boldsymbol{\phi}} . \end{aligned}$$

Upon further expansion of the derivatives involved, the expression can be simplified to

$$\begin{aligned}\nabla \times \mathbf{F} = &\frac{1}{r\sin\theta}\left(\frac{\partial}{\partial\theta}(\sin\theta\, F_\phi) - \frac{\partial}{\partial\phi}(F_\theta)\right)\hat{\mathbf{r}} \\ &+\frac{1}{r}\left(\frac{1}{\sin\theta}\,\frac{\partial F_r}{\partial\phi} - \frac{\partial}{\partial r}(rF_\phi)\right)\hat{\boldsymbol{\theta}} \\ &+\frac{1}{r}\left(\frac{\partial}{\partial r}(rF_\theta) - \frac{\partial}{\partial\theta}(F_r)\right)\hat{\boldsymbol{\phi}}\,. \end{aligned} \tag{1.134}$$

### 1-9.6 Laplacian of a Scalar Field

The Laplacian is a differential operator applied to scalar field quantities. The Laplacian of a differentiable scalar field quantity $\psi$ is defined by

$$\nabla^2\psi = \nabla\cdot\nabla\psi\,. \tag{1.135}$$

Using Eqs. (1.124) and (1.129), it can be shown that

$$\nabla^2\psi = \frac{1}{h_1h_2h_3}\left[\frac{\partial}{\partial u_1}\left(\frac{h_2h_3}{h_1}\,\frac{\partial\psi}{\partial u_1}\right) + \frac{\partial}{\partial u_2}\left(\frac{h_3h_1}{h_2}\,\frac{\partial\psi}{\partial u_2}\right) + \frac{\partial}{\partial u_3}\left(\frac{h_1h_2}{h_3}\,\frac{\partial\psi}{\partial u_3}\right)\right]\,. \tag{1.136}$$

### 1-9.7 Curl of Curl of a Vector Field

When analyzing field quantities, we often encounter the need to evaluate $\nabla\times\nabla\times\mathbf{F}$. We adopt the following identity:

$$\nabla\times\nabla\times\mathbf{F} = \nabla\nabla\cdot\mathbf{F} - \nabla^2\mathbf{F}\,, \tag{1.137}$$

where $\nabla^2\mathbf{F} = \nabla\cdot(\nabla\mathbf{F})$.

Given a vector function $\mathbf{F}$, the quantity on the left-hand side of Eq. (1.137), namely $\nabla\times\nabla\times\mathbf{F}$, can be readily computed by applying the curl operator twice. Similarly, $\nabla\nabla\cdot\mathbf{F} = \nabla(\nabla\cdot\mathbf{F})$ can be computed by applying the divergence operator to $\mathbf{F}$, which would produce a scalar function, and then applying the gradient operator, resulting in a vector function. Such procedures, however, do not apply to the last term in Eq. (1.137) because $\nabla\mathbf{F}$ represents a gradient operator applied to a vector function, which is inconsistent with the rules of vector algebra. The term $\nabla^2\mathbf{F}$ can be computed indirectly by computing the two other terms in Eq. (1.137) and then applying

$$\nabla^2\mathbf{F} = \nabla\nabla\cdot\mathbf{F} - \nabla\times\nabla\times\mathbf{F}\,. \tag{1.138}$$

In Cartesian coordinates the process leads to

$$\nabla\cdot\nabla\mathbf{F} = \nabla^2F_x\,\hat{\mathbf{x}} + \nabla^2F_y\,\hat{\mathbf{y}} + \nabla^2F_z\,\hat{\mathbf{z}}\,. \tag{1.139}$$

## Summary

### Concepts

- Maxwell's equations can be expressed in integral and differential form (with the latter also known as the point form of Maxwell's equations).
- Gauss' laws of electricity and magnetism can be derived from the combination of Ampère's law and Faraday's law.ă
- Faraday's law ($\nabla \times \mathbf{E} = -\partial \mathbf{B}/\partial t$) and the modified Ampère's law ($\nabla \times \mathbf{H} = \mathbf{J} + \partial \mathbf{D}/\partial t$), in addition to the law of conservation of charge, which is expressed by the equation of continuity ($\nabla \cdot \mathbf{J} = -\partial \rho/\partial t$), are the necessary and sufficient equations required for solving for the field quantities **E**, **D**, **B**, and **H**.
- In the general case, the electric flux density **D** and the magnetic flux density **B** in a material medium are each related to both the electric field intensity **E** and the magnetic field intensity **H** in that medium. The relationships depend on the degrees of polarization and magnetization of the molecules comprising the material. Under the small-signal approximation, however, these relations can be expressed in linear form.
- When considering the full range of the electromagnetic spectrum, all materials exhibit a dispersive behavior (the permittivity and permeability are functions of frequency). This is due to the fact that the charges or permanent dipoles (electric or magnetic) have finite masses and cannot react instantaneously to the applied fields.
- Electromagnetic boundary conditions define the relationships between field quantities across a discontinuity in material properties between two adjacent media. These include the continuity of the tangential components of the electric and magnetic fields ($E_t$ and $H_t$) and the continuity of the normal components of the electric and magnetic flux densities ($D_n$ and $B_n$).
- Differential operators such as the gradient, divergence, and curl assume different mathematical forms in different orthogonal coordinate systems. The specific choice of which coordinate system to use depends on the geometry of the boundary value problem under consideration.

## Important Equations

**Point form of Maxwell's equations:**

$$\nabla \times \mathbf{E} = -\frac{\partial \mathbf{B}}{\partial t}$$

$$\nabla \times \mathbf{H} = \frac{\partial \mathbf{D}}{\partial t} + \mathbf{J}$$

$$\nabla \cdot \mathbf{D} = \rho$$

$$\nabla \cdot \mathbf{B} = 0$$

**Law of conservation of charge:**

$$\nabla \cdot \mathbf{J} = -\frac{\partial \rho}{\partial t} \quad \text{(equation of continuity)}$$

**Ohm's law:**

$$\mathbf{J} = \sigma \mathbf{E}$$

**Integral form of Maxwell's equations:**

$$\oint_C \mathbf{E} \cdot d\boldsymbol{\ell} = -\iint_S \frac{\partial \mathbf{B}}{\partial t} \cdot d\mathbf{s} + \oint_C \mathbf{u} \times \mathbf{B} \cdot d\boldsymbol{\ell}$$

$$\oint_C \mathbf{H} \cdot d\boldsymbol{\ell} = \iint_S \frac{\partial \mathbf{D}}{dt} \cdot d\mathbf{s} + I + \iint_S \rho \mathbf{u} \cdot d\mathbf{s} - \oint_C \mathbf{u} \times \mathbf{D} \cdot d\boldsymbol{\ell}$$

$$\oiint_S \mathbf{D} \cdot d\mathbf{s} = \rho$$

$$\oiint_S \mathbf{B} \cdot d\mathbf{s} = 0$$

**Kramers-Krönig relations:**

$$\varepsilon_r'(\omega) - \varepsilon_{r_\infty} = \frac{1}{\pi} \fint_{-\infty}^{+\infty} \frac{\varepsilon_r''(\omega')}{\omega' - \omega}\, d\omega'$$

$$\varepsilon_r''(\omega) = -\frac{1}{\pi} \fint_{-\infty}^{+\infty} \frac{\varepsilon_r'(\omega') - \varepsilon_{r_\infty}}{\omega' - \omega}\, d\omega'$$

**Boundary conditions:**

**Dielectric-dielectric interface:**

$$\hat{\mathbf{n}} \times (\mathbf{E}_1 - \mathbf{E}_2) = 0$$

$$\hat{\mathbf{n}} \times (\mathbf{H}_1 - \mathbf{H}_2) = \mathbf{J}_s$$

$$\hat{\mathbf{n}} \cdot (\mathbf{D}_1 - \mathbf{D}_2) = \rho$$

$$\hat{\mathbf{n}} \cdot (\mathbf{B}_1 - \mathbf{B}_2) = 0$$

**Dielectric-metal interface:**

$$\hat{\mathbf{n}} \times \mathbf{E} = 0$$

$$\hat{\mathbf{n}} \times \mathbf{H} = \mathbf{J}_s$$

$$\hat{\mathbf{n}} \cdot \mathbf{D} = \rho_s$$

$$\hat{\mathbf{n}} \cdot \mathbf{B} = 0$$

**Important Terms** Provide definitions or explain the meaning of the following terms:

anisotropic
bianisotropic
biaxial
boundary conditions
conduction current
constitutive relations
coordinate curve
coordinate surface
curl
current density
diamagnetism
dispersive material
displacement current
divergence theorem
drift current
electric field intensity
electric flux density
electric susceptibility
equation of continuity
Faraday's law
ferromagnetism
Gauss' law for electricity
Gauss' law for magnetism
gradient
Hall effect
homogeneous
induced electric field
inhomogeneous
isotropic homogeneous material
Kramers-Krönig relations
Laplacian
law of conservation of charge
magnetic field intensity
magnetic flux density
magnetization vector
modified Ampère's law
motional induction
ordinary point
paramagnetism
point form of Ohm's law
polarization vector
Stokes' theorem
surface charge density
surface current density
transformer induction
uniaxial
volumetric charge density

## PROBLEMS

### Definitions and Identities

**1.1**

**(a)** Prove the divergence theorem:

$$\iiint_V \nabla \cdot \mathbf{A}\, dV = \oiint_S \mathbf{A} \cdot d\mathbf{S}\,,$$

for a differential vector field $\mathbf{A}$ and a continuous surface $S$ that bounds a volume $V$. (*Hint:* Start from the general definition of divergence.)

**(b)** Prove Stokes' theorem:

$$\iint_S \nabla \times \mathbf{A} \cdot d\mathbf{S} = \oint_C \mathbf{A} \cdot d\boldsymbol{\ell}\,,$$

for a differential vector field $\mathbf{A}$ and a continuous surface $S$ bounded by a continuous contour $C$. (*Hint:* Start from the general definition of curl.)

**1.2** Prove the following vector identities in a generalized coordinate system:

**(a)** $\nabla \cdot \nabla \times \mathbf{A} = 0$ for all $\mathbf{A}$. (*Hint:* Start with the divergence theorem applied to an arbitrary volume $V$ and then use Stokes' theorem.)

**(b)** $\nabla \times \nabla \psi = 0$ for all $\psi$. (*Hint:* Start with Stokes' theorem applied to an arbitrary surface $S$ and note that $d\psi = \nabla \psi \cdot d\boldsymbol{\ell}$.)

**1.3**

**(a)** Suppose $C$ is the closed boundary around an arbitrary surface $S$. Prove that for any scalar function $T$,

$$\iint_S \nabla T \times d\mathbf{S} = -\oint_C T\, d\boldsymbol{\ell}\,.$$

**(b)** Suppose $V$ is a volume bounded by an arbitrary surface $S$. Prove that

$$\iiint_V \nabla T\, d\upsilon = \oiint_S T\, d\mathbf{S}\,.$$

(*Hint:* Start with Stokes' theorem and the divergence theorem assuming $\mathbf{A} = T\mathbf{C}$, where $\mathbf{C}$ is a constant vector.)

**1.4** Construct a nonconstant vector function that has vanishing divergence and curl. Can you find a method for finding such vectors?

**1.5**

**(a)** Prove the "bac-cab" vector identity given by Eq. (C.1) in Appendix C in Cartesian coordinates:

$$\mathbf{A} \times (\mathbf{B} \times \mathbf{C}) = (\mathbf{A} \cdot \mathbf{C})\mathbf{B} - (\mathbf{A} \cdot \mathbf{B})\mathbf{C}\,. \tag{1.140}$$

**(b)** Is the identity given by Eq. (1.141) always valid? If not, find the conditions under which the following identity is valid:

$$\mathbf{A} \times (\mathbf{B} \times \mathbf{C}) = (\mathbf{A} \times \mathbf{B}) \times \mathbf{C}\,. \tag{1.141}$$

**1.6** Consider at time $t$ a surface $S_1$ bounded by contour $C_1$. Let $\mathbf{u}$ be the instantaneous velocity of element $dS$ of the surface. The surface $S_1$ together with the contour $C_1$ may change shape as time elapses so that $\mathbf{u}$ need not be constant for all elements of $S_1$. At time $(t+\Delta t)$, $S_1$ and $C_1$ become $S_2$ and $C_2$, as shown in Fig. P1.6. Use the general integral form of Ampère's law:

$$\oint_C \mathbf{H} \cdot d\boldsymbol{\ell} = I + \frac{d}{dt} \iint_S \mathbf{D} \cdot d\mathbf{s}\,,$$

to show that

$$\oint_C \mathbf{H} \cdot d\boldsymbol{\ell} = I + \iint_S \rho\mathbf{u} \cdot d\mathbf{s} + \iint_S \frac{d\mathbf{D}}{dt} \cdot d\mathbf{s} - \oint_C (\mathbf{u} \times \mathbf{D}) \cdot d\boldsymbol{\ell}\,.$$

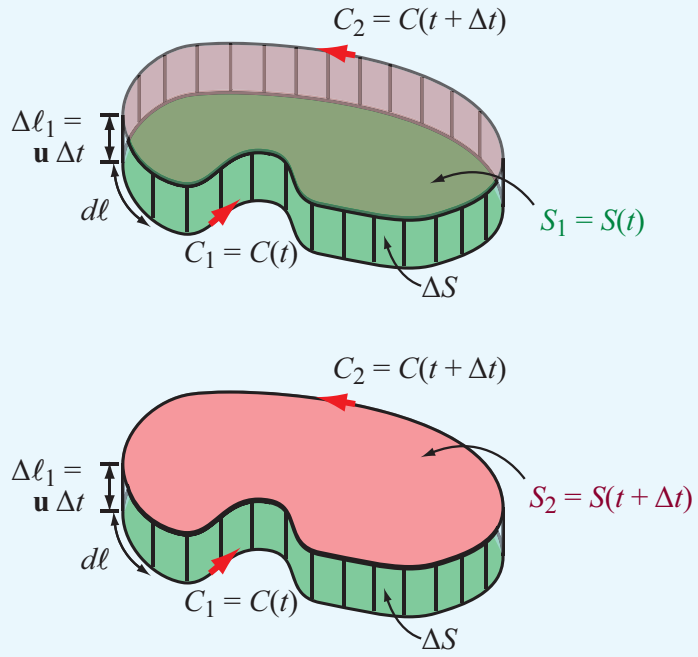


**Figure P1.6:** Surface and contour for Problem 1.6.

## Fields and Currents

**1.7** Suppose a magnet is approaching a conductive loop at a constant velocity, and the loop is connected to a voltmeter as shown in Fig. P1.7.

**(a)** Qualitatively, plot the magnetic flux through the loop as a function of time.

**(b)** Qualitatively, plot the voltage measured by the voltmeter as a function of time.

**(c)** Does the size of the loop relative to that of the magnet have any effect on the results obtained in parts (a) and (b)?

**(d)** Now imagine that you replace the voltmeter with a resistor and repeat the experiment. Plot the current through the loop as a function of time.

**(e)** What is the effect of this current on the magnet?

**1.8** As shown in Fig. P1.8, a dc current of 50 mA passes downward along the negative $z$ axis, enters a thin spherical shell of radius 0.03 m, and at $\theta = 90°$ enters a plane sheet. Write expressions for the current sheet densities in the spherical shell and in the plane.

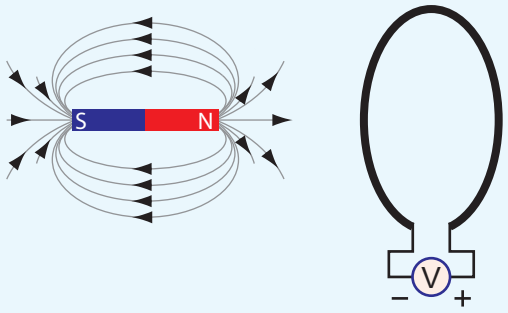


**Figure P1.7:** A permanent magnet is traveling at a constant velocity toward a loop, passes through the loop's center, and continues its travel on a straight line. The loop is attached to a voltmeter that measures the induced voltage.

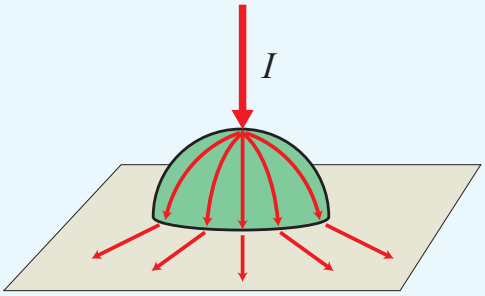


**Figure P1.8:** Geometry of a conducting hemispherical shell attached to a ground plane. A constant current $I$ enters the hemispherical shell at its top.

### 1.9

**(a)** The electric flux density inside a cube is given by $\mathbf{D} = (5+z)\hat{\mathbf{x}} + (3xy)\,\hat{\mathbf{y}}$, as shown in Fig. P1.9. Find the total electric charge enclosed inside the cubical volume.

**(b)** Repeat part (a) for $\mathbf{D} = (5t + xt)\,\hat{\mathbf{x}} + (2t^2 + 2)\,\hat{\mathbf{z}}$ and calculate the total displacement current passing through the cubical surface.

### 1.10

**(a)** Starting from Maxwell's equations, derive the circuit law for inductors, $v = L\,\frac{di}{dt}$.

**(b)** Starting from Maxwell's equations, derive the circuit law for capacitors, $i = C\,\frac{dv}{dt}$.

**(c)** The "quasi-static condition" refers to a condition where the time variation of the fields is very slow, (i.e., $\partial/\partial t \approx 0$). Use Faraday's law to prove Kirchhoff's voltage law under quasi-static conditions.

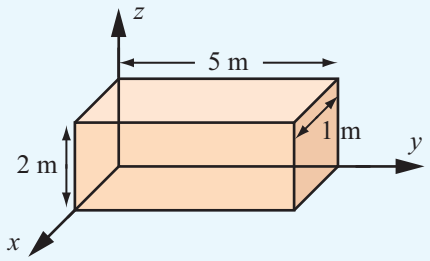


**Figure P1.9:** A cubical volume in a medium with an established flux density.

**1.11** Show whether or not each of the following fields satisfies Maxwell's equations (and is therefore a valid electromagnetic field) in a source-free ($J = 0,\ \rho = 0$) homogeneous region of space. Find the corresponding magnetic field.

**(a)** $\mathbf{E} = \dfrac{1}{4\pi|\mathbf{r}-\mathbf{r}'|}\cos(\omega t - k|\mathbf{r}-\mathbf{r}'|)\,\hat{\mathbf{z}}$, for $\mathbf{r} \neq \mathbf{r}'$.

**(b)** $\mathbf{E} = \sin(\alpha x)\cos(\omega t - \beta z)\,\hat{\mathbf{y}}$ and $\alpha^2 + \beta^2 = \omega^2\mu\varepsilon$.

**1.12**

**(a)** Consider the magnetic flux density given in Cartesian coordinates by

$$\mathbf{B}(x,y) = \frac{B_0}{a}\,(x\,\hat{\mathbf{x}} - y\,\hat{\mathbf{y}}) \qquad (\text{Wb/m}^2).$$

Show that this field obeys Maxwell's equations in free space and sketch the magnetic field lines. (*Hint:* The field lines are given by the differential equation $dy/dx = B_y/B_x$.)

**(b)** Suppose the electric field $\mathbf{E}$ and the magnetic flux density $\mathbf{B}$ are given in spherical coordinates by

$$\mathbf{E}(\mathbf{r},t) = -\frac{q}{4\pi\varepsilon_0 r^2}\,u(vt-r)\hat{\mathbf{r}} \qquad (\text{V/m})$$

and

$$\mathbf{B}(\mathbf{r},t) = 0 \qquad (\text{Wb/m}^2)\,,$$

where $u(x)$ is the step function defined as

$$u(x) \equiv \begin{cases} 1 & x > 0\,, \\ 0 & x < 0\,. \end{cases}$$

Show that these fields satisfy all of Maxwell's equations, and determine $\rho$ and $\mathbf{J}$. (*Hint:* The derivative of the step function $u(x)$ is the Dirac delta function $\delta(x)$.)

**1.13** A square wire loop of side $a$ is placed at distance $s$ from a very long straight wire carrying a current $I$, as shown in Fig. P1.13.

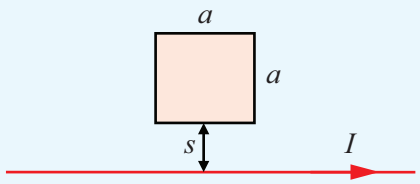


**Figure P1.13:** A square loop with a side parallel to a long wire carrying current $I$.

**(a)** Find the magnetic flux through the square loop.

**(b)** If someone now pulls the loop upwards, directly away from the straight wire, at speed $\upsilon$, what electromotive force $V_{\text{emf}}$ is generated? In which direction (clockwise or counterclockwise) does the current flow in the loop?

**(c)** What if the loop is pulled to the right, instead of upwards, at speed $\upsilon$?

**(d)** Now let us assume a *slowly varying* current $I(t)$ is flowing through the wire. Repeat part (b) for this case.

**1.14** A wire loop in the shape of an isosceles right triangle with side of length $a$ is placed at distance $s$ from a very long straight wire carrying a current $I$, as shown in Fig. P1.14.

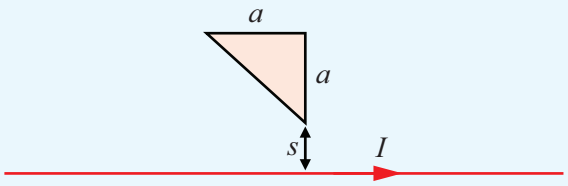


**Figure P1.14:** An isosceles right triangle in the vicinity of a long wire carrying current $I$. The tip of the triangle is at a distance $s$ from the wire.

**(a)** Find the magnetic flux flowing through the wire loop.

**(b)** If someone now pulls the loop upwards directly away from the straight wire, at speed $\upsilon$, what electromotive force $V_{\text{emf}}$ is generated? In which direction (clockwise or counterclockwise) does the current flow in the loop?

**(c)** What if the loop is pulled to the right, instead of upwards, at speed $\upsilon$?

**(d)** Now let us assume a *slowly varying* current $I(t)$ is flowing through the wire. Repeat part (b) for this case.

**1.15** A rectangular loop of wire of linear resistance $\rho$ ($\Omega$/m) is placed in a time-varying magnetic flux density $\mathbf{B}(t)$. If a voltmeter is connected across the loop using the same wire as shown in Fig. P1.15, what voltage does the voltmeter show?

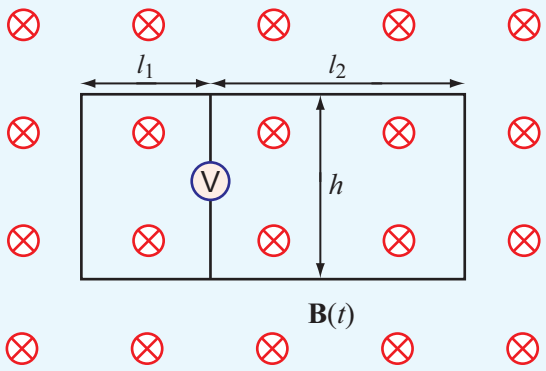


**Figure P1.15:** A rectangular wire loop with a linear resistivity $\rho$ is placed in a medium supporting a time-varying magnetic flux density $\mathbf{B}(t)$. A voltmeter placed at a distance $l_1$ from one end is measuring the induced voltage.

## 1.16

**(a)** A moving rod is rotating with $\omega = 0.4$ rad/s inside a medium with a background magnetic field of $\mathbf{B} = (3t + 4)\,\hat{\mathbf{z}}$, as shown in Fig. P1.16(a). The radius of the semicircle is $R$. Find $V_{\text{emf}}$ at $t = 3$ s. Assume that $\theta$ is 60° at $t = 3$ s.

**(b)** The semicircle (radius $= R$) shown in Fig. P1.16(b) is moving with constant velocity $\mathbf{u} = v_0\,\hat{\mathbf{x}}$ inside a medium with constant magnetic field $\mathbf{B} = B_0\,\hat{\mathbf{z}}$. Find the induced $V_{\text{emf}}$.

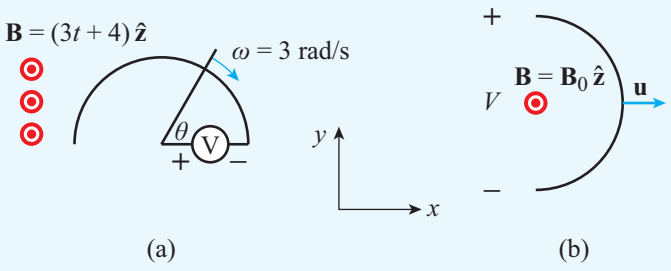


**Figure P1.16:** (a) Configuration of a semicircular wire attached to a moving wire pivoted at the center and moving with a constant angular velocity. A time-varying magnetic flux density perpendicular to the surface of the semicircle is present. (b) A semicircular wire moves with a constant velocity in a constant magnetic field perpendicular to the surface of the semicircle.

**1.17** An air-filled coaxial cable has an inner conductor of radius $a$ and an outer conductor of radius $b$ (with $b \ll \lambda$, where $\lambda$ is the wavelength), as shown in Fig. P1.17. A time-varying current flows along the inner conductor in the $z$-direction:

$$\mathbf{J}_{\text{ac}} = e^{-100(1-r/a)} \cos(\omega t - kz)\, \hat{\mathbf{z}}\,, \qquad 0 < r < a. \qquad (\text{A/m}^2).$$

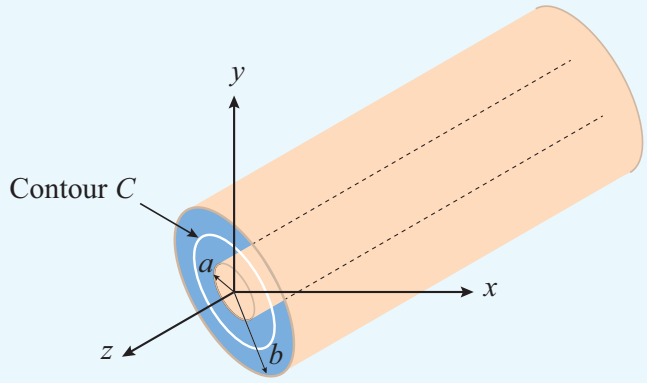


**Figure P1.17:** Configuration of a hollow coaxial cable with inner conductor of radius $a$ and thin outer cylinder of radius $b$. The coaxial line is carrying a sinusoidal time-varying current and a hypothetical uniform volumetric charge density with a constant velocity. This charge density is uniformly distributed over the cross section of only the inner conductor.

Additionally, charged particles with a fictitious volumetric density $\rho_0$ (C/m$^3$) are distributed uniformly over the cross section of the inner conductor, moving with a constant velocity $u\hat{\mathbf{z}}$. These charges only exist on the inner conductor.

**(a)** Determine the total current flowing on the inner conductor (units should be A).

**(b)** Determine the total linear charge density on the inner conductor (units should be C/m).

**(c)** Using the cylindrical symmetry of the problem, determine the magnetic field $\mathbf{H}_0$ in the region $a < r < b$.

**(d)** Calculate the radial electric field.

**(e)** Assume that now your reference contour moves with velocity $\mathbf{u} = v_0\, \hat{\mathbf{z}}$, where $v_0$ is comparable in magnitude to $u$ but much smaller than the velocity of light $c$. Compute the magnetic field $\mathbf{H}$.

## Material Properties

**1.18** Starting from the units of permittivity and electric field intensity, and using the constitutive relations between $\mathbf{E}$ and $\mathbf{D}$ in a homogeneous isotropic medium, show that the unit for the flux density is indeed C/m$^2$.

**1.19** The electric field in a certain region of space is given by $\mathbf{E}(\mathbf{r},t) = \hat{\mathbf{y}}10x^2e^{-\alpha t}\,u(t)$, where $u(t)$ is the step function.

**(a)** Find $\mathbf{D}(\mathbf{r},t)$ if $\varepsilon(\mathbf{r},t) = 3\varepsilon_0 y^2\,\delta(t)$.

**(b)** Find $\mathbf{D}(\mathbf{r},t)$ if $\chi_e(\mathbf{r},t) = 3y^2\,u(t)$.

**(c)** Find $\mathbf{D}(\mathbf{r},t)$ if

$$\varepsilon(\mathbf{r},t) = \varepsilon_0 \begin{pmatrix} 3\,2\,0 \\ 0\,0\,0 \\ 0\,4\,0 \end{pmatrix} \delta(t)\ .$$

**(d)** Chirality is a natural state of symmetry. Many natural substances are chiral materials, such as DNA and many sugars. A chiral material is bi-isotropic and has the following constitutive relation:

$$\mathbf{D} = \varepsilon\left(\mathbf{E} - \chi\,\frac{\partial \mathbf{H}}{\partial t}\right)\ .$$

Using Faraday's law, find $\mathbf{D}$ for $\varepsilon = 7\varepsilon_0$ and $\chi/\mu = 10$.

**1.20** In a given anisotropic medium, the electric permittivity tensor in a certain coordinate system $V$ is given by

$$\overline{\overline{\varepsilon}}_{r_V} = \begin{bmatrix} 7 & -2 & 2 \\ -2 & 4 & -1 \\ 2 & -1 & 4 \end{bmatrix}\ .$$

Let $W$ be the coordinate system where $\overline{\overline{\varepsilon}}_{r_W}$ is diagonal. Find $\overline{\overline{\varepsilon}}_{r_V}$ and the unitary transformation $\overline{\mathbf{Q}}$ that describes the transformation from $V$ to $W$. What type of material is the medium? *Hint:* Find the eigenvalues (roots of the equation $|\overline{\overline{\varepsilon}}_{r_V} - \lambda I| = 0$) and then their corresponding eigenvectors $\{V_n\}$ of $\overline{\overline{\varepsilon}}_{r_V}$. Note that if the eigenvectors of $\overline{\overline{\varepsilon}}_{r_V}$ do not correspond to unique eigenvalues, they may not be mutually orthogonal. In this case, a set of orthogonal unit vectors $\{\mathbf{U}_n\}$ can be found using the Gram-Schmidt process. The transformation matrix $\overline{\mathbf{Q}}$ can be constructed with the three orthonormalized vectors $\overline{\mathbf{Q}} = [\mathbf{U}_1\mathbf{U}_2\mathbf{U}_3]$, and will satisfy $\overline{\mathbf{Q}}^{-1} = \overline{\mathbf{Q}}^{t}$. The diagonal matrix is computed as $\overline{\overline{\varepsilon}}_{r_W} = \overline{\mathbf{Q}}^{-1}\overline{\overline{\varepsilon}}_{r_V}\overline{\mathbf{Q}}$, which has the eigenvalues of $\overline{\overline{\varepsilon}}_{r_V}$ as its nonzero elements.

**1.21** The permittivity for a linear, temporally dispersive medium, with conductivity $\sigma$ and electric susceptibility $\chi_e$, is given by

$$\varepsilon(\omega) = \varepsilon_0\left(1 + \frac{i\sigma}{\omega\varepsilon_0} + \int_0^\infty \chi_e(\tau)\,e^{i\omega\tau}\,d\tau\right)\ .$$

Derive the Kramers-Krönig relation for this medium. *Hint:* Evaluate the integral

$$\oint \frac{\varepsilon(\omega') - \varepsilon_\infty}{\omega' - \omega}\,d\omega'$$

over an appropriate closed contour $C$ using Cauchy's residue theorem, which states that if $f(z)$ is singular at $\{z_n\}_{(n=1)}^{N}$, then

$$\oint_C f(z)\,dz = 2\pi i \sum_{n=1}^{N} \lim_{z\to z_0} (z-z_0)\, f(z_0) \qquad \text{if } \{z_n\}_{n=1}^{N} \text{ are inside the contour } C\,,$$

$$\oint_C f(z)\,dz = \pi i \sum_{n=1}^{N} \lim_{z\to z_0} (z-z_0)\, f(z_0) \qquad \text{if } \{z_n\}_{n=1}^{N} \text{ are on the contour } C,$$

and

$$\oint_C f(z)\,dz = 0 \qquad \text{if } \{z_n\}_{n=1}^{N} \text{ are outside the contour } C.$$

**1.22** Consider a rectangular cuboid volume of height $d$ and base $w \times w$ containing a homogeneous material with permittivity $\varepsilon = \varepsilon_0\varepsilon_r$. Suppose the electric field is perpendicular to the base and is given by $\mathbf{E} = E_z\hat{\mathbf{z}}$, as shown in Fig. P1.22(a).

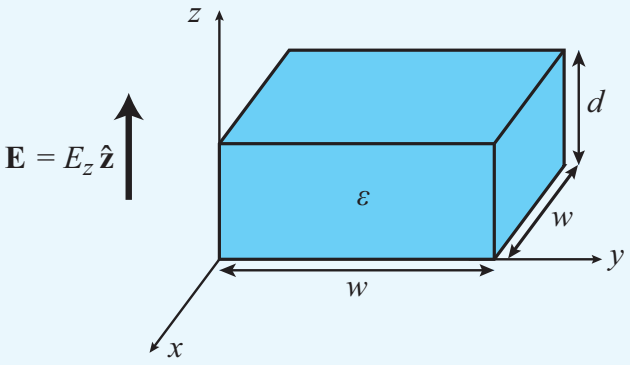


**Figure P1.22(a):** A rectangular cuboid section of a homogeneous medium supporting a constant electric field. The top and bottom surfaces perpendicular to the electric field can be viewed as a parallel-plate capacitor.

**(a)** Noting that the displacement current in the material is defined as $\mathbf{J}_D = \partial\mathbf{D}/\partial t$, find the equivalent capacitance of the cuboid.

**(b)** Now consider a medium with a periodic arrangement of dielectric slabs (parallel to the $x$–$z$ plane) as shown in Fig. P1.22(b). Consider a rectangular cuboid whose width is $w = w_1 + w_2$. Following a similar procedure as in part (a), find the effective dielectric constant of this medium.

**(c)** If the periodicity is now along the $z$-direction as shown in Fig. P1.22(c), choosing the height of the cuboid to be $d = d_1 + d_2$, find the effective dielectric constant of the medium.

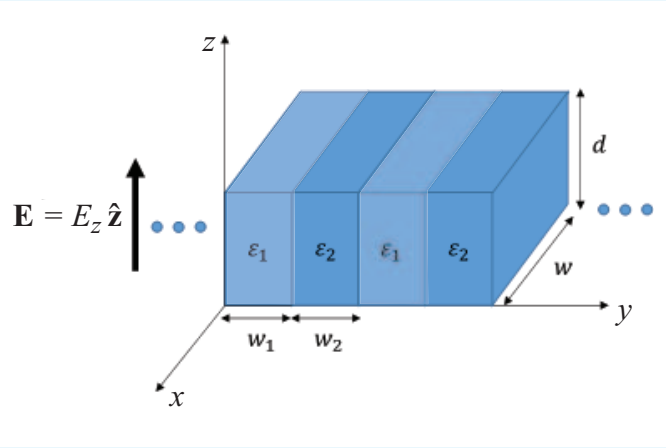


**Figure P1.22(b):** A rectangular cuboid section of a periodic medium supporting a constant eletcric field. The two surfaces perpendicular to the electric field can be viewed as a parallel-plate capacitor.

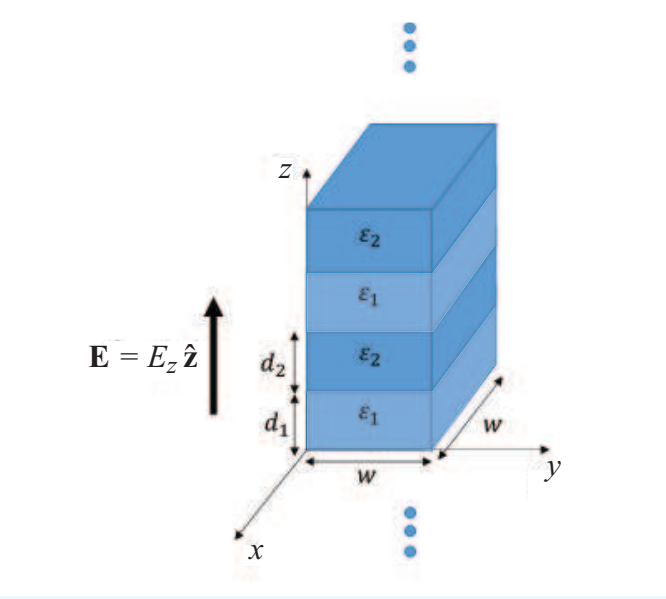


**Figure P1.22(c):** A rectangular cuboid section of a periodic medium supporting a constant eletcric field. The two surfaces perpendicular to the electric field can be viewed as a parallel-plate capacitor.

**1.23** To find the effective dielectric constant of a medium composed of molecules with polarizability $p$ and with a number density of $N$ molecules per unit volume, the following procedure can be followed. Consider the diagrams shown in Fig. P1.23. Part (a) shows the molecules individually in a background dielectric $\varepsilon_0$, and part (b) shows an equivalent homogeneous dielectric medium with permittivity $\varepsilon$ and an isolated single molecule within a void sphere.

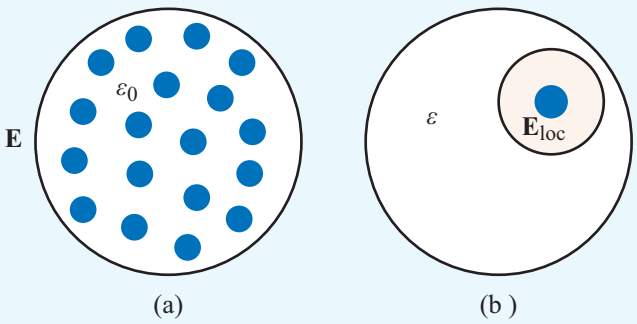


**Figure P1.23:** The configuration of a heterogeneous medium composed of a background medium with permittivity $\varepsilon_0$ and including molecules with dipole moment $p$. This medium can be viewed as a homogeneous medium with effective permittivity $\varepsilon$.

The constitutive relation $\mathbf{D} = \varepsilon\mathbf{E}$ can also be expressed as $\mathbf{D} = \varepsilon_0\mathbf{E} + \mathbf{P}$, where $\mathbf{P}$ is the polarization vector. In the case of induced dipoles, the polarization $\mathbf{P}$ is proportional to the polarizability per unit volume $Np$, where $N$ is the number of dipoles per unit volume and $p$ is the polarizability per dipole. The polarization is given by

$$\mathbf{P} = Np\mathbf{E}_{\text{loc}} ,$$

where $\mathbf{E}_{\text{loc}}$ is the electric field in the void due to the average electric field in the effective medium. Under the quasi-static approximation, it can be shown that the local electric field is given by

$$\mathbf{E}_{\text{loc}} = \mathbf{E} + \frac{\mathbf{P}}{3\varepsilon_0} .$$

Find the effective dielectric constant of the medium ($\varepsilon$). This is the well-known Clausius-Mossotti (or Lorentz-Lorenz) formula.

**1.24** A 3D array of identical metallic spheres rests in a background material with an electric field $\mathbf{E} = \mathbf{E}_0$. The diameter of each sphere is $R$ and the separations between adjacent spheres in the $x$, $y$, and $z$ directions are $a_x$, $a_y$, and $a_z$, respectively. The periodic structure can be viewed as an equivalent dielectric medium. Find the relative permittivity of this structure. Is the relative permeability a function of the radius of the spheres? (*Hint:* A small metallic sphere in a medium under the influence of background electric field $\mathbf{E}$ gets polarized and behaves like a dipole with dipole moment $p = 4\pi_0\varepsilon ER^3$.)

## Boundary Conditions

**1.25** Prove that at the interface between two dielectrics, the relations $\hat{\mathbf{n}} \times (\mathbf{E}_1 - \mathbf{E}_2) = 0$ and $\hat{\mathbf{n}} \times (\mathbf{H}_1 - \mathbf{H}_2) = 0$ are sufficient boundary conditions. That is, $\hat{\mathbf{n}} \cdot (\mathbf{D}_1 - \mathbf{D}_2) = 0$ and $\hat{\mathbf{n}} \cdot (\mathbf{B}_1 - \mathbf{B}_2) = 0$ are satisfied automatically. (*Hint:* Use Cartesian coordinates with a dielectric interface in the $x$–$y$ plane.)

**1.26** Prove that $\partial D_n / \partial t = 0$, where $D_n$ is the normal component of the electric flux density, on the surface of a perfect magnetic conductor. (*Hint:* Start from Ampère's law and use Stokes' theorem for asmall surface on the magnetic surface.)

**1.27**

**(a)** Using the equation of continuity, establish the boundary condition for volumetric current density $\mathbf{J}$ at an interface between two media that can support surface charge density $\rho_s$.

**(b)** If you also include surface current density $\mathbf{J}_s$ at the surface, how will the boundary condition change?

**1.28** A magnetic sphere with relative permeability $\mu_r$ and relative permittivity $\varepsilon_r = 1$ rests in free space. A static magnetic field of $H_0\hat{\mathbf{z}}$ lies within this sphere. Assume no currents or charges exist on the surface of the sphere. Find the magnetic field on the outside surface of the sphere $\mathbf{H}_{ext}(\theta)$, as shown in Fig. P1.28.

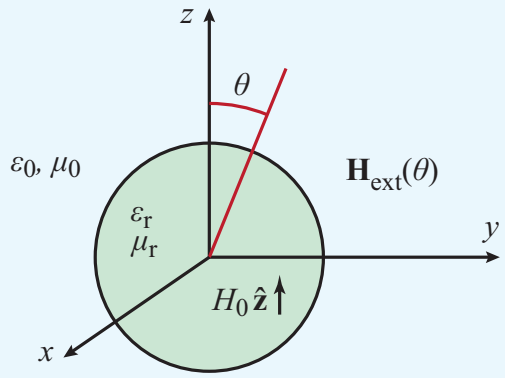


**Figure P1.28:** A spherical magnetic material with permeability $\mu = \mu_0\mu_r$ and permittivity $\varepsilon = \varepsilon_0$ supporting a constant magnetic field inside.

**1.29** Two dielectric media are in contact as shown in Fig. P1.29. An electric field $\mathbf{E}_1$ is incident from medium 1 upon the interface at an angle $\alpha_1$ measured from the common normal.

**(a)** If both media are lossless dielectrics with permittivities $\varepsilon_1$ and $\varepsilon_2$, find the magnitude and direction of $\mathbf{E}_2$ in medium 2.

**(b)** If both media are lossy dielectrics with permittivities and conductivities $(\varepsilon_1, \sigma_1)$ and $(\varepsilon_2, \sigma_2)$:

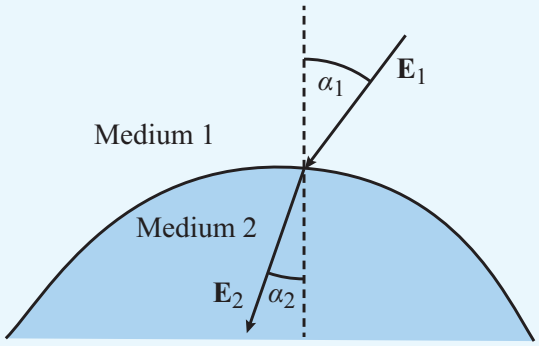


**Figure P1.29:** The interface between two dielectric media.

(i) Find the magnitude and direction of $\mathbf{E}_2$ in medium 2. (*Hint:* There are no surface currents at the discontinuity.)

(ii) Find the surface charge density at the interface.

(iii) Compare the results with part (a).

(iv) What happens if medium 2 is an insulator ($\sigma = 0$)?

## Generalized Coordinates

**1.30** In cylindrical coordinates, we can define the following:

$$r = \sqrt{x^2 + y^2}\,,$$
$$\phi = \arctan\left(\frac{y}{x}\right)\,,$$
$$z = z\,.$$

**(a)** Find the inverse relation for $x(r,\phi,z)$, $y(r,\phi,z)$, and $z(r,\phi,z)$.

**(b)** Find the scaling factors $h_r$, $h_\phi$, and $h_z$ (also known as "metrical coefficients").

**(c)** Derive expressions for each of the following operations in cylindrical coordinates. Confirm your results with those available in Table C-2 in Appendix C.

(i) $\nabla\psi$

(ii) $\nabla\cdot\mathbf{F}$

(iii) $\nabla\times\mathbf{F}$

(iv) $\nabla^2\psi = \nabla\cdot\nabla\psi$

**1.31** Let two fixed points $P_1$ and $P_2$ be located at $x = c$ and $x = -c$ along the $x$-axis, and let $r_1$ and $r_2$ be the distances of a variable point $P$ in the $x$–$y$ plane from $P_1$ and $P_2$, respectively. Let the axes of the coordinate system be defined as

$$u_1 = \xi \ , \quad u_2 = \eta \ , \quad u_3 = z \ ,$$

where

$$\xi = \frac{r_1 + r_2}{2c} \qquad \text{and} \qquad \eta = \frac{r_1 - r_2}{2c} \ .$$

Note that $\xi \geq 1$ and $-1 \leq \eta \leq 1$.

**(a)** Find expressions for $x$ and $y$ in terms of $\xi$ and $\eta$.

**(b)** Let $z = 0$. Plot a few $\xi =$ constant curves and $\eta =$ constant curves to develop a sense for the coordinate system. (*Note:* Beware of sign ambiguity; your plots should cover all four quadrants.)

**(c)** Find the scaling factors $h_\xi$, $h_\eta$, and $h_z$.

**(d)** Define each of the following operations in this coordinate system:

(i) $\nabla\psi$

(ii) $\nabla \times \mathbf{F}$

(iii) $\nabla \cdot \mathbf{F}$

(iv) $\nabla^2\psi$

**1.32** Oblate spheroidal coordinates $(\mu, \nu, \phi)$ belong to a system of curvilinear coordinates in which two sets of coordinate surfaces are obtained by revolving the curves of the elliptic cylindrical coordinates. They are related to Cartesian coordinates by the expressions

$$\begin{aligned} x &= a \cosh\mu \cos\nu \cos\phi \ , \\ y &= a \cosh\mu \cos\nu \sin\phi \ , \\ z &= a \sinh\mu \sin\nu \ , \end{aligned}$$

where $a$ is a constant, and $\mu \in (0, \infty)$, $\nu \in [-\pi/2, +\pi/2]$, and $\phi \in [0, 2\pi)$.

**(a)** Show that the coordinate surfaces are:

$$\text{for } \mu = \text{constant:} \quad \frac{x^2 + y^2}{a^2 \cosh^2\mu} + \frac{z^2}{a^2 \sinh^2\mu} = \cos^2\nu + \sin^2\nu = 1 \ ,$$

$$\text{for } \nu = \text{constant:} \quad \frac{x^2 + y^2}{a^2 \cos^2\nu} + \frac{z^2}{a^2 \sin^2\nu} = \cosh^2\mu - \sinh^2\mu = 1 \ .$$

**(b)** Find the scaling factors $h_\mu$, $h_\nu$, $h_\phi$.

**(c)** Define each of the following operations in oblate spherical coordinates:

(i) $\nabla\psi$
(ii) $\nabla\times\mathbf{F}$
(iii) $\nabla\cdot\mathbf{F}$
(iv) $\nabla^2\psi$

**1.33** Bispherical coordinates $(\xi,\eta,\beta)$ are related to Cartesian coordinates by the expressions

$$x=\frac{a\sin\eta\cos\beta}{\cosh\xi-\cos\eta},$$
$$y=\frac{a\sin\eta\sin\beta}{\cosh\xi-\cos\eta},$$
$$z=\frac{a\sinh\xi}{\cosh\xi-\cos\eta},$$

where $a$ is a constant parameter and $-\infty<\xi<+\infty,\ 0<\eta<\pi$, and $0<\beta<2\pi$.

**(a)** Show that:

(i) the coordinate surfaces $\xi=$ constant represent spheres:

$$x^2+y^2+(z-a\coth\xi)^2=\left(\frac{a}{\sinh\xi}\right)^2.$$

(ii) the coordinate surfaces $\eta=$ constant represent spindle-shaped surfaces of revolution around the $z$-axis:

$$(\sqrt{x^2+y^2}-a\cot\eta)^2+z^2=\left(\frac{a}{\sin\eta}\right)^2.$$

(iii) the coordinate surfaces $\beta=$ constant are semi-infinite planes diverging from the $z$-axis.

**(b)** Find the scaling factors $h_\xi, h_\eta, h_\beta$.

**(c)** Show that the coordinate surfaces are orthogonal to each other.

**(d)** Let $x=0$. Plot a few $\xi=$ constant curves and $\eta=$ constant curves in the $y$–$z$ plane to develop a sense for the coordinate system.

**(e)** Derive the expression for each of the following operations in bispherical coordinates:

(i) $\nabla\psi$
(ii) $\nabla\times\mathbf{F}$
(iii) $\nabla\cdot\mathbf{F}$
(iv) $\nabla^2\psi=\nabla\cdot\nabla\psi$

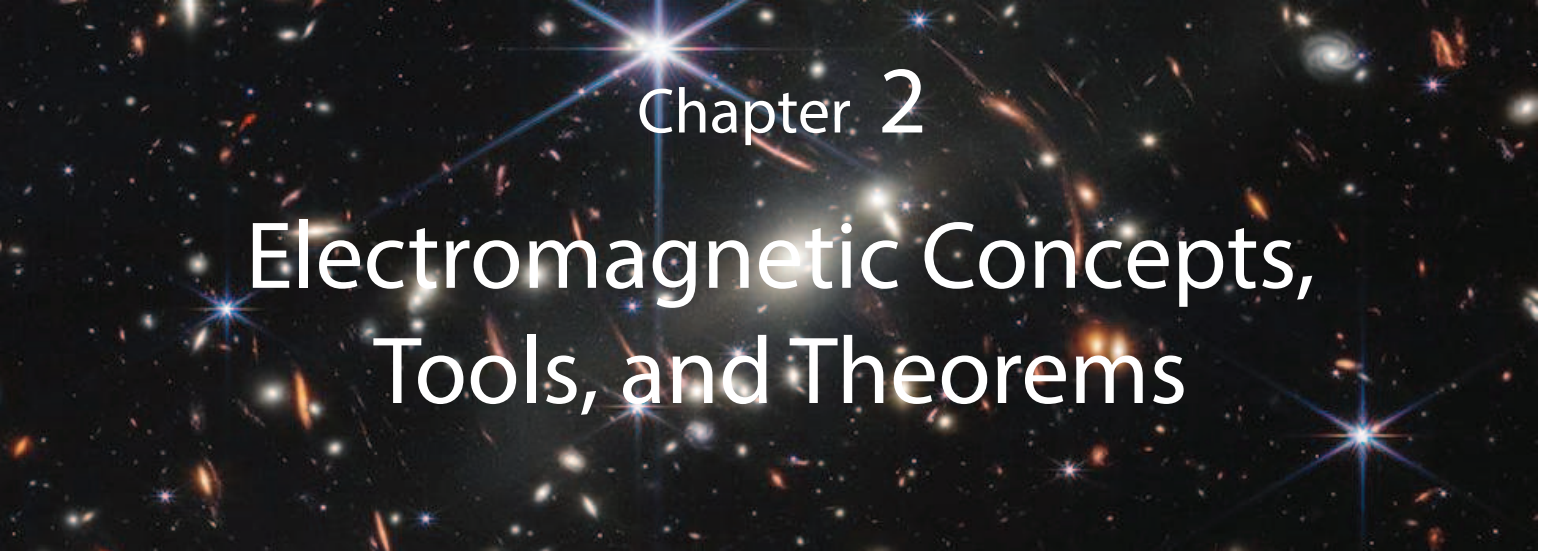

# Chapter 2
# Electromagnetic Concepts, Tools, and Theorems

## Chapter Contents


Overview, 63
2-1 Equivalent Magnetic Charge and Current Densities, 63
2-2 Image Theory, 68
2-3 Method of Images for Other Problems, 71
2-4 Polarization Current, 80
2-5 Stored Electromagnetic Energy, 83
2-6 Flow of Energy, 86
2-7 Superposition Principle, 90
2-8 Uniqueness Theorem, 90
2-9 Equivalence Principle for Electromagnetic Sources, 92
Chapter Summary, 97
Problems, 99


## Objectives

Upon learning the material presented in this chapter, you should be able to:

1. Understand the concept of "fictitious" magnetic charges and magnetic currents and how to incorporate them into Maxwell's equations.
2. Examine the duality relations between the electric and magnetic fields in a material medium.
3. Apply the concept of images to charge and current sources to simplify certain types of boundary value problems.
4. Learn about energy flow and the law of conservation of energy for electromagnetic waves, as well as the conditions that make the solution to Maxwell's equations unique.

## Overview

While undeniably elegant in their mathematical structure, Maxwell's equations and their associated constitutive relations do not lend themselves to straightforward solutions for the electric and magnetic field intensities present in a material medium. In this chapter we explore the use of certain concepts and theorems that will prove helpful in (a) developing intuition about the behavior of the electric and magnetic fields and (b) transforming a complex problem into a simpler version for which we have a readily available solution, or (c) to simply be able to exploit certain symmetries that exist among the field quantities. For example, we will introduce a new concept wherein "artificial" magnetic charges and currents are created to make Maxwell's equations totally symmetric, from which we derive a new duality principle for the electric and magnetic fields. The concept of electromagnetic energy flow and the Poynting theorem are also presented in this chapter to demonstrate how the law of conservation of energy is indeed applicable to electromagnetic fields. The conditions required to make the solution of Maxwell's equations in a homogeneous region of space unique are derived using the Poynting theorem. The concept of equivalent surface sources is presented to show that knowledge of the field quantities outside a source region cannot be used to uniquely identify the sources that produced those fields.

## 2-1 Equivalent Magnetic Charge and Current Densities

We are all familiar with the concept of electric charge density $\rho$ and electric current density $\mathbf{J}$. It is often convenient when solving a certain class of electromagnetic problems involving magnetic materials to introduce the concept of hypothetical or equivalent distributions of ***magnetic charge density*** $\rho_m$ and ***magnetic current density*** $\mathbf{J}_m$.

The foundation for introducing such hypothetical distributions can perhaps be found in the definition of the magnetization vector $\mathbf{M}$ for a magnetic material. From Eq. (1.49) and $\mathbf{B} = \mu\mathbf{H}$, the magnetization vector for a magnetic material with magnetic permeability $\mu$ is given by

$$\mathbf{M} = \frac{1}{\mu_0}\mathbf{B} - \mathbf{H} = \left(\frac{\mu}{\mu_0} - 1\right)\mathbf{H} = (\mu_r - 1)\mathbf{H} \,. \tag{2.1}$$

Here, $\mu$ is the magnetic permeability of the magnetic material. To derive expressions for the hypothetical magnetic charge density $\rho_m$ and magnetic current density $\mathbf{J}_m$, we create an equivalent nonmagnetic medium with permeability $\mu_0$ and then create artificial magnetic charges and currents in that medium so as to generate a magnetization vector equal to that of the real magnetic material. To that end, we employ Faraday's law in the magnetic medium:

$$\nabla \times \mathbf{E} = -\frac{\partial \mathbf{B}}{\partial t} = -\mu_0\mu_r \frac{\partial \mathbf{H}}{\partial t} \,. \tag{2.2}$$

Next, we employ a mathematical divide to break up the quantity on the right-hand side of Eq. (2.2) into two terms:

$$\begin{aligned}\nabla \times \mathbf{E} &= -\mu_0 \frac{\partial \mathbf{H}}{\partial t} - \mu_0(\mu_r - 1)\frac{\partial \mathbf{H}}{\partial t} \\ &= -\mu_0 \frac{\partial \mathbf{H}}{\partial t} - \mu_0 \frac{\partial \mathbf{M}}{\partial t}\,,\end{aligned} \tag{2.3}$$

where we used Eq. (2.1) to replace the second term with the time derivative of the magnetization vector. Equation (2.3) consists of two terms, one representing the relationship between $\mathbf{E}$ and $\mathbf{H}$ in a nonmagnetic medium (with permeability $\mu_0$), and a second term proportional to $\partial\mathbf{M}/\partial t$. This second term has the units of V/m$^2$, and therefore can be interpreted as an ***equivalent magnetic current distribution***:

$$\mathbf{J}_m = \mu_0(\mu_r - 1)\frac{\partial \mathbf{H}}{\partial t} = \mu_0 \frac{\partial \mathbf{M}}{\partial t}\,. \tag{2.4}$$

Using Eq. (2.4), Eq. (2.3) can be rewritten as

$$\nabla \times \mathbf{E} = -\mu_0 \frac{\partial \mathbf{H}}{\partial t} - \mathbf{J}_m\,. \tag{2.5}$$

Next, we use Gauss' law for magnetism

$$\nabla \cdot \mathbf{B} = 0\,. \tag{2.6}$$

Now consider $\mu_0$ as the permeability of an equivalent medium and then seek for a condition that allows the magnetic field $\mathbf{H}$ to remain unchanged throughout the region. Equation (2.6) can be written as

$$\nabla \cdot (\mu_0 \mathbf{H}) = -\mu_0(\mu_r - 1)\nabla \cdot \mathbf{H} = -\mu_0 \nabla \cdot \mathbf{M}\,. \tag{2.7}$$

The quantity $\rho_m = -\mu_0(\mu_r - 1)\nabla \cdot \mathbf{H} = -\mu_0 \nabla \cdot \mathbf{M}$, which has the units webers/m$^3$, can be interpreted as the ***equivalent magnetic charge density***. The preceding expression can be rewritten as

$$\nabla \cdot (\mathbf{H}) = \frac{\rho_m}{\mu_0}\,. \tag{2.8}$$

In conclusion, Maxwell's four equations can now be written in the alternative form

$$\nabla \times \mathbf{E} = -\mu_0 \frac{\partial \mathbf{H}}{\partial t} - \mathbf{J}_m\,, \tag{2.9a}$$

$$\nabla \times \mathbf{H} = \varepsilon \frac{\partial \mathbf{E}}{\partial t} + \mathbf{J}\,, \tag{2.9b}$$

$$\nabla \cdot \mathbf{H} = \frac{\rho_m}{\mu_0}\,, \tag{2.9c}$$

$$\nabla \cdot \mathbf{E} = \frac{\rho}{\varepsilon}\,. \tag{2.9d}$$

It should be emphasized that the notion of equivalent magnetic current density is only applicable to time-varying field quantities. That is, if $\partial \mathbf{H}/\partial t = 0$, then $\mathbf{J}_{\mathrm{m}} = 0$. We also note that in this treatment the magnetic polarization current $\mathbf{J}_{\mathrm{m}}$ and magnetic charge density $\rho_{\mathrm{m}}$ are themselves functions of the unknown magnetic field, but as will be shown later this formulation is useful for setting up an integral equation for the unknowns. Here the four parts of Eq. (2.9) are provided to demonstrate how hypothetical distributions of magnetic charge and current densities can be made part of Maxwell's equations. It should be noted that the choice of $\mu_0$ as the background permeability was arbitrary. In fact any permeability can be assumed as the background material simply by modifying $\mathbf{J}_{\mathrm{m}}$ and $\rho_{\mathrm{m}}$. For example, if we desire a background permeability $\tilde{\mu}_{\mathrm{r}}$ and try to maintain the same $\mathbf{H}$ as that of the original problem, the equivalent magnetic current and charge densities become

$$\mathbf{J}_{\mathrm{m}} = \mu_0(\mu_{\mathrm{r}} - \tilde{\mu}_{\mathrm{r}})\frac{\partial \mathbf{H}}{\partial t} \tag{2.10a}$$

and

$$\rho_{\mathrm{m}} = -\mu_0(\mu_{\mathrm{r}} - \tilde{\mu}_{\mathrm{r}})\nabla \cdot \mathbf{H}\,. \tag{2.10b}$$

Hence, in general Maxwell's equations may be written as

$$\nabla \times \mathbf{E} = -\mu \frac{\partial \mathbf{H}}{\partial t} - \mathbf{J}_{\mathrm{m}}\,, \tag{2.11a}$$

$$\nabla \times \mathbf{H} = \varepsilon \frac{\partial \mathbf{E}}{\partial t} + \mathbf{J}\,, \tag{2.11b}$$

$$\nabla \cdot \mathbf{E} = \frac{\rho}{\varepsilon}\,, \tag{2.11c}$$

$$\nabla \cdot \mathbf{H} = \frac{\rho_{\mathrm{m}}}{\mu}\,, \tag{2.11d}$$

where $\mu = \mu_0\tilde{\mu}_{\mathrm{r}}$.

### 2-1.1 Duality Relations

The set of equations given by Eq. (2.11a)–Eq. (2.11d) is now symmetric. In fact Eq. (2.11a) and Eq. (2.11b) are duals of one another—and the same is true of Eq. (2.11c) and Eq. (2.11d), in the sense that if we make the following substitutions:

$$\mathbf{E} \longrightarrow \mathbf{H}\,, \tag{2.12a}$$

$$\mathbf{H} \longrightarrow -\mathbf{E}\,, \tag{2.12b}$$

$$\mu \longrightarrow \varepsilon\,, \tag{2.12c}$$

$$\varepsilon \longrightarrow \mu\,, \tag{2.12d}$$

$$\mathbf{J} \longrightarrow \mathbf{J}_{\mathrm{m}}\,, \tag{2.12e}$$

$$\mathbf{J}_{\mathrm{m}} \longrightarrow -\mathbf{J}\,, \tag{2.12f}$$

$$\rho \longrightarrow \rho_{\mathrm{m}} \,, \tag{2.12g}$$

$$\rho_{\mathrm{m}} \longrightarrow -\rho \,, \tag{2.12h}$$

then Eq. (2.11a) becomes Eq. (2.11b) and Eq. (2.11b) becomes Eq. (2.11a). Also, Eq. (2.11c) becomes Eq. (2.11d) and vice versa. This correspondence is known as the ***duality principle***. The significance of the duality principle is that if for a medium with parameters $\mu_1, \varepsilon_1$, the solutions ($\mathbf{E}_1$ and $\mathbf{H}_1$) are known for an excitation $\mathbf{J}$, then the solution for excitation $\mathbf{J}_{\mathrm{m}} = \mathbf{J}$ for a medium whose permeability is $\mu_2 = \varepsilon_1$ and permittivity is $\varepsilon_2 = \mu_1$ can be obtained using the duality relations given by

$$\mathbf{E}_2 = -\mathbf{H}_1$$

and

$$\mathbf{H}_2 = \mathbf{E}_1 \,.$$

The duality relations given by Eq. (2.12) are not unique. In fact, for most practical situations these may not be appropriate. For example, the dual of free space with $\mu_0 = 4\pi \times 10^{-7}$ H/m and $\varepsilon_0 = 8.85 \times 10^{-12}$ F/m becomes a medium having a permittivity $\varepsilon = 4\pi \times 10^{-7}$ F/m and a permeability $\mu = 8.85 \times 10^{-12}$ H/m. It is certainly unlikely to encounter such a medium. A more practical set of ***normalized duality relations*** is given by

$$\mathbf{E} \longrightarrow \sqrt{\frac{\mu}{\varepsilon}}\,\mathbf{H} \,, \tag{2.13a}$$

$$\mathbf{H} \longrightarrow -\sqrt{\frac{\varepsilon}{\mu}}\,\mathbf{E} \,, \tag{2.13b}$$

$$\mathbf{J} \longrightarrow \sqrt{\frac{\varepsilon}{\mu}}\,\mathbf{J}_{\mathrm{m}} \,, \tag{2.13c}$$

$$\mathbf{J}_{\mathrm{m}} \longrightarrow -\sqrt{\frac{\mu}{\varepsilon}}\,\mathbf{J} \,, \tag{2.13d}$$

$$\rho \longrightarrow \sqrt{\frac{\varepsilon}{\mu}}\,\rho_{\mathrm{m}} \,, \tag{2.13e}$$

$$\rho_{\mathrm{m}} \longrightarrow -\sqrt{\frac{\mu}{\varepsilon}}\,\rho \,. \tag{2.13f}$$

Note that in this case the units are preserved (the unit of $\sqrt{\mu/\varepsilon}$ is ohms). Substituting the duality relations given by Eqs. (2.13a)–(2.13f) into Eq. (2.11a) leads to

$$\sqrt{\frac{\mu}{\varepsilon}}\,\nabla \times \mathbf{H} = -\mu\,\frac{\partial}{\partial t}\left(-\sqrt{\frac{\varepsilon}{\mu}}\,\mathbf{E}\right) + \sqrt{\frac{\mu}{\varepsilon}}\,\mathbf{J} \,,$$

or equivalently

$$\nabla \times \mathbf{H} = \varepsilon\,\frac{\partial \mathbf{E}}{\partial t} + \mathbf{J} \,,$$

which is Eq. (2.11b). Similarly, Eq. (2.11a) can be obtained from Eq. (2.11b) under the duality relation given by Eqs. (2.13a)–(2.13f), and Eq. (2.11c) can be obtained from Eq. (2.11d) and vice versa.

An important characteristic of the duality relations given by Eqs. (2.13a)–(2.13f) is that the medium parameters are not changed.

### 2-1.2 Modifications to Boundary Conditions

Introducing the concept of magnetic current and charge densities into Maxwell's equations necessitates modification of the boundary conditions derived earlier in Section 1.6. In the presence of a ***surface magnetic current density*** $\mathbf{J}_{sm}$ and a ***surface magnetic charge density*** $\rho_{sm}$, the tangential electric field and the normal component of the magnetic flux density across a surface boundary are no longer continuous. New boundary conditions can be obtained by following the procedure outlined in Section 1.6 or by applying the duality relations given by Eq. (2.12). Application of the duality approach to

$$\hat{\mathbf{n}} \times (\mathbf{H}_1 - \mathbf{H}_2) = \mathbf{J}_s$$

and

$$\hat{\mathbf{n}} \cdot (\mathbf{D}_1 - \mathbf{D}_2) = \rho_s$$

renders

$$\hat{\mathbf{n}} \times (\mathbf{E}_1 - \mathbf{E}_2) = -\mathbf{J}_{sm} \tag{2.15a}$$

and

$$\hat{\mathbf{n}} \cdot (\mathbf{B}_1 - \mathbf{B}_2) = \rho_{sm} \, . \tag{2.15b}$$

The duality relations can also be used to introduce the concept of magnetic conductors and perfect magnetic conductors. Starting from the point form of Ohm's law, namely $\mathbf{J} = \sigma\mathbf{E}$, and then applying the duality relations given by Eq. (2.12), we get

$$\mathbf{J}_m = \sigma_m \mathbf{H} \, , \tag{2.16}$$

where $\sigma_m$ represents the notion of magnetic conductivity. Furthermore, in the same way that we define a perfect electric conductor whose conductivity $\sigma = \infty$, the notion of a ***perfect magnetic conductor*** with $\sigma_m = \infty$ can be introduced as well. Inside a perfect magnetic conductor, $\mathbf{H} = \mathbf{B} = 0$, and therefore on the surface of a perfect magnetic conductor

$$\hat{\mathbf{n}} \times \mathbf{H} = 0 \, , \tag{2.17a}$$

$$\hat{\mathbf{n}} \times \mathbf{E} = -\mathbf{J}_{sm} \, , \qquad \textbf{(perfect magnetic conductor)} \tag{2.17b}$$

$$\hat{\mathbf{n}} \cdot \mathbf{B} = \rho_{sm} \, . \tag{2.17c}$$

These relations constitute the boundary conditions for a perfect magnetic conductor.

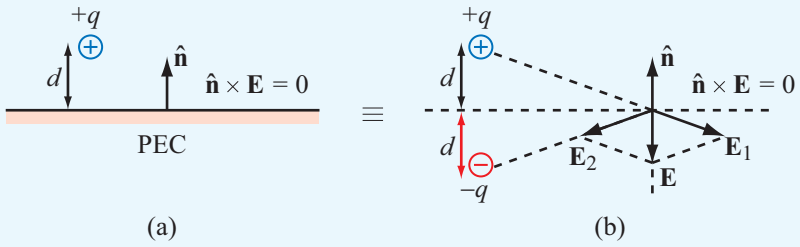


**Figure 2-1:** (a) A positive charge above a perfect electric conductor (PEC) with a planar interface and (b) its equivalent system of charges in the equivalent homogeneous medium.

## 2-2 Image Theory

In certain circumstances involving boundary value problems, it is more convenient to solve the problem in an equivalent homogeneous medium with appropriate modifications of sources and objects than to solve the problem in its actual medium. One simple example where this technique can be applied is a half-space medium composed of a perfect electric conductor with a planar interface and a homogeneous dielectric half-space above it, as shown in Fig. 2-1(a). First, let us consider a stationary positive point charge in the dielectric medium above the perfect conductor. Knowing that the tangential electric field at the interface must be zero (because $\hat{\mathbf{n}} \times \mathbf{E} = 0$), and using Coulomb's law, it can easily be shown that by placing a negative charge of the same magnitude as that of the point charge at the mirror-image point of the charge in the upper medium, as well as removing the conducting medium altogether, leads to an electric field distribution in the upper medium that indeed satisfies the condition $\hat{\mathbf{n}} \times \mathbf{E} = 0$ along the interface points. The equivalent configuration is shown in Fig. 2-1(b).

Since the electric field in the upper-half space, including across the boundary, is the same for both configurations, according to the uniqueness theorem (which will be introduced later), the two configurations are identical so far as the upper space is concerned.

### 2-2.1 Electric Current Filament Parallel to Interface (Fig. 2-2)

Next, let us consider the case of an electric current filament (a current confined in a very thin piece of wire) present in an upper-half space above a perfect conductor (Fig. 2-2(a)). The

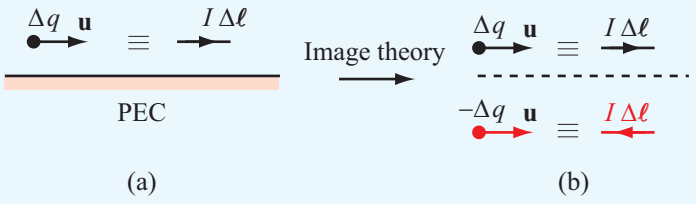


**Figure 2-2:** Image of an electric current over a perfect electric conductor (PEC).

current consists of a filament of length $\Delta\ell$ and intensity $I$. This current can be viewed as the motion of a point charge $\Delta q$ moving along the direction of $\Delta\boldsymbol{\ell}$ with velocity $\mathbf{u}$. Denoting the time that it takes $\Delta q$ to traverse the length of the wire by $\Delta t$, then $\mathbf{u} = \frac{\Delta\boldsymbol{\ell}}{\Delta t}$, and since $I = \Delta q/\Delta t$, it then follows that

$$I\,\Delta\boldsymbol{\ell} = \Delta q\,\mathbf{u}\ .$$

The image of the moving charge $\Delta q$ in a planar perfect conductor is $-\Delta q$ and it moves in the same direction. The image theory techniques allow us to remove the perfect conductor and to replace it with an image current $(-\Delta q\,\mathbf{u})$ flowing in a direction opposite to the direction of the original current (Fig. 2-2(b)). Hence, the image of an electric current over a perfect electric conductor and flowing in a direction parallel to the interface is the same current at the mirror image point flowing in a direction parallel to the interface but in the opposite direction. In general, the current filament can be oriented in any direction relative to the planar interface. Such a current can be divided into two orthogonal components, one parallel to the interface and the other perpendicular to the interface. Hence, we also have to consider the current filament oriented perpendicular to the interface.

### 2-2.2 Electric Current Filament Normal to Interface (Fig. 2-3)

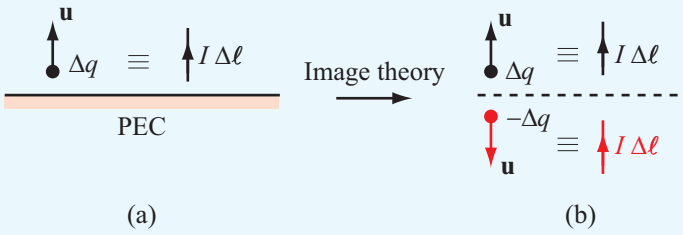


**Figure 2-3:** The image of a current filament normal to a PEC is the same current at the mirror image point along the same direction.

Application of image theory to the configuration shown in Fig. 2-3(a) leads to removal of the perfect conductor and replacing it with charge $-\Delta q$ at the image location of charge $\Delta q$, and as $\Delta q$ moves upwards, $-\Delta q$ has to move downward to maintain image location. Using the equivalent moving charge concept for current filament, it is now obvious that the image of a current flowing normal to the interface is the same current at the mirror image point flowing in the same direction as the original source.

### 2-2.3 Magnetic Current Filament Parallel to Interface (Figs. 2-4 and 2-5)

In many radiation and scattering problems, magnetic current sources are encountered and therefore it is also important to obtain the image of magnetic currents on planar metallic surfaces. In finding the image representation of magnetic currents the duality principle is used. In addition, we use the fact that the normal component of time-varying magnetic fields vanish on the surface of a perfect electric conductor. Applying the duality principle

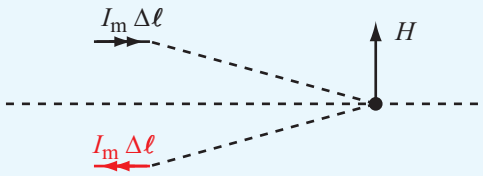


**Figure 2-4:** Magnetic duality applied to the electric charge configuration shown in Fig. 2-2.

(Fig. 2-4) to the problem of two parallel electric currents of equal magnitude and opposite direction, it becomes evident that two parallel magnetic current filaments flowing in opposite directions produce a vanishing tangential magnetic field and a normal electric field along a plane that bisects the medium between the two sources. Conversely, if the directions of the magnetic currents are the same, the normal component of the magnetic field and the tangential component of the electric field will vanish. The latter is the boundary condition for a perfect electric conductor (PEC). Hence, it can be concluded that the image of a magnetic current filament parallel to a planar PEC is a magnetic current filament that flows in the same direction as the original source and located at the mirror image point (Fig. 2-5).

**Figure 2-5:** Equivalent problems (image theory) for a horizontal magnetic current over a planar perfect electric conductor.

### 2-2.4 Magnetic Current Filament Normal to Interface (Fig. 2-6)

To find the image of a perpendicular magnetic current filament over a planar PEC, we can use a similar procedure based on the duality principle applied to two normal electric currents of equal magnitude along the same line and the related boundary conditions. Using the same argument as before, it can be shown that the image of a normal magnetic current filament is a normal magnetic current with the same magnitude at the mirror image point flowing in the opposite direction. The fields produced by this configuration of the magnetic filament currents satisfy the boundary conditions in the perpendicular bisector plane of the line connecting the source and its image.

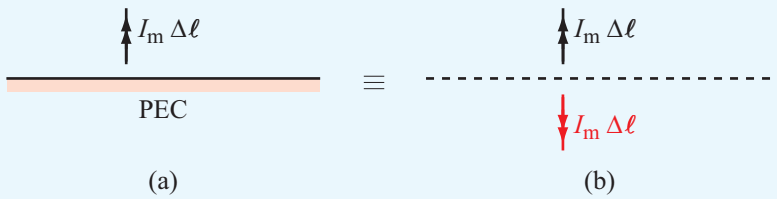


**Figure 2-6:** Equivalent problems (image theory) for a vertical magnetic current over a planar perfect electric conductor.

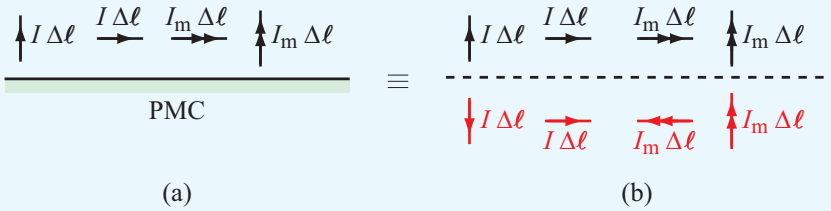


**Figure 2-7:** Image theory for elementary electric and magnetic currents over a planar perfect magnetic conductor (PMC).

### 2-2.5 Electric and Magnetic Current Filaments over a Planar Perfect Magnetic Conductor (Fig. 2-7)

The dual of the perfect electric conductor is the perfect magnetic conductor (PMC) for which $\hat{\mathbf{n}} \times \mathbf{H} = 0$. Also, for time-varying fields, the normal component of the electric fields on PMC is zero. To find the images of electric and magnetic currents over perfect magnetic conductors, the duality relations can be applied to the appropriate cases of currents over a perfect electric conductor. Figure 2-7 shows the images of electric and magnetic sources over a PMC. It should also be mentioned that objects in the upper-half space above a planar PEC or PMC are also mirror-imaged. The reason for this is that objects, whether being conductor or dielectric, can be viewed as surface or polarization current distributions and can be imaged using image theory. For example, the equivalent of the combination of a metallic object and a current source above a PEC, as shown in Fig. 2-8(a), consists of the source, the object, and their images, as shown in Fig. 2-8(b). The method described here is based on the electrostatic concept for charges. However, the results are equally valid for time-varying fields. This can be easily verified once we derive the fields radiated by short current filaments (Hertzian dipole).

## 2-3 Method of Images for Other Problems

In the previous section, image theory was developed for perfect electric and magnetic planar surfaces of infinite extent. The method of images can be developed for a few other objects in the electrostatic or quasi-static regime. For example, for a metallic sphere or a half-space

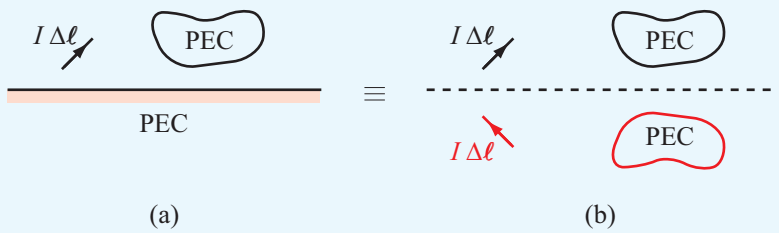


**Figure 2-8:** Equivalent problems for a current source and an object above a perfect electric conductor plane.

dielectric, the image of an external point charge can be obtained using electrostatic field analysis. That is, the value(s) and the location(s) of image charge(s) are sought for in order to establish an equivalence between the electrostatic field produced by the original boundary value problem and those produced by the original point charge and its image charge(s).

### Example 2-1: Reverse Application of Image Theory

Use image theory to show that the $x$-component of the electric field generated by a constant loop current centered at the origin of a Cartesian coordinate system and placed in the $y$-$z$ plane is zero. The geometry of the problem is shown in Fig. 2-9.

**Solution:** The electric current in the loop has circular symmetry. For every point on the loop the following relations exist between the current and its counterpart at the opposite point with respect to the $x$–$y$ plane:

$$I_z(\theta) = I_z\left(\theta + \frac{\pi}{2}\right)$$

and

$$I_y(\theta) = -I_y\left(\theta + \frac{\pi}{2}\right) .$$

This pair of currents defines the relation between a current filament above a perfect electric conductor and its image. Hence the equivalent for a loop of electric current is a half-loop over a PEC surface in the $x$–$y$ plane. Now if we rotate the $y$-$z$ plane about the $x$-axis to form a new Cartesian coordinate system $xy'z'$ (see Fig. 2-9), the same argument can be used to prove that the tangential electric field is zero on the $x$-$y'$ plane. From this argument it can be concluded that the electric field produced by the current loop is always perpendicular to the $x$-axis and has circular symmetry with respect to the $x$-axis.

## 2-3.1 Image of a Point Charge in a Grounded Metallic Sphere

Next, let us consider a metallic sphere of radius $a$ centered around the origin of a Cartesian coordinate system and a point charge $q$ located on the $z$-axis at $Z_0$ outside the metallic sphere,

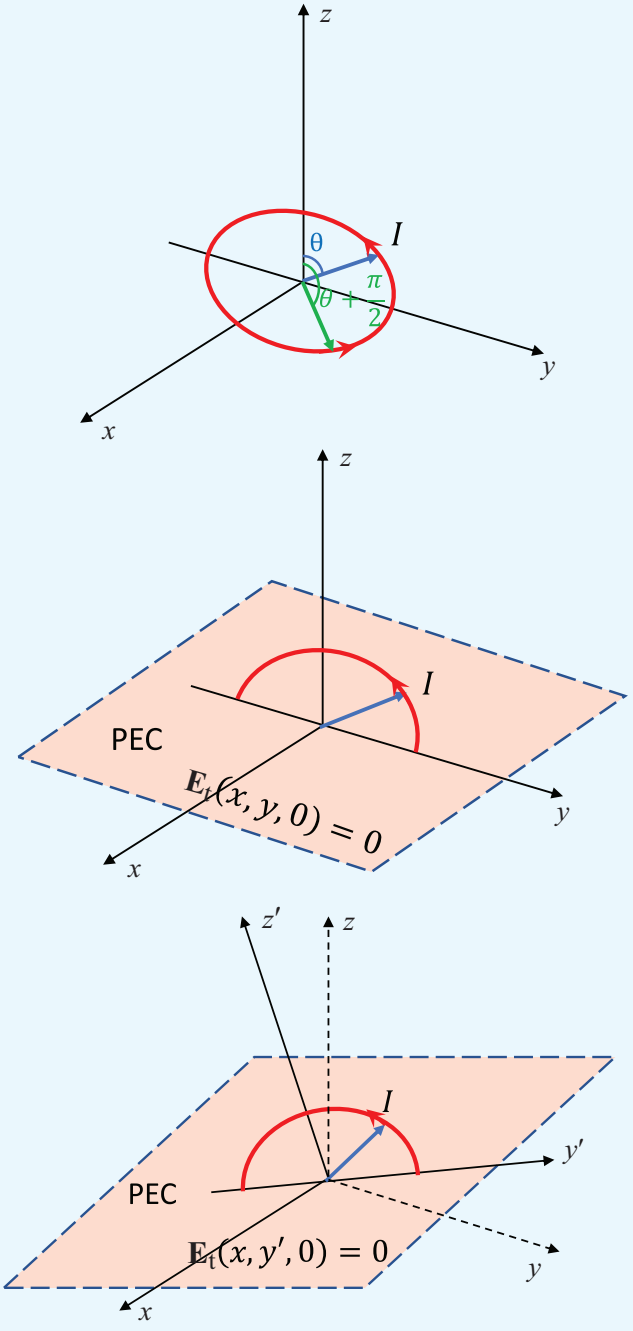


**Figure 2-9:** Reverse application of image theory is used for a wire loop carrying a constant current $I$ to show that the electric field generated from such a source is $\phi$-directed.

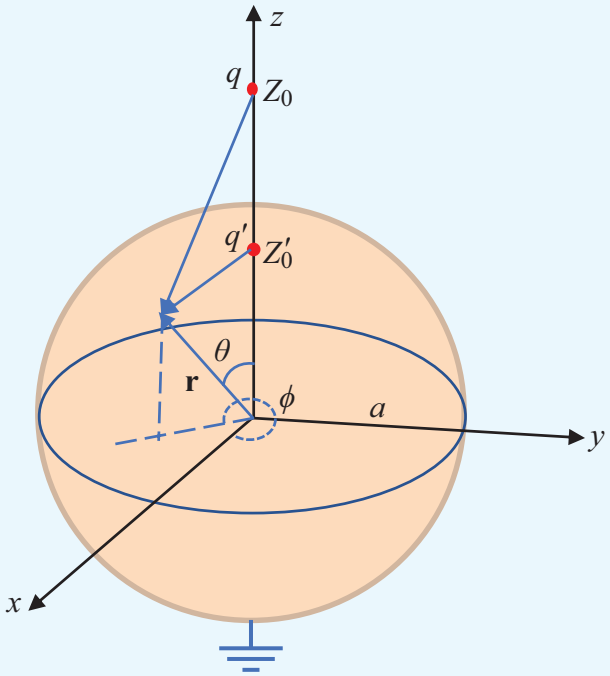


**Figure 2-10:** A point charge $q$ outside a grounded metallic sphere of radius $a$. Using image theory for a static electric field, the conducting sphere can be removed and an image charge $q' = -qa/Z_0$ can be substituted at $Z_0' = a^2/Z_0$.

as shown in Fig. 2-10. Let us first consider a situation where the metallic sphere is grounded (at zero potential). In this case, for a positive point charge, the sphere will be negatively charged and all the positive charges from the sphere are pushed into the ground terminal. Because of the $\phi$-symmetry of the problem, if one can find a point image charge, it should lie on the $z$-axis. Consider a point charge $q'$ on the $z$-axis at $Z_0'$ inside the metallic sphere, representing the image of $q$ inside the metallic sphere. That is, by placing $q'$ on the $z$-axis at $Z_0'$, we can remove the metallic sphere altogether, and therefore the fields produced by the combination of $q$ and $q'$ should be the same as the fields in the original problem insofar as the field at points outside the sphere are concerned. It is emphasized that the image method is applicable only if the sum of the fields from these two charges satisfy the boundary condition on the surface of the metallic sphere. Choosing an arbitrary point on the surface of the sphere at $\mathbf{r} = a(\sin\theta\cos\phi\,\hat{\mathbf{x}} + \sin\theta\sin\phi\,\hat{\mathbf{y}} + \cos\theta\,\hat{\mathbf{z}})$ and calculating the total electric potential there, we have

$$\Phi(\mathbf{r}) = \frac{q}{4\pi\varepsilon|\mathbf{r} - Z_0\,\hat{\mathbf{z}}|} + \frac{q'}{4\pi\varepsilon|\mathbf{r} - Z_0'\,\hat{\mathbf{z}}|}\,. \tag{2.18}$$

This potential can be rewritten as

$$\Phi(\mathbf{r}) = \frac{q/a}{4\pi\varepsilon|\hat{\mathbf{r}} - (Z_0/a)\hat{\mathbf{z}}|} + \frac{q'/Z_0'}{4\pi\varepsilon|(a/Z_0')\hat{\mathbf{r}} - \hat{\mathbf{z}}|} , \tag{2.19}$$

where $\hat{\mathbf{r}} = \mathbf{r}/a$. Inspection of this equation reveals that if

$$\frac{q}{a} = -\frac{q'}{Z_0'} \tag{2.20a}$$

and

$$\frac{Z_0}{a} = \frac{a}{Z_0'} = \alpha , \tag{2.20b}$$

and realizing that

$$|\hat{\mathbf{r}} - \alpha\hat{\mathbf{z}}| = |\alpha\hat{\mathbf{r}} - \hat{\mathbf{z}}| = (1 - 2\alpha\cos\theta + \alpha^2)^{1/2} ,$$

then it is obvious that the potential $\Phi(\mathbf{r}) = 0$ everywhere over the metallic sphere. Hence the location of the image is at

$$Z_0' = \frac{a^2}{Z_0} \tag{2.21a}$$

and the value of the image charge is

$$q' = -q\,\frac{a}{Z_0} . \tag{2.21b}$$

### 2-3.2 Image of a Point Charge in an Isolated Metallic Sphere

Now we consider the case of a point charge outside of an isolated metallic sphere (Fig. 2-11). In this case, placement of a point charge near the metallic sphere polarizes the sphere with a surface charge density of opposite polarity concentrated near the charge and a surface charge density of the same polarity concentrated on the other side of the sphere. For this problem, according to the law of conservation of charge, the net charge on the sphere should add up to zero. The boundary condition still mandates that the potential on the surface of the sphere be a constant. From the previous problem, we concluded that the charge and its image canceled each other's electric potentials on the sphere's surface. A point charge placed at the origin creates a constant potential on the sphere's surface and if placed anywhere else, the electric potential on the surface of the sphere will not be constant. On the other hand, the total charge of the image charges must add up to zero. Hence, the image of a point charge outside a metallic sphere is composed of two equal point charges of opposite polarity, one located at $Z_0' = a^2/Z_0$ with charge $q_1' = -qa/Z_0$ and the other located at the origin with charge $q_2' = qa/Z_0$. Hence, the polarized metallic sphere acts like a dipole with a dipole moment given by

$$p = q'Z_0' = q\,\frac{a^3}{Z_0^2} . \tag{2.22}$$

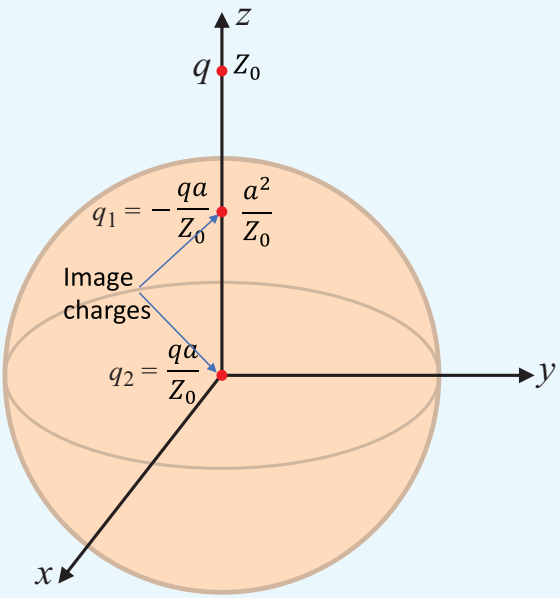


**Figure 2-11:** A point charge $q$ outside an isolated metallic sphere of radius $a$. Also shown are two point charges (image charges) $q_1$ and $q_2$, which can be used to replace the metallic sphere charges $q$, $q_1$, and $q_2$ and produce the same field outside the sphere as the field generated by the original configuration.

The overall electric field can be obtained from the superposition of the fields generated by the three point charges, and is valid only outside or over the surface of the metallic sphere. The surface charge density on the sphere, as dictated by boundary condition, can be calculated from the normal component of the electric flux and is only a function of $\theta$ due to the azimuthal symmetry of the problem. That is,

$$\rho_s(\theta) = \varepsilon\, E_r(a,\theta)\ . \tag{2.23}$$

Using Coulomb's law, the explicit expression for $\rho_s(\theta)$ is given by

$$\rho_s(\theta) = \frac{q}{4\pi a^2}\left[\frac{1-\alpha\cos\theta}{(1+\alpha^2-2\alpha\cos\theta)^3} - \left(\frac{a}{Z_0}\right)\left(\frac{a}{Z_0'}\right)^2 \frac{\alpha-\cos\theta}{(1+\alpha^2-2\alpha\cos\theta)^3} + \frac{1}{\alpha}\right]\ .$$

Further simplification leads to

$$\rho_s(\theta) = \frac{q}{4\pi a^2}\left[\frac{1-\alpha^2}{(1+\alpha^2-2\alpha\cos\theta)^3} + \frac{1}{\alpha}\right]\ . \tag{2.24}$$

Figure 2-12 shows a plot of the normalized surface charge density on an isolated metallic

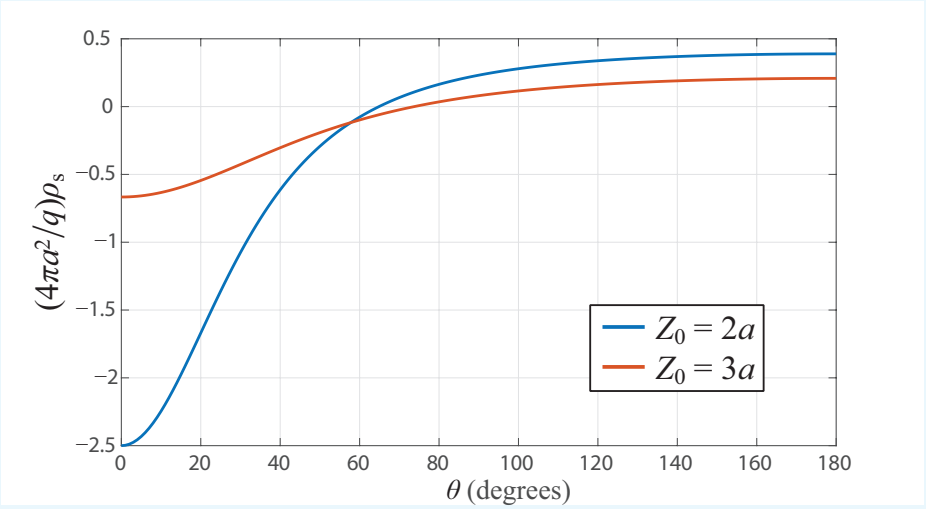


**Figure 2-12:** Normalized surface charge density $(4\pi a^2/q)\rho_s$ due to a point charge $q$ located at $Z_0 = 2a$ and a second plot for a charge at $Z_0 = 3a$.

sphere as a function of $\theta$ for a point charge located at $Z_0 = 2a$, and another plot for a charge located at $Z_0 = 3a$.

## Example 2-2: Force on a Charge outside a Metallic Sphere

Consider a positive point charge $q$ outside a metallic sphere centered around the origin and of radius $a$. Let's assume the charge is located on the $z$-axis at $z = Z_0$, as shown in Fig. 2-11. This charge is attracted towards the metallic sphere. What is the force on charge $q$?

**Solution:** The advantage of image theory is obvious in solving this problem. The equivalent problem is realized by replacing the metallic sphere with the image charges $-qa/Z_0$ and $qa/Z_0$ on the $z$-axis at $a^2/Z_0$ and the origin, respectively. The force on $q$ can easily be computed from the fields generated by the two image charges. Using Coulomb's law, the electric field at $z = Z_0$ is given by

$$\mathbf{E}(Z_0) = \frac{1}{4\pi\varepsilon}\left[\frac{\left(-\dfrac{qa}{Z_0}\right)}{\left(Z_0 - \dfrac{a^2}{Z_0}\right)^2} + \frac{\dfrac{qa}{Z_0}}{Z_0^2}\right]$$

$$= \frac{q}{4\pi\varepsilon}\,\frac{a^3(2Z_0^2 - a^2)}{Z_0^3(Z_0^2 - a^2)^2}\,(-\hat{\mathbf{z}})\,,$$

and therefore the attractive force is given by

$$\mathbf{F}(Z_0) = -\frac{q^2}{4\pi\varepsilon}\,\frac{a^3(2Z_0^2 - a^2)}{Z_0^3(Z_0^2 - a^2)^2}\,\hat{\mathbf{z}}\,.$$

### 2-3.3 Image of a Point Charge over a Half-Space Dielectric Medium with a Planar Interface

By inspection or by solving Poisson's equation directly, it can be shown that the image of a point charge $q$ in a medium with permittivity $\varepsilon_1$ above a half-space dielectric medium with permittivity $\varepsilon_2$ and a planar interface between the two media (Fig. 2-13) is a point charge $q'$ located at the mirror image point (below the interface and equal distance from the interface) having a charge equal to

$$q' = -q\,\frac{\varepsilon_2 - \varepsilon_1}{\varepsilon_2 + \varepsilon_1}\,. \tag{2.25a}$$

The equivalence is for a homogeneous medium having a permittivity equal to that of the upper half-space ($\varepsilon_1$)when the observation point is in the upper half-space. However, if the observation point is in the lower half-space, the image point is at the location of the source and the image charge is

$$q'' = q\frac{\varepsilon_2 - \varepsilon_1}{\varepsilon_2 + \varepsilon_1}\,. \tag{2.25b}$$

That is, the total charge is $q + q'' = 2\varepsilon_2/(\varepsilon_1 + \varepsilon_2)$ and located at the source location in a homogeneous medium with permittivity $\varepsilon_2$. It can easily be shown that both the electric potential and the normal component of the electric flux at any point on the interface right above and right below the interface are equal, as required by the boundary conditions between two dielectric media. This establishes the equivalence between the original problem and the corresponding image problem.

**Example 2-3: Force on a Charge above a Half-Space Dielectric**

For the point charge in a dielectric medium composed of two half-space media with a planar interface, as shown in Fig. 2-13(a), find the force on the charge. Is the force attractive or repulsive? Determine conditions under which the forces are attractive or repulsive.

To find the force on charge $q$ in the upper half-space with dielectric constant $\varepsilon_1$, image theory as shown in Fig. 2-13(b) is used. Assuming the charge is located at $z = Z_0$, the electric field generated by the image charge at $z = Z_0$ is given by

$$\mathbf{E}(Z_0) = -\frac{q(\varepsilon_2 - \varepsilon_1)}{4\pi\varepsilon_1(\varepsilon_2 + \varepsilon_1)}\,\frac{1}{4Z_0^2}\,\hat{\mathbf{z}}\,,$$

and hence the force is

$$\mathbf{F}(Z_0) = -\frac{q^2(\varepsilon_2 - \varepsilon_1)}{4\pi\varepsilon_1(\varepsilon_2 + \varepsilon_1)}\,\frac{1}{4Z_0^2}\,\hat{\mathbf{z}}\,.$$

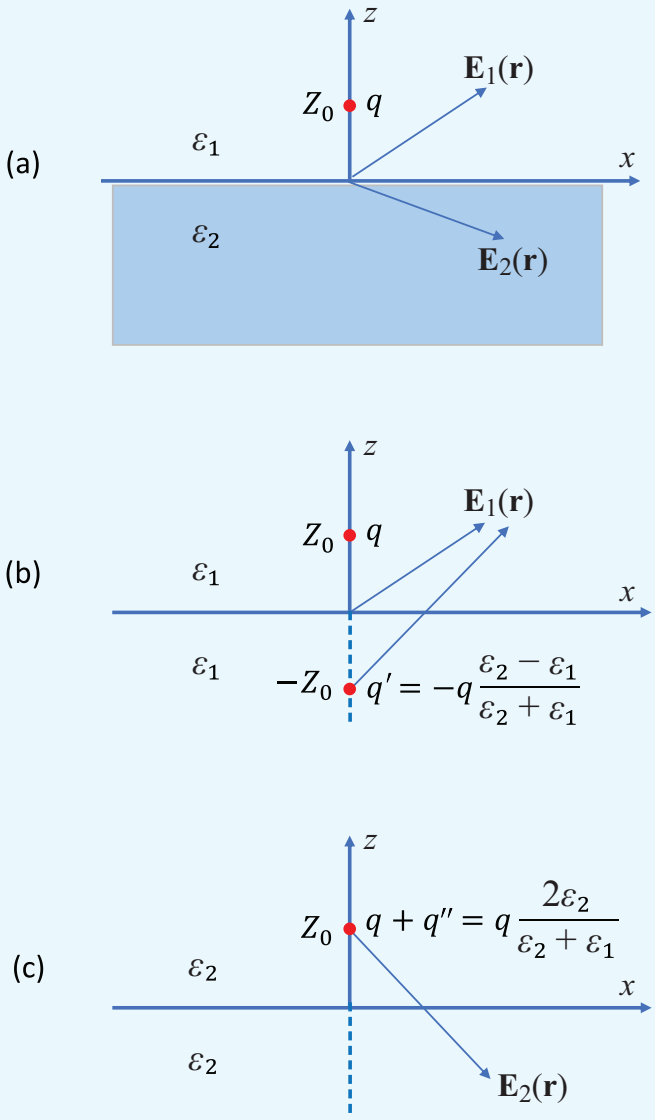


**Figure 2-13:** (a) A point charge in a dielectric medium comprising two half-space media with a planar interface. (b) The original charge and its image, placed in a homogeneous medium having the same permittivity of the upper half-space, produce the same field as the original configuration so far as the points in the upper half-space are concerned. (c) The original charge and its image, placed in a homogeneous medium having the same permittivity of the lower half-space, produce the same field as the original configuration so far as the points in the lower half-space are concerned.

The force is attractive if $\varepsilon_2 > \varepsilon_1$ and is repulsive if $\varepsilon_2 < \varepsilon_1$. It is also interesting to note that if $\varepsilon_2$ is negative then the force is repulsive if $|\varepsilon_2| < \varepsilon_1$ and attractive if $|\varepsilon_2| > \varepsilon_1$. An interesting condition is if $\varepsilon_2 = -\varepsilon_1$, which makes the force infinitely large. In the neighborhood of $\varepsilon_2 = -\varepsilon_1$, this large force can change direction from attractive to repulsive and vice versa.

## 2-4 Polarization Current

To introduce the concepts of hypothetical magnetic current and magnetic charge densities, it was demonstrated in Section 2-2 that the medium permeability can be replaced with a material having an arbitrary permeability, provided that a volumetric magnetic current density proportional to the time rate of change of the magnetic field is embedded throughout the material. The same approach can be applied to the electric field in a dielectric medium. Suppose we try to establish the same electric field $\mathbf{E}$ that exists in an equivalent hypothetical medium with permittivity $\varepsilon$ throughout a medium with a different permittivity $\varepsilon_0$. We start by considering the modified version of Ampère's law:

$$\nabla \times \mathbf{H} = \varepsilon \frac{\partial \mathbf{E}}{\partial t} + \mathbf{J} \,, \tag{2.26}$$

which can be rewritten as

$$\nabla \times \mathbf{H} = \varepsilon_0 \frac{\partial \mathbf{E}}{\partial t} + \varepsilon_0(\varepsilon_r - 1) \frac{\partial \mathbf{E}}{\partial t} + \mathbf{J} \,. \tag{2.27}$$

The middle term on the right-hand side of the preceding equation is equivalent to a ***polarization current*** $\mathbf{J}_p$:

$$\mathbf{J}_p = \varepsilon_0(\varepsilon_r - 1) \frac{\partial \mathbf{E}}{\partial t} = \frac{\partial \mathbf{P}}{\partial t} \,, \tag{2.28}$$

and an associated ***polarization vector***

$$\mathbf{P} = \varepsilon_0(\varepsilon_r - 1)\, \mathbf{E} \,. \tag{2.29}$$

Next we consider Gauss' law:

$$\nabla \cdot \mathbf{D} = \rho \,,$$

which can be rewritten as

$$\begin{aligned} \nabla \cdot \mathbf{E} &= \frac{\rho}{\varepsilon_0} - (\varepsilon_r - 1) \nabla \cdot \mathbf{E} \\ &= \frac{\rho}{\varepsilon_0} - \frac{1}{\varepsilon_0} \nabla \cdot \mathbf{P} \,, \end{aligned}$$

where use was made of Eq. (2.29). Given that the first term is $\rho/\varepsilon_0$, the second term is equivalent to a ***polarization charge density***

$$\rho_p = -\nabla \cdot \mathbf{P} = -\varepsilon_0(\varepsilon_r - 1) \nabla \cdot \mathbf{E} \,. \tag{2.30}$$

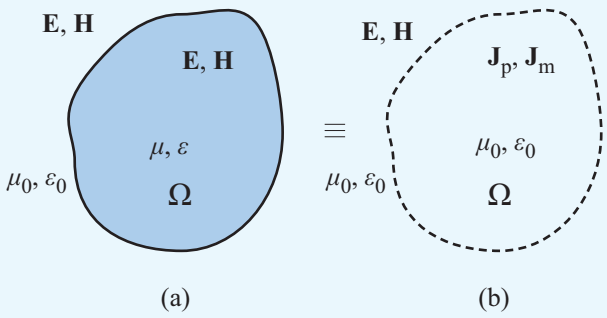


**Figure 2-14:** (a) A background medium with permittivity and permeability $\varepsilon_0$ and $\mu_0$ and an object specified by domain $\Omega$ having permittivity $\varepsilon$ and permeability $\mu$. Certain sources outside or inside the object establish electric and magnetic fields $\mathbf{E}(\mathbf{r})$ and $\mathbf{H}(\mathbf{r})$ throughout the space. (b) An equivalent problem where the object is replaced with electric and magnetic polarization currents within the $\Omega$ domain in a homogeneous medium with permittivity $\varepsilon_0$ and permeability $\mu_0$.

In general, a material with permeability $\mu$ and permittivity $\varepsilon$ can be replaced with vacuum (having permittivity $\varepsilon_0$ and permeability $\mu_0$), and containing magnetic and electric polarization current densities given by

$$\mathbf{J}_{\mathrm{p}} = \varepsilon_0(\varepsilon_{\mathrm{r}} - 1)\,\frac{\partial \mathbf{E}}{\partial t} \tag{2.31a}$$

and

$$\mathbf{J}_{\mathrm{m}} = \mu_0(\mu_{\mathrm{r}} - 1)\,\frac{\partial \mathbf{H}}{\partial t}\,. \tag{2.31b}$$

These polarization currents are distributed throughout the space where the material existed. This equivalence is shown in Fig. 2-14, where an object with permittivity $\varepsilon$ and permeability $\mu$ enclosed within a background medium with permittivity $\varepsilon_0$ and permeability $\mu_0$ is replaced with a homogeneous medium with permittivity $\varepsilon_0$ and permeability $\mu_0$, and containing distributions of electric and magnetic polarization currents across the region where the object existed. It should be noted that a-priori knowledge of the electric and magnetic fields throughout the object is needed to set up the equivalent currents. The original sources that established the fields originally and the polarization currents in the homogeneous background medium will produce the same electric and magnetic fields everywhere as those of the original problem.

It should be noted that the polarization currents and charge densities satisfy the continuity relations, which is a result of the law of conservation of charge. That is,

$$\begin{aligned}\nabla \cdot \mathbf{J}_{\mathrm{p}} &= \varepsilon_0(\varepsilon_{\mathrm{r}} - 1)\,\frac{\partial}{\partial t}\nabla \cdot \mathbf{E} \\ &= -\frac{\partial}{\partial t}\left[-\varepsilon_0(\varepsilon_{\mathrm{r}} - 1)\nabla \cdot \mathbf{E}\right] = -\frac{\partial}{\partial t}\rho_{\mathrm{p}}\,.\end{aligned}$$

Using duality, it can also be shown that

$$\nabla \cdot \mathbf{J}_{\mathrm{m}} = -\frac{\partial}{\partial t}\rho_{\mathrm{m}} \, . \tag{2.32}$$

### 2-4.1 The Relationship between the Electric and Magnetic Polarization Currents

An important point to consider is that the electric and magnetic polarization currents are not independent of each other. Let us denote the domain in which the material exists by $\Omega$ and define a step position function $\Psi(r)$ as

$$\Psi(\mathbf{r}) = \begin{cases} 1 & \mathbf{r} \in \Omega \, , \\ 0 & \mathbf{r} \notin \Omega \, . \end{cases} \tag{2.33}$$

With this definition, $\mathbf{J}_{\mathrm{p}}(\mathbf{r})$ and $\mathbf{J}_{\mathrm{m}}(\mathbf{r})$ can be defined in the entire domain using

$$\mathbf{J}_{\mathrm{p}}(\mathbf{r}) = \varepsilon_0(\varepsilon_{\mathrm{r}} - 1)\, \Psi(\mathbf{r})\, \frac{\partial \mathbf{E}}{\partial t} \tag{2.34a}$$

and

$$\mathbf{J}_{\mathrm{m}}(\mathbf{r}) = \mu_0(\mu_{\mathrm{r}} - 1)\, \Psi(\mathbf{r})\, \frac{\partial \mathbf{H}}{\partial t} \, . \tag{2.34b}$$

Taking $\nabla\times$ of both sides of Eq. (2.34a) yields

$$\nabla \times \mathbf{J}_{\mathrm{p}} = \varepsilon_0(\varepsilon_{\mathrm{r}} - 1)\left(\nabla\Psi \times \frac{\partial \mathbf{E}}{\partial t} + \Psi(\mathbf{r})\, \frac{\partial}{\partial t}\nabla \times \mathbf{E}\right) \, . \tag{2.35}$$

But for $\mathbf{r}$ in $\Omega$

$$\Psi(\mathbf{r})\, \nabla \times \mathbf{E} = -\mu_0\, \Psi(\mathbf{r})\, \frac{\partial \mathbf{H}}{\partial t} - \mathbf{J}_{\mathrm{m}} = -\frac{\mu}{\mu - \mu_0}\, \mathbf{J}_{\mathrm{m}}(\mathbf{r}) \, .$$

Also,

$$\nabla\Psi = -\hat{\mathbf{n}}\, \delta(|\mathbf{r} - \mathbf{r}'|) \, ,$$

where $\mathbf{r}'$ is a position vector on the surface of $\Omega$ and $\hat{\mathbf{n}}$ is an outward unit normal to the surface of $\Omega$. Hence the first term in Eq. (2.35) can be interpreted as a surface current density given by

$$\mathbf{J}_{\mathrm{s}} = -\hat{\mathbf{n}} \times \mathbf{J}_{\mathrm{p}}\, \delta(|\mathbf{r} - \mathbf{r}'|)$$

The relationship between $\mathbf{J}_{\mathrm{m}}$ and $\mathbf{J}_{\mathrm{p}}$ is now given by

$$\frac{1}{\varepsilon_0(\varepsilon_{\mathrm{r}} - 1)}\left[\nabla \times \mathbf{J}_{\mathrm{p}} + \hat{\mathbf{n}} \times \mathbf{J}_{\mathrm{p}}\, \delta(|\mathbf{r} - \mathbf{r}'|)\right] = -\frac{\mu}{\mu - \mu_0}\, \frac{\partial}{\partial t}\, \mathbf{J}_{\mathrm{m}}(\mathbf{r}) \, . \tag{2.36}$$

Using the duality relations, the relationship between $\mathbf{J}_\mathrm{p}$ and $\mathbf{J}_\mathrm{m}$ is given by

$$\frac{1}{\mu_0(\mu_\mathrm{r}-1)}\left[\nabla\times\mathbf{J}_\mathrm{m}+\hat{\mathbf{n}}\times\mathbf{J}_\mathrm{m}\,\delta(|\mathbf{r}-\mathbf{r}'|)\right]=\frac{\varepsilon}{\varepsilon-\varepsilon_0}\frac{\partial}{\partial t}\mathbf{J}_\mathrm{p}(\mathbf{r})\,. \tag{2.37}$$

Equations (2.36) and (2.37) establish the relationship between the magnetic and electric polarization currents.

## 2-5 Stored Electromagnetic Energy

In the static or quasi-static regime, such that the time derivative of the field quantities can be set to zero, the coupled Maxwell's equations become decoupled. Thus, Faraday's law and Ampère's law reduce to

$$\nabla\times\mathbf{E}=0 \tag{2.38a}$$

and

$$\nabla\times\mathbf{H}=\mathbf{J}\,. \tag{2.38b}$$

Since $\nabla\times\mathbf{E}=0$ and $\nabla\times\nabla\Phi=0$ for any scalar function $\Phi$, the electric scalar potential $\Phi(\mathbf{r})$ is defined such that

$$\mathbf{E}(\mathbf{r})=-\nabla\,\Phi(\mathbf{r})\,. \tag{2.39}$$

The choice of negative sign is a convention that ensures the electric field direction points toward regions of low potential from regions of high potential. Inserting Eq. (2.39) into Gauss' law (Eq. (1.1c)) yields the Poisson equation for the scalar electric potential:

$$\nabla^2\,\Phi(\mathbf{r})=-\frac{\rho(\mathbf{r})}{\varepsilon}\,. \tag{2.40}$$

The solution of the Poisson equation, subject to the appropriate boundary conditions, provides the scalar potential function in the desired domain, and then using Eq. (2.39) the electric field can be derived for any specified volumetric charge distribution. The simplest problem to consider is a point charge $q_0$ located at the origin of a coordinate system in a homogeneous, unbounded medium with permittivity $\varepsilon$. This problem was solved in the preceding chapter using Gauss' law, from which the electric field of a point charge was found to be

$$\mathbf{E}(\mathbf{r})=\frac{q_0}{4\pi\varepsilon r^2}\,\hat{\mathbf{r}}\,.$$

Since the electric field has no dependence on the other spherical coordinate parameters ($\theta$ and $\phi$), it is reasonable to expect the potential function $\Phi(\mathbf{r})$ to also be independent of $\theta$ and $\phi$. Using Eq. (2.39), it can be shown that

$$\frac{\partial\Phi}{\partial r}=-E_\mathrm{r}(r)\,,$$

from which we can find the potential of the point charge to be

$$\Phi(r) = \frac{q_0}{4\pi\varepsilon r} + \Phi_0 \,. \tag{2.41}$$

Here, $\Phi_0$ is a constant resulting from the integration. This constant can be determined to be zero ($\Phi_0 = 0$) by specifying the potential to be zero at $r = \infty$. For a volumetric charge distribution, Eq. (2.41) can be generalized to

$$\Phi(\mathbf{r}) = \frac{1}{4\pi\varepsilon} \iiint_V \frac{\rho(\mathbf{r}')}{|\mathbf{r}-\mathbf{r}'|}\, dv' \,.$$

The amount of work required to bring another charge $q$ from $r = \infty$ to location $r$ can be calculated from

$$W = -\int_\infty^r q\mathbf{E}\cdot d\ell = \int_\infty^r q\nabla\Phi\cdot d\ell \,.$$

This is the ***potential energy*** stored in the system composed of two charges. Noting that $\nabla\Phi\cdot d\boldsymbol{\ell} = \partial\Phi$, it can easily be shown that

$$W = q\,\Phi(\mathbf{r}) \,. \tag{2.42}$$

Next, consider $N$ point charges, all in the same medium, at locations $\mathbf{r}_n$. The total electric potential associated with all these charges at location $\mathbf{r}_{N+1}$ ($\mathbf{r}_{N+1} \neq \mathbf{r}_n$, $\forall n \in \{1,2,\ldots N\}$) can be obtained using the superposition principle:

$$\Phi(\mathbf{r}_{N+1}) = \frac{1}{4\pi\varepsilon} \sum_{n=1}^{N} \frac{q_n}{|\mathbf{r}_{N+1}-\mathbf{r}_n|} \,.$$

Moreover, the potential energy required to bring an additional point charge $q_{N+1}$ from infinity to location $\mathbf{r}_{N+1}$ is given by

$$W_{N+1} = \frac{q_{N+1}}{4\pi\varepsilon} \sum_{n=1}^{N} \frac{q_n}{|\mathbf{r}_{N+1}-\mathbf{r}_n|} \,.$$

Now the total potential energy can simply be calculated from

$$W = \sum_{k=1}^{N} W_{k+1} = \frac{1}{4\pi\varepsilon} \sum_{k=1}^{N}\sum_{n=1}^{k} \frac{q_n q_{k+1}}{|\mathbf{r}_{k+1}-\mathbf{r}_n|} \tag{2.43}$$

It is interesting to note that for the summand in Eq. (2.43), the indices are interchangeable without affecting the result (symmetric), which allows us to rewrite Eq. (2.43) as

$$W = \frac{1}{2}\left(\frac{1}{4\pi\varepsilon}\sum_{k=1}^{N}\sum_{\substack{n=1\\ n\neq k}}^{N}\frac{q_n q_{k+1}}{|\mathbf{r}_{k+1}-\mathbf{r}_n|}\right) . \tag{2.44}$$

This representation for the potential can be easily extended to a continuous charge distribution $\rho(\mathbf{r})$ and can be written as

$$W = \frac{1}{2}\iiint\limits_{\upsilon}\iiint\limits_{\upsilon'}\frac{\rho(\mathbf{r})\,\rho(\mathbf{r}')}{4\pi\varepsilon|\mathbf{r}-\mathbf{r}'|}\,d\upsilon'\,d\upsilon .$$

One of the integrals is recognized as the potential function; that is,

$$W = \frac{1}{2}\iiint\limits_{\upsilon}\rho(\mathbf{r})\,\Phi(\mathbf{r})\,d\upsilon . \tag{2.45}$$

Substituting for $\rho$ from the Poisson equation given by (2.40),

$$W = \frac{-\varepsilon}{2}\iiint\limits_{\upsilon}\Phi(\mathbf{r})\,\nabla^2\Phi(\mathbf{r})\,d\upsilon .$$

This can be further modified by using the identity

$$\nabla\cdot(\Phi\nabla\Phi) = \nabla\Phi\cdot\nabla\Phi + \Phi\nabla^2\Phi ,$$

which leads to

$$W = \frac{\varepsilon}{2}\iiint\limits_{\upsilon}|\nabla\Phi(\mathbf{r})|^2\,d\upsilon = \iiint\limits_{\upsilon}\frac{1}{2}\,\varepsilon|\mathbf{E}(\mathbf{r})|^2\,d\upsilon . \tag{2.46}$$

In the derivation of Eq. (2.46), we used the divergence theorem and the fact that the potential at infinity is zero:

$$\iiint\limits_{\upsilon}\nabla\cdot(\Phi\nabla\Phi)\,d\upsilon = \oiint\limits_{S_\infty}\Phi\nabla\Phi\cdot d\mathbf{S} = 0 .$$

Examination of Eq. (2.46) reveals that the quantity

$$w_e(\mathbf{r}) = \frac{1}{2}\,\varepsilon|\mathbf{E}(\mathbf{r})|^2 \tag{2.47}$$

can be interpreted as the ***electric energy density*** (stored electric energy per unit volume). In cases where the medium is anisotropic, it should be recognized that $w_e = \frac{1}{2}\,\varepsilon\mathbf{E}(\mathbf{r})\cdot\mathbf{E}(\mathbf{r}) =$

$\frac{1}{2}\,\mathbf{D}(\mathbf{r})\cdot\mathbf{E}(\mathbf{r})$. Hence the electric energy density in its most general form is given by

$$w_{\mathrm{e}}(\mathbf{r}) = \frac{1}{2}\,\mathbf{E}\cdot\mathbf{D}\,. \tag{2.48}$$

A similar procedure can be followed to derive a relationship for the magnetic energy density by defining the magnetic scalar potential as the dual of the electric scalar potential. Applying duality to Eq. (2.48) leads directly to

$$w_{\mathrm{m}}(\mathbf{r}) = \frac{1}{2}\,\mathbf{H}\cdot\mathbf{B}\,. \tag{2.49}$$

## 2-6 Flow of Energy

It is well established that electromagnetic waves carry power. Of the power radiated by the sun, only a very small fraction reaches planet Earth, and consists of a wide spectrum of electromagnetic waves. To understand how this power is carried by EM waves, in this section we apply Maxwell's equations to derive expressions for power density, power loss, and stored energy. Let us consider a simple region $V$ enclosed by a closed surface $S$, as shown in Fig. 2-15.

The medium inside $S$ is considered to be a homogeneous medium with constitutive parameters $\mu$, $\varepsilon$, and $\sigma$. Enclosed inside $S$ are electric and magnetic current distributions

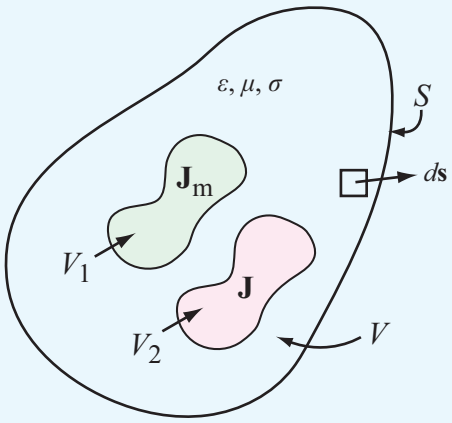


**Figure 2-15:** An enclosed homogeneous region containing volumetric electric and magnetic current distributions $\mathbf{J}$ and $\mathbf{J}_{\mathrm{m}}$, respectively.

$\mathbf{J}(\mathbf{r})$ and $\mathbf{J}_{\mathrm{m}}(\mathbf{r})$. According to Maxwell's equations

$$\nabla \times \mathbf{E} = -\frac{\partial \mathbf{B}}{\partial t} - \mathbf{J}_{\mathrm{m}} \tag{2.50}$$

and

$$\nabla \times \mathbf{H} = \frac{\partial \mathbf{D}}{\partial t} + \sigma \mathbf{E} + \mathbf{J} \,. \tag{2.51}$$

Here $\mathbf{J}$ and $\mathbf{J}_{\mathrm{m}}$ are the impressed electric and magnetic currents (source functions). Application of the inner product on both sides of Eq. (2.50) by $\mathbf{H}$ and on both sides of Eq. (2.51) by $\mathbf{E}$, followed by subtracting the results leads to

$$\mathbf{E} \cdot \nabla \times \mathbf{H} - \mathbf{H} \cdot \nabla \times \mathbf{E} = \mathbf{E} \cdot \frac{\partial \mathbf{D}}{\partial t} + \sigma \mathbf{E} \cdot \mathbf{E} + \mathbf{J} \cdot \mathbf{E} + \mathbf{H} \cdot \frac{\partial \mathbf{B}}{\partial t} + \mathbf{J}_{\mathrm{m}} \cdot \mathbf{H} \,. \tag{2.52}$$

Noting that

$$\nabla \cdot (\mathbf{E} \times \mathbf{H}) = \mathbf{H} \cdot \nabla \times \mathbf{E} - \mathbf{E} \cdot \nabla \times \mathbf{H} \,,$$

$$\mathbf{E} \cdot \frac{\partial \mathbf{D}}{\partial t} = \frac{1}{2} \frac{\partial}{\partial t} (\mathbf{E} \cdot \mathbf{D}) \,,$$

and

$$\mathbf{H} \cdot \frac{\partial \mathbf{B}}{\partial t} = \frac{1}{2} \frac{\partial}{\partial t} (\mathbf{H} \cdot \mathbf{B}) \,,$$

Eq. (2.52) can be rearranged to form

$$\nabla \cdot (\mathbf{E} \times \mathbf{H}) + \frac{1}{2} \frac{\partial}{\partial t} (\mathbf{E} \cdot \mathbf{D} + \mathbf{H} \cdot \mathbf{B}) + \sigma |\mathbf{E}|^2 = -\mathbf{J} \cdot \mathbf{E} - \mathbf{J}_{\mathrm{m}} \cdot \mathbf{H} \,. \tag{2.53}$$

By applying the volume integral to both sides of Eq. (2.53) and then applying the divergence theorem to the first term of the integrand, it can be shown that

$$\begin{aligned} \oiint_S \mathbf{E} \times \mathbf{H} \cdot d\mathbf{s} + \frac{\partial}{\partial t} \iiint_V \left( \frac{\mathbf{E} \cdot \mathbf{D}}{2} + \frac{\mathbf{H} \cdot \mathbf{B}}{2} \right) d\upsilon + \iiint_V \sigma |\mathbf{E}|^2 \, d\upsilon \\ = - \iiint_{V_1} \mathbf{J} \cdot \mathbf{E} \, d\upsilon - \iiint_{V_2} \mathbf{J}_{\mathrm{m}} \cdot \mathbf{H} \, d\upsilon \,. \end{aligned} \tag{2.54}$$

Recalling that the units of $\mathbf{J}$ and $\mathbf{J}_{\mathrm{m}}$ are A/m$^2$ and V/m$^2$, respectively, and the units of $\mathbf{E}$ and $\mathbf{H}$ are V/m and A/m, the unit of the integrals is watts. The right-hand side of Eq. (2.54) is the total power delivered by sources $\mathbf{J}$ and $\mathbf{J}_{\mathrm{m}}$ to the system. The unit of $\sigma |\mathbf{E}|^2$ is W/m$^3$, which represents the instantaneous ***power loss*** in the system. Hence

$$P_{\mathrm{L}} = \iiint_V \sigma |\mathbf{E}|^2 \, d\upsilon \qquad \textbf{(power loss)} \tag{2.55}$$

is the total ***ohmic loss*** in the system due to the medium's finite conductivity $\sigma$. As shown in the previous section, in electrostatic and magnetostatic regimes, the stored electric and magnetic energies per unit volume can be computed from

$$w_e = \frac{1}{2}\mathbf{E}\cdot\mathbf{D} = \frac{1}{2}\varepsilon|\mathbf{E}|^2 \qquad \textbf{(electric energy density)}$$

and

$$w_m = \frac{1}{2}\mathbf{H}\cdot\mathbf{B} = \frac{1}{2}\mu|\mathbf{H}|^2\,. \qquad \textbf{(magnetic energy density)}$$

Hence

$$P_s = \frac{\partial}{\partial t}\iiint_V \left(\frac{\mathbf{E}\cdot\mathbf{D}}{2} + \frac{\mathbf{H}\cdot\mathbf{B}}{2}\right) d\upsilon \qquad \textbf{(stored power)}$$

can be interpreted as the instantaneous time rate of change of ***stored electric and magnetic energies***. The unit of quantity

$$\mathbf{S}(t) = \mathbf{E}\times\mathbf{H} \tag{2.56}$$

is W/m$^2$. Considering that $d\mathbf{s}$ is an outward normal to surface $S$, the first term on the left-hand side of Eq. (2.54) can be interpreted as the net flow of power leaving the system through the closed surface $S$. The vector quantity $\mathbf{S}(t)$ is known as the ***time-dependent Poynting vector***, which may be interpreted as power flow density. Equation (2.54) states the law of conservation of power for electromagnetic waves. It asserts that the power generated by the sources is consumed by ohmic loss, radiated out, and/or getting used to store energy in the medium.

In antenna and scattering problems the integral

$$P_{rad} = \oiint \mathbf{E}\times\mathbf{H}\cdot d\mathbf{s} \tag{2.57}$$

is used to calculate the power radiated by a system of sources.

## Example 2-4: Flow of Energy in a Transmission Line

As shown in Fig. 2-16, in a coaxial line with an inner radius of $a$ and an outer radius of $b$, and filled with a material with permittivity $\varepsilon$ and permeability $\mu$, the electric and magnetic fields are given by

$$\mathbf{E}(\rho,\phi,z,t) = \frac{V_0}{\rho\ln(b/a)}\cos(\omega t - kz)\,\hat{\boldsymbol{\rho}}$$

and

$$\mathbf{H}(\rho,\phi,z,t) = \frac{V_0}{2\pi\eta_0\rho}\cos(\omega t - kz)\,\hat{\boldsymbol{\phi}}\,,$$

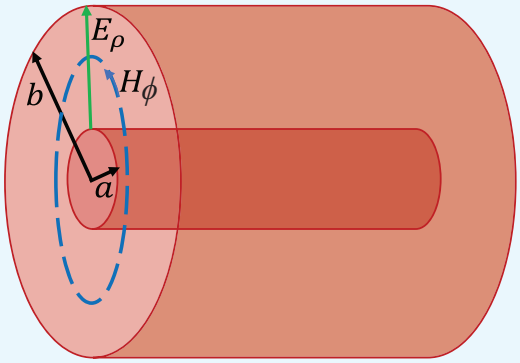


**Figure 2-16:** A coaxial transmission line supporting a traveling electromagnetic wave.

where $\eta_0$ is the ***characteristic impedance*** of the line given by

$$\eta_0 = \frac{1}{2\pi}\sqrt{\frac{\mu}{\varepsilon}}\,\ln\left(\frac{b}{a}\right), \qquad \textbf{(coaxial line)}$$

and $V_0$ is the amplitude of the voltage difference between the inner and outer conductors. Find the time-average power carried by the coaxial line.

**Solution:** To find the time-average power crossing a surface along the coaxial line, say at $z = z_0$, we need to find the power density $\mathbf{S}(\mathbf{r},t)$ at $z_0$:

$$\begin{aligned}\mathbf{S}(\mathbf{r},t) &= \mathbf{E}(\rho,\phi,z_0,t)\times\mathbf{H}(\rho,\phi,z_0,t)\\ &= \frac{V_0^2}{2\pi\ln(b/a)\,\eta_0}\,\frac{\cos^2(\omega t - kz_0)}{\rho^2}\,\hat{\mathbf{z}}\,.\end{aligned}$$

The total power crossing the coaxial line's cross section at $z = z_0$ is given by

$$\begin{aligned}P(t) &= \int_a^b\int_0^{2\pi}\frac{V_0^2}{2\pi\ln(b/a)\,\eta_0}\,\frac{\cos^2(\omega t - kz_0)}{\rho^2}\,\rho\,d\phi\,d\rho\\ &= \frac{V_0^2}{\eta_0}\cos^2(\omega t - kz_0)\,.\end{aligned}$$

The time-average power (net power) at $z_0$ is obtained by

$$P_{\text{avg}} = \frac{1}{T}\int_0^T\frac{V_0^2}{\eta_0}\cos^2(\omega t - kz_0)\,dt\,,$$

where $T = \frac{2\pi}{\omega}$ is one period of $\cos(\omega t - kz_0)$, and therefore

$$P_{\text{avg}} = \frac{1}{2}\frac{V_0^2}{\eta_0}.$$

## 2-7 Superposition Principle

The superposition principle, in general, can be applied to physical problems whose input and output are governed by linear relationships. The curl, divergence, and gradient that are based on spatial differentiations are all linear operators, and thus Maxwell's equations, in general, satisfy the condition for linearity. However, the constitutive relations that relate the electric and magnetic flux densities to the corresponding electric and magnetic field intensities can be nonlinear, depending on the material composition and the magnitude of the field intensities in such media. As discussed in Chapter 1, under the small-signal approximation, the constitutive relations are linear. Considering currents and charges as input and the electric and magnetic fields throughout the region of interest as output, the superposition principle states that if $\mathbf{E}_1(\mathbf{r})$ and $\mathbf{H}_1(\mathbf{r})$ are produced by $\mathbf{J}_1(\mathbf{r})$ and $\mathbf{J}_{1\text{m}}(\mathbf{r})$ according to

$$\nabla \times \mathbf{H}_1(\mathbf{r}) = -i\omega\varepsilon\, \mathbf{E}_1(\mathbf{r}) + \mathbf{J}_1(\mathbf{r})$$

and

$$\nabla \times \mathbf{E}_1(\mathbf{r}) = i\omega\mu\, \mathbf{H}_1(\mathbf{r}) - \mathbf{J}_{1\text{m}}(\mathbf{r}),$$

and $\mathbf{E}_2(\mathbf{r})$ and $\mathbf{H}_2(\mathbf{r})$ are produced by $\mathbf{J}_2(\mathbf{r})$ and $\mathbf{J}_{2\text{m}}(\mathbf{r})$ according to

$$\nabla \times \mathbf{H}_2(\mathbf{r}) = -i\omega\varepsilon\, \mathbf{E}_2(\mathbf{r}) + \mathbf{J}_2(\mathbf{r})$$

and

$$\nabla \times \mathbf{E}_2(\mathbf{r}) = i\omega\mu\, \mathbf{H}_2(\mathbf{r}) - \mathbf{J}_{2\text{m}}(\mathbf{r}),$$

then it follows that $\mathbf{J}_1(\mathbf{r}) + \mathbf{J}_2(\mathbf{r})$ and $\mathbf{J}_{1\text{m}}(\mathbf{r}) + \mathbf{J}_{2\text{m}}(\mathbf{r})$ produce $\mathbf{E}_1(\mathbf{r}) + \mathbf{E}_2(\mathbf{r})$ and $\mathbf{H}_1(\mathbf{r}) + \mathbf{H}_2(\mathbf{r})$.

## 2-8 Uniqueness Theorem

As will be shown later, computation of field quantities generated from electric and magnetic sources present in a homogeneous and unbounded medium can be obtained using electric and magnetic vector and scalar potentials. The same potentials may be used for an inhomogeneous medium made up of a finite number of homogeneous media. To solve such problems, we need to specify the conditions required to make the solution in any given region unique. Let us consider a region with constitutive parameters $\varepsilon$, $\mu$, and $\sigma$, bounded by a closed surface $S$ and containing arbitrary electric and magnetic sources $\mathbf{J}$ and $\mathbf{J}_{\text{m}}$. Suppose there are two sets of solutions that satisfy Maxwell's equations. Let us denote the first set by $\mathbf{E}_1$ and $\mathbf{H}_1$ and the second set by $\mathbf{E}_2$ and $\mathbf{H}_2$. Then, according to the superposition principle, $\mathbf{E} = \mathbf{E}_1 - \mathbf{E}_2$ and

$\mathbf{H} = \mathbf{H}_1 - \mathbf{H}_2$ must satisfy the source-free Maxwell's equations, that is,

$$\nabla \times \mathbf{E} = -\mu \frac{\partial \mathbf{H}}{\partial t} \tag{2.58}$$

and

$$\nabla \times \mathbf{H} = \varepsilon \frac{\partial \mathbf{E}}{\partial t} + \sigma \mathbf{E}. \tag{2.59}$$

Applying the Poynting theorem to the source-free Maxwell's equations given by Eq. (2.58) and Eq. (2.59) leads to

$$\frac{\partial}{\partial t} \iiint_V \left( \frac{1}{2}\, \varepsilon |\mathbf{E}|^2 + \frac{1}{2}\, \mu |\mathbf{H}|^2 \right) d\upsilon = - \iiint_V \sigma |\mathbf{E}|^2 \, d\upsilon - \oiint_S (\mathbf{E} \times \mathbf{H}) \cdot d\mathbf{s} \,. \tag{2.60}$$

If we assume $\hat{\mathbf{n}} \times \mathbf{E} = 0$ or $\hat{\mathbf{n}} \times \mathbf{H} = 0$ on $S$, then

$$\oiint_S (\mathbf{E} \times \mathbf{H}) \cdot d\mathbf{s} = \oiint (\hat{\mathbf{n}} \times \mathbf{E}) \cdot \mathbf{H} \, d\mathbf{s} = - \oiint (\hat{\mathbf{n}} \times \mathbf{H}) \cdot \mathbf{E} \, d\mathbf{s} = 0 \,.$$

That is, if

$$\hat{\mathbf{n}} \times \mathbf{E}_1 = \hat{\mathbf{n}} \times \mathbf{E}_2 \quad \text{or} \quad \hat{\mathbf{n}} \times \mathbf{H}_1 = \hat{\mathbf{n}} \times \mathbf{H}_2 \,,$$

then the surface integral vanishes. Also if $\hat{\mathbf{n}} \times \mathbf{E} = 0$ over a portion of $S$ and $\hat{\mathbf{n}} \times \mathbf{H} = 0$ on the rest, the surface integral vanishes as well. Under any of these conditions the right-hand side of Eq. (2.60) is always a nonpositive quantity. As a result, if $\mathbf{E}_1 = \mathbf{E}_2$ and $\mathbf{H}_1 = \mathbf{H}_2$ at $t = 0$, that is, $\mathbf{E}(t = 0) = \mathbf{H}(t = 0) = 0$, it can be concluded that $\mathbf{E} = \mathbf{H} = 0$ for all values of $t > 0$ and at every point in the domain $V$. The conclusion is based on the argument that the integrand of the left-hand side of Eq. (2.60) is always a positive quantity and its initial value is zero, and hence it cannot have a negative time rate of change. So it is concluded that both sides of Eq. (2.60) are identically zero.

The above-stated conditions are the necessary and sufficient conditions for making the solution of Maxwell's equations unique in region $V$. That is, the solution to Maxwell's equations is unique if the initial values of $\mathbf{E}$ and $\mathbf{H}$ are known throughout the region and if the tangential component of $\mathbf{E}$ or the tangential component of $\mathbf{H}$ is known across a closed surface, or the tangential component of $\mathbf{E}$ is known across part of the surface and the tangential component of $\mathbf{H}$ is known across the remaining part of the surface.

If the medium is unbounded and the surface $S$ approaches infinity, the assumption of having a finite amount of conductivity is required to ensure that $\mathbf{E}$ and $\mathbf{H}$ approach zero on the surface $S$. Alternatively, the application of the radiation boundary condition that will be introduced later can be used to prove that the surface integral vanishes when the surface $S$ is sufficiently far away from the sources.

Oftentimes, when developing a solution involving partial differential equations, the total tangential component of $\mathbf{E}$ or $\mathbf{H}$ is not known, but through the imposition of the boundary conditions across the discontinuities, the uniqueness of the solution throughout the entire region can be established. In certain cases $\hat{\mathbf{n}} \times \mathbf{E} = 0$ for a perfect conductor or $\hat{\mathbf{n}} \times \mathbf{H} = 0$ for

a perfect magnetic conductor, so the values of the tangential components are known per the boundary conditions for those surfaces.

## 2-9 Equivalence Principle for Electromagnetic Sources

The electromagnetic fields established outside a source region can be reproduced by an infinite number of combinations of multiple sources external to the desired region. To demonstrate the validity of this statement, let us first consider a set of electric and magnetic current distributions $\mathbf{J}$ and $\mathbf{J}_m$ confined within a volume $V$, as shown in Fig. 2-17. According to the uniqueness theorem, the tangential components of the electric and magnetic fields on a closed surface $S$ are sufficient to determine the fields outside of $S$. For example, if we consider a scenario where the fields inside $S$ are zero and the fields outside of $S$ are the original fields, according to the boundary conditions for EM fields, we must establish tangential electric and magnetic current sources on $S$ given by

$$\mathbf{J}_s = \hat{\mathbf{n}} \times \mathbf{H} \tag{2.61a}$$

and

$$\mathbf{J}_{ms} = -\hat{\mathbf{n}} \times \mathbf{E}\,, \tag{2.61b}$$

in order for the original tangent electric and magnetic fields to remain the same. The equivalent sources given by Eq. (2.61a) and Eq. (2.61b) are only one of many possible sources that we can choose to satisfy the condition for finding the original fields exterior to $S$. In fact we can place any arbitrary field functions for $\mathbf{E}$ and $\mathbf{H}$ interior to $S$ so long as they are a solution to Maxwell's equation for the homogeneous medium. Suppose $\mathbf{J}'$ and $\mathbf{J}'_m$ produce $\mathbf{E}'$ and $\mathbf{H}'$ in a medium with possibly different constitutive parameters $\mu'$ and $\varepsilon'$ as shown in Fig. 2-18. Another equivalent surface source can then be obtained from

$$\mathbf{J}_s = \hat{\mathbf{n}} \times (\mathbf{H} - \mathbf{H}') \qquad \text{and} \qquad \mathbf{J}_{ms} = -\hat{\mathbf{n}} \times (\mathbf{E} - \mathbf{E}')\,,$$

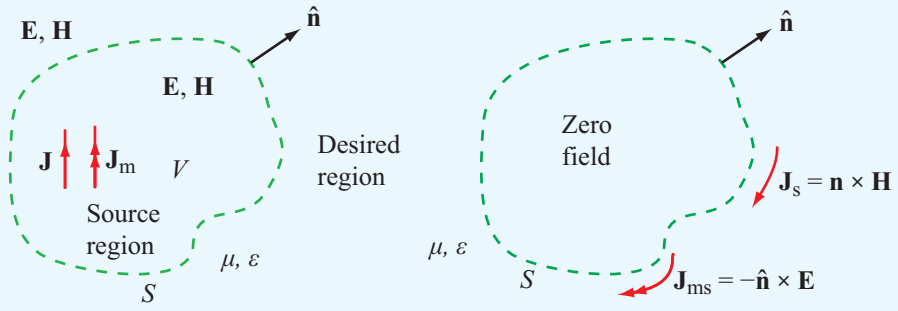


**Figure 2-17:** Equivalent surface electric and magnetic currents $\mathbf{J}_s$ and $\mathbf{J}_{ms}$, respectively, that can produce a null field interior to $S$ as well as the original fields outside of $S$ (in a homogeneous medium with parameters $\mu$ and $\varepsilon$).

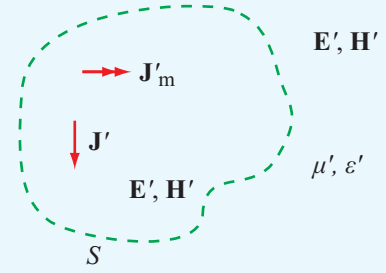


**Figure 2-18:** An arbitrary set of currents and material to establish another set of equivalent sources on the boundary $S$.

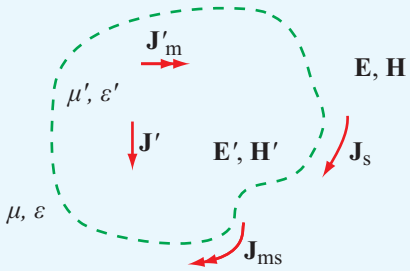


**Figure 2-19:** Another set of equivalent surface currents that produce original fields outside $S$. The medium is now inhomogeneous.

while maintaining the interior fields as $\mathbf{E}'$ and $\mathbf{H}'$ and the exterior fields as $\mathbf{E}$ and $\mathbf{H}$, as shown in Fig. 2-19. Note that we must keep the original sources and the constitutive parameters of the media in the region for which we keep the fields. That is, for the equivalent problem, sources $\mathbf{J}'(\mathbf{r})$ and $\mathbf{J}'_{\mathrm{m}}(\mathbf{r})$ and fields $\mathbf{E}'(\mathbf{r})$ and $\mathbf{H}'(\mathbf{r})$ interior to $S$ must be the same as those in Fig. 2-18.

According to the uniqueness theorem, only the tangential component of the electric field, or the tangential component of the magnetic field, on $S$ is needed to reproduce the fields everywhere in the region of interest. Therefore we should be able to provide the equivalent source condition where only one of the two tangential fields is used. To demonstrate this, consider a problem where surface $S$ is a perfect electric conductor. On this surface, $\hat{\mathbf{n}} \times \mathbf{E} = 0$. To maintain the original tangential electric field on $S$, according to the boundary condition, a surface magnetic current given by $\mathbf{J}_{\mathrm{ms}} = -\hat{\mathbf{n}} \times \mathbf{E}$ is needed, where $\mathbf{E}$ is the original electric field on the surface. Figure 2-20 shows the original and the equivalent configurations, including sources both internal and external to surface $S$. We should note that the equivalent electric surface current ($\mathbf{J}_{\mathrm{s}} = \hat{\mathbf{n}} \times \mathbf{H}$) will be automatically generated on the PEC surface $S$.

Similarly, surface $S$ can be replaced with a magnetic conductor over which $\hat{\mathbf{n}} \times \mathbf{H} = \mathbf{0}$. To maintain the original tangential magnetic field on $S$, an electric surface current $\mathbf{J}_{\mathrm{s}} = \hat{\mathbf{n}} \times \mathbf{H}$ must be placed on $S$. In this case, only the tangential magnetic field on $S$ is needed.

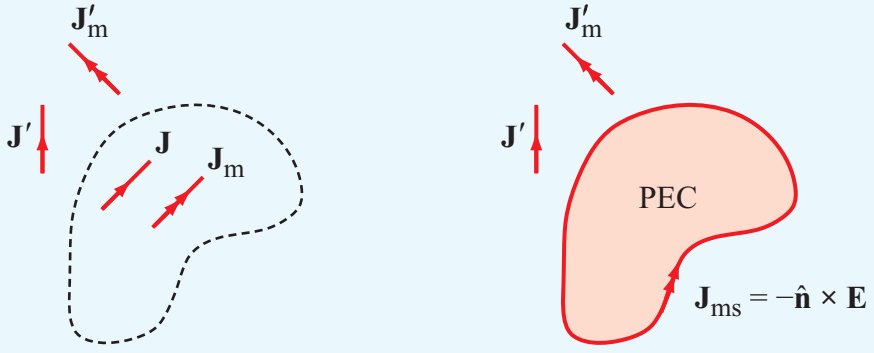


(a) Original configuration (b) Equivalent configuration

**Figure 2-20:** (a) The original configuration includes sources internal and external to a closed surface $S$, and (b) the equivalent configuration wherein external sources are kept unchanged but internal sources are replaced with a PEC surface on $S$ together with an impressed equivalent magnetic surface current on the boundary $S$. In this case only the tangential electric field is used.

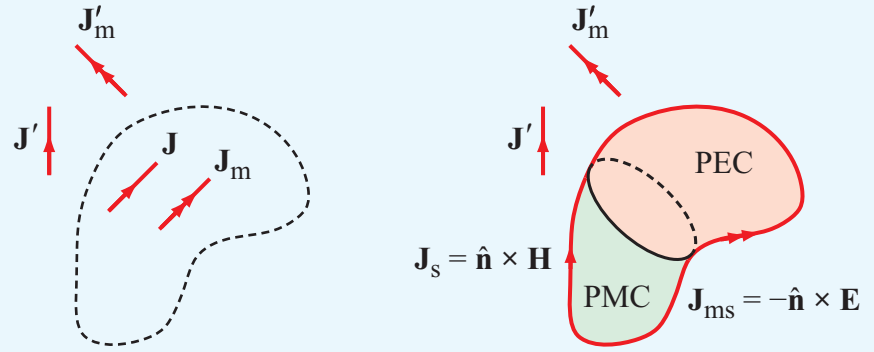


(a) Original configuration (b) Equivalent configuration

**Figure 2-21:** (a) The original configuration includes sources internal and external to a closed surface $S$ and (b) the equivalent configuration wherein external sources are kept unchanged but and internal sources are replaced with a PEC surface on a portion of $S$ with an equivalent magnetic surface current and a PMC surface on the complementary portion of $S$.

Another example is to consider a portion of $S$ as being a perfect electric conductor covered with a magnetic surface current and the complementary portion of $S$ being a perfect magnetic conductor with an electric surface current, as shown in Fig. 2-21.

To better understand how we use equivalent sources, we will explore electric circuits as an analogous model. In a circuit composed of voltage and current sources and passive lumped elements, one can enclose all active components in a block and the passive components in

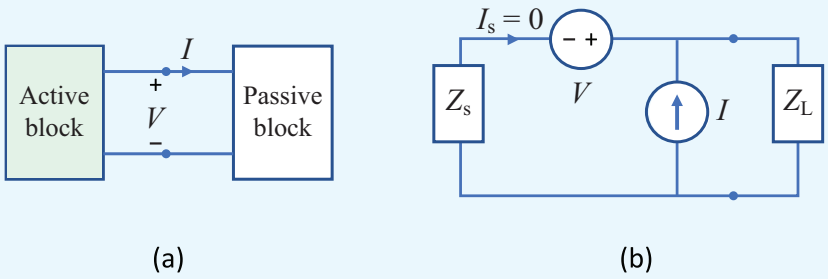


**Figure 2-22:** (a) Block diagram of a circuit with two blocks, one with active sources and one without, and (b) its equivalent circuit with equivalent sources at the designated terminals.

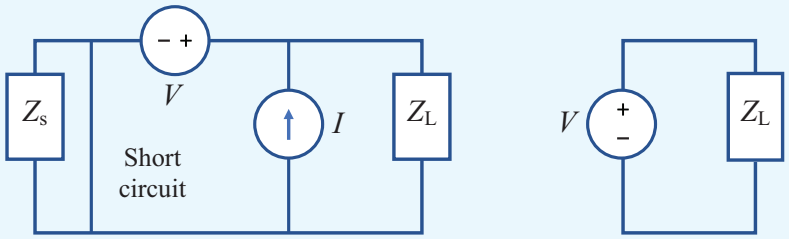


**Figure 2-23:** The equivalent voltage source with a short circuit at the terminal of the source block. This is equivalent to having a PEC on *S*.

another block, as shown in Fig. 2-22(a). Equivalent voltage and current sources can be placed at the terminal between the active and passive blocks, as shown in Fig. 2-22(b), similar to the equivalent magnetic and electric surface current sources on surface *S*. Here $V$ and $I$ are the voltage and current at the terminal, $Z_L$ is the equivalent input impedance of the passive elements, and $Z_s$ is the source impedance. It can easily be shown that the equivalent sources do not produce any voltage across $Z_s$ or any current through it. This is equivalent to null fields within *S*. It can also be shown that placing a short circuit across $Z_s$ (similar to placing PEC over *S*) disables the current source contribution to $Z_L$ and the equivalent source is what is shown in Fig. 2-23. In this case only the voltage source (similar to magnetic surface current on PEC) is sufficient to establish the original current through the passive block. Conversely, by open-circuiting $Z_s$ (similar to placing PMC over *S*), only the current source is sufficient to produce the original voltage across the load, as shown in Fig. 2-24.

The open-circuited voltage source ensures that no current flows through $Z_s$ and the entire current from the current source flows through the load.

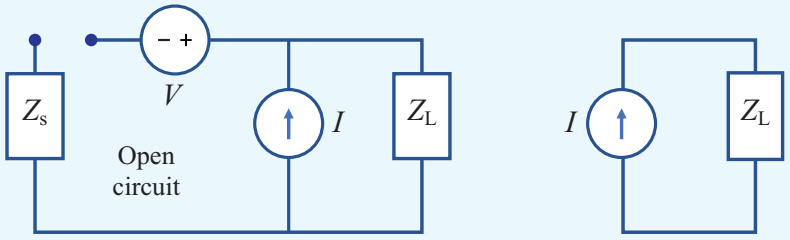


**Figure 2-24:** The equivalent current source with an open circuit across the terminals of the source block. This is equivalent to having a PMC on $S$.

## Example 2-5: Equivalent Source

The electric and magnetic fields for a plane wave are given by

$$\mathbf{E}(\mathbf{r}) = E_0(-\cos\theta\,\hat{\mathbf{y}} + \sin\theta\,\hat{\mathbf{z}})\cos(\omega t - k\sin\theta\,y - k\cos\theta\,z) \tag{2.62a}$$

and

$$\mathbf{H}(\mathbf{r}) = \frac{E_0}{\eta_0}\,\hat{\mathbf{x}}\cos(\omega t - k\sin\theta\,y - k\cos\theta\,z)\ . \tag{2.62b}$$

These fields are generated from certain sources in the $z<0$ half-space. Find equivalent sources on the $x$–$y$ plane that generate the same fields at $z>0$ half-space.

**Solution:** According to Eqs. (2.61a) and (2.61b), equivalent surface electric and magnetic currents can be placed on the $z=0$ surface ($x$–$y$ plane):

$$\mathbf{J}_s(x,y) = \hat{\mathbf{z}}\times\mathbf{H}(x,y,0) \tag{2.63a}$$

and

$$\mathbf{J}_{ms}(x,y) = -\hat{\mathbf{z}}\times\mathbf{E}(x,y,0)\ . \tag{2.63b}$$

Using Eq. (2.62a) in Eq. (2.63a) and Eq. (2.62b) in Eq. (2.63b), we have

$$\mathbf{J}_s^{(1)} = \frac{E_0}{\eta_0}\cos(\omega t - k\sin\theta\,y)\,\hat{\mathbf{y}}$$

and

$$\mathbf{J}_{ms}^{(1)} = -E_0\cos(\theta)\cos(\omega t - k\sin\theta\,y)\,\hat{\mathbf{x}}\ .$$

We can also place a PEC on the $x$–$y$ plane and then just superimpose $\mathbf{J}_{ms}(x,y)$ on it. Since the ground plane is infinite, by applying image theory we can remove the ground plane and double the magnetic current. In this case,

$$\mathbf{J}_{ms}^{(2)} = -2E_0\cos(\theta)\cos(\omega t - k\sin\theta\,y)\,\hat{\mathbf{x}}$$

can produce fields given by Eqs. (2.61a) and (2.61b) in the upper half-space ($z > 0$).

If instead of PEC we use PMC on the $x$–$y$ plane and use image theory, it can be shown that

$$\mathbf{J}_s^{(2)} = \frac{2E_0}{\eta_0} \cos(\omega t - k \sin\theta\, y)\, \hat{\mathbf{y}}$$

can produce fields given by Eqs. (2.61a) and (2.61b) in the upper half-space.

## Summary

### Concepts

- The concepts of fictitious magnetic charge and current distributions are attributed to the magnetization vector $\mathbf{M}$ or the medium permeability $\mu$. The magnetic current distribution can only be defined for time-varying fields.
- Introduction of magnetic charge and current distributions into Maxwell's equations makes them symmetric and results in a set of relations between the electric and magnetic field quantities and their sources known as "duality relations."
- For boundary value problems involving electromagnetic sources (charges and current) and certain objects, such as an infinite planar conducting object, an equivalent problem can be created by replacing the objects with appropriate images of the specified sources.
- Using the concept of electric and magnetic polarization currents for an object with parameters $(\mu, \varepsilon)$, it is possible to construct an equivalent configuration wherein the object is replaced with electric and magnetic polarization currents in the background medium while maintaining the original fields.
- Electric and magnetic polarization currents are not independent of each other. That is, one can be produced from knowledge of the other.
- Maxwell's equations predict that electromagnetic waves can carry energy, in addition to storing energy in material media. The Poynting theorem, derived from Maxwell's equations, states that the law of conservation of energy is applicable to electromagnetic fields.
- The solution to Maxwell's equations is unique if the fields satisfy Maxwell's equations, the initial field values throughout the region of interest are known, and the tangential component of the electric field or the magnetic field over a surface that encloses the region of interest is known.
- It is shown that the electromagnetic fields outside a region that encloses electric and/or magnetic sources can be reproduced by many other equivalent sources. In other words, the knowledge of fields outside the source region cannot be used to uniquely specify the sources that produced them.

## Important Equations

**Equivalent magnetic charge density and current distribution for material with permeability $\mu_0\mu_r$:**

$$\rho_m = -\mu_0(\mu_r - 1)\nabla \cdot \mathbf{H}$$
$$\mathbf{J}_m = \mu_0(\mu_r - 1)\frac{\partial \mathbf{H}}{\partial t}$$

**Maxwell's equations with inclusion of magnetic sources:**

$$\nabla \times \mathbf{E} = -\mu \frac{\partial \mathbf{H}}{\partial t} - \mathbf{J}_m$$
$$\nabla \times \mathbf{H} = \varepsilon \frac{\partial \mathbf{E}}{\partial t} + \mathbf{J}$$
$$\nabla \cdot \mathbf{E} = \frac{\rho}{\varepsilon}$$
$$\nabla \cdot \mathbf{H} = \frac{\rho_m}{\mu}$$

**Duality relations:**

$$\mathbf{E} \to \mathbf{H}, \quad \mathbf{H} \to -\mathbf{E}, \quad \mathbf{J} \to \mathbf{J}_m, \quad \mathbf{J}_m \to -\mathbf{J}$$
$$\rho \to \rho_m, \quad \rho_m \to -\rho, \quad \mu \to \varepsilon, \quad \varepsilon \to \mu$$

**Boundary conditions for a perfect magnetic conductor:**

$$\hat{\mathbf{n}} \times \mathbf{H} = 0$$
$$\hat{\mathbf{n}} \times \mathbf{E} = -\mathbf{J}_{sm}$$
$$\hat{\mathbf{n}} \cdot \mathbf{B} = \rho_{sm}$$

**Polarization current:**

$$\mathbf{J}_p = \varepsilon_0(\varepsilon_r - 1)\frac{\partial \mathbf{E}}{\partial t}$$

**Stored electric and magnetic energy density:**

$$w_e(\mathbf{r}) = \tfrac{1}{2}\,\mathbf{D}(\mathbf{r}) \cdot \mathbf{E}(\mathbf{r})$$
$$w_m(\mathbf{r}) = \tfrac{1}{2}\,\mathbf{B}(\mathbf{r}) \cdot \mathbf{H}(\mathbf{r})$$

**Poynting vector (power density):**

$$\mathbf{S}(\mathbf{r},t) = \mathbf{E}(\rho,t) \times \mathbf{H}(\rho,t)$$

**Equivalent surface currents over a surface enclosing the original source with the assumption that fields are zero inside:**

$$\mathbf{J}_s = \hat{\mathbf{n}} \times \mathbf{H}$$
$$\mathbf{J}_{ms} = -\hat{\mathbf{n}} \times \mathbf{E}$$

## Important Terms

Provide definitions or explain the meaning of the following terms:

boundary conditions (generalized)
duality relations
electric energy density
equivalent source
flow of electromagnetic power
image of currents and charges over a planar conductive surface
image of a point charge over a dielectric half-space medium
image of a point charge over a metallic sphere
magnetic charge density
magnetic current density
normalized duality relations
ohmic loss
perfect electric conductor (PEC)
perfect magnetic conductor (PMC)
polarization charge density
polarization current
potential energy
potential function
Poynting vector
superposition principle
uniqueness theorem

# PROBLEMS

## Equivalent Charges and Currents

**2.1** Consider a point charge $Q$ placed at the center of a metallic sphere filled with a material having permittivity $\varepsilon$. If we want to establish the same electric field inside the sphere but with permittivity $\varepsilon_0$, what charge distribution do we have to establish?

**2.2** The permittivity and permeability tensors for a particular medium are given by

$$\overline{\overline{\varepsilon}}_r = \begin{bmatrix} 3.1 & 0.5 & 0 \\ 0.5 & 3.1 & 0 \\ 0 & 0 & 5 \end{bmatrix} \quad \text{and} \quad \overline{\overline{\mu}}_r = \begin{bmatrix} 1 & 0.1 & 0 \\ 0 & 1 & 0 \\ 0 & 0 & 1.5 \end{bmatrix}.$$

**(a)** For internal fields given by

$$\mathbf{E} = \frac{\hat{\mathbf{x}} + 2\hat{\mathbf{z}}}{\sqrt{5}} \cos(\omega t) \quad \text{and} \quad \mathbf{H} = \hat{\mathbf{z}} \sin(\omega t),$$

what equivalent polarization and magnetic currents are necessary to treat this dielectric medium as a free-space equivalent?

**(b)** Find the total electric and magnetic polarization currents flowing through the depicted surface in Fig. P2.2 at $y = 5$ m.

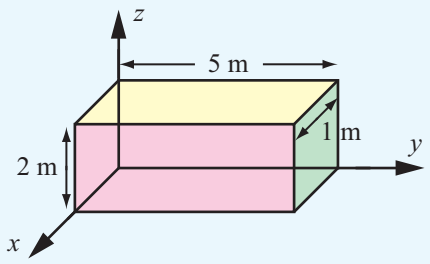


**Figure P2.2:** A block of an anisotropic material in a free-space background.

**2.3** For a general bianisotropic medium, what equivalent polarization and magnetization currents are needed to establish the same fields in a homogeneous medium with permittivity $\varepsilon_0$ and permeability $\mu_0$? Is it possible to find a solution where the bianisotropic medium is replaced with only polarization or magnetization currents in a background medium with permittivity $\varepsilon_0$ and permeability $\mu_0$?

## Duality

**2.4** Consider a homogeneous medium with

$$\mathbf{D} = \varepsilon \mathbf{E} + \xi \mathbf{H}$$

and

$$\mathbf{B} = \xi\mathbf{E} + \mu\mathbf{H}\,,$$

which is called a ***Tellegen medium***. Maxwell's equations are solved for an electric current density $\mathbf{J}$ and a magnetic current density $\mathbf{J}_{\rm m}$, and the fields are found to be $(\mathbf{E}_1, \mathbf{D}_1, \mathbf{B}_1, \mathbf{H}_1)$. The problem is then solved again with $\mathbf{J}$ replaced with $\mathbf{J}_{\rm m}/\eta_0$ and $\mathbf{J}_{\rm m}$ replaced with $-\eta_0\mathbf{J}$, and the fields are found to be $(\mathbf{E}_2, \mathbf{D}_2, \mathbf{B}_2, \mathbf{H}_2)$. Determine the constitutive parameters for the dual problem. Note that $\eta_0$ is the free-space wave impedance and is defined by $\eta_0 = \sqrt{\mu_0/\varepsilon_0}$.

**2.5**

**(a)** Prove that Maxwell's equations are invariant under the following duality transformations:

$$\begin{aligned}
\mathbf{E}' &= \mathbf{E}\cos\alpha + c\mathbf{B}\sin\alpha\,,\\
\mathbf{B}' &= \mathbf{B}\cos\alpha - \frac{1}{c}\,\mathbf{E}\sin\alpha\,,\\
q_{\rm e}' &= q_{\rm e}\cos\alpha + c\varepsilon_0 q_{\rm m}\sin\alpha\,,\\
q_{\rm m}' &= q_{\rm m}\cos\alpha - \frac{1}{c\varepsilon_0}\,q_{\rm e}\sin\alpha\,,
\end{aligned}$$

where $q_{\rm e}$ and $q_{\rm m}$ are electric and magnetic charges (the same relations are true for the charge densities), $c = 1/\sqrt{\mu_0\varepsilon_0}$, and $\alpha$ is an arbitrary angle in "**E**–**B** plane." *Hint:* Show that Maxwell's equations hold for the prime field quantities, and note that in the presence of fictitious magnetic charges we have

$$\nabla\cdot\mathbf{B} = \rho_{\rm m} \qquad \text{and} \qquad \nabla\times\mathbf{E} = -\mathbf{J}_{\rm m} - \frac{\partial\mathbf{B}}{\partial t}\,.$$

**(b)** Then prove that

$$\mathbf{F} = q_{\rm e}(\mathbf{E} + \mathbf{u}\times\mathbf{B}) + q_{\rm m}\left(\frac{\mathbf{B}}{\mu_0} - \varepsilon_0\,\mathbf{u}\times\mathbf{E}\right)$$

is invariant under the above duality transformation.

## Image Theory

**2.6** Consider a 2-D space, infinite along the $z$-direction, defined by the perpendicular intersection of semi-infinite PEC and PMC planes, as shown in Fig. P2.6. Let a point source $\mathbf{J}$ exist in this space. If the origin is defined by the intersection of the two planes, then the expression for the current is given by

$$\mathbf{J} = J_0\,\frac{\hat{\mathbf{y}} - \hat{\mathbf{x}}}{\sqrt{2}}\,\delta(x-a,\, y-a,\, z).$$

**(a)** Draw the equivalent image currents.

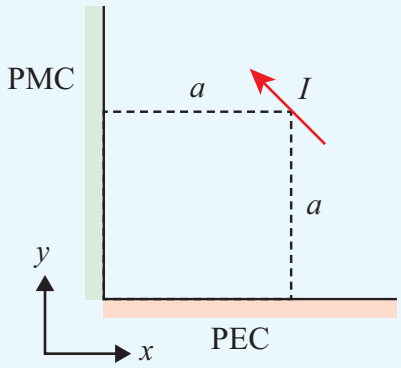


**Figure P2.6:** A filament current placed inside a corner reflector. One side of the reflector is made from a semi-infinite perfect magnetic conductor and the other side is made from a perfect electric conductor.

**(b)** Suppose $\mathbf{J}$ is replaced with $\mathbf{J}_m$, a magnetic current density. Draw the equivalent image currents.

**2.7** Consider a 2-D space, infinite along the $z$-direction. Two PEC planes (both perpendicular to the $x$–$y$ plane) intersect at an angle $\alpha$, as shown in Fig. P2.7. Current $\mathbf{J}$ exists in that space and is given by the following expression:

$$\mathbf{J} = \hat{\mathbf{y}} J_0 \delta(x - a,\ y - b,\ z).$$

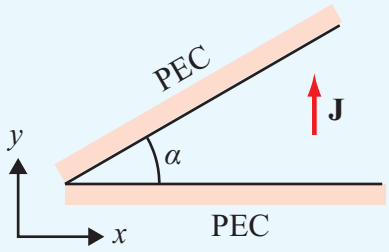


**Figure P2.7:** Configuration of a filament current placed inside of a metallic wedge with interior angle $\alpha$.

**(a)** Suppose $\alpha = 45°$. Draw the equivalent image currents.

**(b)** Suppose $\alpha = 44°$. Draw the equivalent image currents.

**(c)** Comparing your answers to parts (b) and (c), what can you generalize about applying image theory to wedges with angle $\alpha = 360°/N$ or $\alpha \neq 360°/N$ ($N$ = integer)?

**2.8** Consider a 2-D space, infinite along the $z$-direction, and defined by two pairs of parallel PEC and PMC planes, as shown in Fig. P2.8. Let a point source $\mathbf{J}_e$ exist in this space. The expression for the current is given by

$$\mathbf{J}_e = J_0 \frac{\hat{\mathbf{y}} + \hat{\mathbf{x}}}{\sqrt{2}} \delta\left(x - \frac{a}{2}, y - \frac{b}{2}, z\right).$$

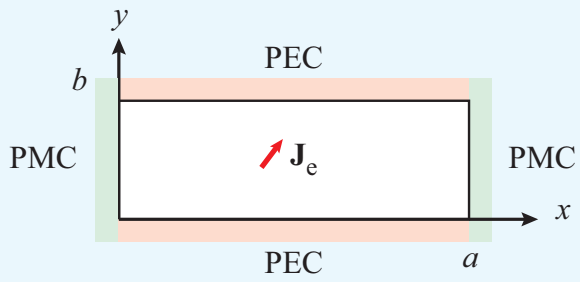


**Figure P2.8:** A filament current inside a rectangular region defined by two vertical PMC walls and two horizontal PEC walls.

**(a)** Draw the equivalent image currents.

**(b)** Suppose $\mathbf{J}_e$ is replaced with a magnetic current density $\mathbf{J}_m$. Draw the equivalent image currents.

**2.9** Consider a loop with radius $a$ that has $N$ turns and carries a current $I$. If the loop is located at the origin and is oriented so that its axis lies along the $z$-direction, the magnetic field due to the loop can be expressed as

$$\mathbf{H} = \frac{NIa^2}{4R^3} (\hat{\mathbf{r}} 2\cos\theta + \hat{\boldsymbol{\theta}} \sin\theta).$$

Use the modified Lorentz law,

$$\mathbf{F} = NI \oint_C d\boldsymbol{\ell} \times \mathbf{B},$$

and image theory to calculate the force on the loop if it is held above a perfect electric conductor at height $z_0$. Assume that the current is time-variant enough to be levitated, but static enough to treat it as such.

**2.10** Consider an arbitrary planar current sheet in the $x$–$y$ plane of a Cartesian coordinate system ($J_s(x,y) = j_s^x(x,y)\,\hat{\mathbf{x}} + j_s^y(x,y)\,\hat{\mathbf{y}}$). Use image theory to prove that the magnetic field generated by this current on the plane that contains the current sheet ($x$–$y$ plane) is normal to the plane; i.e., $\mathbf{H}(\mathbf{r}) = \mathbf{H}_z(\mathbf{r})\,\hat{\mathbf{z}}$.

**2.11** Consider an arbitrary planar magnetic current sheet in the $x$–$y$ plane of a Cartesian coordinate system ($J_{ms}(x,y) = j_{ms}^x(x,y)\,\hat{\mathbf{x}} + j_{ms}^y(x,y)\,\hat{\mathbf{y}}$.) Use image theory to prove that the

electric field generated by this current on the plane that contains the current sheet ($x$–$y$ plane) is normal to the plane; i.e., $\mathbf{H}(\mathbf{r}) = \mathbf{H}_z(\mathbf{r})\,\hat{\mathbf{z}}$.

**2.12** What constitutes the image of a line charge with charge density $\rho_l$ C/m, outside a grounded metallic cylinder at $y = y_0$, as shown in Fig. P2.12? The line charge is parallel to the cylinder axis ($z$-axis).

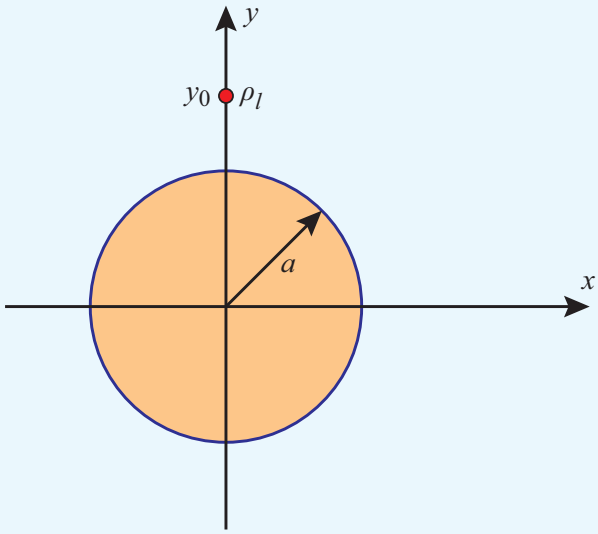


**Figure P2.12:** A geometrical metallic cylinder and a line charge located at $y = y_0$ outside the cylinder. You are asked to find the image source for this problem.

**2.13** A point charge $q$ is placed on the $z$-axis outside of a metallic hemisphere of radius $a$ that sits on an infinite planar conductor in the $x$–$y$ plane. Use image theory to find the equivalent charges. What if the charge is moved to a different location, say in the $y$-$z$ plane at $\theta = \theta_0$ and $r = z_0$?

## Flow of Energy

**2.14** A thick wire of radius $a$ carries a constant current $I$ uniformly distributed over its cross section. A narrow gap in the wire of width $w$ forms a parallel-plate capacitor, as shown in Fig. P2.14.

**(a)** Find the electric and magnetic fields in the gap region as a function of $r$ (distance from the axis) and time.

**(b)** Find the electromagnetic energy ($U_{\text{em}}$) and Poynting vector $\mathbf{S}$ in the gap. Show that

$$-\nabla \cdot \mathbf{S} = \frac{\partial U_{\text{em}}}{\partial t}\,.$$

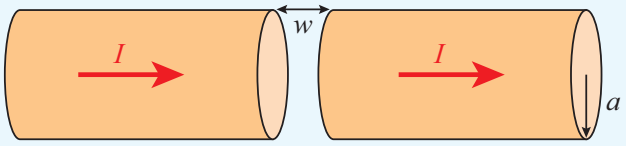


**Figure P2.14:** A cylindrical metallic wire carrying a time-varying current $I$ with a narrow gap that acts as a capacitor. The current density in the cross section of the wire is uniform.

**(c)** Determine the total energy in the gap as a function of time. Calculate the total power flowing in the gap. (Integrate the Poynting vector over the appropriate surface.)

**(d)** Check that the input power is equal to the rate of increase of energy in the gap. Discuss your results.

**2.15** A coaxial cable consists of an inner conductor, a tubular insulating layer, and an outer conductor. The insulating layer has a relative permittivity of $\varepsilon_r$. The electric field intensity inside the insulating layer is given by

$$\mathbf{E} = \frac{V_0}{\rho \ln(b/a)} \cos(\omega t - kz)\, \hat{\boldsymbol{\rho}} \,.$$

Consider a piece of coaxial cable of length $d$ where $0 < z < d$, as shown in Fig. P2.15.

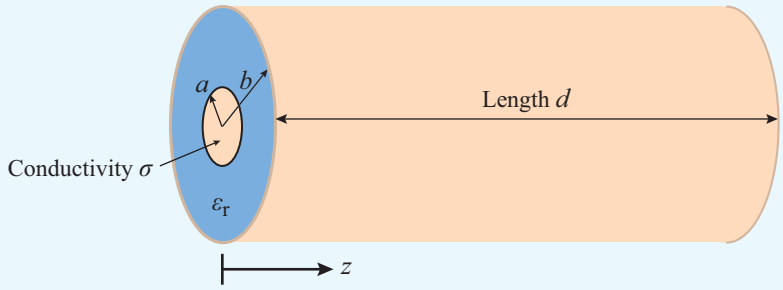


**Figure P2.15:** Configuration of a coaxial transmission line filled with a dielectric material having a relative permittivity $\varepsilon_r$.

**(a)** First assume that the conductors are perfect electric conductors ($\sigma = \infty$).

(i) Find the magnetic field intensity $\mathbf{H}$.

(ii) Find the surface currents on the inner and outer conductors $\mathbf{J}_{sa}$ and $\mathbf{J}_{sb}$, respectively.

(iii) Find the time-dependent Poynting vector $\mathbf{S}(t)$, and calculate the power flow passing through the cross sections at $z = 0$ and $z = d$.

(iv) Find the stored electric and magnetic energy inside the piece of coaxial cable.

(v) Show that conservation of energy is maintained.

**(b)** If the conductors have a finite conductivity $\sigma$ at high frequency, the surface resistivity is given by

$$\rho_S = \sqrt{\frac{\omega\mu_0}{2\sigma}} \quad \text{and} \quad \mathbf{J}_S = \frac{\mathbf{E}}{\rho_S} .$$

We denote the attenuation factor as $\alpha = P_l/(2P_{avg})$, where $P_l$ is the dissipation power per unit length and $P_{avg}$ is the time-average power flowing through the cross section. We can assume in this part of the problem that the length $d$ is an integer multiple of the wavelength $\lambda$; i.e., $d = N\lambda = 2\pi N/k$. Note: $k \gg \alpha$. Use proper approximations to simplify your derivations.

(i) Find the power dissipating on the inner and the outer conductors.

(ii) Find the attenuation factor $\alpha$.

Then the electric field can be modified to

$$\mathbf{E} = \frac{V_0}{\ln(b/a)} \cdot \frac{1}{\rho} \cos(\omega t - kz)\, e^{-\alpha z}\, \hat{\boldsymbol{\rho}} .$$

(iii) Find the power flow passing through the cross sections at $z = 0$ and $z = d$.

(iv) Show that conservation of energy is maintained.

(v) Discuss how to choose the ratio $a/b$ to minimize the attenuation factor $\alpha$.

## Uniqueness Theorem

**2.16** Let the tangential **E**-field and tangential **H**-field on a closed surface $S$ be related by an impedance matrix $\overline{\overline{Z}}(\mathbf{r})$ such that

$$\hat{\mathbf{n}} \times \mathbf{E} = \overline{\overline{Z}}(\mathbf{r}) \cdot (\hat{\mathbf{n}} \times \mathbf{H}) ,$$

where $\hat{\mathbf{n}}$ is the outward normal to the surface $S$ bounding the region of interest $V$ and

$$\overline{\overline{Z}}(\mathbf{r}) = \begin{bmatrix} \hat{\mathbf{s}}_1 z_{11} \hat{\mathbf{s}}_1 & \hat{\mathbf{s}}_1 z_{12} \hat{\mathbf{s}}_2 \\ \hat{\mathbf{s}}_2 z_{21} \hat{\mathbf{s}}_1 & \hat{\mathbf{s}}_2 z_{22} \hat{\mathbf{s}}_2 \end{bmatrix} .$$

$\hat{\mathbf{s}}_1$ and $\hat{\mathbf{s}}_2$ are unit vectors tangential to the surface $S$ such that $\hat{\mathbf{s}}_1$, $\hat{\mathbf{s}}_2$, and $\hat{\mathbf{n}}$ form right-handed orthogonal coordinates and $z_{ij}$ are real constants. Denote $\mathbf{E} = E_1\hat{\mathbf{s}}_1 + E_2\hat{\mathbf{s}}_2 + E_n\hat{\mathbf{s}}_n$ and $\mathbf{H} = H_1\hat{\mathbf{s}}_1 + H_2\hat{\mathbf{s}}_2 + H_n\hat{\mathbf{s}}_n$.

**(a)** Show that

$$E_1 = -z_{21}H_2 + z_{22}H_1$$

and

$$E_2 = z_{11}H_2 - z_{12}H_1 .$$

**(b)** Determine the condition for elements $z_{ij}$ such that the uniqueness theorem holds.

**2.17** A Tellegen medium is a homogeneous medium with constitutive relations

$$\mathbf{D} = \varepsilon\mathbf{E} + \xi\mathbf{H}$$

and

$$\mathbf{B} = \xi\mathbf{E} + \mu\mathbf{H}\,.$$

Consider a special case of a Tellegen medium with $\varepsilon = Mq,\ \xi = q$, and $\mu = q/M$.

**(a)** Show that in the limit as $q \to \infty$ the constitutive relations simplify to $\mathbf{D} = M\mathbf{B}$ and $\mathbf{H} = -M\mathbf{E}$. (*Hint:* Field quantities must remain finite.) Assume $q \to \infty$ for the rest of this problem.

**(b)** Show that the Poynting vector vanishes at all points within such a medium. Using the Poynting theorem, show that for time-varying cases, the stored field energy densities are zero in the absence of sources within the medium.

**(c)** Consider an interface between such a medium and free space. Show that the following boundary conditions must hold at the interface:

$$\hat{\mathbf{n}} \times (\mathbf{H} + M\mathbf{E}) = 0$$

and

$$\hat{\mathbf{n}} \cdot (\mathbf{D} - M\mathbf{B}) = 0\,.$$

| Medium 1 | Medium 2 |
|---|---|
| (Free space) | $\varepsilon = Mq$ |
| $\varepsilon_0$, $\mu_0$ | $\xi = q$ |
| | $\mu = q/M$ |

**(d)** Consider an electric charge $Q_1$ at a distance $d$ from a half-space region (Medium 2). Show that the above boundary conditions can be satisfied if the medium is replaced with two overlaying magnetic and electric charges $Q_2$ and $Q_{2\mathrm{m}}$. Find the values of $Q_2$ and $Q_{2\mathrm{m}}$. (*Hint:* Use Coulomb's law and its dual. Also assume that the interface is at the $x$–$y$ plane, $Q_1$ is placed at $\mathbf{r}_1 = d\hat{\mathbf{z}}$, and $Q_2$ and $Q_{2\mathrm{m}}$ are placed at $\mathbf{r}_2 = -d\hat{\mathbf{z}}$.)

**(e)** Using the uniqueness theorem and the results of part (d), show that image theory can be used to find the solution for an electric current source $\mathbf{J}$ in front of Medium 2. Find the equivalent image currents.

**(f)** Using duality and the results of part (e), find the equivalent image currents for a magnetic current source $\mathbf{J}_{\mathrm{m}}$. Note that the media should not change under the duality transformations.

**(g)** Comment on your results for the special cases of $M = 0,\ M = \infty$, and $M\eta_0 = 1$.

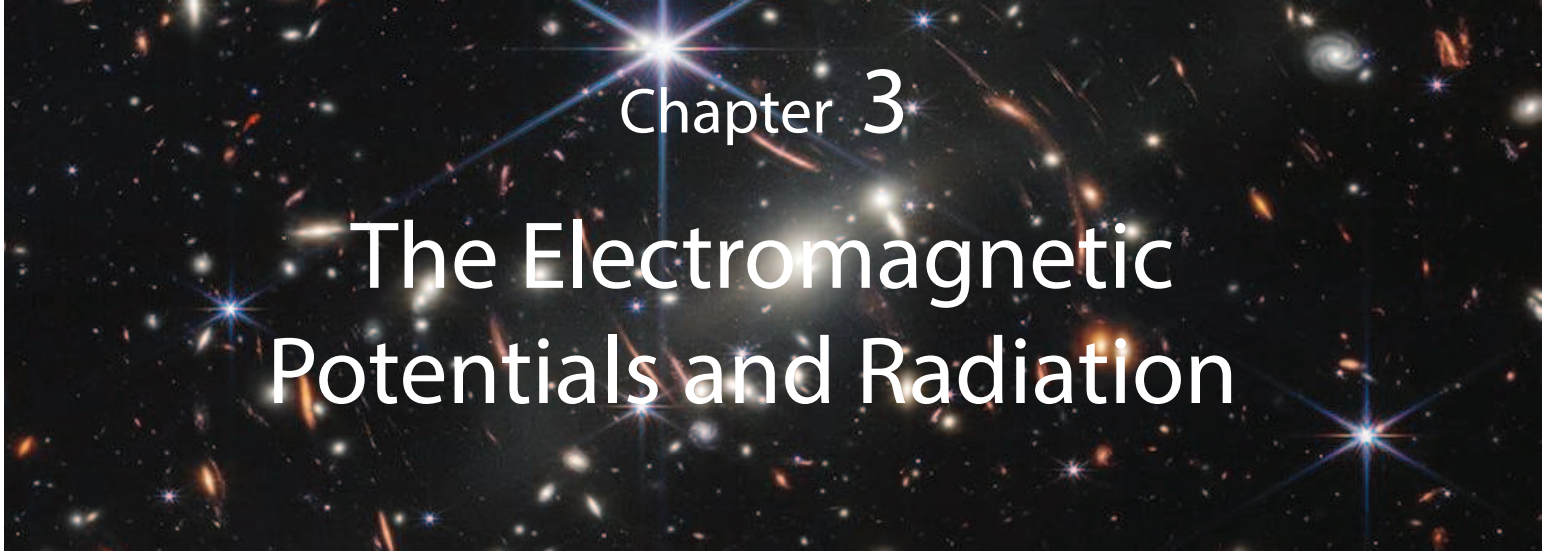

# Chapter 3
# The Electromagnetic Potentials and Radiation

## Chapter Contents


Overview, 108
3-1 Electromagnetic Potentials, 108
3-2 Time-Harmonic Electromagnetic Waves, 122
3-3 Time-Harmonic Retarded Potential, 131
3-4 Far-Field Distance Criterion, 137
3-5 Small Loop of Current: A Hertzian Magnetic Dipole, 139
3-6 Wire Antennas, 144
3-7 Equivalent Circuit for Receiving Antennas, 147
Chapter Summary, 150
Problems, 152


## Objectives

Upon learning the material presented in this chapter, you should be able to:

1. Calculate the radiated electromagnetic fields in a bounded homogeneous medium, given any arbitrary distribution of electric and magnetic currents.
2. Work with the reduced form of Maxwell's equations for time-harmonic sources and fields.
3. Apply the complex Poynting theorem to evaluate the power radiated by antennas of known current distributions.
4. Understand the notion of equivalent current for transmitting and receiving antennas and the far-field criteria for small and large antennas.
5. Explain the equivalence between a small current loop and a magnetic Hertzian dipole perpendicular to the loop surface.

## Overview

The intent of this chapter is to develop a procedure for solving Maxwell's equations to obtain explicit solutions for the electric and magnetic fields in a homogeneous, isotropic, and unbounded medium. In general, the solution to the four-dimensional (space-time) coupled Maxwell's equations, even for a homogeneous and unbounded medium, cannot be derived directly for arbitrary source functions (electric and magnetic currents). To facilitate the solution process, electromagnetic potentials, including electric and magnetic scalar potentials as well as magnetic and electric vector potentials, are defined from which the electric and magnetic fields can be evaluated. It is also shown that such potentials satisfy the wave equation common to all of the aforementioned potential functions. To develop an intuitive approach for the solution of wave equations, the solution for the scalar electric potential for a point charge varying with time dependence $f(t)$ is derived and shown to take the form of $f(t-r/\mathbf{u}_{\rm p})/r$, which represents a wave traveling in space with wave velocity $\mathbf{u}_{\rm p}=1/\sqrt{\mu\varepsilon}$. This result is extrapolated to arrive at general solutions for all potentials associated with arbitrary charge and current distributions, which provides a recipe for field computation for any antenna, so long as the current distributions are known. The notion of the far field for an antenna is introduced, and it is shown that simple expressions can be obtained for the field quantities in terms of current distributions. To further simplify Maxwell's equations, the notion of time-harmonic electromagnetic waves is introduced to reduce the dimensionality of the equations from four (time plus three spatial variables) down to only the three spatial variables. Time-harmonic expressions for the time-average Poynting vector and the stored electric and magnetic energy densities are also obtained and used in the derivation of the complex Poynting theorem, which establishes the law of conservation of energy for time-harmonic fields. Using the time-harmonic expressions for the potentials, we are able to examine the radiation characteristics of basic antennas, such as the Hertzian dipole and wire antennas. Also, an equivalent circuit model for an antenna is introduced and shown to be equally applicable in both the transmitting and receiving modes.

## 3-1 Electromagnetic Potentials

The coupled differential equations provided by Maxwell's equations must be solved for a given set of impressed currents and charges, subject to a set of specific boundary conditions. To arrive at a solution, the set of Maxwell's equations must be simplified as much as possible without losing any embedded information or relation between the EM fields and the associated currents and charges. A viable approach to that end is to make use of electromagnetic vector and scalar potentials. To start, we consider a homogeneous unbounded medium that includes volumetric electric current and charge densities, $\mathbf{J}$ and $\rho$, respectively. At every ordinary point in the medium of interest, the following relationships are applicable:

$$\nabla\times\mathbf{E}=-\frac{\partial\mathbf{B}}{\partial t}\,, \tag{3.1a}$$

$$\nabla\times\mathbf{H}=\frac{\partial\mathbf{D}}{\partial t}+\mathbf{J}\,, \tag{3.1b}$$

$$\nabla\cdot\mathbf{B}=0\,, \tag{3.1c}$$

$$\nabla \cdot \mathbf{D} = \rho \ . \tag{3.1d}$$

Starting from Eq. (3.1c) and noting that $\nabla \cdot \nabla \times \mathbf{A} = 0$ for any arbitrary vector $\mathbf{A}$, it can be concluded that

$$\mathbf{B} = \nabla \times \mathbf{A} \tag{3.2}$$

for some hitherto unknown vector potential that will be referred to as the ***magnetic vector potential***. It should be noted that Eq. (3.2) is not unique; that is, vector $\mathbf{A}' = \mathbf{A} + \nabla\psi$ also satisfies Eq. (3.2) since $\nabla \times \nabla\psi = 0$ for all scalar functions $\psi$. To uniquely define the magnetic vector potential, we need to not only satisfy Eq. (3.2), but to also specify $\nabla \cdot \mathbf{A}$.

Substituting Eq. (3.2) into Eq. (3.1a) gives

$$\nabla \times \left( \mathbf{E} + \frac{\partial \mathbf{A}}{\partial t} \right) = 0 \ , \tag{3.3}$$

which implies

$$\mathbf{E} + \frac{\partial \mathbf{A}}{\partial t} = -\nabla \Phi$$

for some scalar function $\Phi$, known as the ***electric scalar potential***. If $\mathbf{A}$ and $\Phi$ can be determined, then the magnetic flux density $\mathbf{B}$ can be obtained from Eq. (3.2) and the electric field can be obtained from

$$\mathbf{E} = -\nabla \Phi - \frac{\partial \mathbf{A}}{\partial t} \ . \tag{3.4}$$

For a simple homogeneous and isotropic medium we have

$$\mathbf{D} = \varepsilon \mathbf{E} \qquad \text{and} \qquad \mathbf{B} = \mu \mathbf{H} \ ,$$

and therefore the electric flux density and magnetic field can be obtained from

$$\mathbf{D} = -\varepsilon \left( \nabla \Phi + \frac{\partial \mathbf{A}}{\partial t} \right) \tag{3.5a}$$

and

$$\mathbf{H} = \frac{1}{\mu} \nabla \times \mathbf{A} \ . \tag{3.5b}$$

Substituting Eqs. (3.5a) and (3.5b) into Eq. (3.1b) leads to

$$\frac{1}{\mu} \nabla \times \nabla \times \mathbf{A} = -\varepsilon \nabla \frac{\partial \Phi}{\partial t} - \varepsilon \frac{\partial^2 \mathbf{A}}{\partial t^2} + \mathbf{J} \ ,$$

or equivalently

$$\nabla \times \nabla \times \mathbf{A} + \mu\varepsilon \frac{\partial^2 \mathbf{A}}{\partial t^2} + \mu\varepsilon \nabla \frac{\partial \Phi}{\partial t} = \mu \mathbf{J} \ . \tag{3.6}$$

Also, substituting Eq. (3.5a) into Eq. (3.1d) leads to

$$\nabla^2\Phi + \nabla\cdot\frac{\partial \mathbf{A}}{\partial t} = -\frac{\rho}{\varepsilon}\,. \tag{3.7}$$

Noting that for any vector $\mathbf{A}$, $\nabla\times\nabla\times\mathbf{A} = \nabla\nabla\cdot\mathbf{A} - \nabla^2\mathbf{A}$, Eq. (3.6) can be rewritten as

$$-\nabla^2\mathbf{A} + \mu\varepsilon\frac{\partial^2\mathbf{A}}{\partial t^2} + \nabla\left(\nabla\cdot\mathbf{A} + \mu\varepsilon\frac{\partial\Phi}{\partial t}\right) = \mu\mathbf{J}\,. \tag{3.8}$$

As noted earlier, we still need to specify $\nabla\cdot\mathbf{A}$. For simplicity we define

$$\nabla\cdot\mathbf{A} = -\mu\varepsilon\frac{\partial\Phi}{\partial t}\,. \tag{3.9}$$

This relationship is known as the ***Lorenz gauge condition***. Hence

$$\nabla^2\mathbf{A} - \mu\varepsilon\frac{\partial^2\mathbf{A}}{\partial t^2} = -\mu\mathbf{J}\,. \tag{3.10}$$

Also, substituting Eq. (3.9) into Eq. (3.7) leads to

$$\nabla^2\Phi - \mu\varepsilon\frac{\partial^2\Phi}{\partial t^2} = -\frac{\rho}{\varepsilon}\,. \tag{3.11}$$

Equations (3.10) and (3.11) represent wave equations of similar form, except that $\mathbf{A}$ is a vector and $\Phi$ is a scalar. In a Cartesian coordinate system,

$$\nabla^2\mathbf{A} = \nabla^2 A_x\hat{\mathbf{x}} + \nabla^2 A_y\hat{\mathbf{y}} + \nabla^2 A_z\hat{\mathbf{z}}\,.$$

Hence, Eq. (3.10) represents three scalar wave equations similar to Eq. (3.11), given by

$$\nabla^2 A_x - \mu\varepsilon\frac{\partial^2 A_x}{\partial t^2} = -\mu J_x\,, \tag{3.12a}$$

$$\nabla^2 A_y - \mu\varepsilon\frac{\partial^2 A_y}{\partial t^2} = -\mu J_y\,, \tag{3.12b}$$

$$\nabla^2 A_z - \mu\varepsilon\frac{\partial^2 A_z}{\partial t^2} = -\mu J_z\,. \tag{3.12c}$$

If the solution to Eq. (3.11) is known, as will be demonstrated in future sections, the solution to Eq. (3.12) can be obtained by replacing $\rho$ with $\mu\varepsilon J_{\mathrm{i}}$ and $\Phi$ with $A_{\mathrm{i}}$ for $i = x$, $y$, or $z$. The relation between $\mathbf{A}$ and $\Phi$ is also determined by the gauge condition of Eq. (3.9).

### 3-1.1 Hertz Vector Potential

The idea behind developing a vector potential different from the vector potential **A** introduced earlier is to see if a single potential can be defined so that all field quantities can be derived from it directly. Hertz defined such a vector potential $\mathbf{\Pi}$ such that

$$\mathbf{A} = \mu\varepsilon \frac{\partial \mathbf{\Pi}}{\partial t} . \tag{3.13}$$

Hence, according to Eq. (3.9), the scalar electric potential in terms of the Hertz vector potential is given by

$$\Phi = -\nabla \cdot \mathbf{\Pi} . \tag{3.14}$$

From Eq. (3.2),

$$\mathbf{B} = \mu\varepsilon \nabla \times \frac{\partial \mathbf{\Pi}}{\partial t} , \tag{3.15a}$$

or equivalently

$$\mathbf{H} = \varepsilon \nabla \times \frac{\partial \mathbf{\Pi}}{\partial t} , \tag{3.15b}$$

and using Eq. (3.4),

$$\mathbf{E} = \nabla\nabla \cdot \mathbf{\Pi} - \mu\varepsilon \frac{\partial^2 \mathbf{\Pi}}{\partial t^2} . \tag{3.16}$$

It is now obvious that both **E** and **H** can be directly computed once $\mathbf{\Pi}$ has been characterized. To find an equation for $\mathbf{\Pi}$, we note that from Eqs. (3.15a) and (3.16), the modified Ampère's law can be written as

$$\nabla \times \mathbf{H} = \varepsilon \frac{\partial}{\partial t} \nabla \times \nabla \times \mathbf{\Pi} = \varepsilon \frac{\partial}{\partial t} \left( \nabla\nabla \cdot \mathbf{\Pi} - \mu\varepsilon \frac{\partial^2 \mathbf{\Pi}}{\partial t^2} \right) + \mathbf{J} , \tag{3.17a}$$

which can be compacted into

$$\frac{\partial}{\partial t} \left( \nabla \times \nabla \times \mathbf{\Pi} - \nabla\nabla \cdot \mathbf{\Pi} + \mu\varepsilon \frac{\partial^2 \mathbf{\Pi}}{\partial t^2} \right) = \frac{\mathbf{J}}{\varepsilon} , \tag{3.17b}$$

or, using the vector identity $\nabla \times \nabla \times \mathbf{\Pi} - \nabla \cdot \nabla \mathbf{\Pi} = -\nabla^2 \mathbf{\Pi}$,

$$\nabla^2 \mathbf{\Pi} - \mu\varepsilon \frac{\partial^2 \mathbf{\Pi}}{\partial t^2} = -\frac{1}{\varepsilon} \int \mathbf{J}\, dt , \tag{3.18}$$

which indicates that the Hertz vector potential also satisfies the vector wave equation.

### 3-1.2 Potentials for Magnetic Sources

Let us consider a scenario where only magnetic current and charge distributions are present. For such a case, Maxwell's equations can be written as

$$\nabla \times \mathbf{E} = -\frac{\partial \mathbf{B}}{\partial t} - \mathbf{J}_{\mathrm{m}} \,, \tag{3.19a}$$

$$\nabla \times \mathbf{H} = \frac{\partial \mathbf{D}}{\partial t} \,, \tag{3.19b}$$

$$\nabla \cdot \mathbf{D} = 0 \,, \tag{3.19c}$$

$$\nabla \cdot \mathbf{B} = \rho_{\mathrm{m}} \,. \tag{3.19d}$$

Obviously Eq. (3.19a) is the dual of Eq. (3.1b), Eq. (3.19b) is the dual of Eq. (3.1a), Eq. (3.19c) is the dual of Eq. (3.1c), and finally Eq. (3.19d) is the dual of Eq. (3.1d). The ***electric vector potential*** $\mathbf{A}_{\mathrm{m}}$ is now defined as the dual of the magnetic vector potential $\mathbf{A}$, which is defined as the dual of Eq. (3.2) and is given by

$$\mathbf{D} = -\nabla \times \mathbf{A}_{\mathrm{m}} \,. \tag{3.20}$$

Also, the magnetic scalar potential is defined as $\Phi_{\mathrm{m}}$, the dual of the electric scalar potential $\Phi$. Applying the duality relation to Eq. (3.4) gives

$$\mathbf{H} = -\nabla \Phi_{\mathrm{m}} - \frac{\partial \mathbf{A}_{\mathrm{m}}}{\partial t} \,. \tag{3.21}$$

Following a similar procedure, it can be easily shown that the electric vector potential and the magnetic scalar potential satisfy the following wave equations:

$$\nabla^2 \mathbf{A}_{\mathrm{m}} - \mu\varepsilon \frac{\partial^2 \mathbf{A}_{\mathrm{m}}}{\partial t^2} = -\varepsilon \mathbf{J}_{\mathrm{m}} \tag{3.22a}$$

and

$$\nabla^2 \Phi_{\mathrm{m}} - \mu\varepsilon \frac{\partial^2 \Phi_{\mathrm{m}}}{\partial t^2} = -\frac{\rho_{\mathrm{m}}}{\mu} \,, \tag{3.22b}$$

which are the duals of Eqs. (3.10) and (3.11), respectively.

Using the duality relations, we define the ***magnetic Hertz vector potential*** as $\boldsymbol{\Pi}_{\mathrm{m}}$, which satisfies the following wave equation:

$$\nabla^2 \boldsymbol{\Pi}_{\mathrm{m}} - \mu\varepsilon \frac{\partial^2 \boldsymbol{\Pi}_{\mathrm{m}}}{\partial t^2} = -\frac{1}{\mu} \int \mathbf{J}_{\mathrm{m}} \, dt \,. \tag{3.23}$$

The electric and magnetic fields can be obtained in terms of $\mathbf{\Pi}_m$ by applying the duality relations to Eq. (3.15a) and Eq. (3.16), respectively:

$$\mathbf{E} = -\mu \nabla \times \frac{\partial \mathbf{\Pi}_m}{\partial t} \tag{3.24a}$$

and

$$\mathbf{H} = \nabla\nabla \cdot \mathbf{\Pi}_m - \mu\varepsilon \frac{\partial^2 \mathbf{\Pi}_m}{\partial t^2} \, . \tag{3.24b}$$

### 3-1.3 Electric and Magnetic Fields in Terms of Potentials: The Most General Case

Consider a homogeneous medium with constitutive parameters $\mu, \varepsilon$ and time-varying electric and magnetic current distributions $\mathbf{J}$ and $\mathbf{J}_m$. As was shown in previous sections, the electric and magnetic fields can be obtained from the electromagnetic potentials when either electric or magnetic current distributions exist. Using the linearity property of Maxwell's equations, the solution to the simultaneous existence of both electric and magnetic sources can be obtained using the superposition principle. Suppose $\mathbf{A}$ and $\Phi$ are the solutions for the magnetic vector and electric scalar potentials generated by $\mathbf{J}$ and $\rho$, and $\mathbf{A}_m$ and $\Phi_m$ are those generated by $\mathbf{J}_m$ and $\rho_m$, then the total magnetic and electric fields are given by

$$\mathbf{H} = \frac{1}{\mu} \nabla \times \mathbf{A} - \frac{\partial \mathbf{A}_m}{\partial t} - \nabla \Phi_m \tag{3.25a}$$

and

$$\mathbf{E} = -\frac{1}{\varepsilon} \nabla \times \mathbf{A}_m - \frac{\partial \mathbf{A}}{\partial t} - \nabla \Phi \, . \tag{3.25b}$$

Similarly, there are also electric and magnetic Hertz vector potentials associated with $\mathbf{J}$ and $\mathbf{J}_m$. Using the superposition principle, the total electric and magnetic fields in terms of $\mathbf{\Pi}$ and $\mathbf{\Pi}_m$ are given by

$$\mathbf{E} = \nabla\nabla \cdot \mathbf{\Pi} - \mu\varepsilon \frac{\partial^2 \mathbf{\Pi}}{\partial t^2} - \mu \nabla \times \left( \frac{\partial \mathbf{\Pi}_m}{\partial t} \right) \tag{3.26a}$$

and

$$\mathbf{H} = \nabla\nabla \cdot \mathbf{\Pi}_m - \mu\varepsilon \frac{\partial^2 \mathbf{\Pi}_m}{\partial t^2} + \varepsilon \nabla \times \left( \frac{\partial \mathbf{\Pi}}{\partial t} \right) \, . \tag{3.26b}$$

### 3-1.4 Solution of Wave Equation (Retarded Potential)

To demonstrate the application of potentials, we consider the simple example of a point charge at the origin. According to Eq. (3.11) the potentials generated by the charge must satisfy

$$\nabla^2 \Phi - \mu\varepsilon \frac{\partial^2 \Phi}{\partial t^2} = -\frac{\rho}{\varepsilon} \, , \tag{3.27}$$

where in this case

$$\rho(\mathbf{r}) = Q\,\delta(\mathbf{r})\,, \tag{3.28}$$

where $Q$ is the magnitude of the charge and $\delta(\mathbf{r})$ is a delta function specifying that the charge is located at the origin of a coordinate system. First it is noted that the problem has spherical symmetry; that is, $\Phi(r,\theta,\phi) = \Phi(r)$. Therefore $\frac{\partial\Phi}{\partial\theta} = \frac{\partial\Phi}{\partial\phi} = 0$ and

$$\nabla^2\Phi = \frac{1}{r^2}\frac{\partial}{\partial r}\left(r^2\frac{\partial\Phi}{\partial r}\right)\,. \tag{3.29}$$

By introducing the ***regular function*** $\psi(r) = r\Phi(r)$, it can easily be shown that

$$\nabla^2\Phi = \frac{1}{r}\frac{\partial^2\psi}{\partial r^2}\,. \tag{3.30}$$

Equation (3.27) can then be written as

$$\frac{\partial^2\psi}{\partial r^2} - \mu\varepsilon\frac{\partial^2\psi}{\partial t^2} = -\frac{Q}{\varepsilon}\,r\,\delta(\mathbf{r})\,. \tag{3.31}$$

Excluding the location $r = 0$, $\psi$ must satisfy

$$\frac{\partial^2\psi}{\partial r^2} - \mu\varepsilon\frac{\partial^2\psi}{\partial t^2} = 0\,. \tag{3.32}$$

Any function of the form $f(t - r\sqrt{\mu\varepsilon})$ satisfies Eq. (3.32) because it can be shown that

$$\frac{\partial^2 f}{\partial r^2} = \mu\varepsilon f'' \tag{3.33a}$$

and

$$\frac{\partial^2 f}{\partial t^2} = f''\,. \tag{3.33b}$$

The magnitude of the function at a distance $r+\Delta r$ at a later time $t+\Delta t$ is

$$\psi(r+\Delta r,\ \ t+\Delta t) = f(t+\Delta t - (r+\Delta r)\sqrt{\mu\varepsilon})\,.$$

So if $\frac{\Delta r}{\Delta t} = \frac{1}{\sqrt{\mu\varepsilon}}$, then

$$\psi(r+\Delta r,\ \ t+\Delta t) = \psi(r,t)\,. \tag{3.34}$$

This indicates that $\psi(r,t)$ is a propagating signal that has a propagation velocity $\mathbf{u}_\mathrm{p} = \frac{1}{\sqrt{\mu\varepsilon}}$. That is, the scalar potential

$$\Phi(r,t) = \frac{1}{r}\,f(t - r\sqrt{\mu\varepsilon}) \tag{3.35}$$

is a wave. To determine $f(t,r)$, let us examine the quasi-static behavior of the electric potential. Coulomb's equation for the potential due to a point charge $Q(t)$ can be used and

is given by

$$\Phi(r,t) = \frac{Q(t)}{4\pi\varepsilon r} \,. \tag{3.36}$$

By comparing Eqs. (3.35) and (3.36), it is obvious that

$$f(t) = \frac{Q(t)}{4\pi\varepsilon} \,. \tag{3.37}$$

Hence in general, for a time-varying function

$$\Phi(r,t) = \frac{Q\left(t - \dfrac{r}{u_\mathrm{p}}\right)}{4\pi\varepsilon r} \,, \tag{3.38}$$

if the point charge is located at $\mathbf{r}'$, then

$$\Phi(r,t) = \frac{Q\left(t - \dfrac{|\mathbf{r}-\mathbf{r}'|}{u_\mathrm{p}}\right)}{4\pi\varepsilon|\mathbf{r}-\mathbf{r}'|} \,. \tag{3.39}$$

For a distribution of charge density $\rho_\mathrm{v}(\mathbf{r}',t)$, the potential can be obtained from

$$\Phi(r,t) = \frac{1}{4\pi\varepsilon} \iiint_v \frac{\rho_\mathrm{v}(\mathbf{r}',\, t - |\mathbf{r}-\mathbf{r}'|/u_\mathrm{p})}{|\mathbf{r}-\mathbf{r}'|}\, d\mathbf{r}' \,. \tag{3.40}$$

Equation (3.40) was obtained somewhat heuristically, but it can also be obtained from Eq. (3.27) rigorously. Comparing Eq. (3.27) with Eq. (3.12), and noting the similarity of the differential equations, the solution for the vector magnetic potential is deduced to be

$$\mathbf{A}(r,t) = \frac{\mu}{4\pi} \iiint_v \frac{\mathbf{J}(\mathbf{r}',\, t - |\mathbf{r}-\mathbf{r}'|/u_\mathrm{p})}{|\mathbf{r}-\mathbf{r}'|}\, d\mathbf{r}' \,. \tag{3.41}$$

The corresponding electric and magnetic fields can be obtained from Eqs. (3.4).

### 3-1.5 Radiated Field from an Infinitesimal Current Element

Let us consider a very small electric current filament located at the origin of a Cartesian coordinate system with an orientation along $d\boldsymbol{\ell}$, as shown in Fig. 3-1. The volumetric current distribution for this current can be mathematically represented by

$$\mathbf{J}(\mathbf{r},t) = I_0\, d\boldsymbol{\ell}\, \delta(\mathbf{r})\, f(t) \,. \tag{3.42}$$

For this current, the retarded vector potential is found to be

$$\mathbf{A}(\mathbf{r},t) = \frac{\mu I_0\, d\boldsymbol{\ell}}{4\pi r}\, f\left(t - \frac{r}{u_\mathrm{p}}\right) \,. \tag{3.43}$$

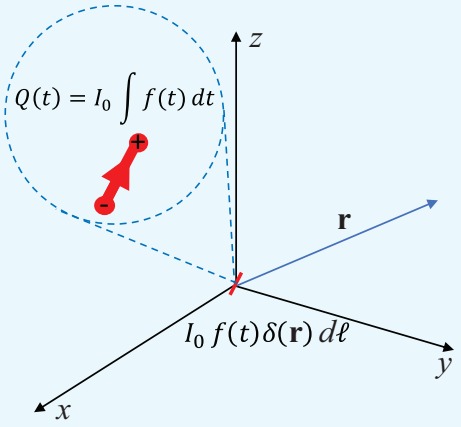


**Figure 3-1:** A very small electric current filament at the origin of the Cartesian coordinate system carries current $I_0\, f(t)$. Also shown in the expanded picture is the current filament and the instantaneous charge accumulations at both ends of the wire.

According to Eq. (3.5b)

$$\mathbf{H} = \frac{I_0}{4\pi} \nabla \times \left[ \frac{d\boldsymbol{\ell}}{r} f\left(t - \frac{r}{u_\mathrm{p}}\right) \right] , \tag{3.44}$$

and since $d\boldsymbol{\ell}$ is a constant vector

$$\mathbf{H} = \frac{I_0}{4\pi} \nabla \left[ \frac{1}{r} f\left(t - \frac{r}{u_\mathrm{p}}\right) \right] \times d\boldsymbol{\ell} \, . \tag{3.45}$$

Also noting that $\nabla f[g(r)] = f' \nabla g$ (for a single variable scalar function $f$), $\nabla r = \hat{\mathbf{r}}$, and $\nabla(1/r) = (-\hat{\mathbf{r}}/r^2)$, it can be easily shown that

$$\mathbf{H} = \frac{I_0}{4\pi} \left[ f'\left(t - \frac{r}{u_\mathrm{p}}\right) \frac{1}{u_\mathrm{p} r} + f\left(t - \frac{r}{u_\mathrm{p}}\right) \frac{1}{r^2} \right] d\boldsymbol{\ell} \times \hat{\mathbf{r}} \, . \tag{3.46}$$

The second term corresponds to the quasi-static solution (wherein $f' \approx 0$), which is the familiar Biot-Savart law that provides the magnetic field intensity generated by a small segment of wire carrying an electric current $I_0$.

As we will show later, the first term inside the square bracket, which varies as $\frac{1}{r}$, is the propagating component of the field that carries with it electromagnetic energy. It is interesting to note that the radiated magnetic field is proportional to the time derivative of the excitation current function. This indicates that a *current* that does not vary with time cannot radiate an electromagnetic field.

The electric field can be obtained from

$$\mathbf{E} = -\nabla \Phi - \frac{\partial \mathbf{A}}{\partial t} \, , \tag{3.47}$$

which requires knowledge of the electric scalar potential. The electric scalar potential can be obtained from the gauge condition given by Eq. (3.9). Using Eq. (3.43), we have

$$\begin{aligned}\nabla\cdot\mathbf{A} &= \frac{\mu I_0}{4\pi}\,\nabla\cdot\left(\frac{f(t-r/u_\mathrm{p})\,d\boldsymbol{\ell}}{r}\right)\\ &= -\frac{\mu I_0}{4\pi}\left(f'(t-r/u_\mathrm{p})\,\frac{1}{u_\mathrm{p}r}+f(t-r/u_\mathrm{p})\,\frac{1}{r^2}\right)\hat{\mathbf{r}}\cdot d\boldsymbol{\ell}\,.\end{aligned}\tag{3.48}$$

From the gauge condition we have

$$\frac{\partial\Phi}{\partial t} = -\frac{\nabla\cdot\mathbf{A}}{\mu\varepsilon}\,,\tag{3.49}$$

which leads to

$$\Phi(\mathbf{r},t) = \frac{I_0}{4\pi\varepsilon}\left[f\left(t-\frac{r}{u_\mathrm{p}}\right)\frac{1}{u_\mathrm{p}r}+\int f\,dt\,\frac{1}{r^2}\right]\hat{\mathbf{r}}\cdot d\boldsymbol{\ell}\,.\tag{3.50}$$

To compute $\mathbf{E}(\mathbf{r},t)$, $\nabla\Phi$ is needed, which after some algebraic manipulation, it is shown that

$$\nabla\Phi = \frac{I_0}{4\pi\varepsilon_0}\left[-\hat{\mathbf{r}}\left(\frac{f'}{u_\mathrm{p}^2r}+\frac{2f}{u_\mathrm{p}r^2}+\frac{2\int f\,dt}{r^3}\right)(\hat{\mathbf{r}}\cdot d\boldsymbol{\ell})+\left(\frac{f}{u_\mathrm{p}r}+\frac{\int f\,dt}{r^2}\right)\nabla(\hat{\mathbf{r}}\cdot d\boldsymbol{\ell})\right]\,,\tag{3.51}$$

and therefore

$$\mathbf{E} = \frac{I_0}{4\pi\varepsilon}\left[\hat{\mathbf{r}}\left(\frac{f'}{u_\mathrm{p}^2r}+\frac{2f}{u_\mathrm{p}r^2}+\frac{2\int f\,dt}{r^3}\right)(\hat{\mathbf{r}}\cdot d\boldsymbol{\ell})-\left(\frac{f}{u_\mathrm{p}r}+\frac{\int f\,dt}{r^2}\right)\nabla(\hat{\mathbf{r}}\cdot d\boldsymbol{\ell})\right]-\frac{\mu I_0}{4\pi}\,\frac{f'}{r}\,d\boldsymbol{\ell}\,.\tag{3.52}$$

It can also be shown that $\nabla(\hat{\mathbf{r}}\cdot d\boldsymbol{\ell})$ is proportional to $\frac{1}{r}$. In fact, after some algebraic manipulation, it can be shown that

$$\nabla(\hat{\mathbf{r}}\cdot\boldsymbol{\ell}) = \frac{1}{r}\,\hat{\mathbf{r}}\times(d\boldsymbol{\ell}\times\hat{\mathbf{r}})\,.\tag{3.53}$$

Denoting $d\boldsymbol{\ell} = \hat{\mathbf{r}}\times(d\boldsymbol{\ell}\times\hat{\mathbf{r}})+(d\boldsymbol{\ell}\cdot\hat{\mathbf{r}})\hat{\mathbf{r}}$ and recalling that $1/u_\mathrm{p}^2 = \mu\varepsilon$, it can be easily shown that

$$\mathbf{E} = \frac{I_0}{2\pi\varepsilon}\left(\frac{f}{u_\mathrm{p}r^2}+\frac{\int f\,dt}{r^3}\right)(\hat{\mathbf{r}}\cdot d\boldsymbol{\ell})\hat{\mathbf{r}}-\frac{I_0}{4\pi}\left(\frac{\sqrt{\mu/\varepsilon}\,f}{r^2}+\frac{\int f\,dt}{\varepsilon r^3}+\frac{\mu f'}{r}\right)\hat{\mathbf{r}}\times(d\boldsymbol{\ell}\times\hat{\mathbf{r}})\,.\tag{3.54}$$

Noting that $I_0\int f(t)\,dt$ represents the instantaneous accumulated charge $Q(t)$ at the end of the filament, the terms with coefficient $1/r^3$ represent the field contribution from the electric dipole. The other terms, $1/r^2$ and $1/r$, are the electrodynamic terms. Specifically, terms proportional to $1/r^2$ result from the Biot-Savart component of the magnetic field. As noted earlier, at far distances from the source, such that only the $\frac{1}{r}$ term remains, the electric field does not have a radial component and is proportional to the time derivative of the current. Note that in such a "far-field" region, the electric field is proportional to the time derivative of

the current source as well. In the far-field region where $1/r \gg 1/r^2 \gg 1/r^3$,

$$\mathbf{H}(\mathbf{r},t) = \frac{I_0\sqrt{\mu\varepsilon}}{4\pi}\frac{f'(t-r/u_\mathrm{p})}{r}\,d\boldsymbol{\ell}\times\hat{\mathbf{r}} \tag{3.55a}$$

and **(far-field region)**

$$\mathbf{E}(\mathbf{r},t) = \frac{\mu I_0}{4\pi}\frac{f'(t-r/u_\mathrm{p})}{r}\,(d\boldsymbol{\ell}\times\hat{\mathbf{r}})\times\hat{\mathbf{r}}\,. \tag{3.55b}$$

It is obvious that no radiation takes place along the axis of the current filament ($d\boldsymbol{\ell}$); that is, both **E** and **H** are zero in the far-field region along the $d\boldsymbol{\ell}$ direction, and **E** and **H** are perpendicular to each other and to the direction of propagation $\hat{\mathbf{r}}$. It is also interesting to note that the ratio of the magnitude of **E** to that of **H** is independent of position and time and the constant of proportionality is given simply by

$$\frac{|\mathbf{E}|}{|\mathbf{H}|} = \sqrt{\frac{\mu}{\varepsilon}} = \eta\,. \tag{3.56}$$

This quantity has the unit of ohms (V/A) and is known as the ***characteristic impedance of the medium***.

## Example 3-1: Electric Field of an Electric Dipole

Derive an expression for the electric field generated by a static dipole with dipole moment $\mathbf{P} = Q\,d\boldsymbol{\ell}$ centered at the origin, as shown in Fig. 3-2.

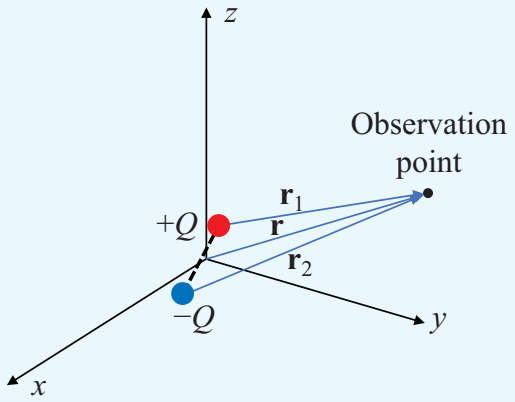


**Figure 3-2:** An electric dipole with dipole moment $\mathbf{P} = Q\,d\boldsymbol{\ell}$ centered at the origin of a coordinate surface.

**Solution:** The electric scalar potential associated with the positive and negative charges is given by

$$\Phi(\mathbf{r}) = \frac{Q}{4\pi\varepsilon}\left(\frac{1}{r_1} - \frac{1}{r_2}\right) . \tag{3.57}$$

Noting that for very small $d\ell$, we can approximate $r_1$ and $r_2$ as

$$r_1 \approx r - \frac{d\boldsymbol{\ell}\cdot\hat{\mathbf{r}}}{2} \tag{3.58a}$$

and

$$r_2 \approx r + \frac{d\boldsymbol{\ell}\cdot\hat{\mathbf{r}}}{2} , \tag{3.58b}$$

and then conclude that

$$\frac{1}{r_1} \approx \frac{1}{r}\left(1 + \frac{d\boldsymbol{\ell}\cdot\hat{\mathbf{r}}}{2r}\right) \tag{3.59a}$$

and

$$\frac{1}{r_2} \approx \frac{1}{r}\left(1 - \frac{d\boldsymbol{\ell}\cdot\hat{\mathbf{r}}}{2r}\right) . \tag{3.59b}$$

Hence the electric scalar potential is given by

$$\Phi(\mathbf{r}) = \frac{Q}{4\pi\varepsilon}\frac{1}{r^2}\,(d\boldsymbol{\ell}\cdot\hat{\mathbf{r}}) . \tag{3.60}$$

The electric field can be obtained from

$$\mathbf{E}(\mathbf{r}) = -\nabla\Phi(\mathbf{r}) = -\frac{Q}{4\pi\varepsilon}\left(\frac{-2}{r^3}(d\boldsymbol{\ell}\cdot\hat{\mathbf{r}}) + \frac{1}{r^2}\,\nabla(d\boldsymbol{\ell}\cdot\hat{\mathbf{r}})\right) . \tag{3.61}$$

Using Eq. (3.53),

$$\mathbf{E}(\mathbf{r}) = \frac{Q}{4\pi\varepsilon}\left[\frac{2}{r^3}\,(d\boldsymbol{\ell}\cdot\hat{\mathbf{r}}) - \frac{1}{r^3}\hat{\mathbf{r}}\times(d\boldsymbol{\ell}\times\hat{\mathbf{r}})\right] . \tag{3.62}$$

Recognizing that $Q = I_0\int f(t)dt$, the field of the dipole is recognized as the two terms in Eq. (3.54) that vary as $1/r^3$.

### 3-1.6 E and H Fields Due to a Distribution of Electric Currents

The expressions for the magnetic and electric fields given by Eqs. (3.46) and (3.54) can be interpreted as the spatial impulse response of the medium (solution to an impulse function of position $\delta(\mathbf{r})$). Consider a time-varying current filament at $\mathbf{r}'$, as shown in Fig. 3-3. According to Eq. (3.46) the magnetic field produced by this current is given by

$$d\mathbf{H} = \frac{I_0}{4\pi}\left(\frac{f'(t-|\mathbf{r}-\mathbf{r}'|/u_\mathrm{p})}{u_\mathrm{p}|\mathbf{r}-\mathbf{r}'|} + \frac{f(t-|\mathbf{r}-\mathbf{r}'|/u_\mathrm{p})}{|\mathbf{r}-\mathbf{r}'|^2}\right) d\boldsymbol{\ell}\times\frac{(\mathbf{r}-\mathbf{r}')}{|\mathbf{r}-\mathbf{r}'|} , \tag{3.63}$$

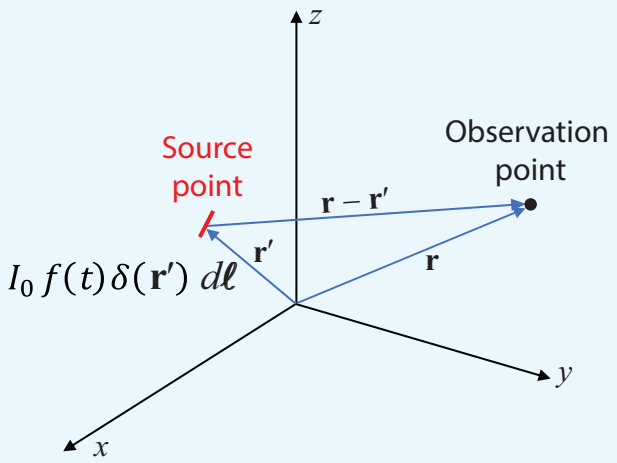


**Figure 3-3:** An infinitesimal time-varying current at $\mathbf{r}'$.

which is obtained from Eq. (3.46) upon substituting $|\mathbf{r}-\mathbf{r}'|$ for $r$ and $(\mathbf{r}-\mathbf{r}')/(|\mathbf{r}-\mathbf{r}'|)$ for $\hat{\mathbf{r}}$. Now let us consider an arbitrary distribution of line currents along a curve defined by $C$, as shown in Fig. 3-4. The current distribution is denoted by $I(\mathbf{r}',t)$. Using superposition, the

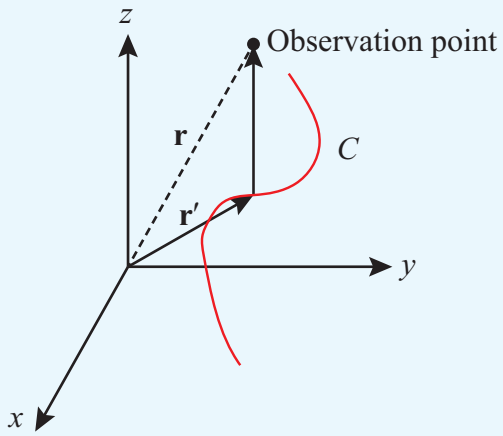


**Figure 3-4:** A wire carrying a time-varying current specified by curve $C$ in a general coordinate system.

magnetic field at the observation point is given by

$$\mathbf{H}=\frac{1}{4\pi}\int_C\left(\frac{I'(\mathbf{r}',t-|\mathbf{r}-\mathbf{r}'|/u_{\rm p})}{u_{\rm p}|\mathbf{r}-\mathbf{r}'|}+\frac{I(\mathbf{r}',t-|\mathbf{r}-\mathbf{r}'|/u_{\rm p})}{|\mathbf{r}-\mathbf{r}'|^2}\right)d\boldsymbol{\ell}'\times\frac{(\mathbf{r}-\mathbf{r}')}{|\mathbf{r}-\mathbf{r}'|}\,. \tag{3.64}$$

where $I'(\cdot) = \frac{\partial}{\partial t} I(\cdot)$. It is obvious that for this current distribution, the electric field can be obtained from Eq. (3.55b) in a similar manner. Duality relations can be used to find the electric and magnetic fields generated by a magnetic current distribution.

Instead of a line current, if the source is a surface or a volumetric current distribution, then we need to make the following substitutions for $I(\mathbf{r}',t)\,d\boldsymbol{\ell}'$:

$$I(\mathbf{r}',t)\,d\boldsymbol{\ell}' \quad\longrightarrow\quad \mathbf{J}_{\mathrm{s}}(\mathbf{r}',t)\,ds' \qquad \text{for surface current, and}$$
$$I(\mathbf{r}',t)\,d\boldsymbol{\ell}' \quad\longrightarrow\quad \mathbf{J}(\mathbf{r}',t)\,dv' \qquad \text{for volumetric current.}$$

For example, the magnetic field for a volumetric current distribution is given by

$$\mathbf{H} = \frac{1}{4\pi} \iiint_V \left( \frac{\mathbf{J}'(\mathbf{r}',t-|\mathbf{r}-\mathbf{r}'|/u_{\mathrm{p}})}{u_{\mathrm{p}}|\mathbf{r}-\mathbf{r}'|} + \frac{\mathbf{J}(\mathbf{r}',t-|\mathbf{r}-\mathbf{r}'|/u_{\mathrm{p}})}{|\mathbf{r}-\mathbf{r}'|^2} \right) \times \frac{(\mathbf{r}-\mathbf{r}')}{|\mathbf{r}-\mathbf{r}'|}\,dv' \,, \tag{3.65}$$

where $J'(\cdot) = \frac{\partial}{\partial t} J(\cdot)$. It is obvious that for a magnetic current distribution the electric field can be obtained from Eq. (3.65) using the duality relation.

The far-field expressions, which are valid at observation points far from the source, are much easier to compute. The far-field criterion is a condition that depends on the dimensions of the current source and the oscillation frequency. This will be discussed in more detail in Section 3-4. For the time being, let us assume that the observation point is in the far-field region of an electric current distribution $\mathbf{J}(r,t)$ and a magnetic current distribution $\mathbf{J}_{\mathrm{m}}(r,t)$. Using the expression given by Eq. (3.55a), Eq. (3.55b) in conjunction with the duality and superposition principles, we can find the total radiated electric and magnetic fields in a homogeneous nondispersive medium with constitutive parameters $\varepsilon$ and $\mu$ using

$$\begin{aligned}\mathbf{H}(\mathbf{r},t) = {} & \frac{\sqrt{\mu\varepsilon}}{4\pi} \iiint_{V_1} \frac{\mathbf{J}'(\mathbf{r}',t-|\mathbf{r}-\mathbf{r}'|/u_{\mathrm{p}})}{|\mathbf{r}-\mathbf{r}'|^2} \times (\mathbf{r}-\mathbf{r}')\,dv' \\ & + \frac{\varepsilon}{4\pi} \iiint_{V_2} \left( \frac{\mathbf{J}'_{\mathrm{m}}(\mathbf{r}',t-|\mathbf{r}-\mathbf{r}'|/u_{\mathrm{p}})}{|\mathbf{r}-\mathbf{r}'|^3} \times (\mathbf{r}-\mathbf{r}') \right) \times (\mathbf{r}-\mathbf{r}')\,dv'\end{aligned} \tag{3.66a}$$

and

$$\begin{aligned}\mathbf{E}(\mathbf{r},t) = {} & \frac{\mu}{4\pi} \iiint_{V_1} \left( \frac{\mathbf{J}'(\mathbf{r}',t-|\mathbf{r}-\mathbf{r}'|/u_{\mathrm{p}})}{|\mathbf{r}-\mathbf{r}'|^3} \times (\mathbf{r}-\mathbf{r}') \right) \times (\mathbf{r}-\mathbf{r}')\,dv' \\ & - \frac{\sqrt{\mu\varepsilon}}{4\pi} \iiint_{V_2} \frac{\mathbf{J}'_{\mathrm{m}}(\mathbf{r}',t-|\mathbf{r}-\mathbf{r}'|/u_{\mathrm{p}})}{|\mathbf{r}-\mathbf{r}'|^2} \times (\mathbf{r}-\mathbf{r}')\,dv' \,.\end{aligned} \tag{3.66b}$$

The expressions given by Eqs. (3.66a) and (3.66b) are the basic time-domain equations governing antenna radiation. Since $|\mathbf{r}| \gg |\mathbf{r}'|$, for simplicity $(\mathbf{r}-\mathbf{r}')$ is often approximated by $\mathbf{r}$ in the denominator and in the vector cross product terms of the integrands of Eqs. (3.66a) and (3.66b). However, this approximation cannot be used in the delay term $|\mathbf{r}-\mathbf{r}'|/u_{\mathrm{p}}$ of the argument of function $f'$ for fast time-varying functions.

## 3-2 Time-Harmonic Electromagnetic Waves

In the preceding sections, it was shown that electromagnetic field quantities and their related potentials can be expressed in terms of coupled partial differential equations in a general four-dimensional space-time vector space. It is often convenient to reduce the dimensionality by resorting to Fourier transformations. That is, the temporal behavior of field quantities can be removed by expressing the fields in the frequency domain and solving the resultant equations in the frequency domain first. In the time-domain treatment of Maxwell's equations, we have so far assumed the medium to be nondispersive. That is, the permittivity and permeability of the medium were assumed to be constant. In Section 1-4.3, it was shown that except for vacuum, all materials are dispersive and thus $\varepsilon$ and $\mu$ are functions of time. To circumvent this difficulty, we can resort to frequency-domain solutions of Maxwell's equations, which are discussed in this section. Once the solution in the frequency domain is obtained, using the linearity properties of Maxwell's equations and inverse Fourier transformations, the temporal behavior of the field quantities can then be reconstructed.

Strictly speaking, Fourier transformations can be applied to "energy" functions, i.e., functions that are square integrable. Basically, for a field quantity $\mathbf{E}(\mathbf{r},t)$ defined at all points in space we require

$$\int_{-\infty}^{+\infty} |\mathbf{E}(\mathbf{r},t)|^2 \, dt < \infty \, .$$

For simplicity, let us assume that all field quantities and source functions are square integrable functions of time and their Fourier transforms are well defined. The Fourier transform of $\mathbf{E}(\mathbf{r},t)$ is defined as

$$\widetilde{\mathbf{E}}(\mathbf{r},\omega) = \int_{-\infty}^{+\infty} \mathbf{E}(\mathbf{r},t)\, e^{i\omega t}\, dt \, , \tag{3.67}$$

where $\widetilde{\mathbf{E}}(\mathbf{r},\omega)$ is in general a complex vector field quantity. Conversely, the temporal field quantity can be obtained from $\widetilde{\mathbf{E}}(\mathbf{r},\omega)$ through an inverse Fourier transformation given by

$$\mathbf{E}(\mathbf{r},t) = \frac{1}{2\pi} \int_{-\infty}^{+\infty} \widetilde{\mathbf{E}}(\mathbf{r},\omega)\, e^{-i\omega t}\, d\omega \, . \tag{3.68}$$

Note that the Fourier transform definitions given by Eqs. (3.67) and (3.68) are different from the conventional definitions, which are the complex conjugate of what we have here. Our definition facilitates integration on the upper half of the complex $\omega$-plane and is consistent with the conventions used in the literature on optics and physics. Equation (3.68) clearly demonstrates that an arbitrary field quantity can be expressed in terms of the superposition of time-harmonic field quantities of the form $\widetilde{\mathbf{E}}(\mathbf{r},\omega)\, e^{-i\omega t}$. Here $\widetilde{\mathbf{E}}(\mathbf{r},\omega)$ in general is a complex quantity.

Confining our attention to field quantities that are real functions of time and space, i.e., $\mathbf{E}^*(\mathbf{r},t) = \mathbf{E}(\mathbf{r},t)$, it can be easily shown that

$$\widetilde{\mathbf{E}}^*(\mathbf{r},\omega) = \widetilde{\mathbf{E}}(\mathbf{r},-\omega)$$

and

$$\mathbf{E}(\mathbf{r},t) = \frac{1}{\pi}\int_0^{+\infty} \Re\mathrm{e}[\widetilde{\mathbf{E}}(\mathbf{r},\omega)\, e^{-i\omega t}]\, d\omega\ . \tag{3.69}$$

Hence any time-domain field quantity can be expressed in terms of the superposition of real time-harmonic functions of the form

$$\mathbf{e}(\mathbf{r},t) = \Re\mathrm{e}[\widetilde{\mathbf{E}}(\mathbf{r},\omega)\, e^{-i\omega t}]\ . \tag{3.70}$$

The complex quantity

$$\widetilde{\mathbf{E}}(\mathbf{r},\omega) = \widetilde{\mathbf{E}}_{\mathrm{r}}(\mathbf{r},\omega) + i\widetilde{\mathbf{E}}_{\mathrm{i}}(\mathbf{r},\omega) \tag{3.71}$$

is referred to as a ***vector phasor***. Similarly, the other time-harmonic fields and sources can be obtained from their frequency-domain counterparts through

$$\mathbf{h}(\mathbf{r},t) = \Re\mathrm{e}[\widetilde{\mathbf{H}}(\mathbf{r},\omega)\, e^{-i\omega t}]\ , \tag{3.72a}$$

$$\mathbf{d}(\mathbf{r},t) = \Re\mathrm{e}[\widetilde{\mathbf{D}}(\mathbf{r},\omega)\, e^{-i\omega t}]\ , \tag{3.72b}$$

$$\mathbf{b}(\mathbf{r},t) = \Re\mathrm{e}[\widetilde{\mathbf{B}}(\mathbf{r},\omega)\, e^{-i\omega t}]\ , \tag{3.72c}$$

$$\mathbf{j}(\mathbf{r},t) = \Re\mathrm{e}[\widetilde{\mathbf{J}}(\mathbf{r},\omega)\, e^{-i\omega t}]\ , \tag{3.72d}$$

and

$$\rho(\mathbf{r},t) = \Re\mathrm{e}[\widetilde{\rho}(\mathbf{r},\omega)\, e^{-i\omega t}]\ . \tag{3.72e}$$

Like any field function, time-harmonic field quantities must satisfy Maxwell's equations. Consider Faraday's law:

$$\nabla\times\mathbf{e}(\mathbf{r},t) = -\frac{\partial\mathbf{b}(\mathbf{r},t)}{\partial t}\ . \tag{3.73}$$

Substituting the phasor forms we have

$$\nabla\times\Re\mathrm{e}[\widetilde{\mathbf{E}}(\mathbf{r},\omega)\, e^{-i\omega t}] = -\frac{\partial}{\partial t}\,\Re\mathrm{e}[\widetilde{\mathbf{B}}(\mathbf{r},\omega)\, e^{-i\omega t}]\ . \tag{3.74}$$

The $\nabla\times$, $\frac{\partial}{\partial t}$, and $\Re\mathrm{e}[\cdot]$ are all linear operators and are commutative; hence

$$\Re\mathrm{e}\{[\nabla\times\widetilde{\mathbf{E}}(\mathbf{r},\omega) - i\omega\widetilde{\mathbf{B}}(\mathbf{r},\omega)]e^{-i\omega t}\} = 0\ . \tag{3.75}$$

Since Eq. (3.75) must be valid for all values of $t$, it follows that the quantity in the square bracket must vanish. Hence

$$\nabla\times\widetilde{\mathbf{E}}(\mathbf{r},\omega) = i\omega\widetilde{\mathbf{B}}(\mathbf{r},\omega)\ . \tag{3.76a}$$

Similarly, the modified Ampère's law yields

$$\nabla \times \widetilde{\mathbf{H}}(\mathbf{r},\omega) = -i\omega\widetilde{\mathbf{D}} + \widetilde{\mathbf{J}}(\mathbf{r},\omega) + \sigma\widetilde{\mathbf{E}}(\mathbf{r},\omega) \; . \tag{3.76b}$$

Gauss' law provides

$$\nabla \cdot \widetilde{\mathbf{D}}(\mathbf{r},\omega) = \widetilde{\rho}(\mathbf{r},\omega) \tag{3.77a}$$

and

$$\nabla \cdot \widetilde{\mathbf{B}}(\mathbf{r},\omega) = 0 \; . \tag{3.77b}$$

Constitutive relations also take on a rather simple form. As mentioned previously, the permittivity and permeability of matter are in general functions of frequency and the relationships between the electric and magnetic flux densities and their corresponding field intensities in the time domain involve mathematical convolutions. Hence, the Fourier transform of the flux densities can be expressed in terms of the product of Fourier transforms of the constitutive parameters and the field intensities. That is,

$$\widetilde{\mathbf{D}}(\mathbf{r},\omega) = \overline{\overline{\varepsilon}}(\omega)\, \widetilde{\mathbf{E}}(\mathbf{r},\omega) \tag{3.78a}$$

and

$$\widetilde{\mathbf{B}}(\mathbf{r},\omega) = \overline{\overline{\mu}}(\omega)\, \widetilde{\mathbf{H}}(\mathbf{r},\omega) \; , \tag{3.78b}$$

where $\overline{\overline{\varepsilon}}(\omega)$ and $\overline{\overline{\mu}}(\omega)$ are in general complex permittivity and permeability tensors.

For simplicity we drop the parameter $\omega$ from the time-independent Maxwell's equations. Allowing generalized time harmonic electric and magnetic sources, the time-independent Maxwell's equations assume the following form:

$$\nabla \times \mathbf{E}(\mathbf{r}) = i\omega\mu\, \mathbf{H}(\mathbf{r}) - \mathbf{J}_{\mathrm{m}}(\mathbf{r}) \; , \tag{3.79a}$$

$$\nabla \times \mathbf{H}(\mathbf{r}) = -i\omega\varepsilon\, \mathbf{E}(\mathbf{r}) + \mathbf{J}(\mathbf{r}) \; , \tag{3.79b}$$

$$\nabla \cdot \mathbf{B}(\mathbf{r}) = \rho_{\mathrm{m}}(\mathbf{r}) \; , \tag{3.79c}$$

$$\nabla \cdot \mathbf{D}(\mathbf{r}) = \rho(\mathbf{r}) \; . \tag{3.79d}$$

Also, the continuity relations are given by

$$\nabla \cdot \mathbf{J}(\mathbf{r}) = i\omega\, \rho(\mathbf{r})$$

and

$$\nabla \cdot \mathbf{J}_{\mathrm{m}}(\mathbf{r}) = i\omega\, \rho_{\mathrm{m}}(\mathbf{r}) \; .$$

For media with finite conductivity where $\sigma \neq 0$, the conductivity can be absorbed into the complex permittivity. From Eq. (3.76b),

$$\nabla \times \mathbf{H} = -i\omega\, \varepsilon\mathbf{E} + \sigma\, \mathbf{E} + \mathbf{J} = -i\omega \left( \varepsilon + \frac{i\sigma}{\omega} \right) \mathbf{E} + \mathbf{J} \; . \tag{3.81}$$

Comparing Eq. (3.81) with Eq. (3.79b), the quantity $\varepsilon + i\sigma/\omega$ can be viewed as an ***effective permittivity*** of the medium:

$$\varepsilon_{\text{eff}} = \varepsilon + \frac{i\sigma}{\omega} \,. \tag{3.82}$$

That is, the medium conductivity adds to the imaginary part of the effective permittivity of the medium.

### 3-2.1 Vector and Scalar Potentials

As mentioned earlier, the time-harmonic potentials can also be defined in terms of their respective phasor quantities. It is then easy to show that

$$\mathbf{B}(\mathbf{r},\omega) = \nabla \times \mathbf{A}(\mathbf{r},\omega) \tag{3.83a}$$

and

$$\mathbf{E}(\mathbf{r},\omega) = -\nabla\Phi(\mathbf{r},\omega) + i\omega\,\mathbf{A}(\mathbf{r},\omega) \,. \tag{3.83b}$$

The gauge condition given by Eq. (3.9) assumes the following form:

$$\nabla \cdot \mathbf{A}(\mathbf{r},\omega) = i\omega\mu\varepsilon\ \Phi(\mathbf{r},\omega) \,, \tag{3.84}$$

from which we obtain

$$\Phi(\mathbf{r},\omega) = -\frac{i\omega}{k^2}\,\nabla\cdot\mathbf{A} \,, \tag{3.85}$$

where $k = \omega\sqrt{\mu\varepsilon}$ is known as the medium's ***wave number***. Hence,

$$\mathbf{E} = \frac{i\omega}{k^2}\,\nabla\nabla\cdot\mathbf{A} + i\omega\mathbf{A} \,. \tag{3.86}$$

In a similar manner, the phasors must satisfy the following frequency-domain wave equations:

$$\nabla^2\mathbf{A} + k^2\mathbf{A} = -\mu\mathbf{J} \tag{3.87a}$$

and

$$\nabla^2\Phi + k^2\Phi = -\frac{\rho}{\varepsilon} \,. \tag{3.87b}$$

Duality relations can be applied to the phasor quantities as well. Hence, in the presence of magnetic sources, the electric vector potential and magnetic scalar potential must satisfy

$$\nabla^2\mathbf{A}_{\text{m}} + k^2\mathbf{A}_{\text{m}} = -\varepsilon\,\mathbf{J}_{\text{m}} \tag{3.88a}$$

and

$$\nabla^2\Phi_{\text{m}} + k^2\Phi_{\text{m}} = -\frac{\rho_{\text{m}}}{\mu} \,. \tag{3.88b}$$

In general, when both electric and magnetic sources are present,

$$\mathbf{H} = \frac{1}{\mu}\nabla\times\mathbf{A} + \frac{i\omega}{k^2}\nabla\nabla\cdot\mathbf{A}_{\mathrm{m}} + i\omega\,\mathbf{A}_{\mathrm{m}} \tag{3.89a}$$

and

$$\mathbf{E} = \frac{i\omega}{k^2}\nabla\nabla\cdot\mathbf{A} + i\omega\mathbf{A} - \frac{1}{\varepsilon}\nabla\times\mathbf{A}_{\mathrm{m}}\,. \tag{3.89b}$$

### 3-2.2 Hertz Potentials

For time-harmonic fields, the phasor forms of the Hertz vector potentials are denoted by $\mathbf{\Pi}(\mathbf{r},\omega)$ and $\mathbf{\Pi}_{\mathrm{m}}(\mathbf{r},\omega)$. These satisfy the following wave equations:

$$\nabla^2\mathbf{\Pi} + k^2\mathbf{\Pi} = \frac{-i\,\mathbf{J}}{\omega\varepsilon} \tag{3.90a}$$

and

$$\nabla^2\mathbf{\Pi}_{\mathrm{m}} + k^2\mathbf{\Pi}_{\mathrm{m}} = \frac{-i\,\mathbf{J}_{\mathrm{m}}}{\omega\mu}\,. \tag{3.90b}$$

Also, the field quantities, in terms of the Hertz vector potentials, are given by

$$\mathbf{H} = -i\omega\varepsilon\,\nabla\times\mathbf{\Pi} + \nabla\nabla\cdot\mathbf{\Pi}_{\mathrm{m}} + k^2\,\mathbf{\Pi}_{\mathrm{m}} \tag{3.91a}$$

and

$$\mathbf{E} = \nabla\nabla\cdot\mathbf{\Pi} + k^2\mathbf{\Pi} + i\omega\mu\,\nabla\times\mathbf{\Pi}_{\mathrm{m}}\,. \tag{3.91b}$$

### 3-2.3 Poynting Vector for Time-Harmonic Fields

Consider a time-harmonic electromagnetic wave given by

$$\mathbf{e}(\mathbf{r},t) = \Re\mathrm{e}[\mathbf{E}(\mathbf{r})\,e^{-i\omega t}] \tag{3.92a}$$

and

$$\mathbf{h}(\mathbf{r},t) = \Re\mathrm{e}[\mathbf{H}(\mathbf{r})\,e^{-i\omega t}]\,. \tag{3.92b}$$

The ***Poynting vector*** for this set of electric and magnetic fields is given by

$$\begin{aligned}\mathbf{s}(\mathbf{r},t) &= \mathbf{e}(\mathbf{r},t)\times\mathbf{h}(\mathbf{r},t)\\ &= \Re\mathrm{e}[\mathbf{E}(\mathbf{r})\,e^{-i\omega t}]\times\Re\mathrm{e}[\mathbf{H}(\mathbf{r})\,e^{-i\omega t}]\,.\end{aligned} \tag{3.93}$$

As mentioned earlier, the phasors $\mathbf{E}(\mathbf{r})$ and $\mathbf{H}(\mathbf{r})$ are, in general, complex quantities that can be written in the following forms:

$$\mathbf{E}(\mathbf{r}) = \mathbf{E}_{\mathrm{r}}(\mathbf{r}) + i\,\mathbf{E}_{\mathrm{i}}(\mathbf{r}) \tag{3.94a}$$

and

$$\mathbf{H}(\mathbf{r}) = \mathbf{H}_{\mathrm{r}}(\mathbf{r}) + i\,\mathbf{H}_{\mathrm{i}}(\mathbf{r})\ . \tag{3.94b}$$

Substituting Eq. (3.94) in Eq. (3.93), and after simple algebraic manipulation, it can be shown that

$$\begin{aligned}\mathbf{s}(\mathbf{r},t) &= [\mathbf{E}_{\mathrm{r}}(\mathbf{r})\ \cos\omega t + \mathbf{E}_{\mathrm{i}}(\mathbf{r})\ \sin\omega t] \times [\mathbf{H}_{\mathrm{r}}(\mathbf{r})\ \cos\omega t + \mathbf{H}_{\mathrm{i}}(\mathbf{r})\ \sin\omega t] \\ &= \mathbf{E}_{\mathrm{r}}(\mathbf{r}) \times \mathbf{H}_{\mathrm{r}}(\mathbf{r})\ \cos^2\omega t + \mathbf{E}_{\mathrm{i}}(\mathbf{r}) \times \mathbf{H}_{\mathrm{i}}(\mathbf{r})\ \sin^2\omega t \\ &\quad + [\mathbf{E}_{\mathrm{r}}(\mathbf{r}) \times \mathbf{H}_{\mathrm{i}}(\mathbf{r}) + \mathbf{E}_{\mathrm{i}}(\mathbf{r}) \times \mathbf{H}_{\mathrm{r}}(\mathbf{r})] \sin\omega t \cos\omega t\ .\end{aligned} \tag{3.95}$$

The ***time-average Poynting vector*** representing the net power density going through at a given point in space can be obtained from

$$\begin{aligned}\mathbf{S}_{\mathrm{avg}}(\mathbf{r}) &= \frac{1}{T}\int_{t}^{t+T} \mathbf{s}(\mathbf{r},t)\ dt \\ &= \frac{1}{2}\left[\mathbf{E}_{\mathrm{r}}(\mathbf{r}) \times \mathbf{H}_{\mathrm{r}}(\mathbf{r}) + \mathbf{E}_{\mathrm{i}}(\mathbf{r}) \times \mathbf{H}_{\mathrm{i}}(\mathbf{r})\right]\ ,\end{aligned} \tag{3.96}$$

where $T = \frac{2\pi}{\omega}$ is a period of the sinusoidal functions. On the other hand, we note that

$$\Re\mathrm{e}[\mathbf{E}(\mathbf{r}) \times \mathbf{H}^*(\mathbf{r})] = \mathbf{E}_{\mathrm{r}}(\mathbf{r}) \times \mathbf{H}_{\mathrm{r}}(\mathbf{r}) + \mathbf{E}_{\mathrm{i}}(\mathbf{r}) \times \mathbf{H}_{\mathrm{i}}(\mathbf{r})\ . \tag{3.97}$$

Comparing Eq. (3.96) with Eq. (3.97), it is obvious now that

$$\mathbf{S}_{\mathrm{avg}}(\mathbf{r}) = \frac{1}{2}\,\Re\mathrm{e}[\mathbf{E}(\mathbf{r}) \times \mathbf{H}^*(\mathbf{r})]\ , \tag{3.98}$$

which states that the time average value of the Poynting vector can be obtained directly from the cross product of the phasor vector field quantities.

In general, the complex Poynting vector or ***complex power flow density*** is defined as

$$\mathbf{S}(\mathbf{r}) = \frac{1}{2}\,\mathbf{E}(\mathbf{r}) \times \mathbf{H}^*(\mathbf{r})\ , \tag{3.99}$$

from which the time-average power density can be obtained:

$$\mathbf{S}_{\mathrm{avg}}(\mathbf{r}) = \Re\mathrm{e}[\mathbf{S}(\mathbf{r})]\ . \tag{3.100a}$$

Also

$$\Im\mathrm{m}[\mathbf{S}(\mathbf{r})] = \frac{1}{2}\,\Im\mathrm{m}[\mathbf{E}(\mathbf{r}) \times \mathbf{H}^*(\mathbf{r})] \tag{3.100b}$$

is related to the flow of reactive power density. In fact this power does not flow out, but oscillates back and forth through a boundary.

### 3-2.4 Energy Density for Time-Harmonic Fields

The stored electric energy per unit volume for a time-harmonic field can be directly computed from

$$\begin{aligned} w_{\rm e}(\mathbf{r},t) &= \frac{1}{2}\,\mathbf{e}(\mathbf{r},t)\cdot\mathbf{d}(\mathbf{r},t) \\ &= \frac{1}{2}\,\Re{\rm e}[\mathbf{E}(\mathbf{r})\,e^{-i\omega t}]\cdot\Re{\rm e}[\mathbf{D}(\mathbf{r})\,e^{-i\omega t}]\,. \end{aligned} \tag{3.101}$$

The complex phasors for the electric flux density and the electric field intensity have real and imaginary vector components denoted by $\mathbf{D}(\mathbf{r}) = \mathbf{D}_{\rm r}(\mathbf{r}) + i\mathbf{D}_{\rm i}(\mathbf{r})$ and $\mathbf{E}(\mathbf{r}) = \mathbf{E}_{\rm r}(\mathbf{r}) + i\,\mathbf{E}_{\rm i}(\mathbf{r})$, respectively. Upon substituting these expressions in Eq. (3.101), it can be shown that

$$\begin{aligned} w_{\rm e}(\mathbf{r},t) = \frac{1}{2}\big\{&\mathbf{E}_{\rm r}(\mathbf{r})\cdot\mathbf{D}_{\rm r}(\mathbf{r})\cos^2(\omega t) + \mathbf{E}_{\rm i}(\mathbf{r})\cdot\mathbf{D}_{\rm i}(\mathbf{r})\sin^2(\omega t) \\ &+ (\mathbf{E}_{\rm r}(\mathbf{r})\cdot\mathbf{D}_{\rm i}(\mathbf{r}) + \mathbf{E}_{\rm i}(\mathbf{r})\cdot\mathbf{D}_{\rm r}(\mathbf{r}))\cos(\omega t)\sin(\omega t)\big\}\,. \end{aligned} \tag{3.102}$$

The time-average electric energy density is given by

$$w_{\rm e}^{\rm avg}(\mathbf{r}) = \frac{1}{T}\int_0^T w_{\rm e}(\mathbf{r},t)\,dt = \frac{1}{4}\left[\mathbf{E}_{\rm r}(\mathbf{r})\cdot\mathbf{D}_{\rm r}(\mathbf{r}) + \mathbf{E}_{\rm i}(\mathbf{r})\cdot\mathbf{D}_{\rm i}(\mathbf{r})\right]\,, \tag{3.103}$$

where $T = 2\pi/\omega$. Noting that for an isotropic medium

$$\mathbf{D}_{\rm r}(\mathbf{r}) = \Re{\rm e}[\varepsilon\,\mathbf{E}(\mathbf{r})] = \varepsilon'\,\mathbf{E}_{\rm r}(\mathbf{r}) - \varepsilon''\,\mathbf{E}_{\rm i}(\mathbf{r}) \tag{3.104a}$$

and

$$\mathbf{D}_{\rm i}(\mathbf{r}) = \Im{\rm m}[\varepsilon\,\mathbf{E}(\mathbf{r})] = \varepsilon'\,\mathbf{E}_{\rm i}(\mathbf{r}) + \varepsilon''\,\mathbf{E}_{\rm r}(\mathbf{r})\,, \tag{3.104b}$$

it can be shown that the time-average electric energy density can be computed from

$$w_{\rm e}^{\rm avg}(\mathbf{r}) = \frac{\varepsilon'}{4}\left(|\mathbf{E}_{\rm r}(\mathbf{r})|^2 + |\mathbf{E}_{\rm i}(\mathbf{r})|^2\right) = \frac{\varepsilon'}{4}|\mathbf{E}(\mathbf{r})|^2\,, \tag{3.105}$$

where $|\mathbf{E}(\mathbf{r})|^2 = \mathbf{E}(\mathbf{r})\cdot\mathbf{E}^*(\mathbf{r})$.

Following a similar procedure, it can be shown that the time-average magnetic energy density can be computed from

$$\begin{aligned} w_{\rm m}^{\rm avg}(\mathbf{r}) &= \frac{\mu'}{4}\left(|\mathbf{H}_{\rm r}(\mathbf{r})|^2 + |\mathbf{H}_{\rm i}(\mathbf{r})|^2\right) \\ &= \frac{\mu'}{4}\,|\mathbf{H}(\mathbf{r})|^2\,. \end{aligned} \tag{3.106}$$

### 3-2.5 Complex Poynting Theorem

The complex Poynting theorem can be obtained from the time-harmonic version of Maxwell's equations given by Eqs. (3.79a) and (3.79b). Starting from

$$\nabla \cdot (\mathbf{E} \times \mathbf{H}^*) = \mathbf{H}^* \cdot \nabla \times \mathbf{E} - \mathbf{E} \cdot \nabla \times \mathbf{H}^*$$

and using Eqs. (3.79a) and (3.79b), it can be shown that

$$\nabla \cdot (\mathbf{E} \times \mathbf{H}^*) = i\omega\mu |\mathbf{H}|^2 - \mathbf{J}_{\mathrm{m}} \cdot \mathbf{H}^* - i\omega\varepsilon^* |\mathbf{E}|^2 - \mathbf{J}^* \cdot \mathbf{E} \,, \tag{3.107}$$

where the medium conductivity is absorbed into the imaginary part of the complex permittivity.

Integrating over a volume $V$ and applying the divergence theorem to the left-hand side, it can be shown that

$$\frac{1}{2} \oiint_S (\mathbf{E} \times \mathbf{H}^*) \cdot d\mathbf{s} = -\frac{1}{2} \iiint_V [\mathbf{E} \cdot \mathbf{J}^* + \mathbf{J}_{\mathrm{m}} \cdot \mathbf{H}^*] \, dv + i\omega \iiint_V \left( \frac{1}{2} \mu |\mathbf{H}|^2 - \frac{1}{2} \varepsilon^* |\mathbf{E}|^2 \right) dv \,. \tag{3.108}$$

The complex time-average input power is given by

$$P_{\mathrm{in}}^{\mathrm{c}} = -\frac{1}{2} \iiint_V (\mathbf{E} \cdot \mathbf{J}^* + \mathbf{J}_{\mathrm{m}} \cdot \mathbf{H}^*) \, dv \,. \tag{3.109}$$

The time-average stored electric field energy (a positive real quantity) is

$$w_{\mathrm{e}} = \frac{1}{2} \iiint_V \frac{1}{2} \varepsilon' |\mathbf{E}|^2 \, dv \,. \qquad \textbf{(stored electric energy)} \tag{3.110a}$$

The time-average stored magnetic field energy is

$$w_{\mathrm{m}} = \frac{1}{2} \iiint_V \frac{1}{2} \mu' |\mathbf{H}|^2 \, dv \,, \qquad \textbf{(stored magnetic energy)} \tag{3.110b}$$

where $\varepsilon'$ and $\mu'$ are the real parts of the complex permittivity and permeability of the medium.

The time-average dissipated power is

$$P_{\mathrm{loss}} = \frac{1}{2} \iiint_V (\omega\mu'' |\mathbf{H}|^2 + \omega\varepsilon'' |\mathbf{E}|^2) \, dv \,. \qquad \textbf{(dissipated power)} \tag{3.111}$$

By denoting the left-hand side of Eq. (3.108) as the "complex" radiated power ($P_{\mathrm{rad}}^{\mathrm{c}}$), we have

$$P_{\mathrm{in}}^{\mathrm{c}} = P_{\mathrm{rad}}^{\mathrm{c}} + P_{\mathrm{loss}} + i2\omega(w_{\mathrm{e}} - w_{\mathrm{m}}) \,. \tag{3.112}$$

Explicitly,

$$\Re\mathrm{e}[P_{\mathrm{in}}^{\mathrm{c}}] = \Re\mathrm{e}[P_{\mathrm{rad}}^{\mathrm{c}}] + P_{\mathrm{loss}} \tag{3.113a}$$

and

$$\Im\mathrm{m}[P_{\mathrm{in}}^{\mathrm{c}}] = \Im\mathrm{m}[P_{\mathrm{rad}}^{\mathrm{c}}] + 2\omega(w_{\mathrm{e}} - w_{\mathrm{m}}) \; . \tag{3.113b}$$

Equation (3.113a) is a statement of the law of conservation of energy and Eq. (3.113b) is the extension of the same law for the reactive power.

### 3-2.6 Time-Harmonic Polarization Currents

As described in Section 2-4, a medium with permittivity $\varepsilon$ and permeability $\mu$ can be replaced with polarization currents in free space. Suppose the fields in the medium are time-harmonic fields given by $\mathbf{e}(\mathbf{r},t)$ and $\mathbf{h}(\mathbf{r},t)$; then the electric and magnetic polarization currents are given by

$$\mathbf{J}_{\mathrm{ep}}(\mathbf{r},t) = \varepsilon_0 \frac{\partial}{\partial t}[(\varepsilon_{\mathrm{r}} - 1)\, \mathbf{e}(\mathbf{r},t)] \tag{3.114a}$$

and

$$\mathbf{J}_{\mathrm{mp}}(\mathbf{r},t) = \mu_0 \frac{\partial}{\partial t}[(\mu_{\mathrm{r}} - 1)\, h(\mathbf{r},t)] \; . \tag{3.114b}$$

The frequency-domain equivalents of Eqs. (3.114a) and (3.114b) are given by

$$\mathbf{J}_{\mathrm{ep}}(\mathbf{r}) = -i\omega\varepsilon_0(\varepsilon_{\mathrm{r}} - 1)\, \mathbf{E}(\mathbf{r}) \tag{3.115a}$$

and

$$\mathbf{J}_{\mathrm{mp}}(\mathbf{r}) = -i\omega\mu_0(\mu_{\mathrm{r}} - 1)\, \mathbf{H}(\mathbf{r}) \; . \tag{3.115b}$$

Using $\varepsilon = \varepsilon' - i\varepsilon''$, we have

$$\mathbf{J}_{\mathrm{ep}}(\mathbf{r}) = \omega\varepsilon_0\varepsilon_{\mathrm{r}}''\, \mathbf{E}(\mathbf{r}) - i\omega\varepsilon_0(\varepsilon_{\mathrm{r}}' - 1)\, \mathbf{E}(\mathbf{r}) \; . \tag{3.116}$$

The first component (in-phase) is known as the ***dissipative current*** and the second component is known as the ***reactive current***, which together with the displacement current in the equivalent free space constitutes the total displacement current $-i\omega\varepsilon_0\varepsilon_{\mathrm{r}}'\, \mathbf{E}(\mathbf{r})$. The quality of a dielectric material can be determined in terms of the relative magnitude of the reactive current to that of the dissipative current, which is independent of the magnitude of the electric field and known as the ***quality factor***

$$\breve{Q} = \frac{\text{displacement current density}}{\text{dissipative current density}} = \frac{\varepsilon_{\mathrm{r}}'}{\varepsilon_{\mathrm{r}}''} \; . \tag{3.117}$$

The reciprocal of this quantity is known as the ***dielectric loss tangent***. It should be noted that the quality factor definition given by Eq. (3.117) is consistent with the definition for the

quality factor of a capacitor filled with the same material, defined by

$$\breve{Q} = \omega \frac{\text{maximum of stored energy}}{\text{average dissipated power}}$$
$$= \omega \frac{\frac{1}{2}\varepsilon'|E|^2}{\frac{1}{2}\omega\varepsilon''|E|^2} = \frac{\varepsilon'}{\varepsilon''} \,. \tag{3.118a}$$

For magnetic materials ($\mu \neq \mu_0$), an analogous magnetic quality factor $\breve{Q}_{\rm m}$ can be defined as

$$\breve{Q}_{\rm m} = \frac{\mu'}{\mu''} \,. \tag{3.118b}$$

## 3-3 Time-Harmonic Retarded Potential

The magnetic vector potential produced by a time-harmonic filament current with

$$\mathbf{j}(\mathbf{r},t) = \delta(\mathbf{r})\, d\boldsymbol{\ell}\, \Re\mathrm{e}[I_0(\omega)\, e^{-i\omega t}] \,, \tag{3.119}$$

noting that $f(t) = \Re\mathrm{e}[I_0(\omega)\, e^{-i\omega t}]$, can be obtained from the Fourier transformation of the time-domain solution obtained in Section 3-1.5. Noting that the Fourier transform of $f(t-t_0)$ is given by

$$\mathcal{F}[f(t-t_0)] = F(\omega)\, e^{i\omega t_0} = I_0(\omega)\, e^{i\omega t_0} \,, \tag{3.120}$$

and recalling that $t_0 = r/u_{\rm p}$, the phasor vector of the corresponding magnetic vector potential is given by

$$\mathbf{A}(\mathbf{r}) = \frac{\mu I_0}{4\pi} \frac{e^{ikr}}{r}\, d\boldsymbol{\ell} \,, \tag{3.121}$$

where, as before, $k = \omega/u_{\rm p}$.

Placing the current filament at location $\mathbf{r}'$, the corresponding magnetic vector potential is given by

$$\mathbf{A}(\mathbf{r}) = \frac{\mu I_0}{4\pi} \frac{e^{ik|\mathbf{r}-\mathbf{r}'|}}{|\mathbf{r}-\mathbf{r}'|}\, d\boldsymbol{\ell} \,. \tag{3.122}$$

Also, using Eq. (3.46), the phasor magnetic field is

$$\mathbf{H}(\mathbf{r}) = \frac{I_0 k^2}{4\pi} \left(-i + \frac{1}{k|\mathbf{r}-\mathbf{r}'|}\right) \frac{e^{ik|\mathbf{r}-\mathbf{r}'|}}{k|\mathbf{r}-\mathbf{r}'|}\, d\boldsymbol{\ell} \times \frac{(\mathbf{r}-\mathbf{r}')}{|\mathbf{r}-\mathbf{r}'|} \,, \tag{3.123}$$

and from Eq. (3.54), the phasor electric field is given by

$$\mathbf{E}(\mathbf{r}) = \frac{I_0 k^2}{4\pi} \eta \frac{e^{ik|\mathbf{r}-\mathbf{r}'|}}{k|\mathbf{r}-\mathbf{r}'|} \left[ \left( \frac{2}{k|\mathbf{r}-\mathbf{r}'|} + \frac{i2}{k^2|\mathbf{r}-\mathbf{r}'|^2} \right) \frac{(\mathbf{r}-\mathbf{r}')\cdot d\boldsymbol{\ell}}{|\mathbf{r}-\mathbf{r}'|^2} (\mathbf{r}-\mathbf{r}') \right.$$
$$\left. - \left( \frac{1}{k|\mathbf{r}-\mathbf{r}'|} + \frac{i}{k^2|\mathbf{r}-\mathbf{r}'|^2} - i \right) \frac{(\mathbf{r}-\mathbf{r}')}{|\mathbf{r}-\mathbf{r}'|} \times \left( d\boldsymbol{\ell} \times \frac{(\mathbf{r}-\mathbf{r}')}{|\mathbf{r}-\mathbf{r}'|} \right) \right] \,. \tag{3.124}$$

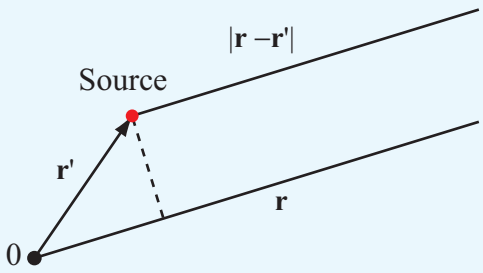


**Figure 3-5:** The geometry of a source at location $\mathbf{r}'$ and an observation point at location $\mathbf{r}$ far from the source.

For a volumetric current distribution with a phasor representation $\mathbf{J}(\mathbf{r})$, the magnetic field can be obtained from Eq. (3.59b):

$$\mathbf{H}(\mathbf{r}) = \frac{k^2}{4\pi} \iiint_V \left(-i + \frac{1}{k|\mathbf{r}-\mathbf{r}'|}\right) \frac{e^{ik|\mathbf{r}-\mathbf{r}'|}}{k|\mathbf{r}-\mathbf{r}'|} \left(\mathbf{J}(\mathbf{r}') \times \frac{(\mathbf{r}-\mathbf{r}')}{|\mathbf{r}-\mathbf{r}'|}\right) dv' \,. \tag{3.125}$$

The far-field expression can be obtained by assuming that

$$k|\mathbf{r}-\mathbf{r}'| \gg 1 \,.$$

Accordingly, the following approximations can be made (see Fig. 3-5):

$$|\mathbf{r}-\mathbf{r}'| \approx r - \mathbf{r}' \cdot \hat{\mathbf{r}} \tag{3.126a}$$

for the phase term and

$$|\mathbf{r}-\mathbf{r}'| \approx r \tag{3.126b}$$

for the magnitude terms. In the far-field region, the expression given by Eq. (3.125) can be approximated as

$$\mathbf{H}(\mathbf{r}) = -\frac{ike^{ikr}}{4\pi r} \iiint_V [\mathbf{J}(\mathbf{r}') \times \hat{\mathbf{r}}] e^{-ik\mathbf{r}'\cdot\hat{\mathbf{r}}} \, dv' \,. \tag{3.127a}$$

The corresponding electric field is given by

$$\mathbf{E}(\mathbf{r}) = -\frac{ik\eta}{4\pi} \frac{e^{ikr}}{r} \iiint_V [\mathbf{J}(\mathbf{r}') \times \hat{\mathbf{r}}] \times \hat{\mathbf{r}} \, e^{-ik\mathbf{r}'\cdot\hat{\mathbf{r}}} \, dv' \,. \tag{3.127b}$$

Careful examination of Eqs. (3.127a) and (3.127b) reveals that

$$\mathbf{E}(\mathbf{r}) = \eta\, \mathbf{H}(\mathbf{r}) \times \hat{\mathbf{r}}\,, \tag{3.128}$$

which indicates that the electric field is perpendicular to the magnetic field and both are perpendicular to the direction of propagation $\hat{\mathbf{r}}$. This type of field configuration is known as a ***transverse electromagnetic wave***. It is also interesting to note that the ratio of the electric field magnitude to that of the magnetic field is a constant, known as the ***characteristic impedance of the medium*** $\eta$.

## Example 3-2: Radiated Power and Antenna Directivity of a Hertzian Dipole

Consider a Hertzian dipole with $I_0\,\Delta\boldsymbol{\ell} = I_0\,\Delta\ell\,\hat{\mathbf{z}}$ at the origin of a Cartesian coordinate system. Find the complex Poynting vector and total power radiated by the Hertzian dipole antenna. Defining ***antenna directivity*** along a given direction in the far-field region as the ratio of the power density in that direction to the power density had the radiated power were to be radiated uniformly, find the directivity function of the Hertzian dipole.

**Solution:** Using Eqs. (3.123) and (3.124) with $\mathbf{r}' = 0$ and $\hat{\mathbf{z}} \times \hat{\mathbf{r}} = \sin\theta\,\hat{\boldsymbol{\phi}}$, the explicit forms of the magnetic and electric fields are given by

$$\mathbf{H}(\mathbf{r}) = \frac{I_0 \Delta\ell k}{4\pi}\frac{e^{ikr}}{r}\left(-i + \frac{1}{kr}\right)\sin\theta\,\hat{\boldsymbol{\phi}} \tag{3.129}$$

and

$$\mathbf{E}(\mathbf{r}) = \eta\,\frac{I_0 \Delta\ell k}{4\pi}\frac{e^{ikr}}{r}\left[2\left(\frac{1}{kr} + \frac{i}{(kr)^2}\right)\cos\theta\,\hat{\mathbf{r}} + \left(-i + \frac{1}{kr} + \frac{i}{(kr)^2}\right)\sin\theta\,\hat{\boldsymbol{\theta}}\right]\,, \tag{3.130}$$

where use was made of the relations $\hat{\mathbf{z}}\cdot\hat{\mathbf{r}} = \cos\theta$ and $\hat{\mathbf{r}} \times (\hat{\mathbf{z}} \times \hat{\mathbf{r}}) = -\sin\theta\,\hat{\boldsymbol{\theta}}$. The complex Poynting vector can now be evaluated from

$$\begin{aligned}\mathbf{S}(\mathbf{r}) &= \frac{1}{2}\,\mathbf{E}(\mathbf{r}) \times \mathbf{H}^*(\mathbf{r}) \\ &= \frac{\eta}{2}\left(\frac{I_0 \Delta\ell k}{4\pi r}\right)^2\left[\frac{-i}{kr}\left(1 + \frac{1}{(kr)^2}\right)\sin 2\theta\,\hat{\boldsymbol{\theta}} + \left(1 + \frac{i}{(kr)^3}\right)\sin^2\theta\,\hat{\mathbf{r}}\right]\,.\end{aligned} \tag{3.131}$$

To calculate the total radiated power, we consider a spherical surface with radius $r$ and evaluate the time-average net power flow through the surface. This can be done by evaluating

$$\begin{aligned}P_{\rm r} &= \int_0^{2\pi}\int_0^{\pi} \Re\mathrm{e}[\mathbf{S}(\mathbf{r})]\cdot\hat{\mathbf{r}}\, r^2 \sin\theta\, d\theta\, d\phi \\ &= \frac{\eta}{2}\frac{|I_0 \Delta\ell|^2 k^2}{(4\pi)^2}\,(2\pi)\int_0^{\pi}\sin^3\theta\, d\theta = \frac{\eta}{3}\frac{|I_0 \Delta\ell|^2 k^2}{4\pi}\,.\end{aligned} \tag{3.132}$$

It is interesting to note that this calculated radiated power is independent of the radius of the sphere, as expected. Another important fact to highlight is that the radiated power is produced entirely by the far-field terms that are proportional to $\frac{1}{kr}$. The directivity of the dipole, per the definition given in the problem statement, can be evaluated from

$$D(\theta,\phi) = \frac{\Re\mathrm{e}[S_\mathrm{r}(\mathbf{r})]}{P_\mathrm{r}/(4\pi r^2)} = \frac{3}{2}\sin^2\theta\ . \qquad \textbf{(short dipole)} \tag{3.133}$$

The directivity pattern is independent of $\phi$, as expected, and assumes its maximum value at $\theta = 90^\circ$.

### Example 3-3: Stored Electromagnetic Energy and Quality Factor for a Hertzian Dipole

Find the time-average stored electric and magnetic energy supplied by the Hertzian dipole and determine its quality factor $\breve{Q}$.

**Solution:** Suppose the antenna and its sources can be enclosed within a sphere of radius $a$. In our example $a$ can be as small as $\Delta\ell/2$. The total time-averaged stored energy can be calculated by integrating Eq. (3.105) and Eq. (3.106) over an infinite volume, excluding the small sphere of radius $a$ around the antenna. As noted in the previous example, the far-field components of the electric and magnetic fields are solely responsible for the radiated power. These fields fill all space, and under steady-state conditions, the source has existed indefinitely and the energy delivered and stored in the space outside the antenna region is infinite. However, excluding the far-field terms, only fields contributing to the reactive power are retained. The time-average stored electric energy per unit volume, excluding the far-field component, can be obtained from Eq. (3.130) and is given by

$$\begin{aligned} w_\mathrm{e}^\mathrm{avg}(\mathbf{r}) &= \frac{1}{4}\varepsilon'\left(\frac{\eta I_0\Delta\ell k}{4\pi}\right)^2\frac{1}{k^2r^4}\left[4\left(1+\frac{1}{(kr)^2}\right)\cos^2\theta+\left(1+\frac{1}{(kr)^2}\right)\sin^2\theta\right] \\ &= \frac{1}{4}\varepsilon'\left(\frac{\eta I_0\Delta\ell}{4\pi}\right)^2\frac{1}{r^4}\left(1+\frac{1}{(kr)^2}\right)(3\cos^2\theta+1)\ . \end{aligned} \tag{3.134}$$

The total electric energy stored outside the antenna can be computed from

$$\begin{aligned} W_\mathrm{e} &= \int_a^\infty\int_0^{2\pi}\int_0^\pi w_\mathrm{e}^\mathrm{avg}(\mathbf{r})\,r^2\sin\theta\,d\phi\,d\theta\,dr \\ &= \frac{1}{4}\,\varepsilon'\left(\frac{\eta I_0\Delta\ell k}{4\pi}\right)^2 8\pi\int_a^\infty\left(\frac{1}{(kr)^2}+\frac{1}{(kr)^4}\right)dr \\ &= \frac{\mu k(I_0\Delta\ell)^2}{8\pi}\left(\frac{1}{(ka)}+\frac{1}{(ka)^3}\right)\ . \end{aligned} \tag{3.135}$$

The time-average stored magnetic energy per unit volume can be evaluated from Eq. (3.129):

$$w_{\mathrm{m}}^{\mathrm{avg}}(\mathbf{r}) = \frac{1}{4}\,\mu' \frac{(I_0 \Delta \ell k)^2}{(4\pi)^2} \frac{1}{r^2} \frac{1}{(kr)^2} \sin^2\theta \ . \tag{3.136}$$

The total magnetic energy stored outside the antenna is therefore given by

$$\begin{aligned} W_{\mathrm{m}} &= \int_a^{\infty} \int_0^{2\pi} \int_0^{\pi} w_{\mathrm{m}}^{\mathrm{avg}}(\mathbf{r})\, r^2 \sin\theta \, d\phi \, d\theta \, dr \\ &= \frac{\mu k (I_0 \Delta \ell)^2}{8\pi} \frac{1}{3ka} \ . \end{aligned} \tag{3.137}$$

Now the quality factor of the dipole can be computed from

$$\begin{aligned} \breve{Q}_{\mathrm{dipole}} &= \frac{\omega(W_{\mathrm{e}} + W_{\mathrm{m}})}{P_{\mathrm{r}}} \\ &= \frac{\dfrac{\eta (I_0 \Delta \ell k)^2}{8\pi} \left( \dfrac{4}{(3ka)} + \dfrac{1}{(ka)^3} \right)}{\dfrac{\eta}{3} \dfrac{(I_0 \Delta \ell k)^2}{4\pi}} \\ &= \frac{1}{ka} + \frac{3}{2} \left( \frac{1}{ka} \right)^3 \ . \end{aligned} \tag{3.138}$$

The maximum value $a$ can assume is $\Delta\ell/2$, and noting that for a Hertzian dipole, $k\Delta\ell/2 \ll 1$, the Hertzian dipole quality factor can be approximated as

$$\breve{Q}_{\mathrm{dipole}} \approx \frac{3\pi^3}{2} \left( \frac{\lambda}{\Delta \ell} \right)^3 \ , \tag{3.139}$$

where $\lambda = u_{\mathrm{p}}/f = 2\pi/k$ is the wavelength.

## Example 3-4: Equivalent Circuit for a Transmitting Hertzian Dipole

An antenna connected to a source presents an equivalent circuit to which the source power is delivered. Using the expressions for the radiated power and reactive power, find the equivalent circuit for the Hertzian dipole.

**Solution:** The radiated power $P_{\mathrm{r}}$ delivered to space is lost power, similar to the power delivered to a resistor. Also referring to Eq. (3.135) the stored reactive energy near the dipole is predominantly electrical or capacitive. It is also noted from Eqs. (3.132) and (3.135) that the dissipative (radiation) power and the reactive energy are proportional to $I_0^2$. This indicates that the same current is flowing through the equivalent resistor and capacitor and therefore these two elements are in series. Figure 3-6 shows the equivalent circuit for the Hertzian dipole.

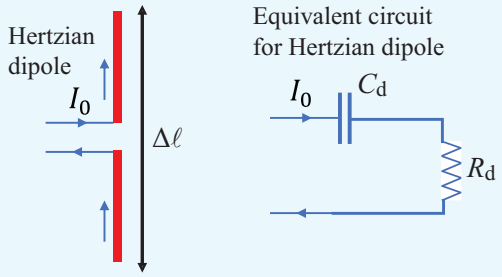


**Figure 3-6:** A source connected to a Hertzian dipole and its equivalent series *RC* circuit.

Noting that the power delivered to the equivalent resistor is $\frac{1}{2} R_d I_0^2$, the equivalent radiation resistance of the Hertzian dipole can be calculated from

$$R_d = \frac{2P_r}{I_0^2} = \frac{2\pi\eta}{3}\left(\frac{\Delta\ell}{\lambda}\right)^2 . \tag{3.140}$$

In free space, $\eta = 120\pi$ and therefore the radiation resistance is

$$R_d = 80\pi^2\left(\frac{\Delta\ell}{\lambda}\right)^2 \quad (\Omega) . \qquad \textbf{(short dipole)}$$

Note that the radiation resistance is a function of frequency (or wavelength) and decreases rapidly with decreasing frequency. The equivalent capacitance is obtained from the reactive power $\omega(W_e + W_m)$. Comparing this reactive power to the reactive power stored in an equivalent capacitor, $I_0^2/(2\omega C_d)$, the dipole equivalent capacitance is given by

$$\begin{aligned} C_d &= \frac{I_0^2}{2\omega^2(W_e + W_m)} \\ &= \frac{1}{\pi\omega\eta\left(\frac{\Delta\ell}{\lambda}\right)^2\left(\frac{4}{(3ka)} + \frac{1}{(ka)^3}\right)} . \end{aligned} \tag{3.141}$$

For a Hertzian dipole, $k\,\Delta\ell/2 \ll 1$, so choosing $a = \Delta\ell/2$ and then ignoring $1/(ka)$ compared with $1/(ka)^3$, a very simple formulation for the capacitance is obtained:

$$C_d = \frac{\pi}{2}\varepsilon\,\Delta\ell . \qquad \textbf{(short dipole)} \tag{3.142}$$

It is interesting to note that this capacitance is not a function of frequency, and thus the antenna's capacitor acts like a lumped capacitor. For free space, $\varepsilon = \frac{1}{36\pi} \times 10^{-9}$ F/m, and

the explicit expression for the Hertzian dipole series capacitance is given by

$$C_{\rm d} = 13.89 \times 10^{-12} \Delta\ell \qquad \text{(F)} \; . \tag{3.143}$$

### 3-3.1 Simplification of Differential Operators in the Far-Field Region

In the far-field region where fields are in the form of transverse electromagnetic waves with spatial functions of the form $e^{ikr}/r$, such as in Eqs. (3.127a) and (3.127b), the differential operators can be simplified by replacing the operator $\nabla$ with $ik\,\hat{\mathbf{r}}$. For example, in the far-field region, the magnetic field intensity can be derived from

$$\mathbf{H}(\mathbf{r}) = \frac{1}{\mu} \nabla \times \mathbf{A}(\mathbf{r}) = \frac{1}{\mu}\, ik\hat{\mathbf{r}} \times \mathbf{A}(\mathbf{r}) \; , \tag{3.144}$$

and we can use Eq. (3.122) to obtain an explicit expression for the far-field approximation for the magnetic field of a Hertzian dipole:

$$\begin{aligned} \mathbf{H}(\mathbf{r}) &= \frac{1}{\mu} ik\hat{\mathbf{r}} \times \left( \frac{\mu I_0}{4\pi} \frac{e^{ik|\mathbf{r}-\mathbf{r}'|}}{|\mathbf{r}-\mathbf{r}'|}\, d\boldsymbol{\ell} \right) \\ &= \frac{ikI_0}{4\pi} \frac{e^{ik|\mathbf{r}-\mathbf{r}'|}}{r}\, \hat{\mathbf{r}} \times \, d\boldsymbol{\ell} \\ &= \frac{ik}{\mu} \left( A_\theta \, \hat{\boldsymbol{\phi}} - A_\phi \, \hat{\boldsymbol{\theta}} \right) \; . \end{aligned} \tag{3.145}$$

Also, Eq. (3.86) in the far-field is reduced to

$$\begin{aligned} \mathbf{E}(\mathbf{r}) &= \frac{i\omega}{k^2} \nabla\nabla \cdot \mathbf{A} + i\omega\mathbf{A} \\ &\approx \frac{i\omega}{k^2} (ik\hat{\mathbf{r}})(ik\hat{\mathbf{r}}) \cdot \mathbf{A}(\mathbf{r}) + i\omega \, \mathbf{A}(\mathbf{r}) \\ &= i\omega[\mathbf{A}(\mathbf{r}) - A_{\rm r}(\mathbf{r}) \, \hat{\mathbf{r}}] = i\omega(A_\theta \, \hat{\boldsymbol{\theta}} + A_\phi \, \hat{\boldsymbol{\phi}}) \; . \end{aligned} \tag{3.146}$$

When both electric and magnetic sources are present, duality and superposition can be invoked to obtain the following far-field expressions for the electric and magnetic fields:

$$\mathbf{E}(\mathbf{r}) = i\omega(A_\theta \, \hat{\boldsymbol{\theta}} + A_\phi \, \hat{\boldsymbol{\phi}}) - \frac{ik}{\varepsilon}(A_{{\rm m}\theta} \, \hat{\boldsymbol{\phi}} - A_{{\rm m}\phi} \, \hat{\boldsymbol{\theta}}) \tag{3.147a}$$

and

$$\mathbf{H}(\mathbf{r}) = \frac{ik}{\mu}(A_\theta \, \hat{\boldsymbol{\phi}} - A_\phi \, \hat{\boldsymbol{\theta}}) + i\omega(A_{{\rm m}\theta} \, \hat{\boldsymbol{\theta}} + A_{{\rm m}\phi} \, \hat{\boldsymbol{\phi}}) \; . \tag{3.147b}$$

## 3-4 Far-Field Distance Criterion

The far-field distance for electromagnetic sources was described qualitatively earlier. To quantify a measure for the far-field distance, we start with small antennas like the short

Hertzian dipole. Consider the magnetic field given by Eq. (3.123). Requiring the first term in the expression to be much larger than the second term, i.e., requiring the Biot-Savart's component of the magnetic field to be much smaller than the radiation term, leads to

$$\frac{1}{k|\mathbf{R}|} \ll 1 \,,$$

where $\mathbf{R} = |\mathbf{r} - \mathbf{r}'|$. If we adopt a factor of 10 for the ratio of the radiation component to the nonradiation component, then

$$R = \frac{10}{k} = \frac{10\lambda}{2\pi} = 1.6\lambda$$

is considered to be the far-field distance for a Hertzian dipole. This criterion can be used for all antennas whose dimensions are small compared to the wavelength. However, for antennas whose dimensions are comparable to or larger than the wavelength, the far-field criterion can be obtained by examining the phase difference between the radiated fields emanating from the center and the edge of the antenna. For an antenna with a maximum dimension of $D$, as shown in Fig. 3-7, the phase difference between the radiated fields emanating from the center and the edge of the antenna can be computed from

$$\begin{aligned} \Delta\phi = k(R_e - R_0) &\approx k\left[R_0\left(1 + \frac{D^2}{8R_0^2}\right) - R_0\right] \\ &= \frac{1}{8}\,k\,\frac{D^2}{R_0} \,. \end{aligned} \tag{3.148}$$

Requiring this phase difference to be less than $\pi/8$, the far-field distance is given by

$$R_0 \geq \frac{2D^2}{\lambda} \,. \tag{3.149}$$

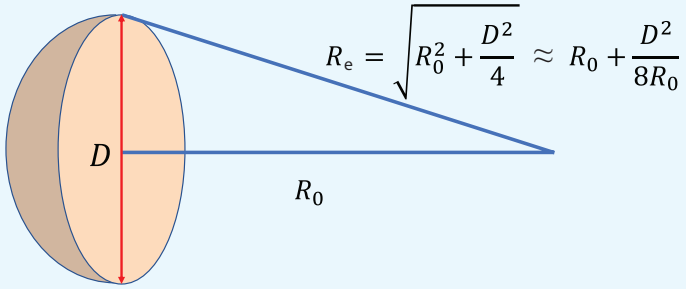


**Figure 3-7:** Geometry of an antenna with maximum dimension $D$ and an observation point at distance $R_0$ from the antenna center.

This criterion ensures that the variations of the field with distance can be expressed as $e^{ikr}/r$ with a maximum phase error of less than 22.5°.

## 3-5 Small Loop of Current: A Hertzian Magnetic Dipole

As was noted earlier, magnetic dipoles observed in certain materials are the result of electron orbital motion, or electron or nuclear spin. The motion of electrons along a closed loop can generate a magnetic field and a permanent magnetic dipole moment. This permanent magnetic dipole moment can react to an external magnetic field excitation. In this section we show that when the loop radius is small (compared with the wavelength as well as with the observation distance from the loop center), the electromagnetic field produced by the loop is the same as what a Hertzian magnetic dipole produces. To establish this equivalence, we consider a small circular loop, carrying a time-harmonic electric current, with radius $a$ centered in the $x$–$y$ plane of a Cartesian coordinate system, as shown in Fig. 3-8. The current distribution can be expressed mathematically as

$$\mathbf{J}(\mathbf{r}) = I_0\,\delta(\rho - a)\,\delta z\,\hat{\boldsymbol{\phi}}\ . \tag{3.150}$$

The magnetic vector potential generated by this current loop is given by

$$\mathbf{A}(\mathbf{r}) = \frac{\mu I_0}{4\pi}\int_0^{2\pi} \frac{e^{ik|\mathbf{r}-\mathbf{r}'|}}{|\mathbf{r}-\mathbf{r}'|}(-\sin\phi'\,\hat{\mathbf{x}} + \cos\phi'\,\hat{\mathbf{y}})a\,d\phi\ . \tag{3.151}$$

Noting that $\mathbf{r}' = a(\cos\phi'\,\hat{\mathbf{x}} + \sin\phi'\,\hat{\mathbf{y}})$ and that

$$\mathbf{r} = r(\sin\theta\cos\phi\,\hat{\mathbf{x}} + \sin\theta\sin\phi\,\hat{\mathbf{y}} + \cos\theta\,\hat{\mathbf{z}})\ ,$$

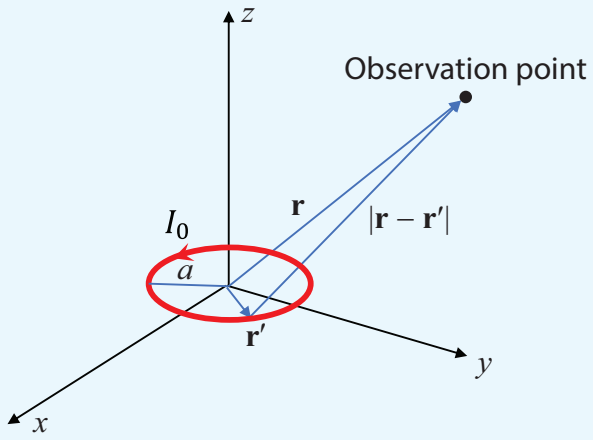


**Figure 3-8:** Geometry of a circular loop antenna of radius $a$ and an observation point at distance $R_0$ from the antenna center.

it follows that

$$|\mathbf{r}-\mathbf{r}'| = \sqrt{r^2+a^2-2ra\sin\theta\cos(\phi-\phi')}\ . \tag{3.152}$$

Using a Taylor series expansion of the integrand around $a=0$ yields

$$\frac{e^{ik|\mathbf{r}-\mathbf{r}'|}}{|\mathbf{r}-\mathbf{r}'|} \approx \frac{e^{ikr}}{r} + \frac{e^{ikr}}{r}\left(-ik+\frac{1}{r}\right)\sin\theta\cos(\phi-\phi')\,a\ . \tag{3.153}$$

After inserting Eq. (3.153) into Eq. (3.151) and noting that the first term will integrate to zero and

$$\int_0^{2\pi} \sin\phi'\cos(\phi-\phi')\,d\phi' = \pi\sin\phi \tag{3.154a}$$

and

$$\int_0^{2\pi} \cos\phi'\cos(\phi-\phi')\,d\phi' = \pi\cos\phi\ , \tag{3.154b}$$

we obtain the following closed-form expression for the magnetic potential:

$$\mathbf{A}(\mathbf{r}) = \frac{\mu I_0\pi a^2}{4\pi}\frac{e^{ikr}}{r}\left(-ik+\frac{1}{r}\right)\sin\theta\ \hat{\boldsymbol{\phi}}\ . \tag{3.155}$$

The electric field can be obtained from Eq. (3.86); however, noting that $\mathbf{A}(\mathbf{r})$ has only one component along $\hat{\boldsymbol{\phi}}$ but it is not a function of $\phi$, it is obvious that $\nabla\cdot\mathbf{A}(\mathbf{r})=0$. Therefore,

$$\mathbf{E}(\mathbf{r}) = \frac{i\omega\mu k I_0\pi a^2}{4\pi}\frac{e^{ikr}}{r}\left(-i+\frac{1}{kr}\right)\sin\theta\ \hat{\boldsymbol{\phi}}\ . \tag{3.156}$$

Also, the magnetic field can be derived from

$$\mathbf{H}(\mathbf{r}) = \frac{1}{\mu}\nabla\times\mathbf{A}(\mathbf{r})\ ,$$

which yields

$$\mathbf{H}(\mathbf{r}) = \frac{-ik^2 I_0\pi a^2}{4\pi}\frac{e^{ikr}}{r}\left[2\left(\frac{1}{kr}+\frac{i}{(kr)^2}\right)\cos\theta\hat{\mathbf{r}} + \left(-i+\frac{1}{kr}+\frac{i}{(kr)^2}\right)\sin\theta\ \hat{\boldsymbol{\theta}}\right]. \tag{3.157}$$

The fields for a Hertzian magnetic dipole, with a current moment $I_{0\mathrm{m}}\,\Delta\ell$, can be obtained from Eqs. (3.129) and (3.130) using the duality relations. These expressions are exactly the same as Eqs. (3.156) and (3.157) if we set

$$I_{0\mathrm{m}}\,\Delta\ell = -ik\eta\pi a^2 I_0\ . \tag{3.158}$$

Hence, we emphasize here that a small current loop acts like a Hertzian magnetic dipole. Considering that $I_{0\mathrm{m}}\,\Delta\ell = -i\omega q_{\mathrm{m}}\,\Delta\ell$, the equivalent magnetic dipole moment of a current

loop is given by

$$p_{\mathrm{m}} = q_{\mathrm{m}}\,\Delta\ell = \mu\pi a^2 I_0 \quad \text{(Wb m)}. \tag{3.159}$$

In the literature, the quantity $m = \pi a^2 I_0$ is referred to as the ***magnetic moment of the loop***. In a medium with $N$ magnetic moments per volume, the magnetization vector $\mathbf{M} = N\mathbf{m}$ A/m, and as was shown before in Eq. (1.49) of Chapter 1, the magnetic flux density can be obtained from $\mathbf{B} = \mu_0\mathbf{H} + \mu_0\mathbf{M}$.

Given the equivalence between a small current loop and a Hertzian magnetic dipole, the radiated power and the equivalent circuit model for a small loop antenna can be easily obtained using duality. The dual of Eq. (3.132), using Eq. (3.158), is given by

$$P_{\mathrm{r}} = \frac{\eta}{3}\frac{|I_{0m}\,\Delta\ell|^2 k^2}{4\pi} = \frac{\eta k^4 A^2 |I_0|^2}{12\pi}\,, \tag{3.160}$$

where $A = \pi a^2$. The radiation resistance, therefore, is

$$R_{\mathrm{loop}} = \frac{8\pi^3\eta}{3}\left(\frac{A}{\lambda^2}\right)^2. \qquad \textbf{(small loop antenna)} \tag{3.161}$$

The dual of the equivalent circuit of Fig. 3-6 is an inductor in series with $R_{\mathrm{loop}}$. The equivalent inductance can be calculated from

$$L_{\mathrm{loop}} = \frac{\omega(W_{\mathrm{e}} + W_{\mathrm{m}})}{\frac{1}{2}\omega|I_0|^2}\,. \tag{3.162}$$

The expressions for $W_{\mathrm{e}}$ and $W_{\mathrm{m}}$ can be obtained by applying duality to Eqs. (3.137) and (3.135), respectively. In the application of the duality principle, the quantity $I_0\,\Delta\ell$ should be replaced with $-ik\eta\pi a^2 I_0$. Choosing the radius of the enclosed volume to be the same as the radius of the loop, and after some simple algebraic manipulations, the loop inductance is found to be

$$L_{\mathrm{loop}} = \frac{\pi}{4}\,\mu a\,. \tag{3.163}$$

In most low-frequency applications, multiturn loops are used quite frequently. In a multiturn loop antenna with $N$ turns, the current contributing to the radiation is $NI_0$, whereas the terminal current is $I_0$. Hence the radiation resistance and loop inductance are given by

$$R_{\mathrm{loop}} = \frac{8\pi^3\eta}{3}\left(N\,\frac{A}{\lambda^2}\right)^2 \tag{3.164a}$$

and $\qquad$ **($N$-turn loop antenna)**

$$L_{\mathrm{loop}} = N^2\,\frac{\pi}{4}\,\mu a\,. \tag{3.164b}$$

### Example 3-5: Magnetic Dipole Moment of Hydrogen Atoms: A Classical Approach

Use the approximate Bohr's model to determine the resulting magnetic moment $m$ for a hydrogen atom. Assume the orbital radius of the electron is $a = 5.3 \times 10^{-11}$ m.

**Solution:** According to Bohr's model, a single electron orbits around the nucleus, which contains a single proton. The motion of the circling electron constitutes an electric current in the opposite direction of the electron motion. If the velocity $u$ and the circumference of the electron orbit $2\pi a$ are known, the equivalent electric current can be obtained from

$$I_0 = \frac{eu}{2\pi a} \,. \tag{3.165}$$

Using classical mechanics, the electron velocity can be estimated by balancing the electrostatic force, between the electron and proton, against the centrifugal force of the electron. That is,

$$\frac{e^2}{4\pi\varepsilon a^2} = \frac{m_e u^2}{a} \,,$$

from which the electron velocity is found to be

$$\begin{aligned} u &= \frac{e}{\sqrt{4\pi\varepsilon m_e a}} \\ &= \frac{1.6 \times 10^{-19}}{\sqrt{4\pi \times 8.86 \times 10^{-12} \times 9.1 \times 10^{-31} \times 5.3 \times 10^{-11}}} \\ &= 2.2 \times 10^6 \quad \text{m/s.} \end{aligned}$$

Here $m_e = 9.1 \times 10^{-31}$ kg is the mass of an electron. Hence the equivalent electric current of a single orbiting electron in a hydrogen atom is

$$I_0 = 1.05 \quad \text{mA} \,,$$

and its magnetic moment is calculated to be

$$\begin{aligned} m = \pi a^2 I_0 &= 3.1415 \times (5.3 \times 10^{-11})^2 \times 1.05 \times 10^{-3} \\ &= 9.26 \times 10^{-24} \quad (\text{A m}^2). \end{aligned}$$

It should be noted that Bohr's model is not an accurate model for atoms with more than a single electron. One contradiction to the above model is that a loop current radiates electromagnetic fields, and therefore the electron should lose its momentum and fall into its nucleus. Bohr explained this contradiction by stating that the orbital radius of an electron around its nucleus is quantized with the smallest radius being $a = 5.3 \times 10^{-11}$, which is known as the "ground state." Hence the electron is not allowed to get closer to the nucleus, and larger orbits can only be achieved if the electron receives specific quantized energy levels from

the electromagnetic waves (photons). Because of its magnetic dipole moment, it seems like hydrogen is a paramagnetic element. However, hydrogen in its natural form appears as an $H_2$ molecule with two electrons having opposite spins, thereby producing a net zero magnetic dipole moment. Monoatomic hydrogen can exist only at extremely high temperatures.

### 3-5.1 Equivalence between Small Current Loops and Short Magnetic Dipoles: An Alternative Method

In the previous section, the equivalence between a small loop carrying an electric current and a short magnetic dipole perpendicular to the loop surface was established by comparing the radiated fields from both. In this section an alternative approach based on Maxwell's equations is presented. Let us denote the field solutions to Maxwell's equations generated by an impressed electric current distribution $\mathbf{J}(\mathbf{r})$ as $\mathbf{E}_1(\mathbf{r})$ and $\mathbf{H}_1(\mathbf{r})$. In this case,

$$\nabla \times \mathbf{E}_1(\mathbf{r}) = i\omega\mu\, \mathbf{H}_1(\mathbf{r}) \tag{3.166a}$$

and

$$\nabla \times \mathbf{H}_1(\mathbf{r}) = -i\omega\varepsilon\, \mathbf{E}_1(\mathbf{r}) + \mathbf{J}(\mathbf{r})\ . \tag{3.166b}$$

By taking the curl of Faraday's law and then using the modified Ampère's law, it can easily be shown that

$$\nabla \times \nabla \times \mathbf{E}_1(\mathbf{r}) - k^2\, \mathbf{E}_1(\mathbf{r}) = i\omega\mu\, \mathbf{J}(\mathbf{r})\ . \tag{3.167}$$

Now let us consider another problem for which the fields are produced entirely by a magnetic current distribution $\mathbf{J}_{\rm m}(\mathbf{r})$. We denote these fields as $\mathbf{E}_2(\mathbf{r})$ and $\mathbf{H}_2(\mathbf{r})$:

$$\nabla \times \mathbf{E}_2(\mathbf{r}) = i\omega\mu\, \mathbf{H}_2(\mathbf{r}) - \mathbf{J}_{\rm m}(\mathbf{r}) \tag{3.168a}$$

and

$$\nabla \times \mathbf{H}_2(\mathbf{r}) = -i\omega\varepsilon\, \mathbf{E}_2(\mathbf{r})\ . \tag{3.168b}$$

Similar to the previous case, by taking the curl of Faraday's law and using Ampère's law, it can be shown that

$$\nabla \times \nabla \times \mathbf{E}_2(\mathbf{r}) - k^2\, \mathbf{E}_2(\mathbf{r}) = -\nabla \times \mathbf{J}_{\rm m}(\mathbf{r})\ . \tag{3.169}$$

If we require the field solutions to be the same, while maintaining the same boundary conditions, then the following relation between the sources must apply:

$$\nabla \times \mathbf{J}_{\rm m}(\mathbf{r}) = -i\omega\mu\, \mathbf{J}(\mathbf{r})\ . \tag{3.170}$$

Consider a small current loop carrying current $I$ and a uniform magnetic current density $\mathbf{J}_{\rm m}$ of height $\Delta\ell$ flowing in a direction perpendicular to the loop with its extent confined to the loop's cross section as shown in Fig. 3-9. Applying a surface integral on both sides of Eq. (3.170) and then applying Stokes' theorem, we have

$$-i\omega\mu \iint_S \mathbf{J}(\mathbf{r})\, ds = \oint_C \mathbf{J}_{\rm m}(\mathbf{r})\, d\ell\ . \tag{3.171}$$

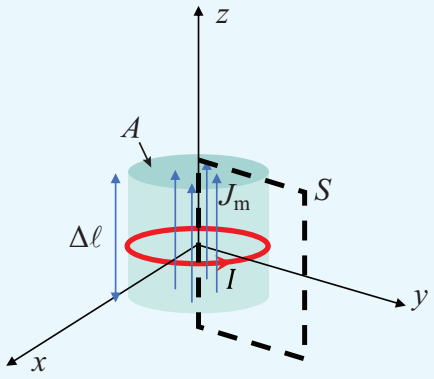


**Figure 3-9:** A circular current loop with a small radius, a cross-section area $A$, and a short uniform magnetic current distribution confined within the loop. This small uniform magnetic current distribution can be approximated as a short magnetic current filament $J_m A = I_m$ at the center of the loop.

Consider $S$ to be a small rectangular surface perpendicular to the surface that contains the current loop and has its contour inside the loop, as shown in Fig. 3-9. It then can be shown that

$$-i\omega\mu I = J_m \, \Delta\ell. \tag{3.172}$$

Multiplying both sides of the above equation by the area of the loop $A$ and noting that the total magnetic current is $I_m = J_m A$, the equivalence between the loop current and the magnetic current filament is found to be

$$I_m \, \Delta\ell = -ik\eta I A \, , \tag{3.173}$$

which is consistent with Eq. (3.158). It is noted that the equivalence of the current loop and a short uniform magnetic current distribution within the loop is exact. Applying the duality principle, it can also be shown that a magnetic current loop carrying current $I_m$ is equivalent to a short Hertzian dipole if the following relation holds:

$$I \, \Delta\ell = \frac{ik}{\eta} I_m A \, . \tag{3.174}$$

## 3-6 Wire Antennas

In the previous sections, we presented the procedures for computing the fields radiated by arbitrary electric and magnetic sources of known distributions. But how are these currents established in space? The currents and voltages generated by active circuits at a desired frequency are used to derive electric current distributions using conductors with very high conductivities. The shapes of these conductors connected to these sources dictate the current distribution function in space. Engineering the desired current distribution function using metallic wires and surfaces, which are referred to as antennas, is a complicated task.

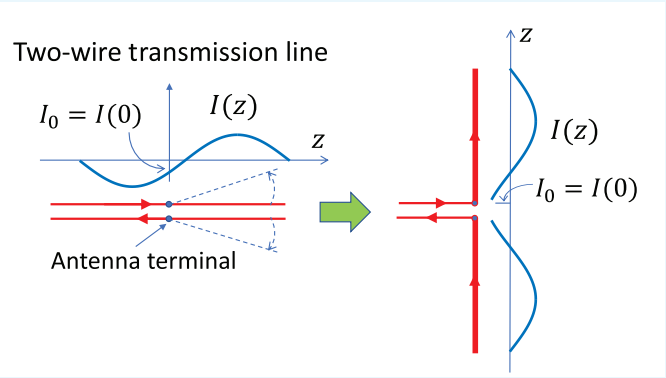


**Figure 3-10:** An open-ended two-wire transmission line supporting a standing-wave current distribution. Shown on the right side is a dipole antenna formed by bending the wires of the transmission line at the antenna terminal points to form a dipole antenna that supports a current distribution similar to that along the transmission line.

However, for certain antenna geometries like straight wires and loops, the current distributions can be accurately estimated. For example, along a dipole antenna of arbitrary length, the current distribution can be approximated from what would have existed on an open-ended transmission line if the dipole wires were straightened along the feeding transmission line, as shown in Fig. 3-10.

Assuming the length of the dipole is $\ell$, the current distribution is approximated by

$$I(z) = \frac{I_0}{\sin(k\ell/2)} \sin[k(\ell/2 - |z|)] \,, \tag{3.175}$$

where $I_0$ is the current at the antenna terminal. This equation ensures that the current at the end of the wires on the dipole goes to zero as expected. This current can be used in Eqs. (3.127a) and (3.127b) to find the electric and magnetic fields in the far-field region. When $\ell \ll \lambda$, the current distribution on the dipole can be approximated by a linear current distribution with the current being $I_0$ at the terminal and going to zero at the end. In this case, the radiated fields can be shown to be proportional to the average current on the antenna $(I_0/2)$ and hence the radiated and reactive powers are reduced by a factor of four compared with what was calculated for a Hertzian dipole with a constant current. In this case the radiation resistance and capacitance are

$$R_{\text{short dipole}} = \frac{\pi\eta}{6}\left(\frac{\ell}{\lambda}\right)^2 = 20\pi^2\left(\frac{\ell}{\lambda}\right)^2 \tag{3.176a}$$

and **(short dipole with linear current distribution)**

$$C_{\text{short dipole}} = 2\pi\varepsilon\ell \,. \tag{3.176b}$$

The half-wave dipole antenna is the most commonly used antenna configuration. The length of this antenna is $\ell = \lambda/2$, and according to Eq. (3.175) the current distribution on this antenna is of the form

$$I(z) = I_0 \cos(kz), \qquad -\lambda/4 \le z \le \lambda/4 \,. \tag{3.177}$$

For this case, $\hat{\mathbf{z}} I(z')\, dz'$ can be substituted for $\mathbf{J}(\mathbf{r}')\, dv'$ in Eq. (3.127b) to find the electric field

$$\begin{aligned}
\mathbf{E}(\mathbf{r}) &= \frac{-ik\eta I_0}{4\pi} \frac{e^{ikr}}{r} \int_{-\lambda/4}^{\lambda/4} (\hat{\mathbf{z}} \times \hat{\mathbf{r}}) \times \hat{\mathbf{r}} \cos(kz')\, e^{-ikz'\cos\theta}\, dz' \\
&= \frac{-ik\eta I_0}{4\pi} \frac{e^{ikr}}{r} \sin\theta\ \hat{\boldsymbol{\theta}} \int_{-\lambda/4}^{\lambda/4} \frac{e^{ikz'} + e^{-ikz'}}{2}\, e^{ikz'\cos\theta}\, dz' \\
&= \frac{-i\eta I_0}{2\pi} \frac{e^{ikr}}{r} \frac{\cos(\frac{\pi}{2}\cos\theta)}{\sin\theta}\, \hat{\boldsymbol{\theta}} \,.
\end{aligned} \tag{3.178a}$$

Similarly, the magnetic field is calculated to be

$$\mathbf{H}(\mathbf{r}) = \frac{-iI_0}{2\pi} \frac{e^{ikr}}{r} \frac{\cos(\frac{\pi}{2}\cos\theta)}{\sin\theta}\, \hat{\boldsymbol{\phi}} \,. \tag{3.178b}$$

The time-average power density can now be easily calculated:

$$S_{\text{avg}}(\mathbf{r}) = \frac{|I_0|^2\eta}{8\pi^2 r^2} \left( \frac{\cos(\frac{\pi}{2}\cos\theta)}{\sin\theta} \right)^2, \qquad \textbf{(}\lambda/2\ \textbf{dipole)} \tag{3.179}$$

from which the total radiated power can be evaluated:

$$P_{\text{r}} = \frac{|I_0|^2\eta}{8\pi^2} \int_0^{2\pi} \int_0^{\pi} \left( \frac{\cos(\frac{\pi}{2}\cos\theta)}{\sin\theta} \right)^2 \sin\theta\, d\theta\, d\phi \,. \tag{3.180}$$

The integral can be evaluated numerically to yield

$$P_{\text{r}} = 36.56 |I_0|^2 \,, \tag{3.181}$$

and noting that $P_{\text{r}} = \frac{1}{2} R_{\text{r}} |I_0|^2$, the radiation resistance for a half-wave dipole is

$$R_{\text{r}} = 73.13\ \Omega \,. \qquad \textbf{(}\lambda/2\ \textbf{dipole)} \tag{3.182}$$

The directivity function defined as

$$D(\theta, \phi) = \frac{4\pi r^2 S_{\text{avg}}(\mathbf{r})}{P_{\text{r}}}$$

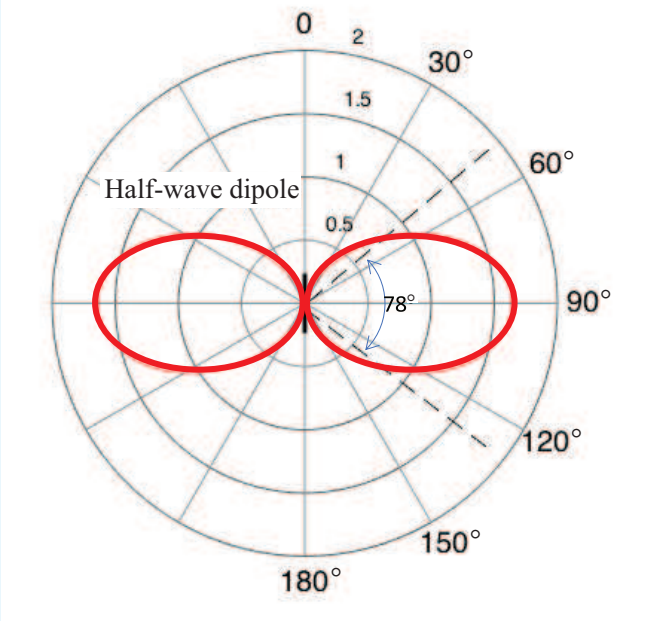


**Figure 3-11:** Radiation pattern of a half-wave dipole in the elevation plane (as a function of $\theta$).

for a half-wave dipole is given by

$$D(\theta,\phi) = 1.64\left(\frac{\cos(\frac{\pi}{2}\cos\theta)}{\sin\theta}\right)^2. \qquad (\lambda/2 \text{ dipole}) \tag{3.183}$$

The radiation pattern of the half-wave dipole is shown in Fig. 3-11. As expected, there is no dependence on $\phi$ and therefore the radiation pattern is uniform in the azimuthal plane. It is also a maximum along $\theta = 90°$, its directivity is 1.64, and the 3-dB beamwidth is 78°.

## 3-7 Equivalent Circuit for Receiving Antennas

It was shown previously that an antenna in transmission mode is viewed by a source as an equivalent load impedance $Z_t$, which is a combination of resistive and reactive lumped elements. Now the question is: Can this equivalent circuit be used for the same antenna when operating in the receiving mode? Electric current is excited on an antenna exposed to a uniform incident electric field. Basically, the ambient electric field is the force function on the free electrons on the surface of a metallic antenna. The receiving antenna is usually connected to a receiver circuit that may be composed of a low-noise amplifier, mixer and a detector. If we represent the input impedance of the receiver by $Z_L$ and the current at the terminal of the antenna by $I_L$, the receive input voltage is $V_L = Z_L I_L$. The Thévenin-equivalent circuit of the

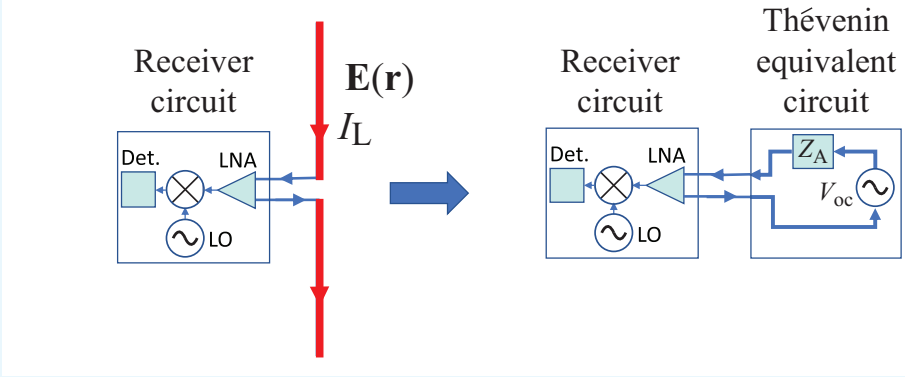


**Figure 3-12:** A receiving antenna connected to a receiver circuit and its equivalent circuit model.

receiving antenna is composed of a voltage source $V_{oc}$ in series with a source impedance $Z_A$, as shown in Fig. 3-12, where $V_{oc}$ is simply the open-circuit voltage that appears at the antenna terminals if the receiver circuit is disconnected.

### 3-7.1 Equivalence of Antenna Impedance in Transmission and Reception Modes

In what follows, it will be shown that the receive antenna impedance $Z_A$ is the same impedance had the antenna been used as a transmitter. To show this equivalence, we consider three experiments. In experiment 1, as shown in Fig. 3-13(1), we consider the antenna in a receiving mode connected to a load impedance $Z_L$ and then we measure a current $I_r$ that goes through it. According to the Thévenin equivalent circuit of the antenna, the measured current is given by

$$I_r = \frac{V_{oc}}{Z_A + Z_L} \,. \tag{3.184}$$

In the second experiment, the same antenna is connected to a source with open-circuit voltage $V_t$ and a source impedance equal to $Z_L$, and the current going through the source ($I_t$) is measured. Since the antenna is in transmitting mode, it presents a load impedance $Z_t$ to the source and the current provided by the source is computed using

$$I_t = \frac{V_t}{Z_t + Z_L} \,.$$

In the third experiment, the antenna is both exposed to the incident electric field and, at the same time, connected to the source. In this experiment we adjust the open-circuit voltage of the source to be

$$V_t = -V_{oc} \,.$$

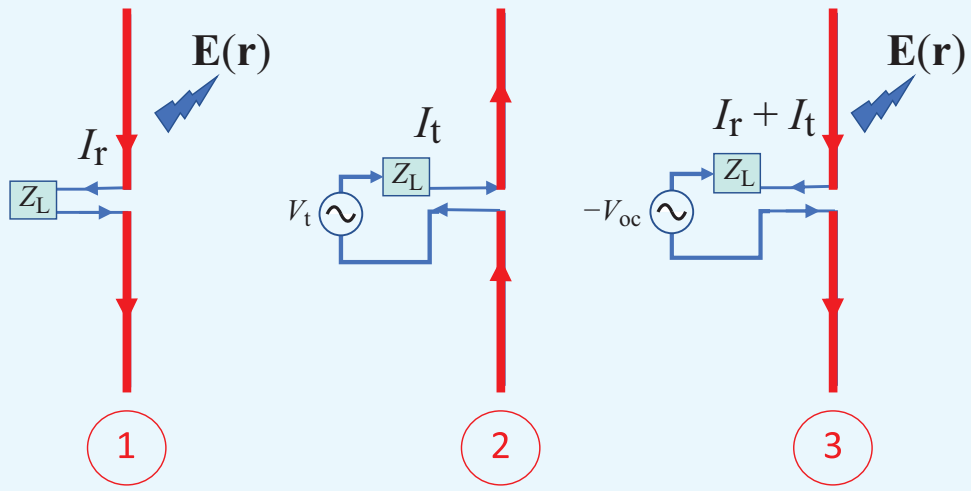


**Figure 3-13:** Configurations of three experiments to show that the antenna equivalent impedance in transmission and reception modes are the same. (1) An antenna in reception mode connected to a load impedance $Z_L$; (2) the antenna of experiment 1 in transmitting mode connected to a source with source impedance $Z_L$; (3) the same antenna in simultaneous reception and transmission modes when the source voltage is adjusted to be $-V_{oc}$.

In this case, because of the opposing voltage sources of equal amplitude and phase, no current will flow through $Z_L$. Using the superposition principle, the total current through $Z_L$ is

$$I_r + I_t = 0 \, .$$

That is,

$$\frac{V_{oc}}{Z_A + Z_L} + \frac{-V_{oc}}{Z_t + Z_L} = 0 \, . \tag{3.185}$$

This can be true only if

$$Z_A = Z_t \, , \tag{3.186}$$

which indicates that the impedance of an antenna is exactly the same for both transmitting and receiving modes. It should be emphasized that the above equation is valid for any arbitrary choice of $Z_L$.

## Summary

### Concepts

- Scalar and vector potential functions are introduced as tools to calculate fields generated by electromagnetic sources (electric and magnetic current and charge distributions).
- It is shown that the scalar and vector potentials satisfy the wave equation, which can be easily solved for a homogeneous and unbounded medium.
- Using the superposition principle, the solution to the wave equation for point sources (retarded potential) is used to find the potentials and the fieds for any arbitrary distribution of electric and magnetic current distributions.
- The notion of time-harmonic electromagnetic waves is introduced to reduce the dimensionality of Maxwell's equations. Expressions for time-average power density and stored electric and magnetic energy density are obtained for time-harmonic waves.
- It is shown that the conductivity of a conducting medium can be included in the imaginary part of the complex permittivity of the medium to create an effective complex dielectric constant.
- Simple expressions for the electric and magnetic fields generated from small current filaments, known as Hertzian dipoles, are obtained. Using the superposition principle, these results are expanded to include the field expressions for arbitrary time-harmonic sources.
- The notion of equivalent circuits for transmitting and receiving antennas in terms of radiation resistance and conductance are obtained, and it is shown that the same equivalent circuit model can be used for an antenna when operated in transmitting or receiving modes.
- The concept of far-field distance for antennas is introduced. At distances larger than the far-field distance the dependence of field expressions with range is of the form $\frac{1}{r}\, e^{ikr}$.
- The equivalence between a small current loop and a magnetic Hertzian dipole, perpendicular to the loop surface, is demonstrated.

## Important Equations

**Magnetic field in terms of magnetic vector potential:**

$$\mathbf{H}(\mathbf{r}) = \frac{1}{\mu}\,\nabla \times \mathbf{A}(\mathbf{r})$$

**Electric field in terms of potentials:**

$$\mathbf{E}(\mathbf{r}) = -\nabla\,\Phi(\mathbf{r}) - \frac{\partial \mathbf{A}(\mathbf{r})}{\partial t}$$

**Lorentz gauge condition:**

$$\nabla \cdot \mathbf{A}(\mathbf{r}) = -\mu\varepsilon\,\frac{\partial \Phi(\mathbf{r})}{\partial t}$$

**Wave equation:**

$$\nabla^2 A(\mathbf{r})\,\mu\varepsilon\,\frac{\partial^2 \mathbf{A}(\mathbf{r})}{\partial t^2} = -\mu\,\mathbf{J}(\mathbf{r})$$

$$\nabla^2\,\Phi(\mathbf{r})\,\mu\varepsilon\,\frac{\partial^2 \Phi(\mathbf{r})}{\partial t^2} = -\frac{\rho(r^2)}{\varepsilon}$$

**Electric and magnetic fields in terms of dielectric and magnetic Hertz potentials:**

$$\mathbf{E} = \nabla\nabla\cdot\mathbf{\Pi} - \mu\varepsilon\,\frac{\partial^2 \mathbf{\Pi}}{\partial t^2} - \mu\nabla\times\left(\frac{\partial \mathbf{\Pi}_{\mathrm{m}}}{\partial t}\right)$$

$$\mathbf{H} = \nabla\nabla\cdot\mathbf{\Pi}_{\mathrm{m}} - \mu\varepsilon\,\frac{\partial^2 \mathbf{\Pi}_{\mathrm{m}}}{\partial t^2} + \varepsilon\nabla\times\left(\frac{\partial \mathbf{\Pi}}{\partial t}\right)$$

**Magnetic vector potential in terms of a volumetric electric current distribution:**

$$\mathbf{A}(r,t) = \frac{\mu}{4\pi}\iiint_v \frac{\mathbf{J}(\mathbf{r}',\, t - |\mathbf{r}-\mathbf{r}'|/u_{\mathrm{p}})}{|\mathbf{r}-\mathbf{r}'|}\,d\mathbf{r}'$$

**Characteristic impedance of a homogeneous medium:**

$$\frac{|\mathbf{E}|}{|\mathbf{H}|} = \sqrt{\frac{\mu}{\varepsilon}} = \eta$$

**Time-harmonic Maxwell's equations:**

$$\nabla\times\mathbf{E}(\mathbf{r}) = i\omega\mu\,\mathbf{H}(\mathbf{r}) - \mathbf{J}_{\mathrm{m}}(\mathbf{r})$$
$$\nabla\times\mathbf{H}(\mathbf{r}) = -i\omega\varepsilon\,\mathbf{E}(\mathbf{r}) + \mathbf{J}(\mathbf{r})$$
$$\nabla\cdot\mathbf{B}(\mathbf{r}) = \rho_{\mathrm{m}}(\mathbf{r})$$
$$\nabla\cdot\mathbf{D}(\mathbf{r}) = \rho(\mathbf{r})$$

**Effective complex permittivity of a conducting medium:**

$$\varepsilon_{\mathrm{eff}} = \varepsilon + i\sigma/\omega$$

**Time-average Poynting vector:**

$$\mathbf{S}_{\mathrm{avg}}(\mathbf{r}) = \tfrac{1}{2}\,\Re\mathrm{e}[\mathbf{E}(\mathbf{r})\times\mathbf{H}^*(\mathbf{r})]$$

**Complex power flow density:**

$$\mathbf{S}(\mathbf{r}) = \tfrac{1}{2}\,\mathbf{E}(\mathbf{r})\times\mathbf{H}^*(\mathbf{r})$$

**Time-average electric and magnetic energy densities:**

$$w_{\mathrm{e}}^{\mathrm{avg}}(\mathbf{r}) = \frac{\varepsilon'}{4}\,|\mathbf{E}(\mathbf{r})|^2\,, \qquad w_{\mathrm{m}}^{\mathrm{avg}}(\mathbf{r}) = \frac{\mu'}{4}\,|\mathbf{H}(\mathbf{r})|^2$$

**Time-average electric and magnetic dissipated power densities:**

$$P_{\mathrm{loss}}^{\mathrm{avg}} = \tfrac{1}{2}\,\omega(\varepsilon''|\mathbf{E}|^2 + \mu''|\mathbf{H}|^2)$$

**Dielectric quality factor:**

$$\breve{Q} = \frac{\varepsilon_{\mathrm{r}}'}{\varepsilon_{\mathrm{r}}''}$$

**Antenna directivity:**

$$D(\theta,\phi) = \frac{S_{\mathrm{avg}}(r,\theta,\phi)}{P_{\mathrm{rad}}/(4\pi r^2)}$$

**Quality factor of an antenna:**

$$\breve{Q}_{\mathrm{ant}} = \frac{\omega(W_{\mathrm{e}} + W_{\mathrm{m}})}{P_{\mathrm{rad}}}$$

**Far-field expansion for field in terms of vector potentials:**

$$\mathbf{E}(\mathbf{r}) = i\omega(A_\theta\,\hat{\boldsymbol{\theta}} + A_\phi\,\hat{\boldsymbol{\phi}}) - \frac{ik}{\varepsilon}(A_{\mathrm{m}\theta}\,\hat{\boldsymbol{\phi}} - A_{\mathrm{m}\phi}\,\hat{\boldsymbol{\theta}})$$
$$\mathbf{H}(\mathbf{r}) = \frac{ik}{\mu}(A_\theta\,\hat{\boldsymbol{\phi}} - A_\phi\,\hat{\boldsymbol{\theta}}) + i\omega(A_{\mathrm{m}\theta}\,\hat{\boldsymbol{\theta}} + A_{\mathrm{m}\phi}\,\hat{\boldsymbol{\phi}})$$

**Far-field distance:**

$R \geq 1.6\lambda$ for small antennas

$R \geq \dfrac{2D^2}{\lambda}$ for large antennas

**Relations between a current loop and Hertzian magnetic dipole:**

$$I_{0\mathrm{m}}\,\Delta\ell = -ik\eta\,\pi a^2 I_0$$

**Directivity of a Hertzian dipole and a $\lambda/2$ dipole:**

$$D_{\mathrm{Hertzian}} = \tfrac{3}{2}\sin^2\theta$$

$$D_{\lambda/2} = 1.64\left[\frac{\cos(\frac{\pi}{2}\cos\theta)}{\sin\theta}\right]$$

**Important Terms** Provide definitions or explain the meaning of the following terms:

antenna directivity
antenna equivalent circuit
antenna quality factor
characteristic impedance
complex power flow density
dielectric loss tangent
dielectric quality factor
effective permittivity
electric scalar potential
electric vector potential
far-field distance
gauge condition
Hertz vector potential
Hertzian dipole
Hertzian magnetic dipole
magnetic Hertz vector potential
magnetic moment of current loop
magnetic scalar potential
magnetic vector potential
quasi-static
radiation resistance
receiving antenna
retarded potential
time-average electric energy density
time-average magnetic energy density
time-average Poynting vector
time-harmonic fields
transverse electromagnetic wave
vector phasor
wave equation
wave number
wire antenna

## PROBLEMS

### Electromagnetic Potentials

**3.1** Consider a region defined by the perpendicular intersection of two semi-infinite PMC and PEC planes. Let a filament current source $\mathbf{I}(t)$ exist in this space, as shown in Fig. P3.1. Suppose the PEC and PMC surfaces coincide with the coordinate surface of a Cartesian coordinate system and the expression for the current is given by

$$\mathbf{I}(t) = I_0 \frac{\hat{\mathbf{y}} - \hat{\mathbf{x}}}{\sqrt{2}} \delta(x-a,\, y-a,\, z)\, f(t)\ .$$

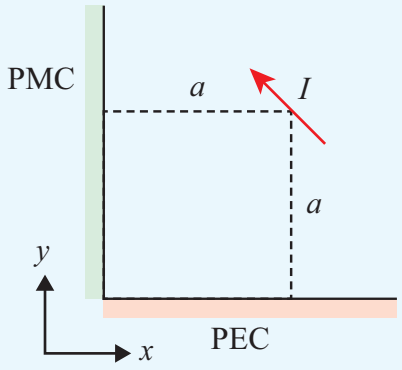


**Figure P3.1:** A small current filament placed inside a corner reflector whose one side is made from a semi-infinite PMC surface and whose other side is made from a semi-infinite PEC surface.

**(a)** Draw the equivalent images and write the expression for the image currents.

**(b)** Find the overall magnetic vector potential in the first quadrant.

**3.2** A fundamental relation used to solve scattering problems states that the total **E**-field is equal to the sum of the incident and scattered fields:

$$\mathbf{E}_{\mathrm{t}} = \mathbf{E}_{\mathrm{i}} + \mathbf{E}_{\mathrm{s}}.$$

Consider a thin vertical cylinder (along the $z$-axis) with relative permittivity $\varepsilon_{\mathrm{r}}$, height $L$, and small area $A$. The polarizability tensor of such a cylinder is given by

$$\overline{\overline{P}} = \begin{bmatrix} \dfrac{2}{\varepsilon_{\mathrm{r}}+1} & 0 & 0 \\ 0 & \dfrac{2}{\varepsilon_{\mathrm{r}}+1} & 0 \\ 0 & 0 & 1 \end{bmatrix} .$$

Remember that the normalized polarizability tensor of a material relates the internal electric field to the incident electric field:

$$\mathbf{E}_{\mathrm{int}} = \overline{\overline{P}} \cdot \mathbf{E}_{\mathrm{i}} \ .$$

Let the incident field be given by

$$\mathbf{E}_{\mathrm{i}} = \frac{\hat{\mathbf{y}} + \hat{\mathbf{z}}}{\sqrt{2}} \cos(\omega t - kx) \ .$$

**(a)** Find the equivalent polarization current so that the medium may be treated as free space.

**(b)** Find the magnetic vector potential in the surrounding space due to the polarization current.

**(c)** Give an expression for the scattered (and thus total) electric field in terms of **A**. You do not need to simplify this expression.

## Fields Radiated by Current Sources (Time Domain)

**3.3** Evaluate $\nabla(\hat{\mathbf{r}} \cdot d\boldsymbol{\ell})$ for any arbitrary differential line element $d\boldsymbol{\ell}$. Show that it is proportional to $1/r$.

**3.4** Image theory has been proven to be valid for electrostatic fields using Coulomb's law. Prove the validity of image theory for a *horizontal* infinitesimal current source above an infinite PEC sheet in the electrodynamic case.

Starting from the following electric field expression:

$$\mathbf{E} = \frac{I_0}{4\pi\varepsilon}\left(\frac{f}{u_{\mathrm{p}} r^2} + \frac{\int f\, dt}{r^3}\right)(\hat{\mathbf{r}} \cdot d\boldsymbol{\ell})\hat{\mathbf{r}} - \frac{I_0}{4\pi}\left(\frac{\sqrt{\varepsilon/\mu}\, f}{r^2} + \frac{\int f\, dt}{\varepsilon r^3} + \frac{\mu f'}{r}\right)\hat{\mathbf{r}} \times (d\boldsymbol{\ell} \times \hat{\mathbf{r}}) \ ,$$

prove that the tangential electric field component vanishes everywhere on the surface. (*Hint:* You can assume that the PEC sheet lies in the $x$–$y$ plane and that the current is along the $\hat{\mathbf{x}}$ direction, and position your test point on the $z$-axis at $z = z_0$.)

**3.5** Let the current on a thin metallic wire of length $L$ be given by

$$\mathbf{I} = \hat{\mathbf{z}}\, I_0 \cos(\omega t), \qquad -\frac{L}{2} < z < \frac{L}{2}\,.$$

**(a)** Find the magnetic vector potential $\mathbf{A}$ in the surrounding space due to the wire.

**(b)** Find the *far-field* electric and magnetic fields from the magnetic vector potential.

**(c)** Compute the Poynting vector $\mathbf{S}(t) = \mathbf{E} \times \mathbf{H}$ and its time average $\langle \mathbf{S} \rangle$.

**3.6** Use the Poynting theorem to derive the expression for the radiated power from an infinitesimal current source (Hertzian dipole).

$$\mathbf{J}(\mathbf{r},t) = \hat{\mathbf{z}}\, I(z)\ \delta(x)\ \delta(y)\ \cos(\omega t)\ ,$$

where $I(z) = I_0(1 - 2|z|/\Delta L)$ for $-\Delta L/2 < z < \Delta L/2$. Find the radiation resistance of a Hertzian dipole. Calculate this for $\Delta \ell = 0.01\lambda$.

**3.7** Derive the general expression for a time-dependent magnetic field along the $z$-axis of an arbitrary loop located in the $x$–$y$ plane and centered around the origin.

**(a)** Assume that the current is uniform along the loop $[I = I_0\, f(t)]$.

**(b)** Assume that the current varies with $\phi$ as $I = I_0 |\sin\phi|\, f(t)$.

## Time-Harmonic Fields

**3.8** One of the most common and elementary types of antenna is the half-wavelength dipole. Evaluate the fields produced by this dipole in the far field, and the corresponding total radiated power, its radiation resistance, and its directivity.

The antenna consists of two thin wires, each of length $h = \lambda/4$, as shown in Fig. P3.8. The signal to be transmitted is fed into the space between the rods. The current distribution can be written as

$$\begin{cases} I = I_0 \cos(\omega t)\cos(kz)\, \hat{\mathbf{z}} & -\lambda/4 < z < \lambda/4, \\ I = 0, & \text{otherwise}. \end{cases}$$

**(a)** Give the phasor form for this current source.

**(b)** Find the far-field vector potential and radiated electric and magnetic fields.

**(c)** Find the Poynting vector $\mathbf{S} = \mathbf{E} \times \mathbf{H}^*$ due to these fields and determine the radiation pattern for this antenna. The radiation pattern is simply $|\mathbf{S}|/[\max(|\mathbf{S}|)]$. Sketch the radiation pattern.

**(d)** Find the total radiated power $P$ by integrating the Poynting vector over a spherical surface. You may need to perform a numerical integration.

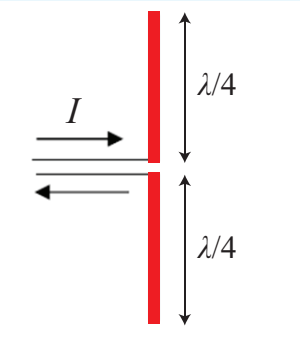


**Figure P3.8:** Configuration of a $\lambda/2$ dipole antenna fed by a two-wire transmission line with terminal current $I$.

**(e)** The radiation resistance for such an antenna is defined as $2P/I_0^2$. Find the radiation resistance.

**(f)** The directivity of an antenna is defined by $4\pi r^2 \max(|\mathbf{S}|)/P$. Find the directivity for this antenna.

**3.9** Consider the dipole described in Problem 3.7. Now, place it in front of an infinite ground plane as shown in Fig. P3.9. Find the radiation pattern (electric field distribution in the far field as a function of $\theta$ and $\phi$) and plot it for (a) $h = \lambda/4$ and (b) $h = \lambda/2$.

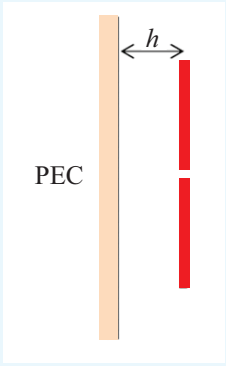


**Figure P3.9:** Geometry of the $\lambda/2$ dipole of Problem 3.8 placed in front of an infinite ground plane at a distance $h$.

**3.10** The magnetic vector potential of a short dipole positioned at the origin can be derived as

$$\mathbf{A} = \frac{\mu I_0}{4\pi} d\boldsymbol{\ell} \frac{e^{ikr}}{r} .$$

Two short vertical dipoles are placed above a perfect electric conductor (PEC) at a height $h$ and separated by a distance $s$, as shown in Fig. P3.10.

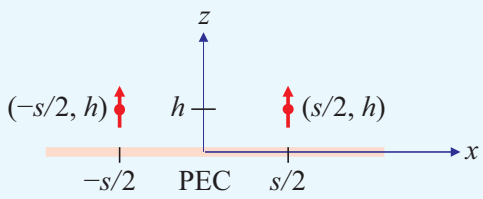


**Figure P3.10:** Two infinitesimal current filaments with separation $s$ placed at a height $h$ above an infinite ground plane. The direction of the currents is perpendicular to the ground plane.

**(a)** Derive an expression for the total magnetic vector potential in $x$–$y$ plane. Simplify the result for when the observation point is in the far-field region of the source.

**(b)** What is the magnetic vector potential in the far-field region when the perfect conductor is replaced with a perfect magnetic conductor?

**3.11** For a small circular loop of current $\mathbf{I} = \hat{\boldsymbol{\phi}}\, I_0 \cos(\omega t)$ and radius $a$ (with $a \ll \lambda$), as shown in Fig. P3.11:

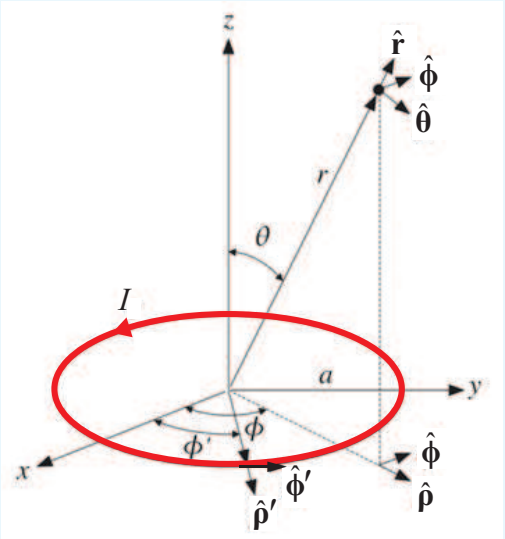


**Figure P3.11:** Configuration of a small loop carrying a constant current $I$.

**(a)** Determine the magnetic vector potential $\mathbf{A}$.

**(b)** Use this vector potential to derive the electric field $\mathbf{E}$ and magnetic field $\mathbf{H}$ and the time-average complex Poynting vector $\mathbf{S} = \frac{1}{2}(\mathbf{E} \times \mathbf{H}^*)$ in the far field.

**(c)** Find the total power $P$ radiated by the small loop by integrating the Poynting vector over a spherical surface centered at the origin with radius $R$ (such that $R \gg \lambda$).

**(d)** The radiation resistance for such an antenna is defined as $2P/I_0^2$. Find the radiation resistance for the small current loop. *Hint:*

(i) $\int_0^{\pi} \cos(n\phi)\, e^{jz\cos\pi}\, d\phi = \pi j^n J_n(z)$

(ii) $J_1(z) \approx z/2$ if $z \ll 1$.

## 3.12

**(a)** For a small loop of radius $r_0$ carrying current $I_1$ and centered at the origin, as shown in Fig. P3.12, show that the far-field magnetic vector potential is given by

$$\mathbf{A} = \frac{-ik_0\mu_0(\pi r_0^2 I_1)}{4\pi r} \sin\theta\, e^{ik_0 r}\, \hat{\boldsymbol{\phi}}\ .$$

**(b)** Using this expression, find the far-field electric and magnetic fields.

**(c)** If a short dipole of length $dl$ carrying current $I_2$ is also placed along the $z$-axis at the origin, choose the radius of the loop $r_0$ so that the total far-field radiation pattern is everywhere circularly polarized ($E_\theta$ and $E_\phi$ equal but 90° out of phase).

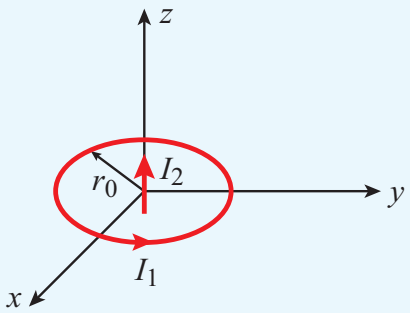


**Figure P3.12:** Geometry of a composite source made of a constant current loop and a vertical Hertzian dipole in the loop center and perpendicular to the surface of the loop.

## 3.13

**(a)** Using your results from Problem 3.12, show that the far-field electric and magnetic fields of a small circular loop of radius $a$ (with $a \ll \lambda$) carrying a time-harmonic current $I$ is the same as that of a short magnetic dipole of current $I_\mathrm{m}$, provided that $I_\mathrm{m}\, dl = -i\omega\mu(\pi a^2)I$.

**(b)** Now consider a small circular loop located at the origin excited by a time-harmonic current

$$\mathbf{I} = \hat{\boldsymbol{\phi}}\, \delta(r-a)\, \delta(z)\, I_0 \cos(\omega t)\ ,$$

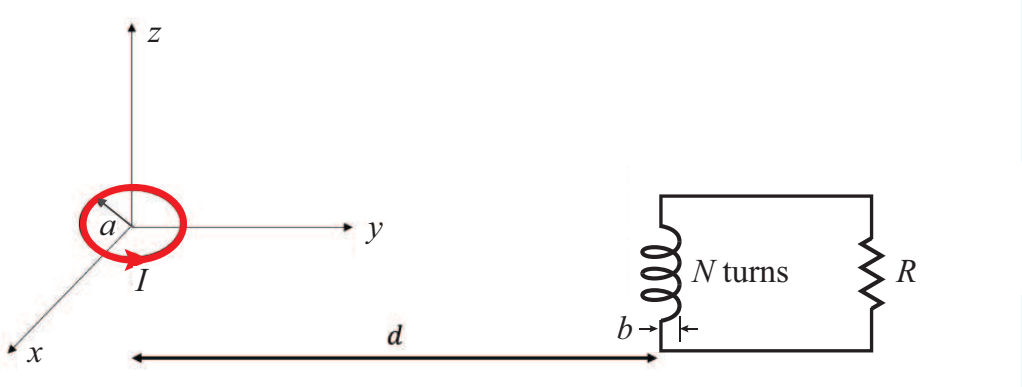


**Figure P3.13:** Configuration of a small loop carrying a uniform current used as a radio transmitter and a solenoid with $N$ turns used as the receiver located at a distance $d$ from the transmitter.

as shown in Fig. P3.13. A solenoid of $N$ turns and radius $b$ is placed in the far field of the excited small loop and is loaded with a resistor $R$.

(i) Assuming that the height of the solenoid is much smaller than the wavelength, calculate the inductance of the solenoid.

(ii) Find the electromotive force in the solenoid.

(iii) Calculate the power delivered to the load.

**3.14** The electric and magnetic fields of a plane wave are given by

$$\mathbf{E} = \hat{\mathbf{x}}\, E_0 e^{-j(\omega t + kz)}$$

and

$$\mathbf{H} = \hat{\mathbf{y}}\, \frac{E_0}{\eta}\, e^{-j(\omega t + kz)}\ .$$

This plane wave is normally incident from $z < 0$ on a square aperture of side length $a$ in an infinite PEC ground screen at $z = 0$ (see Fig. P3.14). Assume that the field in the aperture is identical to the field of the plane wave with the screen absent (this is called the ***Kirchhoff approximation***). Use the equivalence principle to find the corresponding sources. Find the electric vector potential $\mathbf{A}_{\mathrm{m}}$, and from that, determine the electric and magnetic fields in the far field for $z > 0$.

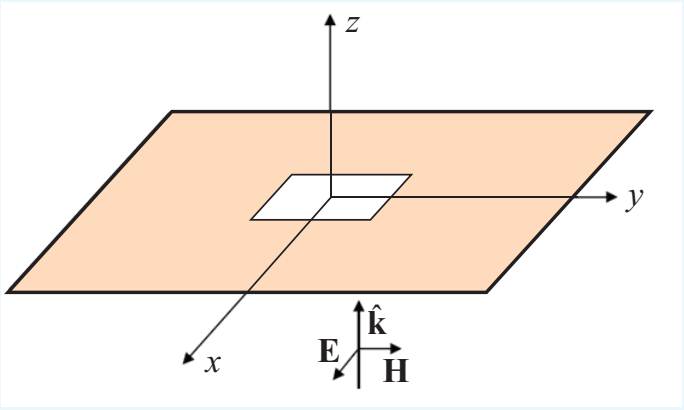


**Figure P3.14:** A rectangular aperture in a planar metallic plate excited by a plane wave illuminating the aperture from the lower half-space.

**3.15**

**(a)** Starting from the general definition of the stored magnetic energy per unit volume:

$$w_{\mathrm{m}} = \frac{1}{2}\,\mathbf{B}(r,t)\cdot\mathbf{H}(r,t),$$

prove that the time-average magnetic energy density is

$$w_{\mathrm{m}}^{\mathrm{avg}} = \frac{1}{4}\,\mu'|\mathbf{H}|^2.$$

**(b)** Prove that the time-average dissipated power is $P_{\mathrm{loss}} = \frac{1}{2}\iiint(\omega\mu''|\mathbf{H}|^2 + \omega\varepsilon''|\mathbf{E}|^2)\,dv$.

**3.16** A cavity is a closed metallic structure that confines electromagnetic fields. The electric field inside the rectangular cavity shown in Fig. P3.16 is given by

$$\mathbf{E} = -jE_0 \sin\frac{\pi x}{l}\sin\frac{\pi y}{a}\,\hat{\mathbf{z}}\,.$$

**(a)** Find the magnetic field distribution inside the cavity, assuming free-space permittivity and permeability for the medium inside the cavity.

**(b)** Find the electric and magnetic stored energy in the cavity.

**(c)** Now assume that the metallic walls of the waveguide are lossy with finite conductivity $\sigma$. The electric field and the surface current on the surface of a lossy conductor are related by the following equation:

$$\hat{\mathbf{n}}\times\mathbf{E} = Z_{\mathrm{s}}\,\hat{\mathbf{n}}\times\mathbf{J}_{\mathrm{s}}\,,$$

where $Z_s$ is the surface impedance given by

$$Z_s = (1+j)\sqrt{\frac{\omega\mu}{2\sigma}}\,.$$

The loss due to the finite conductivity of the metal is equal to the total power passing through the surface penetrating into the metal and given by

$$P = \frac{1}{2}\iint \Re\mathfrak{e}(\mathbf{E}\times\mathbf{H}^*)\cdot d\mathbf{s}\,.$$

Compute the total loss in the cavity for the given field distribution.

**(d)** Calculate the quality factor of the cavity defined as

$$\breve{Q} = \omega\,\frac{W_e + W_m}{P_{loss}}\,.$$

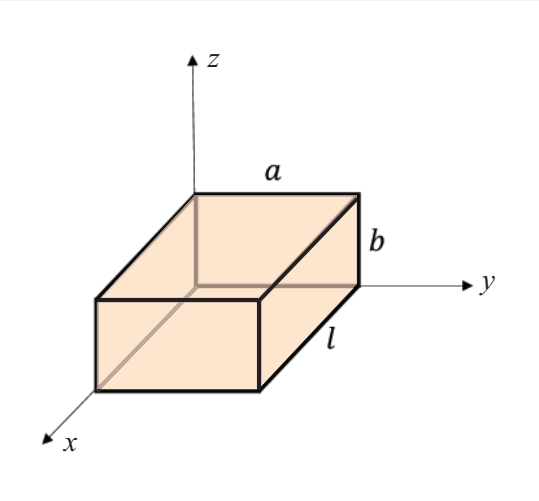


**Figure P3.16:** The geometry of a rectangular cavity with walls made from metallic plates of finite conductivity.

# Chapter 4
# Formal Solutions to Maxwell's Equations and Their Applications

## Chapter Contents


Overview, 162
4-1 Formal Solution of Helmholtz Equation, 162
4-2 Solution of Helmholtz Equation for a Complex Medium, 168
4-3 Integral Equations for Electromagnetic Fields, 176
4-4 Integral Equation Formulation Based on Equivalent Sources, 178
4-5 Integral Equation Formulation for Dielectric Scatterers, 181
4-6 Reciprocity Theorem, 184
4-7 Applications of the Reciprocity Theorem, 189
4-8 Babinet's Principle, 205
Chapter Summary, 216
Problems, 221


## Objectives

Upon learning the material presented in this chapter, you should be able to:

1. Derive expressions for the electromagnetic potentials in a homogeneous medium containing any number of objects with different constitutive parameters.
2. Understand the behavior of the potentials and fields at distances far away from the sources, known as the radiation condition.
3. Set up the integral equation formulations for fields and potentials in a heterogeneous medium.
4. Explain the concept of reciprocity for electromagnetic waves and its applications in antenna and scattering problems.
5. Understand the importance and applications of Babinet's principle in antennas and scattering problems.

## Overview

The focus of this chapter is to use Maxwell's equations to develop rigorous solutions for electromagnetic fields in complex media formed from a heterogeneous mixture of different objects of finite extent embedded in a homogeneous, isotropic, and unbounded medium, in the presence of known electric and magnetic charge and current distributions. We begin by applying the scalar Green's function in a homogeneous unbounded medium to derive wave equations in response to a spatial impulse function. The Green's function is simply the spatial impulse response of the wave equation. Green's theorem is then used to assist in solving the wave equation for the electromagnetic potentials in complex media. Also, the notion of a radiation condition is discussed to express the spatial behavior of the electromagnetic potentials and fields at observation points far from their sources. These solutions are used as a foundation for developing integral equations for the electromagnetic potentials and fields. The process leads to multiple formulations, including the extinction theorem and the electric-field integral equation (EFIE) and magnetic-field integral equation (MFIE) for dielectric and metallic objects, using equivalent sources on the surfaces of the objects. These equations can be solved numerically for a wide range of scattering and antenna problems. Also in this chapter, the reciprocity theorem, which establishes a symmetrical relation between two different sources and their corresponding fields, is introduced. Applications of the reciprocity theorem to antennas are discussed, and it is shown that the radiation pattern of an antenna is the same in both transmission and reception modes. Also the concept of effective area of a receiving antenna is introduced, and its relationship to the antenna directivity is derived. Finally, Babinet's principle for planar metallic structures is introduced, and the relations between the fields of metallic sheets with an opening (aperture) and those forming the complementary metallic sheet are presented. Babinet's principle is used to relate the radiation pattern, polarization, and input impedance of a planar antenna and those for its complementary geometries. Antennas using self-complementary geometries, which makes them frequency-independent, are discussed as well.

## 4-1 Formal Solution of the Helmholtz Equation

This section presents a formal procedure for deriving the solution of the scalar and vector wave equations given by Eqs. (3.87a) and (3.87b). The results presented previously for the retarded potential were obtained somewhat heuristically and are only valid for an unbounded homogeneous medium. The formal solution presented in this section can, in principle, be obtained for far more complicated media. We begin with the derivation of the spatial impulse response of the scalar wave equation for an unbounded homogeneous medium, which is known as ***Green's function***. Consider the following scalar wave equation with an impulse excitation at the origin:

$$\nabla^2 g(\mathbf{r}) + k^2 g(\mathbf{r}) = -\delta(\mathbf{r}) \; . \tag{4.1}$$

The source function (point source) is assumed to have spherical symmetry. In the context of generalized functions, $h(\mathbf{r})$ satisfies the following integral identity:

$$\iiint_V h(\mathbf{r}') \; \delta(\mathbf{r} - \mathbf{r}') \, d\mathbf{r}' = h(\mathbf{r}) \; , \tag{4.2}$$

which is valid for any continuous function $h(\mathbf{r})$. Here $d\mathbf{r}'$ represents the differential volume in a general coordinate system. For example, in the Cartesian, cylindrical, and spherical coordinate systems, $d\mathbf{r}'$ assumes the following definitions, respectively:

$$d\mathbf{r}' = dx'\, dy'\, dz' \,, \tag{4.3a}$$

$$d\mathbf{r}' = \rho'\, d\rho'\, d\phi'\, dz' \,, \tag{4.3b}$$

$$d\mathbf{r}' = r^2 \sin\theta'\, d\theta'\, d\phi'\, dr' \,. \tag{4.3c}$$

To ensure that Eq. (4.2) is satisfied for any continuous function, when expressing $\delta(\mathbf{r})$ in terms of variables of a specific coordinate system, appropriate coefficients must accompany the expanded forms. For example, for the three standard coordinate systems, the following expanded forms for $\delta(\mathbf{r})$ are appropriate:

$$\delta(\mathbf{r}) = \delta(x)\, \delta(y)\, \delta(z) \,, \tag{4.4a}$$

$$\delta(\mathbf{r}) = \frac{1}{\rho}\, \delta(\rho)\, \delta(\phi)\, \delta(z) \,, \tag{4.4b}$$

$$\delta(\mathbf{r}) = \frac{1}{r^2 \sin\theta}\, \delta(\phi)\, \delta(\theta)\, \delta(r) \,. \tag{4.4c}$$

To express spherical symmetry explicitly, one can use

$$\delta(\mathbf{r}) = \frac{\delta(r)}{4\pi r^2} \,, \tag{4.5}$$

since

$$\iiint_V \delta(\mathbf{r})\, d\mathbf{r} = \int_0^R \int_0^{2\pi} \int_0^{\pi} \frac{\delta(r)}{4\pi r^2}\, r^2 \sin\theta\, d\theta\, d\phi\, dr = 1 \,.$$

Using Eq. (4.5) in Eq. (4.1) and noting that $g(\mathbf{r})$ is only a function of $r$, the following second-order differential equation is obtained:

$$\frac{1}{r^2}\frac{\partial}{\partial r}\left(r^2 \frac{\partial\, g(r)}{\partial r}\right) + k^2\, g(r) = \frac{-\delta(r)}{4\pi r^2} \,. \tag{4.6}$$

Equation (4.6) can be rearranged to yield

$$\frac{d^2}{dr^2}\,[r\, g(r)] + k^2 [r\, g(r)] = -\frac{\delta(r)}{4\pi r} \,. \tag{4.7}$$

The general solution of Eq. (4.7) is found to be

$$g(r) = A_1(k)\, \frac{e^{ikr}}{r} + A_2(k)\, \frac{e^{-ikr}}{r} \,. \tag{4.8}$$

Noting that $e^{ikr}$ represents an outward-going wave and $e^{-ikr}$ an incoming wave, it is concluded directly that $A_2 = 0$. Hence,

$$g(r) = A_1(k)\,\frac{e^{ikr}}{r}\,. \tag{4.9}$$

Basically, since it is assumed that there are no sources in the medium except for the point source at the origin, no incoming wave is allowed. To determine coefficient $A_1(k)$, we integrate Eq. (4.1) over a spherical volume of radius $R$ and centered at the origin:

$$\iiint_V \nabla\cdot\nabla\, g(r)\, dv + k^2 \iiint_V g(r)\, dv = -1\,. \tag{4.10}$$

Applying the divergence theorem to the first term leads to

$$\oiint \nabla\, g(r)\cdot d\mathbf{s} + k^2 \iiint g(r)\, dv = -1\,, \tag{4.11}$$

and upon inserting Eq. (4.9), we have

$$\left[A_1\,\frac{\partial}{\partial R}\left(\frac{e^{ikR}}{R}\right)\right] 4\pi R^2 + k^2 4\pi A_1 \int_0^R re^{ikr}\, dr = -1\,. \tag{4.12}$$

In the limit as $R$ approaches zero the left-hand side approaches $-4\pi A_1$, and therefore

$$A_1 = \frac{1}{4\pi}\,. \tag{4.13}$$

Hence,

$$g(r) = \frac{e^{ikr}}{4\pi r}\,. \tag{4.14}$$

To generalize the solution, let us assume that the point source is located at $\mathbf{r}'$. In this case the function representing the point source is expressed by $\delta(\mathbf{r}-\mathbf{r}')$ and simply through a change of variable to $\mathbf{R} = \mathbf{r}-\mathbf{r}'$, a differential equation similar to Eq. (4.6) can be obtained. Denoting the Green's function by $g(\mathbf{r},\mathbf{r}')$ and emphasizing that the observation point is at $\mathbf{r}$ and the source point is at $\mathbf{r}'$, we have

$$g(\mathbf{r},\mathbf{r}') = \frac{e^{ik|\mathbf{r}-\mathbf{r}'|}}{4\pi|\mathbf{r}-\mathbf{r}'|}\,. \tag{4.15}$$

Because of the built-in symmetry of Eq. (4.15), the expression for $g(\mathbf{r},\mathbf{r}')$ would remain unchanged if we were to interchange the locations of the source and observation points. That is,

$$g(\mathbf{r},\mathbf{r}') = g(\mathbf{r}',\mathbf{r})\,. \tag{4.16}$$

This is a statement of ***reciprocity***, which will be explored in more detail later on in this chapter.

### 4-1.1 Green's Theorem

Green's theorem provides the necessary tool to construct the solution for any arbitrary source function once the ***point spread function*** (Green's function) is known. Let $V$ be a closed region of space bounded by a regular surface $S$. Let $\Phi$ and $\psi$ be two scalar functions of position that together with their first and second derivatives are continuous in $V$ and on $S$. By applying the divergence theorem to function $\psi\nabla\Phi$, it can be shown that

$$\iiint_V \nabla\cdot(\psi\nabla\Phi)\,dv = \oiint_S (\psi\nabla\Phi)\cdot d\mathbf{s}\,. \tag{4.17}$$

Recalling that $\nabla\Phi\cdot\hat{\mathbf{n}} = \frac{\partial\Phi}{\partial n}$ for a unit normal vector $\hat{\mathbf{n}}$, and that $\nabla\cdot(\psi\nabla\Phi) = \psi\nabla^2\Phi + \nabla\psi\cdot\nabla\Phi$, Eq. (4.17) can be written as

$$\iiint_V \nabla\psi\cdot\nabla\Phi\,dv + \iiint_V \psi\,\nabla^2\Phi\,dv = \oiint_S \psi\frac{\partial\Phi}{\partial n}\,ds\,. \tag{4.18}$$

Equation (4.18) is ***Green's first identity***. For the special case of $\psi = \Phi$ and $\nabla^2\Phi = 0$, Eq. (4.18) reduces to

$$\iiint_V |\nabla\Phi|^2\,dv = \oiint_S \frac{\partial\Phi}{\partial n}\Phi\,ds\,. \tag{4.19}$$

Equation (4.19) can be used to prove the uniqueness theorem for static problems, which states that the solution to Laplace's equation in a region $V$ is unique if the potential or its normal derivative is known on a closed surface bounding the region.

Now interchanging $\psi$ and $\Phi$ in Eq. (4.18), we have

$$\iiint_V [\nabla\Phi\cdot\nabla\psi + \Phi\,\nabla^2\psi]\,dv = \oiint_S \Phi\frac{\partial\psi}{\partial n}\,ds\,. \tag{4.20}$$

Subtracting Eq. (4.20) from Eq. (4.18) yields

$$\iiint_V [\psi\,\nabla^2\Phi - \Phi\,\nabla^2\psi]\,dv = \oiint_S \left(\psi\frac{\partial\Phi}{\partial n} - \Phi\frac{\partial\psi}{\partial n}\right)\,ds\,. \tag{4.21}$$

Equation (4.21) is ***Green's second identity*** for scalar functions, which is often referred to as ***Green's theorem***.

### 4-1.2 Solution of the Scalar Helmholtz Equation

In this section the solution to the scalar wave equation for an arbitrary source function is obtained through the application of Green's function. Recall that Green's function satisfies

$$\nabla^2\,g(\mathbf{r},\mathbf{r}') + k^2\,g(\mathbf{r},\mathbf{r}') = -\delta(\mathbf{r}-\mathbf{r}')\,, \tag{4.22}$$

and the scalar potential satisfies

$$\nabla^2\,\Phi(\mathbf{r})+k^2\,\Phi(\mathbf{r})=-\frac{\rho(\mathbf{r})}{\varepsilon} \tag{4.23}$$

for a homogeneous region $V$ bounded by a closed surface $S$. According to Green's theorem

$$\iiint_V \left[g(\mathbf{r},\mathbf{r}')\,\nabla^2\,\Phi(\mathbf{r})-\Phi(\mathbf{r})\,\nabla^2\,g(\mathbf{r},\mathbf{r}')\right]\,dv=\oiint\left[g(\mathbf{r},\mathbf{r}')\,\frac{\partial\Phi(\mathbf{r})}{\partial n}-\Phi(\mathbf{r})\,\frac{\partial g(\mathbf{r},\mathbf{r}')}{\partial n}\right]\,ds\,. \tag{4.24}$$

Using Eqs. (4.22) and (4.23) in Eq. (4.24), the left-hand side of Eq. (4.24) simplifies to

$$\iiint_V\left[-k^2\,g(\mathbf{r},\mathbf{r}')\,\Phi(\mathbf{r})-g(\mathbf{r},\mathbf{r}')\,\frac{\rho(\mathbf{r})}{\varepsilon}+k^2\,\Phi(\mathbf{r})\,g(\mathbf{r},\mathbf{r}')+\Phi(\mathbf{r})\,\delta(\mathbf{r}-\mathbf{r}')\right]\,dv$$

$$=\begin{cases}\Phi(\mathbf{r}')-\dfrac{1}{\varepsilon}\displaystyle\iiint_V\rho(\mathbf{r})\,g(\mathbf{r},\mathbf{r}')\,dv & r'\in V\,,\\[2ex] -\dfrac{1}{\varepsilon}\displaystyle\iiint_V\rho(\mathbf{r})\,g(\mathbf{r},\mathbf{r}')\,dv & r'\notin V\,.\end{cases}$$

Interpretation of the case where $r'\notin V$ will be given later in this chapter. Hence, using Eq. (4.15) for $g(\mathbf{r},\mathbf{r}')$ the potential function, when the observation point is within $V$, can be obtained from

$$\Phi(\mathbf{r}')=\frac{1}{4\pi\varepsilon}\iiint\rho(r)\,\frac{e^{ik|\mathbf{r}-\mathbf{r}'|}}{|\mathbf{r}-\mathbf{r}'|}\,dv+\frac{1}{4\pi}\oiint_S\left[\frac{e^{ik|\mathbf{r}-\mathbf{r}'|}}{|\mathbf{r}-\mathbf{r}'|}\,\frac{\partial\,\Phi(r)}{\partial n}-\Phi(r)\,\frac{\partial}{\partial n}\left(\frac{e^{ik|\mathbf{r}-\mathbf{r}'|}}{|\mathbf{r}-\mathbf{r}'|}\right)\right]\,ds\,. \tag{4.25}$$

It is more common to use $\mathbf{r}$ as the observation point and $\mathbf{r}'$ as the source point. Interchanging $\mathbf{r}$ and $\mathbf{r}'$ and using the reciprocity relation $g(\mathbf{r},\mathbf{r}')=g(\mathbf{r}',\mathbf{r})$, Eq. (4.25) is often written as

$$\Phi(\mathbf{r})=\frac{1}{\varepsilon}\iiint_V\rho(\mathbf{r}')\,g(\mathbf{r},\mathbf{r}')\,dv'+\oiint_S\left[g(\mathbf{r},\mathbf{r}')\,\frac{\partial\,\Phi(\mathbf{r}')}{\partial n'}-\Phi(\mathbf{r}')\,\frac{\partial\,g(\mathbf{r}-\mathbf{r}')}{\partial n'}\right]\,ds'\,, \tag{4.26}$$

where $\mathbf{r}$ is the observation point, $\mathbf{r}'$ is the source point and $\hat{\mathbf{n}}'$ is an outward unit vector on surface $S$. It is noted here that $\Phi(r')$ and $\partial\,\Phi(\mathbf{r}')/\partial n'$ can be interpreted as equivalent surface sources. In the absence of charge within volume $V$, the equivalent surface sources generated by the exterior sources, is the reason for the nonvanishing potential $\Phi(\mathbf{r})$ inside $S$. Basically, $\Phi(\mathbf{r}')$ and $\hat{\mathbf{n}}'\cdot\nabla\Phi(\mathbf{r}')$ act as equivalent surface sources for observation points within $S$.

### 4-1.3 Radiation Condition

Let us assume that the charge density $\rho(\mathbf{r}')$ is confined to finite volume $V$. Also assuming that the medium is homogeneous, we can extend the closed surface to infinity. In this case the surface contribution generated entirely by the volumetric charge density $\rho(\mathbf{r}')$ is expected

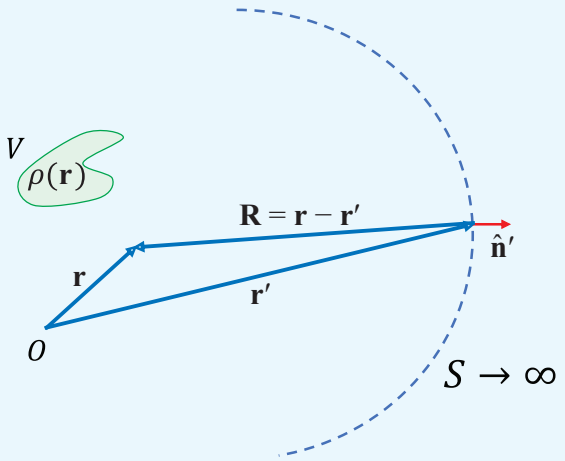


**Figure 4-1:** A volumetric charge density confined within volume $V$ and equivalent surface sources ($\partial\Phi/\partial n$ and $\Phi$) on $S$ that approaches infinity. The contribution from the equivalent surface sources is expected to vanish at observation points far from surface $S$.

to vanish when the surface $S$ is infinitely far away from the observation point and the source function $\rho(\mathbf{r}')$. Let us examine this equivalent surface source contribution more carefully by evaluating

$$I = \oiint_S \left[ g(\mathbf{r},\mathbf{r}') \frac{\partial \Phi(\mathbf{r}')}{\partial n'} - \Phi(\mathbf{r}') \frac{\partial g(\mathbf{r},\mathbf{r}')}{\partial n'} \right] ds' \tag{4.27}$$

as $\mathbf{r}' \to \infty$, as shown in Fig. 4-1.

In this case the scalar Green's function can be simplified to

$$g(\mathbf{r},\mathbf{r}') \approx \frac{e^{ik|\mathbf{r}-\mathbf{r}'|}}{4\pi r'} .$$

Choosing a spherical surface for $S$, we have $\hat{\mathbf{n}}' = \hat{\mathbf{r}}'$ and

$$\frac{\partial g(\mathbf{r},\mathbf{r}')}{\partial n'} \approx \frac{\partial}{\partial r'} \left( \frac{e^{ik|\mathbf{r}-\mathbf{r}'|}}{4\pi r'} \right) = - \left( -\frac{ik}{r'} + \frac{1}{r'^2} \right) \frac{e^{ik|\mathbf{r}-\mathbf{r}'|}}{4\pi} .$$

In this case the surface integral is approximated by

$$I \approx \oiint_S \left[ \frac{e^{ik|\mathbf{r}-\mathbf{r}'|}}{4\pi r'} \frac{\partial \Phi(\mathbf{r}')}{\partial r'} + \Phi(\mathbf{r}') \left( \frac{-ik}{r'} + \frac{1}{r'^2} \right) \frac{e^{ik|\mathbf{r}-\mathbf{r}'|}}{4\pi} \right] ds' . \tag{4.28}$$

We can ignore the $1/r'^2$ term compared with all other $1/r'$ terms, and noting that $ds' = r'^2\, d\Omega'$, we have

$$I \approx \oiint_{S'} \left[ r' \left( \frac{\partial \Phi}{\partial r'} - ik\Phi \right) \frac{e^{ik|\mathbf{r}-\mathbf{r}'|}}{4\pi} \right] d\Omega' \, .$$

The only way to ensure that the contribution due to $I$ vanishes is to require that

$$\lim_{r'\to\infty} r' \left( \frac{\partial\, \Phi(\mathbf{r}')}{\partial r'} - ik\, \Phi(\mathbf{r}') \right) = 0 \, . \tag{4.29}$$

This is known as the ***radiation condition***, which was first introduced by Sommerfeld. It is interesting to note that the free-space Green's function satisfies the radiation condition.

The radiation condition for the electric scalar potential can be extended to the magnetic vector potential in a similar form, as the magnetic vector potential is also a solution to a similar wave equation. This condition is given by

$$\lim_{r'\to\infty} r' \left( \frac{\partial\, \mathbf{A}(\mathbf{r}')}{\partial r'} - ik\, \mathbf{A}(\mathbf{r}') \right) = 0 \, , \tag{4.30}$$

and the magnetic scalar potential $\phi_{\mathrm{m}}$ and the electric vector potential $\mathbf{A}_{\mathrm{m}}(\mathbf{r})$ satisfy similar equations. All these radiation conditions enforce the behavior of potentials as a function of distance to be of the form $e^{ikr}/r$ in the far-field region. This property was used to derive the far-field expressions for the electric and magnetic fields as given by Eqs. (3.147a) and (3.147b). Using these equations, it can easily be shown that the radiation conditions for the electric and magnetic fields take the following forms:

$$\lim_{r\to\infty} r\, [\mathbf{E}(\mathbf{r}) + \hat{\mathbf{r}} \times \eta \mathbf{H}(\mathbf{r})] = 0 \tag{4.31a}$$

and

$$\lim_{r\to\infty} r \left[ \mathbf{H}(\mathbf{r}) - \hat{\mathbf{r}} \times \frac{\mathbf{E}(\mathbf{r})}{\eta} \right] = 0 \, . \tag{4.31b}$$

Equations (4.31a) and (4.31b) indicate that in the far-field region the electric field is perpendicular to the magnetic field and both are perpendicular to the direction of propagation. In addition these equations indicate that the ratio of the electric field to the magnetic field is a constant equal to $\eta = \sqrt{\mu/\varepsilon}$.

## 4-2 Solution of the Helmholtz Equation for a Complex Medium

The formulations provided in the previous section can be extended to include inhomogeneities. For example, let us consider a homogeneous medium with a finite number of inclusions (dielectric or metallic) of finite extent, as shown in Fig. 4-2. Suppose the volumetric charge density exists only in the background medium.

Initially let's assume the background medium to be finite and bounded by a closed surface $S'$. The composite closed surface consisting of the surfaces of the inclusions and the enclosing surface $S'$ encloses the homogeneous surrounding medium denoted by $V$. According

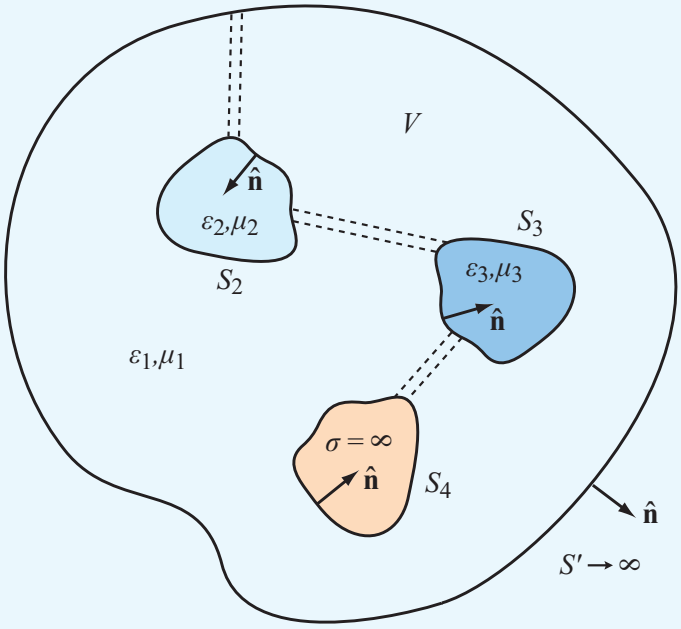


**Figure 4-2:** A complex medium composed of a number of homogeneous segments.

to Eq. (4.25),

$$\Phi(\mathbf{r}) = \frac{1}{\varepsilon_1} \iiint_V \rho(\mathbf{r}')\, g(\mathbf{r},\mathbf{r}')\, dv' + \oiint_{S'+\sum S_i} \left( g(\mathbf{r},\mathbf{r}') \frac{\partial \Phi(\mathbf{r}')}{\partial n'} - \Phi(\mathbf{r}') \frac{\partial\, g(\mathbf{r},\mathbf{r}')}{\partial n'} \right) ds' \,.$$

Now letting $S'$ approach infinity, the surface integral contribution according to the radiation condition vanishes, and therefore

$$\Phi(\mathbf{r}) = \frac{1}{\varepsilon_1} \iiint_V \rho(\mathbf{r}')\, g(\mathbf{r},\mathbf{r}')\, dv' + \oiint_{\sum S_i} \left( g(\mathbf{r},\mathbf{r}') \frac{\partial \Phi(\mathbf{r}')}{\partial n'} - \Phi(\mathbf{r}') \frac{\partial\, g(\mathbf{r},\mathbf{r}')}{\partial n'} \right) ds' \quad (4.32)$$

for any observation point in $V$. Here it should be emphasized that contributions from surfaces connecting $S'$ and other inhomogeneities (shown by dashed lines in Fig. 4-2) cancel each other, as the adjacent surfaces have unit normals opposite to each other. Note that in the absence of inclusions,

$$\Phi_i(\mathbf{r}) = \frac{1}{\varepsilon_1} \iiint_V \rho(\mathbf{r}')\, g(\mathbf{r},\mathbf{r}')\, dv' \,.$$

The surface integral

$$\Phi_s(\mathbf{r}) = \oiint_{\sum S_i} \left( g(\mathbf{r},\mathbf{r}') \frac{\partial\, \Phi(\mathbf{r}')}{\partial n'} - \Phi(\mathbf{r}') \frac{\partial\, g(\mathbf{r},\mathbf{r}')}{\partial n'} \right) ds'$$

can be interpreted as the scattered potential. Here it is assumed that the observation point is within $V$ and outside the volume containing the scatterers. In this case, the total potential $\Phi(\mathbf{r})$ is the superposition of the incident potential and the scattered potential:

$$\Phi(\mathbf{r}) = \Phi_{\mathrm{i}}(\mathbf{r}) + \Phi_{\mathrm{s}}(\mathbf{r}) \ . \tag{4.33}$$

In general we can write

$$\Phi_{\mathrm{i}}(\mathbf{r}) + \Phi_{\mathrm{s}}(\mathbf{r}) = \begin{cases} \Phi(\mathbf{r}) & \mathbf{r} \in V \ , \\ 0 & \mathbf{r} \notin V \ . \end{cases} \tag{4.34}$$

Equation (4.34) is a statement of the ***extinction theorem***. It indicates that when the observation point is within a scatterer ($\mathbf{r} \notin V$), the equivalent surface sources on the scatterers are formed in such a way that the potential produced by them completely eliminates the incident potential everywhere inside the scatterers. This is physically a necessity, as for example if one (or more) of the scatterers is a perfect conductor, the potential is zero (or a constant) on and within the scatterer, and hence the surface charge density $\rho_{\mathrm{s}}(\mathbf{r}) = \hat{\mathbf{n}} \cdot \mathbf{D}(\mathbf{r}) = -\varepsilon \hat{\mathbf{n}} \cdot \nabla \Phi(\mathbf{r})$ must be formed in such a manner as to cancel out the incident potential that was present in the absence of the scatterer.

Also, in the case of dielectric scatterers, the potential inside a dielectric scatterer with dielectric constant $\varepsilon_j$ and closed surface $S_j$ can be obtained using Green's second identity in a similar manner and is given by

$$\oiint_{S_j} \left( g_j(\mathbf{r},\mathbf{r}') \, \frac{\partial \Phi_j(\mathbf{r}')}{\partial n'} - \Phi_j(\mathbf{r}') \, \frac{\partial \, g_j(\mathbf{r},\mathbf{r}')}{\partial n'} \right) ds' = \begin{cases} \Phi_j(\mathbf{r}) & \mathbf{r} \in V_j \ , \\ 0 & \mathbf{r} \notin V_j \ . \end{cases} \tag{4.35}$$

Here we are assuming that there are no charge distributions inside this scatterer and that

$$g_j(\mathbf{r},\mathbf{r}') = \frac{1}{4\pi} \frac{e^{ik_j|\mathbf{r}-\mathbf{r}'|}}{|\mathbf{r}-\mathbf{r}'|}$$

is the scalar Green's function for the medium with dielectric constant $\varepsilon_j$. Again, according to the extinction theorem, the equivalent sources on the surface assume a distribution such that they produce no potential with wave propagation constant $k_j$ outside the scatterer. This is a physical requirement as the wave outside must have a different propagation constant ($k$).

It should be noted that when the observation point is on the surface, it is possible that $\mathbf{r}' = \mathbf{r}$, and this makes the scalar Green's function and its gradient on the surface singular. This singularity can be removed for smooth surfaces by first deforming the surface around the observation point and then evaluating the surface integral contribution around the deformation as the deformation approaches zero. To further elaborate on this point, let's assume that the observation point $\mathbf{r}$ is on $S_j$. We deform this surface around $\mathbf{r}$ by placing a hemispherical surface of radius $a$ centered at $\mathbf{r}$ and then allowing $a \to 0$. This configuration is shown in Fig. 4-3, where $S_j$ is deformed by introducing a vanishing hemispherical surface $S_{\mathrm{s}}$ around

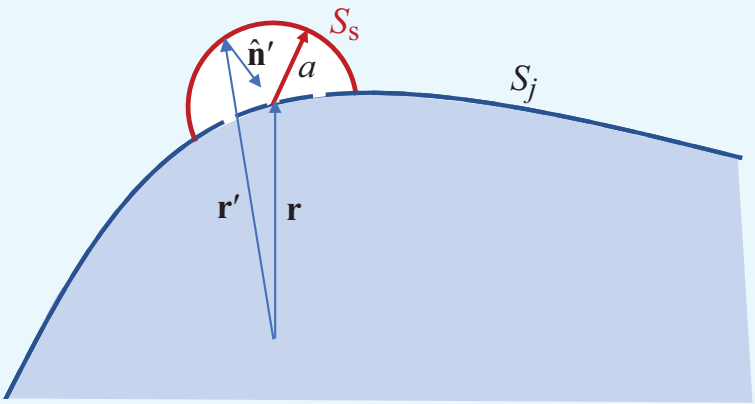


**Figure 4-3:** This figure shows a portion of the interface between the $j$th scatterer and the background medium. To extract the contribution from the singularity of the integrand, the surface is deformed by adding a small hemispherical surface with radius $a$ around the singularity point $\mathbf{r}$ on surface $S_j$. The contribution from this hemispherical surface is calculated analytically in the limit as $a \to 0$.

the observation point. The scattered potential can be calculated from

$$\Phi_s(\mathbf{r}) = \lim_{a\to 0}\left[\oiint_{S_j - S_s}\left(g(\mathbf{r},\mathbf{r}')\frac{\partial\Phi(\mathbf{r}')}{\partial n'} - \Phi(\mathbf{r}')\frac{\partial g(\mathbf{r},\mathbf{r}')}{\partial n'}\right)ds' + \oiint_{S_s}\left(g(\mathbf{r},\mathbf{r}')\frac{\partial\Phi(\mathbf{r}')}{\partial n'} - \Phi(\mathbf{r}')\frac{\partial g(\mathbf{r},\mathbf{r}')}{\partial n'}\right)ds'\right].$$

On $S_s$, the scalar Green's function and its normal derivative are

$$g(\mathbf{r},\mathbf{r}') = \frac{e^{ika}}{4\pi a}$$

and

$$\frac{\partial g(\mathbf{r},\mathbf{r}')}{\partial n'} = -\frac{e^{ika}}{4\pi a}\left(ik - \frac{1}{a}\right).$$

where the negative sign is due to the fact that $\hat{\mathbf{n}}'$ is pointing inward on $S_s$. Also noting that $ds' = a^2 \sin\theta\, d\theta\, d\Phi$, the contribution from the first integrand of the surface integral on $S_s$

vanishes as $a \to 0$ and

$$\lim_{a\to 0} \oiint_{S_s} \left( g(\mathbf{r},\mathbf{r}') \frac{\partial \Phi(\mathbf{r}')}{\partial n'} - \Phi(\mathbf{r}') \frac{\partial g(\mathbf{r},\mathbf{r}')}{\partial n'} \right) ds' = \frac{-\Phi(\mathbf{r})}{4\pi} \int_0^{\pi/2} \int_0^{2\pi} \sin\theta d\theta d\Phi$$
$$= \frac{-\Phi(\mathbf{r})}{2} .$$

Hence Eq. (4.34) should be modified to

$$\Phi_{\mathrm{i}}(\mathbf{r}) + \oiint_{\sum S_i} \left( g(\mathbf{r},\mathbf{r}') \frac{\partial \Phi(\mathbf{r}')}{\partial n'} - \Phi(\mathbf{r}') \frac{\partial g(\mathbf{r},\mathbf{r}')}{\partial n'} \right) ds = \begin{cases} \Phi(\mathbf{r}) & \mathbf{r} \in V , \\ \Phi(\mathbf{r})/2 & \mathbf{r} \text{ on } S_j , \\ 0 & \mathbf{r} \notin V , \end{cases} \tag{4.36}$$

and Eq. (4.35) becomes

$$\oiint \left( g_{\mathrm{i}}(\mathbf{r},\mathbf{r}') \frac{\partial \Phi_j(\mathbf{r}')}{\partial n'} - \Phi_j(\mathbf{r}') \frac{\partial g_j(\mathbf{r},\mathbf{r}')}{\partial n'} \right) ds' = \begin{cases} \Phi_j(\mathbf{r}) & \mathbf{r} \in V_j , \\ \frac{1}{2}\,\Phi_j(\mathbf{r}) & \mathbf{r} \text{ on } S_j , \\ 0 & \mathbf{r} \notin V_j . \end{cases} \tag{4.37}$$

Here $\oiint$ represents the principal-value integral.

Equation (4.36) can be used as an integral equation for metallic objects in order to find the potential in the space on and around the scatterer for an arbitrary incident potential generated by a known charge distribution $\rho(\mathbf{r})$ outside the metallic scatterer. In the quasi-static regime, assuming the scatterer is at potential zero ($\Phi(\mathbf{r}) = 0$, $\mathbf{r}$ on $S$) and solving for $\rho_{\mathrm{s}}(\mathbf{r})$, Eq. (4.36) can be used to form the following integral equation, known as the ***Fredholm integral equation of the first kind***:

$$\Phi_{\mathrm{i}}(\mathbf{r}) = -\Phi_{\mathrm{s}}(\mathbf{r}) = \frac{1}{\varepsilon} \oiint_S \left[ g(\mathbf{r},\mathbf{r}')\, \rho_{\mathrm{s}}(\mathbf{r}') \right] ds' , \tag{4.38}$$

**(metallic scatterers)**

where $\mathbf{r}$ is on the surface of the scatterer $S$. Equation (4.38) is to be solved for $\rho_{\mathrm{s}}(\mathbf{r})$, and once that is found by placing it in the top part of Eq. (4.36), the potential everywhere else ($\mathbf{r} \in V$) can be obtained.

For dielectric objects a coupled integral equation can be formed in terms of the unknown equivalent source on the surface using the boundary conditions

$$\Phi(\mathbf{r}) = \Phi_j(\mathbf{r}) \tag{4.39a}$$

and

$$\varepsilon \hat{\mathbf{n}} \cdot \nabla \Phi(\mathbf{r}) = \varepsilon_j \hat{\mathbf{n}} \cdot \nabla \Phi_j(\mathbf{r}) . \tag{4.39b}$$

These boundary conditions for the scalar potential are derived in Section 4-2.2. Using these in Eqs. (4.36) and (4.37), the desired integral equations are obtained:

$$\Phi_i(\mathbf{r}) + \oiint_{S_j} \left( g(\mathbf{r},\mathbf{r}') \frac{\partial \Phi(\mathbf{r}')}{\partial n'} - \Phi(\mathbf{r}') \frac{\partial g(\mathbf{r},\mathbf{r}')}{\partial n'} \right) ds' = \frac{\Phi(\mathbf{r})}{2} \tag{4.40a}$$

and

$$\oiint_{S_j} \left( \frac{\varepsilon}{\varepsilon_j} g_j(\mathbf{r},\mathbf{r}') \frac{\partial \Phi(\mathbf{r}')}{\partial n'} - \Phi(\mathbf{r}') \frac{\partial g_j(\mathbf{r},\mathbf{r}')}{\partial n'} \right) ds' = \frac{\Phi(\mathbf{r})}{2} \, . \tag{4.40b}$$

**(dielectric scatterers)**

These equations can be solved for $\Phi(\mathbf{r})$ and $\frac{\partial \Phi(\mathbf{r})}{\partial n}$ by discretizing the surface into a number of finite facets and casting the equations in terms of matrix equations that can be solved numerically.

### 4-2.1 Solution for the Vector Helmholtz Equation

For a homogeneous unbounded medium, the magnetic vector potential satisfies

$$\nabla^2 \mathbf{A} + k^2 A = -\mu \mathbf{J} \, .$$

In a Cartesian coordinate system the three components of $\mathbf{A}$ are related to the corresponding components of the volumetric current density by

$$\nabla^2 \begin{pmatrix} A_x \\ A_y \\ A_z \end{pmatrix} + k^2 \begin{pmatrix} A_x \\ A_y \\ A_z \end{pmatrix} = -\mu \begin{pmatrix} J_x \\ J_y \\ J_z \end{pmatrix} \, . \tag{4.41}$$

This constitutes three scalar Helmholtz equations similar to Eq. (4.23). Hence,

$$A_p(\mathbf{r}) = \frac{\mu}{4\pi} \iiint_V J_p(\mathbf{r}') \frac{e^{ik|\mathbf{r}-\mathbf{r}'|}}{|\mathbf{r}-\mathbf{r}'|} dv' \, ,$$

where the subscript $p$ can be $x$, $y$, or $z$. Assembling all three components, the magnetic vector potential for a homogeneous unbounded medium can be calculated from

$$\mathbf{A}(\mathbf{r}) = \frac{\mu}{4\pi} \iiint_V \mathbf{J}(\mathbf{r}') \frac{e^{ik|\mathbf{r}-\mathbf{r}'|}}{|\mathbf{r}-\mathbf{r}'|} dv' \, .$$

For a complex medium composed of discrete metallic or dielectric scatterers the statement for the magnetic vector potential takes the following form:

$$\mathbf{A}_{\mathrm{i}}(\mathbf{r}) + \oiint_{\sum S_j} \left( g(\mathbf{r},\mathbf{r}') \frac{\partial \mathbf{A}(\mathbf{r}')}{\partial n'} - \mathbf{A}(\mathbf{r}') \frac{\partial g(\mathbf{r},\mathbf{r}')}{\partial n'} \right) ds' = \begin{cases} \mathbf{A}(\mathbf{r}) & \mathbf{r} \in V \, , \\ \mathbf{A}(\mathbf{r})/2 & \mathbf{r} \text{ on } S_j \, , \\ 0 & \mathbf{r} \notin V \, , \end{cases} \tag{4.42}$$

where $\mathbf{A}_i(\mathbf{r})$ is the magnetic vector potential due to the sources in the absence of the scatterer and $S_j$ represent the closed surface of the $j$th scatterer. Also inside each dielectric scatterer, assuming no interior current distribution is present, we can get

$$\oiint_{S_j} \left( g_j(\mathbf{r},\mathbf{r}') \frac{\partial \mathbf{A}_j(\mathbf{r}')}{\partial n'} - \mathbf{A}_j(\mathbf{r}') \frac{\partial g_j(\mathbf{r},\mathbf{r}')}{\partial n'} \right) ds'$$

$$= \begin{cases} \mathbf{A}_j(\mathbf{r}) & \mathbf{r} \in V_j \ , \\ \mathbf{A}_j(\mathbf{r})/2 & \mathbf{r} \text{ on } S_j \ , \\ 0 & \mathbf{r} \notin V_j \ . \end{cases} \tag{4.43}$$

For electrodynamics, using Eqs. (4.42) and (4.43), together with enforcing the continuity of the tangential electric field $[\mathbf{E}(\mathbf{r}) = i\omega\ \mathbf{A}(\mathbf{r}) - \nabla\Phi(\mathbf{r})]$ and magnetic field $[\mathbf{H}(\mathbf{r}) = \frac{1}{\mu}\nabla \times \mathbf{A}(\mathbf{r})]$ at the interfaces between the dielectric media as well as using the Lorentz gauge condition $[\nabla \cdot \mathbf{A}(\mathbf{r}) = i\omega\mu\varepsilon\ \Phi(\mathbf{r})]$, leads to a set of coupled integral equations. Derivation of these equations is somewhat lengthy and will not be shown here. Instead another set of integral equations will be derived using the field equations and Green's second identity.

### 4-2.2 Boundary Conditions for Electromagnetic Potentials

In previous chapters we discussed the importance of boundary conditions at interfaces between dielectric and metallic media. In this section we examine how such boundary conditions can be extended to electromagnetic potentials. Let us begin with the electric scalar potential $\Phi(\mathbf{r})$ and the magnetic vector potential $\mathbf{A}(\mathbf{r})$, and their relationships to $\mathbf{E}(\mathbf{r})$ and $\mathbf{B}(\mathbf{r})$:

$$\mathbf{B}(\mathbf{r}) = \nabla \times \mathbf{A}(\mathbf{r}) \tag{4.44a}$$

and

$$\mathbf{E}(\mathbf{r}) = i\omega\ \mathbf{A}(\mathbf{r}) - \nabla\ \Phi(\mathbf{r}) \ . \tag{4.44b}$$

Considering a differential volume $\Delta v$ between two dielectric media, as shown previously in Fig. 1-14 and repeated here as Fig. 4-4, and applying Eq. (1.92b), leads to

$$\iiint_{\Delta v} \mathbf{B}(\mathbf{r})\, dv = \iiint_{\Delta v} \nabla \times \mathbf{A}(\mathbf{r})\, dv = -\oiint_{\Delta S} \mathbf{A}(\mathbf{r}) \times\ d\mathbf{s} \ ,$$

and hence in the limit as $\Delta\ell \to 0$ it can be shown that

$$\hat{\mathbf{n}} \times [\mathbf{A}_1(\mathbf{r}) - \mathbf{A}_2(\mathbf{r})] = 0 \ , \tag{4.45}$$

indicating the continuity of the tangential magnetic vector potential.

To examine the continuity of the normal component of the magnetic vector potential, the Lorenz gauge condition

$$\nabla \cdot \mathbf{A}(\mathbf{r}) = i\omega\mu\varepsilon\ \Phi(\mathbf{r}) \tag{4.46}$$

can be used together with the divergence theorem:

$$\iiint_{\Delta v} \nabla \cdot A \, dv = \oiint_{\Delta S} \mathbf{A} \cdot d\mathbf{s} = i\omega\mu\varepsilon \iiint_{\Delta v} \Phi(\mathbf{r}) \, dv \, . \tag{4.47}$$

Referring to Fig. 4-4, in the limit as $\Delta\ell \to 0$, the right-hand side of Eq. (4.47) vanishes, and we get

$$\hat{\mathbf{n}} \cdot [\mathbf{A}_1(\mathbf{r}) - \mathbf{A}_2(\mathbf{r})] = 0 \, . \tag{4.48}$$

In view of Eqs. (4.45) and (4.48), the magnetic vector potential is shown to be continuous across the interface between two dielectric media; that is,

$$\mathbf{A}_1(\mathbf{r}) = \mathbf{A}_2(\mathbf{r}) \, , \qquad \mathbf{r} \in S \, .$$

To show the continuity of electric scalar potential across two dielectric media, we recall that

$$\hat{\mathbf{n}} \times (\mathbf{E}_1 - \mathbf{E}_2) = 0 \, . \tag{4.49}$$

By combining Eqs. (4.45) and (4.49) in Eq. (4.44b), it becomes obvious that

$$\hat{\mathbf{n}} \times (\nabla\Phi_1 - \nabla\Phi_2) = \hat{\mathbf{n}} \times \nabla(\Phi_1 - \Phi_2) = 0 \, . \tag{4.50}$$

For Eq. (4.50) to hold, it must be true that

$$\Phi_1(\mathbf{r}) = \Phi_2(\mathbf{r}) \, , \qquad \mathbf{r} \in S \, . \tag{4.51}$$

That is, the potential function across the surface must be continuous. Otherwise $\nabla(\Phi_1 - \Phi_2)$ becomes infinite. Equation (4.50) can also be independently derived noting that $\nabla \times \nabla\Phi = 0$ and using Eq. (1.92b) for $\Delta v$ of Fig. 4-4.

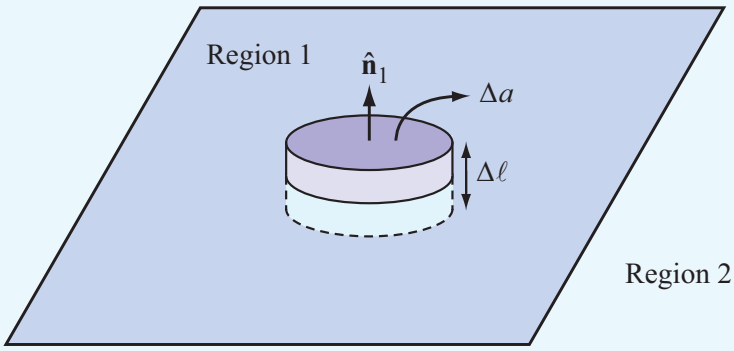


**Figure 4-4:** A small cylindrical volume between two homogeneous media. The base of the cylinder is chosen to be small enough so that the interface can be assumed flat locally.

The boundary condition for the normal component of the electric flux density is given by

$$\varepsilon_1 \, \hat{\mathbf{n}} \cdot \mathbf{E}_1(\mathbf{r}) = \varepsilon_2 \, \hat{\mathbf{n}} \cdot \mathbf{E}_2(\mathbf{r}) \, . \tag{4.52}$$

Using Eq. (4.44b) and noting the continuity of the magnetic vector potential, it can easily be shown that

$$\varepsilon_1 \frac{\partial \Phi_1}{\partial n} = \varepsilon_2 \frac{\partial \Phi_2}{\partial n} \, . \tag{4.53}$$

where as before, $\hat{\mathbf{n}}$ is a unit vector normal to the interface pointing towards medium 1.

Using duality, the continuity of the magnetic scalar potential and electric vector potential across dielectric interfaces can be shown. Also, applying duality to Eq. (4.53), we can show that

$$\mu_1 \frac{\partial \Phi_{\mathrm{m1}}}{\partial n} = \mu_2 \frac{\partial \Phi_{\mathrm{m2}}}{\partial n} \, . \tag{4.54}$$

Now let us consider a situation where the second medium is a perfect electric conductor. According to Eq. (4.44b), since $\mathbf{E}_2(\mathbf{r})$ inside the conductor is zero, it then follows that $\mathbf{A}_2(\mathbf{r}) = 0$ inside the conductor as well. Hence, on the surface of a perfect electric conductor

$$\mathbf{A}_1(\mathbf{r}) = 0 \, , \qquad \mathbf{r} \in S \, .$$

Also, on the surface of a perfect conductor we have

$$\hat{\mathbf{n}} \times \mathbf{E}_1(\mathbf{r}) = 0 \, . \tag{4.55}$$

Using Eq. (4.44b) for $\mathbf{E}_1(\mathbf{r})$ and noting that $\hat{\mathbf{n}} \times \mathbf{A}_1(\mathbf{r}) = 0$, Eq. (4.55) simplifies to

$$\begin{aligned} \hat{\mathbf{n}} \times \nabla \, \Phi_1(\mathbf{r}) &= \hat{\mathbf{n}} \times (\nabla \Phi_1 \cdot \hat{\mathbf{t}} \, \hat{\mathbf{t}} + \nabla \Phi_1 \cdot \hat{\mathbf{n}} \, \hat{\mathbf{n}}) \\ &= \hat{\mathbf{n}} \times \hat{\mathbf{t}} \, \frac{\partial \Phi_1}{\partial t} = 0 \, , \end{aligned} \tag{4.56}$$

where $\hat{\mathbf{t}}$ is a unit vector tangential to the conductor surface. Equation (4.56) indicates that $\partial \Phi_1 / \partial t = 0$, and thus the electric scalar potential on the surface of the conductors must be a constant.

## 4-3 Integral Equations for Electromagnetic Fields

In this section we consider the derivation of integral equations for electromagnetic fields applicable to antennas and scattering problems. In the previous chapter we demonstrated how fields radiated from antennas with known current distribution can be evaluated. However, in practice the determination of the current distribution on antenna surfaces cannot be performed in a straightforward manner. Also, in scattering problems where the goal is to determine the electromagnetic fields scattered by specific objects when illuminated by specific sources, the solution cannot be easily realized except for a very limited number of objects with simple geometries. In principle, integral equation formulations with computer-aided numerical analysis can be used to solve for the current distribution on an antenna of arbitrary

shape, and the same procedure can be used to determine the fields scattered by an arbitrary object. The formulation is derived directly from the fields' wave equation instead of the potentials. Let us consider electric and magnetic sources in a homogeneous and unbounded medium with a finite number of metallic or dielectric objects, as was shown earlier in Fig. 4-2. Maxwell's equations in the background medium with permittivity $\varepsilon_1$ and permeability $\mu_1$ and with electric and magnetic sources $J(\mathbf{r})$, $\rho(\mathbf{r})$, $J_{\rm m}(\mathbf{r})$, and $\rho_{\rm m}(\mathbf{r})$ are given by

$$\nabla \times \mathbf{E}(\mathbf{r}) = i\omega\mu_1\, \mathbf{H}(\mathbf{r}) - \mathbf{J}_{\rm m}(\mathbf{r})\ , \tag{4.57a}$$

$$\nabla \times \mathbf{H}(\mathbf{r}) = -i\omega\varepsilon_1\, \mathbf{E}(\mathbf{r}) + \mathbf{J}(\mathbf{r})\ , \tag{4.57b}$$

$$\nabla \cdot \mathbf{E}(\mathbf{r}) = \frac{1}{\varepsilon_1}\, \rho(\mathbf{r})\ , \tag{4.57c}$$

$$\nabla \cdot \mathbf{H}(\mathbf{r}) = \frac{1}{\mu_1}\, \rho_{\rm m}(\mathbf{r})\ . \tag{4.57d}$$

Taking $\nabla\times$ of both sides of Eq. (4.57a) and using Eq. (4.57b), it can be shown that

$$\nabla \times \nabla \times \mathbf{E}(\mathbf{r}) = k_1^2\, \mathbf{E}(\mathbf{r}) + i\omega\mu_1\, \mathbf{J}(\mathbf{r}) - \nabla \times \mathbf{J}_{\rm m}(\mathbf{r})\ . \tag{4.58}$$

Noting that $\nabla \times \nabla \times \mathbf{E}(\mathbf{r}) = \nabla\nabla \cdot \mathbf{E}(\mathbf{r}) - \nabla^2\mathbf{E}(\mathbf{r})$ and using Eq. (4.57c), we have

$$\nabla \times \nabla \times \mathbf{E}(\mathbf{r}) = \frac{1}{\varepsilon_1}\, \nabla\rho(\mathbf{r}) - \nabla^2\mathbf{E}(\mathbf{r})\ . \tag{4.59}$$

Also, using the equation of continuity ($\nabla \cdot \mathbf{J}(\mathbf{r}) = i\omega\, \rho(\mathbf{r})$) in Eq. (4.59), we have

$$\nabla \times \nabla \times \mathbf{E}(\mathbf{r}) = \frac{1}{i\omega\varepsilon_1}\, \nabla\nabla \cdot \mathbf{J}(\mathbf{r}) - \nabla^2\mathbf{E}(\mathbf{r})\ . \tag{4.60}$$

Finally, using Eq. (4.60) in Eq. (4.58), we obtain the following wave equation for the electric field $\mathbf{E}$:

$$\nabla^2\, \mathbf{E}(\mathbf{r}) + k_1^2\, \mathbf{E}(\mathbf{r}) = -\boldsymbol{\mathcal{F}}(\mathbf{r})\ , \tag{4.61}$$

where

$$\boldsymbol{\mathcal{F}}(\mathbf{r}) = i\omega\mu_1\, \mathbf{J}(\mathbf{r}) - \nabla \times \mathbf{J}_{\rm m}(\mathbf{r}) - \frac{1}{i\omega\varepsilon_1}\, \nabla\nabla \cdot \mathbf{J}(\mathbf{r}) \tag{4.62}$$

is the ***excitation vector*** for the electric field in the background medium. Application of duality leads to the following wave equation for the magnetic field:

$$\nabla^2\, \mathbf{H}(\mathbf{r}) + k_1^2\, \mathbf{H}(\mathbf{r}) = -\boldsymbol{\mathcal{F}}_{\rm m}(\mathbf{r})\ , \tag{4.63}$$

where

$$\boldsymbol{\mathcal{F}}_{\rm m}(\mathbf{r}) = i\omega\varepsilon_1\, \mathbf{J}_{\rm m}(\mathbf{r}) + \nabla \times \mathbf{J}(\mathbf{r}) - \frac{1}{i\omega\mu_1}\, \nabla\nabla \cdot \mathbf{J}_{\rm m}(\mathbf{r})\ . \tag{4.64}$$

Next, by applying Green's second identity, as defined by Eq. (4.20), to Eq. (4.61), the following equations for the electric field are obtained:

$$\iiint_v \boldsymbol{F}(\mathbf{r}')\, g(\mathbf{r},\mathbf{r}')\, dv' + \oiint_{\sum S_i} \left( g(\mathbf{r},\mathbf{r}') \frac{\partial \mathbf{E}(\mathbf{r}')}{\partial n'} - \mathbf{E}(\mathbf{r}') \frac{\partial g(\mathbf{r},\mathbf{r}')}{\partial n'} \right) ds' = \begin{cases} \mathbf{E}(\mathbf{r}) & \mathbf{r} \in V\ , \\ 0 & \mathbf{r} \notin V\ , \end{cases} \tag{4.65}$$

where $g(\mathbf{r},\mathbf{r}')$ is the free-space scalar Green's function. Applying duality to Eq. (4.65), the integral equation for the magnetic fields can be obtained from

$$\iiint_v \boldsymbol{F}_{\mathrm{m}}(\mathbf{r}')\, g(\mathbf{r},\mathbf{r}')\, dv' + \oiint_{\sum S_i} \left( g(\mathbf{r},\mathbf{r}') \frac{\partial \mathbf{H}(\mathbf{r}')}{\partial n'} - \mathbf{H}(\mathbf{r}') \frac{\partial g(\mathbf{r},\mathbf{r}')}{\partial n'} \right) ds' = \begin{cases} \mathbf{H}(\mathbf{r}) & \mathbf{r} \in V\ , \\ 0 & \mathbf{r} \notin V\ . \end{cases} \tag{4.66}$$

The first integral expression in Eqs. (4.65) and (4.66) can be viewed as the incident electric and magnetic fields. These are the fields that would exist in the absence of the scatterers. As shown previously, when the observation point is on the surface, the singularity associated with the scalar Green's function can be removed from the surface integrals, and thus Eqs. (4.65) and (4.66) can be written as

$$\mathbf{E}_{\mathrm{i}}(\mathbf{r}) + \oiint_{\sum S_i} \left( g(\mathbf{r},\mathbf{r}') \frac{\partial \mathbf{E}(\mathbf{r}')}{\partial n'} - \mathbf{E}(\mathbf{r}') \frac{\partial g(\mathbf{r},\mathbf{r}')}{\partial n'} \right) ds' = \begin{cases} \mathbf{E}(\mathbf{r}) & \mathbf{r} \in V\ , \\ \frac{1}{2}\,\mathbf{E}(\mathbf{r}) & \mathbf{r} \text{ on } S_i\ , \\ 0 & \mathbf{r} \notin V\ , \end{cases} \tag{4.67a}$$

and

$$\mathbf{H}_{\mathrm{i}}(\mathbf{r}) + \oiint_{\sum S_i} \left( g(\mathbf{r},\mathbf{r}') \frac{\partial \mathbf{H}(\mathbf{r}')}{\partial n'} - \mathbf{H}(\mathbf{r}') \frac{\partial g(\mathbf{r},\mathbf{r}')}{\partial n'} \right) ds' = \begin{cases} \mathbf{H}(\mathbf{r}) & \mathbf{r} \in V\ , \\ \frac{1}{2}\,\mathbf{H}(\mathbf{r}) & \mathbf{r} \text{ on } S_i\ , \\ 0 & \mathbf{r} \notin V\ , \end{cases} \tag{4.67b}$$

where $\mathbf{E}_{\mathrm{i}}(\mathbf{r})$ and $\mathbf{H}_{\mathrm{i}}(\mathbf{r})$ represent the first integrals in Eqs. (4.65) and (4.66).

## 4-4 Integral Equation Formulation Based on Equivalent Sources

To derive an alternative integral equation based on surface fields using electromagnetic potentials, let us start with the expression for the field quantities in terms of magnetic potentials $\mathbf{A}$ and $\mathbf{A}_{\mathrm{m}}$, as given by Eqs. (3.89a) and (3.89b):

$$\mathbf{E} = \frac{i\omega}{k^2} \nabla\nabla \cdot \mathbf{A} + i\omega\mathbf{A} - \frac{1}{\varepsilon} \nabla \times \mathbf{A}_{\mathrm{m}} \tag{4.68a}$$

and

$$\mathbf{H} = \frac{i\omega}{k^2}\nabla\nabla\cdot\mathbf{A}_{\mathrm{m}} + i\omega\mathbf{A} + \frac{1}{\mu}\nabla\times\mathbf{A}\ , \tag{4.68b}$$

with

$$\mathbf{A}(\mathbf{r}) = \mu \iiint_v \mathbf{J}(\mathbf{r}')\, g(\mathbf{r},\mathbf{r}')\, dv' \tag{4.69a}$$

and

$$\mathbf{A}_{\mathrm{m}}(\mathbf{r}) = \varepsilon \iiint_v \mathbf{J}_{\mathrm{m}}(\mathbf{r}')\, g(\mathbf{r},\mathbf{r}')\, dv'\ , \tag{4.69b}$$

where $g(\mathbf{r},\mathbf{r}')$ is the free-space scalar Green's function. To derive an explicit expression for the fields in terms of the currents, the following observations are in order:

$$\nabla\cdot[\mathbf{J}(\mathbf{r}')\, g(\mathbf{r},\mathbf{r}')] = \mathbf{J}(\mathbf{r}')\cdot\nabla g(\mathbf{r},\mathbf{r}') \tag{4.70a}$$

and

$$\nabla g(\mathbf{r},\mathbf{r}') = -\nabla' g(\mathbf{r},\mathbf{r}')\ , \tag{4.70b}$$

where $\nabla'$ is the gradient operator acting on the prime coordinate variables.

Also, note that

$$\nabla\times[\mathbf{J}_{\mathrm{m}}(\mathbf{r}')\, g(\mathbf{r},\mathbf{r}')] = -\mathbf{J}_{\mathrm{m}}(\mathbf{r}')\times\nabla g(\mathbf{r},\mathbf{r}')\ . \tag{4.71}$$

First we evaluate $\nabla\nabla\cdot\mathbf{A}$ using Eqs. (4.70a) and (4.70b):

$$\nabla\nabla\cdot\mathbf{A}(\mathbf{r}) = -\mu\nabla\iiint_v \mathbf{J}(\mathbf{r}')\cdot\nabla' g(\mathbf{r},\mathbf{r}')\, dv'\ . \tag{4.72}$$

Using the following identity:

$$\nabla'\cdot[\mathbf{J}(\mathbf{r}')\, g(\mathbf{r},\mathbf{r}')] = \mathbf{J}(\mathbf{r}')\cdot\nabla' g(\mathbf{r},\mathbf{r}') + \nabla'\cdot\mathbf{J}(\mathbf{r}')\, g(\mathbf{r},\mathbf{r}')\ ,$$

and employing the divergence theorem, we get

$$\iiint_v \nabla'\cdot[\mathbf{J}(\mathbf{r}')\, g(\mathbf{r},\mathbf{r}')]\, dv' = \oiint_S g(\mathbf{r},\mathbf{r}')\, \mathbf{J}(\mathbf{r}')\cdot\hat{\mathbf{n}}'\, ds'\ . \tag{4.73}$$

The surface $S$ here identifies a closed surface confining the volumetric current $\mathbf{J}(\mathbf{r}')$. Obviously no currents are flowing outside $S$, and therefore $\hat{\mathbf{n}}'\cdot\mathbf{J}(\mathbf{r}') = 0$ along the surface. This renders the right-hand side of Eq. (4.73) equal to zero, and therefore

$$\nabla\nabla\cdot\mathbf{A} = \mu\iiint_v \nabla'\cdot\mathbf{J}(\mathbf{r}')\,\nabla g(\mathbf{r},\mathbf{r}')\, dv'\ . \tag{4.74}$$

Using Eqs. (4.74) and (4.71) in Eq. (4.68a), the explicit expression for the electric field is given by

$$\mathbf{E}(\mathbf{r}) = \frac{i\eta}{k} \iiint_v \left[\nabla' \cdot \mathbf{J}(\mathbf{r}')\, \nabla g(\mathbf{r},\mathbf{r}') + k^2\, \mathbf{J}(\mathbf{r}')\, g(\mathbf{r},\mathbf{r}')\right] dv' + \iiint_v \left[\mathbf{J}_{\mathrm{m}}(\mathbf{r}') \times \nabla g(\mathbf{r},\mathbf{r}')\right] dv' \,. \tag{4.75}$$

Applying duality to Eq. (4.75) gives an explicit expression for the magnetic field:

$$\begin{aligned}\mathbf{H}(\mathbf{r}) = \frac{i}{\eta k} &\iiint_v \left[\nabla' \cdot \mathbf{J}_{\mathrm{m}}(\mathbf{r}')\, \nabla g(\mathbf{r},\mathbf{r}') + k^2\, \mathbf{J}_{\mathrm{m}}(\mathbf{r}')\, g(\mathbf{r},\mathbf{r}')\right] dv' \\ &- \iiint_v \left[\mathbf{J}(\mathbf{r}') \times \nabla g(\mathbf{r},\mathbf{r}')\right] dv' \,.\end{aligned} \tag{4.76}$$

According to the equation of continuity,

$$\nabla' \cdot \mathbf{J}(\mathbf{r}') = i\omega\, \rho(\mathbf{r}')$$

and

$$\nabla' \cdot \mathbf{J}_{\mathrm{m}}(\mathbf{r}') = i\omega\, \rho_{\mathrm{m}}(\mathbf{r}') \,.$$

Equations (4.75) and (4.76) form the basis for the integral equation for scattering and antenna problems. To demonstrate this, let us consider a homogeneous medium with permittivity $\varepsilon$ and permeability $\mu$. Also consider volumetric currents $\mathbf{J}(\mathbf{r})$ and $\mathbf{J}_{\mathrm{m}}(\mathbf{r})$ as excitation. In the absence of any objects in this homogeneous medium, these currents produce $\mathbf{E}_{\mathrm{i}}(\mathbf{r})$ and $\mathbf{H}_{\mathrm{i}}(\mathbf{r})$, and they can be computed from Eqs. (4.75) and (4.76), respectively. In the presence of an object, these fields generate a secondary set of fields that are referred to as the ***scattered fields***. Hence the total fields can be represented by

$$\mathbf{E}(\mathbf{r}) = \mathbf{E}_{\mathrm{i}}(\mathbf{r}) + \mathbf{E}_{\mathrm{s}}(\mathbf{r}) \tag{4.77a}$$

and

$$\mathbf{H}(\mathbf{r}) = \mathbf{H}_{\mathrm{i}}(\mathbf{r}) + \mathbf{H}_{\mathrm{s}}(\mathbf{r}) \,. \tag{4.77b}$$

$\mathbf{E}(\mathbf{r})$ and $\mathbf{H}(\mathbf{r})$ are unknown, but assuming their values are known on the surface of the scatterer, $S_{\mathrm{s}}$, the field equivalence principle can be used by assuming zero fields inside the scatterer and placing the following surface currents on the surface of the scatterer:

$$\mathbf{J}_{\mathrm{s}}(\mathbf{r}) = \hat{\mathbf{n}} \times \mathbf{H}(\mathbf{r}) \,, \qquad \mathbf{r} \in S_{\mathrm{s}} \tag{4.78a}$$

and

$$\mathbf{J}_{\mathrm{ms}}(\mathbf{r}) = -\hat{\mathbf{n}} \times \mathbf{E}(\mathbf{r}) \,, \qquad \mathbf{r} \in S_{\mathrm{s}} \,. \tag{4.78b}$$

Also, equivalent surface charges must be placed on the surface and are given by

$$\rho_{\mathrm{s}}(\mathbf{r}) = \varepsilon\, \hat{\mathbf{n}} \cdot \mathbf{E}(\mathbf{r}) \qquad \text{and} \qquad \rho_{\mathrm{ms}}(\mathbf{r}) = \mu\, \hat{\mathbf{n}} \cdot \mathbf{H}(\mathbf{r}) \,.$$

If these currents are known, they can be used in Eqs. (4.75) and (4.76) to find the scattered fields. Hence the total fields are given by

$$\mathbf{E}(\mathbf{r}) = \mathbf{E}_{\mathrm{i}} + \oiint_{S_{\mathrm{s}}} \left\{ i\eta k[\hat{\mathbf{n}}' \times \mathbf{H}(\mathbf{r}')]\, g(\mathbf{r},\mathbf{r}') - \hat{\mathbf{n}}' \cdot \mathbf{E}(\mathbf{r}')\, \nabla g(\mathbf{r},\mathbf{r}') + [\mathbf{E}(\mathbf{r}') \times \hat{\mathbf{n}}'] \times \nabla g(\mathbf{r},\mathbf{r}') \right\} ds' \tag{4.79a}$$

and

$$\mathbf{H}(\mathbf{r}) = \mathbf{H}_{\mathrm{i}} + \oiint_{S_{\mathrm{s}}} \left\{ \frac{ik}{\eta} [\mathbf{E}(\mathbf{r}') \times \hat{\mathbf{n}}']\, g(\mathbf{r},\mathbf{r}') - \hat{\mathbf{n}}' \cdot \mathbf{H}(\mathbf{r}')\, \nabla g(\mathbf{r},\mathbf{r}') + [\mathbf{H}(\mathbf{r}') \times \hat{\mathbf{n}}'] \times \nabla g(\mathbf{r},\mathbf{r}') \right\} ds' \,. \tag{4.79b}$$

This is valid when the observation point is outside the scatterer (outside $S_{\mathrm{s}}$). In cases where the observation point is on the scatterer, the singularity of the Green's function for the condition $\mathbf{r} = \mathbf{r}'$ must be removed, similarly to what was shown in the previous section. In cases where the observation point is inside the scatterer, the fields must be set to zero according to the equivalence theorem. In general,

$$E_{\mathrm{i}}(\mathbf{r}) + \oiint \left\{ i\eta k[\hat{\mathbf{n}}' \times \mathbf{H}(\mathbf{r}')]\, g(\mathbf{r},\mathbf{r}') - \hat{\mathbf{n}}' \cdot \mathbf{E}(\mathbf{r}')\, \nabla g(\mathbf{r},\mathbf{r}') + [\mathbf{E}(\mathbf{r}') \times \hat{\mathbf{n}}'] \times \nabla g(\mathbf{r},\mathbf{r}') \right\} ds' = \begin{cases} \mathbf{E}(\mathbf{r}) & \mathbf{r} \text{ outside } S_{\mathrm{s}} \,, \\ \frac{1}{2}\,\mathbf{E}(\mathbf{r}) & \mathbf{r} \in S_{\mathrm{s}} \,, \\ 0 & \mathbf{r} \text{ inside } S_{\mathrm{s}} \,, \end{cases} \tag{4.80a}$$

and

$$H_{\mathrm{i}}(\mathbf{r}) + \oiint \left\{ \frac{ik}{\eta} [\mathbf{E}(\mathbf{r}') \times \hat{\mathbf{n}}']\, g(\mathbf{r},\mathbf{r}') - \hat{\mathbf{n}}' \cdot \mathbf{H}(\mathbf{r}')\, \nabla g(\mathbf{r},\mathbf{r}') + [\mathbf{H}(\mathbf{r}') \times \hat{\mathbf{n}}'] \times \nabla g(\mathbf{r},\mathbf{r}') \right\} ds' = \begin{cases} \mathbf{H}(\mathbf{r}) & \mathbf{r} \text{ outside } S_{\mathrm{s}} \,, \\ \frac{1}{2}\,\mathbf{H}(\mathbf{r}) & \mathbf{r} \in S_{\mathrm{s}} \,, \\ 0 & \mathbf{r} \text{ inside } S_{\mathrm{s}} \,. \end{cases} \tag{4.80b}$$

## 4-5 Integral Equation Formulation for Dielectric Scatterers

To examine how Eqs. (4.80a) and (4.80b) can be cast into integral equations, we consider a dielectric object with permittivity $\varepsilon_2$ and permeability $\mu_2$ placed in a homogeneous medium, as shown in Fig. 4-5. As in the previous section, we consider known electric and magnetic current sources $\mathbf{J}(\mathbf{r})$ and $\mathbf{J}_{\mathrm{m}}(\mathbf{r})$ present in the background medium to produce the incident fields $\mathbf{E}_{\mathrm{i}}(\mathbf{r})$ and $\mathbf{H}_{\mathrm{i}}(\mathbf{r})$. The fields outside the scatterer are denoted $\mathbf{E}_1(\mathbf{r})$ and $\mathbf{H}_1(\mathbf{r})$, and those inside the scatterer are denoted $\mathbf{E}_2(\mathbf{r})$ and $\mathbf{H}_2(\mathbf{r})$. The expressions for $\mathbf{E}_1(\mathbf{r})$ and $\mathbf{H}_1(\mathbf{r})$ can

be obtained from Eqs. (4.80a) and (4.80b) by assigning subscript 1 to the fields, to the scalar Green's function, and to the medium parameters. Using a procedure similar to what led to the derivation of Eqs. (4.80a) and (4.80b) for the exterior fields, the following equations are obtained for $\mathbf{E}_2(\mathbf{r})$ and $\mathbf{H}_2(\mathbf{r})$:

$$\oiint \left\{ i\eta_2 k_2 [\hat{\mathbf{n}}_2' \times \mathbf{H}_2(\mathbf{r}')]\, g_2(\mathbf{r},\mathbf{r}') - \hat{\mathbf{n}}_2' \cdot \mathbf{E}_2(\mathbf{r}')\, \nabla g_2(\mathbf{r},\mathbf{r}') + [\mathbf{E}_2(\mathbf{r}') \times \hat{\mathbf{n}}_2'] \times \nabla g_2(\mathbf{r},\mathbf{r}') \right\} ds'$$

$$= \begin{cases} 0 & \mathbf{r} \text{ outside } S_s\,, \\ \frac{1}{2}\,\mathbf{E}_2(\mathbf{r}) & \mathbf{r} \in S_s\,, \\ \mathbf{E}_2(\mathbf{r}) & \mathbf{r} \text{ inside } S_s\,, \end{cases} \tag{4.81a}$$

and

$$\oiint \left\{ \frac{ik_2}{\eta_2} [\mathbf{E}_2(\mathbf{r}') \times \hat{\mathbf{n}}_2']\, g_2(\mathbf{r},\mathbf{r}') - \hat{\mathbf{n}}_2' \cdot \mathbf{H}_2(\mathbf{r}')\, \nabla g_2(\mathbf{r},\mathbf{r}') + [\mathbf{H}_2(\mathbf{r}') \times \hat{\mathbf{n}}_2'] \times \nabla g_2(\mathbf{r},\mathbf{r}') \right\} ds'$$

$$= \begin{cases} 0 & \mathbf{r} \text{ outside } S_s\,, \\ \frac{1}{2}\,\mathbf{H}_2(\mathbf{r}) & \mathbf{r} \in S_s\,, \\ \mathbf{H}_2(\mathbf{r}) & \mathbf{r} \text{ inside } S_s\,. \end{cases} \tag{4.81b}$$

Defining the tangential surface fields as unknown and applying the boundary conditions, we have

$$\hat{\mathbf{n}}_1' \times \mathbf{H}_1(\mathbf{r}') = -\hat{\mathbf{n}}_2' \times \mathbf{H}_2(\mathbf{r}') = \mathbf{J}_s(\mathbf{r}')\,,$$
$$\mathbf{E}_1(\mathbf{r}') \times \hat{\mathbf{n}}_1' = -\mathbf{E}_2(\mathbf{r}') \times \hat{\mathbf{n}}_2' = \mathbf{J}_{ms}(\mathbf{r}')\,,$$
$$\varepsilon_1 \hat{\mathbf{n}}_1 \cdot \mathbf{E}_1(\mathbf{r}') = -\varepsilon_2 \hat{\mathbf{n}}_2' \cdot \mathbf{E}_2(\mathbf{r}') = \frac{\nabla_s' \cdot \mathbf{J}_s(\mathbf{r}')}{i\omega}\,,$$

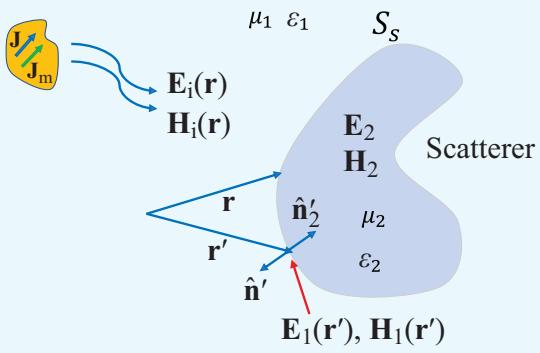


**Figure 4-5:** Geometry of the scattering problem for a dielectric object placed in a homogeneous and unbounded medium illuminated by fields generated by $\mathbf{J}$ and $\mathbf{J}_m$.

$$\mu_1 \hat{\mathbf{n}}_1 \cdot \mathbf{H}_1(\mathbf{r}') = -\mu_2 \hat{\mathbf{n}}_2' \cdot \mathbf{H}_2(\mathbf{r}') = \frac{\nabla_s' \cdot \mathbf{J}_{ms}(\mathbf{r}')}{i\omega} \, .$$

Here $\nabla_s \cdot$ refers to a 2-D divergence operator acting on the surface of the scatterer. The electric-field integral equations can be obtained by requiring the continuity of the tangential electric fields at the boundary of the scatterer using Eqs. (4.80a) and (4.81a); that is,

$$\begin{aligned} &-\frac{1}{2}\mathbf{J}_{ms}(\mathbf{r}) \\ &\quad -\hat{\mathbf{n}} \times \oiint_{S_s} \left( i\eta_1 k_1 \, \mathbf{J}_s(\mathbf{r}') \, g_1(\mathbf{r},\mathbf{r}') + \frac{i\eta_1}{k_1} \, \nabla_s' \cdot \mathbf{J}_s(\mathbf{r}') \, \nabla g_1(\mathbf{r},\mathbf{r}') + \mathbf{J}_{ms}(\mathbf{r}') \times \nabla g_1(\mathbf{r},\mathbf{r}') \right) ds' \\ &= \hat{\mathbf{n}} \times \mathbf{E}_i(\mathbf{r}) \end{aligned} \tag{4.82a}$$

and

$$\begin{aligned} &-\frac{1}{2}\mathbf{J}_{ms}(\mathbf{r}) \\ &\quad +\hat{\mathbf{n}} \times \oiint_{S_s} \left( i\eta_2 k_2 \, \mathbf{J}_s(\mathbf{r}') \, g_2(\mathbf{r},\mathbf{r}') + \frac{i\eta_2}{k_2} \, \nabla_s' \cdot \mathbf{J}_s(\mathbf{r}') \, \nabla g_2(\mathbf{r},\mathbf{r}') + \mathbf{J}_{ms}(\mathbf{r}') \times \nabla g_2(\mathbf{r},\mathbf{r}') \right) ds' \\ &= 0 \, . \end{aligned} \tag{4.82b}$$

Also, the magnetic-field integral equations can be obtained by enforcing the continuity of the tangential magnetic fields at the boundary of the scatterer using Eqs. (4.80b) and (4.81b):

$$\begin{aligned} &\frac{1}{2}\mathbf{J}_s(\mathbf{r}) - \hat{\mathbf{n}} \times \oiint_{S_s} \left( \frac{ik_1}{\eta_1} \, \mathbf{J}_{ms}(\mathbf{r}') \, g_1(\mathbf{r},\mathbf{r}') \right. \\ &\qquad \left. + \frac{i}{k_1\eta_1} \, \nabla_s' \cdot \mathbf{J}_{ms}(\mathbf{r}') \, \nabla g_1(\mathbf{r},\mathbf{r}') - \mathbf{J}_s(\mathbf{r}') \times \nabla g_1(\mathbf{r},\mathbf{r}') \right) ds' \\ &\quad = \hat{\mathbf{n}} \times \mathbf{H}_i(\mathbf{r}) \end{aligned} \tag{4.83a}$$

and

$$\begin{aligned} &\frac{1}{2}\mathbf{J}_s(\mathbf{r}) + \hat{\mathbf{n}} \times \oiint_{S_s} \left( \frac{ik_2}{\eta_2} \, \mathbf{J}_{ms}(\mathbf{r}') \, g_2(\mathbf{r},\mathbf{r}') \right. \\ &\qquad \left. + \frac{i}{k_2\eta_2} \, \nabla_s' \cdot \mathbf{J}_{ms}(\mathbf{r}') \, \nabla g_2(\mathbf{r},\mathbf{r}') - \mathbf{J}_s(\mathbf{r}') \times \nabla g_2(\mathbf{r},\mathbf{r}') \right) ds' \\ &\quad = 0 \, . \end{aligned} \tag{4.83b}$$

The ***magnetic-field integral equations*** (MFIE) given by Eq. (4.83) are duals of the ***electric-field integral equations*** (EFIE). Hence, either EFIE or MFIE is sufficient to find the equivalent surface currents.

The EFIE and MFIE take on a simple form when the scatterer is a metallic object. Noting that $\hat{\mathbf{n}} \times \mathbf{E} = 0$ and $\hat{\mathbf{n}} \cdot \mathbf{H} = 0$ on metallic surfaces, as evident from Eq. (4.82a) by setting

$\mathbf{J}_{ms} = 0$, the EFIE for metallic objects assumes the following form:

$$-i\eta_1 k_1 \hat{\mathbf{n}} \times \oiint_{S_s} \left( \mathbf{J}_s(\mathbf{r}')\, g(\mathbf{r},\mathbf{r}') + \frac{1}{k_1^2} \nabla_s' \cdot \mathbf{J}_s(\mathbf{r}')\, \nabla g(\mathbf{r},\mathbf{r}') \right) dS' = \hat{\mathbf{n}} \times \mathbf{E}_i(\mathbf{r}) \,. \tag{4.84}$$

**(metallic object)**

Also, using Eq. (4.83a) with $\mathbf{J}_{ms} = 0$, the following MFIE for metallic objects is obtained:

$$\frac{1}{2}\mathbf{J}_s(\mathbf{r}) + \hat{\mathbf{n}} \times \oiint_{S_s} \mathbf{J}_s(\mathbf{r}') \times \nabla g_1(\mathbf{r},\mathbf{r}')\, dS' = \hat{\mathbf{n}} \times \mathbf{H}_i(\mathbf{r}) \,. \tag{4.85a}$$

**(metallic object)**

For metallic objects with no sharp edges, the MFIE formulation is preferred and provides a more accurate numerical solution. For surfaces with large radii of curvature, the contribution from the integral becomes negligible compared with $\hat{\mathbf{n}} \times \mathbf{H}_i(\mathbf{r})$ and can be ignored. This is due to the fact that the dominant contribution of the integral comes from source points $\mathbf{r}'$ that are close to the observation point $\mathbf{r}$. When $\mathbf{r}$ is close to $\mathbf{r}'$ for smooth surfaces, $\nabla g(\mathbf{r},\mathbf{r}')$ is almost tangential to the surface, and as a result $\mathbf{J}_s(\mathbf{r}') \times \nabla g(\mathbf{r},\mathbf{r}')$ is almost perpendicular to the surface and its cross product with $\hat{\mathbf{n}}$ is almost zero. Under such assumptions (large radii of surface curvature),

$$\mathbf{J}_s(\mathbf{r}) = 2\hat{\mathbf{n}} \times \mathbf{H}_i(\mathbf{r}) \,, \tag{4.85b}$$

which is known as the ***physical-optics approximation***.

## 4-6 Reciprocity Theorem

The notion of reciprocity was introduced in conjunction with the symmetry property of the scalar Green's function. In circuit theory, reciprocity manifests itself in the symmetry of the impedance matrix of a passive linear network. Consider a two-port network, as shown in Fig. 4-6. It can be easily shown that the short-circuited current at the second port ($I_a$) excited by a voltage source at the first terminal ($V_a$) and the short-circuited current at the first port ($I_b$) excited by a voltage source at the second terminal ($V_b$) satisfy the following relations:

$$I_a V_b = I_b V_a \,. \tag{4.86}$$

The corresponding relationship in electromagnetics is provided by the ***Lorentz reciprocity theorem***. To find the reciprocity relation, let us consider two sets of excitations and their

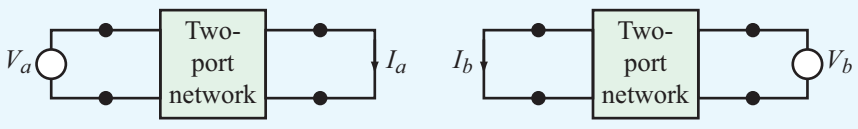


**Figure 4-6:** The concept of reciprocity relationship for a two-port network.

resulting fields in a bounded homogeneous medium specified by volume $V$ and a closed surface $S$. Suppose $\mathbf{E}_a$ and $\mathbf{H}_a$ are generated by electric and magnetic current sources $\mathbf{J}_a$ and $\mathbf{J}_{ma}$ and fields $\mathbf{E}_b$ and $\mathbf{H}_b$ are generated by current sources $\mathbf{J}_b$ and $\mathbf{J}_{mb}$. According to Maxwell's equations,

$$\begin{cases} \nabla \times \mathbf{E}_a = i\omega\mu \mathbf{H}_a - \mathbf{J}_{ma} \,, \\ \nabla \times \mathbf{H}_a = -i\omega\varepsilon \mathbf{E}_a + \mathbf{J}_a \,, \end{cases} \tag{4.87a}$$

and

$$\begin{cases} \nabla \times \mathbf{E}_b = i\omega\mu \mathbf{H}_b - \mathbf{J}_{mb} \,, \\ \nabla \times \mathbf{H}_b = -i\omega\varepsilon \mathbf{E}_b + \mathbf{J}_b \,. \end{cases} \tag{4.87b}$$

Using the following vector identities

$$\nabla \cdot (\mathbf{E}_a \times \mathbf{H}_b) = \mathbf{H}_b \cdot \nabla \times \mathbf{E}_a - \mathbf{E}_a \cdot \nabla \times \mathbf{H}_b \tag{4.88a}$$

and

$$\nabla \cdot (\mathbf{E}_b \times \mathbf{H}_a) = \mathbf{H}_a \cdot \nabla \times \mathbf{E}_b - \mathbf{E}_b \cdot \nabla \times \mathbf{H}_a, \tag{4.88b}$$

and then subtracting Eq. (4.88b) from Eq. (4.88a) and using Eqs. (4.87a) and (4.87b), we have

$$\nabla \cdot (\mathbf{E}_a \times \mathbf{H}_b - \mathbf{E}_b \times \mathbf{H}_a) = -(\mathbf{E}_a \cdot \mathbf{J}_b - \mathbf{H}_a \cdot \mathbf{J}_{mb}) + (\mathbf{E}_b \cdot \mathbf{J}_a - \mathbf{H}_b \cdot \mathbf{J}_{ma}) \,. \tag{4.89}$$

By applying the volume integral to both sides of Eq. (4.89), it can be shown that

$$\oiint_S (\mathbf{E}_a \times \mathbf{H}_b - \mathbf{E}_b \times \mathbf{H}_a) \cdot d\mathbf{s} = -\iiint_V (\mathbf{E}_a \cdot \mathbf{J}_b - \mathbf{H}_a \cdot \mathbf{J}_{mb})\, dv + \iiint_V (\mathbf{E}_b \cdot \mathbf{J}_a - \mathbf{H}_b \cdot \mathbf{J}_{ma})\, dv \,. \tag{4.90}$$

If we let $S \to \infty$, the radiated fields in the far-field region become ***transverse electromagnetic*** (TEM); that is, $\mathbf{E}_{a,b} \perp \mathbf{H}_{a,b} \perp \hat{\mathbf{r}}$, $\mathbf{E}_a = \eta\, \mathbf{H}_a \times \hat{\mathbf{r}}$, and also $\mathbf{E}_b = \eta\, \mathbf{H}_b \times \hat{\mathbf{r}}$. Hence,

$$\begin{aligned} (\mathbf{E}_a \times \mathbf{H}_b - \mathbf{E}_b \times \mathbf{H}_a) \cdot \hat{\mathbf{r}} &= \mathbf{E}_a \cdot (\mathbf{H}_b \times \hat{\mathbf{r}}) - \mathbf{E}_b \cdot (\mathbf{H}_a \times \hat{\mathbf{r}}) \\ &= \frac{1}{\eta} (\mathbf{E}_a \cdot \mathbf{E}_b - \mathbf{E}_b \cdot \mathbf{E}_a) = 0 \,, \end{aligned}$$

which indicates that the left-hand side of Eq. (4.90) vanishes. In this case the reciprocity relation takes the following form:

$$\langle a, b \rangle = \langle b, a \rangle \,, \tag{4.91}$$

where

$$\langle a, b \rangle = \iiint_V (\mathbf{E}_a \cdot \mathbf{J}_b - \mathbf{H}_a \cdot \mathbf{J}_{mb})\, dv \,.$$

As an example, consider elementary sources

$$\mathbf{J}_a = I_0\, \Delta\ell_a\, \delta(\mathbf{r} - \mathbf{r}_1)$$

and

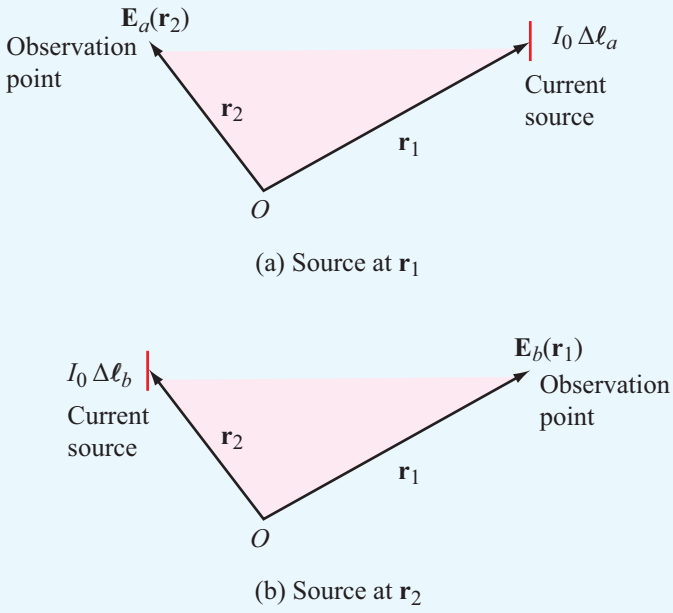


**Figure 4-7:** Geometry of two experiments with elementary sources to demonstrate the reciprocity theorem in a homogeneous unbounded medium.

$$\mathbf{J}_b = I_0\,\Delta\boldsymbol{\ell}_b\,\delta(\mathbf{r}-\mathbf{r}_2)\,,$$

as shown in Fig. 4-7, for which reciprocity dictates that

$$\mathbf{E}_a(\mathbf{r}_2)\cdot\Delta\boldsymbol{\ell}_b = \mathbf{E}_b(\mathbf{r}_1)\cdot\Delta\boldsymbol{\ell}_a\,.$$

That is, if the positions of the source and observation points are interchanged, the same field is produced.

In situations where there are no sources within a finite and bounded medium, it follows that

$$\oiint_S (\mathbf{E}_a\times\mathbf{H}_b - \mathbf{E}_b\times\mathbf{H}_a)\cdot d\mathbf{s} = 0\,, \tag{4.92}$$

which is the statement of ***reciprocity for a source-free region*** (sources are outside $S$).

### 4-6.1 Generalized Form of the Reciprocity Theorem

The statement of reciprocity given by Eq. (4.91) is derived for a homogeneous medium. Considering the symmetry properties discussed earlier for Green's function in homogeneous media, this statement of reciprocity may appear trivial. However, as will be shown in this section, Eq. (4.91) can be extended to very complicated problems, such as a medium composed of many homogeneous regions like the one shown in Fig. 4-8.

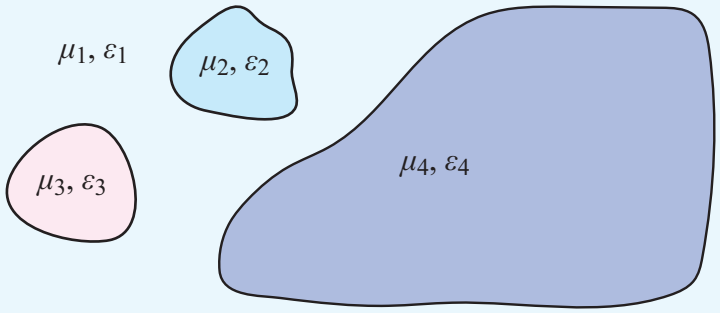


**Figure 4-8:** An inhomogeneous medium composed of many homogeneous segments.

Without loss of generality, we consider a medium composed of only two homogeneous media and we perform two experiments. In the first experiment (Fig. 4-9(a)) we assume that sources $\mathbf{J}_a$ and $\mathbf{J}_{ma}$, which are confined within region 1, produce fields $\mathbf{E}_a$ and $\mathbf{H}_a$. We consider the observation point to be in region 2. In the second experiment (Fig. 4-9(b)) we place sources $\mathbf{J}_b$ and $\mathbf{J}_{mb}$ only in region 2 and observe the fields $\mathbf{E}_b$ and $\mathbf{H}_b$ in the same region.

For the first experiment, Maxwell's equations mandate

$$\nabla \times \mathbf{E}_a = i\omega\mu_2 \mathbf{H}_a \tag{4.93a}$$

and

$$\nabla \times \mathbf{H}_a = -i\omega\varepsilon_2 \mathbf{E}_a \ , \tag{4.93b}$$

because the sources are in region 1. For the second experiment

$$\nabla \times \mathbf{E}_b = i\omega\mu_2 \mathbf{H}_b - \mathbf{J}_{mb} \tag{4.94a}$$

and

$$\nabla \times \mathbf{H}_b = -i\omega\varepsilon_2 \mathbf{E}_b + \mathbf{J}_b \ . \tag{4.94b}$$

In this case, the sources are in region 2. As before, similar to Eq. (4.89), using Eqs. (4.93) and (4.94) we can show that

$$\nabla \cdot (\mathbf{E}_a \times \mathbf{H}_b - \mathbf{E}_b \times \mathbf{H}_a) = \mathbf{H}_a \cdot \mathbf{J}_{mb} - \mathbf{E}_a \cdot \mathbf{J}_b \ . \tag{4.95}$$

Taking the volume integral of Eq. (4.94) in region 2 and using the divergence theorem leads to

$$\oiint_{S_\infty + S} (\mathbf{E}_a \times \mathbf{H}_b - \mathbf{E}_b \times \mathbf{H}_a) \cdot \hat{\mathbf{n}}_2 \, ds = \iiint_{V_2} (\mathbf{H}_a \cdot \mathbf{J}_{mb} - \mathbf{E}_a \cdot \mathbf{J}_b) \, dv \ , \tag{4.96}$$

where $\hat{\mathbf{n}}_2$ is the unit normal to the closed-surface bounding region 2. The closed-surface bounding region 2 in Fig. 4-9 is composed of $S_\infty$ and $S$, which encloses region 1. As shown earlier, the contribution from $S_\infty$ vanishes.

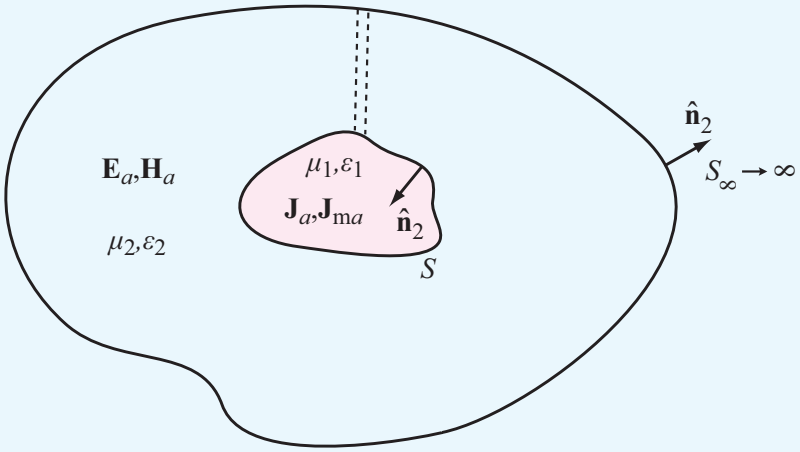


(a) Experiment 1

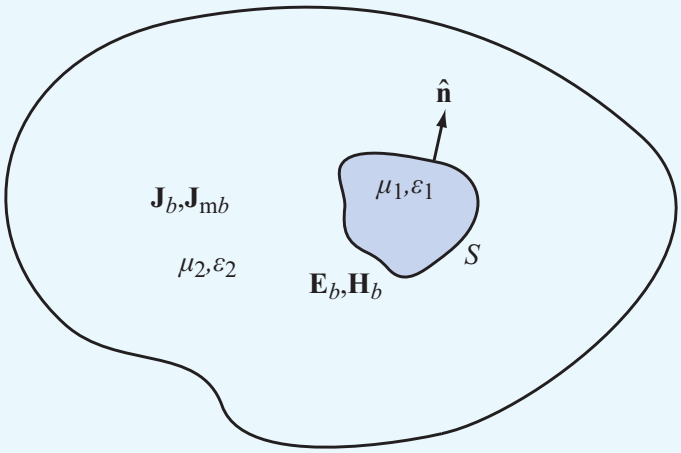


(b) Experiment 2

**Figure 4-9:** Fields and source points used in two experiments.

Next we consider Maxwell's equations in region 1. For the first experiment,

$$\begin{cases} \nabla \times \mathbf{E}_a = i\omega\mu_1 \mathbf{H}_a - \mathbf{J}_{ma} , \\ \nabla \times \mathbf{H}_a = -i\omega\varepsilon_1 \mathbf{E}_a + \mathbf{J}_a , \end{cases} \tag{4.97}$$

for sources in region 1. For the second experiment when the sources are in region 2,

$$\begin{cases} \nabla \times \mathbf{E}_b = i\omega\mu_1 \mathbf{H}_b \ , \\ \nabla \times \mathbf{H}_b = -i\omega\varepsilon_1 \mathbf{E}_b \ . \end{cases} \tag{4.98}$$

Following a similar procedure, it can be shown that

$$\oiint_S (\mathbf{E}_a \times \mathbf{H}_b - \mathbf{E}_b \times \mathbf{H}_a) \cdot \hat{\mathbf{n}}_1 \, ds = -\iiint_{V_1} (\mathbf{H}_b \cdot \mathbf{J}_{ma} - \mathbf{E}_b \cdot \mathbf{J}_a) \, dv \ . \tag{4.99}$$

Now considering that $-\hat{\mathbf{n}}_2 = \hat{\mathbf{n}}_1 = \hat{\mathbf{n}}$ and for surface fields of region 2

$$(\mathbf{E}_a^{(2)} \times \mathbf{H}_b^{(2)}) \cdot \hat{\mathbf{n}} = \mathbf{H}_b^{(2)} \cdot (\hat{\mathbf{n}} \times \mathbf{E}_a^{(2)}) = \mathbf{H}_b^{(2)} \cdot \hat{\mathbf{t}} \, |\hat{\mathbf{n}} \times \mathbf{E}_a^{(2)}| \ ,$$

where $\hat{\mathbf{t}}$ is a unit vector tangential to $S$ given by

$$\hat{\mathbf{t}} = \frac{\hat{\mathbf{n}} \times \mathbf{E}_a^{(2)}}{|\hat{\mathbf{n}} \times \mathbf{E}_a^{(2)}|} \ .$$

Using the boundary conditions

$$\hat{\mathbf{n}} \times \mathbf{E}_a^{(2)} = \hat{\mathbf{n}} \times \mathbf{E}_a^{(1)}$$

and

$$\mathbf{H}_b^{(2)} \cdot \hat{\mathbf{t}} = \mathbf{H}_b^{(1)} \cdot \hat{\mathbf{t}}$$

leads to the result

$$\oiint_S (\mathbf{E}_a^{(2)} \times \mathbf{H}_b^{(2)} - \mathbf{E}_b^{(2)} \times \mathbf{H}_a^{(2)}) \cdot \hat{\mathbf{n}}_2 \, ds = -\oiint_S (\mathbf{E}_a^{(1)} \times \mathbf{H}_b^{(1)} - \mathbf{E}_b^{(1)} \times \mathbf{H}_a^{(1)}) \cdot \hat{\mathbf{n}}_1 \, ds \ .$$

In view of Eqs. (4.96) and (4.99),

$$\iiint_{V_2} (\mathbf{H}_a \cdot \mathbf{J}_{mb} - \mathbf{E}_a \cdot \mathbf{J}_b) \, dv = \iiint_{V_1} (\mathbf{H}_b \cdot \mathbf{J}_{ma} - \mathbf{E}_b \cdot \mathbf{J}_a) \, dv \ , \tag{4.100}$$

which is the same statement as Eq. (4.91). Hence in general

$$\langle a, b \rangle = \langle b, a \rangle \ .$$

## 4-7 Applications of the Reciprocity Theorem

The reciprocity theorem has many applications in antenna theory and scattering problems. In this section we examine a few of its important applications. For example, when the concept of reciprocity was introduced in Section 4-6, we considered the relations between the voltages and currents at the terminals of a two-port network, as shown in Fig. 4-6. Such relations

can also be proven to be true for the voltages and currents at the terminals of two antennas in a communication link. That is, the environment around and in between two antennas can be viewed as a passive circuit network. To show this, consider two metallic antennas in a general isotropic medium at an arbitrary distance from each other. First, Antenna 1 is excited by a voltage source $V_a$ and the second antenna is short-circuited. The short-circuit current on the second antenna, denoted $I_a$, together with Antenna 1 generate fields $\mathbf{E}_a(\mathbf{r})$ and $\mathbf{H}_a(\mathbf{r})$ everywhere in the medium. In a second experiment, the second antenna is excited by a voltage source $V_b$ at its port and the first antenna is short-circuited. The short-circuit current on Antenna 1 is represented by $I_b$ and the fields produced by the ensemble of antennas are denoted $\mathbf{E}_b(\mathbf{r})$ and $\mathbf{H}_b(\mathbf{r})$. The configurations for these experiments are shown in Fig. 4-10. In the application of reciprocity, we consider a composite surface that covers the surfaces of the two antennas plus a large enclosing spherical surface that extends to infinity. As shown before, the contribution from the spherical surface, which is in the far-field region of both antennas, is zero. Also in this case the reciprocity condition for a source-free region given by Eq. (4.92) must be used:

$$\oiint_{S_1+S_2} (\mathbf{E}_a \times \mathbf{H}_b - \mathbf{E}_b \times \mathbf{H}_a) \cdot d\mathbf{s} = 0 \,, \tag{4.101}$$

where $S_1$ and $S_2$ are surfaces covering the surfaces of Antenna 1 and Antenna 2 and their terminals, respectively, as shown in Fig. 4-10. Since $\hat{\mathbf{n}} \times \mathbf{E}_a(\mathbf{r}) = \hat{\mathbf{n}} \times \mathbf{E}_b(\mathbf{r}) = 0$ everywhere on $S_1$ and $S_2$ except for the cylindrical surfaces around the antenna terminals, then Eq. (4.101) simplifies to

$$\oiint_{\mathrm{Cyl}_1+\mathrm{Cyl}_2} (\mathbf{E}_a \times \mathbf{H}_b - \mathbf{E}_b \times \mathbf{H}_a) \cdot d\mathbf{s} = 0 \,. \tag{4.102}$$

In the first experiment, the port of Antenna 2 is short-circuited and thus on cylinder 2 $\hat{\mathbf{n}} \times \mathbf{E}_a(\mathbf{r}) = 0$, and in the second experiment the port of Antenna 1 is short-circuited, which enforces $\hat{\mathbf{n}} \times \mathbf{E}_b(\mathbf{r}) = 0$ on cylinder 1. Hence,

$$\oiint_{\mathrm{Cyl}_1} (\mathbf{E}_a \times \mathbf{H}_b) \cdot d\mathbf{s} = \oiint_{\mathrm{Cyl}_2} (\mathbf{E}_b \times \mathbf{H}_a) \cdot d\mathbf{s} \,. \tag{4.103}$$

Near the terminals of the antennas on the cylindrical segments of $S_1$ and $S_2$, for a very small cylinder radius $\rho_0$ according to Ampère's law

$$\mathbf{H}_b(\rho_0) = \frac{I_b}{2\pi\rho_0}\,\hat{\boldsymbol{\phi}} \tag{4.104a}$$

and

$$\mathbf{H}_a(\rho_0) = \frac{I_a}{2\pi\rho_0}\,\hat{\boldsymbol{\phi}} \,. \tag{4.104b}$$

On the surface of cylinder 1,

$$(\mathbf{E}_a \times \mathbf{H}_b) \cdot \hat{\mathbf{n}} = [H_b(\rho_0)\,\hat{\boldsymbol{\phi}} \times \hat{\boldsymbol{\rho}}] \cdot \mathbf{E}_a(\rho_0) \,.$$

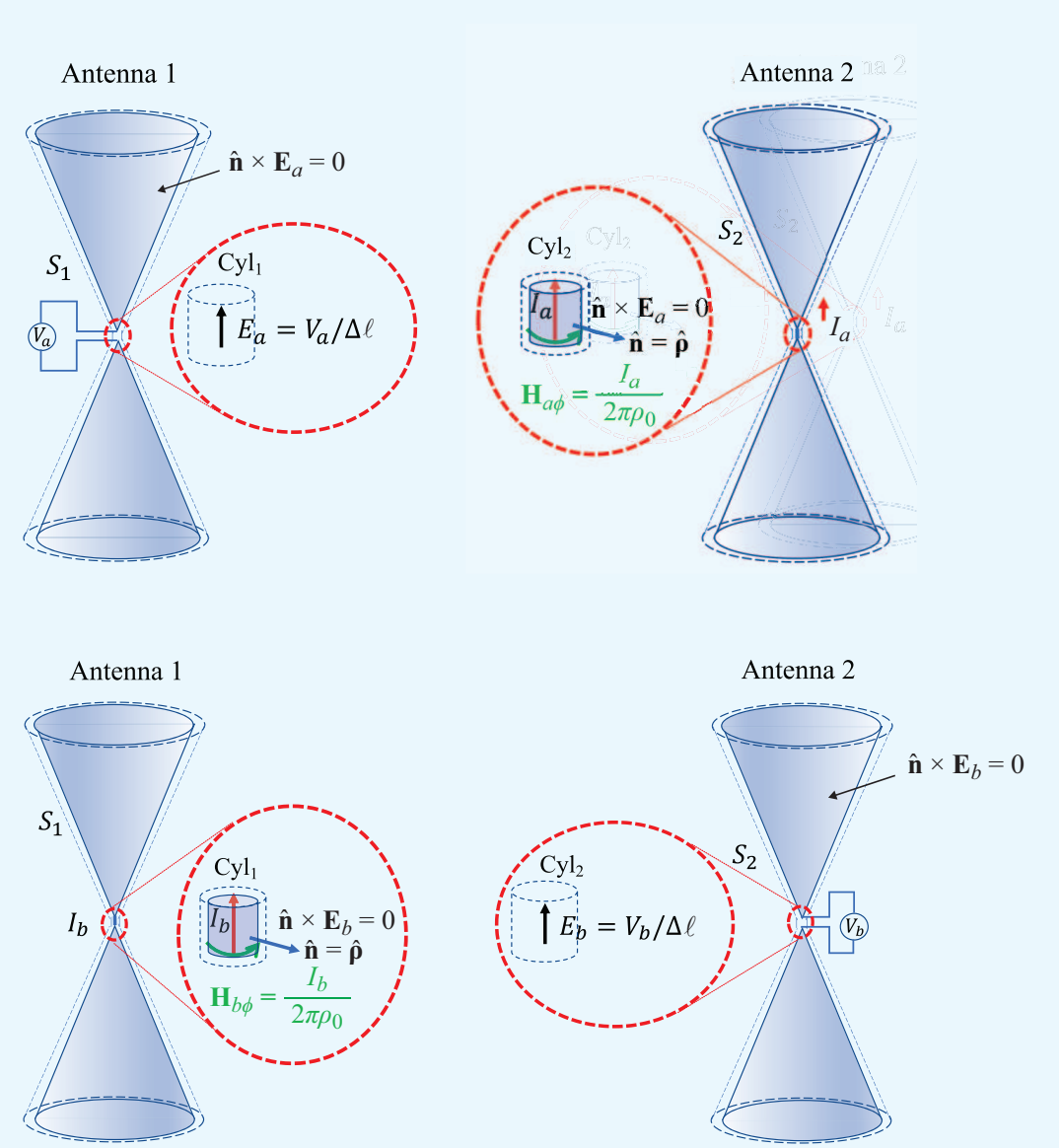


**Figure 4-10:** Configuration of two antennas used for transmission and reception. The reciprocity theorem shows that the two ports of these antennas can be viewed as a two-port passive network.

Noting that $\mathbf{E}_a(\rho_0) = \hat{\mathbf{z}}V_a/\Delta\ell$ and $\mathbf{E}_b(\rho_0) = \hat{\mathbf{z}}V_b/\Delta\ell$, and in view of Eq. (4.104a) and Eq. (4.101), it follows that

$$\oiint_{\text{Cyl}_1} (\mathbf{E}_a \times \mathbf{H}_b) \cdot d\mathbf{s} = -V_a I_b \ . \tag{4.105a}$$

Similarly, using Eq. (4.104b), it can be shown that

$$\oiint_{\text{Cyl}_2} (\mathbf{E}_b \times \mathbf{H}_a) \cdot d\mathbf{s} = -V_b I_a \ . \tag{4.105b}$$

This proves the statement of reciprocity for a general two-port network, namely

$$V_a I_b = V_b I_a \ . \tag{4.106}$$

### 4-7.1 Equivalence of Antenna Patterns in Transmission and Reception

Equation (4.106) can be used to show that the radiation pattern of an antenna in a transmitting mode is the same as its radiation pattern if the antenna were to be used as a receiver. The radiation pattern of an antenna in transmitting mode is defined as the angular $(\theta, \phi)$ variation of the normalized power density of the radiated fields in the far-field region at a fixed distance from the antenna. On the other hand, the radiation pattern of the antenna in the receiving mode is defined as the normalized angular variation of the power received by the antenna if a transmitter at a fixed far-field distance and with fixed transmit power and polarization configuration were to be moved along all possible directions relative to the receive antenna. Figure 4-11 shows the configuration for radiation pattern measurements of an antenna in the transmit and receive modes. Denoting the normalized radiation pattern in the transmitting mode as $D_{\text{t}}(\theta, \phi)$ and that in the receiving mode as $D_{\text{r}}(\theta, \phi)$, we want to show that

$$D_{\text{t}}(\theta, \phi) = D_{\text{r}}(\theta, \phi) \ . \tag{4.107}$$

Consider the geometry of the antenna under test centered at the origin of a spherical coordinate system. This antenna is used as a transmitter and a short dipole placed in the far-field region of the antenna is used as a receiver to measure the received power. In transmission mode, a voltage $V_a$ is at the terminals of the antenna. This voltage induces a short-circuited current $I_a(\theta, \phi)$ at the terminals of the dipole. The received power at each location of the dipole is proportional to $I_a^2(\theta, \phi)$. In another experiment designed to measure the radiation pattern of the antenna in the receiving mode, the dipole is attached to a source and the power received by the antenna is measured as a function of the dipole position. In this case, a fixed $V_b$ is attached to the terminals of the dipole and a short-circuited current $I_b(\theta, \phi)$ flows through the terminals of the antenna. The received power is proportional to $I_b^2(\theta, \phi)$. According to Eq. (4.106),

$$\frac{V_a(\theta, \phi)}{I_a} = \frac{V_b(\theta, \phi)}{I_b} \ . \tag{4.108}$$

Note that $V_a$ and $V_b$ are constant and can be made equal. Also noting that $D_{\text{t}}(\theta, \phi)$ is proportional to $I_a^2(\theta, \phi)$ and $D_{\text{r}}(\theta, \phi)$ is proportional to $I_b^2(\theta, \phi)$, in view of Eq. (4.108) we conclude that Eq. (4.107) holds.

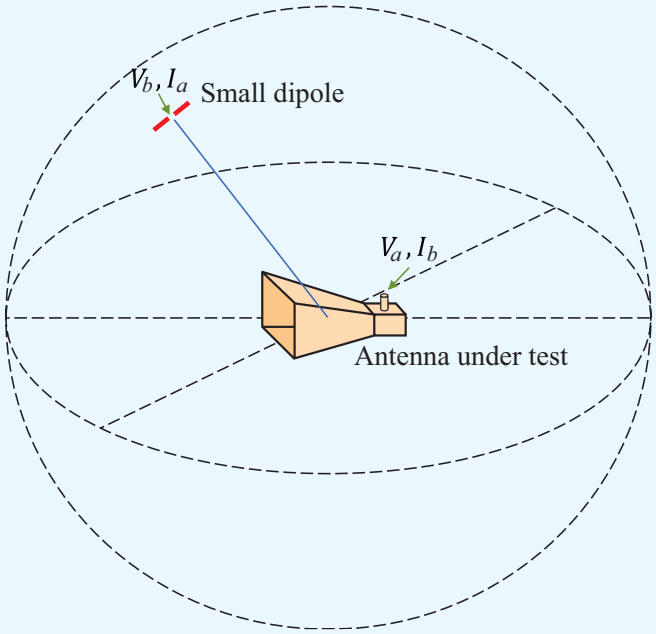


**Figure 4-11:** Configuration of antenna pattern measurement. In the transmit mode a simple antenna like a dipole is placed in the far field of the antenna under test along the $(\theta, \phi)$-direction, and then the received power is measured by the dipole as the dipole is moved over $\theta$–$\phi$ space. The same configuration can be used to measure the radiation pattern of the antenna under test in receiving mode wherein the antenna under test becomes the receiver and the dipole becomes the transmitter. In these experiments the dipole orientation is maintained in $\hat{\boldsymbol{\theta}}$ or $\hat{\boldsymbol{\phi}}$, as the dipole is moved.

## Example 4-1: Application of the Reciprocity Theorem: Show That Tangential Electric Currents near Metallic Surfaces of Arbitrary Shapes Cannot Radiate Electromagnetic Fields

Using the reciprocity theorem, show that the field radiated by an electric current source near and tangential to an arbitrary metallic surface is zero.

**Solution:** Consider a metallic surface $S$ with a dipole of height $\delta h$ above it and located at $\mathbf{r}_s$. Also consider an arbitrary observation point outside $S$, as shown in Fig. 4-12. Let us denote the radiated field from the Hertzian dipole $(I_0 \Delta \ell_t \delta(\mathbf{r} - \mathbf{r}_s))$ in the presence of the surface at the observation point $\mathbf{r}_o$ as $\mathbf{E}_1(\mathbf{r}_o)$. Our objective is to show that

$$\lim_{\delta h \to 0} \mathbf{E}_1(\mathbf{r}_o) = 0 \,.$$

We showed previously that if surface $S$ is an infinite planar surface, image theory can be used. The image of a horizontal Hertzian dipole is a horizontal Hertzian dipole with the

opposite direction of current flow and located at the mirror image point. As $\delta h \to 0$ these opposite currents will totally cancel each other and generate a null field everywhere. This result cannot be directly extended to arbitrary surfaces as we do not know the image of a tangential Hertzian dipole on arbitrary surfaces. To prove a tangential Hertzian dipole right above any metallic surface cannot produce any fields outside the surface, we consider an experiment wherein we place the Hertzian dipole at the observation point $\mathbf{r}_o$ with an arbitrary orientation ($I_0\,\Delta\boldsymbol{\ell}_a\,\delta(\mathbf{r}-\mathbf{r}_0)$) and then evaluate the field at the original source point $\mathbf{r}_s$, which we denote as $\mathbf{E}_2(\mathbf{r}_s)$. According to the reciprocity theorem,

$$\mathbf{E}_2(\mathbf{r}_s)\cdot I_0\,\Delta\boldsymbol{\ell}_t = \mathbf{E}_1(\mathbf{r}_o)\cdot I_0\,\Delta\boldsymbol{\ell}_a\ .$$

But on surface $S$

$$\lim_{\delta h\to 0}\mathbf{E}_2(\mathbf{r}_s)\cdot\Delta\boldsymbol{\ell}_t = 0\ ,$$

since according to boundary conditions, the tangential electric field on the surface of a metallic body must vanish. Hence, we conclude that the component of $\mathbf{E}_1(\mathbf{r}_o)$ along any arbitrary direction is zero, or simply $\mathbf{E}_1(\mathbf{r}_o)=0$.

The result of this example can easily be extended to other similar problems. For example, following the same procedure it can be shown that a Hertzian magnetic dipole placed on and normal to a metallic surface of arbitrary shape cannot radiate electromagnetic fields. This result and that of Example 4-1 can be used in conjunction with the duality principle to prove that tangential magnetic Hertzian dipoles and normal electric Hertzian dipoles placed on a perfect magnetic conductor cannot radiate electromagnetic waves regardless of the shape of the magnetic conductor.

### 4-7.2 Effective Area for Receiving Antennas

The ***effective area*** $A_{\text{eff}}$ of an antenna is defined as a fictitious area around the antenna that allows for the antenna to collect the local incident wave power density and deliver it to

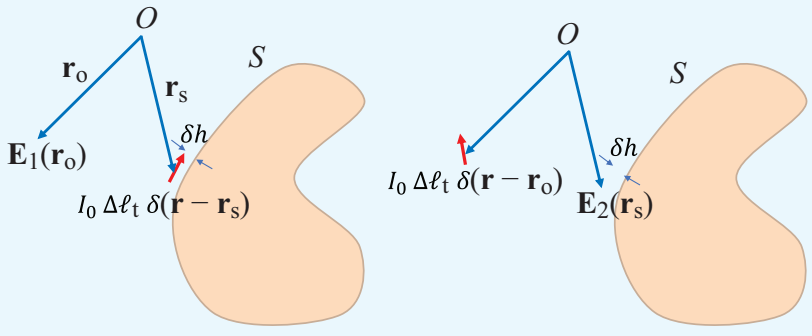


**Figure 4-12:** A short Hertzian dipole radiating near a metallic surface $S$. Also shown is a reciprocal configuration in which the source is moved to the observation position and the field is evaluated at the source position of the original problem.

an impedance-matched transmission line connected to the antenna terminals. Based on this definition,

$$P_{\text{rec}} = A_{\text{eff}}(\theta,\phi)\, S_{\text{inc}} \ , \tag{4.109}$$

where $S_{\text{inc}}$ is the time-average power density of the incident wave. In general, this effective area may be a function of the direction of the incident wave, $(\theta,\phi)$. Our goal here is to relate $A_{\text{eff}}(\theta,\phi)$ to the gain function, $G(\theta,\phi)$, of the antenna in the transmitting mode of operation. To establish this relation we will make use of the reciprocity theorem. Here we assume that the antenna is lossless and impedance-matched. Let us consider two experiments where initially the antenna is used as a transmitter, generating a field at an observation point $\mathbf{r} = (r,\theta,\phi)$ in the far-filed region. We denote this field as $\mathbf{E}_a(\mathbf{r})$. The voltage at the antenna terminals is denoted $V_a$. In the next experiment we use the same antenna as a receiver and measure the short-circuited current $I_b(\theta,\phi)$ when illuminated by an infinitesimal current filament $I_0\,\Delta\ell$ oriented to be parallel to $\mathbf{E}_a(\mathbf{r})$. We emphasize here that the short-circuited current is a function of the infinitesimal current location. The current filament generates an electric field in the vicinity of the antenna, which is represented by $\mathbf{E}_b$, as shown in Fig. 4-13. Now we apply the reciprocity theorem by considering a composite surface that includes the antenna (surface $S$) and a spherical surface that extends to infinity ($S_\infty$). As before, the contribution of $S_\infty$ vanishes due to the fact that fields far away from the antenna and the infinitesimal current filament are TEM. According to Eq. (4.90), we have

$$\oiint_S (\mathbf{E}_a \times \mathbf{H}_b - \mathbf{E}_b \times \mathbf{H}_a)\cdot d\mathbf{s} = -\iiint_V (\mathbf{E}_a \cdot \mathbf{J}_b)\, dv \ . \tag{4.110}$$

Since $\mathbf{E}_b \times \hat{\mathbf{n}} = 0$ on $S$, Eq. (4.110) simplifies to

$$\frac{V_a}{\Delta g} \times \frac{I_b(\theta,\phi)}{2\pi\rho_0} \times 2\pi\rho_0\, \Delta g = I_0\, \Delta\ell\, E_a(\theta,\phi) \ ,$$

noting that $E_a = V_a/\Delta g$, $H_b = I_b/(2\pi\rho)$, the surface of the cylinder is $2\pi\rho_0\,\Delta g$, and that $\mathbf{J}_b = I_0\,\Delta\boldsymbol{\ell}\,\delta(\mathbf{r}-\mathbf{r}')$,

$$V_a I_b(\theta,\phi) = I_0 \Delta\ell E_a(\theta,\phi) \ . \tag{4.111}$$

Assuming that the antenna is impedance-matched under both transmission and reception, and denoting the radiation resistance of the antenna by $R_{\text{A}}$, the radiated power can be calculated from

$$P_{\text{rad}} = \frac{|V_a|^2}{2R_{\text{A}}} \ .$$

Also, the power density at the observation point can be calculated in two ways, once based on the radiated power and directivity and another based on the field power density; hence

$$S_{\text{rad}}(\theta,\phi) = \frac{|V_a|^2}{2R_{\text{A}}(4\pi r^2)}\, G(\theta,\phi) = \frac{|E_a(\theta,\phi)|^2}{2\eta} \ .$$

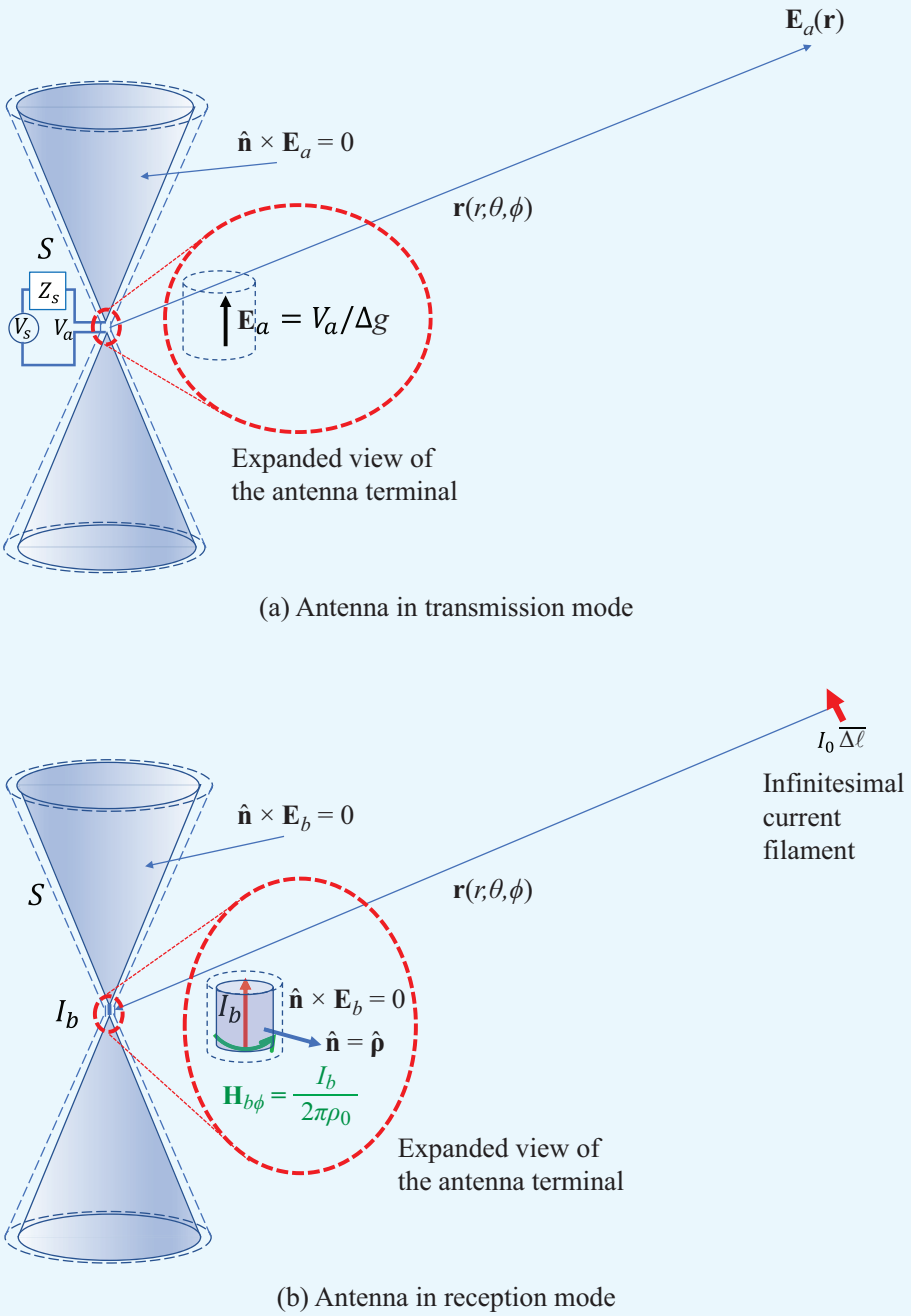


**Figure 4-13:** Configuration of a general antenna in transmission and reception modes. In the transmission mode, a current $I_1$ is excited at the antenna terminal and field $\mathbf{E}_a(\mathbf{r})$ is generated at the observation point $\mathbf{r} = (r, \theta, \phi)$. The same antenna is then illuminated by the fields generated by current filament $I_0 \Delta\ell$ parallel to $\mathbf{E}_a(\mathbf{r})$.

This provides the expression for the electric field in terms of the voltage

$$|E_a(\theta,\phi)|^2 = \frac{\eta|V_a|^2}{R_{\rm A}(4\pi r^2)}\,G(\theta,\phi)\ . \tag{4.112}$$

In the reception mode, the power density generated by the current filament is given by

$$S_{\rm dipole} = \frac{\eta k^2|I_0\,\Delta\ell|^2}{2(4\pi r)^2}\ .$$

The received antenna power according to Eq. (4.109) is

$$P_{\rm rec} = A_{\rm eff}(\theta,\phi)\,\frac{\eta k^2|I_0\,\Delta\ell|^2}{2(4\pi r)^2}\ . \tag{4.113}$$

This is the power delivered to a matched load connected to the receiving antenna. Referring to the match-loaded antenna equivalent circuit shown in Fig. 4-14, the power delivered to the matched load can be calculated from

$$P_{\rm rec} = \frac{|V_{\rm oc}(\theta,\phi)|^2}{8R_{\rm A}}\ . \tag{4.114}$$

This same equivalent circuit can be used to predict the short-circuited current to be

$$I_b(\theta,\phi) = \frac{V_{\rm oc}(\theta,\phi)}{R_{\rm A}}\ .$$

Therefore,

$$P_{\rm rec} = \frac{R_{\rm A}|I_b(\theta,\phi)|^2}{8}\ . \tag{4.115}$$

Substituting Eq. (4.115) into Eq. (4.113),

$$|I_b(\theta,\phi)|^2 = 4A_{\rm eff}(\theta,\phi)\,\frac{\eta k^2|I_0\,\Delta\ell|^2}{R_{\rm A}(4\pi r)^2}\ . \tag{4.116}$$

Using Eq. (4.111), we also have

$$|I_b(\theta,\phi)|^2 = \frac{|I_0\,\Delta\ell|^2|E_a(\theta,\phi)|^2}{|V_a|^2}\ . \tag{4.117}$$

Now, substituting Eq. (4.116) and Eq. (4.112) into Eq. (4.117) provides a relationship between $G(\theta,\phi)$ and $A_{\rm eff}(\theta,\phi)$:

$$A_{\rm eff}(\theta,\phi)\,\frac{\eta k^2|I_0\,\Delta\ell|^2}{R_{\rm A}(4\pi r)^2} = \frac{|I_0\,\Delta\ell|^2}{|V_a|^2}\times\frac{\eta|V_a|^2}{R_{\rm A}(4\pi r^2)}\,G(\theta,\phi)\ ,$$

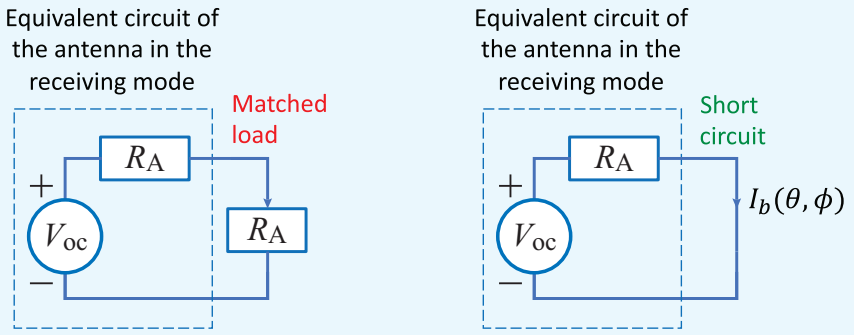


**Figure 4-14:** The antenna equivalent circuit of an antenna in the receiving mode when connected to a matched load $R_A$. Also shown on the right is the equivalent circuit of the antenna in receiving mode when short-circuited at its terminals.

or

$$\frac{k^2}{\pi} A_{\text{eff}}(\theta,\phi) = G(\theta,\phi) \, .$$

Since $k = \frac{2\pi}{\lambda}$, a more familiar relation between antenna directivity and antenna effective area is obtained:

$$A_{\text{eff}}(\theta,\phi) = \frac{\lambda^2}{4\pi} G(\theta,\phi) \, . \tag{4.118}$$

### 4-7.3 Scattering Interaction between Two Adjacent Objects

In this section we examine the application of the reciprocity theorem to understand the mechanics of electromagnetic scattering interaction between objects of various shapes and electrical properties. scattering problems are often solved for objects in isolation. However, when two or more such objects are present simultaneously, the solution for the combination of objects becomes rather complicated and computationally inefficient. In situations where the objects are sufficiently far apart but can be in the near field of each other, the scattering solution can be obtained in an iterative manner. To clarify this, let us consider two objects in a homogeneous and unbounded background medium and illuminated by an incident wave characterized by fields $\mathbf{E}_{\text{i}}(\mathbf{r})$ and $\mathbf{H}_{\text{i}}(\mathbf{r})$, as shown in Fig. 4-15. Let us denote the field scattered by object 1 in isolation as $\mathbf{E}_1^{\text{s}}(\mathbf{r})$ and that by object 2 in isolation as $\mathbf{E}_2^{\text{s}}(\mathbf{r})$. The scattered field $\mathbf{E}_2^{\text{s}}(\mathbf{r})$ can then be considered as a source illuminating object 1, and it causes a secondary scattered field denoted $\mathbf{E}_{12}^{\text{s}}(\mathbf{r})$ in Fig. 4-15. Conversely, the field scattered by object 1 ($\mathbf{E}_1^{\text{s}}(\mathbf{r})$) can be considered a source of illumination for object 2, and it causes a secondary scattered field denoted $\mathbf{E}_{21}^{\text{s}}(\mathbf{r})$. This process continues, and higher-order scattered fields such as $\mathbf{E}_{121}(\mathbf{r})$, $\mathbf{E}_{212}(\mathbf{r})$, and so on are generated. The fields in each scattering iteration become weakened due to propagation path loss, and thus the multiple scattering process converges very quickly. In many practical applications, scattering up to the second order is sufficient to capture important effects such as depolarization or the dominant scattering mechanism. In what follows, the

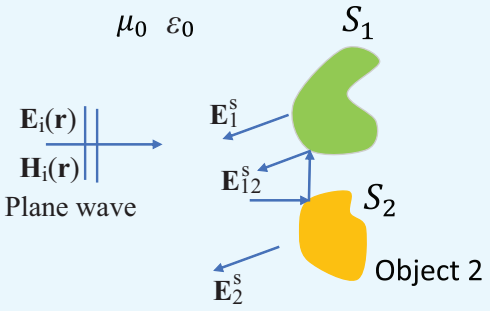


**Figure 4-15:** Adjacent objects in the near field of each other and illuminated by a plane wave. In addition to the direct scattering components $\mathbf{E}_1^s$ and $\mathbf{E}_2^s$, the close proximity of the two objects leads to many multiple scattering components, such as $\mathbf{E}_{12}^s$.

reciprocity theorem is used as a way to analytically obtain the far-field expansion that includes multiple scattering up to second order for two adjacent objects, based solely on the knowledge of the first-order scattering of the individual objects.

### 4-7.4 Perfectly Conducting Objects

In this section we consider a simpler problem wherein the two objects are made from a perfect conducting material. First, consider object 1 in isolation and illuminated by an incident wave. Let us denote the surface current density on object 1 as $\mathbf{J}_1(\mathbf{r})$. To compute the secondary scattered field from object 2, we use $\mathbf{J}_1(\mathbf{r})$ as the source of excitation for object 2. This scenario is depicted in Fig. 4-16(b). Next we consider a scenario where object 1 or, equivalently, surface current distribution $\mathbf{J}_1(\mathbf{r})$ is absent, and an infinitesimal current source given by

$$\mathbf{J}_d(\mathbf{r}) = \hat{\mathbf{p}}\,\delta(\mathbf{r}-\mathbf{r}_0) \tag{4.119}$$

is placed at an observation point $\mathbf{r}_0$ in the far-field region of the objects. The fields produced by the infinitesimal current source in the presence of object 2 are denoted $\mathbf{E}_{d2}(\mathbf{r})$ and $\mathbf{H}_{d2}(\mathbf{r})$, as shown in Fig. 4-17. According to the reciprocity theorem (see Eq. (4.90)),

$$\oiint_{S_2} \left[\mathbf{E}_1^+(\mathbf{r})\times\mathbf{H}_{d2}(\mathbf{r}) - \mathbf{E}_{d2}(\mathbf{r})\times\mathbf{H}_1^+(\mathbf{r})\right]\cdot d\mathbf{s} = \oiint_{S_1} \mathbf{J}_1(\mathbf{r})\cdot\mathbf{E}_{d2}(\mathbf{r})\,ds - \hat{\mathbf{p}}\cdot\mathbf{E}_1^+(\mathbf{r}_0)\,. \tag{4.120}$$

Here the field quantities with superscript "+" ($\mathbf{E}_1^+(\mathbf{r})$, $\mathbf{H}_1^+(\mathbf{r})$) are the direct fields radiated by $\mathbf{J}_1(\mathbf{r})$ ($\mathbf{E}_1^s(\mathbf{r})$, $\mathbf{H}_1^s(\mathbf{r})$) plus the secondary scattered fields ($\mathbf{E}_{21}^s(\mathbf{r})$, $\mathbf{H}_{21}^s(\mathbf{r})$). According to the boundary condition on metallic surfaces, $\hat{\mathbf{n}}\times\mathbf{E}_1^+ = \hat{\mathbf{n}}\times\mathbf{E}_{d2} = 0$, and therefore

$$(\mathbf{E}_1^+\times\mathbf{H}_{d2})\cdot\hat{\mathbf{n}} = (\hat{\mathbf{n}}\times\mathbf{E}_1^+)\cdot\mathbf{H}_{d2} = 0\,, \quad \mathbf{r}\in S_2 \tag{4.121a}$$

and

$$(\mathbf{E}_{d2}\times\mathbf{H}_1^+)\cdot\hat{\mathbf{n}} = (\hat{\mathbf{n}}\times\mathbf{E}_{d2})\cdot\mathbf{H}_1^+ = 0\,, \quad \mathbf{r}\in S_2\,. \tag{4.121b}$$

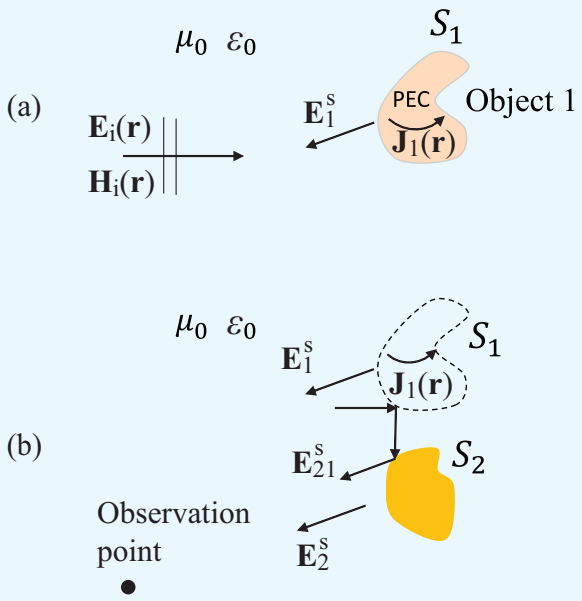


**Figure 4-16:** (a) The incident wave illuminating object 1 in isolation induces a surface current $\mathbf{J}_1(\mathbf{r})$ on the PEC object, and (b) this induced current becomes a source that generates the secondary scattered fields ($\mathbf{E}_{21}^s(\mathbf{r})$, $\mathbf{H}_{21}^s(\mathbf{r})$) from object 2 at the observation point.

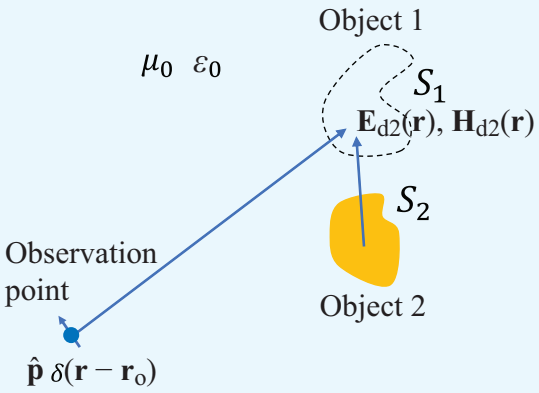


**Figure 4-17:** An infinitesimal current source with orientation $\hat{\mathbf{p}}$ placed at the observation point $\mathbf{r}_0$ is illuminating object 2. The observation point is in the far-field region of the objects, and its field can be locally approximated by a plane wave. $\mathbf{E}_{d2}(\mathbf{r})$ and $\mathbf{H}_{d2}(\mathbf{r})$ represent the sum of the direct field from the source and the near field scattered by object 2.

As a result, the left-hand side of Eq. (4.120) vanishes and we have

$$\hat{\mathbf{p}}\cdot\mathbf{E}_1^+(\mathbf{r}_0) = \oiint_{S_1} \mathbf{J}_1(\mathbf{r})\cdot\mathbf{E}_{d2}(\mathbf{r})\,ds\,. \tag{4.122}$$

As mentioned previously, $\mathbf{E}_1^+(\mathbf{r}_0)$ represents the direct backscatter from object 1 (radiation from $\mathbf{J}_1(\mathbf{r})$) plus the secondary scattered field from object 2 ($\mathbf{E}_{21}^s(\mathbf{r}_0)$); that is,

$$\mathbf{E}_1^+(\mathbf{r}_0) = \mathbf{E}_1^s(\mathbf{r}_0) + \mathbf{E}_{21}^s(\mathbf{r}_0) \ . \tag{4.123}$$

Following a similar procedure, we can compute the first-order scattered field from object 2 plus the second-order scattered field generated by object 1 when illuminated by the first-order scattered field of object 2:

$$\hat{\mathbf{p}} \cdot \mathbf{E}_2^+(\mathbf{r}_0) = \oiint_{S_2} \mathbf{J}_2(\mathbf{r}) \cdot \mathbf{E}_{\mathrm{d}1}(\mathbf{r}) \, ds \ , \tag{4.124}$$

where $\mathbf{E}_{\mathrm{d}1}(\mathbf{r})$ is the incident field from the dipole plus the scattered field from object 1 calculated on the surface of object 2. Thus $\mathbf{E}_1^+(\mathbf{r}_0) + \mathbf{E}_2^+(\mathbf{r}_0)$ represents the total first-order plus the second-order scattered fields from both objects at the observation point $\mathbf{r}_0$. It must be emphasized that the scattered field up to second-order scattering interaction is derived from only the knowledge of the surface currents and the near-field scattered electric field of the isolated objects.

### 4-7.5 Dielectric Objects

In this section we consider a scattering problem composed of two adjacent dielectric objects. For simplicity let us assume the dielectric objects to be nonmagnetic ($\mu = \mu_0$ and $\varepsilon = \varepsilon_0 \varepsilon_i$, $i = 1,2$). The incident wave, in the absence of object 2, creates a polarization current $\mathbf{J}_1(\mathbf{r})$ within object 1. Recall that when the notion of polarization current is used, we are assuming the entire medium is homogeneous and unbounded with permittivity $\varepsilon_0$ and permeability $\mu_0$. This polarization current in the absence of the incident field and presence of object 2 induces a polarization current $\mathbf{J}_{12}(\mathbf{r})$ in object 2. The total fields in this configuration, which represent the first-order scattered field from object 1 and the second-order scattered field from object 2, are denoted $\mathbf{E}_1^+(\mathbf{r})$ and $\mathbf{H}_1^+(\mathbf{r})$. As before, we conduct another experiment in which we place a filament current at the observation point $\mathbf{r}_0$ in the far-field region of the scatterer and keep only object 2. This excitation induces polarization current $\mathbf{J}_{2\mathrm{d}}(\mathbf{r})$ in object 2. The corresponding electric and magnetic fields for this scenario are denoted $\mathbf{E}_{\mathrm{d}2}(\mathbf{r})$ and $\mathbf{H}_{\mathrm{d}2}(\mathbf{r})$. The expressions for the polarization currents in object 2 are given by

$$\mathbf{J}_{12}(\mathbf{r}) = -ik_0 Y_0(\varepsilon_2 - 1)\, \mathbf{E}_1^+(\mathbf{r}) \ , \quad \mathbf{r} \in V_2 \ , \tag{4.125a}$$

and

$$\mathbf{J}_{\mathrm{d}2}(\mathbf{r}) = -ik_0 Y_0(\varepsilon_2 - 1)\, \mathbf{E}_{\mathrm{d}2}(\mathbf{r}) \ , \quad \mathbf{r} \in V_2 \ . \tag{4.125b}$$

Since the medium is homogeneous and unbounded (scatterers are replaced with polarization currents), the reciprocity theorem mandates that

$$\iiint_{V_1} \mathbf{J}_1(\mathbf{r}) \cdot \mathbf{E}_{\mathrm{d}2}(\mathbf{r}) \, dv + \iiint_{V_2} \mathbf{J}_{12}(\mathbf{r}) \cdot \mathbf{E}_{\mathrm{d}2}(\mathbf{r}) \, dv = \iiint_{V_2} \mathbf{J}_{\mathrm{d}2}(\mathbf{r}) \cdot \mathbf{E}_1^+(\mathbf{r}) \, dv + \hat{\mathbf{p}} \cdot \mathbf{E}_1^+(\mathbf{r}_0) \ . \tag{4.126}$$

Using Eqs. (4.125a) and (4.125b) in Eq. (4.126), it can be shown that

$$\iiint_{V_2} \mathbf{J}_{12}(\mathbf{r}) \cdot \mathbf{E}_{\mathrm{d2}}(\mathbf{r})\, dv = \iiint_{V_2} \mathbf{J}_{\mathrm{d2}}(\mathbf{r}) \cdot \mathbf{E}_1^{+}(\mathbf{r})\, dv\,, \tag{4.127}$$

and therefore

$$\hat{\mathbf{p}} \cdot \mathbf{E}_1^{+}(\mathbf{r}_0) = \iiint_{V_1} \mathbf{J}_1(\mathbf{r}) \cdot \mathbf{E}_{\mathrm{d2}}(\mathbf{r})\, dv\,. \tag{4.128}$$

Following a similar procedure by interchanging the roles of objects 1 and 2, it can be easily shown that

$$\hat{\mathbf{p}} \cdot \mathbf{E}_2^{+}(\mathbf{r}_0) = \iiint_{V_2} \mathbf{J}_2(\mathbf{r}) \cdot \mathbf{E}_{\mathrm{d1}}(\mathbf{r})\, dv\,, \tag{4.129}$$

where $\mathbf{E}_2^{+}(\mathbf{r}_0)$ is the first-order scattered field from object 2 plus the second-order scattered field from object 1. Also $\mathbf{J}_2(\mathbf{r})$ represents the polarization current induced in object 2 in the absence of object 1, and $\mathbf{E}_{\mathrm{d1}}(\mathbf{r})$ is the near-field first-order scattered field from object 1 due to the infinitesimal current inside the second scatterer. As before, $\mathbf{E}_1^{+}(\mathbf{r}_0) + \mathbf{E}_2^{+}(\mathbf{r}_0)$ is the total scattered field up to second-order mutual interaction.

## Example 4-2: Radar Cross Section of a Dihedral Using the Reciprocity Theorem

Following the approach outlined for calculating scattering by two adjacent objects up to second-order using the reciprocity theorem, calculate the scattered field in the backscatter direction from two electrically large perpendicular metallic plates, known as a ***dihedral corner reflector***, as shown in Fig. 4-18. Assume the dihedral is illuminated by a plane wave given by $\mathbf{E}_{\mathrm{i}}(\mathbf{r}) = \mathbf{E}_0\, \hat{\mathbf{y}}\, e^{ik_0 x}$. Also calculate the radar cross section of the dihedral corner reflector.

**Solution:** To find the scattered field up to second-order, we need to determine the surface current induced on each plate in isolation when illuminated by the incident wave. Since the plates are electrically large and planar (radii of curvature are infinite), the surface currents can be computed from the physical-optics approximation:

$$\mathbf{J}(\mathbf{r}) = 2\hat{\mathbf{n}} \times \mathbf{H}_{\mathrm{i}}(\mathbf{r})\,. \tag{4.130}$$

The expression for the incident magnetic field is given by

$$\mathbf{H}_{\mathrm{i}}(\mathbf{r}) = \frac{E_0}{\eta_0}\, \hat{\mathbf{z}}\, e^{ik_0 x}\,. \tag{4.131}$$

Let us first consider plate 1, whose unit normal vector is given by

$$\hat{\mathbf{n}}_1 = -\frac{\sqrt{2}}{2}\, \hat{\mathbf{x}} - \frac{\sqrt{2}}{2}\, \hat{\mathbf{y}}\,. \tag{4.132}$$

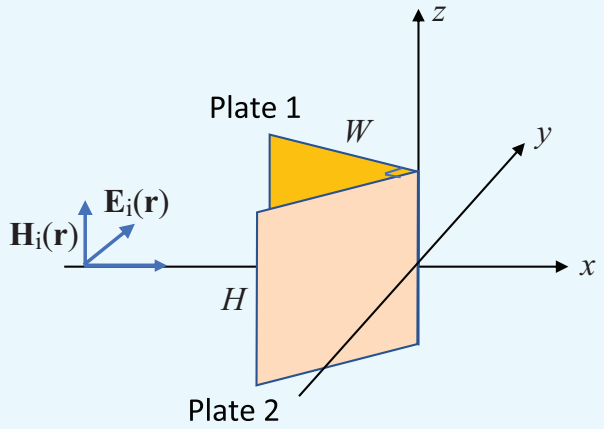


**Figure 4-18:** A dihedral corner reflector composed of two perpendicular planar metallic plates with dimensions $W \times H$, is illuminated by a plane wave. The edge of the dihedral coincides with the $z$-axis. The goal is to compute the scattered field in the backscatter direction ($-x$-axis).

Also, on this object $y = -x$. Hence the surface current is given by

$$\mathbf{J}_1(\mathbf{r}) = (\sqrt{2}\,\hat{\mathbf{y}} - \sqrt{2}\,\hat{\mathbf{x}})\,\frac{E_0}{\eta_0}\,e^{-ik_0 y}\,. \tag{4.133}$$

We also need to find the electric field generated by an infinitesimal dipole at the observation point $\mathbf{r}_0$ orientated along the $y$-axis ($\mathbf{J}_d(\mathbf{r}) = \hat{\mathbf{y}}\,\delta(\mathbf{r} - \mathbf{r}_0)$).

The far field produced by this small dipole can be obtained from Eq. (3.127b) and is given by

$$\mathbf{E}_d(\mathbf{r}) = -ik_0\eta_0\,\frac{e^{ik_0 r_0}}{4\pi r_0}\,[\hat{\mathbf{y}} \times (-\hat{\mathbf{r}}_0)] \times (-\hat{\mathbf{r}}_0)e^{-ik_0\mathbf{r}\cdot\hat{\mathbf{r}}_0}\,. \tag{4.134}$$

Since $\hat{\mathbf{r}}_0 = -\hat{\mathbf{x}}$,

$$\mathbf{E}_d(\mathbf{r}) = ik_0\eta_0\,\frac{e^{ik_0 r_0}}{4\pi r_0}\,e^{ik_0 x}\,\hat{\mathbf{y}}\,. \tag{4.135}$$

To find the scattered field from plate 2 illuminated by $\mathbf{E}_d(\mathbf{r})$, we use the geometric-optics approximation. That is, the scattered field is simply the reflected field, given by Eq. (4.135), on the metallic plate:

$$\mathbf{E}^2_{dr}(\mathbf{r}) = -ik_0\eta_0\,\frac{e^{ik_0 r_0}}{4\pi r_0}\,e^{ik_0 y}\,\hat{\mathbf{x}}\,. \tag{4.136}$$

The total field from the dipole in the presence of plate 2 on plate 1 is given by

$$\begin{aligned}\mathbf{E}_{d2}(\mathbf{r}) &= \mathbf{E}_d(\mathbf{r}) + \mathbf{E}^2_{dr}(\mathbf{r}) \\ &= ik_0\eta_0\,\frac{e^{ik_0 r_0}}{4\pi r_0}\,(e^{ik_0 x}\,\hat{\mathbf{y}} - e^{ik_0 y}\,\hat{\mathbf{x}})\,.\end{aligned} \tag{4.137}$$

Recalling that $x = -y$ for every point on plate 1, we have

$$\mathbf{E}_{\mathrm{d}2}(\mathbf{r}) = ik_0\eta_0 \frac{e^{ik_0 r_0}}{4\pi r_0} \left(e^{-ik_0 y}\,\hat{\mathbf{y}} - e^{ik_0 y}\,\hat{\mathbf{x}}\right) . \tag{4.138}$$

Using Eq. (4.122), the first-order scattered field from plate 1 and the second-order scattered field from plate 2 are related by

$$\begin{aligned}\hat{\mathbf{y}} \cdot \mathbf{E}_1^+(\mathbf{r}_0) &= \int_0^H \int_0^{\sqrt{2}\,W/2} \mathbf{J}_1(\mathbf{r}) \cdot \mathbf{E}_{\mathrm{d}2}(\mathbf{r})\, dz\, dy \\ &= ik_0 E_0 \frac{e^{ik_0 r_0}}{4\pi r_0}\, 2 \int_{-H/2}^{H/2} \int_0^{\sqrt{2}\,W/2} (e^{-i2k_0 y} + 1)\, dy\, dz . \end{aligned} \tag{4.139}$$

After integration the scattered field given by Eq. (4.139) can be written as

$$E_{1y}^+(\mathbf{r}_0) = ik_0 E_0 \sqrt{2}\, \frac{e^{ik_0 r_0}}{4\pi r_0}\, HW \left[1 + e^{-ik_0(\sqrt{2}/2)W}\, \mathrm{sinc}\left(k_0(\sqrt{2}/2)W\right)\right] . \tag{4.140}$$

In a similar manner, we can find the current induced on plate 2 in the absence of plate 1 using the physical-optics approximation, and noting that $y = x$ on plate 2,

$$\mathbf{J}_2(\mathbf{r}) = (\sqrt{2}\,\hat{\mathbf{x}} + \sqrt{2}\,\hat{\mathbf{y}}) \frac{E_0}{\eta_0}\, e^{ik_0 y} . \tag{4.141}$$

The scattered field from plate 1 when illuminated by the fields of the infinitesimal dipole is found to be

$$\mathbf{E}_{\mathrm{d}r}^1(\mathbf{r}) = ik_0\eta_0 \frac{e^{ik_0 r_0}}{4\pi r_0}\, e^{-ik_0 y}\,\hat{\mathbf{x}} . \tag{4.142}$$

Hence the total field from the dipole in the presence of plate 1 on plate 2 is given by

$$\mathbf{E}_{\mathrm{d}1}(\mathbf{r}) = ik_0\eta_0 \frac{e^{ik_0 r_0}}{4\pi r_0} \left(e^{ik_0 y}\,\hat{\mathbf{y}} + e^{-ik_0 y}\,\hat{\mathbf{x}}\right) . \tag{4.143}$$

Using Eqs. (4.141) and (4.143) in Eq. (4.124), we find that

$$\begin{aligned}\hat{\mathbf{y}} \cdot \mathbf{E}_2^+(\mathbf{r}_0) &= \int_{-H/2}^{H/2} \int_{-(\sqrt{2}/2)W}^0 \mathbf{J}_2(\mathbf{r}) \cdot \mathbf{E}_{\mathrm{d}1}(\mathbf{r})\, dy\, dz \\ &= ik_0 E_0 \frac{e^{ik_0 r_0}}{4\pi r_0}\, 2 \int_{-H/2}^{H/2} \int_{-(\sqrt{2}/2)W}^0 [e^{i2k_0 y} + 1]\, dy\, dz . \end{aligned}$$

After performing the integration, we have

$$E_{2y}^+(\mathbf{r}_0) = ik_0 E_0\, \sqrt{2}\, \frac{e^{ik_0 r_0}}{4\pi r_0}\, HW[1 + e^{-ik_0 W\sqrt{2}/2}\, \mathrm{sinc}(k_0 W\sqrt{2}/2)].$$

Hence the total scattered field up to second-order is

$$E_y^s(\mathbf{r}_0) = 2\sqrt{2}\, iAk_0E_0[1 + e^{-ik_0W\sqrt{2}/2}\,\mathrm{sinc}(k_0W\sqrt{2}/2)]\frac{e^{ik_0r_0}}{4\pi r_0}\,, \tag{4.144}$$

where $A = WH$ is the area of each panel. Note that since $W \gg \lambda$, it follows that

$$\mathrm{sinc}(k_0W\sqrt{2}/2) \ll 1$$

and that

$$E_y^s = 2\sqrt{2}\, iAk_0E_0\,\frac{e^{ik_0r_0}}{4\pi r_0}\,. \tag{4.145}$$

The radar cross section of a target is defined as

$$\sigma = \lim_{r\to\infty} 4\pi r^2\,\frac{|E^s|^2}{|E_0|^2}\,.$$

Substituting Eq. (4.145) into Eq. (4.146), the backscatter radar cross section (RCS) of the dihedral is given by

$$\sigma_{\text{dihedral}} = 8\pi\,\frac{A^2}{\lambda_0^2}\,, \qquad \textbf{(dihedral)} \tag{4.146}$$

where we have used $k_0 = 2\pi/\lambda_0$.

## 4-8 Babinet's Principle

In scattering and radiation problems that include planar metallic screens containing apertures (slots), Babinet's principle may prove useful in establishing a relationship to a dual scenario in which magnetic or electric walls with appropriate sources are used in lieu of the slots. One very useful application of Babinet's principle pertains to establishing the relationship between the input impedances of planar complementary antennas. Here, the term "complementary" refers to another antenna structure in which those parts of the antenna made of metallic surfaces are replaced with apertures, and vice versa. There are a number of steps that we need to establish before we can show the relation between a planar antenna and its complementary structure.

**Lemma 1:** Prove that the tangential magnetic field generated by a planar electric current sheet vanishes in the plane that contains the electric current sheet.

**Proof:** To prove this lemma, let us consider an arbitrary planar electric current sheet $\mathbf{J}$ placed in an arbitrary plane $P$, as shown in Fig. 4-19. To show that $H_t = 0$ in $P$, first we evaluate the magnetic vector potential generated by the current distribution $\mathbf{J}$, which is given by

$$\mathbf{A}(\mathbf{r}) = \mu \iint \mathbf{J}(\mathbf{r}')\, g(\mathbf{r},\mathbf{r}')\, ds'\,, \tag{4.147}$$

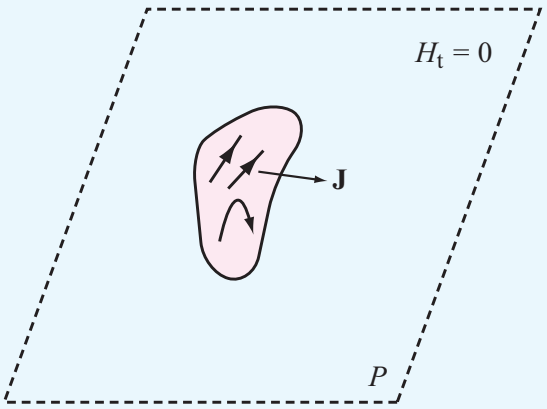


**Figure 4-19:** An arbitrary planar surface current distribution contained in plane $P$.

where in free space

$$g(\mathbf{r},\mathbf{r}') = \frac{1}{4\pi}\frac{e^{ik|\mathbf{r}-\mathbf{r}'|}}{|\mathbf{r}-\mathbf{r}'|} .$$

The magnetic field can be obtained directly from Eq. (4.147) using

$$\mathbf{H}(\mathbf{r}) = \frac{1}{\mu}\nabla\times\mathbf{A} = \iint \nabla\times[\mathbf{J}(\mathbf{r}')\, g(\mathbf{r},\mathbf{r}')]\, ds' . \tag{4.148}$$

Noting that the differentiations in the curl operator are with respect to the unprimed coordinate system

$$\nabla\times[\mathbf{J}(\mathbf{r}')\, g(\mathbf{r},\mathbf{r}')] = \nabla g(\mathbf{r},\mathbf{r}')\times\mathbf{J}(\mathbf{r}') .$$

On the other hand,

$$\nabla g(\mathbf{r},\mathbf{r}') = \left(ik - \frac{1}{|\mathbf{r}-\mathbf{r}'|}\right)\frac{e^{ik|\mathbf{r}-\mathbf{r}'|}}{|\mathbf{r}-\mathbf{r}'|^2}(\mathbf{r}-\mathbf{r}') . \tag{4.149}$$

Evaluating $\mathbf{H}$ at a point in plane $P$ guarantees that the vector $(\mathbf{r}-\mathbf{r}')$ lies in that plane. Also, noting that the current vector $\mathbf{J}(\mathbf{r}')$ is in the $P$ plane, it becomes clear that the integrand of Eq. (4.148) is a vector perpendicular to $P$, and therefore

$$\mathbf{H}_t(\mathbf{r}) = 0, \quad \forall\mathbf{r}\in P .$$

**Lemma 2:** Prove that the tangential electric field generated by a planar magnetic current sheet placed in an arbitrary plane $P$ vanishes everywhere on $P$.

**Proof:** The proof of this lemma can be deduced directly from Lemma 1 by applying the duality relations. These lemmas can also be proven using reverse application of image theory, as described in Problems 2.10 and 2.11 of Chapter 2.

### 4-8.1 Complementary Theorem

Consider a planar metallic sheet consisting of a number of apertures (slots) of arbitrary shapes excited by electric current sources all placed on one side of the metallic sheet, as shown in Fig. 4-20(a). Now consider a second scenario in which identical sources are used as in the first scenario, but the metallic sheet is removed and all apertures are replaced with perfect magnetic conductor sheets, as shown in Fig. 4-20(b). Denote the fields of the first scenario by $\mathbf{E}_1$ and $\mathbf{H}_1$ and those of the second scenario by $\mathbf{E}_2$ and $\mathbf{H}_2$ on the opposite half-space where the sources are located. The ***complementary theorem*** states that

$$\mathbf{E}_1 + \mathbf{E}_2 = \mathbf{E}_\mathrm{i} \tag{4.150a}$$

and

$$\mathbf{H}_1 + \mathbf{H}_2 = \mathbf{H}_\mathrm{i} \ , \tag{4.150b}$$

in the source-free region where $\mathbf{E}_\mathrm{i}$ and $\mathbf{H}_\mathrm{i}$ are the field quantities generated by the same source in the absence of all scatterers (electric and magnetic walls). Application of boundary conditions leads to

$$\hat{\mathbf{n}} \times \mathbf{E}_1 = 0 \qquad \text{on } S_1 \text{ (in Fig. 4-20(a))} \tag{4.151a}$$

and

$$\hat{\mathbf{n}} \times \mathbf{H}_2 = 0 \qquad \text{on } S_2 \text{ (in Fig. 4-20(a))}. \tag{4.151b}$$

The electric current source $\mathbf{J}$ on the left side of the metallic sheet induces a surface current on the metallic surface. This current according to Lemma 1 does not produce any tangential scattered magnetic fields across the apertures (on $S_2$). Hence the total tangential magnetic fields over the apertures are just the incident tangential magnetic fields produced by the source in the absence of the electric conductor; that is,

$$\hat{\mathbf{n}} \times \mathbf{H}_1 = \hat{\mathbf{n}} \times \mathbf{H}_\mathrm{i} \qquad \text{on } S_2 \ . \tag{4.152}$$

Similarly, for the second scenario the electric current source $\mathbf{J}$ induces a magnetic current over the magnetic walls that do not produce a tangential scattered electric field on $S_1$. Hence

$$\hat{\mathbf{n}} \times \mathbf{E}_2 = \hat{\mathbf{n}} \times \mathbf{E}_\mathrm{i} \qquad \text{on } S_1 \ . \tag{4.153}$$

Adding Eqs. (4.153) and (4.151a) yields

$$\hat{\mathbf{n}} \times (\mathbf{E}_1 + \mathbf{E}_2) = \hat{\mathbf{n}} \times \mathbf{E}_\mathrm{i} \qquad \text{on } S_1 \ ,$$

and adding Eqs. (4.151b) and (4.152) yields

$$\hat{\mathbf{n}} \times (\mathbf{H}_1 + \mathbf{H}_2) = \hat{\mathbf{n}} \times \mathbf{H}_\mathrm{i} \qquad \text{on } S_2 \ .$$

Since $S_1$ extends to infinity, $S_1 + S_2$ in addition to a hemisphere at infinity can be considered a closed surface for the source-free region. Since $(\mathbf{E}_1 + \mathbf{E}_2)$ and $(\mathbf{H}_1 + \mathbf{H}_2)$ satisfy Maxwell's equations and since we know the tangential electric field over a portion of the closed surface

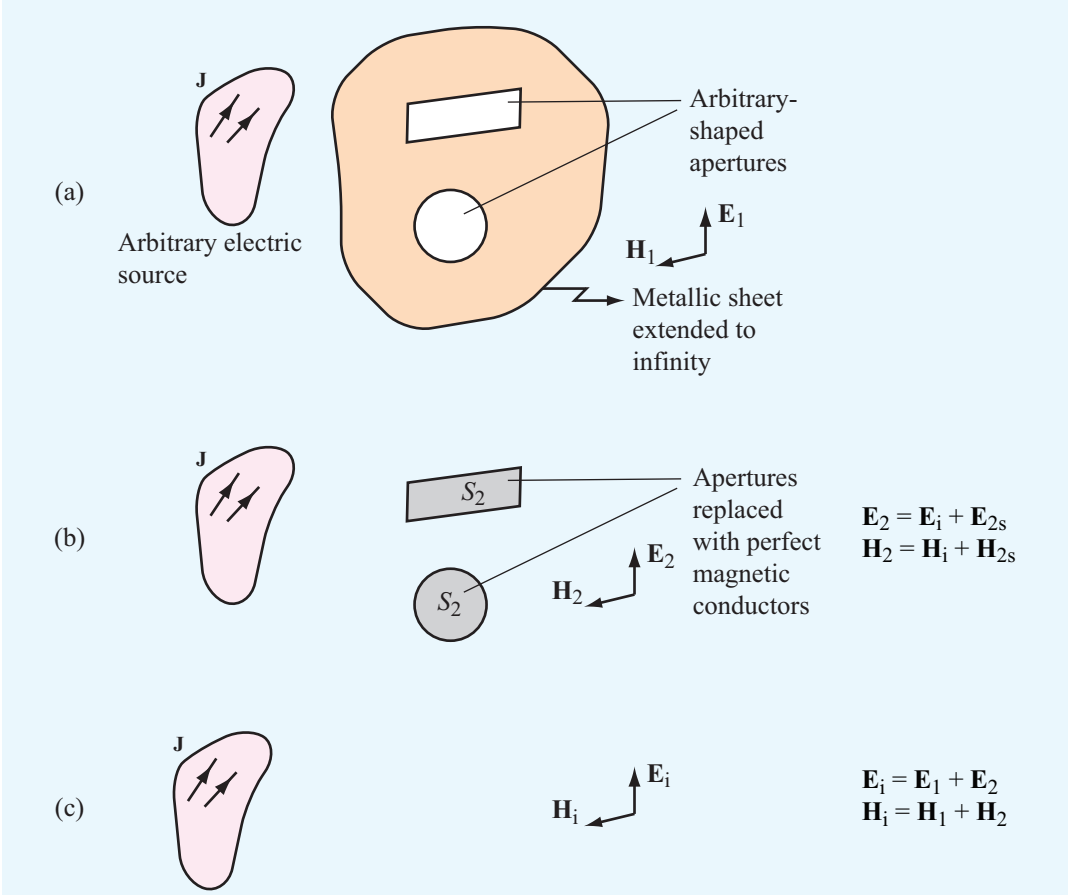


**Figure 4-20:** Three configurations: (a) a planar metallic sheet (which acts like a perfect electric conductor (PEC)) with arbitrary-shaped apertures excited by electric sources; (b) PEC is removed and the apertures are replaced with magnetic conductor sheets; and (c) the source with no scatterers present.

and the tangential magnetic field over the complementary portion of the surface, according to the uniqueness theorem the fields in the source-free region are unique. However, noting that the same tangential fields over $S_1 + S_2$ exist for the third scenario (Fig. 4-20(c)), where there are no scatterers, then Eqs. (4.150a) and (4.150b) hold everywhere in the source-free region.

### 4-8.2 The Babinet Theorem

Consider a planar metallic sheet of infinite extent and a number of apertures of arbitrary shape excited by electric current sources all on one side of the metallic sheet. The electric and magnetic fields in the source-free region in this case will be denoted by $\mathbf{E}_1$ and $\mathbf{H}_1$, as shown in Fig. 4-21(a). In a second experiment, we consider instead the dual of electric current sources as the source of the electromagnetic wave excitation for the metallic sheets instead of

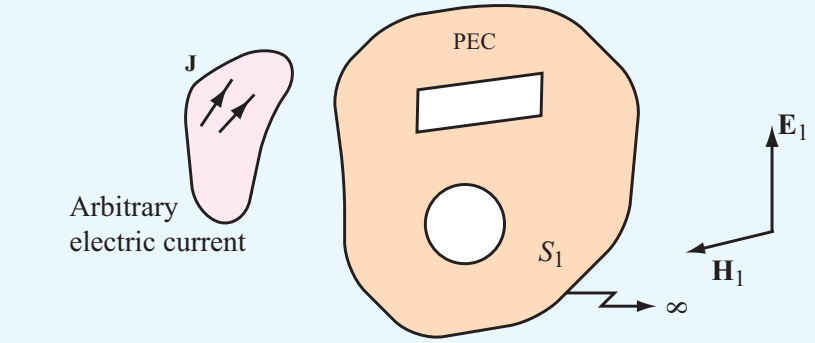


(a) Original configuration

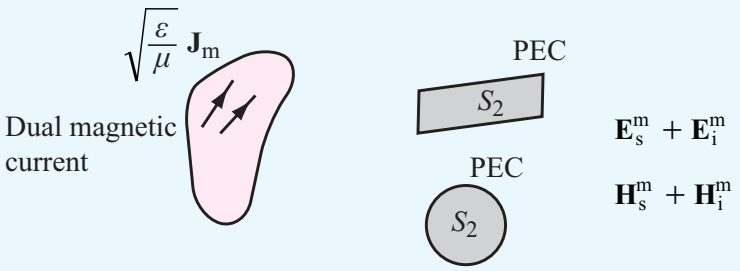


(b) Dual configuration

**Figure 4-21:** Two complementary configurations: (a) a planar metallic sheet with arbitrary-shaped apertures excited by an electric current, and (b) the complementary configuration wherein the apertures are replaced with PECs and excited by the dual magnetic current source.

the apertures in the first experiment, as shown in Fig. 4-21(b). Denoting the scattered fields from these metallic sheets as $\mathbf{E}_s^m$ and $\mathbf{H}_s^m$, the Babinet theorem states that

$$\mathbf{E}_1 = -\sqrt{\frac{\mu}{\varepsilon}}\,\mathbf{H}_s^m \tag{4.154a}$$

and

$$\mathbf{H}_1 = \sqrt{\frac{\varepsilon}{\mu}}\,\mathbf{E}_s^m\,. \tag{4.154b}$$

To prove Eqs. (4.154a) and (4.154b), we apply the complementary theorem to the first experiment. That is, we maintain the same electric current source and replace the apertures with perfect magnetic conductor sheets. This would produce the same electric and magnetic fields in the right-hand side (source-free region) as shown in Fig. 4-20(b). Applying the duality

principle to this problem by simply replacing $\mathbf{J}$ with $\sqrt{\varepsilon/\mu}\,\mathbf{J}_{\mathrm{m}}$ and the perfect magnetic conductors with perfect electric conductors, we obtain the configuration of Fig. 4-21(b). Under the duality relations, $\mathbf{E}_2$ and $\mathbf{H}_2$ of Fig. 4-20(b) must transform to

$$\mathbf{E}_2 \to \sqrt{\frac{\mu}{\varepsilon}}\,(\mathbf{H}_{\mathrm{s}}^{\mathrm{m}} + \mathbf{H}_{\mathrm{i}}^{\mathrm{m}}) \tag{4.155a}$$

and

$$\mathbf{H}_2 \to -\sqrt{\frac{\varepsilon}{\mu}}\,(\mathbf{E}_{\mathrm{s}}^{\mathrm{m}} + \mathbf{E}_{\mathrm{i}}^{\mathrm{m}})\,, \tag{4.155b}$$

where $\mathbf{H}_{\mathrm{s}}^{\mathrm{m}} + \mathbf{H}_{\mathrm{i}}^{\mathrm{m}}$ and $\mathbf{E}_{\mathrm{s}}^{\mathrm{m}} + \mathbf{E}_{\mathrm{i}}^{\mathrm{m}}$ are the total magnetic and electric fields of the configuration in Fig. 4-21(b), decomposed into the incident (in the absence of the conductors) and scattered fields. The superscript "m" denotes that the fields are produced by the dual magnetic sources. Substituting Eqs. (4.155a) and (4.155b) into Eqs. (4.150a) and (4.150b) and noting the duality relations between the incident fields,

$$\mathbf{E}_{\mathrm{i}} \to \sqrt{\frac{\mu}{\varepsilon}}\,\mathbf{H}_{\mathrm{i}}^{\mathrm{m}} \tag{4.156a}$$

and

$$\mathbf{H}_{\mathrm{i}} \to -\sqrt{\frac{\varepsilon}{\mu}}\,\mathbf{E}_{\mathrm{i}}^{\mathrm{m}}\,, \tag{4.156b}$$

it becomes obvious that

$$\mathbf{E}_1 = -\sqrt{\frac{\mu}{\varepsilon}}\,\mathbf{H}_{\mathrm{s}}^{\mathrm{m}} \tag{4.157a}$$

and

$$\mathbf{H}_1 = \sqrt{\frac{\varepsilon}{\mu}}\,\mathbf{E}_{\mathrm{s}}^{\mathrm{m}}\,. \tag{4.157b}$$

### 4-8.3 Complementary Antennas

The Babinet principle provides a useful tool for understanding the concept and application of complementary antennas. Babinet's principle can be used in connection with planar metallic antennas. To make the problem clear, let's consider a simple antenna structure such as a dipole antenna composed of two metallic strips fed by two thin wires (coplanar strips), as shown in Fig. 4-22(a). Such an antenna is similar to wire dipoles in that it radiates most effectively when the overall length of the dipole is about $\lambda/2$. Applying Babinet's principle, a complementary structure is formed as shown in Fig. 4-22(b). Here the areas around the metallic strips of the dipole and its feed (aperture) are replaced with a metallic sheet, and the dipole strip and its feed are left open as an aperture (slot). The antenna so formed is known as the ***slot antenna*** and the feed is known as a ***coplanar waveguide*** (CPW).

Using Babinet's principle, we first establish the relation between the input impedances of these complementary antennas. At the terminal of the wire antenna, the voltage and current

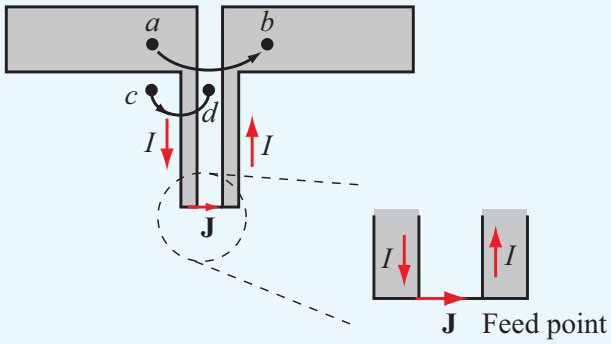


(a) Original configuration

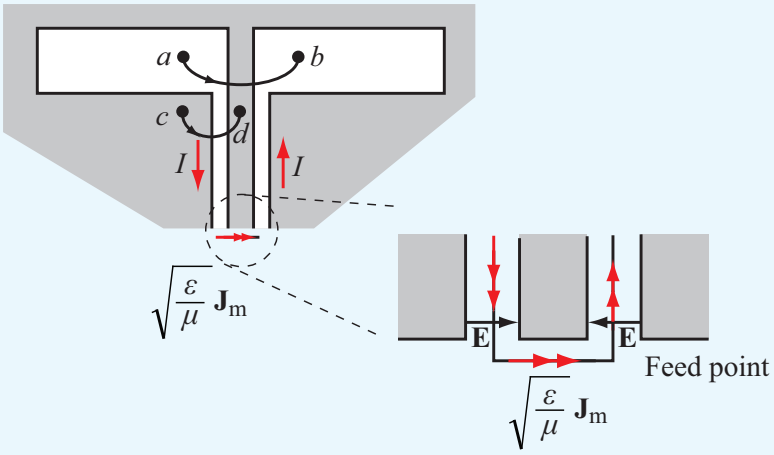


(b) Complementary configuration

**Figure 4-22:** Two complementary configurations: (a) a planar dipole antenna composed of metallic strips fed by a coplanar strip transmission line, and (b) a complementary antenna formed from part (a) by replacing metallic sections with slots and vice versa.

can be obtained from

$$V_{\mathrm{d}} = \int_a^b \mathbf{E}_1 \cdot d\boldsymbol{\ell} \tag{4.158a}$$

and

$$I_{\mathrm{d}} = -2 \int_c^d \mathbf{H}_1 \cdot d\boldsymbol{\ell}\,. \tag{4.158b}$$

In Eq. (4.158b) the symmetry of the problem (with respect to the plane containing the dipole)

is responsible for the factor of 2 in front of the integral. The current and voltage at the terminal are produced by an elementary electric current source at the feed point connected to the terminals of the coplanar strips. For the complementary problem, the feed is an elementary magnetic current source placed adjacent to the center conductor of the CPW line, exciting two opposite magnetic currents in the gaps of the CPW line. These magnetic currents excite the slot antenna by producing a voltage and current at the terminals of the slot antennas, given by

$$I_s = 2\int_a^b \mathbf{H}^m \cdot d\boldsymbol{\ell} \tag{4.159a}$$

and

$$V_s = \int_c^d \mathbf{E}^m \cdot d\boldsymbol{\ell}\ . \tag{4.159b}$$

Again, the symmetry of the problem explains the factor of 2 in front of Eq. (4.159a). According to Eqs. (4.157a) and (4.157b),

$$V_d = -\eta \int_a^b \mathbf{H}^m \cdot d\boldsymbol{\ell}$$

and

$$I_d = -\frac{2}{\eta}\int_c^d \mathbf{E}^m \cdot d\boldsymbol{\ell}\ .$$

Assuming points $a$ and $c$ in Fig. 4-22, and the same for $b$ and $d$, are very close to each other, the input impedance of the dipole antenna can be computed from

$$Z_d = \frac{V_d}{I_d} = \frac{\eta^2}{2}\frac{\int_a^b \mathbf{H}^m \cdot d\boldsymbol{\ell}}{\int_c^d \mathbf{E}^m \cdot d\boldsymbol{\ell}} = \frac{\eta^2}{4}\frac{I_s}{V_s}\ . \tag{4.160}$$

Recognizing the input impedance of the complementary slot $Z_s = V_s/I_s$, it is now easy to show that

$$Z_d Z_s = \eta^2/4\ . \tag{4.161}$$

Although Eq. (4.161) was obtained for a dipole antenna example, this result is valid for any planar antenna and its complementary configuration, since no specific assumptions were made about the operation or geometry of the dipole in deriving Eq. (4.161).

It should also be noted that the electric field radiation pattern of the dipole and the magnetic field radiation pattern of its complementary antenna (slot antenna) are identical and vice versa.

### 4-8.4 Self-Complementary Antennas

In most communication and radar systems, antennas play a very important role in directing the transmitted power along specific directions of interest for the intended application. Across the evolutionary history of wireless devices, multiple bands of operations have been added to each device to enable different types of services and to support high data-rate communication. For

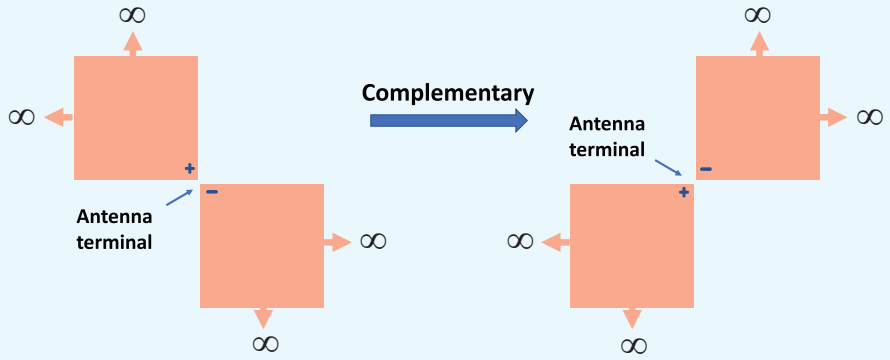


**Figure 4-23:** A planar antenna and its complementary structure. By rotating the antenna counterclockwise by 90°, its complementary geometry is generated. Such an antenna structure is self-complementary.

such devices, small antennas with wide bandwidth are required. The subject of frequency-independent antennas that can provide infinite or, in practice, very wide bandwidth has received significant attention in the recent past. For such antennas, it is desired that the input impedance of the antenna be a real quantity and independent of frequency. In this section it is shown that self-complementary antennas can, in principle, provide infinite bandwidth. Self-complementary antenna structures refer to planar antenna geometries in which the metallic portion of the antenna has exactly the same geometry as the slot or opening on the antenna plane. Basically, for such antennas the complementary geometry can be obtained from the original antenna by simply rotating the antenna by some fixed angle. To demonstrate this concept, let's consider the antenna geometry and its complementary structure shown in Fig. 4-23. The complementary of the antenna geometry can be obtained from the antenna structure itself by rotating the antenna by 90°. Since the geometry of the antenna and its complementary are the same, then it is obvious that the input impedance of the antenna, $Z_A$, and that of its complementary, $Z_C$, are the same. Using Eq. (4.161), it is evident that

$$Z_A Z_C = Z_A^2 = \eta^2/4 \,. \tag{4.162}$$

Hence, the input impedance of a self-complementary antenna is given by

$$Z_A = \eta/2 \,, \qquad \textbf{(self-complementary antenna)} \tag{4.163}$$

which is independent of the antenna geometry and independent of frequency. It is noted that in practice it is not possible to fabricate antennas with metallic sheets that extend to infinity. Depending on the space available, the metallic sheets must be truncated. The size of the truncated metallic sheets that define the antenna determines the low-end of the usable frequency range, and the gap size for the antenna terminals determines the upper end of the

frequency range, yielding a wideband, but of finite bandwidth, antenna. Other geometries for self-complementary antennas can also be considered. For example, a combination of a dipole antenna and its complementary slot can form a self-complementary antenna, as shown in Fig. 4-24. Also shown in the figure is an arbitrarily shaped self-complementary antenna. As an example of a small antenna with a wide bandwidth, let's consider a modified version of the self-complementary dipole. The height of the dipole can be shortened by top-loading it. Placement of an elliptical top-load provides multiple paths for the electric current on the dipole to create a resonant condition and thereby allows for increasing the bandwidth of the dipole inherently. Creating the complementary geometry and feeding the antenna, as shown in Fig. 4-25, provides a very wide bandwidth, as shown in the same figure. This antenna is about $\lambda_m/5$ in height, where $\lambda_m$ is the wavelength at the minimum frequency. The lower frequency is limited by the size of the ground plane, and the high frequency is limited by how faithful the antenna near the feed is to the complementary geometry. One important drawback of self-complementary antennas pertains to their radiation pattern. Although a self-complementary antenna is impedance-matched over a very wide bandwidth, its radiation pattern can change drastically over its bandwidth.

(a) Dipole antenna (b) Zigzag antenna

**Figure 4-24:** A self-complementary dipole antenna and a self-complementary "zigzag" antenna.

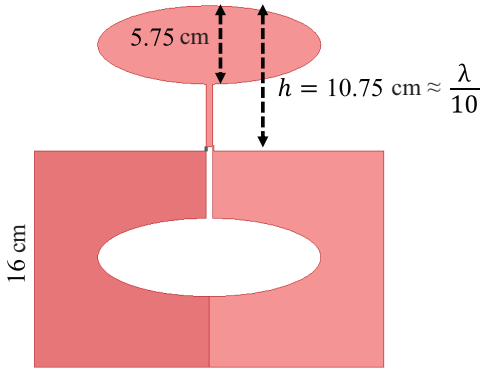


(a) Top-loaded dipole antenna

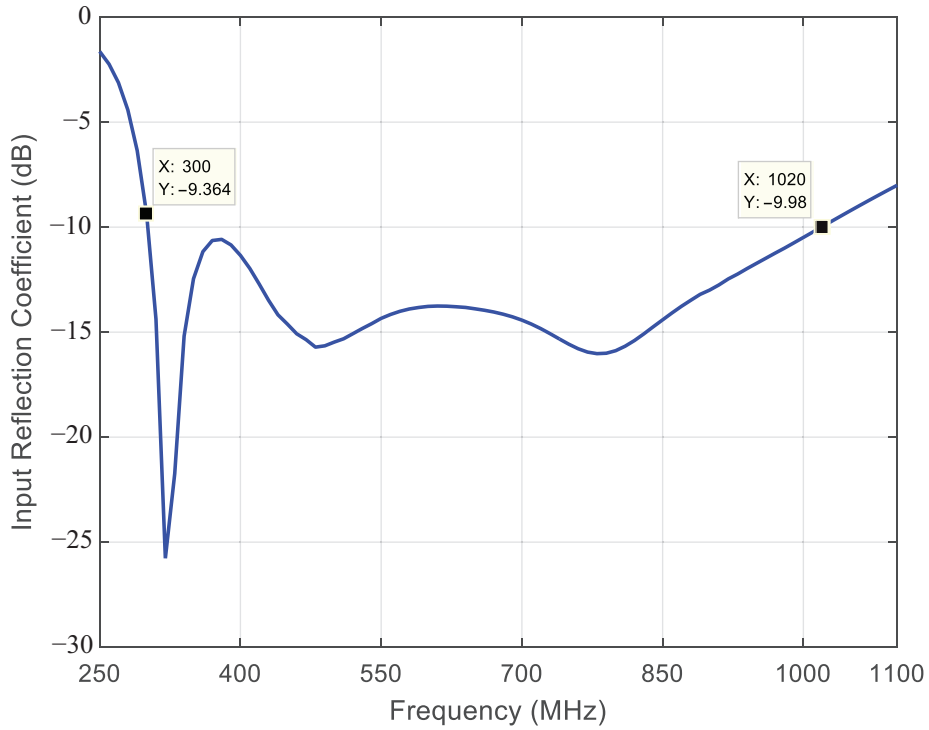


(b) Frequency response of the antenna reflection coefficient

**Figure 4-25:** (a) A self-complementary top-loaded dipole antenna and (b) the antenna reflection coefficient as a function of frequency. The antenna, with dimensions of about $\lambda_m/4$, provides a bandwidth on the order of two octaves. Here, $\lambda_m$ is the wavelength at the lowest frequency of operation, corresponding to $f_m = 300$ MHz.

## Summary

### Concepts

- The concept of Green's function, which presents the spatial impulse response of the wave equation for a homogeneous unbounded medium, is presented.
- Solutions of wave equations for the electromagnetic potentials for arbitrary charge and current distributions are obtained rigorously using Green's function with the help of Green's second identity.
- The solution to wave equations based on Green's function for a homogeneous unbounded medium is extended to include complex media made up of a heterogeneous medium composed of a finite number of objects with different material properties embedded in an otherwise homogeneous unbounded medium.
- The extinction theorem is introduced in the form of an integral equation, which states that the equivalent sources (potentials or fields and their normal derivatives) on the surfaces of the scatterers are formed in such a way as to produce potentials or fields inside the scatterers that can completely cancel out the incident potentials or fields inside the scatterers.
- The extinction theorem is modified for an observation point on the surface of the scatterers to form integral equations for the unknown surface potentials or fields and their normal derivatives on the surfaces of the scatterers.
- Appropriate boundary conditions for the potentials at interfaces between two dielectric media or between a dielectric medium and a metallic one are derived.
- Integral equation formulations based on surface field equivalent sources are derived.
- It is shown that two independent integral equations, namely electric-field integral equations (EFIE) and magnetic-field integral equations (MFIE), can be derived by applying the continuity of the tangential electric field and the tangential magnetic field at the interface between the background medium and the scatterer, respectively.
- A fundamental theorem in electromagnetism known as the reciprocity theorem is presented. This theorem establishes the relationship between two different sources (electric and magnetic current distributions) and their corresponding fields.
- The reciprocity theorem is applied to antennas to show that the radiation pattern of an antenna in the receiving mode is the same as its pattern in the transmitting mode.
- The notion of effective area for a receiving antenna is introduced and its relationship to its directivity function is derived using the reciprocity theorem.
- Babinet's theorem and the complementary theorem that are applicable to planar conducting screens with arbitrary apertures are presented.
- The concept of a complementary antenna, which refers to a planar antenna for which the metallic and aperture areas are the opposite of those of the original antenna, is presented and shown to produce the same radiation pattern as the original antenna with orthogonal polarization. Also the relationship between the input impedances of a planar antenna and its complementary geometry is derived.
- The term "self-complementary antenna" refers to an antenna whose complementary geometry is the same as that of the antenna itself. Such antennas are shown to provide infinite bandwidth (their input impedance is not a function of frequency).

## Important Equations

**Free-space scalar Green's function:**

$$g(\mathbf{r},\mathbf{r}') = \frac{e^{ik|\mathbf{r}-\mathbf{r}'|}}{4\pi|\mathbf{r}-\mathbf{r}'|}$$

**Green's first identity:**

$$\iiint_V \nabla\psi\cdot\nabla\Phi\, dv + \iiint_V \psi\,\nabla^2\Phi\, dv = \oiint \psi\frac{\partial\Phi}{\partial n}\, ds$$

**Green's second identity:**

$$\iiint_V [\psi\,\nabla^2\Phi - \Phi\,\nabla^2\psi]\, dv = \oiint_S \left(\psi\frac{\partial\Phi}{\partial n} - \Phi\frac{\partial\psi}{\partial n}\right) ds$$

**Radiation condition for potentials and fields:**

$$\lim_{r\to\infty} r\left(\frac{\partial\,\Phi(\mathbf{r})}{\partial r} - ik\,\Phi(\mathbf{r})\right) = 0$$

$$\lim_{r\to\infty} r\left(\frac{\partial\,\mathbf{A}(\mathbf{r})}{\partial r} - ik\,\mathbf{A}(\mathbf{r})\right) = 0$$

$$\lim_{r\to\infty} r\,[\mathbf{E}(\mathbf{r}) + \hat{\mathbf{r}}\times\eta\mathbf{H}(\mathbf{r})] = 0$$

$$\lim_{r\to\infty} r\,[n\mathbf{H}(\mathbf{r}) - \hat{\mathbf{r}}\times\mathbf{E}(\mathbf{r})/\eta] = 0$$

**Integral equations for scalar potential based on the extinction theorem:**

$$\Phi_{\mathrm{i}}(\mathbf{r}) + \oiint_{\sum S_i}\left(g(\mathbf{r},\mathbf{r}')\,\frac{\partial\,\Phi(\mathbf{r}')}{\partial n'} - \Phi(\mathbf{r}')\,\frac{\partial\,g(\mathbf{r},\mathbf{r}')}{\partial n'}\right) ds = \begin{cases} \Phi(\mathbf{r}) & \mathbf{r}\in V\,, \\ \Phi(\mathbf{r})/2 & \mathbf{r}\text{ on } S_j\,, \\ 0 & \mathbf{r}\notin V\,, \end{cases}$$

$$\oiint\left(g_{\mathrm{i}}(\mathbf{r},\mathbf{r}')\,\frac{\partial\,\Phi_j(\mathbf{r}')}{\partial n'} - \Phi_j(\mathbf{r}')\,\frac{\partial\,g_j(\mathbf{r},\mathbf{r}')}{\partial n'}\right) ds' = \begin{cases} \Phi_j(\mathbf{r}) & \mathbf{r}\in V_j\,, \\ \frac{1}{2}\,\Phi_j(\mathbf{r}) & \mathbf{r}\text{ on } S_j\,, \\ 0 & \mathbf{r}\notin V_j \end{cases}$$

## Important Equations (continued)

**Boundary conditions for electromagnetic potentials at interface between two dielectric media:**

$$A_1(\mathbf{r}) = A_2(\mathbf{r}) \,, \quad r \in S$$
$$\Phi_1(\mathbf{r}) = \Phi_2(\mathbf{r}) \,, \quad r \in S$$
$$\varepsilon_1 \frac{\partial \Phi_1}{\partial n} = \varepsilon_2 \frac{\partial \Phi_2}{\partial n} \quad r \in S$$

**Boundary conditions at interface between dielectric and metallic media:**

$$A_1(\mathbf{r}) = 0, \quad r \in S$$
$$\Phi_i(\mathbf{r}) = \text{constant}, \quad r \in S$$

**Reciprocity theorem:**

$$\langle a, b \rangle = \langle b, a \rangle$$
$$\langle a, b \rangle = \iiint_V (\mathbf{E}_a \cdot \mathbf{J}_b - \mathbf{H}_a \cdot \mathbf{J}_{\mathrm{m}b}) \, dv$$

**Reciprocity theorem for a source-free region:**

$$\oiint (\mathbf{E}_a \times \mathbf{H}_b - \mathbf{E}_b \times \mathbf{H}_a) \cdot d\mathbf{s} = 0$$

**Two-port network reciprocity relations between voltages and currents at the terminals of two antennas:**

$$V_a I_b = V_b I_a$$

## Important Equations (continued)

**Electric-field integral equations:**

$$
\begin{aligned}
&-\frac{1}{2}\,\mathbf{J}_{\rm ms}(\mathbf{r}) \\
&-\hat{\mathbf{n}}\times\oiint_{S_{\rm s}}\left(i\eta_1 k_1\,\mathbf{J}_{\rm s}(\mathbf{r}')\,g_1(\mathbf{r},\mathbf{r}')+\frac{i\eta_1}{k_1}\,\nabla'_{\rm s}\cdot\mathbf{J}_{\rm s}(\mathbf{r}')\,\nabla g_1(\mathbf{r},\mathbf{r}')+\mathbf{J}_{\rm ms}(\mathbf{r}')\times\nabla g_1(\mathbf{r},\mathbf{r}')\right)ds' \\
&=\hat{\mathbf{n}}\times\mathbf{E}_{\rm i}(\mathbf{r}) \\
&-\frac{1}{2}\,\mathbf{J}_{\rm ms}(\mathbf{r}) \\
&+\hat{\mathbf{n}}\times\oiint_{S_{\rm s}}\left(i\eta_2 k_2\,\mathbf{J}_{\rm s}(\mathbf{r}')\,g_2(\mathbf{r},\mathbf{r}')+\frac{i\eta_2}{k_2}\,\nabla'_{\rm s}\cdot\mathbf{J}_{\rm s}(\mathbf{r}')\,\nabla g_2(\mathbf{r},\mathbf{r}')+\mathbf{J}_{\rm ms}(\mathbf{r}')\times\nabla g_2(\mathbf{r},\mathbf{r}')\right)ds' \\
&=0
\end{aligned}
$$

**Magnetic-field integral equations:**

$$
\begin{aligned}
&\frac{1}{2}\,\mathbf{J}(\mathbf{r})-\hat{\mathbf{n}}\times\oiint_{S_{\rm s}}\left(\frac{ik_1}{\eta_1}\,\mathbf{J}_{\rm ms}(\mathbf{r}')\,g_1(\mathbf{r},\mathbf{r}')\right. \\
&\qquad\left.+\frac{i}{k_1\eta_1}\,\nabla'_{\rm s}\cdot\mathbf{J}_{\rm ms}(\mathbf{r}')\,\nabla g_1(\mathbf{r},\mathbf{r}')-\mathbf{J}_{\rm s}(\mathbf{r}')\times\nabla g_1(\mathbf{r},\mathbf{r}')\right)ds' \\
&\quad=\hat{\mathbf{n}}\times\mathbf{H}_{\rm i}(\mathbf{r}) \\
&\frac{1}{2}\,\mathbf{J}(\mathbf{r})+\hat{\mathbf{n}}\times\oiint_{S_{\rm s}}\left(\frac{ik_2}{\eta_2}\,\mathbf{J}_{\rm ms}(\mathbf{r}')\,g_2(\mathbf{r},\mathbf{r}')\right. \\
&\qquad\left.+\frac{i}{k_2\eta_2}\,\nabla'_{\rm s}\cdot\mathbf{J}_{\rm ms}(\mathbf{r}')\,\nabla g_2(\mathbf{r},\mathbf{r}')-\mathbf{J}_{\rm s}(\mathbf{r}')\times\nabla g_2(\mathbf{r},\mathbf{r}')\right)ds' \\
&\quad=0\,.
\end{aligned}
$$

**Equivalence of antenna patterns in transmission and reception:**

$$D_{\rm t}(\theta,\phi)=D_{\rm r}(\theta,\phi)$$

**Effective area for receiving antenna:**

$$A_{\rm eff}(\theta,\phi)=\frac{\lambda^2}{4\pi}\,G(\theta,\phi)$$

## Important Equations (continued)

**Babinet's theorem in reference to Fig. 4-21:**

$$\mathbf{E}_1 = -\sqrt{\frac{\mu}{\varepsilon}}\,\mathbf{H}_s^m\,, \qquad \mathbf{H}_1 = \sqrt{\frac{\varepsilon}{\mu}}\,\mathbf{E}_s^m$$

**Impedance relation between the input impedances of an antenna ($Z_d$) and its complement antenna ($Z_s$):**

$$Z_d Z_s = \eta^2/4$$

**Input impedance of a self-complementary antenna:**

$$Z_A = \eta/2$$

## Important Terms

Provide definitions or explain the meaning of the following terms:

antenna radiation pattern in receive and transmit modes
antennas as two-port networks
Babinet's principle
boundary conditions for the potentials
complementary antenna
complementary theorem
effective area of a receiving antenna
electric-field integral equation (EFIE)
extinction theorem
Fredholm integral equation
frequency-independent antennas
Friis transmission formula
Green's first identity
Green's function
Green's second identity
Green's theorem
Helmholtz equation
incident potential
magnetic-field integral equation (MFIE)
physical optics current on metallic surfaces
principal-value integral
radiation condition
reciprocity condition for two-port networks
reciprocity theorem
reciprocity theorem for a source-free region
scattered potential
self-complementary antenna
singular point
surface-field integral equations
wave equation

## PROBLEMS

### Integral Equations

**4.1** Follow a procedure similar to that used to derive Eq. (4.36) for electric scalar potential where the observation point $r$ is on the surface of the scatterer to show that the contribution from the singularity of the scalar Green's function in the surface integral of Eq. (4.65) is $\frac{1}{2}\,\mathbf{E}(\mathbf{r})$.

**4.2** Consider a scatterer whose surface is denoted by $S_j$, similar to what is shown in Fig. 4-3. However, this surface has surface slope discontinuities at a finite number of points, as shown in Fig. P4.2. If the observation point happens to be at an edge point, how would you change Eq. (4.36) for this point?

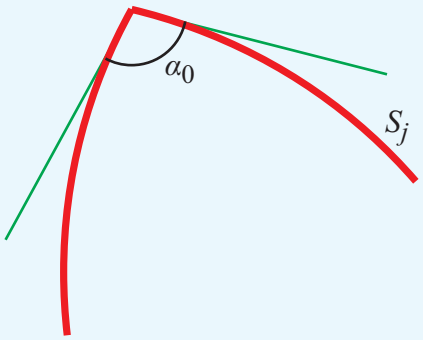


**Figure P4.2:** Surface of an object with a slope discontinuity.

**4.3** Consider a metallic sphere of radius $a$ centered at the origin of a Cartesian coordinate system, as shown in Fig. P4.3. Suppose a plane wave propagating along the $+x$ direction is illuminating the metallic sphere. The electric field expression for the incident field is given by

$$\mathbf{E}_{\mathrm{i}} = E_0\,\hat{\mathbf{y}}\,e^{ik_0 x}\,,$$

with

$$k_0 = \frac{2\pi}{\lambda_0} = \omega\sqrt{\mu_0\varepsilon_0}\,.$$

Assuming $a \gg \lambda_0$, use MFIE for conductors to show that the surface current is approximately $\mathbf{J}(\mathbf{r}) = 2n \times \mathbf{H}_1(\mathbf{r})$.

**(a)** Using this current only on the lit portion of the surface, find the scattered field.

**(b)** Note that the first-order physical-optics current also exists in the shadow area. Show that the first-order physical-optics current produces a magnetic field that almost cancels out the incident magnetic field in the shadow region.

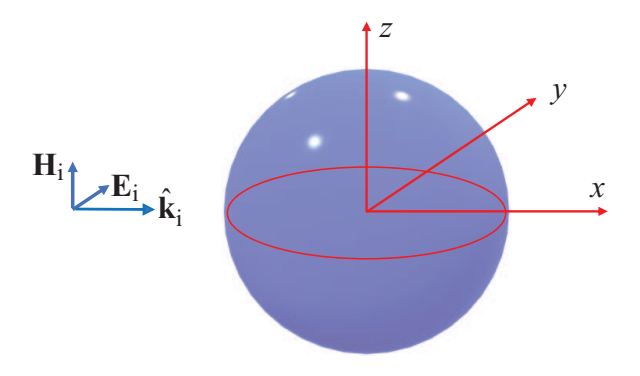


**Figure P4.3:** A metallic sphere illuminated by a plane wave.

## Reciprocity

**4.4** Figure P4.4 shows two antennas with an obstacle. Let $V_1$ be the voltage received at the terminals of antenna (1) when a unit current source is applied at the terminals of antenna (2), and let $V_2$ be the voltage received at antenna (2) when a unit current source is applied at antenna (1). Let $V_1^{\mathrm{i}}$ and $V_2^{\mathrm{i}}$ be the corresponding voltages when the obstacle is absent. Define the scattered voltages as

$$V_1^{\mathrm{s}} = V_1 - V_1^{\mathrm{i}} \quad \text{and} \quad V_2^{\mathrm{s}} = V_2 - V_2^{\mathrm{i}} \,,$$

and show that $V_1^{\mathrm{s}} = V_2^{\mathrm{s}}$.

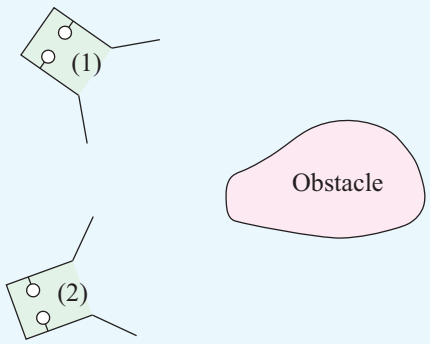


**Figure P4.4:** Diagram for Problem 4.4, showing two antennas that are used as transmit and receive pairs. In one experiment, antenna (1) is the transmitter and antenna (2) is the receiver. In the second experiment, the roles of the two antennas are interchanged.

**4.5** Consider a homogeneous anisotropic medium with permittivity and permeability tensor elements $\overline{\overline{\varepsilon}}$ and $\overline{\overline{\mu}}$, respectively. Following a procedure similar to that used in the proof of the reciprocity theorem, provide the necessary and sufficient conditions for fields to be reciprocal in the anisotropic medium. (*Hint:* For two arbitrary vectors, the dot product $\mathbf{a}\cdot\mathbf{b}$ in matrix notation can be written as $\mathbf{a}^{\mathrm{T}}\mathbf{b}$.)

**4.6** Consider a homogeneous medium with the following constitutive relations:

$$\mathbf{D} = \varepsilon\mathbf{E} + \xi\mathbf{H} \qquad \text{and} \qquad \mathbf{B} = \xi^{*}\mathbf{E} + \mu\mathbf{H}\,,$$

where $\xi$ is related to the Tellegen and Pasteur parameters $\chi$ and $\kappa$ as follows:

$$\xi = \sqrt{\mu\varepsilon}\,(\chi - j\kappa)\,.$$

Find the necessary and sufficient conditions for the fields to be reciprocal in this medium.

**4.7** Consider a typical communications system as shown in Fig. P4.7(a), in which the antennas and the relative separation and orientation are completely arbitrary. The same physical situation is shown in Fig. P4.7(b), except that the transmitter and receiver circuits have been interchanged. We assume that the transmitter and receiver are both connected to the antennas through a length of *single-mode transmission line or waveguide*. The only impressed sources in the problem are located in the transmitter. The fields and currents inside $V$ in each of the two situations of the figure are denoted by ($\mathbf{E}_a$, $\mathbf{H}_a$, $\mathbf{J}_a$) and ($\mathbf{E}_b$, $\mathbf{H}_b$, $\mathbf{J}_b$), respectively. By letting the surface $S$ extend to infinity and applying reciprocity, show that $Z_{12} = Z_{21}$, where $Z_{ij}$'s are the $Z$-parameters of this two-antenna system. (Assume that the transmitter and receiver and feed lines are shielded by a perfect conducting surface.)

$$\begin{bmatrix} V_1 \\ V_2 \end{bmatrix} = \begin{bmatrix} Z_{11}\, Z_{12} \\ Z_{21}\, Z_{22} \end{bmatrix} \begin{bmatrix} I_1 \\ I_2 \end{bmatrix}\,.$$

(*Hint:* You can assume that a coaxial cable connects the antenna to Tx/Rx. Then use the fields distribution inside the coaxial cable (the tangential electric field $E_{\mathrm{t}}$ is proportional to the voltage $V$ and the tangential magnetic field $H_{\mathrm{t}}$ is proportional to the current $I$).)

**4.8** What is the effective area of a Hertzian dipole? If a Hertzian dipole carrying current $I_0$ is placed at the origin of a Cartesian coordinate system and oriented along the $z$-axis, and another one, used as receiver, is placed at location $\mathbf{r}$ and oriented along the $\hat{\boldsymbol{\theta}}$ direction, find the power received by the receiver when the receiver is impedance-matched.

**4.9** Consider a transmitter with power $P_{\mathrm{t}}$ connected to an antenna with gain $G_{\mathrm{t}}(\theta,\phi)$ that is impedance-matched. Another antenna with gain $G_{\mathrm{r}}(\theta,\phi)$ at a distance $R$ from the transmitter is impedance-matched to a receiver. Show that the receiver power can be calculated from

$$P_{\mathrm{r}} = \frac{\lambda^2 G_{\mathrm{t}} G_{\mathrm{r}}}{(4\pi R)^2}\, P_{\mathrm{t}}\,.$$

This equation is known as the ***Friis transmission formula***.

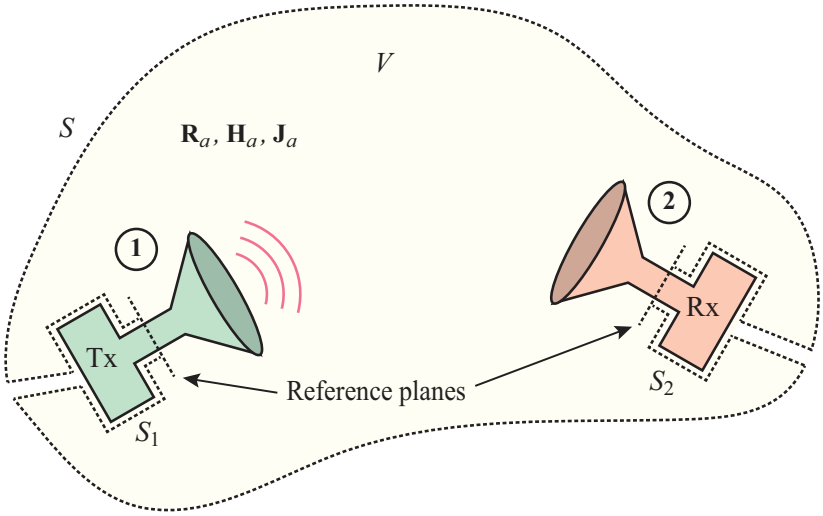


(a) (Tx, Rx) = (Antenna 1, Antenna 2)

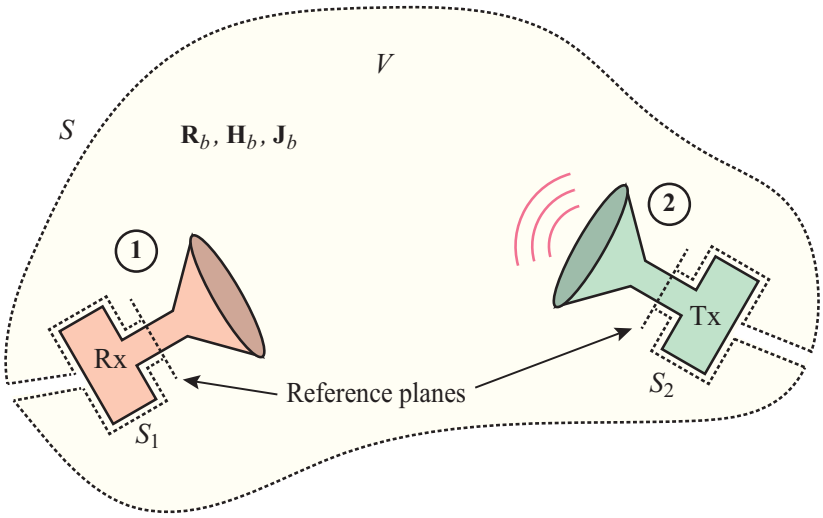


(b) (Tx, Rx) = (Antenna 2, Antenna 1)

**Figure P4.7:** Diagram for Problem 4.7, showing a pair of antennas used as transmitter and receiver in two complementary experiments.

**4.10** Consider the dihedral corner reflector shown in Fig. 4-18 of Example 4-2. Applying reciprocity, calculate the backscatter from the dihedral when it is illuminated by a plane wave given by

$$\mathbf{E}_{\mathrm{i}}(\mathbf{r}) = E_0(-\sin\phi\ \hat{\mathbf{x}} + \cos\phi\ \hat{\mathbf{y}})e^{ik_0(\cos\phi x + \sin\phi y)}\ .$$

**4.11** Find an expression for the radar backscatter cross section of the dihedral corner reflector shown in Fig. 4-18, with the only difference being that the angle between the two plates is $\alpha$. Find out how the RCS decreases when $\alpha$ deviates from 90°.

**4.12** Derive an expression for the scattered field for two adjacent objects in a case where one object is made from a perfect electric conductor and the other object is made from a dielectric.

**4.13** Consider a dielectric sphere of radius $a$ having a permittivity $\varepsilon = 1.05\varepsilon_0$ placed above a metallic plate in the $x$–$y$ plane, as shown in Fig. P4.13. The plate has dimensions $b \times b$, with

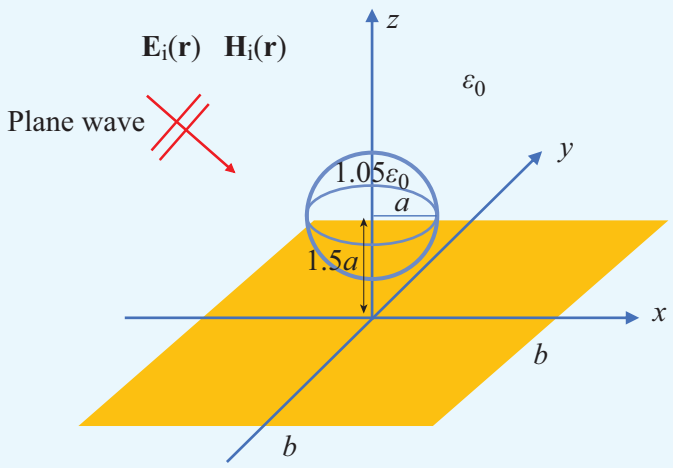


**Figure P4.13:** Diagram for Problem 4.13, showing a dielectric sphere above a finite-size square-shaped metallic plate illuminated by a plane wave.

$b \gg \lambda$. The sphere center is on the $z$-axis at a height $h = 1.5a$. These objects are illuminated by a plane wave given by

$$\mathbf{E}_{\mathrm{i}}(\mathbf{r}) = E_0(\cos\theta\ \hat{\mathbf{x}} + \sin\theta\ \hat{\mathbf{z}})e^{ik(\sin\theta x\cos\theta z)}\ .$$

For $b > 6a$, find the backscatter field from these objects. (*Hint:* Since the permittivity of the sphere is very close to that of the background ($\varepsilon_0$), the Born approximation can be used. Using the Born approximation, the fields inside the dielectric sphere can be approximated by those of the incident wave (in the absence of the sphere).)

## Babinet's Principle

**4.14** Consider an electric source at $z = -\infty$ that produces the following plane wave:

$$\mathbf{E}_{\mathrm{i}} = E_0 e^{ikz}\,\hat{\mathbf{x}}\,,$$

and a metallic sheet in the $z = 0$ plane, with a square aperture of length $L$ located at the origin. The aperture extends from $x = -L/2$ to $x = L/2$ and from $y = -L/2$ to $y = L/2$. Using a high-frequency approximation, the fields for $z > 0$ can be approximately estimated by the following expression:

$$\mathbf{E} = \hat{\mathbf{x}}\,E_0\,\frac{e^{ikr}}{r}\,L^2\,\operatorname{sinc}\left(\frac{Lky}{2r}\right)\operatorname{sinc}\left(\frac{Lkx}{2r}\right)\,.$$

Assume that the source was replaced with a magnetic source and the ground plane with the aperture was replaced with a square metal plate of the same size as the aperture. Use Babinet's principle to find the fields in the $z > 0$ half-space. The $\operatorname{sinc}(\cdot)$ function is defined as $\operatorname{sinc}(x) = (\sin x)/x$.

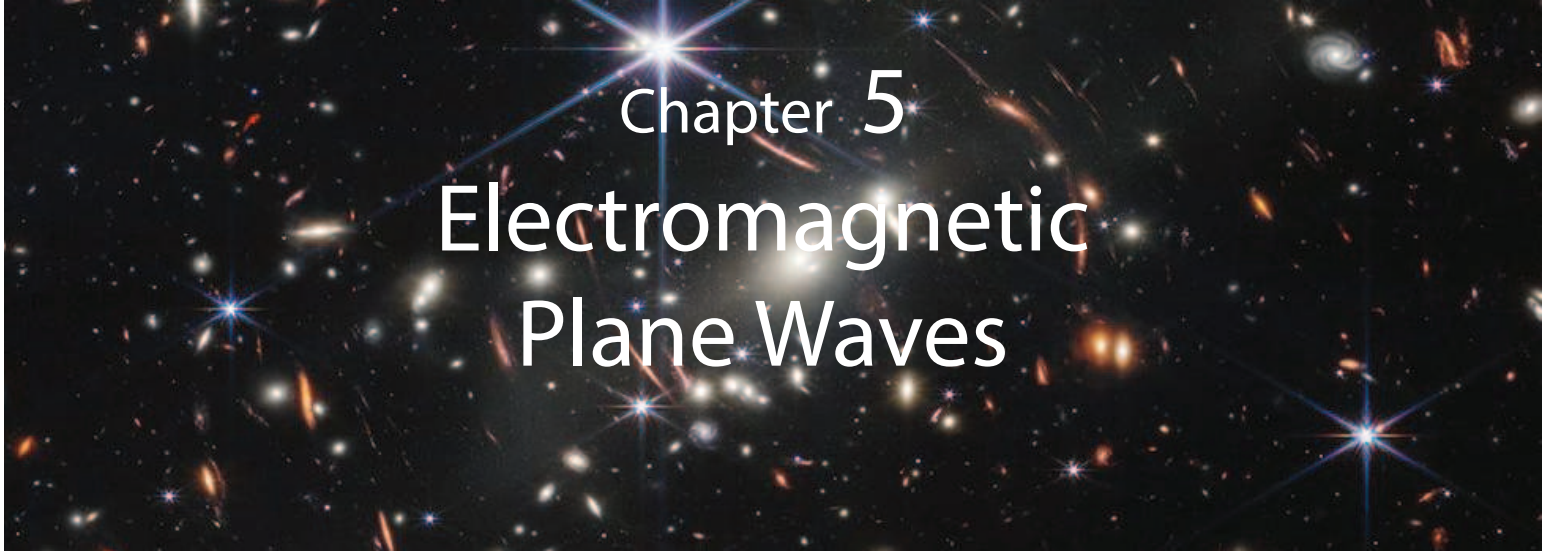

# Chapter 5 Electromagnetic Plane Waves

## Chapter Contents


Overview, 228
5-1 Plane-Wave Propagation in Homogeneous Media, 228
5-2 Polarization of Plane Waves, 238
5-3 Plane Waves in Anisotropic Media, 241
5-4 kDB Coordinate System for Plane Waves in Bianisotropic Media, 247
5-5 Transverse Electric (TE) and Transverse Magnetic (TM) Field Solutions of the Helmholtz Equation, 254
5-6 Plane-Wave Reflection at the Interface between a Dielectric Medium and a Good-Conducting Medium, 264
5-7 Wave Propagation in an Inhomogeneous Medium: Geometric Optics Approximation, 266
5-8 Plane-Wave Reflection by and Transmission through a Half-Space Uniaxial Medium, 275
5-9 Plane Waves in Layered Media, 281
5-10 Plane-Wave Propagation in a Negative-Index Medium, 290
5-11 Negative Refractive-Index Lens, 292
Chapter Summary, 298
Problems, 303


## Objectives

Upon learning the material presented in this chapter, you should be able to:

1. Have an intuitive understanding of the important properties associated with plane-wave propagation in a homogeneous isotropic medium, including the propagation constant of the medium, wave polarization, and phase front.
2. Characterize the field in a source-free region, when generated by sources outside that region, in terms of a continuous spectrum of plane waves.
3. Develop the plane-wave solution in an anisotropic medium using the kDB system.
4. Explain the expansion of fields in terms of transverse electric and transverse magnetic fields.
5. Calculate plane-wave reflection and transmission at planar boundaries between a dielectric medium and another multilayer dielectric medium that may be an isotropic or anisotropic uniaxial medium.
6. Understand the concept of negative-index media and the characteristics of plane waves propagating in such media.

## Overview

In this chapter, we examine the solution to Maxwell's equations for a source-free homogeneous medium. It is shown that the electric and the magnetic fields both satisfy the vector wave equation. Considering an invariant direction for the electric field throughout the medium, the vector wave equation is reduced to a scalar wave equation, which is then solved using the method of separation of variables. The resultant solution is known as a plane wave, as the magnitude and the phase of the electric and magnetic fields are constant in planes perpendicular to the direction of propagation. For such waves, the electric field is perpendicular to the magnetic field and both are perpendicular to the direction of propagation. The notion of nonuniform plane waves is also introduced, for which the planes of constant phase and constant magnitude differ. It is shown that the superposition of all such planes also constitutes a solution to Maxwell's equations, provided that the sum of the square of the propagation constants of the components of these plane waves in the three principal orthogonal directions are equal to the square of the wave number, $k^2$; in other words $K_x^2 + K_y^2 + K_z^2 = k^2 = \omega^2\mu\varepsilon$. Explicit expressions for power and energy density of plane waves are obtained. The notion of plane-wave polarization in terms of parameters of a polarization ellipse is introduced. Then plane-wave solutions for homogeneous but anisotropic media are examined. The dispersion relation that relates different components of the propagation constant along different principal directions to the frequency and tensor elements of permittivity is obtained for the general case, and examples for simpler uniaxial media are discussed in more detail. The kDB coordinate system is presented for plane waves in anisotropic media. This coordinate system facilitates simpler and more intuitive relations between field components. The notion of ordinary and extraordinary waves in a uniaxial medium is introduced in the kDB system, and simplified dispersion relations for them are derived. To study the behavior of plane waves at planar boundaries between two dielectric media, the concepts of transverse electric (TE) and transverse magnetic (TM) field expansion is introduced. It is shown that all field components, in a source-free region, for transverse magnetic fields can be obtained from an electric Hertz vector potential that has only one component along a desired direction of propagation. Also, all field components for TE waves can be generated from a magnetic Hertz vector potential that has only one component along the direction of propagation. The reflection and transmission coefficients of an incident plane wave at an interface between two media, as well as for multilayer media, are obtained using TE and TM wave expansions. These results are extended to include calculation of plane-wave reflection and transmission at planar interfaces between an isotropic and a uniaxial medium with its optical axis parallel to the interface. Finally, plane-wave propagation in negative-index media is examined and the concept of a perfect lens made up of a dielectric slab of negative-index material whose index of refraction is the negative value of the index of refraction of the surrounding medium is presented.

## 5-1 Plane-Wave Propagation in Homogeneous Media

In this section, we consider the solution of Maxwell's equations in an unbounded, source-free, homogeneous medium. Let us consider a medium with constitutive parameters $\varepsilon, \mu$ and free

of currents and charges. For this problem, Maxwell's equations take the following form:

$$\nabla \times \mathbf{E} = i\omega\mu\,\mathbf{H}\,, \tag{5.1a}$$

$$\nabla \times \mathbf{H} = -i\omega\varepsilon\,\mathbf{E}\,, \tag{5.1b}$$

$$\nabla \cdot \mathbf{E} = 0\,, \tag{5.1c}$$

$$\nabla \cdot \mathbf{H} = 0\,. \tag{5.1d}$$

In general $\varepsilon$ and $\mu$ are complex quantities. The equations for the electric and magnetic fields can be decoupled by first taking the curl of Eq. (5.1a) and then using Eq. (5.1b) in the resulting equation:

$$\nabla \times \nabla \times \mathbf{E} = i\omega\mu\,\nabla \times \mathbf{H} = \omega^2\mu\varepsilon\,\mathbf{E}\,. \tag{5.2}$$

But

$$\nabla \times \nabla \times \mathbf{E} = \nabla\nabla \cdot \mathbf{E} - \nabla^2\,\mathbf{E}\,. \tag{5.3}$$

Using Eq. (5.1c) in Eq. (5.3), Eq. (5.2) can be written as

$$\nabla^2\,\mathbf{E} + k^2\,\mathbf{E} = 0\,, \tag{5.4}$$

where $k^2 = \omega^2\mu\varepsilon$. A similar procedure can be followed to show that

$$\nabla^2\,\mathbf{H} + k^2\,\mathbf{H} = 0\,. \tag{5.5}$$

The quantity $k$ is called the ***propagation constant*** of the medium. Equations (5.4) and (5.5) indicate that both the electric and magnetic fields satisfy the vector wave equation. These wave equations are separable in the Cartesian coordinate system and each represents three scalar wave equations for the three components of the fields. That is,

$$\nabla^2 \begin{pmatrix} E_x \\ E_y \\ E_z \end{pmatrix} + k^2 \begin{pmatrix} E_x \\ E_y \\ E_z \end{pmatrix} = 0\,. \tag{5.6}$$

Once the solution for $\mathbf{E}$ is obtained, it is much easier to find the solution for $\mathbf{H}$ directly using Eq. (5.1a) than to repeat the solution process with Eq. (5.5). That is,

$$\mathbf{H} = \frac{1}{i\omega\mu}\,\nabla \times \mathbf{E} = -\frac{i}{k\eta}\,\nabla \times \mathbf{E}\,, \tag{5.7}$$

where $\eta = \sqrt{\frac{\mu}{\varepsilon}}$.

The simplest form of solution that one can conceive for the electric field is of the following:

$$\mathbf{E} = \mathbf{E}_0\,\psi(\mathbf{r})\,, \tag{5.8}$$

where $\mathbf{E}_0$ is a constant vector and $\psi(\mathbf{r})$ is a scalar function of $\mathbf{r}$. Upon substituting Eq. (5.8) into Eq. (5.4), it can be easily shown that

$$\mathbf{E}_0 \nabla^2 \psi(\mathbf{r}) + \mathbf{E}_0 k^2 \psi(\mathbf{r}) = 0 ,$$

which produces a nonvanishing solution if

$$\nabla^2 \psi(\mathbf{r}) + k^2 \psi(\mathbf{r}) = 0 . \tag{5.9}$$

We assume that $\psi(\mathbf{r})$ is separable; i.e.,

$$\psi(\mathbf{r}) = X(x)\, Y(y)\, Z(z) , \tag{5.10}$$

where $X$, $Y$, and $Z$ are single variable functions of $x$, $y$, and $z$, respectively.

Substituting this solution into Eq. (5.9), we have

$$\left( \frac{\partial^2}{\partial x^2} + \frac{\partial^2}{\partial y^2} + \frac{\partial^2}{\partial z^2} \right) XYZ + k^2 XYZ = 0 . \tag{5.11}$$

For points where $\psi(\mathbf{r})$ is nonzero, both sides of Eq. (5.11) can be divided by $XYZ$:

$$\left( \frac{1}{X} \frac{\partial^2}{\partial x^2} X + \frac{1}{Y} \frac{\partial^2}{\partial y^2} Y + \frac{1}{Z} \frac{\partial^2}{\partial z^2} Z \right) + k^2 = 0 . \tag{5.12}$$

The first term in the parenthesis is only a function of variable $x$, the second one is only a function of variable $y$, and the last one is only a function of variable $z$. Hence for Eq. (5.12) to be valid for all values of $x$, $y$, and $z$, each of the three terms in the parenthesis must be equal to a constant; i.e.,

$$\frac{1}{X} \frac{\partial^2}{\partial x^2} X = -K_x^2 , \tag{5.13a}$$

$$\frac{1}{Y} \frac{\partial^2}{\partial y^2} Y = -K_y^2 , \tag{5.13b}$$

$$\frac{1}{Z} \frac{\partial^2}{\partial z^2} Z = -K_z^2 . \tag{5.13c}$$

Equation (5.12) is satisfied if

$$K_x^2 + K_y^2 + K_z^2 = k^2 = \omega^2 \mu \varepsilon . \tag{5.14}$$

Finding solutions to the second-order differential equations given by Eq. (5.13) is straightforward. The solutions are of the following form:

$$X(x) = e^{iK_x x} .$$

$$Y(y) = e^{iK_y y} ,$$

$$Z(z) = e^{iK_z z} .$$

Hence

$$\mathbf{E}(\mathbf{r}) = \mathbf{E}_0 e^{i\mathbf{K}\cdot\mathbf{r}} , \tag{5.15}$$

where

$$\mathbf{K} = K_x\,\hat{\mathbf{x}} + K_y\,\hat{\mathbf{y}} + K_z\,\hat{\mathbf{z}}$$

and

$$|\mathbf{K}| = k = \omega\sqrt{\mu\varepsilon} .$$

For lossless media wherein both $\mu$ and $\varepsilon$ are real, the unit vector $\hat{\mathbf{k}}$ representing the ***direction of propagation*** is

$$\begin{aligned}\hat{\mathbf{k}} = \frac{\mathbf{K}}{|\mathbf{K}|} &= \frac{K_x}{k}\,\hat{\mathbf{x}} + \frac{K_y}{k}\,\hat{\mathbf{y}} + \frac{K_z}{k}\,\hat{\mathbf{z}} \\ &= k_x\,\hat{\mathbf{x}} + k_y\,\hat{\mathbf{y}} + k_z\,\hat{\mathbf{z}} ,\end{aligned} \tag{5.16}$$

where $k_x^2 + k_y^2 + k_z^2 = 1$ and $\hat{\mathbf{k}}$ denotes a direction for which the phase of the electric field in planes perpendicular to that direction is constant. Basically

$$\hat{\mathbf{k}}\cdot\mathbf{r} = \text{const.}$$

defines a plane perpendicular to $\hat{\mathbf{k}}$, as shown in Fig. 5-1.

In this plane, both the phase and magnitude of the electric field are constant, and that is why this specific solution of Maxwell's equations is known as a plane wave. Note that even

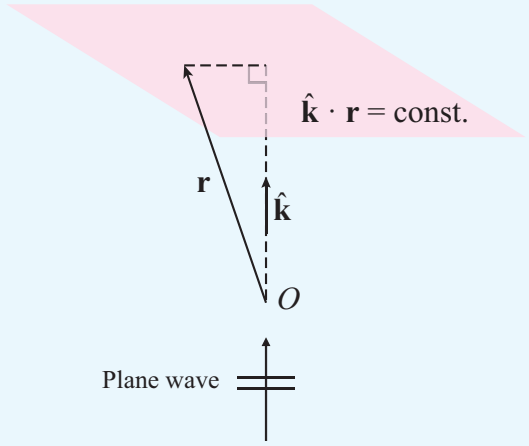


**Figure 5-1:** Phase front of a uniform plane wave is shown to be a plane across which the magnitude and phase of the wave have constant values.

for real values of $\varepsilon$ and $\mu$, Eq. (5.15) may represent a nonpropagating wave. For example, if

$$K_x^2 + K_y^2 > k^2 \ ,$$

then

$$K_z = i\sqrt{K_x^2 + K_y^2 - k^2}$$

and

$$\mathbf{E} = \mathbf{E}_0 e^{i(K_x x + K_y y)} e^{-K_z z} \ .$$

In this case the wave attenuates exponentially along the $z$ direction. The wave is then said to be evanescent along the $+z$ direction. The magnitude $\mathbf{E}_0$ is not entirely a free parameter. Computing the divergence of the electric field shows that

$$\nabla \cdot \mathbf{E} = \mathbf{E}_0 \cdot \nabla e^{i\mathbf{K}\cdot\mathbf{r}} = i\,\mathbf{E}_0 \cdot \mathbf{K}\, e^{i\mathbf{K}\cdot\mathbf{r}} = 0 \ ,$$

which indicates that

$$\mathbf{E}_0 \cdot \hat{\mathbf{k}} = 0 \ . \tag{5.17}$$

Equation (5.17) states that the electric field of the plane wave is normal to the wave's direction of propagation. The corresponding magnetic field can be obtained from Eq. (5.7):

$$\mathbf{H} = \frac{-i}{k\eta} \nabla \times (\mathbf{E}_0 e^{i\mathbf{K}\cdot\mathbf{r}}) = \frac{-i}{k\eta} (i\,\mathbf{K} \times \mathbf{E}_0) e^{i\mathbf{K}\cdot\mathbf{r}} \ ,$$

or

$$\mathbf{H} = \frac{\hat{\mathbf{k}} \times \mathbf{E}_0}{\eta} e^{i\mathbf{K}\cdot\mathbf{r}} \ , \tag{5.18}$$

which indicates that $\mathbf{H}$ is perpendicular to both the electric field and the waves direction of propagation. It is interesting to also note that

$$\frac{|\mathbf{E}|}{|\mathbf{H}|} = \eta = \sqrt{\frac{\mu}{\varepsilon}}$$

at all points in space.

### 5-1.1 Plane Waves in Lossy Media

In situations where either the permittivity $\varepsilon$ or the permeability $\mu$ (or both) is complex, the propagation constant

$$k = \omega\sqrt{\mu\varepsilon} = k' + i\alpha \tag{5.19a}$$

becomes complex, with $k'$ and $\alpha$ representing the real and imaginary parts of $k$. A special case of wave propagation in this case is when the unit vector $\hat{\mathbf{k}}$ is real. Such a plane wave is referred to as a ***uniform*** plane wave. Consider a direction of wave propagation denoted by spherical coordinate angles $\theta$ and $\phi$ for which

$$\hat{\mathbf{k}} = k_x\,\hat{\mathbf{x}} + k_y\,\hat{\mathbf{y}} + k_z\,\hat{\mathbf{z}} = \sin\theta\cos\phi\,\hat{\mathbf{x}} + \sin\theta\sin\phi\,\hat{\mathbf{y}} + \cos\theta\,\hat{\mathbf{z}} \ . \tag{5.19b}$$

In a plane perpendicular to $\hat{\mathbf{k}}$, where

$$\hat{\mathbf{k}} \cdot \mathbf{r} = \xi = \text{const.} ,$$

the phase of $\mathbf{E}$, given by $\xi k'$, is constant. In this same plane the magnitude of the electric field, given by

$$|E| = |\mathbf{E}_0| e^{-\alpha \xi} ,$$

is also constant. Hence, for a uniform plane wave whose direction of propagation is real, both the magnitude and phase of the wave are constant in planes perpendicular to the direction of propagation. In general, the planes of constant phase and magnitude are different. As an example, let us consider a wave for which $K_x$ and $K_y$ are real and

$$K_z = \sqrt{k^2 - K_x^2 - K_y^2} \tag{5.20}$$

is complex (since $k$ is complex). Then

$$K_z = K_z' + iK_z'' .$$

For this wave, the electric field assumes the following form:

$$\mathbf{E} = \mathbf{E}_0 e^{i\mathbf{K}' \cdot \mathbf{r}} e^{-K_z'' z} , \tag{5.21}$$

where now $\mathbf{K}' = K_x \hat{\mathbf{x}} + K_y \hat{\mathbf{y}} + K_z' \hat{\mathbf{z}}$.

Let's define a unit vector

$$\hat{\mathbf{k}}' = \frac{K_x \hat{\mathbf{x}} + K_y \hat{\mathbf{y}} + K_z' \hat{\mathbf{z}}}{\sqrt{K_x^2 + K_y^2 + K_z'^2}} .$$

Then in a plane where

$$\hat{\mathbf{k}}' \cdot \mathbf{r} = \xi = \text{const.}$$

the phase of the wave is constant. Considering that the magnitude of the wave is given by

$$|E| = |E_0| e^{-K_z'' z} ,$$

it is obvious that the magnitude of the plane wave is constant in constant $z$-planes. Therefore in general the constant magnitude and constant phase planes are different for lossy media. Such plane waves are referred to as ***nonuniform*** plane waves.

In general, defining the ***complex phase*** as

$$\phi = \mathbf{K} \cdot \mathbf{r} , \tag{5.22}$$

the vector quantity $\nabla\phi$ specifies a vector that is normal to surfaces of constant $\phi$. In cases where $\mathbf{K}$ is real, $\nabla\phi = \mathbf{K}$, which indicates that ***equiphase surfaces*** are planes perpendicular to $\mathbf{K}$. For a complex $\mathbf{K}$ vector where

$$\mathbf{K} = \mathbf{K}' + i\mathbf{K}'' ,$$

$\nabla\phi = \mathbf{K}' + i\,\mathbf{K}''$, indicating that equiphase surfaces are planes perpendicular to $\mathbf{K}'$ and equiamplitude surfaces are planes perpendicular to $\mathbf{K}''$. Assuming that the medium is lossless,

$$k^2 = \mathbf{K}\cdot\mathbf{K} = |\mathbf{K}'|^2 - |\mathbf{K}''|^2 + 2i\,\mathbf{K}'\cdot\mathbf{K}'' \,, \tag{5.23}$$

which mandates a vanishing imaginary part. The imaginary part of Eq. (5.23) vanishes if $\mathbf{K}'' = 0$ or $\mathbf{K}'\cdot\mathbf{K}'' = 0$. If $\mathbf{K}'' = 0$, a regular uniform plane wave is obtained. Also, $\mathbf{K}'\cdot\mathbf{K}'' = 0$ denotes a possible plane-wave solution in a lossless medium. That is, the equiphase and equiamplitude planes are orthogonal, similar to the example considered earlier. This is known as an ***evanescent wave***. Lossy media can also support evanescent plane waves, but the equiphase and equiamplitude planes are not necessarily orthogonal.

### 5-1.2 Expansion of a Field as a Continuous Spectrum of Plane Waves

In the previous section it was demonstrated that an elementary wave function of the form $\mathbf{E}_0 e^{i\mathbf{K}\cdot\mathbf{r}}$ is a solution to the homogeneous Helmholtz equation for arbitrary parameters $K_x$, $K_y$, and $K_z$, subject to the constraint

$$K_x^2 + K_y^2 + K_z^2 = k^2 \,.$$

That is, any two of the three parameters can be considered as free parameters that may take on real numbers from $-\infty$ to $+\infty$. Hence, there are an infinite number of plane waves that satisfy the wave equation for homogeneous and unbounded media. Since Maxwell's equations are linear, any linear combination of these plane waves is also a solution. That is, the electric field produced by an arbitrary source, in a source-free region, may be written as

$$\begin{aligned}\mathbf{E}(\mathbf{r}) &= \int_{-\infty}^{+\infty}\int_{-\infty}^{+\infty} \mathbf{E}_0(K_x,K_y)\, e^{i\mathbf{K}\cdot\mathbf{r}}\, dK_x\, dK_y \qquad (5.24a)\\ &= \int_{-\infty}^{+\infty}\int_{-\infty}^{+\infty} \left[\mathbf{E}_0(K_x,K_y)\, e^{iK_z z}\right] e^{iK_x x} e^{iK_y y}\, dK_x\, dK_y \,,\end{aligned}$$

and its corresponding magnetic field is given by

$$\mathbf{H}(\mathbf{r}) = \int_{-\infty}^{+\infty}\int_{-\infty}^{+\infty} \frac{\mathbf{K}\times\mathbf{E}_0(K_x,K_y)}{k\eta}\, e^{i\mathbf{K}\cdot\mathbf{r}}\, dK_x\, dK_y \,. \tag{5.24b}$$

Although the elementary field components of the electric and magnetic fields are orthogonal to each other and their magnitude ratios are a constant (and equal to the characteristic impedance of the medium), the same is not true for the overall field quantities. It should also be noted that the choice of $K_x$ and $K_y$ as free parameters is arbitrary; i.e., any two pairs of $K_x$, $K_y$, $K_z$ could have been chosen. Also, as was shown before, the constant magnitude vector $\mathbf{E}_0$ is not entirely arbitrary (see Eq. (5.17)). Equation (5.24a) indicates that in a source-free region the fields produced by arbitrary electric or magnetic currents, outside the region of interest, can be expressed in terms of the superposition of an infinite number of plane waves. It is also interesting to note that Eq. (5.24a) represents a two-dimensional Fourier transformation , and that its inverse can be used to find $\mathbf{E}_0(k_x,k_y)$ in terms of $\mathbf{E}(\mathbf{r})$. Basically, taking the inverse

Fourier transform of Eq. (5.24a), we have

$$\mathbf{E}_0(K_x,K_y)\,e^{iK_z z}=\int_{-\infty}^{+\infty}\int_{-\infty}^{+\infty}\mathbf{E}(x,y,z)\,e^{-iK_x x}e^{-iK_y y}\,dx\,dy\,. \tag{5.25}$$

## Example 5-1: An Application of Plane-Wave Field Expansion

Show that by measuring the tangential electric field in a constant-$z$ plane ($z=z_0$) in the vicinity of an antenna can be used to find the fields at every point where $z>z_0$. This approach can be used to find the radiation pattern of antennas.

**Solution:** When characterizing the radiation pattern of an antenna, traditionally the antenna under test (AUT) is used as a transmitter and another antenna is used as a receiver to measure the power radiated by the AUT. The receiver antenna is moved around the AUT at a constant distance and the recoded power provides the radiation pattern. For proper measurements, the receiving antenna must be placed in the far-field region of the AUT in an environment free of any objects that may perturb the radiated field. This often poses challenging practical conditions for the radiation pattern measurement of large antennas. Alternatively, by measuring the electric field in the vicinity of the antenna on a planar surface, the field outside the surface in the source-free region can be determined. Figure 5-2 shows the configuration for the problem. Let us denote the tangential electric field in the constant-$z$ plane by $\mathbf{E}_t(x,y,z_0)=E_x(x,y,z_0)\,\hat{\mathbf{x}}+E_y(x,y,z_0)\,\hat{\mathbf{y}}$. Assuming that this field is measured and known, we can find the tangential component of the field spectrum from the Fourier transform of the measured tangential electric field:

$$\mathbf{E}_{0t}(K_x,K_y)=e^{-iK_z z_0}\int_{-\infty}^{+\infty}\int_{-\infty}^{+\infty}\mathbf{E}_t(x,y,z_0)e^{-iK_x x}\,e^{-iK_y y}\,dx\,dy\,.$$

In practice the tangential electric field is not measured over the entire constant-$z$ surface due to the fact that fields decay fast for points away from the antenna and thus the limits of the integrals can be truncated at some finite values. It was shown before for plane waves that Gauss's law of electricity mandates $\mathbf{K}\cdot\mathbf{E}_0=0$. This can be used to find the $z$-component of $\mathbf{E}_0$; that is,

$$E_{0z}(K_x,K_y)=-\frac{K_xE_{0x}(K_x,K_y)+K_yE_{0y}(K_x,K_y)}{\sqrt{k^2-K_x^2-K_y^2}}\,.$$

Once all three components of $\mathbf{E}_0(K_x,K_y)$ have been determined, Eq. (5.24a) can be used to find the electric field everywhere ($z>z_0$). This is in agreement with the uniqueness theorem, which states that the fields in a source-free region can be determined from knowledge of the tangential electric field over a closed surface. The closed surface in this example can be regarded as composed of the constant-$z$ surface and an infinite half-sphere closing over the constant-$z$ surface.

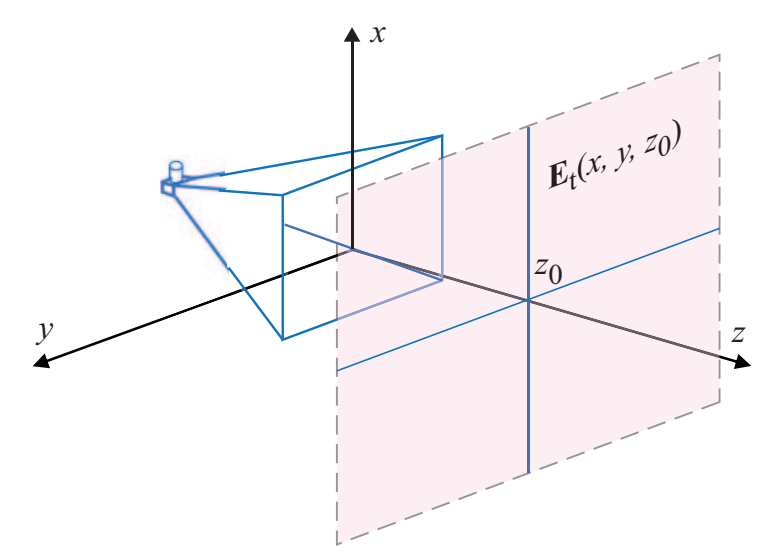


**Figure 5-2:** Configuration for the antenna near-field measurement. The tangential component of the electric field phasor generated by an arbitrary antenna is measured across a planar surface near the antenna. This field is used to characterize the fields everywhere outside the surface in the source-free region.

### 5-1.3 Power and Energy Densities

Consider an elementary plane-wave solution of a Helmholtz equation whose electric and magnetic fields were found to be

$$\mathbf{E} = E_0 e^{i\mathbf{K}\cdot\mathbf{r}}$$

and

$$\mathbf{H} = \frac{\hat{\mathbf{k}} \times E_0}{\eta} e^{i\mathbf{K}\cdot\mathbf{r}} .$$

The ***stored electric energy*** per unit volume is given by

$$w_e = \frac{1}{4}\varepsilon'|\mathbf{E}|^2 = \frac{1}{4}\varepsilon'|E_0|^2 e^{-2\mathbf{K}''\cdot\mathbf{r}} ,$$

and the ***stored magnetic energy*** per unit volume is

$$w_m = \frac{1}{4}\mu'|H|^2 = \frac{1}{4}\mu' \frac{|\hat{\mathbf{k}}|^2|E_0|^2}{|\eta|^2} e^{-2\mathbf{K}''\cdot\mathbf{r}} .$$

In a lossless medium, $\mathbf{K}'' = 0$, and noting that $\mu/\eta^2 = \varepsilon$,

$$w_m = w_e = \frac{1}{4}\varepsilon|E_0|^2 \,. \qquad \textbf{(lossless medium)} \tag{5.26}$$

That is, the stored electric and magnetic energies for a plane wave are independent of position and are equal to each other. In contrast, for a lossy medium the stored energies are functions of position and are not necessarily equal.

The complex power flow density can be obtained from the Poynting vector and is given by

$$\mathbf{S}(\mathbf{r}) = \frac{1}{2}\mathbf{E}\times\mathbf{H}^* = \frac{1}{2}\frac{|E_0|^2\hat{\mathbf{k}}^* - (\mathbf{E}_0\cdot\hat{\mathbf{k}}^*)E_0^*}{\eta^*}\, e^{-2\mathbf{K}''\cdot\mathbf{r}} \,. \tag{5.27}$$

For a uniform plane wave in a lossless medium, the expression becomes much simpler and is given by

$$\mathbf{S}(\mathbf{r}) = \frac{|E_0|^2}{2\eta}\,\hat{\mathbf{k}} \,. \tag{5.28}$$

Considering a uniform plane wave traveling along $\hat{\mathbf{k}}$, the amount of energy delivered to a volume $\Delta v$ along its direction of propagation over an interval $\Delta t$ can be computed using

$$\Delta W = (\mathbf{S}\cdot\hat{\mathbf{k}}\,A)\,\Delta t \,. \tag{5.29}$$

If we assume that the energy of the wave is propagating with ***velocity*** $u_e$ along $\hat{\mathbf{k}}$, then the volume shown in Fig. 5-3 is filled with the wave energy if

$$\Delta r = u_e\,\Delta t \,. \tag{5.30}$$

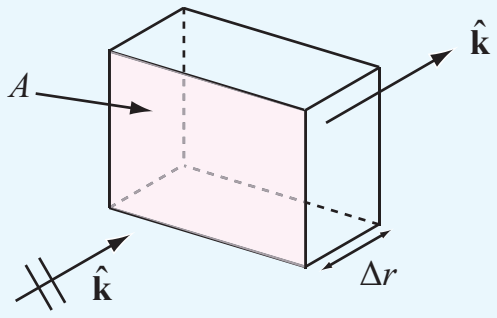


**Figure 5-3:** A fictitious volume in space intercepting an incident plane wave with its front and back faces perpendicular to the direction of propagation. The power density carried by the plane wave fills the volume with electromagnetic energy at the speed of light.

For a differential volume $\Delta v$, the total stored energy is $(w_e + w_m)\,\Delta v = \Delta W$. Hence

$$\mathbf{S}\cdot\hat{\mathbf{k}}\left(A\,\frac{\Delta r}{u_e}\right) = (w_e + w_m)\,\Delta v\,. \tag{5.31}$$

Computing the energy velocity from Eq. (5.31), we have

$$u_e = \frac{S}{w_e + w_m}\,. \tag{5.32}$$

For a uniform plane wave,

$$u_e = \frac{|E_0|^2/\eta}{\frac{1}{2}\,\varepsilon|E_0|^2 + \frac{1}{2}\,\mu|H_0|^2} = \frac{1}{\eta\varepsilon} = \frac{1}{\sqrt{\mu\varepsilon}}\,,$$

indicating that the energy flows at the speed of light.

## 5-2 Polarization of Plane Waves

Let us consider a uniform plane wave in a lossless medium. In such a medium, the plane wave can be fully characterized by the following five quantities:

1. Frequency ($\omega = 2\pi f$).
2. Propagation constant ($k = \omega\sqrt{\mu\varepsilon}$).
3. Direction of propagation ($\hat{\mathbf{k}}_i$).
4. Field intensity ($|\mathbf{E}_0| = \sqrt{\mathbf{E}_0\cdot\mathbf{E}_0^*}$).
5. Polarization ($\hat{\mathbf{p}} = \mathbf{E}_0/|\mathbf{E}_0|$; a complex unit vector).

The time-domain expression for this plane wave can be expressed as

$$\mathbf{E}(\mathbf{r},t) = R_e\left[\mathbf{E}_0 e^{-i[\omega t - k(\hat{\mathbf{k}}_i\cdot\mathbf{r})]}\right]\,,$$

where $\mathbf{r}$ is the position vector. The polarization of a plane wave can be described as the time-varying behavior of the electric field vector at a given point in space. In the most general case, as will be shown in this section, the tip of the electric field traces an ellipse with an angular frequency $\omega$, and the wave is called ***elliptically polarized***. Without loss of generality, let us assume that the direction of propagation is along the $z$-axis in a Cartesian coordinate system. Since in a source-free region $\hat{\mathbf{k}}_i\cdot\mathbf{E}_0 = 0$, the electric field vector can be written as

$$\mathbf{E}_0 = E_1\,\hat{\mathbf{x}} + E_2\,\hat{\mathbf{y}}\,, \tag{5.33}$$

where $E_1$ and $E_2$ are, in general, complex quantities. Hence, the ***polarization vector*** is given by

$$\hat{\mathbf{p}} = \frac{E_1}{\sqrt{|E_1|^2 + |E_2|^2}}\,\hat{\mathbf{x}} + \frac{E_2}{\sqrt{|E_1|^2 + |E_2|^2}}\,\hat{\mathbf{y}}\,. \tag{5.34}$$

Since the reference of the time frame is arbitrary, $E_1$ can be chosen as a real quantity and the ratio of the electric field components can be expressed by

$$\frac{E_2}{E_1} = \alpha e^{j\delta} , \tag{5.35}$$

where both $\alpha$ and $\delta$ are real quantities ($\alpha \geq 0$, $|\delta| \leq \pi$). The time-varying expression for the electric field can now be written in the following form:

$$E(z,t) = E_x\,\hat{\mathbf{x}} + E_y\,\hat{\mathbf{y}} = E_1\left\{\cos(\omega t - kz)\,\hat{\mathbf{x}} + \alpha\cos(\omega t - kz + \delta)\,\hat{\mathbf{y}}\right\} .$$

By eliminating $t$ from the expressions for $E_x$ and $E_y$, the trace of the electric field vector can be obtained. Noting that

$$\cos(\omega t - kz + \delta) = \cos(\omega t - kz)\cos\delta - \sin(\omega t - kz)\sin\delta ,$$

$$\cos(\omega t - kz) = \frac{E_x}{E_1} ,$$

and

$$\sin(\omega t - kz) = \sqrt{1 - \left(\frac{E_x}{E_1}\right)^2} ,$$

it can easily be shown that

$$\left(\frac{E_x}{E_1}\right)^2 - 2\,\frac{\cos\delta}{\alpha}\left(\frac{E_x}{E_1}\cdot\frac{E_y}{E_1}\right) + \frac{1}{\alpha^2}\left(\frac{E_y}{E_1}\right)^2 = \sin^2\delta . \tag{5.36}$$

Equation (5.36) represents an ellipse, as shown in Fig. 5-4. Note that when $\delta > 0$ the tip of the electric field moves clockwise on the ellipse as time proceeds. This wave, by definition, is a ***left-hand elliptically polarized wave***. Conversely, when $\delta < 0$ the tip of the electric field moves counterclockwise and the wave is a ***right-hand elliptically polarized wave***. According to the IEEE definition for handedness of elliptically polarized waves, a wave is called ***right-hand polarized*** when the right-hand fingers of an observer, facing the receding wave, follow the tip of the electric field, his/her thumb points towards the direction of wave propagation. The definition of a left-hand polarized wave is analogous.

Two special cases are noteworthy: (1) $\delta = 0$ and (2) $\delta = \pm\frac{\pi}{2}$ and $\alpha = 1$. In the first case Eq. (5.36) reduces to an equation for a line given by

$$\frac{E_y}{E_x} = \alpha , \qquad (\delta = 0 \;\rightarrow\; \text{linear polarization})$$

for which the handedness is irrelevant. For the second case ($\delta = \pm\pi/2$), the ellipse degenerates into a circle. The ***polarization unit vector*** of the wave is defined as

$$\hat{\mathbf{p}} = \frac{\mathbf{E}}{\sqrt{\mathbf{E}\cdot\mathbf{E}^*}} = \frac{E_x\,\hat{\mathbf{x}} + E_y\,\hat{\mathbf{y}}}{\sqrt{|E_x|^2 + |E_y|^2}} = \frac{\hat{\mathbf{x}} + \alpha e^{i\delta}\,\hat{\mathbf{y}}}{\sqrt{1+\alpha^2}} ,$$

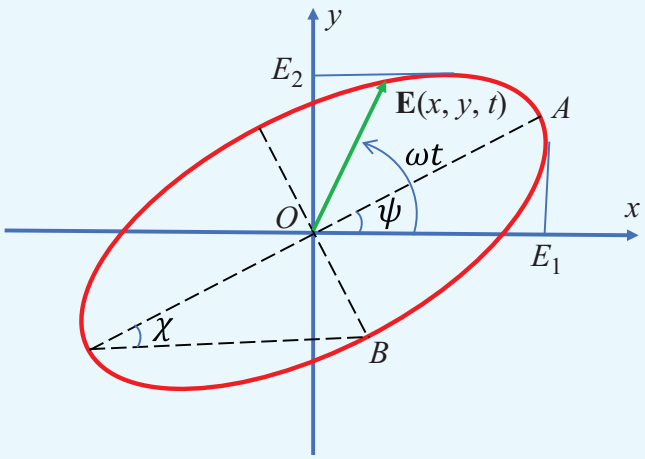


**Figure 5-4:** Polarization ellipse for a plane wave having tilt angle $\psi$ and ellipticity angle $\chi$.

with the $x$-axis as the reference axis.

As shown in Fig. 5-4, the polarization ellipse can be expressed uniquely in terms of two angles known as the ***ellipticity angle*** ($\chi$) and the ***tilt angle*** ($\psi$). The ellipticity angle for an ellipse is defined as

$$\chi = \tan^{-1}\frac{OB}{OA} = \tan^{-1}\frac{1}{\text{AR}} ,$$

where $\text{AR} = OA/OB$ is known as the ***axial ratio***. The ellipticity angle can vary from zero for linear polarization to 45° for circular polarization. The tilt angle $\psi$ can vary from zero to 180° ($0 \le \psi \le 180°$) and the ellipticity angle $\chi$ can vary from $-45°$ to $+45°$. To define the handedness of the polarization, the ellipticity angle is given a sign. *The ellipticity angle is defined as negative for right-hand and positive for left-hand elliptical polarizations, respectively.*

The orientation and ellipticity angles can be expressed in terms of $\alpha$ and $\delta$ and vice versa. Assuming that $\alpha$ and $\delta$ for a wave are known, $\psi$ and $\chi$ can be obtained from

$$\tan(2\psi) = \tan(2\gamma)\cos\delta, \qquad \sin(2\chi) = \sin(2\gamma)\sin\delta , \tag{5.37}$$

where

$$\gamma = \tan^{-1}\alpha .$$

Conversely, if $\psi$ and $\chi$ are known for a wave, $\alpha$ and $\delta$ can be obtained from

$$\tan\delta = \frac{\tan 2\chi}{\sin 2\psi} , \tag{5.38a}$$

$$\cos 2\gamma = \cos 2\chi \cos 2\psi , \tag{5.38b}$$

and

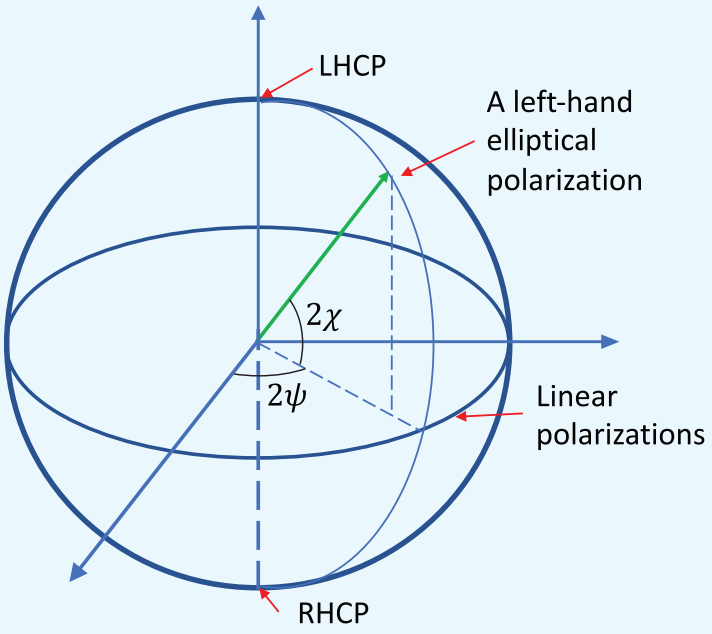


**Figure 5-5:** A Poincaré sphere representing different polarization states of transverse electromagnetic waves. There is a one-to-one relation between a point on the surface of a Poincaré sphere and the polarization state of the wave. Points along the equator represent linear polarizations, the north pole represents left-hand circular polarization (LHCP), and the south pole represents right-hand circular polarization (RHCP).

$$\alpha = \tan\gamma\,. \tag{5.38c}$$

Equations (5.38a) and (5.38c) show that when $\chi = +45^\circ$ then $\delta = 90^\circ$ and $\gamma = 45^\circ$, which implies that $\alpha = 1$. Therefore $\chi = +45^\circ$ is a left-hand circularly polarized wave. Similarly, it can be shown that $\chi = -45^\circ$ corresponds to a right-hand circularly polarized wave.

Since the polarization of a wave is fully characterized by two independent angles, the polarization state of a wave can be uniquely represented by a point on the surface of a sphere, as shown in Fig. 5-5. This sphere is known as the ***Poincaré sphere***. Simple inspections reveal that the linear polarizations are mapped along the equator of the Poincaré sphere and the left-hand polarizations are mapped onto the upper hemisphere, whereas the right-hand polarized waves are mapped on the surface of the lower hemisphere. The left-hand and right-hand circular polarizations are, respectively, mapped on the north and south poles of the Poincaré sphere.

## 5-3 Plane Waves in Anisotropic Media

As mentioned earlier, in certain materials, the directions of the electric field intensity and the electric flux density differ due to some intrinsic material behavior known as ***electric***

***anisotropy***. In this case the electric flux density is related to the electric field intensity by a dielectric permittivity tensor $\varepsilon_0\overline{\overline{\varepsilon}}_r$:

$$\mathbf{D} = \varepsilon_0\overline{\overline{\varepsilon}}_r\,\mathbf{E}\,. \tag{5.39}$$

Similarly for a magnetically anisotropic medium, the magnetic flux density and the magnetic field density are related by

$$\mathbf{B} = \mu_0\overline{\overline{\mu}}_r\,\mathbf{H}\,. \tag{5.40}$$

In this section we are interested in obtaining the possible plane-wave solutions for a source-free homogeneous anisotropic medium. Let us begin with a medium that is only electrically anisotropic whose relative permittivity tensor in Cartesian coordinates is given by

$$\overline{\overline{\varepsilon}}_r = \begin{bmatrix} \varepsilon_{xx} & \varepsilon_{xy} & \varepsilon_{xz} \\ \varepsilon_{yx} & \varepsilon_{yy} & \varepsilon_{yz} \\ \varepsilon_{zx} & \varepsilon_{zy} & \varepsilon_{zz} \end{bmatrix}\,. \tag{5.41}$$

Starting from Maxwell's equations and following the same procedure that led to Eq. (5.2), we can easily show that

$$\nabla\times\nabla\times\mathbf{E} - k^2\overline{\overline{\varepsilon}}_r\,\mathbf{E} = 0\,, \tag{5.42a}$$

where $k^2 = \omega^2\varepsilon_0\mu_0\mu_r$ with $\mu_r$ being the relative permeability of the medium. A similar wave equation for the magnetic field can also be obtained:

$$\nabla\times\left[\overline{\overline{\varepsilon}}_r^{-1}\nabla\times\mathbf{H}\right] - k^2\,\mathbf{H} = 0\,. \tag{5.42b}$$

We are seeking a solution of the following form:

$$\mathbf{E} = \mathbf{E}_0 e^{i\mathbf{K}\cdot\mathbf{r}} \tag{5.43}$$

such that it satisfies Eq. (5.42a). To facilitate a tractable solution, let us consider the curl ($\nabla\times$) operator in the Cartesian coordinate system:

$$\begin{aligned}\nabla\times\mathbf{E} &= \begin{vmatrix} \hat{\mathbf{x}} & \hat{\mathbf{y}} & \hat{\mathbf{z}} \\ \dfrac{\partial}{\partial x} & \dfrac{\partial}{\partial y} & \dfrac{\partial}{\partial z} \\ E_x & E_y & E_z \end{vmatrix} \\ &= \left(\frac{\partial E_z}{\partial y} - \frac{\partial E_y}{\partial z}\right)\hat{\mathbf{x}} - \left(\frac{\partial E_z}{\partial x} - \frac{\partial E_x}{\partial z}\right)\hat{\mathbf{y}} + \left(\frac{\partial E_y}{\partial x} - \frac{\partial E_x}{\partial y}\right)\hat{\mathbf{z}}\,,\end{aligned}$$

which can be reconfigured in the form

$$\nabla \times \mathbf{E} = \begin{pmatrix} 0 & -\dfrac{\partial}{\partial z} & \dfrac{\partial}{\partial y} \\ \dfrac{\partial}{\partial z} & 0 & -\dfrac{\partial}{\partial x} \\ -\dfrac{\partial}{\partial y} & \dfrac{\partial}{\partial x} & 0 \end{pmatrix} \begin{pmatrix} E_x \\ E_y \\ E_z \end{pmatrix} . \tag{5.44}$$

Now it is interesting to note that the $\nabla \times \nabla \times$ operator can easily be represented as the product of two identical matrices, which yields

$$\nabla \times \nabla \times = \begin{pmatrix} -\left(\dfrac{\partial^2}{\partial z^2} + \dfrac{\partial^2}{\partial y^2}\right) & \dfrac{\partial^2}{\partial x\, \partial y} & \dfrac{\partial^2}{\partial x\, \partial z} \\ \dfrac{\partial^2}{\partial y\, \partial x} & -\left(\dfrac{\partial^2}{\partial x^2} + \dfrac{\partial^2}{\partial z^2}\right) & \dfrac{\partial^2}{\partial y\, \partial z} \\ \dfrac{\partial^2}{\partial z\, \partial x} & \dfrac{\partial^2}{\partial z\, \partial y} & -\left(\dfrac{\partial^2}{\partial y^2} + \dfrac{\partial^2}{\partial x^2}\right) \end{pmatrix} . \tag{5.45}$$

Substituting Eq. (5.45) into Eq. (5.42a) and using Eq. (5.43), the differential equation given by Eq. (5.41) reduces to the following linear equation:

$$\begin{pmatrix} K_y^2 + K_z^2 - k^2\varepsilon_{xx} & -(K_yK_x + k^2\varepsilon_{xy}) & -(K_xK_z + k^2\varepsilon_{xz}) \\ -(K_yK_x + k^2\varepsilon_{yx}) & K_x^2 + K_z^2 - k^2\varepsilon_{yy} & -(K_yK_z + k^2\varepsilon_{yz}) \\ -(K_xK_z + k^2\varepsilon_{zx}) & -(K_yK_z + k^2\varepsilon_{zy}) & K_x^2 + K_y^2 - k^2\varepsilon_{zz} \end{pmatrix} \begin{pmatrix} E_x \\ E_y \\ E_z \end{pmatrix} = 0 , \tag{5.46}$$

where as before $\mathbf{K} = K_x\,\hat{\mathbf{x}} + K_y\,\hat{\mathbf{y}} + K_z\,\hat{\mathbf{z}}$. To obtain a nontrivial solution for Eq. (5.46), the determinant of the dispersion matrix must vanish. This will provide a polynomial equation for $K_x$, $K_y$, and $K_z$ whose zeros provide relationships for $K_z$ in terms of $K_x$ and $K_y$.

Using Eq. (5.19b), the wave vector $\mathbf{K} = k\,\hat{\mathbf{k}}$ can be written as

$$\mathbf{K} = kn(\alpha\,\hat{\mathbf{x}} + \beta\,\hat{\mathbf{y}} + \gamma\,\hat{\mathbf{z}}) , \tag{5.47}$$

with

$$\begin{aligned} \alpha &= \sin\theta\cos\phi , \\ \beta &= \sin\theta\sin\phi , \\ \gamma &= \cos\theta , \end{aligned}$$

where $n$ is the index of refraction for a given mode, $k = \omega\sqrt{\mu_0\varepsilon_0}$, and $\theta$ and $\phi$ denote the spherical coordinates of a unit vector along the wave vector $\mathbf{K}$ in the $(x,y,z)$ coordinate system. The determinant of Eq. (5.46) vanishes when the following equation is satisfied:

$$An^4 + Bn^2 + |\overline{\overline{\varepsilon}}_{\mathrm{r}}| = 0 , \tag{5.48}$$

where $|\overline{\overline{\varepsilon}}_r|$ is the determinant of the permittivity tensor, and

$$A = \varepsilon_{xx}\alpha^2 + \varepsilon_{yy}\beta^2 + \varepsilon_{zz}\gamma^2 + (\varepsilon_{xy}+\varepsilon_{yx})\alpha\beta + (\varepsilon_{xz}+\varepsilon_{zx})\alpha\gamma + (\varepsilon_{yz}+\varepsilon_{zy})\beta\gamma \tag{5.49a}$$

and

$$\begin{aligned} B = {} & (\varepsilon_{xx}\varepsilon_{yy} - \varepsilon_{xy}\varepsilon_{yz})(\gamma^2 - 1) + (\varepsilon_{xx}\varepsilon_{zz} - \varepsilon_{xz}\varepsilon_{zx})(\beta^2 - 1) + (\varepsilon_{yy}\varepsilon_{zz} - \varepsilon_{yz}\varepsilon_{zy})(\alpha^2 - 1) \\ & + [\varepsilon_{yx}\varepsilon_{zy} + \varepsilon_{xy}\varepsilon_{yz} - \varepsilon_{yy}(\varepsilon_{xz}+\varepsilon_{zx})]\,\alpha\gamma \\ & + [\varepsilon_{xz}\varepsilon_{zy} + \varepsilon_{yz}\varepsilon_{zx} - \varepsilon_{zz}(\varepsilon_{xy}+\varepsilon_{yx})]\,\alpha\beta \\ & + [\varepsilon_{yz}\varepsilon_{xz} + \varepsilon_{zx}\varepsilon_{xy} - \varepsilon_{xx}(\varepsilon_{yz}+\varepsilon_{zy})]\,\beta\gamma\,. \end{aligned} \tag{5.49b}$$

Since the determinant of Eq. (5.46) is zero, two components of the electric field can be obtained in terms of the third component. Denoting the entries of the dispersion matrix by $d_{ij}$ with $i = 1,2,3$ and $j = 1,2,3$, from Eq. (5.46) we have

$$\begin{pmatrix} d_{11} & d_{12} \\ d_{21} & d_{22} \end{pmatrix} \begin{pmatrix} E_x \\ E_y \end{pmatrix} = -\begin{pmatrix} d_{13} \\ d_{23} \end{pmatrix} E_z\,,$$

or equivalently,

$$\begin{pmatrix} E_x \\ E_y \end{pmatrix} = \frac{-E_z}{d_{11}d_{22} - d_{12}d_{21}} \begin{pmatrix} d_{22} & -d_{12} \\ -d_{21} & d_{11} \end{pmatrix} \begin{pmatrix} d_{13} \\ d_{23} \end{pmatrix}\,. \tag{5.50}$$

Hence,

$$E_x = \frac{d_{12}d_{23} - d_{22}d_{13}}{d_{11}d_{22} - d_{12}d_{21}}\,E_z \tag{5.51a}$$

and

$$E_y = \frac{d_{21}d_{13} - d_{11}d_{23}}{d_{11}d_{22} - d_{12}d_{21}}\,E_z\,. \tag{5.51b}$$

Now Eq. (5.48) can be solved for $n$, with two possible solutions:

$$n_1 = \left( \frac{-B - \sqrt{B^2 - 4A|\overline{\overline{\varepsilon}}_r|}}{2A} \right)^{1/2} \tag{5.52a}$$

and

$$n_2 = \left( \frac{-B + \sqrt{B^2 - 4A|\overline{\overline{\varepsilon}}_r|}}{2A} \right)^{1/2}\,. \tag{5.52b}$$

Note that we are eliminating two other solutions for which the real part of $n$ is negative. Such a medium is referred to as a ***double refracting medium***, which can support two different types of waves simultaneously. The electric field in such a medium can be written as

$$\mathbf{E} = \mathbf{E}_1 e^{ikn_1(\alpha x + \beta y + \gamma z)} + \mathbf{E}_2 e^{ikn_2(\alpha x + \beta y + \gamma z)}\,.$$

The corresponding magnetic field is given by

$$\mathbf{H} = \frac{1}{\omega\mu_0\mu_r}\left(\mathbf{K}_1 \times \mathbf{E}_1 e^{i\mathbf{K}_1\cdot\mathbf{r}} + \mathbf{K}_2 \times \mathbf{E}_2 e^{i\mathbf{K}_2\cdot\mathbf{r}}\right) , \tag{5.53}$$

where $\mathbf{K}_{1,2} = kn_{1,2}(\alpha\,\hat{\mathbf{x}} + \beta\,\hat{\mathbf{y}} + \gamma\,\hat{\mathbf{z}})$.

The case of a magnetically anisotropic medium can be studied using a similar procedure, assuming the permittivity is scalar ($\varepsilon = \varepsilon_0\varepsilon_r$) and the permeability is a tensor $\overline{\overline{\mu}} = \mu_0\overline{\overline{\mu}}_r$ with

$$\overline{\overline{\mu}}_r = \begin{pmatrix} \mu_{xx} & \mu_{xy} & \mu_{xz} \\ \mu_{yx} & \mu_{yy} & \mu_{yz} \\ \mu_{zx} & \mu_{zy} & \mu_{zz} \end{pmatrix} . \tag{5.54}$$

By applying the duality to Eqs. (5.42a) and (5.42a), we obtain

$$\nabla \times \nabla \times \mathbf{H} - k^2\,\overline{\overline{\mu}}_r\,\mathbf{H} = 0 \tag{5.55a}$$

and

$$\nabla \times (\overline{\overline{\mu}}_r^{-1}\,\nabla \times \mathbf{E}) - k^2\,\mathbf{E} = 0\,, \tag{5.55b}$$

where $k^2 = \omega^2\mu_0\varepsilon_0\varepsilon_r$. The dispersion matrix can be obtained from Eq. (5.46) by replacing $\varepsilon_{ij}$ with $\mu_{ij}$. By applying duality, the rest of the problem treatment is similar to what was presented for media with permittivity tensors.

### 5-3.1 Special Case: Homogeneous Isotropic Medium

In an isotropic medium, $\overline{\overline{\varepsilon}}_r = \varepsilon_r\overline{\overline{I}}$, where $\overline{\overline{I}}$ is the identity matrix. Even for this simpler case, calculating the determinant of Eq. (5.46) and simplifying the result can be cumbersome. To simplify the process, an approach based on eigenanalysis can be pursued. As shown earlier in Eq. (5.44) for a plane-wave solution, $\nabla \times \mathbf{E}$ can be represented in terms of an antisymmetric matrix $\overline{\overline{C}}$ given by

$$\overline{\overline{C}} = \begin{pmatrix} 0 & -iK_z & iK_y \\ -iK_z & 0 & -iK_x \\ -iK_y & iK_x & 0 \end{pmatrix} .$$

This matrix can be diagonalized and written as $\overline{\overline{C}} = \overline{\overline{Q}}\,\overline{\overline{\Lambda}}\,\overline{\overline{Q}}^{-1}$, where $\overline{\overline{Q}}$ is the matrix of eigenvectors and $\overline{\overline{\Lambda}}$ is a diagonal matrix whose entries are the eigenvalues of $\overline{\overline{C}}$. It can be shown that

$$\overline{\overline{\Lambda}} = \begin{pmatrix} 0 & 0 & 0 \\ 0 & -\sqrt{K_x^2 + K_y^2 + K_z^2} & 0 \\ 0 & 0 & \sqrt{K_x^2 + K_y^2 + K_z^2} \end{pmatrix} . \tag{5.56}$$

It was also shown that $\nabla \times \nabla \times \mathbf{E}$ can be expressed in terms of a matrix equation whose coefficient is given by $\overline{\overline{C}} \cdot \overline{\overline{C}}$. But

$$\overline{\overline{C}} \cdot \overline{\overline{C}} = \overline{\overline{Q}}\,\overline{\overline{\Lambda}}\,\overline{\overline{Q}}^{-1}\overline{\overline{Q}}\,\overline{\overline{\Lambda}}\,\overline{\overline{Q}}^{-1} = \overline{\overline{Q}}\,\overline{\overline{\Lambda}}^{(2)}\overline{\overline{Q}}^{-1}\,, \tag{5.57}$$

where $\overline{\overline{\Lambda}}^{(2)}$ is a diagonal matrix whose entries are simply the square of the eigenvalues of $\overline{\overline{C}}$. Also, noting that

$$\overline{\overline{\varepsilon}}_{\mathrm{r}} = \varepsilon_{\mathrm{r}}\overline{\overline{I}} = \varepsilon_{\mathrm{r}}\overline{\overline{Q}}\,\overline{\overline{I}}\,\overline{\overline{Q}}^{-1}\,,$$

the operator $(\nabla \times \nabla \times -\omega^2\mu\varepsilon\overline{\overline{I}})$ for the plane-wave solution can be expressed as

$$\overline{\overline{Q}}\begin{pmatrix} -\omega^2\mu\varepsilon & 0 & 0 \\ 0 & -\omega^2\mu\varepsilon + K_x^2 + K_y^2 + K_z^2 & 0 \\ 0 & 0 & -\omega^2\mu\varepsilon + K_x^2 + K_y^2 + K_z^2 \end{pmatrix}\overline{\overline{Q}}^{-1}\,, \tag{5.58}$$

whose determinant is zero if

$$K_x^2 + K_y^2 + K_z^2 = \omega^2\mu\varepsilon\,,$$

which is the expected dispersion relation for the homogeneous isotropic medium.

### 5-3.2 Special Case: Uniaxial Medium

Another case for which a nontrivial solution for the matrix equation (5.46) can be obtained is for a uniaxial medium. For such a medium, the permittivity tensor is diagonal with two of its diagonal elements being equal. Without loss of generality, let us assume that

$$\overline{\overline{\varepsilon}}_{\mathrm{r}} = \begin{pmatrix} \varepsilon_{xx} & 0 & 0 \\ 0 & \varepsilon_{xx} & 0 \\ 0 & 0 & \varepsilon_{zz} \end{pmatrix}\,, \tag{5.59}$$

with $\varepsilon_{xx} \neq \varepsilon_{zz}$. After much algebraic manipulation, the determinant of the matrix given in Eq. (5.46) is found to be

$$\Delta = -k^2(\varepsilon_{xx}k^2 - K_x^2 - K_y^2 - K_z^2)\left[\varepsilon_{xx}(\varepsilon_{zz}k^2 - K_x^2 - K_y^2) - \varepsilon_{zz}K_z^2\right].$$

Setting $\Delta = 0$, two dispersion relations are obtained. The first solution, given by

$$K_x^2 + K_y^2 + K_z^2 = \omega^2\mu\varepsilon_0\varepsilon_{xx}\,, \tag{5.60}$$

is similar to the dispersion relation for an isotropic medium and the plane-wave solution for this mode is referred to as an ***ordinary wave***. The second solution provides the following dispersion relation:

$$K_x^2 + K_y^2 + \frac{\varepsilon_{zz}}{\varepsilon_{xx}}K_z^2 = \omega^2\mu\varepsilon_0\varepsilon_{zz} \tag{5.61}$$

and is known as an ***extraordinary wave***. If the direction of wave propagation in the uniaxial medium is determined by $\theta, \phi$ in such a way that

$$K_x = k \sin\theta \cos\phi \ ,$$
$$K_y = k \sin\theta \sin\phi \ ,$$
$$K_z = k \cos\theta \ ,$$

then substituting these into Eqs. (5.60) and (5.61), for ordinary and extraordinary waves, we have the following dispersion relations respectively:

$$k^2 = \omega^2 \mu \varepsilon_0 \varepsilon_{xx} \tag{5.62a}$$

and

$$k^2 = \omega^2 \mu \varepsilon_0 \left( \frac{\sin^2\theta}{\varepsilon_{zz}} + \frac{\cos^2\theta}{\varepsilon_{xx}} \right)^{-1} . \tag{5.62b}$$

## 5-4 kDB Coordinate System for Plane Waves in Bianisotropic Media

In the preceding sections it was shown that electric and magnetic fields of the form of $\mathbf{E}_0 e^{i\mathbf{K}\cdot\mathbf{r}}$ and $\mathbf{H}_0 e^{i\mathbf{K}\cdot\mathbf{r}}$ represent plane-wave solutions to source-free Maxwell's equations in a homogeneous unbounded medium. Substituting these solutions into Maxwell's equations, it can easily be shown that

$$\mathbf{K} \times \mathbf{E}_0 = \omega \mathbf{B}_0 \ , \tag{5.63a}$$
$$\mathbf{K} \times \mathbf{H}_0 = -\omega \mathbf{D}_0 \ , \tag{5.63b}$$
$$\mathbf{K} \cdot \mathbf{D}_0 = 0 \ , \tag{5.63c}$$
$$\mathbf{K} \cdot \mathbf{B}_0 = 0 \ , \tag{5.63d}$$

where it was assumed that the electric and magnetic flux densities can also be expressed as

$$\mathbf{B} = \mathbf{B}_0 e^{i\mathbf{K}\cdot\mathbf{r}}$$

and

$$\mathbf{D} = \mathbf{D}_0 e^{i\mathbf{K}\cdot\mathbf{r}}.$$

As indicated by Eq. (5.63c) and Eq. (5.63d), it is obvious that $\mathbf{D}_0$ and $\mathbf{B}_0$ are perpendicular to the $\mathbf{K}$ vector. The plane that contains $\mathbf{D}_0$ and $\mathbf{B}_0$ and is perpendicular to $\mathbf{K}$ will be referred to as the ***DB plane***. For isotropic media where $\mathbf{D}_0 = \varepsilon \mathbf{E}_0$ and $\mathbf{B}_0 = \mu \mathbf{H}_0$, the electric field $\mathbf{E}_0$ and magnetic field $\mathbf{H}_0$ are also perpendicular to $\mathbf{K}$. However, for anisotropic media where, for example, $\mathbf{D}_0 = \overline{\overline{\varepsilon}} \mathbf{E}_0$, the electric field is no longer perpendicular to $\mathbf{K}$.

Considering a coordinate system where one of the axes is along $\mathbf{K}$, say the $z'$-axis, then $\mathbf{B}_0$ and $\mathbf{D}_0$ in an anisotropic medium would only have $x'$ and $y'$ components. Hence

$$\mathbf{D}_0 = D_{0x}\,\hat{\mathbf{x}}' + D_{0y}\,\hat{\mathbf{y}}'$$

and

$$\mathbf{B}_0 = B_{0x}\,\hat{\mathbf{x}}' + B_{0y}\,\hat{\mathbf{y}}' \,.$$

In this coordinate system let us denote the bianisotropic constitutive relations as

$$\mathbf{E} = \overline{\overline{\Gamma}}\,\mathbf{D} + \overline{\overline{\vartheta}}\,\mathbf{B} \tag{5.64a}$$

and

$$\mathbf{H} = \overline{\overline{\chi}}\,\mathbf{D} + \overline{\overline{\nu}}\,\mathbf{B}\,, \tag{5.64b}$$

where $\overline{\overline{\Gamma}}$ and $\overline{\overline{\nu}}$ are, for example, the ***impermittivity*** and ***impermeability*** tensors. Using Eqs. (5.64a) and (5.64b) in Eqs. (5.63a) and (5.63b) and noting that $\mathbf{K} = k\,\hat{\mathbf{z}}'$, it can be shown that

$$E_{0x}\,\hat{\mathbf{y}}' - E_{0y}\,\hat{\mathbf{x}}' = \frac{\omega}{k}\,\mathbf{B}_0\,, \tag{5.65a}$$

$$H_{0x}\,\hat{\mathbf{y}}' - H_{0y}\,\hat{\mathbf{x}}' = -\frac{\omega}{k}\,\mathbf{D}_0, \tag{5.65b}$$

and

$$\left.\begin{aligned} \frac{\omega}{k}\,B_{0x} &= -E_{0y} \\ &= -[\gamma_{21}D_{0x} + \gamma_{22}D_{0y} + \vartheta_{21}B_{0x} + \vartheta_{22}B_{0y}]\,, \\ \frac{\omega}{k}\,B_{0y} &= E_{0x} \\ &= \gamma_{11}D_{0x} + \gamma_{12}D_{0y} + \vartheta_{11}B_{0x} + \vartheta_{12}B_{0y}\,, \end{aligned}\right\} \tag{5.66a}$$

$$\left.\begin{aligned} \frac{\omega}{k}\,D_{0x} &= H_{0y} \\ &= \chi_{21}D_{0x} + \chi_{22}D_{0y} + \nu_{21}B_{0x} + \nu_{22}B_{0y}]\,, \\ \frac{\omega}{k}\,D_{0y} &= -H_{0x} \\ &= -[\chi_{11}D_{0x} + \chi_{12}D_{0y} + \nu_{11}B_{0x} + \nu_{12}B_{0y}]\,. \end{aligned}\right\} \tag{5.66b}$$

Denoting $\frac{\omega}{k} = u$ as a ***phase velocity*** and rearranging Eqs. (5.66a) and (5.66b) in matrix notation leads to

$$\begin{pmatrix} u+\vartheta_{21} & \vartheta_{22} \\ -\vartheta_{11} & u-\vartheta_{12} \end{pmatrix} \begin{pmatrix} B_{0x} \\ B_{0y} \end{pmatrix} = \begin{pmatrix} -\gamma_{21} & -\gamma_{22} \\ \gamma_{11} & \gamma_{12} \end{pmatrix} \begin{pmatrix} D_{0x} \\ D_{0y} \end{pmatrix} \tag{5.67a}$$

and

$$\begin{pmatrix} u-\chi_{21} & -\chi_{22} \\ \chi_{11} & u+\chi_{12} \end{pmatrix} \begin{pmatrix} D_{0x} \\ D_{0y} \end{pmatrix} = \begin{pmatrix} \nu_{21} & \nu_{22} \\ -\nu_{11} & -\nu_{12} \end{pmatrix} \begin{pmatrix} B_{0x} \\ B_{0y} \end{pmatrix}. \tag{5.67b}$$

The ***dispersion relation***, an equation for $k$ in terms of the medium parameters, can be obtained by first finding $D_{0x}$ and $D_{0y}$ in terms of $B_{0x}$ and $B_{0y}$ from Eq. (5.67a) and substituting it in Eq. (5.67b). This way, a $(2\times 2)$ matrix coefficient of $B_{0x}$ and $B_{0y}$ is obtained. For a nontrivial solution, the determinant of this $(2\times 2)$ matrix must be set to zero and this will provide the dispersion equation for $k$. As was the case before in Eq. (5.46), finding the solution is not trivial. However, in the kDB system approach we need to find the determinant of a $(2\times 2)$ matrix as opposed to a $(3\times 3)$ matrix.

Let us first consider the simple case of an isotropic medium. For this problem, the constitutive relations, Eqs. (5.64a) and (5.64b), take the following form:

$$\mathbf{E} = \gamma\,\mathbf{D}$$

and

$$\mathbf{H} = \nu\,\mathbf{B}\,.$$

Also, Eqs. (5.67a) and (5.67b) simplify to

$$\begin{pmatrix} u & 0 \\ 0 & u \end{pmatrix}\begin{pmatrix} B_{0x} \\ B_{0y} \end{pmatrix} = \begin{pmatrix} 0 & -\gamma \\ \gamma & 0 \end{pmatrix}\begin{pmatrix} D_{0x} \\ D_{0y} \end{pmatrix} \tag{5.68a}$$

and

$$\begin{pmatrix} u & 0 \\ 0 & u \end{pmatrix}\begin{pmatrix} D_{0x} \\ D_{0y} \end{pmatrix} = \begin{pmatrix} 0 & \nu \\ -\nu & 0 \end{pmatrix}\begin{pmatrix} B_{0x} \\ B_{0y} \end{pmatrix}. \tag{5.68b}$$

Solving for $\mathbf{D}$ from Eq. (5.68b) and substituting in Eq. (5.68a) leads to

$$\begin{aligned} u\begin{pmatrix} B_{0x} \\ B_{0y} \end{pmatrix} &= \begin{pmatrix} 0 & -\gamma \\ \gamma & 0 \end{pmatrix}\begin{pmatrix} 0 & \nu/u \\ -\nu/u & 0 \end{pmatrix}\begin{pmatrix} B_{0x} \\ B_{0y} \end{pmatrix} \\ &= \begin{pmatrix} \gamma\nu/u & 0 \\ 0 & \gamma\nu/u \end{pmatrix}\begin{pmatrix} B_{0x} \\ B_{0y} \end{pmatrix}. \end{aligned}$$

In compact form,

$$\begin{pmatrix} u-\gamma\nu/u & 0 \\ 0 & u-\gamma\nu/u \end{pmatrix}\begin{pmatrix} B_{0x} \\ B_{0y} \end{pmatrix} = 0\,. \tag{5.69}$$

The determinant of Eq. (5.69) is zero if and only if

$$u^2 = \gamma\nu = \frac{1}{\varepsilon\mu}\,,$$

or simply

$$k = \omega\sqrt{\mu\varepsilon}$$

(recall that $u = \omega/k$). Next we consider a uniaxial medium with constitutive relations

$$\mathbf{E} = \overline{\overline{\Gamma}}\,\mathbf{D} \tag{5.70a}$$

and

$$\mathbf{H} = \nu\,\mathbf{B}\,, \tag{5.70b}$$

where the impermittivity matrix takes the following form:

$$\overline{\overline{\Gamma}} = \begin{pmatrix} \gamma & 0 & 0 \\ 0 & \gamma & 0 \\ 0 & 0 & \gamma_z \end{pmatrix}\,. \tag{5.71}$$

In this coordinate system, suppose that the $\hat{\mathbf{k}}$ vector is along an arbitrary direction defined by angles $\theta$ and $\phi$:

$$\hat{\mathbf{k}} = \sin\theta\cos\phi\;\hat{\mathbf{x}} + \sin\theta\sin\phi\;\hat{\mathbf{y}} + \cos\theta\;\hat{\mathbf{z}}\,.$$

Let us choose a kDB coordinate system so that $\hat{\mathbf{k}} = \hat{\mathbf{z}}'$ and $\hat{\mathbf{x}}'$ is parallel to the $x$–$y$ plane, namely

$$\hat{\mathbf{x}}' = \frac{\hat{\mathbf{k}}\times\hat{\mathbf{z}}}{|\hat{\mathbf{k}}\times\hat{\mathbf{z}}|} = \sin\phi\;\hat{\mathbf{x}} - \cos\phi\;\hat{\mathbf{y}}\,.$$

Also,

$$\hat{\mathbf{y}}' = \hat{\mathbf{z}}'\times\hat{\mathbf{x}}' = \cos\theta\cos\phi\;\hat{\mathbf{x}} + \cos\theta\sin\phi\;\hat{\mathbf{y}} - \sin\theta\;\hat{\mathbf{z}}\,.$$

It can easily be shown that any vector in the general coordinate system can be transformed to the kDB system by the transformation matrix $\overline{\overline{T}}$ given by

$$\mathbf{E}' = \overline{\overline{T}}\mathbf{E}\,, \tag{5.72}$$

where

$$\overline{\overline{T}} = \begin{pmatrix} \sin\phi & -\cos\phi & 0 \\ \cos\theta\cos\phi & \cos\theta\sin\phi & -\sin\theta \\ \sin\theta\cos\phi & \sin\theta\sin\phi & \cos\theta \end{pmatrix}\,. \tag{5.73}$$

Conversely, a vector in the kDB coordinate system can be transformed back to the general coordinate system by

$$\mathbf{D} = \overline{\overline{T}}^{-1}\mathbf{D}'\,, \tag{5.74}$$

where, since the transformation is ***unitary***,

$$\overline{\overline{T}}^{-1} = \overline{\overline{T}}^{\mathrm{t}} = \begin{pmatrix} \sin\phi & \cos\theta\cos\phi & \sin\theta\cos\phi \\ -\cos\phi & \cos\theta\sin\phi & \sin\theta\sin\phi \\ 0 & -\sin\theta & \cos\theta \end{pmatrix}\,. \tag{5.75}$$

Using Eqs. (5.72), (5.70), and (5.75), it can be shown that

$$\mathbf{E}' = \overline{\overline{T}}\,\overline{\overline{\Gamma}}\,\overline{\overline{T}}^{-1}\mathbf{D}'\,,$$

and therefore

$$\begin{aligned}\overline{\overline{\Gamma}}' &= \overline{\overline{T}}\,\overline{\overline{\Gamma}}\,\overline{\overline{T}}^{-1} \\ &= \begin{pmatrix} \gamma_{xx} & 0 & 0 \\ 0 & \gamma_{xx}\cos^2\theta + \gamma_{zz}\sin^2\theta & (\gamma_{xx}-\gamma_{zz})\sin\theta\cos\theta \\ 0 & (\gamma_{xx}-\gamma_{zz})\sin\theta\cos\theta & \gamma_{xx}\sin^2\theta + \gamma_{zz}\cos^2\theta \end{pmatrix} . \end{aligned} \tag{5.76}$$

Using Eq. (5.76) in Eq. (5.67a) provides

$$\begin{pmatrix} u & 0 \\ 0 & u \end{pmatrix} \begin{pmatrix} B_{0x} \\ B_{0y} \end{pmatrix} = \begin{pmatrix} 0 & -\gamma_{xx}\cos^2\theta - \gamma_{zz}\sin^2\theta \\ \gamma_{xx} & 0 \end{pmatrix} \begin{pmatrix} D_{0x} \\ D_{0y} \end{pmatrix} , \tag{5.77}$$

and using Eq. (5.76) in Eq. (5.67b) gives

$$\begin{pmatrix} u & 0 \\ 0 & u \end{pmatrix} \begin{pmatrix} D_{0x} \\ D_{0y} \end{pmatrix} = \begin{pmatrix} 0 & \nu \\ -\nu & 0 \end{pmatrix} \begin{pmatrix} B_{0x} \\ B_{0y} \end{pmatrix} . \tag{5.78}$$

Solving for $D$ from Eq. (5.78) and substituting that in Eq. (5.77) results in

$$u^2 \begin{pmatrix} B_{0x} \\ B_{0y} \end{pmatrix} = \begin{pmatrix} \nu(\gamma_{xx}\cos^2\theta + \gamma_{zz}\sin^2\theta) & 0 \\ 0 & \nu\gamma_{xx} \end{pmatrix} \begin{pmatrix} B_{0x} \\ B_{0y} \end{pmatrix}$$

or

$$\begin{pmatrix} u^2 - \nu(\gamma_{xx}\cos^2\theta + \gamma_{zz}\sin^2\theta) & 0 \\ 0 & u^2 - \nu\gamma_{xx} \end{pmatrix} \begin{pmatrix} B_{0x} \\ B_{0y} \end{pmatrix} = 0 . \tag{5.79}$$

A nontrivial solution for Eq. (5.79) can be obtained when either

$$u^2 = \nu\gamma_{xx} \quad \rightarrow \quad k^2 = \omega^2\mu\varepsilon_{xx} \tag{5.80}$$

(recognizing that $k^2 = K_x^2 + K_y^2 + K_z^2$) or

$$u^2 = \nu(\gamma_{xx}\cos^2\theta + \gamma_{zz}\sin^2\theta) , \tag{5.81}$$

which can be written as

$$\omega^2\mu\varepsilon_{zz} = k^2\cos^2\theta\,\frac{\varepsilon_{zz}}{\varepsilon_{xx}} + k^2\sin^2\theta . \tag{5.82}$$

Also, noting that

$$k^2\sin^2\theta = k^2\sin^2\theta\sin^2\phi + k^2\sin^2\theta\cos^2\phi ,$$

Eq. (5.82) can be written as

$$K_x^2 + K_y^2 + \frac{\varepsilon_{zz}}{\varepsilon_{xx}}K_z^2 = \omega^2\mu\varepsilon_{zz} , \tag{5.83}$$

which is in agreement with Eq. (5.61), noting that here $\varepsilon_{xx}$ and $\varepsilon_{zz}$ are the permittivity values and not the relative permittivity values. Equation (5.80) corresponds to a nontrivial solution for Eq. (5.79) for which $B_{0x} = 0$ and $B_{0y} \neq 0$, and since the resulting dispersion relation

corresponds to that of a plane wave in an isotropic medium with permittivity $\varepsilon = \varepsilon_{xx}$, it is referred to as an ***ordinary wave***. On the other hand, the dispersion relation Eq. (5.83) is a solution of Eq. (5.79) for which $B_{0x} \neq 0$ and $B_{0y} = 0$. From Eq. (5.79) we also note that

$$D_{0x} = \frac{v}{u} B_{0y} = \frac{k}{\omega\mu} B_{0y} \tag{5.84a}$$

and

$$D_{0y} = -\frac{v}{u} B_{0x} = -\frac{k}{\omega\mu} B_{0x} \, . \tag{5.84b}$$

Hence for an ordinary wave, $D_{0y} = 0$, and for an extraordinary wave, $D_{0x} = 0$. For ordinary waves

$$E_{0x} = \frac{1}{\varepsilon_{xx}} D_{0x}$$

and

$$H_{0y} = \frac{1}{\mu} B_{0y} \, .$$

That is, the electric field is parallel to the electric flux density and the electric field is perpendicular to the magnetic field intensity, and both are perpendicular to the direction of propagation. The wave impedance is defined as

$$\eta_o = \frac{E_{0x}}{H_{0y}} = \frac{\mu}{\varepsilon_{xx}} \frac{D_{0x}}{B_{0y}} = \frac{\mu}{\varepsilon_{xx}} \frac{k}{\omega\mu} = \sqrt{\frac{\mu}{\varepsilon_{xx}}} \, .$$

For extraordinary waves, using Eq. (5.76), it can be shown that

$$E_{0y} = \left( \frac{\cos^2\theta}{\varepsilon_{xx}} + \frac{\sin^2\theta}{\varepsilon_{zz}} \right) D_{0y} \tag{5.85a}$$

and

$$E_{0z} = \frac{\varepsilon_{zz} - \varepsilon_{xx}}{\varepsilon_{xx}\varepsilon_{zz}} \sin\theta\cos\theta \, D_{0y} \, . \tag{5.85b}$$

Also, since $B_{0y} = 0$,

$$H_{0x} = \frac{1}{\mu} B_{0x} \, .$$

As shown by Eq. (5.85b), the electric field has a component along the direction of propagation so long as $\theta \neq 0$ or $\theta \neq \pi/2$. It should be noted that $\theta = 0$ corresponds to a case where the wave is propagating along the optical axis ($z$-axis). In such a case, the dispersion relation Eq. (5.82) reduces to that for the ordinary wave ($k^2 = \omega^2\mu\varepsilon_{xx}$), or when $\theta = \pi/2$, $K_x^2 + K_y^2 + K_z^2 = \omega^2\mu\varepsilon_{xx}$, the direction of propagation is perpendicular to the optical axis (propagation along $\pm x$-axis) and the dispersion relation simplifies to

$$k^2 = \omega^2\mu\varepsilon_{zz} \, . \tag{5.86}$$

In this case, **E** is also parallel to **D**:

$$E_{0y} = \frac{1}{\varepsilon_{zz}} D_{0y} \,, \tag{5.87}$$

and like ordinary waves, the electric field is perpendicular to the magnetic field and both are perpendicular to the direction of propagation ($\pm x$-axis). The wave impedance is given by

$$\eta_{\rm e}\,(\theta = \pi/2) = -\frac{E_{0y}}{H_{0x}} = \frac{1}{\varepsilon_{zz}} \frac{k}{\omega} = \frac{\sqrt{\mu \varepsilon_{xx}}}{\varepsilon_{zz}} \,. \tag{5.88}$$

Figure 5-6 shows the direction of propagation, the electric and magnetic flux densities as well as the electric and magnetic fields associated with ordinary and extraordinary waves.

As mentioned earlier, the electric field of an extraordinary wave has a component along the direction of propagation. This indicates that the direction of flow of energy and wave propagation are not the same. The complex Poynting vector can be calculated from

$$\begin{aligned} \mathbf{S} = \frac{1}{2}\,\mathbf{E} \times \mathbf{H}^* &= \frac{1}{2}\,(E_{0y}\,\hat{\mathbf{y}}' + E_{0z}\,\hat{\mathbf{z}}') \times H_{0x}^*\,\hat{\mathbf{x}}' \\ &= \frac{1}{2\mu}\,(E_{0z} B_{0x}^*\,\hat{\mathbf{y}}' - E_{0y} B_{0x}^*\,\hat{\mathbf{z}}') \,. \end{aligned} \tag{5.89}$$

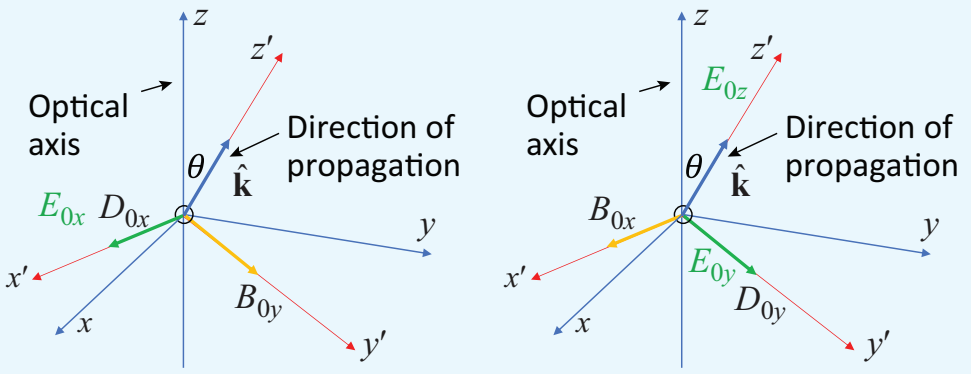


**Figure 5-6:** Configurations of field orientations in a uniaxial dielectric medium with optical axis along $\hat{\mathbf{z}}$: (a) the configuration for an ordinary wave where the direction of the electric flux density and electric field intensity are parallel to each other and perpendicular to the plane formed by the optical axis and the direction of propagation, and (b) the configuration for an extraordinary wave where the electric field intensity and the electric flux intensity lies in the plane formed by the optical axis and the direction of propagation but are no longer parallel to each other.

Noting that $B_{0x} = -\sqrt{\mu/\varepsilon_{xx}}\, D_{0y}$, after some algebraic manipulations it can be shown that the Poynting vector is given by

$$\mathbf{S} = \frac{1}{2}\sqrt{\frac{1}{\mu\varepsilon_{xx}}}\left[\left(\frac{\cos^2\theta}{\varepsilon_{xx}} + \frac{\sin^2\theta}{\varepsilon_{zz}}\right)\hat{\mathbf{z}}' + \frac{\varepsilon_{xx}-\varepsilon_{zz}}{\varepsilon_{xx}\varepsilon_{zz}}\sin\theta\cos\theta\,\hat{\mathbf{y}}'\right]|D_{0y}|^2 \,. \tag{5.90}$$

Here we assumed that the medium is lossless. It is obvious that the Poynting vector has a component along $\hat{\mathbf{y}}'$, in addition to a component along $\hat{\mathbf{z}}'$ (direction of wave propagation). When $\theta = \pi/2$ the Poynting vector has only the $\hat{\mathbf{z}}'$ component. In the case when both $D_{0x}$ and $D_{0y}$ are nonzero, then both ordinary and extraordinary waves can coexist. When $\theta = \pi/2$, $E_{0z} = 0$ for both ordinary and extraordinary waves and the medium is called ***birefringent***, since the phase velocities of the ordinary and extraordinary waves are different. The phase velocity for the ordinary waves can be obtained from

$$u_{\mathrm{p}}^{\mathrm{o}} = \frac{\omega}{k} = \frac{\omega}{\omega\sqrt{\mu\varepsilon_{xx}}} = \frac{1}{\sqrt{\mu\varepsilon_{xx}}} \,, \tag{5.91a}$$

and for the extraordinary wave, Eq. (5.82) leads to

$$u_{\mathrm{p}}^{\mathrm{e}} = \frac{\omega}{k} = \left[\frac{1}{\mu}\left(\frac{\cos^2\theta}{\varepsilon_{xx}} + \frac{\sin^2\theta}{\varepsilon_{zz}}\right)\right]^{1/2} \,. \tag{5.91b}$$

For $\theta = \pi/2$, the phase velocity is

$$u_{\mathrm{p}}^{\mathrm{e}} = \frac{1}{\sqrt{\mu\varepsilon_{zz}}} \,. \tag{5.91c}$$

The electric field propagating in the medium is given by

$$\mathbf{E}(\mathbf{r}) = \frac{D_{0x}}{\varepsilon_{xx}}\exp\left(i\,\frac{\omega}{u_{\mathrm{p}}^{\mathrm{o}}}\,z'\right) + \frac{D_{0y}}{\varepsilon_{zz}}\exp\left(i\,\frac{\omega}{u_{\mathrm{p}}^{\mathrm{e}}}\,z'\right) \,. \tag{5.92}$$

## 5-5 Transverse Electric (TE) and Transverse Magnetic (TM) Field Solutions of the Helmholtz Equation

In the previous section, a special solution of the Helmholtz equation was obtained. In that solution, known as the ***plane-wave solution***, the electric and magnetic fields of elementary waves were found to be orthogonal to each other and to the direction of propagation. That is, both the electric field and magnetic field are in the transverse plane with respect to the direction of propagation, and thus this type of solution is referred to as a ***TEM wave***. This is just one form of many types (modes) of solutions that can satisfy the Helmholtz equation. For example, a class of solutions can be constructed from elementary wave functions where only the electric field or only the magnetic field is in the transverse plane with respect to an arbitrary direction of propagation.

In a source-free region, it was shown that the electric and magnetic fields can be obtained from the electric and magnetic Hertz potentials, which satisfy Helmholtz equations

$$\nabla^2 \mathbf{\Pi} + k^2 \mathbf{\Pi} = 0 \tag{5.93a}$$

and

$$\nabla^2 \mathbf{\Pi}_{\mathrm{m}} + k^2 \mathbf{\Pi}_{\mathrm{m}} = 0 \,, \tag{5.93b}$$

as well as

$$\mathbf{E} = \nabla\nabla \cdot \mathbf{\Pi} + k^2 \mathbf{\Pi} + i\omega\mu \nabla \times \mathbf{\Pi}_{\mathrm{m}} \tag{5.94a}$$

and

$$\mathbf{H} = -i\omega\varepsilon \nabla \times \mathbf{\Pi} + \nabla\nabla \cdot \mathbf{\Pi}_{\mathrm{m}} + k^2 \mathbf{\Pi}_{\mathrm{m}} \,. \tag{5.94b}$$

The TE and TM solutions can be constructed from magnetic and electric Hertz potentials, respectively. Again, to obtain a simple solution we assume the Hertz potential (electric or magnetic) has only one component along the direction of propagation (perpendicular to the transverse plane). Without loss of generality let's assume that the $x$–$y$ plane is the transverse plane. Hence TM modes are generated by an electric Hertz potential

$$\mathbf{\Pi} = \Pi_z \, \hat{\mathbf{z}} \tag{5.95}$$

and $\Pi_{\mathrm{m}} = 0$. Substituting Eq. (5.95) into Eq. (5.94a) gives

$$\mathbf{E} = \nabla \left( \frac{\partial \Pi_z}{\partial z} \right) + k^2 \Pi_z \, \hat{\mathbf{z}} \,. \tag{5.96}$$

Equation (5.96) can be expanded by noting that the $\nabla$ operator may be written as

$$\nabla = \nabla_{\mathrm{t}} + \frac{\partial}{\partial z} \hat{\mathbf{z}} \,,$$

where $\nabla_{\mathrm{t}}$ is a two-dimensional "del" operator in the transverse plane given by

$$\nabla_{\mathrm{t}} = \frac{\partial}{\partial x} \hat{\mathbf{x}} + \frac{\partial}{\partial y} \hat{\mathbf{y}} \,.$$

Hence Eq. (5.96) can be written as

$$\mathbf{E} = \frac{\partial}{\partial z} \nabla_{\mathrm{t}} \Pi_z + \left( \frac{\partial^2 \Pi_z}{\partial z^2} + k^2 \Pi_z \right) \hat{\mathbf{z}} \,. \tag{5.97}$$

Similarly, Eq. (5.94b) can now be expressed as

$$\begin{aligned}\mathbf{H} &= -i\omega\varepsilon\,\nabla\times(\Pi_z\,\hat{\mathbf{z}})\\ &= -i\omega\varepsilon\left(\nabla_{\mathrm{t}}+\frac{\partial}{\partial z}\,\hat{\mathbf{z}}\right)\Pi_z\times\hat{\mathbf{z}}\\ &= -i\omega\varepsilon\,\nabla_{\mathrm{t}}\Pi_z\times\hat{\mathbf{z}}\,.\end{aligned}\tag{5.98}$$

According to Eq. (5.93a), $\Pi_z$ must satisfy the scalar wave equation

$$\nabla^2\Pi_z+k^2\Pi_z=0\,,$$

which can also be written as

$$\nabla_{\mathrm{t}}^2\Pi_z+\frac{\partial^2}{\partial z^2}\,\Pi_z+k^2\Pi_z=0\,.\tag{5.99}$$

Since we chose $z$ as the direction of propagation, we are seeking a solution for $\Pi_z$ of the following form:

$$\Pi_z(\mathbf{r})=\Psi(x,y)\,e^{\pm i\beta z}\,.\tag{5.100}$$

where $\beta$ is the propagation constant along the $z$-axis. Substituting Eq. (5.100) into Eq. (5.99), we get

$$\nabla_{\mathrm{t}}^2\,\Psi+k_{\mathrm{c}}^2\,\Psi=0\,,\tag{5.101}$$

where $k_{\mathrm{c}}^2=k^2-\beta^2$. Equation (5.101) is a two-dimensional wave equation whose solution can be expressed in terms of a wide range of elementary wave functions. For the time being, we assume that appropriate wave functions satisfying Eq. (5.101) are known. Using Eq. (5.100) in Eqs. (5.97) and (5.98) yields

$$\mathbf{E}=(\pm i\beta\,\nabla_{\mathrm{t}}\Psi+k_{\mathrm{c}}^2\,\Psi\,\hat{\mathbf{z}})e^{\pm i\beta z}\tag{5.102a}$$

and **(TM wave)**

$$\mathbf{H}=-i\omega\varepsilon(\nabla_{\mathrm{t}}\Psi\times\hat{\mathbf{z}})e^{\pm i\beta z}\,.\tag{5.102b}$$

Note that $\mathbf{H}$ does not have a $z$-component, and therefore field solutions for Eqs. (5.102a) and (5.102b) are known as ***TM waves***. The ratio of the electric field to the magnetic field components in the transverse plane is independent of position and is known as the ***TM wave impedance***, given by

$$Z_{\mathrm{TM}}=\frac{\hat{\mathbf{z}}\times\mathbf{E}_{\mathrm{t}}}{\mathbf{H}_{\mathrm{t}}}=\frac{\beta}{\omega\varepsilon}\,.\tag{5.103}$$

Another set of modes can be generated from a magnetic Hertz potential $\boldsymbol{\Pi}_{\mathrm{m}}=\Pi_{\mathrm{m}z}\,\hat{\mathbf{z}}$. These modes will be referred to as ***TE modes***. As shown before, the set of fields obtained from a magnetic potential is the dual of those obtained from the dual electric Hertz potential. Thus

we define

$$\Pi_{mz}(r) = \Psi_m(x,y)\, e^{i\beta z}\,, \tag{5.104}$$

whose corresponding fields, using the duality relations, are given by

$$\mathbf{H} = (i\beta\, \nabla_t \Psi_m + k_c^2 \Psi_m\, \hat{\mathbf{z}}) e^{i\beta z} \tag{5.105a}$$

and **(TE wave)**

$$\mathbf{E} = i\omega\mu (\nabla_t \Psi_m \times \hat{\mathbf{z}}) e^{i\beta z} \tag{5.105b}$$

According to the duality relations, the wave admittance, obtained from Eq. (5.103), is given by

$$Y_{TE} = -\frac{\hat{\mathbf{z}} \times \mathbf{H}_t}{\mathbf{E}_t} = \frac{\beta}{\omega\mu}\,. \tag{5.106}$$

### 5-5.1 TM Plane-Wave Reflection and Transmission at Planar Interface between Two Dielectric Media

In this section we consider inhomogeneous media that may be composed of different dielectric or metallic bodies. We begin by first considering simple media whose constitutive parameters are functions of only a single position variable.

As a first example, let's consider an inhomogeneous medium composed of two homogeneous half-space dielectric media with a planar interface, as shown in Fig. 5-7. In this case the permittivity and permeability of the overall medium are only functions of $z$.

Assuming no field variations along the $y$-direction ($\partial/\partial y = 0$), for a TM wave in the upper half-space Eq. (5.101) simplifies to

$$\left(\frac{\partial^2}{\partial x^2} + k_{1c}^2\right) \Psi_1 = 0\,, \tag{5.107a}$$

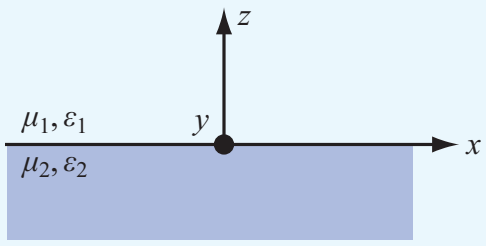


**Figure 5-7:** Wave solution for a half-space dielectric medium.

and for the lower half-space

$$\left(\frac{\partial^2}{\partial x^2}+k_{2c}^2\right)\Psi_2=0\,, \tag{5.107b}$$

where $k_{1c}^2=k_1^2-\beta_1^2$ and $k_{2c}^2=k_2^2-\beta_2^2$. The possible solutions for Eqs. (5.107a) and (5.107b) are of the form $e^{\pm ik_c x}$. Assuming propagation in $+x$-direction and allowing propagation in the $\pm z$-directions, for each half-space, $\Pi_z(r)$ can be obtained from Eq. (5.100):

$$\Pi_1(z)=(A_1e^{-i\beta_1 z}+B_1e^{+i\beta_1 z})e^{ik_{1c}x}$$

and

$$\Pi_2(z)=(A_2e^{-i\beta_2 z}+B_2e^{+i\beta_2 z})e^{ik_{2c}x}\,.$$

The field components can be obtained from Eqs. (5.102a) and (5.102b), and are given by

$$E_{1x}=A_1\beta_1k_{1c}\left(e^{-i\beta_1 z}-\frac{B_1}{A_1}\,e^{i\beta_1 z}\right)e^{ik_{1c}x}\,, \tag{5.108a}$$

$$E_{1z}=k_{1c}^2A_1\left(e^{-i\beta_1 z}+\frac{B_1}{A_1}\,e^{i\beta_1 z}\right)e^{ik_{1c}x}\,, \tag{5.108b}$$

$$H_{1y}=-\omega\varepsilon_1k_{1c}A_1\left(e^{-i\beta_1 z}+\frac{B_1}{A_1}\,e^{i\beta_1 z}\right)e^{ik_{1c}x}\,. \tag{5.108c}$$

The fields in the second medium can be obtained by changing the subscript 1 to 2. Requiring the continuity of tangential electric and magnetic fields at $z=0$ provides the following equations:

$$A_1\beta_1k_{1c}\left(1-\frac{B_1}{A_1}\right)e^{ik_{1c}x}=A_2\beta_2k_{2c}\left(1-\frac{B_2}{A_2}\right)e^{ik_{2c}x} \tag{5.109a}$$

and

$$\varepsilon_1k_{1c}A_1\left(1+\frac{B_1}{A_1}\right)e^{ik_{1c}x}=\varepsilon_2k_{2c}A_2\left(1+\frac{B_2}{A_2}\right)e^{ik_{2c}x}\,. \tag{5.109b}$$

Since Eqs. (5.109a) and (5.109b) must be valid for all $x$, then

$$k_{1c}=k_{2c}\,, \tag{5.110}$$

which is known as the ***phase-matching condition***. Consequently, Eqs. (5.109) simplify to

$$A_1\beta_1\left(1-\frac{B_1}{A_1}\right)=A_2\beta_2\left(1-\frac{B_2}{A_2}\right) \tag{5.111a}$$

and

$$\varepsilon_1A_1\left(1+\frac{B_1}{A_1}\right)=\varepsilon_2A_2\left(1+\frac{B_2}{A_2}\right)\,. \tag{5.111b}$$

Now let's assume these field components are generated by an incident wave

$$\mathbf{H}_{\rm i}(x,z) = \hat{\mathbf{y}} H_0 e^{ik_1 \hat{\mathbf{k}}\cdot\mathbf{r}} = \hat{\mathbf{y}} H_0 e^{ik_1(-\cos\theta_{\rm i}\, z + \sin\theta_{\rm i}\, x)}$$

with $H_0 = -\omega\varepsilon_1 k_{1\rm c} A_1$, and

$$\mathbf{E}_{\rm i}(x,z) = -\eta_1 H_0(\sin\theta_{\rm i}\,\hat{\mathbf{z}} + \cos\theta_{\rm i}\,\hat{\mathbf{x}}) e^{ik_1(-\cos\theta_{\rm i}\, z + \sin\theta_{\rm i}\, x)}\ .$$

This wave excites a mode corresponding to $\beta_1 = k_1\cos\theta_{\rm i}$, $k_{1\rm c} = k_1\sin\theta_{\rm i}$, and

$$\beta_2 = \sqrt{k_2^2 - k_{1\rm c}^2} = \sqrt{k_2^2 - k_1^2\sin^2\theta_{\rm i}}\ . \tag{5.112}$$

Since the second medium is semi-infinite, no upward-going wave is excited, i.e., $B_2 = 0$. Taking the ratio of Eqs. (5.111a) and (5.111b),

$$\frac{\beta_1}{\varepsilon_1}\,\frac{1 - B_1/A_1}{1 + B_1/A_1} = \frac{\beta_2}{\varepsilon_2}\ ,$$

from which $B_1/A_1$ can be obtained and is given by

$$\Gamma_{\rm TM} = \frac{B_1}{A_1} = \frac{\varepsilon_2/\beta_2 - \varepsilon_1/\beta_1}{\varepsilon_2/\beta_2 + \varepsilon_1/\beta_1}\ . \tag{5.113}$$

Hence the total magnetic field in the upper half-space is given by

$$H_{1y} = H_0[e^{-i\beta_1 z} + \Gamma_{\rm TM} e^{i\beta_1 z}] e^{ik_1\sin\theta_{\rm i}\, x}\ . \tag{5.114}$$

The quantity $\Gamma_{\rm TM}$, which is the ratio of upward-going (reflected) wave to incident wave, is known as the ***magnetic reflection coefficient***.

Total electric field:

$$E_{1x} = -\frac{\beta_1}{\omega\varepsilon_1} H_0(e^{-i\beta_1 z} - \Gamma_{\rm TM} e^{i\beta_1 z}) e^{ik_1\sin\theta_{\rm i}\, x} \tag{5.115a}$$

and

$$E_{1z} = -\frac{k_1\sin\theta_{\rm i}}{\omega\varepsilon_1} H_0(e^{-i\beta_1 z} + \Gamma_{\rm TM} e^{i\beta_1 z}) e^{ik_1\sin\theta_{\rm i}\, x}\ . \tag{5.115b}$$

Noting that $\beta_1/\omega\varepsilon_1 = \eta_1\cos\theta_{\rm i}$,

$$\Gamma_{\rm TM} = -\frac{\eta_2\cos\theta_{\rm t} - \eta_1\cos\theta_{\rm i}}{\eta_2\cos\theta_{\rm t} + \eta_1\cos\theta_{\rm i}}\ , \qquad \textbf{(TM reflection coefficient)} \tag{5.116}$$

where the transmission angle $\theta_t$ is related to the incidence angle $\theta_i$ by

$$\cos\theta_t = \frac{\beta_2}{k_2} = \sqrt{1 - \frac{k_1^2}{k_2^2}\sin^2\theta_i}\,. \tag{5.117}$$

To find the fields in the second medium, we note that the lower medium is semi-infinite and cannot produce a reflected wave, that is, $B_2 = 0$. Using Eq. (5.111b), $A_2$ can be found from

$$A_2 = \frac{\varepsilon_1 A_1}{\varepsilon_2}(1+\Gamma_{TM})\,.$$

Hence

$$H_{2y} = H_0(1+\Gamma_{TM})e^{-i\beta_2 z}e^{ik_1\sin\theta_i x}\,. \tag{5.118}$$

The quantity $H_{2y}(z=0)/H_{1y}(z=0)$ is called the ***magnetic transmission coefficient*** and is given by

$$\tau_{TM} = 1+\Gamma_{TM}\,. \tag{5.119}$$

## 5-5.2 TE Plane-Wave Reflection and Transmission at Planar Interface between Two Dielectric Media

To obtain the TE solution, the duality relations can be used. From Eqs. (5.114), (5.115a), and (5.115b),

$$E_{1y} = -E_0(e^{-i\beta_1 z} + \Gamma_{TE}e^{i\beta_1 z})e^{ik_1\sin\theta_i x}\,, \tag{5.120a}$$

$$H_{1x} = -\frac{\cos\theta_i}{\eta_1}E_0(e^{-i\beta_1 z} - \Gamma_{TE}e^{i\beta_1 z})e^{ik_1\sin\theta_i x}\,, \tag{5.120b}$$

$$H_{1z} = -\frac{\sin\theta_i}{\eta_1}E_0(e^{-i\beta_1 z} + \Gamma_{TE}e^{i\beta_1 z})e^{ik_1\sin\theta_i x}\,, \tag{5.120c}$$

and from Eq. (5.118)

$$E_{2y} = -E_0(1+\Gamma_{TE})e^{-i\beta_2 z}e^{ik_1\sin\theta_i x}\,. \tag{5.121}$$

The TE electric field reflection coefficient $\Gamma_{TE}$ can also be obtained using the duality relations:

$$\Gamma_{TE} = \frac{\eta_2/\cos\theta_t - \eta_1/\cos\theta_i}{\eta_2/\cos\theta_t + \eta_1/\cos\theta_i}\,. \qquad \textbf{(TE reflection coefficient)} \tag{5.122}$$

Figure 5-8 shows the magnitude of the reflection coefficient for both TM and TE polarization versus the incident angle for a case where $\varepsilon_1 = \varepsilon_0$ and $\varepsilon_2 = 4\varepsilon_0$.

The well-known Snell's law of refraction can be derived from Eq. (5.110) and is given by

$$n_1\sin\theta_i = n_2\sin\theta_t\,, \tag{5.123}$$

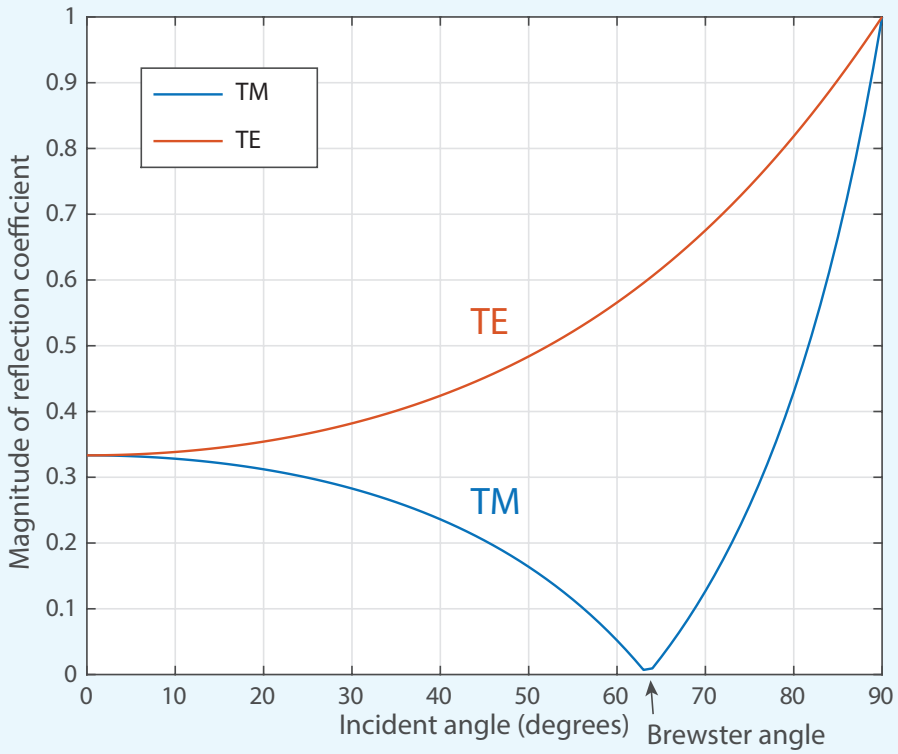


**Figure 5-8:** Magnitude of the plane-wave reflection coefficient at a planar interface between two dielectric media with $\varepsilon_1 = \varepsilon_0$ and $\varepsilon_2 = 4\varepsilon_0$.

where $n_1 = \sqrt{\varepsilon_1 \mu_1}$ and $n_2 = \sqrt{\varepsilon_2 \mu_2}$ are respectively the indices of refraction of the upper and lower media.

### 5-5.3 Brewster Angle

It is interesting to note that the angle at which the reflection coefficient for the TM wave is zero can be obtained from Eq. (5.116):

$$\cos\theta_i = \frac{\eta_2}{\eta_1}\cos\theta_t = \frac{\eta_2}{\eta_1}\sqrt{1 - \frac{k_1^2}{k_2^2}\sin^2\theta_i}\,.$$

This angle is known as the ***Brewster angle*** $\theta_B^{TM}$, which can be explicitly expressed as

$$\theta_B^{TM} = \sin^{-1}\left(\sqrt{\frac{\varepsilon_2(\mu_1\varepsilon_2 - \mu_2\varepsilon_1)}{\mu_1(\varepsilon_2^2 - \varepsilon_1^2)}}\right). \tag{5.124}$$

In the case where the upper and lower half-spaces are nonmagnetic ($\mu_1 = \mu_2 = \mu_0$), Eq. (5.124) takes a simpler form:

$$\theta_B^{TM} = \sin^{-1}\left(\sqrt{\frac{\varepsilon_2}{\varepsilon_2+\varepsilon_1}}\right). \qquad \textbf{(nonmagnetized)}$$

The Brewster angle for TE polarization can be obtained from Eq. (5.124) using duality and is given by

$$\theta_B^{TE} = \sin^{-1}\left(\sqrt{\frac{\mu_2(\varepsilon_1\mu_2 - \varepsilon_2\mu_1)}{\varepsilon_1(\mu_2^2 - \mu_1^2)}}\right). \qquad \textbf{(for magnetic materials only)} \tag{5.125}$$

Note that the Brewster angle for TE polarization does not exist for nonmagnetic materials.

Another interesting observation is the phenomenon of total reflection for lossless media. In situations where $n_1 > n_2$, there exists a critical angle $\theta_i = \theta_c$ for which $\theta_t = \pi/2$ and for $\theta_i > \theta_c$ then $\theta_t$ is pure imaginary. In this case it is easy to show that the magnitudes of the reflection coefficients for both polarizations are unity.

### Example 5-2: Fermat's Principle

Using Snell's law of reflection and refraction, show that ***Fermat's principle***, also known as the ***principle of least time***, is valid for a medium composed of two half-space dielectric media with a planar interface. Consider a point source as the source of radiation and an observation point that could be in either medium.

**Solution:** Let us consider two dielectric media with indices of refraction $n_1$ and $n_2$ and a point source at location $S$ in medium 1 and two observation points, $P_1$ in medium 1 and $P_2$ in medium 2. The geometry of the problem is shown in Fig. 5-9. As shown earlier, the field radiated from a source can be expanded in terms of plane waves propagating in different directions. Each plane wave can be represented by a ray indicating the direction of propagation. The goal here is to show that the point on the surface responsible for reflecting an incident ray that goes through $P_1$ or $P_2$ is a point that minimizes the travel time. Let us first consider the point in medium 1 ($P_1$). According to Snell's law, the point $q$ on the interface between $S$ and $P_1$ is a point such that

$$\hat{\mathbf{n}} \cdot (\hat{\mathbf{k}}_i + \hat{\mathbf{k}}_r) = 0 \tag{5.126a}$$

and

$$\hat{\mathbf{t}} \cdot (\hat{\mathbf{k}}_i - \hat{\mathbf{k}}_r) = 0\,, \tag{5.126b}$$

where $\hat{\mathbf{k}}_i$ and $\hat{\mathbf{k}}_r$ are unit vectors along the $S$–$q$ and $q$–$P_1$ lines respectively, $\hat{\mathbf{n}}$ is a unit normal to the interface, and $\hat{\mathbf{t}}$ is a tangential unit vector to the interface. Now consider another point

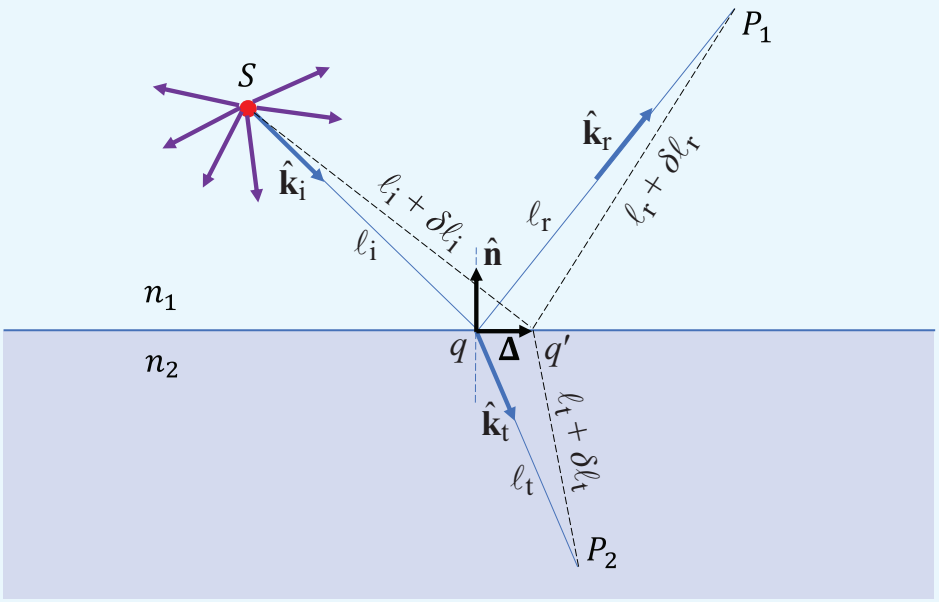


**Figure 5-9:** A source at $S$ above a planar interface between two dielectric media having indices of refraction $n_1$ and $n_2$. According to Fermat's principle, the optical path length between the source and an observation point through reflection or refraction at a point on the interface is stationary with respect to small variations in the path.

$q'$ on the interface that could be responsible for directing the reflected incident ray to $P_1$. We want to show that the travel time through $q$ is shorter than that for $q'$, or $q$ is the stationary point on the surface. Since the speed of light is moderated by the index of refraction, the travel time through a distance $r$ is proportional to a parameter known as the ***optical path length***, defined by $nr$. Hence the minimum travel time corresponds to the minimum optical path length. Representing the optical path length from $S$ to $q$ by $n_1\ell_i$ and that from $q$ to $P_1$ by $n_1\ell_r$, for a point $q'$ near $q$ the corresponding optical pathlengths may be expressed by $n_1(\ell_i+\delta\ell_i)$ and $n_1(\ell_r+\delta\ell_r)$. The vector optical path between $S$ and $q'$ and between $q'$ and $P_1$ can be written as

$$n_1(\ell_i+\delta\ell_i)(\widehat{\mathbf{k}_i+\delta k_i}) = n_1\ell_i\,\hat{\mathbf{k}}_i + n_1\boldsymbol{\Delta} \tag{5.127a}$$

and

$$n_1(\ell_r+\delta\ell_r)(\widehat{\mathbf{k}_r+\delta k_r}) = n_1\ell_r\,\hat{\mathbf{k}}_r - n_1\boldsymbol{\Delta}\,, \tag{5.127b}$$

where $(\widehat{\mathbf{k}_i+\delta k_i})$ and $(\widehat{\mathbf{k}_r+\delta k_r})$ are unit vectors along $Sq'$ and $q'P$, respectively. Also, $\boldsymbol{\Delta}$ is a small tangential vector connecting $q$ to $q'$. Let us now carry out the dot product of Eq. (5.127a) by $\hat{\mathbf{k}}_i$ and the dot product of Eq. (5.127b) by $\hat{\mathbf{k}}_r$, and keeping terms only to the first order in $\delta$,

we have

$$n_1\ell_{\rm i} + n_1\,\delta\ell_{\rm i} = n_1\ell_{\rm i} + n_1\boldsymbol{\Delta}\cdot\hat{\mathbf{k}}_{\rm i} \tag{5.128a}$$

and

$$n_1\ell_{\rm r} + n_1\,\delta\ell_{\rm r} = n_1\ell_{\rm r} - n_1\boldsymbol{\Delta}\cdot\hat{\mathbf{k}}_{\rm r}\ . \tag{5.128b}$$

Note that we have used the fact that to the first-order in $\delta$

$$\hat{\mathbf{k}}_{\rm i}\cdot\widehat{(\mathbf{k}_{\rm i}+\delta k_{\rm i})} = \hat{\mathbf{k}}_{\rm r}\cdot\widehat{(\mathbf{k}_{\rm r}+\delta k_{\rm r})} = 1\ .$$

Now, adding Eqs. (5.128a) and (5.128b) results in

$$(\delta\ell_{\rm i} + \delta\ell_{\rm r}) = \boldsymbol{\Delta}\cdot(\hat{\mathbf{k}}_{\rm i} - \hat{\mathbf{k}}_{\rm r})\ . \tag{5.129}$$

According to Snell's law (see Eq. (5.126)) the right-hand side is zero, so the variational path length difference $\delta\ell_{\rm i} + \delta\ell_{\rm r} = 0$. This indicates that the path $SqP_1$ is stationary (corresponding to the minimum travel time) with respect to small variations in path. This shows that Fermat's principle holds true for reflected rays.

Now let us consider point $P_2$ in the lower half-space. The vector optical path between $q'$ and $P_2$ can be written as

$$n_2(\ell_{\rm t} + \delta\ell_{\rm t})\widehat{(\mathbf{k}_{\rm t}+\delta k_{\rm t})} = n_2\ell_{\rm t}\,\hat{\mathbf{k}}_{\rm t} - n_2\boldsymbol{\Delta}\ . \tag{5.130}$$

Then we evaluate the dot product of Eq. (5.130) with $\hat{\mathbf{k}}_{\rm t}$ and keep terms only to the first order in $\delta$:

$$n_2\ell_{\rm t} + n_2\,\delta\ell_{\rm t} = n_2\ell_{\rm t} - n_2\boldsymbol{\Delta}\cdot\mathbf{k}_{\rm t}\ ,$$

or simply

$$\delta\ell_{\rm t} = -\boldsymbol{\Delta}\cdot\mathbf{k}_{\rm t}\ . \tag{5.131}$$

Adding Eqs. (5.128a) and (5.131) gives

$$\delta\ell_{\rm i} + \delta\ell_{\rm t} = \boldsymbol{\Delta}\cdot(\hat{\mathbf{k}}_{\rm i} - \hat{\mathbf{k}}_{\rm t})\ .$$

According to Snell's law, $\hat{\mathbf{t}}\cdot(\hat{\mathbf{k}}_{\rm i} - \hat{\mathbf{k}}_{\rm t}) = 0$, which indicates that

$$\delta\ell_{\rm i} + \delta\ell_{\rm t} = 0\ .$$

This indicates that the path $SqP_2$ is also stationary with respect to small variations in the path, proving Fermat's principle for the refracted ray.

## 5-6 Plane-Wave Reflection at the Interface between a Dielectric Medium and a Good-Conducting Medium

It can easily be shown that the electric field reflection coefficient of a plane wave reflected by a perfect electric conductor has a magnitude of unity and a phase of 180°, independent of the

incident angle or polarization. This result can be obtained from Eq. (5.122) by noting that for a PEC with conductivity $\sigma = \infty$,

$$\eta_2 = \sqrt{\frac{\mu_0}{\varepsilon_2}} = \left.\sqrt{\frac{\mu_0}{\varepsilon_0\left(1 + i\,\dfrac{\sigma}{\omega\varepsilon_0}\right)}}\right|_{\sigma=\infty} = 0\,. \tag{5.132}$$

However, for most practical situations, good conductors have very high, but not infinite conductivity. Inside such conductors ($\sigma \gg \omega\varepsilon_0$) the electric and magnetic fields have some finite values and, depending on whether we are considering TM or TE incidence, the magnetic or electric fields are given by Eqs. (5.118) or (5.121). The propagation constant in the conductor is given by

$$k_2 = \omega\sqrt{\mu_0\varepsilon_2} \approx \sqrt{\frac{\omega\mu_0\sigma}{2}}\,(1+i) = \sqrt{\pi f\mu_0\sigma}\,(1+i)\,, \tag{5.133}$$

and the medium's characteristic impedance is

$$\eta_2 \approx \sqrt{\frac{\pi f\mu_0}{\sigma}}\,(1-i)\,. \tag{5.134}$$

The refracted angle $\theta_t$ can be computed from

$$\cos\theta_t = \sqrt{1 - \frac{k_0^2\sin^2\theta_i}{k_2^2}} \approx \sqrt{1 - \frac{\omega^2\mu_0\varepsilon_0}{i\omega^2\mu_0\sigma/\omega}\sin^2\theta_i} \approx 1\,,$$

where we used the defining relation $\sigma \gg \omega\varepsilon_0$ for a good conductor. This result indicates that the transmitted wave propagates almost along the unit normal to the interface. According to Eq. (5.133), the attenuation constant $\alpha = \sqrt{\pi f\mu_0\sigma}$, which means that after propagating a distance of

$$\delta_s = \frac{1}{\sqrt{\pi f\mu_0\sigma}}\,, \tag{5.135}$$

the field intensity reaches $e^{-1}$ of its value at the interface. This distance is known as the ***skin depth*** of the conductor, which decreases with increasing frequency and conductivity. Using this definition in Eq. (5.134), the ***wave impedance*** of the conductor may be expressed as

$$\eta_c = \frac{1-i}{\delta_s\sigma}\,. \tag{5.136}$$

Note that the resistive part of the wave impedance, $R_c = 1/(\delta_s\sigma)$, is the dc resistivity of the conducting sheet of the material with cross section of 1 m$^2$ and thickness $\delta_s$. The reactive part of wave impedance represents an inductive impedance. It is interesting to examine the ratio of the total tangential electric field to the total tangential magnetic field in the upper medium at the interface ($z = 0$). Using Eqs. (5.115a) and (5.114) and using (5.116) for a TM wave, we

have

$$\frac{E_{1x}}{H_{1y}} = \frac{\eta_1 \cos\theta_i \,(1-\Gamma_{TM})}{1+\Gamma_{TM}} = \eta_2 \cos\theta_t \approx \eta_c \,, \qquad \textbf{(TM wave)}$$

where $\eta_c$ is as given by Eq. (5.136). Since this ratio is independent of the incident angle, it is valid for any arbitrary source above the conductor, because the fields of the source can be expressed in terms of plane waves propagating in different directions and all these waves would see the same surface impedance. It should be noted here that the same results hold for a TE incident wave using Eqs. (5.120a), (5.120b), and (5.122). Also, if the surface is curved instead of being planar, the incident plane wave at each point on the surface that has a different incident angle would still experience the same surface impedance as long as the radii of surface curvature are much larger than the skin depth. Hence, for electromagnetic boundary value problems, good conductors can be modeled by a surface impedance given by Eq. (5.136) without the need to examine the fields interior to the conductor.

## 5-7 Wave Propagation in an Inhomogeneous Medium: Geometric-Optics Approximation

The problem of wave propagation in inhomogeneous media is of importance for many practical problems, such as atmospheric wave propagation when the permittivity or index of refraction of air can vary gently along the path of propagation. If such permittivity variations as a function of space are slow with a scale much larger than the wavelength, an approximate solution can be obtained. In an approximate formulation inspired by plane-wave characteristics, a solution to Maxwell's equations, known as the ***Eikonal equation***, can be obtained.

Let us consider a medium with permeability $\mu_0$ and inhomogeneous permittivity $\varepsilon(\mathbf{r}) = \varepsilon_0\,\varepsilon_1(\mathbf{r})$. Inspired by the plane-wave solution in a homogeneous medium, we may represent the solution to Maxwell's equations in a source-free region in the following form:

$$\mathbf{E}(\mathbf{r}) = \mathbf{E}_0(\mathbf{r})\, e^{ik_0\,\phi(\mathbf{r})} \tag{5.137a}$$

and

$$\mathbf{H}(\mathbf{r}) = \frac{\mathbf{H}_0(\mathbf{r})}{\eta_0}\, e^{ik_0\,\phi(\mathbf{r})}\,, \tag{5.137b}$$

where $k_0 = 2\pi/\lambda_0 = \omega\sqrt{\mu_0\varepsilon_0}$, and for a lossless medium $\phi(\mathbf{r})$ is a real function that gently varies with $\mathbf{r}$. Note that the unit of $\mathbf{H}_0(\mathbf{r})$ is V/m due to the normalization used in Eq. (5.137b). Applying Faraday's law to the electric field given by Eq. (5.137a), we have

$$\begin{aligned}\nabla\times[\mathbf{E}_0(\mathbf{r})\, e^{ik_0\,\phi(\mathbf{r})}] &= \nabla\, e^{ik_0\,\phi(\mathbf{r})}\times\mathbf{E}_0(\mathbf{r}) + e^{ik_0\,\phi(\mathbf{r})}\nabla\times\mathbf{E}_0(\mathbf{r}) \\ &= ik_0\eta_0\,\frac{\mathbf{H}_0(\mathbf{r})}{\eta_0}\, e^{ik_0\,\phi(\mathbf{r})}\,. \end{aligned} \tag{5.138}$$

Simplifying Eq. (5.138), we get

$$ik_0\,\nabla\phi(\mathbf{r})\times\mathbf{E}_0(\mathbf{r}) + \nabla\times\mathbf{E}_0(\mathbf{r}) = ik_0\,\mathbf{H}_0(\mathbf{r})\,. \tag{5.139}$$

Also, the modified Ampère's law using Eq. (5.137b) gives

$$\nabla \times \left( \frac{\mathbf{H}_0(\mathbf{r})}{\eta_0} \, e^{ik_0 \, \phi(\mathbf{r})} \right) = \frac{1}{\eta_0} \, \nabla e^{ik_0 \, \phi(\mathbf{r})} \times \mathbf{H}_0(\mathbf{r}) + e^{ik_0 \, \phi(\mathbf{r})} \, \frac{1}{\eta_0} \, \nabla \times \mathbf{H}_0(\mathbf{r})$$
$$= -i\omega\varepsilon_0 \varepsilon_{\mathrm{r}}(\mathbf{r}) \, \mathbf{E}_0(\mathbf{r}) \, e^{ik_0 \, \phi(\mathbf{r})} \, . \tag{5.140}$$

Upon simplifying Eq. (5.140) and recalling that $\omega\varepsilon_0 = k_0/\eta_0$, we get

$$ik_0 \, \nabla\phi(\mathbf{r}) \times \mathbf{H}_0(\mathbf{r}) + \nabla \times \mathbf{H}_0(\mathbf{r}) = -ik_0 \, \varepsilon_{\mathrm{r}}(\mathbf{r}) \, \mathbf{E}_0(\mathbf{r}) \, . \tag{5.141}$$

Equations (5.139) and (5.141) must be solved together to find the unknown functions.

For a homogeneous medium, we found $k_0 \, \phi(\mathbf{r}) = \mathbf{K} \cdot \mathbf{r}$ (similar to Eq. (5.22)) and $\mathbf{E}_0$ and $\mathbf{H}_0$ to be constant vectors independent of position, where $\mathbf{K} = k_0 \varepsilon_{\mathrm{r}} \, \hat{\mathbf{k}}_{\mathrm{i}}$ is the propagation vector for a plane wave propagating along $\hat{\mathbf{k}}_{\mathrm{i}}$. We also found that

$$\nabla\phi(\mathbf{r}) = \varepsilon_{\mathrm{r}} \, \hat{\mathbf{k}}_{\mathrm{i}} \, ,$$

indicating that $\mathbf{K}$ is perpendicular to a surface over which the phase front function is constant ($\phi(\mathbf{r}) = C$).

At high frequencies, assuming that $k_0$ is very large compared with the spatial variations of $\mathbf{E}_0(\mathbf{r})$ and $\mathbf{H}_0(\mathbf{r})$, $\nabla \times \mathbf{E}_0(\mathbf{r})$ and $\nabla \times \mathbf{H}_0(\mathbf{r})$ can be ignored compared with other terms in Eqs. (5.139) and (5.141). Therefore, at high frequencies where the wavelength is much smaller than variations in $\varepsilon_{\mathrm{r}}(\mathbf{r})$, $\mathbf{E}_0(\mathbf{r})$, and $\mathbf{H}_0(\mathbf{r})$, Eqs. (5.139) and (5.141) can be expressed as

$$\nabla\phi(\mathbf{r}) \times \mathbf{E}_0(\mathbf{r}) = \mathbf{H}_0(\mathbf{r}) \tag{5.142a}$$

and

$$\nabla\phi(\mathbf{r}) \times \mathbf{H}_0(\mathbf{r}) = -\varepsilon_{\mathrm{r}}(\mathbf{r}) \, \mathbf{E}_0(\mathbf{r}) \, . \tag{5.142b}$$

Also, using Gauss' law of electricity we can show that

$$\nabla \cdot \left[ \varepsilon_0 \, \varepsilon_{\mathrm{r}}(\mathbf{r}) \, \mathbf{E}_0(\mathbf{r}) \, e^{ik_0 \, \phi(\mathbf{r})} \right] = 0 \, ,$$

which can be expanded to show

$$\varepsilon_0 \, \varepsilon_{\mathrm{r}}(\mathbf{r}) \, e^{ik_0 \, \phi(\mathbf{r})} \, \nabla \cdot \mathbf{E}_0(\mathbf{r}) + \left[ \varepsilon_0 \, \nabla\varepsilon_{\mathrm{r}}(\mathbf{r}) \, e^{ik_0 \, \phi(\mathbf{r})} + ik_0 \, \varepsilon_{\mathrm{r}}(\mathbf{r}) \, \nabla\phi(\mathbf{r}) \, e^{ik_0 \, \phi(\mathbf{r})} \right] \cdot \mathbf{E}_0(\mathbf{r}) = 0 \, . \tag{5.143}$$

Again ignoring other terms compared with terms having $k_0$ as a coefficient, Eq. (5.143) is simplified to

$$\mathbf{E}_0(\mathbf{r}) \cdot \nabla\phi(\mathbf{r}) = 0 \, . \tag{5.144}$$

Similarly, Gauss' law for magnetism provides

$$\mathbf{H}_0(\mathbf{r}) \cdot \nabla\phi(\mathbf{r}) = 0 \, . \tag{5.145}$$

Substituting Eq. (5.142a) into Eq. (5.142b), we get

$$\nabla\phi(\mathbf{r}) \times [\nabla\phi(\mathbf{r}) \times \mathbf{E}_0(\mathbf{r})] = -\varepsilon_r(\mathbf{r})\, \mathbf{E}_0(\mathbf{r}) \,. \tag{5.146}$$

Expanding Eq. (5.146) and using Eq. (5.144), we have

$$|\nabla\phi(\mathbf{r})|^2 = \varepsilon_r(\mathbf{r}) = n^2(\mathbf{r}) \,. \qquad \textbf{(Eikonal equation)} \tag{5.147}$$

Equation (5.147) is the famous ***Eikonal equation*** that can be solved to find $\phi(\mathbf{r})$, which represents the phase front of the wave in the inhomogeneous medium. There is some degree of freedom in choosing $\mathbf{E}_0(\mathbf{r})$ so long as Eq. (5.144) is satisfied. Once $\mathbf{E}_0(\mathbf{r})$ is chosen, $\mathbf{H}_0(\mathbf{r})$ can be obtained from Eq. (5.142a).

The Eikonal equation can be solved to find the ray trajectory in the inhomogeneous medium. The ray trajectory represented by a parametric function $\mathbf{r}(s)$, with parameter $s$ denoting the arc length, can be used to find the direction of wave propagation $\hat{\mathbf{k}}$ that is tangent to $\mathbf{r}(s)$. Noting that the direction of wave propagation at each point is perpendicular to $\phi(\mathbf{r})$, we can write

$$\hat{\mathbf{k}}(\mathbf{r}) = \frac{d\mathbf{r}(s)}{ds} = \frac{\nabla\phi(\mathbf{r})}{|\nabla\phi(\mathbf{r})|} \,. \tag{5.148}$$

In view of Eq. (5.148), the Eikonal equation may be written as

$$\nabla\phi(\mathbf{r}) = \hat{\mathbf{k}}(\mathbf{r})\, n(\mathbf{r}) \,. \tag{5.149}$$

The solution to the Eikonal equation can be used to predict interesting phenomena such as a mirage, which happens near the interface between a hot ground surface and air with an increasing index of refraction away from the interface. The atmospheric ducting effect, which happens at the interface between air and warm water bodies, is another example. The equation for the ray trajectory in a medium with a slowly varying index of refraction can be derived by first noting that

$$\frac{d^2\mathbf{r}}{ds^2} = \frac{d}{ds}\left(\frac{d\mathbf{r}}{ds}\right) = \hat{\mathbf{k}} \cdot \nabla\left(\frac{d\mathbf{r}}{ds}\right) = \hat{\mathbf{k}} \cdot \nabla\, \hat{\mathbf{k}} \,, \tag{5.150}$$

according to the definition of gradient. Here we are using a unit vector along the ray path ($\hat{\mathbf{s}} = \hat{\mathbf{k}}$). Using Eq. (5.149) in Eq. (5.150), we have

$$\frac{d^2\mathbf{r}}{ds^2} = \frac{\nabla\phi(\mathbf{r})}{n(\mathbf{r})} \cdot \nabla\left(\frac{\nabla\phi(\mathbf{r})}{n(\mathbf{r})}\right) \,. \tag{5.151}$$

Now consider the vector calculus identity

$$\nabla(\mathbf{U}\cdot\mathbf{V}) = (\mathbf{U}\cdot\nabla)\mathbf{V} + (\mathbf{V}\cdot\nabla)\mathbf{U} + \mathbf{U}\times(\nabla\times\mathbf{V}) + \mathbf{V}\times(\nabla\times\mathbf{U}) \,, \tag{5.152}$$

and choose $\mathbf{U} = \mathbf{V}$ to further simplify Eq. (5.152) to

$$\nabla|\mathbf{U}|^2 = 2(\mathbf{U}\cdot\nabla)\mathbf{U} + 2\mathbf{U}\times(\nabla\times\mathbf{U}) \,. \tag{5.153}$$

Substituting for $\mathbf{U} = \frac{1}{n}\nabla\phi(\mathbf{r})$ into Eq. (5.153), we have

$$\frac{\nabla\phi(\mathbf{r})}{n(\mathbf{r})}\cdot\nabla\frac{\nabla\phi(\mathbf{r})}{n(\mathbf{r})} = \frac{1}{2}\nabla\frac{|\nabla\phi(\mathbf{r})|^2}{n^2} - \frac{\nabla\phi(\mathbf{r})}{n}\times\nabla\times\left(\frac{\nabla\phi(\mathbf{r})}{n(\mathbf{r})}\right) . \tag{5.154}$$

Using Eq. (5.147) in the first term of the right-hand side of Eq. (5.154), in view of Eq. (5.151), it can be shown that

$$\begin{aligned}\frac{d^2\mathbf{r}}{ds^2} &= -\frac{1}{n(\mathbf{r})}\nabla\phi(\mathbf{r})\times\nabla\times\left(\frac{\nabla\phi(\mathbf{r})}{n(\mathbf{r})}\right)\\ &= -\frac{1}{n(\mathbf{r})}\nabla\phi(\mathbf{r})\times\left[\nabla\left(\frac{1}{n(\mathbf{r})}\right)\times\nabla\phi(\mathbf{r})\right]\\ &= -\frac{1}{n(\mathbf{r})}\left(|\nabla\phi(\mathbf{r})|^2\nabla\frac{1}{n(\mathbf{r})} - \nabla\phi(\mathbf{r})\cdot\nabla\frac{1}{n(\mathbf{r})}\nabla\phi(\mathbf{r})\right) ,\end{aligned} \tag{5.155}$$

where we have used the fact that $\nabla\times\nabla\phi(\mathbf{r}) = 0$. Again using Eq. (5.147) in Eq. (5.155), this equation can be simplified to

$$\frac{d^2\mathbf{r}}{ds^2} = \left(\frac{\nabla\phi(\mathbf{r})}{n(\mathbf{r})}\cdot\nabla\frac{1}{n(\mathbf{r})}\right)\nabla\phi(\mathbf{r}) - n(\mathbf{r})\,\nabla\frac{1}{n(\mathbf{r})} . \tag{5.156}$$

Using the definitions given by Eqs. (5.148) and (5.149) in Eq. (5.156), the following differential equation for the trace of rays in the inhomogeneous medium is obtained:

$$n(\mathbf{r})\,\frac{d^2\mathbf{r}}{ds^2} + \left(\nabla\, n(\mathbf{r})\cdot\frac{d\mathbf{r}}{ds}\right)\frac{d\mathbf{r}}{ds} = \nabla\, n(\mathbf{r}) . \tag{5.157}$$

Also, noting that

$$\frac{dn(\mathbf{r})}{ds} = \nabla\, n(\mathbf{r})\cdot\hat{\mathbf{s}} = \nabla\, n(\mathbf{r})\cdot\frac{d\mathbf{r}}{ds} ,$$

Eq. (5.157) can be written in a more compact form as

$$\frac{d}{ds}\left(n(\mathbf{r})\,\frac{d\mathbf{r}}{ds}\right) = \nabla\, n(\mathbf{r}) . \tag{5.158}$$

Equations (5.157) or (5.158) can be used to find the ray trajectory. For example, if $n$ is constant, then from Eq. (5.158) we have

$$\frac{d^2\mathbf{r}}{ds^2} = 0 ,$$

which indicates that $d\mathbf{r}/ds$ is a constant and this represents a line along a fixed direction $\hat{\mathbf{k}}$.

## Example 5-3: Derivation of Snell's Law

Derive Snell's law from the Eikonal equation.

**Solution:** Consider a smooth interface between two media. Let's assume that the local radii of curvature are very large compared with the wavelength. Taking $\nabla\times$ of both sides of Eq. (5.149), we get

$$\nabla \times [\hat{\mathbf{k}}(\mathbf{r})\, n(\mathbf{r})] = 0\ . \tag{5.159}$$

For a small rectangular contour between the two media, as shown in Fig. 5-10, we have

$$\oint_C n\, \hat{\mathbf{k}}(\mathbf{r}) \cdot d\boldsymbol{\ell} = 0\ . \tag{5.160}$$

Letting the length of the sides perpendicular to the interface go to zero, and denoting the angle between $\hat{\mathbf{k}}_1$ and $d\boldsymbol{\ell}$ to be $\theta_\mathrm{i}$ and the angle between $\hat{\mathbf{k}}_2$ and $d\boldsymbol{\ell}$ to be $\theta_\mathrm{t}$, as shown in Fig. 5-10, we have

$$n_1 \sin\theta_\mathrm{i} = n_2 \sin\theta_\mathrm{t}\ .$$

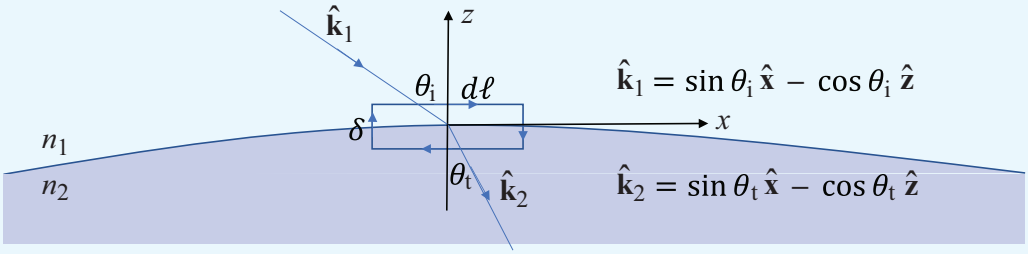


**Figure 5-10:** Proof of Snell's law from the Eikonal equation. A small rectangular contour between the two media is chosen to show that $n_1 \sin\theta_\mathrm{i} = n_2 \sin\theta_2$.

The curl-free property of the ray vector can be used to study how a phase front proceeds as it propagates in an inhomogeneous medium. Consider an initial phase front surface $S_1$ ($\phi(\mathbf{r})$ is constant on this surface), whose radii of curvature are large compared with the wavelength. Suppose the rays emitted from this surface encounter the surface of a perfect conductor ($S_\mathrm{c}$) having a large radius of curvature as well. The reflected rays form a phase front $S_2$. As shown in Fig. 5-11, using Eq. (5.160) on a closed contour $C = p_1 p p_2 q_2 q q_1 p_1$, we have

$$\oint_C n(\mathbf{r})\, \hat{\mathbf{k}}(\mathbf{r}) \cdot d\boldsymbol{\ell} = 0\ .$$

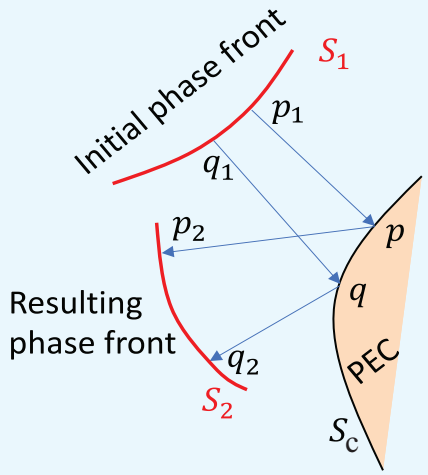


**Figure 5-11:** Phase-front propagation in an inhomogeneous medium based on the Eikonal equation showing that the optical paths for all rays between two phase fronts are the same.

On this contour, $\hat{\mathbf{k}}$ is perpendicular to $d\boldsymbol{\ell}$ on $S_1$ and $S_2$, and on the rest is either parallel or antiparallel. As a result, it can easily be shown that

$$\int_{p_1 p p_2} n(\mathbf{r})\, d\ell = \int_{q_1 q q_2} n(\mathbf{r})\, d\ell\ .$$

That is, $S_2$ is formed in such a way that the optical path lengths for all rays between the two phase fronts are the same.

## Example 5-4: Bending of Rays in an Inhomogeneous Medium

Consider an inhomogeneous medium with index of refraction $n(\mathbf{r}) = n_0 + \alpha z$. Starting with a ray in the $x$–$z$ plane having a direction $\hat{\mathbf{k}} = \sin\theta_0\ \hat{\mathbf{x}} + \cos\theta_0\ \hat{\mathbf{z}}$ at $x = z = 0$, find the ray trajectory in the $x$–$z$ plane using the Eikonal equation.

**Solution:** The starting point is Eq. (5.157), and noting that

$$\nabla\, n(\mathbf{r}) = \alpha\ \hat{\mathbf{z}}\ ,$$

Eq. (5.157) can be written as

$$\frac{d^2\mathbf{r}}{ds^2} + \left(\frac{\alpha}{n(\mathbf{r})}\ \hat{\mathbf{z}} \cdot \frac{d\mathbf{r}}{ds}\right)\frac{d\mathbf{r}}{ds} = \frac{\alpha\ \hat{\mathbf{z}}}{n(\mathbf{r})}\ . \tag{5.161}$$

Finding an exact solution for Eq. (5.161) is not very easy even for this simple linear function for the index of refraction. However, assuming that $\alpha/n_0 \ll 1$, we can proceed with an approximate solution. As shown earlier, when $n$ is a constant the ray trajectory is a line, and thus when $\delta = \alpha/n_0 \ll 1$, $d\mathbf{r}/ds$ may be expanded in terms of its Taylor series expansion in $\delta$:

$$\frac{d\mathbf{r}}{ds} = \sum_{i=0}^{\infty} \left(\frac{d\mathbf{r}}{ds}\right)^{(i)} \delta^i \,, \tag{5.162}$$

where $(d\mathbf{r}/ds)^{(i)}$ is the $i$th-order representation of a ray direction at each point. Also, for all values of $z > 0$,

$$\frac{\alpha}{n_0 + \alpha z} \leq \frac{\alpha}{n_0} = \delta \,. \tag{5.163}$$

To the zeroth order in $\delta$,

$$\frac{d^2\mathbf{r}}{ds^2} = 0$$

and

$$\frac{d\mathbf{r}}{ds} = x'(s)\,\hat{\mathbf{x}} + z'(s)\,\hat{\mathbf{z}} = \hat{\mathbf{k}} \,.$$

If we were to keep the solution to the first order in $\delta$, Eq. (5.161) simplifies to

$$\frac{d^2\mathbf{r}}{ds^2} + \frac{\alpha}{n}\, z'(s)\,\hat{\mathbf{k}} = \frac{\alpha}{n}\,\hat{\mathbf{z}} \,. \tag{5.164}$$

This represents two equations:

$$x''(s) + \frac{\alpha}{n}\, z'(s)\, x'(s) = 0 \tag{5.165a}$$

and

$$z''(s) + \frac{\alpha}{n}\, [z'(s)]^2 = \frac{\alpha}{n} \,. \tag{5.165b}$$

Unfortunately this is still a nonlinear coupled differential equation. However, when $n_0 \gg \alpha z$ (for relatively small values of $z$) these equations simplify to

$$x''(s) + \frac{\alpha}{n_0}\, z'(s)\, x'(s) = 0 \tag{5.166a}$$

and

$$z''(s) + \frac{\alpha}{n_0}\, [z'(s)]^2 = \frac{\alpha}{n_0} \,. \tag{5.166b}$$

To solve this nonlinear coupled differential equation for small values of $z$, $x(s)$ and $z(s)$ may be expanded in terms of their Taylor series; that is,

$$x(s) = a_1 s^2 + a_2 s + a_3 \tag{5.167a}$$

and

$$z(s) = b_1 s^2 + b_2 s + b_3 \ . \tag{5.167b}$$

But we know that $(x(0),\ y(0)) = (0,0)$, which renders the value of unknowns $a_3$ and $b_3$ to be

$$a_3 = b_3 = 0 \ .$$

We also know that

$$\left.\frac{d\mathbf{r}}{ds}\right|_{s=0} = \hat{\mathbf{k}}(0) = \sin\theta_0\ \hat{\mathbf{x}} + \cos\theta_0\ \hat{\mathbf{y}}$$
$$= a_2\ \hat{\mathbf{x}} + b_2\ \hat{\mathbf{y}} \ ,$$

and therefore

$$a_2 = \sin\theta_0$$

and

$$b_2 = \cos\theta_0 \ .$$

Substituting Eq. (5.167b) into Eq. (5.166b), we can find an expression for $b_1$:

$$2b_1 + \frac{\alpha}{n_0}\ (2b_1 s + \cos\theta_0)^2 = \frac{\alpha}{n_0} \ .$$

It is expected that $z''(s)$ be small (proportional to $\alpha/n_0$); that is, $b_1 \ll 1$ and $\alpha/n_0 \ll 1$. Hence,

$$b_1 \approx \frac{\alpha}{2n_0}\ (1 - \cos^2\theta_0) = \frac{\alpha}{2n_0}\ \sin^2\theta_0 \ . \tag{5.168}$$

Now using Eqs. (5.167a) and (5.168) in Eq. (5.166a), we have

$$2a_1 + \frac{\alpha}{n_0}\left(\frac{\alpha s}{n_0}\sin^2\theta_0 + \cos\theta_0\right)(2a_1 s + \sin\theta_0) = 0 \ . \tag{5.169}$$

Also, $a_1$ is expected to be proportional to $\alpha/n_0$, and therefore Eq. (5.169) to the first order in $\alpha/n_0$ can be written as

$$2a_1 + \frac{\alpha}{n_0}\cos\theta_0 \sin\theta_0 = 0 \ , \tag{5.170}$$

or

$$a_1 = -\frac{\alpha}{2n_0}\cos\theta_0 \sin\theta_0 \ . \tag{5.171}$$

Finally, the ray trajectory can be obtained from

$$x(s) = -\frac{\alpha s^2}{2n_0}\cos\theta_0 \sin\theta_0 + s\sin\theta_0 \tag{5.172a}$$

and

$$z(s) = \frac{\alpha s^2}{2n_0} \sin^2\theta_0 + s\cos\theta_0 \ . \tag{5.172b}$$

Note that $d\mathbf{r}/ds = \hat{\mathbf{k}}(s)$ must be a unit vector; that is, we should be able to show that

$$\left|\frac{d\mathbf{r}}{ds}\right| = \sqrt{(x'(s))^2 + (z'(s))^2} = 1 \ . \tag{5.173}$$

Using Eqs. (5.172a) and (5.172b) in Eq. (5.173), we can easily show that

$$\begin{aligned}\left|\frac{d\mathbf{r}}{ds}\right| &= \sqrt{1 + \left(\frac{\alpha}{n_0}\right)^2 s^2 \sin^2\theta_0} \\ &= 1 + \frac{1}{2}\left(\frac{\alpha}{n_0}\right)^2 s^2 \sin^2\theta_0 \approx 1\end{aligned}$$

to the first order in $(\alpha/n_0)$.

Figure 5-12 shows the ray trajectory for a medium with $\alpha/n_0 = 0.05$ and $n_0 = 1.01$.

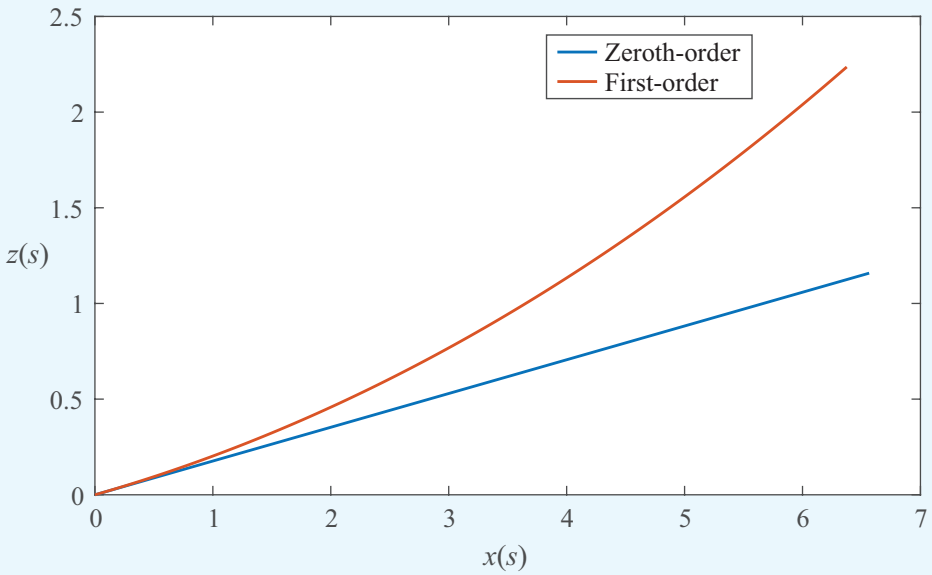


**Figure 5-12:** Ray trajectory calculated from the Eikonal equation for a medium with $n(r) = n_0 + \alpha z$ using a perturbation method for a small value of $\alpha/n_0 = 0.05$. Also shown is the zeroth-order result where the ray trajectory is a line.

## 5-8 Plane-Wave Reflection and Transmission from a Half-Space Uniaxial Medium

As discussed in the previous section, uniaxial media can support two different types of waves, namely ordinary waves and extraordinary waves, depending on the polarization of the electric field with respect to the optical axis. Basically, when the electric field intensity and flux density are perpendicular to the plane formed by the optical axis and the direction of wave propagation, an ordinary wave with a transcendental equation similar to that for a plane wave in an isotropic medium is generated. If the electric field and flux density are parallel to the plane of the optical axis and of the wave propagation direction, an extraordinary wave is generated. Consider two dielectric media with a planar interface in the $x$–$y$ plane at $z = 0$. The $z > 0$ medium is assumed to be isotropic with permittivity $\varepsilon_0\varepsilon_1$ and permeability $\mu_0\mu_1$. The lower half-space medium is chosen to be a uniaxial medium with its optical axis along the $x$ direction. The permittivity of the lower half-space is given by

$$\overline{\overline{\varepsilon}}_2 = \varepsilon_0 \begin{pmatrix} \varepsilon_{x2} & 0 & 0 \\ 0 & \varepsilon_2 & 0 \\ 0 & 0 & \varepsilon_2 \end{pmatrix}, \tag{5.174}$$

and its permeability is $\mu_0\mu_2$. A plane wave propagating along direction

$$\hat{\mathbf{k}}_\mathrm{i} = \sin\theta_\mathrm{i}\,\hat{\mathbf{x}} - \cos\theta_\mathrm{i}\,\hat{\mathbf{z}}$$

is impinging on the lower medium from above, as shown in Fig. 5-13. The plane wave's

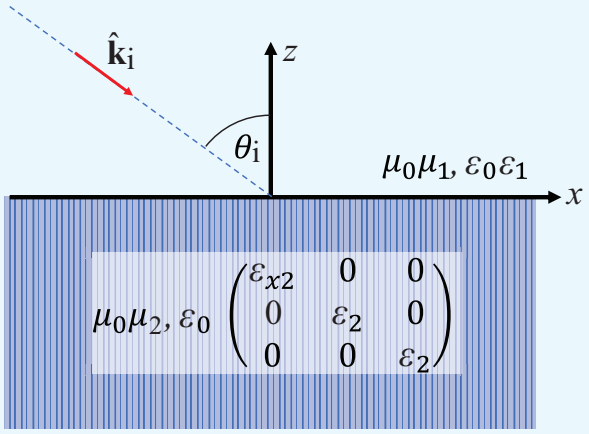


**Figure 5-13:** Geometry of plane-wave reflection from a uniaxial half-space medium with a planar interface. Depending on the polarization of the incident wave, an ordinary wave (for perpendicular polarization) or an extraordinary wave (for parallel polarization) is excited in the lower half-space.

electric and magnetic fields are given by

$$\mathbf{E}_{\rm i}(\mathbf{r}) = \mathbf{E}_0\, e^{ik_1(\sin\theta_{\rm i}\, x - \cos\theta_{\rm i}\, z)} \tag{5.175a}$$

and

$$\mathbf{H}_{\rm i}(\mathbf{r}) = \frac{\hat{\mathbf{k}}_{\rm i} \times \mathbf{E}_0}{\eta_1}\, e^{ik_0(\sin\theta_{\rm i}\, x - \cos\theta_{\rm i}\, z)}\ . \tag{5.175b}$$

Depending on the wave polarization (direction of $\mathbf{E}_0$), ordinary, extraordinary, or both types of waves are generated in the lower half-space medium. Our goal here is to determine the reflected and transmitted waves in the upper and lower media. To simplify the problem, we first assume that $\mathbf{E}_0$ is along the $y$-axis ($\mathbf{E}_0 = E_0\,\hat{\mathbf{y}}$), which excites an ordinary wave. In this case, the mode of propagation is TE, whose fields can be generated from a magnetic Hertz potential $\mathbf{\Pi}^{\rm o}_{\rm m} = \Pi^{\rm o}_j\,\hat{\mathbf{x}}$. Note that here we are expanding the fields in terms of TE and TM to $x$ as opposed to $z$. This choice lends itself to a proper solution for uniaxial media with the optical axis along the $x$-direction. Here the superscript "o" denotes ordinary wave. Since there is no variation with respect to $y$, $\frac{\partial}{\partial y} = 0$ for all field and potential quantities is zero. The Hertz vector potential must satisfy the wave equation

$$\nabla^2\Pi^{\rm o}_{xj} + k_j^2\Pi^{\rm o}_{xj} = 0\ , \tag{5.176}$$

where $j = 1,2$ refers to the upper and lower media, respectively. The electric and magnetic fields can be derived directly from Eqs. (3.91b) and (3.91a) by placing $\mathbf{\Pi} = 0$ and $\mathbf{\Pi}_{\rm m} = \Pi^{\rm o}_{xj}\,\hat{\mathbf{x}}$. The explicit expressions for the fields are given by

$$\mathbf{E}^{\rm o}_j = i\omega\mu_0\mu_j\,\frac{\partial\Pi^{\rm o}_{xj}}{\partial z}\,\hat{\mathbf{y}} \tag{5.177a}$$

and

$$\mathbf{H}^{\rm o}_j = \left(\frac{\partial^2\Pi^{\rm o}_{xj}}{\partial x^2} + k_j^2\Pi^{\rm o}_{xj}\right)\hat{\mathbf{x}} + \frac{\partial^2\Pi^{\rm o}_{xj}}{\partial x\,\partial z}\,\hat{\mathbf{z}}\ . \tag{5.177b}$$

Using Eq. (5.176), Eq. (5.177b) can be simplified to

$$\mathbf{H}^{\rm o}_j = -\frac{\partial^2\Pi^{\rm o}_{xj}}{\partial z^2}\,\hat{\mathbf{x}} + \frac{\partial^2\Pi^{\rm o}_{xj}}{\partial x\,\partial z}\,\hat{\mathbf{z}}\ . \tag{5.178}$$

The extraordinary wave mode is excited when a transverse magnetic (TM) wave perpendicular to the $x$ plane is incident upon the lower half-space. The subscript $j$ here is 2, but it is kept general to allow for treating a multilayer uniaxial lower half-space. TM to $x$ mode can be generated from an electric Hertz vector potential that has only one component along the $x$-axis. That is,

$$\mathbf{\Pi}^{\rm e} = \Pi^{\rm e}_{xj}\,\hat{\mathbf{x}}\ , \tag{5.179}$$

where the superscript "e" means extraordinary. Here we define the electric Hertz vector potential slightly differently from before, because the permittivity can assume two different

values in the uniaxial medium:

$$\mathbf{H}_j^{\mathrm{e}} = -i\omega\varepsilon_0 \nabla \times \mathbf{\Pi}_j^{\mathrm{e}} \,. \tag{5.180}$$

From Faraday's law,

$$\nabla \times \mathbf{E}_j^{\mathrm{e}} = i\omega\mu_j \mathbf{H}_j^{\mathrm{e}} = \omega^2 \varepsilon_0 \mu_0 \mu_j \nabla \times \mathbf{\Pi}_j^{\mathrm{e}} \,, \tag{5.181}$$

or equivalently,

$$\nabla \times [\mathbf{E}_j^{\mathrm{e}} - k_0^2 \mu_j \mathbf{\Pi}_j^{\mathrm{e}}] = 0 \,. \tag{5.182}$$

Hence, the electric field in terms of Hertz vector potential is given by

$$\mathbf{E}_j^{\mathrm{e}} = k_0^2 \mu_j \mathbf{\Pi}_j^{\mathrm{e}} - \nabla \phi_j \,, \tag{5.183}$$

where $\phi_j$ is the scalar electric potential. Also, from Faraday's law in a source-free region, we have

$$\nabla \times \mathbf{H}_j^{\mathrm{e}} = -i\omega \mathbf{D}_j^{\mathrm{e}} \,. \tag{5.184}$$

Upon substitution of Eq. (5.180) into Eq. (5.184), it can easily be shown that

$$\mathbf{D}_j^{\mathrm{e}} = \varepsilon_0 \nabla \times \nabla \times \mathbf{\Pi}_j^{\mathrm{e}} = \varepsilon_0 [\nabla \nabla \cdot \mathbf{\Pi}_j^{\mathrm{e}} - \nabla^2 \mathbf{\Pi}_j^{\mathrm{e}}] \,. \tag{5.185}$$

From the constitutive relation $\mathbf{D} = \overline{\overline{\varepsilon}}\, \mathbf{E}$, we can write

$$\mathbf{D}_j^{\mathrm{e}} = \varepsilon_0 [(\varepsilon_{xj} - \varepsilon_j) E_{xj}^{\mathrm{e}} \, \hat{\mathbf{x}} + \varepsilon_j \mathbf{E}_j^{\mathrm{e}}] \,. \tag{5.186}$$

Using Eqs. (5.186) and (5.183) in Eq. (5.184), the following equation can be obtained:

$$\nabla^2 \mathbf{\Pi}_j^{\mathrm{e}} + k_0^2 \varepsilon_{xj} \mu_j \mathbf{\Pi}_j^{\mathrm{e}} - \nabla (\nabla \cdot \mathbf{\Pi}_j^{\mathrm{e}} + \varepsilon_j \phi_j) - (\varepsilon_{xj} - \varepsilon_j) \frac{\partial \phi_j}{\partial x} = 0. \tag{5.187}$$

By defining $\nabla \cdot \mathbf{\Pi}_j^{\mathrm{e}} = -\varepsilon_j \phi_j$ as a gauge condition, and noting from Eq. (5.179) that $\mathbf{\Pi}_j^{\mathrm{e}}$ has only an $x$ component, the following wave equation for $\Pi_{xj}^{\mathrm{e}}$ is obtained:

$$\nabla^2 \Pi_{xj}^{\mathrm{e}} + k_0^2 \varepsilon_{xj} \mu_j \Pi_{xj}^{\mathrm{e}} + \frac{\varepsilon_{xj} - \varepsilon_j}{\varepsilon_j} \frac{\partial^2 \Pi_{xj}^{\mathrm{e}}}{\partial x^2} = 0 \,, \tag{5.188}$$

where we have used the gauge condition

$$\phi_j = -\frac{1}{\varepsilon_j} \frac{\partial \Pi_{xj}^{\mathrm{e}}}{\partial x} \,. \tag{5.189}$$

Recalling that $\frac{\partial}{\partial y} = 0$ for all potentials, from Eqs. (5.180) and (5.183) we have

$$\mathbf{H}_j^{\mathrm{e}} = -i\omega\varepsilon_0 \frac{\partial \Pi_{xj}^{\mathrm{e}}}{\partial z} \, \hat{\mathbf{y}} \,, \tag{5.190a}$$

and

$$\mathbf{E}_j^{\rm e} = \left( k_0 \mu_j \Pi_{xj}^{\rm e} + \frac{1}{\varepsilon_j} \frac{\partial^2 \Pi_{xj}^{\rm e}}{\partial x^2} \right) \hat{\mathbf{x}} + \frac{1}{\varepsilon_j} \frac{\partial^2 \Pi_{xj}^{\rm e}}{\partial x \, \partial z} \, \hat{\mathbf{z}} \, . \tag{5.190b}$$

The solution to wave equations (5.176) and (5.188) for plane-wave excitation can be expressed in terms of wave functions $\exp[i(k_{xj}^{\rm o} x \pm k_{zj}^{\rm o} z)]$ and $\exp[i(k_{xj}^{\rm e} x \pm k_{zj}^{\rm e} z)]$ for the ordinary and extraordinary waves. Upon substitution of these wave functions into the respective wave equations, the following dispersion relationships are obtained:

$$(k_{xj}^{\rm o})^2 + (k_{zj}^{\rm o})^2 = k_0^2 \mu_j \varepsilon_j \tag{5.191a}$$

and

$$\frac{1}{\varepsilon_j} (k_{xj}^{\rm e})^2 + \frac{1}{\varepsilon_{xj}} (k_{zj}^{\rm e})^2 = k_0^2 \mu_j \, . \tag{5.191b}$$

Note that in the upper half-space we only have ordinary waves, and Eq. (5.191a) is used there. At the interface between the upper medium and lower uniaxial medium ($z = 0$), the continuity of the tangential electric field and magnetic field must be enforced. These relations provide the following phase-matching condition:

$$k_{xj}^{\rm o} = k_{xj}^{\rm e} = k_1 \sin\theta_{\rm i} \, . \tag{5.192}$$

Hence Eqs. (5.191a) and (5.191b) can be used to find

$$k_{zj}^{\rm o} = k_0 \sqrt{\mu_j \varepsilon_j - \mu_1 \varepsilon_1 \sin^2 \theta_{\rm i}} \tag{5.193a}$$

and

$$k_{zj}^{\rm e} = k_0 \sqrt{\frac{\varepsilon_{xj}}{\varepsilon_j}} \sqrt{\mu_j \varepsilon_j - \mu_1 \varepsilon_1 \sin^2 \theta_{\rm i}} \, . \tag{5.193b}$$

The Hertz vector potential for ordinary and extraordinary waves in the $j$th region can be written as

$$\Pi_{xj}^{\rm o} = [A_j^{\rm i} e^{-ik_{zj}^{\rm o} z} + A_j^{\rm r} e^{ik_{zj}^{\rm o} z}] e^{ik_1 \sin\theta_{\rm i} x} \qquad \textbf{(ordinary wave)} \tag{5.194a}$$

and

$$\Pi_{xj}^{\rm e} = [B_j^{\rm i} e^{-ik_{zj}^{\rm e} z} + B_j^{\rm r} e^{ik_{zj}^{\rm e} z}] e^{ik_1 \sin\theta_{\rm i} x} \, , \qquad \textbf{(extraordinary wave)} \tag{5.194b}$$

where the superscripts "i" and "r" refer respectively to incident and reflected waves. The second region is semi-infinite, and thus there is no reflected wave; hence $A_2^{\rm r} = B_2^{\rm r} = 0$. From Eqs. (5.177a) and (5.178), the tangential components of electric and magnetic fields in the upper half-space are given by

$$E_{y1}^{\rm o} = \omega \mu_0 \mu_1 k_{z1}^{\rm o} [A_1^{\rm i} e^{-ik_{z1}^{\rm o} z} - A_1^{\rm r} e^{ik_{z1}^{\rm o} z}] e^{ik_1 \sin\theta_{\rm i} x} \tag{5.195a}$$

and

$$H_{x1}^{\rm o} = (k_{z1}^{\rm o})^2 [A_1^{\rm i} e^{-ik_{z1}^{\rm o} z} + A_1^{\rm r} e^{ik_{z1}^{\rm o} z}] e^{ik_1 \sin\theta_{\rm i} x} \, , \tag{5.195b}$$

and the fields in the lower half-space are given by

$$E_{y2}^{\mathrm{o}} = \omega\mu_0\mu_2 k_{z2}^{\mathrm{o}} A_2^{\mathrm{i}} e^{-ik_{z2}^{\mathrm{o}} z} \tag{5.196a}$$

and

$$H_{x2}^{\mathrm{o}} = (k_{z2}^{\mathrm{o}})^2 A_2^{\mathrm{i}} e^{-ik_{z2}^{\mathrm{o}} z} \,. \tag{5.196b}$$

Enforcing the continuity of the tangential electric and magnetic field components at the interface between two adjacent media provides

$$\mu_1 k_{z1}^{\mathrm{o}} (A_1^{\mathrm{i}} - A_1^{\mathrm{r}}) = \mu_2 k_{z2}^{\mathrm{o}} A_2^{\mathrm{i}} \tag{5.197a}$$

and

$$(k_{z1}^{\mathrm{o}})^2 (A_1^{\mathrm{i}} + A_1^{\mathrm{r}}) = (k_{z2}^{\mathrm{o}})^2 A_2^{\mathrm{i}} \,. \tag{5.197b}$$

Noting that the reflection coefficient for the ordinary wave is $r^{\mathrm{o}} = -A_1^{\mathrm{r}}/A_1^{\mathrm{i}}$, it follows that

$$r^{\mathrm{o}}(\theta_{\mathrm{i}}) = -\frac{\mu_1 k_{z2}^{\mathrm{o}} - \mu_2 k_{z1}^{\mathrm{o}}}{\mu_1 k_{z2}^{\mathrm{o}} + \mu_2 k_{z1}^{\mathrm{o}}} \,, \tag{5.198}$$

where $k_{z2}^{\mathrm{o}}$ and $k_{z1}^{\mathrm{o}}$ are given by Eq. (5.193a). Explicitly,

$$r^{\mathrm{o}}(\theta_{\mathrm{i}}) = -\frac{\mu_1 \sqrt{\mu_2\varepsilon_2 - \mu_1\varepsilon_1 \sin^2\theta_{\mathrm{i}}} - \mu_2 \sqrt{\mu_1\varepsilon_1}\cos\theta_{\mathrm{i}}}{\mu_1 \sqrt{\mu_2\varepsilon_2 - \mu_1\varepsilon_1 \sin^2\theta_{\mathrm{i}}} + \mu_2 \sqrt{\mu_1\varepsilon_1}\cos\theta_{\mathrm{i}}} \,. \tag{5.199}$$

**(reflection coefficient for ordinary wave)**

The transmission coefficient is defined as

$$\tau = \frac{\mu_2 k_{z2}^{\mathrm{o}}}{\mu_1 k_{z1}^{\mathrm{o}}} \frac{A_2^{\mathrm{i}}}{A_1^{\mathrm{i}}} \tag{5.200a}$$

and

$$\tau = 1 + r^{\mathrm{o}}(\theta_1) \,. \tag{5.200b}$$

For an extraordinary wave, the expressions for the electric and magnetic fields in the upper medium can be obtained from Eqs. (5.190a) and (5.190b), and are given by

$$H_{y1}^{\mathrm{e}} = -k_{z1}^{\mathrm{e}} \omega\varepsilon_0 \left( B_1^{\mathrm{i}} e^{-ik_{z1}^{\mathrm{e}} z} - B_1^{\mathrm{r}} e^{ik_{z1}^{\mathrm{e}} z} \right) e^{ik_1 \sin\theta_{\mathrm{i}}\, x} \tag{5.201a}$$

and

$$E_{x1}^{\mathrm{e}} = k_0^2 \mu_1 \left( B_1^{\mathrm{i}} e^{-ik_{z1}^{\mathrm{e}} z} + B_1^{\mathrm{r}} e^{ik_{z1}^{\mathrm{e}} z} \right) \cos^2\theta_{\mathrm{i}}\, e^{ik_1 \sin\theta_{\mathrm{i}}\, x} \,, \tag{5.201b}$$

and in the lower half-space,

$$H_{y2}^{\mathrm{e}} = -k_{z2}^{\mathrm{e}}\omega\varepsilon_0 B_2^{\mathrm{i}} e^{-ik_{z2}^{\mathrm{e}}z} e^{ik_1 \sin\theta_{\mathrm{i}}\, x} \tag{5.202a}$$

and

$$E_{x2}^{\mathrm{e}} = k_0^2 \left( \frac{\mu_2\varepsilon_2 - \mu_1\varepsilon_1 \sin^2\theta_{\mathrm{i}}}{\varepsilon_2} \right) B_2^{\mathrm{i}} e^{-ik_{z2}^{\mathrm{e}}z} e^{ik_1 \sin\theta_{\mathrm{i}}\, x} \,. \tag{5.202b}$$

Enforcing the boundary conditions at $z = 0$ provides

$$k_{z1}^{\mathrm{e}}[B_1^{\mathrm{i}} - B_1^{\mathrm{r}}] = k_{z2}^{\mathrm{e}} B_2^{\mathrm{i}} \tag{5.203a}$$

and

$$\mu_1 \cos^2\theta_{\mathrm{i}}[B_1^{\mathrm{i}} + B_1^{\mathrm{r}}] = \frac{\mu_2\varepsilon_2 - \mu_1\varepsilon_1 \sin^2\theta_{\mathrm{i}}}{\varepsilon_2} B_2^{\mathrm{i}} \,. \tag{5.203b}$$

Solving Eqs. (5.203a) and (5.203b) simultaneously gives the magnetic-field reflection coefficient

$$r^{\mathrm{e}}(\theta_{\mathrm{i}}) = \frac{\sqrt{\varepsilon_2\varepsilon_{x2}}\,\cos\theta_{\mathrm{i}} - \varepsilon_1\sqrt{\mu_2\varepsilon_2 - \mu_1\varepsilon_1\sin^2\theta_{\mathrm{i}}}}{\sqrt{\varepsilon_2\varepsilon_{x2}}\,\cos\theta_{\mathrm{i}} + \varepsilon_1\sqrt{\mu_2\varepsilon_2 - \mu_1\varepsilon_1\sin^2\theta_{\mathrm{i}}}} \,. \tag{5.204}$$

**(reflection coefficient for extraordinary wave)**

Also, it can be shown that the magnetic-field transmission coefficient can be computed from

$$\tau^{\mathrm{e}}(\theta_{\mathrm{i}}) = 1 + r^{\mathrm{e}}(\theta_{\mathrm{i}}) \,. \tag{5.205}$$

It is interesting to note that the phenomenon of no surface reflection at the Brewster angle still occurs for the half-space uniaxial medium. Setting the numerator of Eq. (5.204) to zero, the Brewster angle can be computed from

$$\theta_{\mathrm{B}} = \sin^{-1}\left( \sqrt{\frac{\varepsilon_2(\varepsilon_{x2} - \mu_2\varepsilon_1^2)}{\varepsilon_2\varepsilon_{x2} - \mu_1\varepsilon_1^3}} \right) . \qquad \textbf{(Brewster angle)} \tag{5.206}$$

Note that the permittivity and permeability values in Eq. (5.206) are all relative quantities and are dimensionless. To illustrate with an example, the reflection coefficients for ordinary and extraordinary waves are plotted in Fig. 5-14 as a function of incident angle using Eqs. (5.199) and (5.204), respectively, for an arrangement in which $\mu_1 = \varepsilon_1 = 1$ and $\mu_2 = 1$, $\varepsilon_2 = 4$, and $\varepsilon_{x2}$ having different values of 2, 4, and 6.

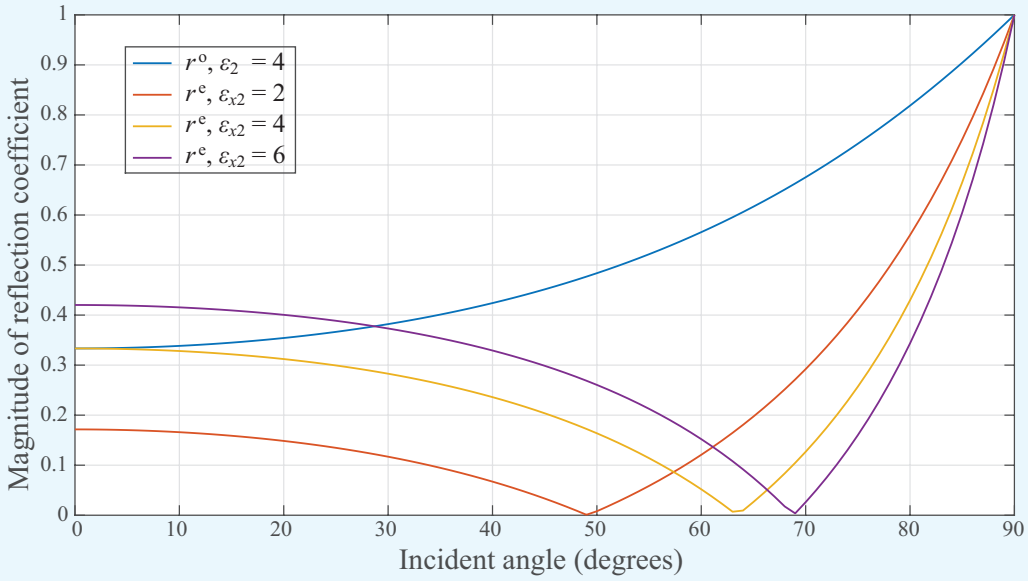


**Figure 5-14:** The magnitude of the reflection coefficient for a plane wave incident upon a uniaxial medium with an optical axis parallel to the interface ($x$-axis), as a function of incident angle. The upper half-space is isotropic with $\varepsilon_1 = \mu_1 = 1$ and the lower half-space is uniaxial with $\varepsilon_2 = 4$ and three different values of $\varepsilon_{x2} = 2$, 4, and 6.

## 5-9 Plane Waves in Layered Media

In many high-frequency circuits and electromagnetic scattering from geophysical media, layered dielectric problems are encountered. To gain some intuition about such problems, we now examine the plane-wave interaction with a layered dielectric medium. Consider a stratified dielectric medium with planar interfaces parallel to the $x$–$y$ plane of a coordinate system. Suppose the constitutive parameters of the $n$th layer are denoted by $\mu_n$ and $\varepsilon_n$, and its boundary with the $(n+1)$th layer is at $z = -d_n$. It is also assumed that the top (region 0) and bottom (region $N+1$) layers are semi-infinite, as shown in Fig. 5-15. Without loss of generality, let us assume that a plane wave is illuminating the interface from above and whose direction of propagation is given by

$$\hat{\mathbf{k}}_\mathrm{i} = \frac{1}{k_0}\left(k_{0x}\hat{\mathbf{x}} - \beta_0\hat{\mathbf{z}}\right) \ , \tag{5.207}$$

where $k_0 = \omega\sqrt{\mu_0\varepsilon_0}$, $k_{0x} = k_0 \sin\theta_\mathrm{i}$, and $\beta_0 = k_0\cos\theta_\mathrm{i}$. For TM waves all field quantities can be expressed in terms of the axial component of the electric field ($E_z$), and for TE waves they can be expressed in terms of the axial component of the magnetic field ($H_z$). Because of the symmetry of the problem, $\partial/\partial y = 0$ for all field components. It is also assumed that the dependence on $z$ in the $n$th layer is of the form $e^{\pm i\beta_n z}$.

For TE waves, $H_{nz}$ can be obtained from the solution to Helmhotz's equation

$$\left(\frac{\partial^2}{\partial x^2} + \left(k_n^2 - \beta_n^2\right)\right) H_{nz} = 0 \,, \tag{5.208}$$

where $k_n = \omega\sqrt{\mu_n \varepsilon_n}$. Other field quantities can be expressed in terms of $H_{nz}$ and are given by

$$H_{nx} = \frac{1}{k_n^2 - \beta_n^2} \frac{\partial^2}{\partial x\, \partial z} H_{nz} \tag{5.209a}$$

and

$$E_{ny} = \frac{-i\omega\mu_n}{k_n^2 - \beta_n^2} \frac{\partial}{\partial x} H_{nz} \,. \tag{5.209b}$$

TE and TM waves are duals of each other under the standard duality relationship $E \to H$, $H \to -E$, and $\mu \rightleftharpoons \varepsilon$. Hence, once the field quantities for TE incidence are obtained, the results for a TM excitation can be obtained using the duality relationships. For an incident TE wave,

$$E_y^{\mathrm{i}} = E_0 e^{-i\beta_0 z} e^{ik_0 \sin\theta_{\mathrm{i}} x} \,. \tag{5.210}$$

The phase-matching condition mandates that the $x$-dependence of all field quantities be the same as that of the incident wave ($e^{ik_0 \sin\theta_{\mathrm{i}} x}$). The total field quantity in region $n$, excluding its dependence on $x$, is given by

$$E_{ny} = A_n e^{i\beta_n z} + B_n e^{-i\beta_n z} \,, \tag{5.211}$$

where $A_n$ and $B_n$ represent the coefficients of the wave components propagating along the positive and negative $z$-directions, respectively. In the zeroth region it is recognized that

$$B_0 = E_0 \tag{5.212a}$$

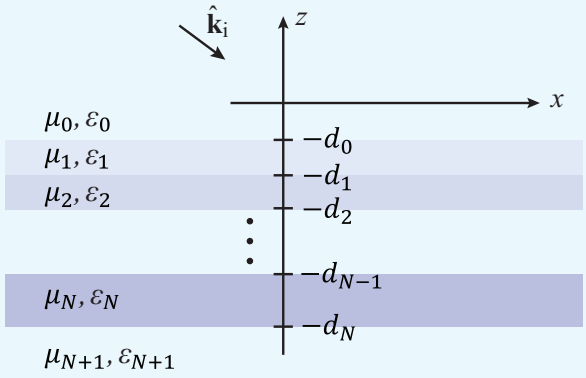


**Figure 5-15:** A layered dielectric medium composed of $N+1$ dielectric media with parallel planar interfaces illuminated by a plane wave from the upper half-space.

and

$$A_0 = R^{\mathrm{TE}} E_0 \ , \tag{5.212b}$$

where $R^{\mathrm{TE}}$ is the total electric field reflection coefficient for TE (***perpendicular polarization***) waves. Since the bottommost region (namely the $(N+1)$th region) is semi-infinite, there would be no upward-traveling wave in that region, i.e.,

$$A_{N+1} = 0 \tag{5.213a}$$

and

$$B_{N+1} = T^{\mathrm{TE}} E_0 \ , \tag{5.213b}$$

where $T^{\mathrm{TE}}$ is the total transmission coefficient.

Evaluating $H_x$ and $E_y$ from Eqs. (5.209a) and (5.209b), and then enforcing the continuity of tangential electric and magnetic fields at the interface between the $n$th and $(n+1)$th region (at $z = -d_n$), we get

$$\frac{\beta_n}{\mu_n}\left[A_n e^{-i\beta_n d_n} - B_n e^{i\beta_n d_n}\right] = \frac{\beta_{(n+1)}}{\mu_{(n+1)}}\left[A_{n+1} e^{-i\beta_{(n+1)} d_n} - B_{n+1} e^{i\beta_{(n+1)} d_n}\right] \tag{5.214a}$$

and

$$\left[A_n e^{-i\beta_n d_n} + B_n e^{i\beta_n d_n}\right] = \left[A_{n+1} e^{-i\beta_{(n+1)} d_n} + B_{n+1} e^{i\beta_{(n+1)} d_n}\right] \ . \tag{5.214b}$$

There are $(N+2)$ regions, and therefore the number of unknowns is $(2N+2)$ (because $B_0$ and $A_{N+1}$ are known). On the other hand, there are $(N+1)$ boundaries and $(2N+2)$ equations for the $(2N+2)$ unknowns. A simple procedure to solve for the unknowns is as follows:

1. Find $\Gamma^{\mathrm{TE}}$ by recursively relating $A_{N+1}/B_{N+1}$ to $A_N/B_N$ (while keeping in mind that $A_{N+1} = 0$), then relating $A_N/B_N$ to $A_{N-1}/B_{N-1}$ and so on until the ratio $A_0/B_0$ is reached.

2. Once $A_0$ is found, relate $A_{n+1}, B_{n+1}$ to $A_n, B_n$ to find all coefficients.

Solving (5.214a), (5.214b) for $A_n$ and $B_n$ results in

$$A_n e^{-i\beta_n d_n} = \frac{1}{2}\left[1 + U_{n(n+1)}\right]\left\{A_{n+1} e^{-i\beta_{(n+1)} d_n} + r^{\mathrm{TE}}_{n(n+1)} B_{n+1} e^{i\beta_{(n+1)} d_n}\right\} \tag{5.215a}$$

and

$$B_n e^{+i\beta_n d_n} = \frac{1}{2}\left[1 + U_{n(n+1)}\right]\left\{r^{\mathrm{TE}}_{n(n+1)} A_{n+1} e^{-i\beta_{(n+1)} d_n} + B_{n+1} e^{i\beta_{(n+1)} d_n}\right\} \ , \tag{5.215b}$$

where

$$U_{n(n+1)} = \frac{\mu_n \beta_{(n+1)}}{\mu_{(n+1)} \beta_n} \ ,$$

and

$$r^{\mathrm{TE}}_{n(n+1)} = \frac{\mu_{n+1}\beta_n - \mu_n \beta_{(n+1)}}{\mu_{n+1}\beta_n + \mu_n \beta_{(n+1)}}$$

is the Fresnel reflection coefficient for a horizontally polarized wave. Taking the ratio of Eqs. (5.215a) and (5.215b), we obtain

$$\frac{A_n}{B_n}\, e^{-2i\beta_n d_n} = \frac{\left[\frac{A_{n+1}}{B_{n+1}}\, e^{-2i\beta_{(n+1)} d_{(n+1)}}\right] e^{2i\beta_{(n+1)}(d_{(n+1)}-d_n)} + r^{\mathrm{TE}}_{n(n+1)}}{\left[\frac{A_{n+1}}{B_{n+1}}\, e^{-2i\beta_{(n+1)} d_{(n+1)}}\right] e^{2i\beta_{(n+1)}(d_{(n+1)}-d_n)} r^{\mathrm{TE}}_{n(n+1)} + 1} \tag{5.216}$$

This is a recurrence relation that can be used to find $A_0/B_0$ starting from $A_{N+1}/B_{N+1} = 0$. In order to solve for $T^{\mathrm{TE}}$ and the rest of the coefficients, we rearrange Eqs. (5.214a) and (5.214b) to obtain $A_{n+1}$ and $B_{n+1}$ in terms of $A_n$ and $B_n$. In matrix notation we have

$$\begin{bmatrix} A_{n+1} e^{-i\beta_{(n+1)} d_{(n+1)}} \\ B_{n+1} e^{i\beta_{(n+1)} d_{(n+1)}} \end{bmatrix} = \overset{=}{F}{}^{\mathrm{TE}}_{(n+1)n} \begin{bmatrix} A_n e^{-i\beta_n d_n} \\ B_n e^{i\beta_n d_n} \end{bmatrix}, \tag{5.217}$$

where $\overset{=}{F}{}^{\mathrm{TE}}_{(n+1)n}$ is referred to as the ***forward propagation matrix***, given by

$$\overset{=}{F}{}^{\mathrm{TE}}_{(n+1)n} = \frac{1}{2}\left(1 + U_{(n+1)n}\right) \begin{bmatrix} e^{-i\beta_{(n+1)}(d_{(n+1)}-d_n)} & r^{\mathrm{TE}}_{(n+1)n}\, e^{-i\beta_{(n+1)}(d_{(n+1)}-d_n)} \\ r^{\mathrm{TE}}_{(n+1)n}\, e^{i\beta_{(n+1)}(d_{(n+1)}-d_n)} & e^{i\beta_{(n+1)}(d_{(n+1)}-d_n)} \end{bmatrix}, \tag{5.218}$$

where

$$U_{(n+1)n} = \frac{\mu_{(n+1)}\beta_n}{\mu_n \beta_{(n+1)}}$$

and

$$r^{\mathrm{TE}}_{(n+1)n} = -r^{\mathrm{TE}}_{n(n+1)} = \frac{\mu_n \beta_{(n+1)} - \mu_(n+1)\beta_n}{\mu_n \beta_{(n+1)} + \mu_{(n+1)}\beta_n}.$$

Knowing $A_0$ and $B_0$, Eq. (5.217) can be used to find $A_n$ and $B_n$ ($n \in \{1,\ldots,N+1\}$). For TM-polarized waves, the duality relations can be used to find the desired quantities.

This formulation for calculating the reflection and transmission properties of plane waves at interfaces between multilayer dielectric media can be used for the design of practical devices in optics and electromagnetics. As discussed in Chapter 1, at very high frequencies such as in the optical regime, the conductivity of metals may not be sufficiently high as to provide surfaces with high reflectivity and minimal loss. However, using multilayer dielectric materials, surfaces with very high reflectivity can be designed. Consider a multilayer periodic layered medium composed of two different materials with indices of refraction $n_2 = \sqrt{\mu_2\varepsilon_2}$ and $n_3 = \sqrt{\mu_3\varepsilon_3}$ and thicknesses $t_2$ and $t_3$, stacked upon each other $N$ times and placed between two half-space media with indices of refraction $n_1 = \sqrt{\mu_1\varepsilon_1}$ and $n_4 = \sqrt{\mu_4\varepsilon_4}$ (see Fig. 5-16). Here $\mu$ and $\varepsilon$ represent the relative permeability and permittivity of each layer. Suppose thicknesses $t_2$ and $t_3$ are chosen such that

$$n_2 t_2 = \frac{\lambda_0}{4} \tag{5.219a}$$

and

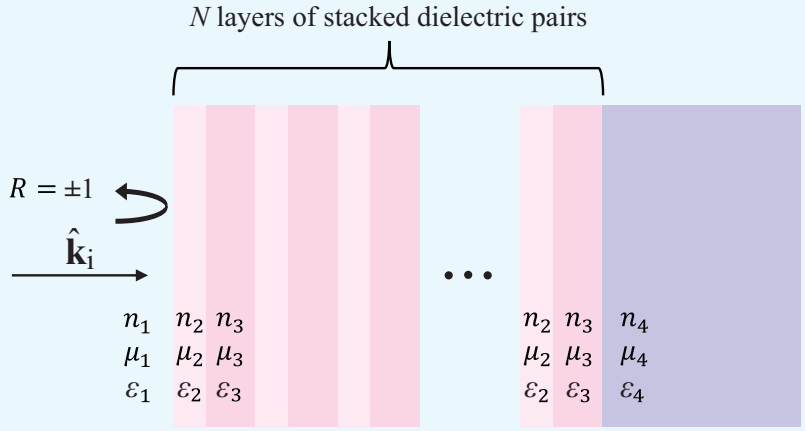


**Figure 5-16:** Periodic $N$-layer stack of dielectric media, each a quarter-wavelength thick, with different indices of refraction, designed to exhibit total reflection.

$$n_3 t_3 = \frac{\lambda_0}{4}\,, \tag{5.219b}$$

where $\lambda_0$ is the free-space wavelength. That is, the thickness of each layer is a quarter-wavelength for $\lambda$ in that medium. In this case it can be shown that the reflection of a plane wave from region 1 is

$$\lim_{N\to\infty} R = \begin{cases} -1 & \text{for } \sqrt{\mu_2/\varepsilon_2} < \sqrt{\mu_3/\varepsilon_3}\,, \\ 1 & \text{for } \sqrt{\mu_2/\varepsilon_2} > \sqrt{\mu_3/\varepsilon_3}\,. \end{cases} \tag{5.220}$$

This structure is known as a ***distributed Bragg reflector*** (***DBR***) or ***Bragg mirror***. In fact, the wave impedance as seen at the interface between region 1 and medium 2 is found to be

$$Z_{\text{in}} = \eta_4 \left(\frac{\eta_2}{\eta_3}\right)^{2N}. \tag{5.221}$$

It is obvious that if $\eta_2 < \eta_3$, then for a sufficiently large number of layers ($N$), one can make $Z_{\text{in}}$ arbitrarily small, and hence $R = -1$. Also, when $\eta_2 > \eta_3$, then $Z_{\text{in}}$ can be made very large, rendering $R = 1$. These conditions correspond to PEC and PMC boundary conditions. This structure is of course band-limited, as we chose each layer to be a quarter-wavelength thick.

The results obtained in Eqs. (5.220) and (5.221) can easily be extended to oblique incidence, noting that the propagation constant and wave impedance in the $j$th layer are given by

$$\beta_j = k_0 n_j \cos\theta_j\,,$$
$$\eta_j^{\text{TE}} = \eta_j \cos\theta_j\,,$$

and

$$\eta_j^{\mathrm{TM}} = \frac{\eta_j}{\cos\theta_j} ,$$

where

$$\cos\theta_j = \sqrt{1 - \left(\frac{n_1}{n_j}\right)\sin^2\theta_1}$$

and $j = 1, 2, 3,$ or 4. In this case the layer thickness should be modified as well:

$$n_j t_j = \frac{\lambda_0}{4\cos\theta_j} .$$

**Example 5-5: Plane-Wave Propagation in an Inhomogeneous Medium (WKB Problem)**

Consider an inhomogeneous medium characterized by permittivity function $\varepsilon(\mathbf{r}) = \varepsilon(z)$ and permeability function $\mu(\mathbf{r}) = \mu$, supporting a linearly polarized plane wave of the form

$$\mathbf{E}(\mathbf{r}) = \hat{\mathbf{y}}\, E_y(z)\, e^{ik_x x} .$$

Derive the wave equation for such a medium and find a possible solution for $E_y(z)$, assuming that $\varepsilon(z)$ is a slowly varying function of $z$. That is, variation of $\varepsilon(z)$ with respect to the "average" wavelength at each point in the medium is slow.

**Solution:** The solution to this problem under the assumption that $\varepsilon(z)$ is a slow-varying function is known as the WKB solution, named after Wentzel, Kramers, and Brillouin. To derive the wave equation for such a medium, we make use of Faraday's law and the modified Ampère's law in a source-free region, i.e.,

$$\nabla \times \mathbf{E} = i\omega\mu\mathbf{H} \tag{5.222a}$$

and

$$\nabla \times \mathbf{H} = -i\omega\, \varepsilon(z)\, \mathbf{E} . \tag{5.222b}$$

Taking $\nabla\times$ of Eq. (5.222a) and then using Eq. (5.222b), we get the following vector wave equation:

$$\nabla \times \nabla \times \mathbf{E} - \omega^2\mu\, \varepsilon(z)\, \mathbf{E} = 0 . \tag{5.223}$$

Note that

$$\nabla \times \nabla \times \mathbf{E} = \nabla(\nabla \cdot \mathbf{E}) - \nabla^2\mathbf{E} . \tag{5.224}$$

Using Gauss' law for electricity ($\nabla \cdot \mathbf{D} = 0$), we have

$$\begin{aligned}\nabla(\nabla \cdot \mathbf{E}) &= \nabla\left[\nabla \cdot \left(\frac{\mathbf{D}}{\varepsilon}\right)\right] \\ &= \nabla\left[\nabla\left(\frac{1}{\varepsilon}\right) \cdot \mathbf{D}\right] \\ &= \nabla\left(-\frac{\nabla\varepsilon}{\varepsilon^2} \cdot \varepsilon\,\mathbf{E}\right) \\ &= -\nabla\left(\frac{\nabla\varepsilon \cdot \mathbf{E}}{\varepsilon}\right) . \end{aligned} \tag{5.225}$$

Noting that

$$\nabla\varepsilon = \frac{d\varepsilon(z)}{dz}\,\hat{\mathbf{z}}$$

and $\mathbf{E} = \hat{\mathbf{y}}\,E_y(z)\,e^{ikx}$, it then follows that for this particular solution, $\nabla(\nabla \cdot \mathbf{E}) = 0$. As a result, the wave equation (5.223) is simplified to

$$[\nabla^2 + \omega^2\mu\,\varepsilon(z)]\,E_y(z)\,e^{ik_x x} = 0\,. \tag{5.226}$$

Since there are no variations with respect to $y$, it follows that $\partial/\partial y = 0$, and therefore Eq. (5.226) can be further simplified to

$$\left(\frac{d^2}{dz^2} + k_z^2(z)\right)\,E_y(z) = 0\,, \tag{5.227}$$

where

$$k_z^2(z) = \omega^2\mu\,\varepsilon(z) - k_x^2\,. \tag{5.228}$$

To proceed further, let us represent $E_y(z) = F(z)\,e^{i\,\phi(z)}$ in its polar form for some slowly varying magnitude function $F(z)$. By substituting this polar form into Eq. (5.227), the following equation is obtained:

$$\frac{d^2F(z)}{dz^2} + 2i\,\frac{dF(z)}{dz}\,\frac{d\phi(z)}{dz} + i\,F(z)\,\frac{d^2\phi(z)}{dz^2} - F(z)\,\left(\frac{d\phi(z)}{dz}\right)^2 + k_z^2(z)\,F(z) = 0\,. \tag{5.229}$$

Since $F(z)$ is a slowly varying function of $z$, $d^2F(z)/dz^2 \approx 0$ compared with other terms in Eq. (5.229). Separating the real and imaginary parts of Eq. (5.229), the following equations for $F(z)$ and $\phi(z)$ are obtained:

$$\left(\frac{d\phi(z)}{dz}\right)^2 - k_z^2(z) = 0 \tag{5.230a}$$

and

$$2\,\frac{dF(z)}{dz}\,\frac{d\phi(z)}{dz} + F(z)\,\frac{d^2\phi(z)}{dz^2} = 0\,. \tag{5.230b}$$

From Eq. (5.230a),

$$\frac{d\phi(z)}{dz} = \pm k_z(z) \ , \tag{5.231}$$

which can be solved to yield

$$\phi(z) = \pm \int_{z_0}^{z} k_z(z')\, dz' \ . \tag{5.232}$$

Now substituting Eq. (5.231) into Eq. (5.230b), we have

$$\frac{1}{F(z)} \frac{dF(z)}{dz} = -\frac{1}{2k_z(z)} \frac{dk_z(z)}{dz} \ . \tag{5.233}$$

Equivalently,

$$\frac{d}{dz}\left[\ln F(z)\right] = \frac{d}{dz}\left(\ln[k_z(z)]^{-1/2}\right) \ ,$$

which can be solved to get

$$F(z) = \frac{E_0}{\sqrt{k_z(z)}} \ .$$

Hence the possible solution to the wave equation takes the following form:

$$E_y(x,z) = \frac{1}{\sqrt{k(z)}} \left(E_0^+ e^{i\int_{z_0}^{z} k(z')\,dz'} + E_0^- e^{-i\int_{z_0}^{z} k(z')\,dz'}\right) e^{ik_x x} \ . \tag{5.234}$$

## Example 5-6: Reflection by and Transmission through a Dielectric Slab

Find expressions for the total reflection and transmission coefficients of a dielectric slab with thickness $t$, permittivity $\varepsilon_1$, and permeability $\mu_1$ sandwiched between two half-space dielectric media with planar interfaces and permittivities and permeabilities of $\varepsilon_0$, $\mu_0$ (top region) and $\varepsilon_2$, $\mu_2$ (bottom region), as shown in Fig. 5-17. Assume that a plane wave propagating along $\hat{\mathbf{k}}_i = (1/k_0)(k_{0x}\,\hat{\mathbf{x}} - \beta_0\,\hat{\mathbf{z}})$ is incident on the slab from the top region.

**Solution:** This is a special case of the general problem for multilayer dielectric media. The electric field expression for a TE wave is given by

$$\mathbf{E}^i = \hat{\mathbf{y}}\, E_0 e^{ik_0 \sin\theta\, x} e^{-i\beta_0 z} \ .$$

The starting point is Eq. (5.216). Recalling that for any layer $n$, $A_n$ represents the magnitude of the electric field of the wave propagating along $+\hat{\mathbf{z}}$ and $B_n$ is associated with the wave moving downward along $-\hat{\mathbf{z}}$, in the present case $A_0$ and $B_0$ represent the fields in the top medium and $A_1$ and $B_1$ pertain to the middle layer. Noting that $A_2 = 0$ in the bottom region, application of Eq. (5.216) for $n = 1$ yields

$$\frac{A_1}{B_1}\, e^{-2i\beta_1 d_1} = r_{12}^{\mathrm{TE}} \ . \tag{5.235}$$

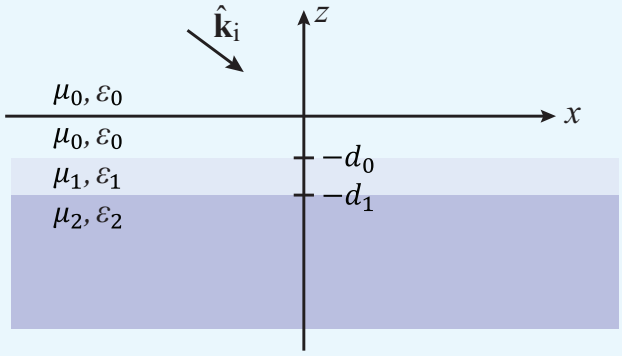


**Figure 5-17:** Dielectric slab with $(\mu_1, \varepsilon_1)$ over a half-space dielectric medium with $(\mu_2, \varepsilon_2)$.

Using Eq. (5.216) again for $n = 0$, we get

$$\frac{A_0}{B_0} e^{-2i\beta_0 d_0} = \frac{\dfrac{A_1}{B_1} e^{-2i\beta_1 d_0} + r_{01}^{\mathrm{TE}}}{\dfrac{A_1}{B_1} e^{-2i\beta_1 d_0} r_{01}^{\mathrm{TE}} + 1} . \tag{5.236}$$

Choosing $d_0 = 0$ and utilizing Eq. (5.235), the total reflection coefficient ($R^{\mathrm{TE}} = A_0/B_0$) can be obtained from Eq. (5.236), noting that $d_1 = t$:

$$R^{\mathrm{TE}} = \frac{r_{12}^{\mathrm{TE}} e^{i2\beta_1 t} + r_{01}^{\mathrm{TE}}}{r_{01}^{\mathrm{TE}} r_{12}^{\mathrm{TE}} e^{i2\beta_1 t} + 1} . \tag{5.237}$$

Also, using Eqs. (5.215a) and (5.215b) twice, it can be shown that

$$\begin{aligned}
\begin{bmatrix} A_0 \\ B_0 \end{bmatrix} &= \left(\frac{1+U_{01}}{2}\right)\left(\frac{1+U_{12}}{2}\right) \begin{bmatrix} e^{i\beta_1 t} & r_{01}^{\mathrm{TE}} e^{-i\beta_1 t} \\ r_{01}^{\mathrm{TE}} e^{i\beta_1 t} & e^{-i\beta_1 t} \end{bmatrix} \begin{bmatrix} 1 & r_{12}^{\mathrm{TE}} \\ r_{12}^{\mathrm{TE}} & 1 \end{bmatrix} \begin{bmatrix} A_2 e^{-i\beta_2 t} \\ B_2 e^{i\beta_2 t} \end{bmatrix} \\
&= \left(\frac{1+U_{01}}{2}\right)\left(\frac{1+U_{12}}{2}\right) \begin{bmatrix} e^{i\beta_1 t} + r_{01}^{\mathrm{TE}} r_{12}^{\mathrm{TE}} e^{-i\beta_1 t} & r_{12}^{\mathrm{TE}} e^{i\beta_1 t} + r_{01}^{\mathrm{TE}} e^{-i\beta_1 t} \\ r_{01}^{\mathrm{TE}} e^{i\beta_1 t} + r_{12}^{\mathrm{TE}} e^{-i\beta_1 t} & e^{-i\beta_1 t} + r_{01}^{\mathrm{TE}} r_{12}^{\mathrm{TE}} e^{i\beta_1 t} \end{bmatrix} \begin{bmatrix} 0 \\ B_2 e^{i\beta_2 t} \end{bmatrix} .
\end{aligned} \tag{5.238}$$

Hence,

$$B_0 = \left(\frac{1+U_{01}}{2}\right)\left(\frac{1+U_{12}}{2}\right)\left(e^{i(\beta_2-\beta_1)t} + r_{01}^{\mathrm{TE}} r_{12}^{\mathrm{TE}} e^{i(\beta_1+\beta_2)t}\right) B_2 . \tag{5.239}$$

Defining the transmission coefficient as

$$T^{\mathrm{TE}} = \frac{B_2}{B_0} = \frac{4e^{i(\beta_1-\beta_2)t}}{(1+U_{01})(1+U_{12})(1+r_{01}^{\mathrm{TE}}r_{12}^{\mathrm{TE}}e^{i2\beta_1 t})} , \tag{5.240}$$

and recognizing that

$$\frac{2}{1+U_{01}} = 1+\frac{1-U_{01}}{1+U_{01}} = 1+r_{01}^{\mathrm{TE}} = \tau_{01}^{\mathrm{TE}} \tag{5.241a}$$

and

$$\frac{2}{1+U_{12}} = 1+\frac{1-U_{12}}{1+U_{12}} = 1+r_{12}^{\mathrm{TE}} = \tau_{12}^{\mathrm{TE}} , \tag{5.241b}$$

we have

$$T^{\mathrm{TE}} = \frac{\tau_{01}^{\mathrm{TE}}\tau_{12}^{\mathrm{TE}}e^{i(\beta_1-\beta_2)t}}{1+r_{01}^{\mathrm{TE}}r_{12}^{\mathrm{TE}}e^{i2\beta_1 t}} . \tag{5.242}$$

## 5-10 Plane-Wave Propagation in a Negative-Index Medium

The constitutive parameters of various types of materials were discussed at some length in Chapter 1. There, the dispersion behavior of permittivity and permeability of materials associated with the spectral response of the induced dipole moments or magnetization vector of molecules revealed the possibility for the real part of the permittivity or permeability of the medium to assume negative values over a certain region of the spectrum. When the real parts of permittivity ($\varepsilon'$) or permeability ($\mu'$) are negative, the propagation constants become imaginary, and the medium inhibits wave propagation over the frequency band where $\varepsilon'$ or $\mu'$ is negative. Such media are referred to as ***bandgap materials***. However, in situations where the real parts of both the permittivity and the permeability of the medium are negative simultaneously, wave propagation is possible but with certain peculiarities that deserve attention. Such media are referred to as ***double-negative*** (DNG) media. One of the intriguing properties of a DNG medium is the fact that its index of refraction is negative, which leads to the possibility that such a medium can potentially overcome the known limitations of conventional lenses, thereby allowing for focusing the entire spectra of plane waves, including the evanescent ones, which constitutes the realization of a perfect lens.

To examine some of these peculiarities, let us consider the behavior of a plane wave propagating in a DNG medium. Similar to a source-free double-positive medium, a plane-wave solution to the wave equation takes the following form:

$$\mathbf{E} = \mathbf{E}_0 e^{i\mathbf{k}\cdot\mathbf{r}} , \tag{5.243}$$

where $\mathbf{k}$, the propagation vector, must satisfy $\mathbf{k}\cdot\mathbf{k} = \omega^2\mu\varepsilon$. For the sake of simplicity let us assume that $\mathbf{k}$ has only a $z$-component and that

$$\mathbf{E} = \mathbf{E}_0 e^{ikz} \tag{5.244}$$

with a dispersion relation

$$k^2 = \omega^2 \mu \varepsilon \ , \tag{5.245}$$

or

$$k = \omega \sqrt{\mu}\, \sqrt{\varepsilon} \ . \tag{5.246}$$

To evaluate $k$ properly, special attention must be given when evaluating the square-root functions. As discussed in Chapter 1, the causality condition mandates that the imaginary parts of $\mu$ and $\varepsilon$ be positive quantities and that the proper branch cut per the chosen time convention $e^{-i\omega t}$ is such that $\sqrt{-1} = i$. Hence for media satisfying the causality condition, $\varepsilon$ and $\mu$ must fall within the upper half-plane of the complex $\mu$ and $\varepsilon$ planes. As a result, for an $\varepsilon$-negative medium, $\varepsilon$ falls in the third quadrant of the complex $\varepsilon$-plane, and the same can be said about a $\mu$-negative medium. Therefore, $\sqrt{\varepsilon}$ and $\sqrt{\mu}$ are each in the first quadrant, and the index of refraction $n = \sqrt{\mu\varepsilon}$ again falls in the third quadrant. That is, the index of refraction has a negative real part. This statement also indicates that

$$\Re\mathrm{e}[k] = k' < 0 \ .$$

Recall that the phase velocity is calculated from

$$\frac{d}{dt}(k'z - \omega t) = 0 \ ,$$

or

$$u_\mathrm{p} = \frac{dz}{dt} = \frac{\omega}{k'} < 0 \ . \tag{5.247}$$

That is, the phase velocity is a negative quantity unlike that for a double-positive medium that has the same but positive values for $\mu$ and $\varepsilon$. The magnetic field can be obtained directly from the modified Ampère's law:

$$\begin{aligned} \mathbf{H} &= \frac{i\mathbf{k} \times \mathbf{E}_0}{i\omega\mu}\, e^{i\mathbf{k}\cdot\mathbf{r}} \\ &= \hat{\mathbf{z}} \times \mathbf{E}_0 \sqrt{\frac{\varepsilon}{\mu}}\, e^{ikz} = \mathbf{H}_0 e^{ikz} \ . \end{aligned} \tag{5.248}$$

But since both $\mu$ and $\varepsilon$ are negative, the characteristic impedance $\eta = \sqrt{\mu/\varepsilon}$ has a positive real part and the direction of the magnetic field would be the same as what it would have been for a double-positive medium. From Gauss' laws for electricity and magnetism it can be shown that $\mathbf{E}_0 \perp \mathbf{H}_0 \perp k'\,\hat{\mathbf{z}}$, similar to a double-positive medium. However, $(\mathbf{E}_0, \mathbf{H}_0, \mathbf{k}')$ form a left-hand system for a DNG, as opposed to a right-hand system for a double-positive system. It is also interesting to examine the behavior of the time-average Poynting vector. As shown in Eq. (5.27), the Poynting vector is given by

$$\begin{aligned} \mathbf{S}(\mathbf{r}) &= \frac{1}{2}\, \Re\mathrm{e}[\mathbf{E} \times \mathbf{H}^*] \\ &= \frac{1}{2}\, \hat{\mathbf{z}}\, |E_0|^2\, \Re\mathrm{e}\left[ \left( \sqrt{\frac{\varepsilon}{\mu}} \right)^* \right] e^{-2k''z} \ , \end{aligned} \tag{5.249}$$

where $k'' = \Im\mathrm{m}[k]$. Noting that $\Re\mathrm{e}[(\sqrt{\varepsilon/\mu})^*] > 0$, and from Eq. (5.249), it is evident that $\mathbf{S}$ is in the positive $z$-direction, whereas the phase velocity is in the negative $z$-direction.

Next we consider a plane wave incident upon a half-space DNG medium. Let us consider a plane wave propagating along $\hat{\mathbf{k}}_\mathrm{i} = \sin\theta_\mathrm{i}\,\hat{\mathbf{x}} + \cos\theta_\mathrm{i}\,\hat{\mathbf{z}}$ in a medium with positive permittivity and permeability $\varepsilon_1$ and $\mu_1$, respectively, incident on a DNG half-space with permeability $\varepsilon_2$ and permeability $\mu_2$, as shown in Fig. 5-18. In the lower half-space the propagation vector is given by

$$\mathbf{k}_1 = k_1 \sin\theta_\mathrm{i}\,\hat{\mathbf{x}} + k_1 \cos\theta_\mathrm{i}\,\hat{\mathbf{z}}\ ,$$

with $k_1 = \omega\sqrt{\mu_1\varepsilon_1}$ . At the interface the phase-matching condition mandates that

$$\mathbf{k}_2 = k_1 \sin\theta_\mathrm{i}\,\hat{\mathbf{x}} + k_2 \cos\theta_\mathrm{t}\,\hat{\mathbf{z}}\ ,$$

with $k_2$ having a negative real value and $\theta_\mathrm{t}$ being defined by Snell's law:

$$\sin\theta_\mathrm{t} = \frac{n_1}{n_2}\sin\theta_\mathrm{i}\ ,$$

and since $n_2 < 0$, $\theta_\mathrm{t}$ is negative, as shown in Fig. 5-18. Also shown in the figure is a double-positive medium and the corresponding phase fronts. Since the wave impedance (TE or TM) of a DNG medium is positive, the expressions for the reflection and transmission coefficients are unchanged and are the same as those obtained for conventional double-positive media.

## 5-11 Negative Refractive-Index Lens

The characteristics of plane-wave propagation in double-negative or negative refractive-index materials were discussed in the previous section. Here we examine qualitatively the propagation of electromagnetic waves emitted from a point source in a double-positive medium placed above a DNG half-space material with a planar interface, as shown in Fig. 5-19. As shown in Section 5-1.2, fields emanating from an arbitrary source can be expressed in terms of a continuous spectrum of plane waves that includes propagating and evanescent plane waves. Propagating plane waves can be represented as rays coming off the point source and then impinge on the interface between the two media. Each plane wave refracts at the interface according to Snell's law, but since the lower medium has a negative index of refraction, the refracted rays form a linear caustic along a line perpendicular to the interface that passes through the point source. In fact, rays on a constant incident angle $\theta_\mathrm{i}$ cone all pass through one point in the DNG medium. The location of these focal points depends on the incident angle, and they all lie on the linear caustics as shown in Fig. 5-19. For example, a ray that impinges on the interface at an angle $\theta_\mathrm{i}$ refracts in a converging manner and meets the perpendicular ray at a depth of $H$, as also shown in Fig. 5-19.

Using Snell's law, and noting that

$$\frac{\tan\theta_\mathrm{i}}{\tan\theta_\mathrm{t}} = \frac{H}{h}\ , \tag{5.250}$$

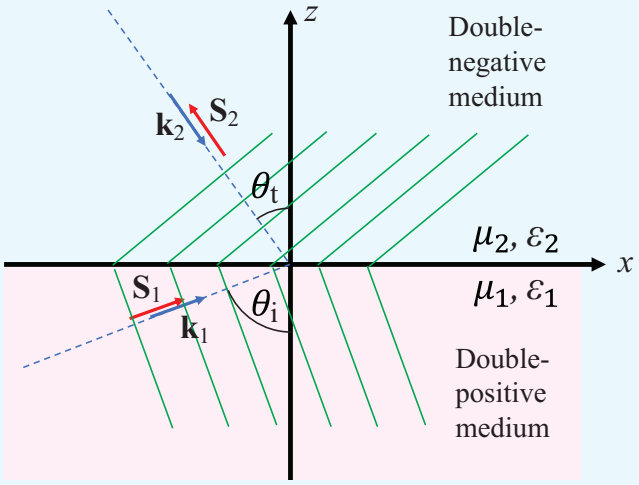


(a) Plane wave incident in a double-positive medium upon a double-negative medium

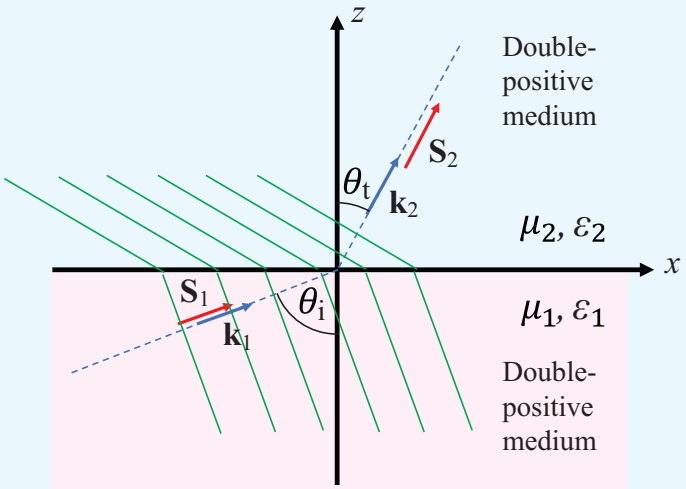


(b) Plane wave incident in a double-positive medium upon a double-positive medium

**Figure 5-18:** (a) A plane wave is incident from a double-positive medium (the lower half-space) upon a planar interface with a double-negative medium (the upper half-space). The phase-matching condition mandates that the tangential components of the $k$-vector ($k_x$) in both media to be the same. However, the normal component of the propagation vector is reversed when compared to a double-positive medium (as shown in (b)).

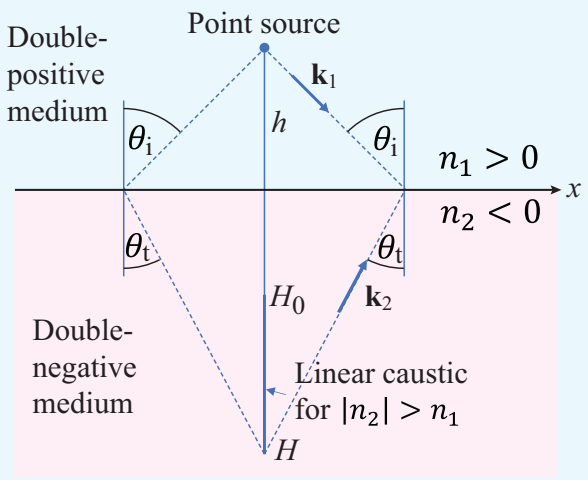


**Figure 5-19:** A point source in a double-positive medium above a double-negative medium. The transmitted rays form a linear caustic in the lower half-space. Rays near normal incidence pass through the caustic point $H_0$.

it can be shown that

$$H = \left|\frac{n_2}{n_1}\right| h \, \frac{\cos\theta_t}{\cos\theta_i} \, . \tag{5.251}$$

For very small values of incident angle ($\theta_i \approx 0$), the starting point of the caustic is located at

$$H_0 = \left|\frac{n_2}{n_1}\right| h \, . \tag{5.252}$$

For $|(n_2/n_1)| > 1$, the linear caustic starts from $z = -H_0$ and goes to $-\infty$. On the other hand, if $|(n_2/n_1)| < 1$, the linear caustic starts from $z = -H_0$ and goes to zero. An interesting condition emerges when $|(n_2/n_1)| = 1$. In this case, the linear caustic collapses to a point and the half-space DNG medium acts like a lens. This is due to the fact that $\theta_t = -\theta_i$, and as a result, all refracted rays must go through the mirror-image point of the source. This particular lens presents a number of advantages over traditional lenses, especially when

$$n_2 = -n_1 \, . \tag{5.253}$$

In this case, the wave impedances for TE and TM waves in the upper half-space, computed from Eqs. (5.103) and (5.106), are given by

$$Z_1^{\mathrm{TM}} = \frac{\beta_1}{\omega\varepsilon_1} \tag{5.254a}$$

and

$$Z_1^{\mathrm{TE}} = \frac{\omega\mu_1}{\beta_1} \, , \tag{5.254b}$$

where $\beta_1 = \sqrt{k_1^2 - k_\rho^2}$ and $k_\rho^2 = k_x^2 + x_y^2$. Also, in the lower half-space we have

$$Z_2^{\mathrm{TM}} = \frac{\beta_2}{\omega \varepsilon_2} \tag{5.255a}$$

and

$$Z_2^{\mathrm{TE}} = \frac{\omega \mu_2}{\beta_2} \,, \tag{5.255b}$$

with

$$\beta_2 = \sqrt{k_2^2 - k_\rho^2} \,.$$

Noting that $\Re\mathrm{e}[k_2] < 0$, it can be shown that also $\Re\mathrm{e}[\beta_2] < 0$. For a lossless case and a propagating wave ($k_2^2 > k_\rho^2$), considering the fact that $\varepsilon_2 < 0$ and $\mu_2 < 0$, it is obvious that the impedances given by Eqs. (5.254) and (5.255) are positive, and that

$$Z_2^{\mathrm{TM}} = Z_1^{\mathrm{TM}} \tag{5.256a}$$

and

$$Z_2^{\mathrm{TE}} = Z_1^{\mathrm{TE}} \,, \tag{5.256b}$$

recalling that $k_2^2 = k_1^2$. The reflection coefficients at the interface are thus calculated to be

$$R^{\mathrm{TE}} = \frac{Z_2^{\mathrm{TE}} - Z_1^{\mathrm{TE}}}{Z_2^{\mathrm{TE}} + Z_1^{\mathrm{TE}}} = 0 \tag{5.257a}$$

and

$$R^{\mathrm{TM}} = \frac{Z_2^{\mathrm{TM}} - Z_1^{\mathrm{TM}}}{Z_2^{\mathrm{TM}} + Z_1^{\mathrm{TM}}} = 0 \,, \tag{5.257b}$$

independent of the incident angle. That is, all power carried by the propagating waves is transferred and focused. It is also interesting to examine the reflection coefficient of the evanescent waves. For the evanescent waves,

$$\beta_1 = \sqrt{k_1^2 - k_\rho^2} = i\sqrt{k_\rho^2 - k_1^2} = i\alpha \,, \tag{5.258}$$

where $\alpha$ is a positive number. If the lower half-space is slightly lossy, then $k_2^2$ is in the fourth quadrant, and for $k_\rho^2 > k_2^2$, we find

$$\beta_2 = \sqrt{k_2^2 - k_\rho^2}$$

in the third quadrant, and in the limit as $k_2 \to -k_1$ we have

$$\beta_2 = i\alpha \,. \tag{5.259}$$

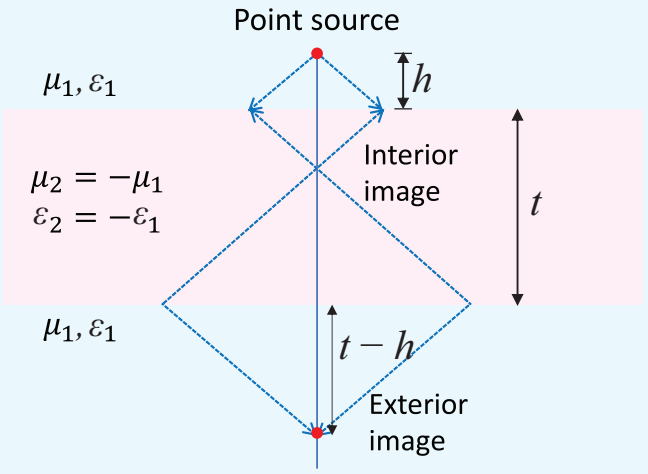


**Figure 5-20:** Configuration of a perfect lens created by a negative-index material having permittivity and permeability equal to the negative of those of the surrounding medium. It is shown that the total reflection from the DNG slab is zero for all propagating and evanescent waves emanating from a point source. Also, all radiating power appears at the image point with a negative phase delay of $2\beta_0 t$.

Thus, for the evanescent waves,

$$Z_1^{\rm TM} = \frac{i\alpha}{\omega\varepsilon_1} \qquad \text{and} \qquad Z_1^{\rm TE} = \frac{\omega\mu_1}{i\alpha}\,, \tag{5.260a}$$

and

$$Z_2^{\rm TM} = -\frac{i\alpha}{\omega\varepsilon_1} \qquad \text{and} \qquad Z_2^{\rm TE} = -\frac{\omega\mu_1}{i\alpha}\,, \tag{5.260b}$$

for which the reflection coefficient of the evanescent wave is found to be

$$R_{\rm eva}^{\rm TE} = R_{\rm eva}^{\rm TM} = \infty\,.$$

This indicates that evanescent waves build up very intensely near the interface.

This configuration for a lens is not very practical, as the focal point (image point) is within the lens. However, a practical lens can be configured from a DNG material slab with thickness $t$ and planar interfaces having permeability and permittivity $\mu_2 = -\mu_1$ and $\varepsilon_2 = -\varepsilon_1$, respectively, as shown in Fig. 5-20. In this configuration, for a source point at a height $h < t$, an interior image point is formed inside the slab, which acts as a source for the second interface. This interior image has a secondary image in the lower half-space at a distance of $t - h$ below the bottom interface. Using the results obtained in Example 5-4, the total reflection coefficient can be obtained from Eq. (5.237). For propagating waves, as shown above

$$r_{01}^{\rm TE} = r_{01}^{\rm TM} = 0\,,$$

which when used in Eq. (5.237) renders

$$R^{\mathrm{TE}} = R^{\mathrm{TM}} = 0 \, .$$

For evanescent waves, it can easily be shown that the reflection coefficients at the interface are infinite; i.e., $r_{01}^{\mathrm{TE}} = r_{01}^{\mathrm{TM}} = \infty$. Rewriting Eq. (5.237) and recalling that $r_{01}^{\mathrm{TE/TM}} = -r_{10}^{\mathrm{TE/TM}}$, the total reflection coefficient for evanescent waves can be written as

$$R_{\mathrm{eva}}^{\mathrm{TE/TM}} = \frac{\left(1 \Big/ r_{01}^{\mathrm{TE/TM}}\right)\left(1 - e^{i2\beta_1 t}\right)}{1 \Big/ \left[\left(r_{01}^{\mathrm{TE/TM}}\right)^2\right] - e^{i2\beta_1 t}} \, .$$

Now it becomes apparent that

$$R_{\mathrm{eva}}^{\mathrm{TE}} = R_{\mathrm{eva}}^{\mathrm{TM}} = 0 \, . \tag{5.261}$$

This indicates that the lens is also matched to all evanescent waves and that all active and reactive power generated by the source appears at the image point. Now examining the transmission coefficient for this lens, we can use Eq. (5.240), and we observe that for propagating waves

$$U_{01} = \frac{\mu_0 \beta_1}{\mu_1 \beta_0} = \frac{\mu_0(-\beta_0)}{(-\mu_0)\beta_0} = 1$$

and

$$U_{12} = \frac{\mu_1 \beta_2}{\mu_2 \beta_1} = \frac{(-\mu_0)\beta_0}{\mu_0(-\beta_0)} = 1 \, ,$$

and $r_{01}^{\mathrm{TE}} = r_{12}^{\mathrm{TE}} = 0$. Thus the total transmission coefficient for propagating waves is given by

$$T^{\mathrm{TE}} = e^{i(-\beta_0 - \beta_0)t} = e^{-i2\beta_0 t} \, . \tag{5.262}$$

For evanescent waves,

$$U_{01} = \frac{\mu_0(i\alpha)}{-\mu_0(i\alpha)} = -1$$

and

$$U_{12} = \frac{-\mu_0(i\alpha)}{\mu_0(i\alpha)} = -1 \, ,$$

and $r_{01}^{\mathrm{TE}} = r_{12}^{\mathrm{TE}} = \infty$. It can also be shown that

$$(1 + U_{01}) r_{01}^{\mathrm{TE}} = 2$$

and

$$(1 + U_{12}) r_{12}^{\mathrm{TE}} = 2 \, ,$$

and as a result, for evanescent waves the total transmission coefficient is given by

$$T_{\text{eva}}^{\text{TE}} = e^{2\alpha t} \ . \tag{5.263}$$

It is interesting to note that the transmitted evanescent waves are amplified through the DNG lens.

## Summary

### Concepts

- The electric field and magnetic field satisfy the vector wave equation in homogeneous, isotropic, and unbounded media.
- A class of solution to the wave equation is known as ***plane waves***, for which the vector directions of the electric and magnetic fields are invariant throughout space.
- The magnitude and phase of plane waves are constant in planes perpendicular to the direction of propagation, and the ratio of the electric field to the magnetic field is constant throughout space. This constant is known as the ***characteristic impedance of the medium*** $\eta = \sqrt{\mu/\varepsilon}$.
- Due to the linearity of Maxwell's equations, fields produced by arbitrary sources, outside the source region, can be expressed in terms of the superposition of an infinite number of plane waves propagating in different directions.
- The polarization of a plane wave is defined as the trace of the tip of an electric field as a function of time in a fixed plane perpendicular to the direction of propagation. In general the polarization of the wave is elliptical, clearly identified by two angles, namely the ellipticity angle ($\chi$) and the orientation angle ($\Psi$).
- A plane-wave solution can also be obtained for propagation in anisotropic media, but the dispersion relations relating components of the propagation vector to the medium wave number are complex.
- A plane-wave solution in anisotropic media is facilitated by kDB coordinate transformation. An example for a simple anisotropic medium, known as a uniaxial medium, is considered, and it is shown that, depending on the polarization of the electric field, two different waves (ordinary and extraordinary) with different propagation constants and characteristics can be supported. For ordinary waves, the electric field and electric flux density are parallel to each other and both are perpendicular to the plane formed by the propagation vector and the optical axis. For the extraordinary wave, **D** and **E** are no longer parallel to each other, and both lie in the plane formed by the propagation vector and the optical axis. In this case the electric field has a component along the direction of propagation.
- Another class of wave expansion, known as ***transverse electric*** and ***transverse magnetic*** fields is presented. Transverse electric (TE) fields are shown to be produced from a magnetic vector potential that has only one component along a desired direction of propagation. Transverse magnetic (TM) fields are obtained from an electric Hertz vector potential that has a single component along the direction of propagation.

### Concepts (continued)

- TE and TM field expansions are used to find the reflection and transmission of incident plane waves at the planar boundaries of layered dielectric media.
- Plane-wave reflection and transmission at the interface of a dielectric and a good conductor are used to show that good conductors can be modeled by an impedance boundary condition.
- For a uniaxial half-space a different gauge condition has to be defined to find the reflected transmission coefficients for TE (ordinary wave) and TM (extraordinary wave).
- Negative-index media or double-negative media (DNG) possess permittivity and permeability values whose real parts are both negative. DNG media can support wave propagation; however, it is shown that their wave number $k$ has a negative real part. Such media have negative phase velocities, and as a result, they demonstrate a negative Doppler shift.
- A dielectric slab of a DNG medium whose index of refraction is equal to but the negative of its surrounding medium is shown to perform like a perfect lens.

### Important Terms

Provide definitions or explain the meaning of the following terms:

axial ratio
bandgap material
birefringent
Bragg mirror
Brewster angle
characteristic impedance
continuous spectrum of plane waves
coordinate transformation matrix
critical angle
DB plane
dielectric slab
dispersion relation
distributed Bragg reflector (DBR)
double-negative media
Eikonal equation
electric reflection coefficient
electric transmission coefficient
ellipticity angle for polarization
elliptic polarization
energy density of plane waves
energy velocity
evanescent wave
extraordinary wave
Fermat's principle
forward propagation matrix
good conductor
impedance boundary condition
impermeability
impermittivity
kDB coordinate
magnetic reflection coefficient
magnetic transmission coefficient
method of separation of variables
negative angle of refraction
negative refractive index
negative refractive index lens
nonuniform plane wave
optical path length
ordinary wave
perpendicular polarization
phase-matching condition
plane wave
Poincaré sphere
polarization unit vector
power density of plane waves
principle of least time
skin depth
Snell's law of reflection
Snell's law of refraction
TEM wave
tilt angle for polarization
transcendental equation
transverse electric fields
transverse magnetic fields
uniform plane wave
unitary transformation
wave polarization
WKB solution

## Important Equations

**Wave equation:**

$$\nabla^2\mathbf{E} + k^2\mathbf{E} = 0$$

**Plane-wave electric and magnetic fields:**

$$\mathbf{E}(\mathbf{r}) = \mathbf{E}_0 e^{i\mathbf{K}\cdot\mathbf{r}} ,$$

$$\mathbf{H} = \frac{\hat{\mathbf{k}} \times \mathbf{E}_0}{\eta}\, e^{i\mathbf{K}\cdot\mathbf{r}}$$

**Dispersion relation for a homogeneous isotropic medium:**

$$k^2 = \mathbf{K}\cdot\mathbf{K} = |\mathbf{K}'|^2 - |\mathbf{K}''|^2 + 2i\,\mathbf{K}'\cdot\mathbf{K}''$$

**Plane-wave stored electric and magnetic energy density:**

$$W_\mathrm{e} = \tfrac{1}{4}\,\varepsilon|E_0|^2 ,$$

$$W_\mathrm{m} = \tfrac{1}{4}\,\mu|H_0|^2$$

**Plane-wave time-average power density:**

$$\mathbf{S}(\mathbf{r}) = \frac{|E_0|^2}{2\eta}\,\hat{\mathbf{k}}$$

**Polarization unit vector:**

$$\hat{\mathbf{p}} = \frac{\mathbf{E}}{\sqrt{\mathbf{E}\cdot\mathbf{E}^*}} = \frac{\hat{\mathbf{x}} + \alpha e^{i\delta}\,\hat{\mathbf{y}}}{\sqrt{1+\alpha^2}}$$

**Polarization tilt and ellipticity angles:**

$$\tan(2\psi) = \tan(2\gamma)\cos\delta, \;\; \sin(2\chi) = \sin(2\gamma)\sin\delta$$

**Dispersion relation for ordinary and extraordinary waves in a uniaxial medium:**

$$K_x^2 + K_y^2 + K_z^2 = \omega^2\mu\varepsilon_{xx} ,$$

$$K_x^2 + K_y^2 + \frac{\varepsilon_{zz}}{\varepsilon_{xx}}\,K_z^2 = \omega^2\mu\varepsilon_{zz}$$

## Important Equations (continued)

**Transverse magnetic fields:**

$$\mathbf{E} = [\pm i\beta\ \nabla_t\Psi + k_c^2\Psi\hat{\mathbf{z}}]e^{\pm i\beta z}\ ,$$
$$\mathbf{H} = -i\omega\varepsilon(\nabla_t\Psi \times \hat{\mathbf{z}})e^{\pm i\beta z}$$

**Transverse electric fields:**

$$\mathbf{H} = [i\beta\ \nabla_t\Psi_m + k_c^2\Psi_m\hat{\mathbf{z}}]e^{i\beta z}\ ,$$
$$\mathbf{E} = i\omega\mu(\nabla_t\Psi_m \times \hat{\mathbf{z}})e^{i\beta z}$$

**TM wave impedance:**

$$Z_{TM} = \frac{\hat{\mathbf{z}} \times \mathbf{E}_t}{\mathbf{H}_t} = \frac{\beta}{\omega\varepsilon}$$

**TE wave admittance:**

$$Y_{TE} = -\frac{\hat{\mathbf{z}} \times \mathbf{H}_t}{\mathbf{E}_t} = \frac{\beta}{\omega\mu}$$

**Magnetic field reflection coefficient:**

$$\Gamma_{TM} = -\frac{\eta_2\cos\theta_t - \eta_1\cos\theta_i}{\eta_2\cos\theta_t + \eta_1\cos\theta_i}$$

**Electric field reflection coefficient:**

$$\Gamma_{TE} = \frac{\eta_2/\cos\theta_t - \eta_1/\cos\theta_i}{\eta_2/\cos\theta_t + \eta_1/\cos\theta_i}$$

**Snell's law of refraction:**

$$n_1\sin\theta_i = n_2\sin\theta_t$$

**Brewster angle:**

$$\theta_B^{TM} = \sin^{-1}\left(\sqrt{\frac{\varepsilon_2(\mu_1\varepsilon_2 - \mu_2\varepsilon_1)}{\mu_1(\varepsilon_2^2 - \varepsilon_1^2)}}\right),$$
$$\theta_B^{TE} = \sin^{-1}\left(\sqrt{\frac{\mu_2(\varepsilon_1\mu_2 - \varepsilon_2\mu_1)}{\varepsilon_1(\mu_2^2 - \mu_1^2)}}\right)$$

**Eikonal equation:**

$$|\nabla\phi(\mathbf{r})|^2 = \varepsilon_r(\mathbf{r}) = n(\mathbf{r})$$

## Important Equations (continued)

**Eikonal equation for ray trajectory:**

$$\frac{d}{ds}\left(n(\mathbf{r})\,\frac{d\mathbf{r}}{ds}\right) = \nabla\, n(\mathbf{r})$$

**Skin depth:**

$$\delta_s = \frac{1}{\sqrt{\pi} f \mu \varepsilon}$$

**Good conductor surface impedance:**

$$\eta_c = \frac{1-j}{\delta_s \sigma}$$

**Reflection coefficient for extraordinary waves:**

$$r^e(\theta_i) = \frac{\sqrt{\varepsilon_2 \varepsilon_{x2}}\cos\theta_i - \varepsilon_1\sqrt{\mu_2\varepsilon_2 - \mu_1\varepsilon_1\sin^2\theta_i}}{\sqrt{\varepsilon_2 \varepsilon_{x2}}\cos\theta_i + \varepsilon_1\sqrt{\mu_2\varepsilon_2 - \mu_1\varepsilon_1\sin^2\theta_i}}$$

**Brewster angle for extraordinary waves:**

$$\theta_B = \sin^{-1}\left(\sqrt{\frac{\varepsilon_2(\varepsilon_{x2} - \mu_2\varepsilon_1^2)}{\varepsilon_2\varepsilon_{x2} - \mu_1\varepsilon_1^3}}\right)$$

**Reflection and transmission coefficients for a dielectric slab:**

$$R^{TE} = \frac{r_{12}^{TE} e^{i2\beta_1 t} + r_{01}^{TE}}{r_{01}^{TE} r_{12}^{TE} e^{i2\beta_1 t} + 1},$$

$$T^{TE} = \frac{\tau_{01}^{TE}\tau_{12}^{TE} e^{i(\beta_1 - \beta_2)t}}{1 + r_{01}^{TE} r_{12}^{TE} e^{i2\beta_1 t}}$$

**Reflection from a DNG perfect lens:**

$$R^{TE} = R^{TM} = 0\,,$$

$$R_{eva}^{TE} = R_{eva}^{TM} = 0$$

**Transmission from a DNG perfect lens:**

$$T^{TE} = e^{-i2\beta_0 t}\,,$$

$$T_{eva}^{TE} = e^{2\alpha t}$$

## PROBLEMS

### Plane Waves

**5.1** Consider a plane wave propagating in a dielectric with a loss tangent of $\tan\delta = \varepsilon''/\varepsilon'$. Let the electric field be $E_0 e^{ikx}$, where $k$ is the complex propagation constant defined by

$$k = \omega\sqrt{\mu\varepsilon}.$$

**(a)** Find the phase difference between the $H$-field and $E$-field.

**(b)** Find the resulting complex Poynting vector. How do you interpret the imaginary and real parts?

**5.2**

**(a)** Can the wave-vector for a plane wave ever be complex in a lossless medium? If so, give an example of such a situation and state what condition has to hold true between the real and imaginary parts. If not, explain why.

**(b)** Give a physical interpretation for the magnitude and direction of the real part of the wave-vector ($\mathbf{K} = \mathbf{K}' + i\,\mathbf{K}''$). Do the same for the imaginary part.

**(c)** Prove that the stored electric and magnetic energies for a plane wave are equal in a lossless medium.

**(d)** Consider a planar interface between two media, Region 1 and Region 2. For a nonmagnetic medium, determine the conditions for a TM incident plane wave to have zero reflectivity at oblique incidence. What about a TE plane wave?

**5.3** A plane wave is normally incident from free space onto a half-space of a material characterized by parameters $\varepsilon$ and $\mu$, as shown in Fig. P5.3.

**(a)** Calculate the transmission and reflection coefficients of the electric field when the material is lossless.

**(b)** Prove power conservation for the incident, reflected and transmitted waves at the interface.

**(c)** Calculate the transmission and reflection coefficients when the material has finite conductivity $\sigma$.

(*Hint:* Assume that the incident plane wave has an electric field vector oriented along the $x$-axis and is propagating along the positive $z$-axis, and then match the boundary conditions for incident, reflected, and transmitted waves.)

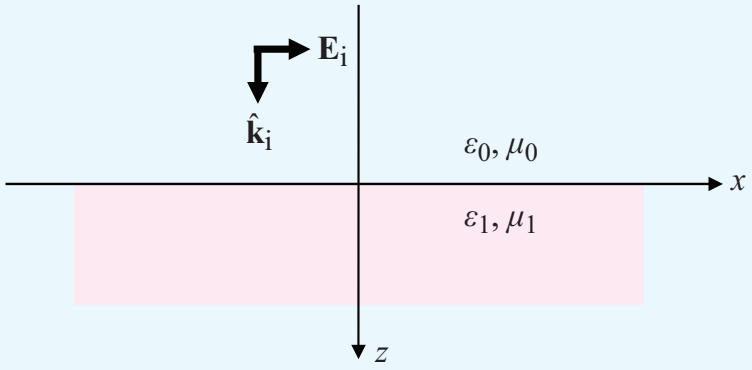


**Figure P5.3:** A planar interface between two half-space dielectric media illuminated by a plane wave of normal incidence.

**5.4** A plane wave of angular frequency $\omega$ and wave number $k$ propagates in a neutral, homogeneous, anisotropic, nonconducting medium with $\mu = 1$.

**(a)** Show that **H** is orthogonal to **E**, **D**, and **K**, and also that **D** and **H** are transverse but **E** is not.

**(b)** Let $\mathbf{D} = \overline{\overline{\varepsilon}}\,\mathbf{E}$, where $\overline{\overline{\varepsilon}}$ is a real symmetric tensor. Choosing the coordinate system parallel to the eigenvectors' directions, the tensor becomes diagonal:

$$\overline{\overline{\varepsilon}} = \begin{bmatrix} \varepsilon_1 & 0 & 0 \\ 0 & \varepsilon_2 & 0 \\ 0 & 0 & \varepsilon_3 \end{bmatrix} .$$

Define $\mathbf{K} = k\,\hat{\mathbf{k}}$, where the components of the unit vector $\hat{\mathbf{k}}$ along the axes are $k_1$, $k_2$, and $k_3$. If $\upsilon = \omega/k$ and $\upsilon_j = 1/\sqrt{\varepsilon_j}$, show that the components of **E** satisfy

$$k_j \sum_{i=1}^{3} k_i E_i + \left( \frac{\upsilon^2}{\upsilon_j^2} - 1 \right) E_j = 0 .$$

Write down the equation for the phase velocity $u$ in terms of $k_j$ and $\upsilon_j$. Show that this equation has two finite roots for $\upsilon^2$, corresponding to two distinct modes of propagation in the direction of $\hat{\mathbf{k}}$.

**5.5** Assume a TE plane wave obliquely incident from free space onto a half-space medium with permittivity $\varepsilon$ and permittivity $\mu_0$, as shown in Fig. P5.5.
Show that

$$P_\mathrm{i} = P_\mathrm{r} + P_\mathrm{t} ,$$

where $P_\mathrm{i}$, $P_\mathrm{r}$, and $P_\mathrm{t}$ are the time-averaged power in the incident, reflected, and transmitted waves respectively. *Hint:* The power density toward or away from the interface is given by the component of the Poynting vector in the direction normal to the interface.

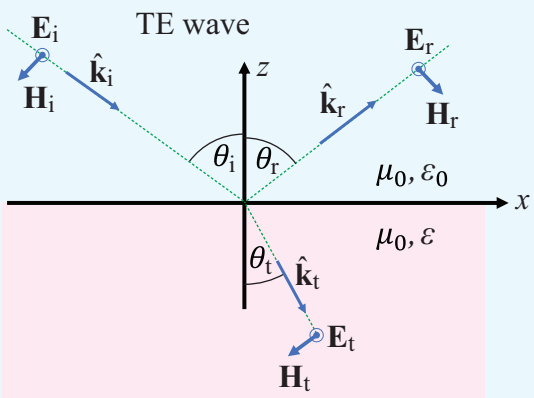


**Figure P5.5:** A planar interface between two half-space dielectric media illuminated by a plane wave illuminating the lower half-space from the top medium at oblique incidence.

**5.6** In this problem, you will derive the well-known ***physical optics*** (***PO***) formalism, used for evaluating the scattered field from an object, assuming a plane-wave incidence on an object. This is applicable only when the object (more specifically, its curvature) is much larger than the wavelength of the incident field, so it is a high-frequency technique.

The idea here is as follows: Given an incident plane wave at a *planar* boundary (see Fig. P5.6(a)), we can easily find the "scattered" (not really called scattering—simply called reflected) field by matching boundary conditions at the planar interface. The fields are computed in terms of Fresnel coefficients, and you will derive them in part (a).

Now, if the scatterer has a large curvature, at every point on the scatterer the surface can be locally approximated by an infinite tangent plane. At each of those points, we can find the scattered field using the Fresnel coefficients and tangent-plane approximation. Using the equivalent surface currents over the entire lit region of the scatterer and using them to find the reradiated fields gives us a good approximation to the total scattered field.

In part (e), you will implement PO to find the scattered field from a PEC cylinder. It is important to note that PEC/PMC makes PO implementation much easier, as the Fresnel coefficients just become constants (part (c)) and field calculation is simpler.

**(a)** Match boundary conditions to derive the Fresnel reflection coefficient for a plane wave incident on a planar dielectric boundary. Derive the reflection coefficient for both TE and TM cases of polarization. Figure P5.6(b) shows the state of polarization for each case.

*Hint 1:* Fields in the TE mode are given by

$$\mathbf{E}_i = E_0 e^{ik_1(x\sin\theta_i - z\cos\theta_i)}\,\hat{\mathbf{y}}\,,$$

$$\mathbf{H}_i = \frac{1}{\eta_1} E_0 e^{ik_1(x\sin\theta_i - z\cos\theta_i)}(\hat{\mathbf{x}}\cos\theta_i + \hat{\mathbf{z}}\sin\theta_i)\,,$$

$$\mathbf{E}_r = r_{TE} E_0 e^{ik_1(x\sin\theta_i + z\cos\theta_i)}\,\hat{\mathbf{y}}\,,$$

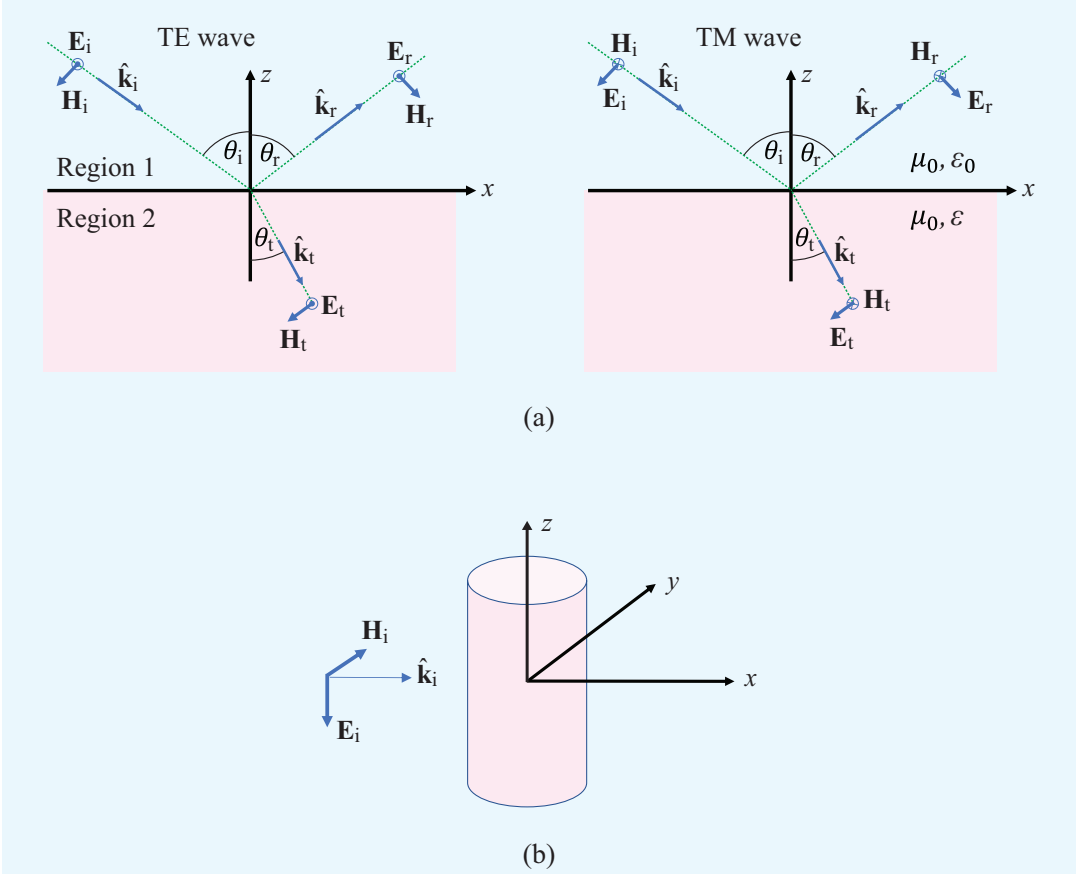


**Figure P5.6:** This figure shows the steps for calculating the PO equivalent current on a smooth surface of objects with large radii of curvature using tangent plane approximation.

$$\mathbf{H}_\mathrm{r} = \frac{r_\mathrm{TE}}{\eta_1} E_0 e^{ik_1(x\sin\theta_\mathrm{i} + z\cos\theta_\mathrm{i})}(-\hat{\mathbf{x}}\cos\theta_\mathrm{i} + \hat{\mathbf{z}}\sin\theta_\mathrm{i}) \,,$$

$$\mathbf{E}_\mathrm{t} = t_\mathrm{TE} E_0 e^{ik_2(x\sin\theta_\mathrm{t} - z\cos\theta_\mathrm{t})}\,\hat{\mathbf{y}} \,,$$

and

$$\mathbf{H}_\mathrm{t} = \frac{t_\mathrm{TE}}{\eta_2} E_0 e^{ik_2(x\sin\theta_\mathrm{t} - z\cos\theta_\mathrm{t})}(\hat{\mathbf{x}}\cos\theta_\mathrm{t} + \hat{\mathbf{z}}\sin\theta_\mathrm{t}) \,.$$

The Fresnel reflection coefficient is defined as

$$r_\mathrm{TE} = \frac{E_0^\mathrm{r}}{E_0^\mathrm{i}}$$

and

$$r_\mathrm{TM} = \frac{H_0^\mathrm{r}}{H_0^\mathrm{i}} \,.$$

*Hint 2:* Use Snell's law: $\theta_i = \theta_r$, $k_1 \sin\theta_i = k_2 \sin\theta_t$.
*Hint 3:* Use duality to get $r_{TM}$ from $r_{TE}$.

It should be noted that our definition of $r_{TM}$ is contrary to the usual convention: the $H$ field is generally assumed to reverse sign upon reflection.

**(b)** Show that $r_{TE} = -1$ and $r_{TM} = 1$ if medium 2 is a PEC.

**(c)** Given a surface (not necessarily planar) with a normal vector $\hat{\mathbf{n}}$, the following plane wave is incident on the surface:

$$\mathbf{E}_i = \mathbf{E}_0 e^{ik\cdot\mathbf{r}}\,, \qquad \mathbf{H}_i = \mathbf{H}_0 e^{ik\cdot\mathbf{r}}\,, \quad \text{and} \quad \mathbf{H}_0 = \frac{\hat{\mathbf{k}}\times\mathbf{E}_0}{\eta}\,.$$

Consider a typical point on the surface. Define a tangent vector

$$\hat{\mathbf{t}} = \frac{\hat{\mathbf{k}}\times\hat{\mathbf{n}}}{|\hat{\mathbf{k}}\times\hat{\mathbf{n}}|}\,.$$

1. Decompose the incident field into two components: one along the tangent $\hat{\mathbf{t}}$ and the other one perpendicular to the tangent ($\hat{\mathbf{k}}\times\hat{\mathbf{t}}$).
2. Compute the reflected fields by applying the appropriate Fresnel coefficient to each component of the incident fields.
3. Compute the following:

$$\hat{\mathbf{n}}\times\mathbf{E}_{total} = \hat{\mathbf{n}}\times(\mathbf{E}_i + \mathbf{E}_r)$$

and

$$\hat{\mathbf{n}}\times\mathbf{H}_{total} = \hat{\mathbf{n}}\times(\mathbf{H}_i + \mathbf{H}_r)\,.$$

**(d)** Use boundary conditions to show that at the surface of a PEC

$$\mathbf{J}_{ms} = 0 \qquad \text{and} \qquad \mathbf{J}_s = 2\hat{\mathbf{n}}\times\mathbf{H}_i\,.$$

The problem of finding the scattered field is now equivalent to the problem of finding the radiated field due to these currents in the homogeneous background medium (in the absence of the scatterer). As such, scattered magnetic and electric fields are given by Eqs. (3.118a) and (3.118b).

**(e)** Given a PEC cylinder of radius $a$ and finite length ranging from $z = -L/2$ to $z = L/2$, located at the center of the coordinate system, assume that the following plane wave is incident on this cylinder, as shown in Fig. P5.6:

$$\mathbf{E}_i = -\hat{\mathbf{z}}\,E_0 e^{ikx}$$

and

$$\mathbf{H}_i = \hat{\mathbf{y}}\,H_0 e^{ikx}\,.$$

Find an expression for $\mathbf{H}_s$. You do not need to solve the integral; however, you should simplify as many terms as you can. Show that the field scattered by PEC cylinders is similar to the radiation pattern of a dipole. (*Hint:* Integrate only over the *lit region* of the cylinder.)

**5.7** Consider a perfect electromagnetic conductor (PEMC). The following boundary conditions hold at the interface of a PEMC and free space:

$$\mathbf{n} \times (\mathbf{H} + Y\mathbf{E}) = 0$$

and

$$\mathbf{n} \cdot (\mathbf{D} - Y\mathbf{B}) = 0 \, .$$

In this problem you will find the reflection coefficients from such an interface.

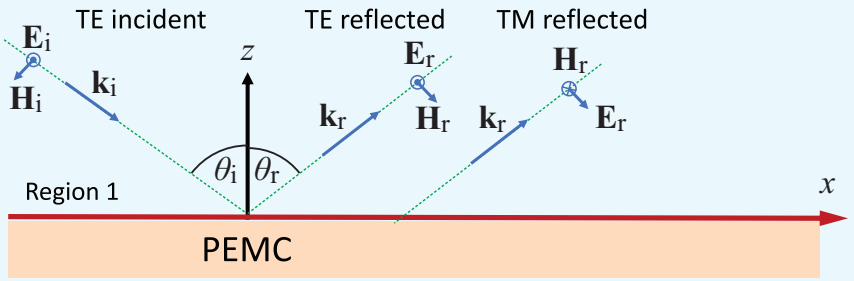


**Figure P5.7:** A planar perfect electromagnetic conductor (PEMC) illuminated by a plane wave at oblique incidence.

**(a)** Assume a TE incident plane wave, as shown in Fig. P5.7. The incident field can be written as $E_i = E_0 e^{ik(x\sin\theta_i - z\cos\theta_i)}\,\hat{\mathbf{y}}$. Find an expression for the incident magnetic field in the given coordinate system. (*Hint:* $\mathbf{H} = \frac{1}{\eta}\,\hat{\mathbf{k}} \times \mathbf{E}$.)

**(b)** The reflected field has both TE and TM components:

$$\mathbf{E}_r = \mathbf{E}_r^{TE} + \mathbf{E}_r^{TM}$$

and

$$\mathbf{H}_r = \mathbf{H}_r^{TE} + \mathbf{H}_r^{TM} \, .$$

Reflection coefficients $R_{TE}^{TE}$ and $R_{TE}^{TM}$ are defined as follows:

$$\mathbf{E}_r^{TE} = R_{TE}^{TE} E_0 e^{ik(x\sin\theta_i + z\cos\theta_i)}\,\hat{\mathbf{y}}$$

and

$$\mathbf{H}_r^{TM} = R_{TE}^{TM} \left(\frac{E_0}{\eta}\right) e^{ik(x\sin\theta_i + z\cos\theta_i)}\,\hat{\mathbf{y}} \, .$$

Find an expression for $\mathbf{E}_{\mathrm{r}}^{\mathrm{TM}}$ and $\mathbf{H}_{\mathrm{r}}^{\mathrm{TE}}$ in the given coordinate system. (*Hint:* $\mathbf{H} = \frac{1}{\eta}\,\hat{\mathbf{k}} \times \mathbf{E}$ and $\mathbf{E} = -\eta\,\hat{\mathbf{k}} \times \mathbf{H}$.)

**(c)** By satisfying the boundary conditions at the interface, find the reflection coefficients and show that $(R_{\mathrm{TE}}^{\mathrm{TM}})^2 + (R_{\mathrm{TE}}^{\mathrm{TE}})^2 = 1$.

**(d)** Find the rotation angle (the angle between $E_{\mathrm{r}}$ and $E_{\mathrm{i}}$). Comment on your results for the cases of $Y = 0$, $Y = \infty$, and $Y\eta = 1$.

**(e)** What can you say about the reflection coefficients, $R_{\mathrm{TM}}^{\mathrm{TM}}$ and $R_{\mathrm{TM}}^{\mathrm{TE}}$, for a TM incident field?

**5.8**

**(a)** A left-handed material is one that has both negative permittivity and negative permeability. For a material with constitutive parameters $(-\mu, -\varepsilon)$, calculate the following:

1. The magnetic field vector if the electric field is given by $\mathbf{E} = \hat{\mathbf{x}}\, E_0 e^{ikz}$.
2. The time-averaged Poynting vector.
3. What are the directions of phase velocity and energy flow?

**(b)** Now consider a planar interface between a right-handed medium with constitutive parameters $(\mu, \varepsilon)$ and the left-handed medium of part (a). For a TE plane wave at oblique incidence from the right-handed medium, draw the rays along the flow of energy.

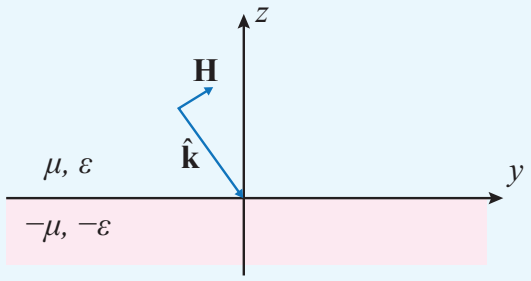


**Figure P5.8:** The geometry of a half-space left-handed material illuminated by a plane wave.

**5.9 Ceramic tile absorbers.** At lower microwave frequencies, and especially at upper VHF bands, the design of absorbers for anechoic chambers based on conductive foams is rather challenging due to the size limitations. At such frequencies, lossy $\mu$–$\varepsilon$ materials are used. For example, combining high-$\mu$ material like Ferrite and high-$\varepsilon$ material like barium titanate having the same permittivity and permissivity ($\mu = \varepsilon$) and reasonable loss, a thin absorber can be designed. Consider a metal-backed lossy $\mu$–$\varepsilon$ material $\mu_{\mathrm{r}} = \varepsilon_{\mathrm{r}} = 100 + i3$.

**(a)** Choose the thickness of the tile so that the reflection coefficient would be less than $-25$ dB at normal incidence.

**(b)** Plot the plane-wave reflection coefficient as a function of incident angle for both polarizations, and find the angular range for which the reflection is below −20 dB.

**(c)** To increase the angular response of the absorber, one more layer with the same thickness can be added. Choose a value for the relative permeability and permittivity of the second layer so as to get the maximum angular range for −20 dB reflection.

**5.10** A thin dielectric slab of complex permittivity $\varepsilon_0\varepsilon_r$ and thickness $t$ can be modeled by an impedance sheet, as shown in Fig. P5.10.

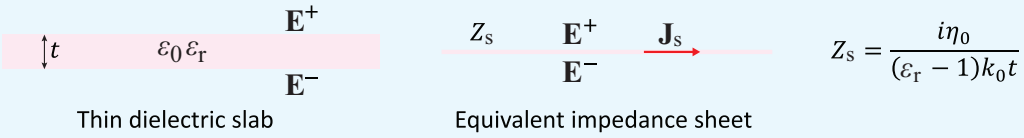


**Figure P5.10:** Impedance sheet equivalent of a thin dielectric slab having a surface impedance $Z_s$.

**(a)** Since the dielectric is thin, using the boundary condition, show that

$$\hat{\mathbf{n}} \times E^+ = \hat{\mathbf{n}} \times E^- \,, \tag{5.264}$$

where $E^+$ is the electric field at a point just above the sheet and $E^-$ is the electric field at the same point just below the sheet.

**(b)** Derive the tangential volumetric polarization current in the thin dielectric slab, and collapse that to a surface electric current ($\mathbf{J}_s$) to show that

$$-\frac{ik_0}{\eta_0}(\varepsilon_r - 1)t\,[(\hat{\mathbf{n}} \times \mathbf{E}) \times \hat{\mathbf{n}}] = \mathbf{J}_s \,,$$

or equivalently,

$$(\hat{\mathbf{n}} \times \mathbf{E}) \times \hat{\mathbf{n}} = Z_s\,\mathbf{J}_s \,, \tag{5.265}$$

where $Z_s$ is the equivalent "sheet impedance" of the thin dielectric slab:

$$Z_s = \frac{i\eta_0}{(\varepsilon_r - 1)k_0 t} \,. \tag{5.266}$$

Here $k_0$ is the wave number in the background and $\eta_0$ is the characteristic impedance. Using the boundary condition for magnetic fields, it can be shown that

$$\hat{\mathbf{n}} \times (H^+ - H^-) = \mathbf{J}_s \,. \tag{5.267}$$

**(c)** Consider an infinite impedance sheet in the $x$–$y$ plane of a Cartesian coordinate system being illuminated by a plane wave from the $Z > 0$ half-space propagating in the direction $\hat{\mathbf{k}}_i = \sin\theta_i\,\hat{\mathbf{x}} - \cos\theta_i\,\hat{\mathbf{y}}$. Find the reflection and transmission coefficients for TE and TM.

**(d)** Compare the results from part (c) with the results obtained from Example 5-6 in the limit as $k_0\sqrt{|\varepsilon|}\,t$ approaches zero.

**5.11** Consider an impedance sheet made from a thin conducting dielectric material with $\varepsilon_r = 1 + i\sigma/\omega\varepsilon$. In this case the impedance sheet becomes a resistive sheet ($R_s$). Choose the conductivity and thickness so that the surface resistivity $R_s = \eta_0$. In the literature this sheet is referred to as a ***Salisbury sheet***. Calculate the plane-wave reflection coefficient at normal incidence for this resistive sheet placed $\lambda/4$ above a perfect electric conductor, as shown in Fig. P5.11.

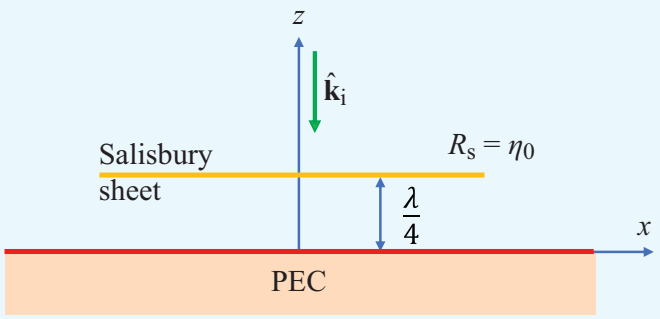


**Figure P5.11:** A Salisbury sheet placed above a perfect electric conductor at a height of $\lambda/4$.

**5.12** The ***polarization matching factor*** for an antenna is defined as

$$\text{PMF} = \hat{\mathbf{p}}_i \cdot \hat{\mathbf{P}}_a\,,$$

where $\hat{\mathbf{p}}_i$ is the polarization unit vector of the wave and $\hat{\mathbf{P}}_a$ is the polarization vector of the receive antenna. Find the polarization matching factor for an antenna with polarization

**(a)** linear vertical polarization,

**(b)** left-hand circular polarization,

**(c)** elliptical polarization with axial ratio AR $= -2$ and tilt angle 30°,

when illuminated by a right-hand circularly polarized plane wave.

**5.13** An elliptically polarized plane wave in air with axial ratio AR $= 3$ is obliquely incident upon a dielectric half-space medium with $\varepsilon_r = 3$ and $\mu_r = 1$. Choose the angle of incidence so that the reflected wave is linearly polarized (along TE polarization).

**5.14** Consider a dielectric slab of thickness $t$ and relative permittivity and permeability $(\varepsilon_2, \mu_2)$ between two media with relative constitutive parameters $(\varepsilon_1, \mu_1)$ and $(\varepsilon_3, \mu_3)$.

**(a)** Find the fields in each region for a normal incident plane wave from region 1 on the slab.

**(b)** Find the ratio of the tangential electric field to the magnetic field at the interface between regions 1 and 2. This is the input wave impedance. Show that when the slab thickness $t = \lambda_0/(4n)$ with $n = \sqrt{\varepsilon_2 \mu_2}$ and $\lambda_0$ being the free-space wavelength, the wave input impedance is

$$Z_{\text{in}} = \frac{\eta_2^2}{\eta_3} .$$

**(c)** Use the result of part (b) to show the input impedance for a Bragg mirror as given by Eq. (5.221).

**5.15** Consider a uniaxial medium with a permittivity matrix

$$\overline{\overline{\varepsilon}} = \varepsilon_0 \begin{pmatrix} \varepsilon_{xx} & 0 & 0 \\ 0 & \varepsilon_{xx} & 0 \\ 0 & 0 & \varepsilon_{zz} \end{pmatrix} .$$

**(a)** Find $n_1$ and $n_2$ as given by Eqs. (5.56) and (5.57) for a plane wave propagating in the direction

$$\hat{\mathbf{k}} = \sin\theta\, \hat{\mathbf{x}} + \cos\theta\, \hat{\mathbf{z}} .$$

**(b)** Find an expression for the electric and magnetic fields.

**5.16** Repeat Problem P5.15 for a uniaxial medium with permittivity tensor

$$\overline{\overline{\varepsilon}} = \varepsilon_0 \begin{pmatrix} \varepsilon_{xx} & 0 & 0 \\ 0 & \varepsilon_{yy} & 0 \\ 0 & 0 & \varepsilon_{yy} \end{pmatrix} .$$

**5.17** Consider a homogeneous isotropic medium with constitutive parameters $\mu_0\mu_1$ and $\varepsilon_0\varepsilon_1$, as shown in Fig. 5-13. The lower half-space is a uniaxial medium with permittivity matrix

$$\overline{\overline{\varepsilon}} = \varepsilon_0 \begin{pmatrix} \varepsilon_2 & 0 & 0 \\ 0 & \varepsilon_2 & 0 \\ 0 & 0 & \varepsilon_{z2} \end{pmatrix}$$

and permeability $\mu_0\mu_2$. Find the reflection and transmission coefficients for a wave impinging on the interface between the two media from above at an oblique incidence angle $\theta_i$.

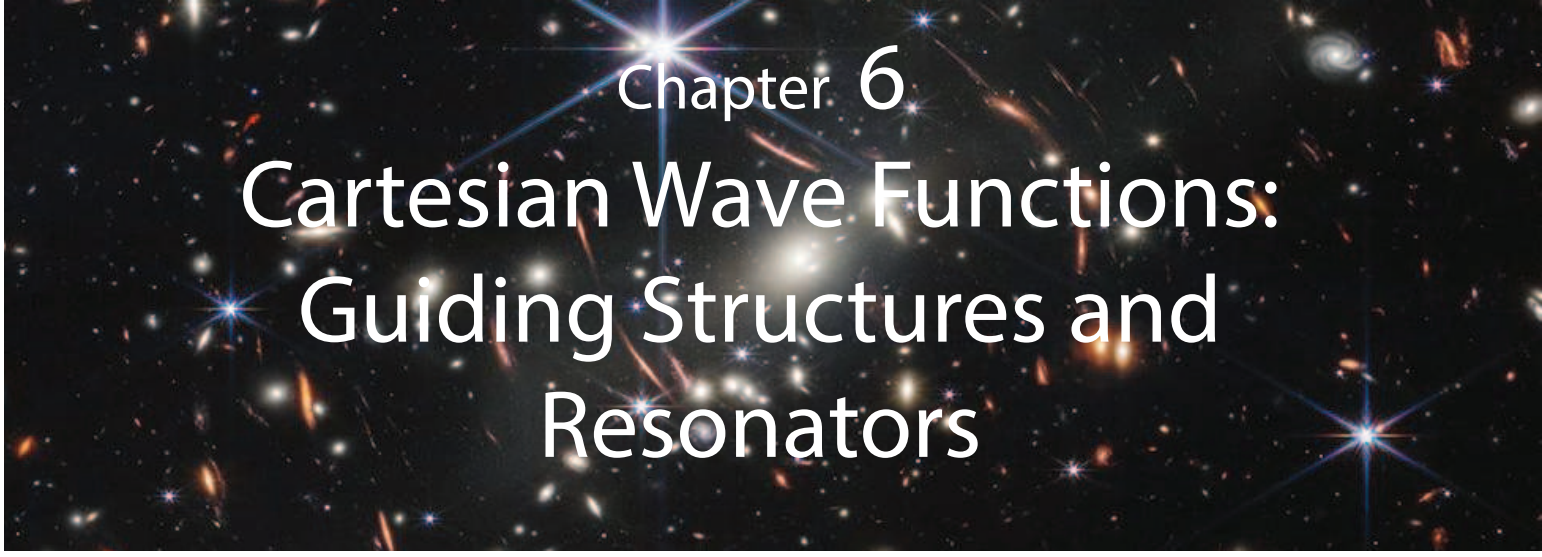

# Chapter 6
# Cartesian Wave Functions: Guiding Structures and Resonators

## Chapter Contents


Overview, 314
6-1 The Dielectric Plate Waveguide, 315
6-2 Guided Waves on Impedance Surfaces, 321
6-3 Practical Realization of Reactive Impedance Surfaces, 324
6-4 Isotropic Reactive Impedance Surfaces, 330
6-5 The Rectangular Waveguide, 335
6-6 Transmission-Line Circuit Model for Waveguides, 357
6-7 Other Modal Solutions for Rectangular Waveguides, 363
6-8 Modal Expansion of Field Quantities, 367
6-9 Calculus of Variation for Estimation of Resonant Frequencies in General Cavities, 382
Chapter Summary, 388
Problems, 393


## Objectives

Upon learning the material presented in this chapter, you should be able to:

1. Develop intuition about wave-guiding structures, other than the standard transmission lines, that can support propagation of electromagnetic waves.
2. Understand the properties of guided electromagnetic waves along dielectric slabs with finite thickness and metallic waveguides, such as cutoff frequencies of different modes, dispersion behavior of wave propagation, low attenuation rate properties, and so on.
3. Realize the orthogonality properties of different modes supported by general waveguides and the fact that power carried in a multimode waveguide is the sum of power carried by the individual modes.
4. Calculate the resonant frequencies of a rectangular cavity and its quality factor when its walls are made from good conductors.
5. Calculate the cutoff frequencies of waveguides and cavities of general shape using a variational formulation.

## Overview

In this chapter we study transverse electric and transverse magnetic guided wave structures that are commonly used in microwave engineering. The chapter begins with a simple nonmetallic dielectric structure known as a dielectric plate waveguide. It is shown that such structures can support both TM and TE modes that can propagate along the dielectric slab with exponentially decaying fields in the medium surrounding it, provided that the index of refraction of the dielectric slab is higher than that of its surrounding medium. It is shown that there are discrete modes of propagation with different propagation constants that are dependent on the slab thickness and indices of refraction of the slab and its surrounding medium. The concept of cutoff frequency for each mode is introduced as the frequency below which that specific mode (with its specific field pattern) cannot propagate along the dielectric slab. It is shown that for the dominant mode ($TM_0$), there is no cutoff frequency. The principle of nonmetallic waveguiding of a dielectric slab is a precursor for fiber optics, which today is the most prevalent waveguide structure in use. Also, the guiding mechanism of the dielectric slab or a modified metal-backed dielectric slab describes the coupling mechanism between different transmission lines and antennas on printed circuit boards. The concept of reactive impedance surface for guiding TE and TM modes is also examined and shown that inductive surfaces can support TM waves and capacitive surfaces can support TE waves. To realize reactive impedance surfaces, metallic surfaces with periodic grooves are introduced and design procedures for creating inductive or capacitive surfaces, using transmission-line theory, are presented. Also, a thin metal-backed substrate with periodic metallic patches on top is shown to act as a reactive impedance surface with reactance values that can be controlled by the substrate thickness, index of refraction, and the gap between the metallic patches.

Next, wave propagation inside closed metallic pipes of fixed cross-sectional geometry along the pipe, known as metallic waveguides, is considered. Specifically, a waveguide with rectangular cross section is considered. The method of separation is used to solve a two-dimensional wave equation for both electric (TM) and magnetic (TE) Hertz vector potentials having only one component along the waveguide axis. The field expressions for different modes of propagation are expressed in terms of the solution to the 2-D wave equation, known as the eigenfunction. It is shown that wave propagation in waveguides is, in general, dispersive. That is, waves at different frequencies propagate with different velocities. Also, the notion of , which represents the speed at which the envelope of a signal propagates in the waveguide, is presented and shown to be different from the phase velocity. A perturbation method that allows for computation of the attenuation rate in a rectangular waveguide is presented as well. Transmission-line circuit models for each waveguide mode are introduced as a means to simplify analysis of certain discontinuities along the length of waveguides. A rectangular cavity structure made from a segment of a rectangular waveguide is also studied. Finally, the properties of eigenfunctions and eigenvalues (cutoff wave number) of metallic waveguides of arbitrary cross section are studied. It is shown that the eigenvalues of the 2-D Laplacian operator that defines the cutoff wave numbers of the waveguide are shown to be always positive and real numbers, and their corresponding eigenfunctions are shown to be orthogonal to each other within the waveguide cross section. Using this property of the eigenfunctions, it is shown that the transverse electric fields for two TM or two TE modes or for one TM and one TE mode are orthogonal. A variational formulation for the calculation

of the eigenvalues of an arbitrary cross section waveguide is presented, and it is shown that such a formulation can be used in a numerical method, known as the ***finite element method***, to find the eigenvalues and eigenfunctions. A similar procedure is presented for estimating the resonant frequencies of a metallic cavity of arbitrary shape.

## 6-1 The Dielectric Plate Waveguide

In this example, an inhomogeneous medium with a step 1-D dielectric variation along the $x$-axis is considered. The resulting geometry is a dielectric plate of thickness $t$, as shown in Fig. 6-1. Let's assume the dielectric plate has a permittivity and permeability given by $\varepsilon_2$ and $\mu_2$, respectively.

### 6-1.1 Transverse Magnetic (TM) Waves

Since we are seeking wave guidance along $z$, and the medium permittivity and permeability variations are independent of $z$ and $y$, for TM waves (see Eq. (5.91))

$$\Pi_{\ell z}(x,z) = \psi_\ell(x)\, e^{i\beta z}$$

with $\psi$ satisfying

$$\frac{d^2\psi_\ell}{dx^2} + k_{\ell c}^2 \psi_\ell = 0\,. \tag{6.1}$$

where subscript $\ell$ refers to regions 1, 2, or 3 and $k_{\ell c}^2 = k_\ell^2 - \beta^2$. Note that the phase-matching condition is implicitly enforced by making $\beta$ independent of the regions. Wave guidance along the $\pm x$-direction is desired to be suppressed, hence $k_{1c}$ and $k_{3c}$ are chosen as pure imaginary quantities; in other words, $k_{1c} = k_{3c} = i\nu$. Solution of Eq. (6.1) can be obtained in terms of two sets of even and odd functions.

#### TM Odd Modes

Considering the odd solutions, $\Pi_{\ell z}^{o}$ in the three regions is given by

$$\Pi_{2z}^{o}(x,z) = A\sin(k_{2c}x)\, e^{i\beta z} \qquad |x| < \frac{t}{2}\,, \tag{6.2a}$$

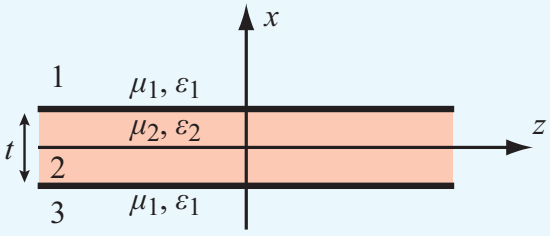


**Figure 6-1:** Geometry of a dielectric slab supporting wave propagation along the $z$-axis.

$$\Pi^{o}_{1z}(x,z) = Be^{-\nu x}\, e^{i\beta z} \qquad x > \frac{t}{2}\,, \tag{6.2b}$$

and

$$\Pi^{o}_{3z}(x,z) = -Be^{\nu x}\, e^{i\beta z} \qquad x < -\frac{t}{2}\,, \tag{6.2c}$$

where

$$k_{2c}^2 = k_2^2 - \beta^2 = \omega^2\mu_2\varepsilon_2 - \beta^2 \tag{6.3a}$$

and

$$\nu^2 = \beta^2 - k_1^2 = \beta^2 - \omega^2\mu_1\varepsilon_1\,. \tag{6.3b}$$

The field components are obtained from Eqs. (5.102a) and (5.102b):

$$\left.\begin{aligned} E_{2z} &= Ak_{2c}^2 \sin(k_{2c}x)\, e^{i\beta z} \\ H_{2y} &= iA\omega\varepsilon_2 k_{2c} \cos(k_{2c}x)\, e^{i\beta z} \end{aligned}\right\} \quad \text{Region 2,}$$

$$\left.\begin{aligned} E_{1z} &= -B\nu^2 e^{-\nu x} e^{i\beta z} \\ H_{1y} &= iB\omega\varepsilon_1(-\nu) e^{-\nu x} e^{i\beta z} \end{aligned}\right\} \quad \text{Region 1,}$$

and

$$\left.\begin{aligned} E_{3z} &= B\nu^2 e^{\nu x} e^{i\beta z} \\ H_{3y} &= iB\omega\varepsilon_1(\nu) e^{\nu x} e^{i\beta z} \end{aligned}\right\} \quad \text{Region 3.}$$

Continuity of tangential electric and magnetic fields must be enforced at $x = \pm t/2$:

$$Ak_{2c}^2 \sin\left(k_{2c}\frac{t}{2}\right) = -B\nu^2 e^{-\nu t/2}$$

and

$$iA\omega\varepsilon_2 k_{2c} \cos\left(k_{2c}\frac{t}{2}\right) = -iB\omega\varepsilon_1 \nu e^{-\nu t/2}\,.$$

The ratio of the above two equations gives an equation relating $k_{2c}$ to $\nu$:

$$\frac{k_{2c}}{\varepsilon_2} \tan\left(k_{2c}\,\frac{t}{2}\right) = \frac{\nu}{\varepsilon_1}\,. \tag{6.4a}$$

Also adding the two equations given by Eq. (6.3), we get

$$k_{2c}^2 + \nu^2 = \omega^2(\mu_2\varepsilon_2 - \mu_1\varepsilon_1)\,. \tag{6.4b}$$

Equations (6.4a) and (6.4b) must be solved simultaneously to find $\nu$ and $k_{2c}$, from which the propagation constant $\beta$ can be obtained. For a given solution $(\nu, k_{2c}, \beta)$, $B$ can be obtained from

$$B = -A\left(\frac{k_{2c}}{\nu}\right)^2 \sin\left(k_{2c}\frac{t}{2}\right) e^{\nu t/2}\,.$$

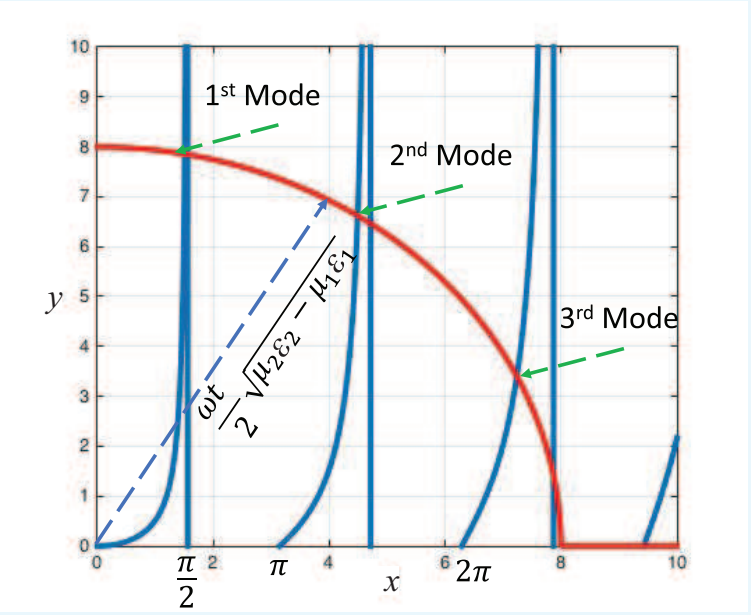


**Figure 6-2:** Graphical solution for determining TM odd modes supported by a dielectric-plate waveguide. The solution consists of the three intersection points between the blue curves representing Eq. (6.5a) and the red curve representing Eq. (6.5b). It is shown that there is no cutoff frequency for TM waves. In this example $\varepsilon_1 = \varepsilon_0,\ \varepsilon_2 = 3\varepsilon_0,\ \mu_1 = \mu_2 = \mu_0$, and $t = 1.8\lambda$.

Defining new variables $X = k_{2c}t/2$ and $Y = \nu t/2$, Eqs. (6.4a) and (6.4b) can be written as

$$\frac{\varepsilon_1}{\varepsilon_2} X \tan X = Y \tag{6.5a}$$

and

$$X^2 + Y^2 = \left(\omega \frac{t}{2}\sqrt{\mu_2\varepsilon_2 - \mu_1\varepsilon_1}\right)^2 . \tag{6.5b}$$

Requiring $\mu_2\varepsilon_2 > \mu_1\varepsilon_1$, the second equation in Eq. (6.5) represents a circle in the $x$–$y$ plane. Plotting both curves and finding the intersection of these curves (for $Y > 0$), the possible solutions for Eq. (6.5) can be obtained graphically (see Fig. 6-2) . It is interesting to note that independent of frequency ($\omega$) and the slab thickness ($t$) there is always a solution for $k_{2c}$ and $\nu$. That is, there is no cutoff frequency for TM odd mode propagation. A ***cutoff frequency*** is defined as a frequency for which $\nu = 0$ (no decay along $x$ axis). Hence the cutoff frequencies for a specific mode correspond to $\nu = 0$ or $\beta = \omega\sqrt{\mu_1\varepsilon_1}$ , which leads to

$$\tan k_{2c}\frac{t}{2} = 0$$

or

$$k_{2c}\,\frac{t}{2} = n\pi \qquad n = 0,1,2,\ldots$$

or

$$\frac{\omega t}{2}\sqrt{\mu_2\varepsilon_2 - \mu_1\varepsilon_1} = n\pi \qquad n = 0,1,2.$$

As noted earlier, there is no cutoff frequency for $\mathrm{TM}_0$. The cutoff frequency for $\mathrm{TM}_n$ is given by

$$f_c^{\mathrm{TM}_n^o} = \frac{n}{t\sqrt{\mu_2\varepsilon_2 - \mu_1\varepsilon_1}} \qquad n = 1,2,\ldots \qquad \textbf{(TM odd modes)} \tag{6.6}$$

## TM Even Modes

For even modes of TM waves, the counterparts of Eqs. (6.2a) through (6.2c) are

$$\Pi_{2z}^{e}(x,z) = A\cos(k_{2c}x)\,e^{i\beta z}\,, \tag{6.7a}$$

$$\Pi_{1z}^{e}(x,z) = Be^{-\nu x}e^{i\beta z}\,, \tag{6.7b}$$

and

$$\Pi_{3z}^{e}(x,z) = Be^{+\nu x}e^{i\beta z}\,. \tag{6.7c}$$

The field components can be obtained as before with the exception of exchanging $\sin(k_{2c}x)$ for $\cos(k_{2c}x)$ and vice versa and keeping track of sign changes. Enforcing the boundary condition at $x = \pm t/2$ results in the following equation:

$$-\frac{k_{2c}t}{2}\cot\left(\frac{k_{2c}t}{2}\right) = \frac{\varepsilon_2}{\varepsilon_1}\,\frac{\nu t}{2}\,. \tag{6.8}$$

Using the same definitions for $X$ and $Y$ as before,

$$\begin{cases} -\dfrac{\varepsilon_1}{\varepsilon_2}\,X\cot X = Y\,, \text{ and} \\ X^2 + Y^2 = \left(\dfrac{\omega t}{2}\sqrt{\mu_2\varepsilon_2 - \mu_1\varepsilon_1}\right)^2\,. \end{cases}$$

Figure 6-3 shows the possible solutions for the even TM modes. The cutoff frequencies correspond to

$$\cot\left(\frac{k_{2c}t}{2}\right) = 0\,,$$

or

$$\frac{k_{2c}t}{2} = \frac{(2n+1)}{2}\,\pi\,,$$

which is equivalent to

$$\frac{\omega t}{2}\sqrt{\mu_2\varepsilon_2 - \mu_1\varepsilon_1} = \left(\frac{2n+1}{2}\right)\pi\,, \qquad n = 0,1,2,\ldots\,,$$

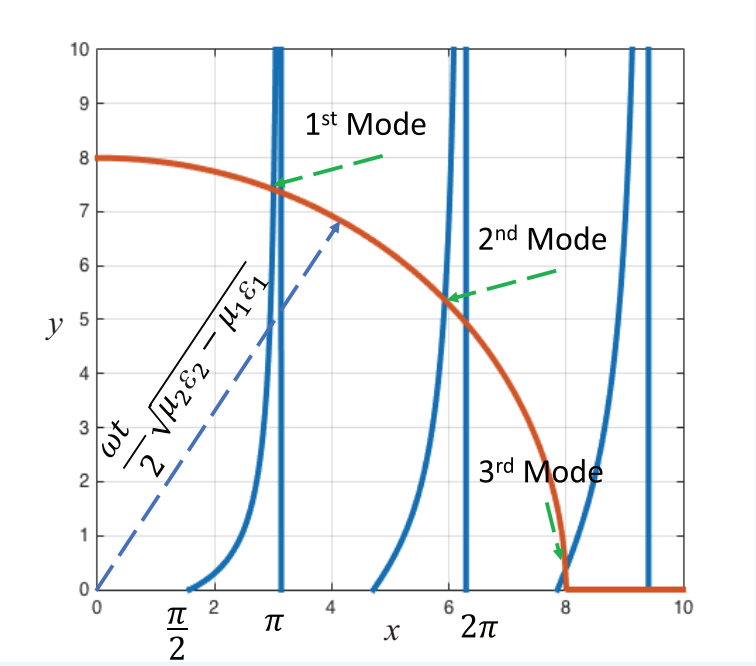


**Figure 6-3:** Graphical solution for determining TM even modes supported by a dielectric-plate waveguide. In this example $\varepsilon_1 = \varepsilon_0$, $\varepsilon_2 = 3\varepsilon_0$, $\mu_1 = \mu_2 = \mu_0$, and $t = 1.8\lambda_0$.

or

$$f_c^{\mathrm{TM}_n^e} = \frac{(2n+1)}{2t\sqrt{\mu_2\varepsilon_2 - \mu_1\varepsilon_1}} \qquad n = 0, 1, 2, \ldots \qquad \textbf{(TM even modes)} \tag{6.9}$$

Combining the even and odd modes, the cutoff frequencies for TM modes are given by

$$f_c^{\mathrm{TM}_n} = \frac{n}{2t\sqrt{\mu_2\varepsilon_2 - \mu_1\varepsilon_1}} \qquad n = 0, 1, 2, \ldots \qquad \textbf{(all TM modes)} \tag{6.10}$$

### 6-1.2 Transverse Electric (TE) Modes

As shown previously, TE modes are the dual of TM modes and the corresponding field distributions can be obtained using the duality relations. As such, the dispersion relations for TE modes are also the dual of their TM counterpart. For the TE modes with odd $\Pi_{mz}(x,z)$ we have

$$\frac{k_{2c}t}{2}\tan\left(\frac{k_{2c}t}{2}\right) = \frac{\mu_2}{\mu_1}\frac{vt}{2}, \qquad \textbf{(TE odd modes)} \tag{6.11a}$$

and for even $\Pi_{mz}(x,z)$,

$$-\frac{k_{2c}t}{2}\cot\left(\frac{k_{2c}t}{2}\right)=\frac{\mu_2}{\mu_1}\frac{\nu t}{2}\,. \qquad \textbf{(TE even modes)} \tag{6.11b}$$

Since Eq. (6.3) is unchanged under the duality relations, *the cutoff frequencies obtained for TM modes are the same as those for the TE modes*. It is emphasized here that guided TE and TM modes propagate unattenuated, independently of both the frequency and the slab thickness.

### 6-1.3 Dielectric-Coated Conductor

The modal analysis of the previous section can easily be extended to solve the waveguide mode analysis for the dielectric-coated planar metallic surface shown in Fig. 6-4. Such a geometry is often encountered in printed circuit boards for high-frequency applications. The boundary condition at $x=0$ mandates that the tangential component of the electric field vanish as $x$ approaches the metal surface. Recalling that the electric field distribution of odd TM modes is given by

$$E_{2z}(x,z)=Ak_{2c}^2\sin(k_{2c}x)\,e^{i\beta z}\,,$$

the required boundary condition for these modes is automatically satisfied. Also, the electric field of even TE modes is given by

$$E_{2y}(x,z)=-i\omega\mu_2 Ak_{2c}\sin(k_{2c}x)\,e^{i\beta z}\,,$$

which also satisfies the boundary condition. For TM modes, the modes of propagation can be obtained from Eq. (6.6), and for TE modes,

$$\left.\begin{aligned}&-\frac{k_{2c}t}{2}\cot\left(\frac{k_{2c}t}{2}\right)=\frac{\mu_2}{\mu_1}\frac{\nu t}{2}\,,\ \text{and}\\&\left(\frac{k_{2c}t}{2}\right)^2+\left(\frac{\nu t}{2}\right)^2=\left(\frac{\omega t}{2}\right)^2(\mu_2\varepsilon_2-\mu_1\varepsilon_1)\,.\end{aligned}\right\} \tag{6.12}$$

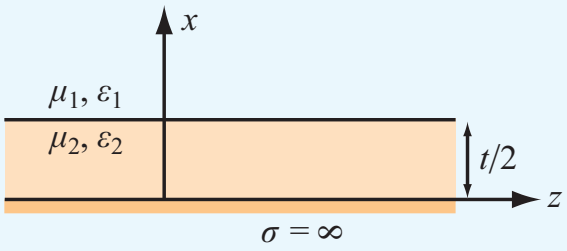


**Figure 6-4:** Geometry of a metal-backed dielectric slab capable of supporting guided waves.

## 6-2 Guided Waves on Impedance Surfaces

In the previous section, we examined TE and TM wave propagation modes on dielectric slabs and dielectric-coated conductors. In the literature, the latter is referred to as ***substrate modes*** or ***surface waves***. In this section we intend to show that surface wave propagation can also be supported by certain nonresistive materials known as ***reactive impedance surfaces***. Mathematically, such surfaces can be represented by an impedance boundary condition that was first introduced by Leontovich for planar surfaces and surfaces with large radii of curvature compared with the wavelength. For such surfaces the tangential electric field is linearly proportional to the tangential magnetic field and the constant of proportionality is known as the ***surface impedance***. Denoting the surface impedance by $Z_s$, the impedance boundary condition for the electric and magnetic fields just above the surface is given by

$$\hat{\mathbf{n}} \times [\hat{\mathbf{n}} \times \mathbf{E}(\mathbf{r})] = -Z_s \, \hat{\mathbf{n}} \times \mathbf{H}(\mathbf{r}) \, . \tag{6.13}$$

Here $Z_s$ can have both the real and imaginary parts but, as will be shown later, surface waves can only propagate along impedance surfaces whose surface impedance is reactive. Using the boundary condition given by Eq. (6.13), the solution to Maxwell's equations can be found using only fields exterior to the object with the impedance surface. This significantly simplifies the solution. In practice, objects with impedance surfaces can only be realized in approximate form. However, it should be emphasized that the impedance boundary condition given by Eq. (6.13) should be independent of the wave attributes and is only a property of the surface itself. To elaborate on this further, let us consider a planar interface between two dielectric half-spaces with indices of refractions $n_1 = \sqrt{\mu_1 \varepsilon_1}$ and $n_2 = \sqrt{\mu_2 \varepsilon_2}$, illuminated by a plane wave from Region 1. For the TM and TE polarizations, referring to Eqs. (5.99) and (5.102), it can be shown that the ratio of the the tangential electric field to tangential magnetic field at the interface ($z = 0$) are given respectively by

$$\frac{E_x}{H_y} = \frac{\beta_2}{\omega \varepsilon_2} \qquad \textbf{(TM)} \tag{6.14a}$$

and

$$\frac{E_y}{H_x} = \frac{\omega \mu_2}{\beta_2} \, . \qquad \textbf{(TE)} \tag{6.14b}$$

Of course, these cannot be used as the surface impedance for the lower medium as the two ratios are functions of wave polarization and incident angle. For an arbitrary source in the upper half-space, the fields can be expanded in terms of a continuous spectrum of plane waves with all propagation directions and polarizations, but because the interface will present different surface impedances, in general the lower half-space cannot be modeled by an impedance surface. However, under the condition that the the index of refraction of the lower medium is much larger than that of the upper medium ($n_2 \gg n_1$), then the application of Snell's law of refraction given by

$$\sin \theta_2 = \frac{n_1}{n_2} \sin \theta_1$$

predicts that $\theta_2 \approx 0$, independently of $\theta_1$, and also $\beta_2 \approx k_2$. Under such a condition, Eqs. (6.14a) and (6.14b) simplify to

$$\frac{E_x}{H_y} = \sqrt{\frac{\mu_2}{\varepsilon_2}} = \eta_2 \qquad \textbf{(TM)}$$

and

$$\frac{E_y}{H_x} = \sqrt{\frac{\mu_2}{\varepsilon_2}} = \eta_2 \,, \qquad \textbf{(TE)}$$

and the lower conducting medium can be modeled by an impedance surface $\eta_c = \eta_2$.

A metallic medium with high but finite conductivity presents itself as a medium with an impedance boundary condition. Suppose the conductivity of the metallic medium is represented by $\sigma$. According to Eq. (1.74), the dielectric constant of this medium is given by

$$\varepsilon_m = \varepsilon_0 + i\,\frac{\sigma}{\omega}\,. \tag{6.15}$$

At frequencies where $\sigma/(\omega\varepsilon_0) \gg 1$, the metallic medium can be approximated by an impedance surface having a surface impedance of

$$\eta_c = \sqrt{\frac{\mu_0}{\varepsilon_0 + i\,\frac{\sigma}{\omega}}} \approx \sqrt{\frac{\omega\mu_0}{i\sigma}} = \sqrt{\frac{\omega\mu_0}{2\sigma}}\,(1-i)\,. \tag{6.16}$$

Hence, the surface is both resistive and inductive.

### 6-2.1 Impedance Surface Waveguide

In this section we demonstrate how an impedance surface can guide TM and TE waves, through which we lay the foundation for the concept of a single-conductor transmission line. Consider a planar impedance surface with surface impedance $Z_s$ placed in the $y$–$z$ plane, as shown in Fig. 6-5. Requiring wave propagation along $z$ and exponential decay along $x$, the scalar potential in the upper half space takes the following form:

$$\psi_1(x,z) = Ae^{-\nu x}e^{i\beta z}\,, \tag{6.17}$$

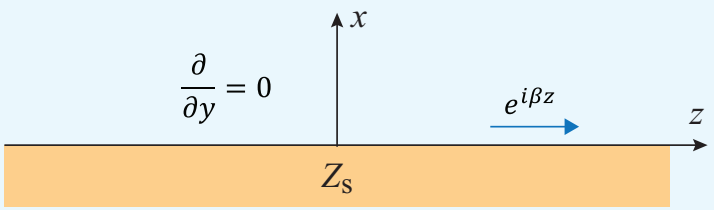


**Figure 6-5:** A planar impedance surface in the $y$–$z$ plane supporting TM and TE guided waves.

where $\nu$ and $\beta$ must satisfy

$$\beta^2 - \nu^2 = k^2 \ . \tag{6.18}$$

For TM waves, the expressions for the tangential electric and magnetic fields can be obtained from Eqs. (5.102a) and (5.102b) and are given by

$$E_z(x,z) = -\nu^2 e^{-\nu x} A e^{i\beta z} \tag{6.19a}$$

and

$$H_y(x,z) = -i\omega\varepsilon\nu A e^{-\nu x} e^{i\beta z} \ . \tag{6.19b}$$

The application of the boundary condition given by Eq. (6.13) to Eq. (6.19a) and Eq. (6.19b) at $z = 0$ provides the following equation for $\nu$:

$$\nu = i\omega\varepsilon Z_s \ . \tag{6.20}$$

This equation indicates that if the surface impedance is pure imaginary and inductive, i.e., if $Z_s = -iX_i$, then $\nu$ becomes a positive real number, which guarantees exponential decay along $x$. In this case the propagation constant is given by

$$\beta = \sqrt{k^2 + \omega^2\varepsilon^2 X_i^2} \ . \qquad \textbf{(TM waves)} \tag{6.21}$$

A similar analysis can be carried out for TE waves by using Eqs. (5.105a) and (5.105b) to find the tangential electric and magnetic fields in the upper half-space:

$$H_z(x,z) = -\nu^2 e^{-\nu x} A e^{i\beta z} \ , \tag{6.22a}$$

$$E_y(x,z) = i\omega\mu\nu A e^{-\nu x} e^{i\beta z} \ , \tag{6.22b}$$

and

$$\nu = \frac{i\omega\mu}{Z_s} \ . \tag{6.22c}$$

Now, note that if the surface impedance is pure imaginary and capacitive, i.e, $Z_s = iX_c$, then $\nu$ becomes a positive real number and TE wave propagation becomes possible. In this case the propagation constant is given by

$$\beta = \sqrt{k^2 + \left(\frac{\omega\mu}{X_c}\right)^2} \ . \qquad \textbf{(TE even waves)} \tag{6.23}$$

In summary, impedance surfaces with purely reactive surface impedance can support surface wave propagation. Surfaces with inductive surface impedance can only support TM waves and surfaces with capacitive surface impedance can only support TE waves.

Example 6-1: Surface Wave on a Lossy Conductor

Good conductors can be represented as impedance surfaces. Can good conductors support surface waves?

**Solution:** From Eq. (6.16), the surface impedance of a good conductor is given by

$$Z_s = \eta_c = \sqrt{\frac{\omega\mu_0}{i\sigma}}\,.$$

This can be used in Eq. (6.20) for TM or Eq. (6.22c) for TE cases to find $\nu$; that is,

$$\nu_{TM} = i\omega\varepsilon\sqrt{\frac{\omega\mu_0}{i\sigma}} = \omega\varepsilon\sqrt{\frac{\omega\mu_0}{2\sigma}}\,(1+i)$$

and

$$\nu_{TE} = \frac{i\omega\mu}{\sqrt{\omega\mu/i\sigma}} = \mu\sqrt{\frac{\omega\sigma}{2\mu_0}}\,(-1+i)\,.$$

Since the decay factor along $x$ is complex, there is some propagation along the $x$ direction, and hence wave propagation along the surface is not supported.

## 6-3 Practical Realization of Reactive Impedance Surfaces

As discussed in Section 6-2.1, surfaces with purely inductive surface impedance can support TM surface waves, and surfaces with purely capacitive surface impedance can support TE surface waves. There are a number of approximate approaches available to realize surfaces with reactive impedances. One conventional approach is through the utilization of a corrugated conductor. Let us consider a one-dimensional periodic surface, as shown in Fig. 6-6, with periodicity in the $z$-direction and the period chosen to be much smaller than the wavelength. Figure 6-6 shows three different periodic surfaces with different groove geometries. Here it is assumed that $w$ and $p$ are much smaller than $\lambda$ at the operating frequency. For the TM case, the electric field has both $z$ and $x$ components and the $z$ component of the electric field can couple between the two sides of the corrugation geometry to form a TEM wave inside the grooves.

### 6-3.1 Rectangular Groove

Considering the geometry shown in Fig. 6-6(a), each groove can be considered a parallel-plate transmission line. This transmission line is filled with a dielectric of constitutive parameters $\mu_0$ and $\varepsilon_0$, and as a result, the propagation constant is $k_0 = \omega\sqrt{\mu_0\varepsilon_0}$. To find the characteristic impedance of this line, the capacitance and inductance per unit length of the line are required. Since the field is uniform along $y$, a finite length $s$ of the line along the $y$-axis can be used to find such a parameter. Consider a segment of the transmission line of length $\ell$, as shown in Fig. 6-7. This forms a parallel-plate capacitor with capacitance

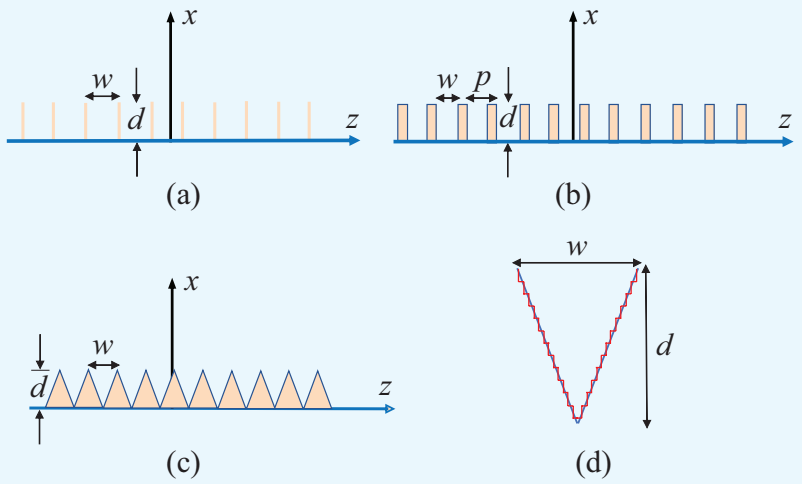


**Figure 6-6:** Geometries for three different periodic surfaces made up of a perfect electric conductor with period $P \ll \lambda$. These surfaces can support TM surface waves.

$$C_{\mathrm{L}} = \frac{\varepsilon_0 s \ell}{w} \qquad \text{(F)}. \tag{6.24}$$

Hence the capacitance per unit length is given simply by

$$C = \frac{C_{\mathrm{L}}}{\ell} = \frac{\varepsilon_0 s}{w} \qquad \text{(F/m)}\ . \tag{6.25}$$

For transmission line, the propagation constant in terms of the capacitance ($C$) and inductance ($L$) per unit length is given by

$$k_0 = \omega \sqrt{LC} = \omega \sqrt{\mu_0 \varepsilon_0}\ . \tag{6.26}$$

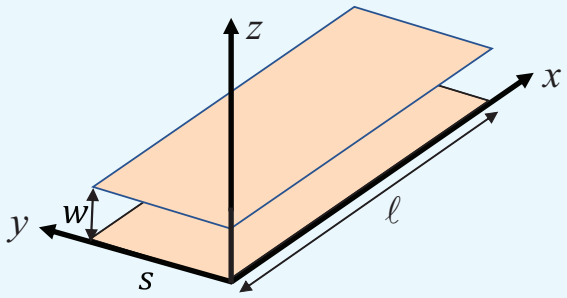


**Figure 6-7:** Geometry of a parallel-plate transmission line of length $\ell$.

Hence, the inductance per unit length of this line can be evaluated from

$$L = \frac{\mu_0 \varepsilon_0}{C} = \frac{\mu_0 w}{s} \qquad \text{(H/m)} \; . \tag{6.27}$$

Using Eqs. (6.25) and (6.26), the characteristic impedance of the parallel-plate transmission line is given by

$$Z_0 = \sqrt{\frac{L}{C}} = \frac{w}{s} \sqrt{\frac{\mu_0}{\varepsilon_0}} = \frac{w}{s} \, \eta_0 \; . \tag{6.28}$$

As depicted in Fig. 6-6(a), these transmission lines are short-circuited at $z = 0$. The input impedance of the short-circuited line can be obtained from

$$Z_{\text{in}} = Z_0 \, \frac{Z_{\text{L}} - iZ_0 \tan k_0 d}{Z_0 - iZ_{\text{L}} \tan k_0 d} \; , \tag{6.29}$$

with $Z_{\text{L}} = 0$. Hence the impedance seen from the aperture of the corrugation is given by

$$Z_{\text{in}} = \frac{V(d)}{I(d)} = -\frac{iw}{s} \, \eta_0 \tan(k_0 d) \; . \tag{6.30}$$

Noting that

$$V(d) = \int_0^w E_z(d,z) \, dz \approx w \, E_z(d) \; ,$$

and noting that the surface current density is proportional to $H_y(x)$, the total current on the metallic strip of width $s$, as shown in Fig. 6-7, is given by

$$I(d) = \int_0^s H_y(d) \, dy \approx s \, H_y(d) \; ,$$

the surface impedance of the corrugated surface, in view of Eq. (6.30), is found to be

$$Z_{\text{s}} = \frac{E_z(d)}{H_y(d)} = \frac{s \, V(d)}{w \, I(d)} = -i\eta_0 \tan(k_0 d) \; . \tag{6.31}$$

Equation (6.31) indicates that when $k_0 d < \pi/2$, or equivalently, when $d < \lambda_0/4$, the reactive impedance surface is inductive and can support TM wave propagation. It is noted that the surface impedance is not a function of the aperture width ($w$). To support TE waves the periodicity of the metallic walls should be along the $y$-direction. In this case, the electric field ($E_y$) can excite a TEM wave inside the grooves and, following a similar procedure, the surface impedance can also be found to be

$$Z_{\text{s}}^{\text{TE}} = \frac{E_y(d)}{H_z(d)} = -i\eta_0 \tan(k_0 d) \; .$$

However, since the surface impedance has to be capacitive, $\pi/2 < k_0 d < \pi$, or equivalently, $\lambda_0/4 < d < \lambda_0/2$. Of course in this case the depth of the grooves is quite large.

Now considering the geometry of Fig. 6-6(b), we realize that over one period the surface

impedance takes on two different values: $Z_s^{(1)} = 0$ and $Z_s^{(2)} = -i\eta_0 \tan(k_0 d)$. Since the period is much smaller than the wavelength, it is reasonable to assume that the effective surface impedance is the weighted average between these two values; that is,

$$Z_s^{\text{eff}} = \frac{0 \times t + Z_s^{(2)} \times w}{p} = \frac{w}{p} Z_s^{(2)} = -i \frac{w}{p} \eta_0 \tan(k_0 d) \ . \tag{6.32}$$

### 6-3.2 Triangular Groove

The computation of surface impedance for the triangular grooves shown in Fig. 6-6(c) is more involved. As in the other cases, for a TM case, a TEM mode is excited inside the grooves, and therefore the transmission line approach can be used to obtain the surface impedance. As shown in Fig. 6-6(d), the triangular groove can be approximated by a staircase geometry where at each step a parallel-plate transmission line can be visualized with a plate separation of

$$w(x) = p \frac{x}{d} \ . \tag{6.33}$$

The capacitance and inductance of this transmission line are now a function of position and are given by Eqs. (6.25) and (6.27). To find the input impedance at the aperture of the groove, transmission-line equations must be used directly. The ***telegrapher's equation*** (considering our time convention of $e^{-i\omega t}$) can be written as

$$\frac{-\partial V(x)}{\partial x} = i\omega \, L(x) \, I(x) \tag{6.34a}$$

and

$$\frac{-\partial I(x)}{\partial x} = i\omega \, C(x) \, V(x) \ , \tag{6.34b}$$

where $L(x)$ and $C(x)$ are respectively the inductance and capacitance per unit length of the line. The negative signs on the left-hand side indicate propagation along the negative $x$-direction. Taking the derivative of Eq. (6.34a) and then using Eq. (6.34b) renders

$$\frac{\partial^2 V(x)}{\partial x^2} - \frac{L'(x)}{L(x)} \frac{\partial V(x)}{\partial x} + \omega^2 \, L(x) \, C(x) \, V(x) = 0 \ . \tag{6.35}$$

In a similar manner, taking the derivative of Eq. (6.34b) and using Eq. (6.34a), we have

$$\frac{\partial^2 I(x)}{\partial x^2} - \frac{C'(x)}{C(x)} \frac{\partial I(x)}{\partial x} + \omega^2 \, L(x) \, C(x) \, I(x) = 0 \ . \tag{6.36}$$

Upon substitution of the inductance and capacitance values and noting that

$$C'(x) = \frac{d}{dx} \left( \frac{\varepsilon_0 s}{(p/d)x} \right) = -\frac{\varepsilon_0 s d}{p} \frac{1}{x^2}$$

and

$$L'(x) = \frac{d}{dx}\left(\frac{p\mu_0 s}{ds}\,x\right) = \mu_0\,\frac{p}{ds}\,,$$

Eqs. (6.35) and (6.36) simplify to

$$\frac{d^2V(x)}{dx^2} - \frac{1}{x}\,\frac{dV(x)}{dx} + k_0^2\,V(x) = 0 \tag{6.37a}$$

and

$$\frac{d^2I(x)}{dx^2} + \frac{1}{x}\,\frac{dI(x)}{dx} + k_0^2\,I(x) = 0\,. \tag{6.37b}$$

Recalling that the Bessel differential equation is of the form

$$\frac{d^2f}{dx^2} + \frac{1}{x}\,\frac{df}{dx} + \left(1 - \frac{n^2}{x^2}\right) f = 0\,,$$

the solution to Eq. (6.37b) is the Bessel function of zeroth order ($n = 0$); that is,

$$I(x) = A\,J_0(k_0x) + B\,Y_0(k_0x)\,. \tag{6.38}$$

Using Fig. 6.34b,

$$V(x) = \frac{-k_0}{i\omega\,C(x)}\,[A\,J_0'(k_0x) + B\,Y_0'(k_0x)]\,. \tag{6.39}$$

The boundary condition mandates that

$$V(0) = 0\,,$$

which requires

$$B = 0\,.$$

Noting that

$$J_0'(k_0x) = -J_1(k_0x)\,,$$

the expression for the voltage inside the triangular grooves simplifies to

$$V(x) = \frac{k_0A}{i\omega\,C(x)}\,J_1(k_0x)\,. \tag{6.40}$$

Also, the expression for the current function is given by

$$I(x) = A\,J_0(k_0x)\,. \tag{6.41}$$

Hence the input impedance at the aperture of the groove ($x = d$) is given by

$$\begin{aligned} Z_{\text{in}} = \frac{V(d)}{I(d)} &= \frac{k_0}{i\omega\,C(d)}\,\frac{J_1(k_0d)}{J_0(k_0d)} \\ &= \frac{-ik_0w}{\omega\varepsilon_0 s}\,\frac{J_1(k_0d)}{J_0(k_0d)} = -i\eta_0\,\frac{w}{s}\,\frac{J_1(k_0d)}{J_0(k_0d)}\,. \end{aligned}$$

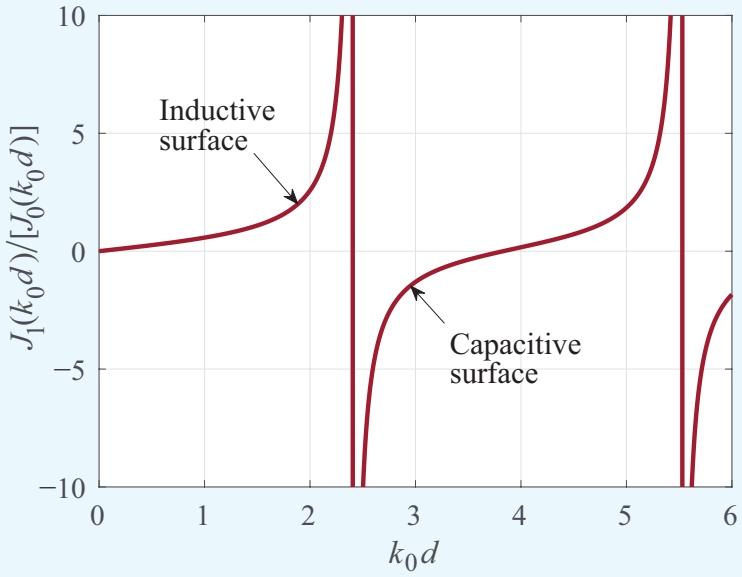


**Figure 6-8:** Plot of the function $J_1(k_0 d)/[J_0(k_0 d)]$ as a function of the triangular groove depth $(k_0 d)$, used for calculating surface impedance.

As in Eq. (6.31), the surface impedance is

$$Z_s = \frac{s}{w}\frac{V(d)}{I(d)} = -i\eta_0 \frac{J_1(k_0 d)}{J_0(k_0 d)} . \tag{6.42}$$

Again the surface impedance of the triangular groove is not a function of aperture width $(w)$. This surface impedance is inductive for values of $k_0 d$ so long as

$$\frac{J_1(k_0 d)}{J_0(k_0 d)} > 0 .$$

It can be shown that this happens when

$$k_0 d < 2.405$$

or

$$d < 0.38\lambda .$$

Figure 6-8 shows a plot of $J_1(k_0 d)/[J_0(k_0 d)]$ as a function of groove depth $(k_0 d)$ and indicates the groove depth values when the surface impedance is inductive or capacitive. It should also be noted here that the one-dimensional corrugated surfaces exhibit anisotropic surface impedances.

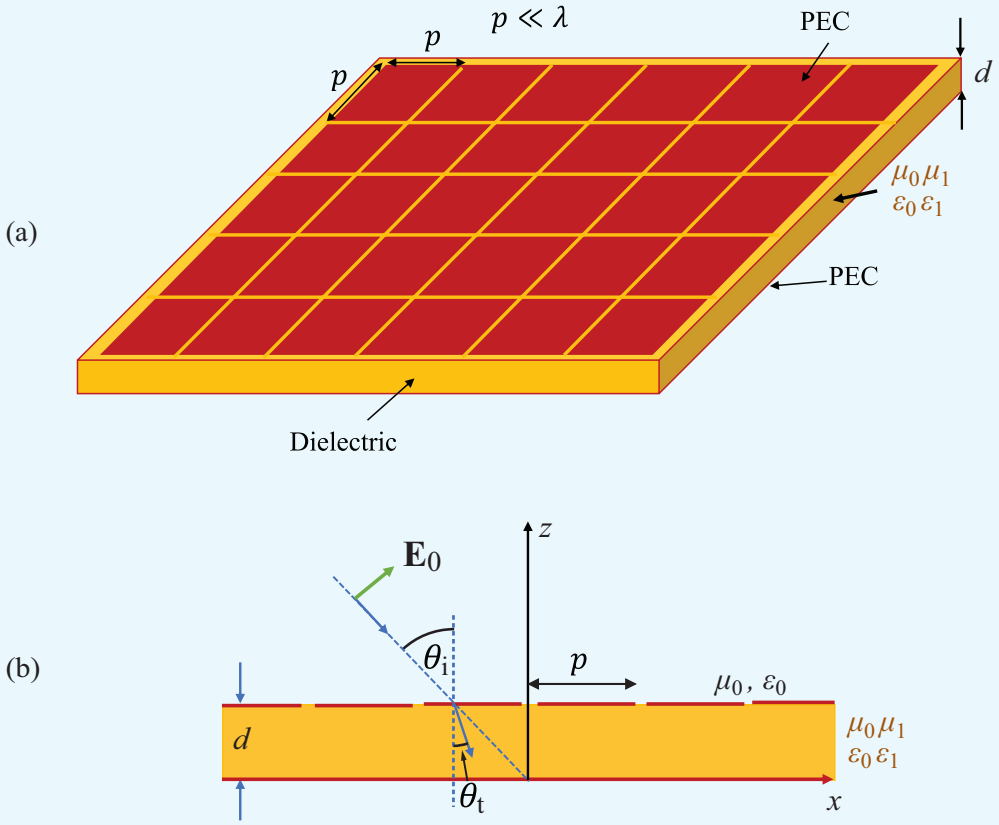


**Figure 6-9:** (a) Isotropic reactive impedance surface created by a periodic array of square metallic patches on a thin metal-backed dielectric substrate, and (b) the same substrate illuminated by a TM-polarized plane wave.

## 6-4 Isotropic Reactive Impedance Surfaces

In the previous section we showed that metals with one-dimensional surface corrugation can support TM and TE surface waves when the electric field is perpendicular to the grooves' walls. Also, to support TE waves we found that the depth of the grooves must be longer than $\lambda_0/4$. For many applications, it is desirable to have reactive impedance surfaces that are isotropic and compact in terms of surface thickness. The cost of fabrication is another issue to consider. In this section we examine the design of capacitive and inductive reactive impedance surfaces using printed circuit technology. The structure is composed of a periodic arrangement of metallic patches over a grounded dielectric substrate with relative permittivity $\varepsilon_1$ and permeability $\mu_1$. The configuration of this structure is shown in Fig. 6-9(a). The metallic square patches form a 2-D periodic surface with a period $p$ that is assumed to be much smaller than a wavelength. To evaluate the performance of this structure, its interaction with an incident plane wave at oblique incidence and TM or TE polarization is considered.

Since the periodicity is much smaller than a wavelength, only reflected and refracted plane waves are generated. Also, to analyze this structure, the behavior of the field over one period can be considered, as depicted in Fig. 6-9(b). Referring to Section 5-4.2, the TM fields in regions 0 ($z \geq d$) and 1 ($0 \leq z \leq d$) can be written as

$$E_{0x}(x,z) = E_0 \cos\theta_\mathrm{i}\ (e^{-ik_0\cos\theta_\mathrm{i}\, z} - \Gamma e^{ik_0\cos\theta_\mathrm{i}\, z}) e^{ik_0\sin\theta_\mathrm{i}\, x}\ , \tag{6.43a}$$

$$H_{0y}(x,z) = -\frac{E_0}{\eta_0}\ (e^{-ik_0\cos\theta_\mathrm{i}\, z} + \Gamma e^{ik_0\cos\theta_\mathrm{i}\, z}) e^{ik_0\sin\theta_\mathrm{i}\, x}\ , \tag{6.43b}$$

$$E_{1x}(x,z) = E_1 \cos\theta_\mathrm{t}\ (e^{-ik_0\cos\theta_\mathrm{t}\, z} - e^{ik_0\cos\theta_\mathrm{t}\, z}) e^{ik_0\sin\theta_\mathrm{i}\, x}\ , \tag{6.43c}$$

and

$$H_{1y}(x,z) = -\frac{E_1}{\eta_1}\ (e^{-ik_1\cos\theta_\mathrm{t}\, z} + e^{ik_1\cos\theta_\mathrm{t}\, z}) e^{ik_0\sin\theta_\mathrm{i}\, x}\ , \tag{6.43d}$$

where we have imposed the phase-matching condition and the fact that $E_{1x}(x,0) = 0$ due to the boundary condition at $z = 0$. Also, as before,

$$\cos\theta_\mathrm{t} = \sqrt{1 - \frac{\sin^2\theta_\mathrm{i}}{\mu_1\varepsilon_1}}\ .$$

The $x$ component of the incident field excites an electric field across the gap between the patches, and the electric field produces the field expressions we have in Eq. (6.43c). Strictly speaking, the electric fields given by Eqs. (6.43a)–(6.43d) are valid for values of $z$ slightly above or below the interface. Since the same voltage gap is exciting the electric fields on both sides of the gaps, the continuity of tangential electric fields at $z = d$ can be imposed; that is,

$$E_0\cos\theta_\mathrm{i}\ (e^{-ik_0\cos\theta_\mathrm{i}\, d} - \Gamma e^{ik_0\cos\theta_\mathrm{i}\, d}) = -2iE_1\cos\theta_\mathrm{t}\sin(k_1\cos\theta_\mathrm{t}\, d)\ . \tag{6.44}$$

The incident field also excites an electric surface current on the metallic patches whose continuity is maintained by the polarization current across the gap. In fact, the gap is acting like a capacitor that facilitates the flow of the electric current. The voltage across this capacitor is given by

$$V \approx E_{0x}(0,d)\ p\ , \tag{6.45}$$

where $p$ is the period. Denoting the capacitance per unit length of the gap by $\widetilde{C}$, the surface current density can be obtained from

$$J_x = -i\omega\widetilde{C}V = -i\omega\widetilde{C}p\ E_{0x}(0,d)\ . \tag{6.46}$$

The boundary condition mandates that

$$\hat{\mathbf{n}} \times (\mathbf{H}_0 - \mathbf{H}_2) = J_x\ . \tag{6.47}$$

Using Eqs. (6.43b) and (6.43d) in Eq. (6.47) provides a second equation for the unknowns:

$$\frac{E_0}{\eta_0}\left(e^{-ik_0\cos\theta_\mathrm{i}\,d}+\Gamma e^{ik_0\cos\theta_\mathrm{i}\,d}\right)-\frac{E_1}{\eta_1}\,2\cos(k_1\cos\theta_\mathrm{t}\,d)=-i\omega\widetilde{C}p[-2iE_1\cos\theta_\mathrm{t}\sin(k_1\cos\theta_\mathrm{t}\,d)]\;. \tag{6.48}$$

According to Eq. (6.13), the surface impedance is defined by

$$Z_\mathrm{s}=-\frac{E_{0x}}{H_{0y}}\;. \tag{6.49}$$

Using Eqs. (6.48) and (6.44), it can be shown that

$$Z_\mathrm{s}^\mathrm{TM}=-i\,\frac{\eta_1\cos\theta_\mathrm{t}\tan(k_1\cos\theta_\mathrm{t}\,d)}{1-\omega\widetilde{C}p\eta_1\cos\theta_\mathrm{t}\tan(k_1\cos\theta_\mathrm{t}\,d)}\;. \tag{6.50}$$

This result is significant because even for a thin substrate where $k_1\cos\theta_\mathrm{t}\,d<1$, the surface can be made to present either an inductive or a capacitive impedance. For example, assuming $k_1\cos\theta_\mathrm{t}\,d<1$, if

$$\omega\widetilde{C}p\eta_1\cos\theta_\mathrm{t}\tan(k_1\cos\theta_\mathrm{t}\,d)<1\;, \tag{6.51}$$

the surface is inductive, and when

$$\omega\widetilde{C}p\eta_1\cos\theta_\mathrm{t}\tan(k_1\cos\theta_\mathrm{t}\,d)>1\;, \tag{6.52}$$

the surface is capacitive. At resonance,

$$\omega\widetilde{C}p\eta_1\cos\theta_\mathrm{t}\tan(k_1\cos\theta_\mathrm{t}\,d)=1\;, \tag{6.53}$$

and the surface acts as a perfect magnetic conductor. Strictly speaking, the surface impedance should not be a function of incident angle. In practice, if $\mu_1\varepsilon_1\gg 1$, then $\cos\theta_\mathrm{t}\approx 1$ and the requirement is satisfied.

The surface impedance presented by Eq. (6.50) can also be obtained by using a transmission-line analogy. The lower medium can be represented by a short-circuited transmission line of length $d$ having a characteristic impedance of

$$Z_1=\eta_1\cos\theta_\mathrm{t} \tag{6.54}$$

and a propagation constant of

$$\beta_1=k_1\cos\theta_\mathrm{t}\;. \tag{6.55}$$

This transmission line is connected to a capacitor ($C$) that represents the gap between two adjacent metallic patches and a semi-infinite transmission line having a characteristic impedance and a propagation constant that are given by

$$Z_0=\eta_0\cos\theta_\mathrm{i} \tag{6.56a}$$

and

$$\beta_0=k_0\cos\theta_\mathrm{i}\;. \tag{6.56b}$$

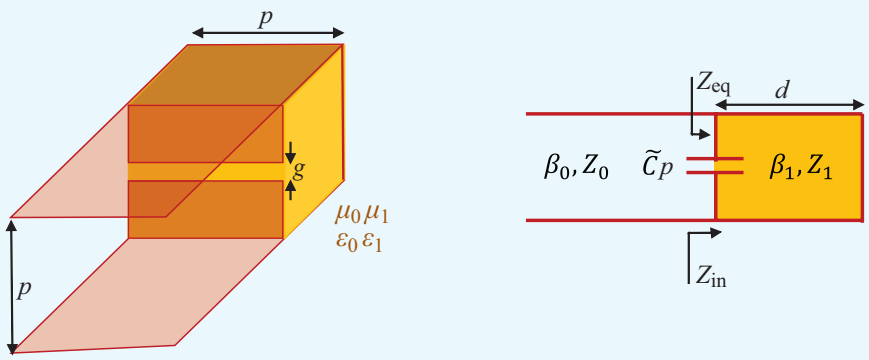


**Figure 6-10:** The equivalent transmission-line representation for one period of metallic square patches over a metal-backed dielectric substrate.

The configuration for this equivalent transmission line is shown in Fig. 6-10. The equivalent impedance of this circuit can be obtained from two shunt impedances, namely the shunt capacitor and the input impedance of the short-circuited segment of the transmission line. The input impedance of the short-circuited transmission line is given by

$$Z_{\text{in}} = -iZ_i \tan\beta_1\, d = -i\eta_1 \cos\theta_t \tan(k_1 \cos\theta_t\, d)\ . \tag{6.57}$$

Hence the equivalent impedance can be obtained simply from

$$\begin{aligned}\frac{V(d)}{I(d)} = Z_{\text{eq}} &= \frac{\left(\frac{1}{-i\omega C}\right)(-iZ_1 \tan\beta_1 d)}{-Z_1 \tan\beta_1 d + \frac{1}{-i\omega C}} \\ &= -i\,\frac{Z_1 \tan\beta_1 d}{1 - \omega C Z_1 \tan\beta_1 d}\ .\end{aligned}$$

Noting that $V(d) = E_{0x}(d)\ p$ and $I(d) = -H_{0y}(d)\ p$, it follows that

$$Z_s^{\text{TM}} = Z_{\text{eq}} = -i\,\frac{\eta_1 \cos\theta_t \tan(k_1 \cos\theta_t d)}{1 - \omega\widetilde{C}p\eta_1 \cos\theta_t \tan(k_1 \cos\theta_t d)}\ . \qquad \textbf{(TM mode)} \tag{6.58}$$

Under the condition given by Eq. (6.51), this surface is inductive and can support a TM surface wave in the upper medium with a propagation constant along $x$ (in our example) given by

$$\beta^{\text{TM}} = \sqrt{\omega^2\mu_0\varepsilon_0 + \omega^2\varepsilon_0^2 X_s^2}$$

with $X_s = iZ_s$.

Now for a TE incident wave with reference to Fig. 6-9(b), the field can be obtained

by applying the duality to Eqs. (6.43a)–(6.43d). However, duality would not apply to the metallic patches unless the metallic patches were to be replaced with magnetic conductors. Nevertheless, using the boundary conditions, continuity of the tangential electric field, and discontinuity of the magnetic field (Eq. (6.47)), the surface impedance can be obtained. Note that in this case the electric field is parallel to the surface. Equivalently, we can use the transmission-line analogy, where the characteristic impedance of the equivalent transmission lines must be modified to

$$Z_0 = \frac{\eta_0}{\cos\theta_\mathrm{i}}$$

and

$$Z_1 = \frac{\eta_1}{\cos\theta_\mathrm{t}} \,.$$

Using these, the surface impedance for this polarization takes the following form:

$$Z_\mathrm{s}^\mathrm{TE} = -i\,\frac{\dfrac{\eta_1}{\cos\theta_\mathrm{t}}\,\tan(k_1\cos\theta_\mathrm{t}\,d)}{1-\omega\widetilde{C}P\,\dfrac{\eta_1}{\cos\theta_\mathrm{t}}\,\tan(k_1\cos\theta_\mathrm{t}\,d)}\,. \qquad \textbf{(TE mode)} \tag{6.59}$$

When $k_1 d \ll 1$, using the first term of the Taylor series expansion of the tangent function in Eq. (6.59) leads to

$$Z_\mathrm{s} = -i\,\frac{\eta_1 k_1 d}{1-\omega\widetilde{C}p\eta_1 k_1 d}\,.$$

This surface impedance is inductive when $\omega\widetilde{C}p\eta_1 k_1 d < 1$. The interesting feature of this polarization is that the surface impedance is independent of the incident angle, as it should be.

An approximate formulation for the capacitance per unit length of coplanar metallic strips can be found in the literature.* For a gap dimension of $g$, the capacitance value is given by

$$\widetilde{C} = \frac{\varepsilon_\mathrm{eff}\,\mathcal{K}[\sqrt{1-(g/p)^2}]}{\mathcal{K}(g/p)}\,, \tag{6.60}$$

where $\mathcal{K}(t)$ is the complete elliptic integral given by

$$\begin{aligned}\mathcal{K}(t) &= \int_0^{\pi/2} \frac{d\alpha}{\sqrt{1-t^2\sin^2\alpha}} \\ &= \frac{\pi}{2}\left(1+\frac{1^2}{2^2}\,t^2+\frac{1^2\cdot 3^2}{2^2\cdot 4^2}\,t^4+\frac{1^2\cdot 3^2\cdot 5^2}{2^2\cdot 4^2\cdot 6^2}\,t^6+\cdots\right)\,.\end{aligned} \tag{6.61}$$

*S. Gevorgian and H. Berg, "Line capacitance and impedance of coplanar strip waveguides on substrates with multiple dielectric layers," 31st European Microwave Conference, 2001.

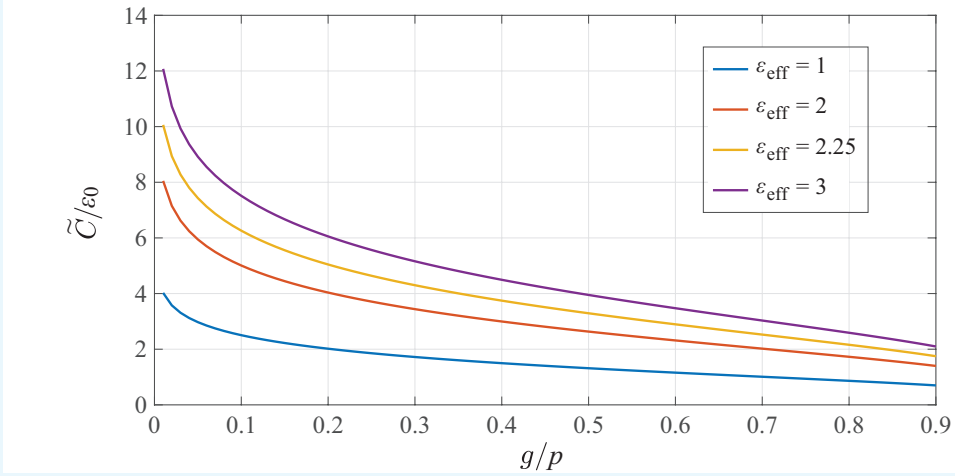


**Figure 6-11:** The normalized capacitance per unit length of coplanar strips over a substrate for different values of $\varepsilon_{\text{eff}}$ as a function of gap-to-strip ratio.

In Eq. (6.60), $\varepsilon_{\text{eff}}$ is the effective dielectric constant formed by the substrate dielectric $\varepsilon_0\varepsilon_1$ and the air $\varepsilon_0$ on both sides of the square patches. Since the electric field is the same on both sides of the gap it can easily be shown that

$$\varepsilon_{\text{eff}} = \varepsilon_0 \frac{1+\varepsilon_1}{2} .$$

Here we are assuming that the substrate thickness $d$ is much larger than the gap $g$, so that the capacitance value is not affected by the ground plane.

Figure 6-11 shows the normalized capacitance $(\widetilde{C}/\varepsilon_0)$ per unit length of a coplanar strip capacitor as a function of gap-over-height ratio $(g/p)$ for different values of $\varepsilon_{\text{eff}}$.

## 6-5 The Rectangular Waveguide

In this section we consider wave propagation inside a hollow metallic pipe of rectangular cross section, as shown in Fig. 6-12. In general, hollow, dielectric-filled, or partially filled, closed metallic pipes of arbitrary cross section but invariant to the $z$-direction are known as ***metallic waveguides***. Here we consider a rectangular waveguide filled with a homogeneous material having permittivity and permeability values denoted by $\varepsilon$ and $\mu$, respectively. The boundary condition over the interior surface of the metallic pipe mandates that the tangential component of the electric field be zero across the waveguide's cross section.

For a TM wave, according to Eq. (5.102a),

$$E_z(x,y,z) = k_c^2 \, \psi(x,y) \, e^{i\beta z} ,$$

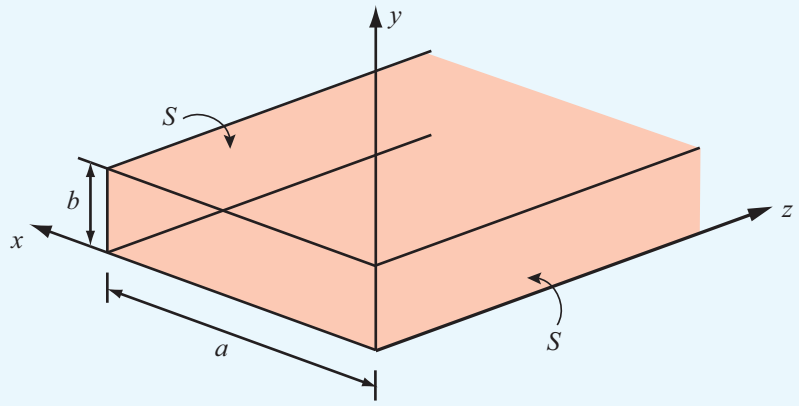


**Figure 6-12:** Geometry of a metallic rectangular waveguide. The cross section geometry is invariant along the waveguide axis.

for a wave traveling along the $+z$-direction. Hence the boundary condition on the waveguide surface $S$, namely $E_z|_{x,y\in S} = 0$, where $S$ encompasses the top and bottom surfaces as well as the side surfaces of the structure shown in Fig. 6-12, mandates that

$$\psi(x,y) = 0\,, \qquad x,y \in S\,, \qquad \textbf{(TM mode)} \tag{6.62}$$

which is known as ***Dirichlet's boundary condition***. For a TE wave according to Eq. (5.105b),

$$\hat{\mathbf{n}} \times \mathbf{E} = i\omega\mu\, \hat{\mathbf{n}} \times (\nabla_t \psi_m \times \hat{\mathbf{z}}) e^{i\beta z}\,.$$

Since $\hat{\mathbf{n}} \cdot \hat{\mathbf{z}} = 0$, it can easily be shown that

$$\hat{\mathbf{n}} \times \mathbf{E} = -i\omega\mu\, \frac{\partial \psi_m}{\partial n}\, e^{i\beta z}\, \hat{\mathbf{z}}\,.$$

Therefore for TE modes the boundary condition mandates that

$$\frac{\partial \psi_m}{\partial n} = 0 \qquad x,y \in s\,. \qquad \textbf{(TE mode)} \tag{6.63}$$

This is known as ***Neumann's boundary condition***.

### 6-5.1 TM Modes

Let's now consider the TM solution for wave propagation in the rectangular waveguide. From Eq. (5.101) in the Cartesian coordinate system, we are seeking a solution for

$$\left(\frac{\partial^2}{\partial x^2} + \frac{\partial^2}{\partial y^2} + k_c^2\right)\, \psi(x,y) = 0\,, \tag{6.64}$$

subject to Dirichlet's boundary condition given by

$$\psi(0,y) = \psi(a,y) = 0$$

on the vertical walls and

$$\psi(x,0) = \psi(x,b) = 0$$

on the horizontal walls. A solution of Eq. (6.64) can be obtained using the method of separation of variables. Assuming

$$\psi(x,y) = X(x)\,Y(y)\ , \tag{6.65}$$

for continuous and differentiable functions of $X(x)$ and $Y(y)$, substituting Eq. (6.65) into Eq. (6.64), and then dividing both sides by $X(x)\,Y(y)$, results in

$$\frac{X''(x)}{X(x)} + \frac{Y''(y)}{Y(y)} + k_c^2 = 0\ . \tag{6.66}$$

Since $X$ is a function of only variable $x$ and $Y$ is a function of only variable $y$, the only possible condition for Eq. (6.66) to be valid is when

$$\frac{X''(x)}{X} = -k_x^2 \tag{6.67a}$$

and

$$\frac{Y''(y)}{Y} = -k_y^2\ . \tag{6.67b}$$

Hence $k_c^2 = k_x^2 + k_y^2$ provides the sufficient and necessary condition for the validity of Eq. (6.66).

Equations (6.67a) and (6.67b) are ordinary second-order differential equations whose solutions are given by

$$X(x) = A\sin(k_x x) + B\cos(k_x x) \tag{6.68a}$$

and

$$Y(y) = C\sin(k_y y) + D\cos(k_y y)\ . \tag{6.68b}$$

The boundary condition for $\psi$ translates into the following conditions for $X(x)$ and $Y(y)$:

$$X(0) = X(a) = 0$$

and

$$Y(0) = Y(b) = 0\ .$$

These conditions provide

$$B = D = 0, \tag{6.69a}$$

$$\sin(k_x a) = 0\,, \tag{6.69b}$$

and

$$\sin(k_y b) = 0\,. \tag{6.69c}$$

Equations (6.69b) and (6.69c) provide discrete solutions (eigenvalues) for $k_x$ and $k_y$:

$$k_x = \frac{m\pi}{a} \qquad m = 1,2,3,\ldots$$

and

$$k_y = \frac{n\pi}{b}\,, \qquad n = 1,2,3,\ldots$$

Therefore

$$\Psi_{mn}(x,y) = E_0 \sin\left(\frac{m\pi}{a}\,x\right) \sin\left(\frac{n\pi}{b}\,y\right)\,. \tag{6.70}$$

where $E_0 = AC$. For each integer pair $(m,n)$ corresponding to mode $\mathrm{TM}_{mn}$, the following propagation constant is obtained:

$$\beta_{mn} = \sqrt{k^2 - \left(\frac{m\pi}{a}\right)^2 - \left(\frac{n\pi}{b}\right)^2}\,. \tag{6.71}$$

The corresponding ***guide wavelength*** (along the $z$-direction), defined by $\lambda_g = 2\pi/\beta$, is given by

$$(\lambda_{gmn})^{-1} = \sqrt{\frac{1}{\lambda^2} - \left(\frac{m}{2a}\right)^2 - \left(\frac{n}{2b}\right)^2}\,. \tag{6.72}$$

The field quantities for TM modes can be directly computed from Eqs. (5.102a) and (5.102b):

$$E_x(x,y,z) = iE_0\beta_{mn}\left(\frac{m\pi}{a}\right)\cos\left(\frac{m\pi}{a}\,x\right)\sin\left(\frac{n\pi}{b}\,y\right)\,e^{i\beta_{mn}z}\,, \tag{6.73a}$$

$$E_y(x,y,z) = iE_0\beta_{mn}\left(\frac{n\pi}{b}\right)\sin\left(\frac{m\pi}{a}\,x\right)\cos\left(\frac{n\pi}{b}\,y\right)\,e^{i\beta_{mn}z}\,, \tag{6.73b}$$

$$E_z(x,y,z) = E_0\left[\left(\frac{m\pi}{a}\right)^2 + \left(\frac{n\pi}{b}\right)^2\right]\sin\left(\frac{m\pi}{a}\,x\right)\sin\left(\frac{n\pi}{b}\,y\right)\,e^{i\beta_{mn}z}\,, \tag{6.73c}$$

$$H_x(x,y,z) = -iE_0\omega\varepsilon\left(\frac{n\pi}{b}\right)\sin\left(\frac{m\pi}{a}\,x\right)\cos\left(\frac{n\pi}{b}\,y\right)\,e^{i\beta_{mn}z}\,, \tag{6.73d}$$

and

$$H_y(x,y,z) = iE_0\omega\varepsilon\left(\frac{m\pi}{a}\right)\cos\left(\frac{m\pi}{a}\,x\right)\sin\left(\frac{n\pi}{b}\,y\right)\,e^{i\beta_{mn}z}\,. \tag{6.73e}$$

The wave impedance is defined by

$$Z_{\mathrm{TM}} = \frac{\hat{\mathbf{z}}\times\mathbf{E}_t}{\mathbf{H}_t} = \frac{E_x}{H_y} = \frac{E_y}{-H_x} = \frac{\sqrt{k^2 - \left(\frac{m\pi}{a}\right)^2 - \left(\frac{n\pi}{b}\right)^2}}{\omega\varepsilon}\,.$$

Among the infinite number of discrete modes, only those for which $\beta_{mn}$ is a real quantity can propagate. The rest are evanescent and do not carry energy. The TM cutoff frequency for the $mn$th mode corresponds to a frequency for which

$$\beta_{mn} = 0$$

and

$$k^2 = (2\pi f_c)^2 \mu\varepsilon = \left(\frac{m\pi}{a}\right)^2 + \left(\frac{n\pi}{b}\right)^2 ,$$

or

$$f_c^{(mn)} = \frac{1}{2\sqrt{\mu\varepsilon}} \sqrt{\left(\frac{m}{a}\right)^2 + \left(\frac{n}{b}\right)^2} . \tag{6.74}$$

The lowest propagating mode corresponds to the smallest cutoff frequency. Assuming $a > b$, the lowest propagating mode corresponds to $m = 1,\ n = 1$:

$$f_c^{(11)} = \frac{1}{2\sqrt{\mu\varepsilon}} \sqrt{\frac{1}{a^2} + \frac{1}{b^2}} . \tag{6.75}$$

Therefore, waveguide structures are high-pass devices that operate at frequencies $f > f_c^{(11)}$. The next propagating mode, in terms of cutoff frequency, is $TM_{21}$, and the mode after that includes $TM_{22}$ or $TM_{31}$ depending on the ratio of $b/a$

### 6-5.2 TE Modes

The TE solution can easily be obtained by using Eqs. (5.105a) and (5.105b) and noting that

$$\psi_{mn}(x,y) = H_0 \cos\left(\frac{m\pi}{a}x\right) \cos\left(\frac{n\pi}{b}y\right) , \tag{6.76}$$

which allows $m$ or $n$ to be zero. The expressions for the TE field quantities are given by

$$H_x(x,y,z) = -iH_0\beta_{mn}\left(\frac{m\pi}{a}\right) \sin\left(\frac{m\pi}{a}x\right) \cos\left(\frac{n\pi}{b}y\right) e^{i\beta_{mn}z} , \tag{6.77a}$$

$$H_y(x,y,z) = -iH_0\beta_{mn}\left(\frac{n\pi}{b}\right) \cos\left(\frac{m\pi}{a}x\right) \sin\left(\frac{n\pi}{b}y\right) e^{i\beta_{mn}z} , \tag{6.77b}$$

$$H_z(x,y,z) = H_0\left[\left(\frac{m\pi}{a}\right)^2 + \left(\frac{n\pi}{b}\right)^2\right] \cos\left(\frac{m\pi}{a}x\right) \cos\left(\frac{n\pi}{b}y\right) e^{i\beta_{mn}z} , \tag{6.77c}$$

$$E_x(x,y,z) = -iH_0\omega\mu\left(\frac{n\pi}{b}\right) \cos\left(\frac{m\pi}{a}x\right) \sin\left(\frac{n\pi}{b}y\right) e^{i\beta_{mn}z} , \tag{6.77d}$$

and

$$E_y(x,y,z) = iH_0\omega\mu\left(\frac{m\pi}{a}\right) \sin\left(\frac{m\pi}{a}x\right) \cos\left(\frac{n\pi}{b}y\right) e^{i\beta_{mn}z} . \tag{6.77e}$$

Hence the lowest-order propagating wave in a rectangular waveguide is a $TE_{10}$ mode ($a > b$) whose cutoff frequency is given by

$$f_c^{(10)} = \frac{1}{2a\sqrt{\mu\varepsilon}} . \tag{6.78}$$

The field expressions given by Eqs. (6.73) and (6.77) are plotted in Fig. 6-13 for four TM and four TE modes in a rectangular waveguide with $a = 2b$. In this figure, the color indicates the intensity of the total field, the solid lines indicate the direction of the electric field, and the dashed lines show the direction of the magnetic field across the cross section of the waveguide.

### 6-5.3 $k$–$\beta$ Diagram

In the preceding subsections, it was shown that for a given propagation mode the ***cutoff wave number*** ($k_c$) is only a function of the waveguide's dimensions $a$ and $b$. For example, for the $mn$th mode,

$$k_{c(mn)}^2 = \left(\frac{m\pi}{a}\right)^2 + \left(\frac{n\pi}{b}\right)^2 .$$

is a fixed quantity independent of frequency. The dispersion relation given by

$$k^2 - \beta^2 = k_c^2 \tag{6.79}$$

provides the relationship between $\beta$ and $k$ (or equivalently $\beta$ and $\omega$). Equation (6.79) describes a hyperbola curve in the $k$–$\beta$ plane, as shown in Fig. 6-14. When $k_c > k$, $\beta$ becomes pure imaginary, $\beta = i\alpha$, and we have

$$k^2 + \alpha^2 = k_c^2 ,$$

which is a circle, and also shown in Fig. 6-14.

The phase velocity in any waveguide is obtained from

$$u_p = \frac{dz}{dt} = \frac{\omega}{\beta} ,$$

which in this case is obviously a nonlinear function of frequency:

$$u_p = \frac{\omega}{\sqrt{k^2 - k_c^2}} .$$

Since $\sqrt{k^2 - k_c^2} < k$ for a propagating mode, then

$$u_p > c .$$

That is, the phase velocity in waveguides is faster than the speed of light. Figure 6-15 shows the $\beta$–$k$ diagram for the first 7 modes of a rectangular waveguide with $a = 2b$.

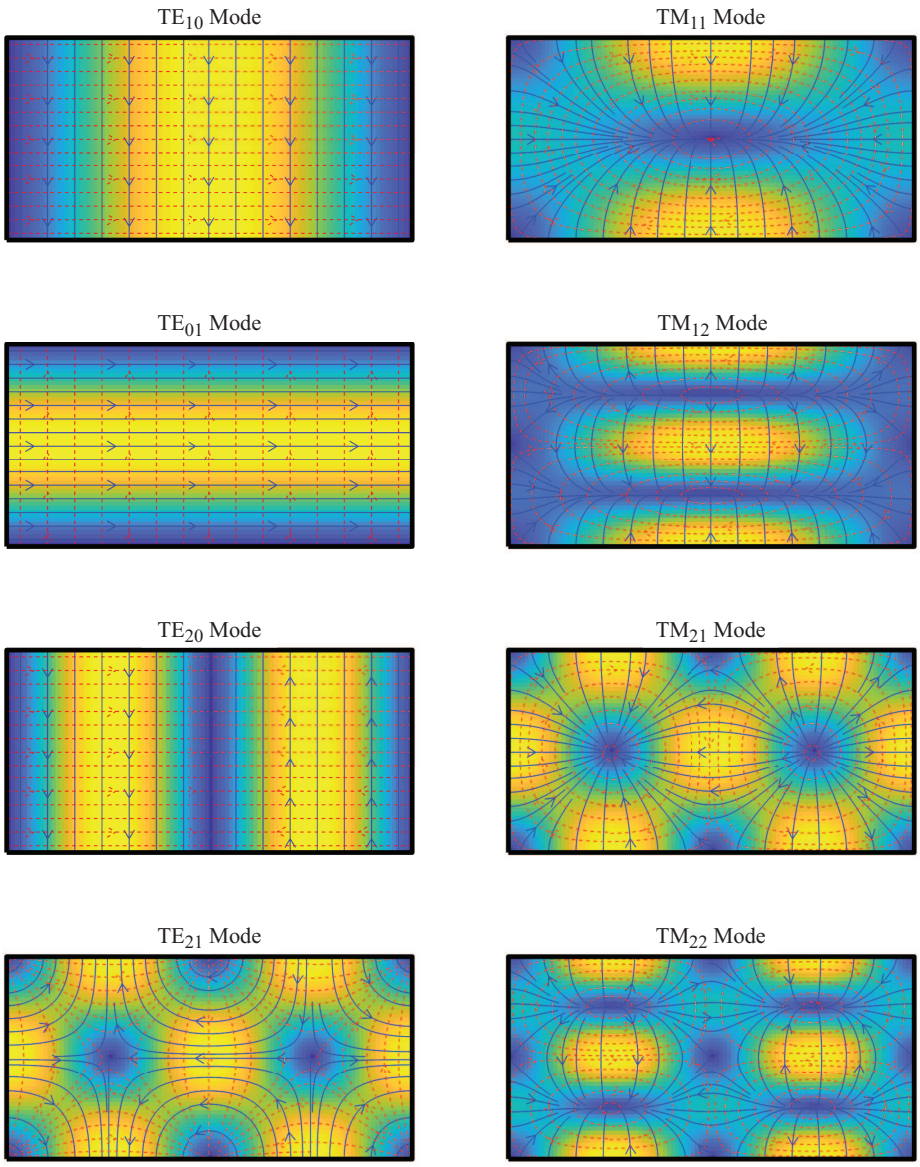


**Figure 6-13:** The TE and TM field distributions across the cross section of a rectangular waveguide. The color indicates the field intensity, the solid lines show the directions of the electric fields, and the dashed lines show the directions of the magnetic fields.

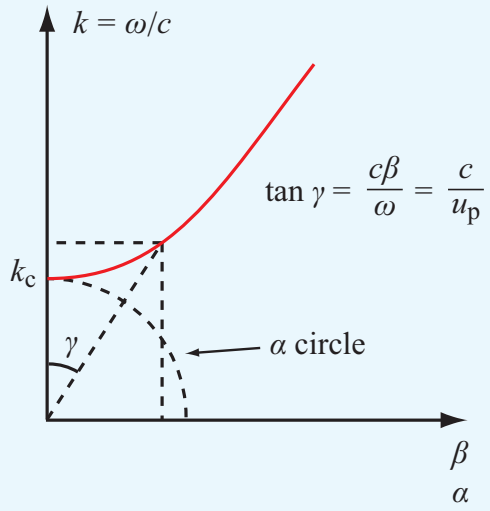


**Figure 6-14:** $\beta$–$k$ diagram for propagation in a metallic waveguide.

### 6-5.4 Group Velocity

The group velocity $u_g$ is the velocity associated with the envelope of the traveling wave. For a monochromatic signal the time-domain expression for the potential is given by

$$\Pi_z(\mathbf{r},t) = \Re\mathrm{e}[\psi(x,y)\, e^{i(\beta z-\omega t)}] \,.$$

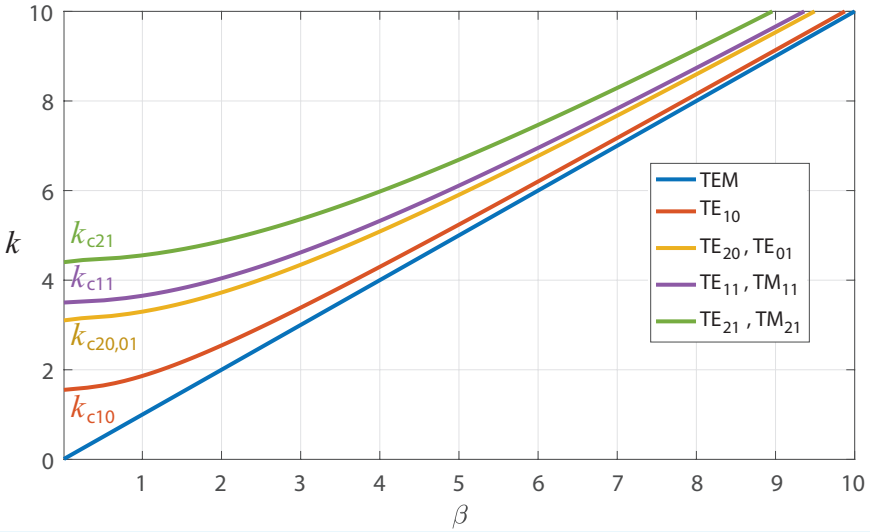


**Figure 6-15:** $\beta$–$k$ diagram for a rectangular waveguide with $a = 2$ and $b = 1$ for the first 7 modes of propagation. The cutoff wave numbers of the various modes are indicated along the $k$-axis. Also shown is the $\beta$–$k$ diagram in free space for a TEM wave.

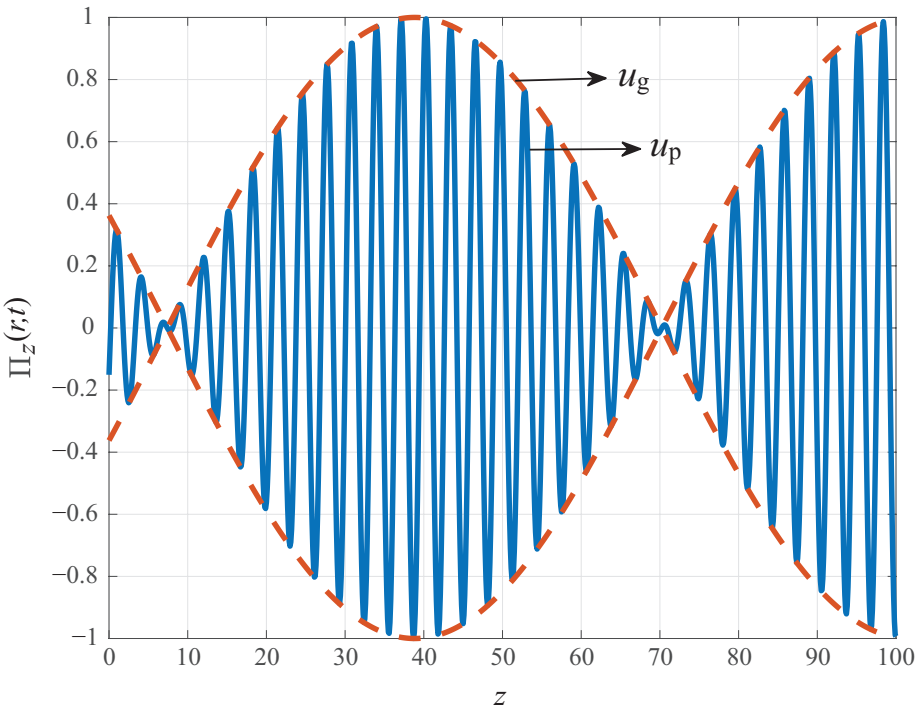


**Figure 6-16:** A time snapshot of a two-tone signal propagating inside a waveguide. The envelope of the wave propagates with velocity $u_g$, which is different from the phase velocity $u_p$.

To demonstrate the concept of group velocity in a waveguide, let us consider two monochromatic signals at angular frequencies

$$\omega_1 = \omega_0 + \Delta\omega \qquad \text{and} \qquad \omega_2 = \omega_0 - \Delta\omega\ .$$

For simplicity we consider the case where the field distributions for both are the same across the waveguide cross section. Hence the total field may be written as

$$\Pi_z(r,t) = \psi(x,y)\ \{\cos[(\omega_0+\Delta\omega)t - (\beta_0+\Delta\beta)z] + \cos[(\omega_0-\Delta\omega)t - (\beta_0-\Delta\beta)z]\}\ . \tag{6.80}$$

Equivalently,

$$\Pi_z(r,t) = 2\,\psi(x,y)\,\cos(\omega_0 t - \beta_0 z)\cos(\Delta\omega t - \Delta\beta z)\ . \tag{6.81}$$

The first cosine term in Eq. (6.81) is the carrier, and the second one, which varies slowly with time and space, is the envelope modulation of the wave, as shown in Fig. 6-16. As shown earlier, the constant phase points in the $z$–$t$ domain correspond to

$$\omega_0 t - \beta_0 z = \text{constant},$$

and hence

$$u_p = \frac{dz}{dt} = \frac{\omega_0}{\beta_0} = \frac{\omega_0}{\sqrt{k_0^2 - k_c^2}} . \tag{6.82}$$

Similarly, constant envelope points in the $z$–$t$ domain can be obtained from

$$\Delta\omega t - \Delta\beta z = \text{constant} ,$$

from which the group velocity can be obtained and is given by

$$u_g = \frac{dz}{dt} = \frac{\Delta\omega}{\Delta\beta} .$$

In the limit as $\Delta\omega \to 0$ and $\Delta\beta \to 0$,

$$u_g = \frac{d\omega}{d\beta} . \tag{6.83}$$

Group velocity can also be expressed in terms of the phase velocity by noting that $\omega = u_p\beta$, which leads to

$$u_g = \frac{d(u_p\beta)}{d\beta} = u_p + \beta\frac{du_p}{d\beta} . \tag{6.84}$$

Also noting that $\beta = 2\pi/\lambda_g$, Eq. (6.84) can be written as

$$u_g = u_p - \lambda_g\frac{du_p}{d\lambda_g} . \tag{6.85}$$

Since in a waveguide

$$\beta = \sqrt{k^2 - k_c^2} = \sqrt{\frac{\omega^2}{c^2} - k_c^2} , \tag{6.86}$$

it can easily be shown that

$$d\beta = \frac{u_p}{c^2}\, d\omega ,$$

and therefore

$$u_p u_g = c^2 , \tag{6.87}$$

independent of the waveguide cross-section geometry and the mode of propagation.

### 6-5.5 Power Flow and Attenuation

Waveguides, like other transmission lines, can transfer power. However, as shown in this section, waveguides can transfer power at much lower attenuation rates compared with other transmission lines that support TEM modes like a coaxial line. The power flow inside a waveguide can be calculated from the Poynting vector. The rate of energy flow in a rectangular

waveguide supporting a $\text{TM}_{mn}$ mode can be established by computing

$$P_{mn}(z) = \frac{1}{2}\,\Re\text{e}\left[\int_0^a\int_0^b (E\times H^*)\cdot\hat{\mathbf{z}}\,dx\,dy\right]$$
$$= \frac{1}{2}\,\Re\text{e}\left[\int_0^a\int_0^b (E_xH_y^* - E_yH_x^*)\,dx\,dy\right]. \tag{6.88}$$

Using the field expressions given by Eq. (6.73),

$$P_{mn}(z) = \frac{1}{2}\,|E_0|^2\left[\omega\varepsilon\left(\frac{m\pi}{a}\right)^2\beta_{mn}\int_0^a\int_0^b \cos^2\left(\frac{m\pi}{a}\,x\right)\,\sin^2\left(\frac{n\pi}{b}\,y\right)\,dx\,dy\right.$$
$$\left. + \omega\varepsilon\left(\frac{n\pi}{b}\right)^2\beta_{mn}\int_0^a\int_0^b \sin^2\left(\frac{m\pi}{a}\,x\right)\,\cos^2\left(\frac{n\pi}{b}\,y\right)\,dx\,dy\right]. \tag{6.89}$$

Fortunately, the integrals can be evaluated analytically, and it can easily be shown that

$$\int_0^a\int_0^b \cos^2\left(\frac{m\pi}{a}\,x\right)\,\sin^2\left(\frac{n\pi}{b}\,y\right)\,dx\,dy = \int_0^a\int_0^b \sin^2\left(\frac{m\pi}{a}\,x\right)\,\cos^2\left(\frac{n\pi}{b}\,y\right)\,dx\,dy$$
$$= \begin{cases} ab/4 & m\neq 0 \text{ and } n\neq 0\,, \\ ab/2 & m=0 \text{ or } n=0\,. \end{cases} \tag{6.90}$$

For a TM mode $m \neq 0$ and $n \neq 0$,

$$P_{mn}^{\text{TM}}(z) = \frac{ab}{8}\,\omega\varepsilon\left[\left(\frac{m\pi}{a}\right)^2 + \left(\frac{n\pi}{b}\right)^2\right]\beta_{mn}|E_0|^2$$
$$= \frac{ab}{8\eta}\,k\beta_{mn}k_{\text{c},mn}^2|E_0|^2\,. \qquad \textbf{(TM mode)} \tag{6.91}$$

The power carried by a TE mode can be obtained by using Eqs. (6.77a) and (6.77b) in Eq. (6.88). Using Eq. (6.90), it can be shown that

$$P_{mn}^{\text{TE}}(z) = \frac{ab}{4}\,|H_0|^2\eta k\beta_{mn}k_{\text{c},mn}^2 \times \begin{cases} \frac{1}{2} & m\neq 0 \text{ and } n\neq 0\,, \\ 1 & m=0 \text{ or } n=0\,. \end{cases} \qquad \textbf{(TE mode)} \tag{6.92}$$

It is interesting to note that in situations where the waveguide is supporting two modes (or more), say a $\text{TM}_{mn}$ and a $\text{TM}_{pq}$, the total power carried by the waveguide is the superposition of power carried by the individual modes; that is,

$$P^{\text{TM}} = P_{mn}^{\text{TM}} + P_{pq}^{\text{TM}}\,.$$

This is the direct result of orthogonality of modes in the waveguide's cross section. For rectangular waveguides,

$$\int_0^a \cos\left(\frac{m\pi}{a}\,x\right)\,\cos\left(\frac{p\pi}{a}\,x\right)\,dx = 0\,, \qquad m \neq p\,,$$

and

$$\int_0^b \sin\left(\frac{n\pi}{b}\,y\right)\,\sin\left(\frac{q\pi}{b}\,y\right)\,dy = 0\,, \qquad n \neq q\,,$$

and because of these properties, the cross product of the fields of different modes does not render a net flow of power along the waveguide. In practice, waveguides are made with metals as opposed to perfect electric conductors. The finite conductivity of metallic walls causes attenuation or loss of power as the wave propagates in the waveguide. Strictly speaking, in this case the modes of propagation cannot be decomposed into TE or TM modes as Dirichlet's or Neumann's boundary conditions are no longer applicable. However, an approximate solution based on a perturbation method can be obtained if the conductivity of the metal is quite high. With this approach, the waveguide walls are initially assumed to be PEC, and the surface currents on the walls are obtained based on that assumption. Then, for good conductors, the surface impedances given by Eq. (5.136) can be used to calculate the power loss:

$$P_{\mathrm{L}} = \frac{1}{2}\,\Re\mathrm{e}\left[\oint_{\mathrm{c}}\int \mathbf{E}^{(1)}\cdot J_{\mathrm{s}}^{*}\,d\ell\,dz\right]\,, \tag{6.93}$$

where the contour integral is over the contour of the waveguide's cross section and $\mathbf{E}^{(1)}$ is the first-order correction to the tangential electric field on a PEC. This electric field is related to the tangential magnetic field through Eq. (6.13) with $Z_{\mathrm{s}} = \eta_{\mathrm{c}}$. Noting that $\mathbf{J}_{\mathrm{s}} = \hat{\mathbf{n}}\times\mathbf{H}$,

$$\hat{\mathbf{n}}\times\hat{\mathbf{n}}\times\mathbf{E}^{(1)} = -\eta_{\mathrm{c}}\,\mathbf{J}_{\mathrm{s}}\,.$$

Hence

$$\hat{\mathbf{n}}\times\mathbf{E}^{(1)} = \eta_{\mathrm{c}}\,\hat{\mathbf{n}}\times\mathbf{J}_{\mathrm{s}}\,. \tag{6.94}$$

In other words,

$$\mathbf{E}_{\mathrm{t}}^{(1)} = \eta_{\mathrm{c}}\,\mathbf{J}_{\mathrm{s}}\,.$$

Substituting Eq. (6.94) into Eq. (6.93) leads to

$$P_{\mathrm{L}} = \frac{1}{2}\;\Re\mathrm{e}\left[\oint_{\mathrm{c}}\int \eta_{\mathrm{c}}|\mathbf{J}_{\mathrm{s}}|^2\,d\ell\,dz\right]\,.$$

The power loss per unit length is given by

$$p_{\mathrm{L}} = \frac{dP_{\mathrm{L}}}{dz} = \frac{1}{2}\,\oint_{\mathrm{c}}\Re\mathrm{e}[\eta_{\mathrm{c}}]|\mathbf{J}_{\mathrm{s}}|^2\,d\ell\,, \tag{6.95}$$

where

$$\Re\mathrm{e}[\eta_c] = \frac{1}{\sigma\delta_s}$$

is the surface resistivity of the metal. To find the attenuation rate in the waveguide, we note that the power as a function of $z$ can be written as

$$P(z) = P_0 e^{-2\alpha z}\,, \tag{6.96}$$

where $\alpha$ is the attenuation rate. The rate of power decrease in the waveguide, power loss per unit length, is given by

$$-\frac{dP(z)}{dz} = 2\alpha P_0 e^{-2\alpha z} = 2\alpha\, P(z) = p_L\,. \tag{6.97}$$

So the attenuation rate for any mode can be obtained from

$$\alpha = \frac{1}{2}\,\frac{p_L}{P(z)} = \frac{\oint |J_s|^2\, d\ell}{4\sigma\delta_s\, P(z)} = \frac{\oint |H_t|^2\, d\ell}{4\sigma\delta_s\, P(z)}\,. \tag{6.98}$$

## Example 6-2: Attenuation Rate for Dominant Mode in a Rectangular Waveguide

Find the attenuation rate in a rectangular waveguide supporting a $\mathrm{TE}_{10}$ mode.

**Solution:** The field expressions for a $\mathrm{TE}_{10}$ mode can be obtained from Eq. (6.77):

$$H_x(\mathbf{r}) = \frac{-i\pi H_0\beta_{10}}{a}\sin\left(\frac{\pi}{a}x\right)\, e^{i\beta_{10}z}\,, \tag{6.99a}$$

$$H_z(\mathbf{r}) = H_0\left(\frac{\pi}{a}\right)^2\cos\left(\frac{\pi}{a}x\right)\, e^{i\beta_{10}z}\,, \tag{6.99b}$$

and

$$E_y(\mathbf{r}) = iH_0\omega\mu\,\frac{\pi}{a}\sin\left(\frac{\pi}{a}x\right)\, e^{i\beta_{10}z}\,. \tag{6.99c}$$

The unperturbed surface current along the walls can be found from $\mathbf{J}_s = \hat{\mathbf{n}}\times\mathbf{H}$ ($\mathbf{r}\in C$). On vertical walls at $x = 0$ and $x = a$,

$$\mathbf{J}_s = \hat{\mathbf{x}}\times\mathbf{H} = -\hat{\mathbf{y}}H_0\left(\frac{\pi}{a}\right)^2 e^{i\beta_{10}z} \qquad x = 0 \tag{6.100a}$$

and

$$\mathbf{J}_s = -\hat{\mathbf{x}}\times\mathbf{H} = -\hat{\mathbf{y}}H_0\left(\frac{\pi}{a}\right)^2 e^{i\beta_{10}z} \qquad x = a\,, \tag{6.100b}$$

and on the horizontal walls

$$\begin{aligned}\mathbf{J}_s &= \hat{\mathbf{y}} \times \mathbf{H} \\ &= H_0 \left[ \hat{\mathbf{z}} \, \frac{i\pi\beta_{10}}{a} \sin\left(\frac{\pi}{a}x\right) + \hat{\mathbf{x}} \left(\frac{\pi}{a}\right)^2 \cos\left(\frac{\pi}{a}x\right) \right] e^{i\beta_{10}z} \qquad y = 0 \end{aligned} \tag{6.101a}$$

and

$$\begin{aligned}\mathbf{J}_s &= -\hat{\mathbf{y}} \times \mathbf{H} \\ &= H_0 \left[ -\hat{\mathbf{z}} \, \frac{i\pi\beta_{10}}{a} \sin\left(\frac{\pi}{a}x\right) - \hat{\mathbf{x}} \left(\frac{\pi}{a}\right)^2 \cos\left(\frac{\pi}{a}x\right) \right] e^{i\beta_{10}z} \qquad y = b \, . \end{aligned} \tag{6.101b}$$

Using Eq. (6.95),

$$\begin{aligned} p_L &= \frac{|H_0|^2}{2\sigma\delta_s} \left[ 2\left(\frac{\pi}{a}\right)^4 b + \left(\frac{\pi\beta_{10}}{a}\right)^2 a + \left(\frac{\pi}{a}\right)^4 a \right] \\ &= \frac{|H_0|^2}{\sigma\delta_s} \left(\frac{\pi}{a}\right)^4 \left[ b + \left(\frac{a\beta_{10}}{\pi}\right)^2 \frac{a}{2} + \frac{a}{2} \right] . \end{aligned} \tag{6.102}$$

From Eq. (6.92) we have

$$P_{10}^{TE}(z) = \frac{ab}{4} |H_0|^2 \eta k \beta_{10} \left(\frac{\pi}{a}\right)^2 . \tag{6.103}$$

Hence, the attenuation rate, using Eq. (6.98), is found to be

$$\alpha = \frac{2\left(\frac{\pi}{a}\right)^2 \left\{ b + \frac{a}{2} \left[ \left(\frac{a\beta_{10}}{\pi}\right)^2 + 1 \right] \right\}}{\sigma\delta_s ab\eta k\beta_{10}} .$$

But

$$\beta_{10}^2 = k^2 - \left(\frac{\pi}{a}\right)^2 ,$$

so

$$\alpha = \frac{2b\left(\frac{\pi}{a}\right)^2 + ak^2}{\sigma\delta_s ab\eta k\beta_{10}} \qquad \text{nepers/m.} \tag{6.104}$$

Note that near cutoff, where $\beta_{10} \to 0$, the attenuation rate $\alpha \to \infty$. Figure 6-17 shows the attenuation rate for a $TE_{10}$ mode inside a waveguide with $a = 2b = 2.28$ cm, with walls made from silver ($\sigma_s = 6.14 \times 10^7$ S/m), copper ($\sigma_c = 5.008 \times 10^7$ S/m), gold ($\sigma_g = 4.1 \times 10^7$ S/m), and aluminum ($\sigma_{Al} = 3.54 \times 10^7$ S/m). It is shown that the attenuation rate increases near the cutoff frequency, and as expected, metals with better conductivity provide lower attenuation rates. In practice, the surface roughness of the walls increases the path length of the surface current and causes the attenuation rates to be higher than what is shown in Fig. 6-17.

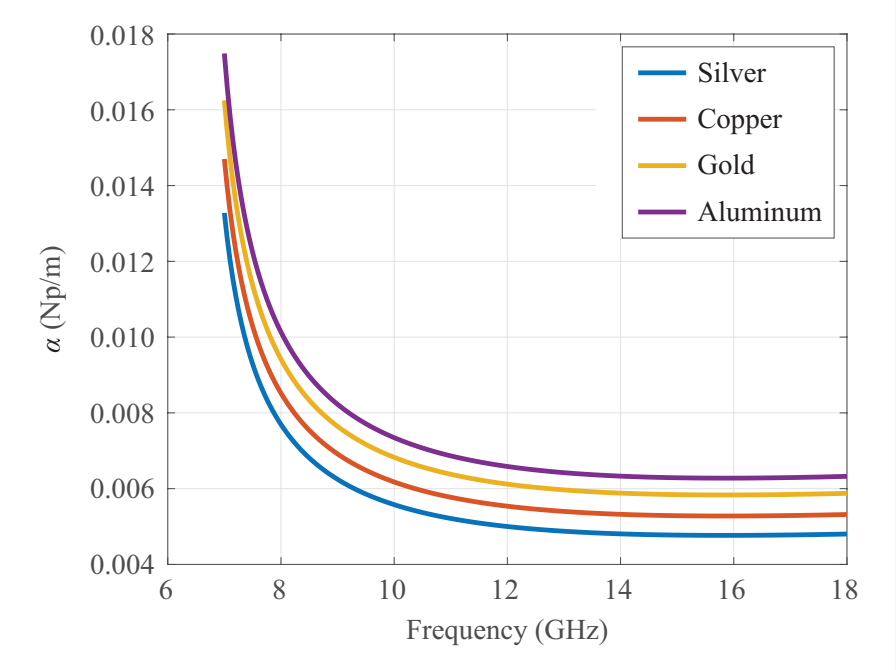


**Figure 6-17:** Attenuation rate inside a rectangular waveguide with $a = 2b = 2.28$ cm, computed using Eq. (6.104). Four different conductivities were used in the calculation corresponding to waveguide walls made from silver, copper, gold, and aluminum.

### 6-5.6 Rectangular Cavity

The term ***cavity resonator*** refers to a region enclosed by a metallic surface within which an electromagnetic field can exist. Such fields can be predicted to exist, without any excitations, at certain frequencies that depend on the shape and size of the cavity. Such frequencies are known as the ***resonant frequencies*** at which the electric and magnetic energies are stored. A rectangular cavity is a cavity made up of a rectangular waveguide terminated at both ends with metallic surfaces, as shown in Fig. 6-18, where the short circuits are placed at $z = 0$ and $z = c$. Similar to the fields in a rectangular waveguide, the fields can be decomposed into TM and TE (with respect to the $z$-axis) modes. In this case, however, the waveguide segment of length $c$ can support both $+z$-going and $-z$-going waves. For TM waves, $E_x(x,y,z)$ can be written as (see Eq. (6.73)):

$$E_x(x,y,z) = E_0 \left(\frac{m\pi}{a}\right) \cos\left(\frac{m\pi}{a}\,x\right) \sin\left(\frac{n\pi}{b}\,y\right) \frac{\partial}{\partial z}\left[Ae^{i\beta_{mn}z} + Be^{-i\beta_{mn}z}\right] . \tag{6.105}$$

The boundary conditions at $z = 0$ and $z = c$ mandate that

$$E_x(x,y,0) = E_x(x,y,c) = 0 .$$

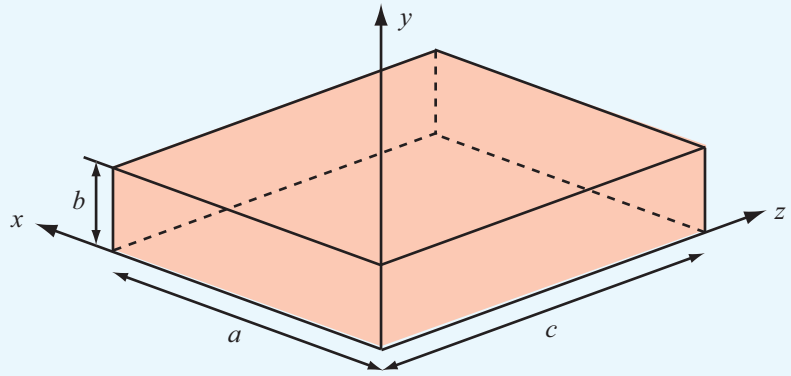


**Figure 6-18:** Geometry of a metallic rectangular cavity.

Hence, $A = B$, and

$$\sin(\beta_{mn} c) = 0 \quad \rightarrow \quad \beta_{mn} = \frac{\ell\pi}{c} \qquad \ell = 1, 2, 3, \ldots$$

According to Eq. (6.71) a nontrivial solution can be obtained when

$$k^2 = \left(\frac{m\pi}{a}\right)^2 + \left(\frac{n\pi}{b}\right)^2 + \left(\frac{\ell\pi}{c}\right)^2 . \tag{6.106}$$

That is, for frequencies at which Eq. (6.106) is satisfied, a resonant mode in the cavity can be established. It is noted that the resonant wave number given by Eq. (6.106) is only a function of the cavity's geometrical parameters $(a, b, c)$. If the material filling the cavity is lossless, the resonant frequencies are all real; otherwise the resonant frequencies are complex so that $k^2 = 4\pi^2 f^2 \mu\varepsilon$ is real. The TM fields in the cavity are given by

$$E_x(x,y,z) = -E_0 \left(\frac{\ell\pi}{c}\right)\left(\frac{m\pi}{a}\right) \cos\left(\frac{m\pi}{a}x\right) \sin\left(\frac{n\pi}{b}y\right) \sin\left(\frac{\ell\pi}{c}z\right) , \tag{6.107a}$$

$$E_y(x,y,z) = -E_0 \left(\frac{\ell\pi}{c}\right)\left(\frac{n\pi}{b}\right) \sin\left(\frac{m\pi}{a}x\right) \cos\left(\frac{n\pi}{b}y\right) \sin\left(\frac{\ell\pi}{c}z\right) , \tag{6.107b}$$

$$E_z(x,y,z) = E_0 \left[\left(\frac{m\pi}{a}\right)^2 + \left(\frac{n\pi}{b}\right)^2\right] \sin\left(\frac{m\pi}{a}x\right) \sin\left(\frac{n\pi}{b}y\right) \cos\left(\frac{\ell\pi}{c}z\right) , \tag{6.107c}$$

$$H_x(x,y,z) = -iE_0\omega\varepsilon \left(\frac{n\pi}{b}\right) \sin\left(\frac{m\pi}{a}x\right) \cos\left(\frac{n\pi}{b}y\right) \cos\left(\frac{\ell\pi}{c}z\right) , \tag{6.107d}$$

and

$$H_y(x,y,z) = -iE_0\omega\varepsilon \left(\frac{m\pi}{a}\right) \cos\left(\frac{m\pi}{a}x\right) \sin\left(\frac{n\pi}{b}y\right) \cos\left(\frac{\ell\pi}{c}z\right) . \tag{6.107e}$$

The field expressions for TE can be obtained from Eq. (6.77) and are given by

$$E_x(x,y,z) = iH_0\omega\mu \left(\frac{n\pi}{b}\right) \cos\left(\frac{m\pi}{a}x\right) \sin\left(\frac{n\pi}{b}y\right) \sin\left(\frac{\ell\pi}{c}z\right) , \tag{6.108a}$$

$$E_y(x,y,z) = iH_0\omega\mu \left(\frac{m\pi}{a}\right) \sin\left(\frac{m\pi}{a}x\right) \cos\left(\frac{n\pi}{b}y\right) \sin\left(\frac{\ell\pi}{c}z\right) , \tag{6.108b}$$

$$H_x(x,y,z) = -H_0 \left(\frac{\ell\pi}{c}\right)\left(\frac{m\pi}{a}\right) \sin\left(\frac{m\pi}{a}x\right) \cos\left(\frac{n\pi}{b}y\right) \cos\left(\frac{\ell\pi}{c}z\right) , \tag{6.108c}$$

$$H_y(x,y,z) = -H_0 \left(\frac{\ell\pi}{c}\right)\left(\frac{n\pi}{b}\right) \cos\left(\frac{m\pi}{a}x\right) \sin\left(\frac{n\pi}{b}y\right) \cos\left(\frac{\ell\pi}{c}z\right) , \tag{6.108d}$$

and

$$H_z(x,y,z) = H_0 \left[\left(\frac{m\pi}{a}\right)^2 + \left(\frac{n\pi}{b}\right)^2\right] \cos\left(\frac{m\pi}{a}x\right) \cos\left(\frac{n\pi}{b}y\right) \sin\left(\frac{\ell\pi}{c}z\right) . \tag{6.108e}$$

According to the Poynting theorem for phasor quantities, the complex power in any region is given by

$$P_{\text{in}}^{\text{c}} = P_{\text{rad}}^{\text{c}} + P_{\text{loss}} + i2\omega(w_{\text{e}} - w_{\text{m}}) . \tag{6.109}$$

In a cavity, there is no radiated power, and assuming no external sources and a loss-free cavity, the conservation of complex power mandates that

$$i2\omega(w_{\text{e}} - w_{\text{m}}) = 0 ,$$

or equivalently, at resonance in a general cavity we have

$$\begin{aligned} w_{\text{e}} = w_{\text{m}} &= \frac{\varepsilon}{4} \iiint_V |\mathbf{E}|^2 \, dv \\ &= \frac{\mu}{4} \iiint_V |\mathbf{H}|^2 \, dv . \end{aligned} \tag{6.110}$$

The time-domain expression for the Poynting theorem is

$$P_{\text{in}}(t) = P_{\text{rad}}(t) + P_{\text{loss}}(t) + \frac{\partial}{\partial t}(w_{\text{e}} + w_{\text{m}}) . \tag{6.111}$$

The law of conservation of power in a lossless cavity provides the following condition:

$$\frac{\partial}{\partial t}(w_{\text{e}} + w_{\text{m}}) = 0 . \tag{6.112}$$

Equation (6.112) indicates that the total stored energy in a cavity is a constant function of time. For a time-harmonic case, if we choose a time for which $\mathbf{H}(t)$ is zero, $w_{\text{m}}$ will be zero as well. In this case the stored electric energy is maximum and twice its average value. In this

case the total stored energy can be computed from

$$w = 2w_{\mathrm{e}} = \frac{\varepsilon}{2} \iiint |\mathbf{E}|^2 \, dv \, . \tag{6.113}$$

In practice, cavity walls are not perfect conductors and they can cause power loss. To compute power loss in a cavity, we can use a perturbation solution similar to what was used in Section 6-5.5 for the calculation of attenuation rates in waveguides. This power loss calculation uses an equation similar to Eq. (6.93) and is given by

$$P_{\mathrm{L}}^{\mathrm{s}} = \frac{1}{2} \, \Re\mathrm{e} \left[ \oiint_{\mathrm{s}} \mathbf{E}^{(1)} \cdot \mathbf{J}_{\mathrm{s}}^{*} \, ds \right] \, , \tag{6.114}$$

where $s$ represents the surface of the cavity. As before, $\mathbf{E}_{\mathrm{t}}^{(1)}$ is the first-order correction to the tangential electric field over the cavity walls and is given by

$$\mathbf{E}_{\mathrm{t}}^{(1)} = \eta_{\mathrm{c}} \, \mathbf{J}_{\mathrm{s}} = \eta_{\mathrm{c}} \, \hat{\mathbf{n}} \times \mathbf{H}(\mathbf{r}) \, , \qquad \mathbf{r} \in s \, .$$

Hence

$$\begin{aligned} P_{\mathrm{L}}^{\mathrm{s}} &= \frac{1}{2} \, \Re\mathrm{e} \left[ \oiint_{\mathrm{s}} \eta_{\mathrm{c}} |\mathbf{H}_{\mathrm{t}}(\mathbf{r})|^2 \, ds \right] \\ &= \frac{1}{2\sigma\delta_{\mathrm{s}}} \oiint_{s} |\mathbf{H}_{\mathrm{t}}(\mathbf{r})|^2 \, ds \end{aligned} \tag{6.115}$$

Equation (6.115) is valid for any cavity of arbitrary geometry. Of course, this expression is proportional to the strength of the fields established inside the cavity. To compare the performance of different cavities or different modes within a specific cavity, a different metric must be used such that it is independent of field strength. One such metric is the quality factor as defined in Eq. (3.149), which is a unitless quantity given by

$$\breve{Q} = \omega \, \frac{\text{maximum of stored energy}}{\text{average dissipated power}} \, . \tag{6.116}$$

Using Eqs. (6.113) and (6.115) in (6.116), the cavity quality factor due to surface loss is given by

$$\breve{Q}_{\mathrm{s}} = \frac{\omega\varepsilon\sigma\delta_{\mathrm{s}} \iiint_{V} |E|^2 \, dv}{\oiint_{\mathrm{s}} |H_{\mathrm{t}}|^2 \, ds} \, . \tag{6.117}$$

This expression for the quality factor assumes that the dielectric filling the cavity is lossless. To consider the effect of dielectric loss as well, we note that the average power loss due to the dielectric loss tangent can be computed from

$$P_{\mathrm{L}}^{\mathrm{d}} = \frac{1}{2} \, \omega\varepsilon'' \iiint_{V} |E|^2 \, dv \, . \tag{6.118}$$

Using Eq. (6.118) in Eq. (6.116), the quality factor due to dielectric loss can easily be computed and is given by

$$\breve{Q}_{\mathrm{d}} = \frac{\varepsilon'}{\varepsilon''} \,. \tag{6.119}$$

The total quality factor using Eq. (6.116) can be written as

$$\breve{Q} = \frac{\omega W}{P_{\mathrm{L}}^{\mathrm{s}} + P_{\mathrm{L}}^{\mathrm{d}}} \,,$$

and thus it can easily be shown that

$$\frac{1}{\breve{Q}} = \frac{1}{\breve{Q}_{\mathrm{s}}} + \frac{1}{\breve{Q}_{\mathrm{d}}} \,. \tag{6.120}$$

According to Eq. (6.94), the eigenvalues of the wave equation subject to Dirichlet's or Neumann's boundary conditions are real and positive quantities. These eigenvalues are a function of the cavity dimensions only. Thus it is interesting to note that for Eq. (6.94) to be true when the cavity is filled with lossy materials, the resonant frequency ($\omega_{mn\ell}$) must be complex so that

$$(\omega_{mn\ell})^2 \mu\varepsilon = C_{mn\ell} \,, \tag{6.121}$$

where $C_{mn\ell}$ is a real and positive number. This establishes a relation between the real and imaginary parts of the resonant frequency to those of the material index of refraction. Representing the complex resonant frequency $\omega_{mn\ell} = \omega'_{mn\ell} - i\omega''_{mn\ell}$ with a negative imaginary part ($\omega''_{mn\ell} > 0$) and the refraction index of the material by $n = \sqrt{\mu\varepsilon} = n' + in''$, from Eq. (6.121) we have

$$(\omega'_{mn\ell} - i\omega''_{mn\ell})^2 (n' + in'')^2 = C_{mn\ell} \,. \tag{6.122}$$

Expanding Eq. (6.122) and setting the imaginary part of the left-hand side equal to zero, we get the following relations:

$$\frac{\omega'^2_{mn\ell} - \omega''^2_{mn\ell}}{\omega'_{mn\ell}\omega''_{mn\ell}} = \frac{n'^2 - n''^2}{n'n''} \,. \tag{6.123}$$

In practice, resonators are filled with low-loss materials; that is, $n'' \ll n'$, which results in a condition where $\omega''_{mn\ell} \ll \omega'_{mn\ell}$. Under this assumption, Eq. (6.123) simplifies to

$$\frac{\omega'_{mn\ell}}{\omega''_{mn\ell}} \approx \frac{n'}{n''} \,. \tag{6.124}$$

For a nonmagnetic material, $\mu = \mu_0$, and with $\varepsilon'' \ll \varepsilon'$, it can be shown that

$$\frac{n'}{n''} \approx \frac{\sqrt{\varepsilon'}}{\varepsilon''/(2\sqrt{\varepsilon'})} = \frac{2\varepsilon'}{\varepsilon''} \,, \tag{6.125}$$

where we use the first-order Taylor expansion of

$$\sqrt{\varepsilon' + i\varepsilon''} \approx \sqrt{\varepsilon'} + i\,\frac{\varepsilon''}{2\sqrt{\varepsilon'}}\,.$$

Recognizing $\varepsilon'/\varepsilon'' = \breve{Q}_{\rm d}$ as the dielectric quality factor, then

$$\breve{Q}_{\rm d}^{mn\ell} = \frac{\omega'_{mn\ell}}{2\omega''_{mn\ell}}\,. \tag{6.126}$$

This result is true for an arbitrarily shaped cavity filled with slightly lossy material.

Due to the presence of losses in the cavity, the stored energy in the cavity decays as a function of time once excitations are removed. Representing the field's ***relaxation time*** by $\tau$ or ***damping factor*** by $\gamma = \frac{1}{\tau}$, the stored energy as a function of time may be represented as

$$W(t) = W_0 e^{-2t/\tau} = W_0 e^{-2\gamma t}\,.$$

Note that the rate of decrease of stored energy must equal the power loss. That is,

$$-\frac{dW}{dt} = 2\gamma W_0 e^{-2\gamma t} = 2\gamma W = P_{\rm L}\,.$$

In other words,

$$\gamma = \frac{P_{\rm L}}{2W} = \frac{\omega}{2}\,\frac{P_{\rm L}}{\omega W} = \frac{\omega}{2\breve{Q}} \tag{6.127}$$

and

$$\tau = \frac{2\breve{Q}}{\omega}\,. \tag{6.128}$$

## Example 6-3: Quality Factor of a Rectangular Cavity

Consider the rectangular cavity shown in Fig. 6-18 with $a = 2.28$ cm, $b = 1.14$ cm, and $c = 3$ cm. Suppose this cavity is supporting the $\rm TE_{101}$ mode. Find the resonant frequency and the quality factor for this cavity, assuming that the walls are made from copper with conductivity $\sigma = 5.8 \times 10^7$ S/m. Also determine the damping factor for this mode.

**Solution:** The field expression can be found from Eq. (6.108) for $m = 1,\ n = 0$, and $\ell = 1$:

$$E_y(x,y,z) = iH_0\omega\mu\,\frac{\pi}{a}\,\sin\left(\frac{\pi}{a}x\right)\,\sin\left(\frac{\pi}{c}\,z\right)\,, \tag{6.129a}$$

$$H_x(x,y,z) = -H_0\frac{\pi^2}{ac}\,\sin\left(\frac{\pi}{a}x\right)\,\cos\left(\frac{\pi}{c}\,z\right)\,, \tag{6.129b}$$

and

$$H_z(x,y,z) = H_0 \left(\frac{\pi}{a}\right)^2 \cos\left(\frac{\pi}{a}x\right) \sin\left(\frac{\pi}{c}z\right) . \tag{6.129c}$$

Note that the electric field and magnetic field are 90° out of phase at every point inside the cavity. This indicates that when the electric field is at its maximum, the magnetic field is zero and vice versa. The time-average stored energy is computed from

$$\begin{aligned} W = 2W_e &= \frac{\varepsilon}{2} \iiint_V |E|^2 \, dv \\ &= \frac{\varepsilon}{2} \int_0^a \int_0^b \int_0^c E_y^2 \, dx \, dy \, dz \\ &= \left(\frac{\varepsilon}{2}\right) |H_0|^2 \omega^2 \mu^2 \left(\frac{\pi}{a}\right)^2 \frac{abc}{4} = \frac{k^2 \mu \pi^2 bc}{8a} |H_0|^2 . \end{aligned} \tag{6.130}$$

To calculate the power loss on the six walls of the cavity, Eq. (6.115) is used:

$$\begin{aligned} P_L = \frac{|H_0|^2}{2\sigma\delta_s} \Bigg\{ & 2 \int_0^a \int_0^c \left[ \frac{\pi^4}{(ac)^2} \sin^2\left(\frac{\pi}{a}x\right) \cos^2\left(\frac{\pi}{c}z\right) + \left(\frac{\pi}{a}\right)^4 \cos^2\left(\frac{\pi}{a}x\right) \sin^2\left(\frac{\pi}{a}x\right) \right] dx \, dz \\ & + 2 \int_0^b \int_0^c \left(\frac{\pi}{a}\right)^4 \sin^2\left(\frac{\pi}{a}z\right) dy \, dz + 2 \int_0^a \int_0^b \frac{\pi^4}{(ac)^2} \sin^2\left(\frac{\pi}{a}x\right) dx \, dy \Bigg\} , \end{aligned}$$

which can easily be integrated to give

$$P_L = \frac{\pi^4}{\sigma\delta_s} \frac{a^3c + c^3a + 2c^3b + 2a^3b}{4a^4c^2} |H_0|^2 . \tag{6.131}$$

Hence, using Eq. (6.117), the quality factor is given by

$$\breve{Q}_s = \frac{(\sigma\delta_s) k_0^3 \eta_0 a^3 b c^3}{2\pi^2 (a^3c + c^3a + 2c^3b + 2a^3b)} . \tag{6.132}$$

The resonant frequency is given by

$$k_0^2 = \left(\frac{\pi}{a}\right)^2 + \left(\frac{\pi}{c}\right)^2 ,$$

or

$$f_0^{\mathrm{TE}_{101}} = \frac{1}{2\sqrt{\mu_0\varepsilon_0}} \sqrt{\frac{1}{a^2} + \frac{1}{c^2}} = 8.263 \text{ GHz}.$$

The quality factor is calculated from Eq. (6.132), which requires calculation of the skin depth:

$$\delta_s = \frac{1}{\sqrt{\pi f \mu \sigma}} = 0.727 \times 10^{-6} \text{ m}.$$

This provides surface conductance $\sigma\delta_s = 42.16$, and finally

$$\breve{Q}_s = 8200.$$

The relaxation time, which is inversely related to the damping factor, is obtained from

$$\tau = \frac{2Q}{\omega} = 316.04 \text{ nsec.}$$

This indicates that after 316.04 nsec an established field in the cavity reaches $e^{-1}$ of its original value. This corresponds to 2611 cycles of oscillation. The damping factor is given by

$$\gamma = \frac{1}{\tau} = 3.16 \times 10^6 \text{ Np/s.}$$

**Example 6-4: Time-Average Stored Electric and Magnetic Energy in a Rectangular Cavity**

Find the expressions for the time-average stored electric and magnetic energy for TM modes in a rectangular cavity with dimensions $a, b, c$, and show that they are equal.

**Solution:** The stored electric energy in the cavity can be calculated from

$$\begin{aligned} w_e &= \frac{1}{4}\varepsilon \int_0^a \int_0^b \int_0^c |\mathbf{E}(x,y,z)|^2 \, dx\, dy\, dz \\ &= \frac{1}{4}\varepsilon \int_0^a \int_0^b \int_0^c \left(|E_x(x,y,z)|^2 + |E_y(x,y,z)|^2 + |E_z(x,y,z)|^2\right) dx\, dy\, dz \, . \end{aligned}$$

Using the field expression given by Eq. (6.109), and noting that the integrals of square of sine or cosine functions over one period are equal to one-half of the period, it can be easily shown that

$$w_e = \frac{\varepsilon}{4} \cdot \frac{abc}{8} \left\{ \left(\frac{\ell\pi}{c}\right)^2 \left(\frac{m\pi}{a}\right)^2 + \left(\frac{\ell\pi}{c}\right)^2 \left(\frac{n\pi}{b}\right)^2 + \left[\left(\frac{m\pi}{a}\right)^2 + \left(\frac{n\pi}{b}\right)^2\right]^2 \right\} |E_0|^2 \, .$$

Making use of Eq. (6.106), this expression can be simplified to

$$\begin{aligned} w_e &= \frac{\varepsilon abc}{32} \left[\left(\frac{m\pi}{a}\right)^2 + \left(\frac{n\pi}{b}\right)^2\right] k^2 |E_0|^2 \\ &= \frac{\varepsilon V}{32} k_{mn}^2 k^2 |E_0|^2 \, , \end{aligned} \tag{6.133}$$

where $V = abc$ is the cavity volume,

$$k_{mn}^2 = \left[\left(\frac{m\pi}{a}\right)^2 + \left(\frac{n\pi}{b}\right)^2\right] \, ,$$

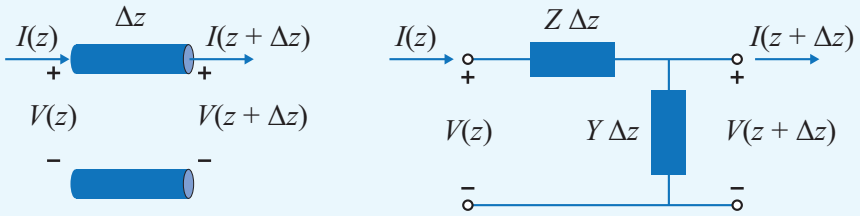


(a) Transmission-line segment (b) Equivalent circuit model

**Figure 6-19:** A differential segment of (a) a transmission line supporting a TEM wave and (b) its equivalent circuit.

and

$$k^2 = \omega^2 \mu \varepsilon = \left[ \left( \frac{m\pi}{a} \right)^2 + \left( \frac{n\pi}{b} \right)^2 + \left( \frac{\ell\pi}{c} \right)^2 \right] .$$

Similarly, the stored magnetic energy can be calculated from

$$\begin{aligned} w_{\mathrm{m}} &= \frac{1}{4} \mu \int_0^a \int_0^b \int_0^c |\mathbf{H}(x,y,z)|^2 \, dx \, dy \, dz \\ &= \frac{1}{4} \mu \int_0^a \int_0^b \int_0^c \left( |H_x(x,y,z)|^2 + |H_y(x,y,z)|^2 \right) \, dx \, dy \, dz. \end{aligned}$$

Inserting the magnetic field expressions from Eqs. (6.107d) and (6.107e),

$$\begin{aligned} w_{\mathrm{m}} &= \frac{\mu abc}{32} \omega^2 \varepsilon^2 \left[ \left( \frac{m\pi}{a} \right)^2 + \left( \frac{n\pi}{b} \right)^2 \right] |E_0|^2 \\ &= \frac{\varepsilon V}{32} k_{mn}^2 k^2 |E_0|^2 . \end{aligned} \tag{6.134}$$

which has the same expression we computed for $w_{\mathrm{e}}$.

## 6-6 Transmission-Line Circuit Model for Waveguides

### 6-6.1 Transmission-Line TEM Mode

In general, circuit models are an easy way to understand the behavior of an electrical system. Strictly speaking, circuit models are applicable for lumped elements and guiding structures that support transverse electromagnetic waves. For example, for a transmission line, such as a coaxial line, supporting a TEM wave, a circuit model for a short section of the line having a differential length $\Delta z$ is represented by a series impedance per unit length denoted by $Z$ and a shunt admittance for unit length represented by $Y$, as shown in Fig. 6-19.

The governing equations for the voltage and current on the line can easily be derived from Kirchhoff's voltage and current laws. They are given by

$$\frac{dV(z)}{dz} = -Z\,I(z) \tag{6.135a}$$

and

$$\frac{dI(z)}{dz} = -Y\,V(z)\,. \tag{6.135b}$$

The voltage and current satisfy one-dimensional wave equations given by

$$\frac{d^2V(z)}{dz} - YZ\,V(z) = 0 \tag{6.136a}$$

and

$$\frac{d^2I(z)}{dz} - YZ\,I(z) = 0\,. \tag{6.136b}$$

Here, the complex propagation constant is defined by

$$\gamma = \sqrt{YZ}\,, \tag{6.137}$$

and the characteristic impedance of the line is defined by

$$Z_0 = \sqrt{\frac{Z}{Y}}\,. \tag{6.138}$$

The transmission line's series impedance per unit length $Z$ is usually represented by an inductance per unit length $L$ in series with a resistance per unit length $R$, and therefore

$$Z = R - i\omega L\,, \tag{6.139a}$$

and the shunt admittance per unit length is represented by a shunt capacitance per unit length $C$ and conductance per unit length $G$:

$$Y = G - i\omega C\,. \tag{6.139b}$$

### 6-6.2 Waveguide TM Modes

Recall that we are using the time convention of $e^{-i\omega t}$. As was shown in the previous section, hollow conductors of infinite length having a constant cross section, namely waveguides, cannot support TEM waves, and the mode of propagation is either TM and/or TE waves. Considering a TM mode of propagation, according to Eqs. (5.102a) and (5.102b) the transverse electric and magnetic fields are given by

$$\mathbf{E}_{\rm t} = \frac{\partial}{\partial z}\,\nabla_{\rm t}\left[\psi(x,y)\,e^{i\beta z}\right] \tag{6.140a}$$

and

$$\mathbf{H}_t = -i\omega\varepsilon\,\nabla_t\left[\psi(x,y)\,e^{i\beta z}\right]\times\hat{\mathbf{z}}\,. \tag{6.140b}$$

It is obvious from Eq. (6.140a) that $\nabla_t\times\mathbf{E}_t = 0$, and therefore in the transverse plane a voltage $V$ can be defined so that

$$\mathbf{E}_t = -\nabla V\,. \tag{6.141}$$

Comparing Eq. (6.141) with Eq. (6.140a) leads to

$$V = -\frac{\partial}{\partial z}\left[\psi(x,y)\,e^{i\beta z}\right]. \tag{6.142}$$

Also, the longitudinal component of the electric field, according to Eq. (5.102a), is given by

$$E_z = k_c^2\,\psi(x,y)\,e^{i\beta z}\,,$$

which, together with Eq. (6.142), can be used to show that

$$\frac{\partial E_z}{\partial z} = -k_c^2 V\,. \tag{6.143}$$

Also, noting that $-i\omega\varepsilon E_z$ represents a longitudinal displacement current density and the fact that $1/k_c^2$ has a unit of $\text{m}^2$, the notion of a longitudinal current along the length of the waveguide can be defined as

$$I = \frac{-i\omega\varepsilon}{k_c^2}\,E_z\,. \tag{6.144}$$

Using Eq. (6.144) in Eq. (6.143), it is now obvious that

$$\frac{\partial I}{\partial z} = i\omega\varepsilon V\,. \tag{6.145}$$

From Eq. (6.142), the rate of change of voltage along the length of the waveguide can be obtained:

$$\frac{\partial V}{\partial z} = \beta^2\,\psi(x,y)\,e^{i\beta z} = \frac{\beta^2}{k_c^2}\,E_z\,. \tag{6.146}$$

Using Eq. (6.144) in Eq. (6.146),

$$\frac{\partial V}{\partial z} = \frac{\beta^2}{-i\omega\varepsilon}\,I = \frac{k^2-k_c^2}{-i\omega\varepsilon}\,I = \left(i\omega\mu + \frac{k_c^2}{i\omega\varepsilon}\right)I\,. \tag{6.147}$$

Equations (6.147) and (6.145) are analogous to Eqs. (6.135a) and (6.135b) for the standard model for a transmission line with

$$Z_{\text{TM}} = \frac{\beta^2}{i\omega\varepsilon} = -i\omega\mu - \frac{k_c^2}{i\omega\varepsilon} \tag{6.148a}$$

and

$$Y_{\text{TM}} = -i\omega\varepsilon\,. \tag{6.148b}$$

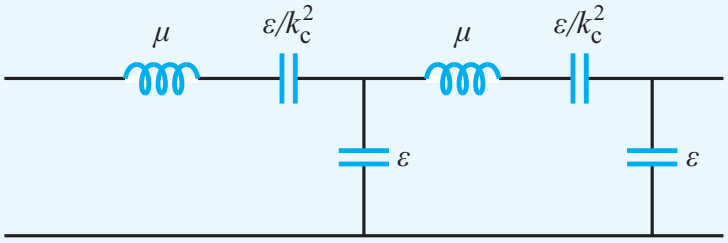


**Figure 6-20:** The transmission-line equivalent circuit model of a waveguide supporting a TM mode.

The transmission-line equivalent circuit model for a TM mode in a waveguide is shown in Fig. 6-20. The complex propagation constant of this waveguide transmission-line equivalent is given by

$$\gamma_{\mathrm{TM}} = \sqrt{Z_{\mathrm{TM}} Y_{\mathrm{TM}}} = \sqrt{-\beta^2} = i\beta \ , \tag{6.149}$$

as expected, and the characteristic impedance of the TM wave is given by

$$Z_0^{\mathrm{TM}} = \sqrt{\frac{Z_{\mathrm{TM}}}{Y_{\mathrm{TM}}}} = \frac{\beta}{\omega\varepsilon} \ , \tag{6.150}$$

which is in agreement with Eq. (5.103). It is clear that this transmission line is a high-pass structure.

### 6-6.3 Waveguide TE Modes

The expressions given in the preceding subsection apply to TM waves. For TE waves, we can apply the duality relations. Basically, by changing $Z_{\mathrm{TM}}$ to $Y_{\mathrm{TE}}$ and $Y_{\mathrm{TM}}$ to $Z_{\mathrm{TE}}$, as well as $\varepsilon$ to $\mu$ and $\mu$ to $\varepsilon$, the following expressions are obtained for the elements of the equivalent circuit for TE waves:

$$Z_{\mathrm{TE}} = -i\omega\mu \tag{6.151a}$$

and

$$Y_{\mathrm{TE}} = -i\omega\varepsilon - \frac{k_{\mathrm{c}}^2}{i\omega\mu} \ . \tag{6.151b}$$

The corresponding expressions for the complex propagation constant $\gamma_{\mathrm{TE}}$ and characteristic impedance $Z_0^{\mathrm{TE}}$ are given by

$$\gamma_{\mathrm{TE}} = i\beta \tag{6.152a}$$

and

$$Z_0^{\mathrm{TE}} = \frac{\beta}{\omega\mu} \ . \tag{6.152b}$$

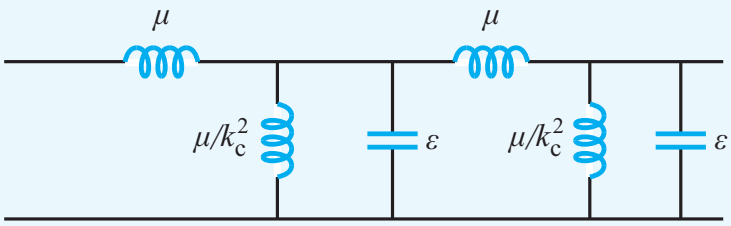


**Figure 6-21:** The transmission-line equivalent circuit model of a waveguide supporting a TE mode.

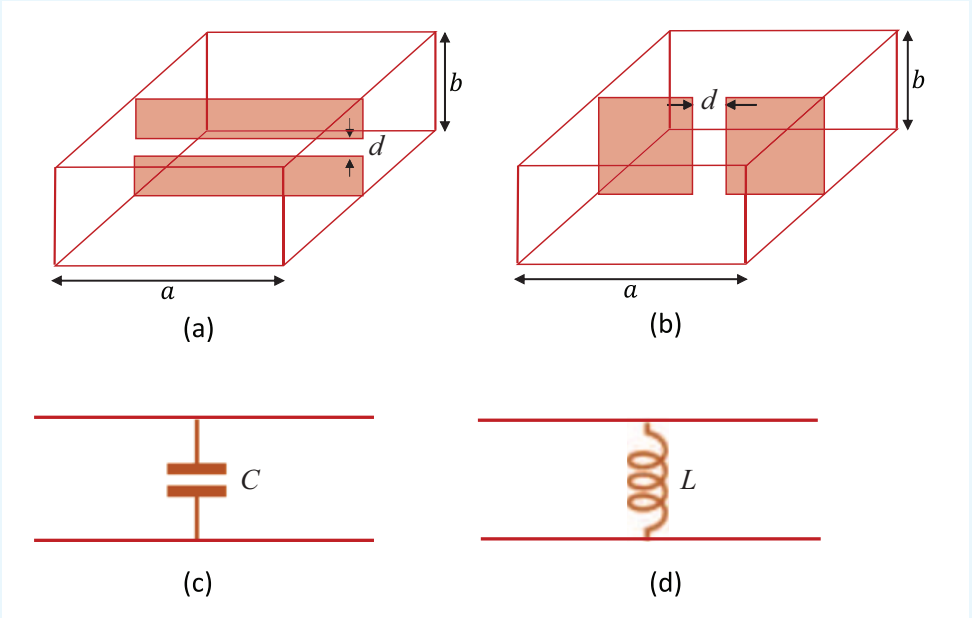


**Figure 6-22:** Metallic septa placed in a rectangular waveguide in a symmetrical manner with a gap between them. The horizontal gap acts like a lumped shunt capacitor, and the vertical gap behaves like a lumped shunt inductor.

Figure 6-21 shows the equivalent circuit model for a waveguide supporting a TE mode.

As will be shown in the following sections, there are discrete modes of propagation for both the TE and TM modes. That is, for a fixed frequency above the dominant cutoff frequency, there are specific discrete values for the propagation constant and the cutoff frequency. Hence the transmission line models presented here are mode-dependent.

The concept of equivalent circuit for waveguides finds application in situations where certain waveguide local discontinuities are present in the cross section of the waveguide. Figure 6-22 shows two such discontinuities where metallic septa with edges perpendicular

and parallel to the electric field of a single-mode $TE_{10}$ waveguide are placed in the waveguide. The metallic septa perpendicular to the electric field shown in Fig. 6-22(a) represent a shunt capacitive lumped element, whereas the septa in Fig. 6-22(b) behave as a shunt inductive element. Figures 6-22(c) and (d) show the transmission-line equivalent circuit for each case. The capacitance and inductance values of the shown septa must be obtained numerically using an integral equation or a mode-matching method. For example, for a symmetrically positioned capacitive septum with gap $d$, the susceptance is given by[†]

$$B = \omega C = Y_0 \frac{4b}{\lambda_g} \left\{ \ln\left[\csc\left(\frac{\pi d}{2b}\right)\right] + \frac{Q_2 \cos^4\left(\frac{\pi d}{2b}\right)}{1 + Q_2 \sin^4\left(\frac{\pi d}{2b}\right)} + \frac{1}{16}\left(\frac{b}{\lambda_g}\right)^2 \left[1 - 3\sin^2\left(\frac{\pi d}{2b}\right)\right] \cos^4\left(\frac{\pi d}{2b}\right) \right\} . \tag{6.153}$$

Also, for a symmetric inductive septum with gap $d$, the reactance is given by[‡]

$$X = \omega L = Z_0 \frac{a}{\lambda_g} \tan^2\left(\frac{\pi d}{2a}\right) \left[1 + \frac{3}{4}\left(\frac{1}{\sqrt{1-(2a/3\lambda)^2}} - 1\right) \sin^2\frac{\pi d}{a} + 2\left(\frac{a}{\lambda}\right)^2 \left(1 - \frac{4}{\pi}\frac{E(\alpha) - \beta^2 F(\alpha)}{\alpha^2} \times \frac{E(\beta) - \alpha^2 F(\beta)}{\beta^2} - \frac{1}{2}\sin^2\frac{\pi d}{a}\right)\right] . \tag{6.154}$$

In Eq. (6.153),

$$Q_2 = \frac{1}{\sqrt{1-(b/\lambda_g)^2}} - 1 ,$$

and in Eq. (6.154),

$$\alpha = \sin\left(\frac{\pi d}{2a}\right) , \qquad \beta = \cos\left(\frac{\pi d}{2a}\right) .$$

It is noted that the expressions given by Eqs. (6.153) and (6.154) are approximate; for more accurate results a full-wave numerical method must be used. Also, in Eq. (6.153) $F(\alpha)$, $E(\alpha)$ are complete elliptic integrals of the first and second kind, respectively; that is,

$$F(\alpha) = \int_0^{\pi/2} \frac{d\phi}{\sqrt{1-\alpha^2\sin^2\phi}}$$

and

$$E(\alpha) = \int_0^{\pi/2} \sqrt{1-\alpha^2\sin^2\phi}\, d\phi .$$

[†]N. Marcuvitz, *Waveguide Handbook*, Peter Peregrinus Ltd., London, U.K., 1986.
[‡]Ibid.

## 6-7 Other Modal Solutions for Rectangular Waveguides

The transverse electric and magnetic field representations with respect to the direction of propagation lend themselves to all waveguides and any arbitrary cross section. In certain waveguide problems, it is not possible to express the modes in terms of only TE or TM modes. For these problems, hybrid TE and TM modes have to be considered to arrive at appropriate solutions. Alternatively, for rectangular waveguides it is possible to generate modes from a single component of the Hertz vector potential that is perpendicular to the direction of propagation. As before, we assume the direction of propagation is along the $z$-axis and the cross section of the waveguide is invariant with respect to $z$. In this section we seek field solutions generated from

$$\boldsymbol{\Pi}(x,y,z) = \psi(x,y)\, e^{i\beta z}\, \hat{\mathbf{x}} \,. \tag{6.155}$$

A similar procedure that led to Eq. (5.101) can be used to show that $\psi(x,y)$ must satisfy the scalar 2-D wave equation

$$\nabla_{\mathrm{t}}^2 \psi(x,y) + k_{\mathrm{c}}^2 \psi(x,y) = 0 \,, \tag{6.156}$$

where $k_{\mathrm{c}}^2 = k^2 - \beta^2$.

### TM Fields

Using Eqs. (5.94a) and (5.94b), it can be shown that

$$E_x = \left( \frac{\partial^2 \psi}{\partial x^2} + k^2 \psi \right) e^{i\beta z} \,, \tag{6.157a}$$

$$E_y = \frac{\partial^2 \psi}{\partial x\, \partial y}\, e^{i\beta z} \,, \tag{6.157b}$$

$$E_z = i\beta\, \frac{\partial \psi}{\partial x}\, e^{i\beta z} \,, \tag{6.157c}$$

and

$$H_x = 0 \,, \tag{6.158a}$$

$$H_y = \omega\varepsilon\beta\psi e^{i\beta z} \,, \tag{6.158b}$$

$$H_z = i\omega\varepsilon\, \frac{\partial \psi}{\partial y}\, e^{i\beta z} \,. \tag{6.158c}$$

As can be seen from Eq. (6.158), this choice for Hertz vector potential generates transverse magnetic with respect to $x$ fields ($\mathrm{TM}_x$). For $\mathrm{TM}_x$ modes, the boundary condition mandates $E_z$ to vanish on the waveguide walls. This is accomplished if

$$\frac{\partial \psi^{\mathrm{TM}_x}(x,y)}{\partial x} = 0 \qquad \text{at } x = 0, a \text{ and } y = 0, b \,.$$

Hence

$$\psi^{\mathrm{TM}_x}(x,y) = \cos\left(\frac{m\pi}{a}\, x\right)\, \sin\left(\frac{n\pi}{b}\, y\right) \,. \tag{6.159}$$

The integer indices are $m = 0, 1, 2, \ldots$ and $n = 1, 2, 3, \ldots$ Using Eqs. (6.157) and (6.158), the field expressions for $\mathrm{TM}_x$ are given by

$$E_x = \left[k^2 - \left(\frac{m\pi}{a}\right)^2\right] \cos\left(\frac{m\pi}{a}\,x\right) \sin\left(\frac{n\pi}{b}\,y\right) e^{i\beta z}, \tag{6.160a}$$

$$E_y = -\left(\frac{m\pi}{a}\right)\left(\frac{n\pi}{b}\right) \sin\left(\frac{m\pi}{a}\,x\right) \cos\left(\frac{n\pi}{b}\,y\right) e^{i\beta z}\,, \tag{6.160b}$$

$$E_z = -i\beta\left(\frac{m\pi}{a}\right) \sin\left(\frac{m\pi}{a}\,x\right) \sin\left(\frac{n\pi}{b}\,y\right) e^{i\beta z}\,, \tag{6.160c}$$

and

$$H_x = 0\,, \tag{6.161a}$$

$$H_y = \omega\varepsilon\beta \cos\left(\frac{m\pi}{a}\,x\right) \sin\left(\frac{n\pi}{b}\,y\right) e^{i\beta z}\,, \tag{6.161b}$$

$$H_z = i\omega\varepsilon\left(\frac{n\pi}{b}\right) \cos\left(\frac{m\pi}{a}\,x\right) \cos\left(\frac{n\pi}{b}\,y\right) e^{i\beta z}\,. \tag{6.161c}$$

## TE Fields

To generate $\mathrm{TE}_x$ fields, a magnetic Hertz vector potential that has only one component along $x$ is chosen. Noting the duality relations of the fields, the $\mathrm{TE}_x$ fields can be evaluated from

$$E_x = 0\,, \tag{6.162a}$$

$$E_y = -\omega\mu\beta\,\psi_{\mathrm{m}} e^{i\beta z}\,, \tag{6.162b}$$

$$E_z = -i\omega\mu\,\frac{\partial\psi_{\mathrm{m}}}{\partial y}\,e^{i\beta z}\,, \tag{6.162c}$$

and

$$H_x = \left(\frac{\partial^2\psi_{\mathrm{m}}}{\partial x^2} + k^2\psi_{\mathrm{m}}\right) e^{i\beta z}\,, \tag{6.163a}$$

$$H_y = \frac{\partial^2\psi_{\mathrm{m}}}{\partial x\,\partial y}\,e^{i\beta z}\,, \tag{6.163b}$$

$$H_z = i\beta\,\frac{\partial\psi_{\mathrm{m}}}{\partial x}\,e^{i\beta z}\,. \tag{6.163c}$$

For $\mathrm{TE}_x$ modes the $E_z = 0$ boundary condition mandates that

$$\frac{\partial\psi^{\mathrm{TE}_x}}{\partial y} = 0 \qquad \text{at } x = 0, a \text{ and } y = 0, b,$$

and therefore

$$\psi^{\mathrm{TE}_x}(x,y) = \sin\left(\frac{m\pi}{a}x\right)\ \cos\left(\frac{n\pi}{b}y\right)\ . \tag{6.164}$$

The indices are $m = 1,2,3,\ldots$ and $n = 0,1,2,\ldots$ Also, the field expressions for $\mathrm{TE}_x$ are given by

$$E_x = 0\ , \tag{6.165a}$$

$$E_y = -\omega\mu\beta\ \sin\left(\frac{m\pi}{a}x\right)\ \cos\left(\frac{n\pi}{b}y\right)\ e^{i\beta z}\ , \tag{6.165b}$$

$$E_z = i\omega\mu\left(\frac{n\pi}{b}\right)\ \sin\left(\frac{m\pi}{a}x\right)\ \sin\left(\frac{n\pi}{b}y\right)\ e^{i\beta z}\ , \tag{6.165c}$$

and

$$H_x = \left[k^2 - \left(\frac{m\pi}{a}\right)^2\right]\ \sin\left(\frac{m\pi}{a}x\right)\ \cos\left(\frac{n\pi}{b}y\right)\ e^{i\beta z}\ , \tag{6.166a}$$

$$H_y = -\left(\frac{m\pi}{a}\right)\left(\frac{n\pi}{b}\right)\ \cos\left(\frac{m\pi}{a}x\right)\ \sin\left(\frac{n\pi}{b}y\right)\ e^{i\beta z}\ , \tag{6.166b}$$

$$H_z = i\beta\left(\frac{m\pi}{a}\right)\ \cos\left(\frac{m\pi}{a}x\right)\ \cos\left(\frac{n\pi}{b}y\right)\ e^{i\beta z}\ . \tag{6.166c}$$

Note that both $\mathrm{TM}_x$ and $\mathrm{TE}_x$ have longitudinal field components along the direction of propagation. As a result, these field expressions may be appropriate for problems for which $\mathrm{TE}_z$ and $\mathrm{TM}_z$ field expansions do not yield satisfactory solutions.

## Example 6-5: Propagation Constant for a Partially Filled Waveguide

Consider a rectangular waveguide filled with two different dielectric materials with a planar interface along the direction of propagation, as shown in Fig. 6-23. Find the propagation constant for different possible modes.

**Solution:** Field solutions based on $\mathrm{TM}_z$ or $\mathrm{TE}_z$ modes do not yield a complete solution. For this problem we examine the $\mathrm{TM}_x$ and $\mathrm{TE}_x$ field solutions. We also note that the phase-matching condition at the interface between media 1 and 2 (at $x = c$) requires the same propagation constant $\beta$ in both regions. For TM to $x$, the solutions for the 2-D scalar potential in regions 1 and 2 take the following form:

$$\psi_1(x,y) = A\cos(k_{x1}x)\ \sin\left(\frac{n\pi}{b}y\right) \tag{6.167a}$$

and

$$\psi_2(x,y) = B\cos[k_{x2}(x-a)]\ \sin\left(\frac{n\pi}{b}y\right)\ , \tag{6.167b}$$

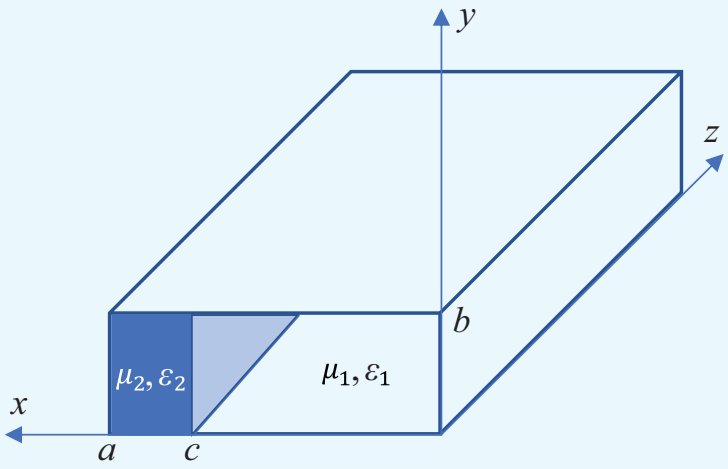


**Figure 6-23:** A partially filled rectangular waveguide.

which satisfy the boundary conditions

$$\left.\frac{\partial \psi_1}{\partial x}\right|_{x=0} = 0$$

and

$$\left.\frac{\partial \psi_2}{\partial x}\right|_{x=0} = 0 \, .$$

The goal is to find $k_{x1}$ and $k_{x2}$ by enforcing the continuity of the tangential electric and magnetic fields at the interface between the two dielectric media ($x = c$). From the dispersion relations we have the following equations:

$$k_{x1}^2 + \left(\frac{n\pi}{b}\right)^2 + \beta^2 = k_1^2 = \omega^2 \mu_1 \varepsilon_1 \tag{6.168a}$$

and

$$k_{x2}^2 + \left(\frac{n\pi}{b}\right)^2 + \beta^2 = k_2^2 = \omega^2 \mu_2 \varepsilon_2 \, . \tag{6.168b}$$

This provides the following equation for $k_{x1}$ and $k_{x2}$:

$$k_{x2}^2 - k_{x1}^2 = \omega^2 (\mu_2 \varepsilon_2 - \mu_1 \varepsilon_1) \, . \tag{6.169}$$

Using Eq. (6.157), the fields $E_z(c,y)$ calculated in each of the two regions are given by

$$E_{z1}(c,y) = -i\beta k_{x1} A \sin(k_{x1} c) \sin\left(\frac{n\pi}{b}\, y\right) e^{i\beta z} \tag{6.170a}$$

and

$$E_{z2}(c,y) = -i\beta k_{x2} B \sin[k_{x2}(c-a)] \sin\left(\frac{n\pi}{b}\, y\right)\, e^{i\beta z}\,. \tag{6.170b}$$

Also, using Eq. (6.158), the tangential magnetic fields in each region at the interface are given by

$$H_{z1}(c,y) = i\omega\varepsilon_1 \left(\frac{n\pi}{b}\right) A\cos(k_{x1}c)\, \sin\left(\frac{n\pi}{b}\, y\right)\, e^{i\beta z} \tag{6.171a}$$

and

$$H_{z2}(c,y) = i\omega\varepsilon_2 \left(\frac{n\pi}{b}\right) B\cos[k_{x2}(c-a)]\, \cos\left(\frac{n\pi}{b}\, y\right)\, e^{i\beta z}\,. \tag{6.171b}$$

From Eqs. (6.170a) and (6.170b), we get

$$k_{x1} A \sin(k_{x1}c) = k_{x2} B \sin[k_{x2}(c-a)]\,, \tag{6.172}$$

and from Eqs. (6.171a) and (6.171b) we get another equation for the unknowns:

$$\varepsilon_1 A\cos(k_{x1}c) = \varepsilon_2 B\cos[k_{x2}(c-a)]\,. \tag{6.173}$$

Taking the ratio of Eqs. (6.172) and (6.173), another equation for $k_{x1}$ and $k_{x2}$ is obtained:

$$\frac{k_{x1}}{\varepsilon_1}\, \tan(k_{x1}c) = \frac{k_{x2}}{\varepsilon_2}\, \tan[k_{x2}(c-a)]\,. \tag{6.174}$$

To find $k_{x1}$ and $k_{x2}$, Eqs. (6.174) and (6.169) must be solved simultaneously. An analytical solution for these equations does not exist and they have to be solved numerically.

A similar procedure can be followed for TE to $x$ modes. Equations (6.162) and (6.163) can be used to find the tangential electric and magnetic fields ($E_z$ and $H_z$) at $x = c$. Using these two equations, the following characteristic equation for $\text{TE}_x$ can be obtained:

$$\frac{k_{x1}}{\mu_1}\cot(k_{x1}a) = \frac{k_{x2}}{\mu_2}\cot[k_{x2}(c-a)]\,. \tag{6.175}$$

Now Eq. (6.175) must be solved together with Eq. (6.169) to find $k_{x1}$ and $k_{x2}$. Then $\beta$ can be found from Eq. (6.168).

## 6-8 Modal Expansion of Field Quantities

In the previous section it was shown that in a closed region, the solution to Maxwell's equations can be expressed in terms of discrete modal wave functions that are solutions to the scalar wave equation, subject to the Dirichlet or Neumann boundary conditions. For waveguide problems the 2-D wave equation is given by

$$\nabla_{\text{t}}^2 \psi + k_{\text{c}}^2 \psi = 0\,, \tag{6.176}$$

where as before $k_c^2 = k^2 - \beta^2$ and $\psi$ is a scalar function of two variables in the cross section of the waveguide. For a rectangular waveguide it was shown that the solution of Eq. (6.176) subject to $\psi = 0$ (TM modes) or $\partial\psi/\partial n = 0$ (TE modes) on the surface of the closed boundary provides a discrete set of solutions. Due to the linearity of Maxwell's equations, any linear combination of the modes is also a solution. In this section we demonstrate that for any arbitrary cross section, the discrete modes constitute an orthogonal and complete set. That is, any solution of Maxwell's equations can be expressed in terms of these modes and the total power can be expressed in terms of the superposition of the powers carried by the individual modes.

The scalar wave equation can be viewed as an eigenfunction problem in which $\psi$ is the eigenfunction of the $\nabla_t^2$ operator with $k_c^2$ as its corresponding eigenvalue. As shown before for a rectangular waveguide, the eigenfunctions for TM modes are given by

$$\psi_{mn}(x,y) = \sin\left(\frac{m\pi}{a}\,x\right)\ \sin\left(\frac{n\pi}{b}\,y\right)\ . \tag{6.177}$$

It can easily be shown that

$$\begin{aligned}\langle \psi_{mn}, \psi_{m'n'} \rangle &= \int_0^a \int_0^b \sin\left(\frac{m\pi}{a}\,x\right)\ \sin\left(\frac{n\pi}{b}\,y\right)\ \sin\left(\frac{m'\pi}{a}\,x\right)\ \sin\left(\frac{n'\pi}{b}\,y\right)\ dx\,dy \\ &= \begin{cases} \frac{1}{4}\,ab & m' = m,\ \ n' = n\ , \\ 0 & m' \neq m \text{ or } n' \neq n\ . \end{cases}\end{aligned} \tag{6.178}$$

That is, the eigenfunctions of TM modes are orthogonal in the cross-section domain. Note that the inner product of functions $\psi_{mn}$ and $\psi_{m'n'}$ is defined as the integral of the product of these functions in the cross section of the waveguide. The same is true for the eigenfunctions of TE modes:

$$\psi_{mn}(x,y) = \cos\left(\frac{m\pi}{a}\,x\right)\ \cos\left(\frac{n\pi}{b}\,y\right)\ . \tag{6.179}$$

The set of eigenfunctions given by Eq. (6.177) or Eq. (6.179) is complete. It is interesting to note that the corresponding eigenvalues for both TE and TM modes, given by

$$k_{mn}^2 = \left(\frac{m\pi}{a}\right)^2 + \left(\frac{n\pi}{b}\right)^2\ ,$$

are real and positive quantities.

These properties hold for waveguides with arbitrary cross-section geometries. To show the orthogonality property, let's consider two possible modes $\psi_{mn}$ and $\psi_{m'n'}$. These must satisfy the scalar wave equation (6.176), i.e.,

$$(\nabla_t^2 + k_{mn}^2)\,\psi_{mn} = 0 \tag{6.180a}$$

and

$$(\nabla_t^2 + k_{m'n'}^2)\,\psi_{m'n'} = 0\ . \tag{6.180b}$$

Multiplying Eq. (6.180a) by $\psi_{m'n'}$, Eq. (6.180b) by $\psi_{mn}$, and then subtracting the resulting equations, we have

$$\psi_{m'n'}\,\nabla_t^2\psi_{mn} - \psi_{mn}\,\nabla_t^2\psi_{m'n'} = (k_{m'n'}^2 - k_{mn}^2)\,\psi_{mn}\,\psi_{m'n'}\ . \tag{6.181}$$

According to Green's second identity

$$\iint_S (\psi_{m'n'}\,\nabla_t^2\psi_{mn} - \psi_{mn}\,\nabla_t^2\psi_{m'n'})\,ds = \oint_C \left(\psi_{m'n'}\frac{\partial\psi_{mn}}{\partial n} - \psi_{mn}\frac{\partial\psi_{m'n'}}{\partial n}\right)\,d\ell\ . \tag{6.182}$$

Since either $\psi = 0$ or $\frac{\partial\psi}{\partial n} = 0$ on the surface of the waveguide, the right-hand side of Eq. (6.182) vanishes, and therefore

$$(k_{m'n'}^2 - k_{mn}^2)\iint_S \psi_{mn}\,\psi_{m'n'}\,ds = 0\ . \tag{6.183}$$

In cases when $m' \neq m$ and $n' \neq n$, then $k_{m'n'} \neq k_{mn}$, which mandates the orthogonality condition:

$$\iint_S \psi_{mn}\,\psi_{m'n'}\,ds = 0\ . \tag{6.184}$$

To prove that $\psi_{mn}$ functions form a complete set (for all $m,n$), let us consider an arbitrary continuous function $f(x,y)$ in the domain $S$ that satisfies the boundary condition. For the set of eigenfunctions to be complete, there must exist coefficients $a_{mn}$ such that

$$f(x,y) = \sum_m \sum_n a_{mn}\ \psi_{mn}(x,y)\ . \tag{6.185}$$

Multiplying both sides of Eq. (6.185) by $\psi_{mn}(x,y)$, integrating over the cross section, and using the orthogonality properties of $\psi_{mn}$, the $a_{mn}$ coefficients can be obtained from

$$a_{mn} = \frac{\displaystyle\iint_S f(x,y)\ \psi_{mn}(x,y)\,ds}{\displaystyle\iint_S \psi_{mn}^2(x,y)\,ds}\ . \tag{6.186}$$

It can also be shown that the eigenvalues $(k_c^2)$ are real and positive. Let's consider the *mn*th mode, for which we can write

$$(\nabla_t^2 + k_{mn}^2)\,\psi_{mn} = 0 \tag{6.187a}$$

and

$$(\nabla_t^2 + k_{mn}^{2\ *})\,\psi_{mn}^* = 0\ , \tag{6.187b}$$

where the superscript $*$ denotes the complex conjugate of the quantity. Multiplying Eq. (6.187a) by $\psi_{mn}^*$ and Eq. (6.187b) by $\psi_{mn}$ and subtracting the resulting equations, we

get

$$\psi_{mn}^{*}\,\nabla_{\mathrm{t}}^{2}\psi_{mn}-\psi_{mn}\,\nabla_{\mathrm{t}}^{2}\psi_{mn}^{*}=(k_{mn}^{2\,*}-k_{mn}^{2})\psi_{mn}\psi_{mn}^{*}\,. \tag{6.188}$$

As in the previous case, integrating both sides of Eq. (6.188) over the cross-sectional area of the waveguide and then invoking Green's second identity, we can show that

$$(k_{mn}^{2\,*}-k_{mn}^{2})\iint_{S}|\psi_{mn}|^{2}\,ds=0\,.$$

Since the integrand is a positive quantity we conclude that

$$k_{mn}^{2}=k_{mn}^{2\,*}\,, \tag{6.189}$$

proving that $k_{mn}^{2}$ is a real quantity. To show that $k_{mn}^{2}$ is a positive quantity, Green's first identity can be used. According to Green's first identity,

$$\iint_{S}(\nabla_{\mathrm{t}}\psi_{mn}\cdot\nabla_{\mathrm{t}}\psi_{mn}+\psi_{mn}\,\nabla_{\mathrm{t}}^{2}\psi_{mn})\,ds=\oint_{C}\psi_{mn}\,\frac{\partial\psi_{mn}}{\partial n}\,d\ell\,. \tag{6.190}$$

Dirichlet's or Neumann's boundary conditions force the right-hand side of Eq. (6.190) to go to zero. Then, using Eq. (6.187a) in the left-hand side of Eq. (6.190), we get

$$k_{mn}^{2}=\frac{\iint(\nabla_{\mathrm{t}}\psi_{mn}\cdot\nabla_{\mathrm{t}}\psi_{mn})\,ds}{\iint\psi_{mn}^{2}\,ds}\,. \tag{6.191}$$

Assuming the eigenfunctions $\psi_{mn}$ are real quantities, it then is obvious that both the numerator and denominator of Eq. (6.191) are positive quantities, which indicates that $k_{mn}^{2}$ is a positive and real quantity. It should be pointed out that the assumption about eigenfunctions being real functions is not necessary to prove that the eigenvalues are real and positive. In fact if $\psi_{mn}=\psi_{mn}'+i\psi_{mn}''$ is complex, then its real and imaginary parts satisfy the wave equation (6.187a) since $k_{mn}^{2}$ is real. Following the above procedure that led to Eq. (6.191) for $\psi_{mn}'$, then it can be shown that $k_{mn}^{2}$ is positive. Alternatively, one can apply Green's first identity to $\psi_{mn}$ and $\psi_{mn}^{*}$ to show that

$$k_{mn}^{2}=\frac{\iint_{S}|\nabla_{\mathrm{t}}\psi_{mn}|^{2}\,ds}{\iint|\psi_{mn}|^{2}\,ds}\,. \tag{6.192}$$

Another interesting property of the eigenfunctions is that not only are they themselves orthogonal, but also their gradients $(\nabla_{\mathrm{t}}\psi_{mn})$ are orthogonal. To show this, we can apply Green's first identity to two distinct eigenfunctions $\psi_{mn}$ and $\psi_{m'n'}$:

$$\iint_{S}(\nabla_{\mathrm{t}}\psi_{mn}\cdot\nabla_{\mathrm{t}}\psi_{m'n'}+\psi_{mn}\nabla_{\mathrm{t}}^{2}\psi_{m'n'})\,ds=\oint\psi_{mn}\,\frac{\partial\psi_{m'n'}}{\partial n}\,d\ell\,.$$

Replacing $-k_{m'n'}^2 \psi_{m'n'}$ for $\nabla_t^2 \psi_{m'n'}$ and using the orthogonality of $\psi_{mn}$ and $\psi_{m'n'}$ and the fact that the right-hand side is zero, it can easily be shown that

$$\iint_S \nabla_t \psi_{mn} \cdot \nabla_t \psi_{m'n'} \, ds = 0 \, . \tag{6.193}$$

### 6-8.1 Waveguide Fields Orthogonality

In the previous subsection we demonstrated the orthogonality of eigenfunctions for an arbitrary waveguide. In this section, we show that the electric fields for two different TM, two different TE, or one TM and one TE mode in the transverse plane of an arbitrary waveguide are orthogonal. Let us first consider two different TM modes. Recalling from Eq. (5.102a) that the transverse electric field can be computed from

$$\mathbf{E}_t^{mn}(\mathbf{r}) = i\beta \, \nabla_t \psi_{mn}(\mathbf{r}) \, e^{i\beta z} \, , \tag{6.194}$$

it follows that the orthogonality of the transverse electric field is established provided that $\nabla_t \psi_{mn}(\mathbf{r})$ is orthogonal to $\nabla_t \psi_{pq}(\mathbf{r})$. This is demonstrated in Eq. (6.193).

For two TE modes, the transverse electric field for any given mode can be obtained from Eq. (5.105b) and is given by

$$\mathbf{E}_t^{mn}(\mathbf{r}) = i\omega\mu [\nabla_t \psi_{mn}(\mathbf{r}) \times \hat{\mathbf{z}}] e^{i\beta z} \, . \tag{6.195}$$

The orthogonality of the transverse electric field for two TE modes can be established if we can show that

$$\iint_S [\nabla_t \psi_{mn}(\mathbf{r}) \times \hat{\mathbf{z}}] \cdot [\nabla_t \psi_{pq}(\mathbf{r}) \times \hat{\mathbf{z}}] \, ds = 0 \, . \tag{6.196}$$

Expanding the integrand of Eq. (6.196), we can show that

$$\begin{aligned} [\nabla_t \psi_{mn}(\mathbf{r}) \times \hat{\mathbf{z}}] \cdot [\nabla_t \psi_{pq}(\mathbf{r}) \times \hat{\mathbf{z}}] &= \hat{\mathbf{z}} \cdot \left\{ [\nabla_t \psi_{pq}(\mathbf{r}) \times \hat{\mathbf{z}}] \times \nabla_t \psi_{mn}(\mathbf{r}) \right\} \\ &= \hat{\mathbf{z}} \cdot [\nabla_t \psi_{mn}(\mathbf{r}) \cdot \nabla_t \psi_{pq}(\mathbf{r}) \, \hat{\mathbf{z}} - \nabla_t \psi_{mn}(\mathbf{r}) \cdot \hat{\mathbf{z}} \, \nabla_t \psi_{pq}(\mathbf{r})] \, . \end{aligned} \tag{6.197}$$

However, $\hat{\mathbf{z}} \cdot \nabla_t \psi_{mn}(\mathbf{r}) = 0$, and hence Eq. (6.196) simplifies to

$$\iint \nabla_t \psi_{mn}(\mathbf{r}) \cdot \nabla_t \psi_{pq}(\mathbf{r}) \, ds = 0 \, , \tag{6.198}$$

which obviously holds according to Eq. (6.193).

Finally, to show that the transverse electric field of a TE mode is orthogonal to the transverse electric field of a TM mode, we need to show that

$$\iint_S (\nabla_t \psi_{mn}^{\mathrm{TE}} \times \hat{\mathbf{z}}) \cdot \nabla_t \psi_{pq}^{\mathrm{TM}} \, ds = 0 \, . \tag{6.199}$$

Consider the following identity:

$$\nabla_t \cdot (\hat{\mathbf{z}}\, \psi_{mn}^{\mathrm{TE}} \times \nabla_t \psi_{pq}^{\mathrm{TM}}) = \nabla_t \times (\hat{\mathbf{z}}\, \psi_{mn}^{\mathrm{TE}}) \cdot \nabla_t \psi_{pq}^{\mathrm{TM}} - \hat{\mathbf{z}}\, \psi_{mn}^{\mathrm{TE}} \cdot \nabla_t \times \nabla_t \psi_{pq}^{\mathrm{TM}} \,. \tag{6.200}$$

But $\nabla_t \times \nabla_t \psi_{pq}^{\mathrm{TM}} = 0$, and applying the surface integral on both sides of Eq. (6.200), and then applying the divergence theorem, leads to

$$\oint_C (\hat{\mathbf{z}}\, \psi_{mn}^{\mathrm{TE}} \times \nabla_t \psi_{pq}^{\mathrm{TM}}) \cdot \hat{\mathbf{n}}\, d\ell = \iint_S \nabla_t \times (\hat{\mathbf{z}}\, \psi_{mn}^{\mathrm{TE}}) \cdot \nabla_t \psi_{pq}^{\mathrm{TM}}\, ds \,, \tag{6.201}$$

where $\hat{\mathbf{n}}$ is the unit normal to the waveguide contour pointing outward. The integrand of the contour integral in Eq. (6.201) can be written as

$$(\hat{\mathbf{z}} \times \nabla_t \psi_{pq}^{\mathrm{TM}}) \cdot \hat{\mathbf{n}} \psi_{mn}^{\mathrm{TE}} = (\hat{\mathbf{n}} \times \hat{\mathbf{z}}) \cdot \nabla_t \psi_{pq}^{\mathrm{TM}} \psi_{mn}^{\mathrm{TE}} \,.$$

Since $\hat{\mathbf{n}} \times \hat{\mathbf{z}}$ is tangential to the waveguide contour and $\nabla_t \psi_{pq}^{\mathrm{TM}} \sim \mathbf{E}_t^{pq}(\mathbf{r})$ is normal to the contour, it follows that

$$\iint_S (\nabla_t \psi_{mn}^{\mathrm{TE}} \times \hat{\mathbf{z}}) \cdot \nabla_t \psi_{pq}^{\mathrm{TM}}\, ds = 0 \,,$$

and hence Eq. (6.199) is satisfied. Note that in this case, $p$ can be equal to $m$ and $q$ can be equal to $n$.

## 6-8.2 Attenuation Rate in Waveguides of Arbitrary Cross Section

The attenuation rate due to losses of metallic walls in a waveguide with arbitrary cross section can be obtained from Eq. (6.98):

$$\alpha = \frac{\oint_C |\mathbf{H}_{\tan}|^2\, d\ell}{4\sigma\delta_s\, P(z)} \,. \tag{6.202}$$

The expressions for $\mathbf{H}_{\tan}$ and $P(z)$ depend on the mode of propagation. For a $\mathrm{TM}_{mn}$ wave, the expressions for fields inside the waveguide are given by Eqs. (5.102a) and (5.102b):

$$\mathbf{E} = E_0 \left[ i\beta_{mn} \nabla_t \psi_{mn} + k_{mn}^2 \psi_{mn}\, \hat{\mathbf{z}} \right] e^{i\beta_{mn} z} \tag{6.203a}$$

and

$$\mathbf{H} = -E_0 i\omega\varepsilon (\nabla_t \psi_{mn} \times \hat{\mathbf{z}}) e^{i\beta_{mn} z} \,. \tag{6.203b}$$

The power carried by the waveguide can be obtained from

$$P(z) = \frac{1}{2}\, \Re\mathrm{e} \iint_S (\mathbf{E} \times H^*) \cdot \hat{\mathbf{z}}\, dz = \frac{1}{2}\, |E_0|^2 \beta_{mn} \omega\varepsilon \iint_S |\nabla_t \psi_{mn}|^2\, ds \,, \tag{6.204}$$

where we have used the fact that $\nabla_t \psi_{mn} \cdot \hat{\mathbf{z}} = 0$. Using Eq. (6.192), we can show that

$$\iint_S |\nabla_t \psi_{mn}|^2 \, ds = k_{mn}^2 \iint \psi_{mn}^2 \, ds \, .$$

Thus Eq. (6.204) is simplified to

$$P(z) = \frac{1}{2} |E_0|^2 \beta_{mn} \omega \varepsilon k_{mn}^2 \iint_S \psi_{mn}^2 \, ds \, . \tag{6.205}$$

The tangential magnetic field on the waveguide wall can be obtained from Eq. (6.203b). Denoting the unit vector on the waveguide wall as $\hat{\mathbf{n}}$,

$$|\mathbf{H}_{\tan}| = |\hat{\mathbf{n}} \times \mathbf{H}| = |E_0 \omega \varepsilon| \frac{\partial \psi_{mn}}{\partial n} \, .$$

As a result, the expression for the attenuation given by Eq. (6.202) can be written as

$$\alpha^{\mathrm{TM}_{mn}} = \frac{\omega \varepsilon \oint_C \left( \dfrac{\partial \psi_{mn}}{\partial n} \right)^2 d\ell}{2\sigma \delta_s \beta_{mn} k_{mn}^2 \iint_S \psi_{mn}^2 \, ds} \, . \tag{6.206}$$

Similarly, the attenuation rate for a $\mathrm{TE}_{mn}$ wave in the waveguide can be computed from the field expressions given by Eqs. (5.105a) and (5.105b):

$$\mathbf{H} = H_0 \left[ i\beta_{mn} \nabla_t \psi_{mn} + k_{mn}^2 \psi_{mn} \, \hat{\mathbf{z}} \right] e^{i\beta_{mn} z} \tag{6.207a}$$

and

$$\mathbf{E} = H_0 (i\omega\mu) \, [\nabla_t \psi_{mn} \times \hat{\mathbf{z}}] \, e^{i\beta_{mn} z} \, . \tag{6.207b}$$

The power carried by the waveguide can be obtained in the manner shown in Eq. (6.204) and is given by

$$\begin{aligned} P(z) &= \frac{1}{2} |H_0|^2 \omega \mu \beta_{mn} \iint_S |\nabla_t \psi_{mn}|^2 \, ds \\ &= \frac{1}{2} |H_0|^2 \beta_{mn} \omega \mu k_{mn}^2 \iint_S \psi_{mn}^2 \, ds \, . \end{aligned} \tag{6.208}$$

Also,

$$|\mathbf{H}_{\tan}|^2 = |\hat{\mathbf{n}} \times \mathbf{H}|^2 = |H_0|^2 \left[ \beta_{mn}^2 \left( \frac{\partial \psi_{mn}}{\partial t} \right)^2 + k_{mn}^4 (\psi_{mn})^2 \right] \, , \tag{6.209}$$

where $\hat{\mathbf{t}}$ is a unit vector tangential to the contour of the waveguide cross section. Hence,

$$\alpha^{\mathrm{TE}_{mn}} = \frac{\oint \left[\beta_{mn}^2 |\hat{\mathbf{n}} \times \nabla_{\mathrm{t}} \psi_{mn}|^2 + k_{mn}^4 \psi_{mn}^2\right] \, d\ell}{2\sigma\delta_s \beta_{mn} \omega\mu k_{mn}^2 \iint_S \psi_{mn}^2 \, ds} \, .$$

### 6-8.3 Expansion of 2-D Scalar Green's Function in Terms of Eigenfunctions

It is somewhat obvious that a $z$-directed electric or magnetic current produces TM or TE modes in a metallic waveguide. Solutions of the wave equation for arbitrary current distributions can be obtained from the scalar Green's function:

$$(\nabla_{\mathrm{t}}^2 + k_{\mathrm{c}}^2)\, g(\boldsymbol{\rho}, \boldsymbol{\rho}') = -\delta(\boldsymbol{\rho} - \boldsymbol{\rho}') \, , \tag{6.210}$$

where $\boldsymbol{\rho} = x\,\hat{\mathbf{x}} + y\,\hat{\mathbf{y}}$ and $\boldsymbol{\rho}' = x'\,\hat{\mathbf{x}} + y'\,\hat{\mathbf{y}}$. Since the set of eigenfunctions is complete,

$$g(\boldsymbol{\rho}, \boldsymbol{\rho}') = \sum_m \sum_n A_{mn}\, \psi_{mn}(\boldsymbol{\rho}) \, . \tag{6.211}$$

Also,

$$\delta(\boldsymbol{\rho} - \boldsymbol{\rho}') = \sum_m \sum_n B_{mn}\, \psi_{mn}(\boldsymbol{\rho}) \, . \tag{6.212}$$

Using Eq. (6.186) it can be shown that

$$B_{mn} = \frac{\psi_{mn}(\rho')}{\iint_S \psi_{mn}^2(\rho)\, ds} \, . \tag{6.213}$$

Substituting Eqs. (6.211) and (6.212) into Eq. (6.210), we have

$$\sum\sum A_{mn}(\nabla_{\mathrm{t}}^2 + k_{\mathrm{c}}^2)\, \psi_{mn}(\rho) = -\sum_m \sum_n \frac{\psi_{mn}(\rho')\, \psi_{mn}(\rho)}{\iint_S \psi_{mn}^2(\rho)\, ds} \, .$$

But $\nabla_{\mathrm{t}}^2 \psi_{mn} = -k_{mn}^2 \psi_{mn}$, which leads to

$$A_{mn} = \frac{1}{k_{mn}^2 - k_{\mathrm{c}}^2} \frac{\psi_{mn}(\rho')}{\iint_S \psi_{mn}^2(\rho)\, d\rho} \, . \tag{6.214}$$

Replacing this value of $A_{mn}$ in Eq. (6.211), the scalar Green's function that satisfies the waveguide boundary condition is then given by

$$g(\boldsymbol{\rho},\boldsymbol{\rho}') = \sum_m \sum_n \frac{\psi_{mn}(\rho')\,\psi_{mn}(\rho)}{(k_{mn}^2 - k_c^2)\iint_S \psi_{mn}^2(\rho)\,d\rho}\,.$$

For example, for a rectangular waveguide carrying a TM mode, the scalar Green's function can be written as

$$g(\boldsymbol{\rho},\boldsymbol{\rho}') = \sum_{m=1}^{\infty}\sum_{n=1}^{\infty} \frac{\sin\left(\frac{m\pi}{a}x\right)\sin\left(\frac{m\pi}{a}x'\right)\sin\left(\frac{n\pi}{b}y\right)\sin\left(\frac{n\pi}{b}y'\right)}{\left[\left(\frac{m\pi}{a}\right)^2 + \left(\frac{n\pi}{b}\right)^2 - k_c^2\right]\left(\frac{ab}{4}\right)}\,.$$

It is also interesting to note that

$$\delta(\boldsymbol{\rho}-\boldsymbol{\rho}') = \sum_{m=1}^{\infty}\sum_{n=1}^{\infty} \frac{4}{ab}\sin\left(\frac{m\pi}{a}x\right)\sin\left(\frac{m\pi}{a}x'\right)\sin\left(\frac{n\pi}{b}y\right)\sin\left(\frac{n\pi}{b}y'\right)\,.$$

### 6-8.4 Calculus of Variations for Estimation of Eigenvalues

The method of separation of variables is available for only a small number of three-dimensional cavity structures and cross-sectional waveguide geometries. For waveguides and cavities of arbitrary geometries, approximate numerical methods must be used to find the cutoff frequencies and resonant frequencies. The method of calculus of variations provides one such method. As shown in Eq. (6.191), the eigenvalues of the scalar wave equation can be obtained from

$$k_c^2 = \frac{\iint_R \nabla_t\psi\cdot\nabla_t\psi\,ds}{\iint_R \psi^2\,ds}\,, \tag{6.215}$$

where $\psi$ is an eigenfunction defined in $R$, the domain specifying the waveguide cross section. Here we want to show among all functions $f$ that are continuous and have a continuous first derivative in $R$, the function that minimizes the ***functional***

$$\frac{N(f)}{D(f)} = \frac{\iint_R \nabla_t f\cdot\nabla_t f\,ds}{\iint_R f^2\,ds} \tag{6.216}$$

is an eigenfunction of the $\nabla_t^2$ operator. The minimum is equal to the lowest eigenvalue $k_{c1}^2$.

Suppose there exists a solution $\psi_1$ that minimizes the functional defined by Eq. (6.216). Then for an arbitrary function $g$ in the class of admissible functions and an arbitrarily small

constant $\delta$,

$$N(\psi_1 + \delta g) > k_{c1}^2 \, D(\psi_1 + \delta g) \, . \tag{6.217}$$

Since $\psi_1$ is the solution to the minimum problem

$$N(\psi_1) = k_{c1}^2 \, D(\psi_1) \, .$$

Noting that

$$N(\psi_1 + \delta g) = N(\psi_1) + \delta^2 \, N(g) + 2\delta \, N(\psi_1, g)$$

and

$$D(\psi_1 + \delta g) = D(\psi_1) + \delta^2 \, D(g) + 2\delta \, D(\psi_1, g) \, ,$$

the inequality in Eq. (6.217) can be written as

$$2\delta[N(\psi_1, g) - k_{c1}^2 \, D(\psi_1, g)] + \delta^2[N(g) - k_{c1}^2 \, D(g)] \geq 0 \, , \tag{6.218}$$

where

$$N(\psi_1, g) = \iint_R \nabla_t \psi_1 \cdot \nabla_t g \, ds$$

and

$$D(\psi_1, g) = \iint_R \psi_1 g \, ds \, .$$

Note here that the second term in Eq. (6.218) is a positive quantity, i.e., $N(g) - k_{c1}^2 \, D(g) > 0$, since $g$ is not minimizing the functional. Since Eq. (6.218) must be valid for any arbitrary positive or negative $\delta$ and any function $g$, then

$$N(\psi_1, g) - k_{c1}^2 \, D(\psi_1, g) = 0 \, , \tag{6.219}$$

Otherwise for a given function $g$, we could choose a sufficiently small $\delta$ with a proper sign so that

$$2\delta[N(\psi_1, g) - k_{c1}^2 \, D(\psi_1, g)] + \delta^2[N(g) - D(g)] \leq 0 \, .$$

Expanding Eq. (6.219), we get

$$\iint_R \nabla_t \psi_1 \cdot \nabla_t g \, ds - k_{c1}^2 \iint_R \psi_1 g \, ds = 0 \, . \tag{6.220}$$

According to Green's first identity

$$\iint_R (\nabla_t \psi_1 \cdot \nabla_t g + g \, \nabla_t^2 \psi_1) \, ds = \oint_C g \, \frac{\partial \psi_1}{\partial n} \, d\ell \, . \tag{6.221}$$

Using Eq. (6.220) in Eq. (6.221), the following relation is obtained:

$$\iint_R g(\nabla_t^2 \psi_1 + k_{c1}^2 \psi_1) \, ds = \oint_C g \, \frac{\partial \psi_1}{\partial n} \, d\ell \, . \tag{6.222}$$

for an arbitrary function $g$. Let us first assume that $g$ is a function with a vanishing value at the waveguide boundary $C$. Then

$$\iint_R g(\nabla_t^2 \psi_1 + k_{c1}^2 \psi_1)\, ds = 0 \tag{6.223}$$

for all arbitrary $g$ functions with a vanishing value at the boundary. The integral given by Eq. (6.223) can vanish if and only if

$$\nabla_t^2 \psi_1 + k_{c1}^2 \psi_1 = 0\ . \tag{6.224}$$

That is, the function that minimizes functional Eq. (6.216) is an eigenfunction of the $\nabla_t^2$ operator with $k_{c1}^2$ as its eigenvalue. If $g$ is not zero on the waveguide boundary, since the left-hand side of Eq. (6.222) vanishes according to Eq. (6.224), then

$$\frac{\partial \psi_1}{\partial n} = 0 \quad \text{on the boundary.} \tag{6.225}$$

Hence $\partial \psi_1 / \partial n = 0$ is called a ***natural boundary condition***. For the TM case where $\psi$ must be zero on the boundary the class of admissible functions ($f$) must also satisfy the boundary condition $f = 0$ on the waveguide boundary. However, for the TE case where $\partial \psi / \partial n = 0$ on the waveguide boundary, the condition that $\partial f / \partial n = 0$ on the boundary to be in the class of admissible functions is not necessary, according to Eq. (6.225).

The next eigenvalue and the corresponding eigenfunction are obtained by minimizing the functional given by Eq. (6.216) subject to the following constraint:

$$\iint_R f \psi_1\, ds = 0\ , \tag{6.226}$$

which requires the orthogonality of the next eigenfunction with that of the first one, as mandated by Eq. (6.224). Since we have added a constraint to the first minimization problem, $k_{c2}^2$ obtained from Eq. (6.216) subject to Eq. (6.226) must be at least as large as $k_{c1}^2$, that is, $k_{c2}^2 > k_{c1}^2$. Now let us assume that this minimization problem has a solution $\psi_2$ such that

$$N(\psi_2) = k_{c2}^2\, D(\psi_2)$$

and

$$D(\psi_2, \psi_1) = 0\ .$$

As before, for an arbitrary function $g$ in the class of admissible function and an arbitrary parameter $\delta$ we must have

$$N(\psi_2 + \delta g) \geq k_{c2}^2\, D(\psi_2 + \delta g)\ . \tag{6.227}$$

It should be noted that the set of admissible functions is constrained by

$$D(\psi_1, g) = 0\ .$$

For a general function $p$ in the class of admissible functions not subject to the orthogonality constraint, we may write

$$g = p - c\psi_1 \ , \tag{6.228}$$

where

$$c = \frac{D(\psi_1, p)}{D(\psi_1)} \ . \tag{6.229}$$

Substituting Eq. (6.228) into Eq. (6.227), the inequality can be written as

$$N(\psi_2 + \delta p - \delta c\psi_1) \geq k_{c2}^2 \, D(\psi_2 + \delta p - \delta c\psi_1) \ .$$

Expanding the functionals $N$ and $D$ and using the argument that $p$ and $\delta$ are arbitrary, the functional coefficient of $\delta$ must vanish for the inequality to hold. That is,

$$N(\psi_2, p) - k_{c2}^2 \, D(\psi_2, p) - c[N(\psi_2, \psi_1) - k_{c2}^2 \, D(\psi_2, \psi_1)] = 0 \ . \tag{6.230}$$

We know that $D(\psi_2, \psi_1) = 0$ and that from the first variational problem for an arbitrary $p$ function

$$N(\psi_1, p) - k_{c1}^2 \, D(\psi_1, p) = 0 \ . \tag{6.231}$$

Choosing $p = \psi_2$, Eq. (6.231) gives the following relations:

$$N(\psi_1, \psi_2) = 0 \ . \tag{6.232}$$

Therefore, Eq. (6.230) reduces to

$$N(\psi_2, p) - k_{c2}^2 \, D(\psi_2, p) = 0 \ . \tag{6.233}$$

But Eq. (6.233) is exactly similar to Eq. (6.220), so with the help of Green's first identity it can be shown that

$$\nabla_t^2 \psi_2 + k_{c2}^2 \psi_2 = 0 \ ,$$

indicating that $k_{c2}^2$ is an eigenvalue and $\psi_2$ is an eigenfunction of the $\nabla_t^2$ operator. We can also get the natural boundary condition

$$\frac{d\psi_2}{dn} = 0 \quad \text{on } C.$$

as before.

This process can be continued to get the $k$th eigenvalue and eigenfunction. That is, we minimize the functional given by Eq. (6.216) subject to

$$\iint_R f \psi_j \, ds = 0 \qquad \text{for } j = 1, 2, \ldots, k-1 \ .$$

This procedure results in obtaining a sequence of eigenvalues $k_{c1}^2 \leq k_{c2}^2 \leq k_{c3}^2 \leq \cdots$ .

### Example 6-6: Estimation of Cutoff Frequency

Use the variation principle by choosing an approximate eigenfunction $\psi$ to find the eigenvalues of the dominant mode in a rectangular waveguide using Eq. (6.215).

Consider a rectangular waveguide with cross-sectional dimensions $a$ and $b$ $(a > b)$ supporting a TE mode. The eigenfunctions for this problem were found to be

$$\psi_{mn}(x,y) = \cos\left(\frac{m\pi}{a}\,x\right)\cos\left(\frac{n\pi}{b}\,y\right)\,,$$

which satisfy the boundary condition $\frac{\partial}{\partial n}\,\psi_{mn} = 0$ on the rectangular contour of the waveguide. The eigenvalues are given by

$$k^2_{c(mn)} = \left(\frac{m\pi}{a}\right)^2 + \left(\frac{n\pi}{b}\right)^2 \qquad n,m = 0,1,2,3,\ldots$$

The lowest eigenvalue corresponds to

$$k^2_{c(10)} = \left(\frac{\pi}{a}\right)^2\,.$$

Let us choose $f(x,y) = (x - \frac{a}{2})$ as an estimate for the first eigenfunction. Then

$$\nabla f = \hat{\mathbf{x}}\,,$$

and using functional Eq. (6.216) an upper bound for the lowest eigenvalue can be obtained from

$$\tilde{k}^2_c = \frac{\displaystyle\int_0^a\int_0^b dx\,dy}{\displaystyle\int_0^a\int_0^b \left(x-\frac{a}{2}\right)^2 dx\,dy} = \frac{a}{\frac{2}{3}\left(\frac{a}{2}\right)^3} = \frac{12}{a^2}\,,$$

which is about 20% higher than the lowest eigenvalue.

## 6-8.5 Numerical Solution

The finite element method offers an efficient numerical procedure for the calculation of the eigenvalues of a waveguide of an arbitrary cross section.[§] This technique is well known and here only a brief discussion of the method is outlined. For homogeneously filled waveguides the longitudinal component of the electric (TM case) or magnetic (TE case) field, denoted by $\psi$, satisfies the homogeneous Helmholtz equation $(\nabla^2 + K_c^2)\psi = 0$, where $K_c$ is the cutoff wave number. It is shown that the solution to the Helmholtz equation minimizes the following

[§]Silvester, P., "A general high-order finite-element waveguide analysis program," *IEEE Transactions Microwave Theory and Technique*, vol. MTT-17, no. 4, April 1969.

functional:

$$F(\psi) = \frac{\iint_S \nabla\psi \cdot \nabla\psi \, ds}{\iint_S \psi^2 \, ds} \, , \tag{6.234}$$

and the minimum is equal to the smallest eigenvalue $\lambda = K_c^2$. To find the minima of the functional, the eigenfunction $\psi$ is approximated by a piecewise linear function. In this approximation the cross section of the waveguide is discretized into small triangular elements with unknown values of $\psi$ at each node of the elements. For the $e$th element the linear function in terms of the node values ($\psi_j^e$) can be represented by[¶]

$$\psi(x,y) = \sum_{j=1}^{3} N_j^e(x,y) \; \psi_j^e \, ,$$

where $N_j^e(x,y)$ constitute the linear basis function given in terms of the element's nodes $x$–$y$ coordinates. That is,

$$N_j^e(x,y) = \frac{1}{2\Delta^e} \left(a_j^e + b_j^e x + c_j^e y\right) , \qquad j = 1,2,3 \tag{6.235}$$

and

$$a_1^e = x_2^e y_3^e - y_2^e x_3^e \, , \qquad b_1^e = y_2^e - y_3^e \, , \qquad c_1^e = x_3^e - x_2^e \, ,$$

where $\Delta^e$ is the area of the triangle given by

$$\Delta^e = \frac{1}{2} \left(b_1^e c_2^e - b_2^e c_1^e\right) ,$$

and the expressions for $a_2^e, \ldots, c_3^e$ are obtained from Eq. (6.235) by cyclic interchange of the subscripts ($1 \to 2, \; 2 \to 3, \; 3 \to 1$).

Substituting the piecewise linear function into the functional defined by Eq. (6.234) and searching for the minima by setting $\delta / \delta \psi_j^e = 0$, the following matrix equation is obtained:

$$\tilde{\mathbf{A}} \tilde{\Psi} = K_c^2 \, \tilde{\mathbf{B}} \, \tilde{\Psi} \, , \tag{6.236}$$

where the elements of $\tilde{\mathbf{A}}$ and $\tilde{\mathbf{B}}$ are given by

$$\tilde{A}_{ij}^e = \frac{1}{4\Delta^e} \left(b_i^e b_j^e + c_i^e c_j^e\right)$$

and

$$\tilde{B}_{ij}^e = \frac{\Delta^e}{12} \left(1 + \delta_{ij}\right) ,$$

and $\delta_{ij}$ is the Kronecker delta. Since some of the nodes are shared among the adjacent

[¶]Jin, J., *The Finite Element Method in Electromagnetics,* New York: John Wiley & Sons, 1993.

elements, the vector $\tilde{\Psi}$ for the unconnected elements must be related to the vector $\Psi$ for connected elements using a connection matrix $\mathbf{C}$.[‖] In this case,

$$\tilde{\Psi} = \mathbf{C}\,\Psi\,,$$

and the matrix equation takes the following form:

$$\mathbf{A}\Psi = K_c^2\,\mathbf{B}\,\Psi\,, \tag{6.237}$$

where $\mathbf{A} = \mathbf{C}^t\,\tilde{\mathbf{A}}\,\mathbf{C}$ and $\mathbf{B} = \mathbf{C}^t\,\tilde{\mathbf{B}}\,\mathbf{C}$. Equation (6.237) is recognized as the generalized eigenvalue problem, which can be solved for $K_c$ numerically using a standard method.[**]

## Example 6-7: Cutoff Frequency of a General Waveguide

Use the formulation given by Eq. (6.237) for the trapezoidal waveguide shown in Fig. 6-24 to find the cutoff frequencies and first two modes' field distribution in the cross section of the waveguide. Such geometry for waveguides is encountered at millimeter-wave (MMW) or sub-MMW bands where silicon micromachining must be used to circumvent the tolerance limitation of traditional milling machines. Chemical etching of silicon wafers with a specific crystal orientation shows different anisotropic etch rates for different planes of the crystal. For example, anisotropic wet etching of a $\langle 100 \rangle$ oriented silicon wafer creates trapezoidal grooves with an angle of 54.74°. Usually ethylenediamine pyrocatechol (EDP) or tetramethylammonium hydroxide (TMAH) etchants are used in this process. The depth of the groove is determined by temperature, concentration, and time of etching. For the waveguide considered here, the larger base of the trapezoid is $b = 2.4$ mm and the groove depth is $h = 1.2$ mm.

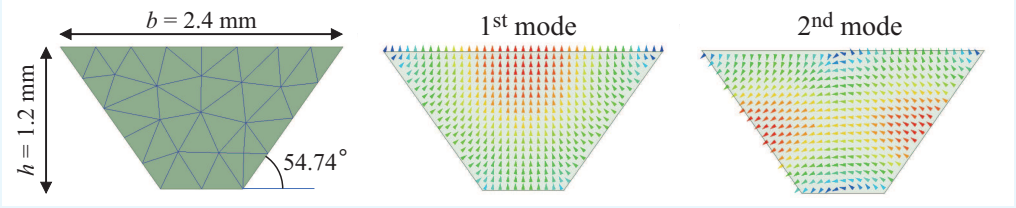


**Figure 6-24:** Configuration of a trapezoidal waveguide and the electric field distribution in the waveguide cross section for the first two modes.

**Solution:** The cross section of the waveguide is discretized by small triangular elements, as shown in Fig. 6-24, and Eq. (6.237) is solved to find the eigenvalues from which the cutoff

[‖] Ibid.

[**] Wilkinson, J. H., *The Algebraic Eigenvalue Problem,* New York: Oxford University Press, 1965.

frequencies are obtained. The process leads to (listed in order)

$$f_c = 84.6 \text{ GHz}, \ \ 117.4 \text{ GHz}, \ \ 165 \text{ GHz}, \ \ 165.4 \text{ GHz}, \ \ 175.5 \text{ GHz}.$$

Also, the field distribution of the first two modes is shown in Fig. 6-24.

## 6-9 Calculus of Variations for Estimation of Resonant Frequencies in General Cavities

In the previous section, we developed a procedure for estimating the eigenvalues and eigenvectors for waveguides of arbitrary cross section. It was also shown that for cavities made from a straight section of such waveguides, of length $c$ along the $z$-axis, the resonant frequencies can be determined from the eigenvalues of the waveguide, $k_{mn}^2$, using

$$k^2 = \omega^2 \mu \varepsilon = k_{mn}^2 + \left(\frac{\ell \pi}{c}\right)^2 . \tag{6.238}$$

However, there are no exact solutions for a general cavity of arbitrary shape. For the best estimation of the resonant frequencies, a stationary formula similar to Eq. (6.215) is needed. To arrive at such a formulation, self-reaction of sources and fields inside a cavity can be used to show that such a functional is stationary. Consider a general-shape cavity filled with a material having permittivity and permeability $\varepsilon$ and $\mu$, as shown in Fig. 6-25. Initially let's assume there exists a volumetric current density $\mathbf{J}_a(\mathbf{r})$ inside the cavity that produces fields $\mathbf{E}_a(\mathbf{r})$ and $\mathbf{H}_a(\mathbf{r})$. These fields must satisfy the modified Ampère's law:

$$\nabla \times \mathbf{H}_a = -i\omega\varepsilon \, \mathbf{E}_a + \mathbf{J}_a \, . \tag{6.239}$$

The boundary condition mandates that $\hat{\mathbf{n}} \times \mathbf{E}_a = 0$ on the surface of the cavity. However, if we consider a magnetic surface current $\mathbf{J}_{\text{ms}a}$ on the cavity walls, then

$$\mathbf{J}_{\text{ms}a} = -\hat{\mathbf{n}} \times \mathbf{E}_a \, , \tag{6.240}$$

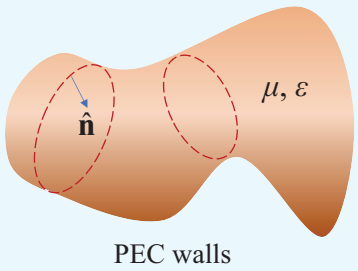


**Figure 6-25:** The geometry of an arbitrary-shaped cavity filled with a homogeneous and isotropic material having parameters $\mu$ and $\varepsilon$.

indicating that the tangential electric field can assume nonvanishing values. Now evaluating the self-reaction of sources and fields using Eq. (4.92), the surface integral vanishes and we have

$$\langle a,a\rangle = \iiint [\mathbf{E}_a(\mathbf{r})\cdot\mathbf{J}_a(\mathbf{r})]\ dv - \oiint [H_a(\mathbf{r})\cdot J_{msa}(\mathbf{r})]\ dS = 0\ . \tag{6.241}$$

Noting that within the volume of the cavity

$$\mathbf{H}_a(\mathbf{r}) = \frac{1}{i\omega\mu}\nabla\times\mathbf{E}_a(\mathbf{r})\ , \tag{6.242}$$

Eq. (6.239) can be rewritten as

$$\mathbf{J}_a(\mathbf{r}) = \frac{1}{i\omega\mu}\nabla\times\nabla\times\mathbf{E}_a(\mathbf{r}) + i\omega\varepsilon\,\mathbf{E}_a(\mathbf{r})\ . \tag{6.243}$$

Substituting Eqs. (6.242) and (6.243) into Eq. (6.241), we get

$$\begin{aligned}\langle a,a\rangle = \frac{1}{i\omega\mu}&\iiint_v \left[\mathbf{E}_a(\mathbf{r})\cdot\nabla\times\nabla\times\mathbf{E}_a(\mathbf{r}) - k^2\,\mathbf{E}_a(\mathbf{r})\cdot\mathbf{E}_a(\mathbf{r})\right]\ dv\\ &+\frac{1}{i\omega\mu}\oiint \{\nabla\times\mathbf{E}_a(\mathbf{r})\cdot[\hat{\mathbf{n}}\times\mathbf{E}_a(\mathbf{r})]\}\ dS\ .\end{aligned} \tag{6.244}$$

To simplify Eq. (6.244), we can make use of

$$\nabla\cdot[\nabla\times\mathbf{E}_a(\mathbf{r})\times\mathbf{E}_a(\mathbf{r})] = \mathbf{E}_a(\mathbf{r})\cdot\nabla\times\nabla\times\mathbf{E}_a(\mathbf{r}) - \nabla\times\mathbf{E}_a(\mathbf{r})\cdot\nabla\times\mathbf{E}_a(\mathbf{r}) \tag{6.245}$$

and

$$\nabla\times\mathbf{E}_a(\mathbf{r})\cdot[\hat{\mathbf{n}}\times\mathbf{E}_a(\mathbf{r})] = \hat{\mathbf{n}}\cdot\{\mathbf{E}_a(\mathbf{r})\times[\nabla\times\mathbf{E}_a(\mathbf{r})]\}\ . \tag{6.246}$$

Also, note that

$$\iiint_v \nabla\cdot[\nabla\times\mathbf{E}_a(\mathbf{r})\times\mathbf{E}_a(\mathbf{r})]\ dv = -\oiint \hat{\mathbf{n}}\cdot[\nabla\times E_a(\mathbf{r})\times\mathbf{E}_a(\mathbf{r})]\ dS\ . \tag{6.247}$$

The reason for the negative sign is that the unit vector $\hat{\mathbf{n}}$ used here is pointing towards the inside of the cavity. Using Eqs. (6.245), (6.246), and (6.247) in Eq. (6.244), the self-reaction expression takes the following form:

$$\begin{aligned}\langle a,a\rangle &= \frac{2}{i\omega\mu}\oiint \hat{\mathbf{n}}\cdot\{\mathbf{E}_a(\mathbf{r})\times[\nabla\times\mathbf{E}_a(\mathbf{r})]\}\ dS\\ &\quad+\frac{1}{i\omega\mu}\iiint [\nabla\times E_a(\mathbf{r})]\cdot[\nabla\times\mathbf{E}_a(\mathbf{r})]\ dv\\ &\quad-\frac{k^2}{i\omega\mu}\iiint [\mathbf{E}_a(\mathbf{r})\cdot\mathbf{E}_a(\mathbf{r})]\ dv\\ &= 0\ .\end{aligned} \tag{6.248}$$

Equation (6.248) can now be used to find the cavity eigenvalue

$$k^2 = \frac{\iiint_v [\nabla \times \mathbf{E}_a(\mathbf{r})] \cdot [\nabla \times \mathbf{E}_a(\mathbf{r})] \; dv + \oiint_S \hat{\mathbf{n}} \cdot \{\mathbf{E}_a(\mathbf{r}) \times [\nabla \times E_a(\mathbf{r})]\} \; dS}{\iiint_v [\mathbf{E}_a(\mathbf{r}) \cdot \mathbf{E}_a(\mathbf{r})] \; dv} \; . \tag{6.249}$$

Of course, inside a cavity at resonance, we can have nonzero field quantities in the absence of any sources like $\mathbf{J}_a(\mathbf{r})$ or $\mathbf{J}_{\mathrm{ms}a}(\mathbf{r})$. In the absence of sources, Eq. (6.241) shows that the self-reaction is zero. However, Eq. (6.249) can still be used to find the eigenvalues ($k^2$) for all modes in the cavity if $\mathbf{E}_a(\mathbf{r})$ is a corresponding field distribution for that mode. Equation (6.249) also indicates that if we were to hypothesize an electric field distribution that could result from certain sources in the cavity, that field distribution can approximately estimate an eigenvalue that has the closest field distribution to the guessed field distribution. This approximate estimate can be accurate if the function given by Eq. (6.249) is stationary with respect to the chosen field function.

To prove the stationarity of the functional, let us assume that

$$\mathbf{E}_a(\mathbf{r}) = \mathbf{E}_{\mathrm{e}}(\mathbf{r}) + \delta \; \mathbf{g}(\mathbf{r}) \; , \tag{6.250}$$

where $\mathbf{E}_{\mathrm{e}}(\mathbf{r})$ is the exact field distribution for a resonant mode, $\mathbf{g}(\mathbf{r})$ is an arbitrary but admissible function ($\hat{\mathbf{n}} \times \mathbf{g}(\mathbf{r}) = 0$ on the boundary), and $\delta$ is a small real number. In this case the estimated value of $k^2$ is a function of $\delta$ and can be written as

$$k^2(\delta) = \frac{N[\mathbf{E}_{\mathrm{e}}(\mathbf{r}) + \delta \; \mathbf{g}(\mathbf{r})]}{D[\mathbf{E}_{\mathrm{e}}(\mathbf{r}) + \delta \; \mathbf{g}(\mathbf{r})]} \; , \tag{6.251}$$

with the exact eigenvalue

$$k^2 = k^2(0) = \frac{N[\mathbf{E}_{\mathrm{e}}(\mathbf{r})]}{D[\mathbf{E}_{\mathrm{e}}(\mathbf{r})]} \; . \tag{6.252}$$

Here $N(\cdot)$ and $D(\cdot)$ refer to the numerator and denominator functionals of Eq. (6.249). To prove stationarity we need to show that

$$\left. \frac{\partial k^2(\delta)}{\partial \delta} \right|_{\delta=0} = 0 \; ,$$

which can be written explicitly as

$$\left. \frac{\partial k^2}{\partial \delta} \right|_{\delta=0} = \left. \frac{\frac{\partial N}{\partial \delta} D - N \frac{\partial D}{\partial \delta}}{D^2} \right|_{\delta=0} \; . \tag{6.253}$$

Using Eq. (6.252) in Eq. (6.253), it can be shown that

$$\left. \frac{\partial k^2}{\partial \delta} \right|_{\delta=0} = \left. \frac{\frac{\partial N}{\partial \delta} - k^2 \frac{\partial D}{\partial \delta}}{D} \right|_{\delta=0} \; . \tag{6.254}$$

But

$$\left.\frac{\partial N}{\partial \delta}\right|_{\delta=0} = 2\iiint_v \nabla\times\mathbf{g}(\mathbf{r})\cdot\nabla\times\mathbf{E}_e(\mathbf{r})\,dv + 2\oiint_S \hat{\mathbf{n}}\cdot\{\mathbf{g}(\mathbf{r})\times[\nabla\times\mathbf{E}_e(\mathbf{r})]\}\,ds + 2\oiint_S \hat{\mathbf{n}}\cdot\{\mathbf{E}_e(\mathbf{r})\times[\nabla\times\mathbf{g}(\mathbf{r})]\}\,ds\,. \tag{6.255}$$

Noting that $\hat{\mathbf{n}}\cdot\{E_e(\mathbf{r})\times[\nabla\times\mathbf{g}(\mathbf{r})]\} = \nabla\times\mathbf{g}(\mathbf{r})\cdot[\hat{\mathbf{n}}\times E_e(\mathbf{r})]$ and the fact that tangential $\mathbf{E}_e(\mathbf{r})$ on $S$ is zero ($\hat{\mathbf{n}}\times\mathbf{E}_e(\mathbf{r}) = 0$), the third integral in Eq. (6.254) vanishes. Also, since $\mathbf{g}(\mathbf{r})$ is an admissible function ($\hat{\mathbf{n}}\times\mathbf{g}(\mathbf{r}) = 0$), the second integral vanishes. Now noting that

$$\nabla\times\mathbf{g}(\mathbf{r})\cdot\nabla\times\mathbf{E}_e(\mathbf{r}) = \nabla\cdot\{\mathbf{g}(\mathbf{r})\times[\nabla\times\mathbf{E}_e(\mathbf{r})]\} + \mathbf{g}(\mathbf{r})\cdot\nabla\times\nabla\times\mathbf{E}_e(\mathbf{r})$$

and the fact that inside the source-free cavity

$$\nabla\times\nabla\times\mathbf{E}_e(\mathbf{r}) = k^2\,\mathbf{E}_e(\mathbf{r})\,,$$

Eq. (6.255) reduces to

$$\left.\frac{\partial N}{\partial \delta}\right|_{\delta=0} = -2\oiint \mathbf{g}(\mathbf{r})\times[\nabla\times\mathbf{E}_e(\mathbf{r})]\cdot\hat{\mathbf{n}}\,dS + 2k^2\iiint_v \mathbf{E}_e(\mathbf{r})\cdot\mathbf{g}(\mathbf{r})\,dv\,. \tag{6.256}$$

Again, the first term evaluates to zero, and we have

$$\left.\frac{\partial N}{\partial \delta}\right|_{\delta=0} = 2k^2\iiint_v \mathbf{E}_e(\mathbf{r})\cdot\mathbf{g}(\mathbf{r})\,dv\,. \tag{6.257}$$

We also need to evaluate

$$\left.\frac{\partial D}{\partial \delta}\right|_{\delta=0} = 2\iiint_v \mathbf{g}(\mathbf{r})\cdot\mathbf{E}_e(\mathbf{r})\,dv\,. \tag{6.258}$$

Using Eqs. (6.257) and (6.258) in Eq. (6.254) shows that

$$\left.\frac{\partial k^2}{\partial \delta}\right|_{\delta=0} = 0\,,$$

which proves that the functional given by Eq. (6.249) is stationary. That is, the function that minimizes Eq. (6.249) is a solution to the vector wave equation

$$\nabla^2\mathbf{E} + k^2E = 0$$

or

$$\nabla\times\nabla\times E - k^2E = 0\,.$$

### Example 6-8: Estimation of Resonant Frequency from the Stationary Formulation

Consider a cavity of spherical shape with radius $a$. Using the stationary formula given by Eq. (6.249) and hypothesizing an appropriate field distribution inside the cavity, find the resonant frequency.

**Solution:** As will be shown later, using the method of separation of variables, an analytical formulation for the field expressions can be obtained. The dominant mode has the simplest field distribution and is generated from a TM to $r$ potential (a set of fields in a spherical coordinate system when the magnetic field does not have an $r$-component). The boundary conditions on the cavity surface are as follows: $E_\theta = E_\phi = 0$ at $r = a$. As will be shown later, these are satisfied when

$$\hat{\mathbf{j}}_n(ka) = 0 \,,$$

where $\hat{\mathbf{j}}_n(kr)$ represents the Schelkunoff spherical Bessel function of the first kind and $n$th order. The dominant mode corresponds to the first zero of $\hat{\mathbf{j}}_1(ka)$; that is, when

$$ka = 2.744 \,.$$

So the exact solution for $k$ is given by

$$k = \frac{2.744}{a} \,.$$

As a guess, we are seeking a solution that is independent of $\phi$ and takes a simple form with $\theta$ and $r$. We should also choose our field distribution so that it satisfies the boundary condition. Let's assume that the electric field is given by

$$\mathbf{E}_a(r,\theta,\phi) = E_r\,\hat{\mathbf{r}} + E_\theta\,\hat{\boldsymbol{\theta}} \,,$$

with

$$E_r = \cos\theta\,\left(\frac{r}{a}\right)^2$$

and

$$E_\theta = \sin\theta\,\left(\frac{r}{a} - 1\right) \,.$$

Obviously $E_\theta(a,\theta,\phi) = 0$ at $r = a$. Using this field distribution, it can be shown that

$$\nabla \times \mathbf{E}_a(\mathbf{r}) = \frac{\sin\theta}{r}\left[1 - 2\left(\frac{r}{a}\right) - \left(\frac{r}{a}\right)^2\right]\,\hat{\boldsymbol{\phi}} \,.$$

Noting that $\hat{\mathbf{n}} = \hat{\mathbf{r}}$ and the fact that $\nabla \times \mathbf{E}_a$ is along $\hat{\boldsymbol{\phi}}$, it can be shown that

$$\hat{\mathbf{r}} \cdot [\mathbf{E}_a(\mathbf{r}) \times (\nabla \times \mathbf{E}_a(\mathbf{r}))] = |\nabla \times \mathbf{E}_a(\mathbf{r})|\,\mathbf{E}_\theta(\mathbf{r}) \,,$$

but $E_\theta(a) = 0$, which makes the second integral in the numerator of Eq. (6.249) vanish. Also, using the fact that

$$\int_0^{\pi/2} \sin^3\theta \, d\theta = \frac{4}{3}$$

and

$$\int_0^{\pi} \cos^2\theta \sin\theta \, d\theta = \frac{2}{3} ,$$

the numerator of Eq. (6.249) is calculated to be

$$N = \frac{52}{45} a = 1.1555a .$$

Also, the denominator is calculated to be

$$D = \frac{88}{630} a^3 = 0.1397a^3 .$$

Hence from Eq. (6.249) we estimate

$$k^2 = \frac{N}{D} = \frac{8.2717}{a^2} ,$$

or

$$k = \frac{2.876}{a} .$$

This value is very close to the exact solution, $k = 2.744/a$, with less than 5% error.

# Summary

## Concepts

- A dielectric slab with planar interfaces and an index of refraction larger than that of its surroundings can support TM and TE propagating waves inside the dielectric slab.
- Different modes of propagation with different field patterns can be supported depending on the index of refraction contrast and the dielectric slab thickness. For each mode there is a cutoff frequency below which that mode cannot be established nor propagate.
- Impedance surfaces with purely reactive impedance can also support TE and TM surface waves. Inductive surfaces can support TM waves and capacitive surfaces can support TE waves.
- Reactive impedance surfaces can be engineered using metallic surfaces with periodic grooves or using a metal-backed substrate with printed metallic patches on top. Both inductive and capacitive reactive impedance surfaces can be realized with the metallic patches over a relatively thin substrate.
- A metallic pipe of rectangular cross section, whether it is hollow or dielectric-filled, can support TE and TM waves. Depending on the geometry of the cross section, different modes with different field patterns and propagation constants may be supported by such structures.
- The attenuation rate of wave propagation in rectangular waveguides is substantially lower than that of ordinary transmission lines.
- Metallic waveguides are dispersive (phase velocity is a function of frequency), and the speed signal envelope known as group velocity is different from the phase velocity inside the waveguide.
- Resonant structures, like rectangular cavities, can support multiple modes at a set of discrete frequencies that depend on the physical dimension of the cavity.
- In practice, cavities are made of good conductors that have high but finite conductivity. For such cavities initial energy established at each mode decays as a function of time and this decay depends on the quality factor of the cavity.
- A transmission-line circuit model for each mode in a rectangular waveguide can be created and used to analyze the effects of localized discontinuities in waveguides.
- For general waveguides with arbitrary cross section, the cutoff wave number is always a positive real number that is only a function of the geometrical shape and dimension of the waveguide's cross section.
- The field generating potentials that satisfy a 2-D wave equation subject to Dirichlet's (TM) or Neumann's (TE) boundary conditions, which are known as eigenfunctions, form an orthogonal and complete set of functions in the 2-D domain of the waveguide's cross section.
- To find the cutoff wave number for waveguides of arbitrary geometry, the calculus of variations is used. A functional is defined from the eigenvalues and shown that the functions that minimize that functional is an eigenfunction and that the value of the functional is an eigenvalue.
- A numerical procedure, known as a finite element procedure, is presented to find the eigenfunctions and eigenvalues.

## Important Equations

**Transcendental equations for different modes of a dielectric-plate waveguide with thickness $t$ and constitutive parameters $\mu_2$, $\varepsilon_2$ in a background medium with constitutive parameters $\mu_1$, $\varepsilon_1$**

$$\begin{cases} \left(\dfrac{k_{2c}t}{2}\right)^2 + \left(\dfrac{vt}{2}\right)^2 = \left(\dfrac{\omega t}{2}\sqrt{\mu_2\varepsilon_2 - \mu_1\varepsilon_1}\right)^2 & \\ \dfrac{\varepsilon_1}{\varepsilon_2}\left(\dfrac{k_{2c}t}{2}\right)\tan\left(\dfrac{k_{2c}t}{2}\right) = \dfrac{vt}{2} & \text{TM odd mode} \\ -\dfrac{\varepsilon_1}{\varepsilon_2}\left(\dfrac{k_{2c}t}{2}\right)\cot\left(\dfrac{k_{2c}t}{2}\right) = \dfrac{vt}{2} & \text{TM even mode} \\ \dfrac{\mu_1}{\mu_2}\left(\dfrac{k_{2c}t}{2}\right)\tan\left(\dfrac{k_{2c}t}{2}\right) = \dfrac{vt}{2} & \text{TE odd mode} \\ -\dfrac{\mu_1}{\mu_2}\left(\dfrac{k_{2c}t}{2}\right)\cot\left(\dfrac{k_{2c}t}{2}\right) = \dfrac{vt}{2} & \text{TE even mode} \end{cases}$$

**Boundary condition for an impedance surface with surface impedance $Z_s$:**

$$\hat{\mathbf{n}} \times [\hat{\mathbf{n}} \times \mathbf{E}(\mathbf{r})] = -Z_s\, \hat{\mathbf{n}} \times \mathbf{H}(\mathbf{r})$$

**Propagation constant of a propagating surface wave ($Z_s = iX_c$) on a capacitance impedance surface:**

$$\beta^{TE} = \sqrt{k^2 + \left(\frac{\omega\mu}{X_c}\right)^2}$$

**and inductive impedance surface ($Z_s = -iX_i$):**

$$\beta^{TM} = \sqrt{k^2 + \omega^2\varepsilon^2 X_i^2}$$

**Surface impedance of a metallic surface with periodic grooves of depth $d$ supporting surface waves:**

$$Z_s = -i\eta_0 \tan(k_0 d) \qquad \text{thin periodic blades}$$

$$Z_s = -i\frac{w}{P}\eta_0 \tan(k_0 d) \qquad \text{thick corrugation with period } P \text{ and groove width } w$$

$$Z_s = -i\eta_0 \frac{J_1(k_0 d)}{J_0(k_0 d)} \qquad \text{triangular groove}$$

## Important Equations (continued)

**Surface impedance of metal-backed dielectric substrate with printed metallic patches with perodicity $P$:**

$$Z_{\mathrm{s}}^{\mathrm{TM}} = -i\,\frac{\eta_1 \cos\theta_{\mathrm{t}} \tan(k_1 \cos\theta_{\mathrm{t}}\, d)}{1 - \omega\widetilde{C}P\eta_1 \cos\theta_{\mathrm{t}} \tan(k_1 \cos\theta_{\mathrm{t}}\, d)}$$

$$Z_{\mathrm{s}}^{\mathrm{TE}} = -i\,\frac{\dfrac{\eta_1}{\cos\theta_{\mathrm{t}}} \tan(k_1 \cos\theta_{\mathrm{t}}\, d)}{1 - \omega\widetilde{C}P\,\dfrac{\eta_1}{\cos\theta_{\mathrm{t}}} \tan(k_1 \cos\theta_{\mathrm{t}}\, d)}$$

**Propagation constant and guided wavelength for a rectangular waveguide with dimensions $a$, $b$ for $mn^{\mathrm{th}}$ mode:**

$$\beta_{mn} = \sqrt{k^2 - \left(\frac{m\pi}{a}\right)^2 - \left(\frac{n\pi}{b}\right)^2}$$

$$(\lambda_{gmn})^{-1} = \sqrt{\frac{1}{\lambda^2} - \left(\frac{m}{2a}\right)^2 - \left(\frac{n}{2b}\right)^2}$$

**Cutoff frequency for $mn^{\mathrm{th}}$ mode:**

$$f_{\mathrm{c}}^{(mn)} = \frac{1}{2\sqrt{\mu\varepsilon}} \sqrt{\left(\frac{m}{a}\right)^2 + \left(\frac{n}{b}\right)^2}$$

**Phase and group velocity:**

$$u_{\mathrm{p}} = \frac{\omega}{\beta} = \frac{\omega}{\sqrt{k^2 - k_{\mathrm{c}}^2}}$$

$$u_{\mathrm{g}} = \frac{d\omega}{d\beta} = u_{\mathrm{p}} + \beta\,\frac{du_{\mathrm{p}}}{d\beta}$$

**Relations between phase velocity and group velocity:**

$$u_{\mathrm{p}} u_{\mathrm{g}} = c^2$$

**Power loss per unit length of a waveguide made with metallic walls of conductivity $\sigma$:**

$$P_{\mathrm{L}} = \frac{1}{2\sigma\delta_{\mathrm{s}}} \oint |H_{\mathrm{t}}|^2\, d\ell$$

## Important Equations (continued)

**Waveguide attenuation rate:**

$$\alpha = \frac{\oint |H_t|^2 \, d\ell}{2\sigma\delta_s P_{mn}}$$

with

$$P_{m,n} = \frac{ab}{p}\,\eta k \beta_{mn} k_{c,\,mn}^2 \times \begin{cases} \frac{1}{2} & m \neq 0 \text{ and } n \neq 0\,, \\ 1 & m = 0 \text{ or } n = 0\,, \end{cases}$$

as power carried by $\mathrm{TE}_{mn}$ mode, and

$$P_{m,n} = \frac{ab}{8\eta}\, k\beta_{mn} k_{c,\,mn}^2$$

as power carried by $\mathrm{TM}_{mn}$ mode.

**Resonant frequency of a rectangular cavity with dimensions $a$, $b$, $c$:**

$$f_{mn\ell} = \frac{1}{2\sqrt{\mu\varepsilon}} \sqrt{\left(\frac{m}{a}\right)^2 + \left(\frac{n}{b}\right)^2 + \left(\frac{\ell}{c}\right)^2}$$

**Quality factor of a cavity due to metallic loss:**

$$\breve{Q}_s = \frac{\omega\varepsilon\sigma\delta_s \iiint_V |E|^2 \, dv}{\oiint_s |H_t|^2 \, ds}$$

**Quality factor of a cavity due to dielectric loss:**

$$\breve{Q}_d = \frac{\varepsilon'}{\varepsilon''}$$

**Total quality factor:**

$$\frac{1}{\breve{Q}} = \frac{1}{\breve{Q}_s} + \frac{1}{\breve{Q}_d}$$

**Damping factor ($\gamma$) and relaxation time of a cavity:**

$$\gamma = \frac{1}{\tau} = \frac{\omega}{2Q}$$

## Important Equations (continued)

**Total stored energy at a resonance:**

$$w = w_{\mathrm{e}} + w_{\mathrm{m}} = 2w_{\mathrm{e}} = \frac{\varepsilon}{2} \iiint |E|^2 \, dv$$

**Series impedance per unit length ($Z$) and shunt admittance per unit length ($Y$) of transmission-line equivalent model for a waveguide:**

$$\left.\begin{aligned} Z &= -i\omega\mu - \frac{k_{\mathrm{c}}^2}{i\omega\varepsilon} \\ Y &= -i\omega\varepsilon \end{aligned}\right\} \quad \text{TM}$$

$$\left.\begin{aligned} Z &= -i\omega\mu \\ Y &= -i\omega\varepsilon - \frac{k_{\mathrm{c}}^2}{i\omega\mu} \end{aligned}\right\} \quad \text{TE}$$

**General waveguide:**

**2-D wave equation for eigenfunctions of a general waveguide:**

$$\nabla_{\mathrm{t}}^2 \psi_{mn} + k_{mn}^2 \psi_{mn} = 0$$

with $\psi_{mn} = 0$ (TM) or $\partial \psi_{mn}/\partial n = 0$ (TE) on the waveguide boundary.

**Properties of eigenfunction $\psi_{mn}$:**

$$\iint_S \psi_{mn}(\mathbf{r}) \; \psi_{m'n'}(\mathbf{r}) \, ds = 0 \qquad \text{orthogonality}$$

$$\iint_S \nabla \psi_{mn}(\mathbf{r}) \cdot \nabla \psi_{m'n'}(\mathbf{r}) \, ds = 0$$

**Properties of eigenvalues ($k_{mn}^2$):**

$$k_{mn}^2 = (k_{mn}^2)^* > 0 \qquad \text{Eigenvalues are real and positive}$$

**Variational formulation:** The function that minimizes the following functional is an eigenfunction and the value of the functional is an eigenvalue:

$$k_{\mathrm{c}}^2 = \frac{\iint_R \nabla_{\mathrm{t}} \psi \cdot \nabla_{\mathrm{t}} \psi \, ds}{\iint_R \psi^2 \, ds}$$

**Variational formulation for a general cavity:**

$$k^2 = \frac{\iiint_v [\nabla \times \mathbf{E}_a(\mathbf{r})] \cdot [\nabla \times \mathbf{E}_a(\mathbf{r})] \, dv + \oiint_S \hat{\mathbf{n}} \cdot \{\mathbf{E}_a(\mathbf{r}) \times [\nabla \times E_a(\mathbf{r})]\} \, dS}{\iiint_v [\mathbf{E}_a(\mathbf{r}) \cdot \mathbf{E}_a(\mathbf{r})] \, dv}$$

**Important Terms** Provide definitions or explain the meaning of the following terms:

attenuation rate
calculus of variations
cavity damping factor
cavity relaxation time
circuit models for waveguides
cutoff frequency
cutoff wave number
dielectric plate waveguide
Dirichlet's boundary condition
eigenfunction
eigenvalue
finite element
functional
generalized eigenvalue problem
group velocity
guided wavelength
isotropic reactive impedance surface
$k$–$\beta$ diagram
metallic septa
natural boundary condition
Neumann's boundary condition
phase velocity
quality factor for cavities
reactive impedance surface
rectangular cavity
rectangular waveguide
stationary formulation
substrate modes
surface impedance
surface resistivity
surface waves
telegrapher's equation
TE mode
TE wave impedance
TM mode
TM wave impedance
waveguide
waveguide discontinuity
waveguide mode

## PROBLEMS

### Waveguides

**6.1** The TE mode fields in and above a metal-backed dielectric slab of thickness $t/2$ (see Fig. P6.1) are given as follows:

$$\text{In region 1:} \quad \begin{cases} E_{1y} = Ai\omega\mu_1 \nu e^{-\nu x} e^{i\beta z}, \\ H_{1x} = -Ai\beta\nu e^{-\nu x} e^{i\beta z}, \\ H_{1z} = -A\nu^2 e^{-\nu x} e^{i\beta z}, \end{cases}$$

$$\text{In region 2:} \quad \begin{cases} E_{2y} = Bi\omega\mu_2 k_{2c} \sin(k_{2c}x)\, e^{i\beta z}, \\ H_{2x} = -Bi\beta k_{2c} \sin(k_{2c}x)\, e^{i\beta z}, \\ H_{2z} = B\beta k_{2c}^2 \cos(k_{2c}x)\, e^{i\beta z}, \end{cases}$$

where $k_{2c}^2 = k_2^2 - \beta^2$, $\nu^2 = \beta^2 - k_1^2$, and $\varepsilon_1 = \varepsilon_2 = \varepsilon_0$.

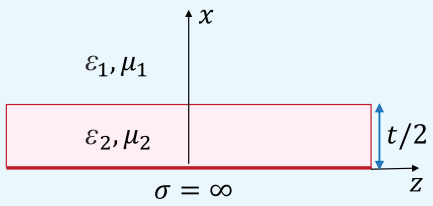


**Figure P6.1:** The geometry of a metal-backed dielectric slab with planar interfaces and infinite extent.

**(a)** Write down the equations that determine $k_{2c}$ and $\nu$.

**(b)** Give the expression for the total $z$-propagating power in the waveguide.

**(c)** Assuming $\mu_2 = 4\mu_1$ and $\mu_1 = \mu_0$, what is the minimum thickness $t$ necessary to support a propagating TE mode?

**6.2** Consider a parallel-plate waveguide formed by conductors covering the planes $y = 0$ and $y = b$, as shown in Fig. P6.2.

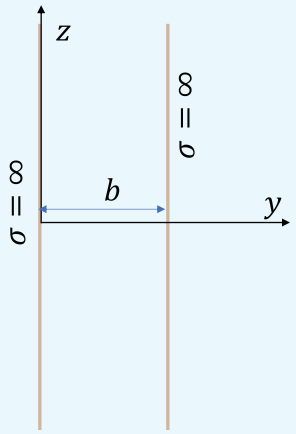


**Figure P6.2:** A parallel-plate waveguide made from infinite metallic sheets separated by a distance $b$ and parallel to the $x$–$z$ plane.

**(a)** Show that the field

$$E_x = E_0 \sin\left(\frac{n\pi y}{b}\right) e^{-\gamma z} \qquad n = 1,2,3,\ldots$$

defines a set of $\text{TE}_n$ modes, and show that the field

$$H_x = H_0 \cos\left(\frac{n\pi y}{b}\right) e^{-\gamma z} \qquad n = 0,1,2,\ldots$$

defines a set of $\text{TM}_n$ modes, where in both cases

$$\gamma = \sqrt{\left(\frac{n\pi}{b}\right)^2 - k^2}\,.$$

**(b)** Show that the cutoff frequencies of the modes are

$$f_c = \frac{n}{2b\sqrt{\varepsilon\mu}}\,.$$

**(c)** Investigate the possibility of propagating a TEM mode (try to derive it from either TM or TE waves).

**6.3** Consider a parallel-plate waveguide, as shown in Fig. P6.3. Regions 0 and 1 have different dielectric constants $\varepsilon_0$ and $\varepsilon_1$. Let the waveguide be infinite in the $y$- and $z$-directions. Consider wave propagation in the $+z$-direction.

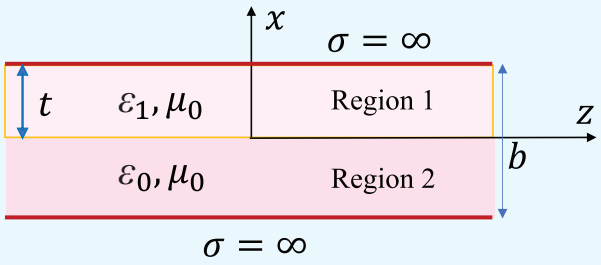


**Figure P6.3:** The geometry of a partially filled parallel-plate waveguide. The load is a dielectric slab with planar interfaces parallel to the waveguide walls.

**(a)** Find the Hertz vector potential $\boldsymbol{\Pi}$ for TM waves in both regions 0 and 1.

**(b)** Find the electric fields in regions 0 and 1.

**(c)** Find the set of equations that can be used to compute the propagation constant inside the waveguide.

**6.4** Consider a rectangular waveguide whose side walls are made from a perfect magnetic conductor, as shown in Fig. P6.4. The waveguide is filled with material 1 for $z < 0$ and with material 2 for $z > 0$. A $\text{TM}_z$ wave is incident from the left (i.e., from material 1). Calculate the reflection and transmission coefficient at the $z = 0$ interface.

*Hint:* For $\text{TM}_z$ modes, the Hertz vector potential is given by $\boldsymbol{\Pi} = \Pi_z\,\hat{\mathbf{z}}$. In region 1, $\Pi_{z,1} = \Psi(x,y)\,(Ae^{i\beta_1 z} + Be^{-i\beta_1 z})$, and in region 2, $\Pi_{z,2} = \Psi(x,y)\,Ce^{i\beta_2 z}$, where $\Psi(x,y)$ satisfies the scalar wave equation $\nabla_t^2 + k_c^2\Psi = 0$.

**6.5** Consider a metallic waveguide with dimensions $a$ and $b$. We place a resistive sheet at $z = 0$ with sheet impedance $Z_s$, as shown in Fig. P6.5. The boundary conditions for resistive sheets are provided in Problem P5.10 (see Eqs. (5.252), (5.253), and (5.255)). The waveguide is supporting $\text{TE}_{10}$ mode. For this mode, find the fields in region 1 and region 2 of the waveguide.

**6.6** Consider a rectangular waveguide with two horizontal PEC walls at $y = 0$ and $y = b$ and two vertical PMC walls at $x = 0$ and $x = a$. Derive the expressions for the appropriate vector potential, electric and magnetic fields, cutoff frequencies, and wave impedance for TM and TE waves. Identify the lowest order modes for each set. Does this structure support TEM modes? (*Hint:* You may need to solve separately for $k_c = 0$.)

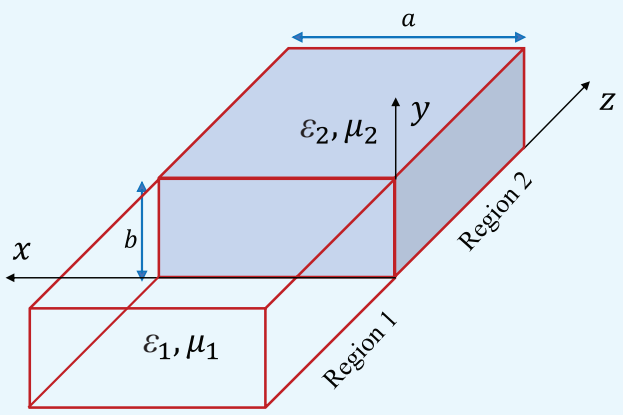


**Figure P6.4:** A rectangular waveguide with PMC walls. Half of the waveguide is filled with a material with constitutive parameters $\mu_1$, $\varepsilon_1$, and the other half is filled with a material with constitutive parameters $\mu_2$, $\varepsilon_2$.

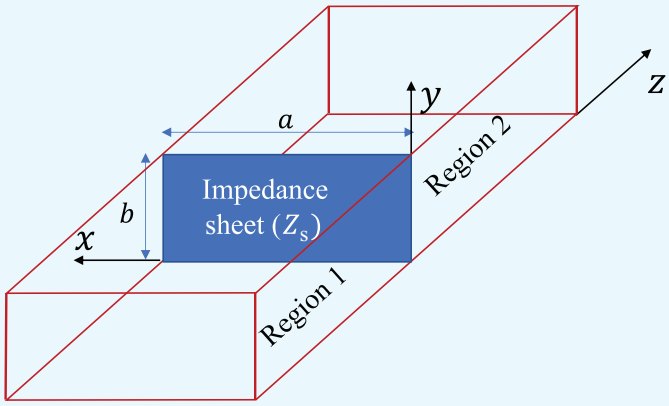


**Figure P6.5:** A thin resistive sheet (impedance sheet) placed in the cross section of the waveguide acts as a discontinuity and reflects some of the incident wave.

**6.7** Consider that the rectangular waveguide shown in Fig. P6.7 is partially filled with dielectric material 2 from $y = 0$ to $y = c$ and partially filled with material 1 from $y = c$ to $y = b$ ($a > b$ and $0 < c < b$).

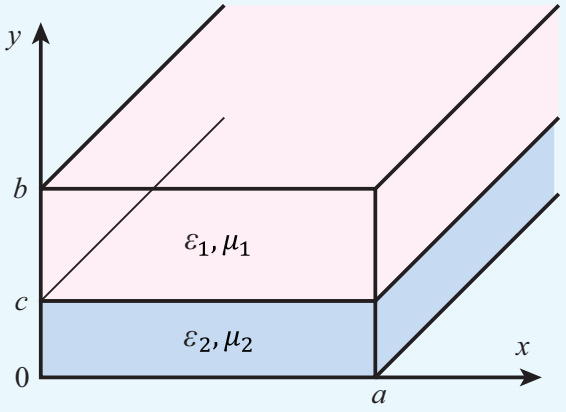


**Figure P6.7:** A partially filled rectangular waveguide with a dielectric slab filling the lower part of the waveguide.

**(a)** Show that $\text{TE}_z$ and $\text{TM}_z$ modes will fail to satisfy the boundary conditions, except for the $\text{TE}z_{0n}$ case. Solve for the $\text{TE}z_{0n}$ mode and find the transcendental equation that governs the propagation constant given by

$$\frac{\mu_2}{k_{2y}}\tan(k_{2y}c) + \frac{\mu_1}{k_{1y}}\tan[k_{1y}(b-c)] = 0\,,$$

where $k_{1y} = \sqrt{k_1^2 - \beta^2}$ and $k_{2y} = \sqrt{k_2^2 - \beta^2}$.

**(b)** For the $\text{TE}_{z_{m0}}$ mode, what are the wave impedances in the two regions?

**(c)** Find the hybrid modes (having both $E_z$ and $H_z$) by solving $\text{TM}_{y_{mn}}$ modes, which have electric Hertz potential in the $y$-direction: $\mathbf{\Pi} = \hat{\mathbf{y}}\,\psi(x,y)\,e^{i\beta z}$.

**(d)** Letting $\varepsilon_1 \approx \varepsilon_2$ and $\mu_1 = \mu_2 = \mu$, show that the cutoff frequency for the dominant $\text{TM}_{x_{mn}}$ mode is obtained by

$$\omega_c = \frac{\pi}{a}\sqrt{\frac{\varepsilon_2(b-c)+\varepsilon_1 c}{\mu\varepsilon_1\varepsilon_2 b}}\,.$$

**6.8** Consider a rectangular waveguide with a centered dielectric slab, as shown in Fig. P6.8. The problem contains three homogeneous regions. We know we cannot find pure $\text{TE}_z$ or $\text{TM}_z$ modes, but for such a structure, $\text{TE}_x$ or $\text{TM}_x$ modes can be introduced.

To solve for these modes, considering $\Pi_x$ and $\Pi_{mx}$ instead of $\Pi_z$ and $\Pi_{mz}$.

**(a)** Derive the equations for the **E** and **H** fields using a procedure that led to Eqs. (5.93) and (5.96).

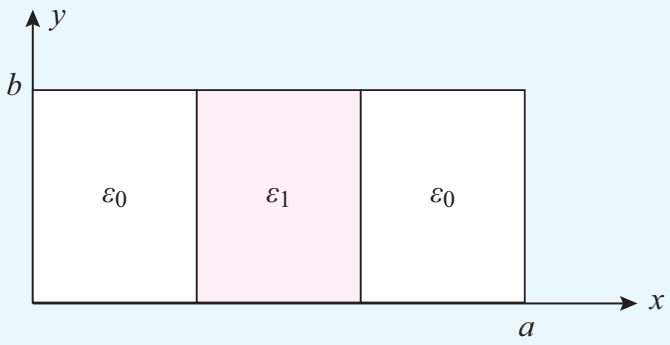


**Figure P6.8:** A partially filled rectangular waveguide with a dielectric slab of thickness $t$ filling the middle part of the waveguide. The planar sides of the slab are parallel to the short side walls of the waveguide.

**(b)** Find $\Pi_x$, $\mathbf{E}$, and $\mathbf{H}$ by applying the boundary condition.

**(c)** Show that the characteristic equations for determining the propagation constants of the $\text{TE}_x$ modes are

$$\frac{k_{x0}}{\mu_0}\cot\left(k_{x0}\frac{a-d}{2}\right)=\frac{k_{x1}}{\mu_1}\tan\left(k_{x1}\frac{d}{2}\right)$$

for the even mode, and

$$\frac{k_{x0}}{\mu_0}\cot\left(k_{x0}\frac{a-d}{2}\right)=-\frac{k_{x1}}{\mu_1}\cot\left(k_{x1}\frac{d}{2}\right)$$

for the odd mode. For $\text{TM}_x$

$$\frac{k_{x0}}{\varepsilon_0}\tan\left(k_{x0}\frac{a-d}{2}\right)=-\frac{k_{x1}}{\varepsilon_1}\tan\left(k_{x1}\frac{d}{2}\right)$$

for the even mode, and

$$\frac{k_{x0}}{\varepsilon_0}\tan\left(k_{x0}\frac{a-d}{2}\right)=\frac{k_{x1}}{\varepsilon_1}\cot\left(k_{x1}\frac{d}{2}\right)$$

for the odd mode, where

$$k_{x0}^2+\left(\frac{n\pi}{b}\right)^2+k_z^2=k_0^2$$

and

$$k_{x1}^2+\left(\frac{n\pi}{b}\right)^2+k_z^2=k_1^2\,.$$

**6.9** Show that the $TM_z$ modes in the isosceles right-triangular waveguide shown in Fig. P6.9, with base side $a$, can be found by specializing the results for a rectangular waveguide to the square case $b = a$, and then finding the linear combinations of the eigenfunctions of the form $f_{mn} = (\psi_{mn} + \alpha\psi_{nm})$ for an appropriate constant $\alpha$ that vanishes on the diagonal side defined by $y = x$ as well as the two sides defined by $y = 0$ and $x = a$. First show why $f_{mn}$ can be an eigenfunction, and then find $\alpha$ by satisfying the boundary conditions. Then find the first five modes of the waveguide. Do the same for $TE_z$ modes. *Note:* The sum of two eigenfunctions is an eigenfunction only if their two eigenvalues are the same.

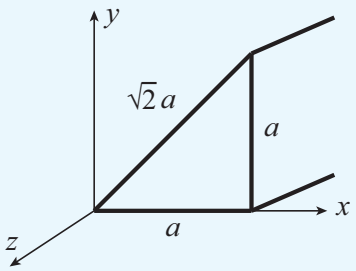


**Figure P6.9:** The configuration of a metallic waveguide with an isosceles cross section.

**6.10** Consider a rectangular waveguide with dimensions $a$ and $b$ with $a > b$, as shown in Fig. P6.10. Suppose the vertical side wall of the waveguide at $x = a$ is a reactive impedance surface with surface impedance $Z_s = -iX_s$. Find the propagation constant for TE modes.

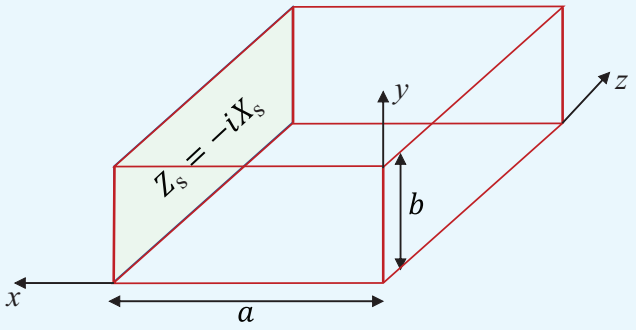


**Figure P6.10:** The geometry of a rectangular waveguide with three sides made from metallic surfaces and one side made from a reactive impedance surface.

**6.11** Suppose a general waveguide is operated at a frequency below its cutoff frequency. Find the time-average net amount of stored energy within a segment of the waveguide of length $L$ in terms of the associated eigenfunction. (*Hint:* Apply the complex Poynting vector to the volume defined by the waveguide walls and the surfaces defined by $z = 0$ and $z = L$.)

**6.12** Following the procedure of Example 6-2, find the attenuation rate in a rectangular waveguide $TE_{20}$ and $TE_{11}$. Plot the attenuation rates for these modes for a rectangular waveguide with $a = 2b = 2.89$ cm as a function of frequency.

## Cavity

**6.13** A rectangular cavity is made from a piece of copper ($\sigma = 5.813 \times 10^7$ S/m) with $a = 4.755$ cm and $b = 2.215$ cm, as shown in Fig. P6.13. The cavity is filled with polyethylene ($\varepsilon_r = 2.25$, $\tan\delta = \varepsilon''/\varepsilon' = 0.0004$). If the resonant frequency of $TE_{101}$ mode is 5 GHz, find the required length $c$ and the $\breve{Q}$ of the cavity.

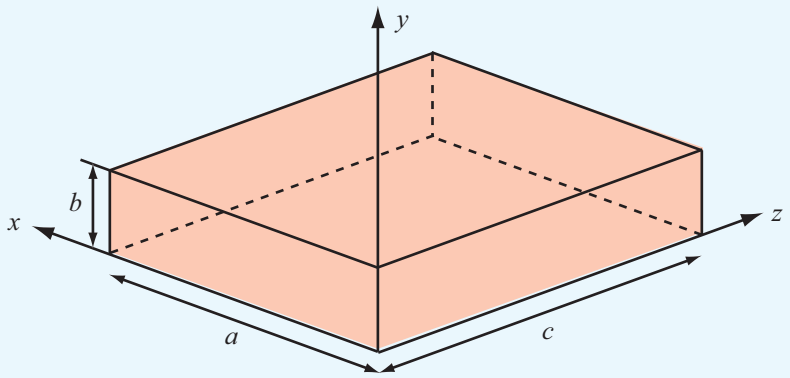


**Figure P6.13:** A metallic rectangular cavity made from copper with finite conductivity.

**6.14** Given a rectangular cavity of dimensions 2 cm × 3 cm × 1 cm:

**(a)** How many electromagnetic modes of wavelength $\lambda$ exist in the cavity in the range $4/\sqrt{5}$ cm $\leq \lambda \leq 8/\sqrt{13}$ cm? Find the wavelengths.

**(b)** Write down the expression for the electric field for each mode.

**(c)** Approximately how many modes are there in the range 0.01 cm $\leq \lambda \leq$ 0.011 cm?

**6.15** Consider an air-filled rectangular cavity with dimensions $a$, $b$, and $c$, and which is partially filled with a dielectric material $\varepsilon$, as shown in Fig. P6.15. Find the resonant frequencies for such a cavity.

## Modal Expansion

**6.16** Consider a standard rectangular waveguide, extending from $z = 0$ to $\infty$, as shown in Fig. P6.16. Suppose we excite the waveguide with a field $\mathbf{H} = H_0\,\hat{\mathbf{x}}$ at the $z = 0$ aperture. Find the amplitudes of the different modes within the waveguide.

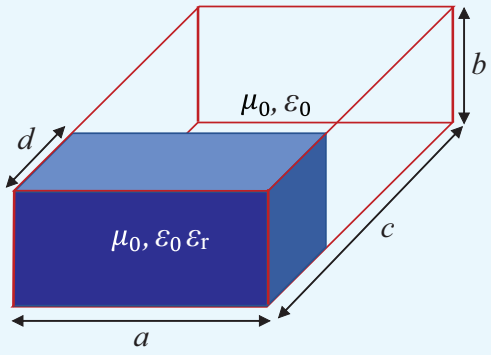


**Figure P6.15:** A rectangular cavity partially filled with a dielectric material.

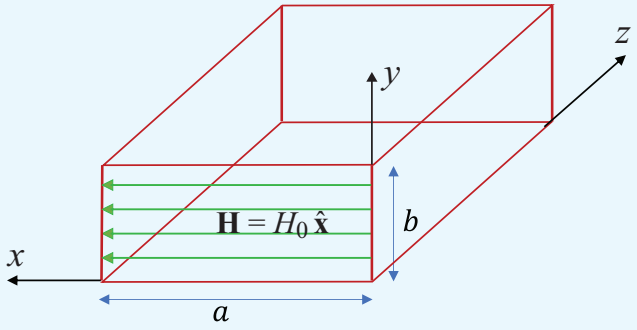


**Figure P6.16:** A rectangular waveguide excited by a uniform magnetic field $\mathbf{H} = H_0\,\hat{\mathbf{x}}$ for $0 < x < a$.

**6.17** Consider an arbitrary waveguide with eigenfunctions $\psi_{mn}$ supporting a $z$-directed current along the waveguide. Suppose the current distribution in the cross section of the waveguide is given by $J_z(\boldsymbol{\rho})\, e^{i\beta z}$. Using Green's function inside the waveguide, find the resulting scalar potential $\psi$, noting that $\psi$ satisfies

$$\nabla_t^2 \psi + k_c^2 \psi = \frac{-i}{\omega\varepsilon}\, \mathbf{J}_z(\boldsymbol{\rho})\ .$$

Also, for a rectangular waveguide, consider a current source of the following form:

$$\mathbf{J}(x,y) = I_0 \delta\left(x - \frac{a}{2}\right) \sin\left(\frac{\pi y}{b}\right) e^{i\beta z}\, \hat{\mathbf{z}}\ .$$

Find the scalar potential $\psi$ and the fields inside the waveguide.

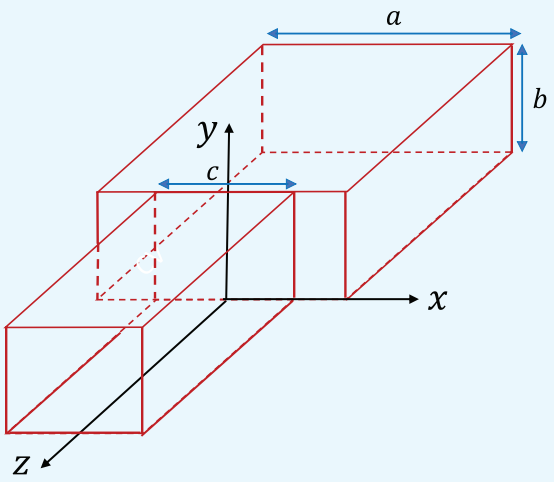


**Figure P6.18:** Configuration of a junction between two rectangular waveguides with dissimilar widths but the same height. The incident wave propagating in the $+z$ direction gets partially reflected at the junction. Away from transition on both sides of the junction only the dominant modes can propagate, but higher-order modes are excited locally.

**6.18** Consider a rectangular waveguide with a discontinuity at $z = 0$ that is terminated in matched loads at both ends, as shown in Fig. P6.18. Assume that the propagating mode in both sections $z < 0$ and $z > 0$ is $\mathrm{TE}^{z}_{10}$. However, in the vicinity of the discontinuity, the fields can be expressed as the superposition of $\mathrm{TE}^{x}_{mn}$ modes. Assuming that $E_y$ at the discontinuity ($z = 0$) is the same as that of the incident wave, find the following:

**(a)** The amplitude of the excited $\mathrm{TE}^{x}_{mn}$ modes at $z = 0$.

**(b)** The aperture susceptance due to this discontinuity, defined as

$$\Im\mathrm{m}[Y_{\mathrm{a}}] = \Im\mathrm{m}\left[\frac{P^*}{|V|^2}\right] ,$$

where $P$ is the $z$-directed complex power at $z = 0$:

$$P = \iint_{z=0} \mathbf{E} \times \mathbf{H}^* \cdot d\mathbf{S} ,$$

and $V$ is the maximum voltage across the aperture:

$$V = \int_{\substack{0 \\ x=0,\ z=0}}^{b} E_y \, dy .$$

**6.19** Suppose the material making a waveguide is such that the boundary condition on its surface is given by

$$\frac{d\psi_{mn}}{dn} + \alpha\psi_{mn} = 0 \,,$$

with $\alpha > 0$. Show that potential $\psi_{mn}$ that satisfies the 2-D wave equation

$$\nabla_{\mathrm{t}}^2\psi_{mn} + k_{mn}^2\psi_{mn} = 0$$

has eigenvalues $k_{mn}^2$ that are real positive numbers.

**6.20** Consider a waveguide with boundary condition

$$\frac{d\psi_{mn}}{dn} + \alpha\psi_{mn} = 0 \,.$$

If $\psi_{mn}$ and $\psi_{m'n'}$ are solutions to the 2-D wave equation with different eigenvalues of $k_{mn}^2$ and $k_{m'n'}^2$, show that

$$\iint_S \psi_{mn}\psi_{m'n'}\, ds = 0 \,.$$

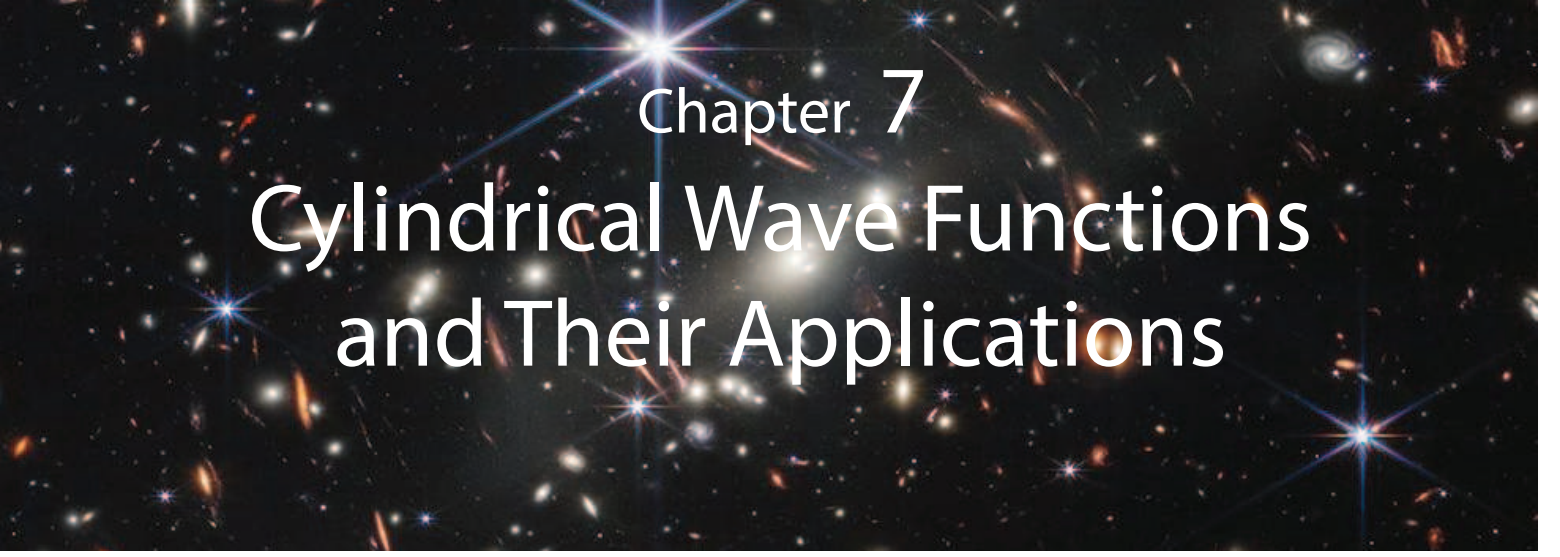

# Chapter 7
# Cylindrical Wave Functions and Their Applications

## Chapter Contents


Overview, 405
7-1 Wave Functions in the Cylindrical Coordinate System, 406
7-2 The Circular Dielectric Waveguide, 427
7-3 Radial and Circumferential Waveguides, 433
7-4 Green's Function Solutions for Some Canonical Problems, 436
7-5 Scattering from a Metallic Circular Cylinder, 455
7-6 Integral Representation of Bessel Functions, 464
7-7 2-D Green's Function for Homogeneous Media in the Presence of a Metallic Wedge, 471
7-8 Asymptotic Evaluation of a Field Diffracted by a Metallic Wedge, 478
Chapter Summary, 490
Problems, 497


## Objectives

Upon learning the material presented in this chapter, you should be able to:

1. Solve boundary-value problems associated with wave equations and objects whose boundary coincides with constant surfaces in a cylindrical coordinate system.
2. Understand the properties of cylindrical wave functions and choose an appropriate set of such functions for the problem at hand.
3. Determine TE and TM modes of propagation and their cutoff frequencies in circular metallic and dielectric (optical-fiber) waveguides.
4. Learn about other forms of cylindrical wave propagation in the radial and circumferential directions.
5. Express Green's function in free space and in circular and sectoral waveguides, as well as external configurations such as metallic cylinders and wedges, in terms of cylindrical wave functions.
6. Use the integral representation of Bessel functions in the asymptotic evaluation of fields scattered by metallic wedges.

## Overview

This chapter deals with the solution of wave equations in a cylindrical coordinate system. TE and TM wave solutions to two-dimensional boundary-value problems are obtained for special cases where the boundary of the object coincides with the coordinate surfaces of a cylindrical coordinate system. Initially the method of separation of variables is applied to the homogeneous scalar wave equation expressed in terms of cylindrical coordinate variables. In situations where such solutions are admissible, the solutions for the $z$-function and $\phi$-function are found to be harmonic functions, whereas the solution for the radial function is a Bessel function. Depending on whether the desired domain includes the entire range $0 \leq \phi \leq 2\pi$ or not, the order of the Bessel functions may or may not be integer number. The properties of cylindrical wave functions are presented so that a proper solution based on the domain of interest can be chosen. A linear combination of cylindrical wave functions, in general, represents the solution to the wave equation. Using the cylindrical wave function, the TE and TM field expressions are obtained for waveguides with a circular cross section and the properties of different modes of such waveguides are examined. It is shown that the different modes of cylindrical waveguides are orthogonal and the total power carried by a wave in the waveguide is the sum of the power carried by the propagating modes of the wave. Cylindrical wave functions are also used to study propagating modes on circular dielectric waveguides, which are known as ***optical fibers***. It is shown that the dominant mode of propagation in a circular dielectric waveguide is a hybrid TE and TM mode. That is, both modes must be considered together when applying the boundary conditions to arrive at a solution. It is also shown that for azimuthally symmetric modes (where fields are independent of $\phi$), the circular dielectric waveguide can support TE and TM modes. Other metallic waveguide geometries, such as angular-sector waveguides that can support Bessel functions of noninteger order, are also considered. The resonant modes and quality factor for a cylindrical cavity are obtained for both TE and TM modes, and an expression for the quality factor of the dominant mode ($TM_{010}$) due to ohmic losses of the walls is found. Other types of waveguides with propagation directions along $\rho$ and $\phi$, known as ***radial waveguides*** and ***circumferential waveguides***, are also presented and the behavior of the fields for such waveguides, which are bounded by two parallel metallic plates perpendicular to the $z$-axis, are studied as well. The responses of the wave equation to a line source (Green's function) in free space, inside a cylindrical waveguide, or outside of a metallic cylinder or infinite wedge, are obtained and studied. The expressions for Green's functions in terms of a series expansion of eigenfunctions are shown to converge poorly. Alternative solutions, referred to as the formal solution, which are derived directly from the wave equation, are presented and shown to be computationally more efficient. A solution based on Fourier transformation of the 2-D free-space Green's function is obtained, from which the ***addition theorem*** for Bessel functions is derived. Plane-wave scattering from a metallic circular cylinder as well as a metallic wedge are presented in terms of a series expansion of appropriate cylindrical wave functions. Then the integral representation of Bessel functions is derived and used to derive an asymptotic solution in the far-field region of a metallic wedge.

## 7-1 Wave Functions in the Cylindrical Coordinate System

In certain scattering and radiation problems where the current distributions' or objects' boundaries coincide with cylindrical coordinate surfaces, solutions may be best obtained using a comparable cylindrical coordinate system. In a source-free and homogeneous region, the scalar potential satisfies the Helmholtz equation given by

$$\nabla^2\psi + k^2\psi = 0\,. \tag{7.1}$$

In cylindrical coordinates, Eq. (7.1) takes the following form:

$$\frac{1}{\rho}\frac{\partial}{\partial\rho}\left(\rho\frac{\partial\psi}{\partial\rho}\right) + \frac{1}{\rho^2}\frac{\partial^2\psi}{\partial\phi^2} + \frac{\partial^2\psi}{\partial z^2} + k^2\psi = 0\,. \tag{7.2}$$

We assume that the scalar potential can be expressed in terms of the product of three functions, each being a function of only $\rho$, $\phi$, or $z$ variables; i.e.,

$$\psi = R(\rho)\,\Phi(\phi)\,Z(z)\,. \tag{7.3}$$

Equation (7.2) can be separated into three differential equations. By substituting Eq. (7.3) into Eq. (7.2) and then dividing both sides by $R\Phi Z$, the process leads to

$$\frac{1}{\rho R}\frac{\partial}{\partial\rho}\left(\rho\frac{\partial R}{\partial\rho}\right) + \frac{1}{\rho^2\Phi}\frac{\partial^2\Phi}{\partial\phi^2} + \frac{1}{Z}\frac{\partial^2 Z}{\partial z^2} + k^2 = 0\,. \tag{7.4}$$

In Eq. (7.4) $(1/Z)(\partial^2 Z/\partial z^2)$ is only a function of $z$, and the rest of the terms are independent of $z$. This can only happen if

$$\frac{1}{Z}\frac{\partial^2 Z}{\partial z^2} = -k_z^2 \tag{7.5}$$

for some constant $k_z^2$.

Equation (7.4) can now be rewritten as

$$\frac{\rho}{R}\frac{d}{d\rho}\left(\rho\frac{dR}{d\rho}\right) + \frac{1}{\Phi}\frac{d^2\Phi}{d\phi^2} + k_\rho^2\rho^2 = 0\,, \tag{7.6}$$

where $k_\rho^2 = k^2 - k_z^2$. Now, in Eq. (7.6), $(1/\Phi)(d^2\Phi/d\phi^2)$ is only a function of $\phi$, and the other terms are independent of $\phi$. In order for Eq. (7.6) to hold, the following must be true:

$$\frac{1}{\Phi}\frac{d^2\Phi}{d\phi^2} = -\nu^2 \tag{7.7}$$

for some constant $\nu$. As a result the following must be true:

$$\rho\frac{d}{d\rho}\left(\rho\frac{dR}{d\rho}\right) + \left[(k_\rho\rho)^2 - \nu^2\right]R = 0\,. \tag{7.8}$$

Clearly, the solution for $R(\rho)$ will depend on $\nu$, and as we will see shortly, the form of the

solution is in terms of Bessel functions of order $\nu$. Hence, to emphasize that fact, we will henceforth add a subscript $\nu$ to $R$.

Upon expanding Eq. (7.8) into

$$(k_\rho\rho)^2\frac{d^2R_\nu}{d(k_\rho\rho)^2}+(k_\rho\rho)\frac{dR_\nu}{d(k_\rho\rho)}+[(k_\rho\rho)^2-\nu^2]R_\nu=0\,, \tag{7.9}$$

and then using a change of variable, namely $\widetilde{\rho}=k_\rho\rho$, Eq. (7.9) can be modified into

$$\frac{d^2R_\nu}{d\widetilde{\rho}^2}+\frac{1}{\widetilde{\rho}}\frac{dR_\nu}{d\widetilde{\rho}}+\left[1-\left(\frac{\nu}{\widetilde{\rho}}\right)^2\right]R_\nu=0\,, \tag{7.10}$$

which is known as ***Bessel's equation of order $\nu$***.

The Helmholtz equation is now separated into three second-order differential equations. Solutions to Eqs. (7.5) and (7.7) are harmonic functions of the form

$$Z(z)=Ae^{ik_zz}+Be^{-ik_zz} \tag{7.11a}$$

and

$$\Phi(\phi)=Ce^{i\nu\phi}+De^{-i\nu\phi}\,. \tag{7.11b}$$

As noted earlier, Eq. (7.8) is a Bessel equation of order $\nu$, whose solution can be expressed in terms of a linear combination of real functions $N_\nu(k_\rho\rho)$ and $J_\nu(k_\rho\rho)$:

$$R_\nu(k_\rho\rho)=AJ_\nu(k_\rho\rho)+BN_\nu(k_\rho\rho)\,, \tag{7.12}$$

where subscript $\nu$ has been added to $R$ to emphasize its order, $J_\nu(k_\rho\rho)$ is the ***Bessel function of the first kind and $\nu$th order*** and $N_\nu(k_\rho\rho)$ is the ***Bessel function of the second kind and $\nu$th order***. The solution of Eq. (7.8) can also be expressed as a linear combination of ***Hankel functions of the first kind*** ($H_\nu^{(1)}(k_\rho\rho)$) and ***Hankel functions of the second kind*** ($H_\nu^{(2)}(k_\rho\rho)$) kind, defined by

$$H_\nu^{(1)}(k_\rho\rho)=J_\nu(k_\rho\rho)+iN_\nu(k_\rho\rho) \tag{7.13a}$$

and

$$H_\nu^{(2)}(k_\rho\rho)=J_\nu(k_\rho\rho)-iN_\nu(k_\rho\rho)\,. \tag{7.13b}$$

In situations where the domain of interest includes points whose $\phi$ coordinate spans the entire domain $[0,2\pi]$, it is necessary that

$$\psi(\rho,\phi,z)=\psi(\rho,\,\phi+2\pi,\,z)\,. \tag{7.14}$$

In other words, $\psi$ must be periodic in $\phi$ if $\psi$ is to be single-valued. In such a case we must choose $\nu=n$, where $n$ is an integer and the possible solutions for $\phi$ are of the following form:

$$\Phi(\phi)=Ae^{in\phi}+Be^{-in\phi}\,, \tag{7.15}$$

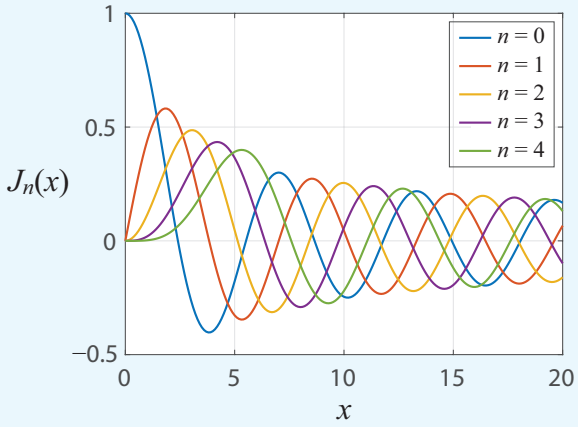


**Figure 7-1:** Bessel functions of the first kind with integer order.

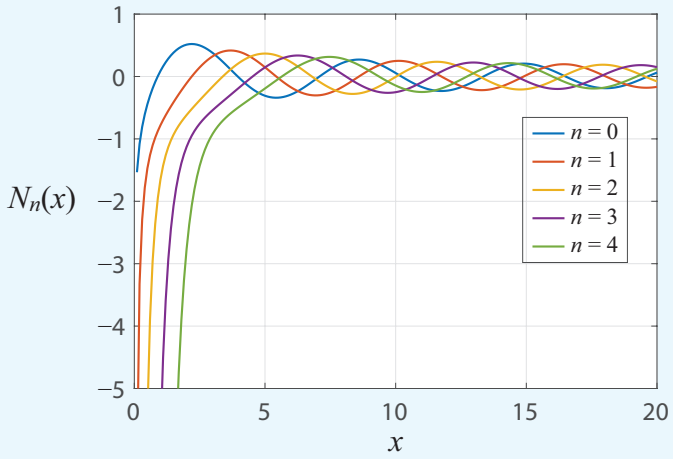


**Figure 7-2:** Bessel functions of the second kind with integer order.

which is a periodic function with period $2\pi$. In this case, the order of Bessel's functions are all integer. Figures 7-1 and 7-2 show the plot of Bessel functions of the first kind and the second kind for integer orders. As shown, the Bessel functions of the first kind are regular everywhere, whereas the Bessel functions of the second kind have singularity at $x = 0$.

To construct proper solutions for $\psi$, certain properties of Bessel functions must be taken into account. Among the possible solutions presented, only $J_n(k_\rho \rho)$ are nonsingular at $\rho = 0$. Also, the asymptotic behavior of Bessel functions as $k_\rho \rho \to \infty$ is of interest to identify

outgoing and incoming waves. The asymptotic behaviors of Bessel functions are given by

$$\lim_{k_\rho \rho \to \infty} J_n(k_\rho \rho) \approx \sqrt{\frac{2}{\pi k_\rho \rho}} \cos\left(k_\rho \rho - \frac{2n+1}{4}\pi\right) , \tag{7.16a}$$

$$\lim_{k_\rho \rho \to \infty} N_n(k_\rho \rho) \approx \sqrt{\frac{2}{\pi k_\rho \rho}} \sin\left(k_\rho \rho - \frac{2n+1}{4}\pi\right) , \tag{7.16b}$$

$$\lim_{k_\rho \rho \to \infty} H_n^{(1)}(k_\rho \rho) \approx \sqrt{\frac{2}{\pi k_\rho \rho}}\, e^{i[k_\rho \rho - (2n+1)\pi/4]} , \tag{7.16c}$$

and

$$\lim_{k_\rho \rho \to \infty} H_n^{(2)}(k_\rho \rho) \approx \sqrt{\frac{2}{\pi k_\rho \rho}}\, e^{-i[k_\rho \rho - (2n+1)\pi/4]} . \tag{7.16d}$$

These expressions are obtained from an asymptotic evaluation of the integral representation of Bessel function. It is clear from the sign of the exponents in their expressions for $H_n^{(1)}(k_\rho \rho)$ that it represents an outgoing cylindrical wave whereas $H_n^{(2)}(k_\rho \rho)$ represents an incoming wave.

The solution to the Helmholtz equations consists of a linear combination of the elementary cylindrical wave functions for all discrete values of $n$ and continuous values of $k_z$. Hence, a solution of the Helmholtz equation may be expanded in terms of the elementary cylindrical functions as

$$\psi(\rho, \phi, z) = \sum_{n=-\infty}^{+\infty} \int_{-\infty}^{+\infty} \left[A_n(k_z)\, J_n(k_\rho \rho) + B_n(k_z)\, N_n(k_\rho \rho)\right] e^{in\phi}\, e^{ik_z z}\, dk_z . \tag{7.17}$$

Noting that

$$k_\rho = \sqrt{k^2 - k_z^2} \tag{7.18}$$

in Eq. (7.17), as $k_z$ varies from $-\infty$ to $+\infty$, $k_\rho$ can become imaginary. For values of $|k_z| < k$ the argument of the Bessel functions is real in a lossless medium and the elementary wave functions can be decomposed into incoming and outgoing propagating cylindrical waves. However, for the rest of $k_z$ values ($|k_z| > k$), the argument of the Bessel functions becomes pure imaginary, and the radial wave function become exponentially decaying. In these cases, it is conventional to use the modified Bessel functions $I_n$ and $K_n$ defined by

$$J_n(i\alpha\rho) = (i)^n\, I_n(\alpha\rho) \tag{7.19a}$$

and

$$H_n^{(1)}(i\alpha\rho) = \frac{2}{\pi}\,(i)^{n+1}\, K_n(\alpha\rho) . \tag{7.19b}$$

Figures 7-3 and 7-4 show the modified Bessel functions of the first and second kind for integer orders, which demonstrate the exponential decay behavior of the modified Bessel functions

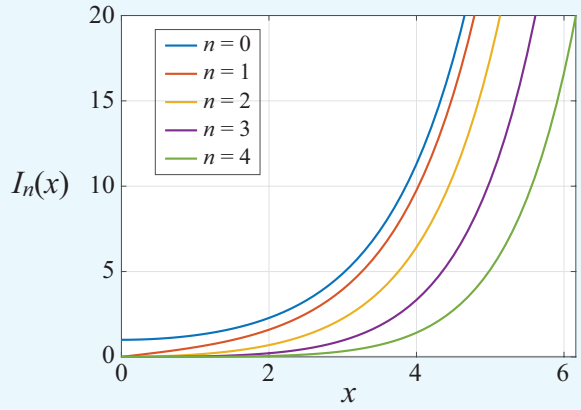


**Figure 7-3:** The modified Bessel functions of the first kind with integer order.

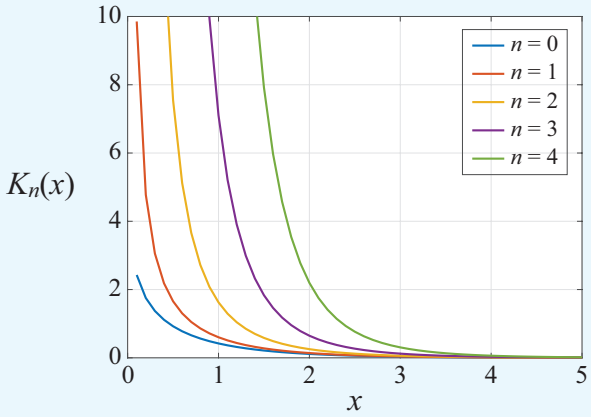


**Figure 7-4:** The modified Bessel functions of the second kind with integer order.

of the second kind as their arguments increase. The large-argument approximation can be obtained from Eqs. (7.16a) and (7.16c):

$$\lim_{\alpha\rho\to\infty} I_n(\alpha\rho) \approx \frac{e^{\alpha\rho}}{\sqrt{2\pi\alpha\rho}} \tag{7.20a}$$

and

$$\lim_{\alpha\rho\to\infty} K_n(\alpha\rho) \approx \sqrt{\frac{\pi}{2\alpha\rho}}\, e^{-\alpha\rho} \,. \tag{7.20b}$$

It should be emphasized here that the modified Bessel functions do not satisfy the Bessel equation given by Eq. (7.10), but they instead satisfy the modified Bessel equation given by

$$\frac{d^2R_\nu}{d\rho^2}+\frac{1}{R_\nu}\frac{dR_\nu}{d\rho}-\left[1+\left(\frac{\nu}{R}\right)^2\right]R_\nu=0\,. \tag{7.21}$$

### 7-1.1 Some Useful Properties of Bessel Functions

As mentioned previously, the radial solution in the cylindrical coordinate system satisfies the following ordinary second-order differential equation:

$$\frac{d^2R_\nu}{d\widetilde{\rho}^2}+\frac{1}{\widetilde{\rho}}\frac{dR_\nu}{d\widetilde{\rho}}+\left(1-\frac{\nu^2}{\widetilde{\rho}^2}\right)R_\nu=0\,, \tag{7.22}$$

where $\widetilde{\rho}$ represents $k_\rho\rho$ in Eq. (7.8). The series solution for $R_\nu$, where $\nu$ can be any real or complex number, is given by

$$R_\nu(\widetilde{\rho})=\sum_{m=0}^{\infty}\frac{(-1)^m}{m!\,\Gamma(\nu+m+1)}\left(\frac{\widetilde{\rho}}{2}\right)^{\nu+2m}\,, \tag{7.23}$$

where the ***gamma function*** is defined as

$$\Gamma(x)=\int_0^\infty t^{x-1}e^{-t}\,dt\,, \tag{7.24}$$

with the well-known property

$$\Gamma(x)=\frac{1}{x}\,\Gamma(x+1)\,.$$

Since Eq. (7.22) is quadratic with respect to $\nu$, a second solution for Eq. (7.22) can easily be obtained simply by replacing $\nu$ with $-\nu$. However, this cannot be done when $\nu$ is an integer. In situations where $\nu=n$, the gamma function $\Gamma$ simplifies to $\Gamma(\nu+m+1)=(n+m)!$, and the resulting solution is the Bessel function of the first kind given by

$$J_n(\rho)=\sum_{m=0}^{\infty}\frac{(-1)^m}{m!\,(n+m)!}\left(\frac{\rho}{2}\right)^{n+2m}\,. \tag{7.25}$$

In this case $J_{-n}(\rho)$ is not independent of $J_n(\rho)$; in fact,

$$J_{-n}(\rho)=(-1)^n\,J_n(\rho)\,. \tag{7.26}$$

This can easily be shown by changing $n$ to $-n$ in Eq. (7.25) and changing index $m$ to $m'+n$ (noting that the reciprocal of the gamma function of a negative integer is zero). In general, the Bessel function of the second kind is defined using

$$N_\nu(\rho)=\frac{1}{\sin\nu\pi}\,[J_\nu(\rho)\cos\nu\pi-J_{-\nu}(\rho)], \tag{7.27}$$

which is independent of Eq. (7.25) even for integer-order $\nu = n$. Also, the following recurrence relation is useful for computation of higher-order Bessel functions in terms of the lower-order counterparts and vice versa:

$$R_{\nu-1} + R_{\nu+1} = \frac{2\nu}{\rho} R_\nu \ . \tag{7.28}$$

To compute the derivatives, the following recurrence relations may be used:

$$\frac{dR_\nu}{d\rho} = \frac{1}{2} \left[R_{\nu-1} - R_{\nu+1}\right] , \tag{7.29a}$$

$$\frac{d}{d\rho} \left[\rho^\nu \, R_\nu(\rho)\right] = \rho^\nu R_{\nu-1} \ , \tag{7.29b}$$

$$\frac{d}{d\rho}[\rho^\nu \, R_\nu(\rho)] = -\rho^{-\nu} R_{\nu+1} \ . \tag{7.29c}$$

Another useful relationship is the ***Wronskian***, given by

$$W = J_\nu(\rho) \, N'_\nu(\rho) - J'_\nu(\rho) \, N_\nu(\rho) = \frac{2}{\pi\rho} \ . \tag{7.30}$$

A similar Wronskian can easily be obtained between $J_\nu(\rho)$ and $H_n^{(1)}(\rho)$:

$$J_\nu(\rho) \, H_\nu^{(1)'}(\rho) - J'_\nu(\rho) \, H_\nu^{(1)}(\rho) = \frac{i2}{\pi\rho} \ . \tag{7.31}$$

The recurrence relations for the modified Bessel functions are given by

$$I_{\nu-1} - I_{\nu+1} = \frac{2\nu}{\rho} I_\nu \tag{7.32a}$$

and

$$K_{\nu-1} - K_{\nu+1} = -\frac{2\nu}{\rho} K_\nu \ , \tag{7.32b}$$

and the derivatives are given by

$$\frac{dI_\nu}{d\rho} = \frac{1}{2} \left[I_{\nu-1} + I_{\nu+1}\right] , \tag{7.33a}$$

$$\frac{dK_\nu}{d\rho} = -\frac{1}{2} \left[K_{\nu-1} + K_{\nu+1}\right] , \tag{7.33b}$$

$$\frac{d}{d\rho} \left[\rho^\nu \, I_\nu(\rho)\right] = \rho^\nu \, I_{\nu-1}(\rho) \ , \tag{7.33c}$$

and

$$\frac{d}{d\rho}\,[\rho^{\nu}\,K_{\nu}(\rho)] = -\rho^{\nu}\,K_{\nu-1}(\rho)\,. \tag{7.33d}$$

### 7-1.2 Orthogonality Relations

Unlike most orthogonal functions and polynomials, the orthogonality of Bessel functions exists among the same kind and same order, but with differently scaled argument. This stems from the fact that

$$\int_0^a J_{\nu}(k_p\rho)\,J_{\nu}(k_q\rho)\,\rho\,d\rho = \frac{a}{k_p^2-k_q^2}\,\left[k_q\,J_{\nu}(k_pa)\,J'_{\nu}(k_qa) - k_q\,J_{\nu}(k_qa)\,J'_{\nu}(k_pa)\right] \tag{7.34}$$

for arbitrary real numbers $k_p$ and $k_q$. Denoting zeros of $J_{\nu}(x)$ by $x_{\nu p}$ and zeros of $J'_{\nu}(x)$ by $x'_{\nu p}$, where $p$ is an integer index ($p = 1,2,3,\ldots$), by choosing

$$k_p = \frac{x_{\nu p}}{a}\,, \tag{7.35a}$$

$$k_q = \frac{x_{\nu q}}{a}\,, \tag{7.35b}$$

or

$$k_p = \frac{x'_{\nu p}}{a}\,, \tag{7.35c}$$

$$k_q = \frac{x'_{\nu q}}{a}\,, \tag{7.35d}$$

the right-hand side of Eq. (7.34) vanishes when $p \neq q$. That is, the orthogonality relations for Bessel functions of the first kind are given by

$$\int_0^a J_{\nu}\left(\frac{x_{\nu p}}{a}\,\rho\right)\,J_{\nu}\left(\frac{x_{\nu q}}{a}\,\rho\right)\,\rho\,d\rho = 0 \tag{7.36a}$$

and

$$\int_0^a J_{\nu}\left(\frac{x'_{\nu p}}{a}\,\rho\right)\,J_{\nu}\left(\frac{x'_{\nu q}}{a}\,\rho\right)\,\rho\,d\rho = 0\,. \tag{7.36b}$$

In cases where $p = q$, both the numerator and the denominator of Eq. (7.34) go to zero. L'Hôpital's rule must be applied to evaluate the value of the integral. Substituting $x$ for $k_pa$ and $x'$ for $k_qa$, Eq. (7.34) can be evaluated from

$$\lim_{x\to x'} \frac{a^2\,[x'\,J_{\nu}(x)\,J'_{\nu}(x') - x\,J_{\nu}(x')\,J'_{\nu}(x)]}{x^2-x'^2} \approx \frac{a^2x\,J'_{\nu}(x)\,\,[J_{\nu}(x)-J_{\nu}(x')]}{2x(x-x')}$$

$$= \frac{a^2x\,J'_{\nu}(x)\,J'_{\nu}(x)\,(x-x')}{2x(x-x')} = \frac{a^2}{2}\,\left[J'_{\nu}(x)\right]^2\,. \tag{7.37}$$

Now, using the recurrence relation

$$J'_\nu(x) = \frac{\nu}{\rho} J_\nu(x) - J_{\nu+1}(x) \ , \tag{7.38}$$

and substituting $x_{\nu p}$ for $x$, it becomes obvious that

$$J'_\nu(x_{\nu p}) = -J_{\nu+1}(x_{\nu p}) \ . \tag{7.39}$$

Therefore the norm of the Bessel functions of the first kind is given simply by

$$\int_0^a J_\nu^2 \left(\frac{x_p}{a}\,\rho\right) \rho \, d\rho = \frac{a^2}{2} \left[J_{\nu+1}(x_{\nu p})\right]^2 \ . \tag{7.40}$$

L'Hôpital's rule can also be applied differently:

$$\begin{aligned} \lim_{x\to x'} \frac{a^2 \left[x' \, J_\nu(x) \, J'_\nu(x') - x \, J_\nu(x') \, J'_\nu(x)\right]}{x^2 - x'^2} &\approx \frac{a^2 x \, J_\nu(x) \ \left[J'_\nu(x) + J''_\nu(x) \ (x'-x) - J'_\nu(x)\right]}{2x(x-x')} \\ &\approx -\frac{a^2}{2} \, J_\nu(x) \, J''_\nu(x) \ . \end{aligned} \tag{7.41}$$

Directly from the Bessel equation we have

$$J''_\nu(x) = -\frac{1}{x} J'_\nu(x) - \left(1 - \frac{\nu^2}{x^2}\right) J_\nu(x) \ . \tag{7.42}$$

Now letting $x = x'_{\nu p}$, it can easily be shown that

$$\int_0^a J_\nu^2 \left(\frac{x'_{\nu p}}{a}\,\rho\right) \rho \, d\rho = \frac{a^2}{2} \left[1 - \left(\frac{\nu^2}{x'_{\nu p}}\right)^2\right] \left[J_\nu(x'_{\nu p})\right]^2 \ , \tag{7.43}$$

which represents the norm of Bessel functions scaled by $x'_{\nu p}/a$ corresponding to Eq. (7.36b).

### 7-1.3 The Cylindrical Waveguide

Consider a metallic waveguide with circular cross-section of radius $a$, as shown in Fig. 7-5. The solution for the field quantities in the source-free region of a circular waveguide can be expressed in terms of TM and TE modes, for which we have respectively the following boundary conditions:

$$\psi(\boldsymbol{\rho}) = 0 \ , \qquad \boldsymbol{\rho} \text{ on } S \ , \qquad \textbf{(TM mode)}$$

and

$$\frac{\partial \psi}{\partial \rho} = 0 \ , \qquad \boldsymbol{\rho} \text{ on } S \ . \qquad \textbf{(TE mode)}$$

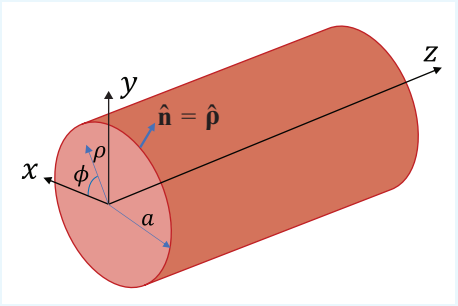


**Figure 7-5:** A metallic circular-cylindrical waveguide of radius $a$.

For a scalar potential $\psi$ that satisfies the 2-D Helmholtz equation in the cylindrical coordinate system,

$$\frac{1}{\rho}\frac{\partial}{\partial\rho}\left(\rho\frac{\partial\psi}{\partial\rho}\right)+\frac{1}{\rho^2}\frac{\partial^2\psi}{\partial\phi^2}+k_\rho^2\psi=0\,. \tag{7.44}$$

The method of separation of variables can be used to express $\psi$ in terms of the elementary wave functions in a cylindrical coordinate system. Since the domain of interest covers the entire range of $\phi$ ($[0,2\pi]$), then (as noted earlier in conjunction with Eq. (7.14)) the order of Bessel function $\nu$ must be an integer ($n$). Also, since the domain includes $\rho=0$, only the Bessel functions of the first kind are admissible. Hence a solution for $\psi$ can be written as

$$\psi(\rho,\phi)=A_n\,J_n(k_\rho\rho)\begin{cases}\sin(n\phi)\,,\\ \cos(n\phi)\,.\end{cases} \tag{7.45}$$

The choice of $\sin(n\phi)$ or $\cos(n\phi)$ is arbitrary, and one can be produced from the other by rotating the $x$–$y$ plane by 90° about the $z$-axis. Because of this circular symmetry of the problem, there is a multiplicity of two for all eigenvalues. That is, the modes are degenerate. For simplicity, we retain only the cosine function from hereon forward. Applying the boundary condition for a TM mode requires that

$$J_n(k_\rho a)=0\,. \tag{7.46}$$

Denoting the zeros of $J_n$ by $x_{np}$, where $p$ is the ascending order of the zeros of $J_n$, $k_\rho$ can be obtained from

$$k_\rho=\frac{x_{np}}{a}\,. \tag{7.47}$$

The propagation constant in the waveguide is therefore given by

$$\beta=\sqrt{k^2-\left(\frac{x_{np}}{a}\right)^2}\,. \tag{7.48}$$

The roots of the first few orders of Bessel function $J_n(X)$ are listed in Table 7-1. The TM cutoff frequency for a specific mode and for a waveguide filled with homogeneous material

**Table 7-1: Roots $x_{np}$ of the first few orders of Bessel function $J_n(x)$ for TM modes. Here, $n$ represents the order of the Bessel function and $p$ represents the order of its zeros $x_{np}$.**

| $p$ ↓ | $n$ | | | | |
|---|---|---|---|---|---|
| | 0 | 1 | 2 | 3 | 4 |
| 1 | 2.405 | 3.832 | 5.138 | 6.380 | 7.588 |
| 2 | 5.520 | 7.016 | 8.417 | 9.761 | 11.065 |
| 3 | 8.654 | 10.173 | 11.620 | 13.015 | 14.372 |
| 4 | 11.792 | 13.324 | 14.796 | | |

**Table 7-2: Roots $x'_{np}$ of the first few orders of $J'_n(x')$ for TE modes. Here, $n$ represents the order of $J'_n(x')$ and $p$ represents the order of its zeros $x'_{np}$.**

| $p$ ↓ | $n$ | | | | |
|---|---|---|---|---|---|
| | 0 | 1 | 2 | 3 | 4 |
| 1 | 3.832 | 1.841 | 3.054 | 4.201 | 5.317 |
| 2 | 7.016 | 5.331 | 6.706 | 8.015 | 9.282 |
| 3 | 10.173 | 8.536 | 9.969 | 11.346 | 12.682 |
| 4 | 13.324 | 11.706 | 13.170 | | |

having permittivity $\varepsilon$ and permeability $\mu$ is given by

$$k_c^{(np)} = k_\rho = \frac{x_{np}}{a} , \tag{7.49a}$$

$$2\pi f_c^{\mathrm{TM}(np)} \sqrt{\mu\varepsilon} = \frac{x_{np}}{a} , \tag{7.49b}$$

and

$$f_c^{\mathrm{TM}(np)} = \frac{x_{np}}{2\pi a \sqrt{\mu\varepsilon}} . \tag{7.49c}$$

Applying the boundary condition for a TE mode, we need to have

$$J'_n(k_\rho a) = 0 .$$

Denoting the roots of $J'_n(X)$ by $x'_{np}$, where again $p$ is an ascending order of zeros of $J'_n(X)$, $k_\rho$ is given by

$$k_\rho^{\mathrm{TE}} = \frac{x'_{np}}{a} . \tag{7.50}$$

The values of these roots for the first few orders of the Bessel functions (first kind) are provided in Table 7-2. The cutoff frequency for TE modes of a homogeneously filled circular

waveguide is given by

$$f_c^{\mathrm{TE}(np)} = \frac{x'_{np}}{2\pi a\sqrt{\mu\varepsilon}}\,. \tag{7.51}$$

The dominant mode of propagation in a circular waveguide corresponds to the smallest value among the roots $x_{np}$ and $x'_{np}$. Referring to Tables 7-1 and 7-2, the dominant mode is $\mathrm{TE}_{11}$. The field distribution of the first few modes of TE and TM modes are shown in Fig. 7-6. The order of propagating modes are $\mathrm{TE}_{11}$, $\mathrm{TM}_{01}$, $\mathrm{TE}_{21}$, ($\mathrm{TM}_{11}$, $\mathrm{TE}_{01}$), $\mathrm{TE}_{31}$, etc. The eigenvalues for $\mathrm{TM}_{11}$ and $\mathrm{TE}_{01}$ are the same, and thus these modes are degenerate.

The field distribution for a TM mode can be obtained from Eqs. (5.102a) and (5.102b), and it is given by

$$E_\rho(\rho,\phi,z) = E_0 i\beta\left(\frac{x_{np}}{a}\right) J'_n\left(\frac{x_{np}}{a}\rho\right)\cos(n\phi)\,e^{i\beta z}\,, \tag{7.52a}$$

$$E_\phi(\beta,\phi,z) = -\frac{E_0 i\beta n}{\rho} J_n\left(\frac{x_{np}}{a}\rho\right)\sin(n\phi)\,e^{i\beta z}\,, \tag{7.52b}$$

$$E_z(\rho,\phi,z) = E_0\left(\frac{x_{np}}{a}\right)^2 J_n\left(\frac{x_{np}}{a}\rho\right)\cos(n\phi)\,e^{i\beta z}\,, \tag{7.52c}$$

$$H_\rho(\rho,\phi,z) = \frac{E_0 i\omega\varepsilon n}{\rho} J_n\left(\frac{x_{np}}{a}\rho\right)\sin(n\phi)\,e^{i\beta z}\,, \tag{7.52d}$$

and

$$H_\phi(\rho,\phi,z) = E_0 i\omega\varepsilon\left(\frac{x_{np}}{a}\right) J'_n\left(\frac{x_{np}}{a}\rho\right)\cos(n\phi)\,e^{i\beta z}\,. \tag{7.52e}$$

The field expressions for ***TE modes*** can be obtained from Eqs. (5.105a) and (5.105b):

$$H_\rho(\rho,\phi,z) = H_0 i\beta\left(\frac{x'_{np}}{a}\right) J'_n\left(\frac{x'_{np}}{a}\rho\right)\cos(n\phi)\,e^{i\beta z}\,, \tag{7.53a}$$

$$H_\phi(\rho,\phi,z) = -\frac{H_0 i\beta n}{\rho} J_n\left(\frac{x'_{np}}{a}\rho\right)\sin(n\phi)\,e^{i\beta z}\,, \tag{7.53b}$$

$$H_z(\rho,\phi,z) = H_0\left(\frac{x'_{np}}{a}\right)^2 J_n\left(\frac{x'_{np}}{a}\rho\right)\cos(n\phi)\,e^{i\beta z}\,, \tag{7.53c}$$

$$E_\rho(\rho,\phi,z) = -\frac{H_0 i\omega\mu n}{\rho} J_n\left(\frac{x'_{np}}{a}\rho\right)\sin(n\phi)\,e^{i\beta z}\,, \tag{7.53d}$$

and

$$E_\phi(\rho,\phi,z) = -H_0 i\omega\mu\left(\frac{x'_{np}}{a}\right) J'_n\left(\frac{x'_{np}}{a}\rho\right)\cos(n\phi)\,e^{i\beta z}\,. \tag{7.53e}$$

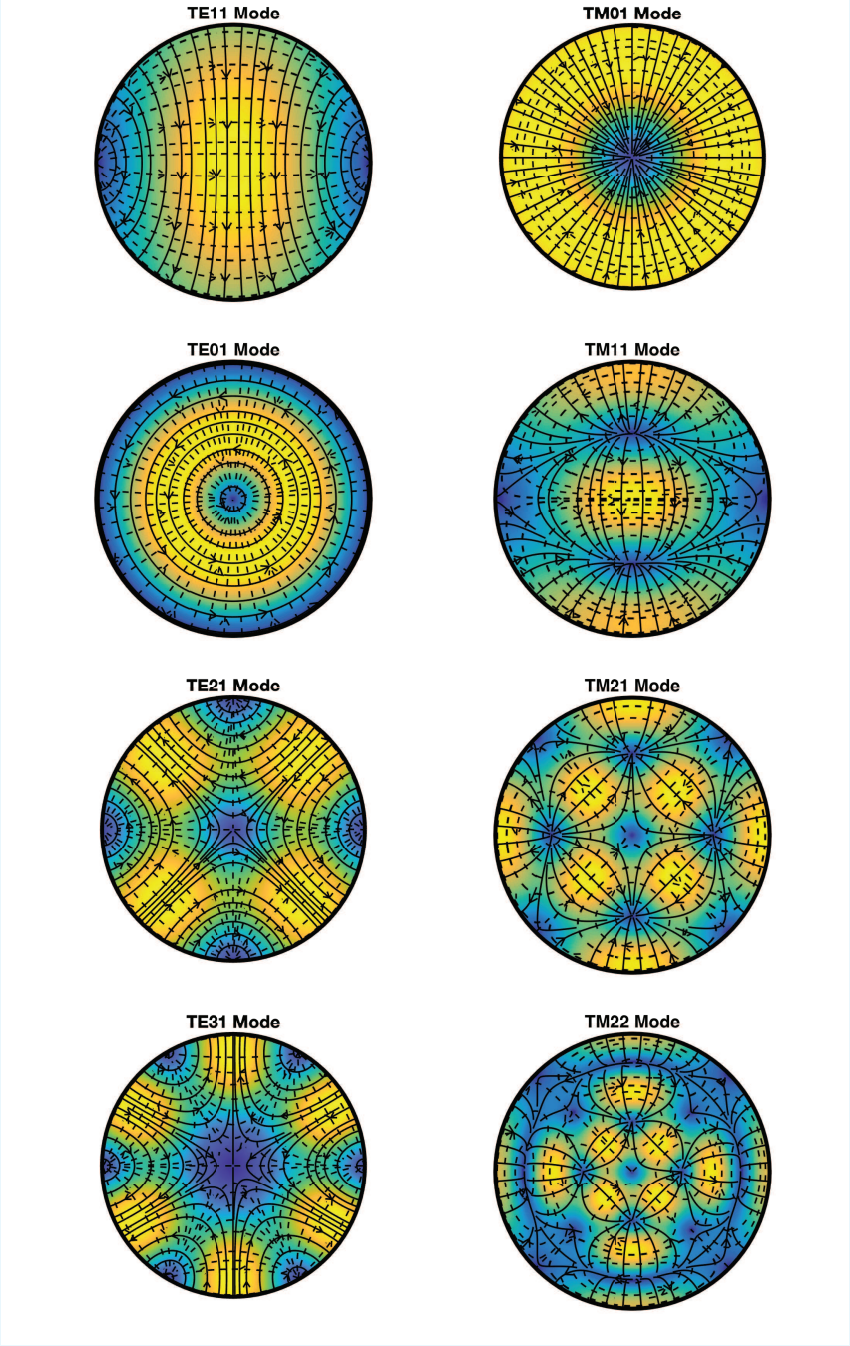


**Figure 7-6:** The field distribution of the first few modes of TE and TM waves in a cylindrical waveguide. The color shows the field intensity, the solid lines indicate the electric field, and the dashed lines indicate the magnetic field.

## Example 7-1: Attenuation Rate in Circular Waveguides

Find an expression for the attenuation rate $\alpha$ due to ohmic losses of the metallic surface of a circular waveguide of radius $a$ for TM and TE modes.

**Solution:** The expression for attenuation rate for a general waveguide is presented in Eqs. (6.206) and (6.209), for TM and TE modes, respectively. Using the following eigenfunctions in these expressions provides the attenuation rate:

$$\psi_{np}^{\mathrm{TM}}(\rho,\phi) = J_n\left(\frac{x_{np}}{a}\,\rho\right)\cos(n\phi) \tag{7.54a}$$

and

$$\psi_{np}^{\mathrm{TE}}(\rho,\phi) = J_n\left(\frac{x'_{np}}{a}\,\rho\right)\cos(n\phi)\ , \tag{7.54b}$$

where as before $x_{np}$ and $x'_{np}$ represent the zeros of $J_n(x)$ and $J'_n(x)$, respectively. The following integrals are needed in Eqs. (6.206) and (6.209):

$$\oint\left(\frac{\partial\psi_{np}^{\mathrm{TM}}}{\partial n}\right)^2 d\ell = \int_0^{2\pi}\left(\frac{\partial\psi_{np}^{\mathrm{TM}}}{\partial\rho}\right)^2 a\,d\phi = a\left(\frac{x_{np}}{a}\right)^2\left[J_{n+1}(x_{np})\right]^2\begin{cases}2\pi & n=0\ ,\\ \pi & n\neq 0\ ,\end{cases} \tag{7.55a}$$

and

$$\begin{aligned}\iint_S(\psi_{np}^{\mathrm{TM}})^2\,ds &= \int_0^{2\pi}\int_0^a\left[J_n\left(\frac{x_{np}}{a}\,\rho\right)\right]^2\cos^2 n\phi\;\rho\,d\rho\,d\phi\\ &= \frac{a^2}{2}\left[J_{n+1}(x_{np})\right]^2\begin{cases}2\pi & n=0\ ,\\ \pi & n\neq 0\ .\end{cases}\end{aligned} \tag{7.55b}$$

In the derivation of Eqs. (7.55a) and (7.55b), we used Eqs. (7.39) and (7.40), respectively. Also, for the TE fields we need to evaluate

$$\begin{aligned}\oint|\hat{\mathbf{n}}\times\nabla_{\mathrm{t}}\psi_{np}|^2\,d\ell &= \int_0^{2\pi}\frac{1}{a^2}\left(\frac{\partial\psi_{np}^{\mathrm{TE}}}{\partial\phi}\right)^2 a\,d\phi\\ &= \frac{n^2}{a}\left[J_n(x'_{np})\right]^2\begin{cases}0 & n=0\ ,\\ \pi & n\neq 0\ ,\end{cases}\end{aligned} \tag{7.56a}$$

$$\begin{aligned}\oint(\psi_{np}^{\mathrm{TE}})^2\,d\ell &= \int_0^{2\pi}\left[J_n(x'_{np})\right]^2\cos^2 n\phi\;a\,d\phi\\ &= a\left[J_n(x'_{np})\right]^2\begin{cases}2\pi & n=0\ ,\\ \pi & n\neq 0\ ,\end{cases}\end{aligned} \tag{7.56b}$$

and

$$\iint_S (\psi_{np})^2 \, ds = \int_0^{2\pi} \int_0^a \left[ J_n\left(\frac{x'_{np}}{a}\,\rho\right)\right]^2 \cos^2 n\phi \; \rho \; d\rho \; d\phi$$
$$= \frac{a^2}{2}\left[1 - \left(\frac{n}{x'_{np}}\right)^2\right] \left[J_n(x'_{np})\right]^2 \begin{cases} 2\pi & n = 0\,, \\ \pi & n \neq 0\,. \end{cases} \tag{7.56c}$$

Substituting Eqs. (7.55a) and (7.55b) into Eq. (6.206) provides the following expression for the attenuation rate of TM waves in a circular waveguide:

$$\alpha^{\mathrm{TM}_{np}} = \frac{\omega\varepsilon}{\sigma\delta_s\beta_{np}a} = \frac{k}{\sigma\delta_s\eta a\,\sqrt{k^2 - \left(\frac{x_{np}}{a}\right)^2}}\,. \tag{7.57}$$

This shows that in cases where $k \gg (x_{np}/a)$, the attenuation rate increases with $\sqrt{f}$ (embedded in $1/\delta_s$).

Similarly, using Eqs. (7.56a), (7.56b), and (7.56c) in Eq. (6.209), the expression for the attenuation rate for TE waves is given by

$$\alpha^{\mathrm{TE}_{np}} = \frac{\beta_{np}n^2}{\sigma\delta_s\omega\mu\left(\frac{x'_{np}}{a}\right)^2 a^3\left[1 - \left(\frac{n}{x'_{np}}\right)^2\right]} + \frac{\left(\frac{x'_{np}}{a}\right)^2}{\sigma\delta_s\omega\mu a\left[1 - \left(\frac{n}{x'_{np}}\right)^2\right]\beta_{np}}$$
$$= \frac{1}{\sigma\delta_s\eta ka\left[1 - \left(\frac{n}{x'_{np}}\right)^2\right]}\left[\frac{n^2\sqrt{k^2 - \left(\frac{x'_{np}}{a}\right)^2}}{a^2\left(\frac{x'_{np}}{a}\right)^2} + \frac{\left(\frac{x'_{np}}{a}\right)^2}{\sqrt{k^2 - \left(\frac{x'_{np}}{a}\right)^2}}\right]. \tag{7.58}$$

It is interesting to note that for $\mathrm{TE}_{0p}$ the attenuation rate simplifies to

$$\alpha^{\mathrm{TE}_{0p}} = \frac{1}{\sigma\delta_s\eta ka}\,\frac{\left(\frac{x'_{0p}}{a}\right)^2}{\sqrt{k^2 - \left(\frac{x'_{0p}}{a}\right)^2}}\,. \tag{7.59}$$

In situations where $k \gg x'_{0p}/a$, the attenuation rate decreases with frequency as $1/f^{3/2}$. Hence the attenuation from such modes can, in principle, go to zero as $f \to \infty$. Note, however, that in such cases the waveguide can support many modes, and maintaining the $\mathrm{TE}_{0p}$ as the only mode becomes very challenging in practice.

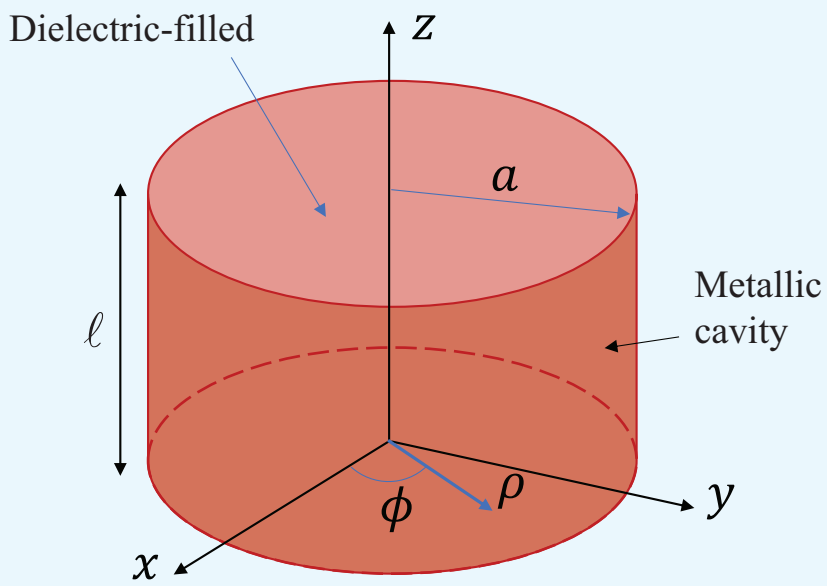


**Figure 7-7:** Configuration of a cylindrical cavity consisting of a metallic cylinder containing a dielectric material.

### 7-1.4 The Cylindrical Cavity

By short-circuiting the two ends of a cylindrical waveguide, we form a cylindrical cavity, as shown in Fig. 7-7. As in the case of the rectangular cavity, the fields can be expressed in terms of TE and TM waveguide modes. In this case, tangential electric fields at $z = 0$ and $z = \ell$ must vanish. The $\rho$-component of the electric field for a TM mode can be written as

$$E_\rho(\rho,\phi,z) = -E_0 \beta k_\rho \, J_n'(k_\rho \rho) \, \cos(n\phi) \, \sin(\beta z) \, . \tag{7.60}$$

Of course, the choice of sine function ensures that $E_\rho(\rho,\phi,0) = 0$. To force $E_\rho(\rho,\phi,z)$, to go to zero as $z$ approaches $\ell$, we need

$$\sin\beta\ell = 0 \quad \rightarrow \quad \beta = \frac{q\pi}{\ell} \, , \qquad q = 0,1,2,3,\ldots$$

The fields can be generated from a potential function

$$\psi_{npq}^{\text{TM}} = J_n\left(\frac{x_{np}}{a}\,\rho\right) \cos(n\phi) \, \cos\left(\frac{q\pi}{\ell}\,z\right) \, , \tag{7.61}$$

and are given by

$$E_\phi(\rho,\phi,z) = \frac{E_0 \beta n}{\rho} \, J_n\left(\frac{x_{np}}{a}\,\rho\right) \cos(n\phi) \, \sin\left(\frac{q\pi}{\ell}\,z\right) \tag{7.62a}$$

and

$$E_z(\rho,\phi,z) = E_0 \left(\frac{x_{np}}{a}\right)^2 J_n\left(\frac{x_{np}}{a}\,\rho\right) \cos(n\phi)\, \cos\left(\frac{q\pi}{\ell}\, z\right) . \tag{7.62b}$$

According to Eq. (7.98a),

$$\left(\frac{q\pi}{\ell}\right)^2 + \left(\frac{x_{np}}{a}\right)^2 = \omega^2 \mu\varepsilon . \tag{7.63}$$

Hence, the resonant frequency of the *npq* mode is given by

$$f_{npq}^{\mathrm{TM}} = \frac{1}{2\pi\sqrt{\mu\varepsilon}} \sqrt{\left(\frac{x_{np}}{a}\right)^2 + \left(\frac{q\pi}{\ell}\right)^2} , \tag{7.64}$$

where $n = 0,1,2,\ldots$, $p = 1,2,3,\ldots$, and $q = 0,1,2,3,\ldots$. The dominant mode is $\mathrm{TM}_{010}$, which has a constant electric field $\mathbf{E} = E_z\,\hat{\mathbf{z}}$. For a TE mode, the field can be generated from potential

$$\psi_{npq}^{\mathrm{TE}} = J_n\left(\frac{x'_{np}}{a}\,\rho\right) \cos(n\phi)\, \sin\left(\frac{q\pi}{\ell}\, z\right) . \tag{7.65}$$

The expressions for the electric field components are given by

$$E_\rho(\rho,\phi,z) = -\frac{H_0 i\omega\mu n}{\rho}\, J_n\left(\frac{x'_{np}}{a}\,\rho\right) \sin(n\phi)\, \sin\left(\frac{q\pi}{\ell}\, z\right) \tag{7.66a}$$

and

$$E_\phi(\rho,\phi,z) = -H_0 i\omega\mu \left(\frac{x'_{np}}{a}\right) J'_n\left(\frac{x'_{np}}{a}\,\rho\right) \cos(n\phi)\, \sin\left(\frac{q\pi}{\ell}\, z\right) . \tag{7.66b}$$

The resonant frequency for TE modes is given by

$$f_{npq}^{\mathrm{TE}} = \frac{1}{2\pi\sqrt{\mu\varepsilon}} \sqrt{\left(\frac{x'_{np}}{a}\right)^2 + \left(\frac{q\pi}{\ell}\right)^2} . \tag{7.67}$$

Here, the index $q = 1,2,3,\ldots$, and thus the dominant resonant frequency is $\mathrm{TE}_{111}$.

The quality factor due to the walls' ohmic loss can be computed in a manner similar to how the attenuation rates for the circular waveguides were estimated. The quality factor for the dominant mode $\mathrm{TM}_{010}$ (this mode is dominant for $d < 2a$) also requires calculation of the stored energy in the cavity. The field expressions for $\mathrm{TM}_{010}$ are given by

$$E_z(\rho,\phi,z) = E_0 \left(\frac{x_{01}}{a}\right)^2 J_0\left(\frac{x_{01}}{a}\,\rho\right) \tag{7.68a}$$

and

$$H_\phi(\rho,\phi,z) = E_0 i\omega\varepsilon \left(\frac{x_{01}}{a}\right) J'_0\left(\frac{x_{01}}{a}\,\rho\right) = -E_0 i\omega\varepsilon \left(\frac{x_{01}}{a}\right) J_1\left(\frac{x_{01}}{a}\,\rho\right) . \tag{7.68b}$$

The stored energy is given by

$$\begin{aligned} W = 2W_{\mathrm{e}} &= \frac{\varepsilon}{2}\int_0^{\ell}\int_0^{a}\int_0^{2\pi} |E_z|^2 \rho \, d\phi \, d\rho \, dz \\ &= \frac{\varepsilon}{2}\,|E_0|^2 \left(\frac{x_{01}}{a}\right)^4 2\pi\ell \int_0^{a} \left[J_0\left(\frac{x_{01}}{a}\,\rho\right)\right]^2 \rho \, d\rho \\ &= \frac{\pi\ell\varepsilon}{2}\,|E_0|^2\,\frac{(x_{01})^4}{a^2}\,[J_1(x_{01})]^2 \ . \end{aligned} \tag{7.69}$$

Because the fields tangential to the lower and upper surfaces of the cylinder (at $z = 0$ and $z = a$) are zero, no ohmic losses occur in those two surfaces. The power loss on the cylinder's walls is computed from

$$\begin{aligned} p_{\mathrm{L}} &= \frac{1}{2\sigma\delta_{\mathrm{s}}} \oiint_S |H_{\tan}|^2 \, ds \\ &= \frac{1}{2\sigma\delta_{\mathrm{s}}}\,|E_0|^2\omega^2\varepsilon^2 \left(\frac{x_{01}}{a}\right)^2 \left\{2\pi a\ell\,[J_1(x_{01})]^2 + 4\pi \int_0^{a} \left[J_1\left(\frac{x_{01}}{a}\,\rho\right)\right]^2 \rho \, d\rho\right\} \\ &= \frac{|E_0|^2\omega^2\varepsilon^2 \left(\frac{x_{01}}{a}\right)^2 \pi a(\ell + a)}{\sigma\delta_{\mathrm{s}}}\,[J_1(x_{01})]^2 \ . \end{aligned} \tag{7.70}$$

In deriving Eq. (7.70) we used the following integral identity for Bessel functions:

$$\int [R_\nu(\rho)]^2 \rho \, d\rho = \frac{\rho^2}{2}\left[\left[R'_\nu(\rho)\right]^2 + \left(1 - \frac{\nu^2}{\rho^2}\right)[R_\nu(\rho)]^2\right] \tag{7.71}$$

and

$$J'_1(\rho) = J_0(\rho) - \frac{1}{\rho}\,J_1(\rho) \ . \tag{7.72}$$

The quality factor for $\mathrm{TM}_{010}$ can now be evaluated using

$$\breve{Q} = \frac{\omega W}{p_{\mathrm{L}}} \ . \tag{7.73}$$

Substituting the expressions for the stored energy from Eq. (7.69) and the power loss from Eq. (7.70), and noting that the cavity resonant wave number is $k_{010}^{\mathrm{TM}} = x_{01}/a$, in Eq. (7.73)

$$\breve{Q} = \frac{\sigma\delta_{\mathrm{s}}\sqrt{\dfrac{\mu}{\varepsilon}}\,x_{01}}{2\left(1 + \dfrac{a}{\ell}\right)} = \frac{\sigma\delta_{\mathrm{s}}\eta 1.202}{2\left(1 + \dfrac{a}{\ell}\right)} \ . \tag{7.74}$$

## Example 7-2: Circular Patch Antenna

Using modal analysis and appropriate boundary conditions, find the operating frequency of a circular patch antenna formed from a circular metallic plate atop an infinite ground plane, as shown in Fig. 7-8.

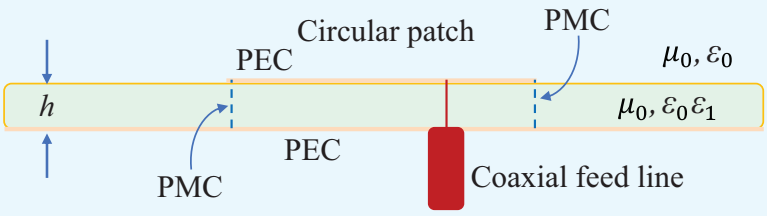


**Figure 7-8:** Configuration of a circular patch antenna fed by a coaxial line. The circular patch is placed on top of a substrate of height $h$ and a relative dielectric constant $\varepsilon_1$. The dotted lines represent equivalent perfect magnetic conductor (PMC) walls.

**Solution:** In practice, patch antennas are fabricated using a metallic-coated low-loss dielectric substrate with a relative permittivity $\varepsilon_1$. The metallic circular plate is attached to the center pin of a coaxial line at an appropriate distance away from the center of the patch, in order to achieve impedance match to the transmission line. The current from the feed flows over the top circular patch in a manner that satisfies the boundary conditions. One boundary condition imposed on the surface current is the one that forces the current normal to the edge of the patch to be zero at the edge. This is not a strict requirement since there are fringing electric fields from the metallic patch to the ground. These fringing electric fields produce a polarization current whose flow is perpendicular to the edge that allow a small amount of conduction current to flow perpendicular to the edge. As a first-order approximation we can ignore the fringing fields around the patch, and in this case the surface current normal to the edge is approximately zero. As a result, the tangential magnetic field near the patch edge is also zero. This constitutes an equivalent PMC wall around the edge of the patch and is a good approximation when the height $h$ of the patch above the ground plane is much smaller than a wavelength. As a result we can consider the circular patch as a circular cavity with the top and bottom faces as PEC and the side wall of the cylinder as PMC.

The boundary conditions for TM and TE waves on PMC are given respectively by

$$\frac{\partial \psi^{\mathrm{TM}}}{\partial n} = \frac{\partial \psi^{\mathrm{TM}}}{\partial \rho}\bigg|_{\rho=a} = 0 \tag{7.75a}$$

and

$$\psi^{\mathrm{TE}}\big|_{\rho=a} = 0\,. \tag{7.75b}$$

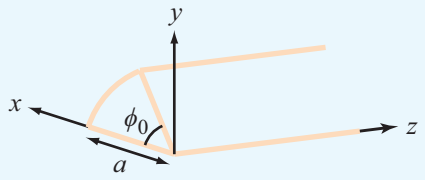


**Figure 7-9:** Geometry of a metallic angular-sector waveguide.

Hence, the TM fields can be generated from a potential function given by

$$\psi_{npq}^{\mathrm{TM}} = J_n\left(\frac{x'_{np}}{a}\,\rho\right)\cos(n\phi)\,\cos\left(\frac{q\pi}{h}\,z\right)\,, \tag{7.76}$$

where $x'_{np}$ represent the $p$th zero of $J'_n(x)$. The TE fields on the other hand can be generated from a potential function given by

$$\psi_{npq}^{\mathrm{TE}} = J_n\left(\frac{x_{np}}{a}\,\rho\right)\cos(n\phi)\,\sin\left(\frac{q\pi}{h}\,z\right)\,. \tag{7.77}$$

The dominant resonant mode (according to Table 7-2) corresponds to $\psi_{110}^{\mathrm{TM}}$, given by

$$\psi_{110}^{\mathrm{TM}} = J_1\left(\frac{1.841}{a}\,\rho\right)\cos\phi\,, \tag{7.78}$$

and the resonant frequency is given by

$$f^{\mathrm{TM}_{110}} = \frac{1.841}{2\pi a\sqrt{\mu_0\varepsilon_0}\sqrt{\varepsilon_1}} = \frac{1.841c}{2\pi a\sqrt{\varepsilon_1}} = \frac{0.879\times 10^8}{a\sqrt{\varepsilon_1}}\,. \tag{7.79}$$

In practice, the resonant frequency is slightly lower than what is calculated from Eq. (7.79) due to the fringing electric field.

### 7-1.5 Angular-Sector Waveguide

In this section, we consider the problem of wave propagation in an angular section of a metallic waveguide as depicted in Fig. 7-9. The region of interest is confined within a metallic pipe whose surface is defined by

$$\rho \le a\,, \quad 0 \le \phi \le \phi_0\,, \quad \text{and} \quad -\infty < z < \infty\,.$$

Similar to the cylindrical waveguide, the scalar potential must satisfy the 2-D Helmholtz equation given by Eq. (7.22), subject to Dirichlet's and Neumann's boundary conditions for TM and TE modes. For this problem the region of interest is not the entire domain but it does include $\rho = 0$. Hence, the admissible solution for radial functions include the Bessel functions

of the first kind and noninteger order given by

$$\psi(\rho,\phi) = (A_n \sin \nu\phi + B_n \cos \nu\phi)\, J_\nu(k_\rho \rho)\ . \tag{7.80}$$

For the TM case, $\psi(\rho,0) = \psi(\rho,\phi_0) = 0$, which enforces

$$B_n = 0$$

and

$$\nu = \frac{n\pi}{\phi_0}\ , \qquad n = 1,2,3,\ldots \tag{7.81}$$

The boundary condition also mandates that $\psi(a,\phi) = 0$, and this condition gives a set of discrete values for $k_\rho$ given by

$$k_{np} = \frac{x_{\nu_p}}{a}\ , \qquad p = 1,2,3,\ldots\ ,$$

where $x_{\nu_p}$ is the $p$th zero of $J_\nu(x)$. Hence the eigenfunctions are given by

$$\psi_{np}^{\mathrm{TM}}(\rho,\phi) = A_{np} \sin\left(\frac{n\pi}{\phi_0}\,\phi\right) J_{n\pi/\phi_0}\left(\frac{x_{\nu_p}}{a}\,\rho\right)\ . \tag{7.82}$$

Explicit expressions for the field quantities can be obtained from Eqs. (5.102a) and (5.102b).

For the TE case for which $\frac{\partial \psi}{\partial n} = 0$ on the waveguide boundary, the admissible solution is given by

$$\psi_{np}^{\mathrm{TE}} = B_{np} \cos\left(\frac{n\pi}{\phi_0}\,\phi\right) J_{n\pi/\phi_0}\left(\frac{x'_{\nu p}}{a}\,\rho\right)\ , \tag{7.83}$$

where $x'_{\nu p}$ is the $p$th zero of $J'_\nu(x)$. The expressions for the field quantities can be obtained from Eqs. (5.105a) and (5.105b).

### 7-1.6 Large Angular-Sector Waveguide

The solution obtained for the angular-sector waveguide can be used to find the possible field solutions in an unbounded angular-sector waveguide with the configuration shown in Fig. 7-10. The domain of interest is now specified by

$$0 < \rho < \infty \quad \text{and} \quad 0 \le \phi \le \phi_0\ .$$

Considering this problem as the limiting case of the previous problem as $a \to \infty$, wave functions similar to Eq. (7.82) can be assumed. However, in this case the domain supports an infinite number of modes with a continuous eigenvalue. To demonstrate that, let us consider the behavior of $J_\nu(k_\rho a)$ as $k_\rho a \to \infty$. Using the large-argument expansion of $J_\nu(k_\rho a)$, it can be shown that

$$\lim_{k_\rho a \to \infty} J_\nu(k_\rho a) = \sqrt{\frac{2}{\pi k_\rho a}} \cos\left(k_\rho a - \frac{(2\nu+1)\pi}{4}\right)\ . \tag{7.84}$$

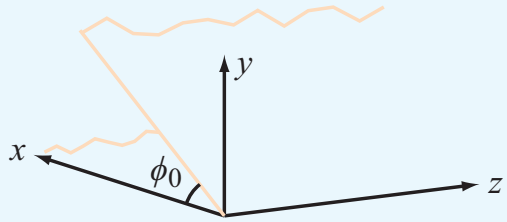


**Figure 7-10:** Geometry of an unbounded angular-sector waveguide (interior wedge).

The eigenvalues (modes) correspond to zeros of $J_\nu(k_\rho a) = 0$. These can be obtained approximately from Eq. (7.84) and are given by

$$x_{\nu_n} = k_{\rho_n} a = \left(n + \frac{\nu}{2} - \frac{1}{4}\right)\pi\,, \qquad n = 1,2,3,\ldots$$

The separation between two successive modes is given by

$$\Delta k_{\rho_n} = k_{\rho_{n+1}} - k_{\rho_n} = \frac{\pi}{a}\,,$$

which goes to zero as $a \to \infty$.

The solution for the scalar potential can be expressed in terms of the superposition of all possible modes:

$$\psi^{\mathrm{TM}}(\rho,\phi) = \lim_{a\to\infty} \sum_n \sum_p A_{np} \sin\left(\frac{n\pi}{\phi_0}\,\phi\right) J_\nu\left(\frac{x_{\nu_p}}{a}\,\rho\right)\,. \tag{7.85}$$

For the unbounded angular-sector waveguide, the summation over $n$ can be replaced by an integral:

$$\psi^{\mathrm{TM}}(\rho,\phi) = \sum_{n=1}^{\infty} \sin\left(\frac{n\pi}{\phi_0}\,\phi\right) \int_0^\infty A_n(k_\rho)\, J_\nu(k_\rho\rho)\, dk_\rho\,. \tag{7.86}$$

The function $\psi(\rho,\phi)$ given by Eq. (7.86) satisfies both the wave equation and the boundary condition, and hence represents a general solution of the problem. The solution for the TE case can easily be constructed from Eq. (7.83) and is given by

$$\psi^{\mathrm{TE}}(\rho,\phi) = \sum_{n=0}^{\infty} \cos\left(\frac{n\pi}{\phi_0}\,\phi\right) \int_0^\infty B_n(k_\rho)\, J_\nu(k_\rho\rho)\, dk_\rho\,. \tag{7.87}$$

## 7-2 The Circular Dielectric Waveguide

In this section we examine how electromagnetic waves are guided by a circular dielectric rod with permittivity $\varepsilon_{\mathrm{d}}$ and permeability $\mu_{\mathrm{d}}$ embedded in a uniform dielectric medium with

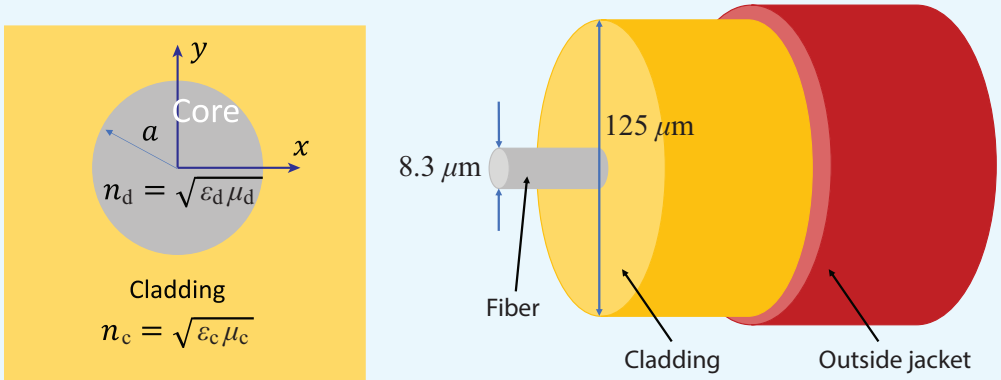


**Figure 7-11:** A single-mode optical fiber with a core of radius $a$ and index of refraction $n_d = \sqrt{\mu_d \varepsilon_d}$ surrounded by a large cladding background with index of refraction $n_c = \sqrt{\mu_c \varepsilon_c}$. At $\lambda = 1500$ nm, a typical value for the index of refraction for a core made from doped silicon is $n \approx 1.45$, and for a cladding made from pure silica a typical value is $n_c \approx 1.44$.

permittivity $\varepsilon_c$ and permeability $\mu_c$, as shown in Fig. 7-11. As in circular metallic waveguides, we are seeking a solution such that all field quantities show a dependence with respect to $z$ of the form $e^{i\beta z}$, which indicates propagation along the $z$-axis. This structure, known as an ***optical fiber***, is the most prevalent structure for data transmission. Optical fibers are used for long-distance (up to a few thousand kilometers) data transfer, and internet communication networks, as well as applications in medicine (such as endoscopy) and other industrial sensors.

The dielectric waveguide modes can be determined by expanding the fields in terms of cylindrical wave functions inside the core and in the cladding region. The fiber is designed so that the wave is confined within the core and the cladding supports only evanescent waves. The cladding around the fiber is chosen to be thick enough so that no fields can reach the outside jacket. The scalar potential in the core region takes the following form:

$$\psi_{\rm I} = J_n(k_\rho^{\rm I}\rho)\, e^{in\phi} \ , \tag{7.88}$$

where

$$(k_\rho^{\rm I})^2 = k_{\rm d}^2 - \beta^2 = \omega^2 \mu_{\rm d}\varepsilon_{\rm d} - \beta^2 \ . \tag{7.89}$$

Since we desire the field to be confined within the core and around it, the potential chosen in cladding must be of the following form:

$$\psi_{\rm II} = H_n^{(1)}(k_\rho^{\rm II}\rho)\, e^{in\phi} \ , \tag{7.90}$$

where

$$(k_\rho^{\rm II})^2 = k_{\rm c}^2 - \beta^2 = -(\beta^2 - \omega^2\mu_{\rm c}\varepsilon_{\rm c}) = -\nu^2 \ , \tag{7.91}$$

for some positive real number $\nu$. The radial function $H_n^{(1)}(k_\rho^{\rm II}\rho) = H_n^{(1)}(i\nu\rho)$ can be written

in terms of the modified Bessel function of the second kind ($K_n$) as defined in Eq. (7.19b) and shown in Fig. 7-4. It turns out that, in the most general case, the field expansion base on TE to $z$ or TM to $z$ alone cannot satisfy all the necessary boundary conditions. Superposition of TE and TM modes must be used to arrive at a satisfactory solution. In region 1 where $r \leq a$, the longitudinal electric and magnetic fields can be written as

$$E_z^{\mathrm{I}}(\rho,\phi) = (k_\rho^{\mathrm{I}})^2 A_n J_n(k_\rho^{\mathrm{I}}\rho)\, e^{in\phi} e^{i\beta z} \tag{7.92a}$$

and

$$H_z^{\mathrm{I}}(\rho,\phi) = (k_\rho^{\mathrm{I}})^2 B_n J_n(k_\rho^{\mathrm{I}}\rho)\, e^{in\phi} e^{i\beta z}\,, \tag{7.92b}$$

and in region 2, $r \geq a$, these fields are expressed as

$$E_z^{\mathrm{II}}(\rho,\phi) = (k_\rho^{\mathrm{II}})^2 C_n H_n^{(1)}(k_\rho^{\mathrm{II}}\rho)\, e^{in\phi} e^{i\beta z} \tag{7.93a}$$

and

$$H_z^{\mathrm{II}}(\rho,\phi) = (k_\rho^{\mathrm{II}})^2 D_n H_n^{(1)}(k_\rho^{\mathrm{II}}\rho)\, e^{in\phi} e^{i\beta z}\,. \tag{7.93b}$$

In view of Eqs. (5.98) and (5.101), the other field components take the following form:

$$E_\rho^{\mathrm{I}}(\rho,\phi) = \left( i\beta k_\rho^{\mathrm{I}} J_n'(k_\rho^{\mathrm{I}}\rho)\, A_n - \frac{n\omega\mu_{\mathrm{d}}}{\rho} J_n(k_\rho^{\mathrm{I}}\rho)\, B_n \right) e^{in\phi} e^{i\beta z}\,, \tag{7.94a}$$

$$E_\phi^{\mathrm{I}}(\rho,\phi) = \left( \frac{-n\beta}{\rho} J_n(k_\rho^{\mathrm{I}}\rho)\, A_n - i\omega\mu_{\mathrm{d}} k_\rho^{\mathrm{I}} J_n'(k_\rho^{\mathrm{I}}\rho)\, B_n \right) e^{in\phi} e^{i\beta z}, \tag{7.94b}$$

$$H_\rho^{\mathrm{I}}(\rho,\phi) = \left( \frac{n\omega\varepsilon_{\mathrm{d}}}{\rho} J_n(k_\rho^{\mathrm{I}}\rho)\, A_n + i\beta k_\rho^{\mathrm{I}} J_n'(k_\rho^{\mathrm{I}}\rho)\, B_n \right) e^{in\phi} e^{i\beta z}\,, \tag{7.94c}$$

and

$$H_\phi^{\mathrm{I}}(\rho,\phi) = \left( i\omega\varepsilon_{\mathrm{d}} k_\rho^{\mathrm{I}} J_n'(k_\rho^{\mathrm{I}}\rho)\, A_n - \frac{\beta n}{\rho} J_n(k_\rho^{\mathrm{I}}\rho)\, B_n \right) e^{in\phi} e^{i\beta z}\,. \tag{7.94d}$$

In region 2 where $r > a$, the field expressions can be obtained in a similar manner and are given by

$$E_\rho^{\mathrm{II}}(\rho,\phi) = \left( i\beta k_\rho^{\mathrm{II}} H_n^{(1)\prime}(k_\rho^{\mathrm{II}}\rho)\, C_n - \frac{n\omega\mu_{\mathrm{c}}}{\rho} H_n^{(1)}(k_\rho^{\mathrm{II}}\rho)\, D_n \right) e^{in\phi} e^{i\beta z}\,, \tag{7.95a}$$

$$E_\phi^{\mathrm{II}}(\rho,\phi) = \left( \frac{-n\beta}{\rho} H_n^{(1)}(k_\rho^{\mathrm{II}}\rho)\, C_n - i\omega\mu_{\mathrm{c}} k_\rho^{\mathrm{II}} H_n^{(1)\prime}(k_\rho^{\mathrm{II}}\rho)\, D_n \right) e^{in\phi} e^{i\beta z}\,, \tag{7.95b}$$

$$H_\rho^{\mathrm{II}}(\rho,\phi) = \left( \frac{n\omega\varepsilon_{\mathrm{c}}}{\rho} H_n^{(1)}(k_\rho^{\mathrm{II}}\rho)\, C_n + i\beta k_\rho^{\mathrm{II}} H_n^{(1)\prime}(k_\rho^{\mathrm{II}}\rho)\, D_n \right) e^{in\phi} e^{i\beta z}\,, \tag{7.95c}$$

and

$$H_\phi^{\mathrm{II}}(\rho,\phi) = \left( i\omega\varepsilon_{\mathrm{c}} k_\rho^{\mathrm{II}} H_n^{(1)\prime}(k_\rho^{\mathrm{II}}\rho)\, C_n - \frac{\beta n}{\rho} H_n^{(1)}(k_\rho^{\mathrm{II}}\rho)\, D_n \right) e^{in\phi} e^{i\beta z}\,. \tag{7.95d}$$

The relations between $A_n$, $B_n$, $C_n$, and $D_n$ for the various modes can be established by applying the boundary conditions at the interface between the core and the surrounding medium (cladding); that is,

$$E_z^{\mathrm{I}}(a,\phi) = E_z^{\mathrm{II}}(a,\phi)\ , \tag{7.96a}$$

$$H_z^{\mathrm{I}}(a,\phi) = H_z^{\mathrm{II}}(a,\phi)\ , \tag{7.96b}$$

$$E_\phi^{\mathrm{I}}(a,\phi) = E_\phi^{\mathrm{II}}(a,\phi)\ , \tag{7.96c}$$

$$H_\phi^{\mathrm{I}}(a,\phi) = H_\phi^{\mathrm{II}}(a,\phi)\ . \tag{7.96d}$$

Using Eqs. (7.92a) and (7.93a) in Eq. (7.96a) and Eqs. (7.92b) and (7.93b) in Eq. (7.96b), we get

$$(k_\rho^{\mathrm{I}})^2\, J_n(k_\rho^{\mathrm{I}} a)\, A_n = (k_\rho^{\mathrm{II}})^2\, H_n^{(1)}(k_\rho^{\mathrm{II}} a)\, C_n \tag{7.97a}$$

and

$$(k_\rho^{\mathrm{I}})^2\, J_n(k_\rho^{\mathrm{I}} a)\, B_n = (k_\rho^{\mathrm{II}})^2\, H_n^{(1)}(k_\rho^{\mathrm{II}} a)\, D_n\ . \tag{7.97b}$$

Also, using Eqs. (7.94b) and (7.95b) in Eq. (7.96c) and using Eqs. (7.94d) and (7.95d) in Eq. (7.96d), two more equations for the unknowns are obtained:

$$\frac{n\beta}{a}\, J_n(k_\rho^{\mathrm{I}} a)\, A_n + i\omega\mu_{\mathrm{d}} k_\rho^{\mathrm{I}}\, J_n'(k_\rho^{\mathrm{I}} a)\, B_n = \frac{n\beta}{a}\, H_n^{(1)}(k_\rho^{\mathrm{II}} a)\, C_n + i\omega\mu_{\mathrm{c}} k_\rho^{\mathrm{II}}\, H_n^{(1)\prime}(k_\rho^{\mathrm{II}} a)\, D_n \tag{7.98a}$$

and

$$i\omega\varepsilon_{\mathrm{d}} k_\rho^{\mathrm{I}}\, J_n'(k_\rho^{\mathrm{I}} a)\, A_n - \frac{n\beta}{a}\, J_n(k_\rho^{\mathrm{I}} a)\, B_n = i\omega\varepsilon_{\mathrm{c}} k_\rho^{\mathrm{II}}\, H_n^{(1)\prime}(k_\rho^{\mathrm{II}} a)\, C_n - \frac{n\beta}{a}\, H_n^{(1)}(k_\rho^{\mathrm{II}} a)\, D_n\ . \tag{7.98b}$$

Equations (7.97a)–(7.98b) constitute four equations for the four unknowns. To arrive at a nonzero solution, the determinant of the coefficients must vanish. That is,

$$\begin{vmatrix} (k_\rho^{\mathrm{I}})^2 J_n(k_\rho^{\mathrm{I}} a) & 0 & -(k_\rho^{\mathrm{II}})^2 H_n^{(1)}(k_\rho^{\mathrm{II}} a) & 0 \\ 0 & (k_\rho^{\mathrm{I}})^2 J_n(k_\rho^{\mathrm{I}} a) & 0 & (k_\rho^{\mathrm{II}})^2 H_n^{(1)}(k_\rho^{\mathrm{II}} a) \\ \frac{n\beta}{a} J_n(k_\rho^{\mathrm{I}} a) & i\omega\mu_{\mathrm{d}} k_\rho^{\mathrm{I}} J_n'(k_\rho^{\mathrm{I}} a) & -\frac{n\beta}{a} H_n^{(1)}(k_\rho^{\mathrm{II}} a) & -i\omega\mu_{\mathrm{c}} k_\rho^{\mathrm{II}} H_n^{(1)\prime}(k_\rho^{\mathrm{II}} a) \\ i\omega\varepsilon_{\mathrm{d}} k_\rho^{\mathrm{I}} J_n'(k_\rho^{\mathrm{I}} a) & -\frac{n\beta}{a} J_n(k_\rho^{\mathrm{I}} a) & -i\omega\varepsilon_{\mathrm{c}} k_\rho^{\mathrm{II}} H_n^{(1)\prime}(k_\rho^{\mathrm{II}} a) & \frac{n\beta}{a} H_n^{(1)}(k_\rho^{\mathrm{II}} a) \end{vmatrix} = 0\ . \tag{7.99}$$

Alternatively, from Eqs. (7.97a) and (7.97b) we find that

$$\frac{B_n}{A_n} = \frac{D_n}{C_n} \tag{7.100}$$

and

$$\frac{A_n}{C_n} = \left(\frac{k_\rho^{\mathrm{II}}}{k_\rho^{\mathrm{I}}}\right)^2 \frac{H_n^{(1)}(k_\rho^{\mathrm{II}} a)}{J_n(k_\rho^{\mathrm{I}} a)}\ . \tag{7.101}$$

Substituting these into Eqs. (7.98a) and (7.98b), the following transcendental equation involving $k_\rho^{\mathrm{II}}$ and $k_\rho^{\mathrm{I}}$ is obtained:

$$\omega^2 \left[ \frac{\mu_\mathrm{d}}{k_\rho^{\mathrm{I}} a} \frac{J_n'(k_\rho^{\mathrm{I}} a)}{J_n(k_\rho^{\mathrm{I}} a)} - \frac{\mu_\mathrm{c}}{k_\rho^{\mathrm{II}} a} \frac{H_n^{(1)\prime}(k_\rho^{\mathrm{II}} a)}{H_n^{(1)}(k_\rho^{\mathrm{II}} a)} \right] \left[ \frac{\varepsilon_\mathrm{d}}{k_\rho^{\mathrm{I}} a} \frac{J_n(k_\rho^{\mathrm{I}} a)}{J_n'(k_\rho^{\mathrm{I}} a)} - \frac{\varepsilon_\mathrm{c}}{k_\rho^{\mathrm{II}} a} \frac{H_n^{(1)\prime}(k_\rho^{\mathrm{II}} a)}{H_n^{(1)}(k_\rho^{\mathrm{II}} a)} \right]$$
$$= n^2 \beta^2 \left[ \left( \frac{1}{k_\rho^{\mathrm{II}} a} \right)^2 - \left( \frac{1}{k_\rho^{\mathrm{I}} a} \right)^2 \right]^2 . \tag{7.102}$$

Using Eq. (7.19b), we can show that

$$\frac{H_n^{(1)\prime}(k_\rho^{\mathrm{II}} a)}{H_n^{(1)}(k_\rho^{\mathrm{II}} a)} = \frac{H_n^{(1)\prime}(i\nu a)}{H_n^{(1)}(i\nu a)} = -i \frac{K_n'(\nu a)}{K_n(\nu a)} .$$

It then follows that the transcendental equation given by Eq. (7.102) can be written as

$$\left[ \frac{\mu_\mathrm{d}}{u} \frac{J_n'(u)}{J_n(u)} + \frac{\mu_\mathrm{c}}{\upsilon} \frac{K_n'(\upsilon)}{K_n(\upsilon)} \right] \left[ \frac{k_\mathrm{d}^2}{u\mu_\mathrm{d}} \frac{J_n'(u)}{J_n(u)} + \frac{k_\mathrm{c}^2}{\upsilon\mu_\mathrm{c}} \frac{K_n'(\upsilon)}{K_n(\upsilon)} \right] = n^2 \beta^2 \left( \frac{1}{\upsilon^2} + \frac{1}{u^2} \right)^2 , \tag{7.103}$$

where $u = k_\rho^{\mathrm{I}} a$ and $\upsilon = \nu a$. We also recall that

$$(k_\rho^{\mathrm{I}})^2 = k_\mathrm{d}^2 - \beta^2$$

and

$$\nu^2 = \beta^2 - k_\mathrm{c}^2 .$$

Hence

$$u^2 + \upsilon^2 = a^2 (k_\mathrm{d}^2 - k_\mathrm{c}^2) . \tag{7.104}$$

Equations (7.103) and (7.104) are solved together to find $k_\rho^{\mathrm{I}}$ and $k_\rho^{\mathrm{II}}$.

For azimuthly symmetric modes $n = 0$, and the transcendental equation given by Eq. (7.102) factors into two equations given by

$$\frac{\mu_\mathrm{d}}{u} \frac{J_0'(u)}{J_0(u)} = -\frac{\mu_\mathrm{c}}{\upsilon} \frac{K_0'(\upsilon)}{K_0(\upsilon)} \tag{7.105a}$$

and

$$\frac{\varepsilon_\mathrm{d}}{u} \frac{J_0'(u)}{J_0(u)} = -\frac{\varepsilon_\mathrm{c}}{\upsilon} \frac{K_0'(\upsilon)}{K_0(\upsilon)} . \tag{7.105b}$$

Using Eq. (7.29c) it can be shown that

$$J_0'(u) = -J_1(u)$$

and

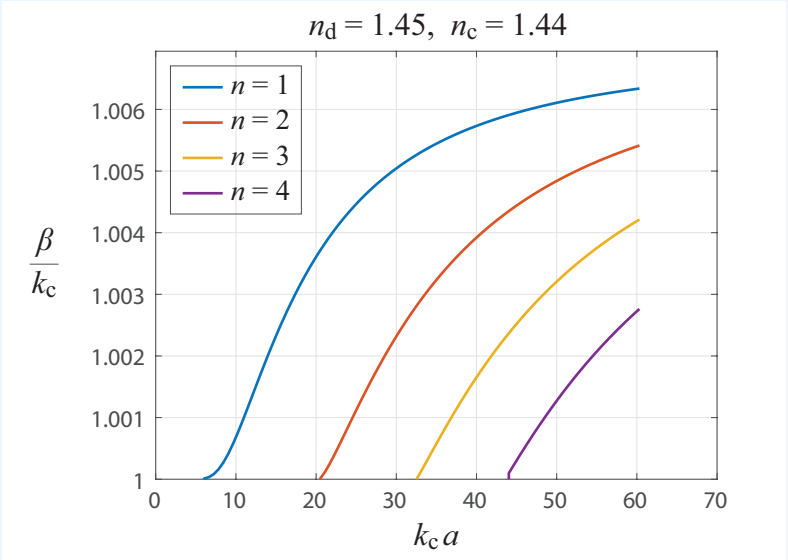


**Figure 7-12:** The normalized propagation constant of hybrid modes inside an optical fiber as a function of $k_c a$ for different mode numbers $n$. Here the index of refraction of the cladding is $n_c = 1.44$ and that of the core is $n_d = 1.45$.

$$K_0'(\upsilon) = -K_1(\upsilon)\ .$$

Hence the two transcendental equations defined by Eqs. (7.105a) and (7.105b) can be written as

$$\frac{\mu_d}{u}\frac{J_1(u)}{J_0(u)} = -\frac{\mu_c}{\upsilon}\frac{K_1(\upsilon)}{K_0(\upsilon)} \tag{7.106a}$$

and

$$\frac{\varepsilon_d}{u}\frac{J_1(u)}{J_0(u)} = -\frac{\varepsilon_c}{\upsilon}\frac{K_1(\upsilon)}{K_0(\upsilon)}\ . \tag{7.106b}$$

Equation (7.105a) (or Eq. (7.106a)) can be obtained from Eqs. (7.97b) and (7.98a) by setting $n = 0$. However, to make sure Eq. (7.98b) is also satisfied, $A_0$ must be zero and, according to Eq. (7.97a), $C_0$ must also be zero. This will constitute a TE wave in the fiber. Also, Eq. (7.105b) (or Eq. (7.106b)) can be obtained directly from Eqs. (7.97a) and (7.98b) by setting $n = 0$. To ensure that Eq. (7.98a) is also satisfied, we must have $B_0 = D_0 = 0$. This corresponds to a TM wave in the fiber.

To examine the behavior of the cutoff frequencies of hybrid modes in optical fibers, we consider an optical fiber with $n_c = 1.44$ and $n_d = 1.45$, and then solve the transcendental equation (Eq. (7.104)) by varying $k_c a$ and the normalized propagation constant $\beta/k_c$ for different values of $n$, as shown in Fig. 7-12. The significance of the results shown in Fig. 7-12 pertains to the bandwidth over which a single mode operation can be maintained. For the

dominant mode corresponding to $n = 1$ from $k_c a \approx 7$ to $k_c a \approx 21$, the fiber can only support the dominant mode. This indicates that the dominant mode, for a fixed fiber radius, has a bandwidth of almost 1.5 octaves.

## 7-3 Radial and Circumferential Waveguides

The transverse electric and magnetic field expansion developed for uniform waveguides can also be applied to structures confined by two planar conductors perpendicular to the $z$-axis. In such cases a standing wave forms along the $z$-axis and propagation can occur in radial or circumferential directions. Since a tangential electric field (transverse electric field) must vanish on planes perpendicular to the $z$-axis, the appropriate boundary condition for the potentials can be obtained from

$$\mathbf{E}_t^{TM} = \frac{\partial}{\partial z} \nabla_t \psi^{TM} \Big|_{r \in z-\text{const. plane}} = 0 \quad \rightarrow \quad \frac{\partial \psi^{TM}}{\partial z} \Big|_{r \in z-\text{const. plane}} = 0 \tag{7.107a}$$

and

$$\mathbf{E}_t^{TE} = i\omega\mu \ \nabla_t \psi^{TE} \big|_{r \in z-\text{const. plane}} = 0 \quad \rightarrow \quad \psi^{TE} \big|_{r \in z-\text{const. plane}} = 0 \, . \tag{7.107b}$$

### 7-3.1 Radial Waveguide

The configuration of a sectoral horn is depicted in Fig. 7-13(a). The sectoral horn is made up of two metallic plates at $\phi = 0$ and $\phi = \alpha$ and two horizontal metallic plates at $z = 0$ and

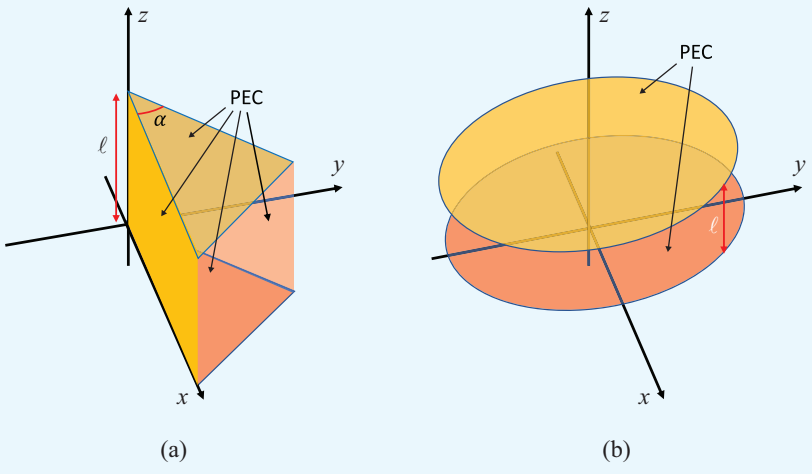


**Figure 7-13:** (a) A sectoral horn waveguide formed by $z = 0$ and $z = \ell$ metallic plates on the top and bottom and $\phi = 0$ and $\phi = \alpha$ metallic plates. (b) A radial waveguide with azimuthal symmetry.

$z = \ell$. The TM radial waves supported by the sectoral horn can be generated from potential

$$\psi^{\mathrm{TM}}(\rho,\phi,z) = H^{(1)}_{n\pi/\alpha}(k_\rho \rho)\, \sin\left(\frac{n\pi}{\alpha}\,\phi\right) \cos\left(\frac{q\pi}{\ell}\,z\right)\,, \qquad n = 1,2,3,\ldots, \quad q = 0,1,2,\ldots \tag{7.108}$$

as this potential satisfies the boundary conditions

$$\psi^{\mathrm{TM}}(\rho,0,z) = \psi(\rho,\alpha,z) = 0 \tag{7.109a}$$

and

$$\left.\frac{\partial \psi^{\mathrm{TM}}}{\partial z}\right|_{\rho,\phi,0} = \left.\frac{\partial \psi^{\mathrm{TM}}}{\partial z}\right|_{\rho,\phi,\ell} = 0\,. \tag{7.109b}$$

In Eq. (7.108), $k_\rho = \sqrt{k^2 - \beta^2} = \sqrt{k^2 - (q\pi/\ell)^2}$ . The choice of Hankel function of the first kind indicates just an outward-traveling wave. In practice, for a sectoral horn of finite dimensions between $\rho = \rho_1$ and $\rho = \rho_2$, the modal solution may be written as

$$\psi^{\mathrm{TM}}_{nq}(\rho,\phi,z) = \left[A_{nq}\, J_{n\pi/\alpha}(k_\rho\rho) + B_{nq}\, N_{n\pi/\alpha}(k_\rho\rho)\right] \sin\left(\frac{n\pi}{\alpha}\,\phi\right) \cos\left(\frac{q\pi}{\ell}\,z\right)\,. \tag{7.110}$$

The unknown coefficients depend on the field distributions at $\rho = \rho_1$ and $\rho = \rho_2$.

Also, for a TE wave, the following potential can be used:

$$\psi^{\mathrm{TE}}_{nq} = H^{(1)}_{n\pi/\alpha}(k_\rho\rho)\, \cos\left(\frac{n\pi}{\alpha}\,\phi\right) \sin\left(\frac{q\pi}{\ell}\,z\right)\,, \qquad n = 0,1,2,\ldots, \quad q = 1,2,\ldots \tag{7.111}$$

Note that for TM waves the lowest-order mode corresponds to $q = 0$, for which $k_\rho = k_0$, and thus there is no cutoff frequency for TM waves. On the other hand, for TE waves the lowest-order mode corresponds to $q = 1$, for which the cutoff wave number is $k_{\mathrm{c}}^{\mathrm{TE}_1} = \pi/\ell$.

A particular type of radial waveguide with azimuthal symmetry is shown in Fig. 7-13(b). For this radial waveguide the lowest-order mode is $\mathrm{TM}_0$ mode, whose fields resemble that of an infinite line source in free space:

$$\psi^{\mathrm{TM}_{0q}}(\rho,\phi,z) = H^{(1)}_0(k_\rho\rho) \cos\left(\frac{q\pi}{\ell}\,z\right)\,, \tag{7.112a}$$

where $k_\rho = [k^2 - (q\pi/\rho)^2]^{1/2}$. For $n = 0$ and $q = 0$, the electric and magnetic fields are given by

$$E_z^{\mathrm{TM}_{00}}(\rho,\phi,z) = k^2\, H_0^{(1)\prime}(k\rho)\,, \tag{7.112b}$$

and

$$H_\phi^{\mathrm{TM}_{00}} = i\omega\varepsilon k\, H_0^{(1)\prime}(k\rho) = -ik^2 \sqrt{\frac{\varepsilon}{\mu}}\, H_1^{(1)}(k\rho)\,. \tag{7.112c}$$

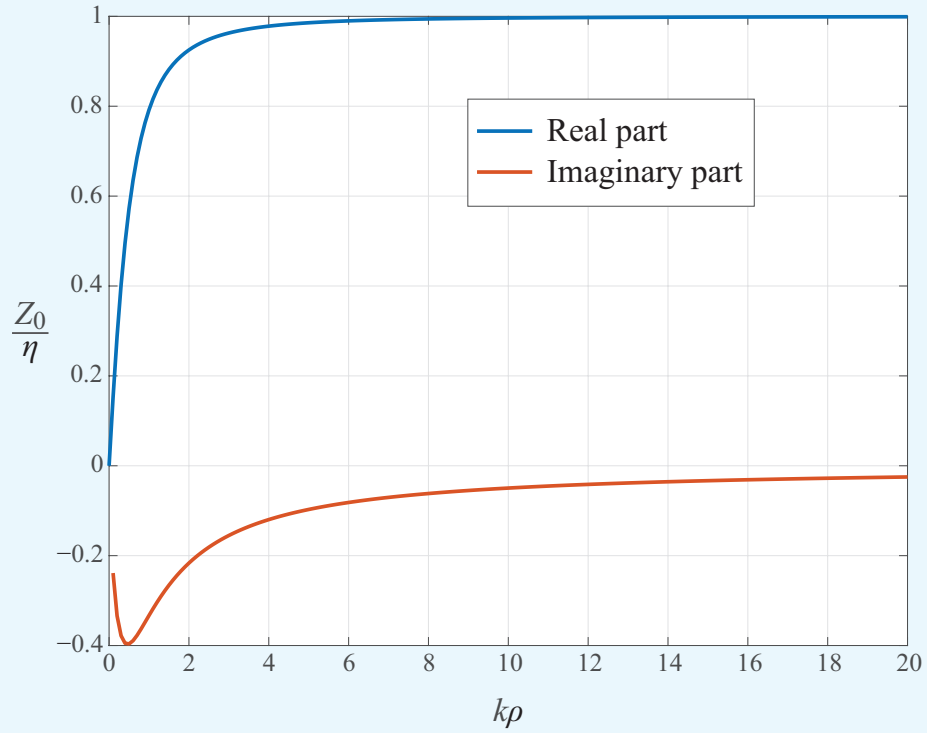


**Figure 7-14:** The complex characteristic impedance of a $TM_0$ mode in a radial waveguide as a function of radial distance ($k\rho$).

In fact, this is a TEM wave propagating in the $\hat{\boldsymbol{\rho}}$-direction, whose characteristic impedance is a function of $\rho$:

$$Z_0 = \frac{E_z^{\mathrm{TM}_{00}}}{-H_\phi^{\mathrm{TM}_{00}}} = \frac{\eta\, H_0^{(1)}(k\rho)}{i\, H_1^{(1)}(k\rho)} \,. \tag{7.113}$$

It can be shown that when $k\rho \gg 1$, the waveguide characteristic impedance is

$$\lim_{k\rho\to\infty} Z_0 = \eta \,.$$

Figure 7-14 shows the complex characteristic impedance of the radial waveguide as a function of $k\rho$.

### 7-3.2 Circumferential Waveguide

The configuration for a circumferential waveguide is shown in Fig. 7-15. In this case, propagation is along $\hat{\boldsymbol{\phi}}$. The geometry shown in this figure is formed by curved metallic walls at $\rho = \rho_1$ and $\rho = \rho_2$, and metallic plates at $z = 0$ and $z = b$. By setting $\rho_2 - \rho_1 = a$, the configuration becomes an H-bent rectangular waveguide for a $TE_{10}$ mode in a rectangular

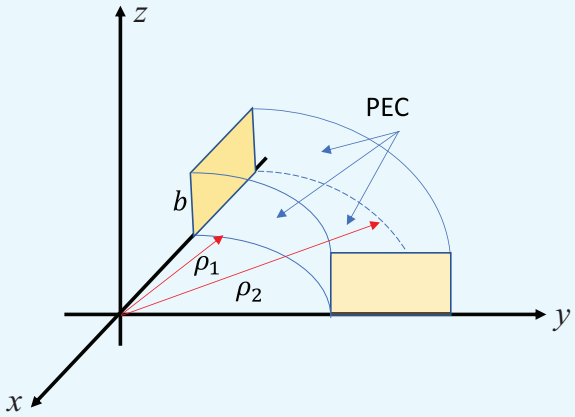


**Figure 7-15:** Configuration of a circumferential waveguide formed by metallic plates at $z = 0$, $z = b$, $\rho = \rho_1$, and $\rho = \rho_2$.

waveguide with $a > b$. The appropriate potential for a $\mathrm{TM}_{v0}$ wave in this circumferential waveguide can be written as

$$\psi^{\mathrm{TM}_{v0}} = [J_v(k\rho)\, N_v(k\rho_1) - J_v(k\rho_1)\, N_v(k\rho)]\,(Ae^{iv\phi} + B^{-iv\phi})\,. \tag{7.114}$$

The choice of radial function is made to ensure that

$$\psi(\rho,\phi,z)\big|_{\rho=\rho_1} = 0\,, \tag{7.115}$$

and coefficients $A$ and $B$ are to be determined depending on the input and output field conditions at the ends of the bent. The boundary condition at $\rho = \rho_2$ is satisfied when

$$F = J_v(k\rho_2)\, N_v(k\rho_1) - J_v(k\rho_1)\, N_v(k\rho_2) = 0\,. \tag{7.116}$$

This provides an equation for the angular propagation constant $v$. Figure 7-16 shows the plot of a function $F$ representing the left-hand side of Eq. (7.116) as a function of $v$ for two cases, one where $\rho_1 = \lambda$ and another where $\rho_1 = 1.1\lambda$, $\rho_2 - \rho_1 = 0.762\lambda$ in both cases. The zeros of Eq. (7.116) are found to be $v = 6.53$ and $v = 7$ for $\rho_1 = \lambda$ and $\rho_1 = 1.1\lambda$, respectively.

## 7-4 Green's Functions Solutions for Some Canonical Problems

The cylindrical wave functions can be used to construct Green's function for waveguides and scattering problems. In what follows we will examine the solution for Green's functions for some canonical problems.

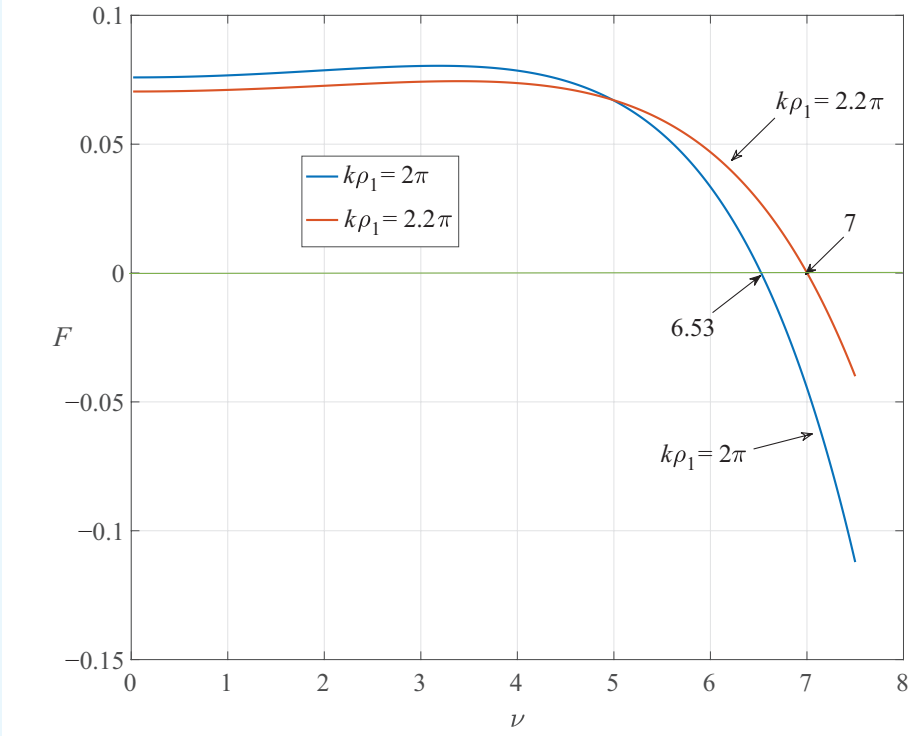


**Figure 7-16:** The transcendental function $F$ given by Eq. (7.116) as a function of $\nu$. The zero crossing of the function indicates the solution of Eq. (7.116). The two graphs correspond to $\rho_1 = \lambda$ and $\rho_1 = 1.1\lambda$, with $\rho_2 - \rho_1 = 0.762\lambda$ in both cases.

### 7-4.1 Green's Function for an Angular-Sector Waveguide

Consider a filament-line current along the $z$-axis located at $\boldsymbol{\rho} = \boldsymbol{\rho}'$ within an angular-sector waveguide, as shown in Fig. 7-17. The current distribution is $\mathbf{J} = \delta(\boldsymbol{\rho} - \boldsymbol{\rho}')\, e^{i\beta z}\, \hat{\mathbf{z}}$, and it excites a TM wave. The Green's function for the problem can be constructed from the eigenvalues and eigenfunction of the waveguide, and is given by

$$g(\boldsymbol{\rho}, \boldsymbol{\rho}') = \sum_n \sum_p \frac{\psi_{np}(\rho')\, \psi_{np}(\rho)}{(k_{np}^2 - k_\rho^2) \iint \psi_{np}^2 \rho\, d\rho\, d\phi}\,,$$

where $k_\rho^2 = k^2 - \beta^2$. Noting that

$$\int_0^{\phi_0} \sin^2\left(\frac{n\pi}{\phi_0}\phi\right) d\phi = \frac{\phi_0}{2} \tag{7.117a}$$

and

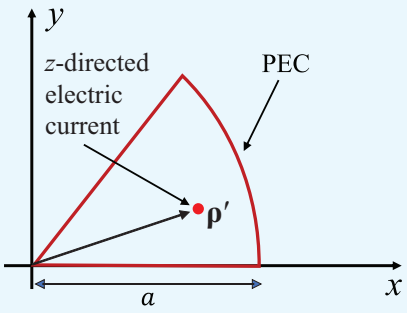


**Figure 7-17:** Configuration of a line source in an angular-sector waveguide. The current distribution is $\mathbf{J} = \delta(\boldsymbol{\rho} - \boldsymbol{\rho}')\, e^{i\beta z}\, \hat{\mathbf{z}}$.

$$\int_0^a \rho\, J_\nu^2\left(\frac{x_{\nu_p}}{a}\rho\right)\, d\rho = \frac{a^2}{2}\, J_{\nu+1}^2(x_{\nu_p})\,, \tag{7.117b}$$

the Green's function takes the following form:

$$g(\boldsymbol{\rho},\boldsymbol{\rho}') = \frac{4}{a^2\phi_0}\sum_{n=1}^{\infty}\sum_{p=1}^{\infty}\frac{\sin\left(\frac{n\pi}{\phi_0}\phi\right)\sin\left(\frac{n\pi}{\phi_0}\phi'\right)\, J_{n\pi/\phi_0}\left(\frac{x_{\nu_p}}{a}\rho\right)\, J_{n\pi/\phi_0}\left(\frac{x_{\nu_p}}{a}\rho'\right)}{(k_{np}^2 - k_\rho^2)\, J_{(n\pi/\phi_0)+1}^2(x_{\nu_p})}\,, \tag{7.118}$$

where

$$k_{np} = \frac{x_{\nu_p}}{a} \qquad \text{for } \nu = \frac{n\pi}{\phi_0}\,.$$

Also, noting that

$$\lim_{x_{\nu_p}\to\infty} J_{\nu+1}(x_{\nu_p}) = (-1)^n\sqrt{\frac{2}{\pi x_{\nu_p}}}\,,$$

the Green's function for the unbounded angular sector can be obtained from

$$g(\boldsymbol{\rho},\boldsymbol{\rho}') = \frac{2}{\phi_0}\sum_{n=1}^{\infty}\sin\left(\frac{n\pi}{\phi_0}\phi\right)\sin\left(\frac{n\pi}{\phi_0}\phi'\right)\int_0^\infty \frac{\alpha}{\alpha^2 - k_\rho^2}\, J_{n\pi/\phi_0}(\alpha\rho)\, J_{n\pi/\phi_0}(\alpha\rho')\, d\alpha\,. \tag{7.119}$$

The Green's function for a circular waveguide with a vane at $\phi = 0$ (see Fig. 7-18) can now easily be obtained from Eq. (7.118) by letting $\phi_0 = 2\pi$ and is given by

$$g(\boldsymbol{\rho},\boldsymbol{\rho}') = \frac{2}{a^2\pi}\sum_{n=1}^{\infty}\sum_{p=1}^{\infty}\frac{\sin\left(\frac{n}{2}\,\phi\right)\sin\left(\frac{m}{2}\,\phi'\right)\, J_{n/2}\left(\frac{x_{np}}{a}\,\rho\right)\, J_{m/2}\left(\frac{x_{np}}{a}\,\rho'\right)}{(k_{np}^2 - k_\rho^2)\, J_{(n+3)/2}^2(x_{np})}, \tag{7.120}$$

where $x_n$ is the $n$th zero of $J_{m/2}(x)$.

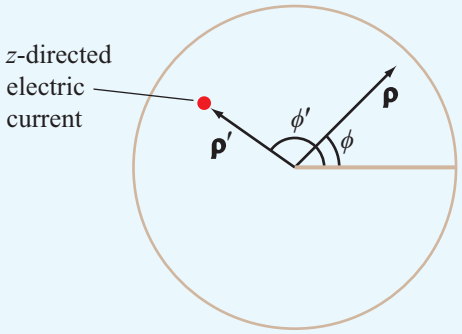


**Figure 7-18:** A circular waveguide with a metallic vane at $\phi = 0$ and a line source at $\boldsymbol{\rho}'$.

### 7-4.2 Formal Solution for Green's Function of an Angular Sector

In the previous section, the solution for Green's function for the angular-sector waveguide was obtained from the formulation based on eigenfunctions. In this section the expression for the Green's function will be derived directly from the solution of the scalar wave function in response to a delta function. The geometry of the problem is shown in Fig. 7-17. The Green's function must satisfy

$$\left[\frac{1}{\rho}\frac{\partial}{\partial\rho}\left(\rho\frac{\partial}{\partial\rho}\right)+\frac{1}{\rho^2}\frac{\partial^2}{\partial\phi^2}+k_\rho^2\right] g(\boldsymbol{\rho},\boldsymbol{\rho}') = -\frac{\delta(\rho-\rho')\,\delta(\phi-\phi')}{\rho}\,, \tag{7.121}$$

and for the TM case, $g(\boldsymbol{\rho},\boldsymbol{\rho}')$ must vanish on the waveguide surface ($\phi = 0$, $\phi = \phi_0$, and $\rho = a$). Using the method of separation of variables, we get

$$g(\boldsymbol{\rho},\boldsymbol{\rho}') = \sum_n g(\rho,\rho')\,F_n(\phi,\phi')\,,$$

and we should note that

$$\delta(\phi-\phi') = \frac{2}{\phi_0}\sum_{n=1}^{\infty}\sin\left(\frac{n\pi}{\phi_0}\phi'\right)\sin\left(\frac{n\pi}{\phi_0}\phi\right)\,. \tag{7.122}$$

The appropriate solution for $F_n(\phi,\phi')$ is similar to the one for $\delta(\phi-\phi')$. Hence

$$\left[\frac{1}{\rho}\frac{\partial}{\partial\rho}\left(\rho\frac{\partial}{\partial\rho}\right)-\left(\frac{n\pi}{\phi_0}\right)^2\frac{1}{\rho^2}+k_\rho^2\right] g(\rho,\rho') = -\frac{\delta(\rho-\rho')}{\rho}\,. \tag{7.123}$$

Direct observation of Eq. (7.123) indicates that $g(\rho,\rho')$ must be continuous at $\rho = \rho'$, but its derivative with respect to $\rho$ at $\rho'$ is discontinuous and the level of discontinuity is $-1/\rho'$. This is the reason for having a delta function on the right-hand side of Eq. (7.123). Let us denote the solution for $g(\rho,\rho')$ where $\rho < \rho'$ by $g_<(\rho,\rho')$, and that for $g(\rho,\rho')$ where $\rho > \rho'$ by

$g_>(\rho,\rho')$. For region $\rho<\rho'$, $g_<$ must be regular. Hence

$$g_< = A\,J_\nu(k_\rho\rho)\;, \tag{7.124}$$

but $g_>$ can be arbitrary in the region $\rho>\rho'$. Hence

$$g_> = B\,J_\nu(k_\rho\rho)+C\,H_\nu^{(1)}(k_\rho\rho)\;, \tag{7.125}$$

where as before $\nu = n\pi/\phi_0$. Continuity of $g$ at $\rho=\rho'$ requires

$$g_< = g_>\;. \tag{7.126}$$

Also,

$$\frac{\partial g_>}{\partial\rho}-\frac{\partial g_<}{\partial\rho} = -\frac{1}{\rho'}\;. \tag{7.127}$$

The boundary condition at $\rho=a$ enforces

$$g_>(a) = B\,J_\nu(k_\rho a)+C\,H_\nu^{(1)}(k_\rho a) = 0\;. \tag{7.128}$$

From Eq. (7.126) and Eq. (7.127),

$$\begin{cases}(A-B)\,J_\nu(k_\rho\rho')-C\,H_\nu^{(1)}(k_\rho\rho') = 0\;,\\ (A-B)\,J_\nu'(k_\rho\rho')-C\,H_\nu^{(1)'}(k_\rho\rho') = \dfrac{1}{k_\rho\rho'}\;.\end{cases} \tag{7.129}$$

Solving Eq. (7.129), we have

$$C = \frac{-J_\nu(k_\rho\rho')}{k_\rho\rho'\left[J_\nu(k_\rho\rho')\,H_\nu^{(1)'}(k_\rho\rho')-J_\nu'(k_\rho\rho')\,H_\nu^{(1)}(k_\rho\rho')\right]}$$

and

$$A-B = \frac{-H_\nu^{(1)}(k_\rho\rho')}{k_\rho\rho'\left[J_\nu(k_\rho\rho')\,H_\nu^{(1)'}(k_\rho\rho')-J_\nu'(k_\rho\rho')\,H_\nu^{(1)}(k_\rho\rho')\right]}\;.$$

Noting the Wronskian relationship

$$W\left[J_\nu(X),\,H_\nu^{(1)}(X)\right] = J_\nu(X)\,H_\nu^{(1)'}(X)-J_\nu'(X)\,H_\nu^{(1)}(X) = \frac{2i}{\pi X} \tag{7.130}$$

and the boundary condition given by Eq. (7.128), we can easily show that

$$C = -\frac{\pi}{2i}\,J_\nu(k_\rho\rho')\;,$$

$$B = -\frac{i\pi}{2}\,\frac{J_\nu(k_\rho\rho')\,H_\nu^{(1)}(k_\rho a)}{J_\nu(k_\rho a)}\;,$$

and

$$A = \frac{\pi i}{2}\left(H_\nu^{(1)}(k_\rho\rho') - \frac{J_\nu(k_\rho\rho')\,H_\nu^{(1)}(k_\rho a)}{J_\nu(k_\rho a)}\right).$$

Consequently,

$$g_<(\boldsymbol{\rho},\boldsymbol{\rho}') = \frac{\pi i}{\phi_0}\sum_{n=1}^{\infty} J_\nu(k_\rho\rho)\left(H_\nu^{(1)}(k_\rho\rho') - \frac{J_\nu(k_\rho\rho')\,H_\nu^{(1)}(k_\rho a)}{J_\nu(k_\rho a)}\right)\sin\nu\phi\sin\nu\phi' \quad (7.131a)$$

and

$$g_>(\boldsymbol{\rho},\boldsymbol{\rho}') = \frac{\pi i}{\phi_0}\sum_{n=1}^{\infty} J_\nu(k_\rho\rho')\left(H_\nu^{(1)}(k_\rho\rho) - \frac{J_\nu(k_\rho\rho)\,H_\nu^{(1)}(k_\rho a)}{J_\nu(k_\rho a)}\right)\sin\nu\phi\sin\nu\phi', \quad (7.131b)$$

where, as before, $\nu = n\pi/\phi_0$.

By comparing Eqs. (7.131a) and (7.131b) with Eq. (7.118), it becomes obvious that reciprocity relations hold and that the expressions obtained from the latter procedure are much easier to compute than Eq. (7.118).

### 7-4.3 Two-Dimensional Green's Function for an Unbounded Homogeneous Medium

In this section we consider the problem of field radiation from an infinitely long time-harmonic filament current. Consider an infinitely long electric current $Ie^{i\beta z}$ located at the origin along the $z$-axis, as shown in Fig. 7-19. The current distribution is given by

$$\mathbf{J}(\mathbf{r}) = Ie^{i\beta z}\,\delta(\boldsymbol{\rho})\,\hat{\mathbf{z}}. \quad (7.132)$$

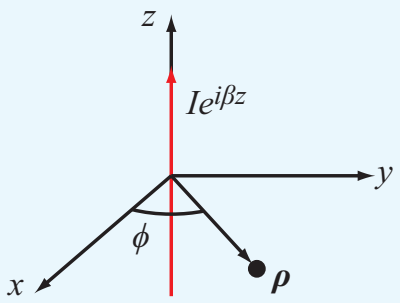


**Figure 7-19:** An infinite current filament along the $z$-axis carrying current $Ie^{i\beta z}$ and an observation point in the $x$–$y$ plane indicated by $\boldsymbol{\rho}$.

This current produces only the $z$-component of the Hertz potential, which satisfies

$$\nabla^2\Pi_z + k^2\Pi_z = \frac{-i}{\omega\varepsilon}\, I e^{i\beta z}\, \delta(\boldsymbol{\rho}) \,. \tag{7.133}$$

As previously stated, since the $z$-dependence of the current is of the form $e^{i\beta z}$, $\Pi(\rho,\phi,z)$ can be written as

$$\Pi_z(\rho,\phi,z) = \Psi(\rho,\phi)\, e^{i\beta z} \,, \tag{7.134}$$

and $\Psi(\rho,\phi)$ is a solution to the following 2-D wave equation:

$$\nabla_{\mathrm{t}}^2\, \Psi(\rho,\phi) + k_\rho^2\, \Psi(\rho,\phi) = \frac{-i}{\omega\varepsilon}\, I\, \delta(\boldsymbol{\rho}) \,, \tag{7.135}$$

where $k_\rho^2 = k^2 - \beta^2$.

Using the method of separation of variables, $\psi$ can be expressed in terms of the product of two functions dependent on only $\phi$ and $\rho$, respectively. Because of the symmetry of the problem, the solution is independent of $\phi$. The dependence on $\rho$ is of the form of Bessel functions, and since the source is at the origin, an outgoing waveform must be chosen. An admissible solution is then of the following form:

$$\Psi(\rho,\phi) = A\, H_0^{(1)}(k_\rho\rho) \,.$$

Since the source is at the origin, a singular behavior of the field at $\rho = 0$ is expected. From Eq. (5.102b), the magnetic field is obtained from

$$\begin{aligned}\mathbf{H}(\rho,\phi) &= -i\omega\varepsilon k_\rho A\, H_0^{(1)'}(k_\rho\rho)\, \hat{\boldsymbol{\rho}} \times \hat{\mathbf{z}} \\ &= i\omega\varepsilon k_\rho A\, H_0^{(1)'}(k_\rho\rho)\, e^{i\beta z}\, \hat{\boldsymbol{\phi}} \,.\end{aligned}$$

According to Ampère's law,

$$\lim_{\rho\to 0} \oint_C H_\phi(\rho,\phi)\, \rho\, d\phi = I \,, \tag{7.136}$$

because

$$\lim_{\rho\to 0} \int_0^{\rho} \int_0^{2\pi} i\omega\varepsilon\, \mathbf{E}\cdot\hat{\mathbf{z}}\, \rho\, d\rho\, d\phi = 0 \,.$$

Using the small-argument expansion of the Hankel function, we have

$$\lim_{X\to 0} H_0^{(1)}(X) \approx -\frac{i2}{\pi}\, \ln\left(\frac{2}{\gamma X}\right) \,,$$

where $\gamma = 1.78107$. As a result it can be easily shown that

$$H_0^{(1)'}(k_\rho\rho) \approx \frac{i2}{\pi}\, \frac{1}{k_\rho\rho} \,. \tag{7.137}$$

Using Eq. (7.137) in Eq. (7.136), we have

$$i\omega\varepsilon k_\rho A \int_0^{2\pi} \frac{i2}{\pi}\,\frac{1}{k_\rho\rho}\,\rho\,d\phi = -4\omega\varepsilon A = I\,,$$

from which $A$ is found to be

$$A = \frac{-I}{4\omega\varepsilon}\,.$$

Hence the magnetic field produced by the filament current is given by

$$\mathbf{H}(\rho,\phi) = \frac{-ik_\rho I}{4}\,H_0^{(1)'}(k_\rho\rho)\,e^{i\beta z}\,\hat{\boldsymbol{\phi}}\,. \tag{7.138}$$

Also, the electric field is found from Eq. (5.102a) to be

$$\mathbf{E}(\rho,\phi) = \frac{-k_\rho^2 I}{4\omega\varepsilon}\,H_0^{(1)}(k_\rho\rho)\,e^{i\beta z}\,\hat{\mathbf{z}} - \frac{iI\beta k_\rho}{4\omega\varepsilon}\,H_0^{(1)'}(k_\rho\rho)\,\hat{\boldsymbol{\rho}}\,. \tag{7.139}$$

Now, positioning the current filament at $\boldsymbol{\rho}'$, we have

$$\Pi_z(\boldsymbol{\rho},\boldsymbol{\rho}') = \frac{-I}{4\omega\varepsilon}\,H_0^{(1)}(k_\rho|\boldsymbol{\rho}-\boldsymbol{\rho}'|)\,e^{i\beta z}\,, \tag{7.140}$$

which can be used to find the Hertz potential for an arbitrary current distribution

$$\mathbf{J}(\boldsymbol{\rho},z) = J(\boldsymbol{\rho})\,e^{i\beta z}\,\hat{\mathbf{z}}\,.$$

The Hertz potential for this current distribution is given by

$$\Pi_z(\rho) = \frac{-e^{i\beta z}}{4\omega\varepsilon}\iint_S J(\boldsymbol{\rho}')\,H_0^{(1)}(k_\rho|\boldsymbol{\rho}-\boldsymbol{\rho}'|)\,\rho'\,d\rho'\,d\phi'\,, \tag{7.141}$$

where $S$ specifies the region for the current distribution. The electric field is given by

$$\mathbf{E}(\rho,\phi) = \frac{-k_\rho}{4\omega\varepsilon}\,e^{i\beta z}\left\{\iint_S\left[k_\rho H_0^{(1)}(k_\rho|\boldsymbol{\rho}-\boldsymbol{\rho}'|)\,\hat{\mathbf{z}} + i\beta\,H_0^{(1)'}(k_\rho|\boldsymbol{\rho}-\boldsymbol{\rho}'|)\,\hat{\boldsymbol{\rho}}\right]J(\boldsymbol{\rho}')\,\rho'\,d\rho'\,d\phi'\right\}, \tag{7.142}$$

where $|\boldsymbol{\rho}-\boldsymbol{\rho}'| = \sqrt{(x-x')^2-(y-y')^2}$ in the Cartesian coordinate system.

Also, the magnetic field can be computed from

$$\mathbf{H}(\rho,\phi) = \frac{-ik_\rho}{4}\iint_S J(\boldsymbol{\rho}')\,H_0^{(1)'}(k_\rho|\boldsymbol{\rho}-\boldsymbol{\rho}'|)\,\frac{\hat{\mathbf{z}}\times(\boldsymbol{\rho}-\boldsymbol{\rho}')}{|\boldsymbol{\rho}-\boldsymbol{\rho}'|}\,\rho'\,d\rho'\,d\phi'\,. \tag{7.143}$$

Note here that $\hat{\boldsymbol{\phi}} = \hat{\mathbf{z}}\times\hat{\boldsymbol{\rho}}$, as used in Eq. (7.138), depends on the origin of the coordinate system, and thus in general its expanded form must be used. That is, once the origin is

translated to $\rho'$, $\hat{\boldsymbol{\phi}}$ is changed accordingly. To track this change, $\hat{\boldsymbol{\phi}}$ is first written as

$$\hat{\boldsymbol{\phi}} = \hat{\mathbf{z}} \times \hat{\boldsymbol{\rho}} = \hat{\mathbf{z}} \times \frac{\boldsymbol{\rho}}{|\boldsymbol{\rho}|} ,$$

and then $\boldsymbol{\rho}$ is translated.

The far-field expressions for Eqs. (7.138) and (7.139) are given by

$$H_\phi(\rho,\phi) \approx k_\rho I \sqrt{\frac{1}{8\pi k_\rho \rho}}\, e^{i(k_\rho \rho - \pi/4)} e^{i\beta z} , \tag{7.144a}$$

$$E_z(\rho,\phi) \approx -\eta\, \frac{k_\rho^2}{k}\, I \sqrt{\frac{1}{8\pi k_\rho \rho}}\, e^{i(k_\rho \rho - \pi/4)} e^{i\beta z} , \tag{7.144b}$$

and

$$E_\rho(\rho,\phi) \approx \eta\, \frac{k_\rho \beta}{k}\, I \sqrt{\frac{1}{8\pi k_\rho \rho}}\, e^{i(k_\rho \rho - \pi/4)} e^{i\beta z} , \tag{7.144c}$$

which show that the equiphase and equiamplitude surfaces are cylinders (constant $\rho$). Also, in the far-field

$$\frac{|\mathbf{E}|}{|H_\phi|} = \eta = \sqrt{\frac{\mu}{\varepsilon}} ,$$

and the fields are TEM.

The total power per unit length radiated by the filament current can be computed by integrating the Poynting vector over the surface of a cylinder of height 1 m:

$$\begin{aligned} P_{\text{rad}} &= \frac{1}{2} \int_0^{2\pi} \int_0^1 R_{\text{e}}(E \times H^*) \cdot \hat{\boldsymbol{\rho}} \rho \, d\phi \, dz \\ &= \frac{1}{2} R_{\text{e}} \left\{ \frac{i\pi k_\rho^3 |I|^2}{8\omega\varepsilon}\, \rho\, H_0^{(1)}(k_\rho \rho)\, \left[ H_0^{(1)'}(k_\rho \rho) \right]^* \right\} . \end{aligned} \tag{7.145}$$

Noting that

$$\begin{aligned} H_0^{(1)}(k_\rho \rho)\, [H_0^{(1)'}(k_\rho \rho)]^* &= H_0^{(1)}(k_\rho \rho)\, J_0'(k_\rho \rho) - i H_0^{(1)}(k_\rho \rho)\, N_0'(k_\rho \rho) \\ &= J_0(k_\rho \rho)\, J_0'(k_\rho \rho) + N_0(k_\rho \rho)\, N_0'(k_\rho \rho) \\ &\quad - i \left[ J_0(k_\rho \rho)\, N_0'(k_\rho \rho) - J_0'(k_\rho \rho)\, N_0(k_\rho \rho) \right] , \end{aligned}$$

and using the Wronskian relation $J_\nu(x)\, N_\nu'(x) - J_\nu'(x)\, N_\nu(x) = \frac{2}{\pi x}$, the radiated power per unit length is given by

$$P_{\text{rad}} = \frac{k_\rho^2}{8\omega\varepsilon}\, |I|^2 \quad \text{W/m.} \tag{7.146}$$

It is interesting to note that the time-average radiated power is independent of distance from the source and proportional to the square of the current.

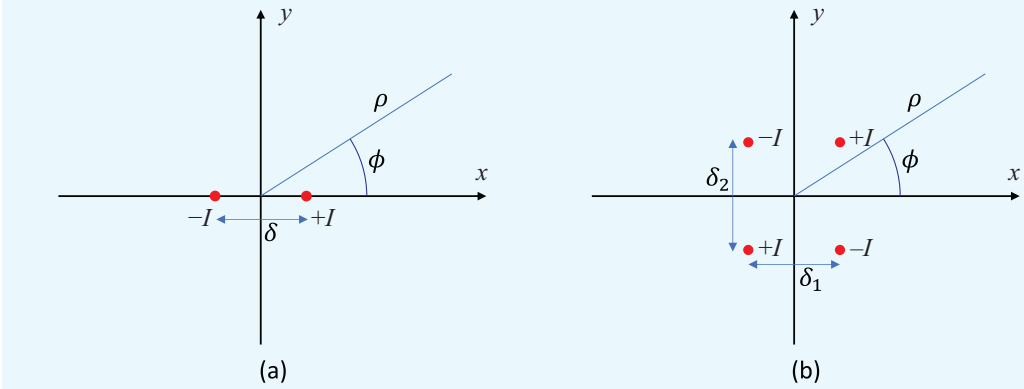


**Figure 7-20:** (a) The configuration of a two-dimensional dipole (line currents flowing in opposite directions) and (b) the configuration of a two-dimensional quadrupole. Here $\delta$, $\delta_1$, and $\delta_2$ are much smaller than a wavelength.

### 7-4.4 Multipole Representation of Cylindrical Wave Functions

In this section, it is shown that an $n$th-order cylindrical wave function of the following form:

$$\psi(\rho,\phi) = H_n^{(1)}(k_\rho \rho) \begin{cases} \cos n\phi & \text{even}, \\ \sin n\phi & \text{odd}, \end{cases} \tag{7.147}$$

represents the Hertz vector potential of an ordered $2n$-element array of closely spaced $z$-directed filament currents of infinite extent flowing in the opposite direction of the adjacent elements. It was shown in the previous section that the Hertz vector potential of an infinite electric current filament is of the form of (see Eq. (7.134))

$$\Pi_z^1(\rho,\phi,z) = \frac{-I}{4\omega\varepsilon} H_0^{(1)}(k_\rho \rho)\, e^{i\beta z} . \tag{7.148}$$

Now let us consider two closely spaced infinite current filaments carrying currents in opposite directions, as shown in Fig. 7-20(a). The separation between the two current lines is denoted by $\delta$, which is much smaller than a wavelength. Obviously, as $\delta \to 0$, the fields emitted from these two currents cancel each other. To ensure a nonzero field, the magnitude of current $I$ can be increased so that $I\delta$ is kept constant as $\delta$ becomes smaller. This configuration of currents is called a ***two-dimensional dipole***. Using superposition, the resulting Hertz vector potential can be obtained from

$$\Pi_z^{2x} = \Pi_z^1\left(x - \frac{\delta}{2}, y\right) - \Pi_z^1\left(x + \frac{\delta}{2}, y\right) . \tag{7.149}$$

In the limit as $\delta \to 0$, Eq. (7.149) can be written as

$$\Pi_z^{2_x} = -\delta \frac{\partial \Pi_z^1}{\partial x} = \frac{I\delta}{4\omega\varepsilon} e^{i\beta z} \frac{\partial}{\partial x} [H_0^{(1)}(k_\rho \rho)]$$
$$= -\frac{k_\rho I\delta}{4\omega\varepsilon} e^{i\beta z} H_1^{(1)}(k_\rho \rho)\cos\phi \ . \tag{7.150}$$

As shown above, the Hertz vector potential of this dipole is entirely expressed by an even cylindrical wave function of order $n = 1$. It can easily be shown that if the two current lines are placed on the $y$-axis, the Hertz vector potential can be expressed by an odd cylindrical wave function of order $n = 1$. Now let us consider the current configuration of Fig. 7-20(b). This current configuration is know as a two-dimensional quadrupole. Using superposition, and in the limit as $\delta_1$ and $\delta_2$ approach zero, the Hertz vector potential for the quadrupole is given by

$$\Pi_z^{4_{x,y}} \approx \delta_1 \delta_2 \frac{\partial^2 \Pi_z^1}{\partial x \, \partial y} = -\delta_2 \frac{\partial \Pi_z^{2_x}}{\partial y} \ . \tag{7.151}$$

Using Eq. (7.150) in Eq. (7.151),

$$\Pi_z^{4_{x,y}} \approx \frac{-Ik_\rho \delta_1 \delta_2}{4\omega\varepsilon} e^{i\beta z} \frac{\partial}{\partial y} [H_1^{(1)}(k_\rho \rho)\cos\phi] \ . \tag{7.152}$$

Carrying out the differentiation of Eq. (7.152) reduces to

$$\Pi_z^{4_{x,y}} \approx \frac{k_\rho^2 I\delta_1 \delta_2}{8\omega\varepsilon} e^{i\beta z} H_2^{(1)}(k_\rho \rho)\sin 2\phi \ . \tag{7.153}$$

Equation (7.153) shows that the Hertz vector potential of a quadrupole line source is a cylindrical wave function of order $n = 2$.

In general, a $2n$-pole line source is defined as $2n$ current lines equally spaced around the surface of a very small cylinder. It can be shown that the Hertz vector potential of the $2n$-pole line source is a cylindrical wave function of order $n$. Of course, duality can be applied to find the magnetic Hertz potential of $2n$-pole magnetic line sources.

### 7-4.5 Fourier Representation of the Two-Dimensional Green's Function

The fields generated by a filament current can be represented in terms of a continuous spectrum of plane waves. This representation can be obtained by expressing the scalar potential function $\psi(x,y)$ in Eq. (7.135) in terms of its Fourier transformation with respect to variable $x$:

$$\psi(x,y) = \frac{1}{2\pi} \int_{-\infty}^{\infty} \tilde{\psi}(k_x, y) \, e^{ik_x x} \, dk_x \ . \tag{7.154}$$

Also, noting that

$$\delta(x) = \frac{1}{2\pi} \int_{-\infty}^{\infty} e^{ik_x x} \, dk_x \ , \tag{7.155}$$

Eq. (7.135) can then be written as

$$\frac{1}{2\pi}\int_{-\infty}^{\infty}\left[\left(-k_x^2+\frac{d^2}{dy^2}\right)\,\widetilde{\psi}(k_x,y)+k_\rho^2\,\widetilde{\psi}(k_x,y)\right]e^{ik_x x}\,dk_x=\frac{1}{2\pi}\int_{-\infty}^{\infty}\frac{-iI}{\omega\varepsilon}\,\delta(y)\,e^{ik_x x}\,dk_x\,. \tag{7.156}$$

This equality holds if the integrands on both sides of Eq. (7.156) are equal; that is,

$$\left(\frac{d^2}{dy^2}+(k_\rho^2-k_x^2)\right)\,\widetilde{\psi}(k_x,y)=-\frac{iI}{\omega\varepsilon}\,\delta(y)\,. \tag{7.157}$$

This is an ordinary second-order differential equation whose solutions are a harmonic function of the following form:

$$\widetilde{\psi}(k_x,y)=\begin{cases}A(k_x)\,e^{ik_y y} & y>0\,,\\ B(k_x)\,e^{-ik_y y} & y<0\,,\end{cases} \tag{7.158}$$

which represent waves traveling outward away from the source. Here

$$k_y=\sqrt{k_\rho^2-k_x^2}\,,$$

and coefficients $A(k_x)$ and $B(k_x)$ are to be found by enforcing the continuity of $\widetilde{\psi}(k_x,y)$ and the jump discontinuity of its derivative at $y=0$. That is,

$$\widetilde{\psi}(k_x,0^+)=\widetilde{\psi}(k_x,0^-) \tag{7.159a}$$

and

$$\frac{\widetilde{\psi}(k_x,0^+)}{dy}-\frac{\widetilde{\psi}(k_x,0^-)}{dy}=\frac{-iI}{\omega\varepsilon}\,. \tag{7.159b}$$

Solving Eq. (7.159) renders

$$A=B=\frac{-I}{2k_y\omega\varepsilon}\,. \tag{7.160}$$

Substituting this solution into Eq. (7.154) provides the Fourier representation of the potential function:

$$\psi(x,y)=\frac{-I}{4\pi\omega\varepsilon}\int_{-\infty}^{\infty}\frac{1}{\sqrt{k_\rho^2-k_x^2}}\,e^{i(k_x x+k_y|y|)}\,dk_x\,. \tag{7.161}$$

The integrand represents a plane wave whose direction of propagation in the $x$-$y$ plane is along $(k_x/k_\rho)\,\hat{\mathbf{x}}+(k_y/k_\rho)\,\hat{\mathbf{y}}$. In Section 7-3.3 it was found that

$$\psi(x,y)=\frac{-I}{2\omega\varepsilon}\,H_0^{(1)}(k_\rho\,\sqrt{x^2+y^2})\,. \tag{7.162}$$

Comparing Eqs. (7.161) and (7.162), the following representation for this Hankel function is obtained:

$$H_0^{(1)}(k_\rho \sqrt{x^2+y^2}) = \frac{1}{\pi} \int_{-\infty}^{\infty} \frac{1}{\sqrt{k_\rho^2 - k_x^2}} e^{i(k_x x + \sqrt{k_\rho^2 - k_x^2}\,|y|)}\, dk_x \,. \tag{7.163}$$

### 7-4.6 Series Solution for the 2-D Green's Function of a Homogeneous Medium

In this section a series solution for the Green's function for a homogeneous medium is obtained in terms of cylindrical wave functions, following the procedure outlined for the formal solution of Green's function for the angular-sector waveguide. Considering the 2-D scalar wave Eq. (7.121) and using the method of separation of variables, we have

$$g(\boldsymbol{\rho}, \boldsymbol{\rho}') = \frac{1}{2\pi} \sum_{m=-\infty}^{\infty} g(\rho, \rho')\, e^{im(\phi - \phi')} \,. \tag{7.164}$$

Note that in this case the entire $\phi$ domain is included in the region of interest. Denoting the solution for $g(\rho, \rho')$ by $g_<$ and $g_>$ for when $\rho \le \rho'$ and $\rho \ge \rho'$, respectively, similar to Eq. (7.124),

$$g_< = A\, J_m(k_\rho \rho) \,.$$

The solution for $g_>$ must be chosen so that only outgoing wave functions are included:

$$g_> = C\, H_m^{(1)}(k_\rho \rho) \,.$$

Requiring the continuity condition for $g(\rho, \rho')$ at $\rho = \rho'$ (similar to Eq. (7.126)) and the jump discontinuity of derivation of $g$ with respect to $\rho$ (similar to Eq. (7.127)), it can be easily shown that

$$A = \frac{\pi i}{2} H_m^{(1)}(k_\rho \rho')$$

and

$$C = \frac{\pi i}{2} J_m(k_\rho \rho') \,.$$

Hence

$$g_<(\boldsymbol{\rho}, \boldsymbol{\rho}') = \frac{i}{4} \sum_{m=-\infty}^{+\infty} H_m^{(1)}(k_\rho \rho')\, J_m(k_\rho \rho)\, e^{im(\phi - \phi')} \tag{7.165a}$$

and

$$g_>(\boldsymbol{\rho}, \boldsymbol{\rho}') = \frac{i}{4} \sum_{m=-\infty}^{+\infty} J_m(k_\rho \rho')\, H_m^{(1)}(k_\rho \rho)\, e^{im(\phi - \phi')} \,. \tag{7.165b}$$

Comparing Eq. (7.165b) with Eq. (7.140), it is now obvious that

$$H_0^{(1)}(k_\rho|\boldsymbol{\rho}-\boldsymbol{\rho}'|) = \begin{cases} \displaystyle\sum_{m=-\infty}^{+\infty} H_m^{(1)}(k_\rho\rho')\, J_m(k_\rho\rho)\, e^{im(\phi-\phi')} & \rho \le \rho' \,, \\ \displaystyle\sum_{m=-\infty}^{+\infty} J_m(k_\rho\rho')\, H_m^{(1)}(k_\rho\rho)\, e^{im(\phi-\phi')} & \rho \ge \rho' \,. \end{cases} \tag{7.166}$$

This result is known as the ***addition theorem*** for the Hankel function of the first kind and zeroth order. A similar result can be obtained for the Hankel function of the first kind and zeroth order by simply conjugating Eq. (7.166). Adding the addition theorem for $H_0^{(1)}$ and $H_0^{(2)}$, we get the addition theorem for Bessel functions of the first kind and zeroth order:

$$J_0(k_\rho|\boldsymbol{\rho}-\boldsymbol{\rho}'|) = \sum_{m=-\infty}^{+\infty} J_{\rm m}(k_\rho\rho')\, J_{\rm m}(k_\rho\rho)\, e^{im(\phi-\phi')} \,. \tag{7.167}$$

### 7-4.7 Addition Theorem

The expressions given by Eqs. (7.166) and (7.167) present the addition theorem for the Hankel function and Bessel function of the first kind and the zeroth order. These can be extended to cylindrical wave functions of any order for a source that is located at $\boldsymbol{\rho}'$, as shown in Fig. 7-21.

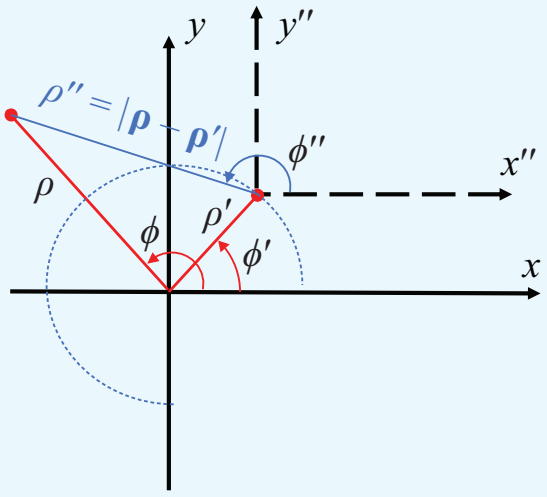


**Figure 7-21:** The geometry of coordinate transformation by translating the origin using translation vector $\boldsymbol{\rho}'$. The cylindrical coordinates in the original coordinate system are denoted by $\rho$ and $\phi$, and in the translated coordinate system by $\rho'' = |\boldsymbol{\rho}-\boldsymbol{\rho}'|$ and $\phi''$.

To specify a cylindrical wave function of arbitrary order "$m$" in the translated coordinate system $(x''-y'')$ in terms of cylindrical wave functions in the original coordinate system $(x-y)$, ***raising or lowering operators*** can be applied to Eqs. (7.166) and (7.167). The raising and lowering operators are defined as

$$\mathcal{R} = -\frac{1}{k_\rho}\left(\frac{\partial}{\partial x} + i\,\frac{\partial}{\partial y}\right) , \tag{7.168a}$$

$$\mathcal{L} = \frac{1}{k_\rho}\left(\frac{\partial}{\partial x} - i\,\frac{\partial}{\partial y}\right) . \tag{7.168b}$$

Recognizing that for any differentiable function $f(\rho,\phi)$,

$$\frac{df(\rho,\phi)}{dx} = \frac{df(\rho,\phi)}{d\rho}\cdot\frac{d\rho}{dx} + \frac{df(\rho,\phi)}{d\phi}\cdot\frac{d\phi}{dx} ,$$
$$\frac{df(\rho,\phi)}{dy} = \frac{df(\rho,\phi)}{d\rho}\cdot\frac{d\rho}{dy} + \frac{df(\rho,\phi)}{d\phi}\cdot\frac{d\phi}{dy} ,$$

and that

$$\frac{d\rho}{dx} = \cos\phi , \qquad \frac{d\rho}{dy} = \sin\phi ,$$
$$\frac{d\phi}{dx} = -\frac{\sin\phi}{\rho} , \qquad \frac{d\phi}{dy} = \frac{\cos\phi}{\rho} , \tag{7.169}$$

it can easily be shown that

$$\begin{aligned}\mathcal{R}\left[R_n(k_\rho\rho'')\,e^{in\phi'}\right] &= -\left[R_n(k_\rho\rho'') - \frac{n}{\rho''}\,R_n(k_\rho\rho'')\right]e^{i(n+1)\phi''} \\ &= R_{n+1}(k_\rho\rho'')\,e^{i(n+1)\phi''} ,\end{aligned} \tag{7.170}$$

where $R_n$ is a Bessel or Hankel function of order $n$. Hence, the raising operator $\mathcal{R}$, once applied to a cylindrical wave function of order $n$, produces a cylindrical wave function one order higher. Similarly, it can be shown that the lowering operator $\mathcal{L}$ can reduce the order of a cylindrical wave funtion by one; that is,

$$\mathcal{L}\left[R_n(k_\rho\rho'')\,e^{in\phi''}\right] = R_{n-1}(k_\rho\rho'')\,e^{i(n-1)\phi''} . \tag{7.171}$$

Noting that the raising and lowering operators are invariant to coordinate translation; i.e.,

$$\frac{\partial}{\partial x''} = \frac{\partial}{\partial x}$$

and

$$\frac{\partial}{\partial y''} = \frac{\partial}{\partial y} ,$$

the raising operator can be applied repetitively ($m$ times) to both sides of Eqs. (7.166) and (7.167) to arrive at the addition theorem for Hankel and Bessel functions of the first kind and $n$th order are given by

$$H_n^{(1)}(k_\rho|\boldsymbol{\rho}-\boldsymbol{\rho}'|)\,e^{in\phi''} = \begin{cases} \displaystyle\sum_{m=-\infty}^{+\infty} H_{m-n}^{(1)}(k_\rho\rho')\,J_m(k_\rho\rho)\,e^{im\phi}e^{-i(m-n)\phi'} & \rho \le \rho' \,, \\ \displaystyle\sum_{m=-\infty}^{+\infty} J_{m-n}(k_\rho\rho')\,H_m^{(1)}(k_\rho\rho)\,e^{im\phi}e^{-i(m-n)\phi'} & \rho \ge \rho' \,, \end{cases} \tag{7.172}$$

and

$$J_n^{(1)}(k_\rho|\boldsymbol{\rho}-\boldsymbol{\rho}'|)\,e^{in\phi''} = \sum_{m=-\infty}^{+\infty} J_{m-n}(k_\rho\rho')\,J_m(k_\rho\rho)\,e^{im\phi}e^{-i(m-n)\phi'} \,. \tag{7.173}$$

## Example 7-3: Application of the Addition Theorem

Use the addition theorem to derive the expression for the Hertz vector potential of the quadrupole shown in Fig. 7-20(b) and compare your result with Eq. (7.153).

**Solution:** We can write the expression for Hertz vector potential of a quadrupole of line currents as the sum of those for each line current translated to the respective line current positions in the diagram; that is,

$$\Pi_z^{4x,y} = -\frac{I}{4\omega\varepsilon}\,e^{i\beta z}\Big[H_0^{(1)}(k_\rho|\boldsymbol{\rho}-\boldsymbol{\rho}_1'|) - H_0^{(1)}(k_\rho|\boldsymbol{\rho}-\boldsymbol{\rho}_2'|)\,e^{i\beta z} + H_0^{(1)}(k_\rho|\boldsymbol{\rho}-\boldsymbol{\rho}_3'|) - H_0^{(1)}(k_\rho|\boldsymbol{\rho}-\boldsymbol{\rho}_4'|)\,e^{i\beta z}\Big] \,.$$

For observation points $\rho \ge \rho'$, the addition theorem for the Hankel function of the first kind and zeroth order is given by:

$$H_0^{(1)}(k_\rho|\boldsymbol{\rho}-\boldsymbol{\rho}'|) = \sum_{m=-\infty}^{\infty} J_m(k_\rho\rho')\,H_m^{(1)}(k_\rho\rho)\,e^{im(\phi-\phi')}.$$

Each line current is positioned such that they lie on a circle of radius $\rho'$ with equal angular spacing, where

$$\rho' = \frac{\sqrt{2}\,\delta}{2} \,.$$

Using this in the above,

$$\begin{aligned}\Pi_z^{4x,y} = -\frac{I}{4\omega\varepsilon}\, e^{i\beta z}\Bigg[ &\sum_{m=-\infty}^{\infty} J_m\left(k_\rho\, \frac{\sqrt{2}\,\delta}{2}\right)\, H_m^{(1)}(k_\rho\rho)\, e^{im\left(\phi-\frac{\pi}{4}\right)} \\ &- \sum_{m=-\infty}^{\infty} J_m\left(k_\rho\, \frac{\sqrt{2}\,\delta}{2}\right)\, H_m^{(1)}(k_\rho\rho)\, e^{im\left(\phi-\frac{3\pi}{4}\right)} \\ &+ \sum_{m=-\infty}^{\infty} J_m\left(k_\rho\, \frac{\sqrt{2}\,\delta}{2}\right)\, H_m^{(1)}(k_\rho\rho)\, e^{im\left(\phi-\frac{5\pi}{4}\right)} \\ &- \sum_{m=-\infty}^{\infty} J_m\left(k_\rho\, \frac{\sqrt{2}\,\delta}{2}\right)\, H_m^{(1)}(k_\rho\rho)\, e^{im\left(\phi-\frac{7\pi}{4}\right)}\Bigg],\end{aligned}$$

which after some simple algebraic steps simplifies to

$$\begin{aligned}\Pi_z^{4x,y} = -\frac{I}{4\omega\varepsilon}\, e^{i\beta z}\Bigg[ &\sum_{m=-\infty}^{\infty} J_m\left(k_\rho\, \frac{\sqrt{2}\,\delta}{2}\right)\, H_m^{(1)}(k_\rho\rho)\, e^{im\phi} e^{im\pi/4}(1+e^{im\pi}) \\ &- \sum_{m=-\infty}^{\infty} J_m\left(k_\rho\, \frac{\sqrt{2}\,\delta}{2}\right)\, H_m^{(1)}(k_\rho\rho)\, e^{im\phi} e^{im\pi/4} e^{im\pi/2}(1+e^{im\pi})\Bigg].\end{aligned}$$

Note that $e^{im\pi/2} = (i)^m$ and $e^{im\pi} = (-1)^m$, and thus

$$\Pi_z^{4x,y} = -\frac{I}{4\omega\varepsilon}\, e^{i\beta z}\left[\sum_{m=-\infty}^{\infty} J_m\left(k_\rho\, \frac{\sqrt{2}\,\delta}{2}\right)\, H_m^{(1)}(k_\rho\rho)\, e^{im\phi} e^{im\pi/4}[1+(-1)^m](1-i^m)\right].$$

$[1+(-1)^m](1-i^m)$ is nonzero for $m = \pm 2, \pm 6, \pm 10$, etc. Since $k_\rho\delta \ll 1$, the small-argument expansion Bessel function of first kind is given by

$$\lim_{k_\rho(\sqrt{2}\,\delta/2)\to 0} J_m\left(k_\rho\, \frac{\sqrt{2}\,\delta}{2}\right) = \frac{1}{m!}\left(\frac{k_\rho\,\sqrt{2}\,\delta}{2}\right)^m.$$

Ignoring terms for $|m| > 2$, we have

$$\begin{aligned}\Pi_z^{4x,y} \approx &-\frac{I}{4\omega\varepsilon}\, e^{i\beta z} \\ &\cdot\left[J_{-2}\left(k_\rho\, \frac{\sqrt{2}\,\delta}{2}\right)\, H_{-2}^{(1)}(k_\rho\rho)\, e^{-i2\phi} e^{-i\pi/2} + J_2\left(k_\rho\, \frac{\sqrt{2}\,\delta}{2}\right)\, H_2^{(1)}(k_\rho\rho)\, e^{i2\phi} e^{i\pi/2}\right].\end{aligned}$$

Using the facts

$$J_{-\nu}(x) = (-1)^\nu\, J_\nu(x)$$

and

$$H_{-\nu}^{(1)}(x) = (-1)^{\nu}\, H_{\nu}^{(1)}(x),$$

we have

$$\Pi_z^{4x,y} \approx -\frac{I}{4\omega\varepsilon}\, e^{i\beta z}\left[J_2\left(k_\rho\, \frac{\sqrt{2}\,\delta}{2}\right) H_2^{(1)}(k_\rho\rho)\,(-i)(\cos 2\phi - i\sin 2\phi)\right.$$
$$\left. + J_2\left(k_\rho\, \frac{\sqrt{2}\,\delta}{2}\right) H_2^{(1)}(k_\rho\rho)\,(i)(\cos 2\phi + i\sin 2\phi)\right],$$
$$\Pi_z^{4x,y} \approx \frac{2I}{4\omega\varepsilon}\, e^{i\beta z}\, J_2\left(k_\rho\, \frac{\sqrt{2}\,\delta}{2}\right) H_2^{(1)}(k_\rho\rho)\,\sin 2\phi\ .$$

Using the first term of the small-argument expansion of $J_m(k_\rho\rho)$, it can be shown that

$$\Pi_z^{4x,y} \approx \frac{(k_\rho)^2 I\delta^2}{8\omega\varepsilon}\, e^{i\beta z}\, H_2^{(1)}(k_\rho\rho)\,\sin 2\phi\ ,$$

which agrees with Eq. (7.153) for $\delta_1 = \delta_2 = \delta$.

### 7-4.8 2-D Green's Function for a Homogeneous Medium in the Presence of a Metallic Cylinder

The field solution for arbitrary sources present in a homogeneous medium next to a metallic cylinder of radius $a$ with its center placed at the origin of a Cartesian system can easily be obtained if the Green's function for the problem is known. Figure 7-22 shows the geometry of the problem where an infinite filament current $Ie^{i\beta z}$ is placed in parallel with the axis of the metallic cylinder at location $\boldsymbol{\rho}'$ with cylindrical coordinates $(\rho', \phi')$. In the absence of the metallic cylinder, the current filament produces the potential $\psi_i(\rho,\phi)$ given by

$$\psi_i(\rho,\phi) = \frac{-I}{4\varepsilon\omega}\, H_0^{(1)}(k_\rho|\boldsymbol{\rho} - \boldsymbol{\rho}'|)\, e^{i\beta z}\ . \tag{7.174}$$

This incident wave scatters off the metallic cylinder and produces the scattered potential $\psi_s(\rho,\phi)$ in such a way as to satisfy the boundary condition

$$\psi_i(a,\phi) + \psi_s(a,\phi) = 0\ . \tag{7.175}$$

The scattered potential can be expressed in terms of cylindrical elementary wave functions as

$$\psi_s(\rho,\phi) = \sum_{m=-\infty}^{+\infty} A_m\, H_m^{(1)}(k_\rho\rho)\, e^{im(\phi-\phi')} e^{i\beta z}\ . \tag{7.176}$$

The choice of Hankel function of the first kind is necessitated by the fact that the scattered potential is an outward-traveling wave. According to Eq. (7.166),

$$\psi_i(a,\phi) = \frac{-I}{4\varepsilon\omega} \sum_{m=-\infty}^{+\infty} H_m^{(1)}(k_\rho \rho)\, J_m(k_\rho a)\, e^{im(\phi-\phi')} e^{i\beta z} \,. \tag{7.177}$$

Using the boundary condition defined by Eq. (7.175), we have

$$\sum_{m=-\infty}^{+\infty} \left( A_m\, H_m^{(1)}(k_\rho a) - \frac{I}{4\varepsilon\omega}\, H_m^{(1)}(k_\rho \rho')\, J_m(k_\rho a)\, e^{im(\phi-\phi')} \right) = 0 \,,$$

from which $a_m$ can be found and is given by

$$A_m = \frac{I}{4\varepsilon\omega} \frac{J_m(k_\rho a)\, H_m^{(1)}(k_\rho \rho')}{H_m^{(1)}(k_\rho a)} \,. \tag{7.178}$$

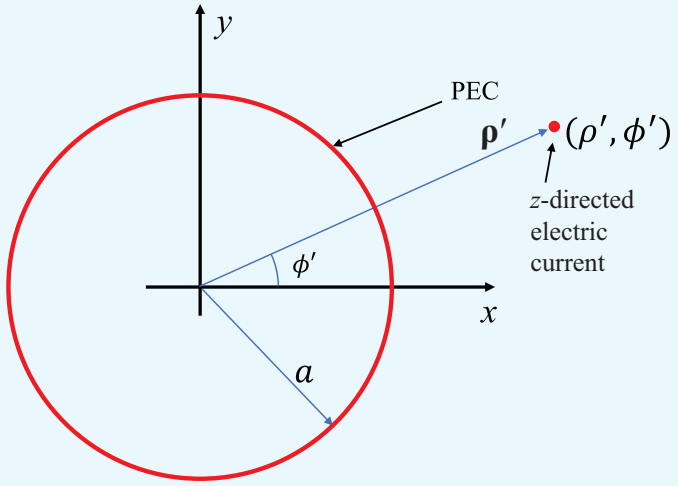


**Figure 7-22:** The geometry for an infinitely long metallic cylinder and an infinitely long filament current positioned at $\boldsymbol{\rho}'$ and directed along $\hat{\mathbf{z}}$.

Hence the total potential $\psi_t(\rho,\phi)$ can be represented by

$$\psi_t(\rho,\phi) = \begin{cases} \dfrac{Ie^{i\beta z}}{4\varepsilon\omega}\displaystyle\sum_{m=-\infty}^{+\infty}\left(\frac{J_m(k_\rho a)}{H_m^{(1)}(k_\rho a)}H_m^{(1)}(k_\rho\rho)-J_m(k_\rho\rho)\right)H_m^{(1)}(k_\rho\rho')\,e^{im(\phi-\phi')} & \rho\le\rho' \\ \dfrac{Ie^{i\beta z}}{4\varepsilon\omega}\displaystyle\sum_{m=-\infty}^{+\infty}\left(\frac{J_m(k_\rho a)}{H_m^{(1)}(k_\rho a)}H_m^{(1)}(k_\rho\rho')-J_m(k_\rho\rho')\right)H_m^{(1)}(k_\rho\rho)\,e^{im(\phi-\phi')} & \rho\ge\rho' \end{cases} \tag{7.179}$$

Note that the reciprocity principle holds. That is, if the observation point $(\rho,\phi)$ and the source point $(\rho',\phi')$ are interchanged, the same expression is obtained.

The expressions for the field quantities can be obtained from Eqs. (5.102a) and (5.102b). Figure 7-23 shows the normalized total $z$-component of the electric field for a problem where the line source is at $\boldsymbol{\rho}'$ and is on the $x$-axis ($\phi'=0$) at different locations $\rho'=0.75\lambda$, $1\lambda$, and $10.5\lambda$, all in the presence of a metallic cylinder with radius $a=0.5\lambda$. The observation point is in the far-field region. For $\rho'=0.75\lambda$, the source is $\lambda/4$ away from the cylinder surface and, as expected, the incident field and the scattered field along the $x$-axis add up coherently. Also, at $\phi=\pm180^\circ$, the incident field and the scattered field cancel each other due to the shadowing effect. For the two other cases, the incident and scattered fields are out of phase along the $x$-axis ($\phi=0$) and interfere destructively.

## 7-5 Scattering from a Metallic Circular Cylinder

Consider a circular metallic cylinder of radius $a$ whose axis coincides with the $z$-axis of the coordinate system, as shown in Fig. 7-24. The cylinder is illuminated by a plane wave whose propagation vector $\hat{\mathbf{k}}_i$ lies in the $x$–$z$ plane with

$$\hat{\mathbf{k}}_i\cdot\hat{\mathbf{x}} = -\sin\theta_i \tag{7.180a}$$

and

$$\hat{\mathbf{k}}_i\cdot\hat{\mathbf{z}} = \cos\theta_i\ . \tag{7.180b}$$

Initially, we consider TM polarization for the incidence field, i.e.,

$$\mathbf{E}^i = E_0(\cos\theta_i\,\hat{\mathbf{x}}+\sin\theta_i\,\hat{\mathbf{z}})e^{ik_0(-\sin\theta_i\,x+\cos\theta_i\,z)}\ . \tag{7.181}$$

The incident field is the total field in the medium in the absence of the metallic cylinder. In the presence of the cylinder the incident field excites a current on the surface of the metallic cylinder, which in turn reradiates elecromagnetic wave. This reradiated field is known as the ***scattered field***, which together with the incident field constitutes the total field in the medium

$$\mathbf{E}_t(\boldsymbol{\rho},z) = \mathbf{E}_i(\boldsymbol{\rho},z)+\mathbf{E}_s(\boldsymbol{\rho},z)\ . \tag{7.182}$$

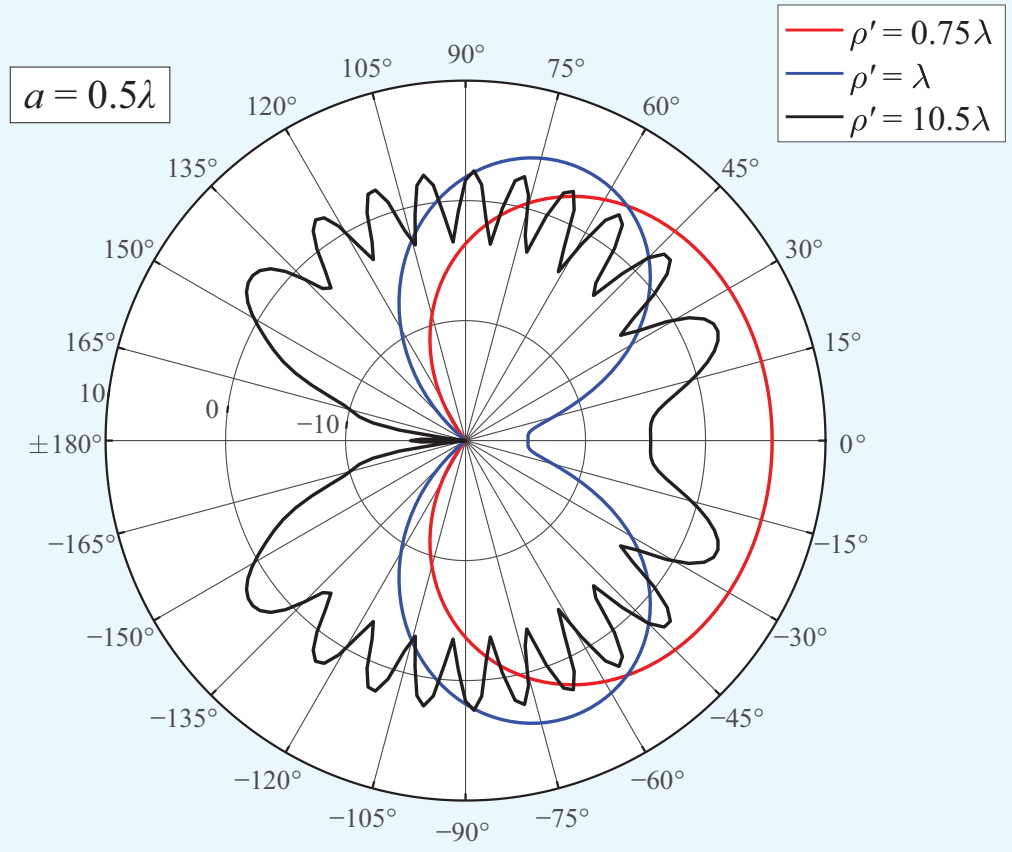


**Figure 7-23:** Normalized total $z$-component of the electric field for a configuration where the line source is at $\boldsymbol{\rho}'$ and is on the $x$-axis ($\phi' = 0$) at different locations: $\rho' = 0.75\lambda$, $1\lambda$, and $10.5\lambda$, in the presence of a metallic cylinder of radius $a = 0.5\lambda$.

The boundary condition on the surface of the cylinder mandates that

$$\hat{\boldsymbol{\rho}} \times \mathbf{E}_{\mathrm{t}}(a\hat{\boldsymbol{\rho}}, z) = 0 \,. \tag{7.183}$$

The incident and scattered fields can be expanded in terms of elementary wave functions in the cylindrical coordinate systems. Since the cylinder cross section does not change with $z$, the scattered field maintains the same $z$-dependence as that of the incident wave

$$\mathbf{E}_{\mathrm{s}}(\boldsymbol{\rho}, z) = \mathbf{E}_{\mathrm{s}}(\boldsymbol{\rho})\, e^{i\beta z} \,,$$

where $\beta = k_0 \cos\theta_{\mathrm{i}}$. The scalar potential $\psi$ generating $\mathbf{E}_{\mathrm{s}}$, in the region $\rho \geq a$, can be written as

$$\psi(\boldsymbol{\rho}) = \sum_{n=-\infty}^{+\infty} A_n\, H_n^{(1)}(k_\rho \rho)\, e^{in\phi} \,, \tag{7.184}$$

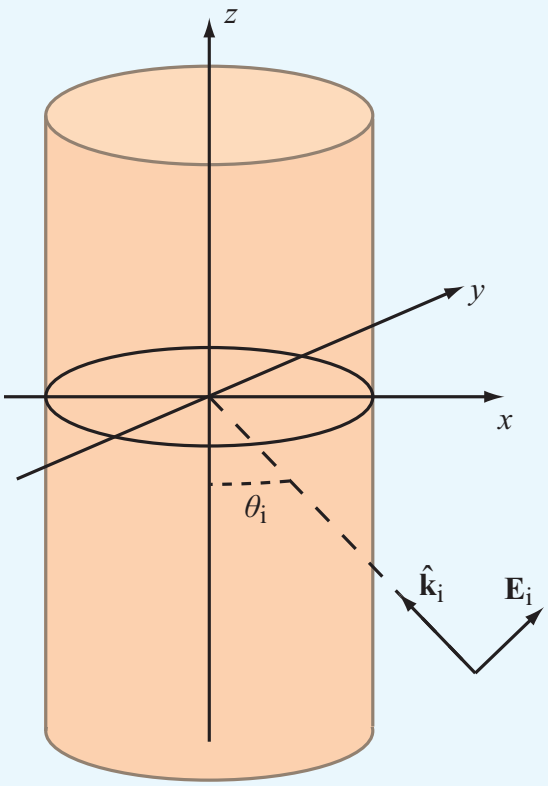


**Figure 7-24:** Geometry of a metallic circular cylinder illuminated by a plane wave.

where $k_\rho = k_0 \sin\theta_i$. The choice of the Hankel function of the first kind is to ensure an outgoing cylindrical wave. Referring to Eq. (5.102a), the components of the scattered electric field are given by

$$E_\rho^s(\rho,\phi,z) = \sum_{n=-\infty}^{+\infty} iA_n \beta k_\rho \, H_n^{(1)'}(k_\rho \rho)\, e^{in\phi} e^{i\beta z}\,, \tag{7.185a}$$

$$E_\phi^s(\rho,\phi,z) = \sum_{n=-\infty}^{+\infty} \frac{-A_n \beta n}{\rho} \, H_n^{(1)}(k_\rho \rho)\, e^{in\phi} e^{i\beta z}\,, \tag{7.185b}$$

and

$$E_z^s(\rho,\phi,z) = \sum_{n=-\infty}^{+\infty} A_n k_\rho^2 \, H_n^{(1)}(k_\rho \rho)\, e^{in\phi} e^{i\beta z} \tag{7.185c}$$

The incident wave can also be expanded in terms of cylindrical eigenfunctions. Using

$$e^{-ik_0 \sin\theta_i\, x} = \sum_{-\infty}^{+\infty} (-i)^n\, J_n(k_\rho \rho)\, e^{in\phi}\ , \tag{7.186}$$

where $k_\rho = \sqrt{k_0^2 - \beta^2} = k_0 \sin\theta_i$, we have

$$E_z^i = E_0 \sin\theta_i\, e^{i\beta z} \sum_{n=-\infty}^{+\infty} (-i)^n\, J_n(k_\rho \rho)\, e^{in\phi}\ , \tag{7.187a}$$

$$E_\phi^i = -E_0 \cos\theta_i \sin\phi\, e^{i\beta z} \sum_{n=-\infty}^{+\infty} (-i)^n\, J_n(k_\rho \rho)\, e^{in\phi}\ , \tag{7.187b}$$

and

$$E_\rho^i = E_0 \cos\theta_i \cos\phi\, e^{i\beta z} \sum_{n=-\infty}^{+\infty} (-i)^n\, J_n(k_\rho \rho)\, e^{in\phi}\ . \tag{7.187c}$$

At the boundary between the cylinder and its surrounding medium,

$$(E_\phi^i + E_\phi^s)\big|_{\rho=a} = 0\ .$$

This condition provides the following equation for the unknown $A_n$:

$$-E_0 \cos\theta_i \sum_{n=-\infty}^{+\infty} (-i)^n\, J_n(ka)\, e^{in\phi} \sin\phi = \sum_{n=-\infty}^{+\infty} \frac{A_n \beta n}{a}\, H_n^{(1)}(k_\rho a)\, e^{in\phi}\ . \tag{7.188}$$

Multiplying both sides of Eq. (7.188) by $e^{-im\phi}$ and integrating the results over 0 to $2\pi$ provides the following equation for $A_m$:

$$\frac{mA_m\beta}{a}\, H_m^{(1)}(k_\rho a) = \frac{-E_0 \cos\theta_i}{2i} \left[(-i)^{m-1}\, J_{m-1}(k_\rho a) - (-i)^{m+1}\, J_{m+1}(k_\rho a)\right]\ .$$

Hence

$$\begin{aligned} A_m &= \frac{-aE_0(-i)^m}{k_0\, H_m^{(1)}(k_\rho a)} \left(\frac{J_{m+1}(k_\rho a) + J_{m-1}(k_\rho a)}{2m}\right) \\ &= \frac{-aE_0(-i)^m}{k_0\, H_m^{(1)}(k_\rho a)}\, \frac{J_m(k_\rho a)}{k_\rho a} = -E_0\, \frac{(-i)^m}{k_0^2 \sin\theta_i}\, \frac{J_m(k_0 \sin\theta_i\, a)}{H_m^{(1)}(k_0 \sin\theta_i\, a)}\ . \end{aligned} \tag{7.189}$$

Similar results can be obtained using the boundary condition

$$(E_z^i + E_z^s)|_{\rho=a} = 0\ . \tag{7.190}$$

Using Eqs. (7.185) and (7.187a) in Eq. (7.190) leads to

$$E_0 \sin\theta_\mathrm{i} \sum_{n=-\infty}^{+\infty} (-i)^n J_n(k_\rho a)\, e^{in\phi} = -\sum_{n=-\infty}^{+\infty} A_n k_\rho^2 H_n^{(1)}(k_\rho a)\, e^{in\phi} \ . \tag{7.191}$$

Multiplying both sides of Eq. (7.191) by $e^{-im\phi}$ and integrating over $\phi$ in the range $[0, 2\pi]$ gives

$$E_0 \sin\theta_\mathrm{i}\, (-i)^m J_m(k_\rho a) = -A_m k_\rho^2 H_m^{(1)}(k_\rho a) \ .$$

Hence

$$A_m = -E_0 \frac{(-i)^m}{k_0^2 \sin\theta_\mathrm{i}} \frac{J_m(k_0 \sin\theta_\mathrm{i}\, a)}{H_m^{(1)}(k_0 \sin\theta_\mathrm{i}\, a)} \ , \tag{7.192}$$

which is consistent with Eq. (7.189).

In the far-field region, simpler expressions for the scattered field quantities can be obtained. Noting that

$$H_n^{(1)'}(x) = \frac{1}{2}\left[H_{n-1}^{(1)}(x) - H_{n+1}^{(1)}(x)\right] \ , \tag{7.193}$$

and using the large-argument expansion of the Hankel function, we have

$$\begin{aligned} \lim_{x\to\infty} H_n^{(1)'}(x) &\approx \frac{1}{2}\sqrt{\frac{2}{\pi x}}\, e^{i\{x-[(2n+1)/4]\pi\}}\left[e^{i\pi/2} - e^{-i\pi/2}\right] \\ &\approx i\sqrt{\frac{2}{\pi x}}\, e^{i\{x-[(2n+1)/4]\pi\}} \ . \end{aligned} \tag{7.194}$$

From Eq. (7.185) it is obvious that $E_\phi^\mathrm{s}$ varies with $\rho$ as $1/\rho^{3/2}$, whereas $E_\rho^\mathrm{s}$ and $E_z^\mathrm{s}$ decay as $1/\rho^{1/2}$. In the far-field region the $E_\phi^\mathrm{s}$-component can be ignored compared with the other two terms. Hence, for points far away from the cylinder axis where $k_\rho \rho = k_0 \sin\theta_\mathrm{i}\, \rho \gg 1$,

$$E_\rho^\mathrm{s}(\rho,\phi,z) = i\beta k_\rho \sqrt{\frac{2}{\pi k_\rho \rho}}\, e^{i(k_\rho \rho - \pi/4)} \left(\sum_{n=-\infty}^{+\infty} iA_n (-i)^n e^{in\phi}\right) e^{i\beta z} \ . \tag{7.195}$$

Recalling that $\beta = k_0 \cos\theta_\mathrm{i}$ and $k_\rho = k_0 \sin\theta_\mathrm{i}$, and using Eq. (7.189) in Eq. (7.195),

$$\begin{aligned} E_\rho^\mathrm{s}(\rho,\phi,z) = E_0 \cos\theta_\mathrm{i} &\sqrt{\frac{2}{\pi k_0 \sin\theta_\mathrm{i}\, \rho}}\, e^{i(k_0 \sin\theta_\mathrm{i}\, \rho - \pi/4)} e^{ik_0 \cos\theta_\mathrm{i}\, z} \\ &\cdot \sum_{n=-\infty}^{+\infty} (-1)^{n+1} \frac{J_n(k_0 \sin\theta_\mathrm{i}\, a)}{H_n^{(1)}(k_0 \sin\theta_\mathrm{i}\, a)}\, e^{in\phi} \ . \end{aligned} \tag{7.196}$$

Also, recalling that for any Bessel function $Z_n$,

$$Z_{-n} = (-1)^n Z_n \ ,$$

Eq. (7.196) can be further reduced to

$$E_\rho^{\rm s}(\rho,\phi,z) = -E_0\cos\theta_{\rm i}\sqrt{\frac{2}{\pi k_0\sin\theta_{\rm i}\,\rho}}\,e^{i(k_0\sin\theta_{\rm i}\,\rho-\pi/4)}e^{ik_0\cos\theta_{\rm i}\,z}$$
$$\cdot\left(\frac{J_0(k_0\sin\theta_{\rm i}\,a)}{H_0^{(1)}(k_0\sin\theta_{\rm i}\,a)}+2\sum_{n=1}^{\infty}(-1)^{n+1}\,\frac{J_n(k_0\sin\theta_{\rm i}\,a)}{H_n^{(1)}(k_0\sin\theta_{\rm i}\,a)}\cos(n\phi)\right).$$

In a similar manner,

$$E_z^{\rm s}(\rho,\phi,z) = E_0\sin\theta_{\rm i}\sqrt{\frac{2}{\pi k_0\sin\theta_{\rm i}\,\rho}}\,e^{i(k_0\sin\theta_{\rm i}\,\rho-\pi/4)}e^{ik_0\cos\theta_{\rm i}\,z}$$
$$\cdot\left(\frac{J_0(k_0\sin\theta_{\rm i}\,a)}{H_0^{(1)}(k_0\sin\theta_{\rm i}\,a)}+2\sum_{n=1}^{\infty}(-1)^{n+1}\,\frac{J_n(k_0\sin\theta_{\rm i}\,a)}{H_n^{(1)}(k_0\sin\theta_{\rm i}\,a)}\cos(n\phi)\right).$$

The total scattered field in the far-zone is therefore

$$\mathbf{E}^{\rm s}(\rho,\phi,z) = (E_0\sin\theta_{\rm i}\,\hat{\mathbf{z}}-E_0\cos\theta_{\rm i}\,\hat{\boldsymbol{\rho}})\sqrt{\frac{2}{\pi k_0\sin\theta_{\rm i}\,\rho}}\,e^{i(k_0\sin\theta_{\rm i}\,\rho-\pi/4)}e^{ik_0\cos\theta_{\rm i}\,z}$$
$$\cdot\left(\frac{J_0(k_0\sin\theta_{\rm i}\,a)}{H_0^{(1)}(k_0\sin\theta_{\rm i}\,a)}+2\sum_{n=1}^{\infty}(-1)^{n+1}\,\frac{J_n(k_0\sin\theta_{\rm i}\,a)}{H_n^{(1)}(k_0\sin\theta_{\rm i}\,a)}\cos(n\phi)\right). \quad (7.197)$$

The direction of propagation is along

$$\hat{\mathbf{k}}_{\rm s} = \sin\theta_{\rm i}\,\hat{\boldsymbol{\rho}}+\cos\theta_{\rm i}\,\hat{\mathbf{z}}\,,$$

which indicates that the propagation of the scattered field is confined to the surface of a cone with a generating angle $\theta_{\rm i}$, as shown in Fig. 7-25. The ***bistatic scattering echo width*** of a 2-D object is mathematically defined as

$$\sigma_2(\phi) = \lim_{\rho\to\infty} 2\pi\rho\,\frac{|\mathbf{E}^{\rm s}|^2}{|\mathbf{E}^{\rm i}|^2}\,, \quad (7.198)$$

which can be interpreted as a fictitious width of an object that captures the incident power density of the incident wave, and if it were to reradiate that power isotropically (uniform in all $\phi$-directions) it would produce the same scattered power density at the observation point as does the scatterer. Using Eq. (7.197) in Eq. (7.198), the radar echo width of a metallic cylinder for a TM polarized incident wave is given by

$$\sigma_2^{\rm TM}(\phi) = \frac{4}{k_0\sin\theta_{\rm i}}\left|\sum_{n=-\infty}^{\infty}(-1)^n\,\frac{J_n(k_0\sin\theta_{\rm i}\,a)}{H_n^{(1)}(k_0\sin\theta_{\rm i}\,a)}\,e^{in\phi}\right|^2. \quad (7.199)$$

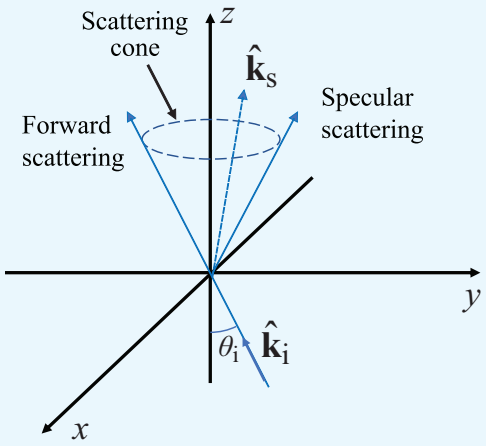


**Figure 7-25:** Ray representation of a scattered field from a metallic cylinder illuminated by a plane wave at oblique incidence. The scattered rays form a cone around the axis of the cylinder with a cone angle equal to the incident angle.

The magnetic field in the far-field region is perpendicular to $\mathbf{E}^s$ and $\hat{\mathbf{k}}_s$ and is given by

$$\mathbf{H}^s(\rho,\phi,s) = \frac{\hat{\mathbf{k}}_s \times \mathbf{E}^s}{\eta_0}\,, \qquad \eta_0 = \sqrt{\frac{\mu_0}{\varepsilon_0}}\,.$$

The solution for TE incidence can be obtained by applying the duality. The electric field is given by

$$\mathbf{E}^s(\rho,\phi,z) = i\omega\mu_0 \left(\frac{\partial}{\partial\rho}\,\psi\hat{\boldsymbol{\rho}} + \frac{1}{\rho}\,\frac{\partial\psi}{\partial\phi}\,\hat{\boldsymbol{\phi}}\right) \times \hat{\mathbf{z}}\, e^{ik_0 \sin\theta_i\, z}\,, \tag{7.200}$$

with $\psi(\rho,\phi)$ given by

$$\psi(\rho,\phi) = \sum_{n=-\infty}^{+\infty} B_n\, H_n^{(1)}(k_\rho\rho)\, e^{in\phi}\,.$$

The components of the scattered electric field are given by

$$E_\rho^s(\rho,\phi,z) = i\omega\mu_0 \sum_{n=-\infty}^{+\infty} \frac{in}{\rho}\, B_n\, H_n^{(1)}(k_\rho\rho)\, e^{in\phi} e^{i\beta z} \tag{7.201a}$$

and

$$E_\phi^s(\rho,\phi,z) = -i\omega\mu_0 \sum_{n=-\infty}^{+\infty} B_n k_\rho\, H_n^{(1)'}(k_\rho\rho)\, e^{in\phi} e^{i\beta z}\,. \tag{7.201b}$$

The incident wave for a TE polarized wave is given by

$$\begin{aligned}\mathbf{E}^{\mathrm{i}}(\rho,\phi,z) &= E_0\hat{\mathbf{y}}\, e^{ik_0(-\sin\theta_{\mathrm{i}}\, x+\cos\theta_{\mathrm{i}}\, z)} \\ &= E_0(\sin\phi\ \hat{\boldsymbol{\rho}}+\cos\phi\ \hat{\boldsymbol{\phi}})e^{ik_0(-\sin\theta_{\mathrm{i}}\, x+\cos\theta_{\mathrm{i}}\, z)}\ .\end{aligned}$$

The boundary condition mandates that

$$E_0\cos\phi\sum_{n=-\infty}^{+\infty}(-i)^n\, J_n(k_0\sin\theta_{\mathrm{i}}\, a)\, e^{in\phi} = -i\omega\mu_0\sum_{n=-\infty}^{+\infty}B_n k_\rho\, H_n^{(1)'}(k_\rho a)\, e^{in\phi}\ . \tag{7.202}$$

Multiplying both sides of Eq. (7.202) by $e^{-im\phi}$ and integrating over $[0,2\pi]$ gives

$$\frac{E_0}{2}\left\{(-i)^{m-1}\, J_{m-1}(k_\rho a)+(-i)^{m+1}\, J_{m+1}(k_\rho a)\right\} = -i\omega\mu_0 k_\rho\, H_m^{(1)'}(k_\rho a)\, B_m$$

and

$$E_0(-i)^m\left(\frac{J_{m-1}(k_\rho a)-J_{m+1}(k_\rho a)}{2}\right) = -\omega\mu_0 k_\rho\, H_m^{(1)'}(k_\rho a)\, B_m\ .$$

Noting that

$$\frac{J_{m-1}(x)-J_{m+1}(x)}{2} = J_m'(x)\ ,$$

the unknown coefficient $B_m$ can be obtained from

$$B_m = -E_0\,\frac{(-i)^m\, J_m'(k_0\sin\theta_{\mathrm{i}}\, a)}{\omega\mu_0 k_0\sin\theta_{\mathrm{i}}\, H_m^{(1)'}(k_0\sin\theta_{\mathrm{i}}\, a)}\ . \tag{7.203}$$

Substituting Eq. (7.203) into Eq. (7.201b),

$$E_\phi^{\mathrm{s}}(\rho,\phi,z) = -iE_0\sum_{n=-\infty}^{+\infty}(-i)^n\frac{J_n'(k_0\sin\theta_{\mathrm{i}}\, a)}{H_n^{(1)'}(k_0\sin\theta_{\mathrm{i}}\, a)}\, H_n^{(1)'}(k_0\sin\theta_{\mathrm{i}}\,\rho)\, e^{in\phi}e^{ik_0\cos\theta_{\mathrm{i}}\, z}\ .$$

In the far field, using Eq. (7.194), $E_\phi^{\mathrm{s}}(\rho,\phi,z)$ is given by

$$\begin{aligned}E_\phi^{\mathrm{s}}(\rho,\phi,z) = E_0\sqrt{\frac{2}{\pi k_0\sin\theta_{\mathrm{i}}\,\rho}}\, e^{i(k_0\sin\theta_{\mathrm{i}}\,\rho-\pi/4)}e^{ik_0\cos\theta_{\mathrm{i}}\, z} \\ \sum_{n=-\infty}^{+\infty}(-1)^n\frac{J_n'(k_0\sin\theta_{\mathrm{i}}\, a)}{H_n^{(1)'}(k_0\sin\theta_{\mathrm{i}}\, a)}\, e^{in\phi}\ .\end{aligned} \tag{7.204}$$

The cylinder echo width can also be obtained from Eq. (7.198) and is given by

$$\sigma_2^{\mathrm{TE}}(\phi) = \frac{4}{k_0 \sin\theta_\mathrm{i}} \left| \sum_{n=-\infty}^{+\infty} (-1)^n \frac{J_n'(k_0 \sin\theta_\mathrm{i}\, a)}{H_n^{(1)'}(k_0 \sin\theta_\mathrm{i}\, a)} e^{in\phi} \right|^2 . \tag{7.205}$$

### 7-5.1 Low-Frequency Approximation

In situations where the cylinder diameter is much smaller than the wavelength; i.e., $k_0 \sin\theta_\mathrm{i}\, a \ll 1$, the asymptotic expansion of Bessel functions can be used to find a closed form solution for the radar echo width of metallic cylinders. Considering the fact that $\lim_{x\to 0} J_n(x) \approx 0$ for $n \neq 0$,

$$J_0(k_0 \sin\theta_\mathrm{i} a) \approx 1$$

and

$$H_0^{(1)}(k_0 \sin\theta_\mathrm{i} a) \approx 1 + i\frac{2}{\pi}\ln(0.8905 k_0 \sin\theta_\mathrm{i} a) .$$

Hence, Eq. (7.199) is reduced to

$$\sigma_2^{\mathrm{TM}} = \frac{1}{2\sin\theta_\mathrm{i}} \frac{\pi\lambda}{(\pi^2/4) + \ln^2(0.8905 k_0 a \sin\theta_\mathrm{i})} . \tag{7.206}$$

Also, noting that

$$\lim_{x\to 0} J_0'(x) \approx x ,$$

$$\lim_{x\to 0} H_0^{(1)\prime}(x) \approx \frac{2}{\pi}\frac{1}{x} ,$$

$$\lim_{x\to 0} J_1'(x) \approx \frac{1}{2} ,$$

and

$$\lim_{x\to 0} H_1^{(1)\prime}(x) \approx i\frac{4}{\pi}\frac{1}{x^2} ,$$

it can be shown that

$$\sigma_2^{\mathrm{TE}} = \frac{\pi^2 a}{\sin\theta_\mathrm{i}} (k_0 a \sin\theta_\mathrm{i})^3 \left(\frac{1}{2} + \cos\phi\right)^2 . \tag{7.207}$$

### 7-5.2 Numerical Simulations

To examine the scattering behavior of a metallic cylinder, the radar backscatter echo width of a metallic cylinder illuminated by a plane wave at normal incidence is plotted in Fig. 7-26 as a function of $ka$ for both TE and TM polarizations. Here the echo width is normalized to its high frequency value, $\pi a$. A similar plot is presented in Fig. 7-27, where the incident wave is now

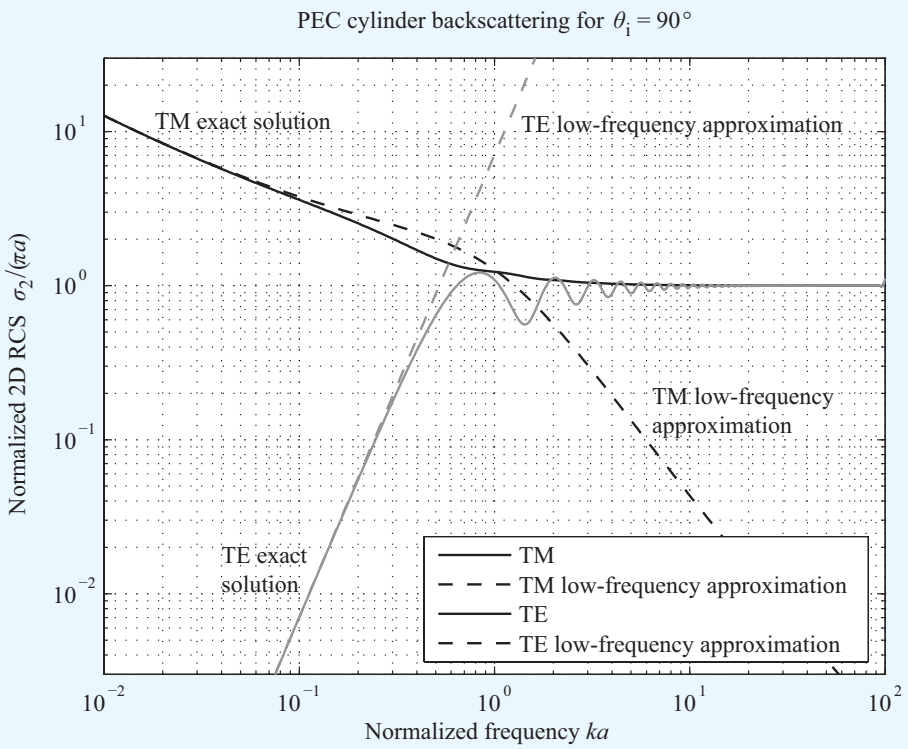


**Figure 7-26:** Normalized backscatter radar echo width of a metallic cylinder at normal incidence for both TE and TM polarizations. Also shown are the low-frequency approximations. The backscatter echo width approaches the high-frequency limit of $\sigma_2 = \pi a$ for values of $ka \geq 10$.

at an oblique incidence $\theta_i = 45°$. Figures 7-28 and 7-29 present the bistatic radar cross section patterns for two metallic cylinder, one with $ka = 1$ and another with $ka = 5$, respectively, at normal incidence ($\theta_i = 90°$) for both TE and TM polarizations. It is interesting to note that the maximum radar cross section is observed in the forward direction. The scattered field in the forward direction is nearly 180° out of phase with respect to the incident wave. In the vicinity of the cylinder the scattered field totally cancels out the incident field, which results in a shadow region near the forward scattering direction. Comparing Fig. 7-28 with Fig. 7-29 shows that bistatic scattering echo width increases with increasing the radius of the cylinder and the scattering lobes become narrower.

## 7-6 Integral Representation of Bessel Functions

The integral representation of Bessel functions is useful in a range of problems related to scattering and antennas. In fact the large-argument approximation for the Bessel functions given in Eqs. (7.16a)–(7.16d) are derived from the asymptotic evaluation of such

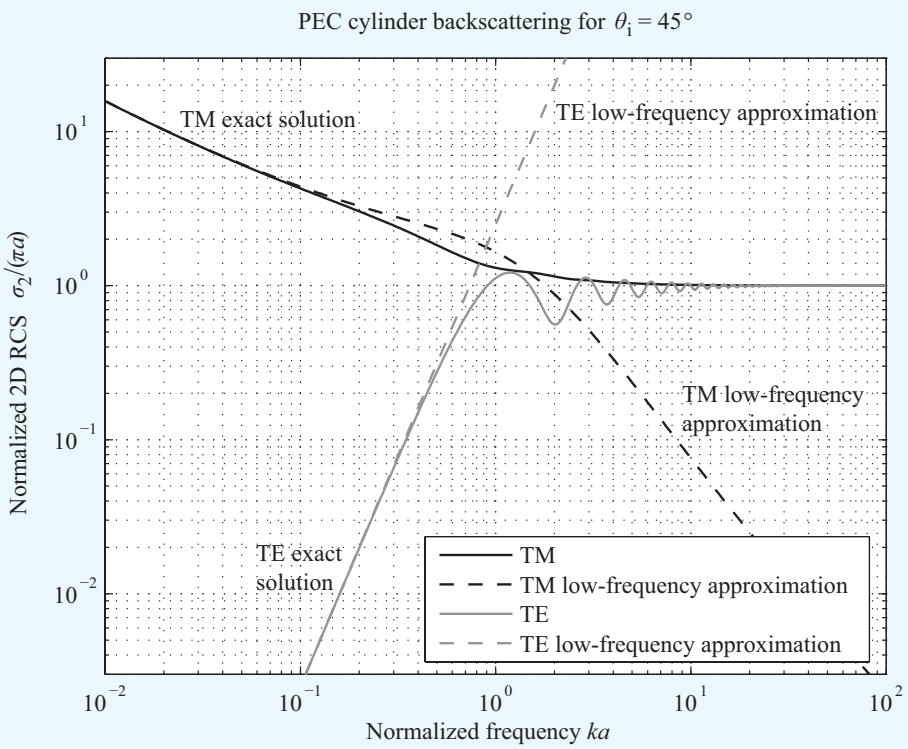


**Figure 7-27:** Normalized backscatter radar echo width of a metallic cylinder at oblique incidence ($\theta_i = 45°$) for both TE and TM polarizations. Also shown are the low-frequency approximations. The backscatter echo width approaches the high-frequency limit of $\sigma_2 = \pi a$ for values of $ka \geq 10$.

representations. It was shown that Bessel functions are solutions to the 2-D wave equation

$$\nabla_t^2 \, \psi(\rho,\phi) + k_\rho^2 \, \psi(\rho,\phi) = 0 \, . \tag{7.208}$$

Following a procedure similar to that in Section 7-2.7, the solution to Eq. (7.208) can be written as

$$\psi(x,y) = \int_{-\infty}^{+\infty} A(k_x) \, e^{i(k_x x + k_y |y|)} \, dk_x \, , \tag{7.209}$$

(see Eq. (7.162)), where $k_y = \sqrt{k_\rho^2 - k_x^2}$. By performing the following change of variables,

$$\begin{aligned} k_x &= k_\rho \cos\gamma \, , \\ k_y &= k_\rho \sin\gamma \, , \end{aligned} \tag{7.210}$$

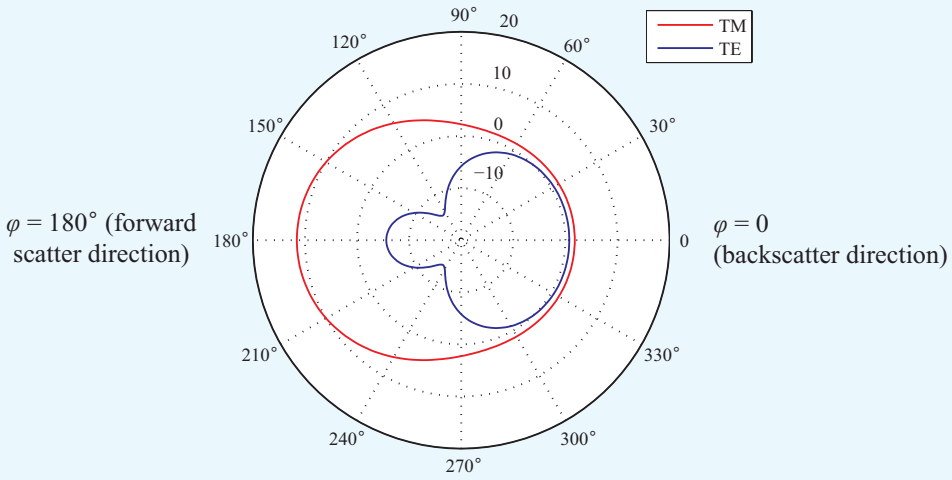


**Figure 7-28:** Bistatic echo width of a metallic cylinder with $ka = 1$ at normal incidence for both TE and TM polarizations.

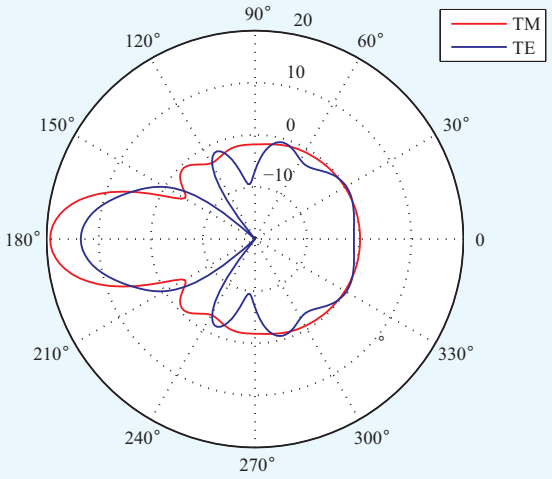


**Figure 7-29:** Bistatic echo width of a metallic cylinder with $ka = 5$ at normal incidence for both TE and TM polarization.

and

$$\begin{aligned} x &= \rho \cos\phi \ , \\ y &= \rho \sin\phi \ , \end{aligned} \tag{7.211}$$

Eq. (7.209) can be rewritten as

$$\psi(\rho,\phi) = \int_C B(\gamma)\, e^{ik_\rho \rho \cos(\gamma \mp \phi)}\, d\gamma \, , \tag{7.212}$$

where $B(\gamma) = -\sin\gamma\, k_\rho\, A(k_\rho \cos\gamma)$, a function to be determined. In Eq. (7.212), the negative sign in the argument of the cosine function corresponds to $y > 0$ and the positive sign corresponds to $y < 0$. The contour $C$ corresponds to a path defined by Eq. (7.210). Another change of variable is used as $\phi' = \gamma \mp \phi$ with $d\gamma = d\phi'$ as

$$\psi(\rho,\phi) = \int_C B(\phi' \pm \phi)\, e^{ik_\rho \rho \cos(\phi')}\, d\phi' \ . \tag{7.213}$$

If $\psi(\rho,\phi)$ is to be represented by the product of two functions, each a function of only one variable, that is, $\psi(\rho,\phi) = F(\phi)\, R(k_\rho \rho)$, then

$$B(\phi' \pm \phi) = F(\phi)\, g(\phi') \ . \tag{7.214}$$

Substitution of Eq. (7.214) into Eq. (7.213) shows that

$$R(k_\rho \rho) = \int_C g(\phi')\, e^{ik_\rho \rho \cos(\phi')}\, d\phi' \ . \tag{7.215}$$

Applying the method of separation of variables to Eq. (7.208) shows that

$$F(\phi) = a e^{i\nu\phi} + b e^{-i\nu\phi} \tag{7.216}$$

and

$$\frac{d^2 R(\widetilde{\rho})}{d\widetilde{\rho}^2} + \frac{1}{\widetilde{\rho}} \frac{dR(\widetilde{\rho})}{d\widetilde{\rho}} + \left(1 - \frac{\nu^2}{\widetilde{\rho}^2}\right) R(\widetilde{\rho}) = 0 \ . \tag{7.217}$$

That is, Eq. (7.215) must satisfy Eq. (7.217) with $\widetilde{\rho} = k_\rho \rho$. Starting from Eq. (7.215),

$$\frac{dR(\widetilde{\rho})}{d\widetilde{\rho}} = \int_C i \cos\phi'\, g(\phi')\, e^{i\widetilde{\rho}\cos\phi'}\, d\phi' \tag{7.218a}$$

and

$$\frac{d^2 R(\widetilde{\rho})}{d\widetilde{\rho}^2} = \int_C -\cos^2\phi'\, g(\phi')\, e^{i\widetilde{\rho}\cos\phi'}\, d\phi' \ . \tag{7.218b}$$

Upon substitution of Eqs. (7.218a) and (7.218b) into Eq. (7.217), the following relation must hold for Eq. (7.215) to satisfy the Bessel differential equation:

$$\int_C g(\phi') \left(\sin^2\phi'\,\widetilde{\rho}^2 + i\cos\phi'\,\widetilde{\rho} - \nu^2\right) e^{i\widetilde{\rho}\cos\phi'}\,d\phi' = 0\,. \tag{7.219}$$

Note that

$$\frac{d^2 e^{i\widetilde{\rho}\cos\phi'}}{d\phi'^2} = -\widetilde{\rho}^2\sin^2\phi'\,e^{i\widetilde{\rho}\cos\phi'} - i\widetilde{\rho}\cos\phi'\,e^{i\widetilde{\rho}\cos\phi'}\,.$$

As a result, Eq. (7.219) can be rewritten as

$$\int_C g(\phi') \left(\frac{d^2 e^{i\widetilde{\rho}\cos\phi'}}{d\phi'^2} + \nu^2 e^{i\widetilde{\rho}\cos\phi'}\right) d\phi' = 0\,. \tag{7.220}$$

Also, we realize that

$$g(\phi')\,\frac{d^2 e^{i\widetilde{\rho}\cos\phi'}}{d\phi'^2} - e^{i\widetilde{\rho}\cos\phi'}\,\frac{d^2 g(\phi')}{d\phi'^2} = \frac{d}{d\phi'}\left(g(\phi')\,\frac{de^{i\widetilde{\rho}\cos\phi'}}{d\phi'} - e^{i\widetilde{\rho}\cos\phi'}\,\frac{dg(\phi')}{d\phi'}\right),$$

which can be used in Eq. (7.220) to arrive at

$$\begin{aligned}\int_C \frac{d}{d\phi'}\left(g(\phi')\,\frac{de^{i\widetilde{\rho}\cos\phi'}}{d\phi'} - e^{i\widetilde{\rho}\cos\phi'}\,\frac{dg(\phi')}{d\phi'}\right) d\phi' \\ + \int e^{i\widetilde{\rho}\cos\phi'}\left(\frac{d^2 g(\phi')}{d\phi'^2} + \nu^2\,g(\phi')\right) d\phi' = 0\,.\end{aligned} \tag{7.221}$$

Equation (7.221) is valid if

$$\left(i\widetilde{\rho}\sin\phi'\,g(\phi') + \frac{dg(\phi')}{d\phi'}\right) e^{i\widetilde{\rho}\cos\phi'}\Big|_{\text{end points}} = 0 \tag{7.222}$$

and

$$\frac{d^2 g(\phi')}{d\phi'^2} + \nu^2\,g(\phi') = 0\,. \tag{7.223}$$

A harmonic function can be chosen for Eq. (7.223) and can be written as

$$g(\phi') = ce^{\pm i\nu\phi'}\,.$$

The constant $c$ is chosen as $c = \frac{1}{\pi}\,e^{-i\nu\pi/2}$ so that the resulting solutions are consistent with the previous expressions for the Bessel function. To satisfy Eq. (7.222), the path of the integral in the complex $\phi'$ plane must be chosen so that at the end points the requirement of Eq. (7.222)

is met. Finally, a general integral representation for the Bessel function can be written as

$$Z_\nu(k_\rho\rho) = \frac{e^{-i\nu\pi/2}}{\pi} \int_C e^{ik_\rho\rho\cos\phi \pm i\nu\phi}\, d\phi \ , \tag{7.224}$$

subject to the following condition on contour $C$:

$$(k_\rho\rho\sin\phi \pm \nu) e^{i(k_\rho\rho\cos\phi\pm\nu\phi)}\Big|_{\text{end points}} = 0 \ . \tag{7.225}$$

For example, if we choose the contour on the complex $\phi$-plane to be a segment of the real axis from $-\pi$ to $\pi$, then for $\nu = n$ (integer),

$$\begin{aligned}\left[k_\rho\rho\sin(\pi)\pm n\right] e^{i(-k_\rho\rho\pm n\pi)} - \left[k_\rho\rho\sin(-\pi)\pm n\right] e^{i(-k_\rho\rho\mp n\pi)} &= \pm n e^{-ik_\rho\rho}(e^{\pm in\pi} - e^{\mp in\pi}) \\ &= \pm 2in e^{-ik_\rho\rho}\sin(\pm n\pi) \\ &= 0 \ ,\end{aligned}$$

and then Eq. (7.225) is satisfied. In fact, if $C$ is any segment of the real axis with length $2\pi$, Eq. (7.225) is satisfied. This can be used to define the Bessel function of the first kind as

$$\mathbf{J}_n(k_\rho\rho) = \frac{(-i)^n}{2\pi} \int_{-\pi}^{\pi} e^{ik_\rho\rho\cos\phi + in\phi}\, d\phi \ . \tag{7.226}$$

Other kinds of Bessel functions of arbitrary order can be obtained by requiring $e^{i(k_\rho\rho\cos\phi+\nu\phi)}$ to vanish at the endpoints on contour $C$ in the complex $\phi$ plane. Let us define

$$\phi = \alpha + i\beta \ ,$$

where $\alpha$ and $\beta$ are respectively the real and imaginary parts of $\phi$. In this case, the exponent can be written as

$$ik_\rho\rho\cos\phi \pm i\nu\phi = \mp\nu\beta + k_\rho\rho\sin\alpha\sinh\beta + i(\pm\nu\alpha + k_\rho\rho\cos\alpha\cosh\beta) \ . \tag{7.227}$$

If contour $C$ is chosen so that $(\mp\nu\beta + k_\rho\rho\sin\alpha\sinh\beta)$ is $-\infty$ at the endpoints of the contour, Eq. (7.224) is a solution to the Bessel differential equation. This can be the case if $\beta \to \infty$ and $\alpha = (2n\pi - \pi/2)$ for any natural number $n$. Also, if $\alpha = (2n\pi + \pi/2)$ and $\beta \to -\infty$, the exponent approaches $-\infty$ again. So it seems that contours with endpoints $[(2n\pi - \pi/2) + i\infty]$ and $[(2n\pi + \pi/2) - i\infty]$ will satisfy the requirement. Sommerfield defined Hankel functions of the first kind and second kind as

$$H_\nu^{(1)}(k_\rho\rho) = \frac{e^{-i\nu\pi/2}}{\pi} \int_{-\pi/2+i\infty}^{\pi/2-i\infty} e^{ik_\rho\rho\cos\phi + i\nu\phi}\, d\phi \tag{7.228a}$$

and

$$H_\nu^{(2)}(k_\rho\rho) = \frac{e^{-i\nu\pi/2}}{\pi} \int_{\pi/2-i\infty}^{3\pi/2+i\infty} e^{ik_\rho\rho\cos\phi + i\nu\phi}\, d\phi \ . \tag{7.228b}$$

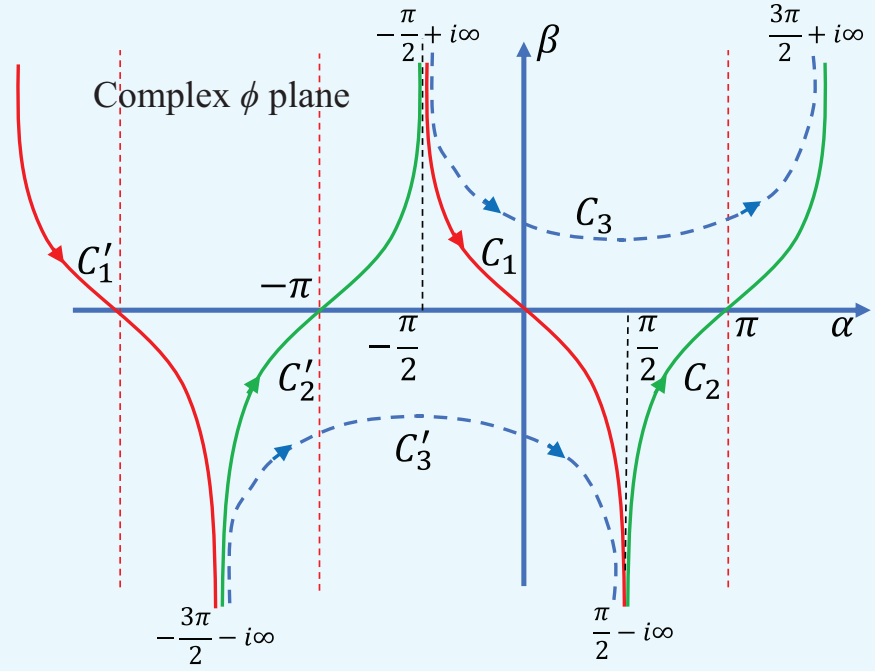


**Figure 7-30:** The complex $\phi$ plane and the appropriate contours for Hankel functions of the first kind ($C_1$) and Hankel functions of the second kind ($C_2$).

These contours are shown in Fig. 7-30 in the complex $\phi$ plane. Note that the actual functions defining the shapes of these contours are not important so long as the endpoints are not changed.

In the asymptotic evaluation of Eq. (7.228a) or Eq. (7.228b) when $k_\rho \rho \gg 1$, the method of stationary-phase approximation or the saddle-point technique is used. For such techniques the contour path is chosen to go through the saddle point or the stationary phase point, near which the variations of the phase of the integrand is slow. The saddle point (stationary phase point) is obtained from the solution

$$\frac{d}{d\phi}\left(k_\rho \rho \cos\phi + \nu\phi\right)\Big|_{\phi_s} = 0\,, \tag{7.229a}$$

$$\phi_s = \sin^{-1}\left(\frac{\nu}{k_\rho \rho}\right) \approx 0, \pm\pi, \pm 2\pi, \ldots \qquad \text{for } \nu \ll k_\rho \rho\,. \tag{7.229b}$$

The contour chosen for Eq. (7.228a), $C_1$, is referred to as the ***steepest descent path***, and it goes through $\phi_s = 0$. The contour chosen for Eq. (7.228b), $C_2$, goes through $\pi$, as shown in Fig. 7-30. Applying the method of steepest descent path, the approximate values of $H_\nu^{(1)}$ and

$H_\nu^{(2)}$ for large values of $k_\rho\rho$ are given by

$$H_\nu^{(1)}(k_\rho\rho) \approx \sqrt{\frac{2}{\pi k_\rho\rho}}\, e^{i\{k_\rho\rho-[(2\nu+1)/4]\pi\}} \tag{7.230a}$$

and

$$H_\nu^{(2)}(k_\rho\rho) \approx \sqrt{\frac{2}{\pi k_\rho\rho}}\, e^{-i\{k_\rho\rho-[(2\nu+1)/4]\pi\}} \tag{7.230b}$$

For details, see Appendix B.

The integral representation for Bessel functions of the first kind and noninteger order can be obtained from the definition

$$J_\nu(k_\rho\rho) = \frac{1}{2}\left[H_\nu^{(1)}(k_\rho\rho) + H_\nu^{(2)}(k_\rho\rho)\right] . \tag{7.231}$$

Noting that contours $C_1$ and $C_2$ can be deformed to coincide anywhere and then follow along $\alpha = \pi/2$ to go to $\pi/2 - i\,\infty$, contour $C_3$ for $J_\nu(k_\rho\rho)$ can be drawn as the one shown in Fig. 7-30. It is noted that $C_2'$ can be used in lieu of $C_2$ to find $H_\nu^{(2)}(k_\rho\rho)$, and therefore $C_3'$ can also be used to find $J_\nu(k_\rho\rho)$:

$$J_\nu(k_\rho\rho) = \frac{e^{-i\nu\pi/2}}{2\pi} \int_{C_3,C_3'} e^{ik_\rho\rho\cos\phi \pm i\nu\phi}\, d\phi . \tag{7.232}$$

## 7-7 2-D Green's Function for Homogeneous Media in the Presence of a Metallic Wedge

Another subject of practical importance is the scattering of electromagnetic waves by a metallic wedge. This problem reveals the behavior of electromagnetic fields near objects with sharp edges. The most general solution for an arbitrary current distribution can be obtained if the solution for a line source is available. Let us consider a metallic wedge of angle $\alpha$ as shown in Fig. 7-31, excited by a current source given by

$$\mathbf{J}(\mathbf{r}) = \frac{I}{\rho}\,\delta(\rho-\rho')\,\delta(\phi-\phi')\,e^{i\beta z}\,\hat{\mathbf{z}} . \tag{7.233}$$

One side of the wedge face is on the $x$–$z$ plane ($\phi = 0$) and the other face is at $\phi = 2\pi - \alpha$. The Hertz vector potential has only a $z$-component and it must satisfy

$$\nabla^2\Pi_z + k^2\Pi_z = \frac{-i}{\omega\varepsilon}\, Ie^{i\beta z}\,\frac{\delta(\rho-\rho')}{\rho}\,\delta(\phi-\phi') . \tag{7.234}$$

As before, since the geometry of the wedge is invariant with respect to $z$, the Hertz potential can be written as

$$\Pi_z(\mathbf{r}) = \Psi(\rho,\phi)\,e^{i\beta z}$$

and

$$\nabla_t^2 \Psi(\rho,\phi) + k_\rho^2 \, \Psi(\rho,\phi) = \frac{-i}{\omega\varepsilon} \, I \, \frac{\delta(\rho-\rho')}{\rho} \, \delta(\phi-\phi') \, . \tag{7.235}$$

The boundary condition for the TM to $z$ field mandates that

$$\Psi(\rho,0) = \Psi(\rho,\, 2\pi-\alpha) = 0 \, .$$

The method of separation of variables can be used in this case since the boundary condition is applied to constant coordinate surfaces $\phi = 0$ and $\phi = 2\pi - \alpha$. The domain of interest includes $0 \le \phi \le 2\pi - \alpha$ and $0 \le \rho < \infty$. We divide the region of interest into two regions: 1) $\rho \le \rho'$ and 2) $\rho \ge \rho'$. In Region 1, which includes $\rho = 0$, the only admissible Bessel function is the Bessel function of the first kind, $J_\nu(k_\rho \rho)$, and in Region 2 the admissible Bessel function is $H_\nu^{(1)}(k_\rho \rho)$, which represents outgoing waves. The admissible solution with respect to $\phi$ is $\sin \nu\phi$, as it satisfies the boundary condition $\psi(\rho,0) = 0$. To satisfy the boundary condition at $\phi = 2\pi - \alpha$, we must have

$$\sin[\nu(2\pi-\alpha)] = 0 \, ,$$

which renders

$$\nu = \frac{m\pi}{2\pi-\alpha} \, , \qquad m = 1,2,3,\ldots$$

For simplicity of carrying indices, let us define $2\pi - \alpha = p\pi$ for some real number $p$. In this case the order of the Bessel function is $\nu = m/p$. Also, recalling that functions $\sin(\frac{m}{p}\,\phi)$ form

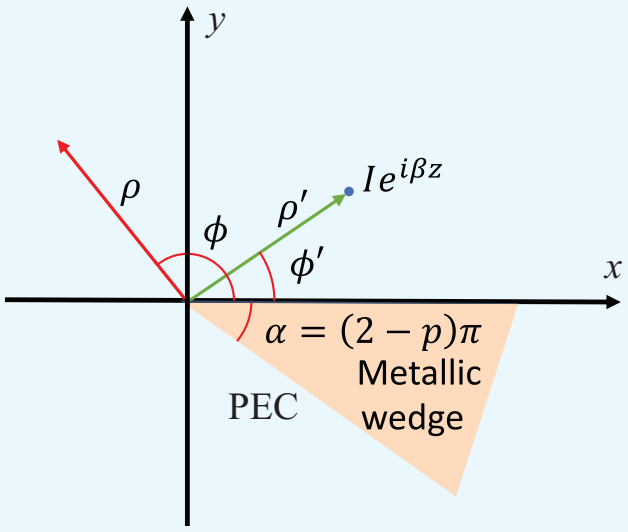


**Figure 7-31:** Configuration of a metallic wedge with angle $\alpha$ excited by a $z$-directed line current at $(\rho', \phi')$.

a set of complete orthogonal functions in the domain $[0, p\pi]$,

$$\delta(\phi - \phi') = \frac{2}{2\pi - \alpha} \sum_{m=1}^{\infty} \sin\left(\frac{m}{p}\,\phi'\right) \sin\left(\frac{m}{p}\,\phi\right) . \tag{7.236}$$

The scalar potential that satisfies Eq. (7.235) in regions $\rho < \rho'$ and $\rho > \rho'$ are given respectively by

$$\Psi_<(\rho, \phi) = \sum_{m=1}^{\infty} A_m\, J_{m/p}(k_\rho \rho) \sin\left(\frac{m}{p}\,\phi'\right) \sin\left(\frac{m}{p}\,\phi\right) \tag{7.237a}$$

and

$$\Psi_>(\rho, \phi) = \sum_{m=1}^{\infty} B_m\, H^{(1)}_{m/p}(k_\rho \rho) \sin\left(\frac{m}{p}\,\phi'\right) \sin\left(\frac{m}{p}\,\phi\right) . \tag{7.237b}$$

Equation (7.235) mandates that

$$\Psi_> - \Psi_<|_{\rho=\rho'} = 0 \tag{7.238a}$$

and

$$\frac{\partial \Psi_>}{\partial \rho} - \frac{\partial \Psi_<}{\partial \rho}\bigg|_{\rho=\rho'} = \frac{-iI}{\omega \varepsilon \rho'}\, \delta(\phi - \phi') . \tag{7.238b}$$

Using Eqs. (7.236), (7.237a), and (7.237b) in Eqs. (7.238a) and (7.238b), the following equations for $A_m$ and $B_m$ are obtained:

$$A_m\, J_{m/p}(k_\rho \rho') = B_m\, H^{(1)}_{m/p}(k_\rho \rho') \tag{7.239a}$$

and

$$B_m k_\rho\, H^{(1)\prime}_{m/p}(k_\rho \rho') - A_m k_\rho\, J'_{m/p}(k_\rho \rho') = \frac{2}{(2\pi - \alpha)\rho'} \left(\frac{-iI}{\omega \varepsilon}\right) . \tag{7.239b}$$

The application of Wronskian

$$J_{m/p}(k_\rho \rho')\, H^{(1)\prime}_{m/p}(k_\rho \rho') - J'_{m/p}(k_\rho \rho')\, H^{(1)}_{m/p}(k_\rho \rho') = \frac{2i}{\pi k_\rho \rho'} \tag{7.240}$$

provides compact expressions for $A_m$ and $B_m$ from Eqs. (7.239a) and (7.239b):

$$A_m = \frac{-I}{p\omega\varepsilon}\, H^{(1)}_{m/p}(k_\rho \rho') \tag{7.241a}$$

and

$$B_m = \frac{-I}{p\omega\varepsilon}\, J_{m/p}(k_\rho \rho') . \tag{7.241b}$$

Hence the potential in each region is given by

$$\Psi_<(\rho,\phi) = \frac{-I}{p\omega\varepsilon} \sum_{m=1}^{\infty} H^{(1)}_{m/p}(k_\rho\rho')\, J_{m/p}(k_\rho\rho)\, \sin\left(\frac{m}{p}\,\phi'\right)\, \sin\left(\frac{m}{p}\,\phi\right) \tag{7.242a}$$

and

$$\Psi_>(\rho,\phi) = \frac{-I}{p\omega\varepsilon} \sum_{m=1}^{\infty} J_{m/p}(k_\rho\rho')\, H^{(1)}_{m/p}(k_\rho\rho)\, \sin\left(\frac{m}{p}\,\phi'\right)\, \sin\left(\frac{m}{p}\,\phi\right)\ . \tag{7.242b}$$

As expected, this solution satisfies the reciprocity requirement. The field expressions can be derived from Eqs. (7.242a) and (7.242b) using Eqs. (5.102a) and (5.102b):

$$E_z(\rho,\phi) = k_\rho^2\ \psi(\rho,\phi)\, e^{i\beta z}\ , \tag{7.243a}$$

$$E_\rho(\rho,\phi) = i\beta\ \frac{\partial}{\partial\rho}\ \psi(\rho,\phi)\, e^{i\beta z}\ , \tag{7.243b}$$

$$E_\phi(\rho,\phi) = i\beta\ \frac{1}{\rho}\ \frac{\partial}{\partial\phi}\ \psi(\rho,\phi)\, e^{i\beta z}\ , \tag{7.243c}$$

$$H_\phi(\rho,\phi) = i\omega\varepsilon\ \frac{\partial}{\partial\rho}\ \psi(\rho,\phi)\, e^{i\beta z}\ , \tag{7.243d}$$

$$H_\rho(\rho,\phi) = -i\omega\varepsilon\ \frac{1}{\rho}\ \frac{\partial}{\partial\phi}\ \psi(\rho,\phi)\, e^{i\beta z}\ . \tag{7.243e}$$

In specific,

$$E_z(\rho,\phi) = \begin{cases} \dfrac{-Ik_\rho^2 e^{i\beta z}}{p\omega\varepsilon} \displaystyle\sum_{m=1}^{\infty} H^{(1)}_{m/p}(k_\rho\rho')\, J_{m/p}(k_\rho\rho)\, \sin\left(\dfrac{m}{p}\,\phi'\right)\, \sin\left(\dfrac{m}{p}\,\phi\right) & \rho<\rho'\ , \\ \dfrac{-Ik_\rho^2 e^{i\beta z}}{p\omega\varepsilon} \displaystyle\sum_{m=1}^{\infty} J_{m/p}(k_\rho\rho')\, H^{(1)}_{m/p}(k_\rho\rho)\, \sin\left(\dfrac{m}{p}\,\phi'\right)\, \sin\left(\dfrac{m}{p}\,\phi\right) & \rho>\rho'\ . \end{cases} \tag{7.244}$$

In the far-field region, as $k_\rho\rho \to \infty$, the large-argument expansion of $H^{(1)}_{m/p}(k_\rho\rho)$ can be used:

$$H^{(1)}_{m/p}(k_\rho\rho) \approx \sqrt{\frac{-2i}{\pi k_\rho\rho}}\ (-i)^{m/p} e^{ik_\rho\rho} \tag{7.245a}$$

and

$$E_z(\rho,\phi) = \frac{-Ik_\rho^2}{p\omega\varepsilon} \sqrt{\frac{-2i}{\pi k_\rho\rho}}\ e^{i(k_\rho\rho+\beta z)} \sum_{m=1}^{\infty} (-i)^{m/p}\, J_{m/p}(k_\rho\rho')\, \sin\left(\frac{m}{p}\,\phi'\right)\, \sin\left(\frac{m}{p}\,\phi\right)\ , \tag{7.245b}$$

where $p = 2-\alpha/\pi$. Other field components can be derived in a similar manner.

As an example, Fig. 7-32(a) and (b) show the $z$-component of the electric field in the far-

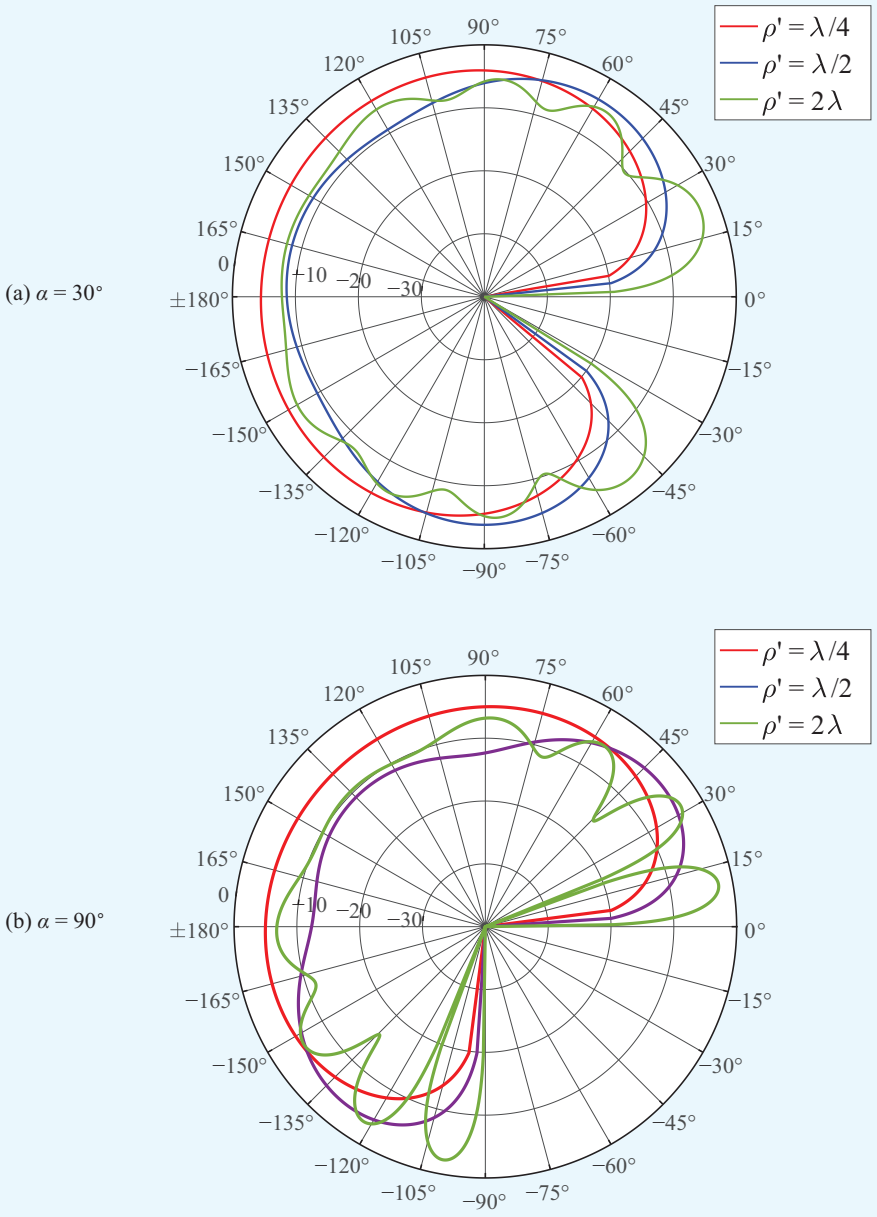


**Figure 7-32:** The $z$-component of the electric field in the far-field region for a metallic wedge with angular extent (a) $\alpha = 30°$ and (b) $al = 90°$.

field region for metallic wedges with interior angles of 30° and 90° when excited by a line source placed at $\phi' = 165°$ and $\phi' = 135°$, respectively, for three different values of $\rho'$. As shown, the total electric field along the wedge surface is zero.

### 7-7.1 The TE Solution

Transverse electric fields are generated by a $z$-directed magnetic filament current (located at $\rho = \rho'$ and $\phi = \phi'$) of the form

$$\mathbf{J}_{\rm m}(\mathbf{r}) = \frac{I_{\rm m}}{\rho}\,\delta(\rho-\rho')\,\delta(\phi-\phi')\,e^{i\beta z}\,\hat{\mathbf{z}}\,. \tag{7.246}$$

The required boundary conditions on the surface of the metallic wedge shown in Fig. 7-31 requires $\partial\psi/\partial n = \partial\psi/\partial\phi = 0$ at $\phi = 0$ and $\phi = 2\pi - \alpha$. This mandates the harmonic wave function with respect to $\phi$ to be of the form of $\cos\nu\phi$ with $\nu = m/p$, where $p = 2 - \alpha/\pi$. Also, noting that

$$\delta(\phi-\phi') = \frac{2}{p\pi}\sum_{m=0}^{\infty}\alpha_m\cos\left(\frac{m}{p}\,\phi'\right)\cos\left(\frac{m}{p}\,\phi\right)\,, \tag{7.247}$$

where

$$\alpha_m = \begin{cases} \frac{1}{2} & m = 0\,, \\ 1 & m \neq 0\,, \end{cases}$$

the appropriate scalar potential can be found by applying duality to Eqs. (7.242a) and (7.242b):

$$\Psi_<(\rho,\phi) = \frac{-I_m}{p\omega\mu}\sum_{m=0}^{\infty}\alpha_m\,H^{(1)}_{m/p}(k_\rho\rho')\,J_{m/p}(k_\rho\rho)\cos\left(\frac{m}{p}\,\phi'\right)\cos\left(\frac{m}{p}\,\phi\right) \tag{7.248a}$$

and

$$\Psi_>(\rho,\phi) = \frac{-I_m}{p\omega\mu}\sum_{m=0}^{\infty}\alpha_m\,J_{m/p}(k_\rho\rho')\,H^{(1)}_{m/p}(k_\rho\rho)\cos\left(\frac{m}{p}\,\phi'\right)\cos\left(\frac{m}{p}\,\phi\right)\,. \tag{7.248b}$$

By applying Eqs. (7.248a) and (7.248b) to the dual of Eqs. (7.243e) and (7.244), all field components can be obtained.

### 7-7.2 Plane-Wave Scattering from a Conducting Wedge

The behavior of the total field in the vicinity of a conducting wedge when illuminated by a plane wave is of interest. To find the solution, consider the wedge shown in Fig. 7-33 when illuminated by a TM plane wave given by

$$\mathbf{E}^{\rm i}(\rho,\phi,z) = E_0\left[\cos\theta'(\cos\phi'\,\hat{\mathbf{x}} + \sin\phi'\,\hat{\mathbf{y}}) + \sin\theta'\,\hat{\mathbf{z}}\right]e^{-ik_0\sin\theta'\,\cos(\phi-\phi')\rho}\,e^{ik_0\cos\theta'\,z}\,. \tag{7.249}$$

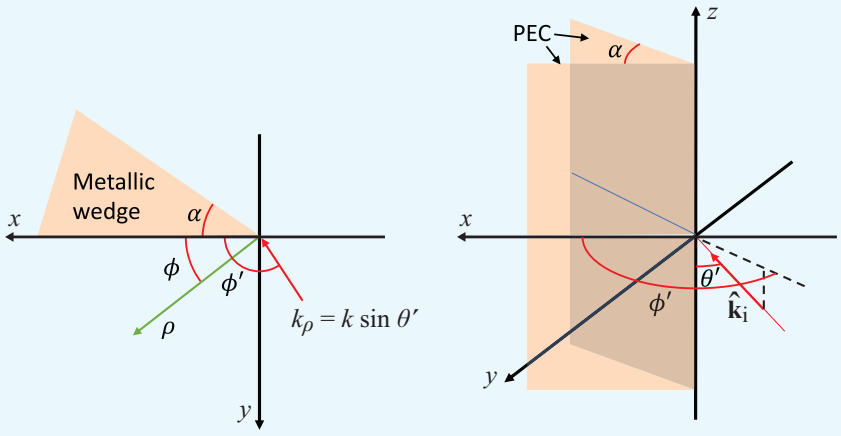


**Figure 7-33:** Configuration of a metallic wedge illuminated by a plane wave of oblique incidence.

For this wave we define $\beta = k_0 \cos\theta'$, $k_\rho = k_0 \sin\theta'$, and $\hat{\boldsymbol{\rho}}' = \cos\phi'\,\hat{\mathbf{x}} + \sin\phi'\,\hat{\mathbf{y}}$. The field generated by an infinite filament current located at $\hat{\boldsymbol{\rho}}'$ was obtained in Section 7-2.6 to be

$$\mathbf{E}(\rho,\phi) = \frac{-k_\rho^2 I}{4\omega\varepsilon} H_0^{(1)}(k_\rho|\boldsymbol{\rho}-\boldsymbol{\rho}'|)\, e^{i\beta z}\,\hat{\mathbf{z}} - \frac{i\beta k_\rho I}{4\omega\varepsilon} H_0^{(1)\prime}(k_\rho|\boldsymbol{\rho}-\boldsymbol{\rho}'|)\, e^{i\beta z}\,\frac{\boldsymbol{\rho}-\boldsymbol{\rho}'}{|\boldsymbol{\rho}-\boldsymbol{\rho}'|} \tag{7.250}$$

(see Eq. (7.139)). By placing the current far away from the origin such that $k_\rho \rho' \gg 1$, the large-argument expansion of the Hankel function can be used to find an approximate field expression in the vicinity of the origin. Noting that

$$|\boldsymbol{\rho}-\boldsymbol{\rho}'| \approx \rho' - \rho\cos(\phi-\phi')\ ,$$

and using the large-argument expansion of Hankel functions,

$$H_0^{(1)}(k_\rho|\boldsymbol{\rho}-\boldsymbol{\rho}'|) \approx \sqrt{\frac{-2i}{\pi k_\rho \rho'}}\, e^{ik_\rho\rho'} e^{-ik_\rho\rho\cos(\phi-\phi')} \tag{7.251a}$$

and

$$H_0^{(1)\prime}(k_\rho|\boldsymbol{\rho}-\boldsymbol{\rho}'|) \approx \sqrt{\frac{-2i}{\pi k_\rho \rho'}}\, ie^{ik_\rho\rho'} e^{-ik_\rho\rho\cos(\phi-\phi')}\ . \tag{7.251b}$$

Also, for $\rho' \gg \rho$, we have

$$\frac{\boldsymbol{\rho}-\boldsymbol{\rho}'}{|\boldsymbol{\rho}-\boldsymbol{\rho}'|} \approx -\hat{\boldsymbol{\rho}}'\ . \tag{7.252}$$

Substituting Eqs. (7.251a), (7.251b), and (7.252) into Eq. (7.250) and comparing the resultant equation with Eq. (7.249), we recognize that if

$$E_0 = -\frac{kk_\rho I}{4\omega\varepsilon}\sqrt{\frac{-2i}{\pi k_\rho \rho'}}\, e^{ik_\rho \rho'}\,, \tag{7.253}$$

then the field of a distant filament current of infinite extent resembles a local plane wave near the tip of the wedge. Hence the total field (incident plus diffracted) can be obtained from Eq. (7.244) for $\rho < \rho'$ using the large-argument expansion of $H_\nu^{(1)}(k_\rho \rho')$. That is,

$$E_z^{\rm t} = \frac{4\sin\theta'}{p} E_0 e^{ik\cos\theta' z} \sum_{m=1}^{\infty} (-i)^{m/p} J_{m/p}(k_\rho \rho) \sin\left(\frac{m}{p}\phi\right) \sin\left(\frac{m}{p}\phi'\right)\,. \tag{7.254}$$

Other field components can be derived from Eq. (7.243). For example,

$$E_\rho^{\rm t} = \frac{4i\cos\theta'}{p} E_0 e^{ik\cos\theta' z} \sum_{m=1}^{\infty} (-i)^{m/p} J'_{m/p}(k_\rho \rho) \sin\left(\frac{m}{p}\phi\right) \sin\left(\frac{m}{p}\phi'\right) \tag{7.255a}$$

and

$$E_\phi^{\rm t} = \frac{4i\cos\theta'}{p} E_0 \frac{e^{ik\cos\theta' z}}{k_\rho \rho} \sum_{m=1}^{\infty} \frac{m}{p} (-i)^{m/p} J_{m/p}(k_\rho \rho) \cos\left(\frac{m}{p}\phi\right) \sin\left(\frac{m}{p}\phi'\right)\,. \tag{7.255b}$$

It is noted that at normal incidence for which $\theta' = \pi/2$, both $E_\rho^{\rm t}$ and $E_\phi^{\rm t}$ vanish.

## 7-8 Asymptotic Evaluation of a Field Diffracted by a Metallic Wedge

In this section we derive a simplified expression for the fields diffracted by a metallic wedge illuminated by a plane wave. The total field expression for the TM wave is given by Eq. (7.254), and that for the TE wave can be obtained by using duality and the potential expression given by Eq. (7.248a). The goal here is to evaluate the infinite summation in these expressions for cases where $k_\rho \rho \gg 1$. Let us denote the infinite summation by

$$S_{\rm TE}^{\rm TM} = \frac{1}{2}\sum_{m=0}^{\infty} \alpha_m (-i)^{m/p} J_{m/p}(k_\rho \rho) \left[\cos\left(\frac{m}{p}(\phi+\phi')\right) \mp \cos\left(\frac{m}{p}(\phi-\phi')\right)\right]\,, \tag{7.256}$$

where, as before,

$$\alpha_m = \begin{cases} 1/2 & m = 0\,, \\ 1 & m \neq 0\,. \end{cases}$$

The negative sign between the two terms inside the square brackets is used for the TM solution and the positive sign is used for the TE solution. We have used the following identities to arrive

at Eq. (7.256):

$$\cos\left(\frac{m}{p}\,(\phi+\phi')\right)-\cos\left(\frac{m}{p}\,(\phi-\phi')\right)=2\sin\left(\frac{m}{p}\phi\right)\sin\left(\frac{m}{p}\phi'\right)$$

and

$$\cos\left(\frac{m}{p}\,(\phi+\phi')\right)+\cos\left(\frac{m}{p}\,(\phi-\phi')\right)=2\cos\left(\frac{m}{p}\phi\right)\cos\left(\frac{m}{p}\phi'\right)\ .$$

Introducing a new variable

$$\gamma^{\pm}=\phi\pm\phi'\ , \tag{7.257}$$

Eq. (7.256) can be written as

$$S^{\mathrm{TM}}_{\mathrm{TE}}=s(k_\rho\rho,\gamma^{+})\mp s(k_\rho\rho,\gamma^{-})\ , \tag{7.258}$$

where

$$\begin{aligned}s(k_\rho\rho,\gamma)&=\sum_{m=0}^{\infty}\frac{\alpha_m}{2}\,(-i)^{m/p}\,J_{m/p}(k_\rho\rho)\cos\left(\frac{m}{p}\,\gamma\right)\\&=\sum_{m=1}^{\infty}\frac{1}{4}\,J_{m/p}(k_\rho\rho)e^{i\frac{m}{p}\,[\gamma-(\pi/2)]}+\sum_{m=0}^{\infty}\frac{1}{4}\,J_{m/p}(k_\rho\rho)e^{-i\frac{m}{p}\,[\gamma+(\pi/2)]}\end{aligned} \tag{7.259}$$

To evaluate Eq. (7.259) asymptotically, we will make use of the integral representation of $J_{m/p}(k_\rho\rho)$ given by Eq. (7.254):

$$J_{m/p}(k_\rho\rho)=\frac{1}{2\pi}\int_{C_3}e^{i[k_\rho\rho\cos\eta+\frac{m}{p}\,(\eta-\pi/2)]}\,d\eta\ , \tag{7.260}$$

where the contour of integration $C_3$ is the one shown in Fig. 7-30. Also noting that

$$J_\nu(k_\rho\rho)=(-1)^\nu\,J_{-\nu}(k_\rho\rho)\ ,$$

Eq. (7.260) can also be written as

$$J_{m/p}(k_\rho\rho)=\frac{1}{2\pi}\int_{C_3'}e^{i[k_\rho\rho\cos\eta-\frac{m}{p}\,(\eta+\pi/2)]}\,d\eta\ . \tag{7.261}$$

Substituting Eqs. (7.260) and (7.261) into the conjugate of Eq. (7.259) and changing the order of summation and integration leads to

$$S^{*}(k_\rho\rho,\gamma)=\frac{1}{8\pi}\int_{C_3}e^{ik_\rho\rho\cos\eta}\sum_{m=1}^{\infty}e^{i\frac{m}{p}\,(\gamma+\eta)}\,d\eta+\frac{1}{8\pi}\int_{C_3'}e^{ik_\rho\rho\cos\eta}\sum_{m=0}^{\infty}e^{-i\frac{m}{p}\,(\gamma+\eta)}\,d\eta\ . \tag{7.262}$$

In the first integral of Eq. (7.262) on contour $C_3$, $\eta$ has a positive imaginary part, and as a result the exponential terms in the summation have exponentially decaying terms. Hence

$$\sum_{m=1}^{\infty} e^{i\frac{m}{p}(\gamma+\eta)} = \frac{e^{i(\gamma+\eta)/p}}{1-e^{i(\gamma+\eta)/p}} = -\frac{1}{1-e^{-i(\gamma+\eta)/p}} \,. \tag{7.263}$$

In the second integral of Eq. (7.262) on contour $C_3'$, $\eta$ has a negative imaginary part, and therefore the exponential terms in the summation have exponentially decaying terms as well. Therefore

$$\sum_{m=0}^{\infty} e^{-i\frac{m}{p}(\gamma+\eta)} = \frac{1}{1-e^{-i(\gamma+\eta)/p}} \,. \tag{7.264}$$

Substituting Eqs. (7.263) and (7.264) into Eq. (7.262) gives

$$S^*(k_\rho\rho),\gamma) = \frac{1}{8\pi} \int_{C_3'-C_3} \frac{e^{ik_\rho\rho\cos\eta}}{1-e^{-i(\gamma+\eta)/p}}\, d\eta \,. \tag{7.265}$$

The integration path is along $C_3'$ and in the opposite direction of $C_3$. It is also noted that

$$\begin{aligned}\frac{1}{1-e^{-i(\gamma+\eta)/p}} = \frac{e^{i(\gamma+\eta)/(2p)}}{e^{i(\gamma+\eta)/(2p)}-e^{-i(\gamma+\eta)/(2p)}} &= \frac{1}{2i}\left(\frac{\cos\left(\frac{\gamma+\eta}{2p}\right)+i\sin\left(\frac{\gamma+\eta}{2p}\right)}{\sin\left(\frac{\gamma+\eta}{2p}\right)}\right) \\ &= \frac{1}{2i}\cot\left(\frac{\gamma+\eta}{2p}\right)+\frac{1}{2} \,. \end{aligned} \tag{7.266}$$

Recognizing

$$\int_{C_3'-C_3} \frac{1}{2\pi}\, e^{ik_\rho\rho\cos\eta}\, d\eta = J_0(k_\rho\rho) - J_0(k_\rho\rho) = 0 \,, \tag{7.267}$$

and in view Eqs. (7.266) and (7.267), Eq. (7.265) can be written as

$$S^*(k_\rho\rho,\gamma) = \frac{1}{16\pi i} \int_{C_3'-C_3} \cot\left(\frac{\gamma+\eta}{2p}\right)\, e^{ik_\rho\rho\cos\eta}\, d\eta \,. \tag{7.268}$$

According to Cauchy's theorem,

$$\oint_C \cot\left(\frac{\gamma+\eta}{2p}\right)\, e^{ik_\rho\rho\cos\eta}\, d\eta = 2\pi i \sum_n R_n \,, \tag{7.269}$$

where $C$ is a closed contour composed of $C_3'$, $C_2$, $-C_3$, and $C_2'$. Here $R$ represents the residue of the integrand evaluated at its poles:

$$R_n = \lim_{\eta\to\eta_n} (\eta-\eta_n)\left[\cot\left(\frac{\gamma+\eta}{2p}\right)\, e^{ik_\rho\rho\cos\eta}\right] \,.$$

Poles of $\cot[(\gamma+\eta)/2p]$ occur at

$$\frac{\gamma+\eta_n}{2p} = n\pi, \qquad n = 0, \pm 1, \pm 2, \dots ,$$

from which $\eta_n$ can be obtained:

$$\eta_n = 2pn\pi - \gamma .$$

Noting that

$$\lim_{\eta\to\eta_n} (\eta - \eta_n) \frac{\cos\left(\frac{\gamma+\eta}{2p}\right)}{\sin\left(\frac{\gamma+\eta}{2p}\right)} e^{ik_\rho \rho \cos\eta} = 2p e^{ik_\rho \rho \cos(2pn\pi-\gamma)} , \tag{7.270}$$

the poles captured by the closed contour are those for which

$$-\pi \le 2pn\pi - \gamma \le \pi ,$$

or equivalently,

$$|2pn\pi - \gamma| \le \pi . \tag{7.271}$$

Therefore

$$\begin{aligned} S^*(k_\rho\rho,\gamma) + \frac{1}{16\pi i}\int_{C_2-C_2'} \cot\left(\frac{\gamma+\eta}{2p}\right) e^{ik_\rho\rho\cos\eta}\, d\eta &= \frac{1}{8}\sum_n R_n \\ &= \frac{p}{4}\sum_n e^{ik_\rho\rho\cos(2pn\pi-\gamma)}\, U(n - |2pn\pi - \gamma|) , \end{aligned} \tag{7.272}$$

where $U(\cdot)$ is the unit step function, which takes a value of unity when its argument is positive and zero when its argument is negative. The right-hand side of Eq. (7.272) represents plane waves corresponding to the incident wave and reflected waves from the faces of the metallic wedge. For $n = 0$ and $\gamma = \phi - \phi'$, the conjugate of the corresponding term for the electric field given by Eq. (7.254) takes the following form:

$$E_z^{0^-} = \sin\theta'\, E_0 e^{ik\cos\theta' z} e^{-ik_\rho\rho\cos(\phi-\phi')}\, U(\pi - |\phi - \phi'|) .$$

This represents the incident wave and is present only in the region where $\phi < \pi + \phi'$. As shown in Fig. 7-34, the half-plane $\phi = \pi + \phi'$ represents the ***shadow boundary***. Basically, the wedge shadows the incident wave for $\phi > \pi + \phi$.

Now, examining the case of $n = 0$ and $\gamma = \phi + \phi'$ gives another contribution of the poles of the integrand:

$$E_z^{0^+} = -\sin\theta'\, E_0 e^{ik\cos\theta' z} e^{-ik_\rho\rho\cos(\phi+\phi')}\, U(\pi - |\phi + \phi'|) . \tag{7.273}$$

This represents the reflected wave from the top face of the wedge, and it only exists in the region where $\phi < \pi - \phi'$. The plane $\phi = \pi - \phi'$ represents the ***reflection boundary***. Finally,

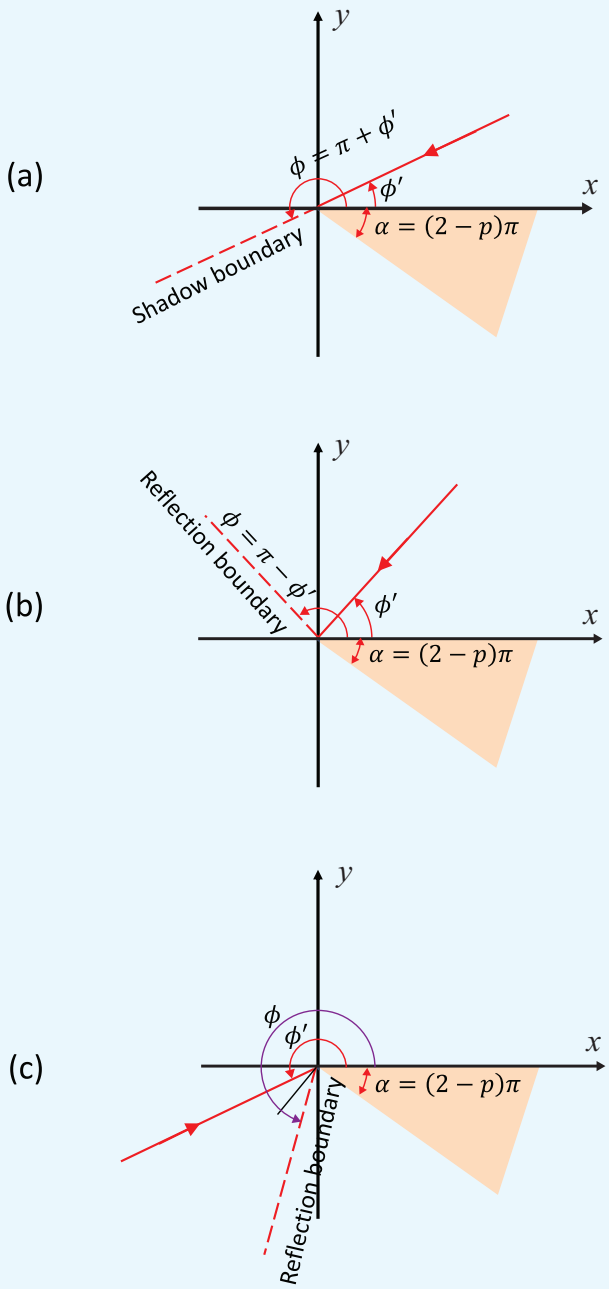


**Figure 7-34:** A metallic wedge with interior angle $\alpha$ illuminated by a plane wave at an angle $\phi'$. Also shown are the shadow boundary condition and reflection boundary.

we need to consider the case of $n = 1$ and $\gamma = \phi + \phi'$. For this case,

$$E_z^{1^+} = -\sin\theta' \, E_0 e^{ik\cos\theta' z} e^{-ik_\rho \rho \cos(\phi+\phi'-2p\pi)} \, U[(\phi+\phi') - (2p-1)\pi] \, , \tag{7.274}$$

which represents a reflected wave from the lower face of the wedge. This reflected wave exists only when

$$\phi \geq (2p-1)\pi - \phi' \, . \tag{7.275}$$

Note that in this case $\phi' > \phi - \alpha = (p-1)\pi$. The plane $\phi = (2p-1)\pi - \phi'$ also represents the reflection boundary for the lower face of the wedge. In general, the contribution from the residues predicts the incident wave and either a reflected ray from the top surface or a reflected ray from the bottom face, depending on the values of $(\phi + \phi')$.

Next we consider the contribution from the integral in Eq. (7.272). Consider

$$I_{C_2,C_2'}(\rho,\gamma) = -\frac{1}{16\pi i} \int_{C_2,C_2'} \cot\left(\frac{\gamma+\eta}{2p}\right) e^{ik_\rho \rho \eta} \, d\eta \, . \tag{7.276}$$

This integral can be evaluated approximately for $k_\rho \rho \gg 1$ using the saddle-point method. The saddle point of the integrand can be obtained from the solution of

$$\frac{d}{d\eta} (i\cos\eta) = 0 \, ,$$

which are found to be $\eta_s = \pm\pi$. The positive solution lies on $C_2$ and the negative solution lies on $C_2'$. The second derivative of the exponent evaluated at the saddle point is given by

$$\frac{d^2}{d\eta^2} (i\cos\eta)\bigg|_{\eta=\pm\pi} = i \, .$$

In conditions in which the saddle point is away from the poles,

$$I_{C_2,C_2'} = -\frac{1}{16\pi i} \left[ \sqrt{\frac{2\pi}{k_\rho \rho}} \, e^{-i(k_\rho \rho + \pi/4)} \cot\left(\frac{\gamma \pm \pi}{2p}\right) \right] \, .$$

Hence

$$I_{C_2} - I_{C_2'} = -\frac{1}{16\pi i} \sqrt{\frac{2\pi}{k_\rho \rho}} \, e^{-i(k_\rho \rho + \pi/4)} \left[ \cot\left(\frac{\gamma+\pi}{2p}\right) - \cot\left(\frac{\gamma-\pi}{2p}\right) \right] \, . \tag{7.277}$$

It further is noted that

$$\cot\left(\frac{\gamma+\pi}{2p}\right) - \cot\left(\frac{\gamma-\pi}{2p}\right) = \frac{\sin\left(\frac{\gamma-\pi}{2p} - \frac{\gamma+\pi}{2p}\right)}{\sin\left(\frac{\gamma+\pi}{2p}\right)\sin\left(\frac{\gamma-\pi}{2p}\right)} = -\frac{2\sin\left(\frac{\pi}{p}\right)}{\cos\left(\frac{\pi}{p}\right) - \cos\left(\frac{\gamma}{p}\right)} \, .$$

The diffracted components of Eq. (7.258), excluding the geometric optics term obtained from the contributions from the poles, are given by

$$S_{\mathrm{d}}^{\mathrm{TE}}{}^{\mathrm{TM}} = \frac{i}{8\pi}\sqrt{\frac{2\pi}{k_\rho \rho}}\, e^{i(k_\rho \rho + \pi/4)} \sin\left(\frac{\pi}{p}\right) \cdot \left[\frac{1}{\cos\left(\frac{\pi}{p}\right) - \cos\left(\frac{\phi+\phi'}{\pi}\right)} \mp \frac{1}{\cos\left(\frac{\pi}{p}\right) - \cos\left(\frac{\phi-\phi'}{p}\right)}\right] . \tag{7.278}$$

Referring to Eq. (7.254), the diffracted $z$-component of the electric field is given by

$$E_z^{\mathrm{d}} = \frac{e^{i(k_\rho \rho - \pi/4)}}{\sqrt{2\pi k_\rho \rho}}\, \sin\theta'\, e^{ik\cos\theta' z} E_0\, \frac{\sin\left(\frac{\pi}{p}\right)}{p} \cdot \left(\frac{1}{\cos\left(\frac{\pi}{p}\right) - \cos\left(\frac{\phi-\phi'}{p}\right)} - \frac{1}{\cos\left(\frac{\pi}{p}\right) - \cos\left(\frac{\phi+\phi'}{p}\right)}\right) . \tag{7.279}$$

For the TE case, a similar expression for the $z$-component of the magnetic field can be obtained. It is noted that when $p = 1$ (corresponding to $\alpha = \pi$, i.e., a flat plane), the diffracted field is zero as expected. It is also interesting to note that when $p = 1/M$ for some integer $M$, again the diffracted field vanishes ($M = 2, 3, 4, \ldots$). These correspond to interior wedges with angles of $\frac{\pi}{2}, \frac{\pi}{3}, \frac{\pi}{4}, \ldots$. The diffracted field becomes indeterminate for values of $\phi - \phi' = \pi$, $\phi + \phi' = \pi$, and $2p\pi - (\phi + \phi') = \pi$ near shadow and reflection boundary conditions.

In summary, the $z$-components of the total electric and magnetic fields can be written as

$$E_z^{\mathrm{t}} = E_z^{\mathrm{d}} + E_z^{\mathrm{GO}} \tag{7.280a}$$

and

$$H_z^{\mathrm{t}} = H_z^{\mathrm{d}} + H_z^{\mathrm{GO}} , \tag{7.280b}$$

where $E_z^{\mathrm{GO}}$ and $H_z^{\mathrm{GO}}$ are geometric optics terms composed of the incident and reflected fields. Oftentimes the diffracted field components are expressed in terms of diffraction coefficients defined by

$$E_z^{\mathrm{d}}(\rho, \phi, z) = E_0 \sin\theta'\, \frac{e^{ik(\sin\theta'\,\rho + \cos\theta'\, z)}}{\sqrt{\rho}}\, D_{\mathrm{s}}(\rho, \phi, \phi') \tag{7.281a}$$

and

$$H_z^{\mathrm{d}}(\rho, \phi, z) = H_0 \sin\theta'\, \frac{e^{ik(\sin\theta'\,\rho + \cos\theta'\, z)}}{\sqrt{\rho}}\, D_{\mathrm{h}}(\rho, \phi, \phi') . \tag{7.281b}$$

The diffraction coefficients for ***soft boundary conditions*** (TM) and for ***hard boundary conditions*** (TE) are given by

$$D_{\mathrm{h}}^{\mathrm{s}}(\rho,\phi,\phi') = \frac{e^{-i\pi/4}}{\sqrt{2\pi k}\sin\theta'}\,\frac{\sin\left(\frac{\pi}{p}\right)}{p} \cdot \left(\frac{1}{\cos\left(\frac{\pi}{p}\right)-\cos\left(\frac{\phi-\phi'}{p}\right)} \mp \frac{1}{\cos\left(\frac{\pi}{p}\right)-\cos\left(\frac{\phi+\phi'}{p}\right)}\right) . \quad (7.282)$$

As an example, the exact solution for the total field given by Eq. (7.254) is computed and the geometric optics terms are subtracted. The resultant field is the diffracted component from which the diffraction coefficients for the TM case are computed. For this example, the wedge angle is chosen to be $\alpha = \pi/6$ and the angles specifying the direction of incidence are chosen to be $\pi' = \pi/4$ and $\theta' = \pi/2$. The diffraction coefficients based on the asymptotic evaluation and the exact solution (using $\rho = 10\lambda$) are compared in Fig. 7-35, where, except at shadow and reflection boundaries, excellent agreement exists between the two solutions.

Of particular interest is the diffraction from half-metallic planes. Half-planes can be modeled as a wedge with angle $\alpha = 0$, for which $p = 2$. The diffraction coefficient for half-planes can be obtained from Eq. (7.282) with $p = 2$, and is given by

$$D_{\mathrm{s}}^{\mathrm{half-plane}}(\phi,\phi') = \frac{i2}{\sqrt{2\pi k}\sin\theta'}\left(\frac{\sin(\phi'/2)\sin(\phi/2)}{\cos\phi+\cos\phi'}\right) \quad (7.283a)$$

and

$$D_{\mathrm{h}}^{\mathrm{half-plane}}(\phi,\phi') = \frac{-i2}{\sqrt{2\pi k}\sin\theta'}\left(\frac{\cos(\phi'/2)\cos(\phi/2)}{\cos\phi+\cos\phi'}\right) . \quad (7.283b)$$

## Example 7-4: Edge Diffraction

Calculate the backscatter echo width of a half-plane illuminated by a TM incident wave.

**Solution:** Let us consider a TM plane wave:

$$E^{\mathrm{i}} = E_0\,\hat{\mathbf{z}}\,e^{-ik_0(\cos\phi' x+\sin\phi' y)} .$$

The diffracted or scattered field is given by

$$E^{\mathrm{d}} = \hat{\mathbf{z}}\,E_0\,\frac{e^{ik\rho}}{\sqrt{\rho}}\,D_{\mathrm{s}}(\phi,\phi') .$$

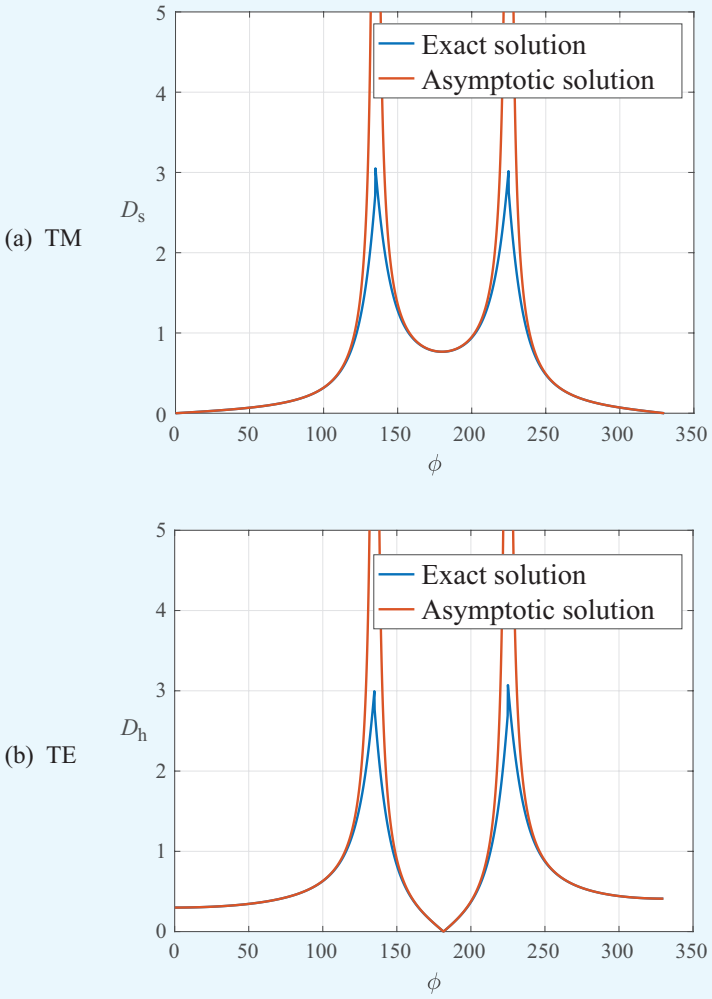


**Figure 7-35:** Diffraction coefficient for a metallic wedge with $\alpha = \pi/6$ when illuminated by (a) a TM plane wave and (b) a TE plane wave, both for $\phi' = \pi/4$ and $\theta' = \pi/2$.

In the case of backscatter, $\phi = \phi'$ and the diffraction coefficient is simplified to

$$D_s(\phi,\phi) = \frac{i}{2\sqrt{2\pi k}}\left(\frac{1}{\cos\phi} - 1\right).$$

The backscatter echo width is defined as

$$\sigma_{2D} = \lim_{\rho\to\infty} 2\pi\rho\,\frac{|E^d|^2}{|E^i|^2} = \frac{\lambda}{8\pi}\left(\frac{1}{\cos\phi} - 1\right)^2.$$

The echo width assumes its minimum at $\phi = 0$ ($\sigma_{2D}(0) = 0$) and is singular at $\phi = \pi/2$ and $\phi = 3\pi/2$ due to the inaccuracy of the diffraction coefficient at the reflection boundary. The echo width at edge-on incidence ($\phi = \pi$) is

$$\sigma_{2D}(\pi) = \frac{\lambda}{2\pi} .$$

## Example 7-5: Diffraction from a Slit in a Metallic Screen

Consider a single slit of width $w$ in a planar metallic plate placed in the $x$–$z$ plane, as shown in Fig. 7-36. Suppose the slit is being illuminated by a plane wave given by

$$\mathbf{E}_i = \hat{\mathbf{z}}\, e^{-ik_0(\cos\phi' x + \sin\phi' y)} . \tag{7.284}$$

Find the diffracted field in the far-field region by ignoring multiple diffraction between the two edges of the slit. Assign coordinate $(\rho, \phi)$ to the observation point.

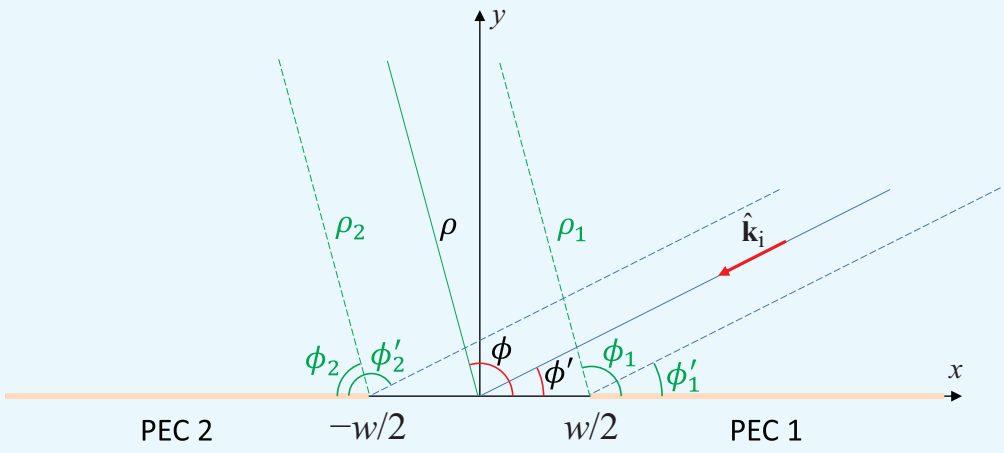


**Figure 7-36:** The geometry of a single metallic slit illuminated by a TM plane wave.

**Solution:** The diffracted field from the half-plane PEC 1 can be evaluated using

$$E_d^{(1)}(\rho, \phi, \phi') = E_0^{(1)} \frac{e^{ik\rho_1}}{\sqrt{\rho_1}} D_s^{(1)} , \tag{7.285}$$

where $E_0^{(1)}$ is the incident field at the edge of the half-plane PEC 1 given by

$$E_0^i = e^{-i(k_0 w/2)\cos\phi'} .$$

The diffraction coefficient can be calculated from Eq. (7.283a) noting that

$$\phi_1' = \phi' \tag{7.286a}$$

and in the far-field region

$$\phi_1 = \phi \tag{7.286b}$$

and

$$\rho_1 \approx \rho - \frac{w}{2}\cos\phi \ . \tag{7.286c}$$

Similarly, the diffracted field from half-plane PEC 2 can be evaluated using

$$E_{\mathrm{d}}^{(2)}(\rho,\phi,\phi') = E_0^{(2)}\ \frac{e^{ik\rho_2}}{\sqrt{\rho_2}}\, D_{\mathrm{s}}^{(2)} \ . \tag{7.287}$$

For this half-plane, the incident field at the edge is

$$E_0^{(2)} = e^{i(k_0 w/2)\cos\phi'}$$

and

$$\phi_2 = \pi - \phi \ , \tag{7.288a}$$

$$\phi_2' = \pi - \phi' \ , \tag{7.288b}$$

$$\rho_2 = \rho + \frac{w}{2}\cos\phi \ . \tag{7.288c}$$

Using Eq. (7.286) in Eq. (7.283a), we have

$$D_{\mathrm{s}}^{(1)} = \frac{i2}{\sqrt{2\pi k}}\ \frac{\sin(\phi'/2)\sin(\phi/2)}{\cos\phi + \cos\phi'} \ . \tag{7.289}$$

Also, using Eq. (7.288) in Eq. (7.283a), we get

$$D_{\mathrm{s}}^{(2)} = \frac{-i2}{\sqrt{2\pi k}}\ \frac{\cos(\phi'/2)\cos(\phi/2)}{\cos\phi + \cos\phi'} \ . \tag{7.290}$$

The total diffracted field can now be calculated from

$$\begin{aligned}\mathbf{E}_{\mathrm{d}} &= \hat{\mathbf{z}}\,\frac{e^{ik\rho}}{\sqrt{\rho}}\left(D_{\mathrm{s}}^{(1)}e^{-i(k_0w/2)(\cos\phi+\cos\phi')}+D_{\mathrm{s}}^{(2)}e^{i(k_0w/2)(\cos\phi+\cos\phi')}\right)\\ &= \hat{\mathbf{z}}\,\frac{-2ie^{ik\rho}}{\sqrt{2\pi k\rho}}\\ &\quad\cdot\left(\frac{\cos(\phi'/2)\cos(\phi/2)e^{i(k_0w/2)(\cos\phi+\cos\phi')}-\sin(\phi'/2)\sin(\phi/2)e^{-i(k_0w/2)(\cos\phi+\cos\phi')}}{\cos\phi+\cos\phi'}\right).\end{aligned} \tag{7.291}$$

It is interesting to note that when $\phi=\pi-\phi'$, the expression for the total diffracted field at the reflection boundary, as given by Eq. (7.291), remains finite. That is,

$$\begin{aligned}\lim_{\phi\to\pi-\phi'}\mathbf{E}_{\mathrm{d}} &= \hat{\mathbf{z}}\,\frac{-2ie^{ik\rho}}{\sqrt{2\pi k\rho}}\left(\frac{\cos(\phi'/2)\cos(\phi/2)-\sin(\phi'/2)\sin(\phi/2)}{2\cos\left(\dfrac{\phi+\phi'}{2}\right)\cos\left(\dfrac{\phi-\phi'}{2}\right)}\right)\\ &= \hat{\mathbf{z}}\,\frac{-ie^{ik\rho}}{\sqrt{2\pi k\rho}}\,\frac{1}{\sin\phi'}\,.\end{aligned}$$

# Summary

## Concepts

- The method of separation of variables is applied to the Helmholtz equation in cylindrical coordinates and the resulting solutions form the cylindrical wave functions.
- The $z$-dependent and $\phi$-dependent solutions for the Helmholtz equation are harmonic functions and the $\rho$-dependent solution is a Bessel function whose order depends on the harmonic number of the $\phi$-dependent function.
- If the domain of interest includes the entire range in $\phi$ ($0 < \phi \leq 2\pi$), the order of the Bessel functions has an integer value. Otherwise, the order of the Bessel functions must be a noninteger.
- The solution to the wave equation consists of a linear combination of cylindrical wave functions.
- A metallic waveguide whose surface coincides with the constant surfaces in a cylindrical coordinate system, such as a circular or angular sector waveguide, supports TE and TM modes whose cutoff frequencies are expressed in terms of zeros of the Bessel functions or their derivatives.
- A segment of a cylindrical waveguide can be capped on both sides to form a cylindrical cavity.
- A circular dieletric waveguide is shown to support hybrid TE and TM modes similar to dielectric plate waveguides. These waveguides have a much lower attenuation rate at optical frequencies and are known as optical fibers.
- Optical fibers can support pure TE or TM modes, but only in cases where the fields have azimuthal symmetry ($n = 0$).
- Other types of waveguides supporting cylindrical wave functions with propagation in radial and circumferential directions can be used to analyze practical problems, such as an H-bent rectangular waveguide.
- Green's functions for both interior cylindrical waveguide problems as well as exterior problems such as metallic cylinders and wedges are derived and expressed in terms of a series summation of appropriate cylidrical wave functions.
- The expression for the 2-D Green's function when the source is displaced from the origin can be expressed in terms of a Hankel function of zeroth order. When solving the Green's function directly, a series solution in terms of a summation of cylidrical wave functions, referenced to the origin of the coordinate system, is also derived. The comparison between the two solutions results in the addition theorem for the Hankel function of the zeroth order.
- The integral representation for Bessel functions of arbitrary order is derived in combination with the saddle-point method and used to find the asymptotic behavior of the scattered field from metallic wedges in the far-field region.

## Important Equations

**Bessel equation:**

$$\frac{d^2R}{d\tilde{\rho}^2}+\frac{1}{\tilde{\rho}}\frac{dR}{d\tilde{\rho}^2}+\left[1-\left(\frac{\nu}{\tilde{\rho}}\right)^2\right]R=0$$

**Hankel functions of the first and second kind in terms of Bessel functions of the first and second kind:**

$$H_\nu^{(1)}(k_\rho\rho)=J_\nu(k_\rho\rho)+iN_\nu(k_\rho\rho)$$
$$H_\nu^{(2)}(k_\rho\rho)=J_\nu(k_\rho\rho)-iN_\nu(k_\rho\rho)$$

**Solution of wave equation in terms of cylindrical wave functions:**

$$\psi(\rho,\phi,z)=\sum_{n=-\infty}^{+\infty}\int_{-\infty}^{+\infty}\left[A_n(k_z)\,J_n(k_\rho\rho)+B_n(k_z)\,N_n(k_\rho\rho)\right]e^{in\phi}e^{ik_zz}\,dk_z$$

**Definition of modified Bessel functions:**

$$J_n(i\alpha\rho)=(i)^n\,I_n(\alpha\rho)$$
$$H_n^{(1)}(i\alpha\rho)=\frac{2}{\pi}\,(i)^{n+1}\,K_n(\alpha\rho)$$

**Gamma function:**

$$\Gamma(x)=\int_0^\infty t^{x-1}e^{-t}\,dt$$

**Recurrence relations for Bessel functions of any kind:**

$$R_{\nu-1}+R_{\nu+1}=\frac{2\nu}{\rho}\,R_\nu$$

**Wronskian relationships:**

$$J_\nu(\rho)\,N_\nu'(\rho)-J_\nu'(\rho)\,N_\nu(\rho)=\frac{2}{\pi\rho}$$

$$J_\nu(\rho)\,H_\nu^{(1)'}(\rho)-J_\nu'(\rho)\,H_\nu^{(1)}(\rho)=\frac{i2}{\pi\rho}$$

## Important Equations (continued)

**Orthogonality of Bessel functions:**

$$\int_0^a J_\nu\left(\frac{x_{\nu p}}{a}\rho\right) J_\nu\left(\frac{x_{\nu q}}{a}\rho\right) \rho\, d\rho = 0$$

$$\int_0^a J_\nu\left(\frac{x'_{\nu p}}{a}\rho\right) J_\nu\left(\frac{x'_{\nu q}}{a}\rho\right) \rho\, d\rho = 0$$

**The norm of Bessel functions:**

$$\int_0^a J_\nu^2\left(\frac{x_{\nu p}}{a}\rho\right) \rho\, d\rho = \frac{a^2}{2}\left[J_{\nu+1}(x_{\nu p})\right]^2$$

$$\int_0^a J_\nu^2\left(\frac{x'_{\nu p}}{a}\rho\right) \rho\, d\rho = \frac{a^2}{2}\left[1-\left(\frac{\nu^2}{x'_{\nu p}}\right)^2\right]\left[J_\nu(x'_{\nu p})\right]^2$$

**Scalar potential function for circular waveguides:**

$$\psi(\rho,\phi) = A_n J_n\left(\frac{x_{np}}{a}\rho\right)\begin{cases}\sin(n\phi)\\ \cos(n\phi)\end{cases} \qquad \text{(TM)}$$

$$\psi(\rho,\phi) = A_n J_n\left(\frac{x'_{np}}{a}\rho\right)\begin{cases}\sin(n\phi)\\ \cos(n\phi)\end{cases} \qquad \text{(TE)}$$

**Cutoff frequency for circular waveguides:**

$$f_c^{\mathrm{TM}(np)} = \frac{x_{np}}{2\pi a\sqrt{\mu\varepsilon}} \qquad \text{(TM)}$$

$$f_c^{\mathrm{TE}(np)} = \frac{x'_{np}}{2\pi a\sqrt{\mu\varepsilon}} \qquad \text{(TE)}$$

## Important Equations (continued)

**Attenuation rate in circular waveguides:**

$$\alpha^{\mathrm{TM}_{np}} = \frac{\omega\varepsilon a}{\sigma\delta_s\beta_{np}x_{np}^2} = \frac{k}{\sigma\delta_s\eta a\sqrt{k^2-\left(\frac{x_{np}}{a}\right)^2}\left(\frac{x_{np}}{a}\right)^2} \qquad \text{(TM)}$$

$$\alpha^{\mathrm{TE}_{np}} = \frac{1}{\sigma\delta_s\eta ka\left[1-\left(\frac{n}{x'_{np}}\right)^2\right]}\left[\frac{n^2\sqrt{k^2-\left(\frac{x'_{np}}{a}\right)^2}}{\left(\frac{x'_{np}}{a}\right)^2}+\frac{\left(\frac{x'_{np}}{a}\right)^2}{\sqrt{k^2-\left(\frac{x'_{np}}{a}\right)^2}}\right] \qquad \text{(TE)}$$

**Transcendental equations for optical fiber:**

$$\left(k_\rho^{\mathrm{II}}\frac{\mu_d}{\mu_c}\frac{J_n'(k_\rho^{\mathrm{I}}a)}{J_n(k_\rho^{\mathrm{I}}a)}+k_\rho^{\mathrm{I}}\frac{K_n'(k_\rho^{\mathrm{II}}a)}{K_n(k_\rho^{\mathrm{II}}a)}\right)\left(k_\rho^{\mathrm{II}}\frac{\varepsilon_d}{\varepsilon_c}\frac{J_n'(k_\rho^{\mathrm{I}}a)}{J_n(k_\rho^{\mathrm{I}}a)}+k_\rho^{\mathrm{I}}\frac{K_n'(k_\rho^{\mathrm{II}}a)}{K_n(k_\rho^{\mathrm{II}}a)}\right) = \frac{\beta^2n^2}{a^2k_c^2}\frac{[(k_\rho^{\mathrm{I}})^2+(k_\rho^{\mathrm{II}})^2]^2}{(k_\rho^{\mathrm{I}})^2(k_\rho^{\mathrm{II}})^2}$$

$$(k_\rho^{\mathrm{I}})^2+(k_\rho^{\mathrm{II}})^2 = k_d^2-k_c^2$$

**Cutoff frequency for cylindrical cavity:**

$$f_{npq}^{\mathrm{TM}} = \frac{1}{2\pi\sqrt{\mu\varepsilon}}\sqrt{\left(\frac{x_{np}}{a}\right)^2+\left(\frac{q\pi}{\ell}\right)^2}$$

$$f_{npq}^{\mathrm{TE}} = \frac{1}{2\pi\sqrt{\mu\varepsilon}}\sqrt{\left(\frac{x'_{np}}{a}\right)^2+\left(\frac{q\pi}{\ell}\right)^2}$$

**Quality factor for $\mathrm{TM}_{010}$ mode in a cylindrical cavity:**

$$\breve{Q} = \frac{\sigma\delta_s\sqrt{\frac{\mu}{\varepsilon}}x_{01}}{2\left(1+\frac{a}{\ell}\right)} = \frac{\sigma\delta_s\eta 1.202}{2\left(1+\frac{a}{\ell}\right)}$$

## Important Equations (continued)

**Modal solution for a radial waveguide:**

$$\psi_{nq}^{\mathrm{TM}}(\rho,\phi,z) = H^{(1)}_{n\pi/\alpha}(k_\rho \rho)\,\sin\left(\frac{n\pi}{\alpha}\,\phi\right)\cos\left(\frac{q\pi}{\ell}\,z\right) \qquad \text{(TM)}$$

$$n = 1,2,3,\ldots, \quad q = 0,1,2,\ldots$$

$$\psi_{nq}^{\mathrm{TE}} = H^{(1)}_{n\pi/\alpha}(k_\rho \rho)\,\cos\left(\frac{n\pi}{\alpha}\,\phi\right)\sin\left(\frac{n\pi}{\ell}\,z\right) \qquad \text{(TE)}$$

$$n = 0,1,2,\ldots, \quad q = 1,2,\ldots$$

**Green's function for an angular sector waveguide:**

$$g_<(\boldsymbol{\rho},\boldsymbol{\rho}') = \frac{\pi i}{\phi_0}\sum_{n=1}^{\infty} J_\nu(k_\rho\rho)\left(H_\nu^{(1)}(k_\rho\rho') - \frac{J_\nu(k_\rho\rho')\,H_\nu^{(1)}(k_\rho a)}{J_\nu(k_\rho a)}\right)\sin\nu\phi\,\sin\nu\phi'$$

$$g_>(\boldsymbol{\rho},\boldsymbol{\rho}') = \frac{\pi i}{\phi_0}\sum_{n=1}^{\infty} J_\nu(k_\rho\rho')\left(H_\nu^{(1)}(k_\rho\rho) - \frac{J_\nu(k_\rho\rho)\,H_\nu^{(1)}(k_\rho a)}{J_\nu(k_\rho a)}\right)\sin\nu\phi\,\sin\nu\phi'$$

**Hankel function in terms of plane waves:**

$$H_0^{(1)}(k_\rho\sqrt{x^2+y^2}) = \frac{1}{\pi}\int_{-\infty}^{\infty}\frac{1}{\sqrt{k_\rho^2-k_x^2}}\,e^{i(k_x x+\sqrt{k_\rho^2-k_x^2}\,|y|)}\,dk_x$$

**Addition theorem for Hankel function:**

$$H_0^{(1)}(k_\rho|\boldsymbol{\rho}-\boldsymbol{\rho}'|) = \begin{cases} \displaystyle\sum_{m=-\infty}^{+\infty} H_m^{(1)}(k_\rho\rho')\,J_m(k_\rho\rho)\,e^{im(\phi-\phi')} & \rho \le \rho' \\ \displaystyle\sum_{m=-\infty}^{+\infty} J_m(k_\rho\rho')\,H_m^{(1)}(k_\rho\rho)\,e^{im(\phi-\phi')} & \rho \ge \rho' \end{cases}$$

**Green's function for a metallic cylinder:**

$$\psi_{\mathrm{t}}(\rho,\phi) = \begin{cases} \dfrac{Ie^{i\beta z}}{4\varepsilon\omega}\displaystyle\sum_{m=-\infty}^{+\infty}\left(\frac{J_m(k_\rho a)}{H_m^{(1)}(k_\rho a)}H_m^{(1)}(k_\rho\rho) - J_m(k_\rho\rho)\right)H_m^{(1)}(k_\rho\rho')\,e^{im(\phi-\phi')} & \rho \le \rho' \\ \dfrac{Ie^{i\beta z}}{4\varepsilon\omega}\displaystyle\sum_{m=-\infty}^{+\infty}\left(\frac{J_m(k_\rho a)}{H_m^{(1)}(k_\rho a)}H_m^{(1)}(k_\rho\rho') - J_m(k_\rho\rho')\right)H_m^{(1)}(k_\rho\rho)\,e^{im(\phi-\phi')} & \rho \ge \rho' \end{cases}$$

## Important Equations (continued)

**Radar echo width:**

$$\sigma_2^{\mathrm{TM}}(\phi) = \frac{4}{k_0 \sin\theta_\mathrm{i}} \left| \sum_{n=-\infty}^{\infty} (-1)^n \frac{J_n(k_0 \sin\theta_\mathrm{i}\, a)}{H_n^{(1)}(k_0 \sin\theta_\mathrm{i}\, a)} e^{in\phi} \right|^2 \qquad \text{(TM)}$$

$$\sigma_2^{\mathrm{TE}}(\phi) = \frac{4}{k_0 \sin\theta_\mathrm{i}} \left| \sum_{n=-\infty}^{+\infty} (-1)^n \frac{J_n'(k_0 \sin\theta_\mathrm{i}\, a)}{H_n^{(1)\prime}(k_0 \sin\theta_\mathrm{i}\, a)} e^{in\phi} \right|^2 \qquad \text{(TE)}$$

**Integral representation of Bessel function of the first kind:**

$$J_n(k_\rho \rho) = \frac{(-i)^n}{2\pi} \int_{-\pi}^{\pi} e^{ik_\rho \rho \cos\phi + in\phi}\, d\phi$$

**Integral representation of Hankel functions:**

$$H_\nu^{(1)}(k_\rho \rho) = \frac{e^{-i\nu\pi/2}}{\pi} \int_{-\pi/2+i\infty}^{\pi/2-i\infty} e^{ik_\rho \rho \cos\phi + i\nu\phi}\, d\phi$$

$$H_\nu^{(2)}(k_\rho \rho) = \frac{e^{-i\nu\pi/2}}{\pi} \int_{\pi/2-i\infty}^{3\pi/2+i\infty} e^{ik_\rho \rho \cos\phi + i\nu\phi}\, d\phi$$

**Total field of a metallic wedge in response to a line source:**

$$E_z(\rho,\phi) = \begin{cases} \dfrac{-Ik_\rho^2 e^{i\beta z}}{p\omega\varepsilon} \displaystyle\sum_{m=1}^{\infty} H_{m/p}^{(1)}(k_\rho \rho')\, J_{m/p}(k_\rho \rho) \sin\left(\frac{m}{p}\phi'\right) \sin\left(\frac{m}{p}\phi\right) & \rho < \rho' \\ \dfrac{-Ik_\rho^2 e^{i\beta z}}{p\omega\varepsilon} \displaystyle\sum_{m=1}^{\infty} J_{m/p}(k_\rho \rho')\, H_{m/p}^{(1)}(k_\rho \rho) \sin\left(\frac{m}{p}\phi'\right) \sin\left(\frac{m}{p}\phi\right) & \rho > \rho' \end{cases} \qquad \text{(TM)}$$

**Far-field plane-wave scattering from a metallic wedge:**

$$E_z^{\mathrm{t}} = \frac{4\sin\theta'}{p} E_0 e^{ik\cos\theta' z} \sum_{m=1}^{\infty} (-i)^{m/p} J_{m/p}(k_\rho \rho) \sin\left(\frac{m}{p}\phi\right) \sin\left(\frac{m}{p}\phi'\right)$$

## Important Equations (continued)

**Diffraction coefficients for a wedge:**

$$D_{\substack{s\\h}}(\rho,\phi,\phi') = \frac{e^{-i\pi/p}}{\sqrt{2\pi k\sin\theta'}}\,\frac{\sin\left(\frac{\pi}{p}\right)}{p} \cdot\left(\frac{1}{\cos\left(\frac{\pi}{p}\right)-\cos\left(\frac{\phi-\phi'}{p}\right)} \mp \frac{1}{\cos\left(\frac{\pi}{p}\right)-\cos\left(\frac{\phi+\phi'}{p}\right)}\right)$$

## Important Terms

Provide definitions or explain the meaning of the following terms:

2-D Green's function for external problem (metallic circular cylinder and wedge)
addition theorem
angular-sector waveguide
Bessel equation
Bessel function of the first kind
Bessel function of the second kind
bistatic echo width
circumferential waveguide
cladding
core
cylindrical cavity
cylindrical waveguide
cylindrical wave functions
diffraction coefficients for metallic wedge
elementary wave functions
formal solution for 2-D Green's function
Fourier representation of 2-D Green's function
gamma function
Green's function for angular-sector waveguide
H-bent rectangular waveguide
Hankel function of the first kind
Hankel function of the second kind
harmonic functions
hybrid mode
integral representation of Bessel function
modified Bessel function of the first kind
modified Bessel function of the second kind
multipole
optical fiber
order of Bessel function
orthogonality of Bessel functions
radial waveguide
reflection boundary
saddle point
saddle-point technique
shadow boundary
stationary phase point
steepest descent path
two-dimensional dipole
Wronskian relationship

## PROBLEMS

**7.1** Show that $\psi(\rho,z) = \ln(\rho)\, e^{ikz}$ satisfies the scalar wave equation.

### Circular Waveguides

**7.2** Consider the coaxial waveguides shown in Fig. P7.2.

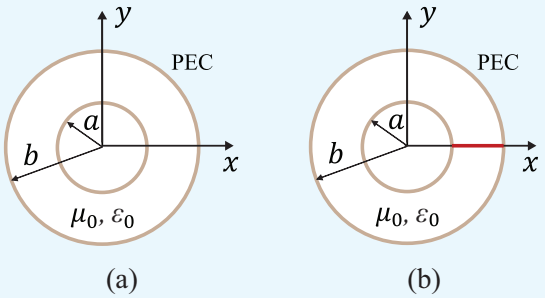


**Figure P7.2:** Configuration of two coaxial waveguide structures with inner and outer radii of $a$ and $b$. For configuration (b) a metallic plate is connecting the inner and outer cylinders.

**(a)** Write down the scalar potential for the proper TM and TE modes inside the coaxial line shown in Fig. P7.2(a).

**(b)** If a PEC plate is inserted between the inner and outer conductors at the position $\phi = 0$, as shown in Fig. P7.2(b), write down the TE and TM modes, and find the lowest TM and the lowest TE modes.

**7.3**

**(a)** For a given radius $a$, what are the TE and TM modes for a circular waveguide with angular extent $0 < \phi < \phi'$? (This structure is called the ***Pacman waveguide***.) Give the potentials only.

**(b)** Now let $\phi' = 270^\circ$ and simplify the form of the potentials. Using information on the roots of Bessel functions, find the lowest-order mode.

**(c)** Find the potentials and fields for TE and TM modes inside a waveguide with a semicircular cross section ($\phi' = 180^\circ$).

**(d)** Find the ***TM Green's function*** inside the waveguide of part (c). This Green's function can be used to find the fields due to an arbitrary electric current source placed along the axis of the waveguide. Find the scalar potential that exist in the waveguide due to the following source:

$$\mathbf{J}(r,\phi) = I_0\, \delta\left(\phi - \frac{\pi}{2}\right)\, e^{ik_c z}\, \hat{\boldsymbol{\rho}}\ .$$

**7.4** Consider a circular metallic waveguide with radius $b$, as shown in Fig. P7.4. Inside the waveguide there exists a concentric dielectric cylinder of radius $a < b$ with parameters $\varepsilon_d$, $\mu_d$.

Except for azimuthly symmetric modes ($\partial/\partial\phi = 0$), $TE_z$ or $TM_z$ modes cannot be supported.

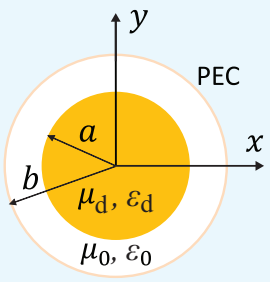


**Figure P7.4:** A circular metallic waveguide loaded with a concentric dielectric cylinder having permittivity $\varepsilon_d$ and permeability $\varepsilon_d$.

**(a)** Find the transcendental equations and the cutoff frequencies for symmetric modes.

**(b)** Find the transcendental equations for the general case.

**7.5** For a circular cylinder of radius $a$ composed of a conductor with conductivity $\sigma$, show that the attentuation rate can be evaluated from

$$\alpha^{TM} = \frac{1}{\sigma\delta_s\eta a\sqrt{1-(f_c/f)^2}}$$

and

$$\alpha^{TE} = \frac{1}{\sigma\delta_s\eta a\sqrt{1-(f_c/f)^2}}\left[\frac{n^2}{(x'_{np})^2-n^2}+\left(\frac{f_c}{f}\right)^2\right].$$

**7.6** For the dielectric-covered conducting rod shown in Fig. P7.6, find the transcendental equations for the $TE_z$ and $TM_z$ modes when $\partial/\partial\phi = 0$. Find transcendental equations for the symmetric modes. Find also the transcendental equations for hybrid modes in the general case.

**7.7** Consider the example of an optical fiber shown in Fig. 7-12. Consider a frequency of operation for which $k_c a = 25$.

**(a)** How many modes can propagate in this fiber?

**(b)** If a portion of the power is carried by the first mode and a portion is carried by the second mode, what is the phase delay between two signals over $100\lambda_c$ of propagation ($\lambda_c$ is the wavelength in the cladding).

## Cylindrical Cavity

**7.8** Consider a cylindrical cavity terminated by conductors at $z = 0$ and $z = d$, with $d = 0.25a$.

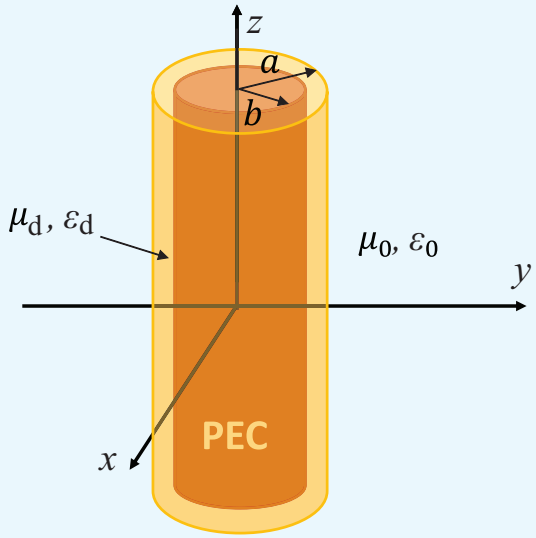


**Figure P7.6:** The geometry of a metallic cylinder of radius $b$ covered uniformly with a dielectric layer with outer radius $a$ and constitutive parameters $\varepsilon_d$ and $\mu_d$. This structure can support guided surface waves.

**(a)** Find the three lowest-order modes for TE and TM waves, respectively, and identify the overall lowest-order mode.

**(b)** For the lowest mode, write down the fields and calculate the quality factor $Q$ for good-conducting cavity walls. The quality factor is given by

$$Q = \frac{\omega W}{P_d},$$

where $W$ is the total energy stored in the cavity and $P_d$ is the power dissipated on the walls, which can be calculated using

$$P_d = \frac{1}{2\sigma\delta_S} |J_S|^2,$$

where $\sigma$ is the conductivity and $d_S$ is skin depth of the conducting material.

**7.9** In Example 7-2, we considered the problem of a circular patch antenna. The operating frequencies of this antenna were determined by finding the resonant frequencies of a cylindrical cavity with metallic top and bottom surfaces and a perfect magnetic conductor on its side. Repeat the problem for a patch antenna whose geometry is shown in Fig. P7.9. Assume that the substrate thickness is $h$ and the dielectric constant of the substrate is $\varepsilon_0\varepsilon_1$.

**7.10** Consider a cylindrical cavity with radius $a$ and height $\ell$. This cavity is loaded by a dielectric rod with constitutive parameters $\mu_d$ and $\varepsilon_d$ and radius $b$ concentric with the cylinder,

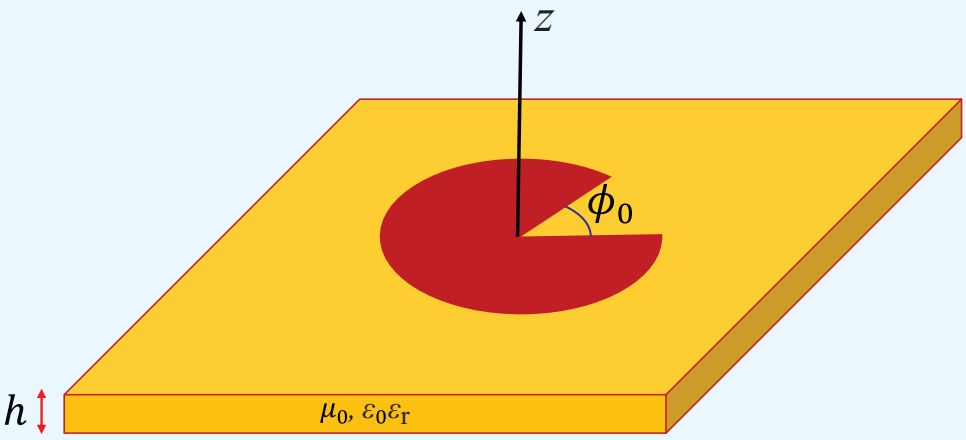


**Figure P7.9:** Geometry of a Pacman patch antenna over a substrate with height $h$ and dielectric constant $\varepsilon_0\varepsilon_r$.

as shown in Fig. P7.10. Find the transcendental equation from which the cavity resonant frequencies can be obtained.

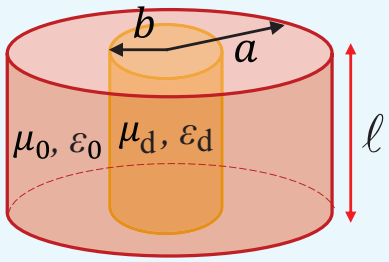


**Figure P7.10:** A partially loaded cylindrical cavity. The resonant frequency is a function of the dielectric parameters and its radius.

**7.11** Consider a cylindrical cavity with radius $a$ and height $\ell$. This cavity is loaded by a dielectric rod having radius $a$, height $d$, and constitutive parameters $\mu_d$ and $\varepsilon_d$, as shown in Fig. P7.11. Find the transcendental equation from which the cavity resonant frequencies can be obtained.

## Radial Waveguide

**7.12** Consider the radial waveguide shown in Fig. P7.12. This waveguide is partially filled with a dielectric slab of thickness $d$ having material parameters $\varepsilon_d$ and $\mu_d$. Find the

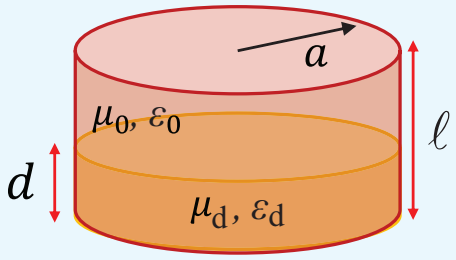


**Figure P7.11:** A partially loaded cylindrical cavity. The resonant frequency is a function of the height of the dielectric disc and its permittivity and permeability.

transcendental equations and the field expressions in this waveguide for both $TM_z$ and $TE_z$ modes.

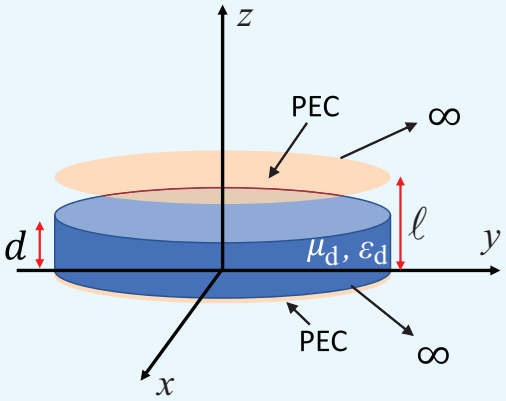


**Figure P7.12:** A dielectric-loaded waveguide. A dielectric slab is placed between two parallel metallic plates.

**7.13** Consider the dielectric radial waveguide shown in Fig. P7.13. The thickness of this dielectric slab is $d$ and its constitutive parameters are $\varepsilon_d$ and $\mu_d$.

**(a)** Find the transcendental equations.

**(b)** Find the field expressions for both $TM_z$ and $TE_z$.

## Multipole

**7.14** Consider the quadrupole shown in Fig. P7.14. Find the corresponding Hertz vector potential and the resulting electric and magnetic field.

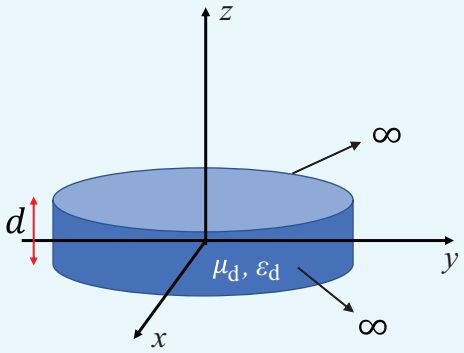


**Figure P7.13:** A radial dielectric waveguide, which is basically a dielectric slab of infinite extent.

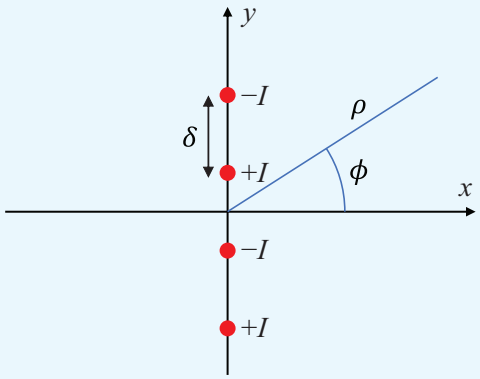


**Figure P7.14:** A two-dimensional quadrupole along the $y$-axis. Note that the separation between the line currents $\delta$ is much smaller than a wavelength.

**7.15** Consider the octopole shown in Fig. P7.15. Find the corresponding Hertz vector potential and the resulting fields. The line currents are equally spaced around a small cylinder.

## Radiation and Scattering

**7.16** Consider a uniform cylindrical $z$-directed current sheet of radius $a$, as shown in Fig. P7.16. Find the electric field throughout the region and radiated power per unit length

$$\mathbf{J}(\rho,\phi) = J_s\,\delta(\rho - a)\,\hat{\mathbf{z}}\,.$$

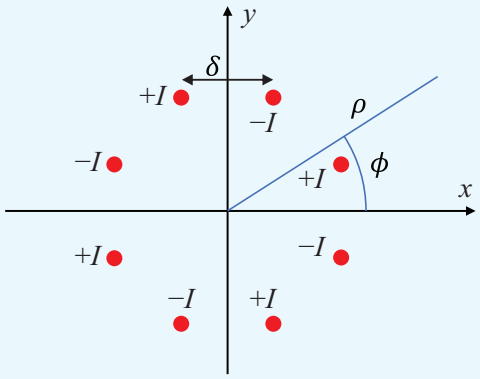


**Figure P7.15:** A two-dimensional octopole arranged symmetrically around the surface of a fictitious small cylinder.

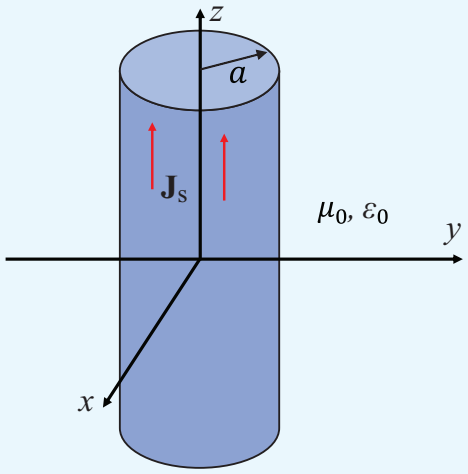


**Figure P7.16:** The geometry of a uniform cylindrical current sheet.

**7.17** Solve Problem 7.16 for a case where the surface current is an arbitrary function of $\phi$:

$$\mathbf{J}(\rho,\phi) = J_s(\phi)\,\delta(\rho-\phi)\,\hat{\mathbf{z}}\,.$$

**7.18** Consider a uniformly distributed cylindrical $z$-directed current sheet of radius $a$ concentric with a dielectric cylinder of radius $b < a$ with constitutive parameters $\varepsilon_d$ and $\mu_d$, as shown in Fig. P7.18. Find the far-field electric field, assuming that

$$\mathbf{J}(\rho,\phi) = J_z\,\delta(\rho-a)\,\hat{\mathbf{z}}\,.$$

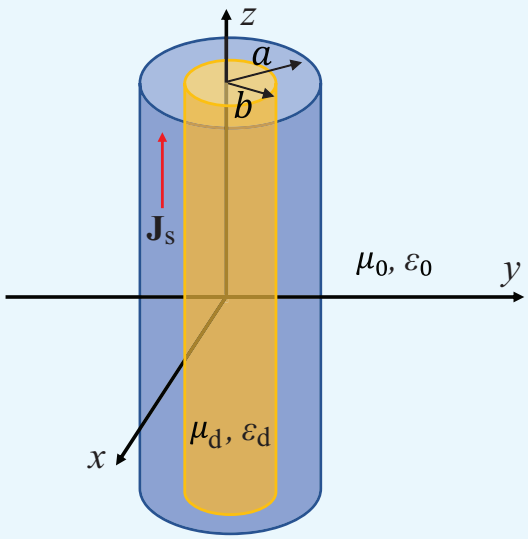


**Figure P7.18:** A uniform cylindrical current sheet around a dielectric cylinder of radius $b$ and parameters $\mu_d$ and $\varepsilon_d$.

**7.19** For Problem 7.19 now consider a case where $b > a$.

**7.20** Consider an infinite $z$-oriented circular metallic cylinder of radius $a$ illuminated by a TM-polarized plane wave whose propagation vector lies in the $x$–$z$ plane, as shown in Fig. P7.20.

**(a)** Compute and plot the backscattering radar cross section (RCS) of this cylinder as a function of frequency over the corresponding wavelength range $0.05a \leq \lambda \leq 50a$ for normal incidence ($\theta_i = 90^\circ$).

**(b)** Compute and plot the RCS of the cylinder in the $x$–$y$ plane for oblique incidence at $\theta_i = 50^\circ$ for $\lambda = 0.5a$, $\lambda = 5a$, and $\lambda = 50a$.

**7.21** Consider the two concentric dielectric cylinders shown in Fig. P7.21. The parameters of the inner dielectric cylinder of radius $a_1$ are $\varepsilon_1$ and $\mu_1$. The outer cylinder has a radius $a_2 > a_1$ with constitutive parameters $\varepsilon_2$ and $\mu_2$. This object is illuminated by a plane wave whose electric field is parallel to the cylinder axis. Find the electric field in each region and the cylinder echo width.

**7.22** Consider a half-plane metallic sheet on the positive $x$-axis ($\phi = 0$) being illuminated by a plane wave whose direction of propagation towards the edge is denoted by $\phi'$. Assuming the $z$-polarized incident plane wave intensity is $E_0$, show that the surface current density on

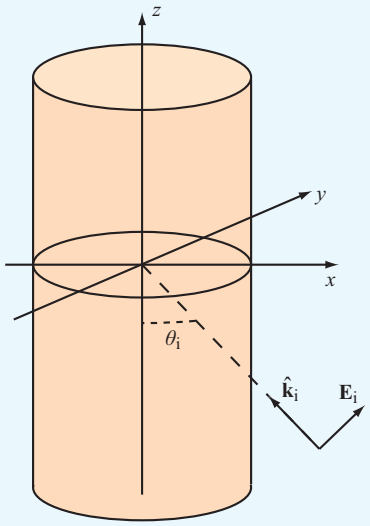


**Figure P7.20:** A metallic cylinder illuminated by a TM-polarized plane wave at oblique incidence.

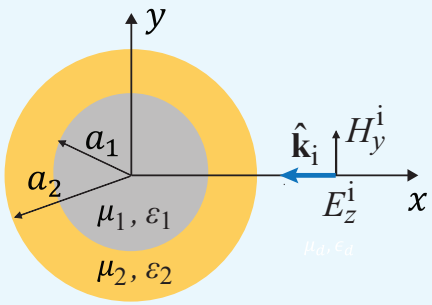


**Figure P7.21:** A two-layer concentric dielectric cylinder illuminated by a plane wave propagating along the $-x$-axis.

the half plane is given by

$$J_z = \frac{2iE_0}{\omega\mu x} \sum_{n=1}^{\infty} n(-i)^{n/2} J_{n/2}(kx) \sin\frac{n\phi'}{2} .$$

# Chapter 8
# Spherical Wave Functions and Their Applications

## Chapter Contents


Overview, 507
8-1 Wave Functions in the Spherical Coordinate System, 508
8-2 Wave Transformation to Spherical Wave Functions, 538
8-3 Multipole Representation of Spherical Waves, 543
8-4 Plane-Wave Scattering from Spheres, 547
8-5 Wave Propagation in a Conical Waveguide, 557
8-6 Biconical Structures, 564
8-7 Other Spherical Waveguides, 572
Chapter Summary, 575
Problems, 583


## Objectives

Upon learning the material presented in this chapter, you should be able to:

1. Solve boundary-value problems associated with wave equations and objects whose boundaries coincide with constant surfaces in a spherical coordinate system.
2. Understand the properties of spherical wave functions composed of special functions, such as Legendre and associated Legendre functions and spherical Hankel functions, and apply them to solve propagation and scattering problems.
3. Determine the resonant frequency of metallic cavities formed by constant coordinate surfaces in a spherical coordinate system and those of a dielectric sphere.
4. Express a plane wave in terms of a summation of spherical wave functions.
5. Calculate the radar cross section of metallic and dielectric spheres.
6. Characterize the fields, and associated wave functions, in conical waveguides and in the region between two cones sharing the same axis (biconical structures).

## Overview

In this chapter we consider the solution of wave equations in a source-free, homogeneous medium, in a spherical coordinate system. We start by showing that under the Lorenz gauge condition, none of the spherical-coordinate components of the magnetic vector potential **A** satisfy the wave equation. To circumvent this difficulty, a magnetic vector potential that has only a radial component ($A_r$) is considered, and a new gauge condition is introduced so that a scalar potential defined by $A_r(r,\theta,\phi)/r$ would indeed satisfy the scalar wave equation. It is shown that such a choice renders a transverse (with respect to $\hat{\mathbf{r}}$) magnetic set of fields (TM-to-$r$). Application of the duality principle leads to an electric vector potential that has only a radial component ($A_{mr}$) and a set of fields TE-to-$r$. Superposition of TM-to-$r$ and TE-to-$r$ can be used to generate any arbitrary set of fields. The solution to the scalar wave equation for the scalar potential proceeds by applying the method of separation of variables. It is shown that such a procedure can produce harmonic functions with respect to the variable $\phi$, Legendre and associated Legendre functions as regarding variable $\theta$, and spherical Bessel functions with respect to $r$. The type and order of such functions depend on the spatial domain of interest. The properties of these functions are presented with some detail to facilitate the choice of the proper solution for the problem at hand. Orthogonality of spherical harmonic functions formed from the product of harmonic functions (sine or cosine) and the corresponding associated Legendre functions are demonstrated. The spherical wave functions are used for canonical problems associated with dielectric or metallic objects whose boundaries coincide with constant coordinate surfaces in the spherical coordinate system. The formulation is applied through examples to illustrate how to compute the resonant frequencies and the corresponding fields in a spherical metallic cavity. For the dominant mode of the resonance, an expression for the quality factor of a metallic spherical cavity with finite conductivity is obtained as well. A similar approach is used to find the resonant frequencies of two concentric metallic spheres, and the results are applied to estimate the resonances that occur at very low frequencies in the atmosphere between the Earth's ground and its ionosphere. Also, spherical dielectric resonators are studied using the spherical wave functions, and it is shown that, in general, the resonant frequencies of such objects are complex even when the dielectric sphere and its surrounding dielectric material are lossless. It is shown that certain higher-order modes can provide very high quality factors. To study scattering problems from spherical objects, expansion of plane waves in terms of the spherical wave function is presented. Also, the addition theorem for spherical wave functions is presented. The solution for bistatic scattering from metallic and dielectric spheres is considered and analytical solutions for the scattered fields and the radar cross section for such scatterers are obtained. Then metallic conical structures are considered. For example, modal expansion of fields inside a conical waveguide is presented and solutions for the order of the associated Legendre function are obtained as a function of the cone angle and azimuthal harmonic orders. Similarly, field modal expansions for biconical structures, made from two metallic cones sharing a common axis, are considered and their applications as antennas are considered. Finally, we examine other spherical waveguide structures formed by the region between two conical surfaces and two constant $\phi$-planes.

## 8-1 Wave Functions in the Spherical Coordinate System

In previous chapters, we examined how electromagnetic waves can be expanded in terms of wave functions in Cartesian and cylindrical coordinate systems. It was shown that using a constant coordinate direction, we can expand the fields in TE and TM modes. For spherical structures, such an expansion does not lend itself to simple construction of solutions for Maxwell's equations. To arrive at an appropriate scalar potential, we need to revisit the magnetic vector potential $\mathbf{A}$ and the scalar electric potential $\Phi$. According to Eqs. (3.6) and (3.7), we have the following relations between $\mathbf{A}$ and $\Phi$:

$$\nabla \times \nabla \times \mathbf{A} - k^2 \mathbf{A} - i\omega\mu\varepsilon \, \nabla\Phi = \mu \mathbf{J} \tag{8.1a}$$

and

$$\nabla^2 \Phi - i\omega \, \nabla \cdot \mathbf{A} = -\frac{\rho}{\varepsilon} \, . \tag{8.1b}$$

Previously we used the Lorenz gauge condition

$$\nabla \cdot A = i\omega\mu\varepsilon\Phi$$

so as to simplify Eq. (8.1a) into the standard form of the wave equation

$$\nabla^2 \mathbf{A} + k^2 \mathbf{A} = -\mu \mathbf{J} \, ,$$

which can be decomposed into three separate scalar wave equations when using the Cartesian coordinate system. The procedure, however, does not work in the spherical coordinate system because the vector components of $\nabla^2 \mathbf{A}$ do not decompose into a Laplacian ($\nabla^2$) for any vector components of $\mathbf{A}$. Let us assume that the magnetic vector potential and the excitation current have only radial components, i.e., $A_\phi = A_\theta = 0$. In this case,

$$\mathbf{A} = A_{\rm r} \hat{\mathbf{r}} \quad \text{and} \quad \mathbf{J} = J_{\rm r} \hat{\mathbf{r}} \, . \tag{8.2}$$

Substituting Eq. (8.2) into Eq. (8.1a), the following scalar equations are obtained:

$$\left[ \frac{1}{r^2 \sin\theta} \frac{\partial}{\partial\theta} \left( \sin\theta \frac{\partial}{\partial\theta} \right) + \frac{1}{r^2 \sin^2\theta} \frac{\partial^2}{\partial\phi^2} + k^2 \right] A_{\rm r} = -i\omega\mu\varepsilon \frac{\partial}{\partial r} \Phi - \mu J_{\rm r} \, , \tag{8.3a}$$

$$\frac{1}{r} \frac{\partial}{\partial\theta} \left( \frac{\partial}{\partial r} A_{\rm r} - i\omega\mu\varepsilon\Phi \right) = 0 \, , \tag{8.3b}$$

and

$$\frac{1}{r\sin\theta} \frac{\partial}{\partial\phi} \left( \frac{\partial}{\partial r} A_{\rm r} - i\omega\mu\varepsilon\Phi \right) = 0 \, . \tag{8.3c}$$

Equations (8.3b) and (8.3c) suggest the use of a different gauge condition, namely

$$\frac{\partial}{\partial r} A_{\rm r} = i\omega\mu\varepsilon\Phi \, . \tag{8.4}$$

Application of Eq. (8.4) leads to satisfactory conditions for Eqs. (8.3b) and (8.3c), and Eq. (8.3a) reduces to

$$\left[\frac{\partial^2}{\partial r^2}+\frac{1}{r^2\sin\theta}\,\frac{\partial}{\partial\theta}\left(\sin\theta\,\frac{\partial}{\partial\theta}\right)+\frac{1}{r^2\sin^2\theta}\,\frac{\partial^2}{\partial\phi^2}+k^2\right]A_{\rm r}=-\mu J_{\rm r}\,. \tag{8.5}$$

Noting that in the spherical coordinate system

$$\nabla^2=\frac{1}{r^2}\,\frac{\partial}{\partial r}\left(r^2\,\frac{\partial}{\partial r}\right)+\frac{1}{r^2\sin\theta}\,\frac{\partial}{\partial\theta}\left(\sin\theta\,\frac{\partial}{\partial\theta}\right)+\frac{1}{r^2\sin^2\theta}\,\frac{\partial^2}{\partial\phi^2}$$

and

$$\frac{1}{r^2}\,\frac{\partial}{\partial r}\left[r^2\,\frac{\partial}{\partial r}\left(\frac{A_{\rm r}}{r}\right)\right]=\frac{1}{r}\,\frac{\partial^2}{\partial r^2}A_{\rm r}\,,$$

Eq. (8.5) can be represented by

$$(\nabla^2+k^2)\,\frac{A_{\rm r}}{r}=-\frac{\mu}{r}\,J_{\rm r}\,, \tag{8.6}$$

which is a scalar wave equation for $A_{\rm r}/r$. By applying the duality relations, a similar equation for the radial component of the electric vector potential can be obtained and is given by

$$(\nabla^2+k^2)\,\frac{A_{\rm mr}}{r}=-\frac{\varepsilon J_{\rm mr}}{r}\,. \tag{8.7}$$

The field quantities can now be obtained from scalar potentials $\psi=A_{\rm r}/r$ and $\psi_{\rm m}=A_{\rm mr}/r$, where both $\psi$ and $\psi_{\rm m}$ are solutions to the wave equation. Recalling that

$$\mathbf{E}=-\nabla\Phi+i\omega\mathbf{A}\,, \tag{8.8}$$

and in view of Eq. (8.4) ,

$$\mathbf{E}=\frac{-1}{i\omega\mu\varepsilon}\,\nabla\frac{\partial}{\partial r}A_{\rm r}+i\omega A_{\rm r}\hat{\mathbf{r}}\,, \tag{8.9}$$

which can be expanded to provide the field components

$$E_{\rm r}=\frac{-1}{i\omega\mu\varepsilon}\left(\frac{\partial^2}{\partial r^2}+k^2\right)A_{\rm r}\,, \tag{8.10a}$$

$$E_\theta=\frac{-1}{i\omega\mu\varepsilon r}\left(\frac{\partial^2}{\partial r\,\partial\theta}\right)A_{\rm r}\,, \tag{8.10b}$$

and

$$E_\phi=\frac{-1}{i\omega\mu\varepsilon}\,\frac{1}{r\sin\theta}\,\frac{\partial^2}{\partial r\,\partial\phi}\,A_{\rm r}\,. \tag{8.10c}$$

Also, the magnetic field in terms of **A** is given by

$$\mathbf{H} = \frac{1}{\mu} \nabla \times \mathbf{A} \, ,$$

which, upon expansion, gives

$$H_\theta = \frac{1}{\mu r \sin\theta} \frac{\partial A_\mathrm{r}}{\partial \phi} \tag{8.11a}$$

and

$$H_\phi = -\frac{1}{\mu r} \frac{\partial A_\mathrm{r}}{\partial \theta} \, . \tag{8.11b}$$

Using the duality relations, the field quantities generated from $\psi_\mathrm{m} = A_\mathrm{mr}/r$ are given by

$$H_\mathrm{r} = \frac{-1}{i\omega\mu\varepsilon} \left( \frac{\partial^2}{\partial r^2} + k^2 \right) A_\mathrm{mr} \, , \tag{8.12a}$$

$$H_\theta = \frac{-1}{i\omega\mu\varepsilon r} \frac{\partial^2}{\partial r \, \partial \theta} A_\mathrm{mr} \, , \tag{8.12b}$$

$$H_\phi = \frac{-1}{i\omega\mu\varepsilon} \frac{1}{r \sin\theta} \frac{\partial^2}{\partial r \, \partial \phi} A_\mathrm{mr} \, , \tag{8.12c}$$

$$E_\theta = \frac{-1}{\varepsilon r \sin\theta} \frac{\partial A_\mathrm{mr}}{\partial \phi} \, , \tag{8.12d}$$

and

$$E_\phi = \frac{1}{\varepsilon r} \frac{\partial A_\mathrm{mr}}{\partial \theta} \, . \tag{8.12e}$$

Superposition must be used to combine Eqs. (8.10), (8.11), and (8.12) when both electric and magnetic sources are present. Equations (8.10), (8.11), and (8.12) produce TM- and TE-to-$\hat{\mathbf{r}}$ modes.

### 8-1.1 Spherical Wave Functions

In this section, we consider the method of separation of variables for the solution of wave equations in the spherical coordinate system. Consider the wave equation

$$(\nabla^2 + k^2) \, \psi(r, \theta, \phi) = 0 \, , \tag{8.13}$$

and assume that the solution can be expressed in terms of the product of three continuous and differentiable functions:

$$\psi(r, \theta, \phi) = R(r) \, Q(\theta) \, F(\phi) \, .$$

By substituting this solution into Eq. (8.13) and then dividing both sides by $RQF/r^2\sin^2\theta$, it can be shown that the process leads to

$$\frac{\sin^2\theta}{R}\frac{d}{dr}\left(r^2\frac{dR}{dr}\right)+\frac{\sin\theta}{Q}\frac{d}{d\theta}\left(\sin\theta\frac{dQ}{d\theta}\right)+\frac{1}{F}\frac{d^2F}{d\phi^2}+k^2r^2\sin^2\theta=0\,. \tag{8.14}$$

Here, only $(1/F)(d^2F/d\phi^2)$ is a function of $\phi$, and the other terms in Eq. (8.14) are not functions of $\phi$. Hence,

$$\frac{1}{F}\frac{d^2F}{d\phi^2}=-\mu^2\,, \tag{8.15}$$

for some constant $\mu$. Substituting Eq. (8.15) into Eq. (8.14) and dividing the resulting equation by $\sin^2\theta$ yields

$$\frac{1}{R}\frac{d}{dr}\left(r^2\frac{dR}{dr}\right)+\frac{1}{\sin\theta\,Q}\frac{d}{d\theta}\left(\sin\theta\frac{dQ}{d\theta}\right)+k^2r^2-\frac{\mu^2}{\sin^2\theta}=0\,. \tag{8.16}$$

Choosing $\nu(\nu+1)$ as the separation constant, we can show that

$$\frac{1}{\sin\theta\,Q}\frac{d}{d\theta}\left(\sin\theta\frac{dQ}{d\theta}\right)-\frac{\mu^2}{\sin^2\theta}=-\nu(\nu+1) \tag{8.17}$$

and

$$\frac{1}{R}\frac{d}{dr}\left(r^2\frac{dR}{dr}\right)-\nu(\nu+1)+k^2r^2=0\,. \tag{8.18}$$

Hence, the three differential equations for $R$, $Q$, and $F$ are given by:

$$\frac{d}{dr}\left(r^2\frac{dR}{dr}\right)+[(kr)^2-\nu(\nu+1)]R=0\,, \tag{8.19a}$$

$$\frac{1}{\sin\theta}\frac{d}{d\theta}\left(\sin\theta\frac{dQ}{d\theta}\right)+\left(\nu(\nu+1)-\frac{\mu^2}{\sin^2\theta}\right)Q=0\,, \tag{8.19b}$$

and

$$\frac{d^2F}{d\phi^2}+\mu^2F=0\,. \tag{8.19c}$$

The solution to Eq. (8.19c) consists of harmonic functions of the form

$$F=Ae^{i\mu\phi}+Be^{-i\mu\phi}\,.$$

As noted previously, if the range for $\phi$ includes the entire domain $[0,2\pi]$, $\mu$ has to be an integer for $\psi$ to be a single-valued function.

The differential equation given by Eq. (8.19a) closely resembles a Bessel equation, and its solutions, known as spherical Bessel functions , are expressed in terms of ordinary Bessel functions:

$$R(kr)=\left(\frac{\pi}{2kr}\right)^{1/2}Z_{n+1/2}(kr)\,, \tag{8.20}$$

where $Z_{n+1/2}(kr)$ represents an ordinary Bessel function of order $(n+\frac{1}{2})$. The spherical Bessel functions behave in a manner similar to their counterpart; i.e., $j_n(kr)$ and $n_n(kr)$ represent standing-wave-type solutions whose large argument expansions are given by

$$\lim_{kr\to\infty} j_n(kr) \approx \frac{1}{kr}\cos\left(kr - \frac{(n+1)\pi}{2}\right) \tag{8.21a}$$

and

$$\lim_{kr\to\infty} n_n(kr) \approx \frac{1}{kr}\sin\left(kr - \frac{(n+1)\pi}{2}\right) . \tag{8.21b}$$

In general, $j_n(kr)$ and $n_n(kr)$ can be expressed in terms of polynomials in $1/kr$ multiplied by $\sin(kr)$ and $\cos(kr)$. Starting from

$$j_0(kr) = \frac{\sin(kr)}{kr} , \qquad j_1(kr) = \frac{\sin(kr)}{(kr)^2} - \frac{\cos(kr)}{(kr)} , \tag{8.22a}$$

$$n_0(kr) = -\frac{\cos(kr)}{kr} , \qquad n_1(kr) = -\frac{\cos(kr)}{(kr)^2} - \frac{\sin(kr)}{(kr)} , \tag{8.22b}$$

and using the recurrence formula

$$R_{n+1}(kr) = \frac{(2n+1)}{kr} R_n(kr) - R_{n-1}(kr) , \tag{8.23}$$

all higher-order spherical Bessel functions can be obtained. The following also provides recurrence relations for the derivatives of the spherical Bessel functions:

$$\frac{d}{dr} R_n(r) = \frac{1}{2n+1} \left[ n\, R_{n-1}(r) - (n+1)\, R_{n+1} \right] , \tag{8.24a}$$

$$\frac{d}{dr} \left( r^{n+1} R_n(r) \right) = r^{n+1} R_{n-1}(r) , \tag{8.24b}$$

and

$$\frac{d}{dr} \left( r^{-n} R_n(r) \right) = -r^{-n} R_{n+1}(r) . \tag{8.24c}$$

It can also be shown that

$$\frac{d}{dr} R_n(r) = -R_{n+1}(r) + \frac{n}{r} R_n(r)$$

and

$$\frac{d}{dr} R_n(r) = R_{n-1}(r) - \frac{n+1}{r} R_n(r) .$$

Similar to the definition of ordinary Hankel functions, the spherical Hankel functions are defined as

$$h_n^{(1)}(kr) = j_n(kr) + i n_n(kr) \tag{8.25a}$$

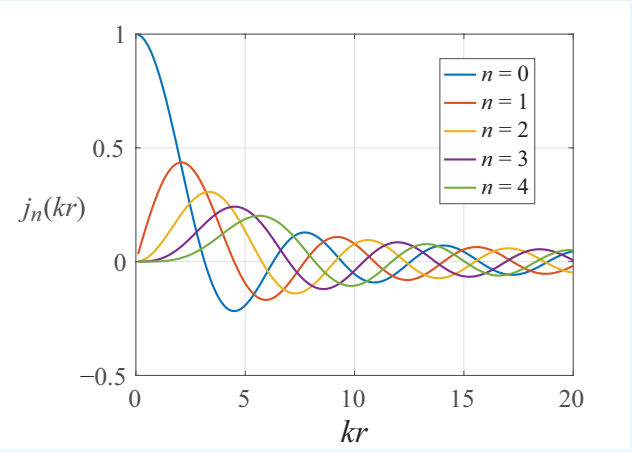


**Figure 8-1:** The spherical Bessel function of the first kind for the first five orders.

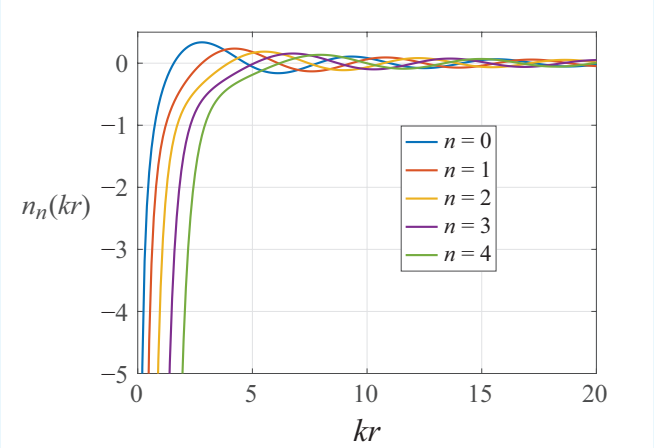


**Figure 8-2:** The spherical Bessel function of the second kind for the first five orders.

and

$$h_n^{(2)}(kr) = j_n(kr) - in_n(kr) \ . \tag{8.25b}$$

Figures 8-1 and 8-2 show the spherical Bessel functions of the first kind and second kind for different orders.

The spherical Hankel function of the first kind represents an outward-going spherical wave and the spherical Hankel function of the second kind represents an incoming spherical

wave:

$$\lim_{kr\to\infty} h_n^{(1)}(kr) \approx \frac{e^{i[kr-\pi(n+1)/2]}}{kr} = (-i)^{n+1}\,\frac{e^{ikr}}{kr} \tag{8.26a}$$

and

$$\lim_{kr\to\infty} h_n^{(2)}(kr) \approx \frac{e^{-i[kr-\pi(n+1)/2]}}{kr} = (i)^{n+1}\frac{e^{-ikr}}{kr}\,. \tag{8.26b}$$

The only spherical Bessel functions that have finite values at $r = 0$ are $j_n(kr)$, and therefore these are the only admissible radial functions if the domain of the problem includes the origin.

The series solutions for the spherical Bessel functions can be obtained from Eq. (7.23) by noting that $\Gamma(\nu+1) = \nu\,\Gamma(\nu)$, $\Gamma(\frac{1}{2}) = \sqrt{\pi}$, and using the duplication formula it can shown that

$$\Gamma\left(\nu+\frac{1}{2}\right) = \frac{\sqrt{\pi}\,\Gamma(2\nu)}{2^{(2\nu-1)}\Gamma(\nu)}\,, \tag{8.27}$$

which leads to

$$j_n(r) = 2^n r^n \sum_{m=0}^{\infty} \frac{(-1)^m (n+m)!}{m!(2n+2m+1)!}\, r^{2m}\,. \tag{8.28}$$

Also, $N_{n+1/2}(r) = (-1)^{n-1}\,J_{-n-1/2}(r)$, and therefore

$$n_n(r) = -\frac{1}{2^n r^{n+1}}\left\{\sum_{m=0}^{n}\frac{\Gamma(2n-2m+1)}{m!\,\Gamma(n-m+1)}\,r^{2m} + \frac{1}{2}\sum_{n=m+1}^{\infty}\frac{(-1)^{m+n}\,\Gamma(m-n)}{m!\,\Gamma(2m-2n)}\,r^{2m}\right\}\,. \tag{8.29}$$

Another useful formula is the Wronskian of the spherical Bessel functions, which can be directly obtained from the Wronskian of the Bessel functions:

$$j_\nu(r)\,n'_\nu(r) - j'_\nu(r)\,n_\nu(r) = \frac{1}{r^2} \tag{8.30a}$$

and

$$j_\nu(r)\,h_\nu^{(1)\prime}(r) - j'_\nu(r)\,h_\nu^{(1)}(r) = \frac{i}{r^2}\,. \tag{8.30b}$$

Equation (8.19b) is the generalized Legendre's equation, and its solutions are known as the ***associated Legendre functions***. Solutions of Eq. (8.19b) can be expressed in terms of the associated Legendre functions of the first kind $P_\nu^\mu(\cos\theta)$ and the associated Legendre functions of the second kind denoted by $Q_\nu^\mu(\cos\theta)$. If $\theta = 0$ and $\theta = \pi$ are in the domain of the problem, the only admissible solution is $P_\nu^\mu(\cos\theta)$.

When $\mu = 0$, the associated Legendre equation given by Eq. (8.19b) reduces to the ordinary Legendre equation given by

$$(1-x^2)\,\frac{d^2y}{dx^2} - 2x\,\frac{dy}{dx} + \nu(\nu+1)y = 0\,, \tag{8.31}$$

where the substitution $x = \cos\theta$ is used in Eq. (8.19b) with $\mu = 0$. The range $0 \le \theta \le \pi$ in the spherical coordinate system corresponds to the range $-1 \le x \le 1$. The solution to Eq. (8.31) can be obtained in terms of an infinite series given by

$$P_\nu(x) = \sum_{m=0}^{N} \frac{(-1)^m(\nu+m)!}{(m!)^2(\nu-m)!}\left(\frac{1-x}{2}\right)^m - \frac{\sin\nu\pi}{\pi} \cdot \sum_{m=N+1}^{\infty} \frac{(m-1-\nu)!(m+\nu)!}{(m!)^2}\left(\frac{1-x}{2}\right)^m , \tag{8.32}$$

where $N$ is the largest integer smaller or equal to $\nu$. It should be noted here that when $\nu$ is a noninteger, $P_\nu(x)$ and $P_\nu(-x)$ become independent of each other and both satisfy Eq. (8.31). However, if $\nu = n$ is an integer, the second term in Eq. (8.32) vanishes and the series solution becomes finite. Using the binomial expansion

$$(1-x)^m = \sum_{k=0}^{m} \binom{m}{k} (-x)^k ,$$

and rearranging the terms,

$$P_n(x) = \sum_{m=0}^{N_2} \frac{(-1)^m(2n-2m)!}{2^n m!\,(n-m)!\,(n-2m)!}\, x^{n-2m} , \tag{8.33}$$

where $N_2 = n/2$ or $(n-1)/2$, depending on whether $n$ is even or odd, respectively. Consequently,

$$P_n(x) = (-1)^n\, P_n(-x) . \tag{8.34}$$

That is, the Legendre polynomials of odd degrees are odd functions and those of even degrees are even functions. Equation (8.34) clearly indicates that $P_n(x)$ and $P_n(-x)$ are no longer independent. Another solution for the Legendre equation, known as the ***Legendre function of the second kind***, is given as

$$Q_\nu(x) = \frac{\pi}{2}\,\frac{P_\nu(x)\cos\pi\nu - P_\nu(-x)}{\sin\nu\pi} . \tag{8.35}$$

This solution when $\nu$ approaches an integer exists and provides a solution independent of $P_n(x)$. However, it should be noted that $Q_n(x)$ become infinite at $x = \pm 1$ (corresponding to $\theta = 0$ and $\theta = \pi$). The series solution for Legendre functions of the second kind is given by

$$Q_n(x) = P_n(x)\left(\frac{1}{2}\ln\frac{1+x}{1-x} - g(n)\right) + \sum_{m=1}^{n} \frac{(-1)^m(n+m)!}{(m!)^2(n-m)!}\, g(m)\left(\frac{1-x}{2}\right)^m , \tag{8.36}$$

where

$$g(n) = \sum_{k=1}^{n} \frac{1}{k} .$$

A compact representation of the Legendre polynomials is given by

$$P_n(x) = \frac{1}{2^n n!}\,\frac{d^n}{dx^n}\,(x^2-1)^n\ , \tag{8.37}$$

with

$$P_0(x) = 1\ , \tag{8.38a}$$

$$P_1(x) = x\ , \tag{8.38b}$$

$$P_2(x) = \tfrac{1}{2}\,(3x^2-1)\ , \tag{8.38c}$$

and

$$P_3(x) = \tfrac{1}{2}\,(5x^3-3x)\ . \tag{8.38d}$$

Also,

$$Q_0(x) = \frac{1}{2}\ln\left(\frac{1+x}{1-x}\right)\ , \tag{8.38e}$$

$$Q_1(x) = \frac{x}{2}\ln\left(\frac{1+x}{1-x}\right) - 1\ , \tag{8.38f}$$

$$Q_2(x) = \frac{3x^2-1}{4}\ln\left(\frac{1+x}{1-x}\right) - \frac{3x}{2}\ , \tag{8.38g}$$

and

$$Q_3(x) = \frac{5x^3-3x}{4}\ln\left(\frac{1+x}{1-x}\right) - \frac{5x^2}{2} + \frac{2}{3}\ . \tag{8.38h}$$

The associated Legendre functions for integer values $\mu = m$ can be expressed in terms of the Legendre functions as shown below:

$$P_n^m(x) = (-1)^m(1-x^2)^{m/2}\,\frac{d^m P_n(x)}{dx^m} \tag{8.39a}$$

and

$$Q_n^m(x) = (-1)^m(1-x^2)^{m/2}\,\frac{d^m Q_n(x)}{dx^m}\ , \tag{8.39b}$$

and they satisfy the following differential equation:

$$(1-x^2)\,\frac{d^2y}{dx^2} - 2x\,\frac{dy}{dx} + \left(n(n+1) - \frac{m^2}{1-x^2}\right)y = 0\ , \tag{8.40}$$

where $y$ can be $P_n^m(x)$ or $Q_n^m(x)$. We note from Eq. (8.39a) that $P_n^m(x) = 0$ for $m > n$. Figures 8-3 and 8-4 show the first few orders of Legendre functions of the first and second kind of integer orders, respectively. Figure 8-5 shows the associated Legendre function of the first kind and third order for $m = 0, 1, 2, 3$.

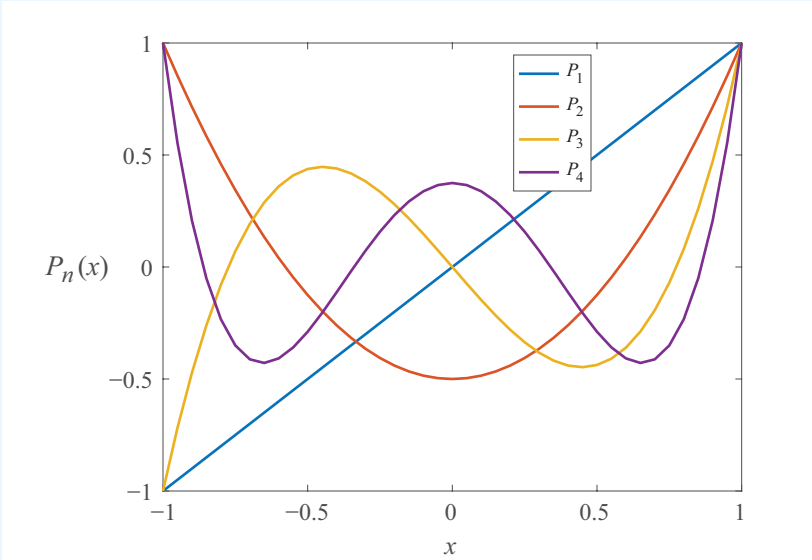


**Figure 8-3:** The first few orders of Legendre functions of the first kind of integer orders.

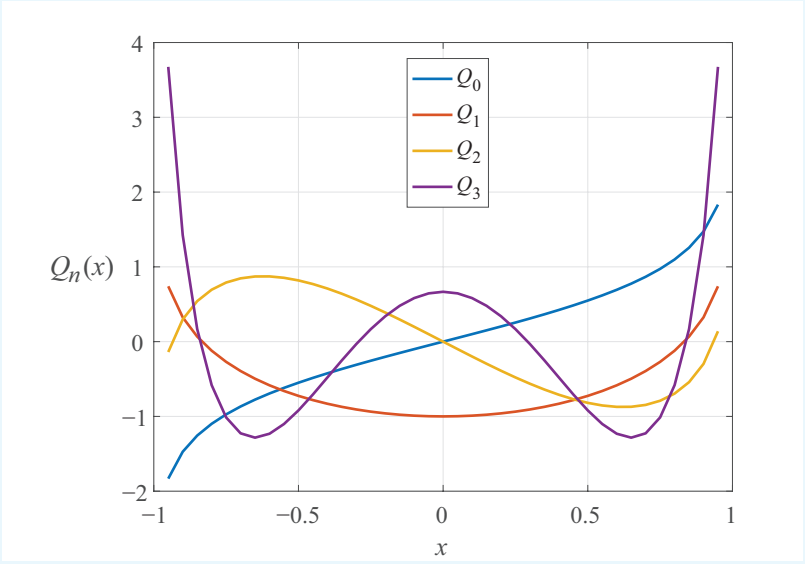


**Figure 8-4:** The first few orders of Legendre function of the second kind of integer orders.

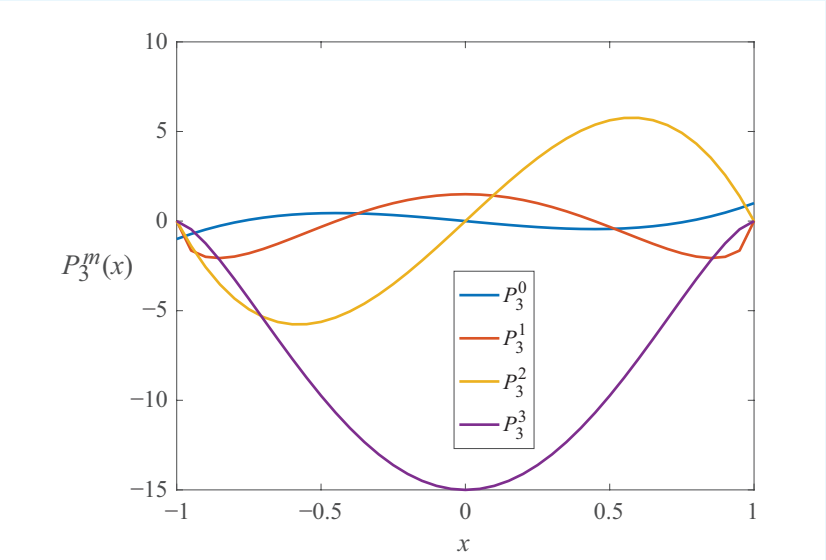


**Figure 8-5:** The associated Legendre function of the first kind and third order for $m = 0, 1, 2, 3$.

The general solution of scalar potential can be expressed in terms of the superposition of elementary spherical Bessel functions:

$$\psi(r,\theta,\phi) = \sum_n \sum_m (a_n j_n(kr) + b_n n_n(kr))\, P_n^m(\cos\theta)\, e^{im\phi} \,, \tag{8.41}$$

for integer values of $m$ and $n$. The superposition can also be expressed in terms of integrals in $\nu$ and $\mu$. The field quantities are expressed in terms of $A_\mathrm{r}$ and $A_\mathrm{mr}$ in Eqs. (8.10) and (8.12), and $A_\mathrm{r}$ and $A_\mathrm{mr}$ are in turn expressed in terms of $r\psi$ and $r\psi_\mathrm{m}$. Sometimes, it is convenient to introduce another kind of spherical Bessel function, which was first introduced by Schelkunoff and defined as

$$\hat{\mathbf{z}}_n(kr) = krz_n(kr) = \sqrt{\frac{\pi kr}{2}}\, Z_{n+1/2}(kr) \,. \tag{8.42}$$

These spherical Bessel functions satisfy the condition

$$\left(\frac{d^2}{d(kr)^2} + 1 - \frac{n(n+1)}{(kr)^2}\right) \hat{\mathbf{z}}_n(kr) = 0 \,. \tag{8.43}$$

## 8-1.2 Orthogonality Properties

To represent an arbitrary wave function in a source-free region in terms of an elementary spherical wave function similar to Eq. (8.41), orthogonality relationships must be established among the elementary functions. For example, it can be shown that the Legendre polynomial $P_n(\cos\theta)$ forms a complete orthogonal set in the $\theta$-domain $[0,\pi]$. Similarly, the two-

dimensional elementary functions

$$U_{nm}^{\mathrm{o}}(\theta,\phi) = P_n^m(\cos\theta)\sin m\phi \tag{8.44a}$$

and

$$U_{nm}^{\mathrm{e}}(\theta,\phi) = P_n^m(\cos\theta)\cos m\phi \tag{8.44b}$$

form a complete orthogonal set over the domain $\theta \in [0,\pi]$ and $\phi \in [0,2\pi]$ and are sometimes referred to as ***spherical harmonic functions***. These are orthogonal functions on the surface of a unit sphere, and thus the orthogonality integral needs a weighting function ($\sin\theta$).

To demonstrate orthogonality of functions $P_n(\cos\theta)$, known as ***zonal harmonics***, we consider two specific elementary wave functions:

$$\psi_1(r,\theta) = j_n(kr)\, P_n(\cos\theta)$$

and

$$\psi_2(r,\theta) = j_m(kr)\, P_m(\cos\theta)\ ,$$

which are solutions to the wave equation (8.13) for $\mu = 0$ and $\nu = n$. Applying Green's second identity to $\psi_1$ and $\psi_2$, we get

$$\iiint (\psi_1 \nabla^2\psi_2 - \psi_2\nabla^2\psi_1)\, dv = \oiint_S \left(\psi_1 \frac{\partial\psi_2}{\partial n} - \psi_2 \frac{\partial\psi_1}{\partial n}\right) ds\ .$$

Using Eq. (8.13), it can be shown that the left-hand side is zero. Considering surface $S$ to be a sphere of radius $r$, we have

$$\int_0^{2\pi}\int_0^{\pi} \left(\psi_1 \frac{\partial\psi_2}{\partial n} - \psi_2 \frac{\partial\psi_1}{\partial n}\right) ds = 0\ . \tag{8.45}$$

Since on this surface the spherical Bessel functions are constant, it can be shown that

$$2\pi kr^2 [j_n(kr)\ j_m'(kr) - j_n'(kr)\ j_m(kr)] \int_0^{\pi} P_n(\cos\theta)\, P_m(\cos\theta)\ \sin\theta\, d\theta = 0\ .$$

It is now obvious that when $n \neq m$,

$$\int_0^{\pi} P_n(\cos\theta)\, P_m(\cos\theta)\sin\theta\, d\theta = 0, \qquad m \neq n\ , \tag{8.46}$$

which proves that $P_n$ and $P_m$ are orthogonal. Noting that

$$P_n(x) = \frac{1}{2^n n!}\frac{d^n}{dx^n}(x^2-1)^n\ ,$$

it can be shown that

$$\int_0^{\pi} [P_n(\cos\theta)]^2 \sin\theta\, d\theta = \frac{2}{2n+1}\ . \tag{8.47}$$

Note that, for any function $f(\theta)$ defined in the domain $\theta \in [0, \pi]$,

$$f(\theta) = \sum_{n=0}^{\infty} a_n \, P_n(\cos\theta) \ ,$$

where

$$a_n = \frac{2n+1}{2} \int_0^{\pi} f(\theta) \, P_n(\cos\theta) \sin\theta \, d\theta \ .$$

To show orthogonality of spherical harmonic functions we consider the following:

$$\psi_1 = U_{nm}(\theta, \phi) \, j_n(kr) \tag{8.48a}$$

and

$$\psi_2 = U_{pq}(\theta, \phi) \, j_p(kr) \ . \tag{8.48b}$$

Obviously $\psi_1$ and $\psi_2$ satisfy the wave equation (8.13). Again, using Green's second identity for a spherical surface, it can be shown that Eq. (8.45) is valid for the new functions $\psi_1$ and $\psi_2$ given in Eq. (8.48). Here the superscript for the spherical harmonic functions $U_{mn}^{\mathrm{o}}$ or $U_{mn}^{\mathrm{e}}$ is suppressed to show an orthogonality relationship that is valid for both.

Direct substitution of Eq. (8.48) into Eq. (8.45) results in

$$kr^2 [j_n(kr) \, j_p'(kr) - j_n'(kr) \, j_p(kr)] \int_0^{2\pi} \int_0^{\pi} U_{nm}(\theta, \phi) \, U_{pq}(\theta, \phi) \, \sin\theta \, d\theta \, d\phi = 0 \ .$$

The term outside the integral vanishes for $n = p$, and hence for $n \neq p$, we have

$$\int_0^{2\pi} \int_0^{\pi} U_{nm}(\theta, \phi) \, U_{pq}(\theta, \phi) \, \sin\theta \, d\theta \, d\phi = 0 \ , \tag{8.49}$$

which is valid for both even and odd functions. Since

$$\int_0^{2\pi} \sin(m\phi) \cos(q\phi) \, d\phi = 0 \ ,$$

it follows that

$$\int_0^{2\pi} \int_0^{\pi} U_{nm}^{\mathrm{o}}(\theta, \phi) \, U_{pq}^{\mathrm{e}}(\theta, \phi) \, \sin\theta \, d\theta \, d\phi = 0 \ ,$$

independently of $n$, $p$, $m$ or $q$. However, in cases where both functions in Eq. (8.49) are either even or odd, and since

$$\int_0^{2\pi} \sin(m\phi) \sin(q\phi) \, d\phi = \int_0^{2\pi} \cos(m\phi) \cos(q\phi) \, d\phi = \begin{cases} 0 & m \neq q \ , \\ \pi & m = q \ , \end{cases} \tag{8.50}$$

it follows that even when $n = p$, unless $m = q$, Eq. (8.49) will still vanish. For $n = p$ and $m = q$, it can be shown that

$$\int_0^{2\pi}\int_0^{\pi} U_{nm}(\theta,\phi)\, U_{pq}(\theta,\phi)\, \sin\theta\, d\theta\, d\phi = \begin{cases} \dfrac{4\pi}{2n+1} & m = 0 \text{ (only even functions)}, \\ \dfrac{2\pi(n+m)!}{(2n+1)(n-m)!} & m \neq 0\ . \end{cases} \tag{8.51}$$

Proof of this result is based on integration by parts using

$$P_n^m(x) = (-1)^m(1-x^2)^{m/2}\,\frac{d^m P_n(x)}{dx^m}\ . \tag{8.52}$$

Figure 8-6 shows the plot of a set of spherical harmonic functions $U_{4m}^{\mathrm{e}}$ as a function of $\theta$ and $\phi$ for $m = 0$, 1, 2, 3, and 4.

### 8-1.3 Fourier-Legendre Expansion

In many problems for which a set of data or a function is known on the surface of a constant sphere, the orthogonality of spherical harmonic functions can be used to express the data or the function in terms of a series expansion. Usually such series can be truncated by keeping only a small number of terms depending on the smoothness of the function with respect to $\theta$ and $\phi$. This way significant compression of data can be achieved. Consider a function $f(\theta,\phi)$ on the surface of a sphere. This function may be expanded in terms of spherical harmonic functions given by

$$f(\theta,\phi) = \sum_{n=0}^{\infty}\sum_{m=0}^{n}[a_{nm}\, U_{nm}^{\mathrm{e}}(\theta,\phi) + b_{nm}\, U_{nm}^{\mathrm{o}}(\theta,\phi)]\ . \tag{8.53}$$

According to Eq. (8.44), Eq. (8.53) may also be written as

$$f(\theta,\phi) = \sum_{n=0}^{\infty}\sum_{m=0}^{n}[(a_{nm}\cos m\phi + b_{nm}\sin m\phi)\, P_n^m(\cos\theta)]\ . \tag{8.54}$$

To find the unknown coefficients $a_{mn}$ and $b_{mn}$, we can multiply both sides of Eq. (8.54) by $U_{pq}^{\mathrm{e}}(\theta,\phi)\sin\theta$ or $U_{pq}^{\mathrm{o}}(\theta,\phi)\sin\theta$ and integrate with respect to $\theta$ and $\phi$ over 0 to $\pi$ and 0 to $2\pi$, respectively. Using the orthogonality relations obtained in the previous section, the following expressions for $a_{nm}$ and $b_{nm}$ are obtained:

$$a_{n0} = \frac{2n+1}{4\pi}\int_0^{2\pi}\int_0^{\pi} f(\theta,\phi)\, P_n(\cos\theta)\, \sin\theta\, d\theta\ , \tag{8.55a}$$

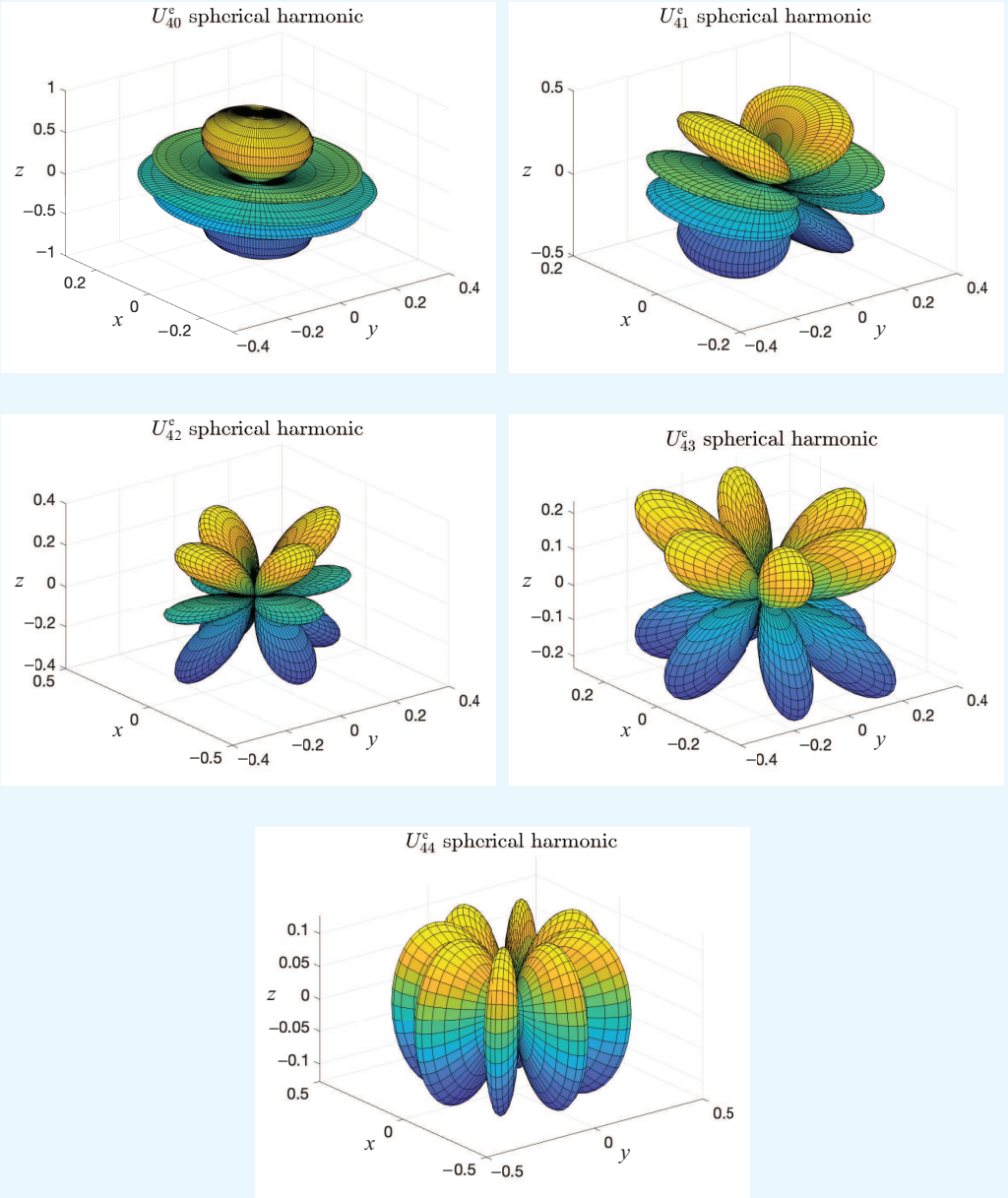


**Figure 8-6:** The plot of spherical harmonic functions for $n = 4$ and $m = 0$, 1, 2, 3, and 4.

$$a_{nm} = \frac{2n+1}{2\pi}\,\frac{(n-m)!}{(n+m)!}\int_0^{2\pi}\int_0^{\pi} f(\theta,\phi)\,P_n^m(\cos\theta)\,\cos m\phi\,\sin\theta\,d\theta\,d\phi\,, \tag{8.55b}$$

and

$$b_{nm} = \frac{2n+1}{2\pi}\frac{(n-m)!}{(n+m)!}\int_0^{2\pi}\int_0^{\pi} f(\theta,\phi)\, P_n^m(\cos\theta)\, \sin m\phi \sin\theta\, d\theta\, d\phi\ . \tag{8.55c}$$

### 8-1.4 Orthogonality of Spherical Harmonic Functions for Vector Fields

Other useful orthogonality relations for spherical harmonic functions applicable to vector fields can also be obtained. These relationships can be derived from the application of the Lorentz reciprocity theorem for a source-free region. Consider a homogeneous region bounded by a spherical surface of radius $r_0$. The Lorentz reciprocity for two sets of vector fields generated by two different sources outside the spherical region can be written as

$$\oiint_S \left[\mathbf{E}^a(\mathbf{r}) \times \mathbf{H}^b(\mathbf{r}) - \mathbf{E}^b(\mathbf{r}) \times \mathbf{H}^a(\mathbf{r})\right] \cdot d\mathbf{s} = 0\ . \tag{8.56}$$

Suppose the fields are generated from an electric current source that has only $\hat{\mathbf{r}}$ component. This, as shown before, creates TM-to-$r$ fields. The potentials in this case can be represented by

$$A_r^a(\mathbf{r}) = \hat{j}_n(kr)\, U_{nm}(\theta,\phi)$$

and

$$A_r^b(\mathbf{r}) = \hat{j}_q(kr)\, U_{pq}(\theta,\phi)\ .$$

$U_{nm}$ and $U_{pq}$ here can be either even or odd functions of $\phi$. It is noted that $d\mathbf{s}$ in Eq. (8.56) is along $\hat{\mathbf{r}}$, hence only the $\theta$ and $\phi$ components of the fields are sufficient in the calculation of Eq. (8.56); that is,

$$\int_0^{2\pi}\int_0^{\pi} \left[(\mathbf{E}_\theta^a \mathbf{H}_\phi^b - \mathbf{E}_\phi^a \mathbf{H}_\theta^b) - (\mathbf{E}_\theta^b \mathbf{H}_\phi^a - \mathbf{E}_\phi^b \mathbf{H}_\theta^a)\right] \sin\theta\, d\theta\, d\phi = 0\ . \tag{8.57}$$

Using Eqs. (8.10b) and (8.10c) together with Eqs. (8.11a) and (8.11b), Eq. (8.56) can be written as

$$\frac{1}{i\omega\mu^2\varepsilon r_0^2}\left[\hat{j}_n'(kr_0)\,\hat{j}_p(kr_0) - \hat{j}_n(kr_0)\,\hat{j}_p'(kr_0)\right] \cdot \int_0^{2\pi}\int_0^{\pi}\left[\sin\theta\,\frac{\partial U_{nm}^{\mathrm{e,o}}}{\partial\theta}\frac{\partial U_{pq}^{\mathrm{e,o}}}{\partial\theta} + \frac{1}{\sin\theta}\frac{\partial U_{nm}^{\mathrm{e,o}}}{\partial\phi}\frac{\partial U_{pq}^{\mathrm{e,o}}}{\partial\phi}\right] d\theta\, d\phi = 0\ . \tag{8.58}$$

If $n \neq q$, the orthogonality relation takes the following form:

$$I = \int_0^{2\pi}\int_0^{\pi}\left[\sin\theta\,\frac{\partial U_{nm}^{\mathrm{e,o}}}{\partial\theta}\frac{\partial U_{pq}^{\mathrm{e,o}}}{\partial\theta} + \frac{1}{\sin\theta}\frac{\partial U_{nm}^{\mathrm{e,o}}}{\partial\phi}\frac{\partial U_{pq}^{\mathrm{e,o}}}{\partial\phi}\right] d\theta\, d\phi = 0\ . \tag{8.59}$$

Also, according to Eq. (8.50), if $m \neq q$, it can easily be shown that the integral will go to zero even when $n = p$. If $n = p$ and $m = q$, then using integration by parts and Eq. (8.51), it can be

shown that

$$I = \begin{cases} \dfrac{4\pi n(n+1)}{2n+1} & m = 0\ , \\ \dfrac{2\pi n(n+1)}{2n+1}\ \dfrac{(n+m)!}{(n-m)!} & m \neq 0\ . \end{cases} \tag{8.60}$$

**Example 8-1: Expansion of Spherical Delta Function**

Find the Fourier-Legendre expansion of $f(\theta,\phi) = \frac{1}{\sin\theta}\ \delta(\theta)\ \delta(\phi)$ and plot the approximate representation of the function by truncating the summation over $n$ to values of $N = 5$, 10, 15, and 20.

**Solution:** Since $f(\theta,\phi)$ is a product of delta functions of $\theta$ and $\phi$, the integrations given by Eqs. (8.55a)–(8.55c) can be carried out easily, and the results are given by

$$a_{n0} = \frac{2n+1}{4\pi}\ P_n(1) = \frac{2n+1}{4\pi}\ ,$$

$$a_{nm} = \frac{2n+1}{2\pi}\ \frac{(n-m)!}{(n+m)!}\ P_n^m(1)\ ,$$

and

$$b_{nm} = 0\ .$$

Hence,

$$\frac{1}{\sin\theta}\ \delta(\theta)\ \delta(\phi) \approx \sum_{n=0}^{N}\sum_{m=0}^{n} \alpha_m\ \frac{2n+1}{4\pi}\ \frac{(n-m)!}{(n+m)!}\ P_n^m(1)\ ,$$

where

$$\alpha_m = \begin{cases} 1 & m = 0\ , \\ 2 & m > 0\ . \end{cases}$$

Figure 8-7(a) shows the normalized truncated expansion of spherical delta function in $\phi = 0$ cut as a function of $\theta$ for four different values of truncation numbers $N = 5$, 10, 15, and 20. Figure 8-7(b) shows the 3-D representation of the truncated spherical delta function for $N = 20$.

### 8-1.5 The Spherical Cavity

To demonstrate the application of the TE-to-$r$ and TM-to-$r$ modes representation of field quantities, let's consider the problem of a spherical cavity. Figure 8-8 shows a metallic sphere of radius $a$ filled with a homogeneous material having permittivity $\varepsilon$ and permeability $\mu$. First, considering TE-to-$r$ modes,

$$A_{\rm mr} = \hat{\mathbf{j}}_n(kr)\ P_n^m(\cos\theta) \begin{cases} \cos m\phi\ , \\ \sin m\phi\ . \end{cases}$$

(a)

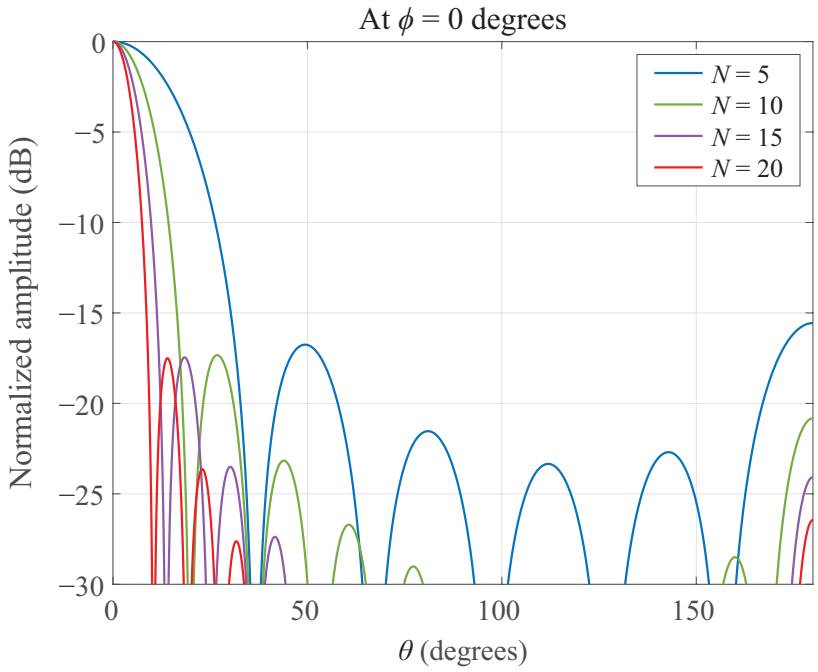


(b)

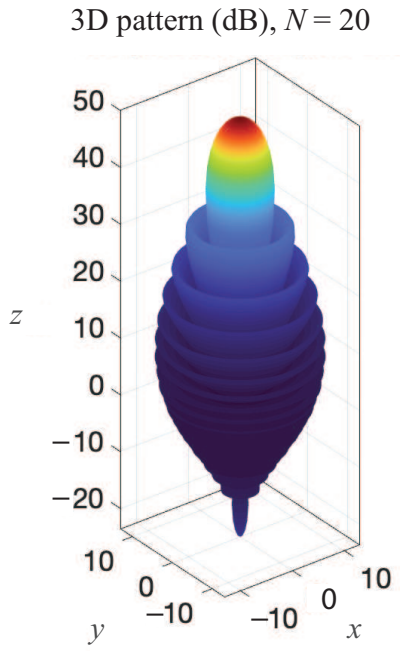


**Figure 8-7:** Plots of the truncated expansion of spherical delta function.

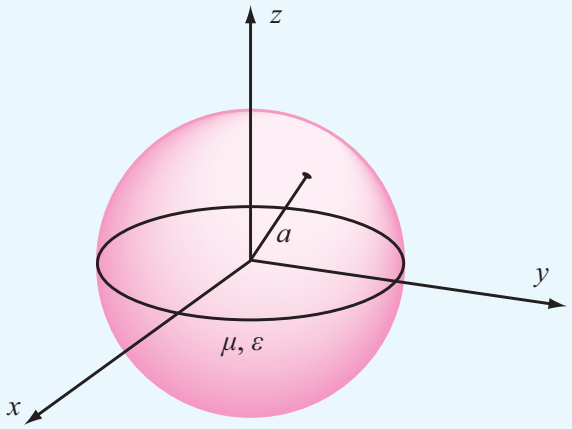


**Figure 8-8:** A metallic sphere filled with a homogeneous material having permittivity $\varepsilon$ and permeability $\mu$.

The tangential electric fields are $E_\theta$ and $E_\phi$, which must vanish on the metallic surface ($r = a$). Referring to Eq. (8.12), the boundary condition is satisfied if

$$\hat{\mathbf{j}}_n(ka) = 0 \, .$$

Denoting the zeros of Schelkunoff's spherical Bessel functions $\hat{\mathbf{j}}_n(x)$ by $x_{np}$, where subscript $p$ represents the order of infinitely many roots of $\hat{\mathbf{j}}_n(x)$, it follows that

$$k = \frac{x_{np}}{a} \qquad \begin{matrix} n = 1,2,3,\ldots \\ p = 1,2,3,\ldots \end{matrix}$$

At a resonance, the potential function $A_{\text{mr}}$ is given by

$$A_{\text{mr}} = \hat{\mathbf{j}}_n \left( x_{np} \frac{r}{a} \right) P_n^m(\cos\theta) \begin{Bmatrix} \cos m\phi \, , \\ \sin m\phi \, . \end{Bmatrix}$$

For TM-to-$r$ modes,

$$A_{\text{r}} = \hat{\mathbf{j}}_n(kr) \, P_n^m(\cos\theta) \begin{Bmatrix} \cos m\phi \\ \sin m\phi \end{Bmatrix} \qquad m \le n \, .$$

According to Eq. (8.10), the tangential electric field on the sphere surface vanishes if

$$\hat{\mathbf{j}}_n'(ka) = 0 \, .$$

**Table 8-1: Ordered zeros of $\hat{\mathbf{j}}_n(x)$.**

| $p$ ↓ | $n$ | | | | | | | |
|---|---|---|---|---|---|---|---|---|
| | 1 | 2 | 3 | 4 | 5 | 6 | 7 | 8 |
| 1 | 4.493 | 5.763 | 6.988 | 8.183 | 9.356 | 10.513 | 11.657 | 12.791 |
| 2 | 7.725 | 9.095 | 10.417 | 11.706 | 12.967 | 14.207 | 15.431 | 16.641 |
| 3 | 10.904 | 12.323 | 13.698 | 15.040 | 16.355 | 17.648 | 18.923 | 20.182 |
| 4 | 14.066 | 15.515 | 16.924 | 18.301 | 19.653 | 20.983 | 22.295 | |
| 5 | 17.221 | 18.689 | 20.122 | 21.525 | 22.905 | | | |
| 6 | 20.371 | 21.854 | | | | | | |

Denoting the roots of $j_n'(x)$ by $x_{np}'$, $k$ is obtained from

$$k = \frac{x_{np}'}{a} .$$

The resonant frequency for TE and TM modes are given respectively by

$$(f)^{\mathrm{TE}_{nmp}} = \frac{x_{np}}{2\pi a\sqrt{\mu\varepsilon}} \tag{8.61a}$$

and

$$(f)^{\mathrm{TM}_{nmp}} = \frac{x_{np}'}{2\pi a\sqrt{\mu\varepsilon}} . \tag{8.61b}$$

Since $m$ and $n$ are independent, there are many degenerate modes. First a set of degenerate modes exist through the choice of $\cos m\phi$ (even mode) or $\sin m\phi$ (odd mode), then for a given $n$ there exist $(n+1)$ degenerate modes corresponding to $P_n^m(\cos\theta)$ for $m \le n$. That is, they all have the same resonant frequency.

It is noted that $n = 0$ is not admissible since $P_0$ is a constant function of $\theta$, and there is no variation with respect to $\phi$ either since $m$ must be zero. According to Eqs. (8.10) and (8.12), the corresponding magnetic and electric fields are zero, and thus no resonance can be established.

Tables 8-1 and 8-2 provide the ordered zeros of the spherical Bessel functions and those of the derivative of spherical Bessel functions, respectively. It is noted that the lowest-order resonant frequency (dominant mode) is $\mathrm{TM}_{1,m,1}$, for $m = 0$ or 1. The next resonant frequencies are for modes $\mathrm{TM}_{2,m,1}$, $\mathrm{TE}_{1,m,1}$, $\mathrm{TM}_{3,m,1}$, and so on.

It is interesting to examine the distribution of the fields of the dominant mode in a spherical cavity. For $\mathrm{TM}_{1,0,1}$ the fields can be computed from Eqs. (8.10) and (8.11) using

$$A_{\mathrm{r}}(r,\theta,\phi) = \hat{\mathbf{j}}_1(kr)\, P_1(\cos\theta) = \hat{\mathbf{j}}_1(kr)\cos\theta , \tag{8.62}$$

**Table 8-2: Ordered zeros of $\hat{\mathbf{j}}_n'(x)$.**

| $p$ ↓ | $n$ | | | | | | | |
|---|---|---|---|---|---|---|---|---|
| | 1 | 2 | 3 | 4 | 5 | 6 | 7 | 8 |
| 1 | 2.744 | 3.870 | 4.973 | 6.062 | 7.140 | 8.211 | 9.275 | 10.335 |
| 2 | 6.117 | 7.443 | 8.722 | 9.968 | 11.189 | 12.391 | 13.579 | 14.763 |
| 3 | 9.317 | 10.713 | 12.064 | 13.380 | 14.670 | 15.939 | 17.190 | 18.425 |
| 4 | 12.486 | 13.921 | 15.314 | 16.674 | 18.009 | 19.221 | 20.615 | 21.894 |
| 5 | 15.644 | 17.103 | 18.524 | 19.915 | 21.281 | 22.626 | | |
| 6 | 18.796 | 20.272 | 21.714 | 23.128 | | | | |
| 7 | 21.946 | | | | | | | |

and are given by

$$E_{\mathrm{r}} = \frac{i}{\omega\mu\varepsilon}\,\frac{n(n+1)}{r^2}\,\hat{\mathbf{j}}_1(kr)\cos\theta\ , \tag{8.63a}$$

$$E_\theta = \frac{-ik}{\omega\mu\varepsilon r}\,\hat{\mathbf{j}}_1'(kr)\sin\theta\ , \tag{8.63b}$$

and

$$H_\phi = \frac{1}{\mu r}\,\hat{\mathbf{j}}_1(kr)\sin\theta\ , \tag{8.63c}$$

where we have used Eq. (8.43) to show that

$$\left(\frac{d^2}{dr^2}+k^2\right)\hat{\mathbf{j}}_n(kr) = \frac{n(n+1)}{r^2}\,\hat{\mathbf{j}}_n(kr)\ . \tag{8.64}$$

In Eqs. (8.63a)–(8.63c), $k = 2.744/a$. The time-average stored energy inside the cavity can be computed from

$$\mathcal{W} = 2\mathcal{W}_{\mathrm{m}} = \iiint_V \frac{1}{2}\,\mu|H(r,\theta,\phi)|^2\,dv\ . \tag{8.65}$$

Noting that

$$\int_0^\pi \sin^3\theta\,d\theta = \int_{-1}^{1}(1-x^2)\,dx = \frac{4}{3}\ , \tag{8.66}$$

it follows that Eq. (8.65) can be written as

$$\mathcal{W} = \frac{4\pi}{3\mu}\int_0^a \left[\hat{\mathbf{j}}_1(kr)\right]^2\,dr\ . \tag{8.67}$$

Using the integral identity

$$\int_0^a \left[\hat{\mathbf{j}}_1(kr)\right]^2 dr = \frac{a}{2}\left\{\left[\hat{\mathbf{j}}_1(ka)\right]^2 - \hat{\mathbf{j}}_0(ka)\,\hat{\mathbf{j}}_2(ka)\right\}, \tag{8.68}$$

and for $ka = 2.744$, Eq. (8.68) is evaluated to be $1.14/k$. Hence,

$$\mathcal{W} = \frac{4\pi \times 1.14}{3\mu k}.$$

The ohmic loss on conducting walls of a cavity can also be computed from the tangential magnetic field, and is given by

$$\begin{aligned} p_{\mathrm{L}} &= \frac{1}{2\sigma\delta_{\mathrm{s}}} \oiint_S |H_\phi|^2\, ds \\ &= \frac{1}{2\sigma\delta_{\mathrm{s}}}\,\frac{1}{\mu^2}\left[\hat{\mathbf{j}}_1(ka)\right]^2 \int_0^{2\pi}\int_0^{\pi} \sin^3\theta\, d\theta\, d\phi \\ &= \frac{4\pi}{3\sigma\delta_{\mathrm{s}}}\,\frac{1}{\mu^2}\left[\hat{j}_1(2.744)\right]^2. \end{aligned}$$

Noting that

$$\hat{j}_1(x) = \frac{\sin(x)}{x} - \cos(x),$$

it is found that $\hat{\mathbf{j}}_1(2.744) = 1.063$. The quality factor of the spherical cavity can be calculated from

$$\breve{Q} = \frac{\omega\mathcal{W}}{p_{\mathrm{L}}} = \frac{\omega\sigma\delta_{\mathrm{s}}\mu \times 1.14}{k \times (1.063)^2} = \sigma\delta_{\mathrm{s}}\eta(1.088),$$

where, as before, $\sigma$ is the conductivity of the metal and $\delta_{\mathrm{s}}$ is the skin depth.

## Example 8-2: Ground Ionosphere Cavity

At low frequencies, the ground acts like a very good conductor and can be approximated as a perfect conductor. The ionosphere, which contains free electrons (but with zero net charge), can also be treated as a perfect conductor at low frequencies (below the plasma frequency). Hence the ground and the ionosphere can be viewed as two concentric metallic spheres having radii represented by $R_{\mathrm{g}}$ (for the ground surface) and $R_{\mathrm{i}}$ (for the ionosphere), respectively, as shown in Fig. 8-9. Find the resonant modes of this cavity.

**Solution:** The modes that can exist in the spherical shell between the ground and the ionosphere are either TE-to-$r$ or TM-to-$r$. Considering TE-to-$r$ modes first, the admissible spherical wave functions that constitute $A_{\mathrm{mr}}$ are given by

$$A_{\mathrm{mr}} = [a_n\,\hat{\mathbf{j}}_n(k_0 r) + b_n\,\hat{\mathbf{h}}_n^{(1)}(k_0 r)]P_n^m(\cos\theta)\begin{cases}\cos m\phi\,, \\ \sin m\phi\,.\end{cases} \tag{8.69}$$

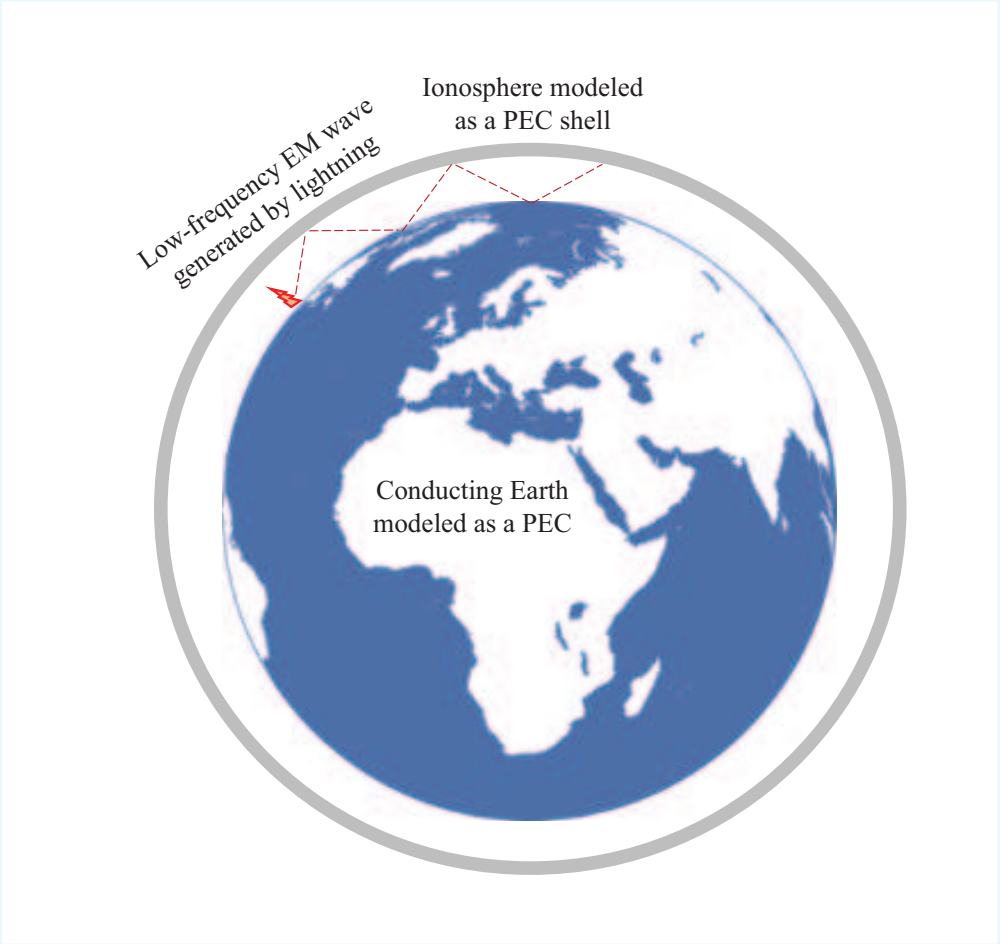


**Figure 8-9:** Configuration of the Earth and ionosphere modeled as a pair of concentric metallic spheres. The resonant fields in the cavity generated by lightning persist at the low frequencies listed in Table 8-3.

The tangential electric fields are given by

$$E_\theta(r,\theta,\phi) = -\frac{1}{\varepsilon_0 r \sin\theta}\,\frac{\partial A_{\mathrm{mr}}(r,\theta,\phi)}{\partial\theta} \tag{8.70a}$$

and

$$E_\phi(r,\theta,\phi) = \frac{1}{\varepsilon_0 r}\,\frac{\partial A_{\mathrm{mr}}(r,\theta,\phi)}{\partial\theta}\,. \tag{8.70b}$$

The boundary condition mandates that

$$E_\theta(R_{\mathrm{e}},\theta,\phi) = E_\theta(R_{\mathrm{i}},\theta,\phi) = 0 \tag{8.71a}$$

and

$$E_\phi(R_\mathrm{e},\theta,\phi) = E_\phi(R_\mathrm{i},\theta,\phi) = 0\ . \tag{8.71b}$$

These boundary conditions are satisfied if

$$A_\mathrm{mr}(R_\mathrm{e},\theta,\phi) = A_\mathrm{mr}(R_\mathrm{i},\theta,\phi) = 0\ ,$$

or equivalently,

$$a_n\,\hat{\mathbf{j}}_n(k_0R_\mathrm{e}) + b_n\,\hat{\mathbf{h}}_n^{(1)}(k_0R_\mathrm{e}) = 0 \tag{8.72a}$$

and

$$a_n\,\hat{\mathbf{j}}_n(k_0R_\mathrm{i}) + b_n\,\hat{\mathbf{h}}_n^{(1)}(k_0R_\mathrm{i}) = 0\ . \tag{8.72b}$$

A nontrivial solution can be found if the determinant of the coefficients of Eqs. (8.72a) and (8.72b) are zero. This provides the following transcendental equation:

$$\hat{\mathbf{j}}_n(k_0^{(n)}R_\mathrm{e})\,\hat{\mathbf{h}}_n^{(1)}(k_0^{(n)}R_\mathrm{i}) - \hat{\mathbf{j}}_n(k_0^{(n)}R_\mathrm{i})\,\hat{\mathbf{h}}_n^{(1)}(k_0^{(n)}R_\mathrm{e}) = 0\ . \tag{8.73}$$

Distinct values of $f_n$ for which $k_0^{(n)} = 2\pi f_n\sqrt{\mu_0\varepsilon_0}$ satisfy Eq. (8.73) are the resonant frequencies. In general, Eq. (8.73) must be solved numerically; however, noting that the ionosphere's height above the ground ranges from 80 km to 650 km and that this is significantly smaller than the Earth's radius, an approximate solution for the resonant frequencies can be obtained. Recall that the Schelkunoff spherical Bessel functions satisfy

$$\left(\frac{d^2}{d(kr)^2} + 1 - \frac{n(n+1)}{(kr)^2}\right)\,\hat{\mathbf{z}}_n(kr) = 0\ . \tag{8.74}$$

For the problem at hand, $R_\mathrm{e} \le r \le R_\mathrm{i}$ and $1/(kr)^2$ can be approximated by $1/(kR_\mathrm{e})^2$. Hence, Eq. (8.74) reduces to the ordinary second-order differential equation given by

$$\left[\frac{d^2}{d(kr)^2} + \left(1 - \frac{n(n+1)}{(kR_\mathrm{e})^2}\right)\right]\,\widetilde{Z}_n(kr) = 0\ , \tag{8.75}$$

which has a solution of the form

$$\widetilde{Z}_n(kr) = \begin{cases}\sin(U_nkr)\ , \\ \cos(U_nkr)\ ,\end{cases} \qquad \text{with } U_n = \sqrt{1 - \frac{n(n+1)}{(k_0^{(n)}R_\mathrm{e})^2}}\ . \tag{8.76}$$

Therefore Eqs. (8.72a) and (8.72b) can be modified to

$$a_n\sin(U_nk_0^{(n)}R_\mathrm{e}) + b_n\cos(U_nk_0^{(n)}R_\mathrm{e}) = 0$$

and

$$a_n\sin(U_nk_0^{(n)}R_\mathrm{i}) + b_n\cos(U_nk_0^{(n)}R_\mathrm{i}) = 0\ .$$

Again requiring that the determinant of the coefficient be zero, we have

$$\sin(U_n k_0^{(n)} R_\mathrm{e}) \cos(U_n k_0^{(n)} R_\mathrm{i}) - \cos(U_n R_\mathrm{e}) \sin(U_n k_0^{(n)} R_\mathrm{i}) = 0 \ ,$$

or

$$\sin[U_n k_0^{(n)} (R_\mathrm{i} - R_\mathrm{e})] = 0 \ . \tag{8.77}$$

Denoting the height of the ionosphere by $h = R_\mathrm{i} - R_\mathrm{e}$, we have

$$k_0^{(n)} U_n = \frac{\ell \pi}{h} \ , \qquad \ell = 1, 2, \ldots \tag{8.78}$$

Substituting Eq. (8.76) into Eq. (8.78), we get

$$f^{n,\ell} = \frac{c}{2\pi} \sqrt{\frac{n(n+1)}{R_\mathrm{e}^2} + \left( \frac{\ell \pi}{h} \right)^2} \ . \tag{8.79}$$

There are $(2n+1)$ degenerate modes corresponding to $m \leq n$ and the choice of $\sin m\phi$ or $\cos m\phi$. The lowest TE-to-$r$ mode corresponds to $n = 0$ and $\ell = 1$:

$$f_{\mathrm{TE_r}}^{01} = \frac{c}{2h} \ . \tag{8.80}$$

For $h = 100$ km, $f_{\mathrm{TE_r}}^{01} = 1.5$ kHz.

Lower-order modes can be excited by TM-to-$r$ modes. These modes are generated by

$$A_\mathrm{r}(r, \theta, \phi) = [a_n \hat{\mathbf{j}}_n(kr) + b_n \hat{\mathbf{h}}_n^{(1)}(kr)] P_n^m(\cos\theta) \begin{cases} \cos m\phi \ , \\ \sin m\phi \ . \end{cases} \tag{8.81}$$

The tangential electric fields $E_\theta$ and $E_\phi$ can be derived from Eq. (8.16). These tangential fields vanish at $r = R_\mathrm{e}$ and $r = R_\mathrm{i}$ if

$$\left. \frac{\partial A(r, \theta, \phi)}{\partial r} \right|_{r=R_\mathrm{e}} = \left. \frac{\partial A(r, \theta, \phi)}{\partial r} \right|_{r=R_\mathrm{i}} = 0 \ . \tag{8.82}$$

Using an approximation for the spherical Bessel functions similar to that in Eq. (8.76), Eq. (8.82) is satisfied if

$$a_n U_n k_0^{(n)} \cos(U_n k_0^{(n)} R_\mathrm{e}) - b_n U_n k_0^{(n)} \sin(U_n k_0^{(n)} R_\mathrm{e}) = 0 \tag{8.83a}$$

and

$$a_n U_n k_0^{(n)} \cos(U_n k_0^{(n)} R_\mathrm{i}) - b_n U_n k_0^{(n)} \sin(U_n k_0^{(n)} R_\mathrm{i}) = 0 \ . \tag{8.83b}$$

Requiring the solution to be nontrivial provides a similar equation to Eq. (8.77):

$$\sin[U_n k_0^{(n)} (R_\mathrm{i} - R_\mathrm{e})] = 0 \ ,$$

**Table 8-3: Resonant frequencies for TM-to-$r$ modes of the cavity between the ionosphere and the Earth's surface.**

| $n$ | 0 | 1 | 2 | 3 | 4 | 5 | $\cdots$ |
|---|---|---|---|---|---|---|---|
| $f$ (Hz) | 0 | 10.45 | 18.27 | 25.89 | 33.36 | 40.86 | $\cdots$ |

from which we find

$$k_0^{(n)} U_n = \frac{\ell\pi}{h}\,, \qquad \ell = 0,1,2,3\,.$$

We note that in this case $\ell = 0$ is admissible, since the solution for $\widetilde{Z}_n(kr)$, in view of Eq. (8.83), is given by

$$\widetilde{Z}_n(kr) = C\cos[k_0^{(n)} U(r - R_e)]$$

for some constant $C$. The resonant frequency has the same form as Eq. (8.79). However, we note that since $h \ll R_e$, the dominant set of modes corresponds to

$$f^{n,0} = \frac{\ell}{2\pi R_e}\sqrt{n(n+1)}\,.$$

Assuming that the Earth's radius is $R_e = 6400$ km, the resonant frequencies for TM-to-$r$ modes are given in Table 8-3. Note that these frequencies are independent of the ionosphere's height, which varies from time to time. For the modes in which the electric field has a radial component, the electric field is a constant function of $r$.

Lightning is a frequent event around the Earth with a frequency of about 40–50 occurrences per second. At low frequencies, lightning is the source of background electric noise whose spectrum peaks around the resonant frequencies reported in Table 8-3.

### 8-1.6 Dielectric Resonators

Microwave and millimeter-wave resonators, such as metallic cavities, are commonly used in filter and oscillator designs as an alternative to resonators made from lumped-circuit elements because of their high quality factor. Another type of resonator is a dielectric resonator that is made entirely from low-loss dielectric material. Such a resonator can provide a higher quality factor than their metallic counterpart, particularly at frequencies in the high microwave and millimeter-wave bands. The spherical dielectric resonator is one of the few geometries for which an exact analytical formulation can be obtained. Consider a dielectric sphere of permittivity $\varepsilon_s$ and permeability $\mu_s$ with radius $a$ placed in a background medium with constitutive parameters $\varepsilon_b$ and $\mu_b$, as shown in Fig. 8-10. We are seeking possible electromagnetic field solutions to this source-free problem. The potential function in regions inside and outside the dielectric sphere must satisfy the wave equation given by Eq. (8.13) with the appropriate wave number for each region. As discussed earlier, a solution to the wave equation given by Eq. (8.13) can be expressed in terms of TM-to-$r$ and TE-to-$r$. Considering first the TM-to-$r$ solution, we recognize that the magnetic vector potential inside and outside

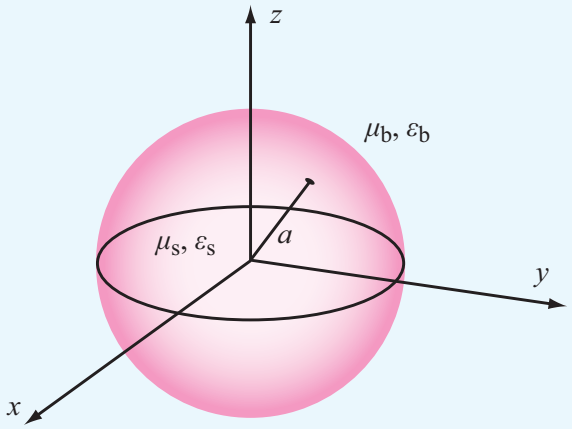


**Figure 8-10:** Geometry of a dielectric sphere of radius $a$ and constitutive parameters $\mu_s$ and $\varepsilon_s$ in a background medium with parameters $\mu_b$ and $\varepsilon_b$.

the sphere must take the following forms:

$$A_r^s(r,\theta,\phi) = a_n\, \hat{j}_n(k_s r)\, P_n^m(\cos\theta) \begin{cases} \sin m\phi, \\ \cos m\phi, \end{cases} \qquad r \le a \tag{8.84a}$$

and

$$A_r^b(r,\theta,\phi) = b_n\, \hat{h}_n^{(1)}(k_b r)\, P_n^m(\cos\theta) \begin{cases} \sin m\phi, \\ \cos m\phi, \end{cases} \qquad r \ge a\,, \tag{8.84b}$$

where

$$k_s = \omega\sqrt{\mu_s \varepsilon_s} \tag{8.85a}$$

and

$$k_b = \omega\sqrt{\mu_b \varepsilon_b}\,. \tag{8.85b}$$

Choice of the sine or cosine functions in Eqs. (8.84a) and (8.84b) is arbitrary due to the symmetry of the sphere. The boundary condition mandates the continuity of tangential electric and magnetic fields. According to Eq. (8.10), tangential electric fields ($E_\theta$ and $E_\phi$) across the boundary ($r = a$) are continuous if

$$\frac{1}{\mu_s \varepsilon_s}\, \frac{\partial A_r^s}{\partial r}\bigg|_{r=a} = \frac{1}{\mu_b \varepsilon_b}\, \frac{\partial A_r^b}{\partial r}\bigg|_{r=a}\,. \tag{8.86}$$

Similarly, according to Eq. (8.11), the continuity of the tangential magnetic fields is satisfied if

$$\frac{1}{\mu_{\rm s}}\ A_r^{\rm s}|_{r=a} = \frac{1}{\mu_{\rm b}}\ A_r^{\rm b}|_{r=a}\ . \tag{8.87}$$

Substituting Eqs. (8.84a) and (8.84b) into Eq. (8.86) renders

$$a_n\ \frac{k_{\rm s}}{\mu_{\rm s}\varepsilon_{\rm s}}\ \hat{j}_n'(k_{\rm s}a) = b_n\ \frac{k_{\rm b}}{\mu_{\rm b}\varepsilon_{\rm b}}\ \hat{h}_n^{(1)\prime}(k_{\rm b}a)\ . \tag{8.88}$$

Also, substituting Eqs. (8.84a) and (8.84b) into Eq. (8.87) provides another equation:

$$a_n\ \frac{1}{\mu_{\rm s}}\ \hat{j}_n(k_{\rm s}a) = b_n\ \frac{1}{\mu_{\rm b}}\ \hat{h}_n^{(1)}(k_{\rm b}a)\ . \tag{8.89}$$

Taking the ratios of Eqs. (8.88) and (8.89), the unknown coefficients $a_n$ and $b_n$ are eliminated and we arrive at the following transcendental equation:

$$\sqrt{\frac{\varepsilon_{\rm s}}{\mu_{\rm s}}}\ \frac{\hat{j}_n(k_{\rm s}a)}{\hat{j}_n'(k_{\rm s}a)} = \sqrt{\frac{\varepsilon_{\rm b}}{\mu_{\rm b}}}\ \frac{\hat{h}_n^{(1)}(k_{\rm b}a)}{\hat{h}_n^{(1)\prime}(k_{\rm b}a)}\ . \qquad \textbf{(TM modes)} \tag{8.90}$$

The solution to Eq. (8.90) reveals all the resonances of the spherical dielectric resonator. It turns out that the solution to this transcendental equation does not have any real roots. The roots are, in general, complex resonant frequencies, and therefore, even for lossless dielectric materials, only finite quality factors can be achieved. If the material properties of the dielectric sphere or those of the background medium are lossy, the resonator will present a lower quality factor. Note that for any value of $n$, all the $m \leq n$ modes are degenerate. The solution for TE-to-$r$ can be obtained using a similar procedure. Noting that TE waves are the dual of TM waves, the transcendental equation for TE modes can be obtained from Eq. (8.90) by changing $\varepsilon$ to $\mu$ and $\mu$ to $\varepsilon$. That is,

$$\sqrt{\frac{\mu_{\rm s}}{\varepsilon_{\rm s}}}\ \frac{\hat{j}_n(k_{\rm s}a)}{\hat{j}_n'(k_{\rm s}a)} = \sqrt{\frac{\mu_{\rm b}}{\varepsilon_{\rm b}}}\ \frac{\hat{h}_n^{(1)}(k_{\rm b}a)}{\hat{h}_n^{(1)\prime}(k_{\rm b}a)}\ . \qquad \textbf{(TE modes)} \tag{8.91}$$

To examine the behavior of the natural resonant frequencies of spherical dielectric resonators, an example is considered: a dielectric sphere with radius $a$, permittivity $\varepsilon_{\rm s} = 9\varepsilon_0$, and permeability $\mu_{\rm s} = \mu_0$ placed in a medium with parameters $\varepsilon_{\rm b} = \varepsilon_0$ and $\mu_{\rm b} = \mu_0$. Solving Eq. (8.90) for TM modes gives complex solutions for $k_{\rm s}a$. Figures 8-11(a) and 8-11(b) show the TM and TE solutions for different values of $n$ in the complex $k_{\rm s}a$ plane. It is shown that for certain high values of $n$, the imaginary part of $(k_{\rm s}a)$ is quite small, which can result in a high quality factor. Referring to Eq. (6.126), the quality factor for each mode can be obtained from

$$Q^{{\rm TE}_n,{\rm TM}_n} = \frac{\omega'}{2\omega''} = \frac{\Re{\rm e}[k_{\rm s}^{{\rm TE}_n,{\rm TM}_n}a]}{2\,\Im{\rm m}[k_{\rm s}^{{\rm TM}_n,{\rm TE}_n}a]}\ . \tag{8.92}$$

Figures 8-12(a) and 8-12(b) show the quality factor of the spherical dielectric resonator for TM and TE modes, respectively. It is shown that the quality factor can get as high as $10^8$

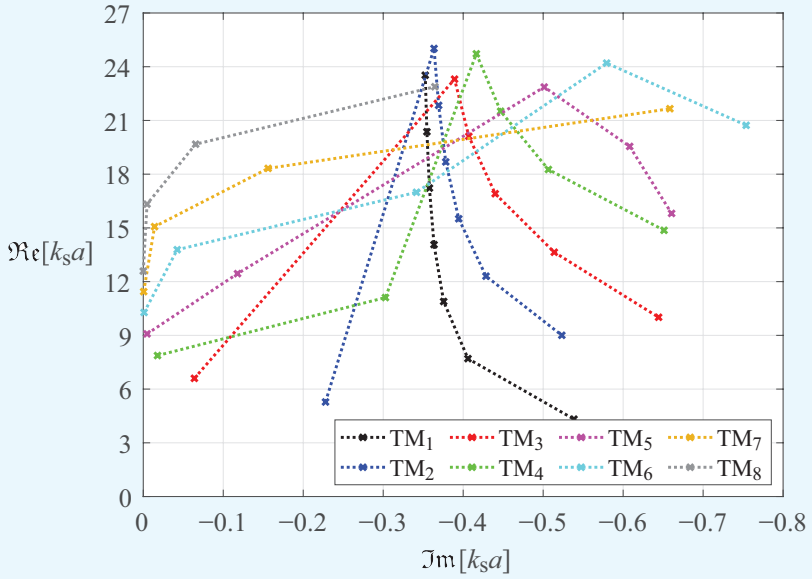


(a) TM modes

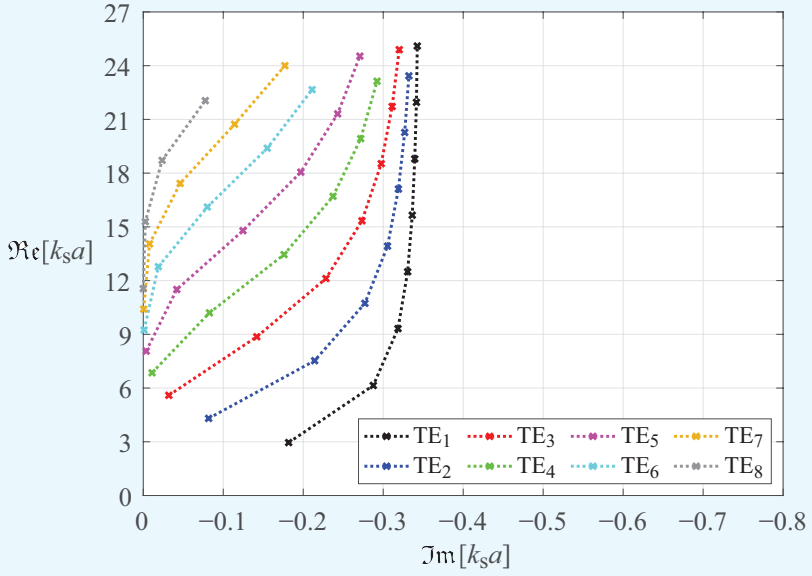


(b) TE modes

**Figure 8-11:** The complex zeros of transcendental equations (a) Eq. (8.90) (for TM) and (b) Eq. (8.91) (for TE) in the complex $k_s a$ plane for a dielectric sphere with $\varepsilon_s = 9$ and $\mu_s = \mu_0$ in a background medium with $\varepsilon_s = \varepsilon_0$ and $\mu_s = \mu_0$. The zeros are obtained for different values of $n$, noting that for each value of $n$ there are many zeros.

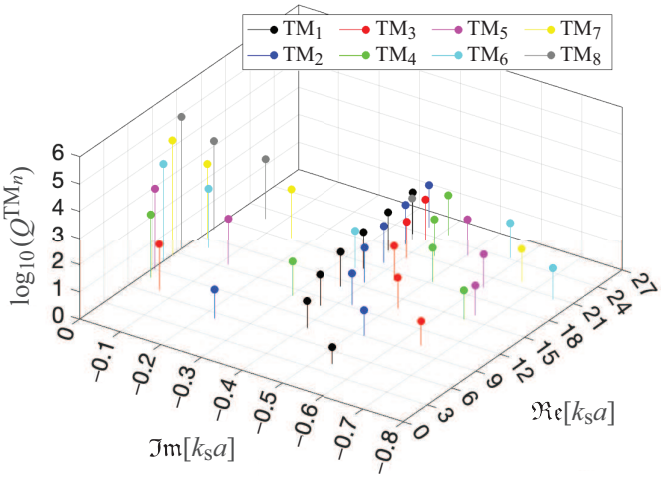


(a) TM modes

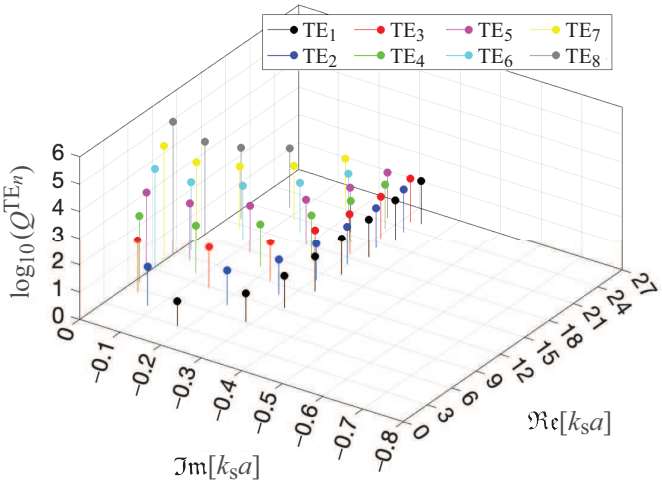


(b) TE modes

**Figure 8-12:** The quality factor of the spherical dielectric resonator for (a) TM and (b) TE resonant modes calculated from Eq. (8.92) in the complex $k_s a$ plane. Note that the quality factor increases for certain zeros for higher values of $n$.

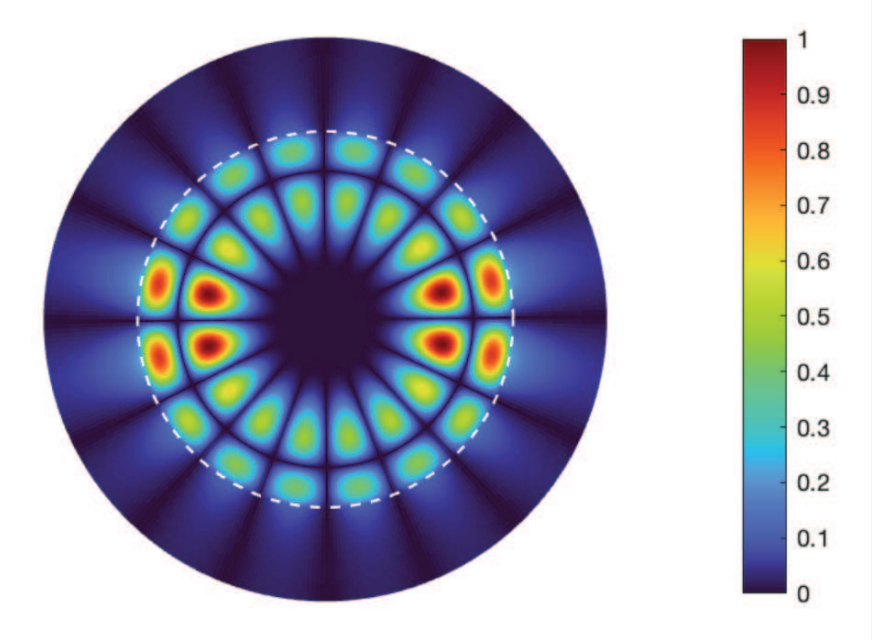


**Figure 8-13:** The magnetic field distribution (normalized to the maximum value) of one of the $TM_8$ modes with the highest $Q$ corresponding to $m = 0$.

for the modes considered in this plot. For higher values of $n$ the quality factor can get higher, but it should be noted that the quality factor is eventually limited by the loss tangent of the dielectric constant of the sphere. Figure 8-13 shows the magnetic field distribution for $TM_8$ mode inside the sphere and its surroundings for $m = 0$.

## 8-2 Wave Transformation to Spherical Wave Functions

To solve boundary value problems in a spherical coordinate system, it is often convenient to express fields in terms of spherical wave functions. In this section, a few useful examples of such transformations are considered.

### 8-2.1 Spherical Wave Function Expansion of a Plane Wave

In scattering problems, the excitation wave is often a plane wave. For scatterers, such as spheres, cones, wedges, etc., whose geometries coincide with the coordinate surfaces, field expansion in terms of spherical wave functions has been proven to be advantageous. Without loss of generality, let's consider a plane wave that is propagating along the $z$-axis and is given by

$$\mathbf{E}_{\mathrm{i}} = \mathbf{E}_0 e^{ikz} \, .$$

Expressing $z = r\cos\theta$ in the spherical coordinate system, we note that the function is independent of $\phi$ and is finite at the origin:

$$e^{ikr\cos\theta} = \sum_{n=0}^{\infty} a_n \, j_n(kr) \, P_n(\cos\theta) \; .$$

To find the unknown coefficients $a_n$, we make use of the orthogonality properties of $P_n(\cos\theta)$ given by Eqs. (8.46) and (8.47). It can easily be shown that

$$\frac{2a_n}{2n+1} \, j_n(kr) = \int_0^{\pi} e^{ikr\cos\theta} \, P_n(\cos\theta) \, \sin\theta \, d\theta \tag{8.93a}$$

and

$$j_n(kr) = 2^n (kr)^n \sum_{m=0}^{\infty} \frac{(-1)^m (n+m)!}{m! \, (2n+2m+1)!} \, (kr)^{2m} \; . \tag{8.93b}$$

To reduce the calculation and evaluate $a_n$ explicitly, the trick is to differentiate both sides of Eq. (8.93a) $n$ times with respect to $r$ and then evaluate the result at $r = 0$. Using the series expansion of $j_n(kr)$, it is easy to show that

$$\frac{d^n}{dr^n} \, j_n(kr) \bigg|_{r=0} = k^n \, \frac{2^n (n!)^2}{(2n+1)!}$$

and

$$\frac{d^n}{dr^n} \, e^{ikr\cos\theta} \bigg|_{r=0} = (i)^n k^n \cos^n\theta \; .$$

Also noting that

$$\int_0^{\pi} \cos^n\theta \, P_n(\cos\theta) \, \sin\theta \, d\theta = \frac{2^{n+1}(n!)^2}{(2n+1)!} \; ,$$

the coefficient $a_n$ is given by

$$a_n = (i)^n (2n+1) \; .$$

Hence

$$e^{ikr\cos\theta} = \sum_{n=0}^{\infty} (i)^n (2n+1) \, j_n(kr) \, P_n(\cos\theta) \; . \tag{8.94}$$

Conversely, using Eq. (8.93a),

$$j_n(kr) = \frac{(i)^{-n}}{2} \int_0^{\pi} e^{ikr\cos\theta} \, P_n(\cos\theta) \, \sin\theta \, d\theta \; , \tag{8.95}$$

which provides a useful formula for direct computation of $j_n(kr)$.

### 8-2.2 Addition Theorem for Spherical Wave Functions

The transformation of wave functions from a spherical coordinate system to another one is encountered in some radiation or scattering problems. The solution to a wave equation for a point source at the origin must satisfy

$$\nabla^2\psi + k^2\psi = -\delta(\mathbf{r}) \; . \tag{8.96}$$

This solution was obtained in Section 4-1 and is referred to as the ***scalar Green's function***:

$$\psi(r,\theta,\phi) = \frac{e^{ikr}}{4\pi r} \; . \tag{8.97}$$

Noting that

$$h_0^{(1)}(kr) = \frac{e^{ikr}}{ikr} \; ,$$

it follows that

$$\psi(r,\theta,\phi) = \frac{ik}{4\pi}\, h_0^{(1)}(kr) \; . \tag{8.98}$$

Now if the source point is moved to $\mathbf{r}'$, the potential function must satisfy

$$\nabla^2\ \psi(\mathbf{r},\mathbf{r}) + k^2\ \psi(\mathbf{r},\mathbf{r}') = -\delta(\mathbf{r}-\mathbf{r}') \; , \tag{8.99}$$

and the solution is found to be

$$\psi(\mathbf{r},\mathbf{r}') = \frac{ik}{4\pi}\, h_0^{(1)}(k|\mathbf{r}-\mathbf{r}'|) \; . \tag{8.100}$$

The solution to Eq. (8.99) can also be written in terms of a summation of spherical wave functions with reference to the origin of the coordinate system and can be written as

$$\psi(\mathbf{r},\mathbf{r}') = \sum_n \sum_m a_{mn}\, \mathcal{R}_n(kr)\, P_n^m(\cos\theta)\, e^{im\phi} \; , \tag{8.101}$$

where $\mathcal{R}_n(kr)$ is a representation of a spherical Bessel function and $a_{mn}$'s are coefficients that depend on $\theta'$ and $\phi'$. Noting that in a spherical coordinate system

$$\delta(\mathbf{r}-\mathbf{r}') = \frac{\delta(r-r')}{r^2\sin\theta'}\, \delta(\theta-\theta')\, \delta(\phi-\phi') \; ,$$

it is possible to express the angular dependence of this function in terms of spherical harmonics:

$$\frac{\delta(\theta-\theta')\, \delta(\phi-\phi')}{\sin\theta'} = \sum_{n=0}^{\infty} \sum_{m=-n}^{n} b_{nm}\, P_n^m(\cos\theta)\, e^{im\phi} \; . \tag{8.102}$$

The unknown coefficients $b_{nm}$'s can easily be obtained using the orthogonality properties of the spherical harmonics and are given by

$$b_{nm} = \frac{(2n+1)(n-m)!}{4\pi(n+m)!} P_n^m(\cos\theta')\, e^{-im\phi'} \,. \tag{8.103}$$

Hence,

$$\delta(\theta-\theta')\,\delta(\phi-\phi') = \frac{\sin\theta'}{4\pi} \sum_{n=0}^{\infty} \sum_{m=-n}^{n} \frac{(2n+1)(n-m)!}{(n+m)!} P_n^m(\cos\theta')\, P_n^m(\cos\theta)\, e^{im(\phi-\phi')} \,.$$

By substituting Eqs. (8.101) and (8.102) into Eq. (8.99), it can be shown that

$$\frac{d}{dr}\left(r^2 \frac{d\mathcal{R}_n(kr)}{dr}\right) + \left[(kr)^2 - n(n+1)\right] \mathcal{R}_n(kr) = -\delta(r-r') \,, \tag{8.104}$$

with

$$a_{nm} = \frac{(2n+1)(n-m)!}{4\pi(n+m)!} P_n^m(\cos\theta')\, e^{-im\phi'} \,. \tag{8.105}$$

The solution to Eq. (8.104) is an appropriate spherical Bessel function. For $r < r'$, the function must be regular, and for $r > r'$ the spherical Bessel function must be an outward-traveling wave, or equivalently

$$\mathcal{R}_{n<}(kr) = c_n\, j_n(kr) \qquad r \le r' \tag{8.106a}$$

and

$$\mathcal{R}_{n>}(kr) = d_n\, h_n^{(1)}(kr) \qquad r \ge r' \,. \tag{8.106b}$$

$\mathcal{R}_n(kr)$ must be continuous at $r = r'$; that is, $\mathcal{R}_{n<}(kr') = \mathcal{R}_{n>}(kr)$ and $r^2\,[d\mathcal{R}_n(kr)/dr]$ must have a jump discontinuity at $r = r'$. In other words,

$$\left.\frac{d\mathcal{R}_{n>}(kr)}{dr}\right|_{r=r'} - \left.\frac{d\mathcal{R}_{n<}(kr)}{dr}\right|_{r=r'} = -\frac{1}{r'^2} \,. \tag{8.107}$$

These two equations can be used to find the unknowns from

$$c_n\, j_n(kr') = d_n\, h_n^{(1)}(kr') \tag{8.108a}$$

and

$$k\, h_n^{(1)\prime}(kr')\, d_n - k\, j_n'(kr)\, c_n = -\frac{1}{r'^2} \,. \tag{8.108b}$$

Using the Wronskian relations,

$$j_n(kr')\, h_n^{(1)\prime}(kr') - j_n'(kr')\, h_n^{(1)}(kr') = \frac{i}{(kr')^2} \,, \tag{8.109}$$

the unknown coefficients are found to be

$$c_n = ik\, h_n^{(1)}(kr') \tag{8.110a}$$

and

$$d_n = ik\, j_n(kr') \; . \tag{8.110b}$$

As a result, Eq. (8.101) can be written as

$$\psi(\mathbf{r},\mathbf{r}') = \frac{ik}{4\pi} \begin{cases} \displaystyle\sum_{n=0}^{\infty}\sum_{m=-n}^{n} \frac{(2n+1)(n-m)!}{(n+m)!}\, h_n^{(1)}(kr')\, j_n(kr)\, P_n^m(\cos\theta')\, P_n^m(\cos\theta)\, e^{im(\phi-\phi')} & r \le r' \; , \\ \displaystyle\sum_{n=0}^{\infty}\sum_{m=-n}^{n} \frac{(2n+1)(n-m)!}{(n+m)!}\, j_n(kr')\, h_n^{(1)}(kr)\, P_n^m(\cos\theta')\, P_n^m(\cos\theta)\, e^{im(\phi-\phi')} & r \ge r' \; . \end{cases} \tag{8.111}$$

Comparing Eq. (8.111) with Eq. (8.104), the expression for the addition theorem is obtained. It turns out that associated Legendre polynomials satisfy the same differential equation whether $m$ is positive or negative. In order for the orthogonality coefficients to work for all positive or negative $m$,

$$P_n^{-m}(x) = (-1)^m\, \frac{(n-m)!}{(n+m)!}\, P_n^m(x) \; .$$

With this definition it can be shown that

$$\frac{(2n+1)(n-m)!}{(n+m)!}\, P_n^m(\cos\theta')\, P_n^m(\cos\theta) = \frac{(2n+1)(n-|m|!)}{(n+|m|!)}\, P_n^{|m|}(\cos\theta')\, P_n^{|m|}(\cos\theta) \; .$$

As a result,

$$h_0^{(1)}(k|\mathbf{r},\mathbf{r}'|) = \begin{cases} \displaystyle\sum_{n=0}^{\infty}\sum_{m=0}^{n} \alpha_m\, \frac{(2n+1)(n-m)!}{(n+m)!}\, j_n(kr)\, h_n^{(1)\prime}(kr)\, P_n^m(\cos\theta')\, P_n^m(\cos\theta)\cos[m(\phi-\phi')] & r \le r' \; , \\ \displaystyle\sum_{n=0}^{\infty}\sum_{m=0}^{n} \alpha_m\, \frac{(2n+1)(n-m)!}{(n+m)!}\, h_n^{(1)}(kr)\, j_n'(kr)\, P_n^m(\cos\theta')\, P_n^m(\cos\theta)\cos[m(\phi-\phi')] & r \ge r' \; , \end{cases}$$

where $\alpha_m$ is Neumann's number defined as

$$\alpha_m = \begin{cases} 1 & m = 0 \; , \\ 2 & m > 0 \; . \end{cases}$$

## 8-3 Multipole Representation of Spherical Waves

In this section we show that spherical wave functions of order $nm$, such as

$$\psi_{nm}(\mathbf{r}) = h_n^{(1)}(kr)\, P_n^m(\cos\theta) \begin{cases} \cos m\phi\ , \\ \sin m\phi\ , \end{cases}$$

can be represented by the magnetic vector potential of an ordered $2n$-element array of closely spaced small Hertzian $z$-directed current elements flowing in the opposite direction of their adjacent elements. An isolated $z$-directed Hertzian current element is referred to as ***monopole*** and two adjacent $z$-directed current elements are referred to as ***dipole***. Figure 8-14 shows the geometry of a monopole, three different dipoles, and a quadrupole. Higher-multipole sources can be realized by induction.

The fields generated by a small current filament were studied extensively in Chapter 3. The magnetic vector potential for such a current was found to be

$$A_z(\mathbf{r}) = \frac{\mu I\, d\ell}{4\pi}\,\frac{e^{ikr}}{r} \tag{8.112}$$

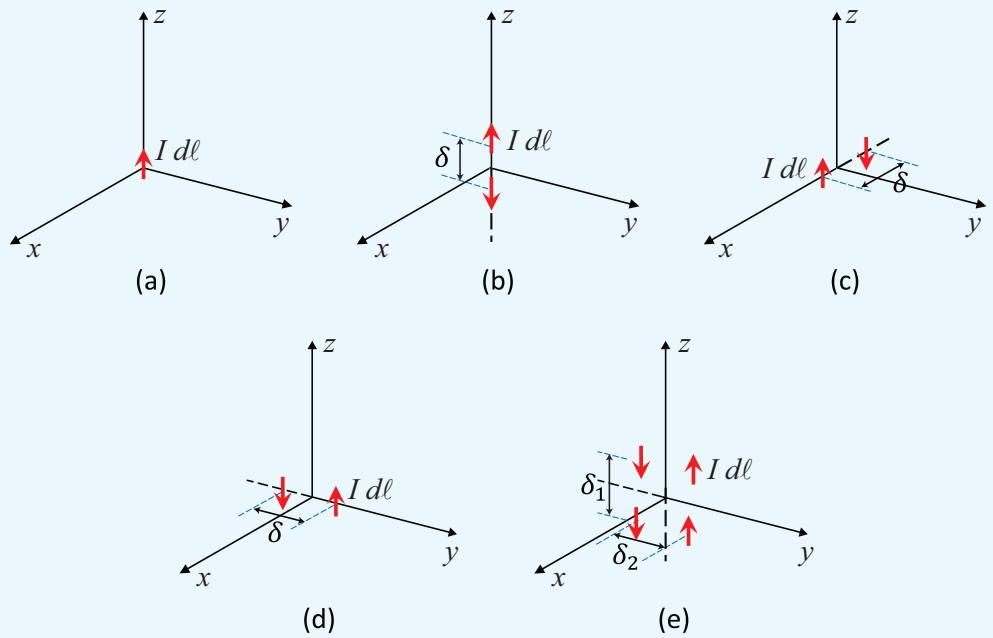


**Figure 8-14:** (a) The geometry of a monopole, (b) a dipole, (c) a different dipole, (d) another different dipole, and (e) a quadrupole.

Recalling that

$$h_0^{(1)}(kr) = \frac{e^{ikr}}{ikr} ,$$

it follows that

$$A_z(\mathbf{r}) = \frac{i\mu kI\, d\ell}{4\pi}\, h_0^{(1)}(kr) . \tag{8.113}$$

This corresponds to a spherical harmonic function of $n = 0$ order. Also, the resulting magnetic field can be obtained from Eq. (3.123) and is given by

$$\mathbf{H}(\mathbf{r}) = \frac{k^2 I\, d\ell}{4\pi} \left(-i + \frac{1}{kr}\right) \frac{e^{ikr}}{r} \sin\theta\, \hat{\boldsymbol{\phi}} . \tag{8.114}$$

Since the current is $r$-directed at $\theta = 0$, the fields can also be generated from $A_r$ (TM-to-$r$). Using Eq. (8.11b), we have

$$H_\phi(\mathbf{r}) = -\frac{1}{\mu r} \frac{\partial A_r}{\partial \theta} . \tag{8.115}$$

Comparing Eqs. (8.114) and (8.115), the expression for $A_r$ is found to be

$$A_r(\mathbf{r}) = \frac{\mu k^2 I\, d\ell}{4\pi} \left(-i + \frac{1}{kr}\right) e^{ikr} \cos\theta . \tag{8.116}$$

Using Eqs. (8.22a), (8.22b), and (8.24a), it can easily be shown that

$$\hat{h}_1^{(1)}(kr) = -\left(1 + \frac{i}{kr}\right) e^{ikr} . \tag{8.117}$$

Also, from Eq. (8.38b),

$$P_1(\cos\theta) = \cos\theta ,$$

therefore, the expression for $A_r$ given by Eq. (8.116) can also be expressed by

$$A_r(\mathbf{r}) = \frac{i\mu k^2 I\, d\ell}{4\pi}\, \hat{h}_1^{(1)}(kr)\, P_1(\cos\theta) . \tag{8.118}$$

Note that in a source-free homogeneous region (with $r > d\ell$), in general, $A_r(\mathbf{r})$ can be written as

$$A_r(\mathbf{r}) = \sum_{n=0}^{\infty} \sum_{m=0}^{n} a_{nm}\, \hat{h}_n^{(1)}(kr)\, P_n^m(\cos\theta) \begin{cases} \cos m\phi , \\ \sin m\phi . \end{cases} \tag{8.119}$$

Comparing Eqs. (8.118) and (8.119), it is noted that

$$a_{nm} = \begin{cases} 0 & n \neq 1 \text{ and for all } m , \\ \dfrac{i\mu k^2 I\, d\ell}{4\pi} & n = 1,\ m = 0 . \end{cases} \tag{8.120}$$

Now let's consider Fig. 8-14(b) for a dipole arrangement along the $z$-axis. The overall magnetic vector potential is the superposition of the vector potentials from each current source

separated by a small distance $\delta$. Representing this magnetic vector potential by $A_z^{2_z}$, it can easily be shown that

$$\begin{aligned} A_z^{2_z} &= A_z^1(x,\, y,\, z-\delta/2) - A_z^1(x,\, y,\, z+\delta/2) \\ &\approx -\delta\, \frac{\partial A_z^1}{\partial z} = -i\, \frac{\mu k I\, d\ell\, \delta}{4\pi}\, \frac{\partial}{\partial z}\, h_0^{(1)}(kr)\ . \end{aligned} \tag{8.121}$$

Noting that

$$\frac{\partial}{\partial z}\, h_0^{(1)}(kr) = k\, h_0^{(1)'}(kr)\, \frac{\partial r}{\partial z} = k\, h_0^{(1)'}(kr)\, \cos\theta\ ,$$

and recognizing that

$$h_0^{(1)'}(kr) = -h_1^{(1)}(kr)\ ,$$

the vector potential for the dipole becomes

$$A_z^{2_z}(\mathbf{r}) = \frac{i\mu k I\, d\ell\, \delta}{4\pi}\, h_1^{(1)}(kr)\, P_1(\cos\theta)\ . \tag{8.122}$$

This corresponds to a spherical wave function with $n = 1$ and $m = 0$. In a similar manner, the magnetic vector potential for the dipole arrangement of Fig. 8-14(c) can be written as

$$\begin{aligned} A_z^{2_x}(\mathbf{r}) \approx -\delta\, \frac{\partial A_z^1}{\partial x} &= \frac{-i\mu k I\, d\ell\, \delta}{4\pi}\, \frac{\partial}{\partial x}\, h_0^{(1)}(kr) \\ &= \frac{-i\mu k I\, d\ell\, \delta}{4\pi}\, h_0^{(1)'}(kr)\, \sin\theta\cos\phi\ . \end{aligned} \tag{8.123}$$

Noting that

$$\sin\theta = P_1^1(\cos\theta)\ ,$$

Eq. (8.123) can be written as

$$A_z^{2_x}(\mathbf{r}) = \frac{i\mu k I\, d\ell\, \delta}{4\pi}\, h_1^{(1)}(kr)\, P_1^1(\cos\theta)\, \cos\phi\ , \tag{8.124}$$

and this corresponds to a spherical wave function with $n = 1$ and $m = 1$ for an even function of $\phi$.

In a similar manner for the dipole configuration of Fig. 8-14(d), the vector potential is given by

$$A_z^{2_y}(\mathbf{r}) = \frac{i\mu k I\, d\ell\, \delta}{4\pi}\, h_1^{(1)}(kr)\, P_1^1(\cos\theta)\, \sin\phi\ , \tag{8.125}$$

which corresponds to a spherical wave function with $n = 1$ and $m = 1$ for an odd function of $\phi$.

For the quadrupole of Fig. 8-14(e), the magnetic vector potential can be obtained by following a similar procedure. Again assuming the separations between the opposing current elements are much smaller than the wavelength, the magnetic vector potential for the

quadrupole can be obtained from

$$A_z^{4_{y,z}}(\mathbf{r}) = \delta_1 \delta_2 \, \frac{\partial^2 A_z^1(\mathbf{r})}{\partial y \, \partial z} \, , \tag{8.126}$$

or alternatively

$$A_z^{4_{y,z}}(\mathbf{r}) = -\delta_2 \, \frac{\partial A_z^{2_z}}{\partial y} \, . \tag{8.127}$$

Noting that

$$\begin{aligned} \frac{\partial}{\partial y}\left[h_1^{(1)}(kr)\cos\theta\right] &= \frac{z}{r}\,\frac{\partial}{\partial y}\left[h_1^{(1)}(kr)\right] + h_1^{(1)}(kr)\,\frac{\partial}{\partial y}\left(\frac{z}{r}\right) \\ &= \frac{z}{r}\,\frac{\partial r}{\partial y}\,\frac{\partial}{\partial r}\left[h_1^{(1)}(kr)\right] + h_1^{(1)}(kr)\left(\frac{-yz}{r^3}\right) \\ &= \frac{yzk}{r^2}\left[h_1^{(1)\prime}(kr) - \frac{1}{kr}\,h_1^{(1)}(kr)\right] \, . \end{aligned} \tag{8.128}$$

Using Eq. (8.24c), it can be shown that

$$h_1^{(1)\prime}(kr) - \frac{1}{kr}\,h_1^{(1)}(kr) = -h_2^{(1)}(kr) \, . \tag{8.129}$$

As a result from Eq. (8.127), the magnetic vector potential for the quadrupole of Fig. 8-14(e) can be obtained from

$$A_z^{4_{y,z}}(\mathbf{r}) = \frac{i\mu k^2 I \, d\ell \, \delta_1 \delta_2}{4\pi} \, h_2^{(1)}(kr) \, \sin\theta\cos\theta\sin\phi \, . \tag{8.130}$$

Using Eqs. (8.38c) and (8.39a), it can be shown that

$$P_2^1(\cos\theta) = -3\sin\theta\cos\theta \, . \tag{8.131}$$

As a result, Eq. (8.130) can be written as

$$A_z^{4_{y,z}}(\mathbf{r}) = \frac{-i\mu k^2 I \, d\ell \, \delta_1 \delta_2}{12\pi} \, h_2^{(1)}(kr) \, P_2^1(\cos\theta)\sin\phi \, . \tag{8.132}$$

In Eq. (8.132) it is shown that the magnetic vector potential of a quadrupole placed in the $y$–$z$ plane is entirely presented by a spherical wave function with $n = 2$ and $m = 1$. In fact, any spherical wave function of order $n$ represents the magnetic vector potential of a multipole of $2n$-element array of $z$-directed current filaments that are closely spaced.

It is interesting to note that if one sets the currents and separations of a collection of multipoles to commensurate the coefficients obtained in Example 8-1 for a truncated expansion of spherical delta function, such an electrically small array can, in principle, produce a highly directive radiation pattern. However, in practice this is quite limited due

to the mutual coupling among the elements and the need for exponentially growing level of currents for high-order multipoles.

## 8-4 Plane-Wave Scattering from Spheres

Spherical objects are among the very few geometries for which analytical solutions can be found for the field scattered in response to plane-wave excitation. In this section we consider plane-wave scattering from metallic and dielectric spherical objects.

### 8-4.1 Scattering from a Metallic Sphere

We are now in a position to tackle the problem of electromagnetic wave scattering from spherical objects. Consider a metallic sphere centered at the origin of a Cartesian coordinate system and having a radius $a$, as shown in Fig. 8-15. Also, consider a plane wave propagating in the $+z$ direction. Without loss of generality, let's assume the electric field is polarized along

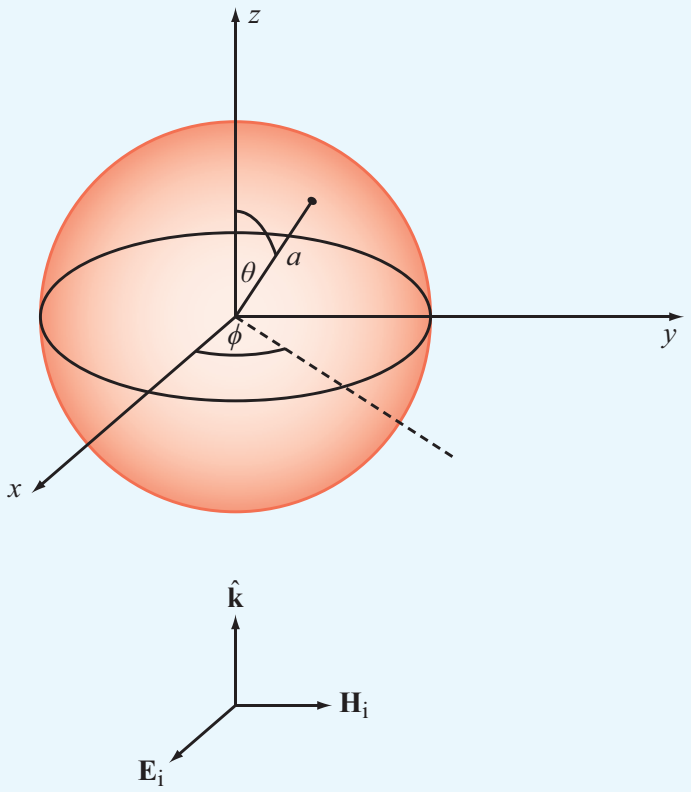


**Figure 8-15:** Geometry of a metallic sphere illuminated by a plane wave.

the $\hat{\mathbf{x}}$ direction. In this case,

$$\mathbf{E}^{\mathrm{i}} = E_0 \hat{\mathbf{x}} e^{ikz} \tag{8.133a}$$

and

$$\mathbf{H}^{\mathrm{i}} = \frac{E_0}{\eta}\, \hat{\mathbf{y}} e^{ikz} \,. \tag{8.133b}$$

The incident field can be expressed in terms of a superposition of TE- and TM-to-$r$ waves. The $r$-component of the incident electric and magnetic fields are found to be

$$\mathbf{E}^{\mathrm{i}}_{\mathrm{r}} = \mathbf{E}^{\mathrm{i}} \cdot \hat{\mathbf{r}} = E_0 \cos\phi \sin\theta\, e^{ikr\cos\theta} = E_0\, \frac{\cos\phi}{-ikr}\, \frac{d}{d\theta}\, e^{ikr\cos\theta}$$

and

$$\mathbf{H}^{\mathrm{i}}_{\mathrm{r}} = \mathbf{H}^{\mathrm{i}} \cdot \hat{\mathbf{r}} = \frac{E_0}{\eta} \frac{\sin\phi}{-ikr} \frac{d}{d\theta}\, (e^{ikr\cos\theta}) \,.$$

Using Eq. (8.39a), it can easily be shown that

$$\frac{d}{d\theta}\, P_n(\cos\theta) = P_n^1(\cos\theta) \,,$$

and using the expansion given by Eq. (8.94), we have

$$E^{\mathrm{i}}_{\mathrm{r}} = \frac{E_0 \cos\phi}{-i(kr)^2} \sum_{n=1}^{\infty} (i)^n (2n+1)\, \hat{j}_n(kr)\, P_n^1(\cos\theta) \tag{8.134a}$$

and

$$H^{\mathrm{i}}_{\mathrm{r}} = \frac{E_0 \sin\phi}{-i(kr)^2\eta} \sum_{n=1}^{\infty} (i)^n (2n+1)\, \hat{j}_n(kr)\, P_n^1(\cos\theta) \,, \tag{8.134b}$$

where $\hat{j}_n(kr)$ is the Schelkunoff spherical Bessel function defined in Eq. (8.32).

According to Eq. (8.10), the corresponding magnetic vector potential that can generate the incident wave is found to be

$$A^i_{\mathrm{r}} = \frac{E_0}{\omega} \cos\phi \sum_{n=1}^{\infty} \frac{(i)^n (2n+1)}{n(n+1)}\, \hat{j}_n(kr)\, P_n^1(\cos\theta) \,,$$

where we have used Eq. (8.43) to show that

$$\frac{d^2}{dr^2}\, \hat{j}_n(kr) = \left( \frac{n(n+1)}{r^2} - k^2 \right)\, \hat{j}_n(kr) \,.$$

In a similar manner the electric vector potential is determined to be

$$A^{\mathrm{i}}_{\mathrm{mr}} = \frac{E_0}{\omega\eta}\,\sin\phi\,\sum_{n=1}^{\infty}\frac{(i)^n(2n+1)}{n(n+1)}\,\hat{j}_n(kr)\,P_n^1(\cos\theta)\;.$$

The scatterer is symmetric with respect to $\phi$; however, as shown above, the incident field has $\phi$-dependency. Using Eq. (8.41) and noting the orthogonality sine and cosine functions, the scattered potential functions can be written as

$$A^{\mathrm{s}}_{\mathrm{r}} = \frac{E_0}{\omega}\,\cos\phi\,\sum_{n=1}^{\infty}a_n\,\hat{h}_n^{(1)}\,(kr)\,P_n^1(\cos\theta)$$

and

$$A^{\mathrm{s}}_{\mathrm{mr}} = \frac{E_0}{\omega\eta}\,\sin\phi\,\sum_{n=1}^{\infty}b_n\,\hat{h}_n^{(1)}\,(kr)\,P_n^1(\cos\theta)\;.$$

Equation (8.10) can be used to find the electric field. For a metallic sphere, boundary conditions mandate that the tangential electric field vanish at the sphere's surface ($r = a$). That is,

$$(E^{\mathrm{i}}_{\theta} + E^{\mathrm{s}}_{\theta})\big|_{r=a} = 0$$

and

$$(E^{\mathrm{i}}_{\phi} + E^{\mathrm{s}}_{\phi})\big|_{r=a} = 0\;.$$

This is satisfied if

$$\left(\frac{\partial}{\partial r}A^{\mathrm{i}}_{\mathrm{r}} + \frac{\partial}{\partial r}A^{\mathrm{s}}_{\mathrm{r}}\right)\bigg|_{r=a} = 0 \tag{8.135}$$

and

$$(A^{\mathrm{i}}_{\mathrm{mr}} + A^{\mathrm{s}}_{\mathrm{mr}})\big|_{r=a} = 0\;. \tag{8.136}$$

Equation (8.135) provides

$$a_n = -\frac{(i)^n(2n+1)}{n(n+1)}\,\frac{\hat{j}_n'(ka)}{\hat{h}_n^{(1)\prime}(ka)}\;. \tag{8.137}$$

Also, Eq. (8.136) provides

$$b_n = -\frac{(i)^n(2n+1)}{n(n+1)}\,\frac{\hat{j}_n(ka)}{\hat{h}_n^{(1)}(ka)}\;. \tag{8.138}$$

The scattered field can easily be computed by combining Eqs. (8.10) and (8.12):

$$E^{\mathrm{s}}_{\mathrm{r}} = \frac{\omega\mu\varepsilon E_0}{(kr)}\cos\phi\,\sum_{n=1}^{\infty}n(n+1)a_n\,\frac{\hat{h}_n^{(1)}(kr)}{(kr)}\,P_n^1(\cos\theta)\;, \tag{8.139a}$$

$$E_\theta^{\rm s} = -E_0 \cos\phi \sum_{n=1}^{\infty} \left( i a_n \frac{\hat{h}_n^{(1)\prime}(kr)}{(kr)} \sin\theta \, P_n^{1\prime}(\cos\theta) + b_n \frac{\hat{h}_n^{(1)}(kr)}{(kr)} \frac{P_n^1(\cos\theta)}{\sin\theta} \right) , \quad (8.139b)$$

and

$$E_\phi^{\rm s} = -E_0 \sin\phi \sum_{n=1}^{\infty} \left( i a_n \frac{\hat{h}_n^{(1)\prime}(kr)}{(kr)} \frac{P_n^1(\cos\theta)}{\sin\theta} + b_n \frac{\hat{h}_n^{(1)}(kr)}{(kr)} \sin\theta \, P_n^{1\prime}(\cos\theta) \right) . \quad (8.139c)$$

The scattered magnetic field components are also found in a similar manner:

$$H_{\rm r}^{\rm s} = \frac{\omega\mu\varepsilon E_0}{(kr)\eta} \sin\phi \sum_{n=1}^{\infty} n(n+1) b_n \frac{\hat{h}_n^{(1)}(kr)}{(kr)} P_n^{(1)}(\cos\theta) , \quad (8.140a)$$

$$H_\theta^{\rm s} = -\frac{E_0}{\eta} \sin\phi \sum_{n=1}^{\infty} \left( i b_n \frac{\hat{h}_n^{(1)\prime}(kr)}{(kr)} \sin\theta \, P_n^{1\prime}(\cos\theta) + a_n \frac{\hat{h}_n^{(1)}(kr)}{(kr)} \frac{P_n^1(\cos\theta)}{\sin\theta} \right) , \quad (8.140b)$$

and

$$H_\phi^{\rm s} = \frac{E_0}{\eta} \cos\phi \sum_{n=1}^{\infty} \left( i b_n \frac{\hat{h}_n^{(1)\prime}(kr)}{(kr)} \frac{P_n^1(\cos\theta)}{\sin\theta} + a_n \frac{\hat{h}_n^{(1)}(kr)}{(kr)} \sin\theta \, P_n^{1\prime}(\cos\theta) \right) . \quad (8.140c)$$

In the far-field region, only the $\theta$ and $\phi$ components of the scattered field remain, noting the large-argument expansion of $\hat{h}_n^{(1)}$ given by Eq. (8.26). Also, noting that

$$\lim_{kr\to\infty} \hat{h}_n^{(1)\prime}(kr) \approx (-i)^n e^{ikr} ,$$

the field expressions in the far-field region are given by

$$E_\theta^{\rm s} = -iE_0 \cos\phi \frac{e^{ikr}}{kr} \sum_{n=1}^{\infty} (-i)^n \left( a_n \sin\theta \, P_n^{1\prime}(\cos\theta) - b_n \frac{P_n^1(\cos\theta)}{\sin\theta} \right) \quad (8.141a)$$

and

$$E_\phi^{\rm s} = -iE_0 \sin\phi \frac{e^{ikr}}{kr} \sum_{n=1}^{\infty} (-i)^n \left( a_n \frac{P_n^1(\cos\theta)}{\sin\theta} - b_n \sin\theta P_n^{1\prime}(\cos\theta) \right) . \quad (8.141b)$$

Equation (8.141) can now be used to find the radar cross section of the sphere. Denoting $E_\theta$ as the co-polarized and $E_\phi$ as the cross-polarized field components, the bistatic radar cross section of a metallic sphere can be computed from

$$\begin{aligned} \sigma_c(\theta,\phi) &= \lim_{r\to\infty} 4\pi r^2 \frac{|E_\theta^{\rm s}|^2}{|E_0|^2} \\ &= \frac{\lambda^2 \cos^2\phi}{\pi} \left| \sum_{n=1}^{\infty} (-i)^n \left( a_n \sin\theta \, P_n^{1\prime}(\cos\theta) - b_n \frac{P_n^1(\cos\theta)}{\sin\theta} \right) \right|^2 \end{aligned} \quad (8.142a)$$

and

$$\sigma_x(\theta,\phi) = \lim_{r\to\infty} 4\pi r^2 \frac{|E_\phi|^2}{|E_0|^2}$$

$$= \frac{\lambda^2 \sin^2\phi}{\pi} \left| \sum_{n=1}^{\infty} (-i)^n \left( a_n \frac{P_n^1(\cos\theta)}{\sin\theta} - b_n \sin\theta \, P_n^{1\prime}(\cos\theta) \right) \right|^2 . \qquad (8.142b)$$

Metallic spheres are often used as calibration targets for radar systems. In such approaches the measured backscatter power by a radar from a target with unknown radar cross section is compared with that from a metallic sphere placed at the same range and location as the unknown target. This radar cross section measurement procedure is known as the ***method of substitution***. Metallic spheres are ideal calibration targets due to their symmetry, and hence they do not need careful positioning and alignment. Equations (8.142a) and (8.142b) can be used to calculate the backscatter radar cross section of a metallic sphere. The backscatter direction is specified by $\theta = \pi$. For the co-polarized component of the scattered field we need to set $\phi = 0$, and for the cross-polarized component $\phi = \pi/2$. To simplify the expression for the backscatter, using Eq. (8.37), we note that $P_n(\pm 1) = (\pm 1)^n$, and using Eq. (8.40) for $m = 0$,

$$\lim_{x\to -1} \frac{dP_n(x)}{dx} = -\frac{n(n+1)}{2} (-1)^n . \qquad (8.143)$$

Also, from Eq. (8.39a),

$$P_n^1(x) = -\sqrt{1-x^2} \, \frac{dP_n(x)}{dx} . \qquad (8.144)$$

Hence

$$\lim_{\theta\to\pi} \frac{P_n^1(\cos\theta)}{\sin\theta} = (-1)^n \frac{n(n+1)}{2} . \qquad (8.145)$$

We also need to simplify $\sin\theta \, P_n^{1\prime}(\cos\theta)$ as $\theta \to \pi$. Using Eq. (8.40) for $m = 1$, it can be shown that

$$\lim_{x\to -1} \sqrt{1-x^2} \, \frac{dP_n^1(x)}{dx} = \lim_{x\to -1} [-P_n''(x) \, (1-x^2) + x P_n'(x)] = (-1)^n \frac{n(n+1)}{2} . \qquad (8.146)$$

Hence, in backscatter,

$$\sigma_c = \frac{\lambda^2}{4\pi} \left| \sum_{n=1}^{\infty} (i)^n n(n+1)(a_n - b_n) \right|^2 , \qquad (8.147)$$

$$\sigma_x = 0 ,$$

but

$$a_n - b_n = \frac{(i)^n(2n+1)}{n(n+1)} \frac{-\hat{j}_n'(ka)\,\hat{h}_n^{(1)}(ka) + \hat{j}_n(ka)\,\hat{h}_n^{(1)\prime}(ka)}{\hat{h}_n^{(1)\prime}(ka)\,\hat{h}_n^{(1)}(ka)}$$
$$= \frac{(i)^{n+1}(2n+1)}{n(n+1)\,\hat{h}_n^{(1)\prime}(ka)\,\hat{h}_n^{(1)}(ka)}\,, \tag{8.148}$$

where the Wronskian relations for the Schelkunoff spherical Bessel functions are used. Substituting Eq. (8.148) into Eq. (8.147), the following equation for the radar cross section of a metallic sphere is obtained:

$$\sigma_c = \frac{\lambda^2}{4\pi} \left| \sum_{n=1}^{\infty} \frac{(-1)^n(2n+1)}{\hat{h}_n^{(1)\prime}(ka)\,\hat{h}_n^{(1)}(ka)} \right|^2 . \tag{8.149}$$

For small values of $ka$ (low-frequency approximation), the following approximation can be used:

$$\lim_{ka\to 0} \frac{1}{\hat{h}_1^{(1)}(ka)} \approx -ka \tag{8.150a}$$

and

$$\lim_{ka\to 0} \frac{1}{\hat{h}_1^{(1)\prime}(ka)} \approx (ka)^2\,, \tag{8.150b}$$

and the summation can be terminated at $n = 1$, as higher terms are proportional to higher powers in $ka$. Hence, when $a \ll \lambda$,

$$\sigma_c^{\mathrm{LF}} = \frac{9\lambda^2}{4\pi}\,(ka)^6\,. \tag{8.151}$$

This equation indicates that the radar cross section of a metallic sphere is proportional to $1/\lambda^4$ and is used to explain why the sky is blue. At high frequencies where the radii of metallic spheres are large compared with the wavelength, it can be shown by using the physical-optics approximation that the co-polarized radar cross section of a metallic sphere is equal to the area of its great circle:

$$\sigma_c^{\mathrm{PO}} = \pi a^2\,. \tag{8.152}$$

Figure 8-16 shows the normalized radar cross section ($\sigma_c/(\pi a^2)$) of a metallic sphere as a function of the normalized radius ($a/\lambda$). Also shown are the low-frequency approximation based on Eq. (8.151) and the high-frequency approximation based on Eq. (8.152). The low-frequency formula given by Eq. (8.151) provides accurate results when $a/\lambda \leq 0.1$. The oscillatory behavior of the RCS around the physical-optics approximation is due to creeping waves. Basically the physical-optics contribution emanates mainly from the specular point on the surface, which is the point closest to the source. The rays at the shadow boundary travel along the surface in the shadow area and emerge from the other side, propagating in

the backscatter direction and can cause constructive or destructive interference. The excess pathlength for the creeping wave is $(2+\pi)a$, and when this is equal to a wavelength, constructive interference occurs. This indicates that the spacing between the peaks or valleys is $\Delta(a/\lambda) \approx 0.2$. The creeping waves shed energy as they travel along the surface. Hence, the larger is the radius, the weaker is the signal that emerges from the other side, and hence the level of the peaks in the RCS as a function of $a/\lambda$ decreases with increasing $a/\lambda$. Figure 8-17 shows the ray representation of the creeping waves around the surface of the metallic sphere.

### 8-4.2 Scattering from a Dielectric Sphere

Electromagnetic scattering from a dielectric sphere can be obtained following a similar procedure. Consider the geometry of the problem given in Fig. 8-15. In this case, however, we assume that the sphere is a homogeneous dielectric material with permittivity $\varepsilon_s$ and permeability $\mu_s$. In addition to the fields outside the sphere we need to consider the interior fields that can be generated from the following TM- and TE-to-$r$ potentials:

$$A_r^d = \frac{E_0}{\omega}\cos\phi \sum_{n=1}^{\infty} c_n \hat{j}_n(k_s r)\, P_n^1(\cos\theta) \tag{8.153a}$$

and

$$A_{mr}^d = \frac{E_0}{\omega\eta}\sin\phi \sum_{n=1}^{\infty} d_n\, j_n(k_s r)\, P_n^1(\cos\theta)\ , \tag{8.153b}$$

where $k_s = \omega\sqrt{\mu_s\varepsilon_s}$. The incident and scattered potentials have the same form as those for the metallic sphere. To find the four sets of unknown coefficients $a_n$, $b_n$, $c_n$, and $d_n$, the boundary condition relationship can be used. Basically,

$$(E_\theta^i + E_\theta^s)\big|_{r=a} = E_\theta^d\big|_{r=a}\ , \tag{8.154a}$$

$$(E_\phi^i + E_\phi^s)\big|_{r=a} = E_\phi^d\big|_{r=a}\ , \tag{8.154b}$$

$$(H_\theta^i + H_\theta^s)\big|_{r=a} = H_\theta^d\big|_{r=a}\ , \tag{8.154c}$$

and

$$(H_\phi^i + H_\phi^s)\big|_{r=a} = H_\phi^d\big|_{r=a}\ . \tag{8.154d}$$

Using Eqs. (8.10)–(8.12), it can easily be shown that Eq. (8.154) is satisfied if

$$\frac{\partial}{\partial r}(A_r^i + A_r^s)\big|_{r=a} = \frac{\partial}{\partial r}A_r^d\big|_{r=a}\ ,$$

$$(A_r^i + A_r^s)\big|_{r=a} = A_r^d\big|_{r=a}\ ,$$

$$\frac{\partial}{\partial r}(A_{mr}^i + A_{mr}^s)\big|_{r=a} = \frac{\partial}{\partial r}A_{mr}^d\big|_{r=a}\ ,$$

and

$$(A_{mr}^i + A_{mr}^s)\big|_{r=a} = A_{mr}^d\big|_{r=a}\ .$$

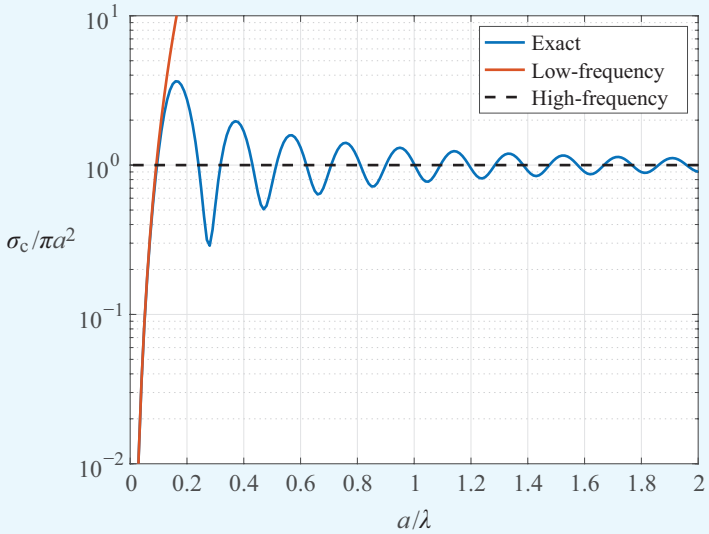


**Figure 8-16:** The normalized backscatter radar cross section of a metallic sphere as a function of the normalized radius ($a/\lambda$). Also shown are the low- and high-frequency approximations.

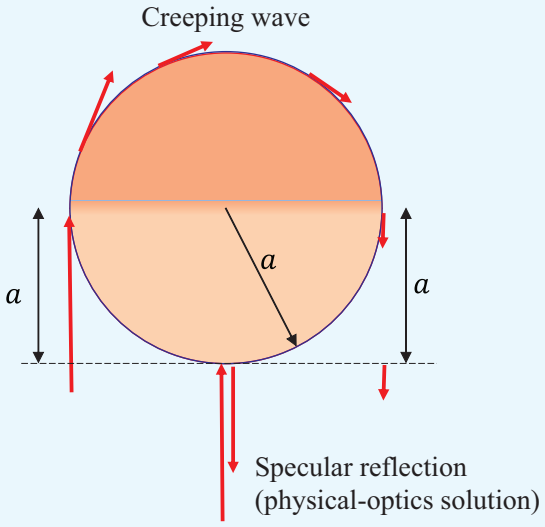


**Figure 8-17:** The ray representation of creeping waves around a metallic sphere. The creeping waves in backscatter interfere with the reflected ray from the specular point and cause the ripple observed in the RCS shown in Fig. 8-16 as a function of $a/\lambda$.

These give four equations for the four unknowns, which can be solved simultaneously to find

$$a_n = \frac{(i)^n(2n+1)}{n(n+1)} \frac{-\sqrt{\varepsilon_s/\varepsilon_0}\,\hat{j}_n'(ka)\,\hat{j}_n(k_s a) + \sqrt{\mu_s/\mu_0}\,\hat{j}_n(ka)\,\hat{j}_n'(k_s a)}{\sqrt{\varepsilon_s/\varepsilon_0}\,\hat{h}_n^{(1)\prime}(ka)\,\hat{j}_n(k_s a) - \sqrt{\mu_s/\mu_0}\,\hat{h}_n^{(1)}(ka)\,\hat{j}_n'(k_s a)}\,, \tag{8.155a}$$

$$b_n = \frac{(i)^n(2n+1)}{n(n+1)} \frac{-\sqrt{\varepsilon_s/\varepsilon_0}\,\hat{j}_n(ka)\,\hat{j}_n'(k_s a) + \sqrt{\mu_s/\mu_0}\,\hat{j}_n'(ka)\,\hat{j}_n(k_s a)}{\sqrt{\varepsilon_s/\varepsilon_0}\,\hat{h}_n^{(1)}(ka)\,\hat{j}_n'(k_s a) - \sqrt{\mu_s/\mu_0}\,\hat{h}_n^{(1)\prime}(ka)\,\hat{j}_n(k_s a)}\,, \tag{8.155b}$$

$$c_n = \frac{(i)^n(2n+1)}{n(n+1)} \frac{i\sqrt{\varepsilon_s/\varepsilon_0}}{\sqrt{\varepsilon_s/\varepsilon_0}\,\hat{h}_n^{(1)\prime}(ka)\,\hat{j}_n(k_s a) - \sqrt{\mu_s/\mu_0}\,\hat{h}_n^{(1)}(ka)\,\hat{j}_n'(k_s a)}\,, \tag{8.155c}$$

and

$$d_n = \frac{(i)^n(2n+1)}{n(n+1)} \frac{-i\sqrt{\mu_s/\mu_0}}{\sqrt{\varepsilon_s/\varepsilon_0}\,\hat{h}_n^{(1)}(ka)\,\hat{j}_n'(k_s a) - \sqrt{\mu_s/\mu_0}\,\hat{h}_n^{(1)\prime}(ka)\,\hat{j}_n(k_s a)}\,. \tag{8.155d}$$

In the limiting case as the sphere dielectric $\varepsilon_s$ approaches that of a PEC ($\varepsilon_s \to \varepsilon_0(1+i\infty)$), $a_n$ and $b_n$ given by Eqs. (8.155a) and (8.155b) reduce to those given by Eqs. (8.137) and (8.138) for a metallic sphere. It is also interesting to note that when

$$\frac{\varepsilon_s}{\varepsilon_0} = \frac{\mu_s}{\mu_0}\,, \tag{8.156}$$

the expressions given by Eqs. (8.155a) and (8.155b) lead to

$$a_n = b_n\,. \tag{8.157}$$

The significance of this result is that in the backscatter direction, for which the co-polarized backscatter radar cross section can be computed from Eq. (8.147), the backscatter goes to zero independently of the sphere radius or its relative permittivity and permeability, so long as $\varepsilon_s/\varepsilon_0 = \mu_s/\mu_0$. In this case, a dielectric sphere becomes invisible to a monostatic radar.

In the general case, the backscatter can be computed from Eq. (8.147) using the $a_n$ and $b_n$ coefficients given by Eqs. (8.155a) and (8.155b). As an example, the normalized backscatter RCS values of dielectric spheres with $\mu_s = \mu_0$ and two different values of $\varepsilon_s = 1.6\varepsilon_0$ and $\varepsilon_s = 2\varepsilon_0$, were evaluated as a function of the normalized radius $(a/\lambda)$ and are shown in Fig. 8-18. The highly oscillatory behavior of the RCS, particularly at higher frequencies (large $a/\lambda$), is due to internal resonances of the dielectric sphere. The oscillatory behavior damps out as the dielectric of the sphere becomes lossy.

A low-frequency approximation for the scattering expressions for dielectric spheres can be obtained by expanding the expressions for $a_n$ and $b_n$ in terms of a truncated power series in $(ka)$. This can be done by noting that

$$\hat{j}_n(ka) \approx 2^n \frac{n!}{(2n+1)!}(ka)^{n+1}\left(1 - \frac{n+1}{(2n+1)(2n+3)}(ka)^2 + \cdots\right) \tag{8.158a}$$

and

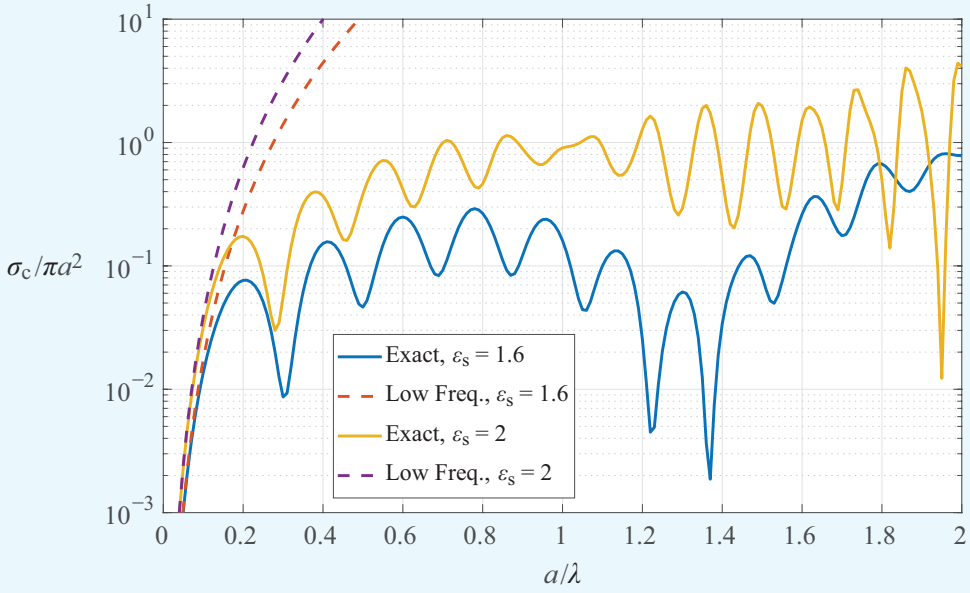


**Figure 8-18:** The normalized backscatter RCS of two dielectric spheres, one with $\varepsilon_s = 1.6\varepsilon_0$ and another with $\varepsilon_s = 2\varepsilon_0$, as a function of the normalized radius $a/\lambda$. Also shown are plots of the low-frequency approximation.

$$\hat{h}_n^{(1)}(ka) \approx \frac{i}{2^n}\,\frac{(2n)!}{n!}\,\frac{1}{(ka)^n} + \cdots \tag{8.158b}$$

Simple expressions can be obtained when $\mu_s = \mu_0$, namely

$$a_1 \approx \frac{1}{30}\left(\frac{\varepsilon_s}{\varepsilon_0} - 1\right)(ka)^5 + \cdots\,, \tag{8.159a}$$

$$a_2 \approx 0\,, \tag{8.159b}$$

$$b_1 \approx i\left[\frac{\varepsilon_s - \varepsilon_0}{\varepsilon_s + 2\varepsilon_0}\,(ka)^3 + \frac{3}{5}\,\frac{(\varepsilon_s - \varepsilon_0)(\varepsilon_s - 2\varepsilon_0)}{(\varepsilon_s + 2\varepsilon_0)^2}\,(ka)^5\right] + \cdots\,, \tag{8.159c}$$

and

$$b_2 \approx \frac{1}{18}\,\frac{\varepsilon_s - \varepsilon_0}{2\varepsilon_s + 3\varepsilon_0}\,(ka)^5 + \cdots \tag{8.159d}$$

For small values of $ka$, the first term of $b_1$ becomes the only significant term. Using $b_1$ only in Eq. (8.76) yields the backscatter RCS for the low-frequency approximation

$$\sigma_c^{\mathrm{LF}} = (\pi a^2)\,4\left|\frac{\varepsilon_s - \varepsilon_0}{\varepsilon_s + 2\varepsilon_0}\right|^2 (ka)^4. \tag{8.160}$$

The computed RCS based on Eq. (8.160) is compared with the results based on the exact solution in Fig. 8-18. Good agreement is observed for $a/\lambda < 0.1$.

For magnetodielectric spheres, it turns out that to the lowest order in $(ka)$, $a_1$ becomes

$$a_1 \approx i\left[\frac{\mu_s - \mu_0}{\mu_s + \mu_0}\right](ka)^3 ,$$

and as a result the low-frequency backscatter RCS for a magneto-dielectric sphere is given by

$$\sigma_c^{LF} = (\pi a^2)\, 4\left|\frac{\varepsilon_s - \varepsilon_0}{\varepsilon_s + 2\varepsilon_0} - \frac{\mu_s - \mu_0}{\mu_s + 2\mu_0}\right|^2 (ka)^4 . \tag{8.161}$$

## 8-5 Wave Propagation in a Conical Waveguide

Consider a metallic cone with a cone angle $\theta_0$ and whose axis coincides with the $z$-axis. We are interested in the fields that can be supported inside the cone portrayed in Fig. 8-19. For an infinite cone, outward-propagating TM waves can be generated from

$$A_r(r,\theta,\phi) = P_{\nu_n^m}^m(\cos\theta)\, \hat{h}_{\nu_n^m}^{(1)}(kr) \begin{cases} \cos m\phi , \\ \sin m\phi , \end{cases} \tag{8.162}$$

where $m$ is an integer, since the domain of interest includes $\phi \in [0, 2\pi]$. The spherical Hankel function of the first kind is chosen for the radial function, since only outward-going waves

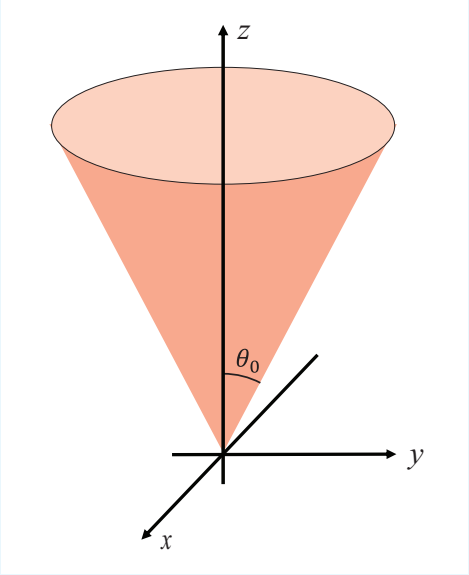


**Figure 8-19:** Geometry of a metallic conical waveguide with cone angle $\theta_0$.

are of interest. The associated Legendre function of the first kind is used, as $\theta = 0$ is included in the domain of interest. Boundary conditions require that $E_\phi = E_r = 0$ at $\theta = \theta_0$. Using Eq. (8.10a) or Eq. (8.10c), it becomes evident that

$$P^m_{\nu^m_n}(\cos\theta_0) = 0 \tag{8.163}$$

for the boundary conditions to be satisfied. Equation (8.163) is the transcendental equation that provides the admissible values of the order of Legendre function of the first kind for different values of $m$ ($\nu^m_n$). Once values of $\nu^m_n$ are found from Eq. (8.163), a potential function constructed from the superposition of modes given by Eq. (8.162) can be used to express a field inside the conical waveguide:

$$A_{\rm r}(r,\theta,\phi) = \sum_{m=0}^{\infty}\sum_{n=1}^{\infty} a_{nm}\, P^m_{\nu^m_n}(\cos\theta)\, \hat{h}^{(1)}_{\nu^m_n}(kr) \begin{cases} \cos m\phi\ , \\ \sin m\phi\ . \end{cases} \tag{8.164}$$

Here $n$ is an index for the ordered zeros of Eq. (8.163), and the superscript $m$ in $\nu^m$ indicates the zeros of Eq. (8.163) for different values of $m$. Note that $\nu^m_n \geq m$. Figure 8-20 shows plots of the transcendental equation for different values of $\theta_0$ and $m$. The zeros of these functions ($\nu^m_n$) are extracted and plotted in Fig. 8-21 as a function of $\theta_0$ for different values of $m$. Considering the fact that

$$\left(\frac{d^2}{dr^2} + k^2\right) \hat{h}^{(1)}_\nu(kr) = \frac{\nu(\nu+1)}{r^2}\, \hat{h}^{(1)}_\nu(kr)\ , \tag{8.165}$$

the field components can be obtained from Eq. (8.10):

$$E_{\rm r} = \frac{-1}{i\omega\mu\varepsilon r^2} \sum_{m=0}^{\infty}\sum_{n=1}^{\infty} a_{mn}\nu^m_n(\nu^m_n+1)\, \hat{h}^{(1)}_{\nu^m_n}(kr)\, P^m_{\nu^m_n}(\cos\theta) \begin{cases} \cos m\phi\ , \\ \sin m\phi\ , \end{cases} \tag{8.166a}$$

$$E_\theta = \frac{k\sin\theta}{i\omega\mu\varepsilon r} \sum_{m=0}^{\infty}\sum_{n=1}^{\infty} a_{mn}\, \hat{h}^{(1)\prime}_{\nu^m_n}(kr)\, P^{m\prime}_{\nu^m_n}(\cos\theta) \begin{cases} \cos m\phi\ , \\ \sin m\phi\ , \end{cases} \tag{8.166b}$$

$$E_\phi = \frac{-k}{i\omega\mu\varepsilon r\sin\theta} \sum_{m=0}^{\infty}\sum_{n=1}^{\infty} m a_{mn}\, \hat{h}^{(1)\prime}_{\nu^m_n}(kr)\, P^m_{\nu^m_n}(\cos\theta) \begin{cases} -\sin m\phi\ , \\ \cos m\phi\ , \end{cases} \tag{8.166c}$$

$$H_\theta = \frac{1}{\mu r\sin\theta} \sum_{m=0}^{\infty}\sum_{n=1}^{\infty} m a_{mn}\, \hat{h}^{(1)}_{\nu^m_n}(kr)\, P^m_{\nu^m_n}(\cos\theta) \begin{cases} -\sin m\phi\ , \\ \cos m\phi\ , \end{cases} \tag{8.166d}$$

and

$$H_\phi = \frac{\sin\theta}{\mu r} \sum_{m=0}^{\infty}\sum_{n=1}^{\infty} a_{mn}\, \hat{h}^{(1)}_{\nu^m_n}(kr)\, P^{m\prime}_{\nu^m_n}(\cos\theta) \begin{cases} \cos m\phi\ , \\ \sin m\phi\ . \end{cases} \tag{8.166e}$$

For the TE-to-$r$ modes, the potential $A_{\rm mr}$ takes a similar form to Eq. (8.162). However, the transcendental equation obtained from Eq. (8.12e) requires that

$$P^{m\prime}_{\nu^m_n}(\cos\theta_0) = 0\ . \tag{8.167}$$

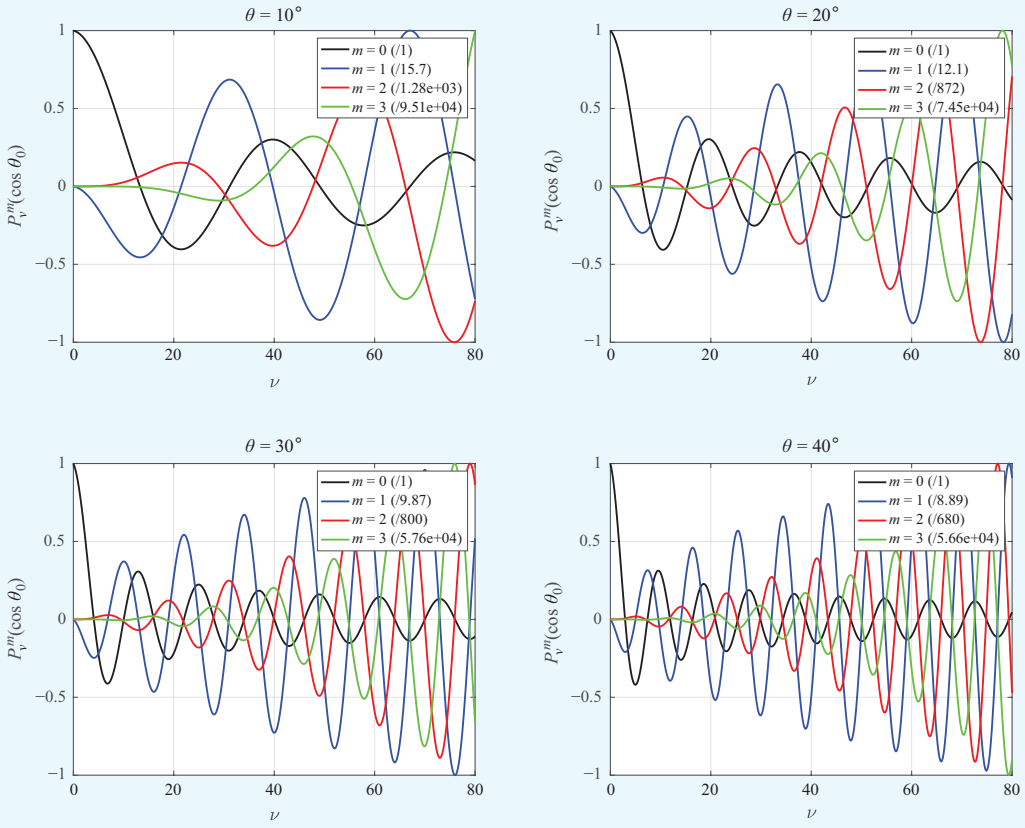


**Figure 8-20:** The plot of transcendental equation Eq. (8.163) for different cone angles $\theta_0 = 10^\circ$, $20^\circ$, $30^\circ$, and $40^\circ$, as a function of $\nu$ for different values of $m$. The zeros of the order $\nu_n^m$ specify the different modes that can be supported in a conical waveguide. The plots shown here for different modes are normalized to their maximum value (noted in the legend) for better viewing.

Once the values of $\nu_n^m$ are obtained for different values of $m$ from Eq. (8.167), the field quantities can be obtained from the dual of Eq. (8.166). Figure 8-23 shows $\nu_n^m$ values as a function of cone angle $\theta_0$ for the TE case. Note that $\nu = 0$ is a solution to Eq. (8.167), but this solution renders null fields inside the conical antenna. In other words, conical antennas cannot support TEM waves, as expected.

A truncated conical waveguide can be used as a horn antenna. Such antennas are usually fed by a circular waveguide. However, it should be noted that modal analysis for such antennas is cumbersome. Figure 8-23 shows the geometry for a conical horn antenna with $\theta_0 = 25^\circ$ and a height of 10 cm, connected to a circular waveguide with a diameter of 3 cm, supporting a $TE_{11}$ mode. The resulting radiation pattern in the far field and the input reflection coefficient as a function of frequency are also shown in this figure. Numerical computation is carried out using an FEM solver.

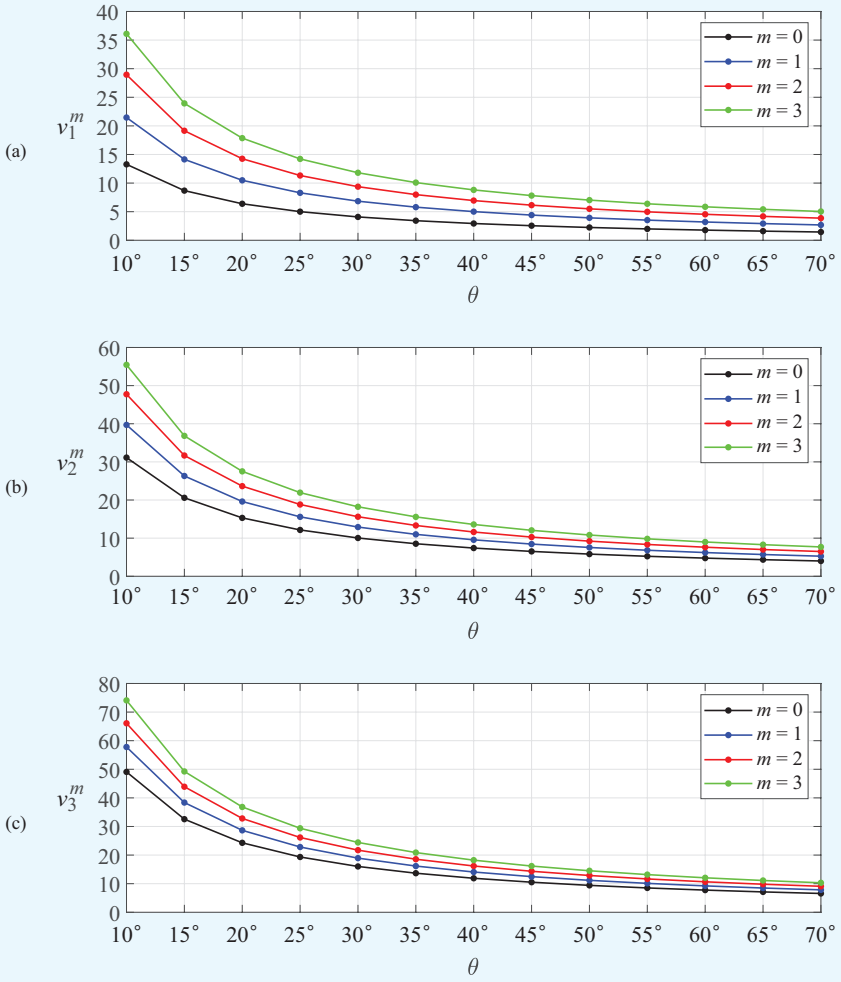


**Figure 8-21:** The zeros of the TM transcendental equation given by Eq. (8.163) are extracted and plotted as a function of the cone angle $\theta$ for multiple values of $m$. (a) shows the first zero $v_1^m$, (b) shows the second zero $v_2^m$, and (c) shows $v_3^m$.

## Example 8-3: Metallic Cone Excited by an External Electric Current

Consider a metallic cone whose axis coincides with the $z$-axis of the Cartesian coordinate system shown in Fig. 8-24. The cone is defined by a constant $\theta_0$ surface. The cone is excited by a spherical surface current that extends between $\theta_1$ and $\theta_2$:

$$\mathbf{J}_s(\mathbf{r}) = \begin{cases} J_0(\theta)\,\hat{\boldsymbol{\phi}} & \theta_1 \le \theta \le \theta_2\,, \\ 0 & \text{otherwise.} \end{cases} \tag{8.168}$$

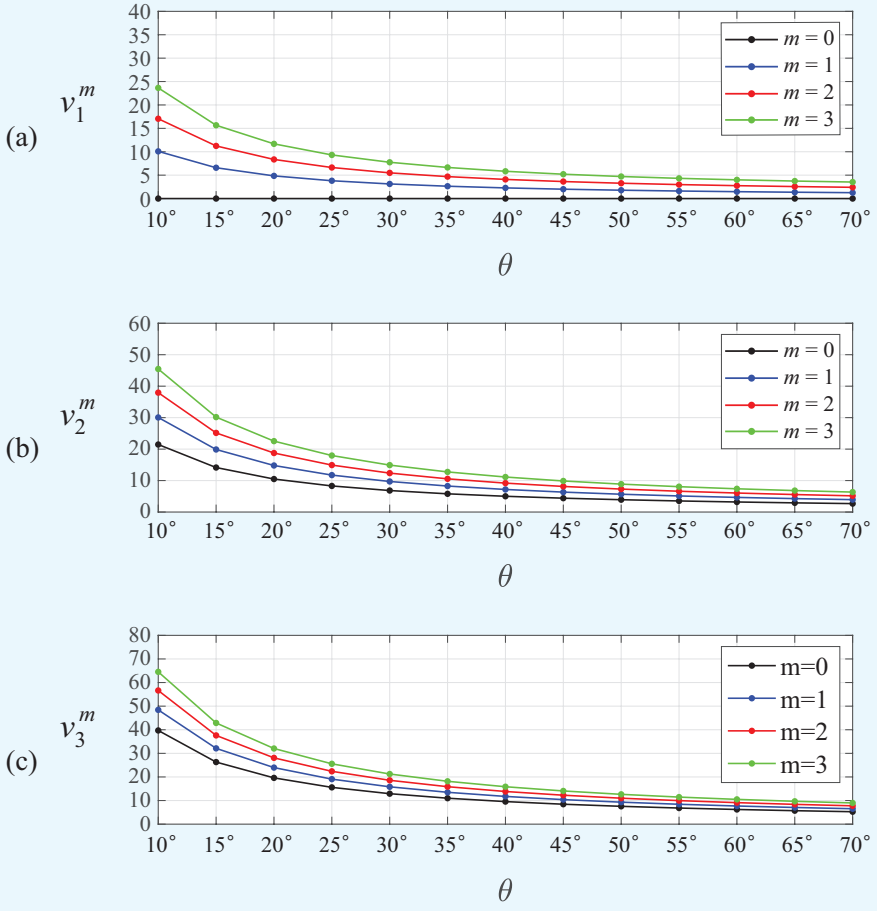


**Figure 8-22:** The zeros of the TE transcendental equation given by Eq. (8.167) are extracted and plotted as a function of the cone angle $\theta$ for multiple values of $m$ values. Part (a) shows the first zero $\nu_1^m$, (b) shows the second zero $\nu_2^m$, and (c) shows $\nu_3^m$.

Find an expression for the electric field.

**Solution:** Since the excitation current is independent of $\phi$ and the cone is also symmetric with respect to $\phi$, all field quantities are independent of variable $\phi$; i.e., $\partial/\partial\phi = 0$. Noting that a $\hat{\boldsymbol{\phi}}$-directed current should produce an electric field that has a $\phi$ component. Noting that for a TM-to-$r$ field, according to Eq. (8.10c), $E_\phi = 0$, it can be concluded that this current can only produce TE-to-$r$ modes, with electric field components given by Eqs. (8.12d) and (8.12e):

$$E_\theta = -\frac{1}{\varepsilon r \sin\theta}\frac{\partial A_{\text{mr}}}{\partial \phi} = 0 \tag{8.169a}$$

and

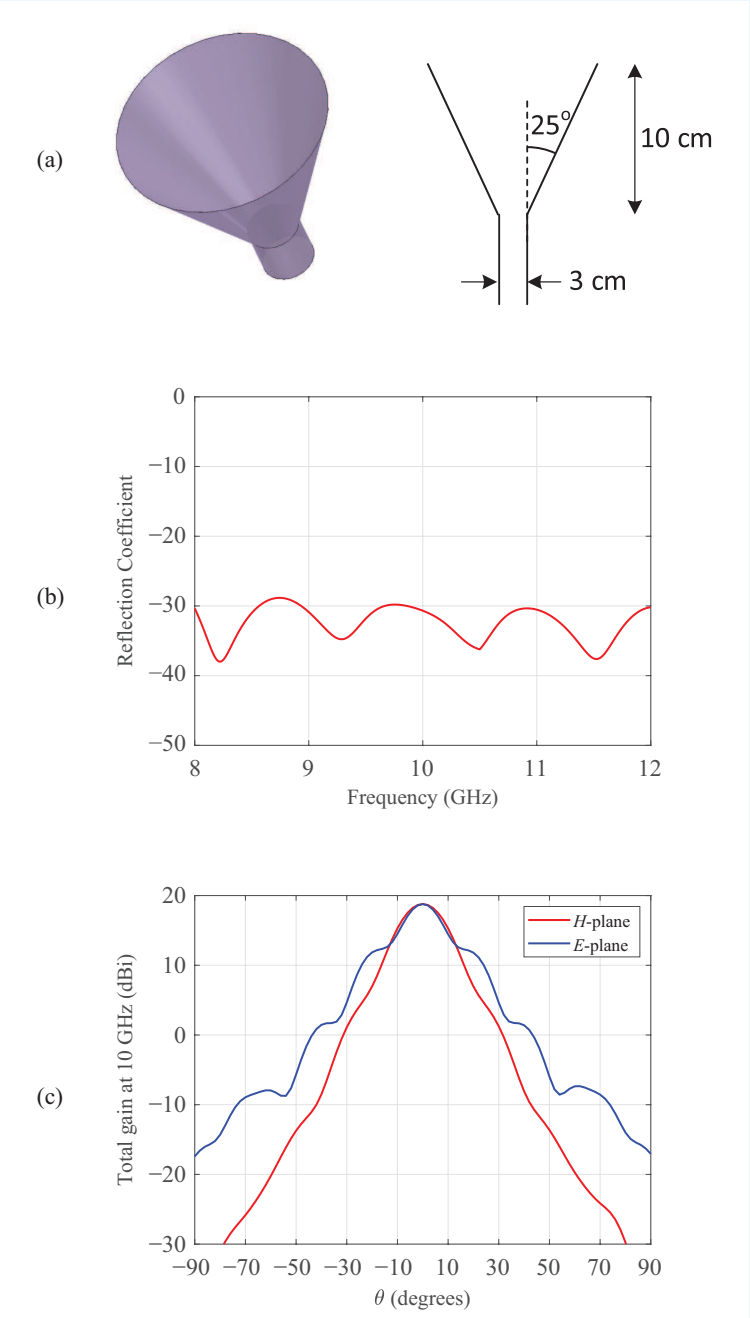


**Figure 8-23:** (a) A conical horn antenna fed by a circular waveguide supporting a $TE_{11}$ mode, (b) the input reflection coefficient as seen by the circular waveguide as a function of frequency, and (c) the far-field radiation pattern in the $E$- and $H$-planes at 10 GHz.

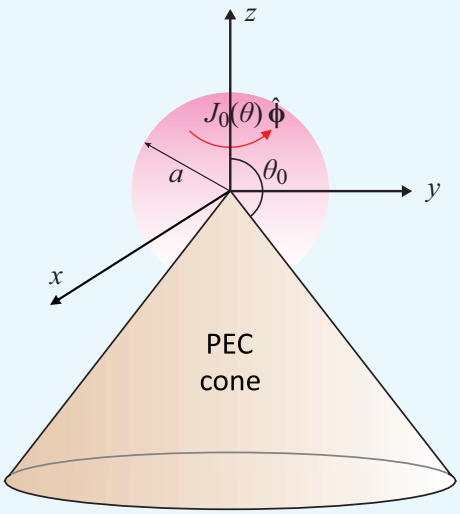


**Figure 8-24:** Geometry of a metallic cone excited by a spherical current sheet flowing in the $\hat{\boldsymbol{\phi}}$-direction with a uniform distribution with respect to $\phi$ but variable along $\theta$. The radius of the spherical current sheet is $a$.

$$E_\phi = \frac{1}{\varepsilon r}\frac{\partial A_{\rm mr}}{\partial \theta}\,. \tag{8.169b}$$

We partition the domain of interest into two regions corresponding to $r < a$ and $r > a$, and for each region we provide an appropriate solution for $A_{\rm mr}(r,\theta)$ in terms of the modes of the conical waveguide. For $r < a$,

$$A^{<}_{\rm mr}(r,\theta) = \sum_{n=1}^{\infty} a_{\nu_n}\, P_{\nu_n}(\cos\theta)\, \hat{j}_{\nu_n}(kr)\,, \tag{8.170a}$$

and for $r > a$,

$$A^{>}_{\rm mr}(r,\theta) = \sum_{n=1}^{\infty} b_{\nu_n}\, P_{\nu_n}(\cos\theta)\, \hat{h}^{(1)}_{\nu_n}(kr)\,. \tag{8.170b}$$

The transcendental equation from which the values of $\nu_n$ are determined is given by Eq. (8.166) for $m = 0$:

$$P'_{\nu_n}(\cos\theta_0) = 0\,, \tag{8.171}$$

which enforces the condition $E_\phi(\theta_0) = 0$ on the surface of the metallic cone. Once the values of $\nu_n$ are determined, Eqs. (8.170a) and (8.170b), in conjunction with the applicable boundary conditions, must be used to find the unknowns $a_{\nu_n}$ and $b_{\nu_n}$. Referring to Eq. (8.169b), continuity of $E_\phi$ at $r = a$ requires

$$A^{<}_{\rm mr}(a,\theta) = A^{>}_{\rm mr}(a,\theta)\,,$$

which provides the following equation relating $a_{\nu_n}$ to $b_{\nu_n}$:

$$a_{\nu_n}\,\hat{j}_{\nu_n}(ka) = b_{\nu_n}\,\hat{h}^{(1)}_{\nu_n}(ka)\ . \tag{8.172}$$

The tangential component of the magnetic field across the surface current must be discontinuous at $r = a$:

$$H_\theta(a^+,\theta) - H_\theta(a^-,\theta) = J_0(\theta)\ . \tag{8.173}$$

Using Eq. (8.12b) for $H_\theta$ and substituting the expressions in Eq. (8.173), we have

$$-\frac{k}{i\omega\mu\varepsilon a}\sum_{n=1}^{\infty}\frac{\partial}{\partial\theta}P_{\nu_n}(\cos\theta)\,[b_{\nu_n}\,\hat{h}^{(1)\prime}_{\nu_n}(ka) - a_{\nu_n}\,\hat{j}'_{\nu_n}(ka)] = J_0(\theta)\ . \tag{8.174}$$

Using Eq. (8.172) in Eq. (8.174) and the Wronskian for the spherical Bessel functions, Eq. (8.174) can be simplified to

$$\frac{1}{\mu\varepsilon a}\sum_{n=1}^{\infty}\frac{\partial}{\partial\theta}P_{\nu_n}(\cos\theta)\,\frac{b_{\nu_n}}{\hat{j}_{\nu_n}(ka)} = J_0(\theta)\ . \tag{8.175}$$

Multiplying both sides of Eq. (8.175) by $(\partial/\partial\theta)\,P_{\nu_m}(\cos\theta)\sin\theta$ and integrating with respect to $\theta$ from 0 to $\theta_0$, we have

$$\frac{1}{\mu\varepsilon\,a}\,\frac{b_{\nu_n}}{\hat{j}_{\nu_n}(ka)}\,C_{\nu_n} = \int_{\theta_1}^{\theta_2} J_0(\theta)\,\frac{\partial}{\partial\theta}P_{\nu_n}(\cos\theta)\sin\theta\,d\theta\ , \tag{8.176}$$

where we have used the orthogonality relations of the Legendre function

$$\int_{\theta_1}^{\theta_2} P_{\nu_n}(\cos\theta)\,\frac{\partial}{\partial\theta}P_{\nu_n}(\cos\theta)\sin\theta\,d\theta = \begin{cases} 0 & m\neq n\ , \\ C_{\nu_n} & m = n\ , \end{cases}$$

with

$$C_{\nu_n} = -\frac{\nu_n(\nu_n+1)}{2\nu_n+1}\left[\sin\theta\,P_{\nu_n}(\cos\theta)\,\frac{\partial^2 P_{\nu_n}}{\partial\theta\,\partial\nu}\right]_{\theta=\theta_0}\ .$$

After finding $b_{\nu_n}$ from Eq. (8.176) and $a_{\nu_n}$ from Eq. (8.172), the field quantities can then be obtained.

## 8-6 Biconical Structures

Biconical structures are formed from two cones of arbitrary angles with a common axis and coinciding apexes at the origin. Figures 8-25(a) and Fig. 8-25(b) show two types of such structures, one structure having one cone in the upper half-space and the other cone in the lower half-space, and the other structure having both cones in the same half-space. Assuming the conical surfaces are metallic and the region of interest is between the surfaces of the cones, such structures can support propagating waves. The outward-traveling TM fields supported by

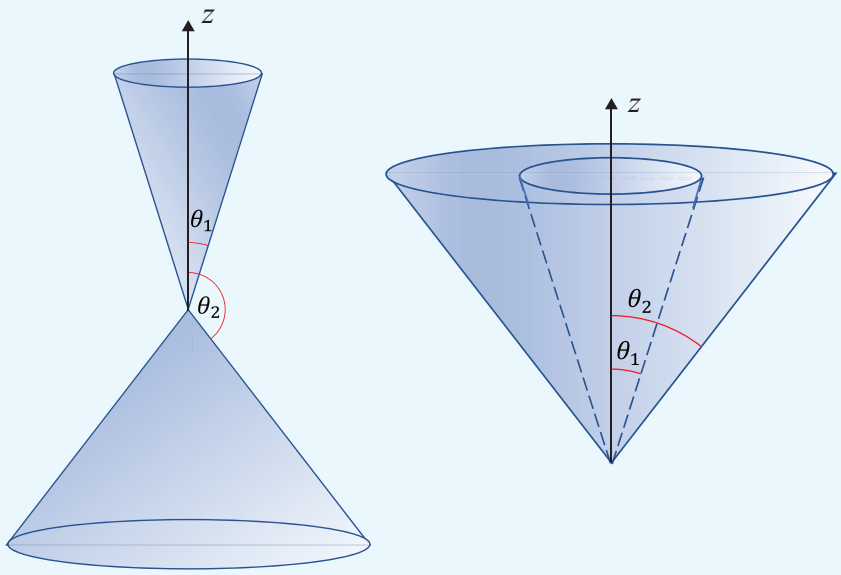


**Figure 8-25:** Biconical structures with the same axis: (a) external cones and (b) coaxial cones.

these structures can be generated from

$$A(r,\theta,\phi) = \hat{h}_\nu^{(1)}(kr)\ [A_\nu P_\nu^m(\cos\theta) + B_\nu Q_\nu^m(\cos\theta)] \begin{cases} \cos m\phi\ , \\ \sin m\phi\ . \end{cases} \tag{8.177}$$

The choice of fraction order for Legendre functions stems from the fact that $\theta = 0$ and/or $\theta = \pi$ are excluded from the domain of interest. The boundary condition mandates that $E_r = E_\phi = 0$ at $\theta = \theta_1$ and $\theta = \theta_2$. Using Eq. (8.10a) or Eq. (8.10c), it can be shown that the required boundary condition at $\theta = \theta_1$ is satisfied when

$$A_\nu = Q_\nu^m(\cos\theta_1) \tag{8.178a}$$

and

$$B_\nu = -P_\nu^m(\cos\theta_1)\ . \tag{8.178b}$$

Imposing the other boundary condition at $\theta = \theta_2$ provides the following transcendental equation:

$$P_{\nu_n}^m(\cos\theta_2)\, Q_{\nu_n}^m(\cos\theta_1) - Q_{\nu_n}^m(\cos\theta_2)\, P_{\nu_n}^m(\cos\theta_1) = 0\ . \tag{8.179}$$

This equation must be solved for $\nu$ to determine the fields supported by the biconical structure. The subscript $n$ here denotes the $n$th zero of Eq. (8.179) for a given $\nu$.

For TE-to-$r$ modes, a similar expression for the electric vector potential can be written. However, the boundary condition requires that

$$E_\phi = \frac{1}{\varepsilon r} \left. \frac{\partial A_{\rm mr}}{\partial \theta} \right|_{\theta=\theta_1 \text{ and } \theta_2} = 0 \,. \tag{8.180}$$

Hence the expression for the electric vector potential takes the following form once the boundary condition at $\theta = \theta_1$ is satisfied:

$$A_{\rm mr}(r,\theta,\phi) = h_\nu^{(1)}(kr) \left( P_\nu^m(\cos\theta) \frac{dQ_\nu^m(\cos\theta_1)}{d\theta_1} - Q_\nu^m(\cos\theta) \frac{dP_\nu^m(\cos\theta_1)}{d\theta_1} \right) \begin{cases} \cos m\phi \,, \\ \sin m\phi \,. \end{cases} \tag{8.181}$$

Enforcing the boundary condition at $\theta = \theta_2$, the following equation for $\nu$ is obtained:

$$\frac{dP_\nu^m(\cos\theta_2)}{d\theta_2} \frac{dQ_\nu^m(\cos\theta_1)}{d\theta_1} - \frac{dQ_\nu^m(\cos\theta_2)}{d\theta_2} \frac{dP_\nu^m(\cos\theta_1)}{d\theta_1} = 0 \,. \tag{8.182}$$

It is interesting to note that $m = 0$ when $\nu = 0$, and therefore the derivative with respect to $\phi$ is zero for all field quantities. Also, we can show that

$$\left( \frac{d^2}{dr^2} + k^2 \right) h_\nu^{(1)}(kr) = \frac{\nu(\nu+1)}{r^2} h_\nu^{(1)}(kr) \,, \tag{8.183}$$

and for $\nu = 0$, $E_r(r,\theta,\phi) = 0$. Therefore in this case the TM electric field has only a $\theta$-component and the TM magnetic field has only a $\phi$-component. That is, the tangential components of the electric field on the surfaces of the cones, independent of the cone angles, are naturally zero. This constitutes a TEM wave with $\mathbf{E} = E_\theta \, \hat{\boldsymbol{\theta}}$ and $\mathbf{H} = H_\phi \, \hat{\boldsymbol{\phi}}$, and the direction of propagation is along $\hat{\mathbf{r}}$. The magnetic vector potential for TM-to-$r$ in this case is written as

$$\begin{aligned} A_r^{00} = \hat{h}_0^{(1)}(kr) \, Q_0(\cos\theta) &= -ie^{ikr} \times \frac{1}{2} \ln \frac{1+\cos\theta}{1-\cos\theta} \\ &= -i \ln[\cot(\theta/2)] \, e^{ikr} \,. \end{aligned} \tag{8.184}$$

Using Eq. (8.184) in Eqs. (8.10b) and (8.11b), the expression for the electric and magnetic fields of the $\rm TM_{00}$ (TEM) mode are given by

$$E_\theta(r,\theta) = \frac{-i\omega}{\sin\theta} \frac{e^{ikr}}{kr}$$

and

$$H_\phi(r,\theta) = \frac{-i\omega}{\eta \sin\theta} \frac{e^{ikr}}{kr} \,.$$

Plots of the functions given by the right-hand side of Eq. (8.179) are shown in Fig. 8-26 for the biconical structures shown in Fig. 8-25(a) when $\theta_1 = \pi - \theta_2$, for different values of $\theta_1$ as a function of $\nu$. The zeros of this function specify the modes of propagation in the

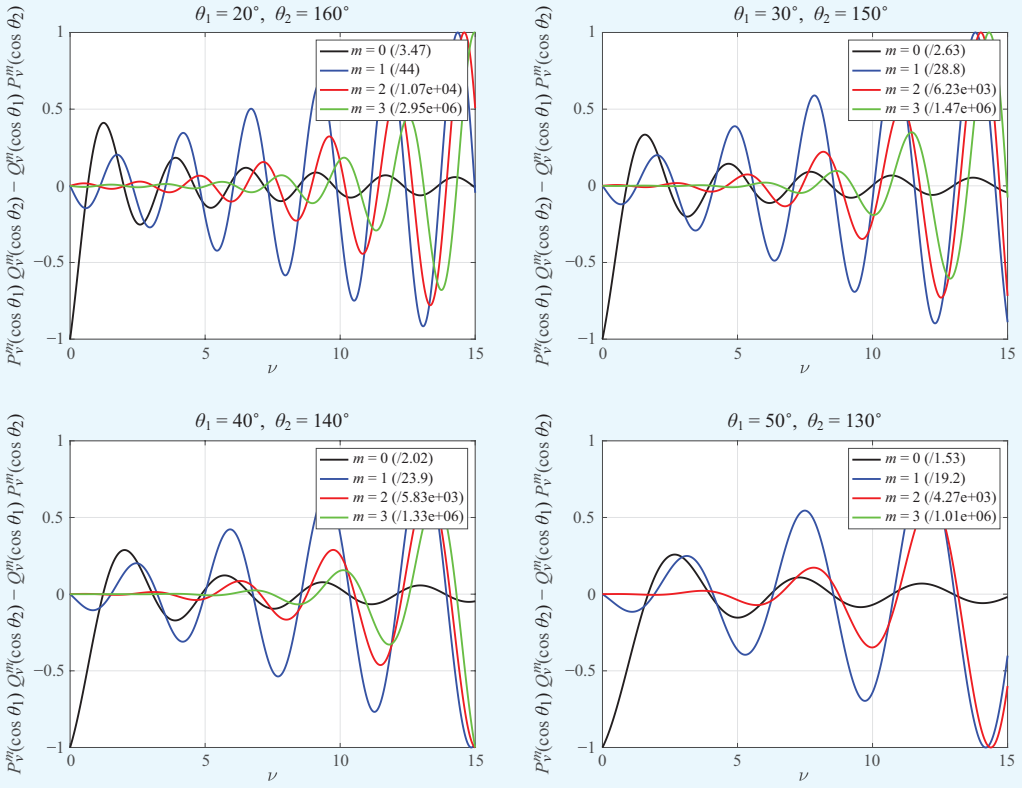


**Figure 8-26:** Plots of the transcendental equation given by Eq. (8.179) for multiple combinations of cone angles as a function of $\nu$. The zeros of the function for different values of $m$ indicate a mode of propagation. The plots shown here for different modes are normalized to their maximum value (noted in the legend) for better viewing.

biconical structure. For each value of $\theta_1 = \pi - \theta_2$, the zeros of the transcendental equation are also functions of $m$, as shown in the plots. Each function is normalized to its maximum value so that the zero crossing can be easily observed for all curves.

The zeros of the TM transcendental equation defined by (8.179) were extracted and are plotted as a function of the cone angle $\theta_1 = \pi - \theta_2$ for different values of $m$, and are shown in Fig. 8-27.

It is interesting to note that the characteristic impedance of the TEM wave defined as

$$Z_0 = \frac{E_\theta}{H_\phi} = \eta$$

is independent of $r$, $\theta$, and $\phi$. When exciting a coaxial biconical structure at its tip by a coaxial transmission line, as shown in Fig. 8-28, the input impedance can be calculated by determining the voltage and current near the tip of the cones. The voltage between the two

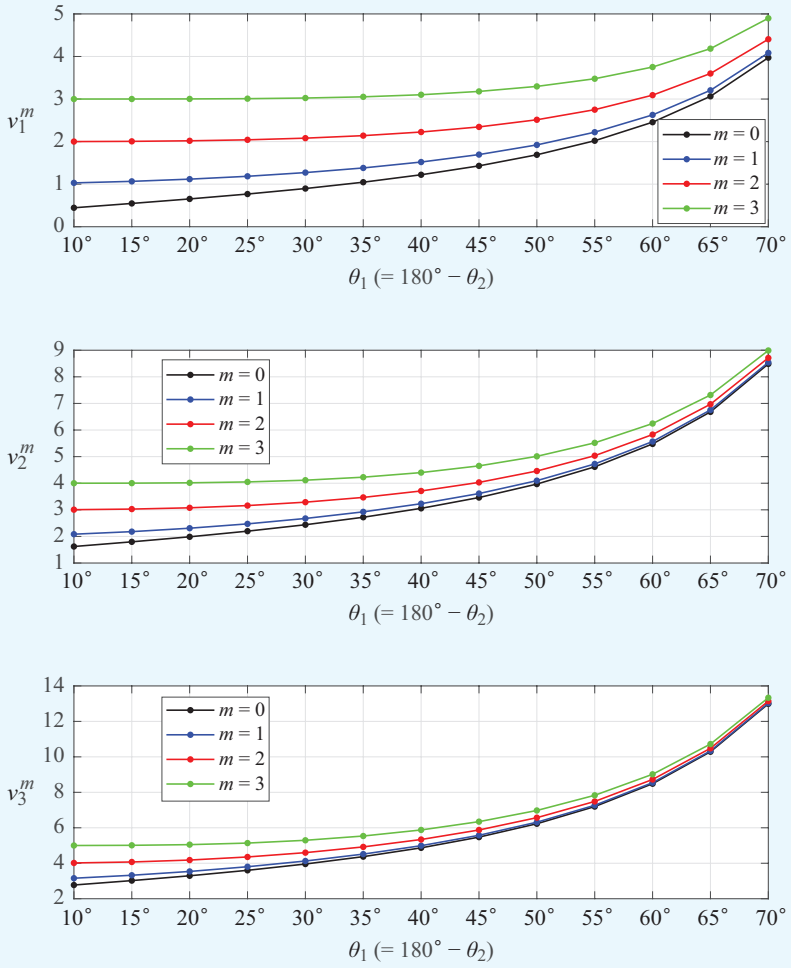


**Figure 8-27:** The zeros of the TM transcendental equation given by Eq. (8.179) were extracted and plotted as a function of the cone angle $\theta_1 = \pi - \theta_2$ for multiple values of $m$.

cones near $r = 0$ is given by

$$V = V(\theta_1) - V(\theta_2) = -\lim_{r\to 0} \int_{\theta_1}^{\theta_2} E_0(r,\theta)\, r\, d\theta = -\lim_{r\to 0} \frac{i\omega}{k}\, e^{ikr} \ln\left(\frac{\cot(\theta_2/2)}{\cot(\theta_1/2)}\right)$$
$$= \frac{-i\omega}{k} \ln\left(\frac{\cot(\theta_2/2)}{\cot(\theta_1/2)}\right) ,$$

where we have used the fact that

$$-\frac{1}{\sin\theta} = \frac{d}{d\theta}\left[\ln(\cot\theta/2)\right] .$$

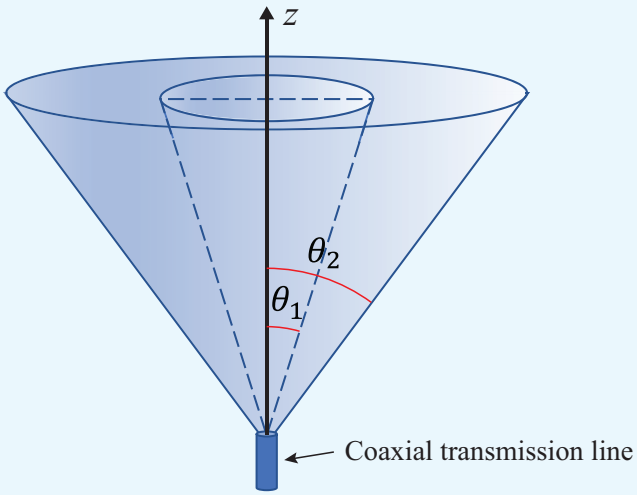


**Figure 8-28:** Geometry of a coaxial biconical antenna fed by a coaxial transmission line supporting $TM^{00}$.

Also, the current flowing over the inner cone can be calculated from

$$I = \lim_{r\to 0} \int_0^{2\pi} H_\phi(r,\theta)\, r\sin\theta\, d\phi = \frac{-i2\pi}{\mu}\ .$$

Hence the input impedance of the biconical structure is given by

$$Z_{\text{in}} = \frac{V}{I} = \frac{\eta}{2\pi} \ln\left[\frac{\cot(\theta_1/2)}{\cot(\theta_2/2)}\right]\ .$$

## Example 8-4: Coaxial Biconical Antenna

For an air-filled coaxial biconical antenna, plot $\theta_2$ in terms of $\theta_1$ so that the antenna is matched to a coaxial cable with each of the following characteristic impedances: 50 Ω, 75 Ω, and 100 Ω.

**Solution:** For an air-filled antenna, $\eta = 120\pi$, and hence

$$Z_0 = Z_{\text{in}} = \frac{120\pi}{2\pi} \ln\left[\frac{\cot(\theta_1/2)}{\cot(\theta_2/2)}\right]\ .$$

Solving this equation for $\theta_2$ yields

$$\theta_2 = 2\cot^{-1}\left[e^{-Z_0/60}\cot(\theta_1/2)\right]\ .$$

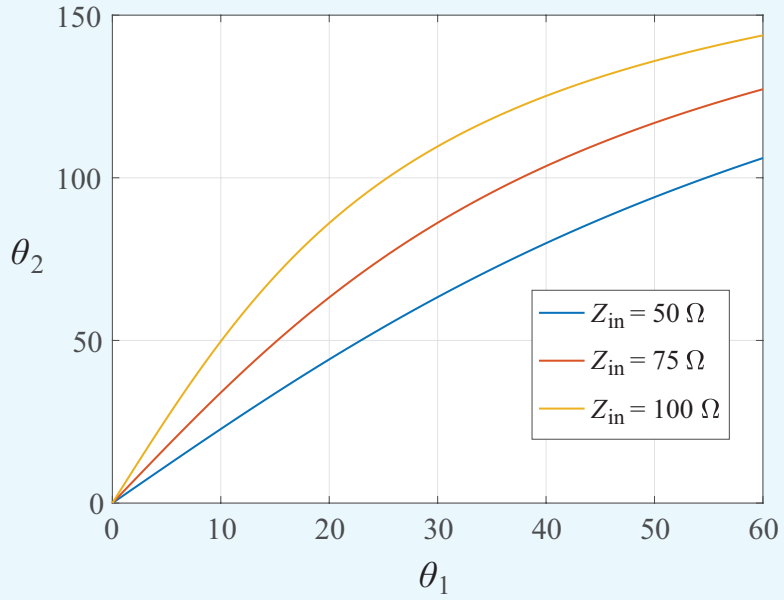


**Figure 8-29:** The variation of $\theta_2$ as a function of $\theta_1$ for a coaxial biconical antenna with cone angles $\theta_1$ and $\theta_2$, for the geometry depicted in Fig. 8-28, for achieving a matched input impedance to a coaxial line for lines with characteristic impedances of $Z_0 = 50\ \Omega$, 75 $\Omega$, and 100 $\Omega$.

Figure 8-29 shows plots of $\theta_2$ versus $\theta_1$ for $Z_0 = 50\ \Omega$, 75 $\Omega$, and 100 $\Omega$. We observe that $\theta_2$ increases with increasing characteristic impedance of the line. It is noted that the antenna produces a wider beam in elevation angle as $\theta_2 - \theta_1$ increases.

Choosing an input impedance of 75 $\Omega$ can provide a wide-angle cone. Choosing $\theta_2 = 65^\circ$ and using Fig. 8-29 for $Z_{in} = 75\ \Omega$ provides an interior cone angle $\theta_1 \approx 20^\circ$. This biconical structure is truncated for a radial length of 3 cm to form a biconical antenna fed by a coaxial line. A numerical method based on FEM is used to simulate the interior field pattern, the input reflection coefficient, and the far-field radiation pattern, which are shown in Figs. 8-30(a), 8-30(b), and 8-30(c), respectively in the frequency range of 10–20 GHz.. The cone angle predicted analytically provides a useful approach to ensuring a very good impedance match to the coaxial line feeding the conical antenna. The 3-dB beamwidth is about 35°, which is smaller than the angular range between the two cones ($\theta_2 - \theta_1 = 45^\circ$).

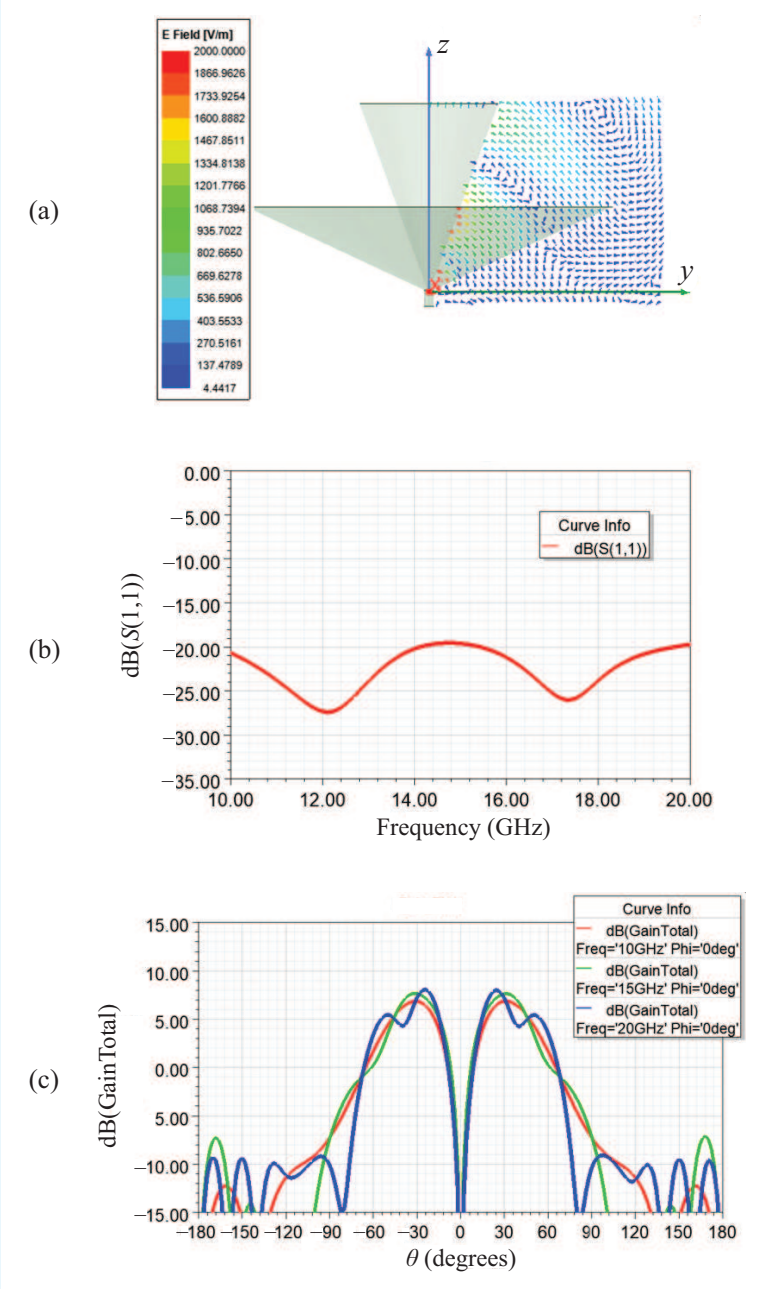


**Figure 8-30:** (a) Configuration of a biconical antenna fed by a 75-$\Omega$ coaxial line and the resultant field distribution. (b) The input reflection coefficient as a function of frequency, which shows a good impedance match over a wide bandwidth. (c) The far-field radiation pattern in a constant $\phi$-plane with omnidirectional characteristic and a 3-dB beamwidth in elevation of about 35°. The angles of the cones are predicted from the results shown in Fig. 8-29.

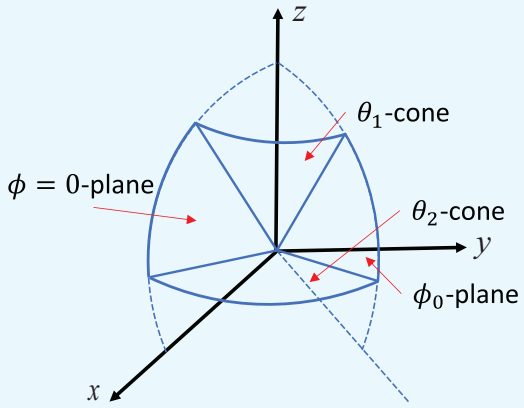


**Figure 8-31:** Geometry of a $\theta$–$\phi$ spherical waveguide. The domain of interest is between $\theta_1$-constant, $\theta_2$-constant, $\phi = 0$-constant, and $\phi_0$-constant surfaces.

## 8-7 Other Spherical Waveguides

Other types of spherical waveguides can also be realized by considering a metallic structure formed by $\phi$-constant surfaces and $\theta$-constant surfaces, as shown in Fig. 8-31. The $\theta$-constant surfaces are conical surfaces with generating angles $\theta_1$ and $\theta_2$. For a TM-to-$r$ mode, the appropriate vector potential takes the following form:

$$A(r,\theta,\phi) = \hat{h}_0^{(1)}(kr)\ \left[a_\nu\, P_\nu^\mu(\cos\theta) + b_\nu\, Q_\nu^\mu(\cos\theta)\right](\sin\mu\phi + C_\mu\cos\mu\phi)\ , \tag{8.185}$$

because the desired domain in $\phi$ is $[0,\phi_0]$ and the domain in $\theta$ is $[\theta_1,\theta_2]$. In this example we consider an outward-propagating mode only. On $\phi$-constant surfaces, the boundary condition requires $E_r$ and $E_\theta$ to vanish at $\phi = 0$ and $\phi = \phi_0$. According to Eqs. (8.10), this requires

$$A(r,\theta,0) = A(r,\theta,\phi_0) = 0\ . \tag{8.186}$$

Enforcing Eq. (8.186) renders the following equations:

$$C_\mu = 0 \tag{8.187}$$

and

$$\sin\mu\phi_0 = 0 \quad\rightarrow\quad \mu = \frac{m\pi}{\phi_0} \qquad m = 1,2,\ldots \tag{8.188}$$

On $\theta$-constant surfaces, $E_r$ and $E_\phi$ must be zero. Referring to Eqs. (8.10) again, their boundary condition is satisfied if

$$A(r,\theta_1,\phi) = A(r,\theta_2,\phi) = 0\ . \tag{8.189}$$

Similar to Eqs. (8.110a) and (8.110b), Eqs. (8.189) is satisfied for $\theta = \theta_1$ if

$$a_\nu = Q_\nu^{m\pi/\phi_0}(\cos\theta_1) \tag{8.190a}$$

and

$$b_\nu = -P_\nu^{m\pi/\phi_0}(\cos\theta_1)\ . \tag{8.190b}$$

In order for Eq. (8.189) to be true at $\theta = \theta_2$, we must enforce

$$Q_{\nu_n^m}^{m\pi/\phi_0}(\cos\theta_1)\, P_{\nu_n^m}^{m\pi/\phi_0}(\cos\theta_2) - P_{\nu_n^m}^{m\pi/\phi_0}(\cos\theta_1)\, Q_{\nu_n^m}^{m\pi/\phi_0}(\cos\theta_2) = 0\ . \tag{8.191}$$

Equation (8.191) is the transcendental equation for the possible modes in the spherical waveguide shown in Fig. 8-31. Here $\nu_n^m$ refers to the $n$th zero of Eq. (8.191) for $\mu_m = m\pi/\phi_0$. For TE-to-$r$ mode, a transcendental equation similar to Eq. (8.182) can be obtained and is given by

$$\frac{d}{d\theta_1} Q_{\nu_n^m}^{m\pi/\phi_0}(\cos\theta_1)\, \frac{d}{d\theta_2} P_{\nu_n^m}^{m\pi/\phi_0}(\cos\theta_2) - \frac{d}{d\theta_1} P_{\nu_n^m}^{m\pi/\phi_0}(\cos\theta_1)\, \frac{d}{d\theta_2} Q_{\nu_n^m}^{m\pi/\phi_0}(\cos\theta_2) = 0\ . \tag{8.192}$$

A truncated $\theta$–$\phi$ spherical waveguide in the radial direction ($r = R_0$) forms a $\theta$–$\phi$ spherical horn. This horn antenna can be fed by a conventional rectangular waveguide or a ridged waveguide at its tip. To examine the performance of such a horn antenna, a transition from a rectangular waveguide to a $\theta$–$\phi$ spherical waveguide is designed, as shown in Fig. 8-32(a). Also shown in Fig. 8-32(a) are the dimensions of a truncated horn antenna for operating at X-band (8–12 GHz). The co-polarized and cross-polarized radiation patterns (at 10 GHz) of this antenna, for both the $E$-plane and the $H$-plane, are shown in Fig. 8-32(b). It is shown that the roll-off of the radiation pattern is not symmetric with angle. This type of horn seems to be appropriate as a feed for an offset reflector antenna.

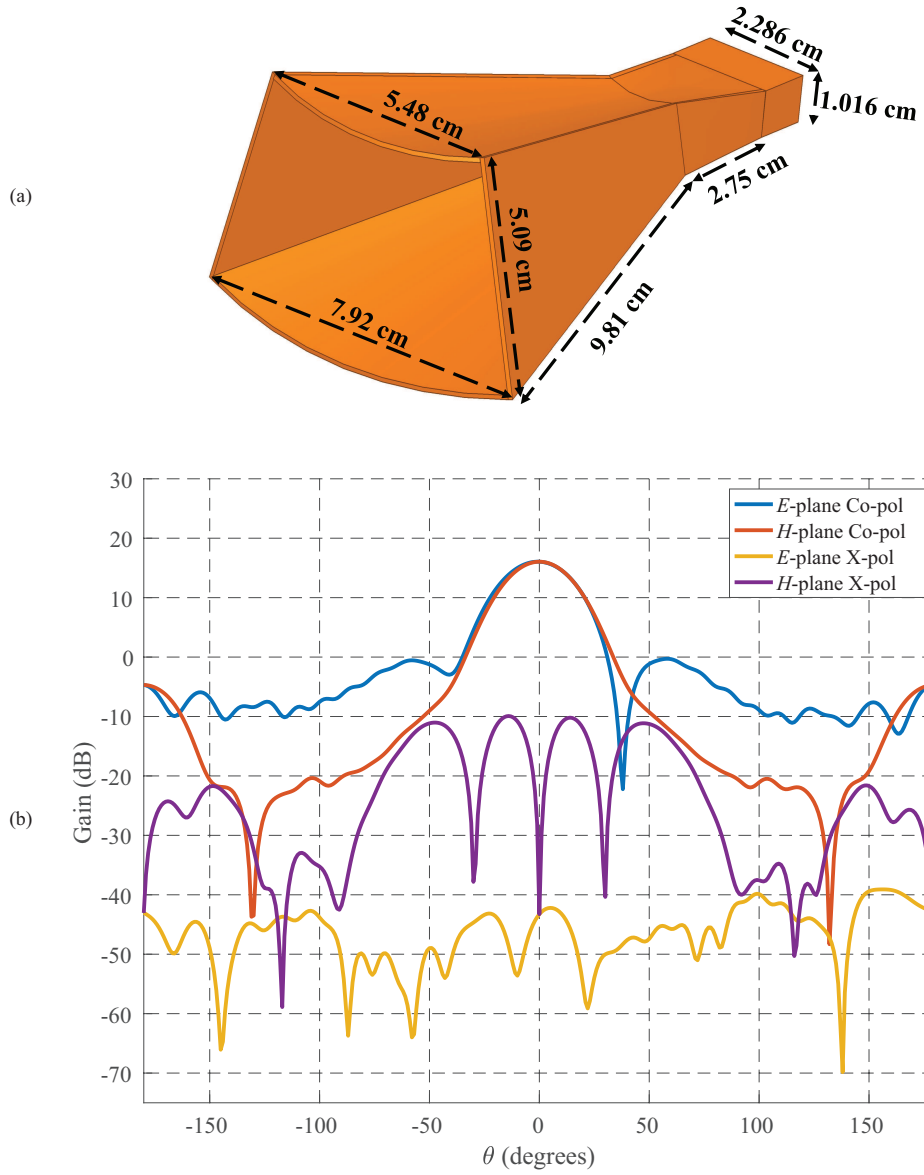


**Figure 8-32:** The geometry and simulated radiation pattern of a truncated $\theta$–$\phi$ spherical waveguide (horn) antenna. A transition to a rectangular waveguide is designed for impedance matching.

# Summary

## Concepts

- In the spherical coordinate system, the vector wave equation for both the magnetic and the electric vector potentials under the Lorentz gauge condition do not yield a scalar wave equation for any component of either vector potential.
- Using a different gauge condition, it is shown that a scalar potential defined by $\psi(r,\theta,\phi) = A_r(r,\theta,\phi)/r$ satisfies the scalar wave equation if the magnetic vector potential has only an $r$ component. This vector potential ($\mathbf{A} = A_r\,\hat{\mathbf{r}}$) generates a set of fields for which the magnetic field has no $r$ component. This set of fields is known as TM-to-$r$ fields.
- Using the duality principle, it is shown that if the electric vector potential has only an $r$ component ($A_m = A_{mr}\,\hat{\mathbf{r}}$), a set of fields can be generated for which the field has no $r$ component. This set of fields is known as TE-to-$r$ fields.
- The method of separation of variables is used to solve the scalar wave equation. This leads to three separate differential equations, one for each of the three spherical coordinate variables. The function of the $\phi$ variable is a harmonic function, that of the $\theta$ variable is a Legendre or associated Legendre function whose order is a function of the domain of interest, and finally the function of the $r$ variable is a spherical Hankel function.
- The characteristics of the spherical wave functions are studied to guide the selection of proper functions suited for the domain of interest.
- Application of the method of separation of variables to problems such as the determination of eigenvalues (resonances) and eigenfunctions (fields for source-free regions) of spherical cavity and dielectric resonator are presented.
- To study plane-wave scattering by metallic and dielectric spherical objects, expansion of plane waves in terms of spherical wave functions is presented. Using such an expansion, the scattering of plane waves by spherical objects is computed and analytical solutions for the bistatic scattering cross sections of such targets are obtained.
- The characteristics of wave propagation in conical waveguides are studied. The field's modal expansion is obtained by first solving a transcendental equation and then using the solution to provide the order of the associated Legendre functions and the spherical Hankel functions.
- Field modal expansion in the region between two metallic cones sharing a common axis (known as a biconical structure) is presented. The characteristics of such fields depend on the order of the associated Legendre functions of the first and second kind, which are found from a transcendental equation obtained by imposing boundary conditions.
- Other spherical waveguide structures formed by four metallic surfaces that coincide with constant $\theta$ (cones) and constant $\phi$ (planes) surfaces are also considered.

## Important Equations

**New gauge condition:**

$$\frac{\partial}{\partial r} A_{\mathrm{r}} = i\omega\mu\varepsilon\Phi$$

**Wave equation for TM-to-*r*:**

$$(\nabla^2 + k^2)\,\frac{A_{\mathrm{r}}}{r} = -\frac{\mu}{r} J_{\mathrm{r}}$$

**Wave equation for TE-to-*r*:**

$$(\nabla^2 + k^2)\,\frac{A_{\mathrm{mr}}}{r} = -\frac{\varepsilon J_{\mathrm{mr}}}{r}$$

**Electric field components for TM-to-*r*:**

$$E_{\mathrm{r}} = \frac{-1}{i\omega\mu\varepsilon}\left(\frac{\partial^2}{\partial r^2} + k^2\right) A_{\mathrm{r}}\,,$$

$$E_\theta = \frac{-1}{i\omega\mu\varepsilon r}\left(\frac{\partial^2}{\partial r\,\partial\theta}\right) A_{\mathrm{r}}\,,$$

$$E_\phi = \frac{-1}{i\omega\mu\varepsilon}\,\frac{1}{r\sin\theta}\,\frac{\partial^2}{\partial r\,\partial\phi} A_{\mathrm{r}}$$

**Magnetic field components for TM-to-*r*:**

$$H_\theta = \frac{1}{\mu r\sin\theta}\,\frac{\partial A_{\mathrm{r}}}{\partial\phi}\,,$$

$$H_\phi = -\frac{1}{\mu r}\,\frac{\partial A_{\mathrm{r}}}{\partial\theta}$$

## Important Equations (continued)

**Electric and magnetic field components for TE-to-*r*:**

$$H_r = \frac{-1}{i\omega\mu\varepsilon}\left(\frac{\partial^2}{\partial r^2} + k^2\right) A_{mr} ,$$

$$H_\theta = \frac{-1}{i\omega\mu\varepsilon r}\frac{\partial^2}{\partial r\,\partial\theta} A_{mr} ,$$

$$H_\phi = \frac{-1}{i\omega\mu\varepsilon}\frac{1}{r\sin\theta}\frac{\partial^2}{\partial r\,\partial\phi} A_{mr} ,$$

$$E_\theta = \frac{-1}{\varepsilon r\sin\theta}\frac{\partial A_{mr}}{\partial\phi} ,$$

$$E_\phi = \frac{1}{\varepsilon r}\frac{\partial A_{mr}}{\partial\theta}$$

**Separation of variables:**

$$\frac{A_r}{r} \text{ or } \frac{A_{mr}}{r} = \psi(r,\theta,\phi) = R(r)\,Q(\theta)\,F(\phi)$$

**The differential equations for *R*, *Q*, and *F*:**

$$\frac{d}{dr}\left(r^2\frac{dR}{dr}\right) + [(kr)^2 - \nu(\nu+1)]R = 0 ,$$

$$\frac{1}{\sin\theta}\frac{d}{d\theta}\left(\sin\theta\frac{dQ}{d\theta}\right) + \left(\nu(\nu+1) - \frac{\mu^2}{\sin^2\theta}\right)Q = 0 ,$$

$$\frac{d^2F}{d\phi^2} + \mu^2 F = 0$$

**Harmonic functions for $F(\phi)$:**

$$F = Ae^{i\mu\phi} + Be^{-i\mu\phi}$$

**Spherical Bessel function for $R(r)$:**

$$R(r) = z_n(kr) = \left(\frac{\pi}{2kr}\right)^{1/2} Z_{n+1/2}(kr)$$

**Recurrence formula for spherical Bessel functions:**

$$z_{n+1}(kr) = \frac{(2n+1)}{kr}\,z_n(kr) - z_{n-1}(kr)$$

## Important Equations (continued)

**Large-argument expansion for spherical Bessel functions:**

$$\lim_{kr\to\infty} h_n^{(1)}(kr) \approx \frac{e^{i[kr-\pi(n+1)/2]}}{kr} = (-i)^{n+1} P\frac{e^{ikr}}{kr}$$

$$\lim_{kr\to\infty} h_n^{(2)}(kr) \approx \frac{e^{-i[kr-\pi(n+1)/2]}}{kr} = (i)^{n+1}\frac{e^{-ikr}}{kr}$$

**Wronskian relations for spherical Bessel functions:**

$$j_\nu(r)\, n'_\nu(r) - j'_\nu(r)\, n_\nu(r) = \frac{1}{r^2}$$

$$j_\nu(r)\, h_\nu^{(1)\prime}(r) - j'_\nu(r)\, h_\nu^{(1)}(r) = \frac{i}{r^2}$$

**Legendre function of the first kind:**

$$P_\nu(x) = \sum_{m=0}^{N} \frac{(-1)^m(\nu+m)!}{(m!)^2(\nu-m)!}\left(\frac{1-x}{2}\right)^m - \frac{\sin\nu\pi}{\pi} \cdot \sum_{m=N+1}^{\infty} \frac{(m-1-\nu)!(m+\nu)!}{(m!)^2}\left(\frac{1-x}{2}\right)^m$$

**Legendre function of the second kind:**

$$Q_n(x) = P_n(x)\left(\frac{1}{2}\ln\frac{1+x}{1-x} - g(n)\right) + \sum_{m=1}^{n} \frac{(-1)^m(n+m)!}{(m!)^2(n-m)!}\, g(m)\left(\frac{1-x}{2}\right)^m$$

**Orthogonality properties of zonal harmonics:**

$$\int_0^\pi P_n(\cos\theta)\, P_m(\cos\theta)\sin\theta\, d\theta = 0, \qquad m \neq n$$

$$\int_0^\pi [P_n(\cos\theta)]^2 \sin\theta\, d\theta = \frac{2}{2n+1}$$

## Important Equations (continued)

**Orthogonality properties of spherical harmonic functions:**

$$\int_0^{2\pi}\int_0^{\pi} U_{nm}(\theta,\phi)\,U_{pq}(\theta,\phi)\,\sin\theta\,d\theta\,d\phi$$
$$= \begin{cases} \dfrac{4\pi}{2n+1} & m=0 \text{ (only even functions)}, \\ \dfrac{2\pi(n+m)!}{(2n+1)(n-m)!} & m\neq 0 \end{cases}$$

**Resonant frequency of a spherical cavity for TE-to-*r* and TM-to-*r* modes:**

$$(f)^{\mathrm{TE}}_{mnp} = \frac{x_{np}}{2\pi a\sqrt{\mu\varepsilon}}\,,$$
$$(f)^{\mathrm{TM}}_{mnp} = \frac{x'_{np}}{2\pi a\sqrt{\mu\varepsilon}}$$

**Transcendental equation for determination of resonant modes for two concentric spherical cavities:**

$$\hat{\mathbf{j}}_n(k_0^{(n)}R_{\mathrm{e}})\,\hat{\mathbf{h}}_n^{(1)}(k_0^{(n)}R_{\mathrm{i}}) - \hat{\mathbf{j}}_n(k_0^{(n)}R_{\mathrm{i}})\,\hat{\mathbf{h}}_n^{(1)}(k_0^{(n)}R_{\mathrm{e}}) = 0\,.$$

**Transcendental equation for determination of resonant modes for TM and TE modes of a spherical dielectric resonator:**

$$\sqrt{\frac{\varepsilon_{\mathrm{s}}}{\mu_{\mathrm{s}}}}\,\frac{\hat{j}_n(k_{\mathrm{s}}a)}{\hat{j}'_n(k_{\mathrm{s}}a)} = \sqrt{\frac{\varepsilon_{\mathrm{b}}}{\mu_{\mathrm{b}}}}\,\frac{\hat{h}_n^{(1)}(k_{\mathrm{b}}a)}{\hat{h}_n^{(1)\prime}(k_{\mathrm{b}}a)}\,, \qquad \text{(TM modes)}$$

$$\sqrt{\frac{\mu_{\mathrm{s}}}{\varepsilon_{\mathrm{s}}}}\,\frac{\hat{j}_n(k_{\mathrm{s}}a)}{\hat{j}'_n(k_{\mathrm{s}}a)} = \sqrt{\frac{\mu_{\mathrm{b}}}{\varepsilon_{\mathrm{b}}}}\,\frac{\hat{h}_n^{(1)}(k_{\mathrm{b}}a)}{\hat{h}_n^{(1)\prime}(k_{\mathrm{b}}a)} \qquad \text{(TE modes)}$$

## Important Equations (continued)

**Plane-wave expansion in terms of spherical wave functions:**

$$\frac{2a_n}{2n+1}\, j_n(kr) = \int_0^{\pi} e^{ikr\cos\theta}\, P_n(\cos\theta)\, \sin\theta\, d\theta\ ,$$

$$j_n(kr) = 2^n (kr)^n \sum_{m=0}^{\infty} \frac{(-1)^m (n+m)!}{m!\,(2n+2m+1)!}\, (kr)^{2m}$$

**Addition theorem for spherical wave functions:**

$$h_0^{(1)}(k|\mathbf{r},\mathbf{r}'|) =$$

$$\begin{cases} \displaystyle\sum_{n=0}^{\infty}\sum_{m=0}^{n} \alpha_m \frac{(2n+1)(n-m)!}{(n+m)!}\, j_n(kr)\, h_n^{(1)\prime}(kr)\, P_n^m(\cos\theta')\, P_n^m(\cos\theta)\cos[m(\phi-\phi')] & r \le r'\ , \\ \displaystyle\sum_{n=0}^{\infty}\sum_{m=0}^{n} \alpha_m \frac{(2n+1)(n-m)!}{(n+m)!}\, h_n^{(1)}(kr)\, j_n'(kr)\, P_n^m(\cos\theta')\, P_n^m(\cos\theta)\cos[m(\phi-\phi')] & r \ge r' \end{cases}$$

**The backscatter radar cross section of a metallic sphere:**

$$a_n - b_n = \frac{(i)^n(2n+1)}{n(n+1)} \frac{\hat{j}_n'(ka)\,\hat{h}_n^{(1)}(ka) - \hat{j}_n(ka)\,\hat{h}_n^{(1)\prime}(ka)}{\hat{h}_n^{(1)\prime}(ka)\,\hat{h}_n^{(1)}(ka)}$$

$$= \frac{(i)^n(2n+1)}{n(n+1)\,\hat{h}_n^{(1)\prime}(ka)\,\hat{h}_n^{(1)}(ka)}$$

**Low-frequency backscatter radar cross section of a metallic sphere:**

$$\lim_{ka\to 0} \frac{1}{\hat{h}_1^{(1)}(ka)}\ , \approx -ka\ ,$$

$$\lim_{ka\to 0} \frac{1}{\hat{h}_1^{(1)\prime}(ka)} \approx (ka)^2$$

**High-frequency backscatter radar cross section of a metallic sphere:**

$$\sigma_c^{\mathrm{LF}} = \frac{9\lambda^2}{4\pi}\, (ka)^6$$

## Important Equations (continued)

**The backscatter radar cross section of a dielectric sphere:**

$$\lim_{x\to -1}\sqrt{1-x^2}\,\frac{dP_n^1(x)}{dx}=\lim_{x\to -1}\frac{1}{2}\,\frac{1}{\sqrt{1-x^2}}\,P_n^1(x)=\lim_{x\to -1}-\frac{1}{2}\,\frac{dP_n(x)}{dx}=(-1)^n\,\frac{n(n+1)}{2}$$

with $a_n$ and $b_n$ given by

$$\left(E_\theta^{\rm i}+E_\theta^{\rm s}\right)\big|_{r=a}=E_\theta^{\rm d}\big|_{r=a}\ ,$$
$$\left(E_\phi^{\rm i}+E_\phi^{\rm s}\right)\big|_{r=a}=E_\phi^{\rm d}\big|_{r=a}$$

**Transcendental equations for TM-to-$r$ and TE-to-$r$ modes for wave propagation in a conical waveguide:**

$$A_{\rm r}(r,\theta,\phi)=P_{\nu_n^m}^m(\cos\theta)\,\hat{h}_{\nu_n^m}^{(1)}(kr)\begin{cases}\cos m\phi\ ,\\ \sin m\phi\ ,\end{cases}$$

$$E_{\rm r}=\frac{-1}{i\omega\mu\varepsilon r^2}\sum_{m=0}^{\infty}\sum_{n=1}^{\infty}a_{mn}\nu_n^m(\nu_n^m+1)\,\hat{h}_{\nu_n^m}^{(1)}(kr)\,P_{\nu_n^m}^m(\cos\theta)\begin{cases}\cos m\phi\ ,\\ \sin m\phi\ ,\end{cases}$$

$$E_\theta=\frac{k\sin\theta}{i\omega\mu\varepsilon r}\sum_{m=0}^{\infty}\sum_{n=1}^{\infty}a_{mn}\,\hat{h}_{\nu_n^m}^{(1)\prime}(kr)\,P_{\nu_n^m}^{m\prime}(\cos\theta)\begin{cases}\cos m\phi\ ,\\ \sin m\phi\ ,\end{cases}$$

$$E_\phi=\frac{-k}{i\omega\mu\varepsilon r\sin\theta}\sum_{m=0}^{\infty}\sum_{n=1}^{\infty}ma_{mn}\,\hat{h}_{\nu_n^m}^{(1)\prime}(kr)\,P_{\nu_n^m}^m(\cos\theta)\begin{cases}-\sin m\phi\ ,\\ \cos m\phi\ ,\end{cases}$$

$$H_\theta=\frac{1}{\mu r\sin\theta}\sum_{m=0}^{\infty}\sum_{n=1}^{\infty}ma_{mn}\,\hat{h}_{\nu_n^m}^{(1)}(kr)\,P_{\nu_n^m}^m(\cos\theta)\begin{cases}-\sin m\phi\ ,\\ \cos m\phi\ ,\end{cases}$$

$$H_\phi=\frac{\sin\theta}{\mu r}\sum_{m=0}^{\infty}\sum_{n=1}^{\infty}a_{mn}\,\hat{h}_{\nu_n^m}^{(1)}(kr)\,P_{\nu_n^m}^{m\prime}(\cos\theta)\begin{cases}\cos m\phi\ ,\\ \sin m\phi\ .\end{cases}$$

## Important Equations (continued)

**Transcendental equations for TM-to-$r$ and TE-to-$r$ modes for wave propagation in a conical waveguide:**

$$A_\nu = Q_\nu^m(\cos\theta_1)\,,$$
$$B_\nu = -P_\nu^m(\cos\theta_1)$$

$$E_\phi = \frac{1}{\varepsilon r}\left.\frac{\partial A_{\rm mr}}{\partial\theta}\right|_{\theta=\theta_1 \text{ and } \theta_2} = 0$$

**Input impedance of a biconical antenna:**

$$Z_{\rm in} = \frac{\eta}{2\pi}\ln\left[\frac{\cot(\theta_1/2)}{\cot(\theta_2/2)}\right]\,, \qquad \theta_2 < \theta_1$$

**Transcendental equations for TM-to-$r$ and TE-to-$r$ modes for a $\theta$–$\phi$ spherical waveguide:**

$$a_\nu = Q_\nu^{m\pi/\phi_0}(\cos\theta_1)\,,$$
$$b_\nu = -P_\nu^{m\pi/\phi_0}(\cos\theta_1)$$

$$Q_{\nu_n^m}^{m\pi/\phi_0}(\cos\theta_1)\,P_{\nu_n^m}^{m\pi/\phi_0}(\cos\theta_2) - P_{\nu_n^m}^{m\pi/\phi_0}(\cos\theta_1)\,Q_{\nu_n^m}^{m\pi/\phi_0}(\cos\theta_2) = 0\,.$$

**Important Terms** Provide definitions or explain the meaning of the following terms:

$\theta$–$\phi$ spherical waveguide
addition theorem for spherical wave functions
associated Legendre functions of the first kind
associated Legendre functions of the second kind
biconical structure
coaxial biconical antenna
concentric spherical cavity
conical horn antenna
conical waveguide
dipole
Fourier-Legendre expansion
Legendre functions
Legendre polynomial
monopole
multipole
quadrupole
radar cross section (RCS)
RCS of dielectric spheres
RCS of metallic spheres
Schelkunoff spherical Bessel functions
spherical Bessel functions of the first kind
spherical Bessel functions of the second kind
spherical cavity
spherical dielectric resonator
spherical Hankel functions of the first kind
spherical Hankel functions of the second kind
spherical harmonic functions
spherical wave functions
transverse electric to $r$ (TE-to-$r$)
transverse magnetic to $r$ (TM-to-$r$)
Wronskian for spherical Bessel functions
zonal harmonic functions

## PROBLEMS

**8.1** Find the Fourier-Legendre expansion of

$$f(\theta,\phi) = \frac{1}{\sin\theta}\,\delta(\theta-\theta_0)\,\delta(\phi-\phi_0)$$

and plot the truncated approximation of $f(\theta,\phi)$ for $N = 10$.

**8.2** Consider a function defined by

$$f(\theta,\phi) = \begin{cases} 1 & 0 < \theta \le \pi/2\ , \\ 0 & \pi/2 < \theta \le \pi\ . \end{cases}$$

Determine the Fourier-Legendre coefficients of $f(\theta,\pi)$.

**8.3** Consider an array of a dipole and a quadrupole as shown Fig. 8-14(c) and Fig. 8-14(e). Choose the ratio of the currents flowing on the dipole and quadrupole so as to maximize the front-to-back ratio of the radiated field.

**8.4** A quadrupole is formed from two dipoles, as shown in Fig. P8.4. Find the magnetic vector potential of such a source. Assuming the observation point is in the far-field region, find the far-field expression for the resulting electric and magnetic fields.

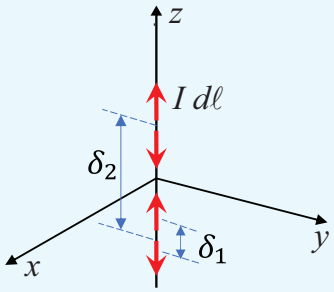


**Figure P8.4:** A quadrupole placed along the $z$-axis. The separations between current elements ($\delta_1$ and $\delta_2$) are much smaller than a wavelength.

## Cavity

**8.5** Consider a hemispherical metallic cavity of radius $a$.

**(a)** Determine the dominant TM-to-$r$ mode and the expression for its resonant frequency.

**(b)** Find the $Q$ of the dominant mode.

**(c)** Compare $Q$ of part (b) with that of a spherical cavity.

**8.6** For a spherical wedge cavity of radius $r$ with PEC boundaries as shown in Fig. P8.6, find the scalar potentials for TE-to-$r$ and TM-to-$r$ and the corresponding resonance frequencies.

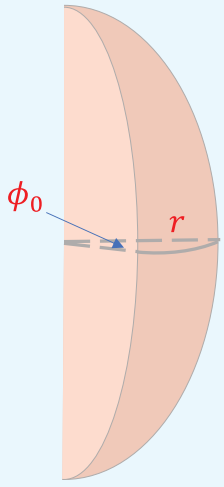


**Figure P8.6:** A spherical sector cavity formed from two $\phi$-constant planes and an $r$-constant surface.

**8.7** A metallic cavity is formed between constant $\phi = 0$ and $\phi = \phi_0$ half-planes, a constant $r = a$ spherical surface, and a constant $\theta = \theta_0$ conical surface, as shown in Fig. P8.7. Find the resonant frequencies for TM-to-$r$ and TE-to-$r$ modes.

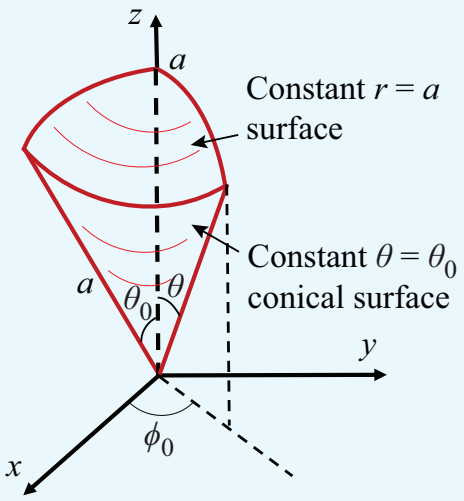


**Figure P8.7:** The geometry of a metallic cavity formed by four surfaces: (1) constant $\phi = 0$ plane, (2) constant $\phi = \phi_0$ plane, (3) constant $\theta = \theta_0$ conical surface, and (4) constant $r = a$ spherical surface.

**8.8** Consider a hemispherical dielectric with radius $a$, permittivity $\varepsilon_d$, and permeability $\mu_d$ placed on an infinite ground plane. Find the natural resonant frequencies of such a dielectric resonator.

**8.9** Consider a cavity lying between concentric conducting spheres at $r = a$ and $r = b$ (with $b > a$). Show that the characteristic equation for TM-to-$r$ modes is given by

$$\frac{\hat{j}_n'(kb)}{\hat{j}_n'(ka)} = \frac{\hat{n}_n'(kb)}{\hat{n}_n'(ka)},$$

and for TE-to-$r$ modes it is given by

$$\frac{\hat{j}_n(kb)}{\hat{j}_n(ka)} = \frac{\hat{n}_n(kb)}{\hat{n}_n(ka)}.$$

**8.10** Consider a spherical cavity of radius $b$ with PMC boundary partially filled with a medium of permittivity $\varepsilon_r$ and permeability $\mu_r$ for $0 < r < a$. A PEC plate is inserted inside the cavity at $\phi = \phi_0$ and $0 < r < b$, as shown in Fig. P8.10. Assuming that $\phi_0 = 0$, find the characteristic equations for TM-to-$r$ and TE-to-$r$ modes.

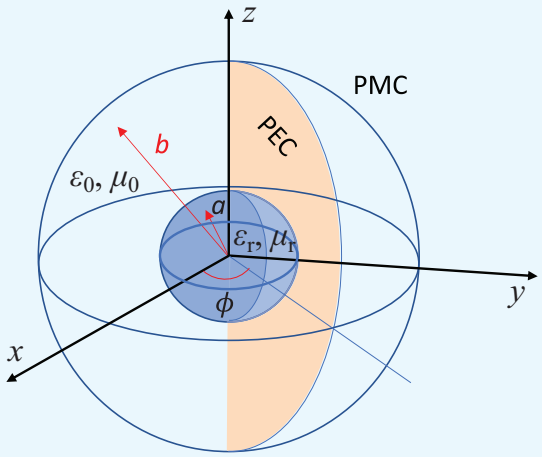


**Figure P8.10:** The configuration of a spherical cavity of radius $b$ made from a PMC having a concentric dieletric sphere of radius $a$ and constitutive parameters $\varepsilon_r$ and $\mu_r$. The cavity also has a $\phi$-constant metallic septum.

## Scattering

**8.11** Consider a conducting sphere of radius $a$ enclosed in a dielectric sphere with radius $b$, as shown in Fig. P8.11. Suppose this object is illuminated by an $x$-polarized plane wave propagating along the $+z$-axis. Find the scattered electric and magnetic fields.

**8.12** Consider a radially directed electric current filament (short-dipole) near a metallic sphere. The goal in this problem is to find the radiated field in the far-field region using reciprocity. Suppose a small dipole is placed at the observation point in the far-field region. The field of this dipole can be approximated, locally, by a plane wave. The scattered field produced by the plane wave at the location of the original source can be computed. According to the reciprocity theorem, the field of the short dipole near the metallic sphere can be computed from the plane-wave scattered field. Derive the expression for the radiated field from a radially directed small dipole in the presence of a metallic sphere of radius $a$.

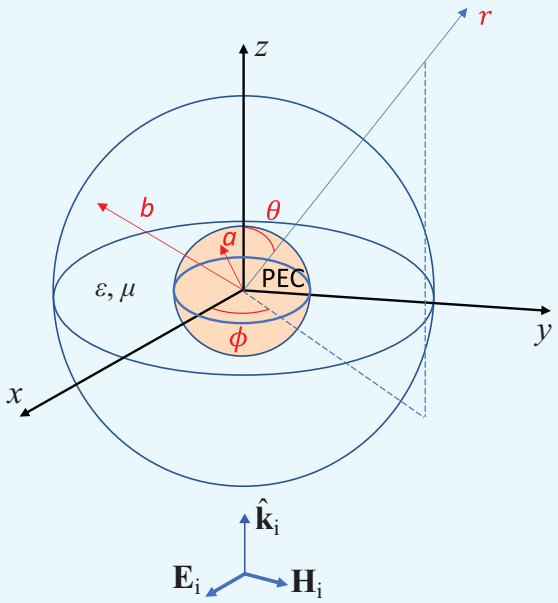


**Figure P8.11:** The geometry of a dielectric-coated metallic sphere illuminated by a plane wave propagating along the $+z$-axis. The radius of the metallic sphere is $a$ and that of the dielectric sphere is $b$.

**8.13** Consider a conducting sphere of radius $a$. A loop of uniform current $\mathbf{I} = I_0\,\hat{\boldsymbol{\phi}}$ and radius $R > \phi$ is placed concentric with the metallic sphere, as shown in Fig. P8.13. Show that the radiation field can be obtained from

$$E_\phi = \frac{\eta I}{r}\, e^{jkr} \sum_{n=1}^{\infty} \frac{2n+1}{2n(n+1)}\, j^{-n} A_n\, P_n^1(0)\, P_n^1(\cos\theta)\ ,$$

where

$$A_n^{-1} = \hat{H}_n^{(1)\prime}(kR) - \frac{\hat{J}_n(ka)\,\hat{N}_n'(kR) - \hat{N}_n(ka)\,\hat{j}_n'(kR)}{\hat{J}_n(ka)\,\hat{N}_n(kR) - \hat{N}_n(ka)\,\hat{J}_n(kR)}\,\hat{H}_n^{(1)}(kR)\ .$$

*Hint:* Find the electric and magnetic fields from the electric vector potential and then apply the boundary and discontinuity conditions.

**8.14** Find the scattered field for a dielectric sphere with parameters $\varepsilon_s$ and $\mu_s$ and radius $a$, placed above an infinite ground plane whose center is at a height of $h > a$ above the ground plane. This object is illuminated by a plane wave given by

$$\mathbf{E}_i = \hat{\mathbf{x}}\, E_0 e^{ik\sin\theta_i\, y - \cos\theta_i\, z}\ .$$

*Hint:* Use image theory and ignore the mutual scattering between the sphere and its image.

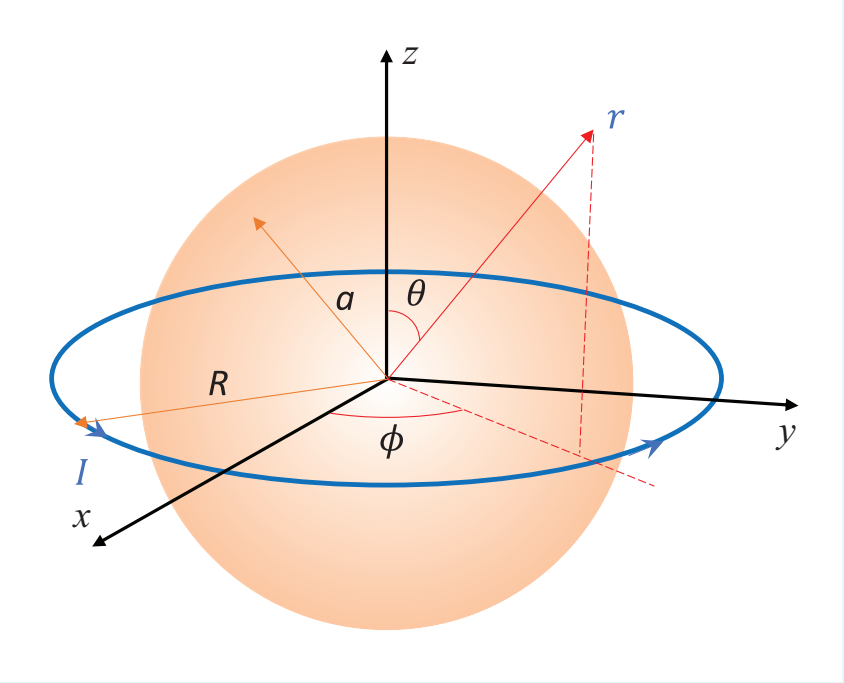


**Figure P8.13:** A metallic sphere of radius $a$ is excited by a concentric loop of constant electric current of radius $R$.

## Conical Structures

**8.15** For a biconical waveguide with a flare angle $\theta$, as shown in Fig. P8.15, calculate the electric vector potential $A_{\text{mr}}$ and the magnetic vector potential $A_r$. The dominant mode of this structure is a TEM. Show that $A_r$ for the TEM mode is defined as

$$A_r = Q_0(\cos\theta)\,\hat{h}_0^{(1)}(kr) = \ln\left(\cot\frac{\theta}{2}\right)\,(\mp i)e^{\pm ikr}\,.$$

**8.16** Consider a coaxial biconical waveguide. Assuming the conductivity of the metal used to make a biconical waveguide suppoorting a TEM mode is $\sigma$, show that an expression for the attenuation rate as a function of radial distance is given by

$$\alpha = \frac{1}{2\eta\sigma}\,\frac{\csc\theta_1 + \csc\theta_2}{\log\dfrac{\cot\theta_1/2}{\cot\theta_2/2}}\,\frac{1}{r}\,.$$

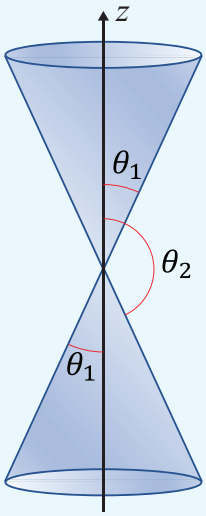


**Figure P8.15:** A metallic biconical structure with $\theta_2 = \pi - \theta_1$.

**8.17** Consider an infinitesimal current filament $I\,d\ell$ placed at the tip of a metallic cone specified by exterior angle $\theta_1$, as shown in Fig. P8.17. Find the radiated electric field for this problem.

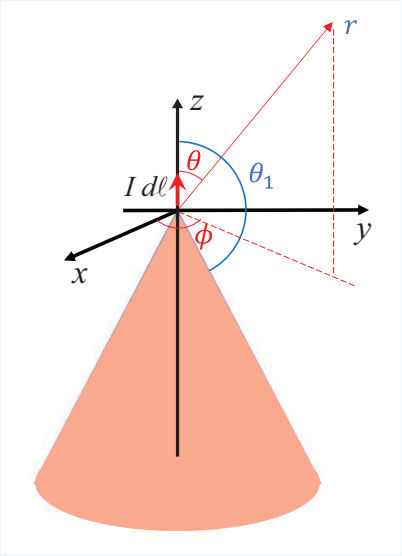


**Figure P8.17:** A metallic cone excited by a $z$-directed infinitesimal current at its tip.

# APPENDIX A: PROPERTIES OF COMPLEX FUNCTIONS

In this appendix important theorems for complex functions are reviewed. To start, basic definitions and properties of complex functions are provided. In general, a function of complex variable $z$ within a domain $\Omega$ in the complex $z$-plane is a collection of ordered complex pairs $(z,w)$, where the first complex number $(z)$ is the independent variable and the second complex number $(w)$ is known as the dependent variable. In complex notation, this relation between the dependent and independent variables is given by

$$w = f(z) \; . \tag{A.1}$$

Function $f(z)$ with domain $\Omega$ is said to be continuous at $z_0 \in \Omega$ if $f(z_0) \neq \infty$ and for any positive real number $\varepsilon > 0$ and for all $z$ in the neighborhood of $z_0$ for which

$$|f(z) - f(z_0)| < \varepsilon \; , \tag{A.2}$$

one can find a real and positive number $\delta$ such that

$$|z - z_0| < \delta \; . \tag{A.3}$$

In this case it can be shown that

$$\lim_{z \to z_0} f(z) = f(z_0) \; . \tag{A.4}$$

A function $w = f(z)$ is said to be differentiable in some $\varepsilon$-neighborhood of a point $z_0$ if the following limit exists and is not infinite:

$$f'(z_0) = \lim_{h \to 0} \frac{f(z_0 + h) - f(z_0)}{h} \; . \tag{A.5}$$

Here $h$, in general, is a complex number and the requirement for differentiability mandates that the same limit should exist independent of the path in the complex plane along which $h \to 0$. Since this definition for differentiation is similar to that for real functions, all differentiation properties, such as linearity and the rules for products and ratios of differentiable functions, apply. Also, the chain rule applies.

## A-1 Cauchy–Riemann Conditions

Consider a differentiable function $w = f(z)$ at $z_0 = x_0 + iy_0$. This function may be expressed in the following manner:

$$f(z) = u(x,y) + i\upsilon(x,y)\ , \tag{A.6}$$

where $u$ and $\upsilon$ are real functions of two variables. The Cauchy–Riemann theorem states that if $f$ is differentiable at $z_0$, the partial derivatives $\frac{\partial u}{\partial x}$, $\frac{\partial u}{\partial y}$, $\frac{\partial \upsilon}{\partial x}$, and $\frac{\partial \upsilon}{\partial y}$ exist at $(x_0, y_0)$, and

$$\frac{\partial u(x_0,y_0)}{\partial x} = \frac{\partial \upsilon(x_0,y_0)}{\partial y} \tag{A.7a}$$

and

$$\frac{\partial u(x_0,y_0)}{\partial y} = -\frac{\partial \upsilon(x_0,y_0)}{\partial x}\ . \tag{A.7b}$$

A function $w = f(z)$ is said to be ***analytic*** in some $\varepsilon$-neighborhood of $z_0$ if and only if it is differentiable in that neighborhood. For example, polynomial functions are analytic everywhere, and rational functions are analytic everywhere except for points where the denominator becomes zero.

It is interesting to note that if $f(z)$ is analytic, using Eqs. (A.7a) and (A.7b), then it can be shown that

$$\nabla_{\mathrm{t}}^2\, u(x,y) = 0 \tag{A.8a}$$

and

$$\nabla_{\mathrm{t}}^2\, \upsilon(x,y) = 0\ , \tag{A.8b}$$

where

$$\nabla_{\mathrm{t}}^2 = \frac{\partial^2}{\partial x^2} + \frac{\partial^2}{\partial y^2}$$

is a 2-D Laplacian operator.

It is noted that analyticity at one point guarantees that the function has all higher-order derivatives, and therefore all partial derivatives of $u(x,y)$ and $\upsilon(x,y)$ exist and are continuous.

## A-2 Conformal Mapping

A function $w = f(z)$ can be considered a mapping from $z = x + iy$ in $z$-plane into $w = u + i\upsilon$ in $w$-plane. If $f(z)$ is analytic in domain $\Omega$ and $f'(z_0) \neq 0$ for a point $z_0$ in $\Omega$, then the mapping is said to be ***conformal***, as it preserves angles between any two curves crossing at $z_0$ in the $z$-plane and those of the mapped curves at $w_0 = f(z_0)$ in magnitude and sense. Small segments of curves passing through $z_0$ are rotated by $\arg[f'(z_0)]$ and a curve length is scaled by $|f'(z_0)|$.

It is also interesting to note that the Laplacian operator is unchanged under a conformal mapping. If $\phi(x,y)$ represents a real function of $x$ and $y$ that satisfies Laplace's equation

$(\nabla_t^2 \phi(x,y) = 0)$, then it can be shown that by conformal mapping from $z$-plane to $w$-plane

$$\nabla_t^2 \phi(u,v) = \frac{\partial^2 \phi}{\partial u^2} + \frac{\partial^2 \phi}{\partial v^2} = \frac{1}{|f'(z)|^2}\left(\frac{\partial^2 \phi}{\partial x^2} + \frac{\partial^2 \phi}{\partial y^2}\right) = 0\,. \tag{A.9}$$

## A-3 Branch Cut and Branch Point

In the definition of complex functions, multiple-valued functions are not allowed. Functions, in general, can be one-to-one and many-to-one. Functions like $e^z$ or $z^2$ are examples of many-to-one functions. For such functions the inverse cannot be defined uniquely, as they become multiple-valued functions. However, if we restrict the domain of many-to-one functions in such a way as to make them one-to-one, then an inverse exists. For example, noting that

$$e^{z+i2n\pi} = e^z\,, \tag{A.10}$$

it is obvious that $f(z) = e^z$ is a many-to-one function. But if we restrict the domain of the function so that $-\pi \le \Im\mathrm{m}(z) \le \pi$, then the function becomes one-to-one. The inverse of this function is

$$g(z) = f^{-1}(z) = \ln z = \ln|z| + i\phi\,, \tag{A.11}$$

where $\phi = \arg(z)$ and $\pi \le \phi \le \pi$. Depending on what restrictions can be placed on $\phi$, to make the function single-valued, many logarithm functions can be defined. Based on the above definition, the logarithm function is discontinuous on the negative real axis. Also, at $z = 0$ the function is undefined; otherwise $\ln(z)$ is analytic. The negative real axis where the function is discontinuous is called a ***branch cut***, and $z = 0$ is called a ***branch point***. It should be noted that the branch cut depends on the restriction put on $\phi$ or definition used for $\phi$ to make the function single-valued. In fact the branch cut does not have to be a straight line and can be an arbitrary curve passing through the branch point.

Other logarithm functions can be defined from

$$\ln(z) = \ln|z| + i(\phi + 2n\pi)\,, \qquad n = 0, \pm 1, \pm 2, \ldots \tag{A.12}$$

The function for $n = 0$ is referred to as the ***principal branch***. Now consider the $n$th value of the logarithm function, the range of argument of $z(\phi)$ must satisfy

$$(2n-1)\pi < \phi < (2n+1)\pi\,. \tag{A.13}$$

The lines corresponding to $\phi = (2n-1)\pi$ are called the branch cuts, as shown in Fig. A-1.

## A-4 Cauchy's Theorem

A region in the complex $z$-plane is called a ***simply connected*** domain if every enclosed contour within this domain encloses only points that are in the domain. Figures A-2(a) and A-2(b) show a simply connected and ***multiply connected*** domains in the complex $z$-plane. Cauchy's theorem states that for a complex function $f(z)$ that is analytic in a simply connected

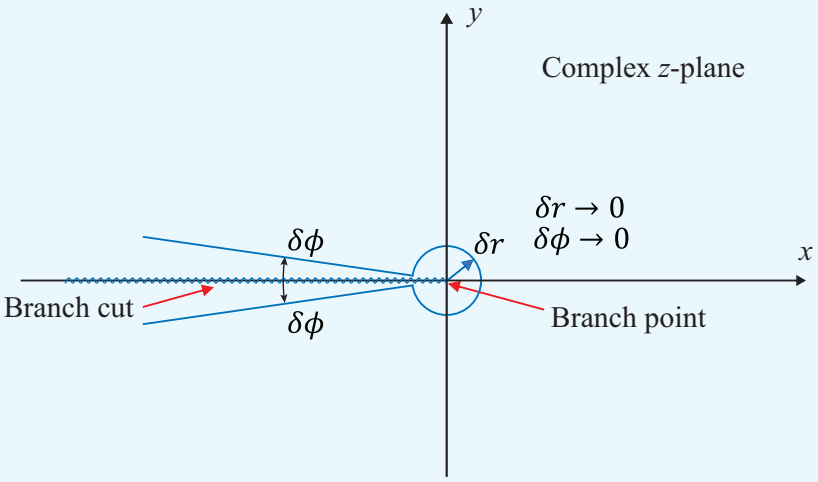


**Figure A-1:** Configuration of a branch cut and the branch point of a logarithm function.

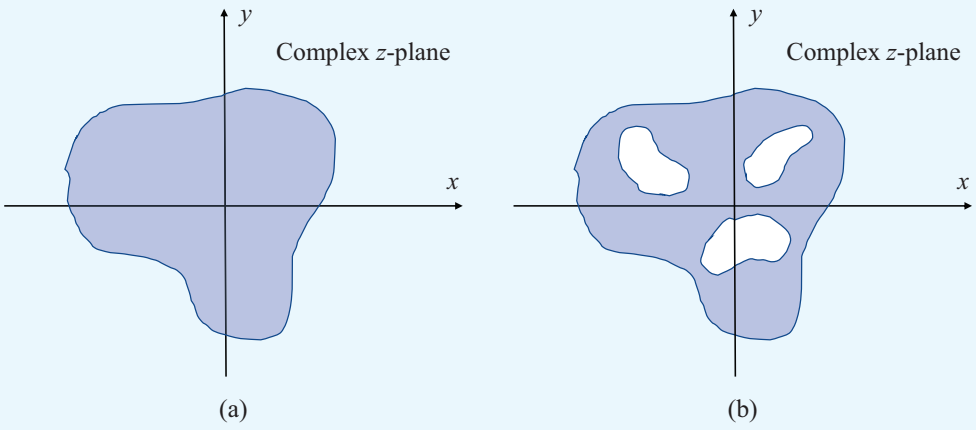


**Figure A-2:** Configuration of (a) a simply connected domain and (b) a multiply connected domain in a complex $z$-plane.

domain $\Omega$ and for any simple closed contour $C$ in $\Omega$, we have

$$\oint_C f(z)\,dz = 0\,. \tag{A.14}$$

## A-5 Cauchy Formulas

Consider a complex function $f(z)$ that is analytic within and on a simple contour $C$. Then for any point $z$ within $C$, we have

$$f(z) = \frac{1}{2\pi i}\oint_{C^+} \frac{f(\zeta)\,d\zeta}{\zeta - z}\,, \tag{A.15}$$

where the direction of integration is in the positive sense (counterclockwise). The result of the first Cauchy formula given by Eq. (A.15) can be used to show that

$$f'(z) = \frac{1}{2\pi i}\oint_{C^+} \frac{f(\zeta)\,d\zeta}{(\zeta - z)^2}\,. \tag{A.16}$$

By differentiating Eq. (A.16), the second derivative of $f(z)$ can be obtained from

$$f''(z) = \frac{2}{2\pi i}\oint_{C^+} \frac{f(\zeta)\,d\zeta}{(\zeta - z)^2}\,. \tag{A.17}$$

In general, it can be shown that

$$f^{(n)}(z) = \frac{n!}{2\pi i}\oint_{C^+} \frac{f(\zeta)\,d\zeta}{(\zeta - z)^{n+1}}\,. \tag{A.18}$$

In fact, Eq. (A.18) can be used to prove that if $f(z)$ is an analytic function in a neighborhood around $z_0$, then $f(z)$ has all derivatives at $z_0$.

## A-6 Poles and Residues

The ***pole*** of a complex function $f(z)$ is defined as a point at which the function is singular (the function becomes infinite). However, the function is analytic in a neighborhood of this point. In this neighborhood the function can be expanded in terms of its Laurent series given by

$$f(z) = \sum_{n=0}^{\infty} a_n (z - z_0)^n + \sum_{m=1}^{M} \frac{b_m}{(z - z_0)^m}\,. \tag{A.19}$$

The second term in this expansion is called the ***principal value*** of $f(z)$ about $z_0$. In situations where the principal part of $f(z)$ about point $z_0$ has an infinite number of terms ($m = \infty$), the point is called an essential singular point.

The coefficient $b_1$ is known as the ***residue*** of $f(z)$ at $z_0$ and is given by

$$b_1 = \frac{1}{2\pi i} \int_C f(z)\, dz\,, \tag{A.20}$$

where $C$ is a small closed cntour around $z_0$ and the direction of integration is in the positive sense (counterclockwise).

The residue theorem states that for an analytic function $f(z)$ within and on a contour $C$ except for a finite number of singular points $z_1, z_2, z_3, \ldots, z_n$ interior to $C$, the integral

$$\oint_{C^+} f(z)\, dz = 2\pi i \sum_{i=1}^{n} K_i\,, \tag{A.21}$$

where $K_i$ is the residue associated with the singular point $z_i$.

## A-7 Jordan's Lemma

Jordan's lemma is often used in connection with the evaluation of integrals of function on the real axis. In such problems the real axis is closed using a semicircle of radius $R$ ($C_R$) centered at the origin in the upper or lower half-plane in the complex $z$-plane to form a closed contour and then let $R$ go to infinity. If the value of the integral over $C_R$ is known, by using the residue theorem, the value of the integral over the real axis can be obtained. This theorem applies to integrands of the form $f(x)\, e^{iax}$ for a positive parameter $a$. For a continuous function $f(z)$ on $C_R$ that satisfies

$$\lim_{R\to\infty} |f(Re^{i\phi})| = 0\,, \tag{A.22}$$

Jordan's lemma states that

$$I_R = \lim_{R\to\infty} \int_{C_R} f(z)\, e^{iaz}\, dz = 0\,. \tag{A.23}$$

In this case,

$$\int_{-\infty}^{\infty} f(x)\, e^{iax}\, dx = 2\pi i \sum_{i=1}^{n} K_i e^{iaz_i}\,. \tag{A.24}$$

where $K_i$ is the residue of $f(z)$ at a finite number of nonreal singular points of $f(z)$ in the upper half-plane.

# APPENDIX B: METHOD OF STEEPEST DESCENT

In radiation and scattering problems we often encounter a certain type of integral of the form

$$I = \int_C g(z)\, e^{\lambda\, h(z)}\, dz\ . \tag{B.1}$$

With some appropriate assumptions, this integral can be evaluated approximately using the method of steepest descent. Here, $C$ represents a fixed path in the complex $z$-plane on which $g(z)$ and $h(z)$ are analytic in some region $\Omega$ that includes $C$. Assuming the integral exists for $\Re\mathrm{e}[\lambda] > 0$ and that its value does not change if the contour $C$ is deformed, the method of steepest descent consists of changing the path of integration to a new path over which the integrand changes most rapidly.

Let us assume that

$$h(z) = u(x,y) + i\upsilon(x,y)\ , \tag{B.2}$$

and consider a point $z_0 = x_0 + iy_0$ in the domain $\Omega$. A direction away from $z = z_0$ along which $u(x,y)$ decreases from $u(x_0,y_0)$ is called a ***direction of descent***, whereas if $u(x,y)$ increases from $u(x_0,y_0)$, the direction is called a ***direction of asscent***. Consider a path $C'$ in $\Omega$ that starts at $z_0$ and ends at $z_1$. If the tangent to $C'$ is always in a direction of descent (ascent), then $C'$ is called a ***path of descent*** (***ascent***). A path of ***steepest descent*** (***ascent***) is a path on which variations $\delta u$ of $u$ are maximum. Noting that for

$$\delta h = h(z) - h(z_0) = \delta u + i\delta\upsilon\ , \tag{B.3}$$

it follows that

$$|\delta h|^2 = |\delta u|^2 + |\delta\upsilon|^2\ . \tag{B.4}$$

To maximize variations of $u$ for a fixed $|\delta h|^2$, variations of $\upsilon$ must be set to zero:

$$\delta\upsilon = 0\ . \tag{B.5}$$

Hence the path of steepest descent or ascent that goes through $z_0 = x_0 + iy_0$ is given by

$$\upsilon(x,y) = \upsilon(x_0,y_0)\ . \tag{B.6}$$

Now consider the exponent function of the integrand of Eq. (B.1) evaluated along the steepest descent or ascent path

$$e^{\lambda\, h(z)} = e^{\lambda[u(x,y)+i\upsilon(x_0,y_0)]}\ . \tag{B.7}$$

The absolute value of $h(z)$, obviously, takes its maximum variation to lower values than $|h(z_0)$ if Eq. (B.6) is chosen to be the steepest descent path, or to higher values than $|h(z_0)|$ if Eq. (B.6) is chosen to be the steepest asscent path.

## B-1 Saddle Point

As mentioned earlier, the path of the contour in Eq. (B.1) can be changed if $g(z)$ and $h(z)$ are analytic functions. The question remains as to which new contour can provide an accurate approximation of Eq. (B.1). In this section, it is shown that if the new contour passes through a point $z_0$ for which

$$h'(z_0) = 0 \,, \tag{B.8}$$

the steepest descent path that goes through $z_0$ provides the maximum variation of $e^{\lambda\, h(z)}$ to lower values. The point $z_0$ that satisfies Eq. (B.8) is known as the ***saddle point*** of function $h(z)$. The reason for choosing the name "saddle point" for $z_0$ is that $h'(z_0) = 0$ does not specify a maximum or minimum for $|h(z)|$, $u(x,y)$, or $\upsilon(x,y)$.

To show that for an analytic function, $|h(z)|$ does not assume its maximum or minimum at $z_0$ where $h'(z_0) = 0$, let us consider the Cauchy integral formula

$$\oint_C \frac{h(z)\, dz}{z - z_0} = 2\pi i\, h(z_0) \tag{B.9}$$

for a point $z_0$ inside $C$. If $C$ is a circle centered at $z_0$ with radius $\rho$, then on $C$

$$z - z_0 = \rho e^{i\phi} \,. \tag{B.10}$$

Using Eq. (B.9), it can be shown that

$$|h(z_0)| = \frac{1}{2\pi} \left| \int_0^{2\pi} h(z)\, i\, d\phi \right| \leq \frac{1}{2\pi} \int_0^{2\pi} |h(z_0 + \rho' e^{i\phi})|\, d\phi \,. \tag{B.11}$$

If $M$ represents the maximum value of $|h(z)|$ on the circle, then the inequality in Eq. (B.11) can be written as

$$|h(z_0)| \leq \frac{1}{2\pi} M \int_0^{2\pi} d\phi = M \tag{B.12}$$

for all values of $z_0$ inside $C$. This result can easily be generalized to any noncircular contour $C$. Equation (B.12) shows that $|h(z)|$ assumes its maximum on the contour and not inside the contour. This is true for all $z_0$ points inside the contour including a point for which $h'(z_0) = 0$.

For a contour in which $h(z)$ has no zero values, $1/h(z)$ is analytic, and therefore $|1/h(z)|$ has no maximum inside $C$. As a result, $|h(z)|$ has no minimum value inside $C$. For this function $z_0$ for which $h(z_0) = 0$ represents a saddle point, as shown in Fig. B-1. This theorem also holds for the real and imaginary parts of $h(z)$. That is, the points of zero derivative of $h(z)$ are saddle points for $u$ and $\upsilon$ functions:

$$u(x_0, y_0) < u_{\max \text{ on } C}$$

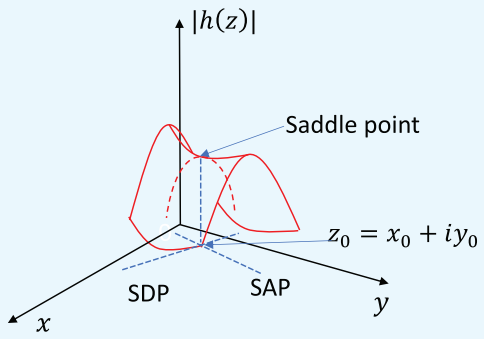


**Figure B-1:** For an analytic function $h(z) = u(x,y) + i\upsilon(x,y)$, the point $z_0$ for which $h'(z_0) = 0$ does not present a maximum or a minimum of $|h(z)|$, $u(x,y)$, or $\upsilon(x,y)$. It simply represents a saddle point for $|h(z)|$, $u(x,y)$, or $\upsilon(x,y)$. The maximum and minimum of such functions in a simply connected domain occur on its boundary.

and

$$\upsilon(x_0, y_0) < \upsilon_{\max \text{ on } C} \, .$$

## B-2 Integration along the Steepest Descent Path

Considering the integral represented by Eq. (B.1) and for contour $C$ shown in Fig. B-2, we first identify the saddle point $z_0$ for function $h(z)$ for which

$$\left.\frac{dh(z)}{dz}\right|_{z=z_0} = 0 \, .$$

Let us also assume that

$$\left.\frac{d^2h(z)}{dz^2}\right|_{z=z_0} = Ae^{i\alpha}$$

and

$$\lim_{z \to C_\infty} g(z)\, e^{\lambda\, h(z)} = 0 \, ,$$

where $C_\infty$ is a circle with a very large radius $\rho \to \infty$. Then according to Cauchy's theorem,

$$\int_C g(z)\, e^{\lambda\, h(z)}\, dz + \int_{\text{SDP}} S(z)\, e^{\lambda\, h(z)}\, dz = 0 \, .$$

The integral on the steepest descent path (SDP) can be evaluated by expanding $h(z)$ in terms of its Taylor series expansion and only retaining the second term of expansion in the exponent.

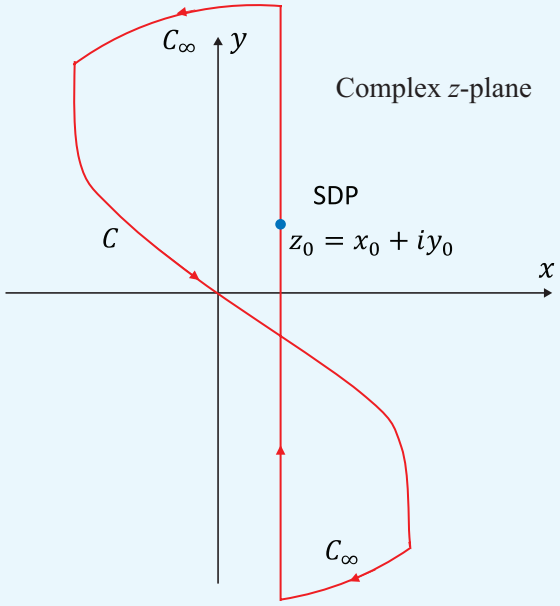


**Figure B-2:** The path of integration method ($C$) for the saddle point method is deformed to the steepest descent path (SDP) noting that the integrand contributionon $C_\infty$ is zero. The integration on SDP is approximated by retaining only the second term of the Taylor series expansion of $h(z)$ and then using the Fresnel integral value.

After some algebraic manipulations, the approximate value of the integral is found to be

$$\int_C g(z)\, e^{\lambda\, h(z)}\, dz \approx \frac{-\sqrt{2\pi}}{\sqrt{\lambda |h''(z_0)|}}\, g(z_0)\, e^{\lambda\, h(z_0)} e^{-i(\alpha-\pi)/2}\,. \tag{B.13}$$

# APPENDIX C:
# USEFUL VECTOR IDENTITIES, OPERATORS, AND COORDINATE TRANSFORMATIONS

**Table C.1:** Useful vector identities.

$$\mathbf{A}\cdot(\mathbf{B}\times\mathbf{C})=\mathbf{B}\cdot(\mathbf{C}\times\mathbf{A})=\mathbf{C}\cdot(\mathbf{A}\times\mathbf{B}) \tag{C.1}$$

$$\mathbf{A}\times(\mathbf{B}\times\mathbf{C})=(\mathbf{A}\cdot\mathbf{C})\mathbf{B}-(\mathbf{A}\cdot\mathbf{B})\mathbf{C} \tag{C.2}$$

$$\nabla(\phi\psi)=\phi\nabla\psi+\psi\nabla\phi \tag{C.3}$$

$$\nabla\cdot(\psi A)=A\cdot\nabla\psi+\psi\nabla\cdot A \tag{C.4}$$

$$\nabla\times(\psi A)=\psi\nabla\times A-A\times\nabla\psi \tag{C.5}$$

$$\nabla(\mathbf{A}\cdot\mathbf{B})=\mathbf{A}\times(\nabla\times\mathbf{B})+\mathbf{B}\times(\nabla\times\mathbf{A})+(\mathbf{A}\cdot\nabla)\mathbf{B}+(\mathbf{B}\cdot\nabla)\mathbf{A} \tag{C.6}$$

$$\nabla\cdot(\mathbf{A}\times\mathbf{B})=\mathbf{B}\cdot(\nabla\times\mathbf{A})-\mathbf{A}\cdot(\nabla\times\mathbf{B}) \tag{C.7}$$

$$\nabla\times(\mathbf{A}\times\mathbf{B})=\mathbf{A}(\nabla\cdot\mathbf{B})-\mathbf{B}(\nabla\cdot\mathbf{A})+(\mathbf{B}\cdot\nabla)\mathbf{A}-(\mathbf{A}\cdot\nabla)\mathbf{B} \tag{C.8}$$

$$(\mathbf{A}\cdot\nabla)\mathbf{A}=\tfrac{1}{2}\nabla|\mathbf{A}|^2+(\nabla\times\mathbf{A})\times\mathbf{A} \tag{C.9}$$

$$\nabla\times\nabla\phi=0 \tag{C.10}$$

$$\nabla\cdot(\nabla\times\mathbf{A})=0 \tag{C.11}$$

$$\nabla\cdot\nabla\phi=\nabla^2\phi \tag{C.12}$$

$$\nabla\times(\nabla\times\mathbf{A})=\nabla(\nabla\cdot\mathbf{A})-\nabla^2\mathbf{A} \tag{C.13}$$

**Table C.2: Gradient, divergence, curl, and Laplacian operators.**

| | Cartesian Coordinates $(x,y,z)$ | Cylindrical Coordinates $(\rho,\phi,z)$ | Spherical Coordinates $(r,\theta,\phi)$ |
|---|---|---|---|
| Gradient $\nabla f$ | $\frac{\partial f}{\partial x}\,\hat{\mathbf{x}}+\frac{\partial f}{\partial y}\,\hat{\mathbf{y}}+\frac{\partial f}{\partial z}\,\hat{\mathbf{z}}$ | $\frac{\partial f}{\partial \rho}\,\hat{\boldsymbol{\rho}}+\frac{1}{\rho}\frac{\partial f}{\partial \phi}\,\hat{\boldsymbol{\phi}}+\frac{\partial f}{\partial z}\,\hat{\mathbf{z}}$ | $\frac{\partial f}{\partial r}\,\hat{\mathbf{r}}+\frac{1}{r}\frac{\partial f}{\partial \theta}\,\hat{\boldsymbol{\theta}}+\frac{1}{r\sin\theta}\frac{\partial f}{\partial \phi}\,\hat{\boldsymbol{\phi}}$ |
| Divergence $\nabla\cdot\mathbf{A}$ | $\frac{\partial A_x}{\partial x}+\frac{\partial A_y}{\partial y}+\frac{\partial A_z}{\partial z}$ | $\frac{1}{\rho}\frac{\partial(\rho A_\rho)}{\partial \rho}+\frac{1}{\rho}\frac{\partial A_\phi}{\partial \phi}+\frac{\partial A_z}{\partial z}$ | $\frac{1}{r^2}\frac{\partial(r^2A_r)}{\partial r}+\frac{1}{r\sin\theta}\frac{\partial(A_\theta\sin\theta)}{\partial\theta}+\frac{1}{r\sin\theta}\frac{\partial A_\phi}{\partial\phi}$ |
| Curl $\nabla\times\mathbf{A}$ | $\left(\frac{\partial A_z}{\partial y}-\frac{\partial A_y}{\partial z}\right)\hat{\mathbf{x}}+\left(\frac{\partial A_x}{\partial z}-\frac{\partial A_z}{\partial x}\right)\hat{\mathbf{y}}+\left(\frac{\partial A_y}{\partial x}-\frac{\partial A_x}{\partial y}\right)\hat{\mathbf{z}}$ | $\left(\frac{1}{\rho}\frac{\partial A_z}{\partial\phi}-\frac{\partial A_\phi}{\partial z}\right)\hat{\boldsymbol{\rho}}+\left(\frac{\partial A_\rho}{\partial z}-\frac{\partial A_z}{\partial\rho}\right)\hat{\boldsymbol{\phi}}+\frac{1}{\rho}\left(\frac{\partial(\rho A_\phi)}{\partial\rho}-\frac{\partial A_\rho}{\partial\phi}\right)\hat{\mathbf{z}}$ | $\frac{1}{r\sin\theta}\left(\frac{\partial}{\partial\theta}(A_\phi\sin\theta)-\frac{\partial A_\theta}{\partial\phi}\right)\hat{\mathbf{r}}+\frac{1}{r}\left(\frac{1}{\sin\theta}\frac{\partial A_r}{\partial\phi}-\frac{\partial}{\partial r}(rA_\phi)\right)\hat{\boldsymbol{\theta}}+\frac{1}{r}\left(\frac{\partial}{\partial r}(rA_\theta)-\frac{\partial A_r}{\partial\theta}\right)\hat{\boldsymbol{\phi}}$ |
| Laplacian $\nabla^2 f$ | $\frac{\partial^2 f}{\partial x^2}+\frac{\partial^2 f}{\partial y^2}+\frac{\partial^2 f}{\partial z^2}$ | $\frac{1}{\rho}\frac{\partial}{\partial\rho}\left(\rho\frac{\partial f}{\partial\rho}\right)+\frac{1}{\rho^2}\frac{\partial^2 f}{\partial\phi^2}+\frac{\partial^2 f}{\partial z^2}$ | $\frac{1}{r^2}\frac{\partial}{\partial r}\left(r^2\frac{\partial f}{\partial r}\right)+\frac{1}{r^2\sin\theta}\frac{\partial}{\partial\theta}\left(\sin\theta\frac{\partial f}{\partial\theta}\right)+\frac{1}{r^2\sin^2\theta}\frac{\partial^2 f}{\partial\phi^2}$ |

## Coordinate Transformation

Consider a field vector $\mathbf{F}$ that can be expressed in Cartesian, cylindrical, and spherical coordinates as

$$\mathbf{F} = f_x\,\hat{\mathbf{x}} + f_y\,\hat{\mathbf{y}} + f_z\,\hat{\mathbf{z}}\,,$$
$$\mathbf{F} = f_\rho\,\hat{\boldsymbol{\rho}} + f_\phi\,\hat{\boldsymbol{\phi}} + f_z\,\hat{\mathbf{z}}\,,$$
$$\mathbf{F} = f_r\,\hat{\mathbf{r}} + f_\theta\,\hat{\boldsymbol{\theta}} + f_\phi\,\hat{\boldsymbol{\phi}}\,.$$

The components of $\mathbf{F}$ in these coordinates systems are related to each other at a given point $\mathbf{p} = (x\,\hat{\mathbf{x}} + y\,\hat{\mathbf{y}} + z\,\hat{\mathbf{z}}) = \rho\,\hat{\boldsymbol{\rho}} + z\,\hat{\mathbf{z}} = r\,\hat{\mathbf{r}}$ as shown below:

**Cartesian to cylindrical:**
$$\begin{bmatrix} f_\rho \\ f_\phi \\ f_z \end{bmatrix} = \begin{bmatrix} \frac{x}{\sqrt{x^2+y^2}} & \frac{y}{\sqrt{x^2+y^2}} & 0 \\ -\frac{y}{\sqrt{x^2+y^2}} & \frac{x}{\sqrt{x^2+y^2}} & 0 \\ 0 & 0 & 1 \end{bmatrix} \begin{bmatrix} f_x \\ f_y \\ f_z \end{bmatrix}$$

**Cylindrical to Cartesian:**
$$\begin{bmatrix} f_x \\ f_y \\ f_z \end{bmatrix} = \begin{bmatrix} \cos\phi & -\sin\phi & 0 \\ \sin\phi & \cos\phi & 0 \\ 0 & 0 & 1 \end{bmatrix} \begin{bmatrix} f_\rho \\ f_\phi \\ f_z \end{bmatrix}$$

**Cartesian to spherical:**
$$\begin{bmatrix} f_r \\ f_\theta \\ f_\phi \end{bmatrix} = \begin{bmatrix} \frac{x}{\sqrt{x^2+y^2+z^2}} & \frac{y}{\sqrt{x^2+y^2+z^2}} & \frac{z}{\sqrt{x^2+y^2+z^2}} \\ \frac{xz}{\sqrt{(x^2+y^2)(x^2+y^2+z^2)}} & \frac{yz}{\sqrt{(x^2+y^2)(x^2+y^2+z^2)}} & \frac{-\sqrt{x^2+y^2}}{\sqrt{x^2+y^2+z^2}} \\ \frac{-y}{\sqrt{x^2+y^2}} & \frac{x}{\sqrt{x^2+y^2}} & 0 \end{bmatrix} \begin{bmatrix} f_x \\ f_y \\ f_z \end{bmatrix}$$

**Spherical to Cartesian:**
$$\begin{bmatrix} f_x \\ f_y \\ f_z \end{bmatrix} = \begin{bmatrix} \sin\theta\cos\phi & \cos\theta\cos\phi & -\sin\phi \\ \sin\theta\sin\phi & \cos\theta\sin\phi & \cos\phi \\ \cos\theta & -\sin\theta & 0 \end{bmatrix} \begin{bmatrix} f_r \\ f_\theta \\ f_\phi \end{bmatrix}$$

## Integral Identities

Surface integral for an arbitrary open surface bounded by the contour $C$:

$$\iint_S \nabla \times \mathbf{A} \cdot d\mathbf{s} = \oint_C \mathbf{A} \cdot \boldsymbol{\ell}$$
$$\iint_S \hat{\mathbf{n}} \times \nabla\phi \, d\mathbf{s} = \oint_C \phi \, d\mathbf{s}$$

Volume integral for an arbitrary volume bounded by closed surface $S$:

$$\iiint_V \nabla \cdot \mathbf{A} \, dv = \oiint_S \mathbf{A} \cdot d\mathbf{s}$$
$$\iiint_V \nabla \times \mathbf{A} \, dv = -\oiint_S \mathbf{A} \times d\mathbf{s}$$
$$\iiint_V \nabla\phi \, dv = \oiint_S \phi \, d\mathbf{s}$$

### Proofs of Integral Relations

Proofs of some of the useful integral identities are provided here:

a. Show that
$$\iiint_V \nabla \times \mathbf{F} \, dv = -\oiint_S \mathbf{F} \times d\mathbf{s} \, .$$

*Proof:* Starting from the vector calculus identity

$$\nabla \cdot (\mathbf{G} \times \mathbf{F}) = \mathbf{F} \cdot \nabla \times \mathbf{G} - \mathbf{G} \cdot \nabla \times \mathbf{F}$$

and assuming $\mathbf{G}$ is a constant vector, we have

$$\iiint_V \nabla \cdot (\mathbf{G} \times \mathbf{F})\, dv = -\mathbf{G} \cdot \iiint_V \nabla \times \mathbf{F}\, dv = \oiint (\mathbf{G} \times \mathbf{F}) \cdot d\mathbf{s}\,,$$

but

$$\mathbf{G} \times \mathbf{F} \cdot d\mathbf{s} = \mathbf{G} \cdot \mathbf{F} \times d\mathbf{s}\,.$$

Since $\mathbf{G}$ is an arbitrary vector, it is now obvious that

$$\iiint_V \nabla \times \mathbf{F}\, dv = -\oiint \mathbf{F} \times d\mathbf{s}\,. \tag{C.14}$$

b. Show that

$$\iiint_V \nabla \psi\, dv = \oiint_S \psi\, d\mathbf{s}\,.$$

*Proof:* In a similar manner, we first note that

$$\nabla \cdot (\psi \mathbf{G}) = \mathbf{G} \cdot \nabla \psi + \psi \nabla \cdot \mathbf{G}\,.$$

Then for some arbitrary constant $\mathbf{G}$,

$$\nabla \cdot (\psi \mathbf{G}) = \mathbf{G} \cdot \nabla \psi\,. \tag{C.15}$$

Taking the volumetric integral from both sides of Eq. (C.15), we have

$$\iiint_V \nabla \cdot (\psi \mathbf{G})\, dv = \mathbf{G} \cdot \oiint \psi\, d\mathbf{s} = \mathbf{G} \cdot \iiint_V \nabla \psi\, dv\,.$$

Hence

$$\iiint_V \nabla \psi\, dv = \oiint_S \psi\, d\mathbf{s}\,. \tag{C.16}$$

c. Show that, for a differentiable scalar function $\psi$ and a surface $S$ having $C$ as its contour,

$$\int_S \hat{\mathbf{n}} \times \nabla \psi\, ds = \oint_C \psi\, d\boldsymbol{\ell}\,. \tag{C.17}$$

*Proof:* According to Stokes' theorem, for a constant vector $\mathbf{a}$,

$$\int_S \nabla \times (\psi \mathbf{a}) \cdot d\mathbf{s} = \oint_C \psi \mathbf{a} \cdot d\boldsymbol{\ell} = \mathbf{a} \cdot \oint_C \psi\, d\boldsymbol{\ell}\,. \tag{C.18}$$

Also,

$$\nabla \times (\psi \mathbf{a}) = \nabla \psi \times \mathbf{a} + \psi \nabla \times \mathbf{a} = \nabla \psi \times \mathbf{a}\,, \tag{C.19}$$

since $\nabla \times \mathbf{a} = 0$. Using Eq. (C.19), we have

$$\int_S \nabla \times (\psi \mathbf{a}) \cdot d\mathbf{s} = \int_S (\nabla \psi \times \mathbf{a}) \cdot \hat{\mathbf{n}}\, ds = \mathbf{a} \cdot \int_S (\hat{\mathbf{n}} \times \nabla \psi)\, ds\,. \tag{C.20}$$

From Eq. (C.18) and Eq. (C.20),

$$\int_S (\hat{\mathbf{n}} \times \nabla \psi)\, ds = \oint_C \psi\, d\boldsymbol{\ell}\,.$$

# Index

*Note:* Page numbers in *italics* refer to occurrences in the end-of-chapter problems.


$\theta$–$\phi$ spherical waveguide, 569, 570, 578
2-D Green's function for external problem, 449–451, 467–474

addition theorem, 405, 449, 490
addition theorem for spherical wave functions, 503, 535–538, 576
angular-sector waveguide, 405, 430–433, 437–441
anisotropic, 2, 17–18, 85, *99*, *223*, 241–245, 247, *304*, 329, 381
antenna directivity, 133–134, 146, 147, 151, *154, 155*, 162, 198
antenna equivalent circuit, 108, 135–137, 141, 147–149, 197, 198
antenna quality factor, 134–135, 151
antenna radiation pattern in receive and transmit modes, 192–194, 219
antennas as two-port networks, 189, 191, 218
associated Legendre functions of the first kind, 510, 512–514, 553
associated Legendre functions of the second kind, 510, 513
attenuation rate, 314, 344, 347–348, 352, 372–374, 391, *400*
axial ratio, 240

Babinet's principle, 162, 205–214, *226*
bandgap material, 290
Bessel equation, 407, 411, 414, 487
Bessel function of the first kind, 407–409, 411, 413–416, 430, 449, 465, 468, 487, 491
Bessel function of the second kind, 407–409, 411, 487
bianisotropic, 18, *99*, 247–254
biaxial, 18
biconical structure, 503, 560–566, *584*
birefringent, 254
bistatic echo width, 456, 460, 462
boundary conditions, 30–33, 67, 70, 74–76, 78, 83, 91–93, 98, *106*, *303*, *305*, *307–310*, 389, *395*, *397–399*, *403*, *583*
boundary conditions for the potentials, 173–176, 218
Bragg mirror, 285, *312*
Brewster angle, 261–264, 280, 301, 302

calculus of variations, 375–379, 382–387
cavity damping factor, 354, 356, 391
cavity relaxation time, 354, 356, 391
characteristic impedance, 118, 133, 151, 234, 265, 291, *310*, 324, 326, 332, 334, 358, 360, 435, 563, 565, 566
circuit models for waveguides, 314, 357–362
circumferential waveguide, 405, 433, 435–436
cladding, 421, 423, 426, *494*
coaxial biconical antenna, 563, 565–566
complementary antenna, 162, 205, 210–212
complementary theorem, 207–208
complex power flow density, 127, 151, 237
concentric spherical cavity, 575
conduction current, 7, 14, 429
conical horn antenna, 556, 558
conical waveguide, 503, 553–560, 577, 578
constitutive relations, 14–28, 90, *99*, *106*, 124, *223*, 248, 249, 277

continuous spectrum of plane waves, 234–235, 292, 321, 446
coordinate curve, 36
coordinate surface, 36, 119, *152*, 405, 406, 468, 503, 533
core, 421, 423, 426
critical angle, 262
curl, 6, 7, 41–43, 90, 143, 206, 229, 242
current density, 3, 63, 100, *104*, 130, 173, 199, 331, 359, 382, *500*
cutoff frequency, 314, 317–320, 339, 340, 348, 361, 375, 379, 381–382, 390, *394, 395*, *397*, *399*
cutoff wave number, 314, 340, 342, 379
cylindrical cavity, 405, 425–430, 489, *494–496*
cylindrical wave functions, 409, 421, 436, 445–446, 448, 450, 487
cylindrical waveguide, 405, 414–420

DB plane, 247
diamagnetism, 17
dielectric loss tangent, 130, *303*, 352, 533
dielectric plate waveguide, 314–320
dielectric quality factor, 130, 151, 354, 531, 533, 534
dielectric slab, 228, 288–290, 302, *310*, *312*
diffraction coefficients for metallic wedge, 480–483, 492
dipole, 108, 117, 134–136, 139, 142–147, 151, *154–157*, 192–194, 201, 203, 204, 210–212, 214, 215, *223*, *308*, 445, 446, 539–541, *579*, *582*
Dirichlet's boundary condition, 336, 337, 346, 353, 367, 370
dispersion relation, 228, 246–248, 251, 252, 278, 291, 300
dispersive material, 18–19, 122
displacement current, 7, 14, 130, 359
distributed Bragg reflector (DBR), 285
divergence theorem, 5, 8, 31, 32, *46, 47*, 85, 87, 129, 164, 165, 175, 179, 187, 372
double-negative media, 290–294, 296, 298, 302
drift current, 14
duality relations, 65–67, 71, 83, 98, 112, 113, 121, 125, 140, 206, 210, 257, 260, 282, 284, 319, 320, 360, 364, 505, 506

effective area of a receiving antenna, 162, 195–198, 219, *223*
effective permittivity, 125, 151
eigenfunction, 314, 368–371, 374–375, 377–380, 392, *399*, *401*
eigenvalue, 314, 338, 353, 368–370, 375–382, 384, 392, *403*
Eikonal equation, 266, 268, 270, 271, 274, 301, 302
electric energy density, 85, 88, *106*, 108, 128, 236–238, 300
electric field intensity, 3, 10, 14, 16, 32, *53*, 63, 90, *104*, 124, 128, 238, 241, 242, 253, 275, 340, 341, 418, *500*
electric flux density, 3, 9, 15, 16, 32, 33, *49*, *58*, 90, 109, 124, 128, 176, 241, 247, 252, 253, 275
electric reflection coefficient, 228, 260, 264, 282, 301, *303*
electric scalar potential, 108, 109, 111–113, 117–119, 125–126
electric susceptibility, 16, 18, *54*
electric transmission coefficient, 228, *303*
electric vector potential, 108, 112, 125–126, 151, *158*
electric-field integral equation (EFIE), 162, 183, 219
elementary wave functions, 409, 415, 450, 453
elliptic polarization, 238–240, *311*
ellipticity angle for polarization, 240, 300
energy density of plane waves, 228, 236–238, 300
energy velocity, 237, 238
equation of continuity, 6, 20, 44, 45, *58*, 177, 180
equivalent source, 71, 92–97, 162, 166, 167, 170, 172, 178–181

evanescent wave, 232, 234, 290, 292, 295–298
extinction theorem, 162, 170, 217
extraordinary wave, 228, 247, 252–254, 275, 276, 278–280, 300, 302

far-field distance, 118, 137–139, 145, 151, *154*, *156, 157*
Faraday's law, 2, 6–8, 10–14, 31, *49*, *54*, 63, 83, 123, 143, 266, 277, 286
Fermat's principle, 262–264
ferromagnetism, 17
finite element, 315, 379, 380
flow of electromagnetic power, 86–90, *104, 105*, 133, 344–348
formal solution for 2-D Green's function, 405, 439–441, 448
forward propagation matrix, 284
Fourier representation of 2-D Green's function, 446–448
Fourier-Legendre expansion, 517–520, *579*
Fredholm integral equation, 172
frequency-independent antennas, 162, 213
Friis transmission formula, *223*
functional, 375–380, 382, 384, 385, 392

gamma function, 411, 487
gauge condition, 110, 117, 125, 151, 174, 277, 503, 504, 572
Gauss' law for electricity, 2, 6, 8, 9, 20, 32, 33, 80, 83, 124, 235, 267, 287, 291
Gauss' law for magnetism, 2, 6, 8, 32, 64, 267, 291
generalized eigenvalue problem, 381
good conductor, 264–266, 302
gradient, 39, 43, 90, 170, 179, 268, 370
Green's first identity, 165, 217, 370, 376, 378
Green's function, 162, 165, 167, 168, 170, 171, 178, 179, 181, 182, 184, 186, 217, *221*, *493*
Green's function for angular-sector waveguide, 437–441, 448, 490
Green's second identity, 165, 170, 174, 178, 217, 369, 370, 515, 516
Green's theorem, 162, 165–166
group velocity, 314, 342–344, 390
guided wavelength, 390

H-bent rectangular waveguide, 435
Hall effect, 20, 35–36
Hankel functions of the first kind, 407, 434, 449, 450, 453, 465, 466, 487
Hankel functions of the second kind, 407, 449, 465, 466, 487
harmonic functions, 405, 407, 447, 464
Helmholtz equation, 162–176, 234, 236, 254–264, 282, 379, 406, 407, 409, 415, 430
Hertz vector potential, 111, 126, 228, 255, 276–278, 314, 363, *395*, *397*, 441, 443, 445, 446, 468, *497, 498*
Hertzian dipole, 108, 133–138, 145, 151, *154*
Hertzian magnetic dipole, 139–144, 151
homogeneous, 2, 3, 15, 31, *50*, *55*, *57*, 68, *99*, *106*, 151, 187, 228–238, 245–246, 300, *397*, 441–444, 448–451, 467–474
hybrid mode, 363, *397*, 405, 425, 426, *494*

image of a point charge over a dielectric half-space medium, 78–80
image of a point charge over a metallic sphere, 72–78
image of currents and charges over a planar conductive surface, 68–71
impermeability, 248
impermittivity, 248, 250
incident potential, 170, 172
inhomogeneous, 2, 15, 90, 93, 168, 187, 257, 266–274, 286–288
integral representation of Bessel function, 405, 409, 460–467, 491
isotropic homogeneous material, 15, 108, 109, 162, 245–246, 300, *312*
isotropic reactive impedance surface, 330–335

$k$–$\beta$ diagram, 340

kDB coordinate, 228, 247–254
Kramers-Krönig relations, 28–30, 45, *54*

Laplacian, 43, 504
law of conservation of charge, 3, 5–6, 8, 45, 75, 81
Legendre functions, 503, 510, 512, 513, 560, 561
Legendre polynomial, 511, 512, 514, 538

magnetic charge density, 63–65, 98
magnetic current density, 63, 65, 67, 80, 100, *101, 102*, 143
magnetic field intensity, 3, 35, 63, 90, *104*, 116, 124, 137, 252
magnetic flux density, 3, 8, 10, 12, 14–16, 32, 35, *50, 51*, 67, 90, 109, 124, 141, 242, 247, 253
magnetic Hertz vector potential, 112, 113, 151, 228, 255, 256, 276, 364, 539–542, 544, 562, *579*, *584*
magnetic moment of current loop, 139–141
magnetic reflection coefficient, 228, 259, 280, 301
magnetic scalar potential, 108, 112, 125–126
magnetic transmission coefficient, 228, 260
magnetic vector potential, 108, 109, 112, 113, 115, 125–126, 131, 139, 151, *153–157*
magnetic-field integral equation (MFIE), 162, 183, 219
magnetization vector, 16–18, 63, 64, 141, 290
metallic septa, 361
method of separation of variables, 228
modified Ampère's law, 2, 6, 14, 32, 80, 83, 111, 124, 143, 190, 267, 286, 291, 382, 442
modified Bessel function of the first kind, 410, 487
modified Bessel function of the second kind, 409, 410, 422, 487
monopole, 539
motional induction, 12
multipole, 538–542

natural boundary condition, 377, 378
negative refractive index, 292–298
negative refractive index lens, 292–298
Neumann's boundary condition, 336, 346, 353, 367, 370, 430
nonuniform plane wave, 228, 233
normalized duality relations, 66

ohmic loss, 88, 525
optical fiber, 405, 421, 425, 426, 489, *494*
optical path length, 263, 271
order of Bessel function, 405, 407, 408, 412, 415, 416, 468
ordinary point, 3, 108
ordinary wave, 228, 246, 252–254, 275, 276, 278, 279, 300
orthogonality of Bessel functions, 413–414, 488

paramagnetic, 17, 143
perfect electric conductor (PEC), 68–72, 93, 94, *101, 102*, *104*, *152, 153*, 156, 176, 208, 210, *225*, 264, *311*, 325, 346
perfect magnetic conductor (PMC), 67, 71, 92, 94, 97, 98, *100–102*, *152*, *156*, 194, 207, 209, 332, *395*, 429, *495*
phase velocity, 314, 340, 343, 344, 390
phase-matching condition, 258, 278, 282, 292, 293, 315, 331, 365
physical-optics current on metallic surfaces, *221*
plane wave, *158*, 199, 200, 202, 203, 221, 222, *225, 226*, 228–298, 321, 330, 446, 447, 452, 456, 459, 472–474, 477, 478, 481–483, 490, *500, 501*, 503, 533–535, 543, *582, 583*
Poincaré sphere, 241
point form of Ohm's law, 19, 20, 45, 67
polarization charge density, 80
polarization current, 65, 71, 80–83, 98, *99*, 130–131, *153*, 201, 202, *310*, 331, 429

polarization unit vector, 239, 300, *311*
polarization vector, 16, 18, 21, 26, 28, *57*, 80, 238, 239, 300, 311
potential energy, 84, 85
potential function, 83, 85, 108, 166, 175, 427, 430, 446, 447, 488, 522, 529, 536, 545, 554
power density of plane waves, 228, 237, 300
Poynting vector, 88, 98, *103, 104*, *106*, 126–127, 133, *154*, *157*, 237, 253, 254, 291, *303, 304*, *309*, 344, *399*, 444
principal-value integral, 172
principle of least time, 262

quadrupole, 539, 541, 542, *579, 580*
quality factor for cavities, 352–356, 391
quasi-static, 114, 116

radar cross section (RCS), 503, 546–549, 551, 576, 577
radial waveguide, 405, 433–435, 490, *496, 497*
radiation condition, 162, 166–169, 217
radiation resistance, 136, 141, 145, 146, *154, 155*, *157*
RCS of dielectric spheres, 551, 552, 577
RCS of metallic spheres, 546–549, 576
reactive impedance surface, 314, 321, 323–335, *399*
receiving antenna, 147–149
reciprocity condition for two-port networks, 192, 218
reciprocity for a source-free region, 190
reciprocity theorem, 162, 184–205, 218, *223*, 519, *582*
reciprocity theorem for a source-free region, 186, 218
rectangular cavity, 314, 349–357, 391, *400, 401*
rectangular waveguide, 314, 335–357, 361, 363–368, 375, 379, 390, *395–402*
reflection boundary, 477, 478, 480–482, 485
retarded potential, 113–115, 131–137

saddle point, 465, 479
saddle-point technique, 465, 479
scattered potential, 170, 171
Schelkunoff spherical Bessel functions, 514, 522, 527, 544, 547
self-complementary antenna, 162, 212–215, 220
shadow boundary, 477, 478
singularity point, 170, 171
skin depth, 265, 266, 302
Snell's law of reflection, 262, 270–271
Snell's law of refraction, 260, 262, 270–271, 301
spherical Bessel functions of the first kind, 507, 509
spherical Bessel functions of the second kind, 507, 509
spherical cavity, 503, 520–529, 575, *580, 581*
spherical dielectric resonator, 503, 529, 531, 533, 534, 575
spherical Hankel functions of the first kind, 508, 509, 553
spherical Hankel functions of the second kind, 508, 509
spherical harmonic functions, 503
spherical wave functions, 503, 506–585
stationary formulation, 382, 386–387
stationary phase point, 465
steepest descent path, 466, 592–595
Stokes' theorem, 7, 14, 31, *46, 47*, *58*, 143
superposition principle, 84, 90, 113, 121, 149
surface charge density, 33, 34, *58, 59*, 67, 75–77, 170
surface current density, 32, 34, *58*, 82, 199, 331, *500*
surface resistivity, 347

TE mode, 314, 319–320, 334, 336, 340, 345, 349, 360–368, 371, 374, 379, 389, *393, 394*, *397*, *399*
TE wave impedance, *395*, *397*
telegrapher's equation, 327
TEM wave, 254
tilt angle for polarization, 240, 300, *311*

time-average electric energy density, 128
time-average magnetic energy density, 128, 135, *159*
time-average Poynting vector, 108, 127, 151, *157*
time-harmonic fields, 108, 122–131, 151, *154–159*
TM mode, 314, 318–324, 326, 333, 336–340, 345, 346, 349, 356, 358–361, 363–364, 368, 371, 374, 375, 389, 391, *394, 395*, *397*, *399*
TM wave impedance, *395*
transcendental equation, 275
transformation matrix, 250
transformer induction, 10, 12
transverse electric fields, 228, 254–264, 301, *304*
transverse electric to *r* (TE-to-*r*), 520, 525, 529, 531, 544, 561, 569, 572, 573, 575, 577, 578, *580, 581*
transverse electromagnetic wave, 133, 137
transverse magnetic fields, 228, 254–264, 301, *304*
transverse magnetic to *r* (TM-to-*r*), 519, 520, 522, 525, 528, 529, 540, 544, 557, 562, 568, 572, 575, 577, 578, *580, 581*

uniaxial, 18, *312*
uniform plane wave, 231–234, 237, 238
uniqueness theorem, 68, 90–93, *105, 106*, 165, 208, 235
unitary transformation, 250

vector phasor, 123, 127, 131
volumetric charge density, 3, 35, *53*, *58*, 108, 166–168

wave equation, 108, 110, 111, 125, 126, 151, 162, 165, 168, 177, 228, 229, 234, 242, 256, 276–278, 286–288, 290, 300, 314, 353, 358, 363, 367, 368, 370, 374, 375, 385, 392, *395*, *403*, 405, 432, 442, 460, 487, *493*, 503–506, 515, 516, 529, 535
wave number, 125, 228, *304*, *310*, 350, 429, 434, 529
wave polarization, 228, 276
waveguide, 314–320, 322–324, 335–367, 371–374, 381–382, 389–392, *393–395*, *397*, *399–403*
waveguide discontinuity, *396*, *402*
waveguide mode, 320
wire antenna, 108, 144–147, *154*
WKB solution, 286–288
Wronskian for spherical Bessel functions, 510, 547, 560, 574
Wronskian relationship, 412, 440, 444, 469, 487

zonal harmonic functions, 515, 536, 574

# Foundations of Applied Electromagnetics

Electromagnetics is credited with the greatest achievements of physics in the 19th century. Despite its long history of development, due to its fundamental nature and broad base, research in applied electromagnetics is still vital and going strong. In recent years electromagnetics played a major role in a wide range of disciplines, including wireless communication, remote sensing of the environment, military defense, and medical applications, among many others. Graduate students interested in such exciting fields of research need a strong foundation in field theory, which was part of the motivation for writing this book on classical electromagnetics but with an eye on its modern applications.

**KAMAL SARABANDI** is the Fawwaz T. Ulaby Distinguished University Professor and the Rufus S. Teesdale Professor of Engineering serving in the Department of Electrical Engineering and Computer Science at the University of Michigan. His research interests include microwave and millimeter-wave radar remote sensing, electromagnetic wave scattering and propagation, antennas, meta-materials, and bio-electromagnetics. Dr. Sarabandi served as a member of NASA's Advisory Council for two consecutive terms (2006-2010) as well as the President of the IEEE Geoscience and Remote Sensing Society (2015-2016). His contributions to the field of electromagnetics have been recognized by many awards including the Humboldt Research Award, the IEEE GRSS Distinguished Achievement Award, the IEEE Judith A. Resnik medal, the IEEE GRSS Education Award, and the NASA Group Achievement Award. He is a Fellow of IEEE and of the American Association for the Advancement of Science (AAAS), and a Fellow of the National Academy of Inventors. He is a member of the National Academy of Engineering.